THE ROLES OF THE MICRORNA 29 FAMILY IN CARTILAGE HOMEOSTASIS AND OSTEOARTHRITIS

LE THI TRUC LINH

THESIS SUBMITTED FOR THE DEGREE OF DOCTOR OF PHILOSOPHY

University of East Anglia

School of biological Sciences

Norwich, United Kingdom

December, 2014

DEDICATION

I would like to dedicate this thesis to my family

my parents

Mr Le Hung Son,

Mrs Le Thi Khanh Hong

my brother

Mr Le Hung Phong

for their constant love, friendship, support and encouragement throughout my life

ABSTRACT

MicroRNAs are short endogenous non-coding RNA molecules, typically 19-25 nucleotides in length, which negatively regulate gene expression. In osteoarthritis (OA), several genes necessary for cartilage homeostasis are aberrantly expressed, with a number of miRNAs implicated in this process. However, our knowledge of the earliest stages of OA, prior to the onset of irreversible changes, remains limited. The purpose of this study was to identify miRNAs involved across the time-course of OA using both a murine model and human cartilage, and to define their function.

Expression profile of miRNAs (Exiqon) and mRNAs (Illumina) on total RNA purified from whole knee joints taken from mice which underwent destabilisation of the medial meniscus (DMM) surgery at day 1, 3 and 7 post-surgery showed: the miRNA expression in whole mouse joints post DMM surgery increased over 7 days; at day 1 and 3, the expression of only 4 miRNAs altered significantly; at day 7, 19 miRNAs were upregulated and 15 downregulated. Among the modulated miRNAs, the miR-29b was the most interesting and was chosen to further investigate since integrating analysis of the miRNA and mRNA expression array data showed the inverse correlation between miR-29b and its potential targets. In end-stage human OA cartilage and in murine injury model, the miR-29 family was found to increase expression. Moreover, the miR-29 family was found to be the negative regulator in both human and murine chondrogenesis, and was also found to involve in murine limb development. Expression of the miR-29 family was found to suppress by SOX9 at least in part through directly binding to the promoter of the primary miR-29a/b1. Also, TGFβ1/3 decreased expression of the miR-29 family whilst Wnt3a did not have any effect. Lipopolysaccharide suppressed the miR-29 family expression in part through NFκB signalling pathway while the IL-1 strongly induced its expression partly through P38 MAKP signalling. Using luciferase reporter assay, the miR-29 family was showed to suppress the TGFβ, NFκB, and WNT/β-catenin signalling pathways. Gene expression profiles of gain- and-loss-of-function revealed regulation of a large number of previously recognised extracellular matrix-associated genes as well as an additional subset of protease and Wnt signalling pathway-related genes. Among these genes, *ADAMTS6, ADAMTS10, ADAMTS14, ADAMTS17, ADAMTS19, FZD3, DVL3, FRAT2, CK2A2* were experimentally validated as direct targets of the miR-29 family.

CONTENTS

LISTS OF TABLES

LISTS OF FIGURES

LISTS OF APPENDICES

Paper: Le et al, 2013

ACKOWNLEGMENTS

I would like to express my special appreciation and thanks to my primary supervisor Professor Ian Clark. I thank him for giving me the opportunity to become a Clark laboratory member and for allowing me to growth as a research scientist as I am now. I deeply appreciate the change to work and study from a great scientist and an honourable person like him. Without his time, support, guidance and encouragement, my PhD project is impossible.

I would also like to thank my second supervisor Professor Andrea Munsterberg for her comments, and suggestion which really helped me to refine my project. I am also in debted to Dr Tracey Swingler, my third supervisor. Her brilliant lab work skills, experiences, and knowledge tremendously help me go through all the obstacles and finish the study. Her time and her availability for all of my constant string of questions during the last 3 years are invaluable.

I am very thankful for all the past and current members of Clark laboratory for helping me on my research and make my PhD journey enjoyable. Special thank you to Dr Natalie Crowe for sharing with me her human osteoarthritis and normal articular cartilage samples, her dedifferentiation model which will take me a lot of time to do it myself. Thanks to Dr Rosemary Davidson for letting me including her DVL3 expression data in my thesis and for her knowledge, advice, support, and encouragement during my PhD. I would like to acknowledge Jonathan Green, Sarah Garner, Yvette Wormstone for their expertise and kind help in mouse injury model, human primary chondrocyte isolation, and cloning.

I would especially thank to Dr Guy Wheeler in Dalmay laboratory, Dr Geoffrey Mok, and Camille Viaut in Munsterberg laboratory for sharing their knowledge and help me through my whole mount in situ hybridization experiment. Thank you to Dr Eleanor Jones in Riley laboratory for kindly sharing with me her data and for her constantly help during my PhD. In addition, a thank you to Dr Helio Pais, who introduced me to bioinformatics analysis using R. His instruction about how to look for miRNA targets in big data set has become priceless to me. I would especially thank to Dr Mathew Barter in David Young laboratory, Newcastle University, members in Professor Tonia Vincent laboratory, Oxford University,

members of Dr Anne Delany laboratory, University of Connecticut, USA for kindly sharing with me their MSCs model, DMM samples, and vectors.

Great thanks to all of my friends for the time they shared with me throughout my PhD journey. I am grateful their incredible friendship which makes the journey to achieve my goal more enjoyable.

Finally, I would like to acknowledge Vietnam Ministry of Education and Training (project 322), University of Each Anglia scholarship for international student for giving me the opportunity to do PhD in the UK. I also deeply thank Arthritis Research UK (program grant #19424, Tracey Swingler, Ian Clark) for supporting my project. Due to the currency exchange rates and the international fees, there are minimal funds from my Vietnam Government Scholarship for laboratory consumables. Thus, my PhD project is impossible without the support from Arthritis Research UK. I also acknowledge the John and Pamela Salter Trust for supporting me with the LNA probe for miR-29b used in my project.

CHAPTER 1
INTRODUCTION

1.1. Synovial joints

In mammals, joints are functionally classified into 3 categories: synarthroses (immovable joints), amphiarthroses (slightly movable joints), and diarthroses (freely movable joints). Most of the main joints of the appendicular skeleton are synovial joints, suggesting this type of joint has a crucial role in the body. The main component of synovial joints includes **the hyaline cartilage**, also known as articular cartilage, covering the bone of the synovial joint providing the cartilage lubricating and shock absorbing characteristics; **a capsule** enclosing the joint in line with **synovial membrane** which contains synovial membrane-resident cells secreting synovial fluid into the synovial cavity helping reduce friction, enabling free movement; **bones**, further held together by **ligaments**. The characteristics of some important components of the synovial joint relevant to this PhD thesis are described below.

1.1.1. Articular cartilage biology

Articular cartilage, a highly specialized tissue with unique mechanical behaviour, consists of **(i) chondrocytes,** the only cells, responsible for the homeostasis of extracellular matrix (ECM), and **(ii) a dense layer of ECM** composed primarily of water, collagen and proteoglycan.

1.1.1.1 Cartilage structural organization

Healthy articular cartilage comprises four different areas: the superficial, intermediate, radial or deep, and calcified zones (Buckwalter *et al.* 2005, Dudhia 2005, Pearle *et al.* 2005, Aigner *et al.* 2006, Martel-Pelletier *et al.* 2008, Umlauf *et al.* 2010, Houard *et al.* 2013) **(Figure 1.0)**. Each is characterized by a particular chondrocyte phenotype, and by distinctive extracellular matrix organization and composition (Buckwalter et al. 2005).

The superficial zone, the articulating surface and the thinnest of the four, makes up 10%-20% of articular cartilage thickness (Buckwalter et al. 2005, Pearle et al. 2005). This

region contains a high amount of collagen (primary type II, and IX) but very low amount of proteoglycan. The collagen fibrils are densely packed and aligned paralleled to the articular surface. Chondrocytes in this layer are characterized by an elongated appearance (Pearle et al. 2005), express many proteins having lubricating and protective functions (e.g. lubricin) but relatively little proteoglycan. This zone is in contact with synovial fluid, and is responsible for most of the tensile properties of cartilage that enable cartilage to resist shear and the tensile and compressive forces imposed by the movement of the articulation (Martel-Pelletier et al. 2008).

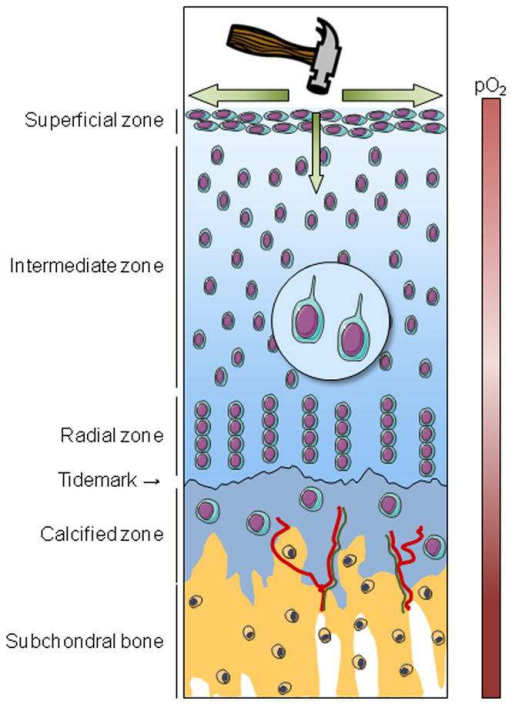

Figure 1.0: Histology of a healthy cartilage structural

The articular cartilage is organized into superficial, intermediate, radial, and calcified zones. Each zone can be distinguished by the difference in chondrocyte morphologies and components of collagen, proteoglycan, mineral and water

The intermediate and the radial zones contain large diameter collagen fibrils oriented perpendicular to the articular surface. These regions also have high amount of proteoglycan which is mainly aggrecan, a large chondroitin sulphate proteoglycan. Chondrocytes in the middle zone are more round than in the superficial zone. In the radial zone, the cells are arranged in columnar fashion (Buckwalter et al. 2005).

The tide mark, a thin line revealed after hematoxylin staining, marks the mineralization front between the calcified and non-calcified articular cartilage (Houard et al. 2013). In **the calcified cartilage zone**, the cell population is very scarce and chondrocytes are hypertrophic (Pearle et al. 2005, Martel-Pelletier et al. 2008). With aging, bloods vessels and nerves can be seen in calcified cartilage arising from the subchondral bones (Lane *et al.* 1977). The main function of this zone seems to be to anchor the cartilage to the bone as collagen fibrils from the radial zone penetrate into the calcified cartilage.

Furthermore, it is noteworthy to know that for mechanical protection purposes, in articular cartilage, the chondrocyte is surrounded by a pericellular matrix and a territorial cartilage matrix forming a capsule-like structure around the cells. Whilst the pericellular matrix is made of a thin layer of non-fibrillar material, which most likely represents the synthetic products of the chondrocytes, such as proteoglycans and glycoproteins, the pericellular matrix also contains a dense meshwork of thin collagen fibers (see below) (Dudhia 2005, Aigner et al. 2006, Martel-Pelletier et al. 2008, Heinegard *et al.* 2011).

1.1.1.2 Biology of chondrocytes

As mention above, chondrocytes are the only cellular components of articular cartilage, make up 5% of the wet weight of articular cartilage, and are surrounded by a pericellular matrix containing type VI collagen, microfibrils, hyaluronic acid, biglycan, and decorin but little or no type II collagen (Buckwalter et al. 2005, Dudhia 2005, Heinegard and Saxne 2011). The arrangement of chondrocytes and articular cartilage specific organisation result from a complex development process called endochondral ossification including four steps e.g. chondrogenesis, chondrocyte differentiation and hypertrophy, mineralization and invasion of bone cells, and finally the formation of bone (DeLise *et al.* 2000, Goldring *et al.* 2006, Goldring 2012). Chondrocytes arise from mesenchymal progenitors as a result of chondrogenesis started with the condensation of mesenchymal stem cell (expressing collagens I, III and V), and followed by the differentiation of chondroprogenitor cell (expressing cartilage-specific collagens II, IX and XI) (Goldring et al. 2006). After chondrogenesis, the chondrocytes remain as resting cells to form the articular cartilage or undergo proliferation, terminal differentiation to chondrocyte hypertrophy, and apoptosis.

There are no blood vessels in articular cartilage, thus the cells rely on diffusion from articular surface or subchondral bone for nutrients and metabolites. Importantly, the oxygen level in the cartilage matrix is quite low, ranging from 10% at the surface to less than 1% in the deep zone (Silver 1975), suggesting the cells have to adapt to this low oxygen level. The mechanisms of this adaption remain unclear but some published data reported the involvement of hypoxia inducible factor -1 alpha (HF-1α) (Schipani *et al.* 2001, Pfander *et al.* 2003). Hipoxia via HIF-1α can stimulate chondrocytes to express a number of genes associated with cartilage anabolism and chondrocyte differentiation like SOX9, TGFβ (Amarilio *et al.* 2007).

1.1.1.3 Biology of cartilage extracellular matrix

Together with chondrocytes, extracellular matrix (ECM) produced by these cells is among the main components of articular cartilage and its integrity is critical for the cartilage biochemical properties and joint physical function.

About structure, the ECM in articular cartilage is organized into pericellular, territorial, interterritorial zones, each of which is represented at specific distance from the chondrocytes (Dudhia 2005, Heinegard and Saxne 2011) (**Figure 1.1**).

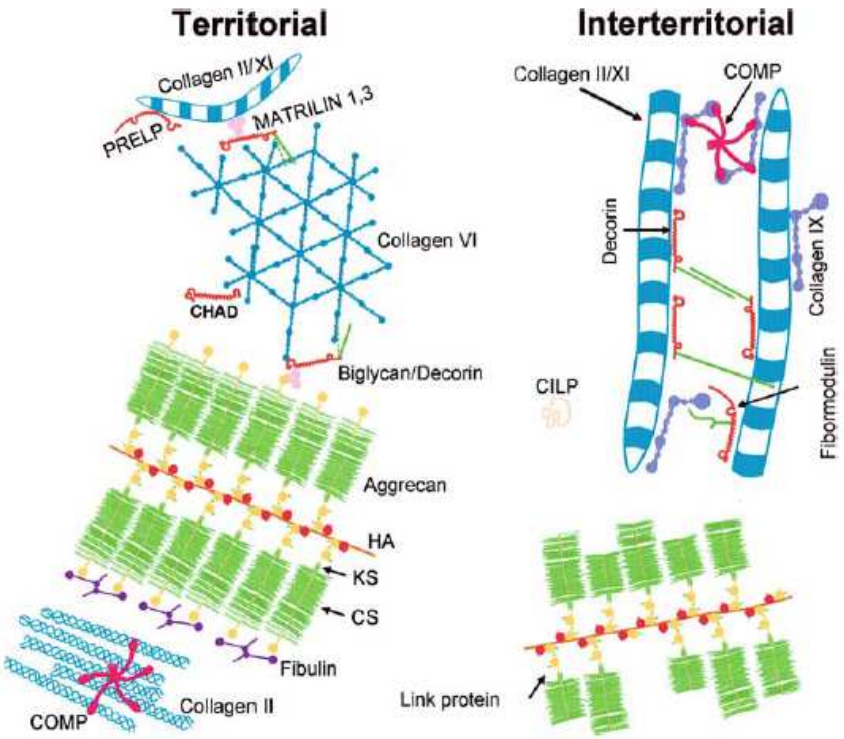

Figure 1.1: **Molecular organisation of normal articular cartilage.**

The cartilage matrix surrounding chondrocytes in healthy articular cartilage is arranged into zones defined by their distance from the cell. Pericellular matrix lies immediately around the cell and is the zone where molecules that interact with cell surface receptors are located. Next to the pericellular matrix, slightly further from the cell, lies the territorial matrix. At largest distance from the cell is the interterritorial matrix (adapted from Heinegard et al, 2011) (Heinegard and Saxne 2011)

Biochemically, of the ECM, approximately 70% is water (Pearle et al. 2005) , and 30% left is solid, of which 5-6% are inorganic compounds (hydroxyapatite), and the remaining 25% are organic compounds. Of the organic components, type II collagen constitutes 68% and the 32% left is formed by proteoglycan (mainly aggrecan) (Martel-Pelletier et al. 2008). The biology of aggrecan and collagen and their functions in articular cartilage are described as below.

1.1.1.3.1 Aggrecan

Molecules made up of a core protein attached to glycosaminoglycan chain are referred as proteoglycan. In articular cartilage, the most abundant proteoglycan is aggrecan, composed of chondroitin sulphate chains and keratan sulphate chains with N- and O-linked oligosaccharides. Aggrecan has three globular domains (G1, G2 and G3) and three extended domains (IGD, KS and CS). The N-terminal G1 domain, responsible for aggrecan-hyaluronan interaction, is followed after the signal peptide. The inter-globular (IGD) connects G1 and G2 domains, whose functions are unclear. Keratan sulphate binding (KS) and chondroitin sulphate (CS) domain lie between G2 and G3 domains (Kiani *et al.* 2002, Dudhia 2005, Martel-Pelletier et al. 2008, Heinegard and Saxne 2011) (Figure 1.2).

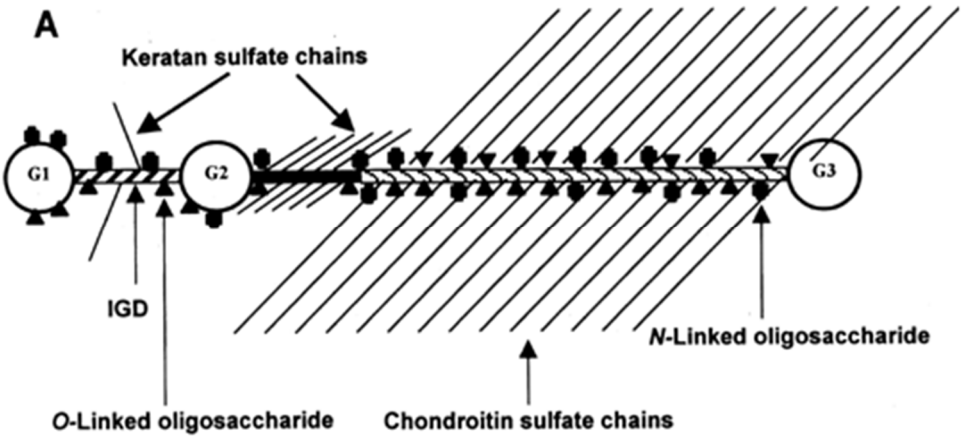

Figure 1.2: Aggrecan structure.

Aggrecan consists of 3 globular domains (G1, G2, and G3) and an attached GAG chain structure. The GAG attachment region is separated into keratin sulphate binding (KS) domain and chondroitin sulphate (CS) domain (Adapted from Kiani et al, 2002) (Kiani et al. 2002).

The chondroitin sulphate domain is the largest domain of aggrecan and is composed of around 100 chondroitin sulphate chains (typically around 2kDa each). Each chain is made up of some 50 disaccharides of glucuronic acid and N-acetylgalactosamine, with a sulphate group in the 4- or 6- position. The negatively-charge chondroitin sulphate chain accounts for the major function of aggrecan as a structural proteoglycan. The function of the keratan sulphate domain is not very clear but may be involved in the tissue distribution of aggrecan. There are about 30 KS chains, usually of small size (5-15 kDa), attached to the mature aggrecan molecule.

Chondroitin sulphate, keratan sulphate, and the interaction of aggrecan and hyaluronic acid are responsible for retaining water the cartilage. The interaction between aggrecan and collagen fibrils makes the ECM highly hydrophilic, leading to high resistance to compressive mechanical loads (Dudhia 2005, Martel-Pelletier et al. 2008).

1.1.1.3.2 Collagen

Collagen fibrils are composed of a protein macromolecular providing cartilage with resistance to tension. Collagen type II constitutes 85% total collagen content in the ECM of articular cartilage. Apart from type II Collagen, ECM also contains other collagens called minor collagens since their concentration is low in comparison with the type II collagen. A list of these collagens is provided in Table 1.1.

All fibril collagens are synthesized in the form of three polypeptide α-chains as a procollagen in which each chain has an N-terminal extension and a C-terminal extension. The three chains are covalently linked via disulphide bridges in the C-terminal propeptide. Following or during secretion of procollagens into the extracellular matrix, the terminal propeptides are cleaved off by specific proteinases e.g. ADAMTS-2, ADAMTS-3, ADAMTS-14 (cleaves the N-terminal) (Lapiere *et al.* 1971, Fernandes *et al.* 2001, Colige *et al.* 2002), and BMP-1 (cleaves the C terminal) (Wermter *et al.* 2007) to produce the mature collagen molecules. The mature collagens then spontaneously self-assemble into

cross-striated fibrils in the extracellular matrix. The fibrils are stabilized by covalent cross-linking (Figure 1.3)

Collagen molecules then associate on a core of two homologous collagen XI and two collagen II molecules to form an outer shell of 10 collagen II molecules of the micro fibril. In addition to collagen type II, fibers contain other collagens, particular collagen type IX. The collagen network is then stabilized by the formation of covalent crosslinks that link the collagen II chains. The links formed are both intra- and inter-molecules, for example, between the chains of collagen XI, between collagens e.g. collagen II and collagen IX.

Many other proteins also have a high affinity for collagens including thrombospondins, leucine-rich repeat proteins (biglycan, decorin, fibromodulin, lumican), matrillins, and fibronectin. Some of these interactions support fibre formation while others modify the collagen fibre surface to provide sites for interactions with neighbouring structures (Heinegard and Saxne 2011).

Collagen types	Characteristics
Type IX	Located on the surface of type II collagen fibrils; promotes the binding of the fibrils to other components of the matrix and to each other; carries a glycosaminoglycan chain.
Type XI	Forms the core of the same fibrosis. Regulates the formation and the diameter of the fibrils
Type V	Sometimes replaces the type XI collagen in cartilage; included in type I collagen fibrils in other tissues. Data on the composition and structure of the third a-chain are contradictory
Type III	Small amount are covalently bound to type II collagen
Type XII	Very small amounts are present on the surface of type II collagen
Type XIV	Very small amounts are present on the surface of type II collagen
Type VI	As in other tissue, forms a network of microfibrils. Concentrated mainly in the pericellular areas, provides a connection between the chondrocytes and the matrix
Type X	Expressed only by hypertrophic chondrocytes in cartilage areas undergoing ossification
Type XXVII	Expressed in cartilage tissue

Table 1.1 Minor collagen of cartilage tissue (adapt from Omelyanenko et al, 2014)(Petrovich *et al.* 2014)

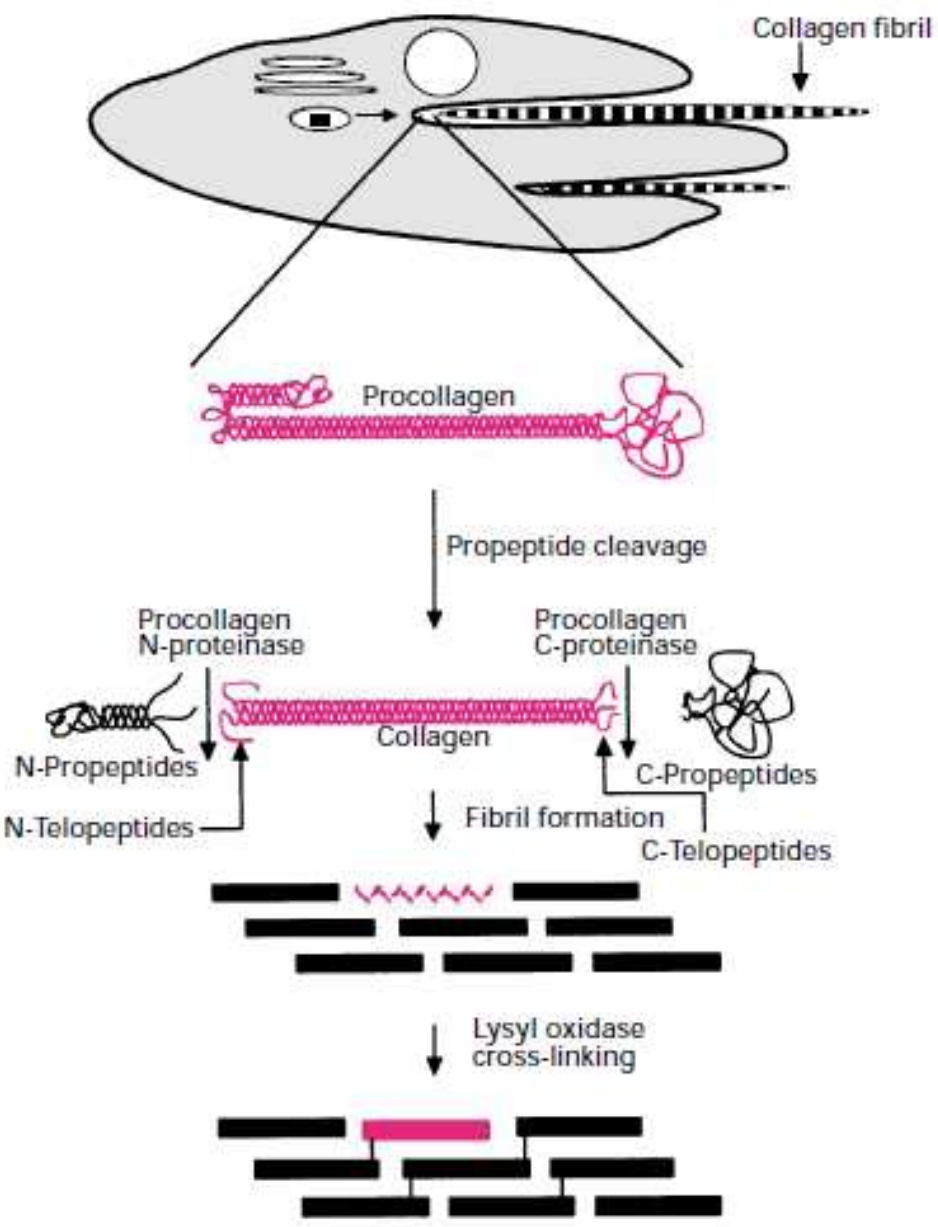

Figure 1.3: The formation of the fibrillar collagens

Procollagen is secreted from cells and converted into collagen by removal of the N- and C-propeptids by pro-collagen metalloproteinases. This produces mature collagen that spontaneously self-assembles into cross-striated fibrils which are stabilized by covalent cross-linking. Taken from (Kadler et al, 1996)(Kadler *et al.* 1996).

1.1.2. Synovium

Synovium is a thin tissue only a few cell layers thick (Fell 1978). The synovium acts as the controller for the environment within the joint where nutrients for chondrocytes can pass into the synovial cavity. Also, the synovium gives the joint its mechanical properties. The synovium can be divided into two compartments e.g. the synovial lining and the sub-lining. The synovial lining contains two cell types e.g. **type A (macrophage-like cells)** clearing all excess materials and potential pathogens from the joint, producing and secreting a number of enzymes and cytokines and chemokines that mediate tissue damage and inflammation in disease; **type B synoviocytes**, **fibroblast like cells**, producing the main component of synovial fluid, hyaluronan. The synovial sublining consists of connective tissue containing blood vessels, fibroblasts, adipocytes, and a limited number of resident immune cells, such as macrophage and mast cells (Smith *et al.* 2003). The synovial fluid has crucial role for lubrication of the joint and for transporting nutrients and oxygen to the cartilage.

1.1.3. Bone

Periarticular bone can be separated into distinct anatomic entities e.g. the subchondral bone plate, the subchondral trabecular bone, and the bone at the joint margins. The subchondral bone plate consists of cortical bone, which is relatively nonporous and poorly vascularized. It is separated from the overlying articular cartilage by the zone of calcified cartilage.

Bone is a very dynamic tissue with constantly undergoing remodelling in which bone resorption is normally followed by new bone formation. The primary cell responsible for bone resorption is the **osteoclast**, a specialized multinucleated cell of hemopoietic origin (Roodman 1999). Bone resorption takes place under a specialized area of the osteoclast cell membrane called “ruffled border,” which comprises a sealed lysosomal compartment where the acidic pH solubilizes the mineral and proteolytic enzymes digest the matrix. On the contrary, **osteoblasts**, the bone forming cells, originally from MSCs committed to osteoblastic lineage. Osteoblasts synthesize and secrete most of the proteins of the bone matrix, including type I collagen and non-collagenous proteins (Caetano-Lopes *et al.* 2007). In normal physiological condition, the amount of bone removed during the resorption and formation phases is balanced such that bone mass is maintained.

1.2. Osteoarthritis

Osteoarthritis (OA) is defined by the American College of Rheumatology as a "heterogeneous group of conditions that lead to joint symptoms and signs which are associated with defective integrity of articular cartilage, in addition to related changes in the underlying bone at the joint margins''.

There are more than 100 types of arthritis. However, OA or degenerative joint disease is the most common type. From a clinical point of view, OA can be classified into two categories e.g. **primary** which refers to its occurrence not related to any prior condition or event which is also referred as idiopathic, and **secondary** which refers to the development of the disease after trauma or pre-existing condition.

The disease most commonly affects the middle-age and elderly, although it may begin earlier as result of injury, obesity or congenitally. As a greater proportion of the population is old aged and with increasing obesity, OA will have a great impact on society in the future with enormous socioeconomic costs.

1.2.1. Osteoarthritis pathology

It is now considered that OA is a disease of the whole joint as an organ resulting in "joint failure" where all major components of the joint e.g. the cartilage, the synovium, and the underlying bone are affected (Loeser *et al.* 2012). The pathologic changes seen in OA include cartilage destruction, fibrosis of the synovial capsule, hyperplasia of the synovial membrane, osteophyte formation, the subchondral bone thickening (**Figure 1.4**) (Aigner et al. 2006, Loeser et al. 2012). These changes result from an incompletely understood series of functional events.

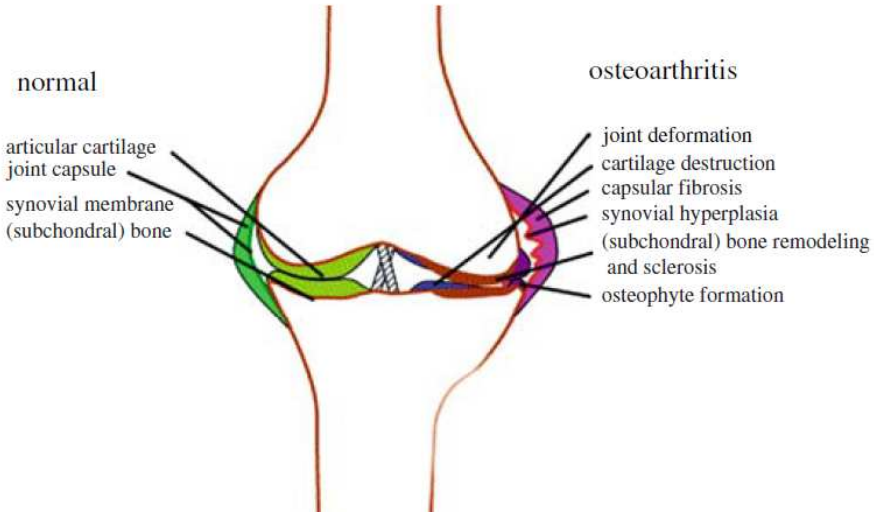

Figure 1.4: Overview of the pathologic changes associated with OA.

In a normal joint, the subchondral bone is covered by a thick layer of articular cartilage and the joint is enclosed in a capsule where the synovial membrane lies. In an OA joint, articular cartilage is destroyed, the subchondral bone is remodelled (thickens), the synovial capsule is fibrosed and osteophytes are formed (reprinted from Aigner et al, 2006) (Aigner et al. 2006)

1.2.1.1.Articular cartilage destruction in osteoarthritis

Biochemical, genetic factors, and mechanical stress contribute to the OA lesion in cartilage, leading to articular cartilage degradation, and chondrocyte metabolism disorders as a consequence. Articular cartilage degeneration is a two phase process controlled mainly by chondrocytes e.g. a short biosynthesis phase where the cells attempt to repair the damaged ECM, followed by the degenerative phase, where the cells destroy the articular cartilage by increasing the synthesis of matrix degradating proteinases and decreasing their synthesis of matrix components, in particular of aggrecan. Besides changes in synthesis and degradation, other aberrant behaviours in cell proliferation and death, and phenotypic modulation are also observed in OA chondrocytes (Sandell *et al.* 2001).

Contrary to normal chondrocytes with no proliferative activity, OA chondrocytes have a low proliferative activity (Meachim *et al.* 1962, Rothwell *et al.* 1973, Lee *et al.* 1993), explained in part due to the better access to proliferation factors from the synovial fluid as well as due to the damage of the ECM (Meachim and Collins 1962, Lee et al. 1993), subsequently causing chondrocyte clustering, a characteristic feature of OA cartilage. Chondrocyte death, caused by apoptosis, necrosis, or other cell death mechanisms such as chondroptosis, is another known feature of OA. Many studies have demonstrated the significant correlations between chondrocyte death and severity of OA and aging. These changes are associated with the production of reactive oxygen species, a lack of growth factors, release of glycosaminoglycan and mechanical injury. However, which of these types of cell death predominate in OA is debatable. The detection of specific form of cell death in articular cartilage is difficult in which current gold standard for detecting chondrocyte death is electron microscopy which suggests that the morphological changes of chondrocytes in OA cartilage are attributed to apoptosis and / or chondroptosis. Chondrocyte death by apoptosis has been reported play an important role: normal cartilage explants or chondrocyte culture exposed to nitric oxide, collagenase, anti CD-59, or mechanical factors e.g. shear strain, loading strain induced apoptosis; cartilage from equine joints have shown that chondrocyte apoptosis is positively correlated with early stages of OA and severity of cartilage damage (Zamli *et al.* 2011).

When the damage occurs, the chondrocytes attempt to repair the damaged matrix by increasing their anabolic activity to enhance ECM synthesis. However, a net loss of ECM content is one of the hallmarks of all stages of OA, suggesting the dominance of ECM degradation over the synthesis. This is characterized by the increase in expression and activation of matrix-degrading enzymes e.g. matrix metalloproteinase (MMPs) and aggrecanases (from the ADAMTS family) (Buckwalter et al. 2005, Pearle et al. 2005, Aigner et al. 2006, Umlauf et al. 2010, Loeser *et al.* 2012). **The MMPs,** belonging to a family of zinc-dependent proteases, show activation correlating with cartilage degradation. Among these, the groups of collagenases 1, 2, 3 (MMP-1, MMP-8, and MMP-13, respectively), stromelysins (MMP-3, MMP-10, MMP-11) and gelatinases (MMP-2, MMP-9) have the highest impact on OA cartilage breakdown (Burrage *et al.* 2006). The MMP-1, MMP-8 and MMP-13 which cleave native fibrillar collagen, contribute to the pathological cleavage of collagen fibrils in OA (Burrage et al. 2006). Of the collagenase group, MMP-13 is deemed to be responsible for most of the collagen II breakdown whilst MMP-1 cleaves type II collagen stronger than MMP-8 (Billinghurst *et al.* 1997) has a pivotal role for collagen cleavage in OA (Knauper *et al.* 1996). In addition to collagenases, others MMPs degrading non-collagen have also been shown to be elevated in OA cartilage e.g. the gelatinases (which cleave denatured collagen, gelatin, type V collagen) and the stromelysins (having substrate preference for proteoglycans, elastin, laminin, fibronectin) (Umlauf et al. 2010) **The aggrecanases** (the ADAMTS family), are also of particular importance in cartilage turnover, and have activity against the proteoglycan aggrecan. Of all ADAMTS members, ADAMTS-4 and ADAMTS-5 are most active against aggrecan (Arner 2002). ADAMTS-5 is constitutively expressed in chondrocytes whereas ADAMTS-4 expression is stimulated by proinflammatory cytokines IL-1β, and TNF-α (Umlauf et al. 2010) (Tortorella *et al.* 2001). In vitro studies with human cartilage show that both ADAMTS-4 and ADAMTS-5 contribute to ECM breakdown during the disease progression even though human recombinant ADAMTS-5 has higher rate of aggrecan cleavage than ADAMTS-4 (Song *et al.* 2007). In mice, ADAMTS-5 has been shown to be the major aggrecanase, by studies with ADAMTS-4 and ADAMTS-5 knockout mice in which only ADAMTS-5 deficiency prevented the mice from cartilage degradation in both inflammatory and a joint-instability model of arthritis (Glasson *et al.* 2005, Stanton *et al.* 2005) .

As mentioned above, despite the attempt at repairing the ECM, the damage to the cartilage becomes irreversible because the adult chondrocytes fail in regenerating the normal cartilage matrix structure. This failure could be, in part, attributed to the phenotypic alteration of chondrocytes. Chondrocyte phenotypes are categorized largely by subtyping collagen expression e.g. chondroprogenitor cells express type IIA procollagen. The alternative splice variant) (Sandell *et al.* 1991), mature chondrocytes are marked by expressing type IIB procollagen, IX, and XI, aggrecan and link protein (Sandell and Aigner 2001), and hypertrophic chondrocytes express type X collagen (Schmid *et al.* 1985). In OA cartilage degeneration, an important proportion of adult articular cartilage chondrocytes, found mostly in the middle zone, re-expressed type IIA procollagen (chondroprogenitor cells) in both early and late OA stages (Sandell and Aigner 2001). Cells in the upper middle zone mainly express type III collagen which is a fibroblast-like phenotype. This phenotype is normally observed in vitro, where the chondrocyte phenotypes are modulated through so-called "dedifferentiation" process by several factors like retinoic acid or IL-1. Dedifferentiated chondrocytes are still very active, express collagen types I, III and V but stop expressing aggrecan and collagen type II (Sandell and Aigner 2001). In the deepest zone of OA cartilage, the cells start to express type X collagen, specific marker for hypertrophy of growth-plate chondrocytes (Girkontaite *et al.* 1996). Indeed, the hypertrophic chondrocytes in OA cartilage and in the growth-plate share similarities and the subsequent functional event associated with hypertrophic differentiation is cartilage mineralization which is also a feature of OA. However, the mechanism involved in pathological cartilage calcification during OA is not completely understood.

1.2.1.2. Synovium in osteoarthritis

Inflammation of the synovial membrane (synovitis) is identified in many OA patients despite lower severity and greater variability as compared to rheumatoid arthritis. It is reported that synovitis can occur even in early stages of the disease (Benito *et al.* 2005). Synovitis is associated with symptoms such as pain, the degree of joint dysfunction, the rapid degeneration of cartilage, and is characterized by the thickening of the synovial lining layer, leukocyte infiltration, and thickening of the sub-lining stroma. The

mechanisms underlying the development of synovitis in OA remain unclear. It is however well known that this inflammatory process is triggered by ECM degradation products, which engage Toll-like receptors and the complement cascade (Scanzello *et al.* 2012). Noteworthy, the synovial reaction may produce a variety of cytokines and chemokines, in turn affecting catabolism of chondrocytes (Scanzello and Goldring 2012).

Of all cell types in the inflamed OA synovium, the macrophages are among the most abundant and depletion of synovial macrophages has been shown to result in decreased osteophyte formation, and IL-1, TNF-α, IL-6, IL-8, MMP-1, MMP-3 production (Bondeson *et al.* 2010). Natural killer cells and dendritic cells are also reported to present in synovial tissue. However, the role of both of them in OA pathogenesis has not yet been elucidated in detail.

1.2.1.3. Subchondral bone in osteoarthritis

Articular cartilage helps to distribute load across the whole joint surface. Any alteration in the properties of cartilage leads to alter load experience by the underlying bone and probably causes a tissue remodelling response. The properties of bone might also modulate how the overlying cartilage reacts to load.

Although OA is often characterized as a disease of articular cartilage, the alteration of bone metabolism is increasingly recognised as a mediator of pain and OA progression. Subchondral bone consists of a dome-like subchondral plate and underlying trabeculae, having a close biomechanical and biochemical relationship with the overlying cartilage. Strong evidence associates subchondral bone alterations with cartilage damage and loss in OA (Karsdal *et al.* 2014). However, there is still an incomplete understanding of the mechanisms for the numerous pathophysiological alterations detected in subchondral bone with OA.

The pathological cascade may be started when the normal subchondral bone suffers from a non-physiological strain. In early-stage OA, the subchondral plate becomes thinner and more porous, together with initial cartilage degeneration. Subchondral trabecular bone also deteriorates, with increased separation and thinner trabeculae. At the same time, microdamage begins to appear in both calcified cartilage and subchondral bone, which will persist throughout the whole pathological process. In late-stage OA, calcified cartilage and the subchondral plate become thicker, with duplicated tidemarks and progressive non-calcified cartilage damage. Subchondral trabecular bone becomes sclerotic (Li *et al.* 2013).

The sclerosis of periarticular mineralized tissues may be a biomechanical compensational adaption to the widespread cysts and microdamage in subchondral bone, which render subchondral bone structure more fragile (Figure 1.5).

Despite increased bone volume density in the sclerotic subchondral bone, its mineralization is reduced and lower than in normal joints. Although collagen synthesis is elevated in subchondral bone, the deposited collagen is hypomineralized and has a markedly reduced calcium-to-collagen ratio [42].

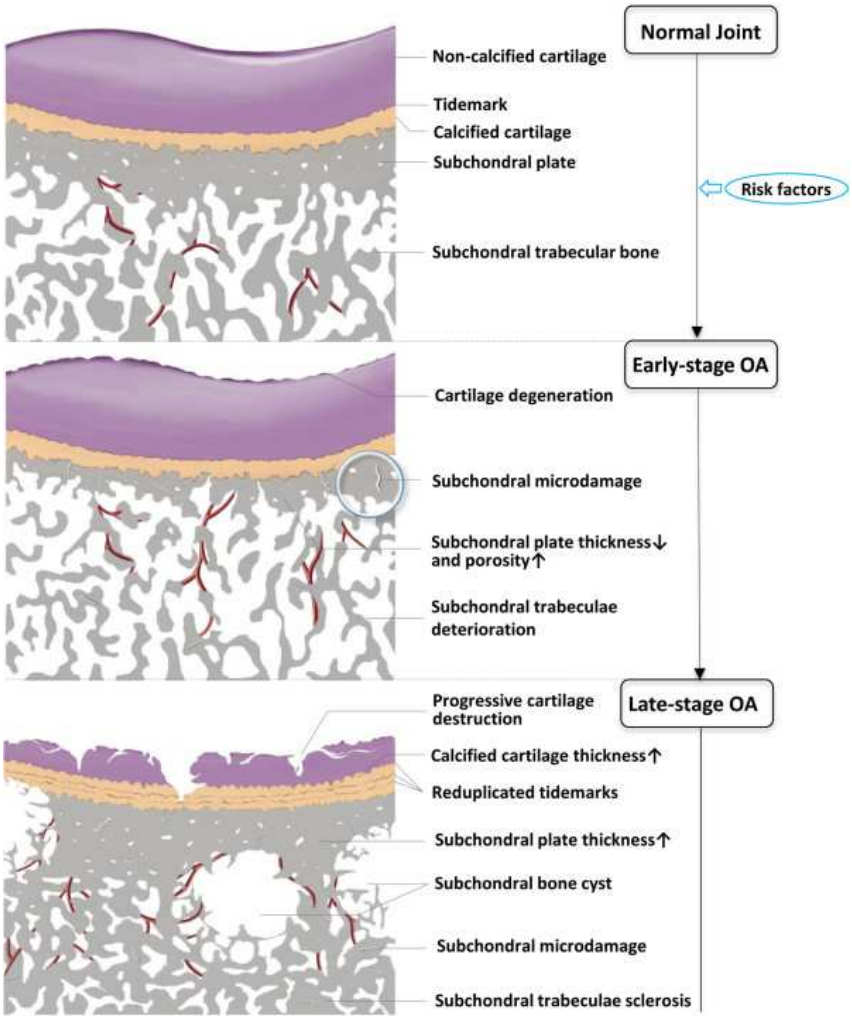

Figure 1.5: Alteration in subchonral bone in Osteoarthritis

In early stage of OA, subchondral microdamage occurs, the subchondral plate is thinner with increased porosity, and subchondral trabeculae are deteriorated. At OA later stage, the calcified cartilage and subchondral plate is thicker, with reduplicated tidemarks. Subchondral trabecular bone becomes sclerotic (adapted from Li et al, 2013)(Li et al. 2013)

1.2.1.4. Osteophytes

Osteophytes, considered as an adaptation to the altered biomechanics, are non-neoplastic osteo-cartilaginous protrusions growing at the margins of OA joints, and represent areas of new cartilage and bone formation. Osteophytes limit joint movement, represent a source of joint pain, and are a radiographic hallmark of OA. However, it is noteworthy that when osteophytes appear in the absence of other bony changes, e.g. subchondral cysts or subchondral sclerosis, they may be a manifestation of aging, rather than of OA.

Osteophytes derive from precursor cells within periosteal or synovial tissue (van der Kraan *et al.* 2007) but the initial stimuli for osteophyte formation remains unclear, probably involving both mechanical and humoral factors as repeated injections of mouse joints with TGFβ or BMP induced or enhanced osteophyte formation in animals with experimentally induced OA (van Beuningen *et al.* 1998).

Osteophytes are composed of cells that express type I procollagen mRNA, mesenchymal prechondrocytes that express type IIA procollagen mRNA, and maturing chondrocytes that express type IIB procollagen mRNA. Based on the spatial pattern of gene expression and cytomorphology, the neochondrogenesis associated with osteophyte formation closely resembles that of healing fracture callus (Matyas *et al.* 1997) and is also similar to the growth plate. Thus, osteophytes may represent an excellent *in vivo* model for induced cartilage repair processes.

1.2.2. Anabolic and catabolic signalling in OA

Anabolic and catabolic activation are largely the result of exposing cells to various cytokines and growth factors e.g. TGFβ, BMPs, IGF-1, TNF-α, IL-1β, Wnt3a. In OA cartilage, the catabolic and anabolic equilibrium is broken and favours the activation of catabolic pathways or mechanisms leading to matrix degradation.

1.2.2.1.Anabolic signalling in OA

As previously mentioned, the early phase of the response to mechanical injury is characterized by the attempt to repair the damage matrix by increasing the anabolic activity of chondrocytes, enhancing synthesis of extracellular matrix components. This is facilitated by enhancing levels of anabolic factors e.g. TGFβ, FGF, and BMPs, and Wnt.

1.2.2.1.1. TGFβ signalling

The TGFβ family, consisting of over 35 members including TGFβ and BMPs, has been widely known to play a crucial role in the development and homeostasis of various tissues. Activated TGFβ (TGFβ-1, -2, -3) binds to their two receptor complex, TGFβ-R1 and TGFβ-RII and phosphorylates members of the receptor-specific Smad family, Smad2 and Smad3. Upon phosphorylation, Smad2/3 subsequently forms a complex with the common mediator Smad4. This complex then translocates into the nucleus where it can act as a transcription factor. Unlike TGFβ-1, -2, -3 which signal via Smad2/3/4, BMPs transduce their signal through Smad-1, -5 and -8 (Miyazawa *et al.* 2002, Verrecchia *et al.* 2002).

Members of the TGFβ family are considered potent mediators of cartilage matrix synthesis, in which they up-regulate the expression of several types of collagens and proteoglycan but down-regulate cartilage degrading enzymes (Verrecchia *et al.* 2001, Verrecchia and Mauviel 2002). Despite such promising data, therapeutic studies with TGFβ revealed major side effects e.g. injection or adenovirus–mediated delivery of TGFβ1 into normal murine knee joint resulted in joint fibrosis and osteophyte formation (van Beuningen et al. 1998) .

1.2.2.1.2. Wnt signalling

The human Wnt family includes 19 members which mostly exert their function by binding to Frizzled (FZD) receptor proteins and LRP-5/6 co-receptor proteins, in turn activating several signal transduction pathways e.g. canonical, and non-canonical signalling pathways. In the canonical Wnt pathway, most β-catenin in the cytoplasm is sequestered and targeted for proteasome-mediated degradation within a multi-protein complex of casein kinase, axin, the adenomatous polyposis coli tumour suppressor protein (APC) and glycogen synthase kinase 3β (GSK3β). With the presence of appropriate Wnt ligands, signalling through the Frizzled receptors inhibits this degradation process, and thereby leads to β-catenin accumulation and translocation into the nucleus (Clevers 2006). Within the nucleus, it acts in concert with Tcf/Lef transcription factors to generate a transcriptionally active complex that regulates a number of genes e.g. MYC, cyclin D1, MMP3 and CD44, E-cadherin, MMP7, MMP26(Dell'accio *et al.* 2008, Umlauf et al. 2010). In contrast to the canonical pathway, non-canonical Wnt signalling is mostly a β-catenin independent mechanism like the Wnt/calcium and Wnt/JNK pathways in vertebrates and the Wnt/planar cell polarity pathway (PCP) in flies (Willert *et al.* 2006). In addition, there

are some natural extracellular inhibitory factors for Wnt signalling. One of the best characterized families is the Dickkopf (Dkk) family which bind to LRP-5/6 and antagonize the canonical pathway. Other antagonists are the secreted frizzled-related protein (sFRP) family which bind directly to Wnt ligands and inhibiting both canonical and non-canonical Wnt pathways (Kawano *et al.* 2003).

A number of published data provide evidence of the critical role of Wnt signalling in OA development. Direct evidences come from animal model studies where β-catenin is conditionally activated or inhibited in articular cartilage chondrocyte of adult mice (Zhu *et al.* 2008, Zhu *et al.* 2009). Mice with β-catenin activated had OA-like cartilage degradation, osteophyte formation, associated with accelerated chondrocyte maturation and MMP13 expression (Zhu et al. 2009). Similarly, selective suppression of β-catenin signalling in Col2a1-ICAT (inhibitor of β-catenin and TCF) transgenic mice also causes OA-like cartilage degradation(Zhu et al. 2008). In line with these reports, in vitro culture of human primary chondrocyte, either activation or blockade of β-catenin signalling all resulted in cartilage loss (Nalesso *et al.* 2011). These data suggest that balanced β-catenin levels are essential for maintaining homeostasis of articular chondrocytes and that any factors impairing this balance could lead to pathological changes. Moreover, LRP5 is located in chromosome 11q12-13, which is thought to be an OA susceptibility locus. LRP5-/- mice displayed increased cartilage degradation, probably due to low bone mass density (Lodewyckx *et al.* 2012). Another study in a mouse OA model also demonstrated that control of Dkk1 expression, a negative regulator of β-catenin/Wnt signalling, prevents joint cartilage deterioration in OA knees through attenuating the apoptosis regulator Bax, MMP3 and RANKL (Weng *et al.* 2010). Also, the inhibition of Dkk1, has been reported to be able to reverse the bone-destructive characteristics of rheumatoid arthritis to the bone-forming characteristics of OA (Diarra *et al.* 2007). This evidence further supports the crucial role of β-catenin/Wnt signalling in OA. Wnt signalling is also reported to function as an OA initiation factor e.g. a down-regulation of Wnt antagonist FRZB and an up-regulation of the ligand Wnt16 and target genes encoding β-catenin, Axin-2, C-JUN and LEF-1 was observed in mouse model of mechanical injury, a major cause of OA; expression of WNT1-inducible signalling protein (WISP-1) was also increased twofold in cartilage lesions compared to healthy intact cartilage (Blom *et al.* 2009).

Human studies also observed the critical role of WNT signalling in OA development. A loss-of-function allelic Arg200Trp and Arg324Gly Frzb variants, encoding sFRP-3, a β-catenin/Wnt signalling inhibitor, contributed to genetic susceptibility of women to hip OA (Loughlin *et al.* 2004, Lane *et al.* 2006). Given the close relationship between bone shape and OA development, Baker-Lepain et al proposed that SNPs in Frzb are associated with the shape of proximal femur and further contribute to hip OA development (Baker-Lepain *et al.* 2012). Moreover, the Frzb knockout mice increased articular cartilage loss during arthritis triggered and this damage was associated with increased WNT signalling and MMP-3 expression and activity. Also, the FRZB deficiency resulted in the cortical bone thickness and density with stiffer bones (Lories *et al.* 2007).

1.2.2.2. Catabolic signalling in OA

Opposing the anabolic effects of growth factors are pro-inflammatory cytokines and a variety of mediators associated with inflammation e.g. NO, prostaglandins, IL-1β, TNF-α, IL-6, IL-8 These factors are first produced by the synovial membrane and diffuse into the cartilage through synovial fluid, together with activate chondrocytes which also have the capacity to produce a variety of cytokines and mediators, responsible for functional alterations in the synovium, the cartilage, and the subchondral bone. Their role in OA has attracted considerable attention.

Of pro-inflammatory cytokines, IL-1β, TNF-α seem prominent and of major importance to cartilage destruction. The biologic activation of cells by IL-1 is mediated through the association with its specific receptors e.g. type I and II IL-1R. Especially, the type I IL-1R, responsible for signal transduction, was found to increase in OA chondrocytes and synovial fibroblasts. IL-1β is a critical mediator, and stimulation of chondrocytes by IL-1β causes gene expression patterns similar to those in OA cartilage (Goldring *et al.* 1988, Lefebvre *et al.* 1990). IL-1β localizes to the site of cartilage degradation in OA joints, providing evidence of its key role in the pathogenesis of OA (Tetlow *et al.* 2001, Pujol *et al.* 2008). IL-1β was reported to suppress aggrecan and collagen and up-regulate the proteolytic enzymes e.g. ADAMTS4 and MMP13 (Goldring 2000, Kobayashi *et al.* 2005). In addition, *IL-1β*, or IL-1β-converting enzyme knockout mice showed the accelerated development of OA lesions in response to OA surgical induced compared to wild type mice (Clements *et al.* 2003). The blocking effects of IL-1β by IL-1 receptor antagonist

(IL-1ra), which is the natural inhibitor of IL-1β by competing with IL-1β for occupancy of the IL-1β cell surface receptors but cannot initiate cellular signals protect against the development of experimentally induced OA lesions in animal models e.g. dogs, horses (Pelletier *et al.* 1997, Frisbie *et al.* 2002). Interestingly, it was reported that the IL-1β concentration is low in inflamed joints and a level from 10-1000 fold excess of IL-1ra over IL-1β was required to efficiency block all of the available IL-1β receptors enough to inhibit joint degradation (Pelletier et al. 1997).

1.2.2.2.1. NFκB Signalling

The transcription factor NFκB is the master regulator of expression of a number of genes critical to innate and adaptive immunity, cell proliferation, and inflammation. NFκB is held in the cytoplasm in an inactive form associated with the inhibitory κB (IκB) protein. A broad range of stimuli, including TNF-α, IL-1β, bacteria and viruses trigger a cascade of signalling, leading to release of NFκB from IκB. The activated NFκB will then translocate to the nucleus, bind to DNA elements present in its target genes and facilitate their transcription.

Numerous published data support the central role of NFκB signalling in cartilage metabolism and development of OA e.g. IκB overexpression in human OA synovial fibroblasts resulted in a decrease in expression of IL-6, IL-8, MPC-1/CCL-2, and MMPs (Amos *et al.* 2006) as well as abolishing the IL-1β-induced effect on expression of ADAMTS-4 (Bondeson *et al.* 2007); In a mouse surgically induced OA model, siRNA inhibiting NFκB/p65 resulted in reducing the amount of IL-1βand TNF-α in synovial fluid, reducing the level of inflammation in the synovium, and decreasing cartilage damage (Chen *et al.* 2008).

1.2.3. Risk factors for Osteoarthritis

The pathogenesis of OA is complex and poorly understood but involves the interaction of multiple factors ranging from genetic predisposition to mechanical and environmental components. Studies are in progress to define the molecular mechanisms involved in initiation and progression of OA.

1.2.3.1.Trauma and altered mechanical load

Mechanical factors and trauma have a central role in the initiation and propagation of OA: Excessive load and trauma which lead to injury of the menisci or ligaments predispose to

the development of the disease; the level and nature of the load experienced might also influence the progression of joint damage: an acute trauma leading to rupture of the meniscus or the cruciate ligaments might precipitate the development of OA. However, the differing contributions to this effect of the initial trauma and the ensuing mechanical instability have not been clearly delineated; also, in immobilized joints, there is lack of OA: further supporting the importance of mechanical triggers in the disease process (Riordan *et al.* 2014).

After joint trauma, the onset and progression of clinical symptoms differs even among groups with the same type of injury and physical activity profile, pointing to the involvement of other factors apart from the trauma.

1.2.3.2. Inflammation

Histologically, the disease was denominated osteoarthrosis, a term that implied the absence of inflammation. However, data acquired using high-sensitivity assays for inflammatory markers (such as C-reactive protein) demonstrate that low-grade inflammation is present (Pearle *et al.* 2007). Numerous inflammatory cytokines are found at increased levels in joint tissues during the acute post-injury phase, including IL-1, IL-6, IL-17, and TNFα (Lee *et al.* 2009). Inflammation seems to be a very early event in OA since the increase of CRP levels precedes the release of other OA indicators or molecular markers of matrix breakdown, and is observed well before clinical disease.

Inflammatory might be of particular importance to the onset and propagation of the primary and secondary OA. However, why the inflammation triggered in OA remains controversial. It was hypothesized that it was caused by traumatic joint injury or an age – related process. Joint injury leads to cartilage degradation and tissue damage. Once degraded, cartilage fragments accumulate in the joint and contact the synovium. Considered foreign bodies, synovial cells react by producing inflammatory mediators, found in synovial fluid. These mediators can activate chondrocytes present in the superficial layer of cartilage, which leads to metalloproteinase synthesis and, eventually, increase cartilage degradation. Published data support for the hypothesis that inflammation was triggered by aging process: advance glycation endproducts (AGEs), produced by a non-enzymatic process in aging tissue, weaken cartilage by modifying its mechanical properties triggering chondrocyte activation by binding to specific receptors present at the

surface of the chondrocytes, called RAGE (receptor for AGEs) lead to an overproduction of proinflammatory cytokines and MMPs (Nah *et al.* 2007); or after a period of vigorous proliferation, chondrocyte division rate declines but has high capacity to synthesize soluble mediators which in turn induces several inflammatory and pro-degradative mediators.

1.2.3.3. Obesity

Obesity is a well known risk factor for the initiation and progression of OA. This association is obvious because any overload on a weight – bearing joint would provoke tear and wear at the surface of the cartilage.

The molecular mechanisms explaining why obesity is one of the major risk factors for OA (Messier *et al.* 2005) is not exactly known. It is possible that the excess weight increases the load borne by all parts of the joint. However, the association between overweight and OA is not simply a question of increased mechanical load because obesity acts as a risk factor for developing hand OA (Grotle *et al.* 2008). Together with this, published data from animal studies: knee cartilage from rabbits fed a high – fat diet showed lower glycosaminoglycan content and aggrecan-1 than cartilage from rabbits fed a normal – fat diet independently of animal weight (Brunner *et al.* 2012); OA surgical induced mice fed a high – fat diet from 4 weeks of age showed higher OA cartilage degeneration at 8 weeks after surgery than those fed a normal diet (Mooney *et al.* 2011); in mice transgenic for human C – reactive protein (CRP) on a high – fat diet, there is a lack of correlation between OA severity and body weight (Gierman *et al.* 2012).

Many studies suggest that systemic inflammatory mediators contribute to the increased risk of OA with obesity. Adipose tissue, especially from the abdomen, is a rich source of pro-inflammatory cytokines, which are often referred to as adipokines. Many adipokines elevated with obesity have also been shown to mediate synovial tissue inflammation. For example, leptin is a 16-kd polypeptide hormone encoded by the obese (*ob*) gene and is primarily secreted by adipocytes. Female C57BL/6J mice with impaired leptin signalling are protected from obesity – induced OA, suggesting elevated body fat in the absence of leptin signalling is insufficient to induce systemic inflammation and OA (Griffin *et al.* 2009). Leptin has been found to exist at higher concentrations in the synovial fluid compared to serum (Presle *et al.* 2006). Leptin, alone or in synergy with IL-1, induced collagen release from bovine cartilage explants and upregulated MMP-1 and MMP-13 expression in bovine chondrocytes(Hui *et al.* 2012).

1.2.3.4. Aging

Aging is the most important risk factor for OA. After 40 year old, many people will appear to have some damage to their joints which may lead to OA, and approximately 50% of individuals greater than the age of 65 suffer from OA. The incidence of the disease through age has been observed: the prevalence of OA rises from 4% in people under the age of 24 to as high as 85% for those at 75-79 years of age. The common justification is the long-term effect of mechanical load on all joint components. Also, the regenerative capability of cartilage is reduced and cellular apoptosis is enhanced with age (Goldring *et al.* 2007).

1.2.3.5.Genetic factors

Evidence from family clustering and twin studies indicates that the risk of OA has an inherited component. Genetic factors may influence between 39% and 65% in radiographic OA of the hand and knee in OA, about 60% in OA of the hip, and about 70% in OA of the spine. Mutations to genes that play a role in the ECM, proteases and inhibitors, cytokines, and growth factors have been found to affect one's susceptibility to develop of OA (Sulzbacher 2013). However, the individual effects are relatively small. For example, a genome – wide association study showing that the C allele of rs3815148 on chr 7q22 was associated with a 1.14- fold increased prevalence of knee and/ or hand OA(Kerkhof *et al.* 2010).

1.3. MicroRNAs in osteoarthritis

1.3.1. The basic biology of miRNA

miRNAs are an abundant class of evolutionarily conserved, short (~22nt long), single – stranded RNA molecules that have emerged as important post transcriptional regulators of gene expression by binding to specific sequences within a target mRNA (Ambros 2004, Bartel 2004). To date, 1424 miRNAs have been identified in human cells and each is predicted to regulate several target genes (Lim *et al.* 2005, Kozomara *et al.* 2011). Computational predictions indicate that more than 50% of all human protein – coding genes are potentially regulated by miRNAs (Lewis *et al.* 2005, Friedman *et al.* 2009). The abundance of mature miRNAs varies extensively from as few as ten to more than 80,000 copies in a single cell, which provides a high degree of flexibility in the regulation of gene expression (Chen *et al.* 2005, Suomi *et al.* 2008). The regulation exerted by miRNAs is

reversible, as feedback/forward regulatory loops have been shown to exert modifying effects during translation (Inui *et al.* 2010) .

1.3.1.1. MicroRNA discovery

In 1981, the first miRNA: *lin-4* was discovered in *Caenorhabditis elegans* (Chalfie 1981). In the early 1990s, Ambros and Ruvkun revealed that *lin-4* controlled a specific step in developmental timing in *C.elegans* by downregulating *lin-14* (a conventional protein – coding gene) (Chalfie 1981, Lee *et al.* 1993, Wightman *et al.* 1993). They recognized that the *lin-14* 3'UTR harbours multiple sites of imperfect complementarity to *lin-4* and proposed that *lin-4* binds to these sites and blocks *lin-14* translation.

Forward genetics also discovered a second miRNA in *C.elegans,* known as *let-7* (Reinhart *et al.* 2000) which targets *lin-41* and *hbl-1* (Abrahante *et al.* 2003, Lin *et al.* 2003). The concept of miRNAs then jumped from worms to higher species, since *let-7* had well-known homologues even in human and fly. In 2001, the term "microRNA" was coined for this class of non-coding gene regulators (Lagos-Quintana *et al.* 2001, Lau *et al.* 2001, Lee *et al.* 2001). The discovery of miRNAs had crossed over to human, and finding miRNA targets became a high priority.

1.3.1.2. MicroRNA biogenesis

Most of the currently known miRNA sequences are located in introns of protein coding genes; a lower percentage of miRNAs originate from exons or non-coding mRNA-like regions (Rodriguez *et al.* 2004). In addition, a significant number of miRNA are found in polycistronic units that encode more than one miRNA. The miRNAs within clusters are often functionally related (Lagos-Quintana et al. 2001, Lau et al. 2001).

Despite the obvious differences between the biology of miRNAs and mRNAs, all available evidence suggests that these transcripts share common mechanisms of transcriptional regulation. Generally, the generation of a miRNA is a multi-step process that starts in the nucleus and finishes in the cytoplasm (Lee *et al.* 2002). First, miRNAs are transcribed by the RNA polymerase II complex (Lee *et al.* 2004) and subsequently capped, polyadenylated, and spliced (Cai *et al.* 2004). Transcription results in a primary miRNA transcript (pri-miRNA) that harbors a hairpin structure (Lee et al. 2002, Kim 2005). Within

the nucleus, the RNAse II–type molecule Drosha and its cofactor DGCR8 process the pri-miRNAs into 70- to 100-nt-long pre-miRNA structures (Lee *et al.* 2003, Han *et al.* 2004), which in turn are exported to the cytoplasm through the nuclear pores by Exportin-5 (Yi *et al.* 2003, Bohnsack *et al.* 2004, Lund *et al.* 2004, Zeng *et al.* 2004). Subsequently, the RNAse III-type protein Dicer generates a double stranded short RNA in the cytoplasm that consists of the leading – strand miRNA and its complementary sequence (Grishok *et al.* 2001, Hutvágner *et al.* 2001, Ketting *et al.* 2001, Chendrimada *et al.* 2005). This duplex miRNA is unwound by a helicase into a single stranded short RNA in the cytoplasm and the leading strand is incorporated into the argonaute protein (Ago 2)-containing ribonucleoprotein complex known as the miRNA-induced silencing complex, mRISC (Hammond *et al.* 2000, Hutvagner *et al.* 2008, Bossé *et al.* 2010). During this process, one strand of the miRNA duplex is selected as the guide miRNA and remains stably associated with mRISC, while the other strand, known as the passenger strand is rapidly removed and degraded (Martinez *et al.* 2002) (Figure 1.5). Selection of the appropriate strand is primarily determined by the strength of base pairing at the ends of the miRNA duplex. The strand with less-stable base pairing at its 5' end is usually destined to become the mature miRNA (Khvorova *et al.* 2003, Schwarz *et al.* 2003, Hutvagner 2005). However, some miRNA passenger strands are thought themselves to negatively regulate gene expression. One hypothesis is that both strands could be used differently in response to extracellular or intracellular cues, to regulate a more diverse set of protein –coding genes as needed, or strand selection could be tissue specific (Ro *et al.* 2007). The mature miRNA guides the RISC complex to the 3'UTR of its target miRNA (Lai 2002, Bartel 2009) . The seed sequence, comprising nucleotides 2-8 at 5'-end of the mature miRNA, is important for binding of the miRNA to its target site in the mRNA (Lewis et al. 2005). Association of miRNA with its target results in mRNA cleavage (if sequence complementarity is high) or more usually in higher eukaryotes, blockade of translation (Zeng and Cullen 2004) (see below).

In an alternative pathway for miRNA biogenesis, short hairpin introns termed mirtrons are spliced and debranched to generate pre-miRNA hairpin mimics (Berezikov *et al.* 2007, Okamura *et al.* 2007, Ruby *et al.* 2007, Westholm *et al.* 2011, Sibley *et al.* 2012). These are then cleaved by Dicer in the cytoplasm and incorporated into typical miRNA silencing

complexes (Berezikov et al. 2007, Okamura et al. 2007, Ruby et al. 2007, Westholm and Lai 2011, Sibley et al. 2012). The presence of mirtrons may be an evolutionary strategy to diversify miRNA-based gene silencing (Lau *et al.* 2009).

1.3.1.3. Mechanisms of action of miRNAs

Mammalian miRNAs often have several isoforms encoded from one or more chromosome, suggesting that they are functionally redundant (Heimberg *et al.* 2008, Kim *et al.* 2009). They may exert variable roles *in vivo* via differences in their expression pattern and 3'-end binding (Ventura *et al.* 2008).

Regulation is mainly exerted by the binding of the miRNA to the 3'UTR of the target mRNA, but binding to other positions on the target mRNA, e.g. in 5'UTR or coding sequence has also been reported (Lytle *et al.* 2007, Lee *et al.* 2009, Li *et al.* 2009). Interestingly, miRNA binding sites within the coding region of a transcript are reported as less effective at mediating translational repression. Aside from the location of miRNA binding sites, factors including the sequence context of the miRNA binding site, the number of target sites within the mRNA, the focal RNA structure, the distance between target sites, all contribute to the efficacy of repression mediated by miRNAs (Brennecke *et al.* 2005, Sætrom *et al.* 2007).

The degree of base pairing between the miRNA and its target in the mRISC complex determines the fate of the transcript. If there is perfect binding between the miRNA and target, the mRNA target is cleaved by Ago2 at the annealing site, with subsequent degradation of the mRNA. In contrast, in cases where the miRNA is only partially complementary to its corresponding 3'UTR, inhibition of target mRNA translation occurs via Ago1. Repression may be exerted either at the initiation step of mRNA translation in which Ago competes with eIF4E or at some stage subsequent to initiation (Kiriakidou *et al.* 2007) (Figure 1.6). This is because miRNA-mRISC complex can bind to actively translating mRNAs, reducing translational elongation and/ or enhancing termination, concomitant with a reduction in ribosome initiation and nascent peptide destablilization (Petersen *et al.* 2006).

Interestingly, besides generally promoting mRNA cleavage or translational repression, miRNA binding to 3'UTR can also induce translation of some target mRNAs. MicroRNAs have been identified which activate translation on cell cycle arrest by directing AGO-containing protein complexes to AU-rich elements in the 3'UTR (Vasudevan *et al.* 2007, Vasudevan *et al.* 2007)

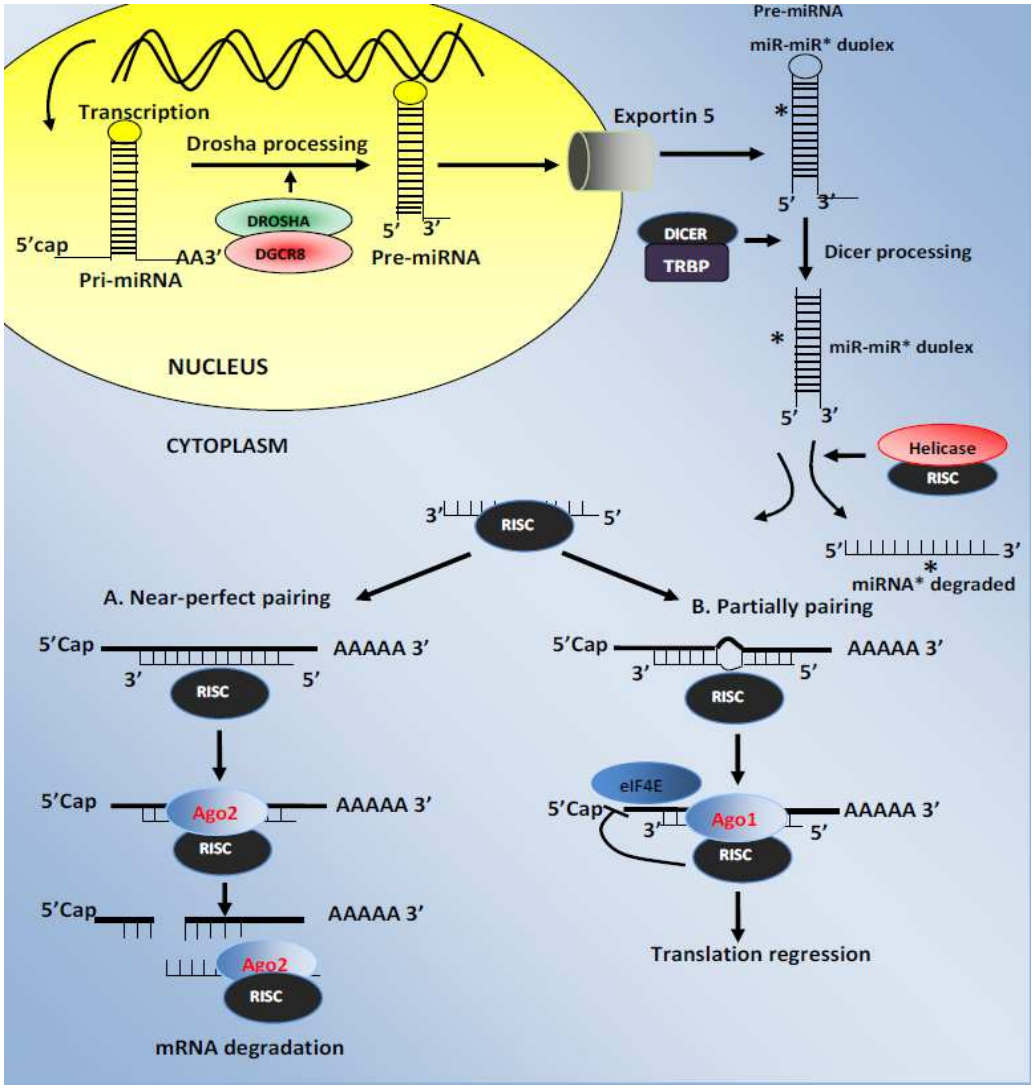

Figure 1.6: Biogenesis of miRNAs.

MicroRNAs are transcribed as RNA precursor molecules (pri-miRNA), which are processed by Drosha and its cofactor DGCR8 into short hairpin structure (pre-miRNA). These are exported into the cytoplasm by Exportin 5, where they are further processed by Dicer and TRBP (Dicer-TAR RNA binding protein) into a miRNA duplex. The duplex is unwound by a helicase and the "guide" strand is incorporated into the RNA–induced silencing complex (RISC) whilst the "passenger" strand undergoes degradation. This miRNA-RISC complex acts by two possible mechanisms: (A) Degradation of target mRNA occurs when miRNA is near-perfectly complementary with 3' untranslated region of target mRNA; (B) Translation inhibition occurs when miRNA is only partially complementary to its target mRNA.

1.3.2. MicroRNAs in skeletal development

It is evident that miRNAs are essential for skeletal development, however, our current knowledge of expression and function of specific miRNAs is still limited. Experimentally removing the majority of miRNAs by a block in miRNA biogenesis through mutating or deleting Dicer, reveals that the miRNA pathway plays a prominent role in skeletal development. An excellent example is the conditional knockout of Dicer in limb mesenchyme at the early stages of embryonic development, which leads to the formation of a much smaller limb. Dicer-null growth plates display a pronounced lack of chondrocyte proliferation in conjunction with enhanced differentiation to postmiototic hypertrophic chondrocytes; this latter may be explained by Dicer having distinct functional effects at different stages of chondrocyte development (Harfe *et al.* 2005). Recently, Kobayashi et al. reported that mice null for Dicer in chondrocytes resulted in skeletal growth defects and premature death (Kobayashi *et al.* 2008), again pointing to essential role of miRNAs in skeletal development.

Further evidence of the important role of miRNAs in skeletogenesis is that some miRNAs were found to exhibit bone-specific and cartilage-specific expression in late development. Wienholds et al. first provided evidence for miR-140 specifically expressed in cartilage of the jaw, head, and fins in zebrafish cartilage during embryonic development (Wienholds *et al.* 2003). Later, Tuddenham et al found that miR-140 is specifically expressed in cartilage tissues during mouse embryonic development (Tuddenham *et al.* 2006). Importantly, Miyaki et al and then Nakamura et al reported that universal knockout of miR-140 lead to mild dwarfism, probably as a result of impaired chondrocyte proliferation (Miyaki *et al.* 2010, Nakamura *et al.* 2011). Recently, Swingler et al found that miR-455-3p was expressed in developing long bones during chick development, restricted to cartilage and perichondrium, and in mouse embryos, where expression was selective in long bones and joints (Swingler *et al.* 2011).

These studies emphasize the importance of the miRNA pathway in skeletal development and revealed that some miRNAs are expressed with precise tissue and developmental stage specificity. Intensive research will uncover a complete spectrum of skeletally associated miRNAs as well as elucidate their biological function.

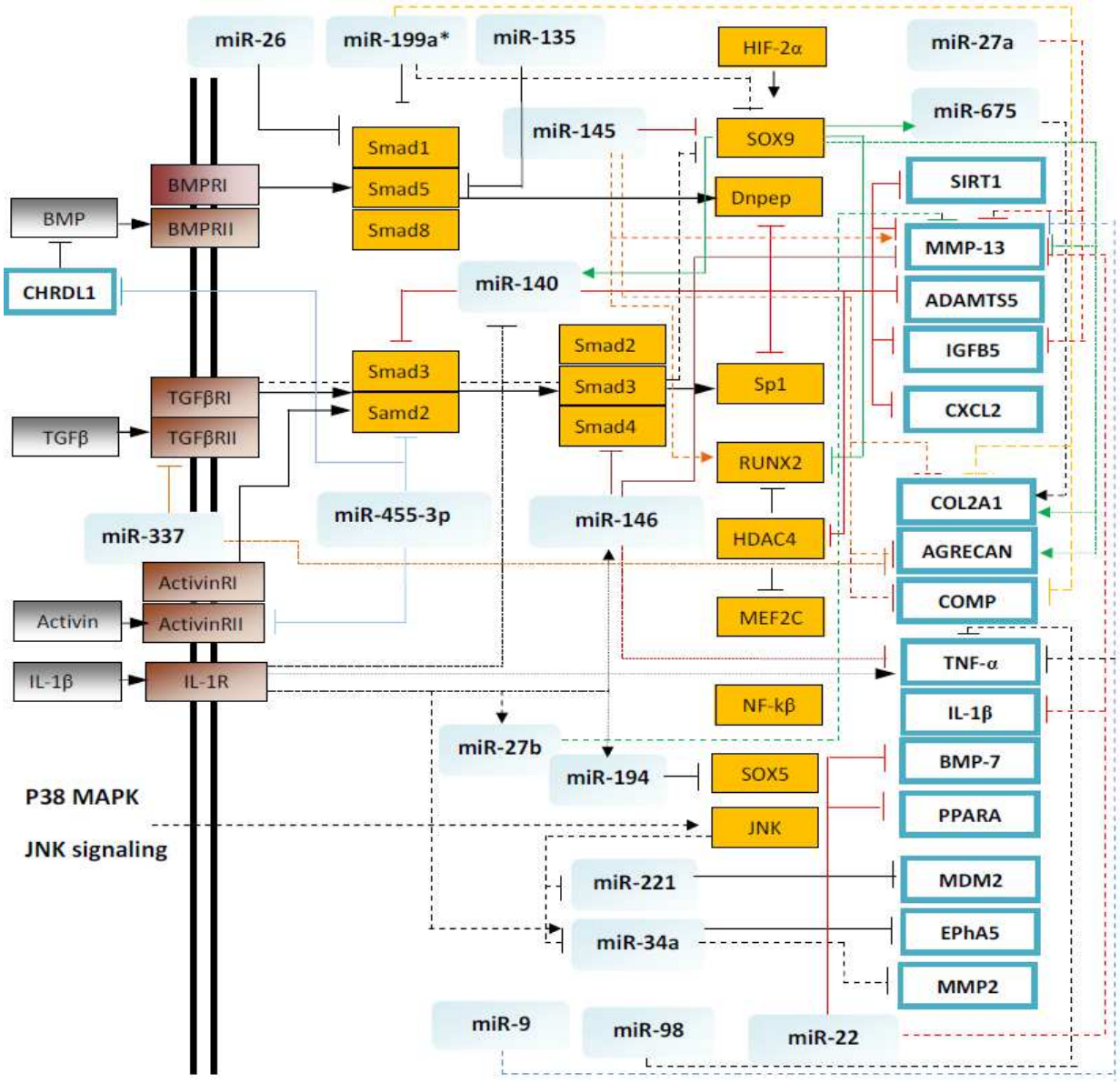

Figure 1.7: An overview of miRNAs involved in chondrogenesis, osteoarthritis and their direct and indirect targets

1.3.3. MicroRNAs in mechanotransduction

Articular cartilage has the unique capacity to resist significant mechanical loading during the lifetime of the organism (Guilak *et al.* 2001). The surface, middle and deep zones within articular cartilage are distinct domains, and they exhibit differential gene expression and attendant functional roles (Neu *et al.* 2007).

Mechano-responsive miRNAs are being identified in chondrocytes, the sole cell type of articular cartilage and evidence that specific miRNAs may impact on stress-related articular cartilage mechanotransduction has also been reported. MicroRNA-365 was the first identified mechanically responsive miRNA in chondrocytes, regulating chondrocyte differentiation through inhibiting HDAC4 (Guan *et al.* 2011). MicroRNA-221, miR-222 were postulated as potential regulators of the articular cartilage mechanotransduction pathway, since their expression patterns in bovine articular cartilage are higher in the weight-bearing anterior medial condyle as compared with the posterior non-weight-bearing medial condyle (Dunn *et al.* 2009). Recently, Li et al. reported that miR-146a was induced by joint instability resulting from medial collateral ligament transection and medial meniscal tear in the knee joints of an OA mouse model, suggesting that miR-146a might be a regulatory factor of the mechanical transduction process in articular cartilage (Li *et al.* 2012). All of these studies are useful for enriching the data on the regulatory mechanism for miRNAs in chondrocyte homeostasis.

1.3.4. MicroRNAs in chondrogenesis

Differential disruption of the Dicer gene in mice resulting in highly abnormal cartilage development suggests miRNAs play a significant role in chondrogenic differentiation. Furthermore, many studies profiled the expression of miRNAs to investigate their function in differentiating MSCs and showed that once they differentiate into chondrocytes, miRNA expression significantly altered (Sorrentino *et al.* 2008, Suomi et al. 2008, Lin *et al.* 2009, Miyaki *et al.* 2009, Karlsen *et al.* 2011, Lin *et al.* 2011, Yan *et al.* 2011, Yang *et al.* 2011) (Table1.2). However, there is no consensus expression signature of any miRNAs amongst these and we attribute this to the design of experiment including inducers of differentiation, cell types, numbers of detected miRNA probes and organism (Table1.2).

Table 1.2: Studies performing miRNA profile comparing between MSC and chondrocytes

	Sorrentino et al 2007	**Suomi et al 2008**	**Lin et al 2009**	**Miyaki et al 2009**	**Yang et al, 2010**	**Lin et al 2011**	**Yang et al 2011**	**Karlsen et al 2011**
Stimulators	-	TGF-β3	BMP-2	BMP-2 TGF-β3	TGF-β3	-	-	-
Cells	BM MSC	BM MSC	C12C2	BM MSC	BM MSC	DAC	BM MSC AC	DAC
Organisms	Human	Mice	-	Human	Mice	Human	Mice	Human
Probes	226	35	-	-	7,815	-	-	875
Cutoff(fold)	1.3	-	1.5	1.5	5	4	-	-
Platform	microarray	qPCR	microarray	microarray	microarray	microarray	microarray	microarray
miRNAs up-regulated	31 32 136 146 149 185 Pre-mir 192 199a-2-5 204 212 Pre-mir-212 Pre-miR-214	24 101 124a 199b 199a	199* 221 298 374 let-7e	15b 16 23b 27b 140 148 197 222 328 505	30a 81a-1 99a 125* 127 140 140* Let-7f	26a 140* 140 222 320a 320d 491* 547-5p 720 1308 let-7d let-7f let-7a	21 22 27b 27a 140 140* 152 291b* 330 431 433 455 let-7b let-7d let-7l	30d 140* 210 451 563
miRNAs down -regulated	10a 10b 21 23a 24-1-3p 24-2 26b 29b 30a-5p 34 100 103-2 107 130a 138-1 Pre-miR-143 145 181a-1 191-5p let-7a-1 let-7a-2 let-7a-3 let-7c let-7d	18 96	21 125a 125b 143 145 210		125b* 132 143 145 212	18a 27a 146a 193b 220b 342-5p 335 365 519e 548e 1248 1284	1 23a 23b 24 26b 99a 99b 99b* 125a-5p 143 144 145 146a 181a 181d 191 199a 199a* 210 320 355-5p 431 503 652 Let-7a Let-7c Let-7g Let-7f	15b 31 132 138 143 145 221 222 379 382 432 494 654* 1308 let-7e

AC: Articular chondrocytes; BM MSC: Bone marrow mesenchymal cells; DAC: dedifferentiated articular chondrocytes.

The regulation of chondrogenesis of murine MSCs in response to stimulation of TGF-β3 was investigated (Suomi et al. 2008, Yang et al. 2011) (Table1.2). Suomi et al compared the expression of 35 miRNAs in chondroblasts derived from MSCs, and found that miR-199a, miR-124a were strongly up-regulated while miR-96 was substantially suppressed (Suomi et al. 2008). They demonstrated how miRNAs and transcription factors could be capable of fine-tuning cellular differentiation by showing that miR-199a, miR-124a, miR-96 could target HIF-α, RFX1, Sox5, respectively (Suomi et al. 2008). Similarly, Yang et al , revealed eight significantly up-regulated and five down-regulated miRNAs (Yang et al. 2011) in this process. The miRNA clusters, miR-143/145 and miR-132/212 were down-regulated, with miR-132 the most down-regulated whilst miR-140* was the most up-regulated (Yang et al. 2011). Similar expression patterns of miR-145, miR-143 were also described in other studies (Lin et al. 2009, Karlsen et al. 2011, Lin et al. 2011, Yan et al. 2011). Corresponding targets of these differentially expressed miRNAs were predicted including: ADAMTS5 (miR-140*), ACVR1B (miR143/145), SMAD family members: SMAD1 (miR-30a), SMAD2 (miR-132/212), SMAD3 and SMAD5 (miR-145), Sox family members: Sox9 (miR-145); Sox6 (miR-143, miR-132/212), Runx2 (miR-30a and miR-140*) (Yang et al. 2011).

Further study has confirmed miR-145 as a key mediator which antagonizes early chondrogenic differentiation in mice via attenuating Sox9 at post-transcriptional level. (Yang *et al.* 2011). Interestingly, cells over-expressing miR-145 significantly decreased the expression of chondrogenic markers at the mRNA level including Col2a1, Agc1, COMP, Col9a2 and Col11a1. Consistent with this,, Martinez-Sanchez et al. reported miR-145 as a direct regulator of Sox9 in normal human articular chondrocytes though binding to a specific site in its 3'UTR, which is not conserved in mice (Martinez-Sanchez *et al.* 2012). Similarly, over-expression of miR-145 in articular cartilage chondrocytes reduced the levels of Sox9, the cartilage matrix components Col2a1 and Agc1 in combination with a significant increase of the hypertrophic markers Runx2 and MMP-13 (Martinez-Sanchez et al. 2012) (Figure 1.7).

This group also reported that miR-675, processed from H19, a non-coding RNA, was tightly regulated by Sox9 during chondrocyte differentiation. MicroRNA-675 could up-regulate expression of Col2a1, albeit indirectly, indicating its potential importance in

maintaining cartilage integrity and homeostasis. Forced over-expression of miR-675 rescued Col2a1 mRNA levels in either Sox9- or H19-depleted primary human articular chondrocytes (Dudek *et al.* 2010). Although its target mRNAs remain unknown, these data suggest that miR-675 may modulate cartilage homeostasis by suppressing a Col2a1 transcriptional repressor (Dudek et al. 2010) (Figure 1.7). Moreover, by performing miRNA expression profile during human primary chondrocyte dedifferentiation, Martinez-Sanchez found that 29 miRNAs were up-regulated more than two-fold and 18 miRNAs were down-regulated. Among these up-regulated miRNAs, miR-1247, transcribed from the DLK1-DIO3 locus, was of particular interest as its expression pattern still increased under hypoxia condition, together with miR-140. Also, miR-1247 level was found to correlate with cartilage-associated miR-675 across a range of 15 different mouse tissues (Martinez-Sanchez *et al.* 2013). Interestingly, SOX9, directly target of miR-1247 via coding sequence, inhibit this miRNA expression, suggesting a negative feedback loop between miR-1247 and its target SOX9 (Martinez-Sanchez and Murphy 2013).

Another study performed miRNA profiling to find expression signatures of nearly 380 miRNAs in C2C12 cells induced by BMP-2 for 24 hours and found that 5 miRNAs including miR-199a* and miR-221 were positively regulated while miR-125a, miR-210, miR-125b, miR-21, miR-145, miR-143 were repressed (Lin et al. 2009). Interestingly, using C3H10T1/2 cells, a well-established *in vitro* cell model of chondrogenesis, showed that miR-199a* expression was reduced significantly within several hours following BMP-2 treatment and then rose dramatically at 24 hours and remained higher thereafter, indicating that miR-199a* may function as a suppressor of the early steps of chondrogenic differentiation (Lin et al. 2009). Indeed, enforced miR-199a* expression in C3H10T1/2 cells or in the prechondrogenic cell line ATDC5, suppresses multiple markers of early chondrogenesis, including Col2a1 and COMP, whereas the antagomir blocking miR-199a* function has the opposite stimulatory effect (Lin et al. 2009). Consistent with these observations, Smad1, a positive downstream mediator of BMP-2 signalling, was shown to be a direct miR-199a* target. Moreover, miR-199a*, through its inhibition of the Smad pathway, is able to inhibit the expression of downstream genes such as p204 (Lin et al. 2009) (Figure 1.7).

The change in expression pattern of miRNAs across the dedifferentiation of chondrocytes also, adds to our understanding of the biology of *in vitro* human chondrogenesis (Karlsen

et al. 2011, Lin et al. 2011). MicroRNA-451, miR-140-3p, miR-210, miR-30d, and miR-563 were reported to be highly expressed on human primary articular chondrocytes at early passage compared with their dedifferentiated counterparts, suggesting their role as inhibitors of differentiation *in vitro* (Lin et al. 2011). Of these miRNAs, miR-140-3p had the highest expression. Conversely, 16 miRNAs were significantly up-regulated in dedifferentiated articular chondrocytes, reflecting their potential as modulators of the chondrogenenic process. Notably, miR-143, miR-145 also had similar expression patterns as previously reported (Lin et al. 2011). A second study also reported a group of 5 miRNAs: miR-451, miR140-3p, miR-210, miR-30d, and miR-563 upregulated on differentiation which may inhibit molecules participating in the dedifferentiation process whilst a further 16 miRNAs were downregulated and may potentially act conversely.

Recently, performing miRNA profiling across ATDC5 cell induced differentiation within 42 days to identify miRNAs with functions in cartilage development, we identified 7 cluster groups of miRNAs which may function cooperatively (Swingler et al. 2011). Among these, 39 miRNAs were found potentially co-regulated with miR-140 with expression increase during chondrogenic process (Swingler et al. 2011). Especially interesting is miR-455, located in an intron of the protein coding gene Col27a1, a cartilage-expressed collagen, which showed similar expression kinetics to collagen XXVII and to miR-140. Consistent with role for miR-140 in modulating TGFβ signalling, miR-455-3p was also found to directly target Smad2, ACVR2B and CHRDL1, again potentially attenuating the TGFβ pathway (Swingler et al. 2011) (Figure 1.7).

MicroRNA-140 shows a generally consistent expression pattern between studies. Indeed, cartilage miRNA research to date has focused heavily on miR-140 and has successfully shown the key roles of miR-140 in chondrocyte proliferation and differentiation. Miyaki et al compared gene expression profiling using miRNA microarrays and quantitative polymerase chain reaction in human articular chondrocytes and human mesenchymal stem cells. They demonstrated that miR-140 had the largest difference in expression between chondrocytes and MSCs (Miyaki et al. 2009), and this is in agreement with latter publications in human, rat and mice (Karlsen et al. 2011, Lin et al. 2011, Yan et al. 2011, Yang et al. 2011). MicroRNA-140 was first shown to target Hdac4, a known co-repressor of Runx2 and MEF2C transcription factors essential for chondrocyte hypertrophy and bone

development (Tuddenham et al. 2006). miR-140 also targets Cxcl12 (Nicolas *et al.* 2008) and Smad3 (Pais *et al.* 2010), both of which are implicated in chondrocyte differentiation. Interestingly, miR-140 is reported to suppress Dnpep, an aspartyl aminopeptidase, which has been suggested to antagonize BMP signalling downstream of Smad activation (Nakamura et al. 2011). Moreover, Sox9 a major transcription factor in maintaining cellular phenotype and preventing hypertrophy, particularly with L-Sox5 and Sox6, (Yamashita *et al.* 2012), is shown to control the expression of miR-140 (Yang *et al.* 2011, Nakamura *et al.* 2012).

The miR-194 is a key mediator during chondrogenic differentiation via suppression of the transcription factor Sox5 (Xu *et al.* 2012). The expression of miR-194 was significantly decreased in chondrogenic differentiation of adipose-derived stem cells (ASCs). Importantly, chondrogenic differentiation of ASCs could be achieved through controlling miR-194 expression (Xu et al. 2012) (Figure 1.7).

Using three rat models e.g. bone matrix gelatin-induced endochondral ossification, collagen-induced arthritis and pristane-induced arthritis, Zhong et al. further demonstrated that miR-337 was directly implicated with chondrogenesis. miR-337 acted as a repressor for TGFBR2 expression at the protein level (Zhong *et al.* 2012). Moreover, aggrecan was differentially expressed in both gain- or loss-of function of miR-337 experiments, providing evidence that miR-337 could influence cartilage specific gene expression in chondrocytes (Zhong et al. 2012) (Figure 1.7).

Kim et al. used chick as a model of chondrogenesis and focused on initiation, namely precartilage condensation, proliferation and migration. They reported that miR-221 and miR-34a, induced by c-Jun N-terminal kinase (JNK) signaling, played pivotal roles (Kim *et al.* 2010, Kim *et al.* 2011). Treatment of chick wing bud MSCs with a JNK inhibitor lead to the suppression of cell migration and stimulation of apoptosis with concurrent significant increase in expression of miR-221 and miR-34a (Kim et al. 2010, Kim et al. 2011). Notably, miR-221 may be involved in apoptosis, since treatment of MSCs with a miR-221 inhibitor increased cell proliferation and this could be rescued by the JNK inhibitor (Kim et al. 2010). MicroRNA-221 is reported to directly target Mdm2, which encodes for an oncoprotein with E3 ubiquitin ligase activity (Kim et al. 2010). Inhibition of Mdm2 expression via miR-221 suppresses ubiquitination leading to accumulation of

Slug protein, whose expression is associated with an increase in apoptosis (Kim et al. 2010). Conversely, miR-34a affects MSC migration, not proliferation (Kim et al. 2011). EphA5, a receptor in Eph/Ephrin signaling which mediates cell-to-cell interaction, has been proven to be a miR-34a target (Kim et al. 2011). Moreover, via regulating RhoA/Rac1 cross-talk, miR-34a negatively modulated reorganization of the actin cytoskeleton (Kim *et al.* 2012), one of the essential processes for establishing chondrocyte-specific morphology. MicroRNA-488 expression is up-regulated at the pre-condensation stage and then down-regulated at the post-condensation stage in chick limb chondrogenesis, suggested a key role in this process (Song *et al.* 2011). Interestingly, mir-488 could regulate cell–to-ECM interaction via modulation of focal adhesion activity by indirectly targeting MMP-2 (Song et al. 2011). More recently, this group reported that miR-142-3p was an important modulator in position-dependent chondrogenesis and was reported to regulate ADAM9 (Kim *et al.* 2011) (Figure 1.7).

1.3.5. MicroRNAs in osteoarthritis

The effects of miRNA deregulation on OA are evident through studies comparing the expression of miRNAs between OA tissues and their normal articular counterparts (Iliopoulos *et al.* 2008, Jones *et al.* 2009). Illopoulos et al. tested the expression of 365 miRNAs and identified a signature of 16 miRNAs, with 9 miRNAs significantly upregulated and 7 miRNAs downregulated in OA cartilage compared with normal controls. Some of these were postulated to be involved in obesity and inflammation (Iliopoulos et al. 2008). Interestingly, functional experiments implicated miR-9 in the regulation of MMP13 expression, as well as miR-9, miR-98 and miR-146 in the control of TNF-α expression, suggesting that these miRNAs may play a protective role in OA. Moreover, miR-22, whose expression correlated with body mass index, directly targets PPARA and BMP-7 at the mRNA and protein levels, respectively. Enforced miR-22 overexpression or siRNA-mediated suppression of either PPARA or BMP-7 resulted in increases in IL-1β and MMP-13 protein levels, again suggesting that miRNA deregulation can have effects on OA (Iliopoulos et al. 2008) (Figure 1.7).

Additionally, Jones et al. investigated the expression of 157 human miRNAs and identified 17 miRNAs whose expression varied by 4-fold or more when comparing normal versus

late-stage OA cartilage (Jones et al. 2009). Consistent with the Illopoulos data, the altered expression of miR-9, miR-98 and miR-146 in OA cartilage are highlighted. The over-expression of these miRNAs also reduced IL-1β-induced TNF-α production, whilst inhibition or over-expression of miR-9 modulated MMP-13 secretion (Jones et al. 2009) (Figure 1.7).

The miR-140 gene, located in an intron of the E3 ubiquitin protein ligase gene Wwp2 on murine chromosome 8 and the small arm of chromosome 16 in humans, is evolutionarily conserved among vertebrates. MicroRNA-140 expression in the cartilage of patients with OA was significantly lower than in normal cartilage (Miyaki et al. 2009, Tardif *et al.* 2009) and decreased miR-140 expression was reported also in OA chondrocytes (Tardif et al. 2009).

Deletion of miR-140 in mice predisposes to the development of age-related OA-like changes (Miyaki et al. 2010, Nakamura et al. 2011) and gives a significant increase in cartilage destruction in surgically induced OA. Conversely, in an antigen-induced arthritis model, transgenic over-expression of miR-140 in chondrocytes protects against cartilage damage (Miyaki *et al.* 2010). The ADAMTS5 gene has been shown to be a direct target of miR-140, whilst reciprocal regulation of ADAMTS5 in the in vivo models above suggests that suppression of OA may involve regulation of ADAMTS5 (Miyaki et al. 2010). Swingler et al. show that miR-140 is increased in expression in hip OA cartilage compared to fracture controls (Swingler et al. 2011), but ADAMTS5 expression is decreased in the former samples. As above, Nakamura et al. identified the aspartyl aminopeptidase Dnpep as a key target for miR-140 essential for skeletal defects in miR-140 null mice (Nakamura *et al.* 2011). Using functional interference, Tardif et al. confirmed IGFBP-5, whose expression in human chondrocytes was significantly higher in OA, as a direct target of miR-140 (Tardif et al. 2009). More recently, miR-140 was shown to directly mediate MMP13 expression *in vitro* by luciferase reporter assay (Liang *et al.* 2012) (Figure 1.7).

The human genome contains two miR-27 genes [mir-27a and miR-27b] on chromosomes 19 and 9, respectively, and their major products differ by only 1 nucleotide in the 3' region. MicroRNA-27a expression was shown to be decreased in OA compared to normal chondrocytes (Tardif et al. 2009). Down-regulation of miR-27a was proposed to be connected with adipose tissue dysregulation in obesity, a strong risk factor for OA. Tardif

et al. suggested that miR-27a may indirectly regulate the levels of both MMP-13 and IGFBP-5 by targeting upstream positive effectors of both genes (Tardif et al. 2009). Conversely, expression miR-27b was found to be significantly lower in OA cartilage samples compared with normal counterparts where it inversely correlated with MMP13, a direct target (Akhtar *et al.* 2010). This points to the possibility of novel avenues for OA therapeutic strategies (Figure 1.7).

MicroRNA-146a was strongly expressed in chondrocytes residing in the superficial layer of cartilage and in low-grade OA cartilage (Yamasaki *et al.* 2009, Li et al. 2012). Its expression level gradually decreased with progressive tissue degeneration. Interestingly, when miR-146 was highly expressed, the expression of MMP13 is low, suggesting that miR-146a has target genes that play a role in OA cartilage pathogenesis (Yamasaki et al. 2009). MicroRNA-146a has recently been implicated in the control of knee joint homeostasis and OA-associated algesia by balancing the inflammatory response in cartilage and synovium with pain-related factors in glial cells (Li *et al.* 2011). As such, it may be useful for the treatment of both cartilage regeneration and the pain symptoms caused by OA (Figure 1.7).

Park et al reported the miR-127-5p, an important mediator in OA whose expression was significant decreased in OA articular cartilage compared to the control counterpart, directly target MMP13. Noteworthy, pre-treatment with MAPK inhibitors and NFκβ inhibitor attenuated the inhibitory effects of IL-1 on miR-127-5p expression while overexpression of miR-127-5p significantly inhibited the phosphorylation of JNK, p38 and Iκβα in the human chondrocytes. These data suggest a reciprocal regulatory loop between NFκβ, MAP kinase, and IL-1β in controlling MMP13 expression (Park *et al.* 2013).

1.3.6. MicroRNAs in inflammation

Some miRNAs could be of importance in the inflammatory events of osteoarthritis. MicroRNA-140 was suppressed by IL-1β signaling, and transfection of human chondrocytes with miR-140 downregulated IL-1β driven induction of ADAMTS5 (Miyaki et al. 2009). However, contrary to this, Liang et al. reported that expression of miR-140

and MMP-13 was elevated in IL-1β-stimulated C28/I2 and expression of miR-140 was shown to be NF-κB-dependent (Liang *et al.* 2012) (Figure 1.7).

Expression of miR-34a was significantly induced by IL-1β while antagonism of miR-34a prevented IL-1β-induced chondrocyte apoptosis (Abouheif *et al.* 2010), as well as IL-1β-induced down regulation of type II collagen in rat chondrocytes (Abouheif et al. 2010). Other relevant miRNAs reported to be induced by IL-1β are miR-146a (Yamasaki et al. 2009, Li et al. 2012), miR-34a (Abouheif et al. 2010), miR-194 (Xu et al. 2012), miR-27b (Akhtar et al. 2010) (Figure 1.7).

1.3.7. Utility of microRNAs for diagnosis

It is evident that miRNAs in serum may become a powerful tool in the development of diagnostic biomarkers. MicroRNAs are relatively stable with enzymatic, freezing, thawing or extreme pH conditions (Mitchell *et al.* 2008, Link *et al.* 2010) due to lipid or lipoprotein complexes (Esau *et al.* 2006). Moreover, extracellular miRNAs are detectable in almost all body fluids and excretions including urine, faeces, saliva, tears, ascetic, pleural and amniotic fluid (Chen *et al.* 2008, Gilad *et al.* 2008). Interestingly, miRNAs in plasma have the capacity to interact with intact cells with some degree of specificity, and modify recipient cell gene expression and protein production via a miRNA-related mechanism (Arroyo *et al.* 2011). This opens up the possibility of genetic exchange between cells and the exogenous regulation of gene expression. MicroRNA-21 was the first serum miRNA biomarker to be discovered: patients with diffuse large B cell lymphoma had high serum levels of miR-21, which was associated with increased relapse-free survival (Lawrie *et al.* 2008). Subsequently, the usefulness of serum miRNAs for diagnosis and prognosis has been reported for solid cancers and leukemia (Ferracin *et al.* 2010, Kosaka *et al.* 2010, Wittmann *et al.* 2010). For OA, Murata et al. examined the potential of miRNA as diagnostic biomarkers and found a number of miRNA in plasma some of which were found at different levels between RA and OA patients (Murata *et al.* 2010). Recently, let-7e, miR-454, miR-886 were identified differentially expressed crilculating miRNAs in OA patient necessitating arthroplasty in a large, population – based cohort. Especially, let – 7e emerged as potential predictor for severe knee or hip OA (Beyer *et al.* 2014).

Besides the measurement of miRNAs in plasma, PBMCs could also be useful in developing a biomarker for OA. Circulating PBMCs such as macrophages and T cells accumulate in the synovium of OA patients, producing proinflammatory cytokines and proteinases associated with synovitis, linked to the early stages of OA progression. It has been demonstrated that the high expression of miR-146a, miR-155, miR-181a and miR-223 in PBMCs from OA patients versus normal controls may be related to the pathogenesis of OA (Okuhara *et al.* 2011). Interestingly, miR-146 and miR-223 are highly expressed in early-stage OA (Yamasaki et al. 2009), with expression gradually decreasing with OA progression with the promise for diagnosis of early OA is specificity can be demonstrated.

Taken together, there is growing evidence for future miRNA-based diagnostics. However, there is a requirement for detailed investigations directed at diagnostic performance (sensitivity, specificity, accuracy) of these promising novel biomarkers before the measurement of miRNAs can enter the clinic.

1.3.8. Utility of microRNAs in therapeutic treatment

Currently there is no disease-modifying therapeutics available for patients suffering from OA. Therapeutic options are limited to oral and intra-articularly injected analgesic medications, and joint replacement surgery (Wieland *et al.* 2005). OA patients often present with cartilage that already exhibits a damaged matrix, and in which repair/regeneration is. Although cartilage seems a relatively simple tissue type to engineer because of its single cell type and its lack of a blood, nerve or lymph system, regenerating cartilage in a form that can function effectively after implantation has proven difficult. Several approaches are currently being investigated to utilize a miRNA-based therapy to overcome these problems, and these may represent a novel therapeutic application for pharmacological control. Currently there are over 70 clinical trials worldwide based on miRNA manipulation to treat a range of conditions including various cancers and cardiovascular disease; however, none of these to date are for arthritis.

The targeting of miRNAs represents a novel therapeutic opportunity for OA treatment in which miRNA deficiencies could be corrected by either antagonizing (antagomirs) or

restoring (mimics) miRNA function. Poorly expressed miRNAs could be restored by over expression using stable vector transfection or transfection by double-stranded miRNA, whilst over-expressed miRNAs could be antagonized by modified DNA oligonucleotides. Particularly, it has been proven that the systematic administration of antagonist miRNAs modified with locked nucleic acids (LNA) could function without toxicity in non-human primates (Elmen *et al.* 2008). Evidence on efficacy was also demonstrated in mouse models using miR-122 antisense oligonucleotides, which resulted in a decrease in hepatic fatty acid and cholesterol synthesis (Esau et al. 2006). In man, when miR-143/miR-145 activity was restored in pancreatic cancer cells (in which their levels were repressed), the cell was no longer tumourigenic (Kent *et al.* 2010). Although this type of therapy has not been applied in OA, there is very promising evidence for therapeutic potential, e.g. the silencing of miR-34a by LNA-modified antisense oligonucleotides could effectively reduce rat chondrocyte apoptosis induced by IL-1β (Kongcharoensombat *et al.* 2010). This study revealed that silencing of miR-34a might be a novel intervention for OA treatment if this could be appropriately targeted.

Another approach is to combine miRNA technology with stem cell engineering. *In vivo* MSCs participate in chondrogenesis. MSCs can be conveniently obtained with less injury than primary cells and manipulated *in vitro* and hence they are promising cells in cartilage regeneration. At present, autologous MSCs have been transplanted in human injured or osteoarthritis knees for repair of articular cartilage defects. However, unexpected results from the ectopic transplantation of MSCs also have been reported, such as hypertrophy, mineralization, and vascularisation. Deciphering the role of miRNA regulation in the chondrogenesis of MSCs may open a new era of research and pave the way for the development of new treatments for OA

A growing body of evidence indicates that miRNAs convey a novel and efficient way for the regulation of gene expression, being involved in multiple aspects of cellular processes. Understanding their expression profile and dynamic regulation may be the key to enhancing chondrogenic differentiation, or maintaining phenotype in the treatment of OA. Recent advances in miRNA research have provided new perspectives on the regulation of OA and novel insight into the potential development of therapeutic treatments. Using miRNAs as therapeutic targets may well become a powerful tool in the development of

new therapeutic approaches. However, numerous questions including potential off-target effects and efficient and targeted delivery *in vivo* need to be solved before using miRNAs in therapeutics

SCOPE OF THE THESIS

OA is the most prevalent degenerative joint pathology leading to considerable problems with disability and pain in a huge number of people, especially the elderly population. As the population ages and with increased life expectancy, the burden of osteoarthritis will continue to rise. However, there is currently a lack of biomarkers and sensitive techniques for identifying and assessing patients with early changes. Also, clinical treatment for OA still remains unsatisfactory. Thus, deepening our understanding and gain further insights into the molecular mechanisms in OA would be very important for long term purpose of diagnosis and therapeutic treatment.

Several hundred miRNAs have been identified so far and initial studies have linked specific miRNAs to OA. However, there are no key miRNAs identified so far which functionally impact on early human OA onset and disease progression. Thus, I undertook this project to identify miRNAs mediating initiation and progression of OA and dissect their biological function in order to identify new signalling pathways involved in the pathogenesis of OA. The hypothesis and specific aims of the project were:

Hypothesis: The dysregulated expression of specific microRNAs contributes to the onset or progression of OA.

Specific aim 1: Profile miRNA and mRNA expressions in whole knee joint in DMM model to identify the potential miRNAs involved in the early stage of OA

Specific aim 2: Determine the involvement of the miRNA in human end stage OA cartilage, in murine injury model, in chondrogenesis.

Specific aim 3: Identify factors control the miRNA expression in articular cartilage

Specific aim 4: Identify miRNA direct targets to identify new signaling pathways involved in homeostasis of articular cartilage.

CHAPTER 2
MATERIALS AND METHODS

2.1.Materials

2.1.1. Murine models

2.1.1.1. Destabilization of the medial meniscus murine model (DMM model)

Induction of OA by destabilization of the medial meniscus (DMM) was kindly performed by Professor Tonia Vincent Kennedy Institute for Rheumatology, Oxford University, U.K. Protocols using C57Bl/6 mice were as described previously in (Burleigh *et al.* 2012, Chong *et al.* 2013).

Briefly, C57Bl/6 male mice were housed 3-5 per cage in 63x54x30 cm^3 standard individually vented cages and maintained with a 12h/12h light/dark cycle at an ambient temperature of 21ºC. Mice were fed a certified mouse diet (RM3 from Special Dietary Systems, Essex, UK) and water ad libitum. 10 week old mice were anaesthetized by intra-peritoneal injection of a 1:1:2 mixture of Hypnorm (0.315mg/ml fentanyl citrate and 10mg/ml fluanisone; VetaPharma Ltd, Leeds, UK), Hypnovol (5mg/ml midazolam; Roche), and sterile water for injection, at a dose of 10ml/kg body weight. The ventral portion of the right knee was shaved and swabbed with iodine to prepare a sterile surgical field. The medial meniscus was identified and the attachment of its anterior horn to the tibial plateau was cut. Care was taken to avoid injury to the anterior cruciate ligament and the cartilage surfaces. The mice were fully mobile within 2-4 hours after surgery. After 1, 3, 7 days after surgery, the mice were culled and knees harvested.

2.1.1.2. Murine hip avulsion injury model

The femoral caps of C57Bl/6 mice ages 4 weeks were avulsed using forceps as described in (Chong et al. 2013). After washing three times with sterile phosphate-buffered saline (PBS) (Life Technologies, 10010023), the femoral caps were immediately put in either 500µl Trizol® reagent (Invitrogen, 15569-026) (for time point 0) or in 24-well plate for (other time points e.g. 3, 6, 12, 48 hours). 200µl of Dulbecco's modified Eagle's medium (DMEM) (Life Technologies, 10566-016) containing 100 IU/ml penicillin and 100µg/ml

streptomycin (Sigma, P4333) was added to each well and the plate was incubated at 37ºC in 5% (v/v) CO_2. At the desired time points, the femoral caps were harvested (with Trizol reagent) and total RNA was isolated.

2.1.2. Human end stage OA specimens and normal counterparts

Ethical Committee approval for using discarded human tissue was received prior to the initiation of the studies. Full informed consent was obtained from all donors. Human articular cartilage was obtained from patients undergoing total hip/ knee replacement surgery at the Norfolk and Norwich University Hospital. In total, 8 hip and 7 knee OA cartilage samples were collected. 7 healthy articular cartilages were harvested from total hip replacement following fracture to the neck of femur. None of the healthy individuals had a clinical history of arthritis or other diseases affecting cartilage, no macroscopic lesions to the cartilage were seen.

2.1.3. Cell lines

All cell lines were maintained in DMEM high glucose, GlutaMAX supplement (Life Technologies, 10566-016) containing 10% (v/v) heat-inactivated fetal bovine serum (FCS) (PAA, UK), 100U/ml penicillin, and 100µg/ml streptomycin (Sigma, P4333) at 37ºC in 5% (v/v) CO_2.

2.1.3.1. Chondrosarcoma SW1353

The SW1353 cell line was initiated from a primary grade II chondrosarcoma of the right humerus obtained from a 72 year old female Caucasian. SW1353 cells were purchased from the American Type Culture Collection (ATCC) (no.HTB-94).

2.1.3.2. Chicken dermal fibroblasts DF1

DF-1 is a spontaneously immortalized chicken fibroblast cell line without viral or chemical treatment derived from 10 day old East Lansing Line (ELL-0) embryo. DF1 was a kind gift from Professor Andrea Munsterberg, University of East Anglia, U.K.

2.1.3.3. Dicer knockdown cell lines

DLD-1 Parental and DLD-1 Dicer null_cell lines were a kind gift from Professor Tamas Dalmay, University of East Anglia, U.K. These cell lines were originally purchased from Horizon Discovery (Cambridge, U.K.). Both cell lines were originally isolated from a colorectal adenocarcinoma.

2.2.Methods

2.2.1. Molecular biology- based methods

2.2.2.2. Human genomic DNA isolation

Buffer

Extraction Buffer: 10mM Tris-HCl pH 8 (Fisher Scientific, BP152-500), 5mM NaCl (Fisher Scientific, BP3581), 0.5% (w/v) SDS (Fisher Scientific, 10356463).

DNA extraction protocol

Human chondrosarcoma SW1353 cells were harvested from a 75cm^2 flask by trypsin-EDTA treatment (Life Technologies, 25200072) and pelleted by centrifugation at 17.3xg, 5 minutes.

The cell pellet was mixed well with 100µl nuclease-free water (Sigma, W4502), 400µl extraction buffer, 10µl Proteinase K (20mg/ml) (Sigma, P6556) and incubated at 50^{o}C, 2 hours.

500µl of PCI (phenol: chloroform: isoamyl alcohol 25:24:1) (Sigma, P2069) was added, mixed gently and centrifuged, 10 minutes at 130,000xg.

The top phase was transferred to a new tube, 1 ml of chloroform (Sigma, 288306) was added and after vortex, the mixture was again centrifuged at 130,000xg for 10 minutes.

The upper phase was transferred to a new tube and two volumes of 100% (v/v) ethanol (Sigma, 459844) were added, followed by centrifugation at 130,000xg for 5 minutes.

The DNA pellet was washed with 700µl of 70% (v/v) ethanol, and then centrifuged at 130,000xg for 1 minute. Discard the ethanol.

Finally, the pellet was dried at room temperature and dissolved in 100µl of nuclease-free water (Sigma, W4502).

2.2.2.3. PCR amplification for 3'UTR regions

3'UTR regions of all genes including *ADAMTS6, ADAMTS14, ADAMTS17, ADAMTS19, FZD3, FZD5, DVL3, FRAT2,* and *CK2A2* were downloaded from the Ensembl Genome Browser: http://www.ensembl.org/index.html. Primers were specifically designed to amplify a 1-2 kb region of 3'UTR of these genes including the miR-29 family binding sites. A restriction site of *Sac*I (5'GAGCTC3'), XbaI (5'TCTAGA3') or *Sal*I (5'GTCGAC3') are added to the 5' end of each primer. Primer sequences are listed in Appendix, Table 1.

All 3'UTR regions were amplified from human genomic DNA, isolated from the SW1353 cell line. 100ng genomic DNA was added together with 5µl 10X reaction buffer, 5 units accuTaq^{TM} LA DNA polymerase (Sigma, D8045), 0.5µl dNTP 10µM (Bioline, BIO-39044), 1µl forward primer 10µM (Sigma), 1µl reverse primer 10µM (Sigma) in a 50µl reaction volume. The reaction was run on a Veriti^{R} 96-well thermal cycler (Applied Biosystems, 4375786) at 98^{o}C, 30 seconds to denature DNA and follows by 32 cycles: 10 seconds at 98^{o}C, 20 seconds at annealing temperature (depending on each primer pair), 1-2 minutes at 68^{o}C. Finally, the reaction was left 2 minutes at 68^{o}C for final extension.

The PCR reaction was confirmed by loading 3µl PCR product on 1% (w/v) agarose gels, which were prepared by heating 1% (w/v) agarose (Sigma, A9639) in Tris-acetate-EDTA (TAE) buffer, and run at 120V. After staining in ethidium bromide solution (Sigma, E1510) for 20 minutes, the product was visualized under UV-light.

2.2.2.4. Phenol/chloroform clean up

Nuclease- free water (Sigma, W4502) was added to a PCR reaction to 200µl, followed by 200µl of phenol: chloroform: isoamyl alcohol (Sigma, P2069). The reaction was mixed well and centrifuged at 130,000xg for 10 minutes. The upper phase was collected to a fresh tube and a 2.5 volume of 100% (v/v) ethanol (Sigma, 459844) and 1/10 volume of 5M NaOAc (sodium acetate, Sigma, S2889) were added, followed by centrifugation at 130,000xg for 10 minutes. The DNA pellet was washed with 500µl of 70% (v/v) ethanol (Sigma, 459844), and centrifuged at 130,000xg for 10 minutes. Finally, the pellet was dried at room temperature for 5 minutes and dissolved in 27µl nuclease- free water (Sigma, W4502).

2.2.2.5. Plasmid isolation

A single colony from LB (Luria Bertani) agar plate supplemented with 100µg/ml ampicillin (Sigma, A0166) was inoculated into 5ml of LB broth medium also supplemented with 100µg/ml ampicillin incubated at 37°C, 180rpm overnight. The bacterial culture was pelleted by centrifugation at maximum speed for 5 minutes. Plasmids were isolated using the QIAprep Spin Miniprep Kit (Qiagen, 27104): The pellet was resuspended in 250µl of P1 buffer. 250µl of P2 buffer was added to the suspension which was then mixed thoroughly by vigorously inverting 4-6 times and incubated at room temperature for 5 minutes. After that, 50µl of P3 buffer was added and the mixture was inverted until a homogenous suspension containing a white flocculate was formed. The bacterial lysate was cleared by centrifugation at 130,000xg, 10 minutes and the supernatant was transferred to a spin column. The column was washed two times with 500µl of wash buffer. Finally, the plasmid was then eluted with 30µl nuclease free water (Sigma, W4502).

For preparation of large quantities of plasmid DNA, the QIAGEN Plasmid MIDI Kit was used (Qiagen, 12143): A single colony from LB ampicillin agar plate was inoculated into 100ml of LB medium supplemented with 100µg/ml ampicillin (Sigma, A0166), incubated at 37°C, 180rpm overnight and harvested by centrifugation at maximum speed for 10 minutes at 4°C. The bacterial pellet was resuspended in 4 ml of P1 buffer, followed by 4 ml of P2 buffer, and the suspension was thoroughly mixed by vigorously inverting the sealed tube 4-6 times and incubated at room temperature for 5 minutes. 4 ml of chilled P3 buffer was added, and the suspension was thoroughly mixed by vigorously inverting 4-6 times and incubated on ice for 15 min, followed by centrifugation at 130,000xg for 30 minutes at 4°C. The QIAGEN-tip was equilibrated by applying 3 ml of QBT buffer, and the column was allowed to empty by gravity flow. The supernatant (above) was applied to the QIAGEN-tip. The QIAGENtip was washed twice with 10ml of wash buffer. The DNA was eluted with 5 ml of elution buffer and precipitated by adding 5 ml of room temperature 100% (v/v) isopropanol (Sigma, 190764) to the eluted DNA, followed by centrifugation immediately at 130,000xg for 10 minutes at 4 °C. The supernatant was carefully decanted. The DNA pellet was washed with 2 ml of room temperature 70% (v/v) ethanol (Sigma, 459844), followed by centrifugation at 130,000xg for 5 minutes. The supernatant was carefully decanted without disturbing the pellet. The pellet was dried for

5-10 min. Finally, the plasmid pellet was dissolved in 500µl of nuclease free water and the plasmid concentration was determined using a Nanodrop spectrophotometer.

2.2.2.6. Digestion

2µg of plasmid pmiR-Glo or all PCR products after phenol/chloroform clean up was incubated with 1µl either *Sal*I (10 units/ µl) (Promega, R6061), *Sac*I (10 units/ µl) (Promega, R6051), or *Xba*I (Promega, R6181) in the recommended buffer in a final volume 20µl for 3 hours at 37ºC. The digestion reaction was terminated by heating at 75ºC for 15 minutes.

After digestion, the 5' phosphate of plasmid was removed to prevent self-ligating by incubating the digestion mix with 1µl Antarctic Phosphatase (5 units/µl) (NEB, M0289S) and 3µl Antarctic Phosphatase buffer 10X, in a final volume 30µl.The reaction was carried out at 37ºC for 15 minutes and followed 5 minutes at 70ºC to inactivate the enzyme.

2.2.2.7. Gel purification

The digestion mix was applied to 1% (w/v) SeaKem® LE Agarose (Lonza, 50002). DNA fragments were visualized by staining with ethidium bromide (Sigma, E1510). Under UV-light, the appropriate DNA band was excised from the gel with a clean scalpel and transferred into an Eppendorf tube. The Zymoclean Gel DNA Recovery Kit (Zymo Research, D4001) was used to purify DNA from the agarose gel. Briefly, 3 volumes of ADB were added to each volume of agarose excised from the gel and incubated at 37-55ºC for 5-10 minutes until the gel slice was completely dissolved. For DNA fragments higher than 8kb, 1 addition volume of water was also added to the agarose. The dissolved agarose solution was transferred to the Zymo-spin column and centrifuged for 30 seconds at full speed. The flow-though was discarded. The column was washed two times with 200µl DNA wash buffer and centrifuged at full speed at 30 seconds. The flow-though was discarded. DNA was eluted with 13µl nuclease-free water (Sigma, W4502) and quantified using a NanoDrop spectrophotometer.

2.2.2.8. Ligation

Ligation of DNA fragments was performed with a ratio of 1:3 of plasmid DNA: insert. The reaction mixture was incubated with 1µl of T4-DNA Ligase (1 unit/µl) (Life Technologies, 15224-017), 1µl of ligation buffer (10X) in a final volume of 10µl ddH2O. The reaction was left at 14^{o}C for 24hours.

2.2.2.9. Transformation

To 100µl of competent E.coli DH5α, either 50-100ng of plasmid DNA or 10 µl of ligation reaction were added and incubated for 20 minutes on ice. A heat shock at 42°C for 30 seconds was followed by incubation on ice for another 2 minutes. 500µl of LB medium was added to the bacteria and the bacterial suspension was shaken at 37°C and 180rpm for 60 minutes. The bacteria were then spread on LB-agar plates containing 100µg/ml ampicillin (Sigma, A9393). Plates were incubated at 37°C overnight.

2.2.2.10. MicroRNA 29 family binding site mutagenesis

QuikChange II XL site-directed mutagenesis kit (Agilent, 200521) was used to replace 5 nucleotides in the binding site of the miR-29 family to either *Xba*I (5'TCTAGA3'), *Sal*I (5'GTCGAC3'), *Sac*I (5'GAGCTC3') depending on which restriction enzymes were used in subcloning. The basic procedure utilizes PfuUltra high fidelity (HF) DNA polymerase for extending two mutagenic oligonucleotide primers which have desire mutations in the middle of their sequences and the rest of the sequence complementary to opposite strands of miR-GLO- 3'UTR. After cycling, PfuUltra HF DNA polymerase will generate a mutated plasmid containing staggered nicks (Figure 2.1). The product is then treated with *Dpn* I nuclease targeting sequence 5'-Gm^{6}ATC-3'. *Dpn* I, specific for methylated and hemimethylated DNA, will digest the parental DNA template and select for mutant-containing synthesized DNA. The nicked vector DNA incorporating the desire mutant of the miR-29 family binding site is then transformed into XL10 Gold ultracompetent cells (Figure 2.1).

Mutangenic primers were designed using Agilent's website: QuikChange primer design program: www.agilent.com/genomics/qcpd. The lists of primer mutants used are listed in Appendix, Table 2.

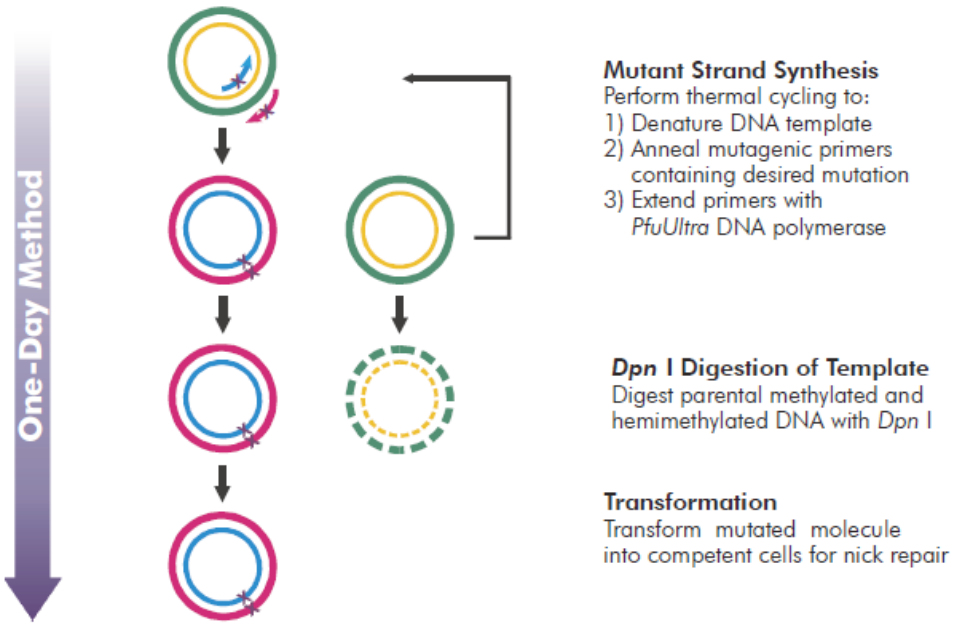

Figure 2.1: QuikChange II XL site-direct mutagenesis method

The reaction is prepared in a final volume of 50µl with 10ng of pmiR-Glo-3'UTR, 1.5µl primer mutant forward (100ng/µl), 1.5µl primer mutant reverse (100ng/µl), 1µl of dNTP mix (10mM), 5µl of reaction buffer (10X), 1µl of PfuUltra HP DNA polymerase (2.5 units/µl). The reaction is cycled at 1 minute at 95ºC, followed by 18 cycles at 95ºC 50 seconds, 68ºC 1 minute/1 kb plasmid length, and finally extension at 68ºC for 7 minutes. The amplification reaction was further incubated with 1µl of *Dpn*I restriction enzyme (10units/µl) at 37ºC for another 1 hour. To 50µl of XL10-Gold Ultracompetent cells, 5µl of *Dpn* I-treated DNA was added and the transformation protocol followed as above.

2.2.2.11. Sequencing

DNA Sequencing was performed by Source BioScience (http://www.lifesciences.sourcebioscience.com/). The sequencing signal was read by Chromas 2.4.

2.2.2.12. Total RNA isolation

2.2.2.12.1. Total RNA isolation from cultured cells

500ml of Trizol® reagent (Invitrogen, 15569-026) were added directly to adherent cells after removing the growth media from a 6-well plate. The cells were lysed by pipetting up and down several times. 250µl chloroform (Sigma, 288306) was added per 500µl Trizol®, vortexed for 15 seconds and incubated at room temperature for 10mins. The Trizol®/Chloroform mixture was centrifuged at 130,000xg, 10min, at 4°C and the aqueous layer recovered into a fresh tube. 500µl of 100% (v/v) isopropanol (Sigma, 190764) was added, mixed, left 10min at room temperature and centrifuged at 130,000xg, 10min, at 4°C then the supernatant was discarded. RNA pellets were washed with 75% (v/v) ethanol (Sigma, 459844), and centrifuged at 130,000xg, 2min, at 4°C. The supernatant was discarded, the pellet air dried and then suspended in 50µl RNase-free water and stored at -80°C until further use.

2.2.2.12.2. Total RNA isolation from murine whole knee joint

All materials used were RNase free. Whole knee joints were ground under liquid nitrogen using BioPulverizer (Biospec). Trizol® reagent (Invitrogen, 15569-026) were added immediately to ground samples (1.5ml/50mg samples) and mixed thoroughly for 5 minutes. Ground knee joints were pelleted at 130,000xg for 2min at 4°C and the supernatant recovered. 250µl chloroform (Sigma, 288306) was added per 500µl Trizol®, vortexed for 15 seconds and incubated at room temperature for 10mins. Samples were then treated as cultured cells above.

2.2.2.12.3. Total RNA isolated from murine hip or knee cartilage

Murine hip femoral caps were fully homogenized with 500µl Trizol® reagent (Invitrogen, 15569-026) using a disposable pestle. Then, 200µl chloroform (Sigma, 288306) was added, vortexed for 15 seconds, and left at room temperature for 10mins. The Trizol®/chloroform mixture was centrifuged at 130,000xg for 10 minutes at 4°C, and the aqueous layer collected into a fresh tube. The RNA purification step was performed using *mir*Vana™ miRNA Isolation Kit (AM1560, Life Technology) according to the manufactures recommendation for total RNA recovery. Briefly, 1.25x aqueous layer volume of 100% (v/v) RT ethanol was added to the aqueous phase and the samples were loaded onto

columns. The flow through was discarded after centrifuging 15 seconds at 130,000xg. Then three wash steps were followed by applying wash solution 1 (700µl), and then wash solution 2/3 (500µl) (twice) to the column. For each washing, the column was centrifuged at 130,000xg for 15 seconds followed by discarding the flow through. The columns was then placed in RNase-free collection tubes and 30µl of RNas-free water added. Columns were then left to stand for 2 minutes and centrifuged at 2 minutes, 13,000xg. RNA was then stored at -80^{o}C until used.

2.2.2.13. MicroRNA quantification and integrity

The concentration of RNA samples was determined by measuring the absorbance at 260nm using the NanoDrop spectrophotometer (NanoDrop Technologies). The purity of RNA is determined from the ratio A_{260}/A_{280} and A_{260}/A_{230}.

The integrity of total RNA was determined using the Experion^{TM} automated electrophoresis system (Bio-Rad, USA). This method measures fluorescence of a fluorophore bound to RNA. RNA integrity can be evaluated automatically by comparing the area of the peaks corresponding to the rRNAs. A 28S/18S rRNA ratio close to 2 indicates for intact RNA.

2.2.2.14. cDNA synthesis

2.2.2.14.1. SuperScript II reverse transcriptase cDNA synthesis

Total RNA was isolated from cells, whole knee joints, human or murine cartilages as above and reverse transcribed to cDNA using SuperScript II reverse transcriptase (Life Technologies, 18064-014). Briefly, in a total volume of 11µl in 96-well PCR plate, 1µg total RNA and 0.2µg random hexamer primer (Life Technologies, 48190-011) was mixed together and the plate was incubated at 70^{o}C for 10mins. Samples were chilled on ice, then, a master mix containing 1µl SuperScript II reverse transcriptase (200 units/µl) (Life Technologies, 18064-014), 4µl First Strand buffer (5X) (Life Technologies, 28028-013), 2µl 0.1M dithiothreitol (DTT) (Life Technologies, 18057-018), 2µl of 10mM dNTP mix (Bioline, BIO-39044), 1µl Recombinant RNasin Ribonuclease Inhibitor (20-40 units/µl) (Promega, N2511) was added to the randomly primed RNA to give a total volume of 20µl and incubated for 1 hour at 42^{o}C followed by a heat inactivation step at 70^{o}C, for 10mins.

cDNA was diluted to 0.5µg/ml in nuclease-free water (Sigma, W4502). 5µg cDNA was used for qRT-PCR analysis of genes of interest and 1µg cDNA was used for analysis of 18S rRNA. QRT-PCR is described in 2.2.2.15.

2.2.2.14.2. M-MLV reverse transcriptase cDNA synthesis

Moloney Murine Leukemia Virus (M-MLV) reverse transcriptase was used to perform cDNA synthesis straight from cell lysate without the need of purifying total RNA. This method was used for cell plated in 96-well plate where a number of cells are too small for RNA extraction.

Briefly, medium was removed and the cells in 96-well plate were washed with ice cold PBS (Life Technologies, 10010023). Then, 30µl cells to Cells-II-cDNA lysis buffer (Life Technologies, AM8723) was added to each well, providing a cell lysate which can immediately be reverse transcribed without the need for RNA isolation. Lysates were transferred to 96-well PCR plate and heated to 75ºC for 15 minutes to inactivate RNases. Lysates can be stored at -80ºC until reverse transcription. For genomic DNA digestion, 1µl DNase I 1 units/µl (Life Technologies, AM2222) and 3µl DNase I buffer (10X) were added per well. The plate was heated to 37ºC for 15 minutes, followed by an inactivation step at 75ºC for 5 minutes.

For reverse transcription, 8µl of DNase-treated samples were transferred to a new ice cold PCR plate. Following this, 3µl of 10mM dNTP mix (Bioline, BIO-39044) and 0.2µg random hexamer primers (50µM) (Life Technologies, 48190-011) were added per well and samples were heated to 70ºC for 5 minutes. Samples were chilled on ice and a master mix including 0.5µl Moloney Murine Leukemia Virus (M-MLV) reverse transcriptase 200 units/µl (Life Technologies, 28028-013), 4µl First Strand buffer (5X) (Life Technologies, 28028-013), 2µl 0.1M dithiothreitol (DTT) (Life Technologies, 18057-018), 0.5µl Recombinant RNasin Ribonuclease Inhibitor (20-40 units/µl) (Promega, N2511), 1µl nuclease-free water (Sigma, W4502) was added per well. Samples were then heated to 37ºC for 50 minutes, followed by an inactivation step of 75ºC for 15 minutes. After that, 30µl of nuclease-free water (Sigma, W4502) was added per sample. For quantitative real-time PCR (qRT-PCR) analysis of genes of interest, 5µl of each sample was used. For the

house keeping gene 18S rRNA, samples were diluted 1:10 and 5µl was used. QRT-PCR is described in 2.2.2.15.

2.2.2.14.3. miRCURY LNA™ Universal cDNA synthesis

MicroRNA cDNA was synthesized by the miRCURY LNA™ Universal cDNA synthesis kit (Exiqon, 203300). This step provides templates for all miRNA real-time PCR assays by one first-strand cDNA synthesis reaction. The basis principal is in Figure 2.2.

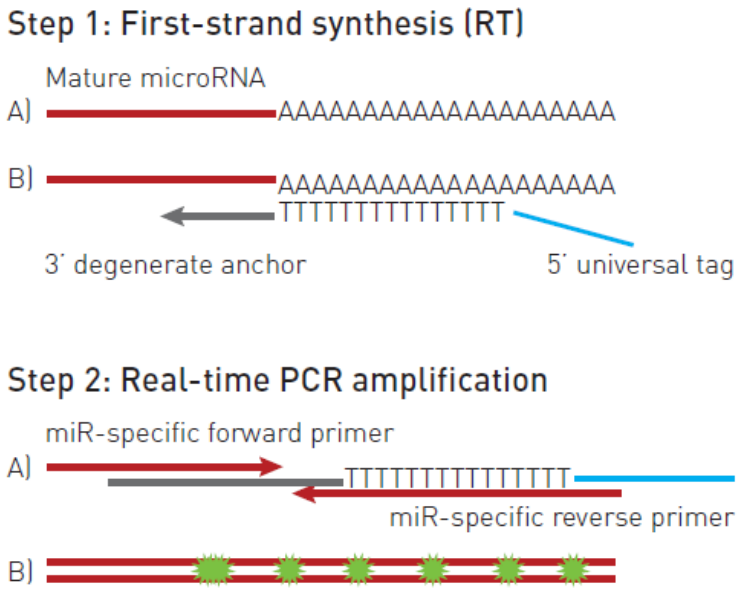

Figure 2.2: Outline of the miRCURY LNA Universal RT miRNAsynthesis.

A poly-A tail is added to the mature miRNA template (step 1A). cDNA was synthesized using a poly-T primer with a 3'degenerate anchor and a 5'universal tag (step1B). Then the cDNA template is amplified using miRNA-specific and LNA^{TM}-enhanced forward and reverse primers (step 2A). Sybr green is used for detection (step 2B). *Reprinted from miRCURY LNA^{TM} Universal RT microRNA PCR instruction manual (Exiqon).*

Total RNA was adjusted to 5ng/µl using nuclease-free water (Sigma, W4502). 10ng of RNA was transferred to an ice cold 96-well PCR plate. A master mix contained 2µl Reaction Buffer (5X) (Exiqon, 203300), 1µl enzyme mix was added to each well. The reaction was brought to 10µl with nuclease-free water and the plate was heated to 42^{o}C for 1 hour followed by a heat inactivation step at 95^{o}C for 5minutes. cDNA was then diluted to 12.5 pg/µl by nuclease free water (Sigma, W4502) and 50pg of cDNA was used for qRT-PCR analysis of miRNA of interest.

2.2.2.15. Real-time quantitative RT-PCR

2.2.2.15.1. Universal Probe Library Real-Time qRT-PCR

The Universal Probe Library (UPL) (Roche Diagnostics) enables extensive transcript coverage due to the short 8-9 nucleotide-long probes. Each probe has a fluorescein (FAM™) label at the 5' end and a dark quencher dye at the 3' end; shorter (typically 8-9 nucleotide) than conventional probe (25-35 nucleotides); locked nucleic acids (LNA™) are incorporated into it sequence. Each probe can detect ~7,000 transcripts and each transcript is detected by ~16 probes.

Primers were designed using the freely available ProbeFinder web-based software provided by Roche Applied Science in which the 'exon boundary spanning' option was selected. Primers were subjected to short sequence BLASTn search to confirm specificity. All the primers were purchased from Sigma and reconstituted in nuclease free water (Sigma, W4502) at 100nM. Primer sequences and UPL probe numbers are in Appendix, Table 3.

For quantitative RT-PCR using the universal primers and probes, the qRT-PCR was carried out using the ABI Prism 7900 HT Sequence Detector (Applied Biosystems) in a microAmp® optical 96-well plate (Life technologies, N8010560). When RNA quantity was known, the qRT-PCR was run using 5ng cDNA for genes of interest and 1ng cDNA for 18S rRNA. For M-MLV-reverse-transcribed- cDNA transcript samples, 5µl samples was used for gene of interest or diluted 1:10 and used 5µl for detecting 18S rRNA.

Each qRT-PCR reaction contained Kappa Fast Universal qPCR Master Mix (2X) (Kappa Biosystems, KK4703), a final concentration of 100nM of each of forward and reverse primers, 200nM of Universal Probe (Roche Diagnostics). The reaction was carried out in a final volume of 25µl. The plate was sealed with microAmp® optical adhesive film (Life Technologies, 4311971) and run with the following PCR cycles: 50°C 2 minutes, 95°C 10 minutes, 40 cycles for 95°C 15 seconds, 60°C 1 minute.

2.2.2.15.2. Standard probe-based Real-time qRT-PCR

The probe-based quantitative real-time PCR method was used to detect the expression of ADAMTS genes including *ADAMTS4, ADAMTS6, ADAMTS10, ADAMTS14, ADAMTS17, ADAMTS19*. These primer and probe sequences were described in (Davidson *et al.* 2006). Briefly, the primers and probes were designed by Primer Express® 1.0 software (Life Technologies, 4363991) and were closed to intron/exon boundaries to control amplification of genomic DNA. Where possible, the probes were designed to span two neighbouring exons. Specificity of primers and probes were validated thought BLASTn. Primer sequences and probe sequences are in Appendix, Table 4

The qRT-PCR reaction was also carried out in a final volume 25µl of Kappa Fast Universal qPCR Master Mix (2X) (Kappa Biosystems, KK4703), 100nM final concentration of each of forward and reverse primers, 200nM genes of interest-specific probe. Reaction set up and cycling conditions were as in 2.2.2.15.1.

2.2.2.15.3. SYBR® Green Real-time PCR

A combination of SYBR® green dye fluorescence with gene-of-interest specific primers enabled double stranded-DNA amplification measurement during PCR. SYBR® green real-time qRT-PCR was used to detect primary and pre sequences of the miR-29 family (which were described in (Eyholzer *et al.* 2010)) and other genes as below. Full primer sequences and list of genes detected by SYBR® green real-time PCR are listed in Appendix, Table 5. All primers were purchased from Sigma.

For SYBR® green qRT-PCR reaction, the amount of cDNA for genes of interest and 18S rRNA is as 2.2.2.15.1. The reaction contained 0.18µl SYBR® green I dye, Kappa Fast Universal qPCR Master Mix (2X) (Kappa Biosystems, KK4703), 100nM final concentration of each of forward and reverse primers. The PCR cycle conditions are as 2.2.2.15.1 followed by another dissociation step which produces the melting curve for the PCR amplification product.

2.2.2.15.4. SYBR® Green Real-time PCR for the mature miR-29 family detection

LNA primers for detecting miR-29 family mature sequence

All LNA primers were designed for optimal performance with the miRCURY LNA™ Universal cDNA synthesis kit. The LNA primers are Hsa-miR-29b-3p LNA™ PCR primer sets (Exiqon, 204679), Hsa-miR-29a-3p LNA™ PCR primer sets (Exiqon, 204698), Hsa-miR-29c-3p LNA™ PCR primer sets (Exiqon, 204729).

Real-time PCR protocol

The qRT-PCR reaction used SYBR® green I dye in combination with LNA™ PCR primer sets to quantify the original mature miR-29 family. The reactions contained 50pg of miRCURY-LNA™-Universal cDNAs for either the miR-29 family or U6. The PCR reaction mix contained 0.18µl SYBR® Green I dye, 5µl Kappa Fast Universal qPCR Master Mix (2X) (Kappa Biosystems, KK4703), and 1µl of forward and reverse primer mix (as recommend by the manufacture (Exiqon)) in a final volume of 10µl. PCR cycles: 10 minutes at 95°C, 40 cycles for 10 seconds at 95°C, 1 minute at 60°C and a dissociation step. The dissociation step produces a melting curve for the PCR amplification product and ensures there is only amplification of the target gene.

2.2.2.15.5. Quantitative RT-PCR Data analysis

2.2.2.15.5.1. Control genes

The constitutively expressed "housekeeping" 18S rRNA was used as the control for relative mRNA gene expression while U6 was used as endogenous control for relative miRNA gene expression.

2.2.2.15.5.2. Relative gene expression – comparative C_t method

Raw fluorescence data was analyzed by the 7000HT SDS 2.2 software to produce threshold cycle (C_t) values, which is the cycle number at which the signal is detectable above the baseline. The C_t values were transformed using the comparative C_t method to obtain relative quantification (RQ) of gene expression:

$$RQ=2^{-\Delta Ct}$$

Where: for mRNA expression: ΔC_t= target gene C_t - 18S C_t

Or for miRNA expression: ΔC_t= the miR-29 family C_t - U6 C_t

This method assumed that all primers and probe sets are working at the same efficiency.

2.2.2.15.6. Western Blot

Buffer and antibody

Radio immunoprecipitation assay (RIPA) buffer: The buffer was made (final concentration) with 50mM Tris base (Fisher Scientific, BP152-500) (which was adjusted to pH 7.6 with hydrochloric acid (Sigma, 258148)),150mM NaCl (Fisher Scientific, BP3581), 1% (v/v) Triton X-100 (Sigma, X100), 1% (w/v) sodium deoxycholate (Sigma, D6750), 0.1% (w/v) sodium dodecyl sulfate (SDS) (Fisher Scientific, 10356463), 10mM sodium fluoride (NaF) (Sigma, 201154), 2mM sodium orthovanadate (Na_3VO_4) (Sigma, S6508), 1X protease inhibitor cocktail (Fisher Scientific, PI-78410).

Resolving buffer: To make up 4X buffer: 91g Tris base (Fisher Scientific, BP152-500) was dissolved in Milli-Q Ultrapure water (Merck Millipore) and adjusted to pH 8.8 with hydrochloric acid (Sigma, 258148). The solution was then made up to 500ml. 2g SDS (Fisher Scientific, 10356463) was added and dissolved.

Staking buffer: To make up 4X buffer: 6.05g Tris base (Fisher Scientific, BP152-500) was dissolved in Milli-Q Ultrapure water and adjusted to pH 6.8 with hydrochloric acid (Sigma, 258148). Milli-Q water was added to 100ml volume. 0.4g SDS (Fisher Scientific, 10356463) was added and dissolved.

Running buffer: To make up 10X buffer: 30.2g Tris base (Fisher Scientific, BP152-500), 144g glycine (Fisher Scientific, 10467963), 10g SDS (Fisher Scientific, 10356463) were dissolved in Milli-Q water to a final volume 1L.

Transfer buffer: To make up 1X buffer: 5.8g Tris base (Fisher Scientific, BP152-500), 2.9g glycine (Fisher Scientific, 10467963), 0.37g SDS (Fisher Scientific, 10356463) were dissolved in Milli-Q water, 200ml 100% (v/v) methanol (Sigma, 322415) were added then Milli-Q water to a final volume of 1L.

Tris-buffered saline (TBS): To make up 10X buffer: 24.2g Tris base (Fisher Scientific, BP152-500), 80g NaCl (Fisher Scientific, BP3581) were dissolved in 900ml Milli-Q water and adjusted to pH 7.6 with hydrochloric acid (Sigma, 258148). Milli-Q water was added to 1L volume.

Blocking buffer: For 150ml, 15ml 10X TBS was diluted in 135ml Milli-Q water. 7,5g non-fat dry milk (OXOID, LP0031) was added and stirred to mix. Finally, 0.15ml Tween®-20 was added (Sigma, P5927).

Primary antibody dilution buffer: For 20 ml, 2 ml 10X TBS was diluted to 18 ml with Milli-Q water. 1.0 g BSA (Sigma, A9418) was added and dissolved by stirring. While stirring, 20µl Tween-20 (Sigma, P5927) was added.

Wash Buffer (TBST): TBS with a final concentration 0.1% (v/v) Tween-20 (Sigma, P5927).

Antibody: GAPDH antibody (Cell Signaling, #2118S), DVL3 antibody (Cell Signaling, #3218), FZD5 antibody (Cell Signaling, #3795)

Western blot protocol

SW1353 cells were plated in 6-well plates ($1.5x10^5$cells/well) and transfected with Syn-Hsa-miR-29b miScript miRNA mimic (Qiagen, MSY0000100) as referred in 2.2.2.7.2.5. At desired time post transfection, cells in each well of 6-well plate were washed twice with ice cold PBS (Life Technologies, 10010023) before adding 100µl RIPA buffer to each well and harvesting by scraping. The cell lysate was transferred to a fresh ice-cold 1.5ml tube and centrifuged at full speech in 10 minutes. The supernatant was collected and stored at -20^{o}C.

Protein was quantified using the Bio-Rad Protein Assay (Bio-Rad, #500-0006) which is based on the method of Bradford. Briefly, 200µl dye reagent concentrate was diluted 5 times with Milli-Q water before adding 20µl sample lysate. The mixture was incubated at room temperature for 10 minutes and absorbance measured at 595nm. Comparison of this value to a standard curve provided a relative concentration of solubilized protein. The

standard curve was created with five dilutions of proteins standards of bovine serum albumin (Bio-Rad, 500-0002) from 0.2 to 0.9 mg/ml.

Samples was adjusted to 20µg solubilized protein in a 30µl with nuclease-free water (Sigma, W4502), followed by adding 20ng/µl Bromophenol Blue (Sigma, 114391) and 1.2µl 1M DTT (Thermal Scientific, # R0861). The sample was gently mixed and heated to 95ºC for 5 minutes. Samples were then electrophoresed on 10% (w/v) polyacrylamide gels. The resolving gel was cast with the following components: 5ml 30% (w/v) Acrylamide/ Bis Acrylamide solution 37:5:1 (Bio-Rad, #161-0154), 3.75ml resolving buffer (4X), 6.25ml Milli-Q water, 50µl 10% (w/v) ammonium persulfate (APS) (Sigma, A3678), 10µl TEMED (Sigma, T9281). Resolving gels were topped with isopropanol (Sigma, 190764) until set. Then isopropanol was removed and the stacking gel was cast on top of the resolving gel and a comb was inserted. For 1 gel, the stacking gel was made with 0.71ml stacking buffer (4X), 0.41ml 30% (w/v) acrylamide/ bis acrylamide solution 37:5:1 (Bio-Rad, #161-0154), 1.91ml Milli-Q water, 16µl 10% (w/v) APS (Sigma, A3678), 3.2µl TEMED (Sigma, T9281). Samples were loaded on the gel and were electrophoresed at 50V until the bromophenol blue passed through the stacking gel and then 80V for 1.5 hours.

Immobilon®-FL PVDF membrane (Merck Millipore, IPFL00010) was incubated in 100% (v/v) methanol (Sigma, 322415) for 15 seconds and washed with Milli-Q water. Then, Immobilon®-FL PVDF membrane, gel, extra thick blotting paper (Bio-Rad, #170-3966) were incubated in transfer buffer for 5 minutes. The gel was plated on top of Immobilon®-FL PVDF membrane in Trans-blot® SD semi-Dry Electrophoretic transfer cell (Bio-Rad, #170-3940) with extra thick blotting paper underneath and on top and run for 25V for 30 minutes (for 2 gels,1 mm thick).

After transfer, the membranes were briefly washed with TBS and incubated in blocking buffer for 1 hour, with gently rocking at room temperature. Membranes were then washed in TBST three times for 5 minutes. Primary antibody and membrane was incubated with gentle agitation overnight at 4ºC. Membranes were then washed in TBST three times for 5 minutes and incubated with IRDye® 800CW goat polyclonal anti-rabbit IgG (Li-Cor, 926-32211) (50µg) for 1 hour at room temperature with gently rock. Membranes were washed

with TBST for another three times for 5 minutes. The membrane was visualized using a Li-Cor Odyssey InfraRed Scanner.

2.2.2.15.7. Whole mount *in situ* hybridization

Reagents and buffers

Sodium chloride (NaCl) (Fisher Scientific, BP3581), tri-sodium citrate (Fisher Scientific, 10637174), magnesium chloride hexahydrate ($MgCl_2.6.H_2O$) (Fisher Scientific, M35-500), potassium chloride (KCl) (Fisher Scientific, BP366-500), heparin (Sigma, H3393), yeast tRNA (Fisher Scientific, 10523043), paraformaldehyde (Sigma, P6148), normal goat serum (heat inactivated), Triton-X100 (Sigma, X100), Tween-20 (Sigma, P5927), BSA (Sigma, A9418)

Saline sodium citrate buffer (SSC): 20X SSC buffer was made up with 175.3 g of NaCl and 88.2 g of sodium citrate, pH 7, in a total volume of 1000ml.

Development solution (DS): The solution was made up with: 100 mM Tris-HCl pH9.5, 50mM magnesium chloride hexahydrate (MgCl2.6.H2O), 100mM sodium chloride (NaCl) + 0.1% (v/v)Tween 20.

Blocking solution: The solution was made up with: 2% (v/v) NGS, 2 mg/ml BSA, 0.1% (v/v) Triton X-100 + 0.05%)v/v) Tween 20 in PBS.

Hybridisation Buffer (HB): The buffer was made up with 50% (v/v) formamide, 5xSSC, 0.1% (v/v) Tween 20 + 10 mM citric acid pH6.0 + 50 µg/ml heparin + 100 µg/ml tRNA in PBS

Tris-buffered saline with Tween 20 (TBST): for 100ml (10X) buffer was made up with 8g NaCl, 25ml Tris-HCl pH7.5, 0.2g KCl, 10ml Tween 20

Phosphate-buffered saline with Tween 20 (PBST): PBS with 0.1% (v/v) Tween 20

Probe: miRCURY LNA™ miR-29b-3p detection probe, 250pmol, 5'-DIG and 3'-DIG labelled (Exiqon, 38131-15)

Fixation

Mouse embryos at desired stages were dissected and fixed in 4% PFA-PBS on a rolling platform overnight at 4^{o}C. Then next day, the embryos were washed 4 times with PBST and dehydrated through increasing MeOH concentration washes e.g. 25%, 50%, 75% and 100% MeOH on the gentle rocking platform. The embryos can then store in 100% MeOH at -20^{o}C until required.

In situ hybridization protocol

On a gently rocking platform, the embryos were washed with decreasing MeOH concentration i.e. 75% (v/v), 50% (v/v), 25% (v/v), 0 (v/v) % MeOH for 15 minutes each time to dehydrate. After that, the embryos were digested with Proteinase K (10µg/ml final concentration) for 30 minutes, followed by rinsing twice in PBST and fixing in 4% (v/v) PFA for 20 minutes. To get rid of the remaining PBST, the embryo was washed 4 times in PBST for 5-7 minutes. The embryo was prehybridized in hybridization buffer at 54^{o}C for 3 hours and the "nape" of the neck of embryo was pricked to facilitate the probe penetration. After prehybridisation step, the buffer was removed and replaced with fresh warm hybridisation buffer containing 20 pmol of the miR-29b LNA probe (Exiqon, 38131-15) and left at 54^{o}C overnight with gentle rocking. The probe hybridisation solution was removed followed by washes at 54^{o}C and 15 minutes each wash e.g. 75% HB: 25% 2xSSC, 50% HB:50% 2xSSC, 25% HB:75% 2xSSC, 2xSSC, 0.2xSSC. Following these washes, at room temperature, another 4 washes were carried on gently rocking platform, 10 minutes for each wash e.g. 75% 0.2xSSC:25% PBST, 50% 0.2xSSC:50% PBST, 25% 0.2xSSC:75% PBST, PBST. The embryo was then put in blocking solution for several hours at room temperature and incubated at 4°C O/N with the pre-absorbed antibody at a final dilution of 1:5000 in Blocking Solution. After that, the Blocking Solution was removed and washed throughout 2 or 3 days at RT in PBST with gentle rocking. To get rid of all remaining PBST, the embryos were washed twice with TBST and with development solution for 15 minutes each wash. Colour development was carried out at room temperature in 3.5ml development solution plus 15-50µl substrates.

The antibody was pre-adsorbed using previously fixed and dehydrated tissue that is not suitable for in situ hybridization. These tissues were dehydrated and washed 15 minutes in

blocking solution, followed by incubating with blocking solution containing the antibody at 1:1000 dilution for three hours.

2.2.2. Cell culture and cell-based assays

2.2.2.1. Human primary chondrocyte isolation

Human cartilage chips were incubated with digestion medium including DMEM GlutaMAX^{TM} (Life Technologies, 10566-016), 1mg/ml collagenase (Sigma, C1639), 0.4% (w/v) Hepes (Fisher Scientific, BP310-100), 100 IU/ml penicillin, 100µg/ml streptomycin (Sigma, P4333) at 37^{o}C, 180rpm overnight. The digestion mixture was then strained through a 70µm cell strainer. Cells were plated at 4x10^{4}cells/cm^{2} and grown to 80% confluence. Cells were used by passage 2.

2.2.2.2. Human de-differentiation assay

Human primary chondrocytes were isolated from human knee OA articular cartilage as described in 2.2.2.1. The cells were then subjected to serial subculture in monolayer. The de-differentiation assay was performed by Dr Natalie Crowe (Clark lab, University of East Anglia).

2.2.2.3. Chondrogenesis model

The human chondrogenesis model was performed by Dr Matthew Barter, Newcastle University. Briefly, human bone marrow stem cells (from seven donors, 18-25 years of age) were isolated from human bone marrow mononuclear cells (purchased from Lonza Biosciences) and resuspended in chondrogenic culture medium consisting of high glucose Dulbecco's modified Eagle's medium containing 100 µg/ml sodium pyruvate (Lonza), 10 ng/ml TGF-β3 (Peprotech), 100 nM dexamethasone, 1x ITS-1 premix, 40 µg/ml proline, and 25 µg/ml ascorbate-2-phosphate (Sigma). 5x10^{5} hMSC in 100µl medium were pipetted onto 6.5mm diameter, 0.4-µm pore size polycarbonate Transwell filters (Merck Millipore), centrifuged in a 24-well plate (200g, 5 minutes), then 0.5 ml of chondrogenic medium was added to the lower well as described. Media were replaced every 2 or 3 days up to 14 days.

The murine chondrogenesis model was performed by Dr Tracey Swingler, University of East Anglia. Briefly, ATDC5 cells were seeded at $6x10^4$/well of a 6-well plate in DMEM/Ham's F-12 medium (Life technologies, 11320-033) containing 5% (v/v) FCS (PAA), 2mM glutamine, 100 IU/ml penicillin, 100µm/ml streptomycin (Sigma, P4333), 5ng/ml sodium selenite, 10µg/ml human transferrin (Sigma, I3146), and 10µg/ml bovine pancreatic insulin at 37°C, in an atmosphere of 5% CO_2. Media was replaced every 2 days up to 42 days. After 21 days, the medium was replaced with α-minimal essential medium with the same supplements, and the atmosphere was changed to 3% CO_2.

2.2.2.4. Monolayer cell culture and storage

All cells were cultured at 37°C with 5% (v/v) CO_2. Cells were usually grown in Dulbecco's modified Eagle's medium (DMEM) High Glucose, GlutaMAX supplement (Life technologies, 10566-016) with 10% (v/v) heat-inactivated Fetal Calf Serum (FCS) (PAA) and 100 IU/ml penicillin and 100µg/ml streptomycin (Sigma, P4333). For maintenance, medium was refreshed at least three times weekly. Cells were passaged at around 80-90% confluence. Adherent cells were detached by washing x2 with HBSS (Life Technologies, 14025092) then treated with 2 ml of trypsin/EDTA (Life Technologies, 25200072) for 2-3 minutes at 37°C. After centrifugation (17.3xg, 5 minutes), the cell pellet was gently resuspended in fresh medium. Cells were replated at a ratio of 1: 20. For long term storage, cells were detached and pelleted by centrifugation at 17.3xg for 5 minutes. The pellets were resuspended in cryo-preservation medium including 90% (v/v) FCS (ATCC) and 10% (v/v) DMSO (Fisher, BP231-100), slowly frozen down at approximately 1°C/minute, and stored in liquid nitrogen.

2.2.2.5. Micromass culture

Media

Growth medium: Dulbecco's modified Eagle's medium (DMEM) High Glucose, GlutaMAX supplement (Life technologies, 10566-016) with 10% (v/v) heat-inactivated Fetal Calf Serum (FCS) (ATCC) and 100 IU/ml penicillin and 100µg/ml streptomycin (Sigma, P4333).

Different medium were prepared: the DMEM high glucose, GlutaMAX supplement (Life technologies, 10566-016) adding 1X Insulin- Transferrin-Selenium (ITS-G) (Life Technologies, 41400-045).

Micromass culture

The protocol was described in (Greco *et al.* 2011) with some modifications. Human primary chondrocytes was isolated from human OA knee cartilage as described in 2.2.2.1 and cultured in monolayer with growth medium. Whenever reaching confluence, the cells were passaged two times. Confluent passage 2 monolayer culture of human primary chondrocytes were released by trypsin/EDTA (Life Technologies, 25200072), and resuspended in growth media at a density of $2.5x10^7$ cells/ml. Micromass was obtained by pipetting 20µl of cell suspension into individual wells of 24 well-plates and leaving for 3 hours to attach without additional medium. Then, 1ml growth medium was gently added and the micromass was left for another 24 hours before stimulating with cytokines or growth factors.

2.2.2.6.Induction cells with regulatory factors: major cytokines and growth factors

Cytokines and growth factors:

Human recombinant TGFβ1 (R&D Systems, 240-B-002/CF) and **human recombinant TGFβ3** (R&D Systems, 243-B-002/CF) were reconstituted in sterile 4mM HCl (Sigma, 258148) containing 0.5% (w/v) bovine serum albumin (Sigma, A2058).

Human recombinant Wnt3a (R&D Systems, 5036-WN-010/CF) was reconstituted in sterile Phosphate Buffered Saline (PBS) (Life Technologies, 10010023).

Human Recombinant Interleukin-1β (IL-1β) (First Link, ILB4551) was reconstituted in sterile Phosphate Buffered Saline (PBS) containing 0.5% (w/v) bovine serum albumin (Sigma, A2058).

NFκB activation inhibitor II JSH-23 (Calbiochem, 481408) is a cell-permeable diamino compound that selectively blocks nuclear translocation of NF-κB p65 and its transcription activity without affecting IκB degradation.

Lipopolysaccharides (LPS) (Sigma, L3012) are components of the cell wall of gram negative bacteria. LPS are extracted from *E.coli* serotype O111:B4 and purified by gel filtration. LPS is reconstituted in sterile (PBS) (Life Technologies, 10010023).

P38 inhibitor SB203580 (Sigma, S8307) is a pyridinyl imidazole that suppresses the activation of MAPKAP kinase-2. The P38 inhibitor, therefore, inhibits the MAPKAP kinase-2 cascade which is activated by cellular stress, bacterial infection and pro-inflammatory cytokines. SB203580 was resuspended in DMSO (Fisher, BP231-100).

2.2.2.6.1. Stimulation of cells in monolayer with cytokines and growth factors

Human chondrosarcoma SW1353 and human primary chondrocytes were maintained as described above. For stimulation, either $5x10^3$ SW1353 cells or 10^4 human primary chondrocytes were seeded into each well of a 96-well plate with 100µl DMEM GlutaMax (Life Technologies, 10566-016) with 10% (v/v) FCS (ATCC) and 100 units/ml penicillin and 100µg/ml streptomycin (Sigma, P4333). Cells were serum starved for 14 hours and were stimulated with different cytokines and growth factors at final concentration: TGFβ1, TGFβ3 4ng/ml, IL-1 5ng/ml, Wnt3a 100ng/ml, LPS 1µg/ml at 4, 8, 12, 24, 48 hours. All treatments were performed in triplicate. At each time point, cells in each well were washed with ice cold PBS (Life Technologies, 10010023) and harvested with 30µl Cells-to-cDNA lysis buffer (Life Technologies, AM8723).

2.2.2.6.2. Stimulation of cells in micromass culture with cytokines and growth factors

After the micromass was rested in growth medium for 24 hours, the different medium with either TGFβ1 (10ng/ml), IL-1 (20ng/ml), Wnt3a (50ng/ml) or LPS (1µg/ml) was added. All treatments were performed in triplicate. After different time points as desired, some of micromasses were harvested for Alcian blue matrix staining and others for quantitative RT-PCR.

2.2.2.7. Mammalian cell transfection

2.2.2.7.1. Plasmids, constructs, siRNAs and microRNA mimic and inhibitor

Sox9 expression vector: The vector was kindly provided by Dr Simon Tew (University of Liverpool, UK). The vector was described in (Lefebvre *et al.* 1997). Briefly, an almost full-length coding sequence of human SOX9 which is from codon 27 (directly from the first ATG associated with the Kozak sequence) up to 39bp of 3'unstranslated region was subcloned into pCDNA-5'UT-FLAG. pCDNA-5'UT-FLAG is pCDNA 3.1 with a FLAG sequence.

The miR-29a/b1 promoter construct: The construct was kindly provided by Dr Anne Delany (University of Connecticut Health Center, US) and was described in (Kapinas *et al.* 2010). The 2kb region upstream from the transcriptional start site of the human miR-29a/b1 putative promoter (EU154353) was subcloned into the luciferase reporter pGL4.10 (Promega).

p(CAGA)$_{12}$-luc plasmid: The construct was a kind gift of Dr Andrew Chantry, University of East Anglia, UK and is described in (Pais *et al*. 2010). 12 binding sites of the complex Smad3/4 (GAGAC) was cloned upstream of the luciferase encoding gene in luciferase reporter pGL3 (Promega).

IκBα promoter reporter plasmid: The plasmid was a kind gift from Prof. Derek Mann, (Newcastle University, UK), (originally from Prof. Ronald Hay, University of Dundee, UK). The plasmid contains 5 binding sites of P65 cloned upstream of the luciferase gene.

TOPflash and FOPflash reporter plasmids: The TOPflash reporter is a kind gift from Prof. Andrea Munsterberg (University of East Anglia, UK), and was originally from Prof. Randall Moon (University of Washington, USA). The FOPflash vector is provided by Dr Sarah Snelling (University of Oxford, UK). TOPflash contains 7 binding sites of TCF/LEF (AGATCAAAGG) driving the expression of the firefly luciferase. The back bone is the pTA-luc vector. The FOPflash vector is the control of TOPflash where all 7 binding sites of TCF/LEF are mutated.

The miR-29 mimic:

- Syn-hsa-miR-29a-3p miScript miRNA mimic (Qiagen, MSY000086): 5'UAGCACCAUCUGAAAUCGGUUA
- Syn-hsa-miR-29b miScript miRNA mimic (Qiagen, MSY0000100): 5'UAGCACCAUUUGAAAUCAGUGUU
- Syn-hsa-miR-29c miScript miRNA mimic (Qiagen, MSY0000681) 5'UAGCACCAUUUGAAAUCGGUUA
- AllStars negative control siRNA (Qiagen, SI03650318)

The 29b inhibitor control

- Anti-hsa-miR-29b miScipt miRNA inhibitor (Qiagen, MIN000100)
- miScript Inhibitor negative control (Qiagen, 1027271)

siRNA

- SOX9 siRNA: Dharmacon siRNA SMARTpool® (Fisher Scientific)
- Control: non-targeting siRNA 2 (Dharmacon, 001210-02)

2.2.2.7.2. Transient transfection protocol

2.2.2.7.2.1. SOX9 overexpression

SW1353 cells were plated in a 96-well plate ($5x10^3$cells/well) in growth medium without antibiotics one day before transfection. The cells were 80% confluent at the time of transfection. Before addition of the transfection complexes, the growth medium was removed from the cells and the cells were covered with 50µl of fresh growth medium without antibiotics. For each transfection, two tubes are prepared as follows: **Tube 1:** 100ng SOX9 expression vector was diluted in 25µl DMEM GlutaMax (Life Technologies, 10566-016) without serum and antibiotics; **Tube 2:** 0.2µl transfection reagent Lipofectamine 2000 (Life Technologies, 11668027) was diluted in 25µl DMEM GlutaMax (Life technologies, 10566-016) no serum and antibiotics. After 5 min of incubation, the diluted DNA and the diluted transfection reagent were combined and incubated at room temperature for 20 min. Then, 50µl of complexes were added to each well. The plate was

gently rocked back and forth and incubated at 37°C in a CO_2 incubator. All transfection was performed in triplicate. The pcDNA3.1 vector was used as control. After 6 hours of transfection, transfection medium was replaced with fresh growth medium without antibiotics for another 24 hours. For harvesting, cells were washed with ice cold PBS (Life Technologies, 10010023) and harvested with 30µl Cells-to-cDNA lysis buffer (Life Technologies, AM8723).

2.2.2.7.2.2. SOX9 and miR-29a/b1 promoter cotransfection

To cotransfect SOX9 and the promoter miR-29a/b1, the SW1353 cells were prepared as described above one day before transfection. For each transfection, two tubes are prepared as follows: **Tube 1:** 100ng of 29a/b1 promoter, and either 100ng SOX9/200ng pcDNA3 or 300ng SOX9/100ng pcDNA3 was diluted in 25µl DMEM GlutaMax (Life Technologies, 10566-016) without serum and antibiotics; **Tube 2:** 0.2µl transfection reagent Lipofectamine 2000 (Life Technologies, 11668027) was diluted in 25µl DMEM GlutaMax (Life Technologies, 10566-016) no serum and antibiotics. The diluted DNA and the diluted transfection reagent were combined after 5 min of incubation and incubated at room temperature for another 20 min. Then, 50µl of complexes were added to each well. The plate was incubated at 37°C in a CO_2 incubator and transfection medium was changed with fresh medium without antibiotics for another 24 hours. Then, cells were washed with ice cold PBS (Life Technologies, 10010023) and a luciferase assay performed. All transfection were performed in triplicate.

2.2.2.7.2.3. Transfection of the miR-29a/b1 promoter with cytokines and growth factors

SW1353 cells were plated and transfected with 100ng miR-29a/b1 promoter as described above. Cells were incubated with the promoter for 24 hours. The medium was then removed and replaced with serum, antibiotic-free DMEM GlutaMAX medium (Life technologies, 10566-016), and cells were serum-starved overnight. Cells was stimulated for 6 hours with TGFβ1/3 (4ng/ml), IL-1 (5ng/ml), Wnt3a (100ng/ml), LPS (1µg/ml) in the presence or absence of 50nM NFκB inhibitor or 10nM p38 inhibitor (Sigma, S8307). Medium was removed 6 hours post stimulation and cells were washed twice with ice cold PBS (Life Technologies, 10010023) and then harvested for luciferase assay.

2.2.2.7.2.4. Short interfering RNA SOX9 mRNA knockdown

SW1353 cells were plated and transfected with either 100nM SOX9 siRNA (Dharmacon) or non-targeting siRNA 2 (Dharmacon, 001210-02) as section 2.2.2.7.2.1. To detect siRNA-mediated mRNA SOX9 knockdown, cells were incubated for 48 hours post transfection, then harvested in 30µl Cells-to-cDNA lysis buffer (Life Technologies, AM8723).

2.2.2.7.2.5. Human primary chondrocyte gain- and loss-of-function experiments

One day before transfection, human primary chondrocytes at passage 1 was plated in 6-well plate at $2x10^5$ cells/ wells in fresh growth medium without antibiotics so that the cells will be around 80% confluent. Complexes were prepared as followed for transfection: **Tube 1**: miR-29b mimic/ inhibitor/ AllStar negative control/ inhibitor negative control (50nM) was diluted in 250µl of serum, antibiotic-free DMEM GlutaMAX (Life Technologies, 10566-016). **Tube 2**: 5µl of Lipofectamine 2000 (Life Technologies, 11668027) was diluted in 250µl serum, antibiotic-free DMEM GlutaMax (Life technology, 10566-016). Time for incubation and transfection mixture was prepared similar to section 2.2.2.7.2.2. The original medium was aspirated from the wells, 500µl transfection mixture was added to each well and the final volume was made to 1ml with DMEM GlutaMAX with 10% (v/v) heat-inactivated FCS, without antibiotics. All transfections were performed in triplicated. Cells were incubated for 48 hours, then, supernatant was removed and cells was washed with ice cold PBS and 1ml Trizol reagent was added. Samples were stored at -20^{o}C until RNA extraction.

2.2.2.7.2.6. Transfection of human primary chondrocytes with miR-29 family mimics and treatment cytokines and growth factors

50nM either miR-29a/b/c mimics or AllStar negative control was transfected to human primary chondrocytes in 6-well plate as in section 2.2.2.7.2.5. After 24 hours, medium was removed from the wells and replaced with DMEM GlutaMAX with 0.5% (v/v) heat inactivated FCS overnight. Then, cells were stimulated with TGFβ1 (4ng/ml), IL-1 (5ng/ml), Wnt3a (100ng/ml). At desired times post stimulation as in Chapter 5, medium was removed, the cells were washed with ice cold PBS and harvested in 1ml Trizol reagent.

2.2.2.7.2.7. Transfection of the miR-29b mimic in micromass culture with cytokines and growth factors

Confluent passage 2 monolayer culture of human primary chondrocytes were released by trypsin/EDTA and plated in 175 cm^2 flask with growth medium with 10% (v/v) heat inactivated FCS, no antibiotics one day before transfection to give cells at 90-100% confluence. 100nM miR-29b mimic or non-targeting control was diluted in 500µl medium (tube1) and 4 µl Lipofectamine 2000 was also diluted in 500µl medium (tube 2). Transfection was carried out as in 2.2.2.7.2.2. The original medium from the flask was removed before adding 1ml transfection mixture and the flask was further covered with another 14ml growth medium with 10% (v/v) heat inactivated FCS. After incubating with miR-29b mimic for 48 hours, cells was detached by trypsin/EDTA and put in micromass culture as in 2.2.2.5. After 24 hours of resting, miR-29b transfected micromasses were treated with either TGFβ1 (10ng/ml), IL-1 (5ng/ml), Wnt3a (100ng/ml) in different media (referred in 2.2.2.5) with 10% (v/v) heat inactivated FCS without antibiotics. At desired time, micromasses were harvested in 500µl Trizol reagent.

2.2.2.7.2.8. Co-transfection of reporter vectors with the miR-29 family mimic/ miR-29b inhibitor and stimulation with cytokines and growth factors

SW1353 were seeded into 96-well plate 1 day before transfection as in 2.2.2.7.2.1 and transiently co-transfected with: (1)100ng of reporter plasmids of either $p(CAGAC)_{12}$- luc, $I\kappa B_3$-luc, TOPflash, FOPflash, (2) 10ng of renilla luciferase reporter, and (3) 50nM of either miR-29a/b/c mimic, AllStar non-targeting negative control, miR-29b inhibitor, or inhibitor negative control. The protocol for transfection is as in 2.2.2.7.2.5. After 24 hours of transfection, cells was serum starved overnight and were treated with recombinant human TGFβ1 (4ng/ml), IL-1β (5ng/ml), Wnt3a (100ng/ml) for 6 hours. After stimulation, cells were harvested and a luciferase assay performed as in 2.2.2.8.

2.2.2.7.2.9. Cotransfection of pmiR-Glo-3'UTR reporter with the miR-29 family mimic

Chicken fibroblasts DF1 were plated in a 96-well plate (10^4cells/well) in antibiotic free growth media with 10% (v/v) FCS overnight. 100ng of either pmiR-Glo-3'UTR wild type

or mutant constructs were co-transfected with 50nM miR-29a/b/c mimic using the non-targeting Allstars as control. The protocol for transfection was described in 2.2.2.7.2.5. After 24 hours post transfection. DF1 cells were harvested for luciferase assay as in 2.2.2.8.

2.2.2.8. Luciferase reporter assay

At desire times post transfection, the plate was removed from the incubator. Luminescence was detected using the Dual-Luciferase Reporter Assay system (Promega, E1980). Briefly, the medium on the cells was removed. The cells were washed twice with ice cold PBS and 70µl of cell lysis buffer provided in the kit (Promega, E1980) was added to each well. The plate was gently rocked back and forth for 30 minutes. Then, 10µl cell lysates were transferred to a 96- well white microplate. For measuring firefly luciferase activity, 50µl of Dual Luciferase Reagent was added to each well. The firefly luminescence was measured using a microplate reader. For measuring Renilla luciferase activity, 50 µl of Dual Stop & Glo Reagent was added to each well and mixed gently then the luminescence measured.

After measurement of the firefly luciferase luminescence and Renilla luciferase luminescence, the relative luciferase activity was calculated as the ratio of the firefly activity normalized to the Renilla luciferase activity.

2.2.3. MicroRNA and mRNA microarray

2.2.3.1. MicroRNA and mRNA microarray for destabilization of medial menicus (DMM) model

Whole knee joints from mice which underwent DMM surgery (e.g. DMM-operated right knee and unoperated left knee) were subjected to total RNA isolation and grouped as DMM left (referred to as control) or DMM right (referred as treatment). At each time point (1, 3, 7 days after surgery), equal amounts of total RNA from each sample in the same group was pooled together. The integrity of the new pooled samples was checked before sending to Exiqon Services (Denmark) or Source Bioscience (UK) to perform miRNA microarray or mRNA microarray, respectively.

The miRCURY LNA^{TM} microRNA Hi-Power Labelling Kit Hy3^{TM}/Hy5^{TM} was used for miRNA microarray in which the Hy3^{TM} labelled samples and Hy5^{TM} labelled samples

were mixed pair-wise and hybridized to capture probes targeting all miRNAs or human, mouse and rat registered in the miBASE 18.0. For whole genome array, Illumina's BeadArray-based technology was employed by using MouseWG-6 v2.0 Expression BeadChips whose feature content derived mainly from NCBI reference sequence (NCBI refseq), and simultaneously profiles more than 45,000 mouse transcripts. The BeadChips consists of oligonucleotides immobilized to bead held in microwells on the surface of any array substrate, and made up with 50-mer-gene-specific probe plus 29-mer address sequences. Especially, the chip has high level of bead type redundancy (average 30 beads per probe) to control the quality and reproducibility of the direct hybridization assay.

2.2.3.2. Whole genome array for miR-29b gain and loss-of-function experiment

Human primary chondrocytes were transiently transfected with either miR-29b mimic or miR-29b inhibitor for 48 hours in triplicate. Then, total RNA was isolated and equal amounts of total RNA of each sample in the triplicate was pooled together. After checking the quality and integrity, the new pooled samples were sent to Source Bioscience (UK) to perform human whole genome profile. Again, the Illumina's BeadArray-based technology was employed but using humanHT-12 V4.0 expression BeadChips. Similarly, the feature content derived mainly from NCBI reference sequence (NCBI refseq) which simultaneously profile more than 47,000 human transcripts.

2.2.4. Data analysis

2.2.4.1. Pre-processing microRNA array data

2.2.4.1.1. VST transformation and quantile normalization

It is necessary to do background correction to remove non-specific signal from total signal. However, the initial data-pre-processing in the Illumina GenomeStudio solfware provides users with bead summary data in the form of a single signal intensity value for each probe. This value is calculated by subtracting the local background from the signal intensity of each bead, then taking the means of all beads containing a given probe. This means BeadStudio output data has undergone background correction. Thus, no further background correction need to be done for the Bead summary data, received from Source Bioscience (UK).

To reliably detect changes in expression from the whole genome array, it is important to remove sources of variation of non-biological origin between arrays to make data comparable. There are two types of variations might be seen when comparing arrays e.g. interesting variation (biological differences), and obscuring variation. Sources of obscuring variation were introduced during the process of carrying out the experiments e.g. **during preparing the samples** including mRNA extraction and isolation, variation in introduction and incorporation of dye, effected by pipetting error, temperature fluctuations and reagent quality; **during manufacturing of the array** including variation in the amount of probe present at each feature or spot and variation in the hybridization efficiency of the probes for their mRNA targets; **during hybridization of the sample on the array** including variation in the amount of samples applied to the array and variation in the amount of target hybridized to the probe; and after array hybridization including variation in optical measurement and intensity computed from the scan image. So, comparisons between different biological samples can be made, it is important to remove these obscuring variations to ensure the values being analysed reflect the biology. For Beadchip array data, the two steps to achieve this are commonly referred to as between-array normalization, and transformation. Two popular methods that implement these steps are VST transformation and quantile normalization for the Lumi packages. Briefly, for analysing, bead summary array data was imported into R studio (http://www.rstudio.com/). Array data was then transformed and normalized using Lumi package.

2.2.4.1.2. Sequence data

The miR-29 family mature sequence data was retrieved from miRbase database (http://www.mirbase.org/). 3'UTR sequences were downloaded from UCSC (https://genome.ucsc.edu/) and Ensembl (http://www.ensembl.org/index.html). RefSeq IDs were used to map probe sets to UCSC database and Ensembl Gene IDs were used to map probesets to the Ensembl database.

2.2.4.1.3. The MicroRNA-29 family target prediction

Three types of seed matches in the 3'UTR were considered when predicting direct miRNA-29 targets e.g. **6-mer seed match** which is 6nt in length and was complementary

to nucleotides 2 to 7 in the miR-29 family; **7-mer seed match** which is 7nt length and is complementary to nucleotides 1–7 in the miRNA or nucleotides 2–7 in the miRNA with "A" at the first position; and **8-mer seed match** which is 8nt length, and matched nucleotides 1–8 in the miRNA or nucleotides 2–8 in the miRNA with an "A" at the first position. For searching these seed matches in the 3'UTR, 3'UTR sequences were imported and read in R studios using the "*readDNAStringSet*" function in Biostring package. Also, three types of miR-29 family seed matches were searched using "*vcountPattern*"function.

In line with using R studios, some miRNA target prediction programs available were also used to predict targets for miR-29 including TargetScan (http://www.targetscan.org/), miRNA body map (http://www.mirnabodymap.org/), miRDB (http://mirdb.org/miRDB/), DIANA (http://diana.cslab.ece.ntua.gr/), Pictar (http://pictar.mdc-berlin.de/), miRbase (http://www.mirbase.org/).

2.2.4.1.4. Functional pathway analysis

DAVID (Database for Annotation, Visualization and Integrated Discovery) functional annotation tool (http://david.abcc.ncifcrf.gov/) was used to perform functional analysis for particular gene groups.

2.2.4.1.5. Statistical analysis

Unless otherwise stated, for the whole thesis, Student's unpaired t-test (two-tail) was performed to compare difference between two groups. All values are given as mean values of replicates with error bar representing the standard error of the mean. The statistical analysis was carried using GraphPad Prism version 4.0 for Windows. Levels of statistical significant are represented as * $\leq$ 0.05, ** $\leq$ 0.01, *** $\leq$ 0.001.

CHAPTER III
IDENTIFICATION OF THE MIR-29 FAMILY IN CARTILAGE HOMEOSTASIS AND OSTEOARTHRITIS

3.1. Introduction

MicroRNAs are referred to as the master regulators for gene expression: they exert their suppressive functions on targeting genes at the post transcriptional level through a sequence-complementary mechanism (Bartel 2009). In human chondrocytes, many different miRNAs are found and each of them are shown to directly and/or indirectly regulate hundreds of target genes, implicating a complex gene regulatory network in which miRNAs are involved (Le *et al.* 2013). This means that miRNAs take a crucial part in controlling the balance of the mRNA network in cartilage homeostasis; and the dysregulation of miRNA expression could trigger OA onset by disrupting this regulatory network.

Indeed, an essential role of miRNAs has been reported in various aspects of cartilage development, cartilage homeostasis, and also in OA pathogenesis (Le et al. 2013). For instance, knockout of Dicer, the pre-miRNA processing enzyme, in a cartilage-specific manner resulted in skeletal growth defects, premature death of mice, reduction in growth plate chondrocytes, and an increase in hypertrophic chondrocytes (Kobayashi et al. 2008). Mutation of the Dnm3 locus, transcribing the miRNAs miR-199a, miR-199*, and miR-214, resulted in growth retardation including craniofacial hypoplasia (Watanabe *et al.* 2008). Universal knockout of miR-140, a cartilage and skeletal-restricted miRNA lead to: mild craniofacial deformities and dwarfism; early onset of age-related OA development; greater susceptibility to OA with accelerated proteoglycan loss and fibrillation of articular cartilage (Miyaki et al. 2010, Nakamura et al. 2011). Transgenic mice overexpressing miR-240 in cartilage were resistant to antigen-induced arthritis-associated loss of proteoglycan and type II collagen (Miyaki et al. 2010). Other specific miRNAs: miR-9, miR-98, and miR-146 were highlighted to be expressed differentially in miRNA profiles between human OA cartilage and its normal articular counterpart (Iliopoulos et al. 2008, Jones *et al.* 2009); miR-199a, miR-675, miR-145, miR-140, miR-455 have been proven to function in chondrogenesis and cartilage homeostasis (Lin *et al.* 2009, Miyaki *et al.* 2009, Dudek *et al.* 2010, Martinez-Sanchez *et al.* 2012, Swingler *et al.* 2012); miR-222 is

reported to play a potential role in the articular cartilage mechanotransduction pathway (Dunn *et al.* 2009); miR-146a and miR-146b, whose expression is regulated by NFκB, appear to be the key miRNAs in the inflammatory response (Taganov *et al.* 2006); miR-34a, miR-194, miR-27b were reported to be induced by IL-1β (Abouheif et al. 2010, Akhtar *et al.* 2010, Xu et al. 2012). All of these data reveal miRNAs as important modulators of various aspects of articular cartilage homeostasis and OA pathogenesis.

OA develops slowly with time and may not be symptomatic until significant joint damage has occurred. Currently, there is a lack of effective approaches to OA prevention or treatment. Available treatments are limited to pain management, and joint replacement surgery, this latter in the late phase of the disease. MicroRNAs, with the ability to fine-tune the expression of multiple genes, could be a promising tool for therapeutic applications for a complex disease like OA. The down regulation of gene expression by miRNAs is relatively modest, thus the approach of combining multiple miRNAs to simultaneously target OA pathogenesis-relevant networks may be needed. Furthermore, There is growing evidence for future miRNA-based diagnostics: a number of miRNA in plasma were found at different levels between RA and OA patients (Murata *et al.* 2010); let-7e, miR-454, miR-886 were identified as differentially expressed circulating miRNAs in OA patients necessitating arthroplasty, especially, let–7e emerged as potential predictor for severe knee or hip OA (Beyer et al. 2014). However, there is a requirement for detailed investigations directed at diagnostic performance (sensitivity, specificity, accuracy) of these promising novel biomarkers before the measurement of miRNAs can enter the clinic.

With all of the above information, the essential roles of miRNAs in cartilage homeostasis and OA are shown with potential for clinical application. The insights into the roles of miRNAs in chondrogenesis, articular cartilage homeostasis, and OA initiation and progression are, nevertheless, still insufficient. Thus, there is a continuing need to deepen our understanding of the molecular mechanisms miRNAs are involved in cartilage homeostasis and OA. Investigating the disease directly in man is challenging due to e.g. the inability to harvest articular tissue at an early stage; the slow disease progression; the absence of symptoms in the early stage of the disease; the variety of symptoms; the variety of causes and environmental influence. Animal models mimicking features of OA are, therefore, an important alternative solution.

In an effort to identify novel miRNAs important in the development of OA, the murine Destabilization of Medial Meniscus (DMM) model was used to identify miRNAs differentially expressed at 1, 3, 7 days (i.e. early stages) after the surgery. Performing miRNA and mRNA profiling followed with an integrated analysis highlighted miR-29b as a candidate miRNA participating in the early onset of OA in DMM model. Alongside the DMM model, the role of the miR-29 family in cartilage homeostasis and OA was also investigated in other human and mouse models e.g. human end-stage OA cartilage, the murine hip avulsion injury model, a human primary chondrocyte dedifferentiation model, a human chondrogenesis model, and murine limb development.

Aims

- Performing miRNA and mRNA profiling in DMM model at very early time points 1, 3, 7 days after surgery
- Identifying miRNA potentially involve in OA onset by bioinformatics analysis
- Investigating the regulation of the miR-29 family which is highlighted from bioinformatics analysis above in human end-stage OA cartilage
- Determining the expression pattern of the miR-29 family in injury model
- Establishing if the miR-29 family involving in chondrocyte phenotype
- Determining the role of miR-29 in human and murine chondrogenesis
- Investigating the involvement of miR-29 in murine limb development

3.2. Results

3.2.1. The microRNA profile in the DMM model at 1, 3, 7 days after surgery

As little is known about the involvement of miRNAs at the early stage of OA, identifying miRNAs modulated in OA initiation was a major aim. Since mRNA profiles have shown large changes in gene expression even at 24 hours post surgery, the DMM model was used to investigate this.

Alongside DMM mice (mice whose medial meniscal tibial ligament of the right knee was transected whilst the left knee was untouched), naïve mice (receiving no treatment), and sham-operated mice (mice whose right knees were operated to visualize the medial meniscal tibia ligament but not transected) were used. Total RNA was first isolated from the whole knee joints of DMM mice (both right and left knees) and their controls at 3 different time points i.e. 1, 3, 7 days after surgery, and subsequently checked for quality and integrity. Unfortunately, RNA from naïve mice was degraded and not further studied. For miRNA profiling, an equal amount of total RNA from individual in each triplicate in the DMM right knee and DMM left knee group at 1, 3, and 7 days after surgery was pooled and these pools were subsequently subjected to miRNA microarray using the miRCURY LNA^{TM} microRNA Hi-Power Labelling Kit Hy3^{TM}/Hy5^{TM}, containing probes targeting all human, mouse and rat miRNAs registered in the miRBase 18.0.

Clustering analysis showed that: the miRNA profiles of the DMM right or left knees were clustered quite closely to each other at day 1 and 3 but far apart at day 7 (Appendix, Figure 1), suggesting that more miRNAs were modulated at the later time point than the earlier. In line with this, calculating the number of miRNAs which changed expression at each time point revealed the same pattern: only small changes were observed until 7 days post-surgery (Figure 3.1). Using 1.5 fold-change (FC) as the cut off, only four miRNAs significantly increased expression at day 1 and 3 whilst more than 30 miRNAs were modulated at day 7. The list of miRNAs which changed expression is listed in Table 3.1.

To visualize the expression pattern of miRNAs across the time course of the DMM model, unsupervised hierarchical clustering analysis was carried out for miRNAs that met the filtering criteria e.g. absolute FC > 1.3 in each time point. Several clusters of miRNAs were identified comparing between DMM right and left knee i.e. (i) miRNAs which **increased** expression across the time course (cluster 1, 2, 3) (Figure 3.2a, b, c), (ii)

miRNAs which **decreased** expression across the time course (cluster 5, 6) (Figure 3.2.e, f), (iii) miRNAs **which decreased** expression across 3 days but **increased** at day 7 (cluster 4) (Figure 3.2d) and (iv) miRNAs which **increased** until 3 days but **decreased** at day 7 (cluster 7) (Figure 3.2.g).

A subset of miRNA differentially expressed by microarray analysis was selected for revalidating the array data by quantitative real-time RT-PCR. The result confirmed the miRNA array data since a similar expression pattern between the two platforms for miR-140, miR-455 (data not shown) and miR-29b (which will be discussed below) was observed.

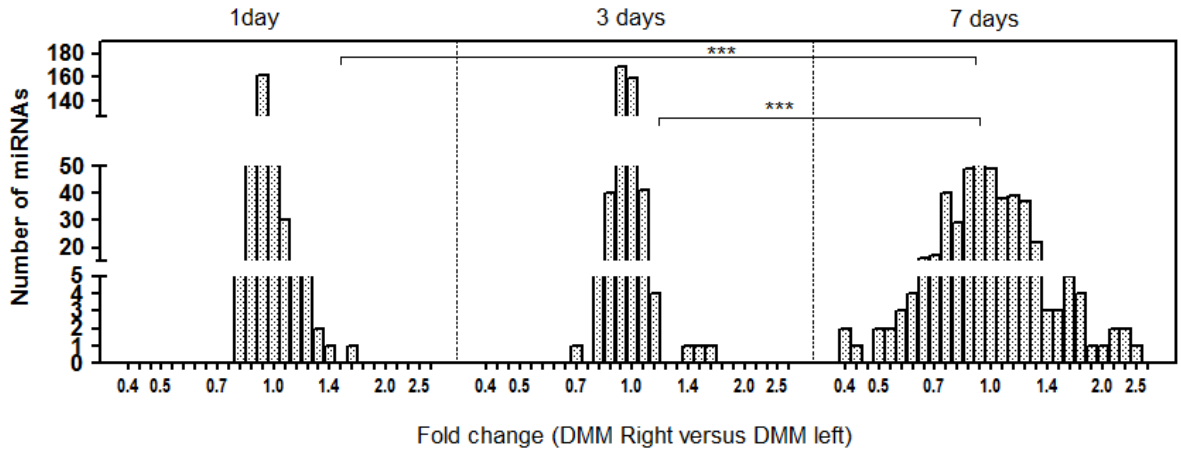

Figure 3.1: Modulation of miRNA expression across a 7 day time course

From the array data, for each miRNA, fold change (FC) was calculated by comparing its expression level in DMM right versus left knee. The number of regulated miRNAs were calculated for each of 0.05 interval of a (0.4, 2.5) range of FC. FC: > 1: increase expression; < 1: decrease expression. The difference in number of miRNAs modulated was calculated by unpaired two-tailed t test: * $p<0.05$, ** $p < 0.01$, *** $p<0.001$.

Day 1		Day 7	
miRNA	**FC**	**miRNA**	**FC**
miR-144-3p	1.7	miR-379-5p	2.6
miR-29b-3p	1.5	miR-127-3p	2.4
		miR-335-5p	2.4
		miR-370-5p	2.2
Day 3		miR-214-3p	2.2
miRNA	**FC**	miR-21-5p	2.1
miR-370-5p	1.7	miR-3073-3p	2.0
miR-21-5p	1.6	miR-199a-3p	1.9
		miR-214-5p	1.8
		miR-210-3p	1.8
		miR-455-3p	1.8
		miR-199a-5p	1.7
		miR-2137	1.7
		miR-199b-5p	1.7
		miR-136-5p	1.7
		miR-34a-5p	1.6
		miR-99b-5p	1.6
		miR-152-3p	1.5
		miR-34c-5p	1.5
		miR-144-3p	-1.5
		miR-3100-3p	-1.5
		miR-669c-3p	-1.6
		miR-378-3p	-1.6
		miR-3473b	-1.6
		miR-133a-5p	-1.6
		miR-3474	-1.7
		miR-378b	-1.7
		miR-133a-3p	-1.8
		miR-133b-3p	-1.8
		miR-1952	-1.9
		miR-491-3p	-1.9
		miR-1a-3p	-2.2
		miR-706	-2.3
		miR-3572	-2.3

Table 3.1: The list of miRNAs regulated in the DMM model with fold change higher than 1.5 (increase or decrease) at 1, 3, and 7 days after surgery.

Fold change (FC) was calculated by comparing between the DMM operated right and un-operated left knee. Down-regulated miRNAs are presented as negative FC.

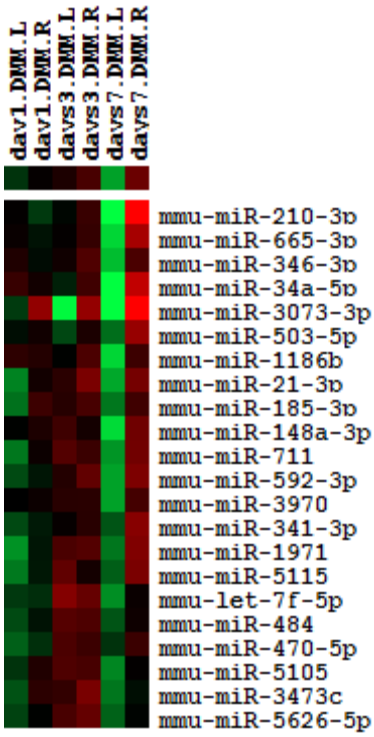
dav1.DMM.L
dav1.DMM.R
davs3.DMM.L
davs3.DMM.R
davs7.DMM.L
davs7.DMM.R
mmu-miR-210-3p
mmu-miR-665-3p
mmu-miR-346-3p
mmu-miR-34a-5p
mmu-miR-3073-3p
mmu-miR-503-5p
mmu-miR-1186b
mmu-miR-21-3p
mmu-miR-185-3p
mmu-miR-148a-3p
mmu-miR-711
mmu-miR-592-3p
mmu-miR-3970
mmu-miR-341-3p
mmu-miR-1971
mmu-miR-5115
mmu-let-7f-5p
mmu-miR-484
mmu-miR-470-5p
mmu-miR-5105
mmu-miR-3473c
mmu-miR-5626-5p

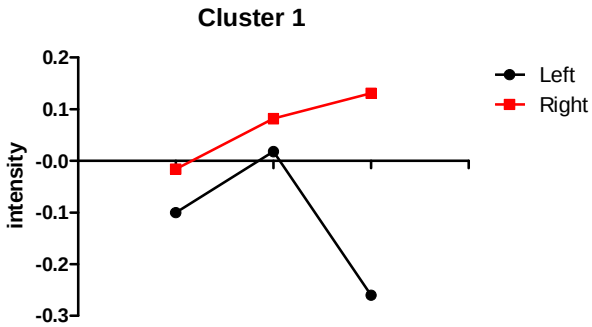
Cluster 1
intensity
0.2
0.1
-0.0
-0.1
-0.2
-0.3
Left
Right

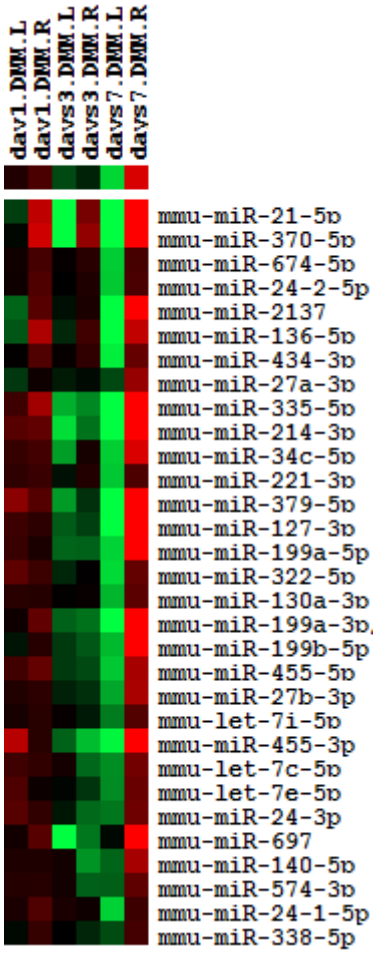
dav1.DMM.L
dav1.DMM.R
davs3.DMM.L
davs3.DMM.R
davs7.DMM.L
davs7.DMM.R
mmu-miR-21-5p
mmu-miR-370-5p
mmu-miR-674-5p
mmu-miR-24-2-5p
mmu-miR-2137
mmu-miR-136-5p
mmu-miR-434-3p
mmu-miR-27a-3p
mmu-miR-335-5p
mmu-miR-214-3p
mmu-miR-34c-5p
mmu-miR-221-3p
mmu-miR-379-5p
mmu-miR-127-3p
mmu-miR-199a-5p
mmu-miR-322-5p
mmu-miR-130a-3p
mmu-miR-199a-3p
mmu-miR-199b-5p
mmu-miR-455-5p
mmu-miR-27b-3p
mmu-let-7i-5p
mmu-miR-455-3p
mmu-let-7c-5p
mmu-let-7e-5p
mmu-miR-24-3p
mmu-miR-697
mmu-miR-140-5p
mmu-miR-574-3p
mmu-miR-24-1-5p
mmu-miR-338-5p

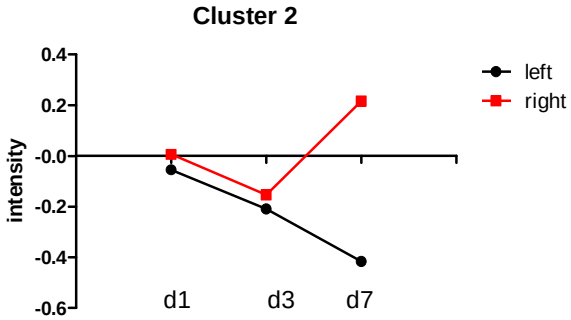
Cluster 2
intensity
0.4
0.2
-0.0
-0.2
-0.4
-0.6
d1
d3
d7
left
right

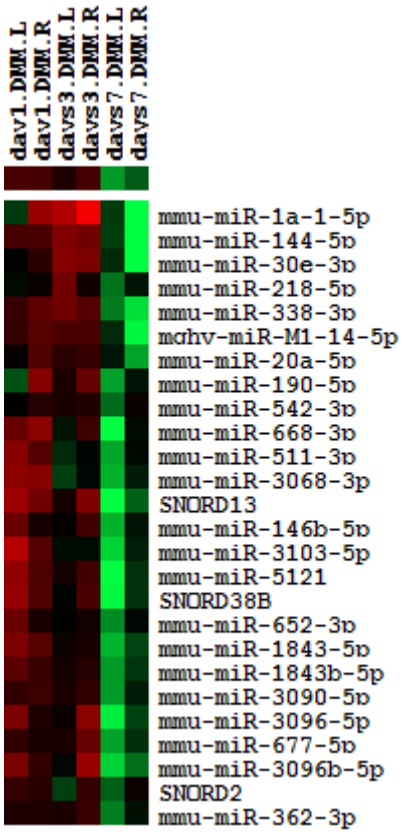
dav1.DMM.L
dav1.DMM.R
davs3.DMM.L
davs3.DMM.R
davs7.DMM.L
davs7.DMM.R
mmu-miR-1a-1-5p
mmu-miR-144-5p
mmu-miR-30e-3p
mmu-miR-218-5p
mmu-miR-338-3p
mghv-miR-M1-14-5p
mmu-miR-20a-5p
mmu-miR-190-5p
mmu-miR-542-3p
mmu-miR-668-3p
mmu-miR-511-3p
mmu-miR-3068-3p
SNORD13
mmu-miR-146b-5p
mmu-miR-3103-5p
mmu-miR-5121
SNORD38B
mmu-miR-652-3p
mmu-miR-1843-5p
mmu-miR-1843b-5p
mmu-miR-3090-5p
mmu-miR-3096-5p
mmu-miR-677-5p
mmu-miR-3096b-5p
SNORD2
mmu-miR-362-3p

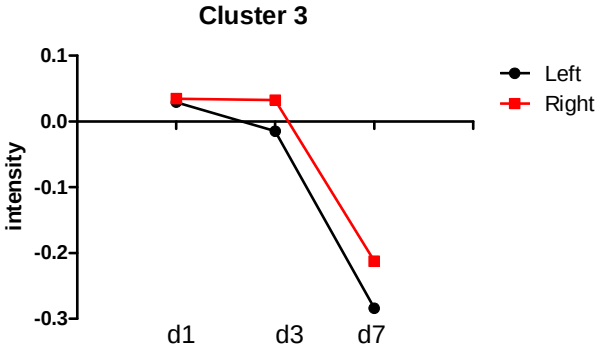
Cluster 3
0.1
0.0
-0.1
-0.2
-0.3
intensity
d1
d3
d7
Left
Right

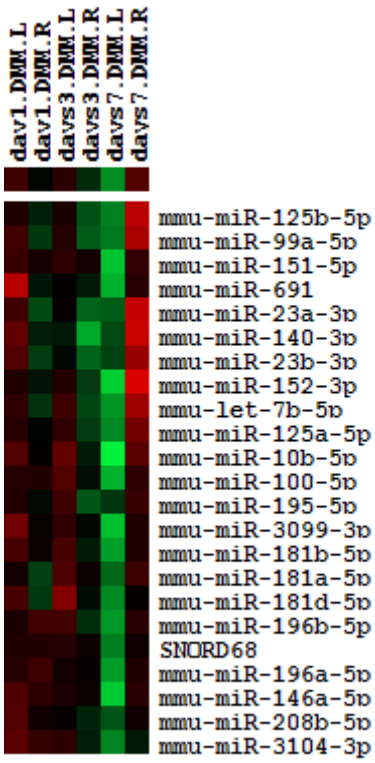
dav1.DMM.L
dav1.DMM.R
davs3.DMM.L
davs3.DMM.R
davs7.DMM.L
davs7.DMM.R
mmu-miR-125b-5p
mmu-miR-99a-5p
mmu-miR-151-5p
mmu-miR-691
mmu-miR-23a-3p
mmu-miR-140-3p
mmu-miR-23b-3p
mmu-miR-152-3p
mmu-let-7b-5p
mmu-miR-125a-5p
mmu-miR-10b-5p
mmu-miR-100-5p
mmu-miR-195-5p
mmu-miR-3099-3p
mmu-miR-181b-5p
mmu-miR-181a-5p
mmu-miR-181d-5p
mmu-miR-196b-5p
SNORD68
mmu-miR-196a-5p
mmu-miR-146a-5p
mmu-miR-208b-5p
mmu-miR-3104-3p

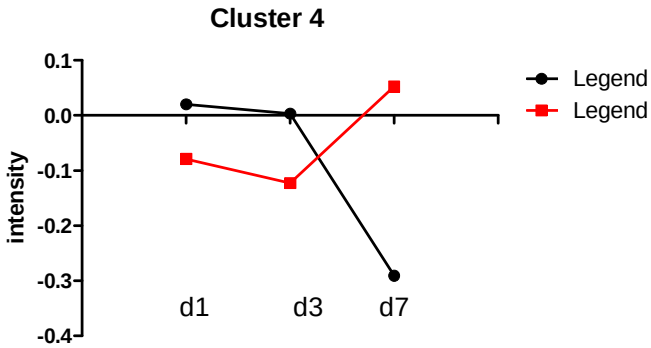
Cluster 4
0.1
0.0
-0.1
-0.2
-0.3
-0.4
intensity
d1
d3
d7
Legend
Legend

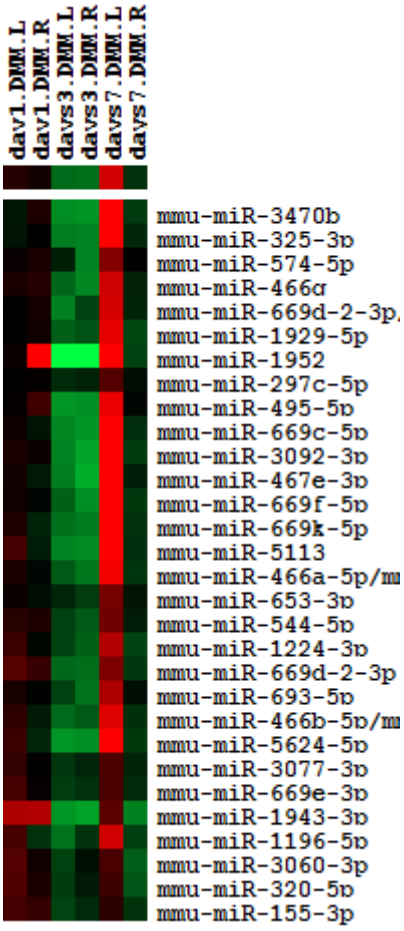
dav1.DMM.L
dav1.DMM.R
davs3.DMM.L
davs3.DMM.R
davs7.DMM.L
davs7.DMM.R
mmu-miR-3470b
mmu-miR-325-3p
mmu-miR-574-5p
mmu-miR-466a
mmu-miR-669d-2-3p
mmu-miR-1929-5p
mmu-miR-1952
mmu-miR-297c-5p
mmu-miR-495-5p
mmu-miR-669c-5p
mmu-miR-3092-3p
mmu-miR-467e-3p
mmu-miR-669f-5p
mmu-miR-669k-5p
mmu-miR-5113
mmu-miR-466a-5p/m
mmu-miR-653-3p
mmu-miR-544-5p
mmu-miR-1224-3p
mmu-miR-669d-2-3p
mmu-miR-693-5p
mmu-miR-466b-5p/m
mmu-miR-5624-5p
mmu-miR-3077-3p
mmu-miR-669e-3p
mmu-miR-1943-3p
mmu-miR-1196-5p
mmu-miR-3060-3p
mmu-miR-320-5p
mmu-miR-155-3p

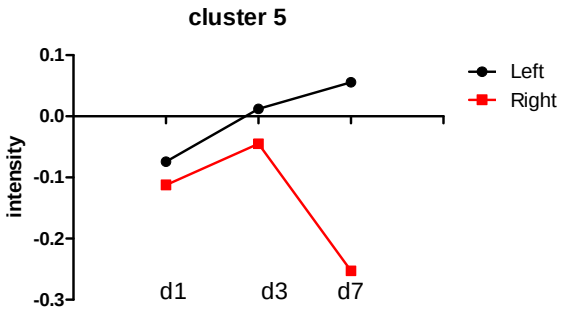
cluster 5
0.1
0.0
-0.1
-0.2
-0.3
intensity
d1
d3
d7
Left
Right

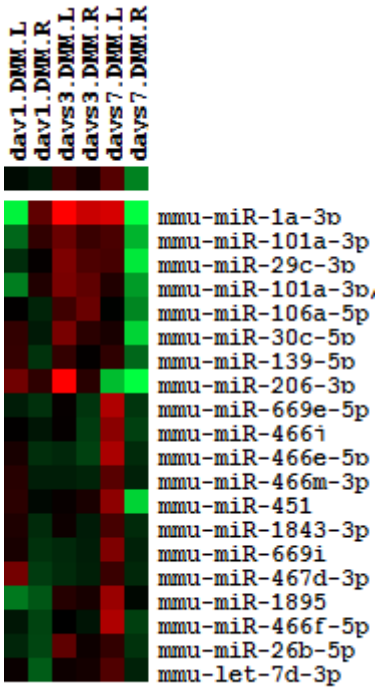
dav1.DMM.L
dav1.DMM.R
davs3.DMM.L
davs3.DMM.R
davs7.DMM.L
davs7.DMM.R
mmu-miR-1a-3p
mmu-miR-101a-3p
mmu-miR-29c-3p
mmu-miR-101a-3p,
mmu-miR-106a-5p
mmu-miR-30c-5p
mmu-miR-139-5p
mmu-miR-206-3p
mmu-miR-669e-5p
mmu-miR-466i
mmu-miR-466e-5p
mmu-miR-466m-3p
mmu-miR-451
mmu-miR-1843-3p
mmu-miR-669i
mmu-miR-467d-3p
mmu-miR-1895
mmu-miR-466f-5p
mmu-miR-26b-5p
mmu-let-7d-3p

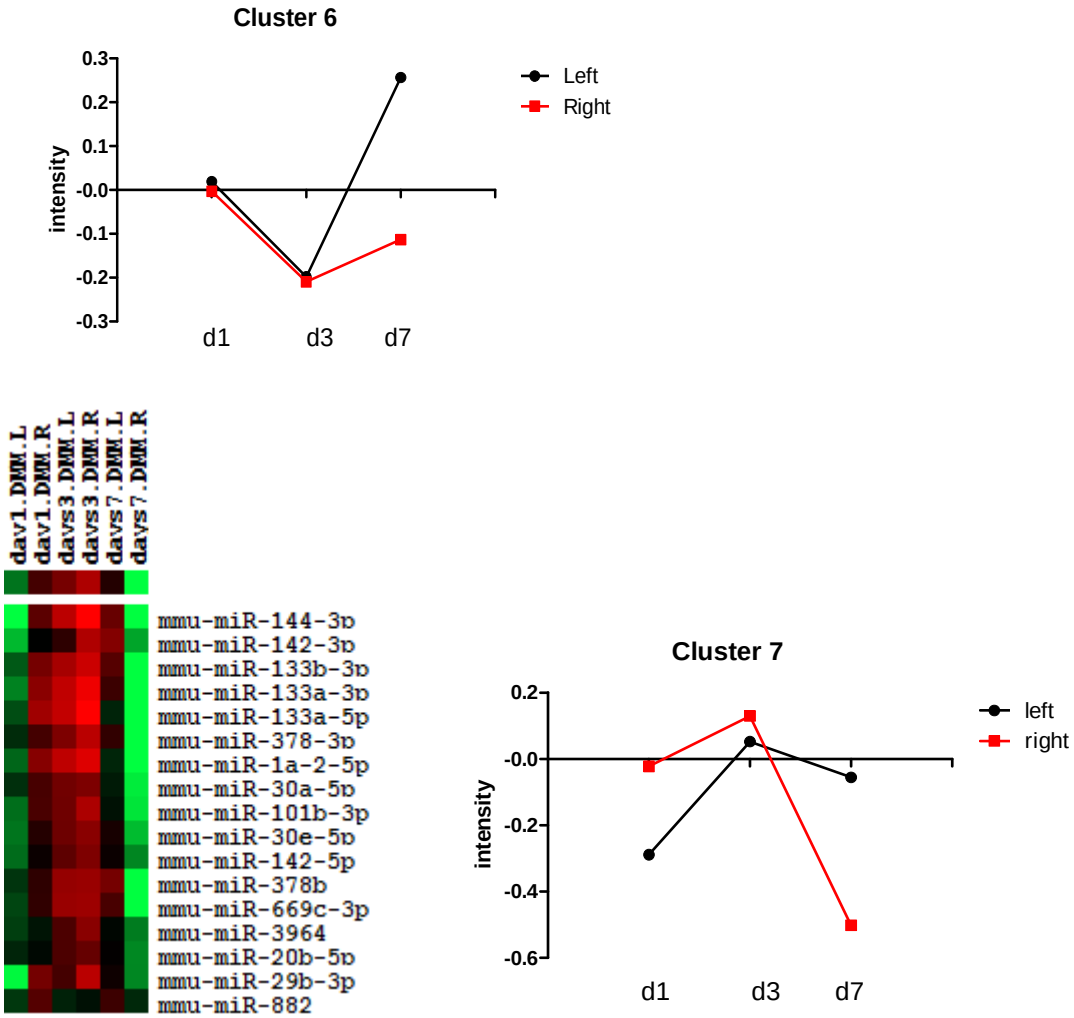

Figure 3.2: Unsupervised hierarchical clustering analysis for miRNAs with absolute fold change higher than 1.3.

Comparing DMM right versus left knee at 1, 3, 7 day time points: cluster 1, 2, 3: all the miRNAs induced expression; cluster 5, 6: all miRNAs decreased expression; cluster 4: miRNAs decreased across 3 days but increased at day 7; cluster 7: miRNAs increased across 3 days but decreased at day 7. Comparing between three time points: cluster 1: miRNAs increased across 7 days; cluster 2, 6: miRNAs decreased at day 3; cluster 3, 5: miRNAs decreased at day 7. SNORD: small nucleolar RNA.

3.2.2. Expression profile of mRNAs in DMM right and left knee

The microRNA microarray profiling revealed approximately 35 miRNAs modulated in the DMM model at 3 different time points, and whilst changes in expression are small, this may suggest that these miRNAs may have a role in regulating the onset of OA. For further filtering of miRNAs having important roles amongst these modulated miRNAs, examining the mRNA expression profile would be useful since miRNAs exert their function by directly targeting and subsequently inhibiting mRNA expression. Additionally, since no major modulation of miRNA expression level was observed until 7 days after DMM surgery, it was sufficient to profile mRNA expression for two time points i.e. 1 and 7 day following DMM surgery.

The Illumina BeadArray-based: MouseWG-6 v2.0 Expression BeadChip was used to profile more than 45,000 mouse transcripts in the pooled total RNA samples (DMM right and left knee), previously subjected to miRNA profiling. Consistent with the miRNA profile, mRNA array data also showed a similar expression pattern: no major change in mRNA expression level until day 7 when comparing between DMM right and left knee (Figure 3.3). If the absolute fold change cutoff is set at 1.5, only 30 mRNAs changed expression at day 1 whilst at day 7, more than 683 mRNAs were modulated. The full lists of mRNA which changed expression are in Appendix, Table 6, 7.

A subset of mRNA differentially expressed by microarray analysis was selected for revalidating the array data. Comparison of the expression levels between the mRNA microarray and quantitative real-time qRT-PCR demonstrated a similar expression pattern between the two platform for 4 genes i.e. *CCL2, IL6, SAA3, Arginase-1* (Appendix, Figure 2). These results confirmed the mRNA array data.

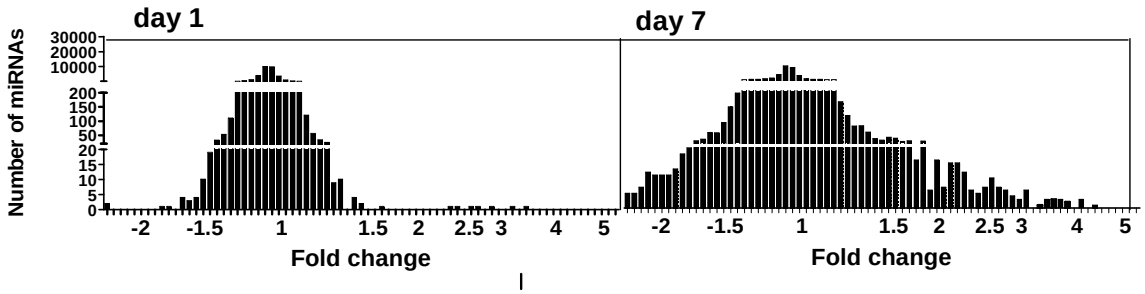

Figure 3.3 Total numbers of mRNAs at different fold change value at day 1 and day 7 following surgery in DMM model.

At each time point, Fold change = intensity value in DMM right - intensity value in DMM left. Numbers of mRNAs were calculated as fold change ranging from -3 to 7 for each increase of 0.05. Fold change: > 1: increase expression; < 1: decrease expression.

3.2.3. Integrated miRNA and mRNA expression profiles of the DMM model identify miR-29b as a miRNA associated with OA onset

To prioritize miRNAs which might have a role in OA onset in the DMM model, an integrated analysis between miRNA and mRNA profiles at 1 and 7 day of the DMM model was performed. This approach took advantage of inverse correlation analysis in which a miRNA was considered as a potential candidate if it was differentially expressed, and inversely correlated with the expression of its putative targets in the same biological samples.

Steps for the miRNA and mRNA profile integrating analysis include: (i) predicting miRNA putative targets by searching for 4 different types of seed sequences e.g. 6-, 7 match 8-, 7 A1-, and 8-mer seed sequences located in the 3' UTR; (ii) integrating expression levels at each time point in the DMM model for all miRNA targets; (iii) searching for a miRNA's putative target enrichment which is given more detail below.

If a miRNA has an impact in the pathological changes in the DMM model and could exert its suppressive function on variety of targets, then when it is down-regulated, there should be an enrichment of its predicted targets among up-regulated mRNA and vice versa. This means that for downregulated miRNAs, a greater percentage of upregulated mRNAs will be their targets and the inverse pattern will be observed for an upregulated miRNA. This should also be true when comparing between different time points, 1 and 7 days in the DMM model. For instance, if a miRNA was repressed across the 7 day time course, the percentage of its targets amongst up-regulated mRNA at day 7 should be higher than at day 1. Together with this, for a downregulated miRNA, an enrichment of miRNA targets in up-regulated mRNAs over unmodulated mRNAs should also be observed at each time point or across the time course.

Additionally, fold change threshold is another challenge faced in integrating analysis. In fact, it is almost impossible to choose the "right" cut off as the normal 1.5 fold change would be too stringent, and consequently, the power to detect potential miRNAs would be very low. To overcome this, in this study, all calculations were done for all fold change values greater than 1 at 0.05 fold intervals.

The integrating analysis for the miRNA and mRNA array data in the DMM model showed that amongst the differentially expressed miRNAs, miRNA-29b is the most interesting. Indeed, a substantial enrichment of miR-29b putative targets which was inversely correlated

with the miRNA expression level was observed at each time points (Figure 3.4, Figure 3.5). At day 1, when miR-29b increased expression, 6mer- and 7mer match 8- targets in the down-regulated section were dominant compared with the up-regulated section (Figure 3.4). Conversely, at day 7, when miR-29b decreased expression, there was a strong enrichment of targets with 4 different types of seed sites in the up-regulated section over the down-regulated (figure 3.4). Also at day 7, the ratio up-regulated targets/unchanged targets was substantially higher than the ratio down-regulated targets/unchanged targets (Figure 3.5).

The inverse correlation between miR-29b and its potential targets was also observed across the time course: whilst miR-29b level was down-regulated from day 1 to day 7, there was a substantial increase of miR-29 targets in the up-regulated mRNAs at day 7 compared with day 1. Consistent with this, the ratio up-regulated targets/unchanged targets showed an enrichment at day 7 (Figure 3.5). All of the data above suggest that miRNA-29b has a potential functional role in OA onset in the DMM model and was selected as the candidate miRNA for further functional studies.

From miRNA microarray data, miR-29b is the one on two miRNAs increased expression with 1.5 fold change at day 1 following DMM surgery. Real-time qRT-PCR was used to re-measure expression level of miR-29b in the DMM samples and sham surgery samples. The Real-time qRT-PCR data confirmed miRNA microarray data and showed a significant increase of miR-29b expression level in DMM right compared with left knee or sham surgery (Figure 3.6).

MicroRNA-29b is a member of the miR-29 family including miR-29a and miR-29c with the mature sequences differing at nucleotide positions 10, 18, 21, 22, or 23 but sharing a common seed sequence for target recognition. We hypothesized that not just miR-29b but all members of miR-29s may contribute to OA onset, as all miRNA-29s showed a downward trend at all 3 time points even though the difference did not reach statistical significance. Therefore, in this study, we investigated the link between all miR-29 members with OA rather than just miR-29b alone.

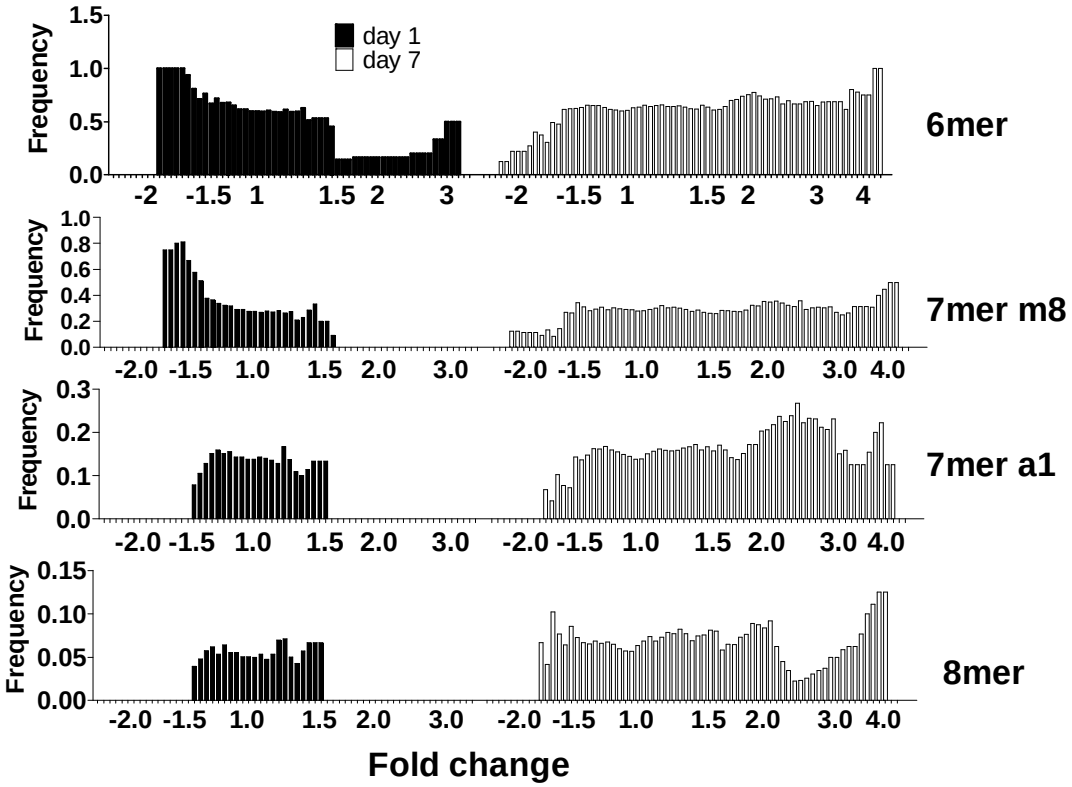

Figure 3.4 Percentage of miR-29 predicted targets in differentially expressed mRNA at day 1 and day 7 after surgery in DMM model.

The calculation was done for all the fold changes ± 0.05 from -2.5 to 4.0 and for each type of seed sequence e.g. 6mer, 7mer match 8, 7mer a1, 8mer. The mRNA having more than one binding site for each type of seed sequence was always assigned as 1. At k fold change, the percentage of 6mer-seed-site targets in modulated mRNAs was calculated: **a_6mer**= sum of mRNA having 6mer-seed site sequence in their 3'UTR with the fold change in the range (k, k+0.05); **b_k**= sum of mRNA with the fold change in the rank (k, k+0.05); **Freq= a_6mer/b_k**. The percentage of other seed site targets was calculated similarly. Day1: closed bar, day 7: opened bar.

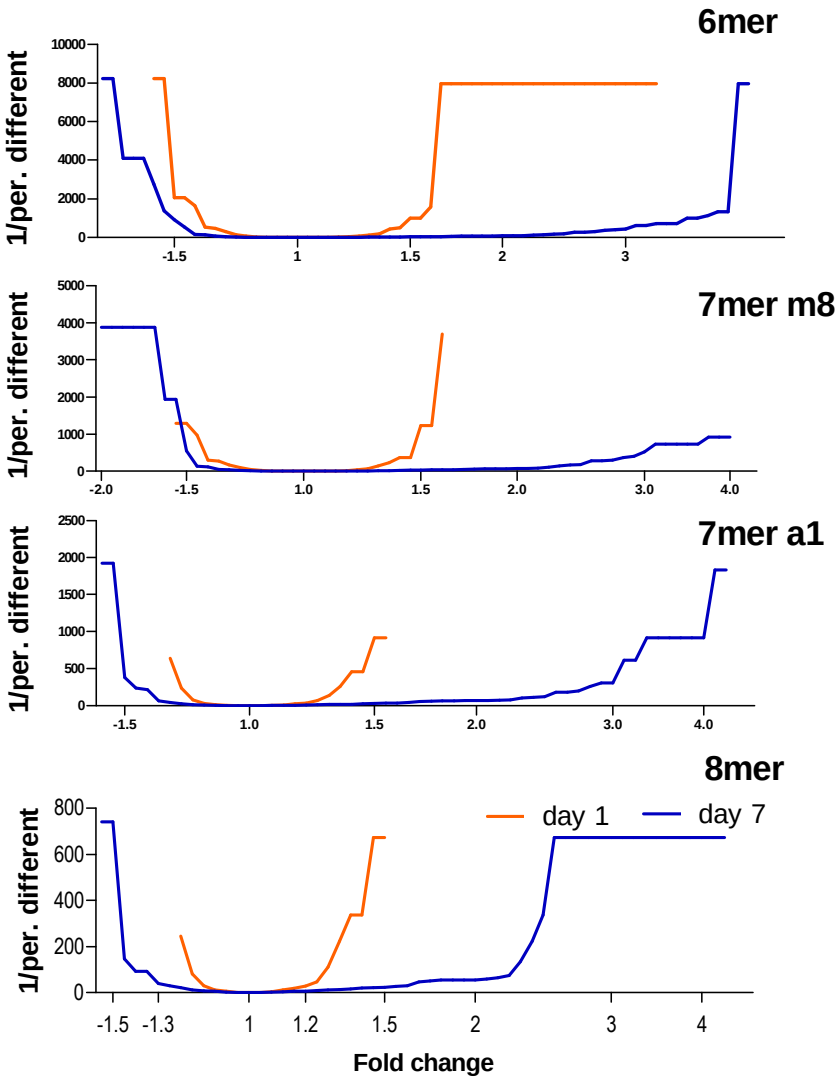

Figure 3.5 Percentage of miR-29 targets that changed expression compared to unchanged expression at day 1 and day 7 after surgery in DMM model.

The calculation was done for all the fold change (FC) ± 0.05 from each other from -2.5 to 4.0 and for each types of seed sequence e.g. 6mer, 7mer match 8, 7mer a1, 8mer. The mRNA having more than one binding site for each type of seed sequence was always assigned as 1. When FC=k, the percentage of 6mer-seed-site targets which increased or decreased expression was calculated: **6mer_changed** = sum of mRNA having 6mer-seed site sequence in their 3'UTR with FC in the range (k, FC max) if k >0, or (FC min, k) if k<0; **6mer_unchanged** = sum of mRNA having 6mer-seed site sequence in their 3'UTR with FC range in (0,k] if k>0, or (k, 0] if k< 0; **1/Per.different = 6mer_unchange/6mer_changed.** The percentage of other seed site targets was calculated similarly. Day1: red line, day 7: blue line.

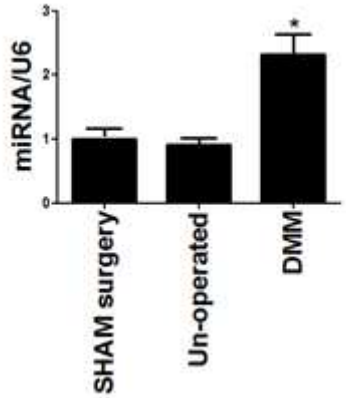

Figure 3.6: MicroRNA 29b was significantly induced in the DMM model at 1 day after surgery

Total RNA was reversed transcribed to cDNA and miR-29b expression was measured by real-time qRT-PCR in individual samples of sham right knee (sham surgery), DMM left knee (un-operated), and DMM right knee (DMM) at 1 day after surgery. U6 was used as endogenous control. Expression level of miR-29b in DMM and sham surgery was normalized to un-operated control. The data show mean +/- SEM, n=3. The expression of miR-29b between each group was analysed by unpaired two-tailed t test * $p<0.05$, ** $p < 0.01$, *** $p<0.001$.

3.2.4. Up-regulation of miR-29s in the murine hip avulsion injury model

Traumatic joint injury and joint magliment are linked to OA initiation. Patients with traumatic joint injury show an increased risk of OA, implicating the early events post-injury as important in the long term. To investigate the role of miR-29s in the onset of OA, a murine hip cartilage avulsion injury model, where the murine hip femoral cap cartilage was sub-cultured in serum-free media across a 48 hour-time course, was used. Total RNA was isolated from the explants using Trizol, reverse transcribed to cDNA by either SuperScript II reverse transcriptase (for mRNA detection) or miRCURY LNA^{TM} Universal cDNA synthesis (for miRNA detection). Expression levels were measured by real-time qRT-PCR.

The majority of the genes rapidly induced in murine joints following surgical destabilization (DMM model) were also regulated in murine hip cartilage explants upon injury (Chong et al. 2013). Interestingly, some genes such as *Dkk3, Ccl2, Il6* were significantly regulated after 3 hours in culture (Appendix, Figure 3) though likely regulating genes which are modulated at later time points. The expression pattern of the miR-29 family is similar to each other and tends to increase across the 48 hour time course (Figure 3.7): miR-29b and 29c significantly increased expression after 12 hours in culture; miR-29a significantly after 6 hours. This suggests that the regulation of the miR-29s may contribute to the molecular mechanism underlying the initiation of OA.

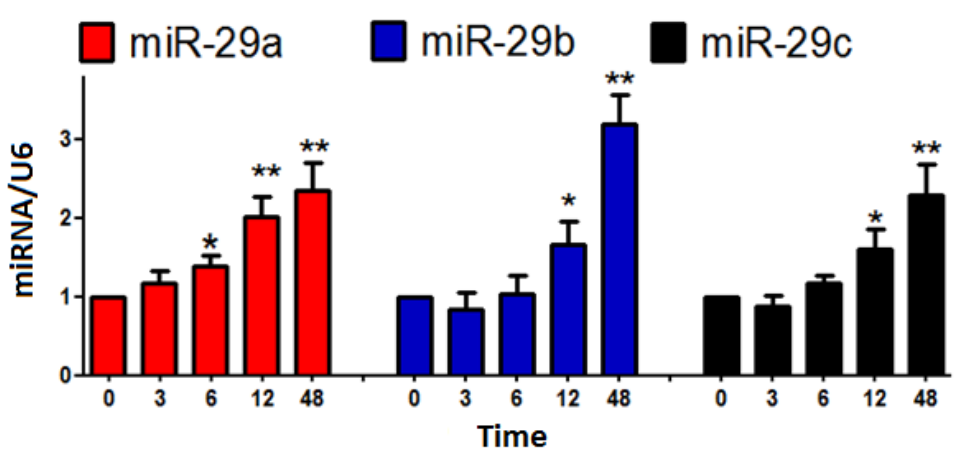

Figure 3.7: Expression of the miR-29 family in the hip avulsion injury model

The femoral caps of C57Bl/6 mice aged 4 weeks were avulsed and put in culture. At each of 3, 6, 12, 48 hour time points, the femoral caps were harvested. Total RNA was isolated using Trizol and reverse transcribed to cDNA. Expression of the mature miR-29 family was measured by real-time q-RTPCR where U6 was used as an endogenous control. At least triplicate samples were measured at each time. Means ± standard errors are presented, n=6. Difference in expression between each time point against control (t=0) was calculated by unpaired two-tailed t test. * $p<0.05$, ** $p < 0.01$, *** $p<0.001$.

3.2.5. Up-regulation of the miR-29 family in human end-stage OA cartilage

To determine whether the miR-29 family could play a role in human OA, its expression level was compared between hip / knee OA cartilage and non-disease tissue controls (hip cartilage followingfracture to the neck of femur).

Human articular cartilage samples (total: 8 hip and 7 knee OA cartilage, 7 healthy fracture to the neck of femur) were obtained from patients undergoing total hip/ knee replacement surgery at the Norfolk and Norwich University Hospital. Total RNA was isolated from all cartilage samples using Trizol and followed by a purification step through column using miRVana kit. The total RNA was reverse transcribed to cDNA using miRCURY LNA™ Universal cDNA synthesis. Expression of all miR-29 members was measured by real-time qRT-PCR with U6 as the endogenous control.

Data (Figure 3.8) showed an increase in miR-29 expression in hip OA but decrease in knee OA cartilage compared to fracture control. This reached significance, or close to significance in each case. Whilst there is no comparison with normal knee cartilage, these data show that the miR-29 family is regulated in human end-stage OA cartilage.

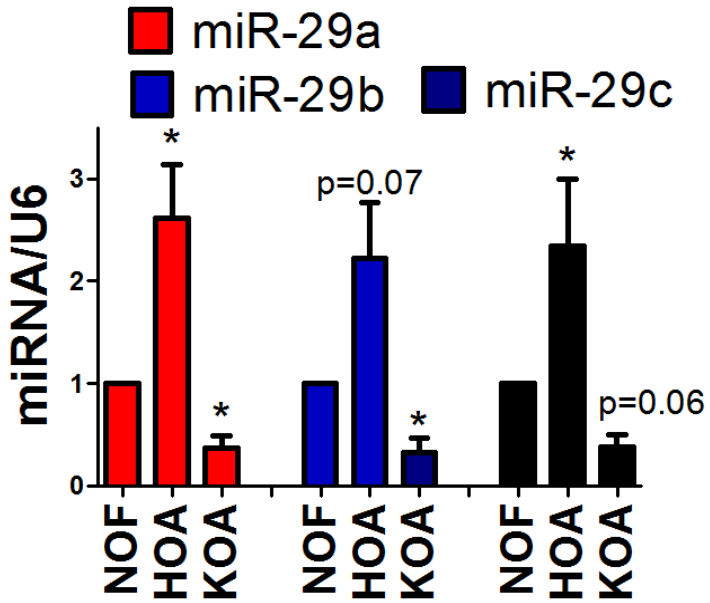

Figure 3.8: Expression of the miR-29 family in human OA cartilage

Total RNA was isolated from human articular cartilage of either end-stage OA patients or healthy controls and reverse transcribed to cDNA. Expression of the mature miR-29 family was measured by real-time qRT-PCR using U6 as an endogenous control. HOA (hip osteoarthritis cartilage, n=8), KOA (knee osteoarthritis, n=7), NOF (neck of the femur, n=7). Means ± standard errors are presented. Difference in expression between each time point against control (NOF) was calculated by unpaired two-tailed Student's t test. * $p<0.05$, ** $p < 0.01$, *** $p<0.001$.

3.2.6. The miR-29 family is regulated with chondrocyte phenotype

Dedifferentiation and the loss of phenotype is an obstacle in expanding human chondrocytes: the cells stop expressing aggrecan and collagen type II, and this limits capacity to form cartilage. In line with this, alteration chondrocyte phenotype is one of the characteristics of OA. As compared with normal articular cartilage, the chondrocytes embedded in different zones of OA cartilage were shown to express different markers of chondrocyte differentiation: chondrocytes in the middle zone re-expressing chondroprogenitor phenotype; cells in the upper middle zone expressing type III collagen (dedifferentiated phenotype) (Aigner *et al.* 1993). Assessing whether the miR-29 family is regulated with chondrocyte phenotype, therefore, would help to further determine the relevance of the miR-29 family in cartilage function.

This was investigated using human primary chondrocyte dedifferentiation model. After isolation from human knee OA cartilage by collagenase (collagenase-post digested HACs (PD)), primary chondrocytes were cultured in monolayer (primary culture HACs (P0), and three sequential passages were performed at 1: 3 dilution of cells (passage 1 to passage 3). Total RNA was isolated from cartilage, PD, P0 to P3 chondrocytes and reverse transcribed to cDNA. The expression level of all the miR-29 family was then measured by real-time qRT-PCR.

The expression of the miR-29 family was found to significantly decrease when HACs were passaged in monolayer (Figure 3.9), indicating the putative role of the miR-29 family in chondrocytic phenotype.

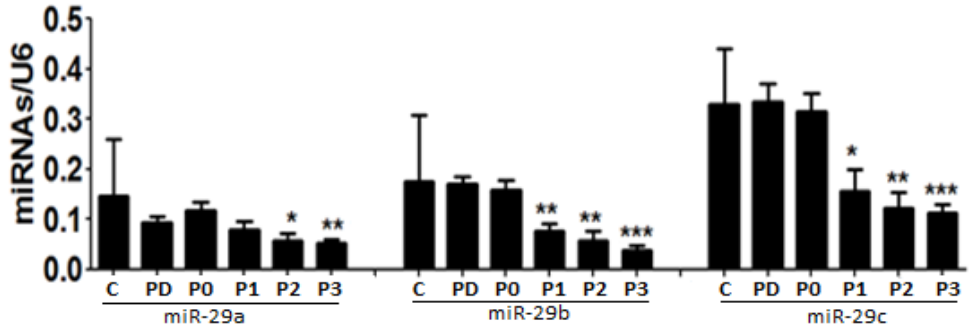

Figure 3.9: Expression of the miR-29 family in a chondrocyte dedifferentiation model

Human primary chondrocytes were isolated from the articular cartilage of 8 knee OA patients using collagenase digest. The cells were put in culture and passaged 3 times. Total RNA was isolated from either human articular cartilage (cart) or chondrocytes post digestion with collagenase (PD) or each passage 0, 1, 2, 3 (P0, P1, P2, P3). After reverse transcribing to cDNA, expression of the mature miR-29 family was measured by real-time qRT-PCR (U6 was used as an endogenous control). Mean ± standard errors are presented, n=8. Different in expression between was calculated by unpaired two-tailed t test. * $p<0.05$, ** $p < 0.01$, *** $p<0.001$.

3.2.7. MicroRNA-29s expression in chondrogenesis

Chondrogenesis is the earliest phase of skeletal development, occuring as a result of: mesenchymal cell condensation, chondroprogenitor cell differentiation, chondrocyte differentiation and maturation. Chondrogenesis results in the formation of cartilage and bone in the process of endochondral ossification (Goldring *et al.* 2006). It is pertinent to examine the role of miR-29 in chondrogenesis, particularly since the replay of this developmental process may contribute to osteoarthritis.

To determine the expression and therefore possible role of the miR-29 family in chondrogenesis both human and mouse chondrogenesis models were used. **Human chondrogenesis model**: human bone marrow stem cells were differentiated to form a cartilage disc (the model was kindly developed by Dr Matt J. Barter (Newcastle University, UK)); **Mouse chondrogenesis model**: the embryonic carcinoma cell line ATDC5 was stimulated to from chondrocytes using insulin for 42 days (this model was developed by Dr Tracey Swingler (University of East Anglia)). Total RNA was isolated, reverse transcribed to cDNA and used for measuring expression level of the miRNA by real-time qRT-PCR.

In the human chondrogenesis model, a significant down-regulation of the miR-29s after 3 days of differentiation was observed; after that, miR-29s return to the original expression levels (Figure 3.10). A similar expression pattern was also observed in the murine ATDC5 chondrocyte differentiation model: significantly decreased expression of all the miR-29 members after 14 days differentiation; with a return after 36 days, to the original level (Appendix, Figure 4). These data imply that miR-29 may be a negative regulator of the early stage of chondrogenesis.

Indeed, the miR-29 family was not the only miRNA regulated in either the human or murine chondrogenic process, many other miRNAs were strongly modulated e.g. (Barter et al, unpublished data) (Swingler et al. 2012). However, it can be postulated that the miRNA would have a functional role in chondrogenesis if it had affected on mRNA expression. To test this hypothesis, again an integrating analysis approachs (using mRNA expression profile data to analyse miR-29 putative target genes) was used. A substantial enrichment of miR-29 targets was inversely associated with the expression of miR-29s was observed (Data not shown). Together, these data suggest that the miR-29 family acts as the negative regulator of chondrogenesis, leading to an increase in mRNA to enable the process.

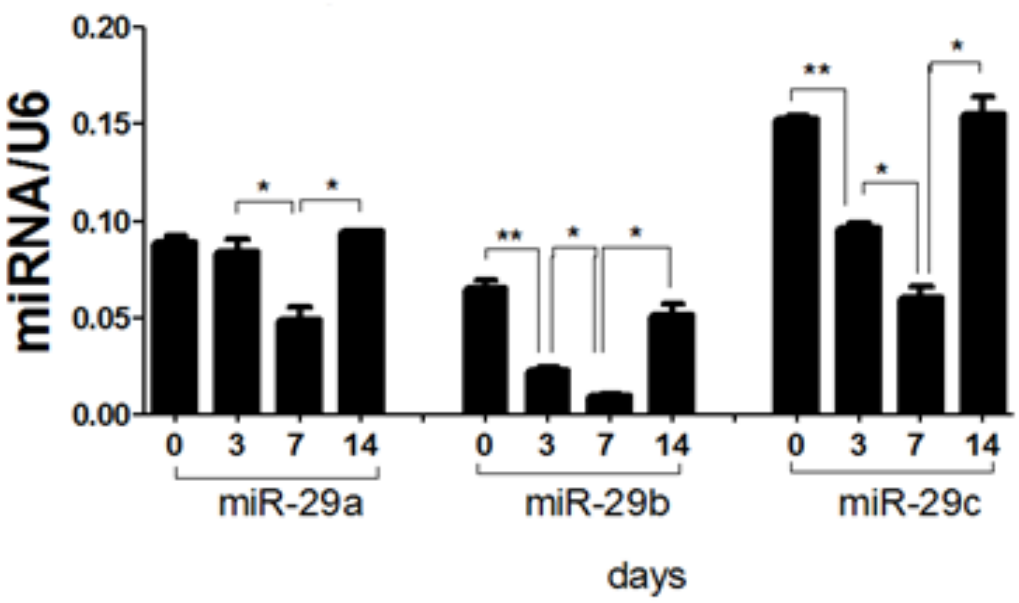

Figure 3.10: Expression of the miR-29 family in the human chondrogenesis model.

Human bone marrow stem cells (from 3 donors, 18-25 years of age, $5x10^5$ cells in 100µl growth medium) were put into polycarbonate Transwell filters and centrifuged in 24 well plates. 0.5ml chondrogenic culture medium containing 100µg/ml sodium pyruvate, 10ng/ml TGFβ3, 100nM dexamethasone, 1x ITS, 40µg/ml proline, and 25µg/ml ascorbate-2 phosphate was added to the lower well. Media were replaced every 2 or 3 days up to 14 days. At 0, 3, 7, 14 days, the cells were harvested and total RNA was extracted using Trizol. The RNA was then reverse transcribed to cDNA and was used for measuring the expression level of the mature miR-29 family by real-time qRT-PCR (U6 was used as an endogenous control). Assays were repeated 3 times. At least triplicate samples were in each time. Means ± standard errors are presented. Difference in expression between each time point was calculated by unpaired two-tailed t test. * $p<0.05$, ** $p < 0.01$, *** $p<0.001$.

3.2.8. The miR-29b is expressed in murine limb development

The formation of the skeleton first is initiated with the formation of a precartilage condensation (anlagen) which is followed by chondrogenesis triggered in the precartilage condensation and ultimately cartilage is formed. This process involves the cooperation of many cell activities e.g. migration, adhesion, intracellular signalling, and proliferation (Goldring et al. 2006). Given the likely involvement of the miR-29 family in chondrogenesis, it is pertinent to ask whether miR-29s are expressed in murine limb development. Additionally, the miR-29 family or its members have been shown to control cell proliferation and apoptosis in different tumour types. A murine model would thus be a useful model to study the role of the miR-29 family in cell proliferation and apoptosis limb development.

In mice, the forelimb starts to develop at stage E9.5 whilst the hindlimb starts behind by about half a day. Five days later, a miniature model of the adult limb is formed (E14.5 and E15 for fore and hindlimb, respectively). At stage E11, a distinct apical ectodermal ridge at the limb tip is formed in the forelimb and the handplate is beginning to form at E11.5. Similarly events happen in the hindlimb at half a day later (at E11.5 and E12) (Martin 1990).

Whole mount *in situ* hybridization was conducted using amiRCURY LNA^{TM} miR-29b-3p double-DIG labelled probe to detect the expression of miR-29b in the mouse embryo stage E11.5 and E15. The data showed that: at stage E11.5, miR29b was expressed in the cartilage of both fore and hindlimb; at stage E15 when the small scale the adult limb was formed, miR-29b was strongly expressed, implicating miR-29b playing a role in murine limb development. Besides limbs, miR-29b was also found on the brain and the spine of embryo stage E11.5 (Figure 3.11).

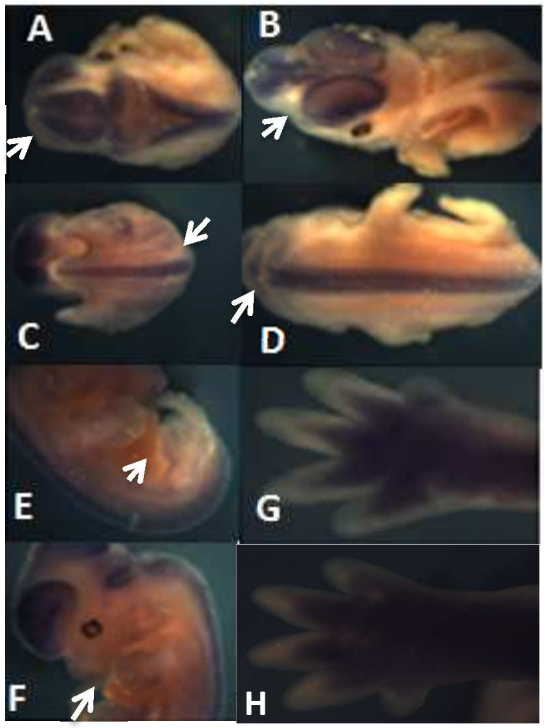

Figure 3.11: Whole mount *in situ* hybridization of miRNA-29b in murine embryo stage E11.5 and E.15.

Using a miRCURY LNA^{TM} double-DIG labelled miR-29b probe, miR-29b was found to be expressed: in the embryo stage E11.5 in the brain (A), mouth (B), spine (C-D), hindlimb (E), forelimb (F); in the embryo stage E15 in hindlimb (G) and forelimb (H).

3.3. DISCUSSION

The principal aim of this study was to begin to identify the miRNAs which were implicated in the early stages of OA and elucidate their function. Whilst there have been a number of studies on the role of miRNAs in OA pathogenesis, they have not focused on the disease onset. In the present study, for the first time, the miRNA expression profile was reported for the DMM mouse model at early time points e.g. 1, 3, 7 days following surgery. The fact that only a small number of miRNAs changed expression across the first three days after DMM surgery might indicate miRNAs mainly contribute in disease progression rather than initiation. However, there are some limitations of the study which prevent a firm conclusion about the role of miRNAs in the early stages of the disease. Total RNA for the miRNA microarray was isolated from whole knee joints of DMM mice. Thus, if a miRNA is expressed in a single tissue e.g. cartilage, bone, meniscus, ligament or synovium, pooling of tissues will reduce the signal to a lower level than in the individual tissue and that could be the explanation for the overall low levels of modulated miRNAs observed in the present study. Moreover, insufficient controls, e.g. naïve samples and genes responding to sham surgery in this study may also have been problematic. The DMM model does not completely recapitulate human OA pathogenesis, e.g. with more synovial involvement in the latter.

However, it remains unlikely that the miRNA microarray data acquired from the DMM model in this study is incorrect. The DMM left knee (no surgery) used as a control would show the consequence of surgery, even if it can't distinguish injury per se from early OA. Moreover, Burleigh et al (2012) reported a large and significant difference in expression levels of e.g. *Ccl2, Arg1e, Il6, Saa-3* in the same DMM model just 6 hours following surgery, which was interpreted as response to surgical destabilization rather than reaction to injury (Burleigh *et al.* 2012). In this study, such an increase in expression was also observed when comparing between the DMM right and DMM left, suggesting that the DMM left knee can act as a suitable control. Hence, it was expected that the changes in miRNA expression at early time points would be greater.

MicroRNA-29b, one of only two miRNAs significantly increased in expression at day one post-surgery and inversely correlated with expression of its putative targets, was investigated in detail. The miR-29b is encoded by two loci in the human genome e.g. the primary miR-29-a/b1 cluster in chromosome 7, and the primary miR-29b2/c cluster in chromosome 1.

Normally, clustered miRNAs in humans work in combination to accomplish their function. At the transcriptional level, at least one of the other miR-29 family members i.e. miR-29a or miR-29c will be co-transcribed with miR-29b. In addition, miR-29b is reported to have a short half-life (the time taken for the miRNA to fall to half of its original value) which is linked to the presence of uracil bases at positions 9-11, compared with miR-29a (more stable with a reported half-life of > 12 hours) (Zhang *et al.* 2011). Thus, in the DMM model at 1 day after surgery it would be expected that a significant increase in either miR-29a or miR-29c would accompany that of miR-29b. However, only miR-29b increased in expression (1.5 fold change in array data) but not any of the other miR-29 family members, perhaps implicating another post-transcriptional regulatory mechanism controlling miRNA processing. In line with the DMM model data, in a murine hip avulsion injury model, an increasing expression level was also observed for all miR-29 members post injury. Interestingly, a similar pattern of expression of some genes strongly induced in the DMM model at 6 hours after surgery (Burleigh et al. 2012) was seen in the injury model suggesting some molecular similarities between the two models. In line with this, Chong et al (2013) also observed a similar pattern when measuring the expression of the set of gene induced expression in DMM model 6 hours after surgery and in murine injury model in which the hip cartilages cultured for 6 hours (Chong et al. 2013). Since mechanical factors following traumatic joint injury may mediate OA onset, these data suggest for the first time an important role for the miR-29 family in the initiation of OA. The fact that the miR-29 family increased in expression in human OA end-stage cartilage supports a role for the miR-29s in the disease. In this study, human knee cartilage normal controls were not available, and the difference in hip and knee cartilage may explain in part why the miR-29 family levels increased in hip but decreased in knee OA cartilage compared to human hip fracture control. Also, in this project, the miR-29 family expression level is very variable across a human tissue panel e.g. heart, brain, lung, spleen (data not shown). In supporting these data, previous published data also demonstrated the different expression level of the miR-29 family in different tissues in zebrafish (Wienholds *et al.* 2005). These data suggest that the mechanisms controlling the miR-29 family expression in different tissues are not similar. The fact that miR-29 family expression was modulated in different mouse models and in human OA cartilage implies a role for the miR-29 family in cartilage, and suggest that the two pri-miR-29a/b1 and pri-miR-29b2/c clusters may be involved in both early and late stages of the disease. The direct mechanism

controlling miR-29 family expression and the extent to which each cluster contributes to OA remains unknown and is worthy of further investigation.

This study also provides evidence for the role of the miR-29 family in cartilage formation as its expression was regulated during human and mouse chondrogenesis and inversely correlated with its putative targets. In fact, such decreased expression level at an early stage of chondrogenesis is in line with published data e.g. Guerit et al (2013) showed the decreased expression of miR-29a is essential for chondrogenesis via its regulation of FOXO3a (Guerit *et al.* 2014); Sorentino et al (2008) found miR-29b was among miRNAs down-regulated when differentiating human MSCs through chondrogenesis (Sorrentino et al. 2008); Yan et al (2011) demonstrated that both miR-29a and miR-29b were significantly decreased in a chondrogenesis model where mouse MSC were grown on polyhydroxyalkanoates (Yan et al. 2011). However, I have demonstrated for the first time that all miR-29 family members are involved in chondrogenesis, stressing the important role of both miR-29 clusters in controlling cartilage homeostasis in human and mouse. In contrast to this data, there are others studies profiling the expression of miRNAs in murine and human chondrogenesis model (Suomi et al. 2008, Lin et al. 2009, Miyaki *et al.* 2009, Lin et al. 2011, Yang et al. 2011). The miR-29 family, nevertheless, was not amongst the miRNAs which had altered expression. This is not surprising and could be attributed to differing design of experiments including inducers of differentiation, cell type, numbers of detected miRNA probes and organism. In addition, despite of being a negative regulator of chondrogenesis, miR-29b was found to express in murine limb development. A number of published data report that the miR-29 family can act as oncogenes whose expression induces cell proliferation but inhibits apoptosis. Whether the miR-29 family is involved in murine limb development through inducing chondrocyte proliferation in the growth plate remains unknown. Therefore, examination of the role of miR-29 family in limb development in vivo will be a priority for future studies.

Another piece of data supporting the role of the miR-29 family in OA comes from the fact that expression of the miR-29 family is decreased during chondrocyte dedifferentiation. Again, other groups have profiled miRNAs in human dedifferentiation models (Karlsen et al. 2011, Lin et al. 2011) but the miR-29 family has not shown up in any of them. As mentioned above, this could be attributed to many different factors.

Taken together, all of these data show that the miR-29 family may modulate both cartilage homeostasis and OA and make a compelling case for further investigation. In this PhD thesis, for the first time, the whole miR-29 family is reported to be involved in OA although the increase of the miR-29b in OA had been shown (Moulin *et al.* 2012). Nevertheless, the miRNA-29 family has been implicated in many other areas of pathology. Many publications have reported the involvement of the miR-29 family in cancers where the miRNA family or a single member could serve as either a tumour suppressor or an oncogene. In rhabdomyosarcoma (Wang *et al.* 2008), nasopharyngeal carcinoma (Sengupta *et al.* 2008), hepatocellular carcinoma (Xiong *et al.* 2010), acute myeloid leukemia (Eyholzer et al. 2010) , multiple myeloma (Zhang *et al.* 2011, Amodio *et al.* 2012), chronic lymphocytic leukemia (Santanam *et al.* 2010), glioblastoma (Cortez *et al.* 2010), and lung (Fabbri *et al.* 2007) and pancreatic cancer (Muniyappa *et al.* 2009), miR-29 was described as a tumor suppressor whilst in acute myeloid leukemia , colorectal liver metastasis (Wang *et al.* 2012), and breast cancer (Chou *et al.* 2013) , miR-29 was shown to be as tumour promoter.

Besides cancers, the miR-29 family has been shown to participate in a number of physiological processes including (i) **muscle development** e.g. knockdown of miR-29b in vivo induced cardiac fibrosis in mice; miR-29a/b1 inhibition induced vascular smooth muscle cell calcification; miR-29 family expression was developmentally up-regulated in porcine skeletal muscle from fetal to adult, and this was also true in mice and human; the miR-29 family was found to be down-regulated in myotonic dystrophy type I and Duchenne muscular dystrophy (Wei *et al.* 2013), (ii) **bone formation** e.g. miR-29a increased bone mass, induced osteoblast differentiation, and inhibited osteoclast differentiation; reduced miR-29a expression was associated with low bone mass and poor skeletal microarchitecture in rats treated with glucocorticoids (Wang *et al.* 2013), (iii) **HIV virus infection** e.g. ectopic expression of miRNA-29a resulted in reduction of HIV virus levels, implicating this miRNA as a potential strategy in developing anti-HIV therapeutics (Ahluwalia *et al.* 2008), (iv) **aging** e.g. miR-29 family up-regulation was observed in a number of different organs e.g. liver, muscle, and brain of several aging models (Ugalde *et al.* 2011, Fenn *et al.* 2013, Hu *et al.* 2014), (v) **diabetes** e.g. the miR-29 family was up-regulated in diabetic rats and forced expression of miR-29 inhibited insulin induced glucose imported by 3T3-L1 adipocytes (He *et al.* 2007); reduced miR-29b in plasma samples of type 2 diabetes patients anticipated the

manifestation of the disease (Zampetaki *et al.* 2010); miR-29c was found up-regulated the kidney glomeruli from diabetic mice (Long *et al.* 2011); the continued expression of miR-29 isoforms in the pancreatic β-cell seems to be required for normal and selective stimulation of insulin secretion by glucose (Pullen *et al.* 2011); (vi) **fibrosis development**, the miR-29 family has been shown to be implicated in the development of fibrosis of many organs including heart, kidney, lung, liver, and systemic sclerosis; (vii) **Alzheimer disease,** the miR-29a/b1 cluster or miR-29a was significantly decreased in Alzheimer patients (Hebert *et al.* 2008, Shioya *et al.* 2010).

In conclusion, with all of the data above, the miR-29 family may play a key role in Osteoarthritis and of is worthy of further investigation. The mechanisms which control its expression together with its function in chondrocytes will be described in the next chapters.

CHAPTER IV
FACTORS THAT CONTROL EXPRESSION OF THE MICRORNA-29 FAMILY

4.1. Introduction

In the previous chapter, evidence for the involvement of the miR-29 family in cartilage homeostasis and OA was presented. The increased expression of the all family members is apparent in both early and late stages of OA. However, which factors or mechanisms are responsible for miR-29 induction or repression in chondrocytes remains unknown and is worthy of further investigation.

The miR-29 family is intergenic miRNAs and is encoded in two gene clusters e.g. one for the primary miR-29a/b1 on chr.7q32, and the other for the primary miR-29b2/c on chr.1q32.2 (Saini *et al.* 2007, Chang *et al.* 2008). The miR-29b1 and miR-29a precursors are processed from the pri-miR-29a/b1 last intron (Genbank accession EU154353) whist the miR-29b2 and miR-29c precursors are from the pri-miR-29b2/c last exon (Genbank accession EU154352 and EU154351) (Chang et al. 2008) (Figure 4.1). These precursors are all transcribed as polycistronic primary transcripts (Chang et al. 2008, Mott *et al.* 2010) upon which various transcriptional regulators e.g. NFκB (Liu *et al.* 2010, Mott et al. 2010), supressors (c-Myc (Mott et al. 2010, Parpart *et al.* 2014), Sp1(Liu et al. 2010, Amodio *et al.* 2012), Gli (Mott et al. 2010), Yin-Yang-1, Smad3 (Qin *et al.* 2011), Ezh, H3K27, HDAC1, HDAC3), or inducers (Gli, SRF, Mef2, TCF/LEF, GATA3 (Chou et al. 2013), CEBPA (Eyholzer et al. 2010)), and signalling pathways e.g, Wnt , TGFβ, TLR/NFκB, TNFα/NFκB, hedgehog signalling have been reported to be directly and/or indirectly involved. For instance, **both canonical and non-canonical Wnt signalling** was reported to induce the miR-29 family level in different cellular contexts: Wnt3a rapidly induces miR-29 levels in osteoblastic cells (Kapinas *et al.* 2009, Kapinas et al. 2010) or in muscle progenitor cells (MPCs) (Hu *et al.* 2014), respectively, at least in part through the two putative TCF/LEF-binding sites in the miR-29a promoter (Kapinas et al. 2010); non-canonical Wnt signalling through Wnt7a/Frizzled 9 resulted in increased expression of only the mature miR-29b but not miR-29a or c or any miR-29b primary or precursor forms in non-small lung cancer cell lines H661 and H15 (Avasarala *et al.* 2013). In addition, ERK5 and PPARγ, key effectors of the Wnt7a/Frizzled 9 pathway, were also observed to be strong inducers of miR-29b expression (Avasarala et al.

2013). In contrast to Wnt signalling, **TGFβ/Smad3 signalling** was shown to negatively regulate miR-29 family expression in different cell lines e.g. human aortic adventitial

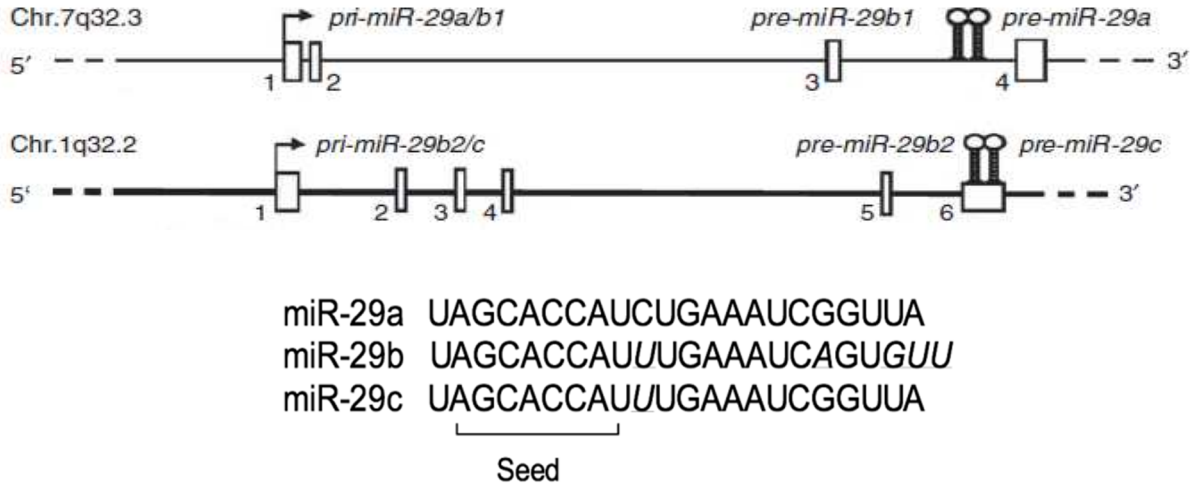

Figure 4.1: Genomic organization of the miR-29 family

The miR-29 family includes three members miR-29a, miR-29b and miR-29c. The primary pri-29a/b1 is located in chromosome 7 containing pre-29a and pre-29b1. The primary pri-29b2/c is located in chromosome 1 including pre-29b2 and pre-29c. The hairpins indicate the locations of the sequence encoding precursors of miR-29s. Pre-29a and pre-29c will process into mature miR-29a and miR-29c, respectively. Pre-29b1 and pre-29b2 will process into mature miR29b. The mature sequences of the miR-29 family members share identical seed regions. Nucleotides that differ among miR-29s are indicated in italics.

fibroblasts (Maegdefessel *et al.* 2012), renal fibrosis cells (Wang *et al.* 2012, Ramdas *et al.* 2013), murine hepatic stellate cells (Roderburg *et al.* 2011), rat hepatic stellate cells (Kwiecinski *et al.* 2011), human skin fibroblasts (Maurer *et al.* 2010), human tenon's fibroblast (Li *et al.* 2012), human lung fibroblast cell line (Cushing *et al.* 2011, Yang *et al.* 2013). The suppressive effect of TGFβ/Smad3 signalling on miR-29 expression was partly mediated through a Smad3 binding site in the highly conserved region around 22kb upstream of the miR-29b2/c promoter as showed by chromatin immunoprecipitation assay (Qin et al. 2011, Ramdas et al. 2013). Similar to TGFβ, **Toll-like receptor (TLR) signalling and TNFα signalling** have been shown to mediate suppressive effects on miR-29 family expression. In man, treating human cholangiocarcinoma cells with TLR ligands e.g. TLR3 (Poly (I:C)), TLR4 (LPS), TLR5 (flagellin), TLR6 (MALP-2) showed a significant decrease in the miR-29 level beginning after 4 hours of LPS treatment but increasing to 24 hours (Mott et al. 2010); treating human stellate cells with LPS strongly decreased all miR-29 family expression after 1 hour (Roderburg et al. 2011); treating C2C12 myoblasts with TNFα substantially reduced miR-29b and miR-29c expression (Wang et al. 2008); stimulating the choroidal-retinal pigment epithelial cell line ARPE-19 with TNFα resulted in significant down regulation of all miR-29s; conversely, transfecting with a synthetic NFκB decoy, (NFκB inhibitor), rescued the down regulation of miR-29 by TNFα (Χαι *εϖ αλ.* 2014). The activation of NFκB through TLR signalling with its three binding sites in the miR-29a/b1 cluster promoter (-561, -110, and +134) was proven to be the mechanism for the suppression of miR-29a/b1 promoter function (Mott et al. 2010). In mice, miR-29a and miR-29b significantly decreased expression in murine natural killer (NK) cells stimulated with the TLR3 ligand (Poly (I:C)) or phorbol ester (PMA) as well as in splenocytes, NK and T cells of mice infected with L. *monocytogenes* or *Mycobacterium bovis* bacillus Calmette-Guérin (Ma *et al.* 2011). Consistent with the human miRNA, a region about 25 kb upstream of the murine promoter of miR-29a/b1 contains two NFκB binding sites. The second binding site is more conserved between human and mouse and it has been shown to be key for suppression of the miR-29a/b1 promoter (Ma et al. 2011). Importantly, other transcriptional factors, co-operating with NFκB to suppress or induce miR-29 family expression, have also been reported e.g. YY1, Sp1, Ezh, H3K27, HDAC1, HADC3, Mef2, SFR. Forced expression of YY1 in C2C12 lead to a 2-fold decrease of miR-29b and miR-29c levels; similarly, siRNA knockdown of YY1 significantly enhanced expression of miRNA expression. ChIP analysis showed that YY1 did not bind to the miR-29b2/c locus in cells in the absence of NFκB,

suggesting that both pathways are necessarye for silencing the miR-29b2/c locus. Amongst 4 putative binding sites of YY1 in highly a conserved region ~20kb upstream of miR-29b2/c, only one site is bound by YY1 on ChIP assay whereas all 4 sites produced a binding complex with EMSAs using nucleus extract from C2C12. Notably, Ezh, H3K27, HDAC1, whose expression is associated with repression of muscle-specific genes, and recruited by YY1, was also detected by ChIP assay. In line of these transcription factors, Mef2 and SFR, well-known for activating muscle genes, were also found binding to the miR-29b2/c promoter. Again using luciferase reporter assay, a reporter containing a 4.5 kb fragment spanning YY1, Mef2, SFR binding sites was repressed by YY1 or loss of the YY1 binding site but stimulated with either YY1 knockdown or SRF or Mef2 (Wang et al. 2008). In addition, forced expression of Sp1 or NFκB (p65) reduced miR-29b expression; conversely, knockdown of Sp1 or NFκB (p65) by siRNAs resulted in induced miR-29b level (Liu et al. 2010). EMSA assay using probes spanning the -125/-75 miR-29b sequence yielded two major complexes, suggesting Sp1/NFκB acts as a repressive complex interacting with an element of the miR-29b enhancer (Liu et al. 2010). Interestingly, histone deacetylase (HDAC) 1 and 3 contribute to the repressor activity of Sp1/NFκB on miR-29b expression (Liu et al. 2010). Incubation of HDAC1/HDAC3 with ^{32}P-labelled probe from the miR-29a/b1 cluster region together with NFκB p50/p65 and Sp1 showed a delayed and more intense band; HDAC1/3 inhibitors increase miR-29b expression, supporting the interaction of HDAC1 and 3 and Sp1/NFκB with the miR-29b regulatory sequence (Liu et al. 2010). Similar to other signalling mentioned previously, **hedgehog signalling pathway** was also shown to repress miR-29 expression: cells treated with cyclopamine, an inhibitor of Smoothened (a hedgehog signalling component), or transfected with siRNA to knockdown Gli-3, the expression of miR-29b increased (Mott et al. 2010). Along with the transcription factors mentioned above, there are other transcriptional factors controlling miR-29 family expression. The serum alphafetoprotein (AFP), a membrane-secreted protein associated with poor patient outcome in hepatocellular carcinoma, was reported to inhibit miR-29a expression through facilitating c-MYC binding to the promoter of the pri-miR-29a/b. This conclusion was supported by: the inability of AFP to decrease the miR-29a level in the absence of c-MYC protein; c-MYC was abundantly bound to the miR-29a/b1 promoter in the presence of AFP, but did not bind without AFP (Parpart et al. 2014); c-MYC promoter binding protein (MBP), originally described to bind to and repress c-MYC promoter function, up-regulated miR-29b expression

by 6 fold in prostate cancer cells (Steele *et al.* 2010). The haematopoietic master transcription factor, CCAAT/enhancer-binding protein-α (CEBPA), was also reported to activate the expression of miR-29a and miR-29b. Forced expression of CEBPA in acute myeloid leukaemic cells lead to two-fold induced expression of the primary miR-29a/b1 and the mature miR-29a and miR-29b whereas the expression of miR-29b2/c primary transcript remained stable. Using luciferase reporter assays, the sequence, having the conserved region spanning -682 bp upstream to +296 bp downstream of the miR-29a/b1 transcriptional start site and containing 6 potential CEBPA sites, was also strongly induced with CEBPA. Among these binding sites, the one located at +15 to +29 bp was identified to be responsible for CEBPA-mediated activation of the pri-miR-29a/b1 promoter on ChIP assay (Eyholzer et al. 2010). Another transcriptional factor, GATA3, specifying and maintaining luminal epithelial cell differentiation in the mammary gland, was also found to induce miR-29 expression directly by binding to three GATA3 sites in the miR-29a/b1 promoter. Interestingly, GATA3 can induce miR-29s expression by inhibiting the TGFβ and NFκB signalling pathway. Additionally, STAT1 (signal transducer and activator of transcription) a transcription factor induced by interferon γ signalling, was reported to upregulate primary 29a/b1, the pre-29a, pre-29b1, and the mature miR-29a, miR-29b in melanoma cell and T cells (Schmitt *et al.* 2013).

With all the information above, it is likely that in different cellular contexts, the miR-29 family expression is controlled by different transcription factors and signalling pathways. Which factors control its expression in human chondrocytes remains unknown. The effects of a variety of anabolic and catabolic factors e.g. TGFβ, Wnt3a, IL-1, LPS on miR-29 family expression in human chondrocytes were thus investigated. Also, the effect of SOX9, a major specifier of chondrocyte phenotype was also investigated.

Aims:

- Analyse the promoter region (approximately 2kb upstream of the transcription starting site) of the miR-29 family for SOX9 binding sites. Experimentally validate the impact of SOX9 on miR-29 expression.
- Test major anabolic and catabolic cytokines controlling the miR-29 expression in chondocytes.

4.2. Results

4.2.1. The master regulator of chondrogenesis SOX9 suppresses expression of the miR-29 family

The master regulator for chondrogenesis SOX9 has a critical function in a number of development processes e.g. skeletal formation, sex determination, pre-B and T cell development. *SOX9* was found to be expressed in all chondroprogenitors and differentiated chondrocytes, but not in hypertrophic chondrocytes (Ng *et al.* 1997, Zhao *et al.* 1997). Importantly, SOX9 is considered as the critical transcriptional factor for chondrogenic differentiation, partly owing to the fact that its functions are required for differentiating chondrogenic mesenchymal condensations into chondrocytes, and for all stages of chondrocyte differentiation: in mouse chimera, *Sox9* knockout cells were excluded from all cartilage and no cartilage developed in teratomas derived from *Sox9* -/- embryonic stem cells (Bi *et al.* 1999); *Sox9* deletion from chondrocytes at later stages of development resulted in decrease in chondrocyte development, cartilage matrix gene transcriptional inhibition, and prematurely conversion from proliferating chondrocytes to hypertrophic chondrocytes (Akiyama *et al.* 2002). Considering the critical role of SOX9 in chondrocytes, I explored the connection between this factor and expression of the miR-29 family. Initial evidence suggested a link: in the DMM model mRNA profiling data, at 7 days after the surgery, *Sox9* expression was greatly induced (Appendix, Table 7) whilst the miR-29s expression was suppressed; in both human and mouse chondrogenesis models, the level of Sox9 was inversely correlated with the level of miR-29 expression (data not shown). Thus, SOX9 could be a miRNA-29 target or SOX9 could regulate miRNA-29 expression.

To test the postulate **that SOX9 is a miR-29 target**, the effect of the miR-29 members on SOX9 transcriptional expression was examined: after sub-cloning the *SOX9* 3'UTR downstream of the luciferase gene, this SOX9-3'UTR reporter vector was co-transfected with the miR-29 family into SW1353 cells; 24 hours after transfection, luciferase activity was measured. Luciferase activity showed that miR-29 family have no effect on the *SOX9* 3'UTR even though bioinformatics analysis found one 6-mer seed site for miR-29 in the *SOX9* 3'UTR (data not shown), suggesting that SOX9 is not a miR-29 family direct target. Also, whether SOX9 is a miR-29 indirect target was also determined: relative expression of SOX9 was checked in human primary chondrocytes transfected with miR-29 family for 48 hours. Quantitative RT-PCR confirmed that the SOX9 level was not changed with miR-29

transfection in chondrocytes (data not shown). Thus, SOX9 is not a direct or indirect target of miR-29s at least at the transcriptional level.

For testing the second hypothesis **SOX9 is a suppressor of miR-29 expression**, the effect of overexpression or knockdown of SOX9 on miR-29 expression was studied: a SOX9 expression construct or siRNA was transiently transfected into the human chondrosarcoma SW1353, 48 hours after transfection, the level of the mature miR-29 family was measured by quantitative RT-PCR. The data (Figure 4.2) show that SOX9 suppressed miR-29 transcription: the miR-29 family levels were significantly reduced when SOX9 was overexpressed (Figure 4.2.a,c) but induced when SOX9 was knocked down (Figure 4.2.b,c).

To further explore the regulatory mechanism by which SOX9 suppressed miR-29 expression, the 2kb region upstream from the primary miR-29a/b1 and miR-29b2/c transcription start sites were analysed by searching for the SOX9 DNA-binding motif ([A/T][A/T]CAA[A/T]). This analysis revealed 5 putative binding sites for SOX9 in the promoter regions of pri-miR-29a/b1 and pri-miR-29b2/c, respectively (Figure 4.3.a). A reporter construct with the primary miR-29a/b1 2kb promoter, kindly provided by Dr Anne Delany (University of Connecticut, USA) was used to further validate the direct effect of SOX9: the reporter was co-transfected with increasing amounts of SOX9-expression plasmid into SW1353 cells and luciferase activity measured after 24 hours of transfection. Luciferase activity in SW1353 cells significantly decreased in a dose-dependent manner (Figure 4.3.b) showing that SOX9 directly regulated the primary miR-29a/b1 promoter.

The data above demonstrate that SOX9 is a miR-29 family suppressor.

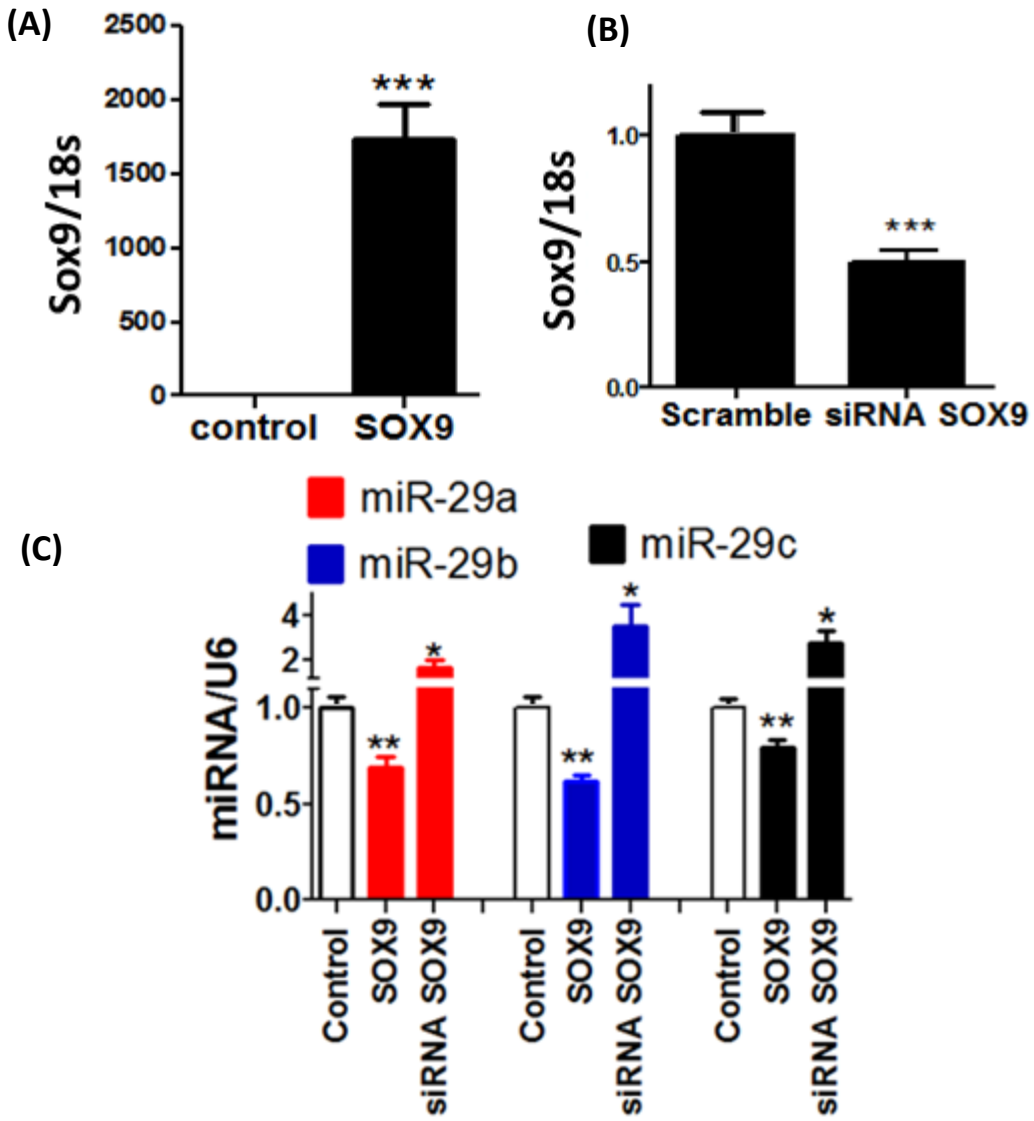

Figure 4.2: **Sox9 suppresses miR-29 family expression**.

(A) SOX9 gain-of-function: transiently transfection of a SOX9-expression vector or pcDNA3 empty vector (control) into SW1353 cells; (B) SOX9 loss-of-function: transiently transfection of SOX9 siRNA or a non-targeting control into SW1353 cells. Relative expression of SOX9 in (A) and (B) was measured 48 hours after transfection by quantitative RT-PCR using18S as the endogenous control; (C) The miR-29 family expression levels after overexpression or knockdown of SOX9 in SW1353 cells was measured by quantitative RT-PCR. Using U6 as the endogenous control. Red bar: miR-29a, green bar: miR-29b, black bar: miR-29c, open bar: control. Means ± standard errors are presented. Difference in expression was analysed by unpaired two-tailed Student's t test. * $p<0.05$, ** $p < 0.01$, *** $p<0.001$, n=3.

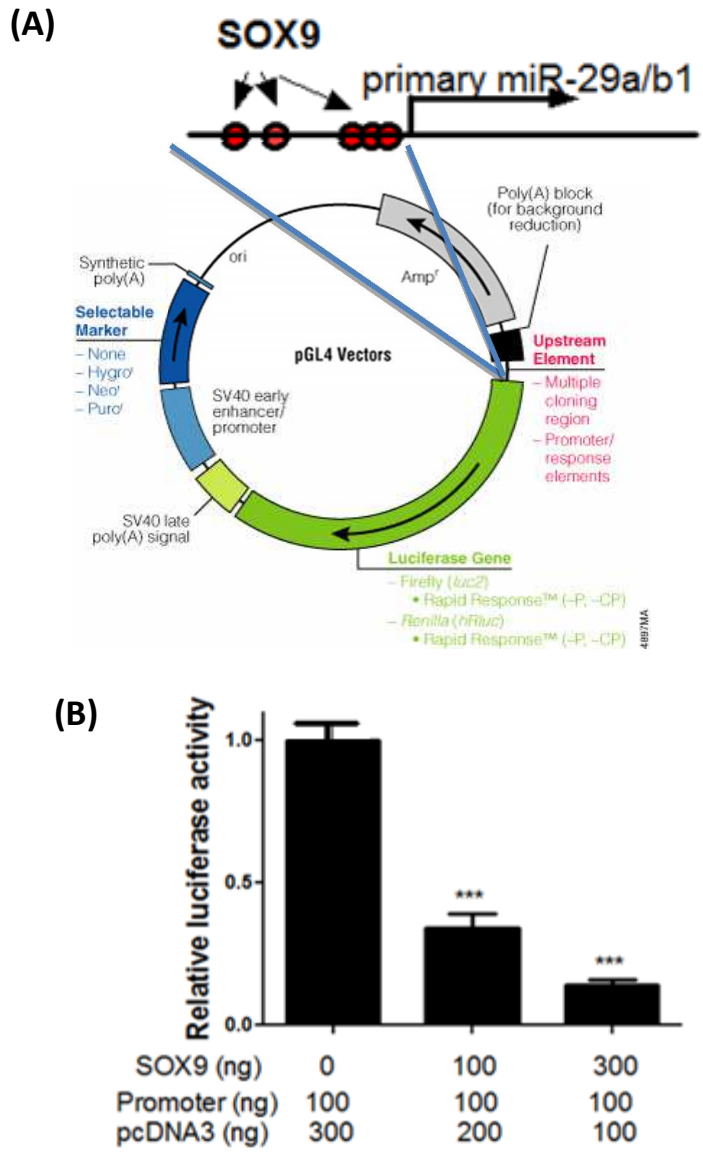

Figure 4.3: **Sox9 suppresses primary miR-29a/b1 transcription by directly binding to the proximal miR-29a/b1 promoter.**

(A) Structure of the miR-29a/b1 promoter reporter: 5 putative binding sites of SOX9 were identified by analysing the 2kb region upstream of the transcription start site of miR-29a/b1 by JASPAR. This 2kb region was sub-cloned upstream of the luciferase gene in a pGL4 vector.
(B) Suppressive effect of SOX9 on the primary miR-29a/b1 promoter reporter: transiently co-transfection of primary miR-29a/b1 promoter (100ng) with increasing amount of SOX9-expression vector (0, 100, 300ng) or pcDNA.3 to equalise DNA into SW1353. A constitutively expressed Renilla lucierase was used as a control for transfection efficiency. Luciferase activity was measured 24 hours after transfection. Means ± standard errors are presented. The difference in luciferase activity was analysed by unpaired two-tailed Student's t test. * $p<0.05$, ** $p < 0.01$, *** $p<0.001$, n=6.

4.2.2. TGFβ1 inhibits expression of the miR-29 family

TGFβ signalling has many important roles in chondrocytes and articular cartilage: TGFβ induces extracellular matrix formation; stimulates chondrocyte proliferation; inhibits the terminal differentiation of chondrocytes; retains chondrocytes in the pre hypertrophic stage; increases total glycosaminoglycan synthesis; maintains the matrix component in immature cartilage (Li *et al.* 2005). Animal studies showed that: transgenic mice overexpressing a cytoplasmically truncated, dominant-negative form of the TβRII in cartilage, resulted in a joint disease similar to human osteoarthritis (Serra *et al.* 1997); Smad3 deficient mice showed premature chondrocyte maturation with increased length of the hypertrophic region, disorganization of the chondrocyte columns, early expression of collagen type X in the growth plate; and null mice gradually developed an end-stage OA phenotype (Li et al. 2005). These essential roles of TGFβ signalling in chondrocytes suggest the necessity of examining whether the miR-29 family is regulated by TGFβ signalling in human chondrocytes. Moreover, a number of published data show that TGFβ signalling negatively regulates miR-29 family expression in different human fibroses e.g. renal, lung, liver fibrosis. The impact of TGFβ signalling in human chondrocytes on the miR-29 family was thus checked.

To address the above question, expression of the miR-29 family with TGFβ1 treatment in human primary chondrocytes was compared both in monolayer and micromass culture. **In monolayer culture**: HACs were put in high glucose media containing 10% (v/v) FCS until the cells reached 90% confluence; medium was replaced with that containing 0.5% (v/v) FCS) prior to stimulating with 4ng/ml TGFβ or vehicle control (4mM HCl with 0.5% (w/v) BSA). **In micromass culture**: HACs were put in high glucose media containing 10% (v/v) FCS in monolayer following two sequential passages to increase cell number; the micromass ($2.5x10^7$cells/ml) was cultured in high glucose media with 10% (v/v) FCS for 24 hours before treating with 10ng/ml TGFβ or vehicle control (4mM HCl with 0.5% (w/v) BSA). Cells were harvested for qRT-PCR after 24 hours or 48 hours treatment in monolayer or micromass cultures, respectively. Quantitative RT-PCR primers for measuring the miR-29 family were described before. For the primary transcripts: two primer pairs specific for exon 1 and exon 3 were used; for the precursor transcripts: primers directly bind to the precursor sequence (Appendix, Table 5); the mature transcripts were measure by LNA-primers.

The qRT-PCR data show that expression of the miR-29 family was suppressed by TGFβ signalling (Figure 4.4). However, each culture system gave a different response. The pri-29b2/c transcript was significantly decreased after stimulating HACs for 24 hours with TGFβ1 in monolayer culture, whilst the pri-29a/b1 transcript was unchanged (Figure 4.4 a); the pri-29a/b1 transcript was significantly decreased in micromass culture after 48 hours with TGFβ1 whilst the pri-29b2/c transcript was unchanged or even increased (Figure 4.4 b). Notably, the levels of all mature forms of miR-29 were significantly decreased by TGFβ1 in both systems. These data suggest a hypothesis that the primary and the precursor miRNAs may be rapidly regulated and then processed into mature miRNAs. In order to test this hypothesis, SW1353 cells were treated with TGFβ1 (4ng/ml) in monolayer in a time course. Since the expression levels of the primary and pre miRNAs modulated by TGFβ1 in human primary chondrocyte were similar and ahead the mature miRNAs, it might be sufficient to measure only the pre-miRNA rather than both the primary and precursor sequences. Consistent with above data, qRT-PCR showed that TGFβ1 suppressed miR-29 family expression in SW1353 cells (Figure 4.5). Interestingly, significantly suppressive effects of TGFβ1 on precursor miRNAs were observed after 4 hours till the end of the time course (Figure 4.5.a) whilst significant change in the mature miRNAs was only seen after 12 hour treatment (Figure 4.5.b). This data, thus, confirms the hypothesis above. Together with TGFβ1, the effect of TGFβ3 on the miR-29 family expression also checked on SW1353 in monolayer across the time course. Quantitative RT-PCR data (Figure 4.5) showed that TGFβ3 also strongly supressed the expression of the miR-29s. However, the TGFβ3 significant decrease the precursor and the mature miRNAs were observed at 12 hour time point though at 4 hours a

The suppressive effect of TGFβ on expression of the miR-29 family was also investigated on the proximal promoter of the primary miR-29a/b1 gene. The promoter-reporter was transfected into SW1353 cells, cells were serum starved for 24 hours and treated with TGFβ1 (4ng/ml) for another 6 hours before performing the luciferase assay. In line with the expression data, TGFβ1 significantly suppressed the promoter activity of pri-miR-29a/b1 (Figure 4.6).

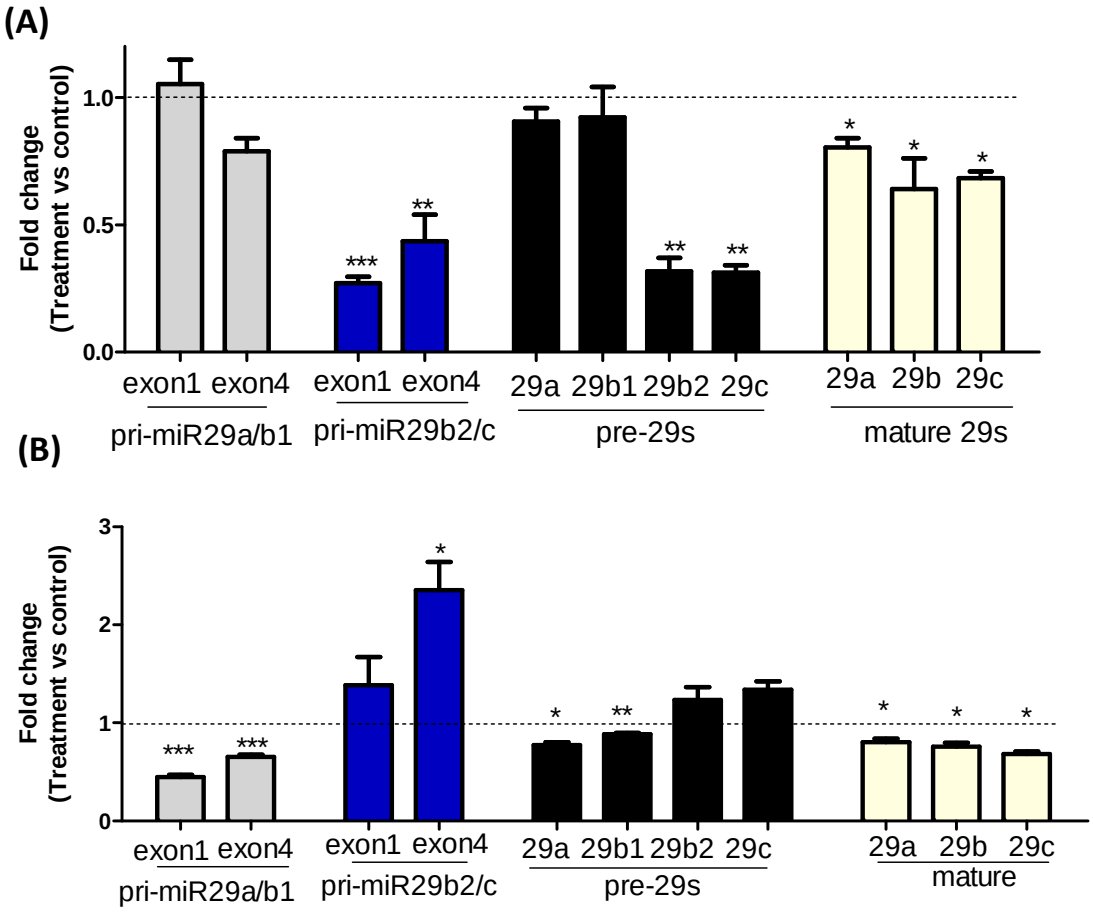

Figure 4.4 TGFβ1 suppresses expression of the miR-29 family in human primary chondrocyte

(A) TGFβ1suppresses expression of the miR-29 family in monolayer culture: Human primary chondrocytes were cultured in high glucose media with 10% (v/v) FCS in monolayer until 90% confluence. Cells were switched to high glucose media with 0.5% (v/v) FCS for 24 hours before treating with TGFβ1 (4ng/ml) or vehicle (4mM HCl+0.5% (w/v) BSA) for another 24 hours.

(B) TGFβ1suppresses expression of the miR-29 family in micromass culture: Human primary chondrocytes were cultured in high glucose media with 10% (v/v) FCS in monolayer. After 2 sequential passages, cells were put in micromass culture ($2.5x10^7$cells/ml) in high glucose media with 10% (v/v) FCS. After 24 hours in micromass, cells were stimulated for 48 hours with TGFβ (10ng/ml) or vehicle (4mM HCl+0.5% (w/v) BSA) in 10% (v/v) FCS media.

Relative expression of the primary miR-29a/b1, -29b2/c, precursor miR-29a, -29b1, -29b2, -29c, the mature miR-29a, b, c were measured by quantitative RT-PCR. 18S rRNA was the endogenous control for measuring primary and precursor transcripts; U6 was the endogenous control for measuring miR-29 mature transcripts. The horizontal line at 1 represents the mean of the vehicle control. Brown bar, pri-miR-29a/b1 transcripts; blue bar, pri-miR-29b2/c transcripts; black bar, precursor transcripts; yellow bar, mature transcripts. Means ± standard errors are presented. The difference between the treatment and the control was analysed by unpaired two-tailed t test. * $p<0.05$, ** $p < 0.01$, *** $p<0.001$, n=3.

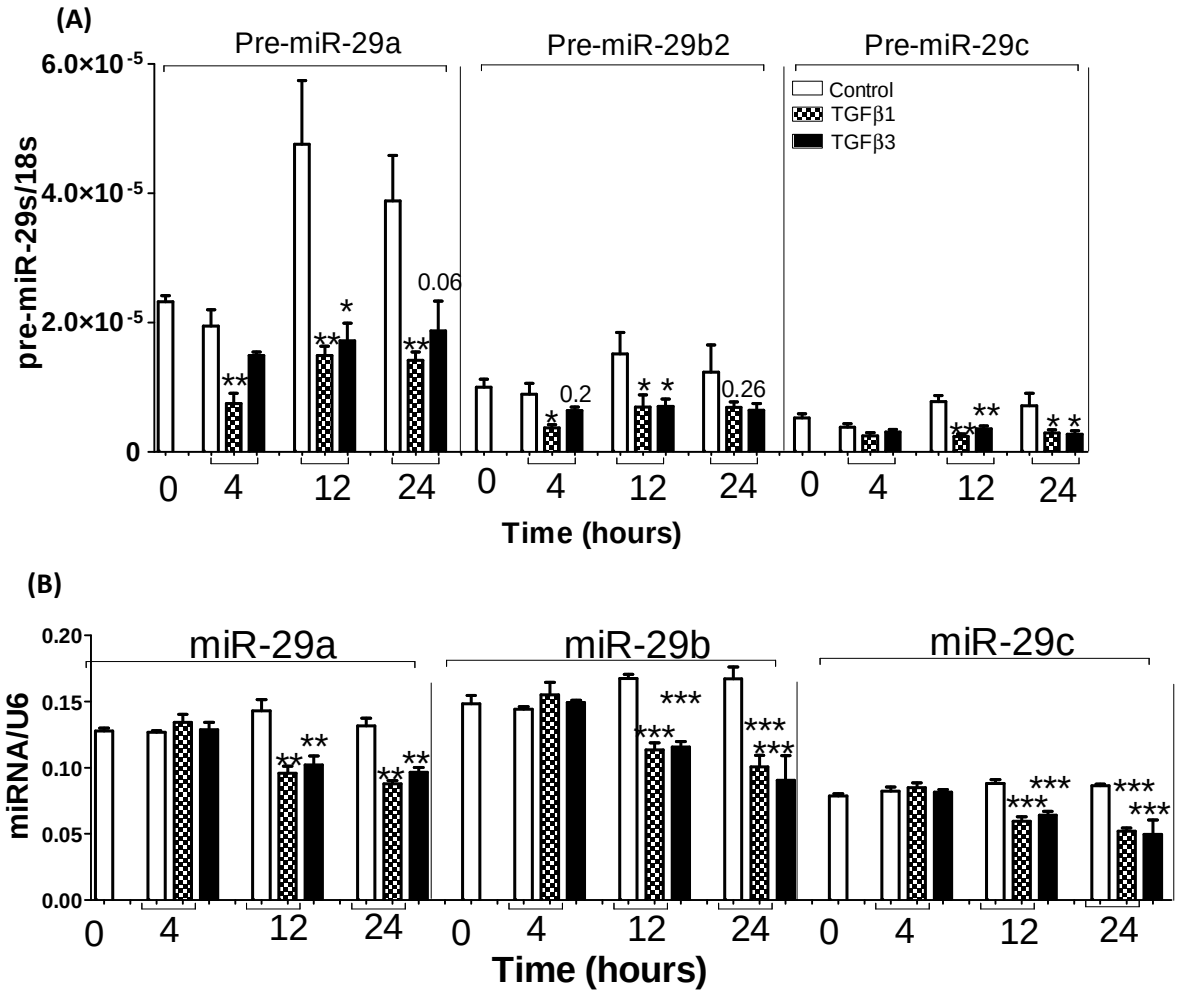

Figure 4.5 TGFβ1/3 suppresses expression of the miR-29 family in SW1353 cells

SW1353 cells were cultured in high glucose media with 10% (v/v) FCS in monolayer until 90% confluence. Cells were serum starved for 24 hours before treating with TGFβ1or TGFβ3 (4ng/ml) or vehicle (4mM HCl+0.5% (w/v) BSA) across 24 hour course.

Relative expression of the precursor miR-29a, -29b2, -29c, the mature miR-29a, b, c were measured by quantitative RT-PCR. 18S rRNA was the endogenous control for measuring the precursor transcripts; U6 was the endogenous control for measuring miR-29 mature transcripts. Open bar, control; brick bar, TGFβ1; close bar, TGFβ3. (A) Expression level of pre-miR-29a, 29b2, 29c. (B) Expression level of mature miR-29a, b, c. Means ± standard errors are presented. The difference between the treatment and the control was analysed by unpaired two-tailed t test. * $p<0.05$, ** $p < 0.01$, *** $p<0.001$, n=3.

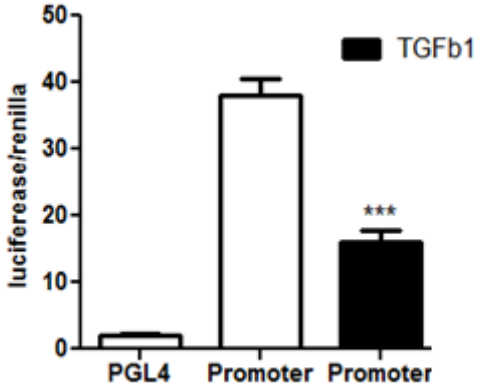

Figure 4.6: TGFβ1decreases expression from the primary miR-29a/b1 promoter

The pri-miR-29a/b1 promoter-reporter (100ng) or the empty vector pGL4 (control, 100ng) were transfected into SW1353 cells. After transfection, cells were serum starved for 24 hours, followed by stimulating for another 6 hours with TGFβ1 (4ng/ml), or vehicle (4mM HCl+0.5% BSA) before measuring luciferase activity. Renilla was use as endogenous control. Open bar: vehicle, black bar: TGFβ1. Means ± standard errors are presented. The difference of luciferase activity was analysed by unpaired two-tailed Student's t test. * $p<0.05$, ** $p < 0.01$, *** $p<0.001$, n=6.

4.2.3. Expression of the miR-29 family is not regulated by canonical Wnt signalling

As shown in the section above, the TGFβ signalling pathway, stimulated by TGFβ1 (or TGFβ3, data not shown), negatively regulated the expression of themiR-29 family. Signalling cross talk between TGFβ and Wnt signalling pathways has been previously reported, e.g. after TGFβ stimulation, Smad3 interacts with LEF1 to activate target gene transcription independently of β-catenin (Letamendia *et al.* 2001); TGFβ was shown to up-regulate the expression of many Wnt ligands e.g. Wnt2, 4, 5a, 7a, 10a, and Wnt co-receptors e.g. LRP5 (Zhou *et al.* 2004); TGFβ was found to increase nuclear accumulation and stability of β-catenin; interestingly, working synergistically with Wnt signalling pathways, TGFβ was reported to stimulate chondrocyte differentiation from mesenchymal cell (Zhou et al. 2004). Wnt signalling is also known to have a key role in cartilage homeostasis and osteoarthritis (Zhu et al. 2008, Zhu et al. 2009). Thus, it was pertinent to investigate the effect of Wnt signalling onexpression of the miR-29 family in chondrocytes, and then potential synergy with TGFβ signalling.

The effect of canonical Wnt signalling stimulated by Wnt3a (50 or 100ng/ml) on the miR-29 family was investigated in HACs cultured in monolayer or micromass after 24 hours or 48 hours, respectively; or in SW1353 cells in monolayer culture across a 24 hour time course. In addition, the effect of Wnt3a on the proximal pri-miR-29a/b1 promoter was also examined after 6 hour treatment with Wnt3a (50 or 100ng/ml). Quantitative RT-PCR data for all transcripts of miR-29 family and luciferase assay data for the miR-29a/b1 promoter showed canonical Wnt signalling did not regulate expression of the miR-29 family (Appendix, Figure 5). Wnt3a did regulate Axin2 expression in the same experiments, showing induction of the canonical Wnt pathway (Appendix, Figure 6).

4.2.4. IL-1 induces expression of the miR-29 family in part via the p38 signalling pathway.

IL-1 is a catabolic and anti-anabolic cytokines, it down regulates the expression of cartilage matrix components e.g. aggrecan and type II collagen and induces expression of matrix degrading enzymes e.g. MMP-3, MMP-13, ADAMTS4 (Koshy *et al.* 2002). *Il-1β*, or Il-1β-converting enzyme knockout mice showed the accelerated development of OA lesions in response to OA surgical induced in compared with wide type mice (Clements et al. 2003). It is considered to be a major cytokine driving the pathology of OA (Goldring *et al.* 2004). Thus, it was pertinent to examine whether IL-1 controls the expression of the miR-29 family in human chondrocytes.

The effect of IL-1 on the expression of the miR-29 family was first measured in IL-1-treated SW1353 for 48 hour time course in monolayer culture: SW1353 cells were cultured in high glucose media with 10% (v/v) FCS until reach confluence and followed by serum starved for 24 hours before treating with 5ng/ml IL-1 or vehicle (0.5% (w/v) BSA) for 48 hour time course. Relative expressions of the precursor and mature miRNA-29 transcripts were measured by qRT-PCR. Data (Figure 4.7) showed that IL-1 induced the expression of miR-29 family: the biggest induction on miR-29 precursors was observed at 4 hours; at later time point, the level of miR-29a precursors was decreased as compare with 4 hours (pre-29a) whilst other precursors did not change expression (Figure 4.7a); the induction of mature miR-29s were only observed significantly after 48 hours (Figure 4.7b). These data suggested that the increase in expression after IL-1 treatment of the miR-29 derivatives is time-dependent. The induction of IL-1 on the miR-29 family was again checked on the HACs in micromass culture: The micromass containing ($2.5x10^7$cells/ml) of passage 2 HAC was cultured in high glucose media with 10% (v/v) FCS for 48 hours before treating with 20ng/ml IL-1 or vehicle control (0.5% (w/v) BSA). Quantitative RT-PCR primers for measuring the miR-29 family were described before (Appendix, Table 5). Real-time RT-PCR data (Figure 4.8) showed that IL-1 strongly induced expression of the miR-29 family, with all processed transcripts significantly up-regulated by IL-1. The fold increase was highest for the pri-miR-29a/b1 locus in which the primary miR-29a/b1 and pre-miR29a and b1 were increased with 9 and 5 fold, respectively.

The molecular pathways induced by IL-1 can be the three classical MAPK-signalling pathways i.e. ERK, p38, JNK and through NFκB (Aigner *et al.* 2006, Fan *et al.* 2007). The

signalling pathway through which IL-1 regulated miR-29 family expression was investigated. SW1353 cells were stimulated with IL-1 together with an NFκB inhibitor (10μM) or a p38 inhibitor (SB203580) (10μM) or 6 hours in monolayer and the relative expression of the precursor miRNAs were again measured. The data showed that inhibition of the NFκB pathway further induced expression of the pre-miR-29a and b1 (Figure 4.9). Inhibition of p38 suppressed IL-1 induction of pre-miR-29a and b1, with a similar pattern for pre-miR-29b2 and c (Figure 4.10), suggesting that IL-1 induces expression of the miR-29 family at least in part through p38 MAPK signalling.

Furthermore, the effect of IL-1 on the promoter of pri-miR-29a/b1 was also examined by luciferase assay. The pri-miR-29a/b1 promoter-reporter was transfected into SW1353 cells for 24 hours before stimulation with IL-1 (5ng/ml) with or without the NFκB inhibitor (10nM) or p38 inhibitor (10μM) for another 6 hours. Luciferase data showed that the activity of the pri-miR-29a/b1 promoter was significantly decreased by IL-1 and that this effect was abolished by treatment with the NFκB inhibitor (Figure 4.11). However, the p38 inhibitor had no effect on the suppressive effect of IL-1 on the promoter of pri-miR-29a/b1 (data not shown).

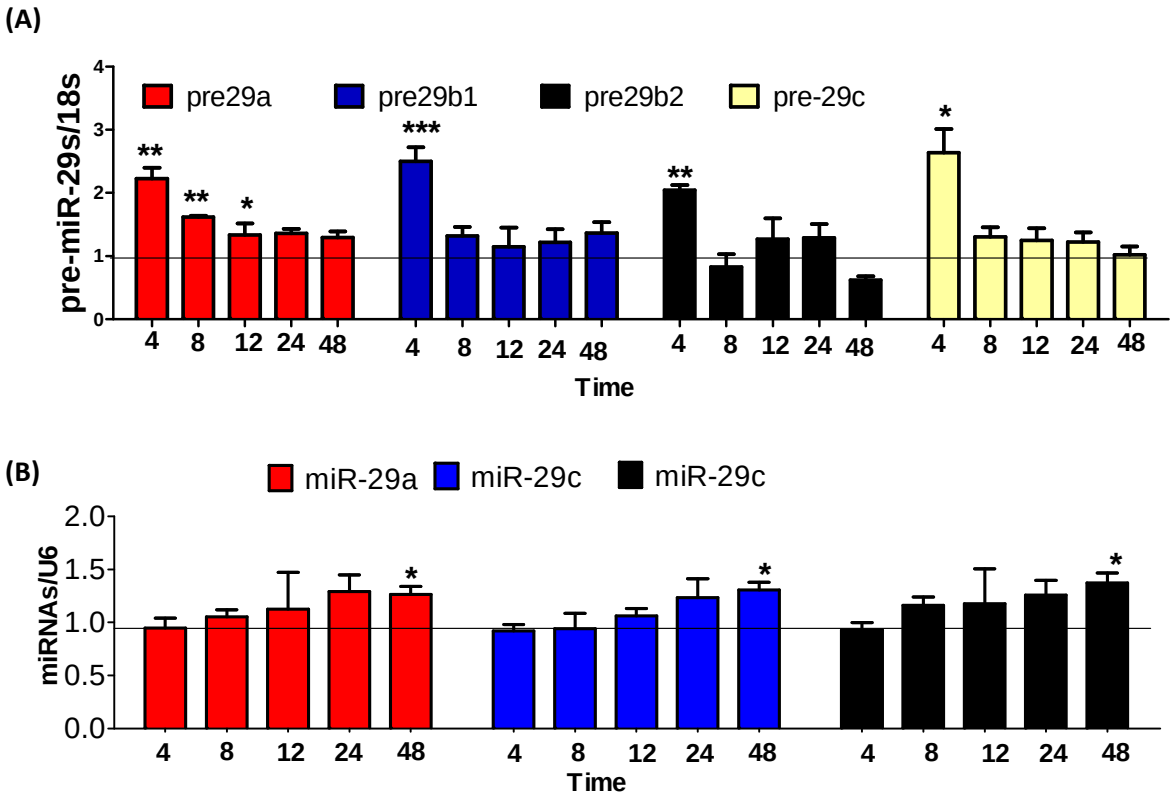

Figure 4.7: IL-1 induces expression of the miR-29 family in SW1353 in monolayer culture

SW1353 cells were cultured in high glucose media with 10% (v/v) FCS in monolayer until 90% confluence. Cells were serum starved for 24 hours before treating with IL-1 (5ng/ml) or vehicle (0.5% (w/v) BSA) across 48 hour course.
Relative expression of the precursor miR-29a, -b1, -b2, -c, the mature miR-29a, b, c were measured by quantitative RT-PCR. 18S rRNA was the endogenous control for measuring the precursor transcripts; U6 was the endogenous control for measuring miR-29 mature transcripts. The horizontal line at 1 serves as the vehicle control.
(A) Expression level of pre-miR-29a, 29b2, 29c. Red bar, pre-miR-29a; blue bar, pre-miR-29b1; black bar, pre-miR-29b2; yellow bar, pre-miR-29c
(B) Expression level of mature miR-29a, b, c. Red bar, miR-29a; blue bar, miR-29b; black bar, miR-29c
Means ± standard errors are presented. The difference between the treatment and the control was analysed by unpaired two-tailed t test. * $p<0.05$, ** $p < 0.01$, *** $p<0.001$, n=3.

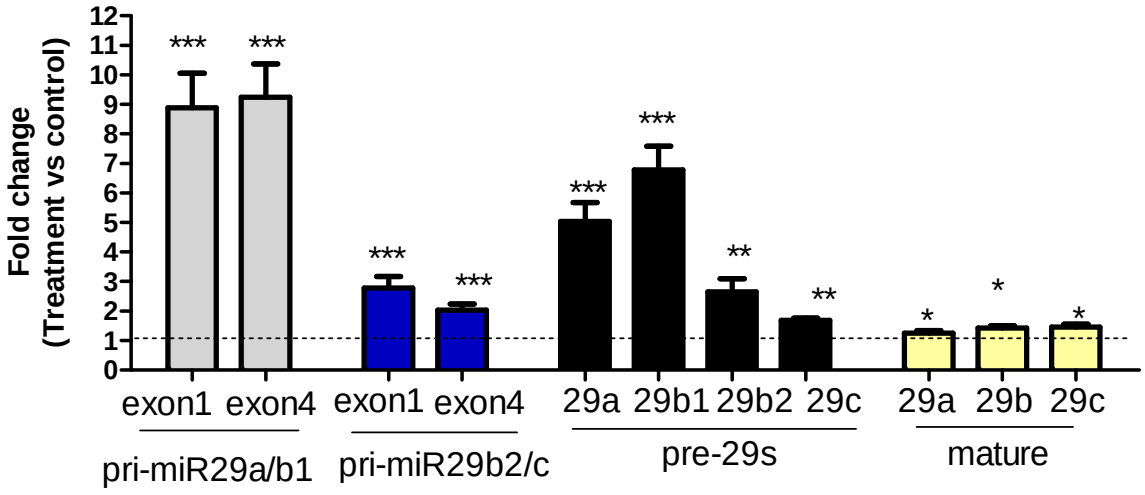

Figure 4.8: IL-1 induces expression of the miR-29 family in human primary chondrocyte in micromass culture

Human primary chondrocytes were cultured in high glucose media with 10% (v/v) FCS in monolayer. After 2 sequential passages, cells were put in micromass culture ($2.5x10^7$cells/ml) in high glucose media with 10% (v/v) FCS. After 24 hours in micromass, cells were stimulated for 48 hours with IL-1β (10ng/ml) or vehicle (0.5% (w/v) BSA).
Relative expression of the primary miR-29a/b1, -29b2/c, precursor miR-29a, -29b1, -29b2, -29c, the mature miR-29a,- 29b, -29c were measured by quantitative RT-PCR. 18S rRNA was the endogenous control for measuring primary and precursor transcripts; U6 was the endogenous control for measuring miR-29 mature transcripts. The horizontal line at 1 serves as the vehicle control. Brown bar, pri-miR-29a/b1 transcripts; blue bar, pri-miR-29b2/c transcripts; black bar, precursor transcripts; yellow bar, mature transcripts. Means ± standard errors are presented. The difference between the treatment and the control was analysed by unpaired two-tailed Student's t test. * $p<0.05$, ** $p < 0.01$, *** $p<0.001$, n=3.

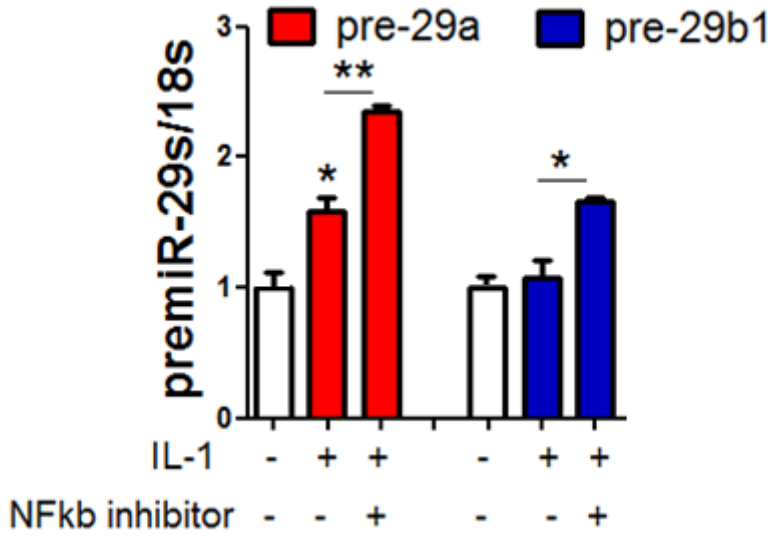

Figure 4.9 NFκB inhibition further increases the IL-1-induced expression of pre-miR-29a and pre-miR-29b1

SW1353 cells were plated in high glucose media with 10% (v/v) FCS in a 6 well-plate in monolayer and serum starved for 24 hours before treating with IL-1β (10ng/ml) in the presence or absence of NFκB inhibitor JSH-23 (10μM) for a further 8 hours. Cells were then harvested and the total RNA was isolated by Trizol. Relative expression of pre-miR-29a, -29b1 were measured by quantitative RT-PCR. 18S rRNA was the endogenous control. Red bar, pre-miR-29a; blue bar, pre-miR-29b1. Means ± standard errors are presented. The difference between the treatment and the control was analysed by unpaired two-tailed Student's t test * $p<0.05$, ** $p < 0.01$, *** $p<0.001$, n=6.

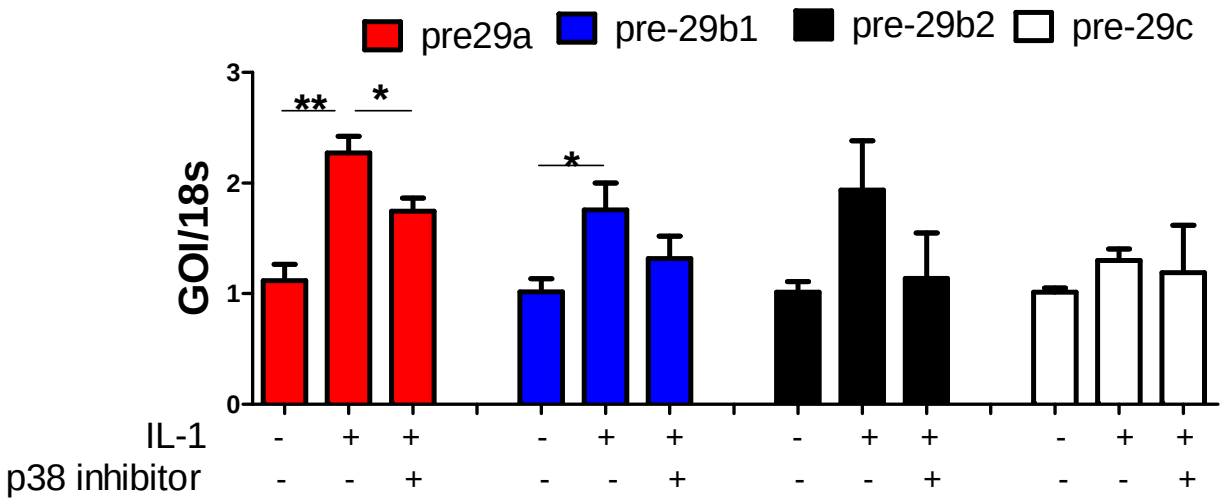

Figure 4.10 P38 inhibition suppresses the IL-1 induction of pre-miR-29s

SW1353 cells were plated in high glucose media with 10% (v/v) FCS in a 6 well-plate in monolayer and serum starved for 24 hours before treating with IL-1β (10ng/ml) in the presence or absence of p38 inhibitor SB203580 (10µM) for a further 8 hours. Cells were then harvested and the total RNA was isolated by Trizol. Relative expression of pre-miR-29a, -29b1, -29b2, -29c were measured by quantitative RT-PCR. 18S rRNA was the endogenous control. Red bar, pre-miR-29a; blue bar, pre-miR-29b1; black bar, pre-miR-29b2; white bar, pre-miR-29c. Means ± standard errors are presented. The difference between the treatment and the control was analysed by unpaired two-tailed Student's t test * $p<0.05$, ** $p < 0.01$, *** $p<0.001$, n=3.

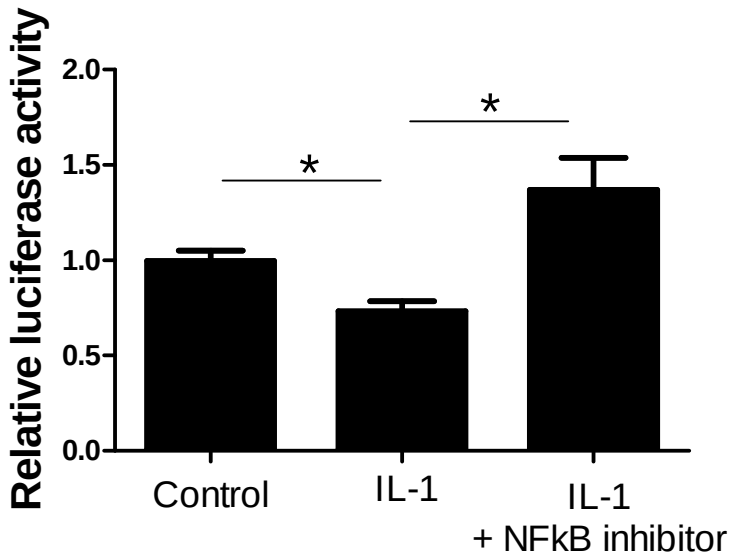

Figure 4.11: IL-1 suppresses the primary miR-29a/b1 promoter through NFκB

Pri-miR-29a/b1 promoter reporter (100ng) or pGL4 (control, 100ng) were transfected into SW1353 cells. After transfection, cells were serum starved for 24 hours, and followed by stimulating for another 6 hours with IL-1β (5ng/ml), IL-1β and NFκB inhibitor JSH-23 (10μM) or vehicle (0.5% (w/v) BSA) before measuring luciferase activity. Renilla was the endogenous control. Means ± standard errors are presented. The difference of luciferase activity was analysed by unpaired two-tailed Student's t test. * $p<0.05$, ** $p < 0.01$, *** $p<0.001$, n=6.

4.2.1. LPS suppressed the miR-29 family expression through NFκB signalling pathway

Toll-like receptors (TLRs) have important roles in activation of the innate and adaptive host defence against infections. TLR can bind to various damage-associated molecular patterns, which are endogenous danger signals or alarmins, leading to autoinflammatory conditions, and contributing to production of co-stimulatory signals necessary for adaptive immune reactions (Janeway *et al.* 2002). Lipopolysaccharide (endotoxin) (LPS) from bacteria is an example of a TLR-stimulating molecule. Chondrocytes are a potential source of several proinflammatory substances which may be TLR ligands: high-mobility group box 1, heat-shock proteins, and several components of the cartilage extracellular matrix (ECM) - e.g. low-molecular-weight hyaluronan, heparin sulphate, biglycan, and fibronectin fragments (Konttinen *et al.* 2012). From this point of view, OA could be considered as an autoinflammatory disease with the chondrocyte as its primary inflammatory cell (Konttinen et al. 2012). On this basis it was hypothesized that the activation of TLR-4, a receptor for LPS, may directly affect the biosynthetic activity of chondrocytes, including expression of the miR-29 family.

The level of miR-29 family expression was measured by qRT-PCR in HACs stimulated LPS (1µg/ml) in monolayer or micromass culture for a 24 hours or a 48 hour time course, respectively. Real-time PCR showed that the miR-29 family was significantly suppressed by LPS (Figure 4.12). Interesting, the levels of all processed miRNAs were strongly regulated by LPS in a time dependent manner: a significant decrease of the two miR-29 family clusters and their precursors were detected after 4 hours of treatment whilst decrease of the mature miRNAs was not detected until 24 hours. However, after 48 hours treating with LPS, all miR-29 family was tended to increase (Figure 4.12)

Again, the effect of LPS on the promoter of pri-miR-29a/b1 was also examined by luciferase assay. The pri-miR-29a/b1 promoter reporter was transfected into SW1353 cells for 24 hours before stimulation with LPS (1µg/ml) in the presence or absence of an NFκB inhibitor JSH-23 (10µM) for another 6 hours. Luciferase assay data showed that promoter activity of pri-miR-29a/b1 was significantly decreased by LPS and this effect was abolished with the NFκB inhibitor (Figure 4.13).

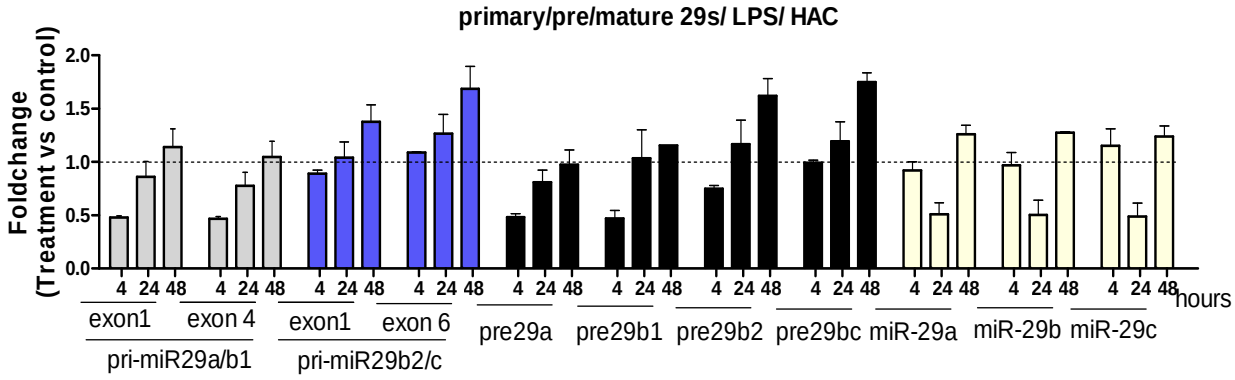

Figure 4.12: LPS suppresses expression of the miR-29 family

Human primary chondrocytes were cultured in high glucose media with 10% (v/v) FCS in monolayer. After 2 sequential passages, cells were put in micromass culture ($2.5x10^7$cells/ml) in high glucose media with 10% (v/v) FCS. After 24 hours in micromass, cells were stimulated for 4, 24, and 48 hours with LPS (1µg/ml) or vehicle (0.5% (w/v) BSA).
Relative expression of the primary miR-29a/b1, -29b2/c, precursor miR-29a, -29b1, -29b2, -29c, the mature miR-29a,- 29b, -29c was measured by quantitative RT-PCR. 18S rRNA was the endogenous control for measuring primary and precursor transcripts; U6 was the endogenous control for measuring miR-29 mature transcripts. The horizontal line at 1 serves as the vehicle control. Brown bar, pri-miR-29a/b1 transcripts; blue bar, pri-miR-29b2/c transcripts; black bar, pre-miR transcripts; yellow bar, mature miR transcripts. Means ± standard errors are presented. The difference between the treatment and the control was analysed by unpaired two-tailed Student's t test. * $p<0.05$, ** $p < 0.01$, *** $p<0.001$, n=3.

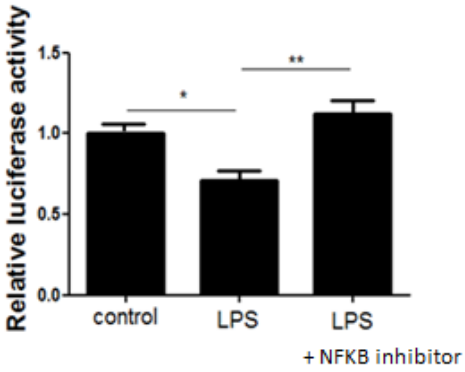

Figure 4.13: LPS suppresss the primary miR-29a/b1 promoter through NFκB

Pri-miR-29a/b1 promoter-reporter (100ng) or pGL4 (control, 100ng) was transfected into SW1353 cells. After transfection, cells were serum starved for 24 hours, followed by stimulatiion for another 6 hours with LPS (1µg/ml) in the absence or presence of an NFκB inhibitor JSH-23 (10µM) before measuring luciferase activity. Renilla was the endogenous control. Means ± standard errors are presented. The difference of luciferase activity was analysed by unpaired two-tailed Student's t test. * $p<0.05$, ** $p < 0.01$, *** $p<0.001$, n=6.

4.2.2. The microRNA-29 family targets Dicer giving a negative feedback loop for maturation of pre-miR-29

Previous data showed that expression of the miR-29 family was regulated by TGFβ, IL-1, LPS in which primary microRNA and precursor microRNA were modulated far ahead the mature microRNAs. In order to explain this, the 3'UTR regions of genes encoding for proteins involved in miRNA biogenesis were searched for putative binding site of the miR-29 family. Among these, of particular interest is the ribonuclease III enzyme Dicer, renowned for its central role in the biogenesis of microRNAs, converting the stem-loop pre-miRNA to mature miRNA (Bartel 2004). Bioinformatic analysis showed that there was a putative binding site of miR-29 in the *DICER* 3'UTR, suggesting the miR-29 family may regulate Dicer expression leading to the down-regulation of the Dicer level and as the consequence, the processing from precursors to mature miRNAs would potentially be slowed down. The 3'UTR region of *DICER* was therefore sub-cloned downstream of the firefly luciferase gene in the pmiR-GLO vector. The effect of the miR-29 family on the *DICER* 3'UTR was measured by luciferase assay after 24 hour co-transfection of the *DICER* 3'UTR- pmiR-GLO and the miR-29 family in SW1353 cells. Dual-luciferase reporter analysis showed the co-transfection of miR-29s significantly inhibited the wild type construct, whereas when the target site was mutated, the construct was not inhibited (Figure 4.14). This indicates that miR-29 may suppress expression of Dicer. The effect of the miR-29 family in *DICER* expression at transcriptional level was also investigated. Human primary chondrocyte was transfected with either miR-29b mimic (50nM) or non – targeting control (50nM). The transfected cells were then put in either monolayer or micromass culture for a further 48 hours. The expression of *DICER* was measured by qRT-PCR. Real-time qRT-PCR data showed that the expression of Dicer was not affected by miR-29s (data not shown), suggesting that the miR-29s does not control Dicer expression at mRNA level.

There is a growing body of work demonstrating that microRNAs can be processed independently of Dicer via Argonaute2 (Dueck *et al.* 2010). To evaluate whether or not miR-29s required Dicer to mature, the level of pre-miR-29s and mature miR-29s were measured in DLD, a Dicer-knockdown cell line. Data (Figure 4.15) showed that the levels of mature miR-29s were strongly reduced whilst the level of pre-miR-29s was not affected (Figure 4.15), demonstrating miR-29 processing is Dicer-dependent.

Taken together, these data show that the miR-29 family targets Dicer giving a negative feedback loop for its maturation.

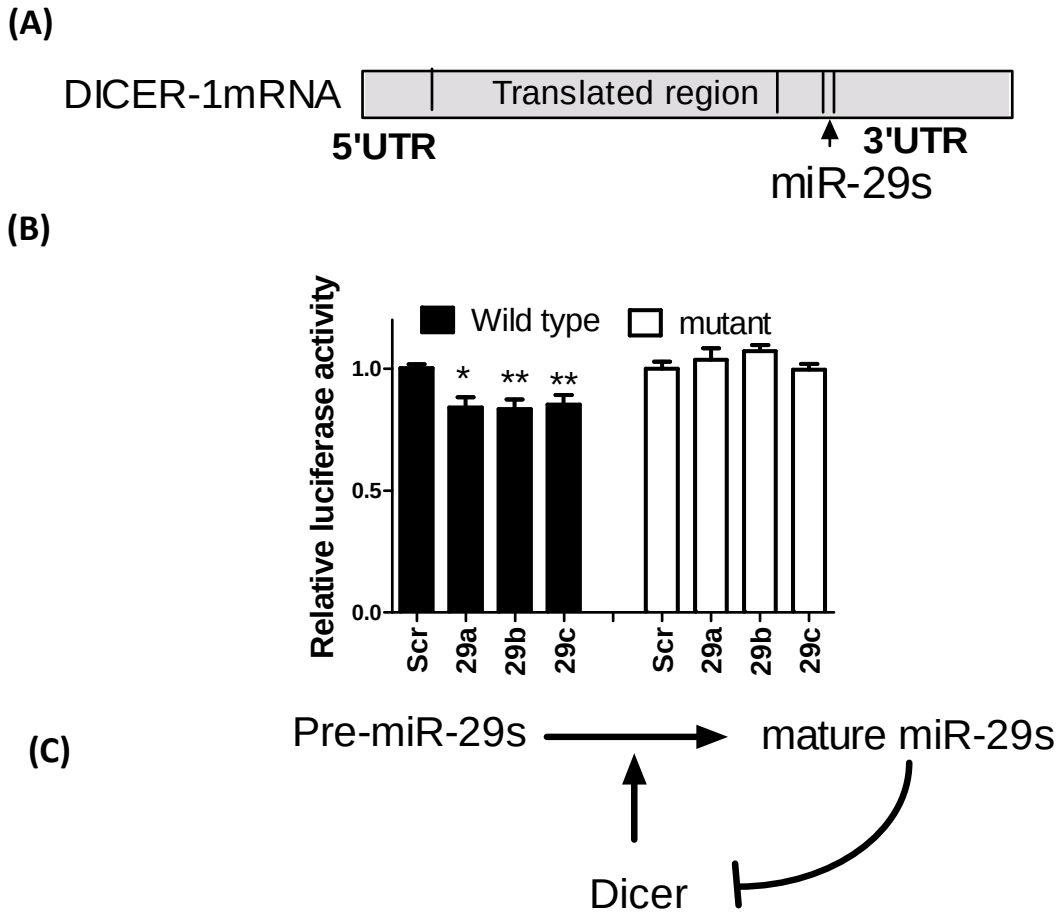

Figure 4.14: The miR-29 family targets Dicer

(A) Bioinformatic analysis reveals one binding site of the miR-29 family in the 3'UTR of Dicer. (B) miR-29 family targets Dicer: The Dicer 3'UTR containing the binding site of the miR-29 family (wild type) or a mutated, non-functional binding site for miR-29 family (mutant) were sub-cloned into the pmiR-GLO vector and were co-transfected with either miR-29a, -29b, -29c mimic (50nM) or non-targeting control (50nM) into SW1353 cells for 24 hours and luciferase activity was measured. Renilla was the endogenous control. (C) miR-29 targets Dicer giving a negative feedback loop for its maturation. Means ± standard errors are presented. The difference of luciferase activity was analysed by unpaired two-tailed Student's t test. * $p<0.05$, ** $p < 0.01$, *** $p<0.001$, n=6.

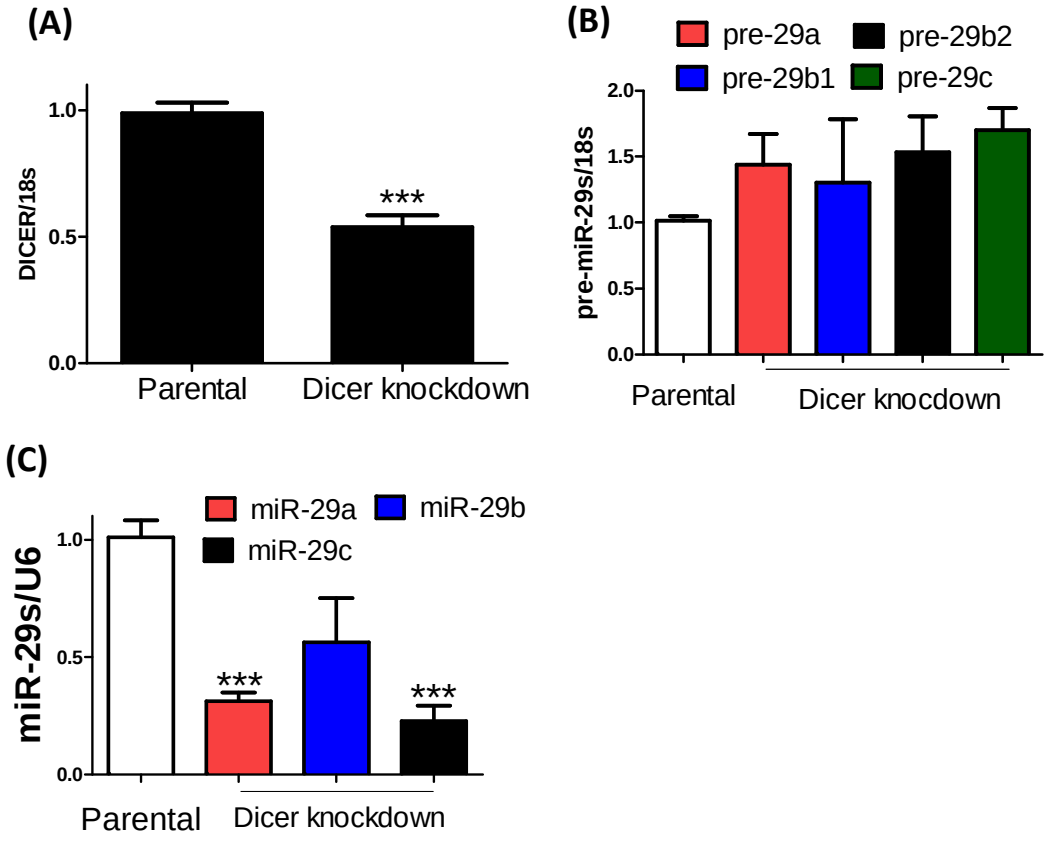

Figure 4.15: Dicer is required for the miR-29 family maturation

2

Level of Dicer, precursor and mature miR-29 were measured in DLD, Dicer knockdown cell line or parental control by quantitative RT-PCR. (A) Relative expression of Dicer; (B) Relative expression of precursor miR-29s (normalised to expression in parental control). 18S rRNA is endogenous control. Red, pre-29a; blue, pre-29b1; black, pre-29b2; green, pre-29c; white, levels of all precursors in control (set at 1); (C) Relative expression of mature miR-29 family (normalised to expression in parental control). U6 is endogenous control. Red, miR-29a; blue, miR-29b; black, miR-29c; white, levels of all mature miR-29 in control (set at 1). Means ± standard errors are presented. The difference of relative expression was analysed by unpaired two-tailed Student's t test. * $p<0.05$, ** $p < 0.01$, *** $p<0.001$, n=3.

4.3. Discussion

Since miRNAs have broad effects on cartilage homeostasis, and OA, it is particularly interesting to work out how miRNAs themselves are being regulated. Such data could provide crucial information for further understanding the mechanism underlying OA and for being able to manipulate these miRNAs in chondrocytes therapeutically. Generally, the expression of miRNAs can be regulated transcriptionally, epigenetically, or controlled by different stimuli e.g. cytokines and growth factors. In this study, just transcription factors, cytokines, and growth factors controlling the miR-29 family expression in chondrocytes were for the first time investigated. These studies were able to show that, in human chondrocytes, the master transcriptional regulator SOX9, TGFβ and LPS suppressed whilst IL-1 strongly induced the miRNA-29 family expression.

Several published data report the suppressive effect of SOX9 on the expression of individual members of the miR-29 family in other cellular contexts: in murine stem cells, overexpression of SOX9 or knockdown SOX9 in cell lines e.g. C3H10T1/2 or ATDC5 leads to suppression or induction of miR-29a and miR-29b expression (Yan et al. 2011), respectively; in human C-20/A4 chondrocytes, overexpression of SOX9 strongly down-regulated the level of miR-29a (Guerit et al. 2014). Herein, for the first time, suppressive effect of SOX9 on the expression of all members of the miR-29 family in primary human chondrocytes was shown. The effect was exerted, at least in part, through directly targeting the promoter of the miR-29a/b1 locus. In line with these data, Guerit et al (2014) reported that SOX9 can physically bind to at least 3 out of 4 putative binding sites within the proximal promoter of miR-29a/b1 cluster; also, another transcription factor YY1, was shown not to bind directly to the miR-29a/b1 promoter, but, physically interacted with SOX9 to suppress miR-29a/b1 expression (Guerit et al. 2014). The mechanism by which SOX9 negatively regulates the pri-miR-29b2/c cluster is still unknown. Several putative binding sites of SOX9 are found in the promoter of the pri-miR-29b2/c cluster, implicating a possible direct mechanism. However, this needs further investigation.

Alongside SOX9, other transcriptional regulatory mechanisms responsible for expression of the miR-29 family have also been reported: the pri-miR-29a/b1 locus was stimulated by the transcription factors CEBPA (Eyholzer et al, 2010), GATA3 (Chou et al. 2013), STAT1 (Schmitt et al, 2012) but suppressed by c-MYC (Mott et al. 2010, Parpart et al. 2014), NFκB

(Liu et al. 2010, Mott et al. 2010), Sp1(Liu et al. 2010, Amodio et al. 2012), HDAC1, HDAC3, and Gli (Mott et al. 2010); the pri-miR-29b2/c locus was inhibited by Smad3 (Qin et al. 2011), NFκB, YY1, Ezh2, H3K37, HDAC1 (Wang et al. 2008). Thus, it is likely that the transcriptional regulation of the miR-29a/b1 cluster is controlled by a combination of different transcription factors. Interestingly, in the chondrocyte context, miR-1247 together with miR-145 were reported to directly target and repress expression of SOX9 (Yang et al. 2011, Martinez-Sanchez and Murphy 2013), suggesting these miRNAs could contribute to the induction of the miR-29 family level in chondrocytes. Additionally, throughout the current project, the miR-29 family members exhibit different expression levels between the primary miR-29a/b1 and primary miR-29b2/c loci in different cellular contexts. This discrepancy could be explained in part by different transcription factor binding to each promoter.

Together with SOX9, TGFβ signalling was found to suppress the expression of all miR-29 family members in chondrocytes. Since TGFβ signalling induces SOX9 expression (Greco et al. 2011), the suppressive effect of TGFβ on the miR-29 family could be exerted through SOX9 and this TGFβ-SOX9 signalling could in part explain the down-regulation of the miR-29 family by TGFβ. The suppressive effect of TGFβ on the miR-29 family expression has also been observed in various cell types associated with fibrosis e.g. human aortic adventitial fibroblasts (Maegdefessel et al. 2012), renal fibrosis cells (Wang et al. 2012, Ramdas et al. 2013), murine hepatic stellate cells (Roderburg et al. 2011), rat hepatic stellate cells (Kwiecinski et al. 2011), human skin fibroblasts (Maurer et al. 2010), human tenon's fibroblast (Li et al. 2012), human lung fibroblast cell line (Cushing et al. 2011, Yang et al. 2013) in which either some members or the whole miR-29 family significantly decreased expression with TGFβ treatment. Apart from TGFβ-SOX9 signalling, the mechanism for the inhibition of TGFβ on the miR-29 family expression is currently unknown. There is some evidence that TGFβ inhibits miR-29 expression through SMAD3 signalling e.g. the inhibition effect of TGFβ on miR-29 expression was abolished when *Smad3* was knocked out in mouse embryonic fibroblast (Qin et al. 2011); SMAD3 could directly interact with at least two conserved SMAD3-binding sites in the promoter region of miR-29b2/c locus (Qin et al. 2011); activated TGFβ signalling induced SMAD3 translocate into nucleus and bind to miR-29b2/c promoter, resulting in the dissociation of MyoD and the stabilization of YY1 whose expression negatively regulated the miR-29b2/c expression through a conserved binding site

(Qin et al. 2011). However, this needs to be validated in chondrocytes. Besides the suppressive role, TGFβ also exerted an inductive effect on miR-29 expression at late time points. For instance, the primary miR-29b2/c locus was induced in human primary chondrocyte in micromass cultured with TGFβ1 for 48 hours (Figure 4.4b) though this increase did not reach significantly; the miR-29 family expression was increased at a late stage in the human chondrogenesis model with TGFβ3 as the major driver among others (Figure 3.12). That TGFβ induces miR-29 family expression suggests that there are may be several TGFβ-triggered signalling pathways, apart from TGFβ-SOX9, regulating the miRNA-29 expression. However, in this project, the molecular mechanisms by which TGFβ controls expression of the miR-29s are again not fully understood.

The TLR4 ligand, LPS, was found to repress the miR-29 family expression in chondrocytes. Importantly, this inhibition was facilitated by NFκB (p50/p65). Supporting the finding of this study, published data in cholangiocarcinoma cells and murine hepatic stellate cells also showed that LPS down-regulated expression of the miR-29 family (Mott et al. 2010, Roderburg et al. 2011) . Moreover, NFκB, activated by TLR ligands, was revealed to both directly or indirectly (cooperating with YY1) suppress the miR-29a/b1 or the miR-29b2/c locus, respectively (Wang et al. 2008, Mott et al. 2010). In contrast to LPS, it was surprising to find that IL-1β increased miR-29 expression and this stimulation was not NFκB but p38-dependent. However, the effect of inhibiting p38 signalling was only observed for miR-29a and miR-29b but not miR-29c, although all miR-29 family members were found strongly induced by IL-1β. Since IL-1β could activate the NFκB signalling pathway alongside p38 MAPK signalling (Aigner et al. 2006), the fact that an NFκB inhibitor further increased the IL-1 induction of the miR-29a/b1 locus implicates NFκB signalling in suppressing miR-29. It is likely that in human chondrocyte, for the period of time examined (48 hours), induction through 38 MAPK signalling was dominant over the NFκB, explaining why IL-1β induced (not suppressed) miR-29 expression. It therefore, made sense to expect a similar induction of the proximal promoter of miR-29a/b1 by IL-1β. However, a suppressive effect was observed. These data could be explained if the inductive p38-dependent transcription factors do not work through this 2kb proximal promoter of the miR-29a/b1, whilst several binding sites of NFκB in this promoter region are seen. This hypothesis needs experimental data to validate it. The mechanism responsible for the IL-1β induced miR-29b2/c cluster is still unclear and needed to be further explored. Notably, the IL-1β mRNA expression level was increased by

LPS/ TLR-4 and this is mediated by p38 MAP kinase in human chondrocytes (Bobacz *et al.* 2007). Therefore, that the miR-29 family expression was increased after 48 hours treatment with LPS could be explained in part by the accumulation of IL-1β which in turn up-regulated the miR-29 family expression.

This study also showed that the expression of all miR-29 members was not modulated by Wnt3a (β-catenin, canonical Wnt signalling), neither at the mRNA level by qRT-PCR or in the promoter assay. There are, several publications which have reported that either some members or the whole miR-29 family were Wnt3a-induced: In osteoblasts, Wnt3a positively modulates the expression of miR-29a and miR-29c though two T-cell factor/LEF-binding sites within the miR-29a/b1 promoter (Kapinas et al. 2009, Kapinas et al. 2010); in muscle progenitor cells (MPCs), Wnt3a treatment increased miR-29s expression in a time dependent manner (Hu et al. 2014); the promoter activities of both the miR-29a/b1 and miR-29b2/c cluster were strongly induced in MPCs where Wnt3a was overexpressed or added to media (Hu et al. 2014).Therefore, an interesting question that remains to be answered is why miR-29 expression is not modulated by Wnt3a in chondrocytes.

In contrast to the rapid change in expression of the pri-miR-29 or pre-miR-29 in response to stimuli, the modulation of the miR-29 family mature is quite slow. The posttranscriptional processing from the precursor to the mature form of the miR-29 family may be tightly controlled. Since the miR-29s has significant impact on a functional phenotype by regulating multiple genes that fall into the same or related pathways (which will be discussed more in Chapter 5), its expression must be regulated, potentially at more than one level. Interestingly, herein, Dicer was found to be the direct target of the miR29 family, suggesting a negative feedback loop for its maturation. In supporting this data, in T47D breast cancer cells, Dicer 1 was also reported as a miR-29a target (Cochrane *et al.* 2010). Apart from Dicer, other components of the microRNA precursor processing machinery e.g. Helicase, Exportin 4 and 5 are also predicted to be putative targets of the miR-29s as they have several binding sites in their 3'UTR regions (data not shown). Even though these have not been experimentally validated as the direct targets, this further supports the idea that miR-29 is involved in a negative feedback loop for its maturation.

In conclusion, the miR-29 family was found to be negatively regulated by the master regulator of chondrogensis SOX9, by TGFβ signalling and by LPS-NFκB signalling. It is

positively regulated by IL-1-p38 MAPK signalling. Interestingly, the canonical Wnt signalling pathway does not control expression of the miR-29 family. Furthermore, expression of the miR-29 family was tightly controlled at the level of posttranscriptional processing in which miR-29 directly targets Dicer, giving a negative feedback loop for its maturation.

CHAPTER 5
FUNCTIONS OF THE MICRORNA 29 FAMILY IN CHONDROCYTES

5.1 Introduction

The ability of a single miRNA to target multiple mRNAs especially those that function in the same intracellular pathways and/or diseases, adds an additional layer of regulation to gene expression. The aberrant expression of the miR-29 family has been found in multiple malignancies and fibroses, carcinogenesis. Also, an understanding of how miR-29 contributes to these processes has been revealed: miR-29 targets genes are involved in cellular proliferation, cell cycle, cell differentiation, and apoptosis at genetic and epigenetic levels. The following summarizes some functions of miR-29s in human disease.

In chondrogenesis or OA, around 30 miRNAs have been shown to have functions in cartilage homeostasis (Le et al, 2013), which is relatively small compared to the total number of miRNAs. Moreover, as mentioned in the previous chapter, for any potential miRNA therapeutic application, a combination of different miRNAs might be required for a complex disease like OA. Identifying novel miRNA targets and the cell signalling pathways and networks by which miRNAs exert their functions on disease phenotype are therefore, of particular importance both to have an insight into OA pathogenesis and also to ensure the specificity in any miRNA-based drug delivery method. Thus, this chapter places emphasis on identifying the function of the miR-29 family in chondrocytes including identifying the function of the miR-29 family in TGFβ/Smad, NFκB, and Wnt/β-catenin signalling pathways and novel targets of the miR-29s.

Aims:

- Investigate signalling pathways involved in chondrogenesis and osteoarthritis which are regulated by the miR-29 family
- Perform gain-and-loss of function of miR-29b experiments to identify potential targets of the miR-29 family
- Identify and validate novel direct targets of the miR-29 family

5.2 Results

5.2.1 The miR-29 family supress TGFβ/Smad signalling pathway

In articular cartilage, the canonical TGFβ/Smad signalling pathway has been shown to play a pivotal role in the maintenance of normal cartilage: it up-regulates the expression of several types of collagens and proteoglycan; and it down-regulates cartilage degrading enzymes. Importantly, disruption of the TGFβ pathway has been shown to lead to OA. Mice expressing a dominant negative TGFβRII exhibit articular cartilage degeneration similar to that observed in human OA with abnormal expression of type X collagen, an indicator of chondrocyte hypertrophy; mutant mice with targeted disruption of Smad3 (Smad3−/−) show a similar pathology in chondrocytes, including aberrant type X collagen expression in vivo; primary chondrocytes isolated from Smad3−/− mice demonstrate an accelerated differentiation process with up-regulated BMP signalling.

In Chapter 4, expression of the miR-29 family was found to be suppressed by TGFβ signalling. Here, I measure the impact of the miR-29 family on Smad signalling. The TGFβ/Smad signalling reporter (CAGA)12-luc (Figure 5.1a) containing 12 binding sites of the Smad2/3/4 (GAGAC) binding site upstream of the firefly luciferase-encoding gene was used. The principle of this experiment is based on the fact that: signals are transduced from TGFβ ligands to the Smad2/3/4 complex which subsequently regulates gene expression; the miR-29 family may change the expression or transcriptional activity of Smad2/3/4; thus altering luciferase levels. $(CAGA)_{12}$-luc (100ng) and Renilla (10ng) were co-transfected with either miR-29 mimic (50nM) or non-targeting control (50nM) into SW1353 cells for 24 hours and followed by serum starvation for another 24 hours. Cells were then treated with either TGFβ1 or TGFβ3 (4ng/ml) for another 6 hours before measuring the luciferase activity. Luciferase assay data (Figure 5.1b) showed that: stimulating cells with TGFβ1 strongly induced luciferase activity as compared with non-treatment control; pre-treatment with all members of the miR-29 family significantly decreased the luciferase activity at this 6 hour time point. A similar pattern was observed when treating cells with TGFβ3 (Appendix, Figure 7a). These data demonstrate that Smad signalling was successfully activated in SW1353 cells by TGFβ1or TGFβ3 and that the miR-29 family is a negative regulator of this signalling. As all miR-29 family members supressed the signalling, an experiment using only an inhibitor of miR-29b (50nM) was performed. Consistent with the mimic data above,

luciferase activity was significantly increased with the miR-29b inhibitor compared to control (Figure 5.1c and Appendix, Figure 7b).

The suppressive effect of the miR-29 family on the TGFβ signalling pathway was further confirmed by measuring the effect of the miR-29 family on a TGFβ responsive gene. ADAMTS4 was chosen since it is induced by TGFβ in chondrocytes, but was not a putative direct target of the miR-29 family. Human primary chondrocytes were transfected with miR-29 family mimics (50nM) in monolayer for 24 hours with 10% (v/v) FCS. The media was then replaced with media with 0.5% (v/v) FCS for another 24 hours before stimulating with TGFβ (4ng/ml) for a further 6 hours. The expression of ADAMTS4 was measured by qRT-PCR (Figure 5.2) showing that ADAMTS4 was strongly induced by TGFβ; the miR-29 mimics significantly decreased the expression of ADAMTS4 as compared with non-targeting control. These data again confirmed the suppressive effect of the miR-29 family on TGFβ signalling pathway.

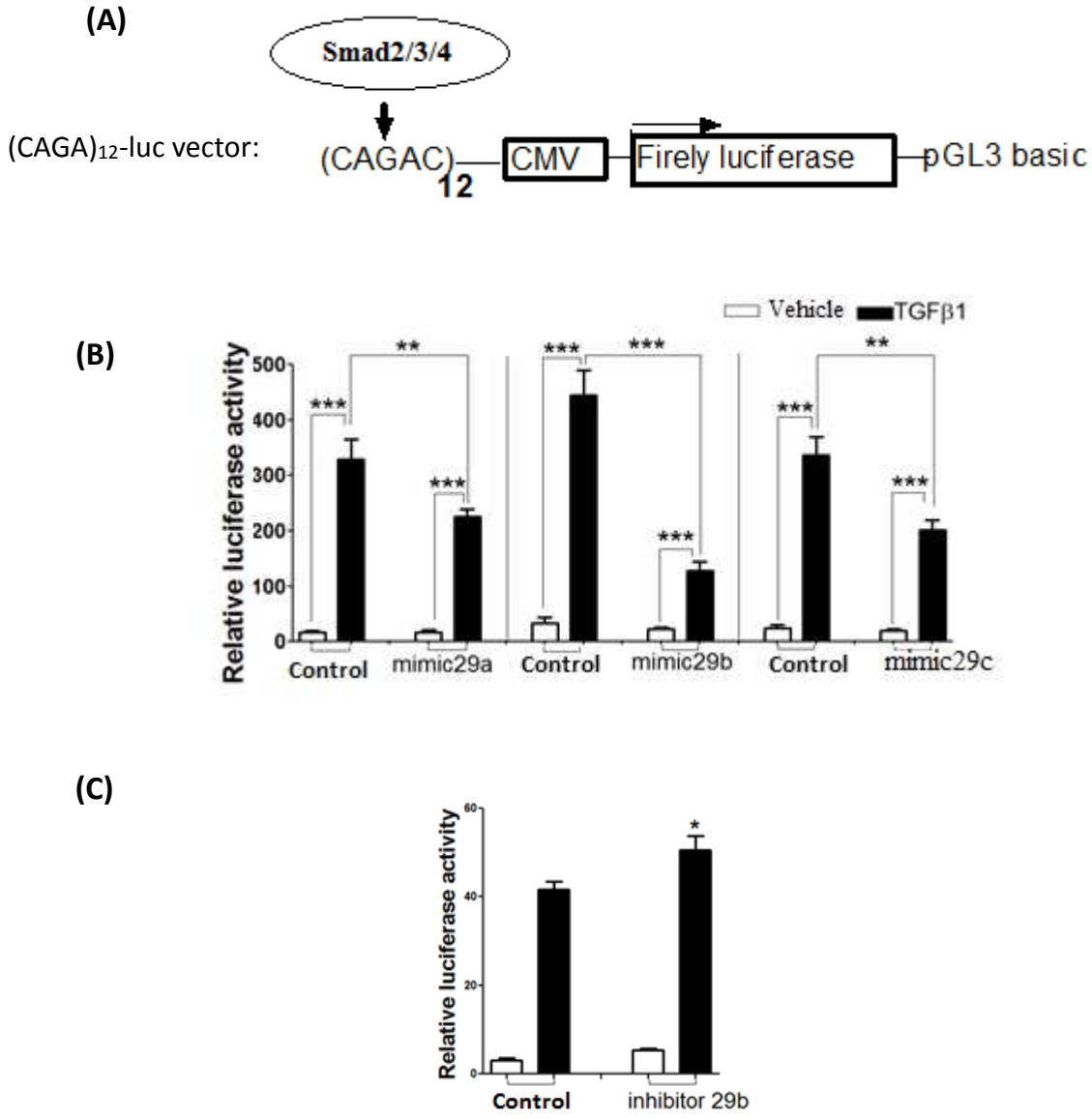

Figure 5.1 The miR-29 family suppress TGFβ signalling pathway

(A) The TGFβ signalling reporter ($CAGA_{12}$-luc) contains 12 binding sites of the Smad2/3/4 (GAGAC) binding consensus upstream of the firely luciferase-encoding gene in pGL3100ng $CAGA_{12}$-luc vector, and 10ng Renilla vector were co-transfected with either miR-29 family mimic (B) or miR-29b inhibitor (C) into SW1353 cells in monolayer. The non-targeting control (50nM) was also used as the negative control. 24 hours after transfection, cells were serum starved for another 24 hours, followed by treatment with TGFβ (4ng/ml) for another 6 hours before measuring luciferase activity. Renilla is the loading control for luciferase assay. Open bar: non – treatment control, close bar: TGFβ treatment. Means ± standard errors are presented, n=6. The difference of luciferase activity was analysed by Student's unpaired two-tailed t test. * $p<0.05$, ** $p < 0.01$, *** $p<0.001$

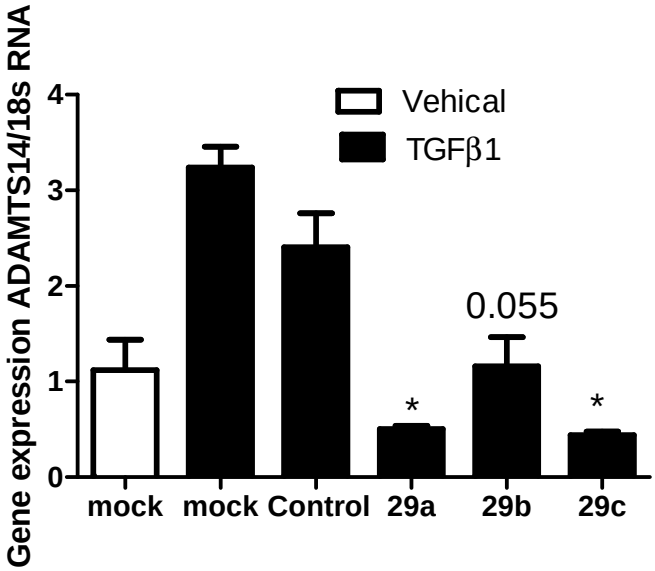

Figure 5.2 The miR-29 family suppresses the TGFβ induced gene ADAMTS4

Human primary chondrocytes were transfected with either miR-29 family mimics (50nM) or non – targeting control (50nM) for 24 hours. Cells were then changed into 0.5% (v/v) FCS for 24 hours and followed by stimulating with TGFβ1 (4ng/ml) for another 6 hours. Total RNA was isolated and the expression level of ADAMTS4 was measured by qRT-PCR. 18S rRNA was used as the endogenous control. Data were normalized to untreated, mock transfected cells. Open bar: non – treatment control, close bars: TGFβ treatment. Means ± standard errors are presented, n=3. The difference in expression level of ADAMTS was analysed by Student's unpaired two-tailed t test. * $p<0.05$, ** $p < 0.01$, *** $p<0.00$

5.2.2 The miR-29 family suppresses the NFκB signalling pathway

In Chapter 4, IL-1β was found to increase expression of the miR-29 family. It is, therefore, of importance to investigate how the miR-29 family regulates the signalling pathways triggered by IL-1β. There are at least three pathways triggered by IL-1β including NFκB, JNK, and p38 MAPK pathways. Nevertheless, in this project, just the interaction between the miR-29 family and NFκB signalling was investigated. The transcription factor NFκB is held in the cytoplasm in an inactive form associated with the inhibtory κB (IκB) protein. In response to IL-1β binding of the receptor, NFκB releases from IκB and the activated NFκB will then translocate to the nuclear, bind to DNA elements present in its target genes and facilitate their transcription.

Similar to the experiment for investigating the interacting between the miR-29 family and TGFβ signalling, the NFκB signalling reporter containing multiple binding sites for NFκB upstream of a luciferase-encoding gene was utilized (Figure 5.3a). The signal cascade from IL-1β will activate NFκB which consequently induces the transcription of the luciferase gene in the reporter and this may be modulated by the miR-29 family. The luciferase assay was set up similar to the experiment in 5.1.1 except the cells were treated with IL-1β (5ng/ml) instead of TGFβ1 (4ng/ml). Luciferase data (Figure 5.3b, c) showed that IL-1β strongly induced the luciferase activity of the κB reporter; all miR-29 family mimics significantly decreased activity (B) but the miR-29b inhibitor induced activity (C). These data show that NFκB signalling was successfully triggered in SW1353 cells by IL-1and that the miR-29 family is a negative regulator of the NFκB signalling pathway.

The suppressive effect of the miR-29 family on the NFκB signalling pathway was further confirmed by measuring the effect of the miR-29 family on an NFκB responsive gene. MMP3, which is induced expression by IL-1 and is not a putative direct target of the miR-29 family, was chosen. Again, the experiment was set up similar to the experiment in 5.1.1 except cells were stimulated with IL-1 (5ng/ml). The Taqman qRT-PCR (Figure 5.4) showed that MMP3 was strongly induced expression by IL-1β; the miR-29b and miR-29c mimics significantly decreased the expression of MMP3 as compared with non-targeting control, though the miR-29a mimic had no effect.

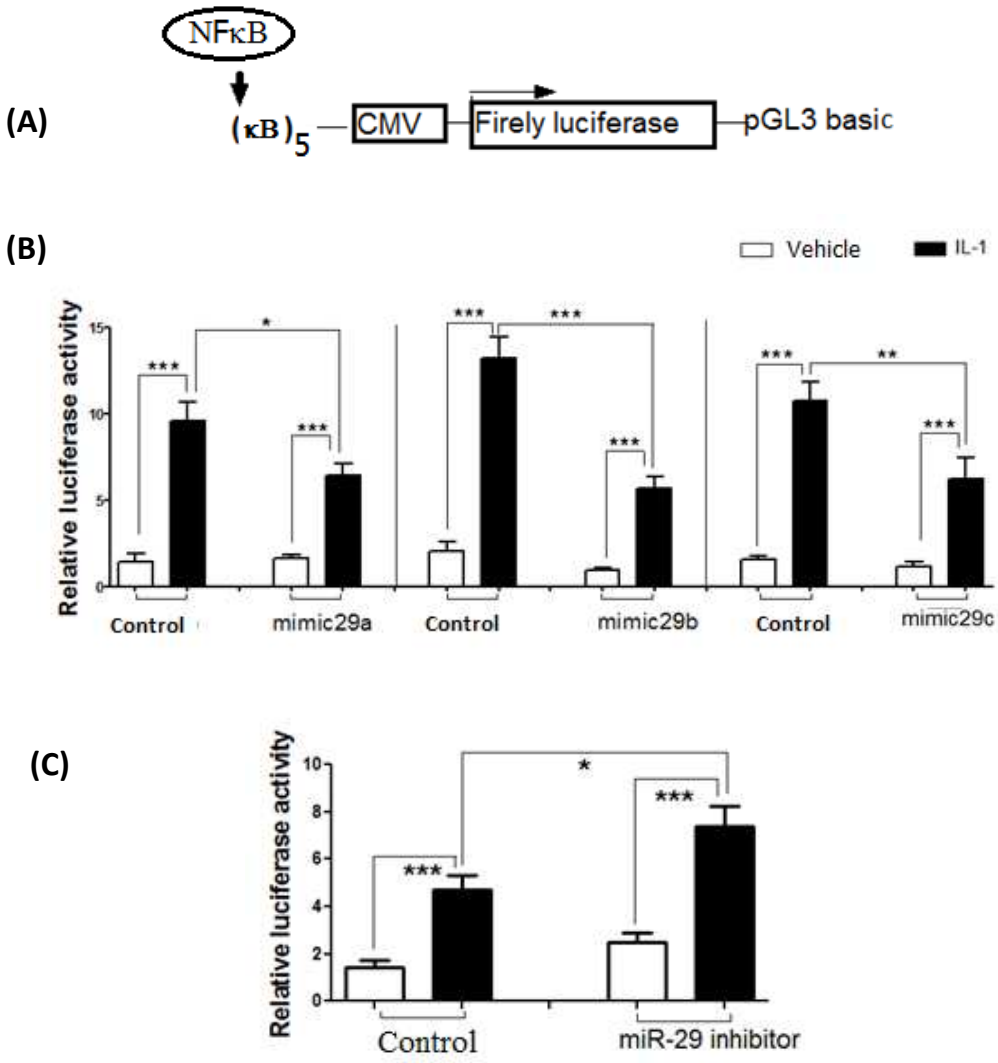

Figure 5.3 The miR-29 family suppresses NFκB signalling pathway

(A) The NFκB signalling reporter (κB vector) contains 5 binding sites of NFκB upstream of the firely luciferase-encoding gene in pGL3

100ng κB vector, and 10ng Renilla expression vector were co-transfected with either miR-29 family mimic (B) or miR-29b inhibitor (C) into SW1353 cells in monolayer. The non-targeting control (50nM) was also used as a negative control. 24 hours after transfection, cells were serum starved for further 24 hours, and followed by treating with IL-1 (5ng/ml) for another 6 hours before measuring luciferase activity. Renilla is the endogenous control for luciferase assay. Means ± standard errors are presented, n=6. The difference of luciferase activity was analysed by Student's unpaired two-tailed t test. * $p<0.05$, ** $p < 0.01$, *** $p<0.001$

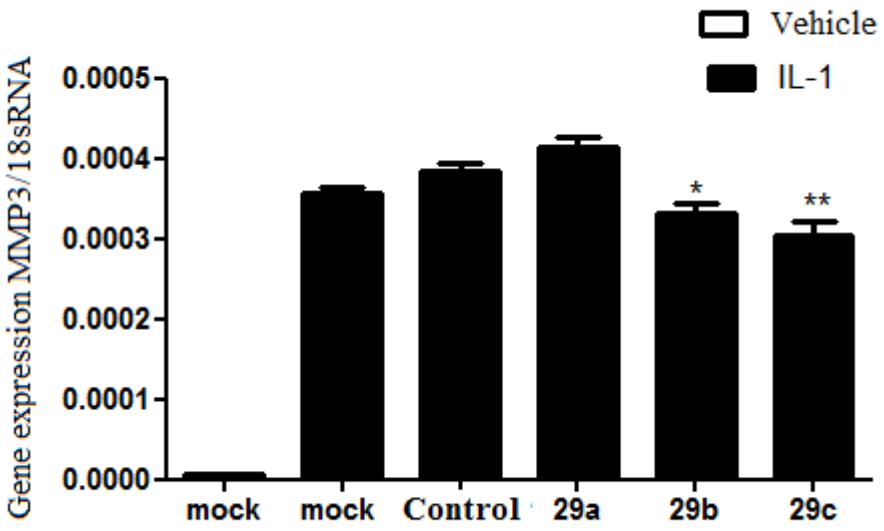

Figure 5.4 The miR-29 family suppresses expression of the IL-1-induced gene MMP3
Human primary chondrocytes were transfected with either miR-29 family mimic (50nM) or non – targeting control (50nM) for 24 hours. Cells were then changed into 0.5% (v/v) FCS for 24 hours, followed by stimulating with IL-1β (5ng/ml) for a further 6 hours. Total RNA was isolated and the expression of MMP3 was measured by qRT-PCR. 18S rRNA expression was used as the housekeeping gene. Open bar: non – treatment control, close bar: IL-1β treatment. Means ± standard errors are presented, n=3. The difference in expression level of IL-1β was analysed by unpaired two-tailed t test. * $p<0.05$, ** $p < 0.01$, *** $p<0.001$

5.2.3 The miR-29 family supresses the canonical Wnt signalling pathway

Even though expression of the miR-29 family is not regulated by Wnt3a in human chondrocyte, it is still of interest to investigate whether the WNT/β-catenin signalling is modulated by the miR-29 family because of the critical role of this signalling in OA development: balanced β-catenin levels are essential for maintaining homeostasis of articular cartilage and any factors impairing this balance could lead to pathological changes.

For investigating the interaction between the miR-29 family with the WNT/β-catenin signalling, the TOPFlash reporter (containing 7 binding sites of TCF/LEF driving the expression of the luciferase encoding gene) and FOPFlash reporter (control for TOPFlash where all the TCF/LEF binding sites are mutated) were used (Figure 5.5a). With the presence of e.g. Wnt3a, the signal transduced from the FZD receptor and LRP-5/6 co-receptor proteins will lead to the accumulation of β-catenin in the nucleus where it acts in concert with TCF/LEF transcription factors to generate a transcriptionally active complex inducing the expression of cognate genes and also therefore the TOPFlash reporter. Thus, any modulation of luciferase activity in the presence of the miR-29 family indicates that the miRNA family impacts on canonical signalling. Again the luciferase assay experiment was set up similarly to the assay in 5.1.1 but the TOPFlash (100ng) or FOPFlash (100ng) and Wnt3a (50ng/ml) were utilized. Luciferase assay data (Figure 5.5b, c) showed that Wnt3a strongly induced the luciferase activity from TOPFlash but not FOPFlash reporters; all members of the miR-29 family significantly decreased luciferase activity, whilst a miR-29b inhibitor increased the luciferase activity compared to control. These data show that the WNT/β-catenin pathway was induced in SW1353 cell with Wnt3a and that the miR-29 family is a negative regulator of this signalling.

The suppressive effect of the miR-29 family on the WNT/β-catenin signalling pathway was further confirmed by measuring the effect of the miR-29 family on the expression of *AXIN2*, a WNT/β-catenin responsive gene and not a putative direct target of the miR-29 family. The experiment was set up similarly to the experiment in 5.1.1 except cells were stimulated with Wnt3a (50ng/ml). The qRT-PCR data (Figure 5.6) showed that *AXIN2* expression was strongly induced by Wnt3a; the miR-29 family mimics significantly decreased the expression of *AXIN2* as compared with non-targeting control.

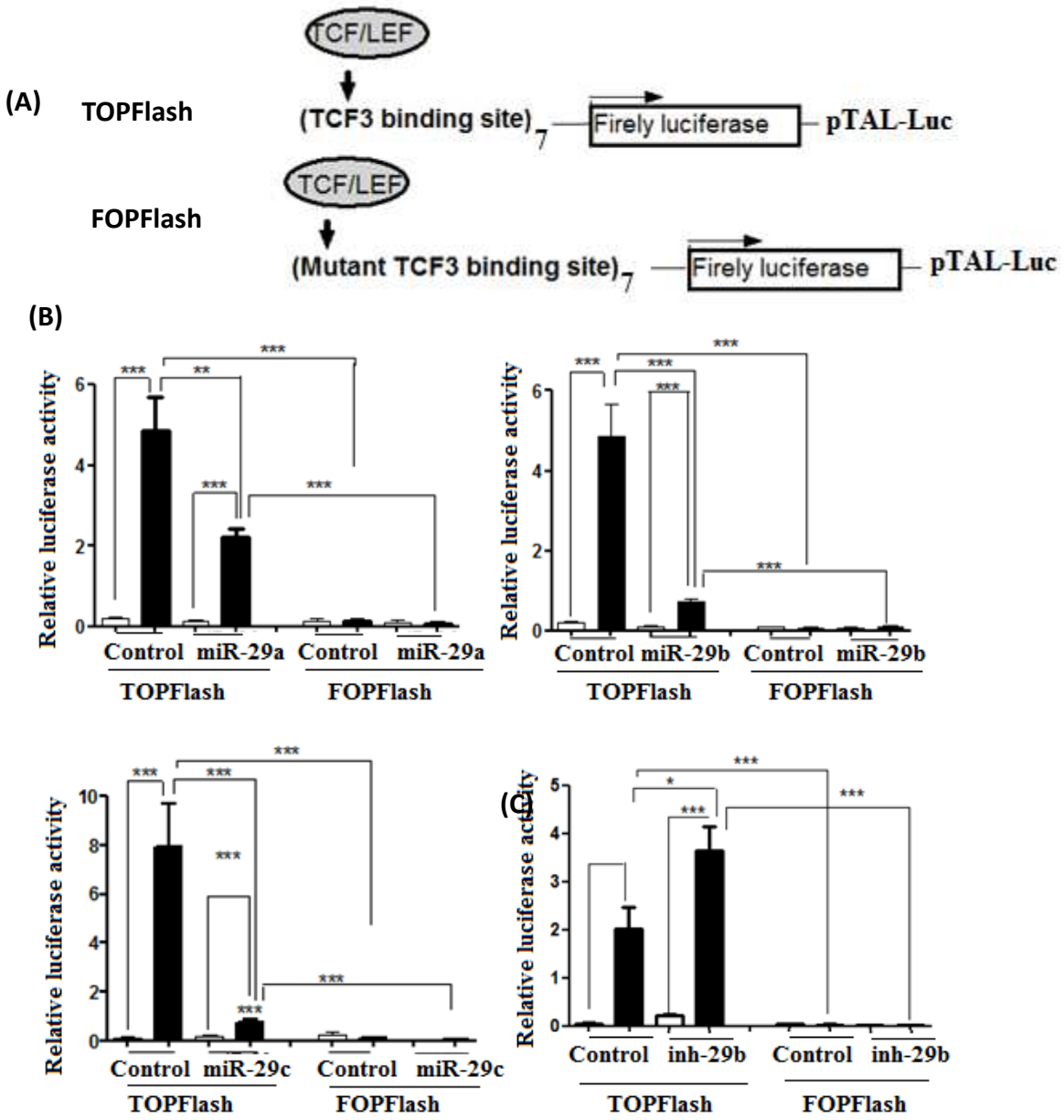

Figure 5.5 The miR-29 family suppresses the WNT/β-catenin signalling pathway

(A) The canonical WNT signalling reporter (TOPFlash vector) contains 7 binding sites of TCF/LEF upstream of the firely luciferase encoding gene in the pTAL-Luc vector. The FOPFlash vector is the control in which all binding sites of TCF/LEF are mutated.

100ng TOPFlash or FOPFlash vectors, and 10ng Renilla vector was co-transfected with either miR-29 family mimic (50nM) (B) or miR-29b inhibitor (50nM) (C) into SW1353 cells in monolayer. The non-targeting control (50nM) was also used as the control. 24 hours after transfection, cells were serum starved for another 24 hours, and followed by treatment with WNT3a (50ng/ml) for another 6 hours before measuring luciferase activity. Renilla is the endogenous control for luciferase assay. Means ± standard errors are presented, n=6. The difference of luciferase activity was analysed by Student's unpaired two-tailed t test. * $p<0.05$, ** $p < 0.01$, *** $p<0.001$

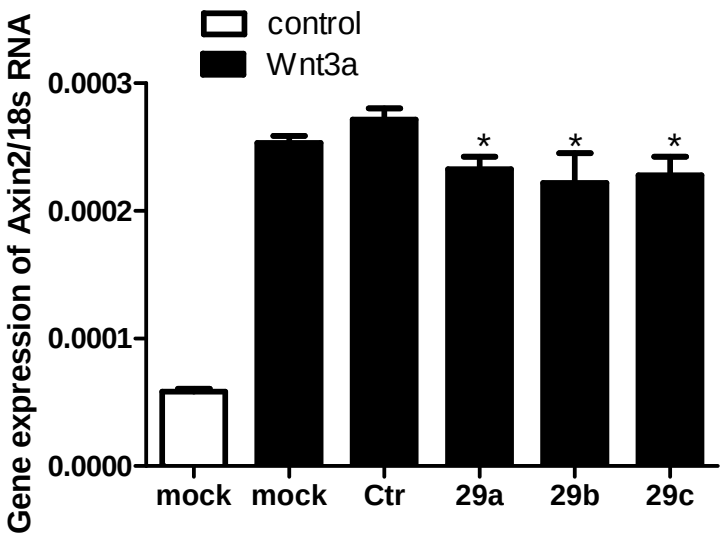

Figure 5.6 The miR-29 family suppresses expression of the WNT/β-catenin induced gene *AXIN2*

Human primary chondrocytes were transfected with either miR-29 family mimic (50nM) or non – targeting control (50nM) for 24 hours. Cells were then serum starved for 24 hours and followed by stimulating with Wnt3a (50ng/ml) for another 6 hours. The expression level of Axin2 was measured by qRT-PCR. 18S rRNA was used as the housekeeping gene. Open bar: non – treatment control, close bar: WNT3a treatment. Means ± standard errors are presented, n=3. The difference in expression level of *AXIN2* was analysed by unpaired two-tailed t test. * $p<0.05$, ** $p < 0.01$, *** $p<0.001$

5.2.4 Identification of miR-29 family targets

The miR-29 family was found to suppress the TGFβ/Smad, NFκB, and WNT/β-catenin signalling pathways. Nonetheless, it still remained unclear the direct mechanism by which the miR-29 family controlled these pathways. I therefore sought to identify novel targets of the miR-29 family to explain how the miR-29 family interacts with these pathways.

5.2.4.1 Gain- and loss- of function of miR-29b

For identifying new targets, a gain- and loss- of function experiment was performed. Since the miR-29 family shares the same seed binding site, it was deemed sufficient just to overexpress or silence miR-29b rather than all members of the family. Human primary chondrocytes were transiently transfected with miR-29b mimic or miR-29b inhibitor (50nM) and their non-targeting controls for 48 hours in triplicate and then total RNA was isolated. The transfection experiment was validated by measuring the miR-29b level by qRT-PCR. The data (data not shown) showed that the level of miR-29b strongly increased or decreased after transfection with either miR-29b mimic or inhibitor, respectively. These data suggest a good transfection efficiency into human chondrocytes. For performing a whole genome profile, an equal amount of total RNA from each sample in the triplicate was pooled together. These pooled samples were then subjected to whole genome array using Illumina human HT-12 V4.0 expression BeadChips to profile more than 47,000 human transcripts.

The global effect of the miR-29b mimic and inhibitor transfection on whole genome expression was first investigated by plotting the distribution of different expression values for all mRNAs in the miR-29b overexpression or knockdown experiments. Since the miRNA will exert its function by suppressing target gene expression, it was expected that the overexpression of miR-29b would significantly suppress target gene expression; conversely, a strong induction of target gene expression would be observed with the silencing of the miR-29b. Consistent with this hypothesis, data (Figure 5.7A) showed that in the miR-29b silencing experiment, the distribution of modulated genes was slightly skewed towards higher expression. Using an absolute 1.3 fold change (FC) as the cut off, there are 213 and 144 mRNA going up and down, respectively in this experiment (whilst just 9 and 10 mRNA going up and down respectively if the FC cut off was 1.5). Surprisingly, this pattern was also observed with the overexpression of the miR-29b (Figure 5.7B) with 703 and 518 mRNA

going up and down with 1.5 FC cut off, respectively. These data suggest that the miR-29b mimic has stronger effect than miR-29b inhibitor in chondrocytes and that the transfection with the miR-29b mimic strongly induced rather than supressed gene expression. Further analysis of the mRNAs strongly increased with miR-29b overexpression showed that the majority of these induced genes do not contain a binding site for the miR-29 family in their 3'UTR, suggesting that they are not direct targets of the miR-29 family. Indeed, a number of interferon responsive genes were strongly increased (Appendix, Table 7), suggesting a non-specific response to the synthetic oligonucleotide. This has been previously noted even for small RNAs (Karlsen et al. 2011). Interestingly, these genes were not modulated in the miR-29b silencing experiment, suggesting that a specific sequence in the miR-29b mimic is responsible.

The effect of the miR-29b mimic or inhibitor on whole genome expression was further analysed by examining the potential targets of the miR-29 family. The array data (Figure 5.8) revealed there were 12215 mRNAs in the intersection of the two experiments that increased in the miR-29b knockdown and decreased in miR-29b overexpression experiments. To further explore the effect of modulation of miR-29b on the transcriptome, the percentage of mRNAs containing seed sites (e.g. 6-mer, 7-mer, 8-mer) was calculated. It was a postulated that potential direct targets of miR-29s (those mRNA containing miR-29 seed sites) should be enriched in mRNA down-regulated by miR-29b and in mRNA up-regulated by miRNA-29b silencing. Particularly, this enrichment should be highest in genes that are decreased by miR-29b mimic and increased by miR-29b inhibitor. Data (Figure 5.8) showed that regardless of the length of the seed sequence, the percentage of mRNAs with seed sites is higher in the mRNAs which are decreased on overexpression or increased on silencing of miR-29b than in total mRNA. The percentage of mRNAs with seed sites is the highest in the intersection of the two experiments. These data confirm the hypothesis that taking the intersection containing mRNAs which decrease with the overexpression and increase with silencing of miR-29b is an effective way to filter the relevant miRNA targets.

Also, a subset of mRNA which was differentially expressed in the microarray analysis was selected for validating using RT-qPCR. Comparison of the expression levels between the microarray and RT-PCR results demonstrated a similar expression pattern between the two platforms (data not shown). These results confirmed the mRNA array data.

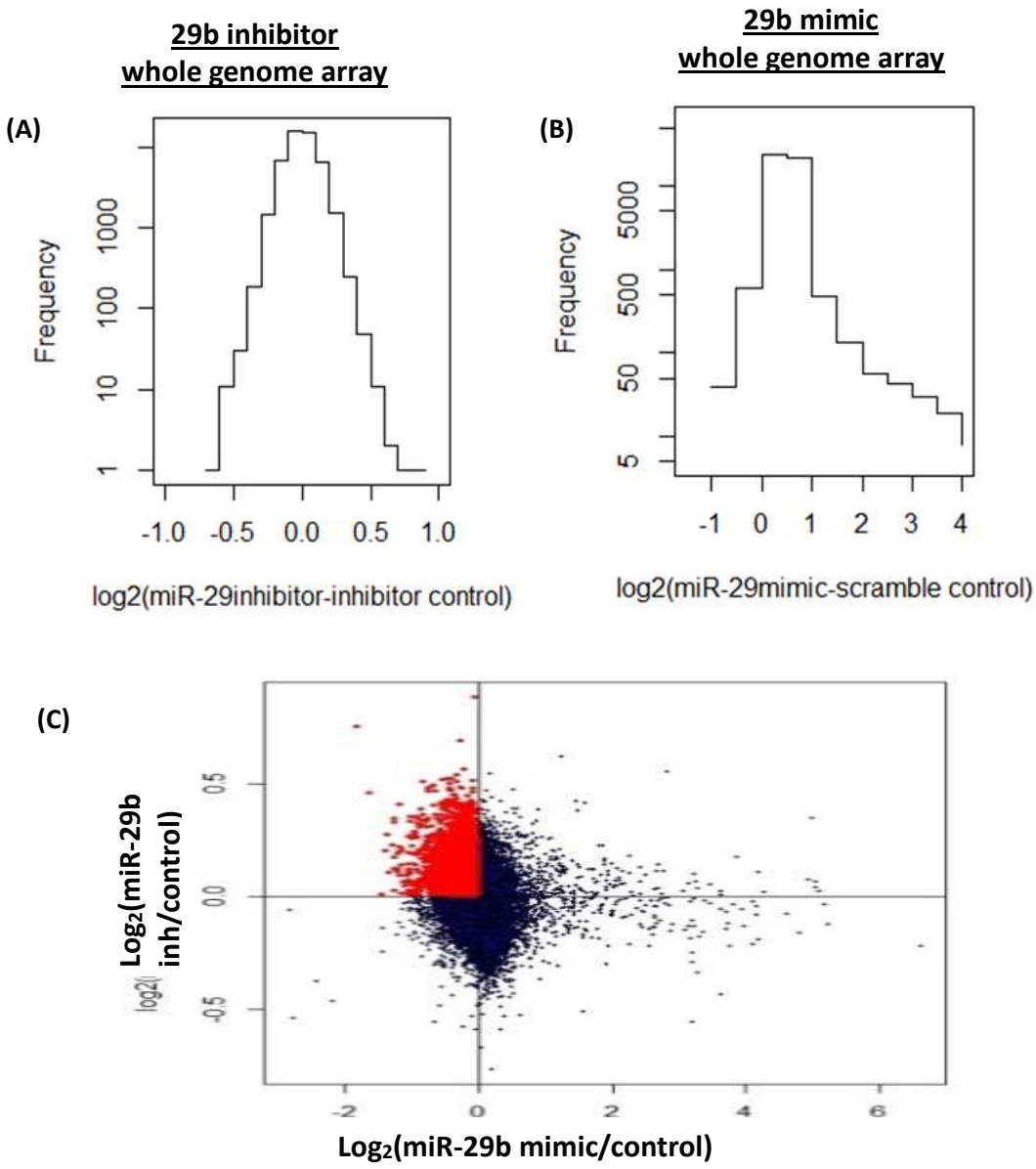

Figure 5.7 Gain- and loss- of function of miR-29b experiments

Human primary chondrocytes were cultured in high glucose media with 10% (v/v) FCS in monolayer until reaching 90% confluence. Cells were transfected with miR-29b mimic (50nM), miR-29b inhibitor (50nM), or non – targeting control (50nM) for 48 hours in triplicate. Cells were then harvested and total RNA was isolated from each sample. An equal amount of total RNA from each sample was pooled together. Pooled samples were subjected to whole genome array using Illumina humanHT-12 V4.0 expression BeadChip array. The Global effect of the miR-29b overexpression or silencing on whole genome expression was presented in (A) for the miR-29b silencing experiment and in (B) for the miR-29b overexpression experiment. Both datasets were plotted together on the same chart (C). The mRNAs which decreased in the miR-29 overexpression and increased in the miR-29b silencing experiment are highlighted in red.

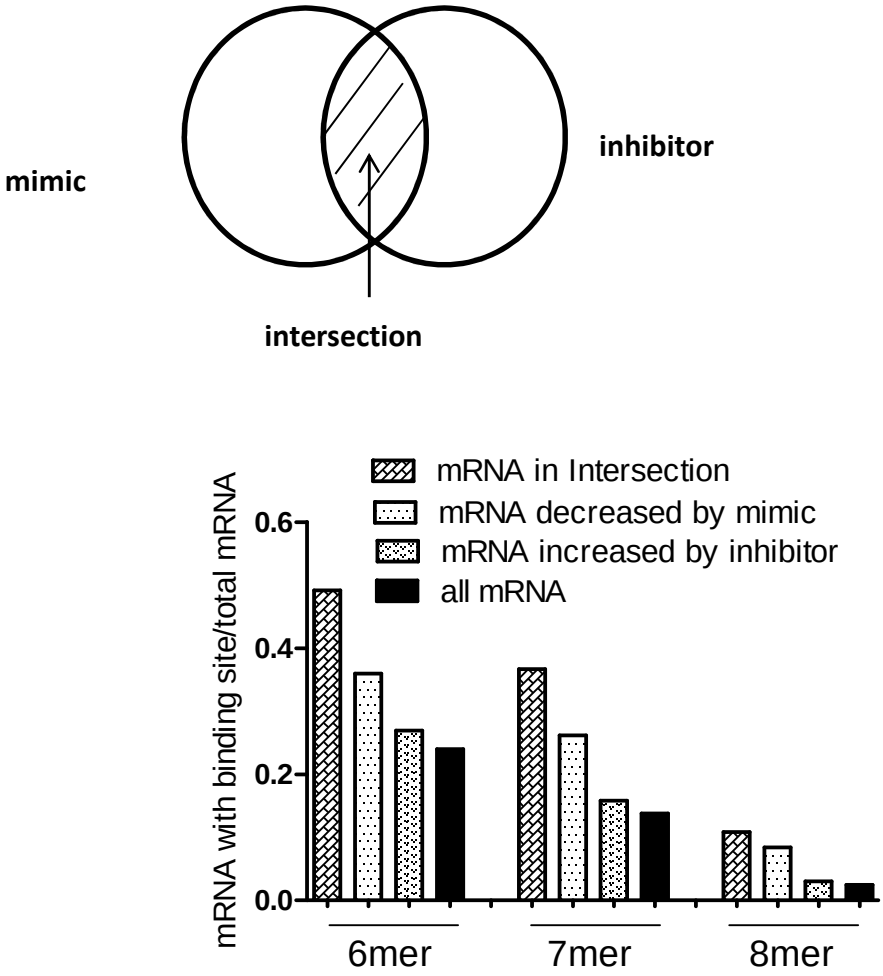

Figure 5.8: Enrichment of miR-29 putative direct targets in miR-29b gain – and loss – of function experiment.

From whole genome array data, the percentage of miR-29 putative direct targets was calculated for (i) mRNA decreased by the miR-29b mimic ; (ii) mRNA increased by the miR-29b inhibitor ; (iii) mRNA in the intersection of the two (decreased by miRN-29b mimic and increased by inhibitor) (iv) all the mRNAs detected from the whole genome array. The calculation was performed for the range of fold change (FC) and for each types of seed sequence e.g. 6-mer, 7-mer, 8-mer. The mRNA having more than one binding site for each type of seed sequence was always assigned as 1. When FC=k, the percentage of 6mer-seed-site targets increasing or decreasing expression was calculated: **6mer** = sum of mRNA having 6mer-seed site sequence in the 3'UTR with FC in the range of (k, FC max) if k >0, or (FC min, k) if k<0; **Total mRNA** = sum of mRNA with FC in the range of (k, FC max) if k>0, or (FC min, k) if k< 0; **mRNA with binding site/ total mRNA = 6mer/total mRNA.** The percentage of other seed site targets was calculated similarly. Here, calculation for the absolute FC 1.3 is presented.

5.2.4.2 Known targets of the miR-29 family

The miR-29 family has emerged as an important miRNA in a number of pathologic settings by regulating multiple genes that fall into the same or related pathways.

In the whole genome array of the overexpression and silencing of the miR-29b, a number of known direct targets of the miR-29 family were also identified in human chondrocytes (e.g. Table 5.1).

Gene	Binding sites				Fold change mimic (decrease)	Fold change inhibitor (increase)
	s6	s7m8	s7a1	s8		
COL1A1	**3**	**1**	**3**	**1**	**2.53**	**1.69**
COL1A2	**3**	**1**	**2**	**1**	**1.26**	**1.05**
COL2A1	**1**	**1**	**1**	**1**	**1.17**	**1.39**
COL3A1	**3**	**2**	**2**	**2**	**1.36**	**1.26**
COL4A1	**2**	**1**	**2**	**1**	**1.22**	**1.41**
COL5A1	**5**	**4**	**2**	**2**	**1.15**	**1.15**
COL5A2	**2**	**1**	**2**	**1**	**2.20**	**1.27**
COL6A1	**1**	**0**	**1**	**0**	**1.27**	**1.08**
COL6A2	**1**	**1**	**1**	**1**	**1.12**	**1.01**
COL6A3	**1**	**1**	**1**	**1**	**1.20**	**1.14**
COL8A1	**1**	**1**	**1**	**1**	**1.35**	**1.07**
COL11A1	**2**	**2**	**0**	**0**	**1.80**	**1.25**
COL15A1	**2**	**1**	**1**	**1**	**1.73**	**1.22**
COL16A1	**1**	**1**	**0**	**0**	**1.35**	**1.05**
COL20A1	**3**	**0**	**0**	**0**	**1.01**	**1.13**
ADAM19	**6**	**2**	**0**	**0**	**1.64**	**1.28**
CDK6	**3**	**2**	**1**	**0**	**1.61**	**1.07**

Table 5.1: Fold change expression of known targets of the miR-29 family in the miR-29b gain- and loss- of function experiment in human articular chondrocytes

5.2.4.3 Novel targets of the miR-29 family

5.2.4.3.1 The ADAMTS family

The miR-29 family is one example of the fact that a miRNA can regulate many functionally related genes. As shown above, a number of extracellular matrix-related genes were found to be direct targets of the miR-29 family. Since a miRNA can regulate the expression of several hundred genes, it was likely that the miR-29 family could directly target sets of novel genes within families. In chapter 4, TGFβ was found to suppress miR-29 family expression and the miR-29 family itself was also found to supress TGFβ signalling. These data suggest that the level of miR-29 and TGFβ-induced genes, may be inversely correlated and the miR-29 family might further inhibit the effect of TGFβ signalling on gene expression by exerting a second suppressive effect on the pathway through directly targeting inducible genes. This means that a number of TGFβ-inducible genes could potentially be direct targets of the miR-29 family. Herein, the ADAMTS family investigated as TGFβ inducible genes (except *ADAMTS 19*) (Figure 5.9) and genes which have roles in cartilage.

Human primary chondrocytes were stimulated with TGFβ1 for 24 hours in monolayer culture. The expression levels of members of the ADAMTS families were measured by qRT-PCR showing that *ADAMTS6*, *ADAMTS10*, *ADAMTS14* and *ADAMTS17* were significantly induced by TGFβ (Figure 5.9). Moreover, bioinformatic analysis found that there were a number of miR-29 binding sites in the 3'UTR regions of these ADAMTS genes (Table 5.2). Together with this, these TGFβ induced ADAMTS genes were predicted to be miR-29 potential direct targets by different bioinformatics algorithms e.g. Diana, Targetscan, Microcosm, miRDB, Picta (Table 5.2). Taken together, all of these data demonstrated that ADAMTS genes, including *ADAMTS6, ADAMTS10, ADAMTS14, ADAMTS17, ADAMTS19* are miR-29 potential direct targets.

In order to validate these ADAMTS genes as miR-29 direct targets, the expression levels of these genes were measured by qRT-PCR in human chondrocytes transfected with the miR-29b mimic for 48 hours. qRT-PCR (Figure 5.10) showed that the expression of these ADAMTS genes was significantly suppressed by overexpression of the miR-29b, again supporting that these genes are the miR-29 direct targets. To further validate these ADAMTS genes as miR-29 direct targets, the 3'UTR regions containing the miR-29 binding sties were

subcloned downstream of the luciferase encoding gene in pmiRGLO. These ADAMTS3'UTR-pmiRGLO reporter vectors (100ng) were co-transfected with the miR-29 family mimic (50nM) to DF1 cells. After 24 hours of transfection, the cells were harvested and luciferase assays were performed. Together with the ADAMTS 3'UTR-pmiRGLO reporter vectors, mutant vectors in which the miR-29 binding sites were mutated were constructed and tested. A 3'UTR was a direct target for the miR-29 family if the luciferase activity was suppressed with the overexpression of the miRNA in the wild-type construct and this effect was abolished when the miRNA binding sites were mutated. Luciferase assay data showed that *ADAMTS6* (Figure 5.14), *ADAMTS10* (Figure 5.15*), ADAMTS14* (Figure 5.11), *ADAMTS17* (Figure 5.12), *ADAMTS19* (Figure 5.13) were all direct targets of the miR-29 family.

Genes	8 -mer	7 -mer	6 -mer	Bioinformatic algorithm
ADAMTS6		2		Diana, Targetscan, Microcosm, miRDB,Picta
ADAMTS10		2		Diana, Microcosm, Picta
ADAMTS14		2	2	Diana, Picta
ADAMTS17		2	3	Targetscan, Microcosm, miRDB,Picta
ADAMTS19		2		Picta

Table 5.2: *ADAMTS6, ADAMTS10, ADAMTS14, ADAMTS17, ADAMTS19* are predicted to be miR-29 targets

A number of different binding sites for miR-29 were found in the 3'UTR regions of *ADAMTS6, ADAMTS10, ADAMTS14, ADAMTS17,* and *ADAMTS19*. These ADAMTSs were predicted to be miR-29 family targets by different bioinformatics algorithms.

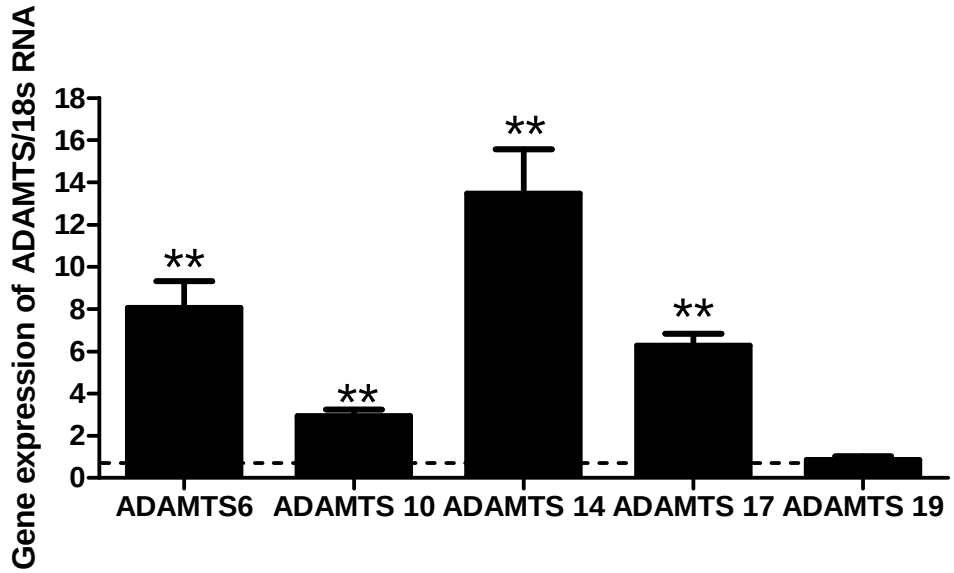

Figure 5.9 Members of ADAMTS family are TGFβ inducible genes

Human primary chondrocytes was cultured with 10% (v/v) FCS in monolayer until 90% confluence. Cells were switched to media with 0.5% (v/v) FCS for 24 hours before treating with TGFβ1 (4ng/ml) or vehicle (4mM HCl+0.5% (w/v) BSA) for another 24 hours. Cells were harvested and subjected to total RNA isolation. Relative expression of the ADAMTS genes was measured by quantitative RT-PCR. 18S rRNA was the housekeeping control. Relative expression value of each of the ADAMTSs in TGFβ stimulated cells was normalized to the vehicle control. The horizontal line at 1 serves as the vehicle control. Closed bar: TGFβ treatment, open bar: vehicle. Means ± standard errors are presented, n=3. The difference between the treatment and the control was analysed by Student's unpaired two-tailed t test. * $p<0.05$, ** $p < 0.01$, ***, $p<0.001$.

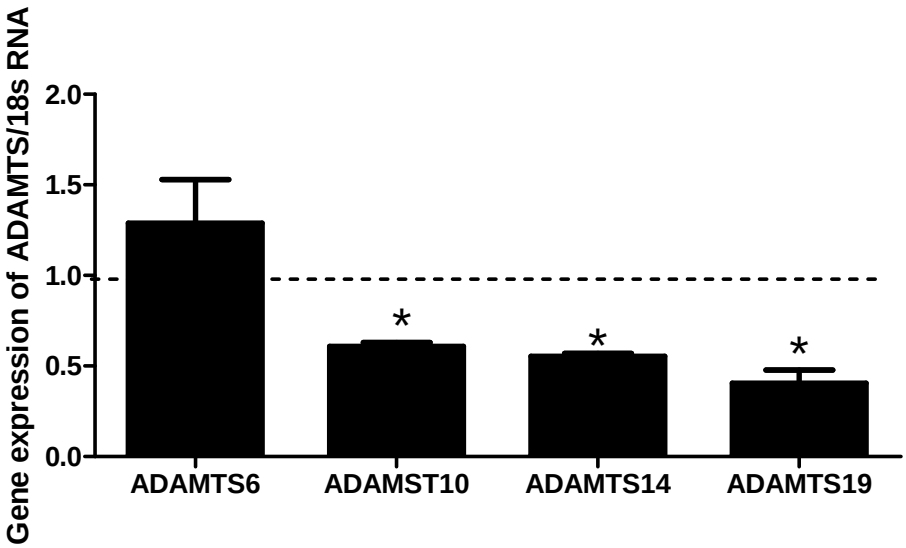

Figure 5.10 The expressions of members of the ADAMTS family were suppressed by miR-29b mimic

Human primary chondrocytes was cultured in media with 10% (v/v) FCS in monolayer until 90% confluence. Cells were then transfected with either miR-29b mimic (50nM) or non – targeting control (50nM) for 48 hours. Total RNA was isolated and the expression levels of the ADAMTS genes were measured by qRT-PCR. 18S rRNA was the housekeeping control. Relative expression value of each of the ADAMTS genes was normalized to non – targeting control. The horizontal line at 1 serves as the non-targeting control. Means ± standard errors are presented, n=3. The difference in expression between miR-29b overexpression and non – targeting control was analysed by Student's unpaired two-tailed t test. * $p<0.05$, ** $p < 0.01$, ***, $p<0.001$

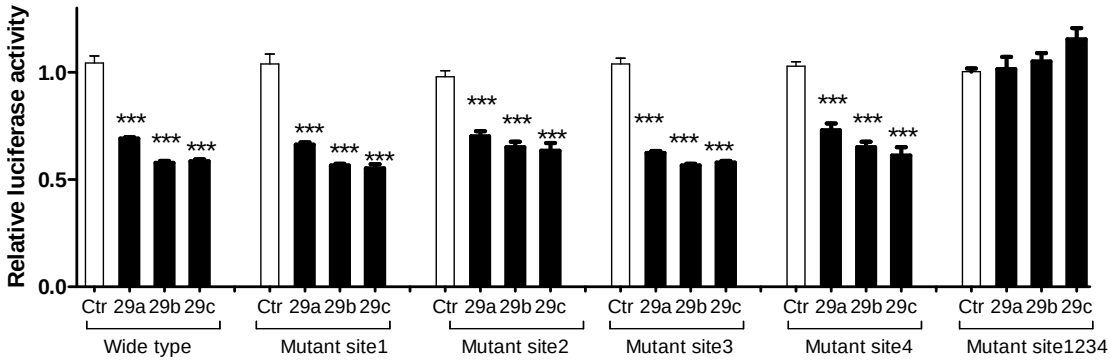

Figure 5.11: ADAMTS14 is a direct target of the miR-29 family

The ADAMTS14 3'UTR region containing 4 binding sites of the miR-29 family was subcloned downstream of the luciferase encoding gene in the pmiRGLO vector to create the ADAMTS14 3'UTR-pmiRGLO wide type (WT) vector. The mutant vectors were created from WT vector in which just single or quadruplicate binding sites of the miR-29 family were mutated. Either the WT or the mutants vectors (100ng) were co-transfected into chicken fibroblast DF1 cells with either miR-29b mimic (50nM) or non – targeting control (50nM). Luciferase assays were performed 24 hours after transfection. The relative luciferase value was normalised to the non-targetting control Open bar: non-targetting control, closed bar: miR-29 family mimic. Means ± standard errors are presented, n=6. The difference of luciferase activity was analysed by Student's unpaired two-tailed t test. * $p<0.05$, ** $p < 0.01$, *** $p<0.001$, Ctr, non-targetting control, 29a, 29b, 29c: miR-29a,-b,-c mimic.

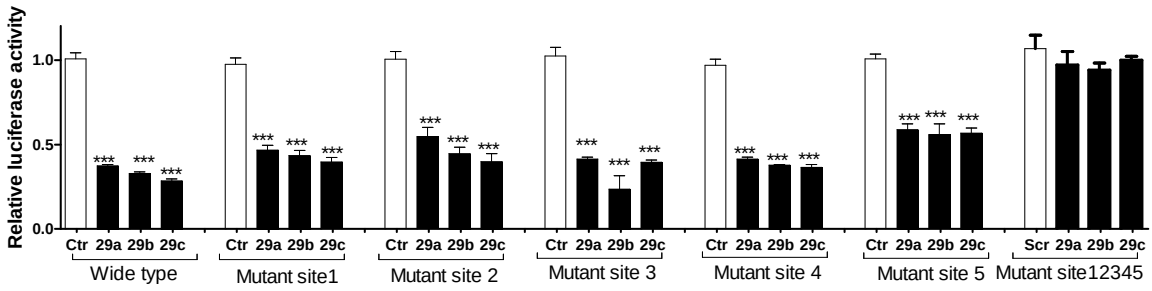

Figure 5.12: ADAMTS17 is a direct target of the miR-29 family

The ADAMTS17 3'UTR region containing 5 binding sites of the miR-29 family was subcloned downstream of the luciferase encoding gene in the pmiRGLO vector to create the ADAMTS17 3'UTR-pmiRGLO wide type (WT) vector. The mutant vectors were created from WT vector in which just single or quadruplicate binding sites of the miR-29 family were mutated. Either the WT or the mutants vectors (100ng) were co-transfected into chicken fibroblast DF1 cells with either miR-29b mimic (50nM) or non – targeting control (50nM). Luciferase assays were performed 24 hours after transfection. The relative luciferase value was normalised to the non-targetting control Open bar: non-targetting control, closed bar: miR-29 family mimic. Means ± standard errors are presented, n=6. The difference of luciferase activity was analysed by Student's unpaired two-tailed t test. * $p<0.05$, ** $p < 0.01$, *** $p<0.001$, Ctr, non-targetting control, 29a, 29b, 29c: miR-29a,-b,-c mimic.

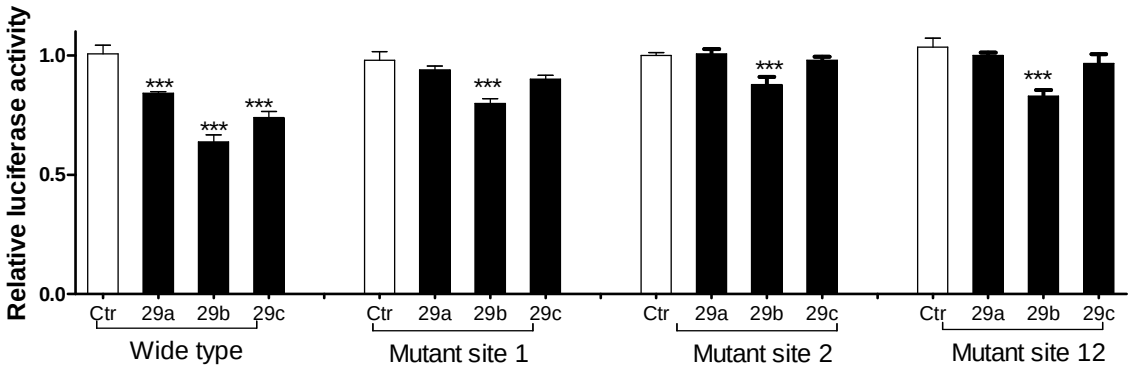

Figure 5.13: ADAMTS19 is a direct target of the miR-29 family

The ADAMTS19 3'UTR region containing 2 binding sites of the miR-29 family was subcloned downstream of the luciferase encoding gene in the pmiRGLO vector to create the ADAMTS19 3'UTR-pmiRGLO wide type (WT) vector. The mutant vectors were created from WT vector in which just single or duplicate binding sites of the miR-29 family were mutated. Either the WT or the mutants vectors (100ng) were co-transfected into chicken fibroblast DF1 cells with either miR-29b mimic (50nM) or non – targeting control (50nM). Luciferase assays were performed 24 hours after transfection. The relative luciferase value was normalised to the non-targetting control Open bar: non-targetting control, closed bar:

miR-29 family mimic. Means ± standard errors are presented, n=6. The difference of luciferase activity was analysed by Student's unpaired two-tailed t test. * $p<0.05$, ** $p < 0.01$, *** $p<0.001$, Ctr, non-targetting control, 29a, 29b, 29c: miR-29a,-b,-c mimic.

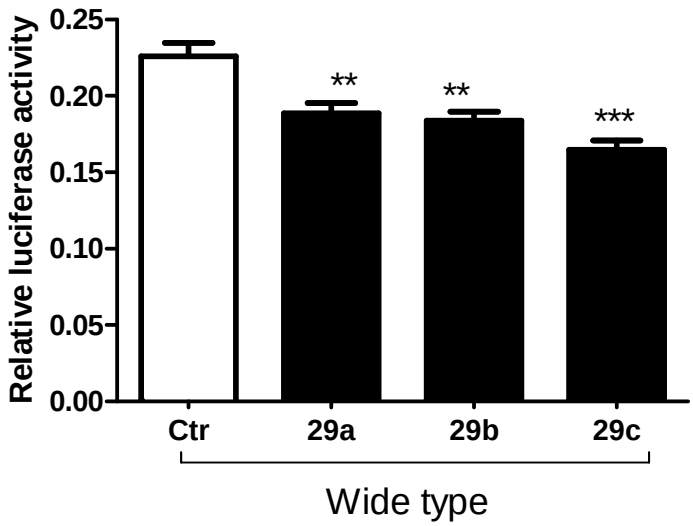

Figure 5.14: ADAMTS6 is a direct target of the miR-29 family

The ADAMTS6 3'UTR region containing 2 binding sites of the miR-29 family was subcloned downstream of the luciferase encoding gene in the pmiRGLO vector to create the ADAMTS6 3'UTR-pmiRGLO wide type (WT) vector. The WT vector (100ng) was co-transfected into chicken fibroblast DF1 cells with either miR-29b mimic (50nM) or non – targeting control (50nM). Luciferase assays were performed 24 hours after transfection. The relative luciferase value was normalised to the non-targeting control Open bar: non-targeting control, closed bar: miR-29 family mimic. Means ± standard errors are presented, n=6. The difference of luciferase activity was analysed by Student's unpaired two-tailed t test. * $p<0.05$, ** $p < 0.01$, *** $p<0.001$, Ctr, non-targeting control, 29a, 29b, 29c: miR-29a,-b,-c mimic.

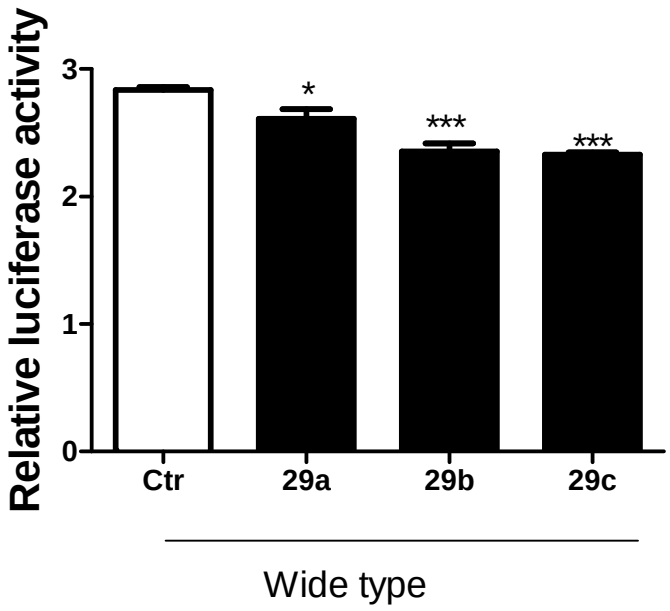

Figure 5.15: ADAMTS10 is a direct target of the miR-29 family
The ADAMTS10 3'UTR region containing 2 binding sites of the miR-29 family was subcloned downstream of the luciferase encoding gene in the pmiRGLO vector to create the ADAMTS10 3'UTR-pmiRGLO wide type (WT) vector. The WT vector (100ng) was co-transfected into chicken fibroblast DF1 cells with either miR-29b mimic (50nM) or non – targeting control (50nM). Luciferase assays were performed 24 hours after transfection. The relative luciferase value was normalised to the non-targeting control Open bar: non-targeting control, closed bar: miR-29 family mimic. Means ± standard errors are presented, n=6. The difference of luciferase activity was analysed by Student's unpaired two-tailed t test. * $p<0.05$, ** $p < 0.01$, *** $p<0.001$, Ctr, non-targeting control, 29a, 29b, 29c: miR-29a,-b,-c mimic.

5.2.4.3.2 WNT signalling pathway related genes

As shown previously, the miR-29 family was found to negatively regulate the TGFβ, NFκB, and WNT/β-catenin signalling pathways. The remaining question is how the miR-29 family supress these signalling pathways.

The whole genome array from the miR-29b gain – and loss – of function experiment found 12215 mRNAs that were the miR-29 putative targets. These consisted of 6925 mRNAs containing at least one 6-mer, 3400 mRNAs containing 7-mer, and 728 mRNAs containing 8-mer binding sites in their 3'UTR. Those mRNAs with miR-29 binding sites were considered as putative direct targets of the miR-29 family; the others without the miR-29 binding site were considered as indirect targets.

The miR-29 family suppression of TGFβ, NFκB, and WNT/β-catenin signalling pathways could be through a direct mechanism by targeting the mRNAs in the signalling cascade. In order to verify how miR-29 suppresses these signalling pathways, both putative miRNA-29 indirect and direct targets were analysed with DAVID functional analysis (web address) software to identify the most represented gene ontology (GO) categories. Analysing the miR-29 direct target sections found the enrichment for the Wnt signalling pathway together with MAPK kinase signalling pathway, apoptosis pathways, P53 signalling pathways. Since, NFκB and TGFβ pathways did not come up in this analysis, the miR-29 indirect targets were further analysed. However, neither NFκB nor TGFβ signalling pathways were enriched. In the scope of this project, the mechanisms by which the miR-29 suppressed these two signalling pathways remains unclear and need to be further explored.

All the miR-29 putative direct targets were selected regardless of the fold change cut off. In this manner, the Wnt signalling-related direct targets e.g. Dishevelled 3 (DVL3), casein kinase 2 alpha 2 polypeptide (CSNK2A2), GSK-3 binding protein frat2 (FRAT2), Frizzled family receptor 3 (FZD3), and Frizzled family receptor 5 (FZD5) were only modulated with a small fold change in the array (Fold change between 1 to 1.2). The expression of these mRNAs were measured by qRT-PCR, however in triplicate samples these data showed that the modulation of these genes under the control of the miR-29b did not reach statistical significance (Appendix, Figure 8).

Even though expression of these Wnt-related genes was not significantly modulated at the mRNA level, the genes were explored as miR-29 direct targets since miR-29 might exert its functions on these genes at the protein level. To verify these genes as the miR-29 direct targets, 3'UTR regions containing miR-29 binding sites of these genes were subcloned downstream of a luciferase encoding gene in the pmiRGLO vector. Constructs in which the miR-29 binding sites were mutated were also created. Either the 3'UTR-pmiRGLO vectors or the mutant 3'UTR-pmiRGLO vectors were co-transfected with the miR-29 family mimic (50nM) into DF1 cells for 24 hours. Then cells were harvested and the luciferase assays were performed. Luciferase assay data showed that FZD3 (Figure 5.19), FZD5 (Figure 5.18), FRAT2 (Figure 5.17), CK2A2 (Figure 5.16), DVL3 (Figure 5.15) were the direct targets of the miR-29 family since the luciferase activities were significantly decreased with the miR-29 family mimics and this effects were abolished when the miR-29 binding sites were mutated.

As mentioned above, qRT-PCR showed that the expression levels of these WNT signalling related genes were not significantly modulated with the miR-29b mimic at the mRNA level. However, the luciferase assay showed that miR-29 family could directly bind to the 3'UTR regions of these genes. It was postulated that the miR-29 family could directly target these genes at the protein level. Since all members of the miR-29 family directly targeted these genes, it was sufficient to check the effect of the miR-29b mimic on these genes at the protein level. In order to test this hypothesis, SW1353 cells were transfected with miR-29b mimic for 72 hours. Cells were then harvested and subjected to western blot. Time limitations meant that only expression levels of DVL3 were examined. Western blot data (Figure 5.15) showed that miR-29b supressed DVL3 expression level to 50% as compared to the non – targeting control, again confirming DVL3 is a direct target of miR-29 family.

Taken together, all of these data provide good evidence that the miR-29 family can inhibit the Wnt signalling, at least in part, via repression of these targets. Interestingly, DVL3, CSNK2A2 and FRAT2 were decreased in expression in hip OA cartilage compared to fracture controls, where the miR-29 family were increased in expression. Fzd3 expression however, was higher in expression in hip OA (Figure 5.20).

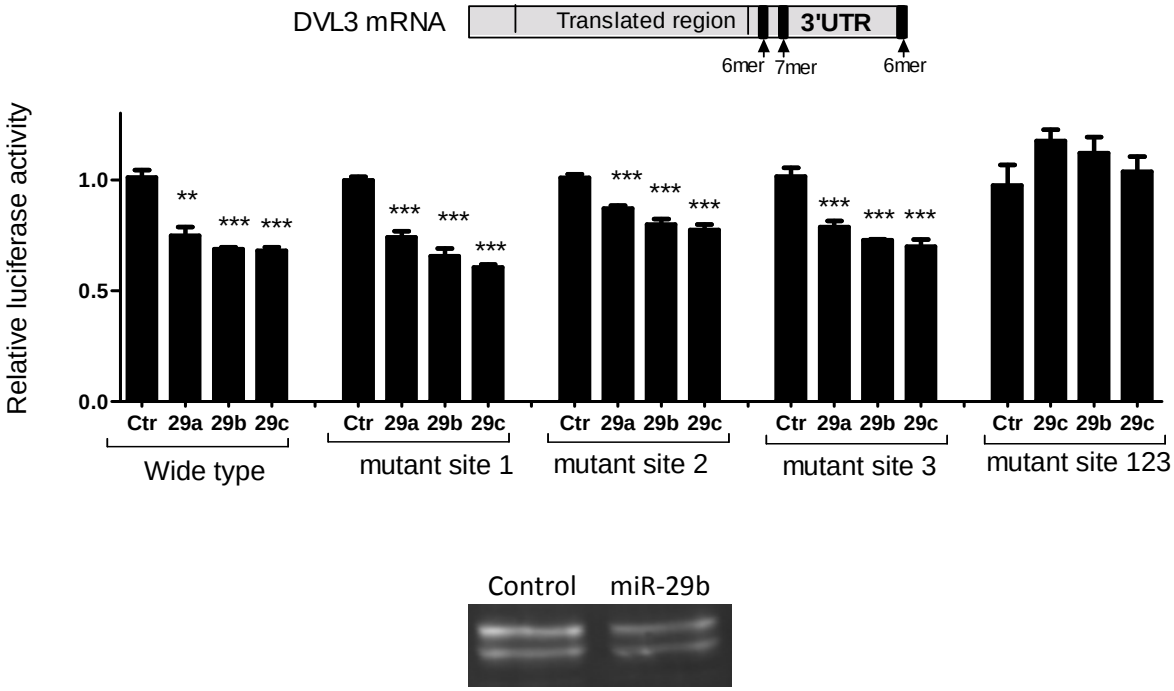

Figure 5.16: DVL3 is a direct target of the miR-29 family

(A) The DVL3 3'UTR region containing 3 binding sites of the miR-29 family was subcloned downstream of the luciferase encoding gene in the pmiRGLO vector to create the DVL3 3'UTR-pmiRGLO wide type (WT) vector. The mutant vectors were created from WT vector in which just single or triplicate binding sites of the miR-29 family were mutated. Either the WT or the mutants vectors (100ng) were co-transfected into chicken fibroblast DF1 cells with either miR-29b mimic (50nM) or non – targeting control (50nM). Luciferase assays were performed 24 hours after transfection. The relative luciferase value was normalised to the non-targetting control. Means ± standard errors are presented, n=6. The difference of luciferase activity was analysed by Student's unpaired two-tailed t test. * $p<0.05$, ** $p < 0.01$, *** $p<0.001$, Ctr, non-targetting control, 29a, 29b, 29c: miR-29a,-b,-c mimic.

(B) SW1353 was transfected with a miR-29b mimic (50nM) or non-targeting control (50nM) for 3 days. Protein was extracted and separated on 10 (w/v) SDS-PAGE, blotted onto PVDF and probed with an anti DVL3 antibody. The blot was stripped and re-probed with a GAPDH antibody to assess loading, n=2.

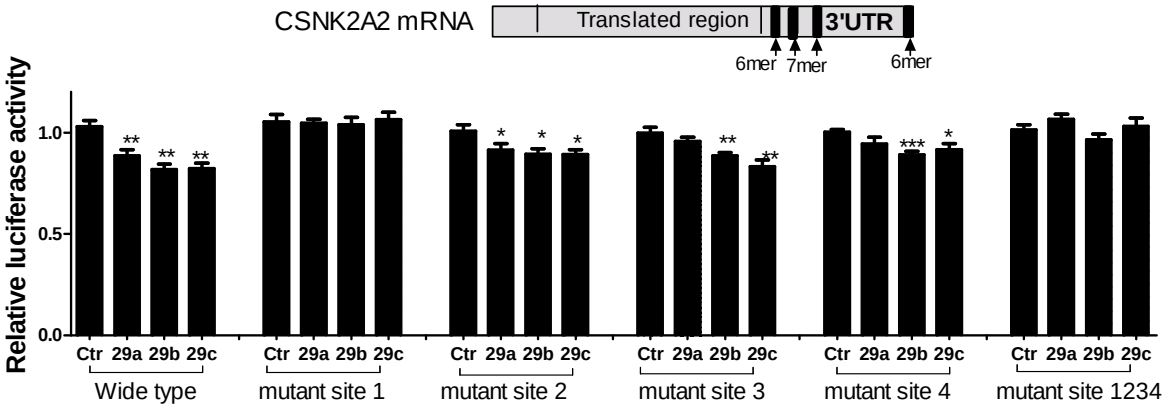

Figure 5.17: CK2A2 is a direct target of the miR-29 family

The CK2A2 3'UTR region containing 4 binding sites of the miR-29 family was subcloned downstream of the luciferase encoding gene in the pmiRGLO vector to create the CK2A2 3'UTR-pmiRGLO wide type (WT) vector. The mutant vectors were created from WT vector in which just single or quadruplicate binding sites of the miR-29 family were mutated. Either the WT or the mutants vectors (100ng) were co-transfected into chicken fibroblast DF1 cells with either miR-29b mimic (50nM) or non – targeting control (50nM). Luciferase assays were performed 24 hours after transfection. The relative luciferase value was normalised to the non-targeting control. Means ± standard errors are presented, n=6. The difference of luciferase activity was analysed by Student's unpaired two-tailed t test. * $p<0.05$, ** $p < 0.01$, *** $p<0.001$, Ctr, non-targeting control, 29a, 29b, 29c: miR-29a,-b,-c mimic.

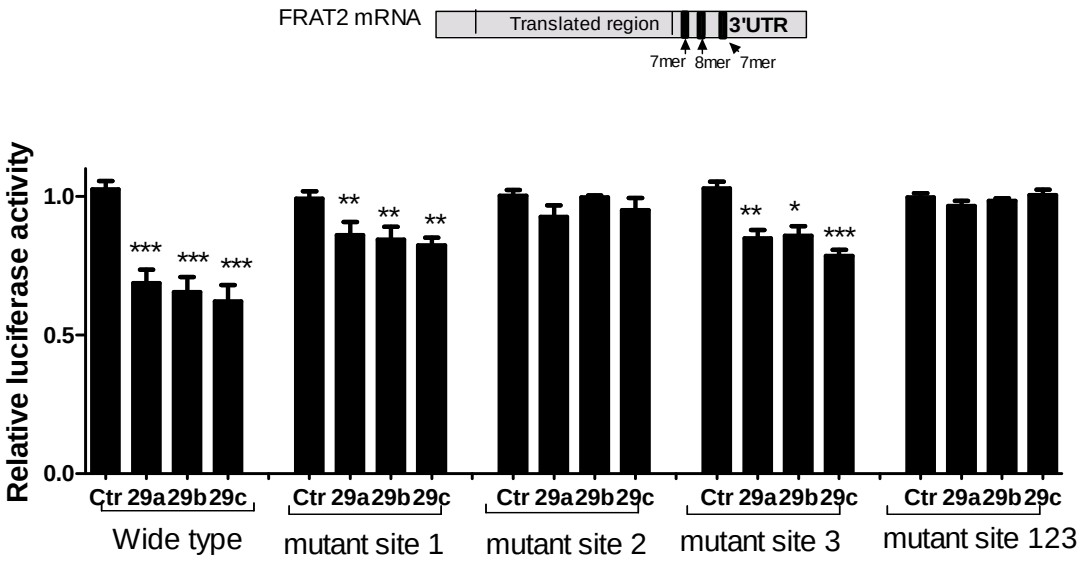

Figure 5.18: *FRAT2* is a direct target of the miR-29 family

The *FRAT2* 3'UTR region containing 4 binding sites of the miR-29 family was subcloned downstream of the luciferase encoding gene in the pmiRGLO vector to create the *FRAT2* 3'UTR-pmiRGLO wide type (WT) vector. The mutant vectors were created from WT vector in which just single or triplicate binding sites of the miR-29 family were mutated. Either the WT or the mutants vectors (100ng) were co-transfected into chicken fibroblast DF1 cells with either miR-29b mimic (50nM) or non – targeting control (50nM). Luciferase assays were performed 24 hours after transfection. The relative luciferase value was normalised to the non-targeting control. Means ± standard errors are presented, n=6. The difference of luciferase activity was analysed by Student's unpaired two-tailed t test. * $p<0.05$, ** $p < 0.01$, *** $p<0.001$, Ctr, non-targeting control, 29a, 29b, 29c: miR-29a,-b,-c mimic.

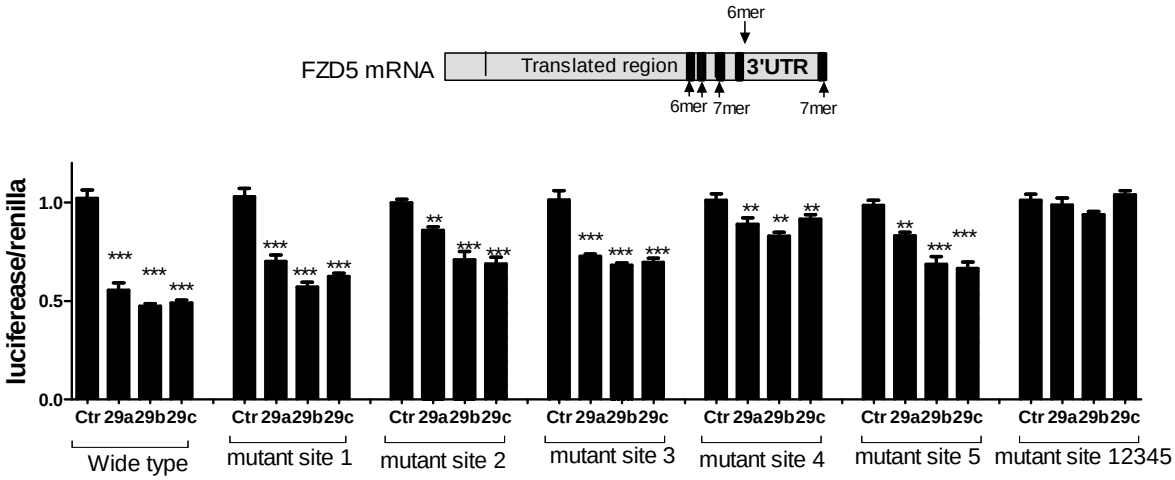

Figure 5.19: *FZD5* is a direct target of the miR-29 family

The *FZD5* 3'UTR region containing 5 binding sites of the miR-29 family was subcloned downstream of the luciferase encoding gene in the pmiRGLO vector to create the *FZD5* 3'UTR-pmiRGLO wide type (WT) vector. The mutant vectors were created from WT vector in which just single or quintuplicate binding sites of the miR-29 family were mutated. Either the WT or the mutants vectors (100ng) were co-transfected into chicken fibroblast DF1 cells with either miR-29b mimic (50nM) or non – targeting control (50nM). Luciferase assays were performed 24 hours after transfection. The relative luciferase value was normalised to the non-targeting control. Means ± standard errors are presented, n=6. The difference of luciferase activity was analysed by Student's unpaired two-tailed t test. * $p<0.05$, ** $p < 0.01$, *** $p<0.001$, Ctr, non-targeting control, 29a, 29b, 29c: miR-29a,-b,-c mimic.

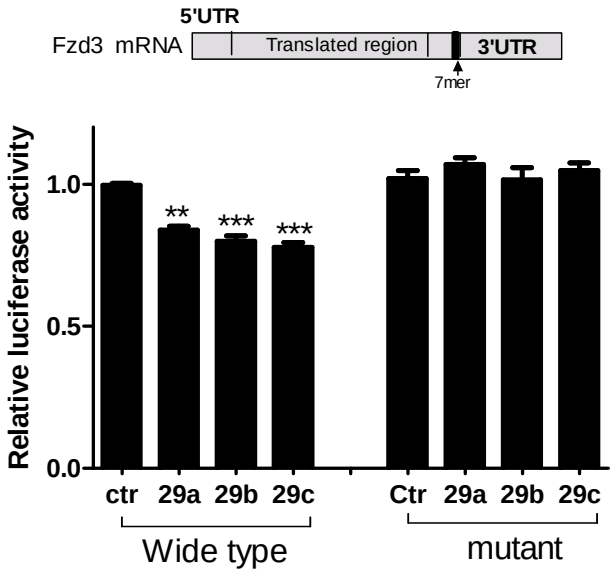

Figure 5.20: *FZD3* is a direct target of the miR-29 family

The *FZD3* 3'UTR region containing 1 binding sites of the miR-29 family was subcloned downstream of the luciferase encoding gene in the pmiRGLO vector to create the *FZD3* 3'UTR-pmiRGLO wide type (WT) vector. The mutant vectors were created from WT vector in which binding site of the miR-29 family were mutated. Either the WT or the mutants vectors (100ng) were co-transfected into chicken fibroblast DF1 cells with either miR-29b mimic (50nM) or non – targeting control (50nM). Luciferase assays were performed 24 hours after transfection. The relative luciferase value was normalised to the non-targeting control. Means ± standard errors are presented, n=6. The difference of luciferase activity was analysed by Student's unpaired two-tailed t test. * $p<0.05$, ** $p < 0.01$, *** $p<0.001$, Ctr, non-targeting control, 29a, 29b, 29c: miR-29a,-b,-c mimic.

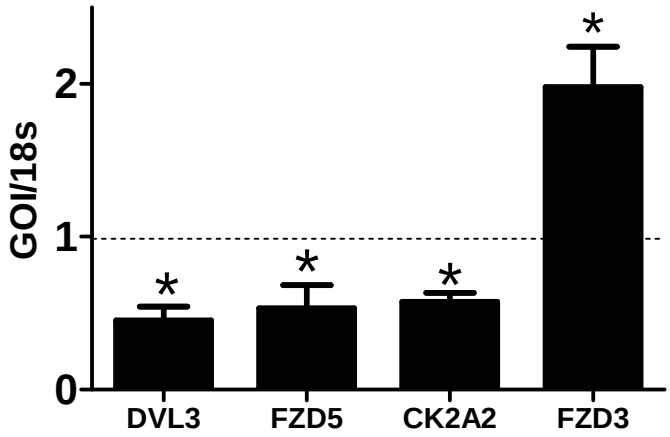

Figure 5.21: Expression of *FZD3, FZD5, DVL3,* and *CK2A2* in human cartilage

Total RNA was isolated from human hip articular cartilage of either end-stage OA patients or fracture controls and reverse transcribed to cDNA. Relative expressions of *FZD3, FZD5, DVL3,* and *CK2A2* were measured by real-time PCR where 18S rRNA was used as housekeeping control in hip osteoarthritis cartilage (HOA, n=8) and fracture to the neck of the femur (NOF, n=7). The horizontal line at 1 is the expression of these genes in NOF. Means ± standard errors are presented. Different in expression between HOA and control NOF was calculated by Student's unpaired two-tailed t test. * $p<0.05$, ** $p < 0.01$, *** $p<0.001$

5.3 Discussion

Previously, the miR-29 family has been shown to negatively interact with TGFβ signalling in several pathologic settings in which fibrosis development was the outcome of the disease such as liver, cardiac, renal fibrosis (van Rooij *et al.* 2008, Kwiecinski et al. 2011, Qin et al. 2011). In line with these studies, in the present study, the miR-29 family was also found to suppress the TGFβ signalling pathway in human chondrocytes. Noteworthy, miR-29 is one downstream mediator of TGFβ signalling in which the miRNA blocks the effect of the growth factor on gene expression. However, the direct mechanism by which miR-29 interferes with TGFβ signalling remains unclear in human chondrocytes. In fact, Smad3 was demonstrated to be a direct target of miR-29 in thyroid cells (Leone *et al.* 2012). In human chondrocytes, nevertheless, with transfection of miR-29 family mimics, the Smad3 mRNA level was not changed (data not shown); similarly, any decrease in luciferase activity when co-transfecting a Smad3-3'UTR reporter with miR-29 mimics was not statistically significant (data not shown), suggesting that Smad3 is not the target of miR-29 in the context of the chondrocyte. In addition, no obvious components of TGFβ signalling were regulated in the miR-29b gain- and loss-of function experiment with the whole genome array. This leads to the hypotheses that miR-29 may directly targets TGFβ signalling components at the protein level rather than mRNA level (similar to miR-140 (Pais et al. 2010)) or that the inhibition of miR-29 on TGFβ signalling is the consequence of the direct suppression of other factors inducing TGFβ signalling. To test this hypothesis, it may be best to perform miR-29b gain- and loss-of function experiment together with a proteomic assay. It may also be instructive to perform array experiments in the presence or absence of TGFβ itself

It has been shown that in the development and progression of OA, NFκB plays an active role e.g. mediating articular chondrocyte responses to proinflammatory cytokines (IL-1, TNF-α); inducing MMPs (e.g. MMP-1, MMP-3, MMP-13), cytokines (e,g, IL-6, IL-8) and chemokine expression (Marcu *et al.* 2010). Thus, NFκB is an attractive target for the treatment of OA. In this project, for the first time, NFκB signalling was confirmed as negatively regulated by the miR-29 family and miR-29 is also likely to serve as a downstream inhibitor of the signalling. Similar to TGFβ signalling, it is still not clear the direct mechanism by which miR-29 regulates NFκB signalling pathway. However, it suggests a potential therapeutic strategy for targeting NFκB signalling using miR-29. Further studies are needed to dissect the direct mechanism by which miR-29 interferes with NFκB signalling.

In this project, the miR-29 family was found to suppress the Wnt/β-catenin signalling pathway. In line with my data, the negative effect of the miR-29 on this signalling pathway is also reported. In human non-small-cell lung cancer cells, miR-29 directly targets DNMTs which in turn inhibited the methylation of Wnt inhibitory factor-1 (WIF-1) promoter; accordingly, miR-29 over-expression down-regulated β-catenin expression (Tan *et al.* 2013). In human colorectal cancer cells, miR-29b negatively regulated Wnt signalling and targeted B-cell CLL/lymphoma 9-like (BCL9L), thus decreasing its expression with a consequent decrease in nuclear translocation of β-catenin (Subramanian *et al.* 2014). In contrast to these studies, published data reports that the miR-29 family positively regulated canonical Wnt signalling by directly targeting its inhibitors in human embryonic kidney cells (Liu *et al.* 2011) and human fetal osteoblastic cells (Kapinas et al. 2010). This contradiction is not surprising as many miRNAs are known to act in a context-dependent manner depending on the relative availability of their targets in any cell type and this discordance could be a reflection of the differences in the miR-29 family regulatory networks in different cell lines.

Besides exerting function on several crucial signalling pathways implicated on chondrogenesis and OA, the crucial role of the miR-29 family was clearly shown through their target genes. In this project, miR-29b gain- and loss-of-function was applied to find miR-29 potential targets. Together with some novel and known targets which will be discussed later, the liposome – mediated transient transfection of the miR-29b-3p mimic surprisingly induced the expression of a number of immune genes which are not the miRNA targets. The Qiagen miR-29b-3p mimic used in the present study is double-stranded, 23 nucleotides in length with sequence identical to the sequence of the mature endogenous miRNA-29b-3p and does not contain any chemical modifications or overhangs, which makes it unlikely for any sequence difference between endogenous miRNA and Qiagen mimic to be responsible for the immune response. Moreover, the lack of immune response against the controls and the miR-29b inhibitor confirms that the immune response was specific and not due to a general response to small RNA. Indeed, it is likely that some specific GU- rich 4-mer sequences e.g. AUUU, UUGA, UGUU in the miR-29b-3p mature sequence (5'UAGCACCAUUUGAAAUCAGUGUU3') might be important for the immune gene up-regulation since these sequences have been shown to be potent immunostimulatory motifs mediated through TLR7 or TLR7/8 (Forsbach *et al.* 2008). Especially, it has been shown that the main effects induced upon activation of TLR7 in human immune cells are IFN- dependent

effects, proinflammatory cytokines and chemokines from cell expression only TLR7 or both TLR7 and 8 (Hertzog *et al.* 2003). Also, it is possible that this up-regulation of the immune genes could be attributed to the liposome alone besides the sequence of the synthetic miRNA since the levels of the immune genes were higher than the levels obtained for electroporation, and those observed in un-transfected controls (Karlsen *et al.* 2013). The explanation for this could be because liposomes fuse with the plasma membrane, which may trigger membrane – associated lipid receptors and/or distort the actin cytoskeleton which in turn up-regulates immune genes. However, it may depend on cellular context since electroporation could strongly trigger the increase of the immune genes in some cell types.

This study identifies FZD3, FZD5, FRAT2, CK2A2 and DVL3 as the critical targets of the miR-29 family in the Wnt signalling pathway. These genes have important roles in both canonical and/or non-canonical Wnt signalling pathways. **FZD3** and **FZD5** belong to the Frizzled proteins, which are the receptors for Wnt ligands. Wnt3a, Wnt5a, and Wnt2 can bind to FZD3 which in turn can activate both canonical and non-canonical WNT signalling pathways: Wnt3a activates the TOPFlash reporter in HEK293 cells overexpressing Wnt3a/FZD3/LRP6 (Lu *et al.* 2004) whist Wnt5a binding to FZD3 triggers downstream pathways independent of β-catenin (Hansen *et al.* 2009); Wnt2 can interact with FZD3 in human cumulus cells, but it is not known which downstream signalling pathways are activated after this binding interaction (Wang *et al.* 2009). **FZD5** functions as the receptor for Wnt5a, Wnt9b, and Wnt7a. Co-injection of hFZD5 and XWnt-5a induced the formation of dorsal axis duplication in *X. laevis* embryos; this axis duplication was suppressed after co-injection of RNA for human GSK-3β, suggesting the involvement β-catenin-dependent signalling in this receptor – ligand combination (He *et al.* 1997). Wnt9b was found in HEK293 cells as a binding partner for FZD5 to activate the TOPFlash reporter (Liu *et al.* 2008). Wnt7a was found to bind to FZD5 to activate the β-catenin signalling pathway and increase the proliferation of epithelial cells in the endometrium (Carmon *et al.* 2008). By targeting these two Frizzled proteins, miR-29 can interfere with Wnt signalling pathways. However, it will depend on the cellular context, whichWnt ligands are available to partner with, which will determine outcome. In line with these Frizzled proteins, another novel target of the miR-29 family, DVL3 (Disheveled 3), belonging to the Disheveled family including DVL1, 2 and 3, is a central component in mediating downstream events of both canonical and non-canonical Wnt signalling. Wnt ligands binding to Frizzled protein recruit Disheveled to the plasma membrane which leads to activation of downstream pathways. Disheveleds

includes DIX, PD2, and DEP domains: DIX and PDZ domains function together in canonical Wnt signalling to stabilize β-catenin; the DIX domain binds with Axin and results in inhibition of the β-catenin degradation complex in canonical Wnt signalling; PDZ and DEP domains cooperate in different subpathways of noncanonical Wnt signalling. Moreover, the other two targets FRAT2 and CSNK2A2 are potent activators of canonical Wnt signalling. **FRAT2** (Frequently rearranged in advanced T-cell lymphomas -2) belongs to the FRAT family including FRAT 1, 2, 3. By binding to GSK3, Frat prevents the phosphorylation and concomitant degradation of β – catenin (van Amerongen *et al.* 2005). **CSNK2A2** encodes for the subunit CK2α' of casein kinase 2 (CK2). CK2 has been shown to act as a positive modulator of WNT/β-catenin pathway, suppressing β-catenin degradation and β-catenin binding to APC (Price 2006). Several keys components of the WNT/β-catenin signalling are known substrates of CK2 in vitro including DVL (Willert *et al.* 1997), TEF/TCF (Homma *et al.* 2002, Miravet *et al.* 2002, Hammerlein *et al.* 2005), and β-catenin (Song *et al.* 2003). Taken together, it is likely that by directly targeting FZD3, FZD5, DVL3, FRAT2 and CSNK2A2, miR-29 could in part or in specific contexts, suppress the Wnt signalling pathway. Interestingly, in human cartilage, the expression levels of FZD5, CSNK2A2, and DLV3 were found to be down regulated in human OA, inversely correlating with the miR-29 expression level, suggesting a direct mechanism in which the suppression of these genes are controlled by miR-29 in human OA cartilage. However, FZD3 expression level was up-regulated in human OA cartilage which could be explained by the fact that there are many other factors which are involved in controlling gene expression together with miRNAs. Since the dys-regulation (either up-regulation or down-regulation) of the canonical Wnt signalling pathway can both lead to OA, there is a possible explanation for the disease development: the excessive amount of the miR-29 down-regulates the expression levels of a number of Wnt signalling related genes which consequently suppress the Wnt signalling pathway. Nevertheless, whether miR-29 targets all of these genes at the same time and the level at which the suppression of each gene contributing to the disease are still not explained in this project.

MicroRNA 29 has been suggested to serve as a master regulator in complex regulatory networks through fine-tuning a large set of functionally related genes, probably best illustrated by its extracellular matrix-related targets, whereby at least 16 ECM related genes are experimentally validated including collagen isoforms (van Rooij et al. 2008, Luna *et al.*

2009, Kwiecinski et al. 2011, Qin et al. 2011, Wang et al. 2012), laminin γ1 (Luna et al. 2009, Nishikawa *et al.* 2014), fibrillin 1, elastin (van Rooij et al. 2008), integrin β1 (Cushing et al. 2011). In line with these data, in this project, a number of ECM- related genes were highlighted as the direct targets of the miR-29 in human OA chondrocytes. However, there is not complete overlap since there are a number of genes that have been experimentally validated as direct targets of miR29 but not regulated when miR-29b was overexpressed or inhibited in human chondrocytes. For example, validated miR-29 direct target genes include DNMT3A, DNMT3B (Fabbri et al. 2007, Garzon *et al.* 2009, Amodio et al. 2012, Morita *et al.* 2013, Tan et al. 2013, Parpart et al. 2014), MMP2 (Liu et al. 2010, Steele et al. 2010, Fang *et al.* 2011), MMP9, ADAM12, ADAM19 (Luna et al. 2009, Ramdas et al. 2013), ADAMTS9 (Cushing et al. 2011). Nonetheless, in human chondrocyte, the expression levels of these genes were not modulated by the miR-29 family. The precise explanation for this difference is still not clear.

In this PhD thesis, members of ADAMTS family including *ADAMTS6, ADAMTS10 ADAMTS14, ADAMTS17, ADAMTS19* have been confirmed as novel direct targets of the miR-29 family. Interestingly, the miR-29 family is suppressed by TGFβ whist its direct targets, the ADAMTS family are strongly induced by TGFβ. However, except ADAMTS14 described as a procollagen N-propeptidase for pro-collagen type I, type II, and type III, the functions of ADAMTS 6, -17, and-19 remain unknown. Thus, further investigating the suppressive effect of miR-29 family on these ADAMTS becomes difficult both in vitro and in vivo. Moreover, ADAMTS14 and ADAMTS17 levels were reported to largely increase in hip OA cartilage and hip OA synovium, respectively (Davidson et al. 2006); the rs4747096 nsSNP in ADAMTS14 was over-represented in women requiring joint replacement because of knee OA and in patients with symptomatic hand OA (Rodriguez-Lopez *et al.* 2009, Poonpet *et al.* 2013), implicating the involvement of these ADAMTS on OA. The microRNA 29 family is, nevertheless, found to increase expression in hip OA cartilage in our sample set. Again, this could be explained in part by the fact that in cellular context, a miRNA is just one factor amongst others e.g. transcription, epigenetic silencing, differential biosynthesis, and extracellular stimuli controlling gene expression.

In summary, the miR-29 family was found to suppress the TGFβ/Smad3, NFκB, and Wnt/β-catenin signalling pathways. Gene expression profiles of gain- and-loss-of-function revealed the regulation of a large number of previously recognised extracellular matrix-associated

genes as well as an additional subset of protease and Wnt signalling pathway-related genes. Among these genes, the ADAMTS family e.g. *ADAMTS6, ADAMTS10, ADAMTS14, ADAMTS17, ADAMTS19,* and Wnt signalling related genes e.g. *FZD3, FZD5, DVL3, FRAT2, CK2A2* were validated as direct targets of the miR-29 family.

CHAPTER 6
GENERAL DISCUSSION

6.1 Summary

This project has identified the miR-29 family as important miRNAs involved in both cartilage homeostasis and OA (Chapter 3). In the murine DMM model of OA at 1, 3, and 7 days after surgery, miRNA profile data from total RNA isolated from the whole knee joints showed that miR-29b was significantly increased at day 1 and showed a trend to decrease at day 3 and 7 after surgery. Integrating analysis between the mRNA profiling and miRNA profiling data from the DMM model strongly highlighted the role of the miR-29 family since the expression of its putative targets inversely correlated with its expression across the time course. In human end-stage hip OA cartilage, the miR-29 family was increased compared with the facture to neck of femur controls. Furthermore, in a murine hip injury model, the expression of the miR-29 family was increased across a 48 hour time course. The miR-29 family was also found to be involved in chondrocyte phenotype since the expression of all members of the miR-29 family decreased across dedifferentiation of human chondrocytes. In chondrogenesis, the miR-29 family was found to significantly decrease at an early stage, suggesting a negative role in this phase of chondrogenesis in both human and murine models. The miR-29 family was also found to be expressed in murine limb development.

The factors controlling miR-29 family expression are another important finding of this project (Chapter 4). The master regulator of chondrogenesis SOX9 was found to negatively regulate miR-29 expression, at least in part through directly binding to the promoter region of miR-29a/b1. A number of growth factors and cytokines were identified which regulate expression of the miR-29 family in both human primary chondrocytes and SW1353 cell line: TGFβ supressed miR-29 family expression; IL-1 strongly increased the miRNA expression through the p38 MAPK signalling pathway; treatment with LPS for less than 24 hours decreased expression of miR-29 through NFκB signalling whilst treatment with LPS for longer times increased miR-29 expression. Interestingly, in response to cytokines and growth factors, the miR-29 primary and precursor transcripts were regulated ahead the mature transcripts. This was explained in part by the fact that several components taking part in the miRNA precursor processing were possibly the miR-29 targets. Among these, Dicer-1 was proven as a miR-29 direct target.

Crucially, the functions of the miR-29 family in chondrocyte were also revealed in which miR-29 served as the negative regulator of the TGFβ/SMAD, NFκB and WNT/β-catenin signalling pathways. A number of novel direct targets of the miR-29 family have been found e.g. the ADAMTS family (*ADAMTS6, -10, -14, -17, -19*) and components of the Wnt signalling pathway (*FZD3, -5, FRAT2, CK2A2, DVL3*) (Chapter 5).

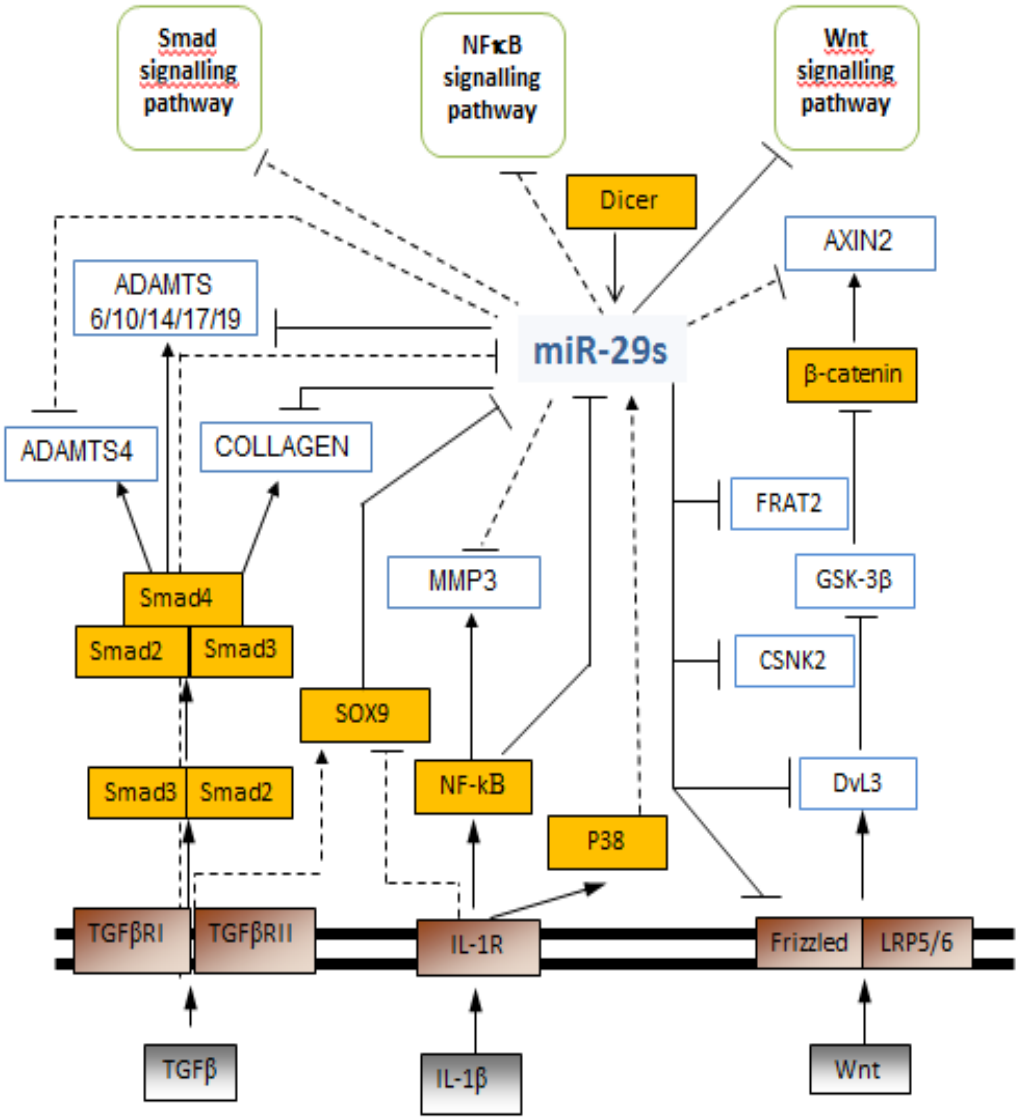

Figure 6.1. Summary of the role of the miR-29 family in chondrocytes

6.2 General discussion

6.2.1 Increased expression of the miR-29 family may contribute to the onset or progression of OA

The tight regulation of miRNA expression is crucial for cartilage homeostasis since the dysregulation of miRNAs may lead to OA. Especially, it has been shown that the aberrant expression of a single miRNA could have a profound effect on cartilage i.e. miR-140, with absence of miR-140 leading to premature OA (Miyaki et al. 2010). In the present study, all members of the miR-29 family have been implicated in cartilage homeostasis and OA. In both early and late stages of OA, an increase level of the miR-29 family was observed, suggesting that miR-29 may be involved in the onset of the disease. Moreover, in this study, the molecular mechanisms controlling this increased expression of miR-29 and the mechanisms by which increased miR-29 expression may lead to OA have been investigated: the miR-29 expression was up-regulated by IL-1, which is induced in both early and end stage OA, consequently suppressing both TGFβ and WNT/β-catenin signalling pathways. Since alteration of these two signalling pathways has been shown to be involved in OA development (Verrecchia et al. 2001, Verrecchia and Mauviel 2002, Zhu et al. 2008, Zhu et al. 2009), the increased expression level of the miR-29 family may contribute to this. In line with this, the miR-29 family was found to strongly suppress a number of ECM-related genes, especially collagens. Aggrecan was also found to be indirectly decreased by miR-29 (data not shown). However, more evidence is required to support this premise. If the increased expression level of miR-29 is a common observation in different OA models, this may also suggest that circulating miR-29 could be a biomarker for detecting early stage OA and also offers the possibility of using a miR-29 inhibitor as a novel treatment for OA. We are investigating the expression of the miR-29 family in the Str/ort model in collaboration with Dr Blandine Poulet (University College London, UK) and Professor Andy Pitsillides (Royal Veterinary College, London, UK).

The increased level of the miR-29 family may not be the only microRNA underlying the development of OA. In this project, miRNA profiling in the DMM model at 1, 3, and 7 days after surgery found a number of miRNAs modulated apart from miR-29s, suggesting these may also contribute to the pathogenesis of OA. Also, a number of miRNAs have been identified as differently expressed in human end stage OA cartilage as compared to the control counterparts. It is clear that in order to maintain cartilage homeostasis, miRNAs will interact with each other and mRNAs in a complex network that is tightly regulated. Thus, the up-regulation of miR-29 might be either the reason or the consequence of the deregulation of other networks of miRNAs. The question is how the other miRNAs interact with miR-29 and the effect of the increase expression of miR-29 on the miRNA/mRNA network in OA. This requires a computer modelling approach to resolve.

6.2.2 The signalling cascade IL-1/p38, IL-1/NFκB and the miR-29 family

Interestingly, in this study, it was found that whist IL-1 induced miR-29 expression through p38/MAPK, the NFκB pathway appears suppressive to miR-29 expression. In addition, the miRNA itself was found to suppress NFκB signalling. These data suggest that in response to the signalling cascade triggered by IL-1, the miR-29 expression level was induced through (i) induced expression of p38 MAPK and (ii) escape from the suppressive effect of NFκB through inhibiting the NFκB signalling pathway. However, the mechanism by which miR-29 suppressed NFκB signalling was not fully understood since the miR-29b gain- and loss- of function mRNA profiling experiment in human primary chondrocytes did not identify any potential targets related to the NFκB signalling pathway. It is a hypothesis that this suppressive effect could be an indirect effect or some potential targets could alter only at the protein level. Also, the direct mechanism through which p38 induced the miR-29 expression is not clear, even though in the promoter of miR-29a/b1 there are several binding sites for AP1 (data not shown). Interestingly, it is reported that p38 activation was found to induce NFκB activity in a dual way: by reducing IκB levels and by potentiating the translocation of p65/p50 (Baeza-Raja *et al.* 2004). Though evidence for this activation in human chondrocytes was not clear, the network controlling miR-29 expression in response to IL-1 becomes more complicated if this interaction is true in chondrocytes. Moreover, in this study, miR-29 was found to inhibit the pre-miRNA processing machinery to target Dicer and may also directly target other pre-miRNA processing genes, suggesting another regulatory layer for tightly

controlling the level of miR-29 in human chondrocytes. This could partly explain that the excessive amount of the miRNA in chondrocytes may lead to OA. Multiple regulatory layers are therefore needed for controlling miR-29 levels, clearly showed when the level of the primary miR-29 family was induced ahead of the level of mature miR-29 in chondrocytes stimulated with IL-1, TGFβ, and LPS. In the DMM model, miR-29 expression was induced 1 day after surgery together with the IL-1β expression level though this latter was not significant (data not shown), suggesting one possible explanation for the increase level of miR-29. However, it is unlikely that miR-29 was solely induced by IL-1 in the DMM model since the IL-1 level would have to be induced very early in order to then stimulate miR-29 expression. In line with this, mRNA profiling of DMM model 6 hours after surgery did not find a strongly induced expression of IL-1 (Burleigh et al. 2012). Similarly, in the murine hip injury model, the miR-29 expression level was also found to increase across the time course (reaching significance at 12 hours in culture). The precise mechanism for the increase expression of miR-29s in both DMM model and murine hip injury model are not clear and require further investigation.

6.2.3 The signalling cascade TGFβ/ Smad3 signalling pathway and the miR-29 family

In contrast with IL-1, TGFβ suppresses miR-29 expression. Since the miR-29 family directly targets a number of ECM-related genes, the suppressive effect TGFβ exerted on the miR-29 family is consistent with the well described protective effect of TGFβ in chondrocytes (Li et al. 2005). Interestingly, the miRNA itself gave a negative feedback loop on the TGFβ/Smad signalling pathway. This could be explained as an attempt to maintain miR-29 at homeostatic levels as TGFβ signalling becomes aberrant. This may also in part support the fact that an excessive amount of the miR-29 family could lead to OA: through suppressing Smad signalling and directly inhibiting responsive genes e.g. ECM related genes, the up-regulation of the miR-29s could strongly diminish the function of TGFβ in chondrocytes.

The precise mechanism by which TGFβ suppressed miR-29 expression and the mechanism by which miR-29 inhibited the TGFβ/Smad signalling were unclear. The miR-29b gain- and loss- of function mRNA profiling did not identify any TGFβ related potential targets, suggesting that this may also be at the protein level. Moreover, regarding the cellular context, when both IL-1 and TGFβ may be present, the cross talk between the two cytokines as well

as with other cytokines and growth factors in controlling the miR-29s expression levels are still unclear.

6.2.4 The canonical Wnt signalling and the miR-29 family

In this project, expression of the miR-29 family was not controlled by Wnt3a in chondrocytes. Since Wnt3a could trigger both canonical Wnt/β-catenin and CaMKII signalling pathways (Nalesso et al. 2011), it is likely that these two signalling pathways do not modulate the miR-29 levels in chondrocyte. However, expression ofmiR-29 was found to be induced by WNT3a in osteoblasts, suggesting a different mechanism controlling the miRNA-29 expression in the two cells types. The answer to this difference remains unknown and needs further investigation.

The canonical Wnt/β-catenin signalling pathway was inhibited by the miR-29 family in which some Wnt signalling related genes were validated as direct targets of the miRNA. Both over-activation and inhibition of Wnt signalling can lead to skeletal deformities and an early onset OA (Zhu et al. 2008, Zhu et al. 2009), illustrating that Wnt signalling needs to be tightly regulated in cartilage homeostasis. However, whether the decreasing of these direct targets is the mechanism for inhibition of the Wnt/β-catenin signalling pathway has not been confirmed in this study. This could be facilitated by utilizing siRNA to suppress the expression of each of these genes and measure this effect on the signalling though TOPFlash reporter.

6.2.5 Therapeautic applications for treating OA by targeting the miR-29 family

MicroRNAs have many advantages as a therapeutic modality. The mature miRNA sequences are short and often completely conserved across species. These characteristics make miRNAs relatively easy to target therapeutically and allow for using the same miRNA-modulating compound in preclinical efficacy and safety studies as well as in clinical trials. Moreover, miRNAs have typically many targets within cellular networks, which, in turn, enable modulation of entire pathways in a disease state via therapeutic targeting of disease – associated miRNAs.

The increase of the miR-29 family in OA potentially opens the door to develop a novel therapeutic strategy for OA. The therapeutic approach using **miRNA sponges** (transgenic

overexpression of RNA molecules harbouring complementary binding sites to a miRNA) or **miRNA-29 antagonists** to block the function of the endogenous miRNA-29s may have great promise as a novel treatment. The miRNA sponges have been proved to be successful in vivo whist the antagonists might have greater promise from a therapeutic perspective.

However, detailed examination of the miRNA therapy should be conducted before clinical use. Especially, the antagonists should have high binding affinity, and bio-stability. Indeed, this could be facilitated by chemically modifying them to increase the duplex melting temperature and improving nuclease resistance. Sugar modifications e.g. the 2'-O-methyl (2'-O-Me), 2'-O-Methoxyethyl (2'-MOE) 2'-fluoro and the bicyclic locked nucleic acid (LNA) modification are commonly used. Among these, the LNA exhibits the highest affinity toward complementary RNA with an increase in Tm of +2-8^{o}C per introduced LNA modification. In addition, by substituting the phosphodiester (PO) backbone linkages with phosphorothioate (PS) linkages in the antagonist oligonucleotides or by using peptide nucleic acid (PNA) or morpholino oligomers, respectively, their nuclease resistance properties might increase. Apart from nuclease resistance, PS backbone modifications also enhance binding to plasma proteins, leading to reduced clearance by glomerular filtration and urinary excretion. PNA oligomers are uncharged oligonucleotide analogues, in which the sugar-phosphate backbone has been replaced by a peptide-like backbone consisting of N-(2-aminoethyl)-glycine units. Polylysine-conjugated and nanoparticle-encapsulated PNA antimiRs have been shown to efficiently inhibit miRNA function in cultured cells and in mice (van Rooij *et al.* 2014). Morpholinos are uncharged and with slightly increased binding affinity to complementary miRNAs.

An effective way to deliver the miRNA-29 inhibitor to the arthritis joint to inhibit the endogenous miRNA-29 is needed. In particular, it is likely that the uptake of a synthetic antagonist into chondrocytes surrounded by the abundant matrix would be difficult in the treatment of damaged cartilage. The main challenge for development of miRNA - based therapeutics is efficient and safe delivery. Two strategies have been utilized to enhance in vivo delivery of antagonists: cholesterol conjugation and modification of the phosphate backbone with PS linkages. The 3' cholesterol conjugated, 2'-O-Me-modified antagonists have become a well-validated experimental tool for in vivo inhibition of miRNAs. PS backbone linkages can be employed to enhance the pharmacokinetic properties of antisense

oligonucleotides. The antagonist approach contains 2 PS modifications at the 5' end and 4 at the 3' end, which have been shown to be important for their in vivo activity, whereas complete replacement of the PO backbone by PS linkages decreased the antagonist efficiency. An increasing number of reports have described silencing of miRNA in vivo by unconjugated LNA-modified antagonists ranging from 8nt to 16nt in length as described in previous section. Administration of such antimiRs is either by intraperitoneal or subcutaneous injection resulted in antimiR uptake in the tissue of interest, which led to inhibition of miRNA function and derepression of direct target mRNAs. However, the mechanism of cellular uptake and distribution are still poorly understood. Directing uptake to cartilage is likely still to be difficult, and delivery by injection not pragmatic in OA.

6.3 Future direction

6.3.1 The modulation of the miR-29 family in OA

The miR-29 family was found to modulate expression in different animal models e.g. the DMM model, hip avulsion injury model, as well as human end stage OA cartilage. These data suggest that the increase in expression of the miR-29 family could be a common event in both early onset and end stage OA. However, care must be applied to conclude the up-regulation of miR-29s will lead to OA, with the expression level of miR-29s during OA progression remaining unclear. Thus, it is of importance to examine miR-29 expression in naturally occurring OA models too.

The miR-29 expression pattern increased in the hip avulsion injury across the time course in this study. Nonetheless, whether miR-29 potential targets were inversely correlated with the miR-29 expression level in this model has not been proven. Thus, we are performing mRNA profiling in the same samples in which the miR-29 expression was found to increase. This may also reveal additional mechanisms which lead to the increased expression of miR-29.

6.3.2 Biological functions of the miR-29 family in chondrocytes

The miR-29 family was found to suppress TGFβ/Smad, NFκB, and Wnt/β-catenin signalling pathways through using the reporters of these pathways together with measuring expression level of the responsive genes. However, whether interfering with the miR-29 effect on these signalling will lead to alter chondrocyte phenotype remains unclear. Overexpression and

knockdown of the miR-29 family in HACs in micromass culture in combination with measurement of chondrocyte markers e.g. *MMP13, COL2A1, SOX9, ADAMTS5* will help to address this.

From the miR-29b gain- and loss- of function mRNA data, apart from the Wnt signalling pathway, enrichment of some miR-29 potential targets which are related to MAPK signalling and apoptosis pathways was evident. Thus, validating these genes as the direct targets of the miR-29s is a priority in the future. It is now clear that miRNAs regulate gene expression at both mRNAs and protein levels. Also, the direct mechanisms the miR-29 supressing the two TGFβ and NFκB signalling pathways are unclear. Therefore, there is a need for proteomic analysis of the miR-29b gain- and loss- of function in HACs, likely in micromass culture. In addition, performing miR-29b gain – and loss - of function together with treatment with IL-1 and TGFβ could greatly help to find the mechanism miR-29 family interfering with NFκB and Smad signalling pathways. All of these experiments will give more information about biological functions of miR-29 in chondrocyte and the complex regulatory network the miR-29 is within.

A key step in understanding the biological functions of the miR-29 family in cartilage homeostasis and OA will be the development of multiple in vivo molecular tools to access gain – of – functions or loss – of – function in mouse models: A number of gain- of –function where the miR-29 family members are overexpressed through a transgenic model, such as the B cell – specific overexpression of the miR-29a/b1 cluster (Santanam et al. 2010), a viral transfection model such as the retroviral transfection of bone-marrow stem cells with miR-29a (Han *et al.* 2010) or systemic delivery of miR-29a have been reported (Wang *et al.* 2012). Also, loss-of-function models have been developed as a Cre-Lox-inducible knockout of the miR-29a/b-1 cluster or the expression of the miR-29 “sponge” sequence (either by transgene or lentivirus) (Ma et al. 2011). However, there is no information whether gain – and loss- of function of the miR-29s lead to OA in these models. Therefore, future studies in which these mice put on OA models e.g. DMM will provide more detail about the function of the miR-29 family.

6.3.3 The involvement of the miR-29 family expression in chick limb bud development and Zebrafish cartilage development.

The miR-29 family was suggested to be a negative regulator of early stage of chondrogenesis in both human and murine chondrogenesis models in this study. Nearly 16 collagen genes were validated as miR-29 direct targets in this study and others. Also, this miRNA was also expressed in murine limb development. It is likely that miR-29 would have a crucial role in cartilage and limb bud development and it is worthy of further investigation. This could be facilitated by again using the gain- and loss- of function of all members of the miR-29 family: a 500bp region around the mature sequence of the miR-29s or a sequence complementary to miR-29 can be subcloned and injected into the chicken limb. However, the involvement of the miR-29 family in chick limb development by in situ hybridization might be required to determine the stage in which miR-29 was expressed in the development process. In addition, ADAMTS14, a pro-collagen pro-peptidase, was validated as the miR-29 direct target. Overexpression or knockdown of the miR-29 family in chick limb could help to further investigate the functional outcome of the suppressive effect of the miR-29s on ADAMTS14 though the ADAMTS14 will need to be verified to be expressed in the chick limb first. This method could be useful for investigating the functional outcome of the interaction between miR-29 and other novel targets.

Interesting, the miR-29 family was found to be express in the cartilage of zebrafish (Wienholds et al. 2005). Thus, zebrafish might be a useful model for investigating the role of the miR-29s in cartilage development. Overexpression and knockdown of the miR-29 family could greatly help for answering this question.

6.3.4 The miR-29 family as the biomarker for OA

MicroRNAs exist in human body fluids such as plasma, urine, and saliva in a stable form which has the potential to be a novel diagnostic and prognostic biomarker. OA can be difficult to diagnose, but it is important to diagnose OA early and start treatment to prevent joint destruction in which the miR-29 based therapy could be an option. Indeed, there is growing evidence for future miRNA-based diagnostics: a number of miRNA in plasma were found at different levels between RA and OA patients. For examples, let-7e, miR-454, miR-886 were identified as differentially expressed circulating miRNAs in OA patients who underwent arthroplasty especially, let–7e emerged as potential predictor for severe knee or hip OA (Beyer et al. 2014). Since the miR-29 family was modulated at an early stage in DMM model, it could be a useful biomarker for OA in clinical use. Thus the expression level

of the miR-29 family in plasma should be determined to have an overview expression pattern of the miRNA.

REFERENCES

Abouheif, M., T. Nakasa, H. Shibuya, T. Niimoto, W. Kongcharoensombat and M. Ochi (2010). "Silencing microRNA-34a inhibits chondrocyte apoptosis in a rat osteoarthritis model in vitro." Rheumatology (Oxford, England) **49**(11): 2054-2060.

Abrahante, J., A. Daul, M. Li, M. Volk, J. Tennessen, E. Miller and A. Rougvie (2003). "The Caenorhabditis elegans hunchback-like Gene lin-57/hbl-1 Controls Developmental Time and Is Regulated by MicroRNAs." Developmental Cell **4**(5): 625-637.

Ahluwalia, J. K., S. Z. Khan, K. Soni, P. Rawat, A. Gupta, M. Hariharan, V. Scaria, M. Lalwani, B. Pillai, D. Mitra and S. K. Brahmachari (2008). "Human cellular microRNA hsa-miR-29a interferes with viral nef protein expression and HIV-1 replication." Retrovirology **5**: 117.

Aigner, T., W. Bertling, H. Stoss, G. Weseloh and K. von der Mark (1993). "Independent expression of fibril-forming collagens I, II, and III in chondrocytes of human osteoarthritic cartilage." J Clin Invest **91**(3): 829-837.

Aigner, T., A. Sachse, P. M. Gebhard and H. I. Roach (2006). "Osteoarthritis: pathobiology-targets and ways for therapeutic intervention." Adv Drug Deliv Rev **58**(2): 128-149.

Aigner, T., S. Soeder and J. Haag (2006). "IL-1beta and BMPs--interactive players of cartilage matrix degradation and regeneration." Eur Cell Mater **12**: 49-56; discussion 56.

Akhtar, N., Z. Rasheed, S. Ramamurthy, A. Anbazhagan, F. Voss and T. Haqqi (2010). "MicroRNA-27b regulates the expression of matrix metalloproteinase 13 in human osteoarthritis chondrocytes." Arthritis & Rheumatism **62**(5): 1361-1371.

(2010). "MicroRNA-27b regulates the expression of matrix metalloproteinase 13 in human osteoarthritis chondrocytes." Arthritis and rheumatism **62**(5): 1361-1371.

Akiyama, H., M. C. Chaboissier, J. F. Martin, A. Schedl and B. de Crombrugghe (2002). "The transcription factor Sox9 has essential roles in successive steps of the chondrocyte differentiation pathway and is required for expression of Sox5 and Sox6." Genes Dev **16**(21): 2813-2828.

Amarilio, R., S. V. Viukov, A. Sharir, I. Eshkar-Oren, R. S. Johnson and E. Zelzer (2007). "HIF1alpha regulation of Sox9 is necessary to maintain differentiation of hypoxic prechondrogenic cells during early skeletogenesis." Development **134**(21): 3917-3928.

Ambros, V. (2004). "The functions of animal microRNAs." Nature **431**(7006): 350-355.

Amodio, N., M. T. Di Martino, U. Foresta, E. Leone, M. Lionetti, M. Leotta, A. M. Gulla, M. R. Pitari, F. Conforti, M. Rossi, V. Agosti, M. Fulciniti, G. Misso, F. Morabito, M. Ferrarini, A. Neri, M. Caraglia, N. C. Munshi, K. C. Anderson, P. Tagliaferri and P. Tassone (2012). "miR-29b sensitizes multiple myeloma cells to bortezomib-induced apoptosis through the activation of a feedback loop with the transcription factor Sp1." Cell Death Dis **3**: e436.

Amodio, N., M. Leotta, D. Bellizzi, M. T. Di Martino, P. D'Aquila, M. Lionetti, F. Fabiani, E. Leone, A. M. Gulla, G. Passarino, M. Caraglia, M. Negrini, A. Neri, A. Giordano, P. Tagliaferri and P. Tassone (2012). "DNA-demethylating and anti-tumor activity of synthetic miR-29b mimics in multiple myeloma." Oncotarget **3**(10): 1246-1258.

Amos, N., S. Lauder, A. Evans, M. Feldmann and J. Bondeson (2006). "Adenoviral gene transfer into osteoarthritis synovial cells using the endogenous inhibitor IkappaBalpha reveals that most, but not all, inflammatory and destructive mediators are NFkappaB dependent." Rheumatology (Oxford) **45**(10): 1201-1209.

Arner, E. C. (2002). "Aggrecanase-mediated cartilage degradation." Curr Opin Pharmacol **2**(3): 322-329.

Arroyo, J., J. Chevillet, E. Kroh, I. Ruf, C. Pritchard, D. Gibson, P. Mitchell, C. Bennett, E. Pogosova-Agadjanyan, D. Stirewalt, J. Tait and M. Tewari (2011). "Argonaute2 complexes carry a

population of circulating microRNAs independent of vesicles in human plasma." Proceedings of the National Academy of Sciences **108**(12): 5003-5008.
Avasarala, S., M. Van Scoyk, J. Wang, M. Sechler, K. Vandervest, C. Brzezinski, C. Weekes, M. G. Edwards, J. Arcaroli, R. E. Davis, R. K. Bikkavilli and R. A. Winn (2013). "hsa-miR29b, a critical downstream target of non-canonical Wnt signaling, plays an anti-proliferative role in non-small cell lung cancer cells via targeting MDM2 expression." Biol Open **2**(7): 675-685.
Baeza-Raja, B. and P. Munoz-Canoves (2004). "p38 MAPK-induced nuclear factor-kappaB activity is required for skeletal muscle differentiation: role of interleukin-6." Mol Biol Cell **15**(4): 2013-2026.
Baker-Lepain, J. C., J. A. Lynch, N. Parimi, C. E. McCulloch, M. C. Nevitt, M. Corr and N. E. Lane (2012). "Variant alleles of the Wnt antagonist FRZB are determinants of hip shape and modify the relationship between hip shape and osteoarthritis." Arthritis Rheum **64**(5): 1457-1465.
Bartel, D. (2004). "MicroRNAs: genomics, biogenesis, mechanism, and function." Cell **116**(2): 281-297.
(2009). "MicroRNAs: target recognition and regulatory functions." Cell **136**(2): 215-233.
Benito, M. J., D. J. Veale, O. FitzGerald, W. B. van den Berg and B. Bresnihan (2005). "Synovial tissue inflammation in early and late osteoarthritis." Ann Rheum Dis **64**(9): 1263-1267.
Berezikov, E., W.-J. Chung, J. Willis, E. Cuppen and E. Lai (2007). "Mammalian mirtron genes." Mol Cell **28**(2): 328-336.
Beyer, C., A. Zampetaki, N. Y. Lin, A. Kleyer, C. Perricone, A. Iagnocco, A. Distler, S. R. Langley, K. Gelse, S. Sesselmann, R. Lorenzini, A. Niemeier, B. Swoboda, J. H. Distler, P. Santer, G. Egger, J. Willeit, M. Mayr, G. Schett and S. Kiechl (2014). "Signature of circulating microRNAs in osteoarthritis." Ann Rheum Dis.
Bi, W., J. M. Deng, Z. Zhang, R. R. Behringer and B. de Crombrugghe (1999). "Sox9 is required for cartilage formation." Nat Genet **22**(1): 85-89.
Billinghurst, R. C., L. Dahlberg, M. Ionescu, A. Reiner, R. Bourne, C. Rorabeck, P. Mitchell, J. Hambor, O. Diekmann, H. Tschesche, J. Chen, H. Van Wart and A. R. Poole (1997). "Enhanced cleavage of type II collagen by collagenases in osteoarthritic articular cartilage." J Clin Invest **99**(7): 1534-1545.
Blom, A. B., S. M. Brockbank, P. L. van Lent, H. M. van Beuningen, J. Geurts, N. Takahashi, P. M. van der Kraan, F. A. van de Loo, B. W. Schreurs, K. Clements, P. Newham and W. B. van den Berg (2009). "Involvement of the Wnt signaling pathway in experimental and human osteoarthritis: prominent role of Wnt-induced signaling protein 1." Arthritis Rheum **60**(2): 501-512.
Bobacz, K., I. G. Sunk, J. G. Hofstaetter, L. Amoyo, C. D. Toma, S. Akira, T. Weichhart, M. Saemann and J. S. Smolen (2007). "Toll-like receptors and chondrocytes: the lipopolysaccharide-induced decrease in cartilage matrix synthesis is dependent on the presence of toll-like receptor 4 and antagonized by bone morphogenetic protein 7." Arthritis Rheum **56**(6): 1880-1893.
Bohnsack, M., K. Czaplinski and D. Gorlich (2004). "Exportin 5 is a RanGTP-dependent dsRNA-binding protein that mediates nuclear export of pre-miRNAs." RNA (New York, N.Y.) **10**(2): 185-191.
Bondeson, J., A. B. Blom, S. Wainwright, C. Hughes, B. Caterson and W. B. van den Berg (2010). "The role of synovial macrophages and macrophage-produced mediators in driving inflammatory and destructive responses in osteoarthritis." Arthritis Rheum **62**(3): 647-657.
Bondeson, J., S. Lauder, S. Wainwright, N. Amos, A. Evans, C. Hughes, M. Feldmann and B. Caterson (2007). "Adenoviral gene transfer of the endogenous inhibitor IkappaBalpha into human osteoarthritis synovial fibroblasts demonstrates that several matrix metalloproteinases and aggrecanases are nuclear factor-kappaB-dependent." J Rheumatol **34**(3): 523-533.
Bossé, G. and M. Simard (2010). "A new twist in the microRNA pathway: Not Dicer but Argonaute is required for a microRNA production." Cell Res **20**(7): 735-737.

Brennecke, J., A. Stark, R. Russell and S. Cohen (2005). "Principles of MicroRNA–Target Recognition." PLoS Biol **3**(3): e85.

Brunner, A. M., C. M. Henn, E. I. Drewniak, A. Lesieur-Brooks, J. Machan, J. J. Crisco and M. G. Ehrlich (2012). "High dietary fat and the development of osteoarthritis in a rabbit model." Osteoarthritis Cartilage **20**(6): 584-592.

Buckwalter, J. A., H. J. Mankin and A. J. Grodzinsky (2005). "Articular cartilage and osteoarthritis." Instr Course Lect **54**: 465-480.

Burleigh, A., A. Chanalaris, M. Gardiner, C. Driscoll, O. Boruc, J. Saklatvala and T. Vincent (2012). "Joint immobilisation prevents murine osteoarthritis, and reveals the highly mechanosensitive nature of protease expression in vivo." Arthritis Rheum: n/a-n/a.

Burleigh, A., A. Chanalaris, M. D. Gardiner, C. Driscoll, O. Boruc, J. Saklatvala and T. L. Vincent (2012). "Joint immobilization prevents murine osteoarthritis and reveals the highly mechanosensitive nature of protease expression in vivo." Arthritis Rheum **64**(7): 2278-2288.

Burrage, P. S., K. S. Mix and C. E. Brinckerhoff (2006). "Matrix metalloproteinases: role in arthritis." Front Biosci **11**: 529-543.

Caetano-Lopes, J., H. Canhao and J. E. Fonseca (2007). "Osteoblasts and bone formation." Acta Reumatol Port **32**(2): 103-110.

Cai, J., G. Yin, B. Lin, X. Wang, X. Liu, X. Chen, D. Yan, G. Shan, J. Qu and S. Wu (2014). "Roles of NFkappaB-miR-29s-MMP-2 circuitry in experimental choroidal neovascularization." J Neuroinflammation **11**: 88.

Cai, X., C. Hagedorn and B. Cullen (2004). "Human microRNAs are processed from capped, polyadenylated transcripts that can also function as mRNAs." RNA (New York, N.Y.) **10**(12): 1957-1966.

Carmon, K. S. and D. S. Loose (2008). "Secreted frizzled-related protein 4 regulates two Wnt7a signaling pathways and inhibits proliferation in endometrial cancer cells." Mol Cancer Res **6**(6): 1017-1028.

Chalfie, M. (1981). "Mutations that lead to reiterations in the cell lineages of C. elegans." Cell **24**(1): 59-69.

Chang, T. C., D. Yu, Y. S. Lee, E. A. Wentzel, D. E. Arking, K. M. West, C. V. Dang, A. Thomas-Tikhonenko and J. T. Mendell (2008). "Widespread microRNA repression by Myc contributes to tumorigenesis." Nat Genet **40**(1): 43-50.

Chen, C., D. Ridzon, A. Broomer, Z. Zhou, D. Lee, J. Nguyen, M. Barbisin, N. Xu, V. Mahuvakar, M. Andersen, K. Lao, K. Livak and K. Guegler (2005). "Real-time quantification of microRNAs by stem–loop RT–PCR." Nucleic Acids Res **33**(20): e179-e179.

Chen, L. X., L. Lin, H. J. Wang, X. L. Wei, X. Fu, J. Y. Zhang and C. L. Yu (2008). "Suppression of early experimental osteoarthritis by in vivo delivery of the adenoviral vector-mediated NF-kappaBp65-specific siRNA." Osteoarthritis Cartilage **16**(2): 174-184.

Chen, X., Y. Ba, L. Ma, X. Cai, Y. Yin, K. Wang, J. Guo, Y. Zhang, J. Chen, X. Guo, Q. Li, X. Li, W. Wang, Y. Zhang, J. Wang, X. Jiang, Y. Xiang, C. Xu, P. Zheng, J. Zhang, R. Li, H. Zhang, X. Shang, T. Gong, G. Ning, J. Wang, K. Zen, J. Zhang and C.-Y. Zhang (2008). "Characterization of microRNAs in serum: a novel class of biomarkers for diagnosis of cancer and other diseases." Cell Res **18**(10): 997-1006.

Chendrimada, T., R. Gregory, E. Kumaraswamy, J. Norman, N. Cooch, K. Nishikura and R. Shiekhattar (2005). "TRBP recruits the Dicer complex to Ago2 for microRNA processing and gene silencing." Nature **436**(7051): 740-744.

Chong, K. W., A. Chanalaris, A. Burleigh, H. Jin, F. E. Watt, J. Saklatvala and T. L. Vincent (2013). "Fibroblast growth factor 2 drives changes in gene expression following injury to murine cartilage in vitro and in vivo." Arthritis Rheum **65**(9): 2346-2355.

Chou, J., J. H. Lin, A. Brenot, J. W. Kim, S. Provot and Z. Werb (2013). "GATA3 suppresses metastasis and modulates the tumour microenvironment by regulating microRNA-29b expression." Nat Cell Biol **15**(2): 201-213.

Clements, K. M., J. S. Price, M. G. Chambers, D. M. Visco, A. R. Poole and R. M. Mason (2003). "Gene deletion of either interleukin-1beta, interleukin-1beta-converting enzyme, inducible nitric oxide synthase, or stromelysin 1 accelerates the development of knee osteoarthritis in mice after surgical transection of the medial collateral ligament and partial medial meniscectomy." Arthritis Rheum **48**(12): 3452-3463.

Clevers, H. (2006). "Wnt/beta-catenin signaling in development and disease." Cell **127**(3): 469-480.

Cochrane, D. R., D. M. Cittelly, E. N. Howe, N. S. Spoelstra, E. L. McKinsey, K. LaPara, A. Elias, D. Yee and J. K. Richer (2010). "MicroRNAs link estrogen receptor alpha status and Dicer levels in breast cancer." Horm Cancer **1**(6): 306-319.

Colige, A., I. Vandenberghe, M. Thiry, C. A. Lambert, J. Van Beeumen, S. W. Li, D. J. Prockop, C. M. Lapiere and B. V. Nusgens (2002). "Cloning and characterization of ADAMTS-14, a novel ADAMTS displaying high homology with ADAMTS-2 and ADAMTS-3." J Biol Chem **277**(8): 5756-5766.

Cortez, M. A., M. S. Nicoloso, M. Shimizu, S. Rossi, G. Gopisetty, J. R. Molina, C. Carlotti, Jr., D. Tirapelli, L. Neder, M. S. Brassesco, C. A. Scrideli, L. G. Tone, M. M. Georgescu, W. Zhang, V. Puduvalli and G. A. Calin (2010). "miR-29b and miR-125a regulate podoplanin and suppress invasion in glioblastoma." Genes Chromosomes Cancer **49**(11): 981-990.

Cushing, L., P. P. Kuang, J. Qian, F. Shao, J. Wu, F. Little, V. J. Thannickal, W. V. Cardoso and J. Lu (2011). "miR-29 is a major regulator of genes associated with pulmonary fibrosis." Am J Respir Cell Mol Biol **45**(2): 287-294.

Davidson, R. K., J. G. Waters, L. Kevorkian, C. Darrah, A. Cooper, S. T. Donell and I. M. Clark (2006). "Expression profiling of metalloproteinases and their inhibitors in synovium and cartilage." Arthritis Res Ther **8**(4): R124.

DeLise, A. M., L. Fischer and R. S. Tuan (2000). "Cellular interactions and signaling in cartilage development." Osteoarthritis Cartilage **8**(5): 309-334.

Dell'accio, F., C. De Bari, N. M. Eltawil, P. Vanhummelen and C. Pitzalis (2008). "Identification of the molecular response of articular cartilage to injury, by microarray screening: Wnt-16 expression and signaling after injury and in osteoarthritis." Arthritis Rheum **58**(5): 1410-1421.

Diarra, D., M. Stolina, K. Polzer, J. Zwerina, M. S. Ominsky, D. Dwyer, A. Korb, J. Smolen, M. Hoffmann, C. Scheinecker, D. van der Heide, R. Landewe, D. Lacey, W. G. Richards and G. Schett (2007). "Dickkopf-1 is a master regulator of joint remodeling." Nat Med **13**(2): 156-163.

Dudek, K., J. Lafont, A. Martinez-Sanchez and C. Murphy (2010). "Type II collagen expression is regulated by tissue-specific miR-675 in human articular chondrocytes." The Journal of biological chemistry **285**(32): 24381-24387.

(2010). "Type II collagen expression is regulated by tissue-specific miR-675 in human articular chondrocytes." Journal of Biological Chemistry **285**(32): 24381-24387.

Dudhia, J. (2005). "Aggrecan, aging and assembly in articular cartilage." Cell Mol Life Sci **62**(19-20): 2241-2256.

Dueck, A. and G. Meister (2010). "MicroRNA processing without Dicer." Genome Biol **11**(6): 123.

Dunn, W., G. DuRaine and H. Reddi (2009). "Profiling microRNA expression in bovine articular cartilage and implications for mechanotransduction." Arthritis & Rheumatism **60**(8): 2333-2339.

(2009). "Profiling microRNA expression in bovine articular cartilage and implications for mechanotransduction." Arthritis and rheumatism **60**(8): 2333-2339.

Elmen, J., M. Lindow, S. Schutz, M. Lawrence, A. Petri, S. Obad, M. Lindholm, M. Hedtjarn, H. Hansen, U. Berger, S. Gullans, P. Kearney, P. Sarnow, E. Straarup and S. Kauppinen (2008). "LNA-mediated microRNA silencing in non-human primates." Nature **452**(7189): 896-899.

Esau, C., S. Davis, S. Murray, X. X. Yu, S. Pandey, M. Pear, L. Watts, S. Booten, M. Graham, R. McKay, A. Subramaniam, S. Propp, B. Lollo, S. Freier, F. Bennett, S. Bhanot and B. Monia (2006). "miR-122 regulation of lipid metabolism revealed by in vivo antisense targeting." Cell Metabolism **3**(2): 87-98.

Eyholzer, M., S. Schmid, L. Wilkens, B. U. Mueller and T. Pabst (2010). "The tumour-suppressive miR-29a/b1 cluster is regulated by CEBPA and blocked in human AML." Br J Cancer **103**(2): 275-284.

Fabbri, M., R. Garzon, A. Cimmino, Z. Liu, N. Zanesi, E. Callegari, S. Liu, H. Alder, S. Costinean, C. Fernandez-Cymering, S. Volinia, G. Guler, C. D. Morrison, K. K. Chan, G. Marcucci, G. A. Calin, K. Huebner and C. M. Croce (2007). "MicroRNA-29 family reverts aberrant methylation in lung cancer by targeting DNA methyltransferases 3A and 3B." Proc Natl Acad Sci U S A **104**(40): 15805-15810.

Fan, Z., S. Soder, S. Oehler, K. Fundel and T. Aigner (2007). "Activation of interleukin-1 signaling cascades in normal and osteoarthritic articular cartilage." Am J Pathol **171**(3): 938-946.

Fang, J. H., H. C. Zhou, C. Zeng, J. Yang, Y. Liu, X. Huang, J. P. Zhang, X. Y. Guan and S. M. Zhuang (2011). "MicroRNA-29b suppresses tumor angiogenesis, invasion, and metastasis by regulating matrix metalloproteinase 2 expression." Hepatology **54**(5): 1729-1740.

Fell, H. B. (1978). "Synoviocytes." J Clin Pathol Suppl (R Coll Pathol) **12**: 14-24.

Fenn, A. M., K. M. Smith, A. E. Lovett-Racke, M. Guerau-de-Arellano, C. C. Whitacre and J. P. Godbout (2013). "Increased micro-RNA 29b in the aged brain correlates with the reduction of insulin-like growth factor-1 and fractalkine ligand." Neurobiol Aging **34**(12): 2748-2758.

Fernandes, R. J., S. Hirohata, J. M. Engle, A. Colige, D. H. Cohn, D. R. Eyre and S. S. Apte (2001). "Procollagen II amino propeptide processing by ADAMTS-3. Insights on dermatosparaxis." J Biol Chem **276**(34): 31502-31509.

Ferracin, M., A. Veronese and M. Negrini (2010). "Micromarkers: miRNAs in cancer diagnosis and prognosis." Expert review of Molecular Diagnostics **10**(3): 297-308.

Forsbach, A., J. G. Nemorin, C. Montino, C. Muller, U. Samulowitz, A. P. Vicari, M. Jurk, G. K. Mutwiri, A. M. Krieg, G. B. Lipford and J. Vollmer (2008). "Identification of RNA sequence motifs stimulating sequence-specific TLR8-dependent immune responses." J Immunol **180**(6): 3729-3738.

Friedman, R., K. Farh, C. Burge and D. Bartel (2009). "Most mammalian mRNAs are conserved targets of microRNAs." Genome Res **19**(1): 92-105.

Frisbie, D. D., S. C. Ghivizzani, P. D. Robbins, C. H. Evans and C. W. McIlwraith (2002). "Treatment of experimental equine osteoarthritis by in vivo delivery of the equine interleukin-1 receptor antagonist gene." Gene Ther **9**(1): 12-20.

Garzon, R., C. E. Heaphy, V. Havelange, M. Fabbri, S. Volinia, T. Tsao, N. Zanesi, S. M. Kornblau, G. Marcucci, G. A. Calin, M. Andreeff and C. M. Croce (2009). "MicroRNA 29b functions in acute myeloid leukemia." Blood **114**(26): 5331-5341.

Gierman, L. M., F. van der Ham, A. Koudijs, P. Y. Wielinga, R. Kleemann, T. Kooistra, R. Stoop, M. Kloppenburg, G. J. van Osch, V. Stojanovic-Susulic, T. W. Huizinga and A. M. Zuurmond (2012). "Metabolic stress-induced inflammation plays a major role in the development of osteoarthritis in mice." Arthritis Rheum **64**(4): 1172-1181.

Gilad, S., E. Meiri, Y. Yogev, S. Benjamin, D. Lebanony, N. Yerushalmi, H. Benjamin, M. Kushnir, H. Cholakh, N. Melamed, Z. Bentwich, M. Hod, Y. Goren and A. Chajut (2008). "Serum MicroRNAs Are Promising Novel Biomarkers." PLoS One **3**(9): e3148.

Girkontaite, I., S. Frischholz, P. Lammi, K. Wagner, B. Swoboda, T. Aigner and K. Von der Mark (1996). "Immunolocalization of type X collagen in normal fetal and adult osteoarthritic cartilage with monoclonal antibodies." Matrix Biol **15**(4): 231-238.

Glasson, S. S., R. Askew, B. Sheppard, B. Carito, T. Blanchet, H. L. Ma, C. R. Flannery, D. Peluso, K. Kanki, Z. Yang, M. K. Majumdar and E. A. Morris (2005). "Deletion of active ADAMTS5 prevents cartilage degradation in a murine model of osteoarthritis." Nature **434**(7033): 644-648.

Goldring, M., K. Tsuchimochi and K. Ijiri (2006). "The control of chondrogenesis." J Cell Biochem **97**(1): 33-44.

Goldring, M. B. (2000). "Osteoarthritis and cartilage: the role of cytokines." Curr Rheumatol Rep **2**(6): 459-465.

(2012). "Chondrogenesis, chondrocyte differentiation, and articular cartilage metabolism in health and osteoarthritis." Ther Adv Musculoskelet Dis **4**(4): 269-285.

Goldring, M. B., J. Birkhead, L. J. Sandell, T. Kimura and S. M. Krane (1988). "Interleukin 1 suppresses expression of cartilage-specific types II and IX collagens and increases types I and III collagens in human chondrocytes." J Clin Invest **82**(6): 2026-2037.

Goldring, M. B. and S. R. Goldring (2007). "Osteoarthritis." J Cell Physiol **213**(3): 626-634.

Goldring, M. B., K. Tsuchimochi and K. Ijiri (2006). "The control of chondrogenesis." J Cell Biochem **97**(1): 33-44.

Goldring, S. R. and M. B. Goldring (2004). "The role of cytokines in cartilage matrix degeneration in osteoarthritis." Clin Orthop Relat Res(427 Suppl): S27-36.

Greco, K. V., A. J. Iqbal, L. Rattazzi, G. Nalesso, N. Moradi-Bidhendi, A. R. Moore, M. B. Goldring, F. Dell'Accio and M. Perretti (2011). "High density micromass cultures of a human chondrocyte cell line: a reliable assay system to reveal the modulatory functions of pharmacological agents." Biochem Pharmacol **82**(12): 1919-1929.

Griffin, T. M., J. L. Huebner, V. B. Kraus and F. Guilak (2009). "Extreme obesity due to impaired leptin signaling in mice does not cause knee osteoarthritis." Arthritis Rheum **60**(10): 2935-2944.

Grishok, A., A. E. Pasquinelli, D. Conte, N. Li, S. Parrish, I. Ha, D. L. Baillie, A. Fire, G. Ruvkun and C. C. Mello (2001). "Genes and mechanisms related to RNA interference regulate expression of the small temporal RNAs that control C. elegans developmental timing." Cell **106**(1): 23-34.

Grotle, M., K. B. Hagen, B. Natvig, F. A. Dahl and T. K. Kvien (2008). "Obesity and osteoarthritis in knee, hip and/or hand: an epidemiological study in the general population with 10 years follow-up." BMC Musculoskelet Disord **9**: 132.

Guan, Y.-J., X. Yang, L. Wei and Q. Chen (2011). "MiR-365: a mechanosensitive microRNA stimulates chondrocyte differentiation through targeting histone deacetylase 4." FASEB Journal **25**(12): 4457-4466.

Guerit, D., J. M. Brondello, P. Chuchana, D. Philipot, K. Toupet, C. Bony, C. Jorgensen and D. Noel (2014). "FoxO3a regulation by miRNA-29a controls chondrogenic differentiation of mesenchymal stem cells and cartilage formation." Stem Cells Dev.

Guilak, F., D. L. Butler and S. A. Goldstein (2001). "Functional tissue engineering: the role of biomechanics in articular cartilage repair." Clin Orthop Relat Res(391 Suppl).

Hammerlein, A., J. Weiske and O. Huber (2005). "A second protein kinase CK1-mediated step negatively regulates Wnt signalling by disrupting the lymphocyte enhancer factor-1/beta-catenin complex." Cell Mol Life Sci **62**(5): 606-618.

Hammond, S. M., E. Bernstein, D. Beach and G. J. Hannon (2000). "An RNA-directed nuclease mediates post-transcriptional gene silencing in Drosophila cells." Nature **404**(6775): 293-296.

Han, J., Y. Lee, K.-H. Yeom, Y.-K. Kim, H. Jin and N. Kim (2004). "The Drosha-DGCR8 complex in primary microRNA processing." Genes Dev **18**(24): 3016-3027.

Han, Y. C., C. Y. Park, G. Bhagat, J. Zhang, Y. Wang, J. B. Fan, M. Liu, Y. Zou, I. L. Weissman and H. Gu (2010). "microRNA-29a induces aberrant self-renewal capacity in hematopoietic progenitors, biased myeloid development, and acute myeloid leukemia." J Exp Med **207**(3): 475-489.

Hansen, C., J. Howlin, A. Tengholm, O. Dyachok, W. F. Vogel, A. C. Nairn, P. Greengard and T. Andersson (2009). "Wnt-5a-induced phosphorylation of DARPP-32 inhibits breast cancer cell migration in a CREB-dependent manner." J Biol Chem **284**(40): 27533-27543.

Harfe, B., M. McManus, J. Mansfield, E. Hornstein and C. Tabin (2005). "The RNaseIII enzyme Dicer is required for morphogenesis but not patterning of the vertebrate limb." Proc Natl Acad Sci U S A **102**(31): 10898-10903.

He, A., L. Zhu, N. Gupta, Y. Chang and F. Fang (2007). "Overexpression of micro ribonucleic acid 29, highly up-regulated in diabetic rats, leads to insulin resistance in 3T3-L1 adipocytes." Mol Endocrinol **21**(11): 2785-2794.

He, X., J. P. Saint-Jeannet, Y. Wang, J. Nathans, I. Dawid and H. Varmus (1997). "A member of the Frizzled protein family mediating axis induction by Wnt-5A." Science **275**(5306): 1652-1654.

Hebert, S. S., K. Horre, L. Nicolai, A. S. Papadopoulou, W. Mandemakers, A. N. Silahtaroglu, S. Kauppinen, A. Delacourte and B. De Strooper (2008). "Loss of microRNA cluster miR-29a/b-1 in sporadic Alzheimer's disease correlates with increased BACE1/beta-secretase expression." Proc Natl Acad Sci U S A **105**(17): 6415-6420.

Heimberg, A., L. Sempere, V. Moy, P. Donoghue and K. Peterson (2008). "MicroRNAs and the advent of vertebrate morphological complexity." Proceedings of the National Academy of Sciences **105**(8): 2946-2950.

Heinegard, D. and T. Saxne (2011). "The role of the cartilage matrix in osteoarthritis." Nat Rev Rheumatol **7**(1): 50-56.

Hertzog, P. J., L. A. O'Neill and J. A. Hamilton (2003). "The interferon in TLR signaling: more than just antiviral." Trends Immunol **24**(10): 534-539.

Homma, M. K., D. Li, E. G. Krebs, Y. Yuasa and Y. Homma (2002). "Association and regulation of casein kinase 2 activity by adenomatous polyposis coli protein." Proc Natl Acad Sci U S A **99**(9): 5959-5964.

Houard, X., M. B. Goldring and F. Berenbaum (2013). "Homeostatic mechanisms in articular cartilage and role of inflammation in osteoarthritis." Curr Rheumatol Rep **15**(11): 375.

Hu, Z., J. D. Klein, W. E. Mitch, L. Zhang, I. Martinez and X. H. Wang (2014). "MicroRNA-29 induces cellular senescence in aging muscle through multiple signaling pathways." AGING **6**(3): 15.

Hu, Z., J. D. Klein, W. E. Mitch, L. Zhang, I. Martinez and X. H. Wang (2014). "MicroRNA-29 induces cellular senescence in aging muscle through multiple signaling pathways." Aging (Albany NY) **6**(3): 160-175.

Hui, W., G. J. Litherland, M. S. Elias, G. I. Kitson, T. E. Cawston, A. D. Rowan and D. A. Young (2012). "Leptin produced by joint white adipose tissue induces cartilage degradation via upregulation and activation of matrix metalloproteinases." Ann Rheum Dis **71**(3): 455-462.

Hutvagner, G. (2005). "Small RNA asymmetry in RNAi: function in RISC assembly and gene regulation." FEBS Lett **579**(26): 5850-5857.

Hutvágner, G., J. McLachlan, A. Pasquinelli, É. Bálint, T. Tuschl and P. Zamore (2001). "A Cellular Function for the RNA-Interference Enzyme Dicer in the Maturation of the let-7 Small Temporal RNA." Science **293**(5531): 834-838.

Hutvagner, G. and M. Simard (2008). "Argonaute proteins: key players in RNA silencing." Nature Reviews. Molecular Cell Biology **9**(1): 22-32.

Iliopoulos, D., K. Malizos, P. Oikonomou and A. Tsezou (2008). "Integrative microRNA and proteomic approaches identify novel osteoarthritis genes and their collaborative metabolic and inflammatory networks." PLoS One **3**(11): e3740.

Inui, M., G. Martello and S. Piccolo (2010). "MicroRNA control of signal transduction." Nature Reviews. Molecular Cell Biology **11**(4): 252-263.

Janeway, C. A., Jr. and R. Medzhitov (2002). "Innate immune recognition." Annu Rev Immunol **20**: 197-216.

Jones, S. W., G. Watkins, N. Le Good, S. Roberts, C. L. Murphy, S. M. Brockbank, M. R. Needham, S. J. Read and P. Newham (2009). "The identification of differentially expressed microRNA in osteoarthritic tissue that modulate the production of TNF-alpha and MMP13." Osteoarthritis and Cartilage **17**(4): 464-472.

(2009). "The identification of differentially expressed microRNA in osteoarthritic tissue that modulate the production of TNF-alpha and MMP13." Osteoarthritis and cartilage / OARS, Osteoarthritis Research Society **17**(4): 464-472.

Kadler, K. E., D. F. Holmes, J. A. Trotter and J. A. Chapman (1996). "Collagen fibril formation." Biochem J **316 (Pt 1)**: 1-11.

Kapinas, K., C. Kessler and A. Delany (2009). "miR-29 suppression of osteonectin in osteoblasts: regulation during differentiation and by canonical Wnt signaling." J Cell Biochem **108**(1): 216-224.

Kapinas, K., C. Kessler, T. Ricks, G. Gronowicz and A. M. Delany (2010). "miR-29 modulates Wnt signaling in human osteoblasts through a positive feedback loop." J Biol Chem **285**(33): 25221-25231.

Karlsen, T., A. Shahdadfar and J. Brinchmann (2011). "Human primary articular chondrocytes, chondroblasts-like cells, and dedifferentiated chondrocytes: differences in gene, microRNA, and protein expression and phenotype." Tissue engineering. Part C, Methods **17**(2): 219-227.

Karlsen, T. A. and J. E. Brinchmann (2013). "Liposome delivery of microRNA-145 to mesenchymal stem cells leads to immunological off-target effects mediated by RIG-I." Mol Ther **21**(6): 1169-1181.

Karsdal, M. A., A. C. Bay-Jensen, R. J. Lories, S. Abramson, T. Spector, P. Pastoureau, C. Christiansen, M. Attur, K. Henriksen, S. R. Goldring and V. Kraus (2014). "The coupling of bone and cartilage turnover in osteoarthritis: opportunities for bone antiresorptives and anabolics as potential treatments?" Ann Rheum Dis **73**(2): 336-348.

Kawano, Y. and R. Kypta (2003). "Secreted antagonists of the Wnt signalling pathway." J Cell Sci **116**(Pt 13): 2627-2634.

Kent, O., R. Chivukula, M. Mullendore, E. Wentzel, G. Feldmann, K. Lee, S. Liu, S. Leach, A. Maitra and J. Mendell (2010). "Repression of the miR-143/145 cluster by oncogenic Ras initiates a tumor-promoting feed-forward pathway." Genes Dev **24**(24): 2754-2759.

Kerkhof, H. J., R. J. Lories, I. Meulenbelt, I. Jonsdottir, A. M. Valdes, P. Arp, T. Ingvarsson, M. Jhamai, H. Jonsson, L. Stolk, G. Thorleifsson, G. Zhai, F. Zhang, Y. Zhu, R. van der Breggen, A. Carr, M. Doherty, S. Doherty, D. T. Felson, A. Gonzalez, B. V. Halldorsson, D. J. Hart, V. B. Hauksson, A. Hofman, J. P. Ioannidis, M. Kloppenburg, N. E. Lane, J. Loughlin, F. P. Luyten, M. C. Nevitt, N. Parimi, H. A. Pols, F. Rivadeneira, E. P. Slagboom, U. Styrkarsdottir, A. Tsezou, T. van de Putte, J. Zmuda, T. D. Spector, K. Stefansson, A. G. Uitterlinden and J. B. van Meurs (2010). "A genome-wide association study identifies an osteoarthritis susceptibility locus on chromosome 7q22." Arthritis Rheum **62**(2): 499-510.

Ketting, R. F., S. E. Fischer, E. Bernstein, T. Sijen, G. J. Hannon and R. H. Plasterk (2001). "Dicer functions in RNA interference and in synthesis of small RNA involved in developmental timing in C. elegans." Genes Dev **15**(20): 2654-2659.

Khvorova, A., A. Reynolds and S. Jayasena (2003). "Functional siRNAs and miRNAs exhibit strand bias." Cell **115**(2): 209-216.

Kiani, C., L. Chen, Y. J. Wu, A. J. Yee and B. B. Yang (2002). "Structure and function of aggrecan." Cell Res **12**(1): 19-32.

Kim, D., J. Song and E.-J. Jin (2010). "MicroRNA-221 Regulates Chondrogenic Differentiation through Promoting Proteosomal Degradation of Slug by Targeting Mdm2." Journal of Biological Chemistry **285**(35): 26900-26907.
Kim, D., J. Song, S. Kim, C.-H. Chun and E.-J. Jin (2011). "MicroRNA-34a regulates migration of chondroblast and IL-1β-induced degeneration of chondrocytes by targeting EphA5." Biochem Biophys Res Commun **415**(4): 551-557.
Kim, D., J. Song, S. Kim, C.-H. Chun, J. Sonn and E.-J. Jin (2012). "MicroRNA-34a modulates cytoskeletal dynamics through regulating RhoA/Rac1 crosstalk in chondroblasts." The Journal of biological chemistry.
Kim, D., J. Song, S. Kim, S.-S. Kang and E.-J. Jin (2011). "MicroRNA-142-3p regulates TGF-β3-mediated region-dependent chondrogenesis by regulating ADAM9." Biochem Biophys Res Commun **414**(4): 653-659.
Kim, N. (2005). "MicroRNA biogenesis: coordinated cropping and dicing." Nature Reviews. Molecular Cell Biology **6**(5): 376-385.
Kim, N., J. Han and M. Siomi (2009). "Biogenesis of small RNAs in animals." Nature reviews. Molecular cell biology **10**(2): 126-139.
Kiriakidou, M., G. Tan, S. Lamprinaki, M. De Planell-Saguer, P. Nelson and Z. Mourelatos (2007). "An mRNA m7G cap binding-like motif within human Ago2 represses translation." Cell **129**(6): 1141-1151.
Knauper, V., C. Lopez-Otin, B. Smith, G. Knight and G. Murphy (1996). "Biochemical characterization of human collagenase-3." J Biol Chem **271**(3): 1544-1550.
Kobayashi, M., G. R. Squires, A. Mousa, M. Tanzer, D. J. Zukor, J. Antoniou, U. Feige and A. R. Poole (2005). "Role of interleukin-1 and tumor necrosis factor alpha in matrix degradation of human osteoarthritic cartilage." Arthritis Rheum **52**(1): 128-135.
Kobayashi, T., J. Lu, B. Cobb, S. Rodda, A. McMahon, E. Schipani, M. Merkenschlager and H. Kronenberg (2008). "Dicer-dependent pathways regulate chondrocyte proliferation and differentiation." Proc Natl Acad Sci U S A **105**(6): 1949-1954.
Kongcharoensombat, W., T. Nakasa, M. Ishikawa, A. Nakamae, M. Deie, N. Adachi, A. Mohamed and M. Ochi (2010). "The effect of microRNA-21 on proliferation and matrix synthesis of chondrocytes embedded in atelocollagen gel." Knee Surgery, Sports Traumatology, Arthroscopy **18**(12): 1679-1684.
Konttinen, Y. T., T. Sillat, G. Barreto, M. Ainola and D. C. Nordstrom (2012). "Osteoarthritis as an autoinflammatory disease caused by chondrocyte-mediated inflammatory responses." Arthritis Rheum **64**(3): 613-616.
Kosaka, N., H. Iguchi and T. Ochiya (2010). "Circulating microRNA in body fluid: a new potential biomarker for cancer diagnosis and prognosis." Cancer Sci **101**(10): 2087-2092.
Koshy, P. J., C. J. Lundy, A. D. Rowan, S. Porter, D. R. Edwards, A. Hogan, I. M. Clark and T. E. Cawston (2002). "The modulation of matrix metalloproteinase and ADAM gene expression in human chondrocytes by interleukin-1 and oncostatin M: a time-course study using real-time quantitative reverse transcription-polymerase chain reaction." Arthritis Rheum **46**(4): 961-967.
Kozomara, A. and S. Griffiths-Jones (2011). "miRBase: integrating microRNA annotation and deep-sequencing data." Nucleic Acids Research **39**(Database issue): D152-D157.
Kwiecinski, M., A. Noetel, N. Elfimova, J. Trebicka, S. Schievenbusch, I. Strack, L. Molnar, M. von Brandenstein, U. Tox, R. Nischt, O. Coutelle, H. P. Dienes and M. Odenthal (2011). "Hepatocyte growth factor (HGF) inhibits collagen I and IV synthesis in hepatic stellate cells by miRNA-29 induction." PLoS One **6**(9): e24568.
Lagos-Quintana, M., R. Rauhut, W. Lendeckel and T. Tuschl (2001). "Identification of novel genes coding for small expressed RNAs." Science (New York, N.Y.) **294**(5543): 853-858.

Lai, E. (2002). "Micro RNAs are complementary to 3' UTR sequence motifs that mediate negative post-transcriptional regulation." Nat Genet **30**(4): 363-364.
Lane, L. B., A. Villacin and P. G. Bullough (1977). "The vascularity and remodelling of subchondrial bone and calcified cartilage in adult human femoral and humeral heads. An age- and stress-related phenomenon." J Bone Joint Surg Br **59**(3): 272-278.
Lane, N. E., K. Lian, M. C. Nevitt, J. M. Zmuda, L. Lui, J. Li, J. Wang, M. Fontecha, N. Umblas, M. Rosenbach, P. de Leon and M. Corr (2006). "Frizzled-related protein variants are risk factors for hip osteoarthritis." Arthritis Rheum **54**(4): 1246-1254.
Lapiere, C. M., A. Lenaers and L. D. Kohn (1971). "Procollagen peptidase: an enzyme excising the coordination peptides of procollagen." Proc Natl Acad Sci U S A **68**(12): 3054-3058.
Lau, N. C., L. P. Lim, E. G. Weinstein and D. P. Bartel (2001). "An abundant class of tiny RNAs with probable regulatory roles in Caenorhabditis elegans." Science (New York, N.Y.) **294**(5543): 858-862.
Lau, P.-W. and I. MacRae (2009). "The molecular machines that mediate microRNA maturation." J Cell Mol Med **13**(1): 54-60.
Lawrie, C., S. Gal, H. Dunlop, B. Pushkaran, A. Liggins, K. Pulford, A. Banham, F. Pezzella, J. Boultwood, J. Wainscoat, C. Hatton and A. Harris (2008). "Detection of elevated levels of tumour-associated microRNAs in serum of patients with diffuse large B-cell lymphoma." Br J Haematol **141**(5): 672-675.
Le, L. T., T. E. Swingler and I. M. Clark (2013). "Review: the role of microRNAs in osteoarthritis and chondrogenesis." Arthritis Rheum **65**(8): 1963-1974.
Lee, D. A., G. Bentley and C. W. Archer (1993). "The control of cell division in articular chondrocytes." Osteoarthritis Cartilage **1**(2): 137-146.
Lee, I., S. Ajay, J. I. Yook, H. S. Kim, S. H. Hong, N. H. Kim, S. Dhanasekaran, A. Chinnaiyan and B. Athey (2009). "New class of microRNA targets containing simultaneous 5'-UTR and 3'-UTR interaction sites." Genome Res **19**(7): 1175-1183.
Lee, J. H., T. Ort, K. Ma, K. Picha, J. Carton, P. A. Marsters, L. S. Lohmander, F. Baribaud, X. Y. Song and S. Blake (2009). "Resistin is elevated following traumatic joint injury and causes matrix degradation and release of inflammatory cytokines from articular cartilage in vitro." Osteoarthritis Cartilage **17**(5): 613-620.
Lee, R. and V. Ambros (2001). "An Extensive Class of Small RNAs in Caenorhabditis elegans." Science **294**(5543): 862-864.
Lee, R. C., R. L. Feinbaum and V. Ambros (1993). "The C. elegans heterochronic gene lin-4 encodes small RNAs with antisense complementarity to lin-14." Cell **75**(5): 843-854.
Lee, Y., C. Ahn, J. Han, H. Choi, J. Kim, J. Yim, J. Lee, P. Provost, O. Radmark, S. Kim and N. Kim (2003). "The nuclear RNase III Drosha initiates microRNA processing." Nature **425**(6956): 415-419.
Lee, Y., K. Jeon, J.-T. Lee, S. Kim and N. Kim (2002). "MicroRNA maturation: stepwise processing and subcellular localization." The EMBO Journal **21**(17): 4663-4670.
Lee, Y., M. Kim, J. Han, K.-H. Yeom, S. Lee, S. Baek and N. Kim (2004). "MicroRNA genes are transcribed by RNA polymerase II." The EMBO Journal **23**(20): 4051-4060.
Lefebvre, V., W. Huang, V. R. Harley, P. N. Goodfellow and B. de Crombrugghe (1997). "SOX9 is a potent activator of the chondrocyte-specific enhancer of the pro alpha1(II) collagen gene." Mol Cell Biol **17**(4): 2336-2346.
Lefebvre, V., C. Peeters-Joris and G. Vaes (1990). "Modulation by interleukin 1 and tumor necrosis factor alpha of production of collagenase, tissue inhibitor of metalloproteinases and collagen types in differentiated and dedifferentiated articular chondrocytes." Biochim Biophys Acta **1052**(3): 366-378.

Leone, V., D. D'Angelo, P. Pallante, C. M. Croce and A. Fusco (2012). "Thyrotropin regulates thyroid cell proliferation by up-regulating miR-23b and miR-29b that target SMAD3." J Clin Endocrinol Metab **97**(9): 3292-3301.

Letamendia, A., E. Labbe and L. Attisano (2001). "Transcriptional regulation by Smads: crosstalk between the TGF-beta and Wnt pathways." J Bone Joint Surg Am **83-A Suppl 1**(Pt 1): S31-39.

Lewis, B., C. Burge and D. Bartel (2005). "Conserved Seed Pairing, Often Flanked by Adenosines, Indicates that Thousands of Human Genes are MicroRNA Targets." Cell **120**(1): 15-20.

Li, G., J. Yin, J. Gao, T. S. Cheng, N. J. Pavlos, C. Zhang and M. H. Zheng (2013). "Subchondral bone in osteoarthritis: insight into risk factors and microstructural changes." Arthritis Res Ther **15**(6): 223.

Li, H., H. Xie, W. Liu, R. Hu, B. Huang, Y.-F. Tan, K. Xu, Z.-F. Sheng, H.-D. Zhou, X.-P. Wu and X.-H. Luo (2009). "A novel microRNA targeting HDAC5 regulates osteoblast differentiation in mice and contributes to primary osteoporosis in humans." The Journal of clinical investigation **119**(12): 3666-3677.

Li, J., J. Huang, L. Dai, D. Yu, Q. Chen, X. Zhang and K. Dai (2012). "MiR-146a, an interleukin-1beta responsive microRNA, induces vascular endothelial growth factor and chondrocyte apoptosis by targeting Smad4." Arthritis Res Ther **14**(2): R75.

Li, N., J. Cui, X. Duan, H. Chen and F. Fan (2012). "Suppression of type I collagen expression by miR-29b via PI3K, Akt, and Sp1 pathway in human Tenon's fibroblasts." Invest Ophthalmol Vis Sci **53**(3): 1670-1678.

Li, T. F., R. J. O'Keefe and D. Chen (2005). "TGF-beta signaling in chondrocytes." Front Biosci **10**: 681-688.

Li, X., G. Gibson, J.-S. Kim, J. Kroin, S. Xu, A. van Wijnen and H.-J. Im (2011). "MicroRNA-146a is linked to pain-related pathophysiology of osteoarthritis." Gene **480**(1-2): 34-41.

Liang, Z.-J., H. Zhuang, G.-X. Wang, Z. Li, H.-T. Zhang, T.-Q. Yu and B.-D. Zhang (2012). "MiRNA-140 is a negative feedback regulator of MMP-13 in IL-1β-stimulated human articular chondrocyte C28/I2 cells." Inflammation Research **61**(5): 503-509.

(2012). "MiRNA-140 is a negative feedback regulator of MMP-13 in IL-1β-stimulated human articular chondrocyte C28/I2 cells." Inflammation research: 1-7.

Lim, L., N. Lau, P. Garrett-Engele, A. Grimson, J. Schelter, J. Castle, D. Bartel, P. Linsley and J. Johnson (2005). "Microarray analysis shows that some microRNAs downregulate large numbers of target mRNAs." Nature **433**(7027): 769-773.

Lin, E., L. Kong, X.-H. Bai, Y. Luan and C.-J. Liu (2009). "miR-199a, a bone morphogenic protein 2-responsive MicroRNA, regulates chondrogenesis via direct targeting to Smad1." The Journal of biological chemistry **284**(17): 11326-11335.

(2009). "miR-199a, a bone morphogenic protein 2-responsive MicroRNA, regulates chondrogenesis via direct targeting to Smad1." Journal of Biological Chemistry **284**(17): 11326-11335.

Lin, L., Q. Shen, C. Zhang, L. Chen and C. Yu (2011). "Assessment of the profiling microRNA expression of differentiated and dedifferentiated human adult articular chondrocytes." Journal of Orthopaedic Research **29**(10): 1578-1584.

Lin, S.-Y., S. Johnson, M. Abraham, M. Vella, A. Pasquinelli, C. Gamberi, E. Gottlieb and F. Slack (2003). "The C elegans hunchback homolog, hbl-1, controls temporal patterning and is a probable microRNA target." Developmental Cell **4**(5): 639-650.

Link, A., F. Balaguer, Y. Shen, T. Nagasaka, J. J. Lozano, R. Boland and A. Goel (2010). "Fecal MicroRNAs as novel biomarkers for colon cancer screening." Cancer Epidemiol Biomarkers Prev **19**(7): 1766-1774.

Liu, C., Y. Wang, P. M. Smallwood and J. Nathans (2008). "An essential role for Frizzled5 in neuronal survival in the parafascicular nucleus of the thalamus." J Neurosci **28**(22): 5641-5653.

Liu, S., L. C. Wu, J. Pang, R. Santhanam, S. Schwind, Y. Z. Wu, C. J. Hickey, J. Yu, H. Becker, K. Maharry, M. D. Radmacher, C. Li, S. P. Whitman, A. Mishra, N. Stauffer, A. M. Eiring, R. Briesewitz, R. A.

Baiocchi, K. K. Chan, P. Paschka, M. A. Caligiuri, J. C. Byrd, C. M. Croce, C. D. Bloomfield, D. Perrotti, R. Garzon and G. Marcucci (2010). "Sp1/NFkappaB/HDAC/miR-29b regulatory network in KIT-driven myeloid leukemia." Cancer Cell **17**(4): 333-347.

Liu, Y., T. Huang, X. Zhao and L. Cheng (2011). "MicroRNAs modulate the Wnt signaling pathway through targeting its inhibitors." Biochem Biophys Res Commun **408**(2): 259-264.

Lodewyckx, L., F. P. Luyten and R. J. Lories (2012). "Genetic deletion of low-density lipoprotein receptor-related protein 5 increases cartilage degradation in instability-induced osteoarthritis." Rheumatology (Oxford) **51**(11): 1973-1978.

Loeser, R., S. Goldring, C. Scanzello and M. Goldring (2012). "Osteoarthritis: A disease of the joint as an organ." Arthritis & Rheumatism: n/a-n/a.

Loeser, R. F., S. R. Goldring, C. R. Scanzello and M. B. Goldring (2012). "Osteoarthritis: a disease of the joint as an organ." Arthritis Rheum **64**(6): 1697-1707.

Long, J., Y. Wang, W. Wang, B. H. Chang and F. R. Danesh (2011). "MicroRNA-29c is a signature microRNA under high glucose conditions that targets Sprouty homolog 1, and its in vivo knockdown prevents progression of diabetic nephropathy." J Biol Chem **286**(13): 11837-11848.

Lories, R. J., J. Peeters, A. Bakker, P. Tylzanowski, I. Derese, J. Schrooten, J. T. Thomas and F. P. Luyten (2007). "Articular cartilage and biomechanical properties of the long bones in Frzb-knockout mice." Arthritis Rheum **56**(12): 4095-4103.

Loughlin, J., B. Dowling, K. Chapman, L. Marcelline, Z. Mustafa, L. Southam, A. Ferreira, C. Ciesielski, D. A. Carson and M. Corr (2004). "Functional variants within the secreted frizzled-related protein 3 gene are associated with hip osteoarthritis in females." Proc Natl Acad Sci U S A **101**(26): 9757-9762.

Lu, D., Y. Zhao, R. Tawatao, H. B. Cottam, M. Sen, L. M. Leoni, T. J. Kipps, M. Corr and D. A. Carson (2004). "Activation of the Wnt signaling pathway in chronic lymphocytic leukemia." Proc Natl Acad Sci U S A **101**(9): 3118-3123.

Luna, C., G. Li, J. Qiu, D. L. Epstein and P. Gonzalez (2009). "Role of miR-29b on the regulation of the extracellular matrix in human trabecular meshwork cells under chronic oxidative stress." Mol Vis **15**: 2488-2497.

Lund, E., S. Güttinger, A. Calado, J. Dahlberg and U. Kutay (2004). "Nuclear Export of MicroRNA Precursors." Science **303**(5654): 95-98.

Lytle, R., T. Yario and J. Steitz (2007). "Target mRNAs are repressed as efficiently by microRNA-binding sites in the 5′ UTR as in the 3′ UTR." Proceedings of the National Academy of Sciences **104**(23): 9667-9672.

Ma, F., S. Xu, X. Liu, Q. Zhang, X. Xu, M. Liu, M. Hua, N. Li, H. Yao and X. Cao (2011). "The microRNA miR-29 controls innate and adaptive immune responses to intracellular bacterial infection by targeting interferon-gamma." Nat Immunol **12**(9): 861-869.

Maegdefessel, L., J. Azuma, R. Toh, D. R. Merk, A. Deng, J. T. Chin, U. Raaz, A. M. Schoelmerich, A. Raiesdana, N. J. Leeper, M. V. McConnell, R. L. Dalman, J. M. Spin and P. S. Tsao (2012). "Inhibition of microRNA-29b reduces murine abdominal aortic aneurysm development." J Clin Invest **122**(2): 497-506.

Marcu, K. B., M. Otero, E. Olivotto, R. M. Borzi and M. B. Goldring (2010). "NF-kappaB signaling: multiple angles to target OA." Curr Drug Targets **11**(5): 599-613.

Martel-Pelletier, J., C. Boileau, J. P. Pelletier and P. J. Roughley (2008). "Cartilage in normal and osteoarthritis conditions." Best Pract Res Clin Rheumatol **22**(2): 351-384.

Martin, P. (1990). "Tissue patterning in the developing mouse limb." Int J Dev Biol **34**(3): 323-336.

Martinez-Sanchez, A., K. Dudek and C. Murphy (2012). "Regulation of human chondrocyte function through direct inhibition of cartilage master regulator SOX9 by microRNA-145 (miRNA-145)." Journal of Biological Chemistry **287**(2): 916-924.

(2012). "Regulation of human chondrocyte function through direct inhibition of cartilage master regulator SOX9 by microRNA-145 (miRNA-145)." The Journal of biological chemistry **287**(2): 916-924.
Martinez-Sanchez, A. and C. L. Murphy (2013). "miR-1247 functions by targeting cartilage transcription factor SOX9." J Biol Chem **288**(43): 30802-30814.
Martinez, J., A. Patkaniowska, H. Urlaub, R. Lührmann and T. Tuschl (2002). "Single-stranded antisense siRNAs guide target RNA cleavage in RNAi." Cell **110**(5): 563-574.
Matyas, J. R., L. J. Sandell and M. E. Adams (1997). "Gene expression of type II collagens in chondro-osteophytes in experimental osteoarthritis." Osteoarthritis Cartilage **5**(2): 99-105.
Maurer, B., J. Stanczyk, A. Jungel, A. Akhmetshina, M. Trenkmann, M. Brock, O. Kowal-Bielecka, R. E. Gay, B. A. Michel, J. H. Distler, S. Gay and O. Distler (2010). "MicroRNA-29, a key regulator of collagen expression in systemic sclerosis." Arthritis Rheum **62**(6): 1733-1743.
Meachim, G. and D. H. Collins (1962). "Cell counts of normal and osteoarthritic articular cartilage in relation to the uptake of sulphate (35SO4) in vitro." Ann Rheum Dis **21**: 45-50.
Messier, S. P., D. J. Gutekunst, C. Davis and P. DeVita (2005). "Weight loss reduces knee-joint loads in overweight and obese older adults with knee osteoarthritis." Arthritis Rheum **52**(7): 2026-2032.
Miravet, S., J. Piedra, F. Miro, E. Itarte, A. Garcia de Herreros and M. Dunach (2002). "The transcriptional factor Tcf-4 contains different binding sites for beta-catenin and plakoglobin." J Biol Chem **277**(3): 1884-1891.
Mitchell, P., R. Parkin, E. Kroh, B. Fritz, S. Wyman, E. Pogosova-Agadjanyan, A. Peterson, J. Noteboom, K. O'Briant, A. Allen, D. Lin, N. Urban, C. Drescher, B. Knudsen, D. Stirewalt, R. Gentleman, R. Vessella, P. Nelson, D. Martin and M. Tewari (2008). "Circulating microRNAs as stable blood-based markers for cancer detection." Proceedings of the National Academy of Sciences **105**(30): 10513-10518.
Miyaki, S., T. Nakasa, S. Otsuki, S. Grogan, R. Higashiyama, A. Inoue, Y. Kato, T. Sato, M. Lotz and H. Asahara (2009). "MicroRNA-140 is expressed in differentiated human articular chondrocytes and modulates interleukin-1 responses." Arthritis & Rheumatism **60**(9): 2723-2730.
(2009). "MicroRNA-140 is expressed in differentiated human articular chondrocytes and modulates interleukin-1 responses." Arthritis and rheumatism **60**(9): 2723-2730.
Miyaki, S., T. Nakasa, S. Otsuki, S. P. Grogan, R. Higashiyama, A. Inoue, Y. Kato, T. Sato, M. K. Lotz and H. Asahara (2009). "MicroRNA-140 is expressed in differentiated human articular chondrocytes and modulates interleukin-1 responses." Arthritis Rheum **60**(9): 2723-2730.
Miyaki, S., T. Sato, A. Inoue, S. Otsuki, Y. Ito, S. Yokoyama, Y. Kato, F. Takemoto, T. Nakasa, S. Yamashita, S. Takada, M. Lotz, H. Ueno-Kudo and H. Asahara (2010). "MicroRNA-140 plays dual roles in both cartilage development and homeostasis." Genes Dev **24**(11): 1173-1185.
Miyaki, S., T. Sato, A. Inoue, S. Otsuki, Y. Ito, S. Yokoyama, Y. Kato, F. Takemoto, T. Nakasa, S. Yamashita, S. Takada, M. K. Lotz, H. Ueno-Kudo and H. Asahara (2010). "MicroRNA-140 plays dual roles in both cartilage development and homeostasis." Genes Dev **24**(11): 1173-1185.
Miyazawa, K., M. Shinozaki, T. Hara, T. Furuya and K. Miyazono (2002). "Two major Smad pathways in TGF-beta superfamily signalling." Genes Cells **7**(12): 1191-1204.
Mooney, R. A., E. R. Sampson, J. Lerea, R. N. Rosier and M. J. Zuscik (2011). "High-fat diet accelerates progression of osteoarthritis after meniscal/ligamentous injury." Arthritis Res Ther **13**(6): R198.
Morita, S., T. Horii, M. Kimura, T. Ochiya, S. Tajima and I. Hatada (2013). "miR-29 represses the activities of DNA methyltransferases and DNA demethylases." Int J Mol Sci **14**(7): 14647-14658.
Mott, J. L., S. Kurita, S. C. Cazanave, S. F. Bronk, N. W. Werneburg and M. E. Fernandez-Zapico (2010). "Transcriptional suppression of mir-29b-1/mir-29a promoter by c-Myc, hedgehog, and NF-kappaB." J Cell Biochem **110**(5): 1155-1164.

Moulin, D., V. Salone, M. Koufany, T. Clement, P. Netter, I. Behm-Ansmant, B. Charpentier, C. Branlant and J.-Y. Jouzeau (2012). "miR-29b is overexpressed in osteoarthritic patients and targets type II collagen." Osteoarthritis and Cartilage **20**: S139 - S140.

Muniyappa, M. K., P. Dowling, M. Henry, P. Meleady, P. Doolan, P. Gammell, M. Clynes and N. Barron (2009). "MiRNA-29a regulates the expression of numerous proteins and reduces the invasiveness and proliferation of human carcinoma cell lines." Eur J Cancer **45**(17): 3104-3118.

Murata, K., H. Yoshitomi, S. Tanida, M. Ishikawa, K. Nishitani, H. Ito and T. Nakamura (2010). "Plasma and synovial fluid microRNAs as potential biomarkers of rheumatoid arthritis and osteoarthritis." Arthritis Res Ther **12**(3): R86.

Murata, K., H. Yoshitomi, S. Tanida, M. Ishikawa, K. Nishitani, H. Ito and T. Nakamura (2010). "Plasma and synovial fluid microRNAs as potential biomarkers of rheumatoid arthritis and osteoarthritis." Arthritis Res Ther **12**(3): R86.

Nah, S. S., I. Y. Choi, B. Yoo, Y. G. Kim, H. B. Moon and C. K. Lee (2007). "Advanced glycation end products increases matrix metalloproteinase-1, -3, and -13, and TNF-alpha in human osteoarthritic chondrocytes." FEBS Lett **581**(9): 1928-1932.

Nakamura, Y., X. He, H. Kato, S. Wakitani, T. Kobayashi, S. Watanabe, A. Iida, H. Tahara, M. L. Warman, R. Watanapokasin and J. H. Postlethwait (2012). "Sox9 is upstream of microRNA-140 in cartilage." Appl Biochem Biotechnol **166**(1): 64-71.

Nakamura, Y., J. Inloes, T. Katagiri and T. Kobayashi (2011). "Chondrocyte-specific microRNA-140 regulates endochondral bone development and targets Dnpep to modulate bone morphogenetic protein signaling." Mol Cell Biol **31**(14): 3019-3028.

Nakamura, Y., J. B. Inloes, T. Katagiri and T. Kobayashi (2011). "Chondrocyte-specific microRNA-140 regulates endochondral bone development and targets Dnpep to modulate bone morphogenetic protein signaling." Mol Cell Biol **31**(14): 3019-3028.

Nalesso, G., J. Sherwood, J. Bertrand, T. Pap, M. Ramachandran, C. De Bari, C. Pitzalis and F. Dell'accio (2011). "WNT-3A modulates articular chondrocyte phenotype by activating both canonical and noncanonical pathways." J Cell Biol **193**(3): 551-564.

Neu, C., A. Khalafi, K. Komvopoulos, T. Schmid and H. Reddi (2007). "Mechanotransduction of bovine articular cartilage superficial zone protein by transforming growth factor β signaling." Arthritis & Rheumatism **56**(11): 3706-3714.

Ng, L. J., S. Wheatley, G. E. Muscat, J. Conway-Campbell, J. Bowles, E. Wright, D. M. Bell, P. P. Tam, K. S. Cheah and P. Koopman (1997). "SOX9 binds DNA, activates transcription, and coexpresses with type II collagen during chondrogenesis in the mouse." Dev Biol **183**(1): 108-121.

Nicolas, F. E., H. Pais, F. Schwach, M. Lindow, S. Kauppinen, V. Moulton and T. Dalmay (2008). "Experimental identification of microRNA-140 targets by silencing and overexpressing miR-140." RNA (New York, N.Y.) **14**(12): 2513-2520.

Nishikawa, R., Y. Goto, S. Kojima, H. Enokida, T. Chiyomaru, T. Kinoshita, S. Sakamoto, M. Fuse, M. Nakagawa, Y. Naya, T. Ichikawa and N. Seki (2014). "Tumor-suppressive microRNA-29s inhibit cancer cell migration and invasion via targeting LAMC1 in prostate cancer." Int J Oncol **45**(1): 401-410.

Okamura, K., J. Hagen, H. Duan, D. Tyler and E. Lai (2007). "The mirtron pathway generates microRNA-class regulatory RNAs in Drosophila." Cell **130**(1): 89-100.

Okuhara, A., T. Nakasa, H. Shibuya, T. Niimoto, N. Adachi, M. Deie and M. Ochi (2011). "Changes in microRNA expression in peripheral mononuclear cells according to the progression of osteoarthritis." Modern rheumatology / the Japan Rheumatism Association: 1-12.

Pais, H., E. Francisco, S. Soond, T. Swingler, I. Clark, A. Chantry, V. Moulton and T. Dalmay (2010). "Analyzing mRNA expression identifies Smad3 as a microRNA-140 target regulated only at protein level." RNA **16**(3): 489-494.

Pais, H., F. E. Nicolas, S. M. Soond, T. E. Swingler, I. M. Clark, A. Chantry, V. Moulton and T. Dalmay (2010). "Analyzing mRNA expression identifies Smad3 as a microRNA-140 target regulated only at protein level." RNA **16**(3): 489-494.

Park, S. J., E. J. Cheon, M. H. Lee and H. A. Kim (2013). "MicroRNA-127-5p regulates matrix metalloproteinase 13 expression and interleukin-1beta-induced catabolic effects in human chondrocytes." Arthritis Rheum **65**(12): 3141-3152.

Parpart, S., S. Roessler, F. Dong, V. Rao, A. Takai, J. Ji, L. X. Qin, Q. H. Ye, H. L. Jia, Z. Y. Tang and X. W. Wang (2014). "Modulation of miR-29 expression by alpha-fetoprotein is linked to the hepatocellular carcinoma epigenome." Hepatology **60**(3): 872-883.

Pearle, A. D., C. R. Scanzello, S. George, L. A. Mandl, E. F. DiCarlo, M. Peterson, T. P. Sculco and M. K. Crow (2007). "Elevated high-sensitivity C-reactive protein levels are associated with local inflammatory findings in patients with osteoarthritis." Osteoarthritis Cartilage **15**(5): 516-523.

Pearle, A. D., R. F. Warren and S. A. Rodeo (2005). "Basic science of articular cartilage and osteoarthritis." Clin Sports Med **24**(1): 1-12.

Pelletier, J. P., J. P. Caron, C. Evans, P. D. Robbins, H. I. Georgescu, D. Jovanovic, J. C. Fernandes and J. Martel-Pelletier (1997). "In vivo suppression of early experimental osteoarthritis by interleukin-1 receptor antagonist using gene therapy." Arthritis Rheum **40**(6): 1012-1019.

Petersen, C., M.-E. Bordeleau, J. Pelletier and P. Sharp (2006). "Short RNAs repress translation after initiation in mammalian cells." Mol Cell **21**(4): 533-542.

Petrovich, O. n., S. L. llyich and M. S. Pavlovich (2014). "Connectic tissue: Histophysiology, Biochemistry, Molecular Biology ".

Pfander, D., T. Cramer, E. Schipani and R. S. Johnson (2003). "HIF-1alpha controls extracellular matrix synthesis by epiphyseal chondrocytes." J Cell Sci **116**(Pt 9): 1819-1826.

Poonpet, T., S. Honsawek, N. Tammachote, S. Kanitnate and R. Tammachote (2013). "ADAMTS14 gene polymorphism associated with knee osteoarthritis in Thai women." Genet Mol Res **12**(4): 5301-5309.

Presle, N., P. Pottie, H. Dumond, C. Guillaume, F. Lapicque, S. Pallu, D. Mainard, P. Netter and B. Terlain (2006). "Differential distribution of adipokines between serum and synovial fluid in patients with osteoarthritis. Contribution of joint tissues to their articular production." Osteoarthritis Cartilage **14**(7): 690-695.

Price, M. A. (2006). "CKI, there's more than one: casein kinase I family members in Wnt and Hedgehog signaling." Genes Dev **20**(4): 399-410.

Pujol, J.-P., C. Chadjichristos, F. Legendre, C. Bauge, G. Beauchef, R. Andriamanalijaona, P. Galera and K. Boumediene (2008). "Interleukin-1 and transforming growth factor-beta 1 as crucial factors in osteoarthritic cartilage metabolism." Connect Tissue Res **49**(3): 293-297.

Pullen, T. J., G. da Silva Xavier, G. Kelsey and G. A. Rutter (2011). "miR-29a and miR-29b contribute to pancreatic beta-cell-specific silencing of monocarboxylate transporter 1 (Mct1)." Mol Cell Biol **31**(15): 3182-3194.

Qin, W., A. C. Chung, X. R. Huang, X. M. Meng, D. S. Hui, C. M. Yu, J. J. Sung and H. Y. Lan (2011). "TGF-beta/Smad3 signaling promotes renal fibrosis by inhibiting miR-29." J Am Soc Nephrol **22**(8): 1462-1474.

Ramdas, V., M. McBride, L. Denby and A. H. Baker (2013). "Canonical transforming growth factor-beta signaling regulates disintegrin metalloprotease expression in experimental renal fibrosis via miR-29." Am J Pathol **183**(6): 1885-1896.

Reinhart, B. J., F. J. Slack, M. Basson, A. E. Pasquinelli, J. C. Bettinger, A. E. Rougvie, H. R. Horvitz and G. Ruvkun (2000). "The 21-nucleotide let-7 RNA regulates developmental timing in Caenorhabditis elegans." Nature **403**(6772): 901-906.

Riordan, E. A., C. Little and D. Hunter (2014). "Pathogenesis of post-traumatic OA with a view to intervention." Best Pract Res Clin Rheumatol **28**(1): 17-30.

Ro, S., C. Park, D. Young, K. Sanders and W. Yan (2007). "Tissue-dependent paired expression of miRNAs." Nucleic Acids Res **35**(17): 5944-5953.
Roderburg, C., G. W. Urban, K. Bettermann, M. Vucur, H. Zimmermann, S. Schmidt, J. Janssen, C. Koppe, P. Knolle, M. Castoldi, F. Tacke, C. Trautwein and T. Luedde (2011). "Micro-RNA profiling reveals a role for miR-29 in human and murine liver fibrosis." Hepatology **53**(1): 209-218.
Rodriguez-Lopez, J., M. Pombo-Suarez, J. Loughlin, A. Tsezou, F. J. Blanco, I. Meulenbelt, P. E. Slagboom, A. M. Valdes, T. D. Spector, J. J. Gomez-Reino and A. Gonzalez (2009). "Association of a nsSNP in ADAMTS14 to some osteoarthritis phenotypes." Osteoarthritis Cartilage **17**(3): 321-327.
Rodriguez, A., S. Griffiths-Jones, J. Ashurst and A. Bradley (2004). "Identification of mammalian microRNA host genes and transcription units." Genome Res **14**(10A): 1902-1910.
Roodman, G. D. (1999). "Cell biology of the osteoclast." Exp Hematol **27**(8): 1229-1241.
Rothwell, A. G. and G. Bentley (1973). "Chondrocyte multiplication in osteoarthritic articular cartilage." J Bone Joint Surg Br **55**(3): 588-594.
Ruby, G., C. Jan and D. Bartel (2007). "Intronic microRNA precursors that bypass Drosha processing." Nature **448**(7149): 83-86.
Sætrom, P., B. Heale, O. Snøve, L. Aagaard, J. Alluin and J. Rossi (2007). "Distance constraints between microRNA target sites dictate efficacy and cooperativity." Nucleic Acids Res **35**(7): 2333-2342.
Saini, H. K., S. Griffiths-Jones and A. J. Enright (2007). "Genomic analysis of human microRNA transcripts." Proc Natl Acad Sci U S A **104**(45): 17719-17724.
Sandell, L. J. and T. Aigner (2001). "Articular cartilage and changes in arthritis. An introduction: cell biology of osteoarthritis." Arthritis Res **3**(2): 107-113.
Sandell, L. J., N. Morris, J. R. Robbins and M. B. Goldring (1991). "Alternatively spliced type II procollagen mRNAs define distinct populations of cells during vertebral development: differential expression of the amino-propeptide." J Cell Biol **114**(6): 1307-1319.
Santanam, U., N. Zanesi, A. Efanov, S. Costinean, A. Palamarchuk, J. P. Hagan, S. Volinia, H. Alder, L. Rassenti, T. Kipps, C. M. Croce and Y. Pekarsky (2010). "Chronic lymphocytic leukemia modeled in mouse by targeted miR-29 expression." Proc Natl Acad Sci U S A **107**(27): 12210-12215.
Scanzello, C. R. and S. R. Goldring (2012). "The role of synovitis in osteoarthritis pathogenesis." Bone **51**(2): 249-257.
Schipani, E., H. E. Ryan, S. Didrickson, T. Kobayashi, M. Knight and R. S. Johnson (2001). "Hypoxia in cartilage: HIF-1alpha is essential for chondrocyte growth arrest and survival." Genes Dev **15**(21): 2865-2876.
Schmid, T. M. and T. F. Linsenmayer (1985). "Developmental acquisition of type X collagen in the embryonic chick tibiotarsus." Dev Biol **107**(2): 373-381.
Schmitt, M. J., C. Margue, I. Behrmann and S. Kreis (2013). "MiRNA-29: a microRNA family with tumor-suppressing and immune-modulating properties." Curr Mol Med **13**(4): 572-585.
Schwarz, D., G. Hutvágner, T. Du, Z. Xu, N. Aronin and P. Zamore (2003). "Asymmetry in the assembly of the RNAi enzyme complex." Cell **115**(2): 199-208.
Sengupta, S., J. A. den Boon, I. H. Chen, M. A. Newton, S. A. Stanhope, Y. J. Cheng, C. J. Chen, A. Hildesheim, B. Sugden and P. Ahlquist (2008). "MicroRNA 29c is down-regulated in nasopharyngeal carcinomas, up-regulating mRNAs encoding extracellular matrix proteins." Proc Natl Acad Sci U S A **105**(15): 5874-5878.
Serra, R., M. Johnson, E. H. Filvaroff, J. LaBorde, D. M. Sheehan, R. Derynck and H. L. Moses (1997). "Expression of a truncated, kinase-defective TGF-beta type II receptor in mouse skeletal

tissue promotes terminal chondrocyte differentiation and osteoarthritis." J Cell Biol **139**(2): 541-552.
Shioya, M., S. Obayashi, H. Tabunoki, K. Arima, Y. Saito, T. Ishida and J. Satoh (2010). "Aberrant microRNA expression in the brains of neurodegenerative diseases: miR-29a decreased in Alzheimer disease brains targets neurone navigator 3." Neuropathol Appl Neurobiol **36**(4): 320-330.
Sibley, C., Y. Seow, S. Saayman, K. Dijkstra, S. El Andaloussi, M. Weinberg and M. Wood (2012). "The biogenesis and characterization of mammalian microRNAs of mirtron origin." Nucleic Acids Res **40**(1): 438-448.
Silver, I. A. (1975). "Measurement of pH and ionic composition of pericellular sites." Philos Trans R Soc Lond B Biol Sci **271**(912): 261-272.
Smith, M. D., E. Barg, H. Weedon, V. Papengelis, T. Smeets, P. P. Tak, M. Kraan, M. Coleman and M. J. Ahern (2003). "Microarchitecture and protective mechanisms in synovial tissue from clinically and arthroscopically normal knee joints." Ann Rheum Dis **62**(4): 303-307.
Song, D. H., I. Dominguez, J. Mizuno, M. Kaut, S. C. Mohr and D. C. Seldin (2003). "CK2 phosphorylation of the armadillo repeat region of beta-catenin potentiates Wnt signaling." J Biol Chem **278**(26): 24018-24025.
Song, J., D. Kim and E.-J. Jin (2011). "MicroRNA-488 suppresses cell migration through modulation of the focal adhesion activity during chondrogenic differentiation of chick limb mesenchymal cells." Cell Biology International **35**(2): 179-185.
Song, R. H., M. D. Tortorella, A. M. Malfait, J. T. Alston, Z. Yang, E. C. Arner and D. W. Griggs (2007). "Aggrecan degradation in human articular cartilage explants is mediated by both ADAMTS-4 and ADAMTS-5." Arthritis Rheum **56**(2): 575-585.
Sorrentino, A., M. Ferracin, G. Castelli, M. Biffoni, G. Tomaselli, M. Baiocchi, A. Fatica, M. Negrini, C. Peschle and M. Valtieri (2008). "Isolation and characterization of CD146+ multipotent mesenchymal stromal cells." Exp Hematol **36**(8): 1035-1046.
Stanton, H., F. M. Rogerson, C. J. East, S. B. Golub, K. E. Lawlor, C. T. Meeker, C. B. Little, K. Last, P. J. Farmer, I. K. Campbell, A. M. Fourie and A. J. Fosang (2005). "ADAMTS5 is the major aggrecanase in mouse cartilage in vivo and in vitro." Nature **434**(7033): 648-652.
Steele, R., J. L. Mott and R. B. Ray (2010). "MBP-1 upregulates miR-29b that represses Mcl-1, collagens, and matrix-metalloproteinase-2 in prostate cancer cells." Genes Cancer **1**(4): 381-387.
Subramanian, M., S. R. Rao, P. Thacker, S. Chatterjee and D. Karunagaran (2014). "MiR-29b downregulates canonical Wnt signaling by suppressing coactivators of beta-catenin in human colorectal cancer cells." J Cell Biochem **115**(11): 1974-1984.
Sulzbacher, I. (2013). "Osteoarthritis: histology and pathogenesis." Wien Med Wochenschr **163**(9-10): 212-219.
Suomi, S., H. Taipaleenmäki, A. Seppänen, T. Ripatti, K. Väänänen, T. Hentunen, A.-M. Säämänen and T. Laitala-Leinonen (2008). "MicroRNAs regulate osteogenesis and chondrogenesis of mouse bone marrow stromal cells." Gene Regulation and Systems Biology **2**: 177-191.
Swingler, T., G. Wheeler, V. Carmont, H. Elliott, M. Barter, M. Abu-Elmagd, S. Donell, R. Boot-Handford, M. Hajihosseini, A. Münsterberg, T. Dalmay, D. Young and I. Clark (2011). "The expression and function of microRNAs in chondrogenesis and osteoarthritis." Arthritis & Rheumatism: n/a-n/a.
(2012). "The expression and function of microRNAs in chondrogenesis and osteoarthritis." Arthritis & Rheumatism **64**: 1909-1919.
Taganov, K., M. Boldin, K.-J. Chang and D. Baltimore (2006). "NF-kappaB-dependent induction of microRNA miR-146, an inhibitor targeted to signaling proteins of innate immune responses." Proc Natl Acad Sci U S A **103**(33): 12481-12486.

Tan, M., J. Wu and Y. Cai (2013). "Suppression of Wnt signaling by the miR-29 family is mediated by demethylation of WIF-1 in non-small-cell lung cancer." Biochem Biophys Res Commun **438**(4): 673-679.

Tardif, G., D. Hum, J.-P. Pelletier, N. Duval and J. Martel-Pelletier (2009). "Regulation of the IGFBP-5 and MMP-13 genes by the microRNAs miR-140 and miR-27a in human osteoarthritic chondrocytes." BMC Musculoskelet Disord **10**: 148.

Tetlow, L., D. Adlam and D. Woolley (2001). "Matrix metalloproteinase and proinflammatory cytokine production by chondrocytes of human osteoarthritic cartilage: Associations with degenerative changes." Arthritis & Rheumatism **44**(3): 585-594.

Tortorella, M. D., A. M. Malfait, C. Deccico and E. Arner (2001). "The role of ADAM-TS4 (aggrecanase-1) and ADAM-TS5 (aggrecanase-2) in a model of cartilage degradation." Osteoarthritis Cartilage **9**(6): 539-552.

Tuddenham, L., G. Wheeler, S. Ntounia-Fousara, J. Waters, M. Hajihosseini, I. Clark and T. Dalmay (2006). "The cartilage specific microRNA-140 targets histone deacetylase 4 in mouse cells." FEBS Lett **580**(17): 4214-4217.

Ugalde, A. P., A. J. Ramsay, J. de la Rosa, I. Varela, G. Marino, J. Cadinanos, J. Lu, J. M. Freije and C. Lopez-Otin (2011). "Aging and chronic DNA damage response activate a regulatory pathway involving miR-29 and p53." EMBO J **30**(11): 2219-2232.

Umlauf, D., S. Frank, T. Pap and J. Bertrand (2010). "Cartilage biology, pathology, and repair." Cellular and Molecular Life Sciences **67**(24): 4197-4211.

van Amerongen, R. and A. Berns (2005). "Re-evaluating the role of Frat in Wnt-signal transduction." Cell Cycle **4**(8): 1065-1072.

van Beuningen, H. M., H. L. Glansbeek, P. M. van der Kraan and W. B. van den Berg (1998). "Differential effects of local application of BMP-2 or TGF-beta 1 on both articular cartilage composition and osteophyte formation." Osteoarthritis Cartilage **6**(5): 306-317.

van der Kraan, P. M. and W. B. van den Berg (2007). "Osteophytes: relevance and biology." Osteoarthritis Cartilage **15**(3): 237-244.

van Rooij, E. and S. Kauppinen (2014). "Development of microRNA therapeutics is coming of age." EMBO Mol Med **6**(7): 851-864.

van Rooij, E., L. B. Sutherland, J. E. Thatcher, J. M. DiMaio, R. H. Naseem, W. S. Marshall, J. A. Hill and E. N. Olson (2008). "Dysregulation of microRNAs after myocardial infarction reveals a role of miR-29 in cardiac fibrosis." Proc Natl Acad Sci U S A **105**(35): 13027-13032.

Vasudevan, S. and J. Steitz (2007). "AU-rich-element-mediated upregulation of translation by FXR1 and Argonaute 2." Cell **128**(6): 1105-1118.

Vasudevan, S., Y. Tong and J. Steitz (2007). "Switching from repression to activation: microRNAs can up-regulate translation." Science (New York, N.Y.) **318**(5858): 1931-1934.

Ventura, A., A. Young, M. Winslow, L. Lintault, A. Meissner, S. Erkeland, J. Newman, R. Bronson, D. Crowley, J. Stone, R. Jaenisch, P. Sharp and T. Jacks (2008). "Targeted deletion reveals essential and overlapping functions of the miR-17 through 92 family of miRNA clusters." Cell **132**(5): 875-886.

Verrecchia, F., M. L. Chu and A. Mauviel (2001). "Identification of novel TGF-beta /Smad gene targets in dermal fibroblasts using a combined cDNA microarray/promoter transactivation approach." J Biol Chem **276**(20): 17058-17062.

Verrecchia, F. and A. Mauviel (2002). "Transforming growth factor-beta signaling through the Smad pathway: role in extracellular matrix gene expression and regulation." J Invest Dermatol **118**(2): 211-215.

Wang, B., R. Komers, R. Carew, C. E. Winbanks, B. Xu, M. Herman-Edelstein, P. Koh, M. Thomas, K. Jandeleit-Dahm, P. Gregorevic, M. E. Cooper and P. Kantharidis (2012). "Suppression of

microRNA-29 expression by TGF-beta1 promotes collagen expression and renal fibrosis." J Am Soc Nephrol **23**(2): 252-265.
Wang, F. S., P. C. Chuang, C. L. Lin, M. W. Chen, H. J. Ke, Y. H. Chang, Y. S. Chen, S. L. Wu and J. Y. Ko (2013). "MicroRNA-29a protects against glucocorticoid-induced bone loss and fragility in rats by orchestrating bone acquisition and resorption." Arthritis Rheum **65**(6): 1530-1540.
Wang, H., R. Garzon, H. Sun, K. J. Ladner, R. Singh, J. Dahlman, A. Cheng, B. M. Hall, S. J. Qualman, D. S. Chandler, C. M. Croce and D. C. Guttridge (2008). "NF-kappaB-YY1-miR-29 regulatory circuitry in skeletal myogenesis and rhabdomyosarcoma." Cancer Cell **14**(5): 369-381.
Wang, H. X., F. R. Tekpetey and G. M. Kidder (2009). "Identification of WNT/beta-CATENIN signaling pathway components in human cumulus cells." Mol Hum Reprod **15**(1): 11-17.
Wang, L., L. Zhou, P. Jiang, L. Lu, X. Chen, H. Lan, D. C. Guttridge, H. Sun and H. Wang (2012). "Loss of miR-29 in myoblasts contributes to dystrophic muscle pathogenesis." Mol Ther **20**(6): 1222-1233.
Wang, L. G. and J. Gu (2012). "Serum microRNA-29a is a promising novel marker for early detection of colorectal liver metastasis." Cancer Epidemiol **36**(1): e61-67.
Watanabe, T., T. Sato, T. Amano, Y. Kawamura, N. Kawamura, H. Kawaguchi, N. Yamashita, H. Kurihara and T. Nakaoka (2008). "Dnm3os, a non-coding RNA, is required for normal growth and skeletal development in mice." Dev Dyn **237**(12): 3738-3748.
Wei, W., H. B. He, W. Y. Zhang, H. X. Zhang, J. B. Bai, H. Z. Liu, J. H. Cao, K. C. Chang, X. Y. Li and S. H. Zhao (2013). "miR-29 targets Akt3 to reduce proliferation and facilitate differentiation of myoblasts in skeletal muscle development." Cell Death Dis **4**: e668.
Weng, L. H., C. J. Wang, J. Y. Ko, Y. C. Sun and F. S. Wang (2010). "Control of Dkk-1 ameliorates chondrocyte apoptosis, cartilage destruction, and subchondral bone deterioration in osteoarthritic knees." Arthritis Rheum **62**(5): 1393-1402.
Wermter, C., M. Howel, V. Hintze, B. Bombosch, K. Aufenvenne, I. Yiallouros and W. Stocker (2007). "The protease domain of procollagen C-proteinase (BMP1) lacks substrate selectivity, which is conferred by non-proteolytic domains." Biol Chem **388**(5): 513-521.
Westholm, J. and E. Lai (2011). "Mirtrons: microRNA biogenesis via splicing." Biochimie **93**(11): 1897-1904.
Wieland, H., M. Michaelis, B. Kirschbaum and K. Rudolphi (2005). "Osteoarthritis — an untreatable disease?" Nature Reviews Drug Discovery **4**(4): 331-344.
Wienholds, E., W. P. Kloosterman, E. Miska, E. Alvarez-Saavedra, E. Berezikov, E. de Bruijn, H. R. Horvitz, S. Kauppinen and R. H. Plasterk (2005). "MicroRNA expression in zebrafish embryonic development." Science **309**(5732): 310-311.
Wienholds, E., M. Koudijs, F. van Eeden, E. Cuppen and R. Plasterk (2003). "The microRNA-producing enzyme Dicer1 is essential for zebrafish development." Nat Genet **35**(3): 217-218.
Wightman, B., I. Ha and G. Ruvkun (1993). "Posttranscriptional regulation of the heterochronic gene lin-14 by lin-4 mediates temporal pattern formation in C. elegans." Cell **75**(5): 855-862.
Willert, K., M. Brink, A. Wodarz, H. Varmus and R. Nusse (1997). "Casein kinase 2 associates with and phosphorylates dishevelled." EMBO J **16**(11): 3089-3096.
Willert, K. and K. A. Jones (2006). "Wnt signaling: is the party in the nucleus?" Genes Dev **20**(11): 1394-1404.
Wittmann, J. and H.-M. Jäck (2010). "Serum microRNAs as powerful cancer biomarkers." Biochim Biophys Acta **1806**(2): 200-207.
Xiong, Y., J. H. Fang, J. P. Yun, J. Yang, Y. Zhang, W. H. Jia and S. M. Zhuang (2010). "Effects of microRNA-29 on apoptosis, tumorigenicity, and prognosis of hepatocellular carcinoma." Hepatology **51**(3): 836-845.
Xu, J., Y. Kang, W.-m. Liao and L. Yu (2012). "MiR-194 Regulates Chondrogenic Differentiation of Human Adipose-Derived Stem Cells by Targeting Sox5." PLoS One **7**(3): e31861.

Yamasaki, K., T. Nakasa, S. Miyaki, M. Ishikawa, M. Deie, N. Adachi, Y. Yasunaga, H. Asahara and M. Ochi (2009). "Expression of MicroRNA-146a in osteoarthritis cartilage." Arthritis and rheumatism **60**(4): 1035-1041.

Yamashita, S., S. Miyaki, Y. Kato, S. Yokoyama, T. Sato, F. Barrionuevo, H. Akiyama, G. Scherer, S. Takada and H. Asahara (2012). "L-Sox5 and Sox6 enhance chondrogenic miR-140 expression by strengthening dimeric Sox9 activity." Journal of Biological Chemistry.

Yan, C., Y. Wang, X.-Y. Shen, G. Yang, J. Jian, H.-S. Wang, G.-Q. Chen and Q. Wu (2011). "MicroRNA regulation associated chondrogenesis of mouse MSCs grown on polyhydroxyalkanoates." Biomaterials **32**(27): 6435-6444.

Yang, B., H. Guo, Y. Zhang, L. Chen, D. Ying and S. Dong (2011). "MicroRNA-145 Regulates Chondrogenic Differentiation of Mesenchymal Stem Cells by Targeting Sox9." PLoS One **6**(7): e21679.

Yang, B., H. Guo, Y. Zhang, S. Dong and D. Ying (2011). "The microRNA expression profiles of mouse mesenchymal stem cell during chondrogenic differentiation." BMB Reports **44**(1): 28-33.

Yang, J., S. Qin, C. Yi, G. Ma, H. Zhu, W. Zhou, Y. Xiong, X. Zhu, Y. Wang, L. He and X. Guo (2011). "MiR-140 is co-expressed with Wwp2-C transcript and activated by Sox9 to target Sp1 in maintaining the chondrocyte proliferation." FEBS Lett **585**(19): 2992-2997.

Yang, T., Y. Liang, Q. Lin, J. Liu, F. Luo, X. Li, H. Zhou, S. Zhuang and H. Zhang (2013). "miR-29 mediates TGFbeta1-induced extracellular matrix synthesis through activation of PI3K-AKT pathway in human lung fibroblasts." J Cell Biochem **114**(6): 1336-1342.

Yi, R., Y. Qin, I. Macara and B. Cullen (2003). "Exportin-5 mediates the nuclear export of pre-microRNAs and short hairpin RNAs." Genes Dev **17**(24): 3011-3016.

Zamli, Z. and M. Sharif (2011). "Chondrocyte apoptosis: a cause or consequence of osteoarthritis?" Int J Rheum Dis **14**(2): 159-166.

Zampetaki, A., S. Kiechl, I. Drozdov, P. Willeit, U. Mayr, M. Prokopi, A. Mayr, S. Weger, F. Oberhollenzer, E. Bonora, A. Shah, J. Willeit and M. Mayr (2010). "Plasma microRNA profiling reveals loss of endothelial miR-126 and other microRNAs in type 2 diabetes." Circ Res **107**(6): 810-817.

Zeng, Y. and B. Cullen (2004). "Structural requirements for pre-microRNA binding and nuclear export by Exportin 5." Nucleic Acids Res **32**(16): 4776-4785.

Zhang, Y. K., H. Wang, Y. Leng, Z. L. Li, Y. F. Yang, F. J. Xiao, Q. F. Li, X. Q. Chen and L. S. Wang (2011). "Overexpression of microRNA-29b induces apoptosis of multiple myeloma cells through down regulating Mcl-1." Biochem Biophys Res Commun **414**(1): 233-239.

Zhang, Z., J. Zou, G. K. Wang, J. T. Zhang, S. Huang, Y. W. Qin and Q. Jing (2011). "Uracils at nucleotide position 9-11 are required for the rapid turnover of miR-29 family." Nucleic Acids Res **39**(10): 4387-4395.

Zhao, Q., H. Eberspaecher, V. Lefebvre and B. De Crombrugghe (1997). "Parallel expression of Sox9 and Col2a1 in cells undergoing chondrogenesis." Dev Dyn **209**(4): 377-386.

Zhong, N., J. Sun, Z. Min, W. Zhao, R. Zhang, W. Wang, J. Tian, L. Tian, J. Ma, D. Li, Y. Han and S. Lu (2012). "MicroRNA-337 is associated with chondrogenesis through regulating TGFBR2 expression." Osteoarthritis and Cartilage.

Zhou, S., K. Eid and J. Glowacki (2004). "Cooperation between TGF-beta and Wnt pathways during chondrocyte and adipocyte differentiation of human marrow stromal cells." J Bone Miner Res **19**(3): 463-470.

Zhu, M., M. Chen, M. Zuscik, Q. Wu, Y. J. Wang, R. N. Rosier, R. J. O'Keefe and D. Chen (2008). "Inhibition of beta-catenin signaling in articular chondrocytes results in articular cartilage destruction." Arthritis Rheum **58**(7): 2053-2064.

Zhu, M., D. Tang, Q. Wu, S. Hao, M. Chen, C. Xie, R. N. Rosier, R. J. O'Keefe, M. Zuscik and D. Chen (2009). "Activation of beta-catenin signaling in articular chondrocytes leads to osteoarthritis-

like phenotype in adult beta-catenin conditional activation mice." J Bone Miner Res **24**(1): 12-21.

ENDICES

Genes	Accession number	Sequences (5'->3')
ADAMTS6	ENSG00000049192	Forward: ACGTGAGCTCTCTCATCGTCATGGTTCTGC Reverse: ACGTGAGCTCCAAGCAGGAGAATGAATGTAGG
ADAMTS14	ENSG00000138316	Forward: GAGCTCGCTGTGCCCTGCCATC GAGCTCGGGTCCAATGGCGATGTTA
ADAMTS17	ENSG00000140470	Forward: ACGTTCTAGAAACATGAGCGTGGACTTGG Reverse: ACGTTCTAGATGTAATGCAAGTTAACGAATGG
ADAMTS19	ENSG00000145808	Forward: ACGTGAGCTCAATCACAGCTCCAGGTAATC Reverse: ACGTGAGCTCCCAAGAGACATACTATCTTCCAAGG
FZD3	ENSG00000104290	Forward: ATGCGTCGACTATTAGATGCCCAGCCTTTCTC Reverse: ATGCGTCGACATGCCTACCAAGAGGATAACATTC
FZD5	ENSG00000163251	Forward: ATGCGTCGACGGCATCGGCTACAACCTGAC Reverse: ATGCGTCGACAGACCACACAGTTCAAAGA AACCTG
FRAT2	ENSG00000181274	Forward: ATGCGTCGACCAACAGCGTCCAGTTCCTAC Reverse: ATGCGTCGACGCCGTCAAGTTTCATACAGC
CK2A2	ENSG00000070770	Forward: ATGCGTCGACATGCAGGTACTAGAGTTGTGTGG Reverse: ATGCGTCGACAATAAGTTTGCTTGTTTCTGTGG
DVL3	ENSG00000161202	Forward: ATGCGTCGACGCTGCGTTCCTCTCTCCATC Reverse: ATGCGTCGACTACCATTTATTGAGCACCTACTCTACTG TG

Table 1: Primer sequences for PCR amplification 3'UTR region of potential targets of the miR-29 family. For subcloning purpose, restriction sites (bases underlined) were added to the 5'P of the primers. *Sac*I (GAGCTC), *Sal*I (GTCGAC), *Xba*I (TCTAGA).

Genes	Mutant	Primer sequence (5'->3')
ADAMTS6	Site 1	Forward: TATGTGATGCACTGACATGTAATTTAAGAAGCTTATGATGGAATCAAGTCAAACATGCTGTTTAACTGAAAG Reverse: CTTTCAGTTAAACAGCATGTTTGACTTGATTCCATCATAAGCTTCTTAAATTACATGTCAGTGCATCACATA
	Site 2	Forward: TATTTATTTCACCAGGGCACATTAAGCTTAAGTTAACTGTTCTTTGAAAAGGCGCAAGGGAATTCAGT Reverse: ACTGAATTCCCTTGCGCCTTTTCAAAGAACAGTTAACTTAAGCTTAATGTGCCCTGGTGAAATAAATA
ADAMTS10	Site 1	Forward: GGGGACACAGACCCGTTTGTAAGCTTACCCCTTGTCGATGGTGTGCG Reverse: CGCACACCATCGACAAGGGGTAAGCTTACAAACGGGTCTGTGTCCCC
	Site 2	Forward: GCTCGGTCCGGGCCAAGCTTATGACGATGAGAGATGCATTAATCGGTCC Reverse: GGACCGATTAATGCATCTCTCATCGTCATAAGCTTGGCCCGGACCGAGC
ADAMTS14	Site 1	Forward: GTTTGTCTTTGCTGGCCAGAAGAGTCGACTCATGGCCATACTCTGGCCTTG Reverse: CAAGGCCAGAGTATGGCCATGAGTCGACTCTTCTGGCCAGCAAAGAC
	Site 2	Forward: GGGTGCCAGCCCCTGGCCGTCGACTGGAGTGGGGAAGACAC Reverse: GTGTCTTCCCCACTCCAGTCGACGGCCAGGGGCTGGCACCC
	Site 3	Forward: CTAAACTCCTGCCAGGTGATAGAGAGCTCTCTCACTTCTTCCTTCCCCAAGGC

		Reverse: GCCTTGGGGAAGGAAGAAGTGAGAGAGCTCTCTATCACCTGGCAGGAGTTTAG
	Site 4	Forward: CTAAACTCCTGCCAGGTGATAGAGAGCTCTCTCACTTCTTCCTTCCCCAAGGC Reverse: GCCTTGGGGAAGGAAGAAGTGAGAGAGCTCTCTATCACCTGGCAGGAGTTTAG
ADAMTS17	Site 1	Forward: GCAATTACCGTTTCTTATGTCACAGTCGACTGAAGAGAGGCCCTTCTGTTTCCC Reverse: GGGAAACAGAAGGGCCTCTCTTCAGTCGACTGTGACATAAGAAACGGTAATTGC
	Site 2	Forward: CACCAACTTGGTGGGCATTTCATGTCGACTTATGTTCTAGGACTTTACCGTA Reverse: TACGGTAAAGTCCTAGAACATAAGTCGACATGAAATGCCCACCAAGTTGGTG
	Site 3	Forward: TAACAAAACAAAACACAGAAACACAGTCGACATAAATCAAGAAGCACAGGGAGATGATCCCATGG Reverse: CCATGGGATCATCTCCCTGTGCTTCTTGATTTATGTCGACTGTGTTTCTGTGTTTTGTTTTGTTA
	Site 4	Forward: GAAGTGTTGAGAAACTTCCGTGTCGACTCTGTGGAAAGAACCGAGGGT Reverse: ACCCTCGGTTCTTTCCACAGAGTCGACACGGAAGTTTCTCAACACTTC
	Site 5	Forward: CCAGAGTCTCACGACCCTACGGTCGCCTTTTTATTGGTGCAAAATTAAACC Reverse: GGTTTAATTTTGCACCAATAAAAAGGCGACCGTAGGGTCGTGAGACTCTGG
ADAMTS	Site 1	Forward: ATCAAATTAATTTATTTTTTTGCCTGCCAAACATCCAATGGTCGACTTGTTTTGGTTACACAAACATTTTGATTTATACTATATG

19		Reverse: CATATAGTATAAATCAAAATGTTTGTGTAACCAAAACAAGTCGACCATTGGATGTTTGGCAGGCAAAAAAATAAATTAATTTGAT
	Site 2	Forward: GTTGTTTGTTAGGGCTATCTCTAAGTCGACCCTCTCTCCCCACCAATAACATTGAATTATC Reverse: ATAATTCAATGTTATTGGTGGGGAGAGAGGGTCGACTTAGAGATAGCCCTAACAAACAACG
FZD3		Forward: GGATTTAGTCTAACTCACAGCTAAGGTAGAAAAGTACTCTGATGGCAAGAGAATGTCCAGACTAATATTTTC Reverse: GAAAATATTAGTCTGGACATTCTCTTGCCATCAGAGTACTTTTCTACCTTAGCTGTGAGTTAGACTAAATCC
FZD5	Site 1	Forward: CGGCGTCGCGGCCCAAGCTTGGGAGGCGGTCGCAG Reverse: CTGCGACCGCCTCCCAAGCTTGGGCCGCGACGCCG
	Site 2	Forward: GTGGACGTGGAGATGAAGCACAAGCTTGACCACAGGCCTATCCAGAAGG Reverse: CCTTCTGGATAGGCCTGTGGTCAAGCTTGTGCTTCATCTCCACGTCCAC
	Site 3	Forward: GCCCACCAGCAGGTAGAAGCTTAGCGGGCCCAGCACGAAGCC Reverse: GGCTTCGTGCTGGGCCCGCTAAGCTTCTACCTGCTGGTGGGC
	Site 4	Forward: CACATGAAGTACTTGAGCATGAAGCTTCAGTACTCGGGCTTGGCGCGCG Reverse: CGCGCGCCAAGCCCGAGTACTGAAGCTTCATGCTCAAGTACTTCATGTG
	Site 5	Forward: CGGGAGGGGGCAACAAGCTTATGAAGGTAAACGGAAGTGACCTTGGCA Reverse: TGCCAAGGTCACTTCCGTTTACCTTCATAAGCTTGTTGCCCCCTCCCG
FRAT2	Site 1	Forward: GCGTGGAGAAATGTATGCGCCAGAAGCTTTCCGTGGGGCATGAG

		AATTTCC Reverse: GGAAATTCTCATGCCCCACGGAAAGCTTCTGGCGCATACATTTCTCCACGC
	Site 2	Forward: CTTATTTTCTGGTGGAGGAGCTTAGTAAGTAAGCTTACAATTGCTGTGCAAAGAAATTCCAGAGG-3' Reverse: CCTCTGGAATTTCTTTGCACAGCAATTGTAAGCTTACTTACTAAGCTCCTCCACCAGAAAATAAG
	Site 3	Forward: GGGAGACTCCAAGCGGTGGTAAAAGCTTAACAGGGCTCTTCTTGGAGCAAG Reverse: CTTGCTCCAAGAAGAGCCCTGTTAAGCTTTTACCACCGCTTGGAGTCTCCC
CK2A2	Site 1	Forward: AGAGGAATATACAAGGGGCTTGGGGAAGAAAATAAGCTTCCCGGAGCAAGTGTTG Reverse: CAACACTTGCTCCGGGAAGCTTATTTTCTTCCCCAAGCCCCTTGTATATTCCTCT
	Site 2	Forward: TCTCCTCTAATCTATCAGTCTGAGAAGCTTTTCCTCTCTGCAAGGGAACACATTTGC Reverse: GCAAATGTGTTCCCTTGCAGAGAGGAAAAGCTTCTCAGACTGATAGATTAGAGGAGA
	Site 3	Forward: GCGCCTGACTCGAGAAGCTTACCTTTCAGTCCACTGGGACCAATCCA Reverse: TGGATTGGTCCCAGTGGACTGAAAGGTAAGCTTCTCGAGTCAGGCGC
	Site 4	Forward: CTGCTTCCATCCTTATCAACAGAAGCTTTGGGAGAACCTAAGTCATTTCCCTGAG Reverse: TCAGGGAAATGACTTAGGTTCTCCCAAAGCTTCTGTTGATAAGGATGGAAGCAG
DVL3	Site 1	Forward: GTGCGCTAACTGCTCGCAGAAGCTTGCGAGGGTGGGGTGCACC

		Reverse: GGTGCACCCCACCCTCGCAAGCTTCTGCGAGCAGTTAGCGCAC
	Site 2	Forward: CCCTTTTGTCTCTGGGACCAGACTTGTTAAGCTTACCCCTTACTCCCCTCTGC Reverse: GCAGAGGGGAGTAAGGGGTAAGCTTAACAAGTCTGGTCCCAGAGACAAAAGGG
	Site 3	Forward: GCACAGTGCCTGGCACACAGTAGAGTAAAGCTTCAATAAATGGTAGTCGACC Reverse: GGTCGACTACCATTTATTGAAGCTTTACTCTACTGTGTGCCAGGCACTGTGC
DICER		Forward: ACGTGAGCTCGTGTGCAGTAGTGCCAGTCC Reverse: ACGTGAGCTCTGCAATCACAGGAACACAGG

Table 2: Primers for mutating the binding sites of the miR-29 family

Genes	Accession number	Primer sequence (5'->3')	Probe
Arginase-1	ENSMUST00000020161	Forward: CCTGAAGGAACTGAAAGGAAAG Reverse: TTGGCAGATATGCAGGGAGT	2
IL-6	ENSMUST00000026845	Forward: TGATGGATGCTACCAAACTGG Reverse: TTCATGTACTCCAGGTAGCTATGG	6
SAA3	ENAMUST00000006956	Forward: GCTCGGGGGAACTATGATG Reverse: AACTTCTGAACAGCCTCTCTGG	26
Axin2		Forward: GCTGACGGATGATTCCATGT Reverse: ACTGCCCACACGATAAGGAG	56
SOX9	ENST00000245479	Forward: TACCCGCACTTGCACAAC Reverse: TCTCGCTCTCGTTCAGAAGTC	61
FZD3	NM_017412	Forward: ACAGCAAAGTGAGCAGCTACC Reverse: CTGTAACTGCAGGGCGTGTA	75
FZD5	NM_003468	Forward:ACCCCAGGGGAGAGAAACT Reverse: TGCAAATTGGGGGAAGTAAG	83
DVL3	NM_004423	Forward:CCCTGAGCACCATCACCT Reverse: GGATGGACAAGTGGAAGTCG	17
FRAT2		Forward: GTTCAAGGTCACGGTTTGCT Reverse: GAAAAGACTCCGGGGTGAGT	14
CK2A2	NM_001896	Forward: CCATGGAGCACCCATACTTC Reverse: CACAGCATTGTCTGCACAAG	68

Table 3: Primer sequence and the Universal Probe Library probe for gene of interest

Genes	Accession number	Primer sequence (5'-3')
ADAMTS4	MM_005099	Forward: CAAGGTCCCATGTGCAACGT Reverse: CATCTGCCACCACCAGTGTCT Probe: FAM-CCGAAGAGCCAAGCGCTTTGCTTC-TAMRA
ADAMTS6	NM_014273	Forward: GGCTGAATGACACATCCACTGTT Reverse: CAAACCGTTCAATGCTCACTGA Probe: FAM-AAGCGCTTCCGCCTCTGCAACC-TAMRA
ADAMTS10	NM_030957	Forward: AGAGAACGGTGTGGCTAACCA Reverse: TCTCTCGCGCTCACACATTC Probe: FAM-CAGTGCTCATCACACGCTATGACATCTGC-TAMRA
ADAMTS14	AF366351	Forward: CGCTGGATGGGACTGAGTGT Reverse: CGCGAACATGACCCAAACTT Probe: FAM-CCCGGCAAGTGGTGCTTCAAAGGT-TAMRA
ADAMTS17	NM_139057	Forward: GGTCTCAATTTGGCCTTTACCAT Reverse: GACCTGCCAGCGGCAAGAT Probe: FAM-CCACAACTTGGGCATGAACCACGA-TAMRA
ADAMTS19	AJ311904	Forward: GGTGTAAGGCTGGAGAATGTACCA Reverse: TGCGCTCTCGACTGCTGAT Probe: FAM-CCTCAGCACCTGAACATCTGGCCG-TAMRA
MMP3	NM002422	Forward: TTCCGCCTGTCTCAAGATGATAT Reverse: AAAGGACAAAGCAGGATCACAGTT Probe: FAM-TCAGTCCCTCTATGGACCTCCCCCTGAC-TAMRA

Table 4: Primer pairs and probe for gene of interest

Genes	Primer sequences (5'->3')
Pri-miR-29a/b1exon 1	Forward: TACTGAACTGTCACGGCAGA Reverse: TGTAGTTAGCGACCTCTGCT
Pri-miR-29a/b1Exon4	Forward: TTGCACCCTCACGACATGCT Reverse: TGACTCTCAGCAGGCCTCA
Pri-miR-29b2/c exon 1	Forward: ACTTCTTTAGGGGTGTGCGTA Reverse: ACCCATCTCCCTAGCATTCT
Pri-miR-29b2/c Exon6	Forward: TCAGACTTGCCACCTGGACT Reverse: AGTTGGCATGAGGCTTCGA
Pre-29a	Forward: CTGATTTCTTTTGGTGTTCAG Reverse: AACCGATTTCAGATGGTGC
Pre-29b1	Forward: CATATGGTGGTTTAGATTT Reverse: AACACTGATTTCAAATGGTG
Pre-29b2	Forward: GCTGGTTTCACATGGTGGC Reverse: AACACTGATTTCAAATGGTG
Pre-29c	Forward: CGATTTCTCCTGGTGTTCA Reverse: ACCGATTTCAAATGGTGC

Table 5: Primers for detecting the primary and the premature sequence of the miR-29 family

Names	24_DMM_R	24_DMM_L	log2 Fold change	Fold change
CYP2E1	9.0	10.2	-1.2	2.3
CES3	8.1	9.3	-1.2	2.3
TMEM45B	7.9	8.6	-0.8	1.7
CFD	12.9	13.6	-0.7	1.6
SCD1	10.1	10.7	-0.6	1.6
IGFBP6	8.9	9.6	-0.6	1.5
CHAD	12.4	13.0	-0.6	1.5
LOC100045005	9.6	10.2	-0.6	1.5
TENS1	8.5	9.1	-0.6	1.5
C130045I22RIK	8.2	8.8	-0.6	1.5
LOC667337	9.4	9.9	-0.6	1.5
CXCL1	9.1	7.3	1.9	3.6
CCL7	9.2	7.5	1.8	3.4
SAA3	8.9	7.3	1.6	3.1
TIMP1	12.0	10.5	1.5	2.9
SERPINA3N	11.2	9.7	1.5	2.8
GP38	10.8	9.4	1.4	2.6
MMP3	8.9	7.6	1.3	2.5
ARG1	8.0	7.1	0.8	1.8
CXCL14	9.4	8.8	0.7	1.6
MB	11.9	11.2	0.7	1.6
ANGPTL4	9.5	8.9	0.6	1.6
MT1	13.5	12.9	0.6	1.6
ANKRD23	9.5	8.9	0.6	1.5
MS4A6D	9.9	9.3	0.6	1.5
LOC386330	9.9	9.4	0.5	1.5
LOC270589	8.9	8.4	0.5	1.5
CCL9	11.2	10.6	0.5	1.5
CKM	12.3	11.8	0.5	1.5
LOC386144	9.6	9.1	0.5	1.4

Table 6: List genes changed expression at day 1 in DMM model

GENES	7_DMM_R	7_DMM_L	log2 Fold change	Fold change
MYL3	9.8	11.0	-1.2	2.3
ATP1A2	9.0	10.1	-1.2	2.3
NDRG2	10.0	11.2	-1.2	2.3
CKMT2	11.7	12.8	-1.2	2.2
ANKRD23	10.2	11.4	-1.2	2.2
2310003M01RIK	9.5	10.6	-1.1	2.2
ACTN2	11.1	12.2	-1.1	2.2
2310042D19RIK	9.2	10.3	-1.1	2.2
MYH2	11.0	12.1	-1.1	2.2
PFKM	11.5	12.6	-1.1	2.2
ABRA	8.6	9.7	-1.1	2.1
COX7A1	11.4	12.5	-1.1	2.1
ANKRD2	8.0	9.1	-1.1	2.1
COX8B	11.8	12.8	-1.1	2.1
MB	12.0	13.1	-1.1	2.1
ENO3	12.9	14.0	-1.1	2.1
DUSP26	8.1	9.2	-1.1	2.1
RTN2	10.0	11.1	-1.0	2.1
PKIA	10.4	11.5	-1.0	2.1
TCAP	12.5	13.6	-1.0	2.1
MYOZ1	10.4	11.5	-1.0	2.0
MYOM1	9.9	10.9	-1.0	2.0
ACTN3	11.3	12.3	-1.0	2.0
2310002L09RIK	8.6	9.6	-1.0	2.0
HRC	10.3	11.3	-1.0	2.0
MYOM2	9.1	10.1	-1.0	2.0
CKM	13.0	14.0	-1.0	2.0
CSRP3	8.5	9.5	-1.0	2.0
TMEM38A	9.3	10.3	-1.0	2.0
1110012N22RIK	9.2	10.2	-1.0	2.0
TPM2	11.3	12.3	-1.0	2.0
RYR1	10.1	11.1	-1.0	2.0
MLF1	9.5	10.5	-1.0	2.0
TTN	9.7	10.7	-1.0	2.0
TMOD4	10.7	11.7	-1.0	2.0
DYSFIP1	8.7	9.7	-1.0	2.0
NRAP	9.1	10.1	-1.0	2.0
CMYA5	10.8	11.8	-1.0	2.0
SMTNL2	8.5	9.5	-1.0	1.9
MYLK2	9.2	10.2	-1.0	1.9

MYL2	9.3	10.3	-0.9	1.9
LOC669660	8.6	9.6	-0.9	1.9
KBTBD10	9.8	10.7	-0.9	1.9
ASB2	10.6	11.5	-0.9	1.9
A530098C11RIK	8.7	9.6	-0.9	1.9
F730003H07RIK	9.3	10.3	-0.9	1.9
ZMYND17	8.5	9.4	-0.9	1.9
CPT1B	8.3	9.2	-0.9	1.9
2310079P10RIK	8.5	9.4	-0.9	1.9
EEF1A2	10.7	11.6	-0.9	1.9
YIPF7	8.5	9.4	-0.9	1.9
SCL0003151.1_1374	8.9	9.8	-0.9	1.9
INMT	7.6	8.5	-0.9	1.9
CES3	8.8	9.7	-0.9	1.9
PYGM	9.2	10.1	-0.9	1.8
MYBPC2	11.6	12.5	-0.9	1.8
8030451F13RIK	8.6	9.5	-0.9	1.8
FABP3	10.6	11.4	-0.9	1.8
NEURL	9.5	10.4	-0.9	1.8
PDLIM3	10.4	11.3	-0.9	1.8
SYPL2	9.6	10.5	-0.9	1.8
4833419K08RIK	9.0	9.9	-0.9	1.8
AMPD1	11.1	12.0	-0.8	1.8
CACNA1S	8.6	9.5	-0.8	1.8
SCL0002069.1_48	8.1	9.0	-0.8	1.8
C130073O12RIK	9.0	9.9	-0.8	1.8
GM1157	7.8	8.6	-0.8	1.8
MYH1	9.2	10.1	-0.8	1.8
SLC25A37	11.8	12.6	-0.8	1.8
LOC638935	8.1	9.0	-0.8	1.8
LOC386360	10.4	11.2	-0.8	1.8
BC030476	9.0	9.8	-0.8	1.8
MYH4	10.0	10.8	-0.8	1.7
SCL000959.1_2	13.3	14.1	-0.8	1.7
RPL3L	12.2	13.0	-0.8	1.7
COX6A2	12.7	13.5	-0.8	1.7
MTDNA_ND4L	8.7	9.5	-0.8	1.7
TNNT3	13.1	13.9	-0.8	1.7
AK1	9.8	10.6	-0.8	1.7
DES	11.1	11.9	-0.8	1.7
A2BP1	8.4	9.2	-0.8	1.7
KY	9.1	9.8	-0.8	1.7

UNC45B	8.4	9.2	-0.8	1.7
AI595366	8.7	9.4	-0.8	1.7
D830037I21RIK	7.3	8.1	-0.8	1.7
PGM2	12.0	12.8	-0.8	1.7
4933421G18RIK	9.7	10.4	-0.8	1.7
MYF6	8.3	9.0	-0.8	1.7
SCN4B	8.3	9.1	-0.8	1.7
ALPK3	8.5	9.3	-0.8	1.7
PGAM2	12.3	13.1	-0.8	1.7
ITGA2B	8.9	9.7	-0.8	1.7
CRYAB	9.8	10.6	-0.7	1.7
LOC386144	9.1	9.8	-0.7	1.7
LOC100047934	10.8	11.6	-0.7	1.7
SRL	9.3	10.0	-0.7	1.7
PHKG1	8.8	9.5	-0.7	1.7
ATP1B1	9.5	10.2	-0.7	1.7
HSPB7	8.2	8.9	-0.7	1.7
TNNC1	8.3	9.0	-0.7	1.6
CHCHD10	12.4	13.1	-0.7	1.6
GMPR	9.0	9.7	-0.7	1.6
S3-12	9.3	10.0	-0.7	1.6
9930004G02RIK	9.4	10.1	-0.7	1.6
TCEA3	10.3	11.0	-0.7	1.6
PPP1R3C	10.7	11.4	-0.7	1.6
TRIM54	9.0	9.7	-0.7	1.6
FBP2	8.3	9.0	-0.7	1.6
COQ10A	8.8	9.5	-0.7	1.6
TXLNB	7.8	8.5	-0.7	1.6
XIRP2	8.4	9.1	-0.7	1.6
FSD2	8.6	9.3	-0.7	1.6
PDE4DIP	9.9	10.6	-0.7	1.6
NDUFC1	10.9	11.6	-0.7	1.6
MSCP	11.9	12.6	-0.7	1.6
EG433229	9.2	9.9	-0.7	1.6
SMARCD3	8.2	8.9	-0.7	1.6
SCL0003073.1_164	8.2	8.8	-0.7	1.6
HHATL	8.6	9.3	-0.7	1.6
DNAJC7	8.9	9.6	-0.7	1.6
USP13	7.9	8.6	-0.7	1.6
ADSSL1	11.5	12.2	-0.7	1.6
ACADM	11.2	11.9	-0.7	1.6
MT-ATP6	11.3	12.0	-0.7	1.6
6430573H23RIK	8.2	8.9	-0.7	1.6
TUBA8	8.6	9.3	-0.7	1.6

DEDD2	9.8	10.4	-0.7	1.6
LOC100041835	12.3	12.9	-0.7	1.6
1300013J15RIK	7.9	8.6	-0.7	1.6
MACROD1	9.1	9.8	-0.7	1.6
ALDOA	13.2	13.9	-0.7	1.6
LOC667034	8.5	9.2	-0.7	1.6
MDH2	10.0	10.6	-0.7	1.6
PDK4	9.3	10.0	-0.7	1.6
ART5	7.7	8.4	-0.7	1.6
JSRP1	7.9	8.6	-0.7	1.6
PPM1L	8.4	9.0	-0.7	1.6
MFN2	10.1	10.8	-0.7	1.6
RILPL1	8.8	9.4	-0.6	1.6
EHBP1L1	8.8	9.4	-0.6	1.6
NDUFA5	10.3	10.9	-0.6	1.6
MTDNA_ND2	11.5	12.2	-0.6	1.6
MTDNA_ND5	11.5	12.2	-0.6	1.6
TRIM72	9.7	10.4	-0.6	1.6
B930008G03RIK	10.0	10.7	-0.6	1.6
2310040G24RIK	7.9	8.5	-0.6	1.6
ALAD	12.0	12.7	-0.6	1.6
SGCA	8.4	9.0	-0.6	1.5
LOC385959	8.3	8.9	-0.6	1.5
LOC547380	8.3	8.9	-0.6	1.5
NDUFS7	11.8	12.4	-0.6	1.5
1300017J02RIK	8.9	9.5	-0.6	1.5
LOC381792	7.7	8.3	-0.6	1.5
FLNC	8.5	9.1	-0.6	1.5
DHRS7C	8.1	8.7	-0.6	1.5
ART1	8.0	8.6	-0.6	1.5
EG245190	8.8	9.5	-0.6	1.5
A530020A01RIK	7.9	8.5	-0.6	1.5
PRKAA2	7.8	8.4	-0.6	1.5
VLDLR	8.7	9.3	-0.6	1.5
1110002E22RIK	8.1	8.7	-0.6	1.5
NDUFB9	7.8	8.4	-0.6	1.5
MYO18B	8.1	8.7	-0.6	1.5
ITGB1BP3	8.3	8.9	-0.6	1.5
PHLDA3	9.4	10.0	-0.6	1.5
GPT2	8.5	9.1	-0.6	1.5
LOC386256	7.9	8.5	-0.6	1.5
TSC22D3	9.4	10.0	-0.6	1.5
NDUFA4	12.4	13.0	-0.6	1.5

4CYTL1	9.4	10.0	-0.6	1.5
PTP4A3	9.0	9.6	-0.6	1.5
FBXO32	7.9	8.5	-0.6	1.5
CNKSR1	7.7	8.3	-0.6	1.5
ZXDA	9.0	9.6	-0.6	1.5
LOC100044934	8.4	9.0	-0.6	1.5
KBTBD5	7.8	8.4	-0.6	1.5
SRR	11.0	11.6	-0.6	1.5
CACNG1	8.1	8.7	-0.6	1.5
SCL0002124.1_39	7.7	8.3	-0.6	1.5
DEB1	11.0	11.6	-0.6	1.5
LMOD3	7.9	8.5	-0.6	1.5
9830134C10RIK	8.2	8.8	-0.6	1.5
TYKI	9.3	9.9	-0.6	1.5
UFSP1	8.6	9.2	-0.6	1.5
SMPX	7.7	8.2	-0.6	1.5
LOC100047214	9.1	9.7	-0.6	1.5
VGLL2	7.6	8.2	-0.6	1.5
CAR3	10.3	10.9	-0.6	1.5
SLC25A12	9.1	9.7	-0.6	1.5
EG622339	13.4	14.0	-0.6	1.5
CIB2	9.4	9.9	-0.6	1.5
A630006E02RIK	9.5	10.1	-0.6	1.5
UGP2	9.4	10.0	-0.6	1.5
4933428A15RIK	8.6	9.2	-0.6	1.5
CHKA	9.4	10.0	-0.6	1.5
SNTA1	8.5	9.0	-0.6	1.5
SLC6A9	9.3	9.9	-0.6	1.5
2410076I21RIK	8.4	8.9	-0.6	1.5
TPI1	12.1	12.6	-0.6	1.5
SMTNL1	7.9	8.4	-0.6	1.5
TMOD1	8.7	9.3	-0.6	1.5
TSPAN8	8.5	9.1	-0.6	1.5
MTDNA_COXII	12.8	13.4	-0.6	1.5
NDUFS2	8.7	9.3	-0.6	1.5
SLC2A4	8.1	8.7	-0.6	1.5
MYOT	7.8	8.4	-0.6	1.5
A230005G17RIK	8.3	8.9	-0.6	1.5
TNNT1	8.9	9.4	-0.6	1.5
FHL1	11.6	12.1	-0.6	1.5
SPNB1	9.5	10.0	-0.6	1.5
5830496L11RIK	9.1	9.6	-0.6	1.5
ENSMUSG00000054212	9.5	10.1	-0.6	1.5

5430434G16RIK	8.9	9.4	-0.6	1.5
IDH3A	8.9	9.4	-0.6	1.5
SLC38A5	11.1	11.7	-0.6	1.5
LDB3	8.1	8.6	-0.6	1.5
E430039I23RIK	11.1	11.6	-0.6	1.5
KEL	10.5	11.0	-0.6	1.5
2310039E09RIK	8.2	8.7	-0.6	1.5
D530007E13RIK	8.9	9.4	-0.6	1.5
1110018J23RIK	7.9	8.5	-0.6	1.5
TMEM45B	8.2	8.7	-0.6	1.5
BC022224	10.2	10.7	-0.6	1.5
RBM38	9.9	10.5	-0.6	1.5
2810484G07RIK	10.9	11.5	-0.5	1.5
ACO2	10.8	11.4	-0.5	1.5
1700021F05RIK	10.3	10.8	-0.5	1.5
VEGFB	9.8	10.4	-0.5	1.5
STXBP3	8.2	8.7	-0.5	1.5
AGL	9.3	9.8	-0.5	1.5
TAL1	9.3	9.8	-0.5	1.5
MYOZ2	7.7	8.2	-0.5	1.5
NCTC1	7.8	8.3	-0.5	1.5
ABCA7	9.4	10.0	-0.5	1.5
SAR1B	10.3	10.9	-0.5	1.5
3632431M01RIK	8.6	9.1	-0.5	1.5
FCHO1	10.0	10.5	-0.5	1.5
P2RY1	8.8	9.3	-0.5	1.5
B230387C07RIK	9.1	9.7	-0.5	1.5
TRIM63	7.5	8.0	-0.5	1.5
1810020D17RIK	9.5	10.0	-0.5	1.4
FYCO1	8.1	8.6	-0.5	1.4
RABGEF1	10.3	10.8	-0.5	1.4
ITGB1BP2	8.2	8.8	-0.5	1.4
IFT140	9.1	9.6	-0.5	1.4
SAMD11	8.2	8.7	-0.5	1.4
ABCB10	8.2	8.8	-0.5	1.4
LOC100046690	9.0	9.5	-0.5	1.4
PFN2	8.9	9.5	-0.5	1.4
C1QTNF3	11.0	7.5	3.5	11.3
LRRC15	10.6	8.4	2.2	4.7
ANGPTL1	9.7	7.6	2.1	4.4
MFAP5	10.2	8.1	2.1	4.4
THBS2	11.8	9.7	2.1	4.3
FSTL1	11.1	9.0	2.0	4.1

COL6A2	10.4	8.4	2.0	4.1
MMP2	13.7	11.7	2.0	3.9
COL6A1	12.4	10.4	2.0	3.9
CAPN6	9.7	7.7	2.0	3.9
COL3A1	9.8	7.9	1.9	3.8
MMP3	9.3	7.4	1.9	3.8
TIMP1	11.8	9.9	1.9	3.8
COL5A1	12.6	10.7	1.9	3.7
CTHRC1	9.5	7.6	1.9	3.7
AEBP1	10.9	9.1	1.9	3.6
COL18A1	9.8	8.0	1.8	3.5
DKK3	10.2	8.5	1.7	3.4
COL14A1	9.3	7.6	1.7	3.3
E430002G05RIK	9.9	8.1	1.7	3.3
PCOLCE	10.9	9.2	1.7	3.3
LUM	12.2	10.5	1.7	3.3
DPT	10.3	8.6	1.7	3.2
MMP14	11.9	10.2	1.7	3.2
GP38	11.0	9.3	1.7	3.2
FCRLS	9.9	8.2	1.6	3.1
MFAP4	9.2	7.6	1.6	3.1
CSRP2	11.0	9.4	1.6	3.1
LOX	11.4	9.8	1.6	3.1
SPON2	11.2	9.6	1.6	3.0
ITM2A	9.8	8.2	1.6	3.0
LY6A	12.8	11.3	1.6	3.0
DDAH1	9.3	7.7	1.6	3.0
MUP2	9.7	8.2	1.6	3.0
GPNMB	9.5	8.0	1.6	3.0
CD248	9.9	8.3	1.5	2.9
ANTXR1	9.9	8.3	1.5	2.9
6330406I15RIK	9.7	8.1	1.5	2.9
LOXL1	10.8	9.2	1.5	2.9
MUP1	9.2	7.7	1.5	2.9
NBL1	10.3	8.8	1.5	2.9
MFAP2	9.2	7.7	1.5	2.8
CCL21A	10.6	9.1	1.5	2.8
FN1	10.4	8.9	1.5	2.8
MEST	8.8	7.3	1.5	2.8
MRGPRF	9.5	8.0	1.5	2.8
CCL21C	10.0	8.5	1.5	2.8
SAA3	8.7	7.2	1.5	2.8
LOC100048554	9.2	7.7	1.5	2.8
THY1	10.0	8.5	1.5	2.7

HTRA1	10.5	9.1	1.5	2.7
OSR2	9.3	7.8	1.5	2.7
LOC100041504	9.9	8.4	1.4	2.7
GPX7	9.8	8.4	1.4	2.7
KDELR3	10.4	8.9	1.4	2.7
H19	11.4	10.0	1.4	2.7
PDLIM4	10.3	8.9	1.4	2.6
C1QTNF2	9.3	7.9	1.4	2.6
COL6A3	11.3	9.9	1.4	2.6
FBLN2	9.4	8.0	1.4	2.6
MXRA8	10.5	9.1	1.4	2.6
SCL0001849.1_2273	9.0	7.6	1.4	2.6
VKORC1	11.1	9.7	1.3	2.5
PPIC	12.3	11.0	1.3	2.5
ITGBL1	9.6	8.3	1.3	2.5
EMP1	12.7	11.4	1.3	2.5
KNSL5	11.8	10.5	1.3	2.5
SERPINH1	12.8	11.5	1.3	2.5
2310016C16RIK	10.3	9.0	1.3	2.5
WISP2	10.4	9.1	1.3	2.5
MAGED1	11.6	10.3	1.3	2.5
COL16A1	11.6	10.3	1.3	2.5
LEPREL2	9.2	7.9	1.3	2.4
GPX8	10.7	9.4	1.3	2.4
BGN	14.3	13.0	1.3	2.4
SRPX2	10.2	8.9	1.3	2.4
ITGA11	9.9	8.6	1.3	2.4
CCDC80	11.0	9.7	1.3	2.4
CLEC11A	10.4	9.2	1.3	2.4
SMOC1	9.7	8.5	1.2	2.4
OGN	10.3	9.0	1.2	2.4
CRTAP	10.1	8.9	1.2	2.4
VIM	11.1	9.8	1.2	2.3
COL4A2	11.3	10.0	1.2	2.3
FKBP11	10.0	8.7	1.2	2.3
CD276	9.3	8.1	1.2	2.3
PRKCDBP	10.1	8.9	1.2	2.3
CCL7	8.4	7.2	1.2	2.3
NFATC4	9.4	8.1	1.2	2.3
ECM1	10.8	9.6	1.2	2.3
COL15A1	9.4	8.2	1.2	2.3
2610027C15RIK	10.0	8.8	1.2	2.3

PRELP	13.1	11.9	1.2	2.3
TIMP2	12.6	11.4	1.2	2.3
GRB10	9.4	8.2	1.2	2.3
FBN1	9.6	8.4	1.2	2.3
COPZ2	10.0	8.8	1.2	2.3
SCARF2	12.0	10.8	1.2	2.3
ENPP1	9.6	8.4	1.2	2.3
COL4A1	11.7	10.5	1.2	2.3
IGF1	9.6	8.4	1.2	2.2
SULF2	9.2	8.0	1.2	2.2
SERPINA3N	10.2	9.0	1.2	2.2
FKBP9	11.1	9.9	1.2	2.2
RNASE4	9.8	8.6	1.2	2.2
COMP	12.8	11.6	1.2	2.2
MS4A6D	9.8	8.6	1.2	2.2
CPXM1	9.3	8.2	1.1	2.2
DAB2	9.7	8.5	1.1	2.2
EFEMP2	10.0	8.9	1.1	2.2
LOC100047053	8.4	7.3	1.1	2.2
COL8A1	9.5	8.4	1.1	2.2
SERPING1	11.9	10.7	1.1	2.2
ANGPTL4	10.2	9.1	1.1	2.2
THBS3	8.7	7.6	1.1	2.1
HSPG2	10.5	9.4	1.1	2.1
PTN	8.9	7.8	1.1	2.1
GM22	9.3	8.2	1.1	2.1
NNMT	9.6	8.6	1.1	2.1
LGMN	10.9	9.8	1.1	2.1
4930533K18RIK	9.8	8.7	1.1	2.1
VASN	10.9	9.8	1.1	2.1
ELN	8.5	7.5	1.1	2.1
FMOD	10.2	9.1	1.1	2.1
LOC100046883	10.8	9.8	1.1	2.1
CLEC4N	8.6	7.6	1.1	2.1
NDN	10.0	8.9	1.1	2.1
ACAN	9.7	8.6	1.1	2.1
OLFML1	8.8	7.8	1.1	2.1
C1QTNF1	8.7	7.6	1.1	2.1
SOCS3	9.3	8.3	1.0	2.1
1500015O10RIK	11.9	10.8	1.0	2.0
FKBP10	9.7	8.7	1.0	2.0
TREM2	9.4	8.4	1.0	2.0
MGP	13.5	12.5	1.0	2.0
COL10A1	10.7	9.6	1.0	2.0

ADAMTS12	8.7	7.7	1.0	2.0
CRLF1	8.5	7.5	1.0	2.0
HTRA3	9.6	8.6	1.0	2.0
P4HA2	9.0	8.0	1.0	2.0
FSCN1	9.0	8.1	1.0	2.0
NUPR1	12.0	11.0	1.0	2.0
SCARA3	11.9	10.9	1.0	2.0
SYNPO	10.1	9.1	1.0	2.0
NID2	8.8	7.8	1.0	2.0
TSPAN6	8.9	7.9	1.0	2.0
LGALS1	12.5	11.5	1.0	2.0
IGFBP7	10.5	9.5	1.0	2.0
TMEM119	9.7	8.7	1.0	2.0
COL2A1	13.6	12.6	1.0	2.0
MS4A7	8.8	7.8	1.0	2.0
ANXA5	12.4	11.4	1.0	2.0
RAMP2	10.0	9.1	1.0	2.0
MMP23	9.5	8.5	1.0	1.9
SLC1A4	8.5	7.6	1.0	1.9
LOC100047856	9.1	8.2	1.0	1.9
AHNAK2	9.1	8.2	1.0	1.9
CDKN1C	11.0	10.0	1.0	1.9
APOE	11.0	10.0	1.0	1.9
SPARC	13.1	12.1	1.0	1.9
BC020108	8.5	7.5	0.9	1.9
C1QB	11.5	10.5	0.9	1.9
FNDC3B	10.2	9.3	0.9	1.9
IGSF10	8.8	7.9	0.9	1.9
COL12A1	9.1	8.2	0.9	1.9
9030024J15RIK	9.7	8.7	0.9	1.9
1110036O03RIK	8.9	8.0	0.9	1.9
LRIG3	9.4	8.5	0.9	1.9
FAM129B	10.2	9.3	0.9	1.9
EDNRA	9.5	8.5	0.9	1.9
IL33	8.3	7.4	0.9	1.9
IGFBP6	10.0	9.0	0.9	1.9
LGALS3BP	10.8	9.9	0.9	1.9
OLFML3	11.5	10.6	0.9	1.9
COL1A2	11.1	10.2	0.9	1.9
GPR176	8.4	7.5	0.9	1.9
CERCAM	9.9	9.0	0.9	1.9
CNRIP1	9.7	8.8	0.9	1.9
GALNTL1	8.5	7.7	0.9	1.9

KERA	8.2	7.3	0.9	1.9
PRG4	12.7	11.8	0.9	1.9
IGKV3-2_X16954_IG_KAPPA_VARIABLE_3-2_18	9.0	8.1	0.9	1.9
LOC676136	9.5	8.6	0.9	1.9
ABI3BP	8.6	7.7	0.9	1.9
PKD2	8.9	8.0	0.9	1.8
COL1A1	13.2	12.3	0.9	1.8
SCX	8.6	7.7	0.9	1.8
IGF2	10.3	9.4	0.9	1.8
SFRP1	8.3	7.4	0.9	1.8
KCTD17	9.1	8.2	0.9	1.8
IGFBP4	12.0	11.2	0.9	1.8
MFGE8	12.3	11.5	0.9	1.8
EFS	9.2	8.4	0.9	1.8
BC064033	8.4	7.6	0.9	1.8
LOC243431	9.8	9.0	0.9	1.8
MAGED2	11.1	10.2	0.9	1.8
DPYSL3	9.3	8.4	0.9	1.8
ANPEP	8.4	7.6	0.9	1.8
A430110N23RIK	8.2	7.4	0.9	1.8
CXCL1	8.1	7.2	0.8	1.8
LTBP3	9.0	8.2	0.8	1.8
LRRC17	8.3	7.4	0.8	1.8
LOC100047583	9.3	8.5	0.8	1.8
UTS2R	8.3	7.4	0.8	1.8
TNN	8.3	7.5	0.8	1.8
CALU	10.0	9.2	0.8	1.8
BMP1	9.9	9.1	0.8	1.8
SCARA5	9.7	8.9	0.8	1.8
TXNDC5	10.7	9.9	0.8	1.8
SDC2	10.4	9.6	0.8	1.8
IFITM2	12.1	11.3	0.8	1.8
PRDX4	11.0	10.1	0.8	1.8
DLK1	8.2	7.3	0.8	1.8
0610007N19RIK	9.4	8.6	0.8	1.8
TPST1	9.9	9.0	0.8	1.8
NT5DC2	9.1	8.3	0.8	1.8
SULF1	8.9	8.1	0.8	1.8
HTRA4	9.0	8.2	0.8	1.8
AKR1B8	8.3	7.4	0.8	1.8
SRPX	8.8	8.0	0.8	1.8

MARCKS	11.2	10.4	0.8	1.8
PARVA	9.6	8.8	0.8	1.7
TGFB3	8.8	8.0	0.8	1.7
LOC232060	8.7	7.9	0.8	1.7
WISP1	9.5	8.7	0.8	1.7
LXN	10.0	9.2	0.8	1.7
D14ERTD449E	9.2	8.5	0.8	1.7
MDK	8.6	7.8	0.8	1.7
TGFBI	11.3	10.5	0.8	1.7
SH3PXD2B	9.4	8.6	0.8	1.7
EMP2	9.0	8.2	0.8	1.7
IGHG	9.7	9.0	0.8	1.7
RIN2	9.1	8.3	0.8	1.7
1700023M03RIK	9.9	9.2	0.8	1.7
WBP5	10.9	10.1	0.8	1.7
CD68	10.3	9.5	0.8	1.7
1200009O22RIK	8.6	7.8	0.8	1.7
IL1RL1	8.1	7.3	0.8	1.7
ADAMTS2	11.0	10.2	0.8	1.7
A730054J21RIK	8.3	7.5	0.8	1.7
4732462B05RIK	10.0	9.3	0.8	1.7
LBP	9.9	9.1	0.8	1.7
IL13RA1	8.7	7.9	0.8	1.7
FER1L3	8.4	7.6	0.8	1.7
C4A	10.0	9.2	0.8	1.7
SOX9	9.8	9.0	0.8	1.7
1810055G02RIK	10.2	9.4	0.8	1.7
PANX3	10.7	10.0	0.8	1.7
FKBP14	8.5	7.7	0.8	1.7
SERPINF1	12.8	12.1	0.8	1.7
TUBB6	9.9	9.2	0.8	1.7
C1QC	10.8	10.0	0.8	1.7
OLFML2B	11.5	10.7	0.8	1.7
TCEAL8	9.9	9.2	0.8	1.7
PDGFRA	9.4	8.6	0.8	1.7
NOX4	8.3	7.5	0.8	1.7
SFRP2	8.1	7.3	0.7	1.7
6720469N11RIK	10.1	9.3	0.7	1.7
LOC380799	8.7	8.0	0.7	1.7
CSTB	12.6	11.8	0.7	1.7
CYB561	8.7	8.0	0.7	1.7
LHFPL2	9.7	9.0	0.7	1.7
LOC98434	10.3	9.5	0.7	1.7

CD14	8.5	7.7	0.7	1.7
PMP22	9.4	8.7	0.7	1.7
RBP1	8.6	7.8	0.7	1.7
2310008M10RIK	11.4	10.6	0.7	1.7
MT1	13.4	12.7	0.7	1.7
EXT1	9.9	9.2	0.7	1.7
LIMA1	9.0	8.3	0.7	1.7
MATN4	8.3	7.5	0.7	1.7
EDG5	9.3	8.6	0.7	1.7
SPSB1	8.7	8.0	0.7	1.7
ARMCX2	9.4	8.7	0.7	1.7
SVEP1	8.3	7.6	0.7	1.7
HMGN3	10.5	9.8	0.7	1.6
GPR23	8.7	8.0	0.7	1.6
FOLR2	8.6	7.8	0.7	1.6
UBE2E2	9.3	8.6	0.7	1.6
RHOJ	9.4	8.7	0.7	1.6
PROS1	9.9	9.2	0.7	1.6
STAB1	9.6	8.9	0.7	1.6
LOC637227	9.6	8.8	0.7	1.6
MYADM	10.8	10.1	0.7	1.6
ANXA8	8.4	7.7	0.7	1.6
PLOD1	8.3	7.6	0.7	1.6
MEOX2	8.9	8.2	0.7	1.6
LOC381629	10.7	10.0	0.7	1.6
LOC384413	9.4	8.7	0.7	1.6
TAX1BP3	10.5	9.8	0.7	1.6
6330404C01RIK	9.3	8.6	0.7	1.6
FRMD6	9.8	9.1	0.7	1.6
COL9A2	10.6	9.9	0.7	1.6
NT5E	9.0	8.3	0.7	1.6
MYO1E	9.0	8.3	0.7	1.6
LMAN1	9.5	8.8	0.7	1.6
GRN	12.1	11.4	0.7	1.6
LOC669053	9.3	8.6	0.7	1.6
CUL7	9.5	8.8	0.7	1.6
P4HB	13.1	12.4	0.7	1.6
TWSG1	10.1	9.4	0.7	1.6
D4BWG0951E	8.3	7.7	0.7	1.6
BICC1	9.6	8.9	0.7	1.6
WTIP	9.3	8.6	0.7	1.6
IL11RA1	11.3	10.7	0.7	1.6
LOC636944	9.9	9.3	0.7	1.6
PLVAP	10.2	9.5	0.7	1.6

EGFR	8.5	7.8	0.7	1.6
RFTN2	8.6	8.0	0.7	1.6
TMED3	9.9	9.2	0.7	1.6
TUBB2B	8.7	8.1	0.7	1.6
C130021I20	7.9	7.3	0.7	1.6
CXCL16	8.2	7.5	0.7	1.6
CDON	8.2	7.6	0.7	1.6
SDC3	11.1	10.5	0.7	1.6
5430435G22RIK	8.4	7.8	0.7	1.6
ADRA2A	8.6	7.9	0.7	1.6
C1QA	9.3	8.7	0.7	1.6
PRRC1	9.8	9.2	0.7	1.6
TPBG	8.3	7.7	0.6	1.6
BOK	8.5	7.8	0.6	1.6
NID1	8.8	8.1	0.6	1.6
FXYD6	11.3	10.7	0.6	1.6
TGFBR2	9.8	9.2	0.6	1.6
LAMC1	9.2	8.5	0.6	1.6
ZFP521	8.4	7.7	0.6	1.6
GPR125	9.4	8.8	0.6	1.6
COL5A2	8.0	7.4	0.6	1.6
PAPSS2	9.2	8.6	0.6	1.6
BDH2	9.5	8.9	0.6	1.6
MIA1	10.1	9.4	0.6	1.6
SOCS2	9.9	9.2	0.6	1.6
GLT8D1	9.4	8.8	0.6	1.6
PLOD2	8.5	7.9	0.6	1.6
FSTL	8.0	7.4	0.6	1.6
IGFBP3	8.1	7.5	0.6	1.5
2410146L05RIK	8.0	7.3	0.6	1.5
GSTM2	10.2	9.5	0.6	1.5
ISLR	8.0	7.4	0.6	1.5
PPIB	11.3	10.7	0.6	1.5
PDGFRB	8.6	7.9	0.6	1.5
DLG5	9.5	8.9	0.6	1.5
CAV1	10.4	9.8	0.6	1.5
CCL4	8.2	7.6	0.6	1.5
TMEM176B	10.1	9.4	0.6	1.5
RAB34	8.4	7.7	0.6	1.5
CDKN1A	8.7	8.1	0.6	1.5
CYB5R3	9.6	9.0	0.6	1.5
SEPN1	10.2	9.6	0.6	1.5
LOC630253	8.2	7.6	0.6	1.5

PRRX2	8.1	7.5	0.6	1.5
RHOC	8.4	7.8	0.6	1.5
PRSS35	8.8	8.2	0.6	1.5
GPRC5B	8.4	7.8	0.6	1.5
PDIA5	8.1	7.5	0.6	1.5
PMEPA1	8.2	7.6	0.6	1.5
ADAMTS4	7.9	7.3	0.6	1.5
RRBP1	9.3	8.7	0.6	1.5
FAM171B	8.4	7.8	0.6	1.5
SERTAD4	8.1	7.5	0.6	1.5
CRABP2	7.8	7.2	0.6	1.5
5430433G21RIK	9.4	8.9	0.6	1.5
RAB11FIP5	9.3	8.7	0.6	1.5
4933421H10RIK	8.7	8.1	0.6	1.5
DCN	12.3	11.7	0.6	1.5
2610009E16RIK	9.1	8.5	0.6	1.5
3110079O15RIK	12.8	12.2	0.6	1.5
VAT1	9.6	9.1	0.6	1.5
COL8A2	8.2	7.6	0.6	1.5
LOC100047162	9.9	9.4	0.6	1.5
HOXC6	9.1	8.5	0.6	1.5
ZFYVE21	10.3	9.7	0.6	1.5
BGLAP-RS1	13.8	13.2	0.6	1.5
9430028L06RIK	7.9	7.3	0.6	1.5
ACTA2	10.3	9.7	0.6	1.5
GLT25D1	10.7	10.1	0.6	1.5
RCN3	8.3	7.7	0.6	1.5
CLEC3B	8.2	7.6	0.6	1.5
GMDS	8.8	8.2	0.6	1.5
BMPER	8.3	7.7	0.6	1.5
2300002D11RIK	8.0	7.4	0.6	1.5
PLAT	8.0	7.4	0.6	1.5
TWIST1	8.4	7.8	0.6	1.5
6230400G14RIK	8.8	8.2	0.6	1.5
PLOD3	10.2	9.7	0.6	1.5
CAPG	10.0	9.5	0.6	1.5
LOC626583	8.1	7.5	0.6	1.5
ALG14	8.9	8.4	0.6	1.5
MMP12	7.8	7.2	0.6	1.5
TNXB	8.5	7.9	0.6	1.5
TUBA1A	9.4	8.9	0.6	1.5
CD81	12.8	12.2	0.6	1.5
TMEM86A	9.9	9.4	0.6	1.5
C1QTNF5	7.9	7.3	0.6	1.5

ERGIC1	9.4	8.8	0.6	1.5
5031439A09RIK	8.9	8.4	0.6	1.5
S100A10	9.2	8.6	0.6	1.5
CBR2	9.1	8.6	0.6	1.5
FBLN7	7.8	7.3	0.6	1.5
B9D1	8.3	7.7	0.6	1.5
ALG5	9.6	9.1	0.6	1.5
RRAS	9.9	9.3	0.6	1.5
CHMP4B	10.4	9.8	0.6	1.5
GNS	10.9	10.4	0.6	1.5
H47	10.8	10.3	0.6	1.5
IFITM5	9.2	8.7	0.6	1.5
WWTR1	8.8	8.2	0.5	1.5
CRIP2	11.0	10.4	0.5	1.5
ANXA2	13.6	13.1	0.5	1.5
A730017D01RIK	8.5	7.9	0.5	1.5
PRRX1	8.1	7.6	0.5	1.5
COL22A1	10.4	9.9	0.5	1.5
MANBAL	10.3	9.8	0.5	1.5
POFUT2	8.1	7.6	0.5	1.5
APLNR	8.3	7.7	0.5	1.5
FBLIM1	8.7	8.2	0.5	1.5
LMNA	10.4	9.9	0.5	1.5
PLCD1	8.7	8.1	0.5	1.5
RHBDF1	9.9	9.4	0.5	1.5
LOC100039175	8.8	8.2	0.5	1.5
EBPL	8.8	8.3	0.5	1.5
KDELR2	8.5	8.0	0.5	1.5
FAH	8.9	8.3	0.5	1.5
PDIA3	11.7	11.1	0.5	1.5
PLA1A	8.1	7.6	0.5	1.5
GAS6	11.3	10.8	0.5	1.5
BC065085	8.3	7.8	0.5	1.5
D10ERTD610E	8.6	8.1	0.5	1.4
IFIT3	8.5	8.0	0.5	1.4
PDGFRL	7.9	7.4	0.5	1.4
3632451O06RIK	8.0	7.5	0.5	1.4
TPM4	11.3	10.8	0.5	1.4
PLP2	10.0	9.5	0.5	1.4
C4B	8.7	8.1	0.5	1.4

Table 7: Genes changed expression in DMM model at day 7

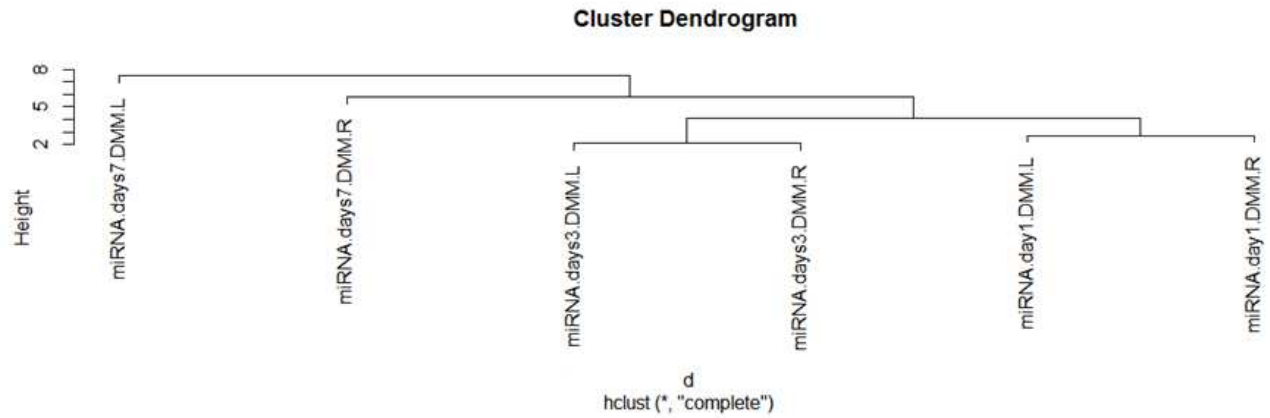

Figure 1: Hierarchical cluster analysis for DMM models at 1, 3, and 7 days after surgery

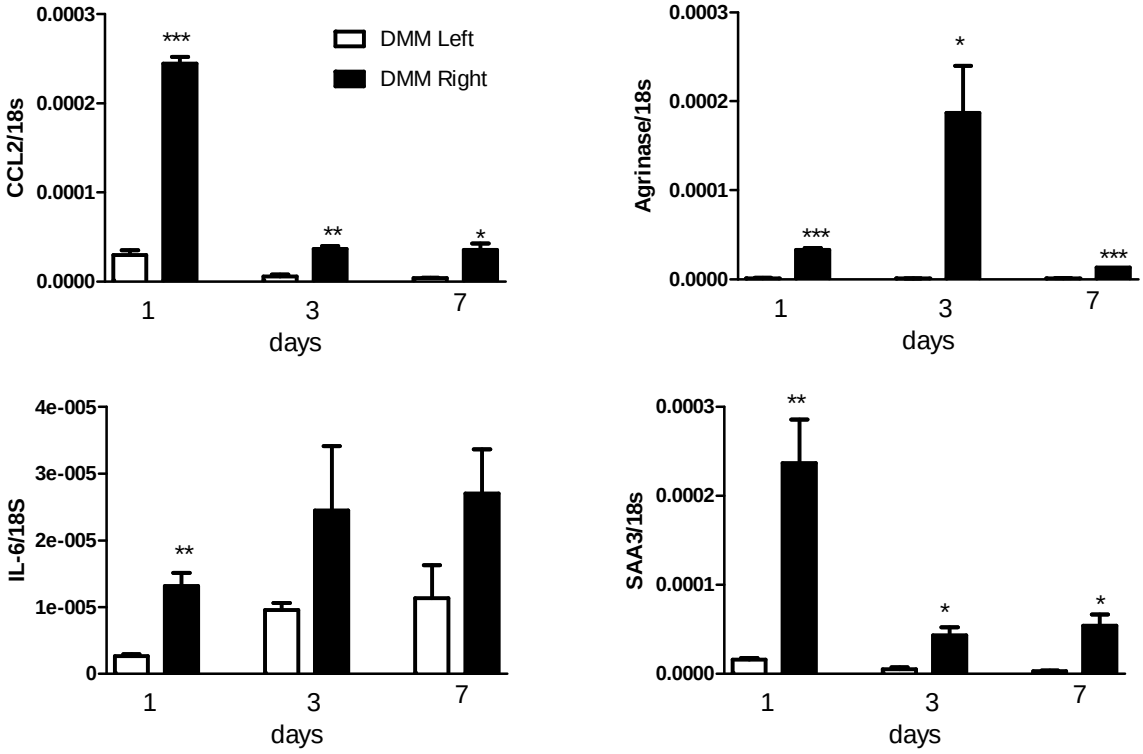

Figure 2: CCL2, Agrinase, IL-6 and SAA-3 were significantly induced expression in DMM model at 1, 3, and 7 days after surgery

Total RNA was reversed transcribed to cDNA and gene expression was measured by real-time qRT-PCR in individual samples of DMM left knee (un-operated, open bar), and DMM right knee (DMM, close bar). 18S was used as endogenous control. The data show mean +/- SEM, n=3. The expression of genes of interest between each group was analysed by unpaired two-tailed t test * $p<0.05$, ** $p < 0.01$, *** $p<0.001$.

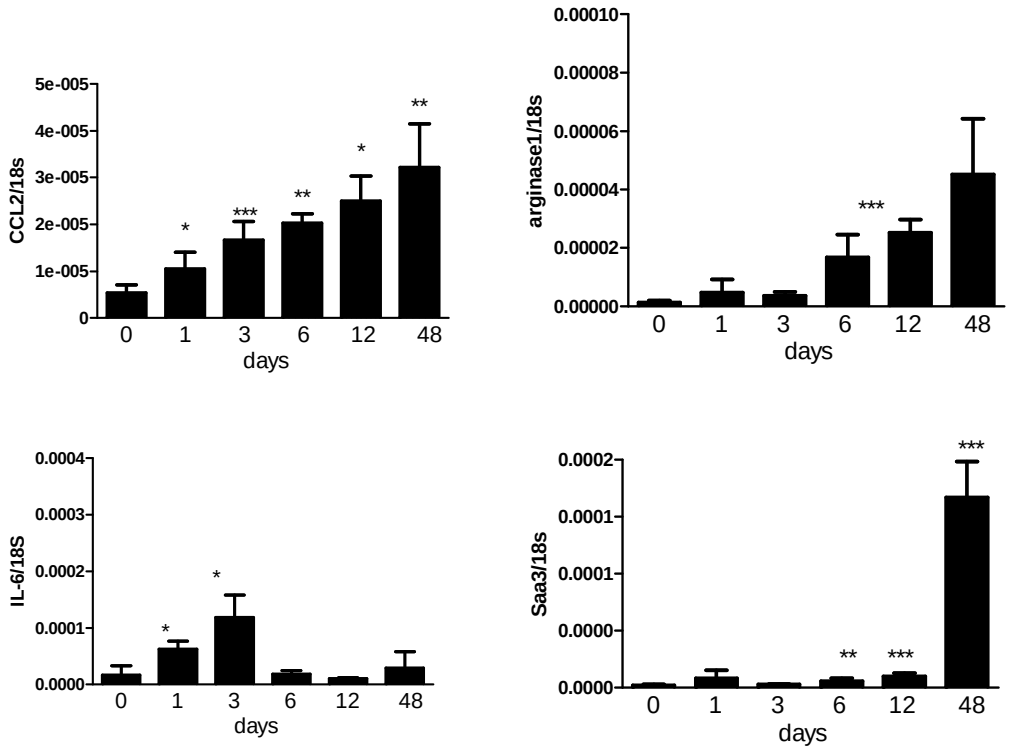

Figure 3: Gene expression in hip avulsion injury model

The femoral caps of C57Bl/6 mice aged 4 weeks were avulsed and put in culture. At each of 3, 6, 12, 48 hour time points, the femoral caps were harvested. Total RNA was isolated using Trizol and reverse transcribed to cDNA. Gene expression was measured by real-time qRT-PCR where 18S was used as an endogenous control. Assays were repeated 3 times. At least triplicate samples were measured at each time. Means ± standard errors are presented. Difference in expression between each time point against control (t=0) was calculated by unpaired two-tailed t test. * $p<0.05$, ** $p < 0.01$, *** $p<0.001$.

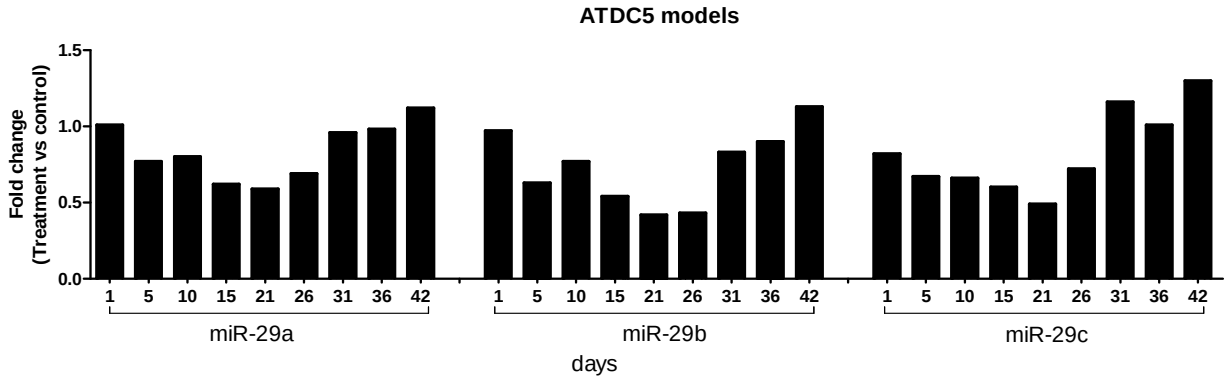

Figure 4: The expression of the miR-29 family in ATDC5 model

The embryonic carcinoma cell line ATDC5 was stimulated to from chondrocytes using insulin for 42 days. Total RNA was isolated, reverse transcribed to cDNA and used for miRNA microarray.

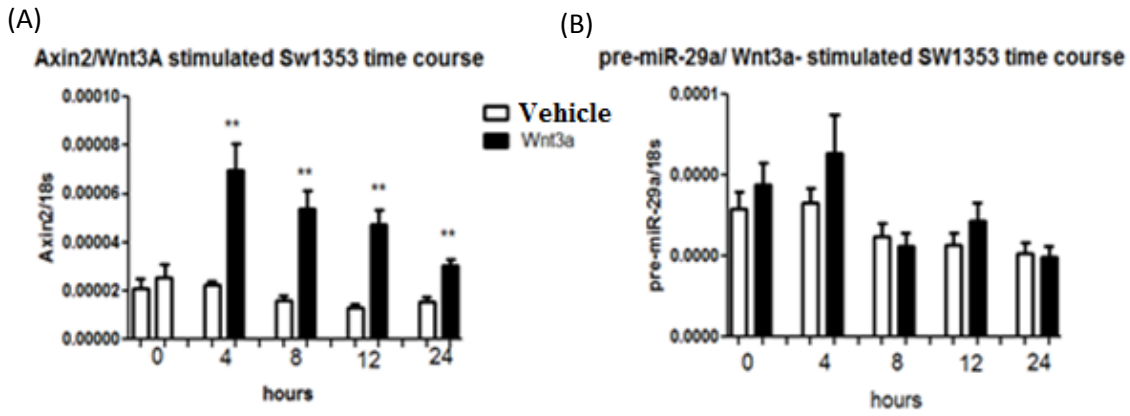

Figure 5: Expression of the miR-29 family was not controlled by Wnt3a

SW1353 cells were cultured in high glucose media with 10% (v/v) FCS in monolayer until 90% confluence. Cells were serum starved for 24 hours before treating with Wnt3a or vehicle (0.5% (w/v) BSA) across 24 hour course.

Relative expression of the precursor miR-29a and axin2 was measured by quantitative RT-PCR. 18S rRNA was the endogenous control for measuring the precursor transcripts. Open bar, control; close bar, WNT3a. (A) Expression level of axin2. (B) Expression level of precursor miR-29a. Means ± standard errors are presented. The difference between the treatment and the control was analysed by unpaired two-tailed t test. * $p<0.05$, ** $p < 0.01$, *** $p<0.001$, n=3.

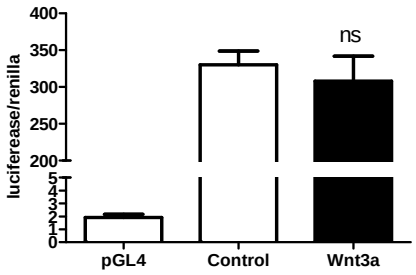

Figure 6: Wnt3a does not control the expression from the primary miR-29a/b1 promoter

The pri-miR-29a/b1 promoter-reporter (100ng) or the empty vector pGL4 (control, 100ng) were transfected into SW1353 cells. After transfection, cells were serum starved for 24 hours, followed by stimulating for another 6 hours with WNT3a (100ng/ml), or vehicle (0.5% BSA) before measuring luciferase activity. Renilla was use as endogenous control. Open bar: vehicle, black bar: Wnt3a. Means ± standard errors are presented, n=3. The difference of luciferase activity was analysed by unpaired two-tailed Student's t test. * $p<0.05$, ** $p < 0.01$, *** $p<0.00$.

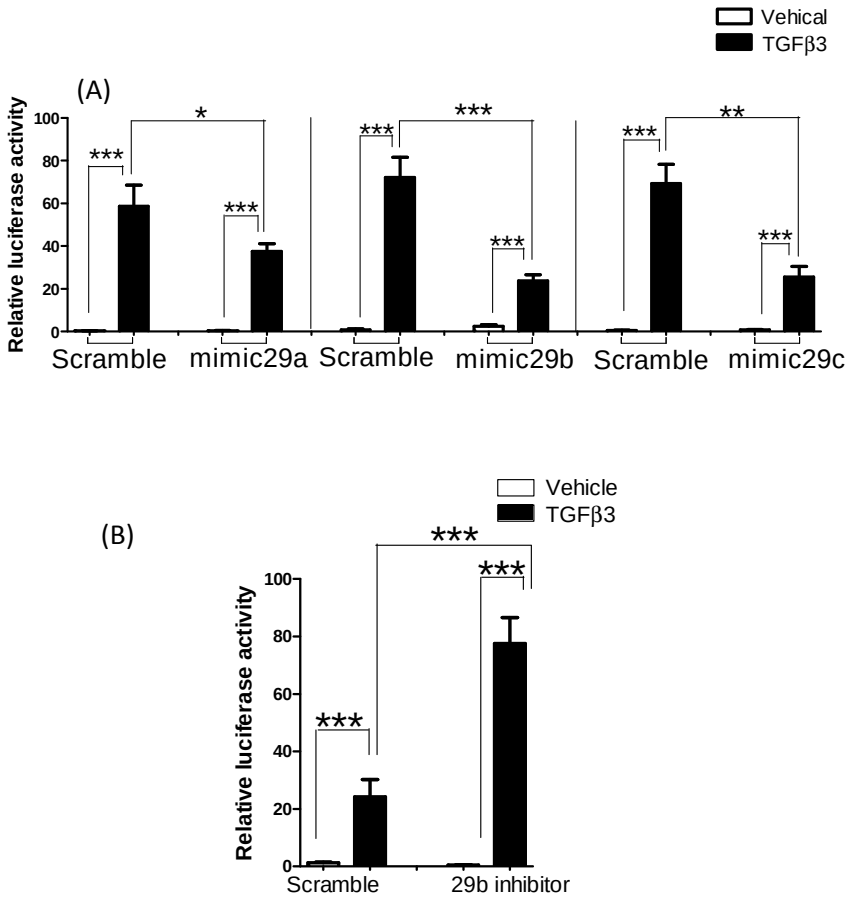

Figure 7 The miR-29 family suppress TGFβ signalling pathway

(A) The TGFβ signalling reporter ($CAGA_{12}$-luc) contains 12 binding sites of the Smad2/3/4 (GAGAC) binding consensus upstream of the firely luciferase-encoding gene in pGL3100ng $CAGA_{12}$-luc vector, and 10ng Renilla vector were co-transfected with either miR-29 family mimic (B) or miR-29b inhibitor (C) into SW1353 cells in monolayer. The non-targeting control (50nM) was also used as the negative control. 24 hours after transfection, cells were serum starved for another 24 hours, followed by treatment with TGFβ3 (4ng/ml) for another 6 hours before measuring luciferase activity. Renilla is the loading control for luciferase assay. Open bar: non – treatment control, close bar: TGFβ3 treatment. Means ± standard errors are presented, n=6. The difference of luciferase activity was analysed by Student's unpaired two-tailed t test. * $p<0.05$, ** $p < 0.01$, *** $p<0.001$

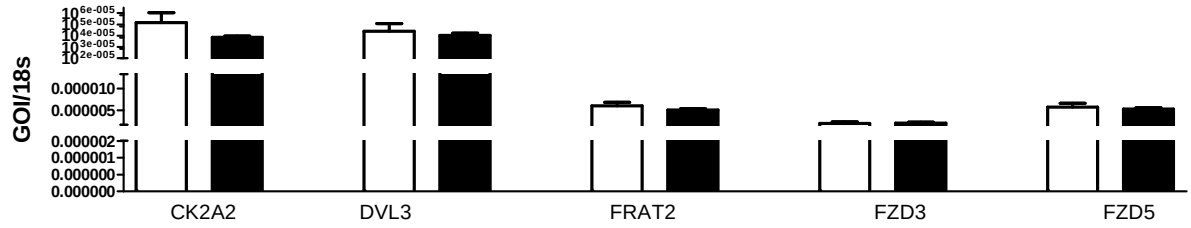

Figure 8 The miR-29 family does not target some of its putative targets at mRNA level Human primary chondrocytes was cultured in media with 10% (v/v) FCS in monolayer until 90% confluence. Cells were then transfected with either miR-29b mimic (50nM) or non – targeting control (50nM) for 48 hours. Total RNA was isolated and the expression levels of GOI were measured by qRT-PCR. 18S rRNA was the housekeeping control. Relative expression value of each of these genes was normalized to non – targeting control. Means ± standard errors are presented, n=3. The difference in expression between miR-29b overexpression and non – targeting control was analysed by Student's unpaired two-tailed t test. * $p<0.05$, ** $p < 0.01$, ***, $p<0.001$

THE ROLES OF THE MICRORNA 29 FAMILY IN CARTILAGE HOMEOSTASIS AND OSTEOARTHRITIS

LE THI TRUC LINH

THESIS SUBMITTED FOR THE DEGREE OF DOCTOR OF PHILOSOPHY

University of East Anglia

School of biological Sciences

Norwich, United Kingdom

December, 2014

DEDICATION

I would like to dedicate this thesis to my family

my parents

Mr Le Hung Son,

Mrs Le Thi Khanh Hong

my brother

Mr Le Hung Phong

for their constant love, friendship, support and encouragement throughout my life

ABSTRACT

MicroRNAs are short endogenous non-coding RNA molecules, typically 19-25 nucleotides in length, which negatively regulate gene expression. In osteoarthritis (OA), several genes necessary for cartilage homeostasis are aberrantly expressed, with a number of miRNAs implicated in this process. However, our knowledge of the earliest stages of OA, prior to the onset of irreversible changes, remains limited. The purpose of this study was to identify miRNAs involved across the time-course of OA using both a murine model and human cartilage, and to define their function.

Expression profile of miRNAs (Exiqon) and mRNAs (Illumina) on total RNA purified from whole knee joints taken from mice which underwent destabilisation of the medial meniscus (DMM) surgery at day 1, 3 and 7 post-surgery showed: the miRNA expression in whole mouse joints post DMM surgery increased over 7 days; at day 1 and 3, the expression of only 4 miRNAs altered significantly; at day 7, 19 miRNAs were upregulated and 15 downregulated. Among the modulated miRNAs, the miR-29b was the most interesting and was chosen to further investigate since integrating analysis of the miRNA and mRNA expression array data showed the inverse correlation between miR-29b and its potential targets. In end-stage human OA cartilage and in murine injury model, the miR-29 family was found to increase expression. Moreover, the miR-29 family was found to be the negative regulator in both human and murine chondrogenesis, and was also found to involve in murine limb development. Expression of the miR-29 family was found to suppress by SOX9 at least in part through directly binding to the promoter of the primary miR-29a/b1. Also, TGFβ1/3 decreased expression of the miR-29 family whilst Wnt3a did not have any effect. Lipopolysaccharide suppressed the miR-29 family expression in part through NFκB signalling pathway while the IL-1 strongly induced its expression partly through P38 MAKP signalling. Using luciferase reporter assay, the miR-29 family was showed to suppress the TGFβ, NFκB, and WNT/β-catenin signalling pathways. Gene expression profiles of gain- and-loss-of-function revealed regulation of a large number of previously recognised extracellular matrix-associated genes as well as an additional subset of protease and Wnt signalling pathway-related genes. Among these genes, *ADAMTS6, ADAMTS10, ADAMTS14, ADAMTS17, ADAMTS19, FZD3, DVL3, FRAT2, CK2A2* were experimentally validated as direct targets of the miR-29 family.

CONTENTS

LISTS OF TABLES

LISTS OF FIGURES

LISTS OF APPENDICES

Paper: Le et al, 2013

ACKOWNLEGMENTS

I would like to express my special appreciation and thanks to my primary supervisor Professor Ian Clark. I thank him for giving me the opportunity to become a Clark laboratory member and for allowing me to growth as a research scientist as I am now. I deeply appreciate the change to work and study from a great scientist and an honourable person like him. Without his time, support, guidance and encouragement, my PhD project is impossible.

I would also like to thank my second supervisor Professor Andrea Munsterberg for her comments, and suggestion which really helped me to refine my project. I am also in debted to Dr Tracey Swingler, my third supervisor. Her brilliant lab work skills, experiences, and knowledge tremendously help me go through all the obstacles and finish the study. Her time and her availability for all of my constant string of questions during the last 3 years are invaluable.

I am very thankful for all the past and current members of Clark laboratory for helping me on my research and make my PhD journey enjoyable. Special thank you to Dr Natalie Crowe for sharing with me her human osteoarthritis and normal articular cartilage samples, her dedifferentiation model which will take me a lot of time to do it myself. Thanks to Dr Rosemary Davidson for letting me including her DVL3 expression data in my thesis and for her knowledge, advice, support, and encouragement during my PhD. I would like to acknowledge Jonathan Green, Sarah Garner, Yvette Wormstone for their expertise and kind help in mouse injury model, human primary chondrocyte isolation, and cloning.

I would especially thank to Dr Guy Wheeler in Dalmay laboratory, Dr Geoffrey Mok, and Camille Viaut in Munsterberg laboratory for sharing their knowledge and help me through my whole mount in situ hybridization experiment. Thank you to Dr Eleanor Jones in Riley laboratory for kindly sharing with me her data and for her constantly help during my PhD. In addition, a thank you to Dr Helio Pais, who introduced me to bioinformatics analysis using R. His instruction about how to look for miRNA targets in big data set has become priceless to me. I would especially thank to Dr Mathew Barter in David Young laboratory, Newcastle University, members in Professor Tonia Vincent laboratory, Oxford University,

members of Dr Anne Delany laboratory, University of Connecticut, USA for kindly sharing with me their MSCs model, DMM samples, and vectors.

Great thanks to all of my friends for the time they shared with me throughout my PhD journey. I am grateful their incredible friendship which makes the journey to achieve my goal more enjoyable.

Finally, I would like to acknowledge Vietnam Ministry of Education and Training (project 322), University of Each Anglia scholarship for international student for giving me the opportunity to do PhD in the UK. I also deeply thank Arthritis Research UK (program grant #19424, Tracey Swingler, Ian Clark) for supporting my project. Due to the currency exchange rates and the international fees, there are minimal funds from my Vietnam Government Scholarship for laboratory consumables. Thus, my PhD project is impossible without the support from Arthritis Research UK. I also acknowledge the John and Pamela Salter Trust for supporting me with the LNA probe for miR-29b used in my project.

CHAPTER 1
INTRODUCTION

1.1. Synovial joints

In mammals, joints are functionally classified into 3 categories: synarthroses (immovable joints), amphiarthroses (slightly movable joints), and diarthroses (freely movable joints). Most of the main joints of the appendicular skeleton are synovial joints, suggesting this type of joint has a crucial role in the body. The main component of synovial joints includes **the hyaline cartilage**, also known as articular cartilage, covering the bone of the synovial joint providing the cartilage lubricating and shock absorbing characteristics; **a capsule** enclosing the joint in line with **synovial membrane** which contains synovial membrane-resident cells secreting synovial fluid into the synovial cavity helping reduce friction, enabling free movement; **bones**, further held together by **ligaments**. The characteristics of some important components of the synovial joint relevant to this PhD thesis are described below.

1.1.1. Articular cartilage biology

Articular cartilage, a highly specialized tissue with unique mechanical behaviour, consists of **(i) chondrocytes,** the only cells, responsible for the homeostasis of extracellular matrix (ECM), and **(ii) a dense layer of ECM** composed primarily of water, collagen and proteoglycan.

1.1.1.1 Cartilage structural organization

Healthy articular cartilage comprises four different areas: the superficial, intermediate, radial or deep, and calcified zones (Buckwalter *et al.* 2005, Dudhia 2005, Pearle *et al.* 2005, Aigner *et al.* 2006, Martel-Pelletier *et al.* 2008, Umlauf *et al.* 2010, Houard *et al.* 2013) **(Figure 1.0)**. Each is characterized by a particular chondrocyte phenotype, and by distinctive extracellular matrix organization and composition (Buckwalter et al. 2005).

The superficial zone, the articulating surface and the thinnest of the four, makes up 10%-20% of articular cartilage thickness (Buckwalter et al. 2005, Pearle et al. 2005). This

region contains a high amount of collagen (primary type II, and IX) but very low amount of proteoglycan. The collagen fibrils are densely packed and aligned paralleled to the articular surface. Chondrocytes in this layer are characterized by an elongated appearance (Pearle et al. 2005), express many proteins having lubricating and protective functions (e.g. lubricin) but relatively little proteoglycan. This zone is in contact with synovial fluid, and is responsible for most of the tensile properties of cartilage that enable cartilage to resist shear and the tensile and compressive forces imposed by the movement of the articulation (Martel-Pelletier et al. 2008).

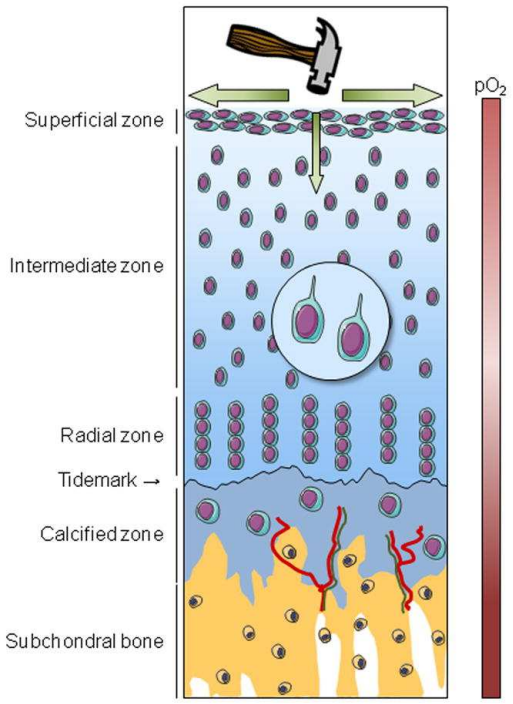

Figure 1.0: Histology of a healthy cartilage structural

The articular cartilage is organized into superficial, intermediate, radial, and calcified zones. Each zone can be distinguished by the difference in chondrocyte morphologies and components of collagen, proteoglycan, mineral and water

The intermediate and the radial zones contain large diameter collagen fibrils oriented perpendicular to the articular surface. These regions also have high amount of proteoglycan which is mainly aggrecan, a large chondroitin sulphate proteoglycan. Chondrocytes in the middle zone are more round than in the superficial zone. In the radial zone, the cells are arranged in columnar fashion (Buckwalter et al. 2005).

The tide mark, a thin line revealed after hematoxylin staining, marks the mineralization front between the calcified and non-calcified articular cartilage (Houard et al. 2013). In **the calcified cartilage zone**, the cell population is very scarce and chondrocytes are hypertrophic (Pearle et al. 2005, Martel-Pelletier et al. 2008). With aging, bloods vessels and nerves can be seen in calcified cartilage arising from the subchondral bones (Lane *et al.* 1977). The main function of this zone seems to be to anchor the cartilage to the bone as collagen fibrils from the radial zone penetrate into the calcified cartilage.

Furthermore, it is noteworthy to know that for mechanical protection purposes, in articular cartilage, the chondrocyte is surrounded by a pericellular matrix and a territorial cartilage matrix forming a capsule-like structure around the cells. Whilst the pericellular matrix is made of a thin layer of non-fibrillar material, which most likely represents the synthetic products of the chondrocytes, such as proteoglycans and glycoproteins, the pericellular matrix also contains a dense meshwork of thin collagen fibers (see below) (Dudhia 2005, Aigner et al. 2006, Martel-Pelletier et al. 2008, Heinegard *et al.* 2011).

1.1.1.2 Biology of chondrocytes

As mention above, chondrocytes are the only cellular components of articular cartilage, make up 5% of the wet weight of articular cartilage, and are surrounded by a pericellular matrix containing type VI collagen, microfibrils, hyaluronic acid, biglycan, and decorin but little or no type II collagen (Buckwalter et al. 2005, Dudhia 2005, Heinegard and Saxne 2011). The arrangement of chondrocytes and articular cartilage specific organisation result from a complex development process called endochondral ossification including four steps e.g. chondrogenesis, chondrocyte differentiation and hypertrophy, mineralization and invasion of bone cells, and finally the formation of bone (DeLise *et al.* 2000, Goldring *et al.* 2006, Goldring 2012). Chondrocytes arise from mesenchymal progenitors as a result of chondrogenesis started with the condensation of mesenchymal stem cell (expressing collagens I, III and V), and followed by the differentiation of chondroprogenitor cell (expressing cartilage-specific collagens II, IX and XI) (Goldring et al. 2006). After chondrogenesis, the chondrocytes remain as resting cells to form the articular cartilage or undergo proliferation, terminal differentiation to chondrocyte hypertrophy, and apoptosis.

There are no blood vessels in articular cartilage, thus the cells rely on diffusion from articular surface or subchondral bone for nutrients and metabolites. Importantly, the oxygen level in the cartilage matrix is quite low, ranging from 10% at the surface to less than 1% in the deep zone (Silver 1975), suggesting the cells have to adapt to this low oxygen level. The mechanisms of this adaption remain unclear but some published data reported the involvement of hypoxia inducible factor -1 alpha (HF-1α) (Schipani *et al.* 2001, Pfander *et al.* 2003). Hipoxia via HIF-1α can stimulate chondrocytes to express a number of genes associated with cartilage anabolism and chondrocyte differentiation like SOX9, TGFβ (Amarilio *et al.* 2007).

1.1.1.3 Biology of cartilage extracellular matrix

Together with chondrocytes, extracellular matrix (ECM) produced by these cells is among the main components of articular cartilage and its integrity is critical for the cartilage biochemical properties and joint physical function.

About structure, the ECM in articular cartilage is organized into pericellular, territorial, interterritorial zones, each of which is represented at specific distance from the chondrocytes (Dudhia 2005, Heinegard and Saxne 2011) (**Figure 1.1**).

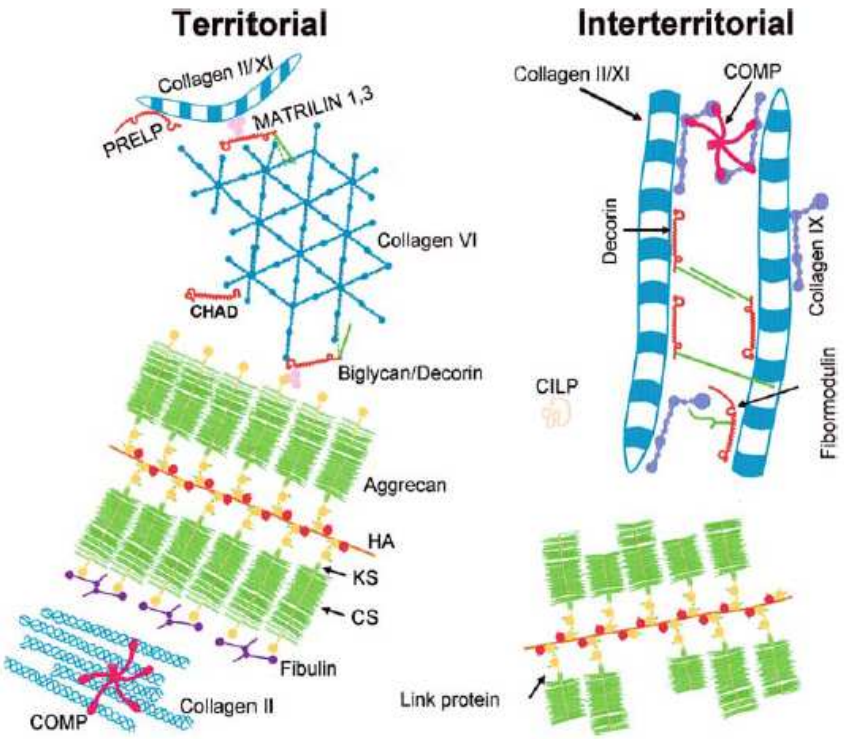

Figure 1.1: **Molecular organisation of normal articular cartilage.**

The cartilage matrix surrounding chondrocytes in healthy articular cartilage is arranged into zones defined by their distance from the cell. Pericellular matrix lies immediately around the cell and is the zone where molecules that interact with cell surface receptors are located. Next to the pericellular matrix, slightly further from the cell, lies the territorial matrix. At largest distance from the cell is the interterritorial matrix (adapted from Heinegard et al, 2011) (Heinegard and Saxne 2011)

Biochemically, of the ECM, approximately 70% is water (Pearle et al. 2005) , and 30% left is solid, of which 5-6% are inorganic compounds (hydroxyapatite), and the remaining 25% are organic compounds. Of the organic components, type II collagen constitutes 68% and the 32% left is formed by proteoglycan (mainly aggrecan) (Martel-Pelletier et al. 2008). The biology of aggrecan and collagen and their functions in articular cartilage are described as below.

1.1.1.3.1 Aggrecan

Molecules made up of a core protein attached to glycosaminoglycan chain are referred as proteoglycan. In articular cartilage, the most abundant proteoglycan is aggrecan, composed of chondroitin sulphate chains and keratan sulphate chains with N- and O-linked oligosaccharides. Aggrecan has three globular domains (G1, G2 and G3) and three extended domains (IGD, KS and CS). The N-terminal G1 domain, responsible for aggrecan-hyaluronan interaction, is followed after the signal peptide. The inter-globular (IGD) connects G1 and G2 domains, whose functions are unclear. Keratan sulphate binding (KS) and chondroitin sulphate (CS) domain lie between G2 and G3 domains (Kiani *et al.* 2002, Dudhia 2005, Martel-Pelletier et al. 2008, Heinegard and Saxne 2011) (Figure 1.2).

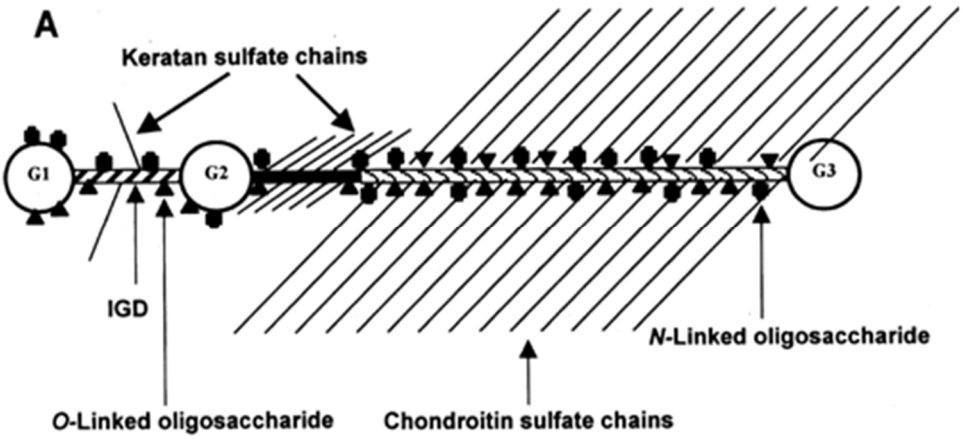

Figure 1.2: Aggrecan structure.

Aggrecan consists of 3 globular domains (G1, G2, and G3) and an attached GAG chain structure. The GAG attachment region is separated into keratin sulphate binding (KS) domain and chondroitin sulphate (CS) domain (Adapted from Kiani et al, 2002) (Kiani et al. 2002).

The chondroitin sulphate domain is the largest domain of aggrecan and is composed of around 100 chondroitin sulphate chains (typically around 2kDa each). Each chain is made up of some 50 disaccharides of glucuronic acid and N-acetylgalactosamine, with a sulphate group in the 4- or 6- position. The negatively-charge chondroitin sulphate chain accounts for the major function of aggrecan as a structural proteoglycan. The function of the keratan sulphate domain is not very clear but may be involved in the tissue distribution of aggrecan. There are about 30 KS chains, usually of small size (5-15 kDa), attached to the mature aggrecan molecule.

Chondroitin sulphate, keratan sulphate, and the interaction of aggrecan and hyaluronic acid are responsible for retaining water the cartilage. The interaction between aggrecan and collagen fibrils makes the ECM highly hydrophilic, leading to high resistance to compressive mechanical loads (Dudhia 2005, Martel-Pelletier et al. 2008).

1.1.1.3.2 Collagen

Collagen fibrils are composed of a protein macromolecular providing cartilage with resistance to tension. Collagen type II constitutes 85% total collagen content in the ECM of articular cartilage. Apart from type II Collagen, ECM also contains other collagens called minor collagens since their concentration is low in comparison with the type II collagen. A list of these collagens is provided in Table 1.1.

All fibril collagens are synthesized in the form of three polypeptide α-chains as a procollagen in which each chain has an N-terminal extension and a C-terminal extension. The three chains are covalently linked via disulphide bridges in the C-terminal propeptide. Following or during secretion of procollagens into the extracellular matrix, the terminal propeptides are cleaved off by specific proteinases e.g. ADAMTS-2, ADAMTS-3, ADAMTS-14 (cleaves the N-terminal) (Lapiere *et al.* 1971, Fernandes *et al.* 2001, Colige *et al.* 2002), and BMP-1 (cleaves the C terminal) (Wermter *et al.* 2007) to produce the mature collagen molecules. The mature collagens then spontaneously self-assemble into

cross-striated fibrils in the extracellular matrix. The fibrils are stabilized by covalent cross-linking (Figure 1.3)

Collagen molecules then associate on a core of two homologous collagen XI and two collagen II molecules to form an outer shell of 10 collagen II molecules of the micro fibril. In addition to collagen type II, fibers contain other collagens, particular collagen type IX. The collagen network is then stabilized by the formation of covalent crosslinks that link the collagen II chains. The links formed are both intra- and inter-molecules, for example, between the chains of collagen XI, between collagens e.g. collagen II and collagen IX.

Many other proteins also have a high affinity for collagens including thrombospondins, leucine-rich repeat proteins (biglycan, decorin, fibromodulin, lumican), matrillins, and fibronectin. Some of these interactions support fibre formation while others modify the collagen fibre surface to provide sites for interactions with neighbouring structures (Heinegard and Saxne 2011).

Collagen types	Characteristics
Type IX	Located on the surface of type II collagen fibrils; promotes the binding of the fibrils to other components of the matrix and to each other; carries a glycosaminoglycan chain.
Type XI	Forms the core of the same fibrosis. Regulates the formation and the diameter of the fibrils
Type V	Sometimes replaces the type XI collagen in cartilage; included in type I collagen fibrils in other tissues. Data on the composition and structure of the third a-chain are contradictory
Type III	Small amount are covalently bound to type II collagen
Type XII	Very small amounts are present on the surface of type II collagen
Type XIV	Very small amounts are present on the surface of type II collagen
Type VI	As in other tissue, forms a network of microfibrils. Concentrated mainly in the pericellular areas, provides a connection between the chondrocytes and the matrix
Type X	Expressed only by hypertrophic chondrocytes in cartilage areas undergoing ossification
Type XXVII	Expressed in cartilage tissue

Table 1.1 Minor collagen of cartilage tissue (adapt from Omelyanenko et al, 2014)(Petrovich *et al.* 2014)

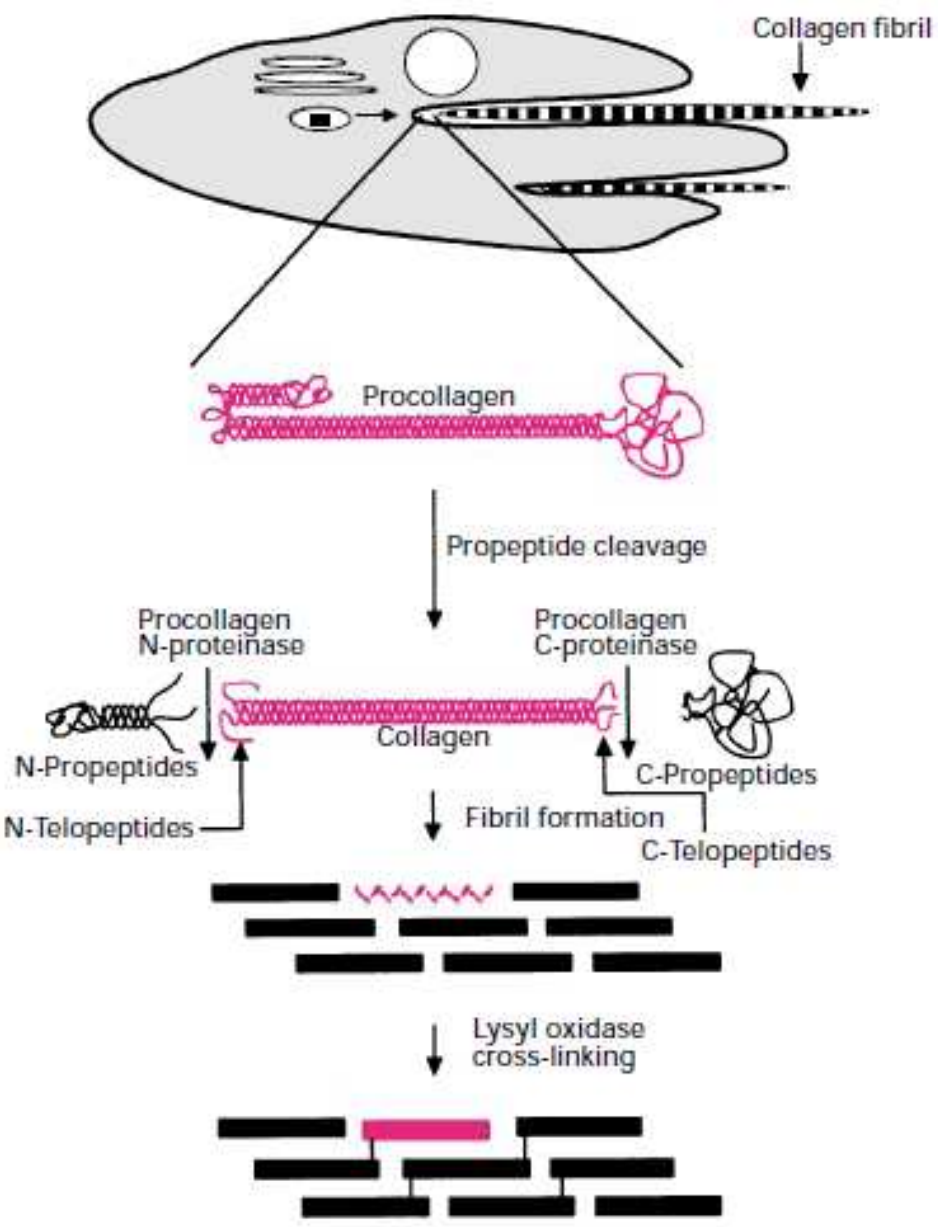

Figure 1.3: The formation of the fibrillar collagens

Procollagen is secreted from cells and converted into collagen by removal of the N- and C-propeptids by pro-collagen metalloproteinases. This produces mature collagen that spontaneously self-assembles into cross-striated fibrils which are stabilized by covalent cross-linking. Taken from (Kadler et al, 1996)(Kadler *et al.* 1996).

1.1.2. Synovium

Synovium is a thin tissue only a few cell layers thick (Fell 1978). The synovium acts as the controller for the environment within the joint where nutrients for chondrocytes can pass into the synovial cavity. Also, the synovium gives the joint its mechanical properties. The synovium can be divided into two compartments e.g. the synovial lining and the sub-lining. The synovial lining contains two cell types e.g. **type A (macrophage-like cells)** clearing all excess materials and potential pathogens from the joint, producing and secreting a number of enzymes and cytokines and chemokines that mediate tissue damage and inflammation in disease; **type B synoviocytes**, **fibroblast like cells**, producing the main component of synovial fluid, hyaluronan. The synovial sublining consists of connective tissue containing blood vessels, fibroblasts, adipocytes, and a limited number of resident immune cells, such as macrophage and mast cells (Smith *et al.* 2003). The synovial fluid has crucial role for lubrication of the joint and for transporting nutrients and oxygen to the cartilage.

1.1.3. Bone

Periarticular bone can be separated into distinct anatomic entities e.g. the subchondral bone plate, the subchondral trabecular bone, and the bone at the joint margins. The subchondral bone plate consists of cortical bone, which is relatively nonporous and poorly vascularized. It is separated from the overlying articular cartilage by the zone of calcified cartilage.

Bone is a very dynamic tissue with constantly undergoing remodelling in which bone resorption is normally followed by new bone formation. The primary cell responsible for bone resorption is the **osteoclast**, a specialized multinucleated cell of hemopoietic origin (Roodman 1999). Bone resorption takes place under a specialized area of the osteoclast cell membrane called “ruffled border,” which comprises a sealed lysosomal compartment where the acidic pH solubilizes the mineral and proteolytic enzymes digest the matrix. On the contrary, **osteoblasts**, the bone forming cells, originally from MSCs committed to osteoblastic lineage. Osteoblasts synthesize and secrete most of the proteins of the bone matrix, including type I collagen and non-collagenous proteins (Caetano-Lopes *et al.* 2007). In normal physiological condition, the amount of bone removed during the resorption and formation phases is balanced such that bone mass is maintained.

1.2. Osteoarthritis

Osteoarthritis (OA) is defined by the American College of Rheumatology as a "heterogeneous group of conditions that lead to joint symptoms and signs which are associated with defective integrity of articular cartilage, in addition to related changes in the underlying bone at the joint margins''.

There are more than 100 types of arthritis. However, OA or degenerative joint disease is the most common type. From a clinical point of view, OA can be classified into two categories e.g. **primary** which refers to its occurrence not related to any prior condition or event which is also referred as idiopathic, and **secondary** which refers to the development of the disease after trauma or pre-existing condition.

The disease most commonly affects the middle-age and elderly, although it may begin earlier as result of injury, obesity or congenitally. As a greater proportion of the population is old aged and with increasing obesity, OA will have a great impact on society in the future with enormous socioeconomic costs.

1.2.1. Osteoarthritis pathology

It is now considered that OA is a disease of the whole joint as an organ resulting in "joint failure" where all major components of the joint e.g. the cartilage, the synovium, and the underlying bone are affected (Loeser *et al.* 2012). The pathologic changes seen in OA include cartilage destruction, fibrosis of the synovial capsule, hyperplasia of the synovial membrane, osteophyte formation, the subchondral bone thickening (**Figure 1.4**) (Aigner et al. 2006, Loeser et al. 2012). These changes result from an incompletely understood series of functional events.

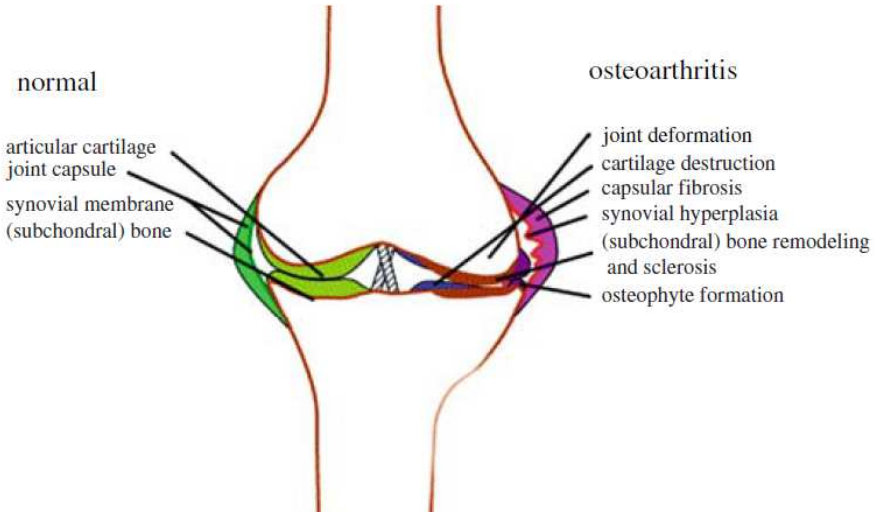

Figure 1.4: Overview of the pathologic changes associated with OA.

In a normal joint, the subchondral bone is covered by a thick layer of articular cartilage and the joint is enclosed in a capsule where the synovial membrane lies. In an OA joint, articular cartilage is destroyed, the subchondral bone is remodelled (thickens), the synovial capsule is fibrosed and osteophytes are formed (reprinted from Aigner et al, 2006) (Aigner et al. 2006)

1.2.1.1.Articular cartilage destruction in osteoarthritis

Biochemical, genetic factors, and mechanical stress contribute to the OA lesion in cartilage, leading to articular cartilage degradation, and chondrocyte metabolism disorders as a consequence. Articular cartilage degeneration is a two phase process controlled mainly by chondrocytes e.g. a short biosynthesis phase where the cells attempt to repair the damaged ECM, followed by the degenerative phase, where the cells destroy the articular cartilage by increasing the synthesis of matrix degradating proteinases and decreasing their synthesis of matrix components, in particular of aggrecan. Besides changes in synthesis and degradation, other aberrant behaviours in cell proliferation and death, and phenotypic modulation are also observed in OA chondrocytes (Sandell *et al.* 2001).

Contrary to normal chondrocytes with no proliferative activity, OA chondrocytes have a low proliferative activity (Meachim *et al.* 1962, Rothwell *et al.* 1973, Lee *et al.* 1993), explained in part due to the better access to proliferation factors from the synovial fluid as well as due to the damage of the ECM (Meachim and Collins 1962, Lee et al. 1993), subsequently causing chondrocyte clustering, a characteristic feature of OA cartilage. Chondrocyte death, caused by apoptosis, necrosis, or other cell death mechanisms such as chondroptosis, is another known feature of OA. Many studies have demonstrated the significant correlations between chondrocyte death and severity of OA and aging. These changes are associated with the production of reactive oxygen species, a lack of growth factors, release of glycosaminoglycan and mechanical injury. However, which of these types of cell death predominate in OA is debatable. The detection of specific form of cell death in articular cartilage is difficult in which current gold standard for detecting chondrocyte death is electron microscopy which suggests that the morphological changes of chondrocytes in OA cartilage are attributed to apoptosis and / or chondroptosis. Chondrocyte death by apoptosis has been reported play an important role: normal cartilage explants or chondrocyte culture exposed to nitric oxide, collagenase, anti CD-59, or mechanical factors e.g. shear strain, loading strain induced apoptosis; cartilage from equine joints have shown that chondrocyte apoptosis is positively correlated with early stages of OA and severity of cartilage damage (Zamli *et al.* 2011).

When the damage occurs, the chondrocytes attempt to repair the damaged matrix by increasing their anabolic activity to enhance ECM synthesis. However, a net loss of ECM content is one of the hallmarks of all stages of OA, suggesting the dominance of ECM degradation over the synthesis. This is characterized by the increase in expression and activation of matrix-degrading enzymes e.g. matrix metalloproteinase (MMPs) and aggrecanases (from the ADAMTS family) (Buckwalter et al. 2005, Pearle et al. 2005, Aigner et al. 2006, Umlauf et al. 2010, Loeser *et al.* 2012). **The MMPs,** belonging to a family of zinc-dependent proteases, show activation correlating with cartilage degradation. Among these, the groups of collagenases 1, 2, 3 (MMP-1, MMP-8, and MMP-13, respectively), stromelysins (MMP-3, MMP-10, MMP-11) and gelatinases (MMP-2, MMP-9) have the highest impact on OA cartilage breakdown (Burrage *et al.* 2006). The MMP-1, MMP-8 and MMP-13 which cleave native fibrillar collagen, contribute to the pathological cleavage of collagen fibrils in OA (Burrage et al. 2006). Of the collagenase group, MMP-13 is deemed to be responsible for most of the collagen II breakdown whilst MMP-1 cleaves type II collagen stronger than MMP-8 (Billinghurst *et al.* 1997) has a pivotal role for collagen cleavage in OA (Knauper *et al.* 1996). In addition to collagenases, others MMPs degrading non-collagen have also been shown to be elevated in OA cartilage e.g. the gelatinases (which cleave denatured collagen, gelatin, type V collagen) and the stromelysins (having substrate preference for proteoglycans, elastin, laminin, fibronectin) (Umlauf et al. 2010) **The aggrecanases** (the ADAMTS family), are also of particular importance in cartilage turnover, and have activity against the proteoglycan aggrecan. Of all ADAMTS members, ADAMTS-4 and ADAMTS-5 are most active against aggrecan (Arner 2002). ADAMTS-5 is constitutively expressed in chondrocytes whereas ADAMTS-4 expression is stimulated by proinflammatory cytokines IL-1β, and TNF-α (Umlauf et al. 2010) (Tortorella *et al.* 2001). In vitro studies with human cartilage show that both ADAMTS-4 and ADAMTS-5 contribute to ECM breakdown during the disease progression even though human recombinant ADAMTS-5 has higher rate of aggrecan cleavage than ADAMTS-4 (Song *et al.* 2007). In mice, ADAMTS-5 has been shown to be the major aggrecanase, by studies with ADAMTS-4 and ADAMTS-5 knockout mice in which only ADAMTS-5 deficiency prevented the mice from cartilage degradation in both inflammatory and a joint-instability model of arthritis (Glasson *et al.* 2005, Stanton *et al.* 2005) .

As mentioned above, despite the attempt at repairing the ECM, the damage to the cartilage becomes irreversible because the adult chondrocytes fail in regenerating the normal cartilage matrix structure. This failure could be, in part, attributed to the phenotypic alteration of chondrocytes. Chondrocyte phenotypes are categorized largely by subtyping collagen expression e.g. chondroprogenitor cells express type IIA procollagen. The alternative splice variant) (Sandell *et al.* 1991), mature chondrocytes are marked by expressing type IIB procollagen, IX, and XI, aggrecan and link protein (Sandell and Aigner 2001), and hypertrophic chondrocytes express type X collagen (Schmid *et al.* 1985). In OA cartilage degeneration, an important proportion of adult articular cartilage chondrocytes, found mostly in the middle zone, re-expressed type IIA procollagen (chondroprogenitor cells) in both early and late OA stages (Sandell and Aigner 2001). Cells in the upper middle zone mainly express type III collagen which is a fibroblast-like phenotype. This phenotype is normally observed in vitro, where the chondrocyte phenotypes are modulated through so-called "dedifferentiation" process by several factors like retinoic acid or IL-1. Dedifferentiated chondrocytes are still very active, express collagen types I, III and V but stop expressing aggrecan and collagen type II (Sandell and Aigner 2001). In the deepest zone of OA cartilage, the cells start to express type X collagen, specific marker for hypertrophy of growth-plate chondrocytes (Girkontaite *et al.* 1996). Indeed, the hypertrophic chondrocytes in OA cartilage and in the growth-plate share similarities and the subsequent functional event associated with hypertrophic differentiation is cartilage mineralization which is also a feature of OA. However, the mechanism involved in pathological cartilage calcification during OA is not completely understood.

1.2.1.2. Synovium in osteoarthritis

Inflammation of the synovial membrane (synovitis) is identified in many OA patients despite lower severity and greater variability as compared to rheumatoid arthritis. It is reported that synovitis can occur even in early stages of the disease (Benito *et al.* 2005). Synovitis is associated with symptoms such as pain, the degree of joint dysfunction, the rapid degeneration of cartilage, and is characterized by the thickening of the synovial lining layer, leukocyte infiltration, and thickening of the sub-lining stroma. The

mechanisms underlying the development of synovitis in OA remain unclear. It is however well known that this inflammatory process is triggered by ECM degradation products, which engage Toll-like receptors and the complement cascade (Scanzello *et al.* 2012). Noteworthy, the synovial reaction may produce a variety of cytokines and chemokines, in turn affecting catabolism of chondrocytes (Scanzello and Goldring 2012).

Of all cell types in the inflamed OA synovium, the macrophages are among the most abundant and depletion of synovial macrophages has been shown to result in decreased osteophyte formation, and IL-1, TNF-α, IL-6, IL-8, MMP-1, MMP-3 production (Bondeson *et al.* 2010). Natural killer cells and dendritic cells are also reported to present in synovial tissue. However, the role of both of them in OA pathogenesis has not yet been elucidated in detail.

1.2.1.3. Subchondral bone in osteoarthritis

Articular cartilage helps to distribute load across the whole joint surface. Any alteration in the properties of cartilage leads to alter load experience by the underlying bone and probably causes a tissue remodelling response. The properties of bone might also modulate how the overlying cartilage reacts to load.

Although OA is often characterized as a disease of articular cartilage, the alteration of bone metabolism is increasingly recognised as a mediator of pain and OA progression. Subchondral bone consists of a dome-like subchondral plate and underlying trabeculae, having a close biomechanical and biochemical relationship with the overlying cartilage. Strong evidence associates subchondral bone alterations with cartilage damage and loss in OA (Karsdal *et al.* 2014). However, there is still an incomplete understanding of the mechanisms for the numerous pathophysiological alterations detected in subchondral bone with OA.

The pathological cascade may be started when the normal subchondral bone suffers from a non-physiological strain. In early-stage OA, the subchondral plate becomes thinner and more porous, together with initial cartilage degeneration. Subchondral trabecular bone also deteriorates, with increased separation and thinner trabeculae. At the same time, microdamage begins to appear in both calcified cartilage and subchondral bone, which will persist throughout the whole pathological process. In late-stage OA, calcified cartilage and the subchondral plate become thicker, with duplicated tidemarks and progressive non-calcified cartilage damage. Subchondral trabecular bone becomes sclerotic (Li *et al.* 2013).

The sclerosis of periarticular mineralized tissues may be a biomechanical compensational adaption to the widespread cysts and microdamage in subchondral bone, which render subchondral bone structure more fragile (Figure 1.5).

Despite increased bone volume density in the sclerotic subchondral bone, its mineralization is reduced and lower than in normal joints. Although collagen synthesis is elevated in subchondral bone, the deposited collagen is hypomineralized and has a markedly reduced calcium-to-collagen ratio [42].

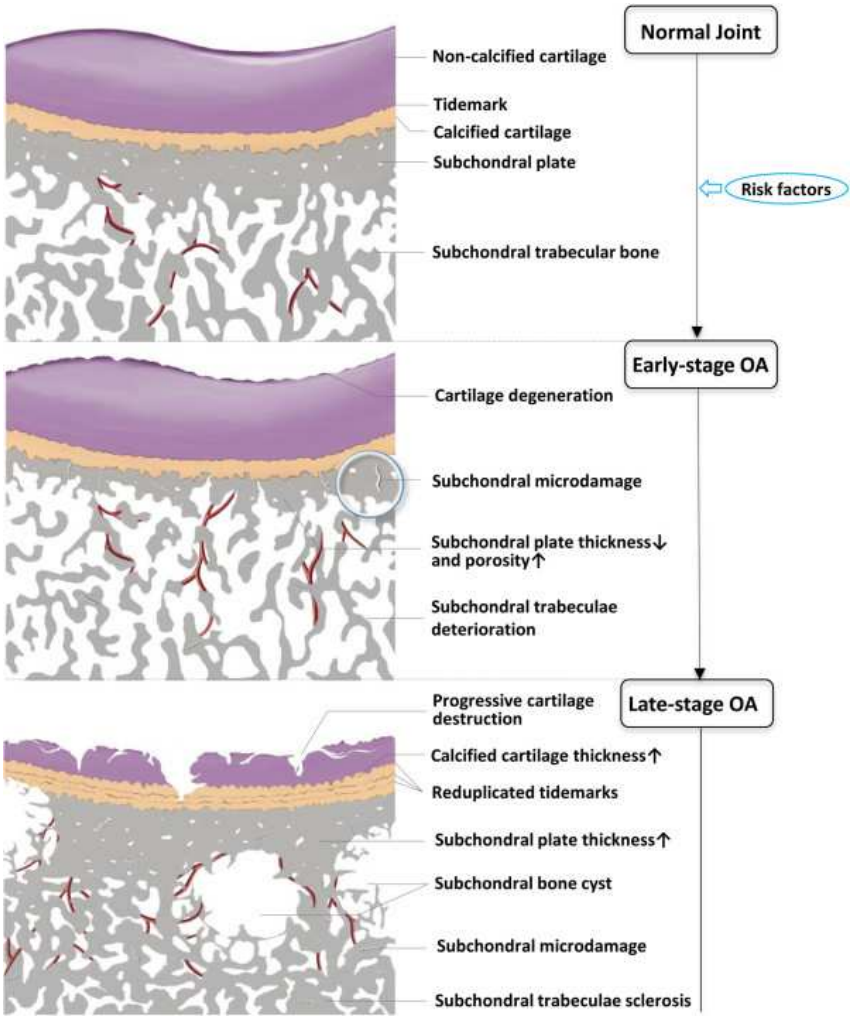

Figure 1.5: Alteration in subchonral bone in Osteoarthritis

In early stage of OA, subchondral microdamage occurs, the subchondral plate is thinner with increased porosity, and subchondral trabeculae are deteriorated. At OA later stage, the calcified cartilage and subchondral plate is thicker, with reduplicated tidemarks. Subchondral trabecular bone becomes sclerotic (adapted from Li et al, 2013)(Li et al. 2013)

1.2.1.4. Osteophytes

Osteophytes, considered as an adaptation to the altered biomechanics, are non-neoplastic osteo-cartilaginous protrusions growing at the margins of OA joints, and represent areas of new cartilage and bone formation. Osteophytes limit joint movement, represent a source of joint pain, and are a radiographic hallmark of OA. However, it is noteworthy that when osteophytes appear in the absence of other bony changes, e.g. subchondral cysts or subchondral sclerosis, they may be a manifestation of aging, rather than of OA.

Osteophytes derive from precursor cells within periosteal or synovial tissue (van der Kraan *et al.* 2007) but the initial stimuli for osteophyte formation remains unclear, probably involving both mechanical and humoral factors as repeated injections of mouse joints with TGFβ or BMP induced or enhanced osteophyte formation in animals with experimentally induced OA (van Beuningen *et al.* 1998).

Osteophytes are composed of cells that express type I procollagen mRNA, mesenchymal prechondrocytes that express type IIA procollagen mRNA, and maturing chondrocytes that express type IIB procollagen mRNA. Based on the spatial pattern of gene expression and cytomorphology, the neochondrogenesis associated with osteophyte formation closely resembles that of healing fracture callus (Matyas *et al.* 1997) and is also similar to the growth plate. Thus, osteophytes may represent an excellent *in vivo* model for induced cartilage repair processes.

1.2.2. Anabolic and catabolic signalling in OA

Anabolic and catabolic activation are largely the result of exposing cells to various cytokines and growth factors e.g. TGFβ, BMPs, IGF-1, TNF-α, IL-1β, Wnt3a. In OA cartilage, the catabolic and anabolic equilibrium is broken and favours the activation of catabolic pathways or mechanisms leading to matrix degradation.

1.2.2.1.Anabolic signalling in OA

As previously mentioned, the early phase of the response to mechanical injury is characterized by the attempt to repair the damage matrix by increasing the anabolic activity of chondrocytes, enhancing synthesis of extracellular matrix components. This is facilitated by enhancing levels of anabolic factors e.g. TGFβ, FGF, and BMPs, and Wnt.

1.2.2.1.1. TGFβ signalling

The TGFβ family, consisting of over 35 members including TGFβ and BMPs, has been widely known to play a crucial role in the development and homeostasis of various tissues. Activated TGFβ (TGFβ-1, -2, -3) binds to their two receptor complex, TGFβ-R1 and TGFβ-RII and phosphorylates members of the receptor-specific Smad family, Smad2 and Smad3. Upon phosphorylation, Smad2/3 subsequently forms a complex with the common mediator Smad4. This complex then translocates into the nucleus where it can act as a transcription factor. Unlike TGFβ-1, -2, -3 which signal via Smad2/3/4, BMPs transduce their signal through Smad-1, -5 and -8 (Miyazawa *et al.* 2002, Verrecchia *et al.* 2002).

Members of the TGFβ family are considered potent mediators of cartilage matrix synthesis, in which they up-regulate the expression of several types of collagens and proteoglycan but down-regulate cartilage degrading enzymes (Verrecchia *et al.* 2001, Verrecchia and Mauviel 2002). Despite such promising data, therapeutic studies with TGFβ revealed major side effects e.g. injection or adenovirus–mediated delivery of TGFβ1 into normal murine knee joint resulted in joint fibrosis and osteophyte formation (van Beuningen et al. 1998) .

1.2.2.1.2. Wnt signalling

The human Wnt family includes 19 members which mostly exert their function by binding to Frizzled (FZD) receptor proteins and LRP-5/6 co-receptor proteins, in turn activating several signal transduction pathways e.g. canonical, and non-canonical signalling pathways. In the canonical Wnt pathway, most β-catenin in the cytoplasm is sequestered and targeted for proteasome-mediated degradation within a multi-protein complex of casein kinase, axin, the adenomatous polyposis coli tumour suppressor protein (APC) and glycogen synthase kinase 3β (GSK3β). With the presence of appropriate Wnt ligands, signalling through the Frizzled receptors inhibits this degradation process, and thereby leads to β-catenin accumulation and translocation into the nucleus (Clevers 2006). Within the nucleus, it acts in concert with Tcf/Lef transcription factors to generate a transcriptionally active complex that regulates a number of genes e.g. MYC, cyclin D1, MMP3 and CD44, E-cadherin, MMP7, MMP26(Dell'accio *et al.* 2008, Umlauf et al. 2010). In contrast to the canonical pathway, non-canonical Wnt signalling is mostly a β-catenin independent mechanism like the Wnt/calcium and Wnt/JNK pathways in vertebrates and the Wnt/planar cell polarity pathway (PCP) in flies (Willert *et al.* 2006). In addition, there

are some natural extracellular inhibitory factors for Wnt signalling. One of the best characterized families is the Dickkopf (Dkk) family which bind to LRP-5/6 and antagonize the canonical pathway. Other antagonists are the secreted frizzled-related protein (sFRP) family which bind directly to Wnt ligands and inhibiting both canonical and non-canonical Wnt pathways (Kawano *et al.* 2003).

A number of published data provide evidence of the critical role of Wnt signalling in OA development. Direct evidences come from animal model studies where β-catenin is conditionally activated or inhibited in articular cartilage chondrocyte of adult mice (Zhu *et al.* 2008, Zhu *et al.* 2009). Mice with β-catenin activated had OA-like cartilage degradation, osteophyte formation, associated with accelerated chondrocyte maturation and MMP13 expression (Zhu et al. 2009). Similarly, selective suppression of β-catenin signalling in Col2a1-ICAT (inhibitor of β-catenin and TCF) transgenic mice also causes OA-like cartilage degradation(Zhu et al. 2008). In line with these reports, in vitro culture of human primary chondrocyte, either activation or blockade of β-catenin signalling all resulted in cartilage loss (Nalesso *et al.* 2011). These data suggest that balanced β-catenin levels are essential for maintaining homeostasis of articular chondrocytes and that any factors impairing this balance could lead to pathological changes. Moreover, LRP5 is located in chromosome 11q12-13, which is thought to be an OA susceptibility locus. LRP5-/- mice displayed increased cartilage degradation, probably due to low bone mass density (Lodewyckx *et al.* 2012). Another study in a mouse OA model also demonstrated that control of Dkk1 expression, a negative regulator of β-catenin/Wnt signalling, prevents joint cartilage deterioration in OA knees through attenuating the apoptosis regulator Bax, MMP3 and RANKL (Weng *et al.* 2010). Also, the inhibition of Dkk1, has been reported to be able to reverse the bone-destructive characteristics of rheumatoid arthritis to the bone-forming characteristics of OA (Diarra *et al.* 2007). This evidence further supports the crucial role of β-catenin/Wnt signalling in OA. Wnt signalling is also reported to function as an OA initiation factor e.g. a down-regulation of Wnt antagonist FRZB and an up-regulation of the ligand Wnt16 and target genes encoding β-catenin, Axin-2, C-JUN and LEF-1 was observed in mouse model of mechanical injury, a major cause of OA; expression of WNT1-inducible signalling protein (WISP-1) was also increased twofold in cartilage lesions compared to healthy intact cartilage (Blom *et al.* 2009).

Human studies also observed the critical role of WNT signalling in OA development. A loss-of-function allelic Arg200Trp and Arg324Gly Frzb variants, encoding sFRP-3, a β-catenin/Wnt signalling inhibitor, contributed to genetic susceptibility of women to hip OA (Loughlin *et al.* 2004, Lane *et al.* 2006). Given the close relationship between bone shape and OA development, Baker-Lepain et al proposed that SNPs in Frzb are associated with the shape of proximal femur and further contribute to hip OA development (Baker-Lepain *et al.* 2012). Moreover, the Frzb knockout mice increased articular cartilage loss during arthritis triggered and this damage was associated with increased WNT signalling and MMP-3 expression and activity. Also, the FRZB deficiency resulted in the cortical bone thickness and density with stiffer bones (Lories *et al.* 2007).

1.2.2.2. Catabolic signalling in OA

Opposing the anabolic effects of growth factors are pro-inflammatory cytokines and a variety of mediators associated with inflammation e.g. NO, prostaglandins, IL-1β, TNF-α, IL-6, IL-8 These factors are first produced by the synovial membrane and diffuse into the cartilage through synovial fluid, together with activate chondrocytes which also have the capacity to produce a variety of cytokines and mediators, responsible for functional alterations in the synovium, the cartilage, and the subchondral bone. Their role in OA has attracted considerable attention.

Of pro-inflammatory cytokines, IL-1β, TNF-α seem prominent and of major importance to cartilage destruction. The biologic activation of cells by IL-1 is mediated through the association with its specific receptors e.g. type I and II IL-1R. Especially, the type I IL-1R, responsible for signal transduction, was found to increase in OA chondrocytes and synovial fibroblasts. IL-1β is a critical mediator, and stimulation of chondrocytes by IL-1β causes gene expression patterns similar to those in OA cartilage (Goldring *et al.* 1988, Lefebvre *et al.* 1990). IL-1β localizes to the site of cartilage degradation in OA joints, providing evidence of its key role in the pathogenesis of OA (Tetlow *et al.* 2001, Pujol *et al.* 2008). IL-1β was reported to suppress aggrecan and collagen and up-regulate the proteolytic enzymes e.g. ADAMTS4 and MMP13 (Goldring 2000, Kobayashi *et al.* 2005). In addition, *IL-1β*, or IL-1β-converting enzyme knockout mice showed the accelerated development of OA lesions in response to OA surgical induced compared to wild type mice (Clements *et al.* 2003). The blocking effects of IL-1β by IL-1 receptor antagonist

(IL-1ra), which is the natural inhibitor of IL-1β by competing with IL-1β for occupancy of the IL-1β cell surface receptors but cannot initiate cellular signals protect against the development of experimentally induced OA lesions in animal models e.g. dogs, horses (Pelletier *et al.* 1997, Frisbie *et al.* 2002). Interestingly, it was reported that the IL-1β concentration is low in inflamed joints and a level from 10-1000 fold excess of IL-1ra over IL-1β was required to efficiency block all of the available IL-1β receptors enough to inhibit joint degradation (Pelletier et al. 1997).

1.2.2.2.1. NFκB Signalling

The transcription factor NFκB is the master regulator of expression of a number of genes critical to innate and adaptive immunity, cell proliferation, and inflammation. NFκB is held in the cytoplasm in an inactive form associated with the inhibitory κB (IκB) protein. A broad range of stimuli, including TNF-α, IL-1β, bacteria and viruses trigger a cascade of signalling, leading to release of NFκB from IκB. The activated NFκB will then translocate to the nucleus, bind to DNA elements present in its target genes and facilitate their transcription.

Numerous published data support the central role of NFκB signalling in cartilage metabolism and development of OA e.g. IκB overexpression in human OA synovial fibroblasts resulted in a decrease in expression of IL-6, IL-8, MPC-1/CCL-2, and MMPs (Amos *et al.* 2006) as well as abolishing the IL-1β-induced effect on expression of ADAMTS-4 (Bondeson *et al.* 2007); In a mouse surgically induced OA model, siRNA inhibiting NFκB/p65 resulted in reducing the amount of IL-1βand TNF-α in synovial fluid, reducing the level of inflammation in the synovium, and decreasing cartilage damage (Chen *et al.* 2008).

1.2.3. Risk factors for Osteoarthritis

The pathogenesis of OA is complex and poorly understood but involves the interaction of multiple factors ranging from genetic predisposition to mechanical and environmental components. Studies are in progress to define the molecular mechanisms involved in initiation and progression of OA.

1.2.3.1.Trauma and altered mechanical load

Mechanical factors and trauma have a central role in the initiation and propagation of OA: Excessive load and trauma which lead to injury of the menisci or ligaments predispose to

the development of the disease; the level and nature of the load experienced might also influence the progression of joint damage: an acute trauma leading to rupture of the meniscus or the cruciate ligaments might precipitate the development of OA. However, the differing contributions to this effect of the initial trauma and the ensuing mechanical instability have not been clearly delineated; also, in immobilized joints, there is lack of OA: further supporting the importance of mechanical triggers in the disease process (Riordan *et al.* 2014).

After joint trauma, the onset and progression of clinical symptoms differs even among groups with the same type of injury and physical activity profile, pointing to the involvement of other factors apart from the trauma.

1.2.3.2. Inflammation

Histologically, the disease was denominated osteoarthrosis, a term that implied the absence of inflammation. However, data acquired using high-sensitivity assays for inflammatory markers (such as C-reactive protein) demonstrate that low-grade inflammation is present (Pearle *et al.* 2007). Numerous inflammatory cytokines are found at increased levels in joint tissues during the acute post-injury phase, including IL-1, IL-6, IL-17, and TNFα (Lee *et al.* 2009). Inflammation seems to be a very early event in OA since the increase of CRP levels precedes the release of other OA indicators or molecular markers of matrix breakdown, and is observed well before clinical disease.

Inflammatory might be of particular importance to the onset and propagation of the primary and secondary OA. However, why the inflammation triggered in OA remains controversial. It was hypothesized that it was caused by traumatic joint injury or an age – related process. Joint injury leads to cartilage degradation and tissue damage. Once degraded, cartilage fragments accumulate in the joint and contact the synovium. Considered foreign bodies, synovial cells react by producing inflammatory mediators, found in synovial fluid. These mediators can activate chondrocytes present in the superficial layer of cartilage, which leads to metalloproteinase synthesis and, eventually, increase cartilage degradation. Published data support for the hypothesis that inflammation was triggered by aging process: advance glycation endproducts (AGEs), produced by a non-enzymatic process in aging tissue, weaken cartilage by modifying its mechanical properties triggering chondrocyte activation by binding to specific receptors present at the

surface of the chondrocytes, called RAGE (receptor for AGEs) lead to an overproduction of proinflammatory cytokines and MMPs (Nah *et al.* 2007); or after a period of vigorous proliferation, chondrocyte division rate declines but has high capacity to synthesize soluble mediators which in turn induces several inflammatory and pro-degradative mediators.

1.2.3.3. Obesity

Obesity is a well known risk factor for the initiation and progression of OA. This association is obvious because any overload on a weight – bearing joint would provoke tear and wear at the surface of the cartilage.

The molecular mechanisms explaining why obesity is one of the major risk factors for OA (Messier *et al.* 2005) is not exactly known. It is possible that the excess weight increases the load borne by all parts of the joint. However, the association between overweight and OA is not simply a question of increased mechanical load because obesity acts as a risk factor for developing hand OA (Grotle *et al.* 2008). Together with this, published data from animal studies: knee cartilage from rabbits fed a high – fat diet showed lower glycosaminoglycan content and aggrecan-1 than cartilage from rabbits fed a normal – fat diet independently of animal weight (Brunner *et al.* 2012); OA surgical induced mice fed a high – fat diet from 4 weeks of age showed higher OA cartilage degeneration at 8 weeks after surgery than those fed a normal diet (Mooney *et al.* 2011); in mice transgenic for human C – reactive protein (CRP) on a high – fat diet, there is a lack of correlation between OA severity and body weight (Gierman *et al.* 2012).

Many studies suggest that systemic inflammatory mediators contribute to the increased risk of OA with obesity. Adipose tissue, especially from the abdomen, is a rich source of pro-inflammatory cytokines, which are often referred to as adipokines. Many adipokines elevated with obesity have also been shown to mediate synovial tissue inflammation. For example, leptin is a 16-kd polypeptide hormone encoded by the obese (*ob*) gene and is primarily secreted by adipocytes. Female C57BL/6J mice with impaired leptin signalling are protected from obesity – induced OA, suggesting elevated body fat in the absence of leptin signalling is insufficient to induce systemic inflammation and OA (Griffin *et al.* 2009). Leptin has been found to exist at higher concentrations in the synovial fluid compared to serum (Presle *et al.* 2006). Leptin, alone or in synergy with IL-1, induced collagen release from bovine cartilage explants and upregulated MMP-1 and MMP-13 expression in bovine chondrocytes(Hui *et al.* 2012).

1.2.3.4. Aging

Aging is the most important risk factor for OA. After 40 year old, many people will appear to have some damage to their joints which may lead to OA, and approximately 50% of individuals greater than the age of 65 suffer from OA. The incidence of the disease through age has been observed: the prevalence of OA rises from 4% in people under the age of 24 to as high as 85% for those at 75-79 years of age. The common justification is the long-term effect of mechanical load on all joint components. Also, the regenerative capability of cartilage is reduced and cellular apoptosis is enhanced with age (Goldring *et al.* 2007).

1.2.3.5.Genetic factors

Evidence from family clustering and twin studies indicates that the risk of OA has an inherited component. Genetic factors may influence between 39% and 65% in radiographic OA of the hand and knee in OA, about 60% in OA of the hip, and about 70% in OA of the spine. Mutations to genes that play a role in the ECM, proteases and inhibitors, cytokines, and growth factors have been found to affect one's susceptibility to develop of OA (Sulzbacher 2013). However, the individual effects are relatively small. For example, a genome – wide association study showing that the C allele of rs3815148 on chr 7q22 was associated with a 1.14- fold increased prevalence of knee and/ or hand OA(Kerkhof *et al.* 2010).

1.3. MicroRNAs in osteoarthritis

1.3.1. The basic biology of miRNA

miRNAs are an abundant class of evolutionarily conserved, short (~22nt long), single – stranded RNA molecules that have emerged as important post transcriptional regulators of gene expression by binding to specific sequences within a target mRNA (Ambros 2004, Bartel 2004). To date, 1424 miRNAs have been identified in human cells and each is predicted to regulate several target genes (Lim *et al.* 2005, Kozomara *et al.* 2011). Computational predictions indicate that more than 50% of all human protein – coding genes are potentially regulated by miRNAs (Lewis *et al.* 2005, Friedman *et al.* 2009). The abundance of mature miRNAs varies extensively from as few as ten to more than 80,000 copies in a single cell, which provides a high degree of flexibility in the regulation of gene expression (Chen *et al.* 2005, Suomi *et al.* 2008). The regulation exerted by miRNAs is

reversible, as feedback/forward regulatory loops have been shown to exert modifying effects during translation (Inui *et al.* 2010) .

1.3.1.1. MicroRNA discovery

In 1981, the first miRNA: *lin-4* was discovered in *Caenorhabditis elegans* (Chalfie 1981). In the early 1990s, Ambros and Ruvkun revealed that *lin-4* controlled a specific step in developmental timing in *C.elegans* by downregulating *lin-14* (a conventional protein – coding gene) (Chalfie 1981, Lee *et al.* 1993, Wightman *et al.* 1993). They recognized that the *lin-14* 3'UTR harbours multiple sites of imperfect complementarity to *lin-4* and proposed that *lin-4* binds to these sites and blocks *lin-14* translation.

Forward genetics also discovered a second miRNA in *C.elegans,* known as *let-7* (Reinhart *et al.* 2000) which targets *lin-41* and *hbl-1* (Abrahante *et al.* 2003, Lin *et al.* 2003). The concept of miRNAs then jumped from worms to higher species, since *let-7* had well-known homologues even in human and fly. In 2001, the term "microRNA" was coined for this class of non-coding gene regulators (Lagos-Quintana *et al.* 2001, Lau *et al.* 2001, Lee *et al.* 2001). The discovery of miRNAs had crossed over to human, and finding miRNA targets became a high priority.

1.3.1.2. MicroRNA biogenesis

Most of the currently known miRNA sequences are located in introns of protein coding genes; a lower percentage of miRNAs originate from exons or non-coding mRNA-like regions (Rodriguez *et al.* 2004). In addition, a significant number of miRNA are found in polycistronic units that encode more than one miRNA. The miRNAs within clusters are often functionally related (Lagos-Quintana et al. 2001, Lau et al. 2001).

Despite the obvious differences between the biology of miRNAs and mRNAs, all available evidence suggests that these transcripts share common mechanisms of transcriptional regulation. Generally, the generation of a miRNA is a multi-step process that starts in the nucleus and finishes in the cytoplasm (Lee *et al.* 2002). First, miRNAs are transcribed by the RNA polymerase II complex (Lee *et al.* 2004) and subsequently capped, polyadenylated, and spliced (Cai *et al.* 2004). Transcription results in a primary miRNA transcript (pri-miRNA) that harbors a hairpin structure (Lee et al. 2002, Kim 2005). Within

the nucleus, the RNAse II–type molecule Drosha and its cofactor DGCR8 process the pri-miRNAs into 70- to 100-nt-long pre-miRNA structures (Lee *et al.* 2003, Han *et al.* 2004), which in turn are exported to the cytoplasm through the nuclear pores by Exportin-5 (Yi *et al.* 2003, Bohnsack *et al.* 2004, Lund *et al.* 2004, Zeng *et al.* 2004). Subsequently, the RNAse III-type protein Dicer generates a double stranded short RNA in the cytoplasm that consists of the leading – strand miRNA and its complementary sequence (Grishok *et al.* 2001, Hutvágner *et al.* 2001, Ketting *et al.* 2001, Chendrimada *et al.* 2005). This duplex miRNA is unwound by a helicase into a single stranded short RNA in the cytoplasm and the leading strand is incorporated into the argonaute protein (Ago 2)-containing ribonucleoprotein complex known as the miRNA-induced silencing complex, mRISC (Hammond *et al.* 2000, Hutvagner *et al.* 2008, Bossé *et al.* 2010). During this process, one strand of the miRNA duplex is selected as the guide miRNA and remains stably associated with mRISC, while the other strand, known as the passenger strand is rapidly removed and degraded (Martinez *et al.* 2002) (Figure 1.5). Selection of the appropriate strand is primarily determined by the strength of base pairing at the ends of the miRNA duplex. The strand with less-stable base pairing at its 5' end is usually destined to become the mature miRNA (Khvorova *et al.* 2003, Schwarz *et al.* 2003, Hutvagner 2005). However, some miRNA passenger strands are thought themselves to negatively regulate gene expression. One hypothesis is that both strands could be used differently in response to extracellular or intracellular cues, to regulate a more diverse set of protein –coding genes as needed, or strand selection could be tissue specific (Ro *et al.* 2007). The mature miRNA guides the RISC complex to the 3'UTR of its target miRNA (Lai 2002, Bartel 2009) . The seed sequence, comprising nucleotides 2-8 at 5'-end of the mature miRNA, is important for binding of the miRNA to its target site in the mRNA (Lewis et al. 2005). Association of miRNA with its target results in mRNA cleavage (if sequence complementarity is high) or more usually in higher eukaryotes, blockade of translation (Zeng and Cullen 2004) (see below).

In an alternative pathway for miRNA biogenesis, short hairpin introns termed mirtrons are spliced and debranched to generate pre-miRNA hairpin mimics (Berezikov *et al.* 2007, Okamura *et al.* 2007, Ruby *et al.* 2007, Westholm *et al.* 2011, Sibley *et al.* 2012). These are then cleaved by Dicer in the cytoplasm and incorporated into typical miRNA silencing

complexes (Berezikov et al. 2007, Okamura et al. 2007, Ruby et al. 2007, Westholm and Lai 2011, Sibley et al. 2012). The presence of mirtrons may be an evolutionary strategy to diversify miRNA-based gene silencing (Lau *et al.* 2009).

1.3.1.3. Mechanisms of action of miRNAs

Mammalian miRNAs often have several isoforms encoded from one or more chromosome, suggesting that they are functionally redundant (Heimberg *et al.* 2008, Kim *et al.* 2009). They may exert variable roles *in vivo* via differences in their expression pattern and 3'-end binding (Ventura *et al.* 2008).

Regulation is mainly exerted by the binding of the miRNA to the 3'UTR of the target mRNA, but binding to other positions on the target mRNA, e.g. in 5'UTR or coding sequence has also been reported (Lytle *et al.* 2007, Lee *et al.* 2009, Li *et al.* 2009). Interestingly, miRNA binding sites within the coding region of a transcript are reported as less effective at mediating translational repression. Aside from the location of miRNA binding sites, factors including the sequence context of the miRNA binding site, the number of target sites within the mRNA, the focal RNA structure, the distance between target sites, all contribute to the efficacy of repression mediated by miRNAs (Brennecke *et al.* 2005, Sætrom *et al.* 2007).

The degree of base pairing between the miRNA and its target in the mRISC complex determines the fate of the transcript. If there is perfect binding between the miRNA and target, the mRNA target is cleaved by Ago2 at the annealing site, with subsequent degradation of the mRNA. In contrast, in cases where the miRNA is only partially complementary to its corresponding 3'UTR, inhibition of target mRNA translation occurs via Ago1. Repression may be exerted either at the initiation step of mRNA translation in which Ago competes with eIF4E or at some stage subsequent to initiation (Kiriakidou *et al.* 2007) (Figure 1.6). This is because miRNA-mRISC complex can bind to actively translating mRNAs, reducing translational elongation and/ or enhancing termination, concomitant with a reduction in ribosome initiation and nascent peptide destablilization (Petersen *et al.* 2006).

Interestingly, besides generally promoting mRNA cleavage or translational repression, miRNA binding to 3'UTR can also induce translation of some target mRNAs. MicroRNAs have been identified which activate translation on cell cycle arrest by directing AGO-containing protein complexes to AU-rich elements in the 3'UTR (Vasudevan *et al.* 2007, Vasudevan *et al.* 2007)

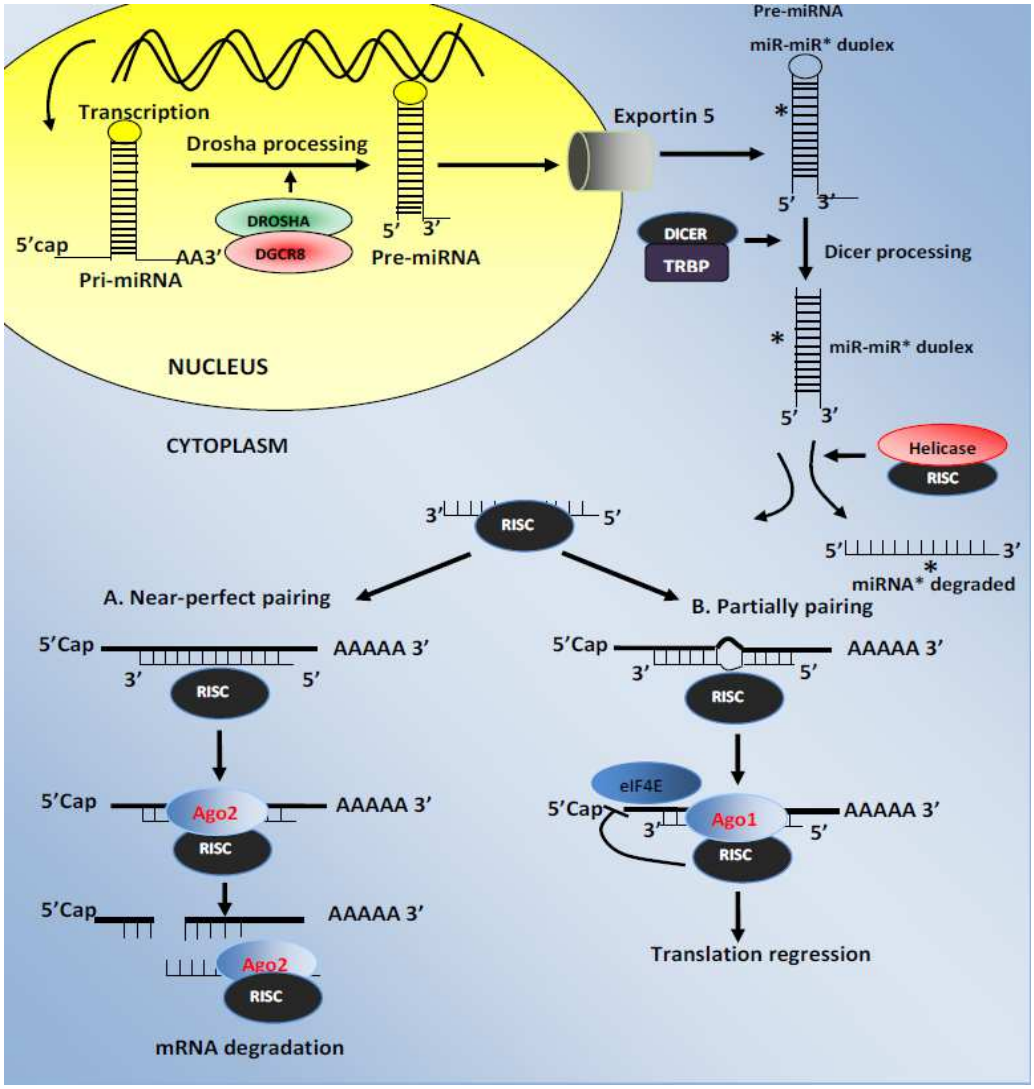

Figure 1.6: Biogenesis of miRNAs.

MicroRNAs are transcribed as RNA precursor molecules (pri-miRNA), which are processed by Drosha and its cofactor DGCR8 into short hairpin structure (pre-miRNA). These are exported into the cytoplasm by Exportin 5, where they are further processed by Dicer and TRBP (Dicer-TAR RNA binding protein) into a miRNA duplex. The duplex is unwound by a helicase and the "guide" strand is incorporated into the RNA–induced silencing complex (RISC) whilst the "passenger" strand undergoes degradation. This miRNA-RISC complex acts by two possible mechanisms: (A) Degradation of target mRNA occurs when miRNA is near-perfectly complementary with 3' untranslated region of target mRNA; (B) Translation inhibition occurs when miRNA is only partially complementary to its target mRNA.

1.3.2. MicroRNAs in skeletal development

It is evident that miRNAs are essential for skeletal development, however, our current knowledge of expression and function of specific miRNAs is still limited. Experimentally removing the majority of miRNAs by a block in miRNA biogenesis through mutating or deleting Dicer, reveals that the miRNA pathway plays a prominent role in skeletal development. An excellent example is the conditional knockout of Dicer in limb mesenchyme at the early stages of embryonic development, which leads to the formation of a much smaller limb. Dicer-null growth plates display a pronounced lack of chondrocyte proliferation in conjunction with enhanced differentiation to postmiototic hypertrophic chondrocytes; this latter may be explained by Dicer having distinct functional effects at different stages of chondrocyte development (Harfe *et al.* 2005). Recently, Kobayashi et al. reported that mice null for Dicer in chondrocytes resulted in skeletal growth defects and premature death (Kobayashi *et al.* 2008), again pointing to essential role of miRNAs in skeletal development.

Further evidence of the important role of miRNAs in skeletogenesis is that some miRNAs were found to exhibit bone-specific and cartilage-specific expression in late development. Wienholds et al. first provided evidence for miR-140 specifically expressed in cartilage of the jaw, head, and fins in zebrafish cartilage during embryonic development (Wienholds *et al.* 2003). Later, Tuddenham et al found that miR-140 is specifically expressed in cartilage tissues during mouse embryonic development (Tuddenham *et al.* 2006). Importantly, Miyaki et al and then Nakamura et al reported that universal knockout of miR-140 lead to mild dwarfism, probably as a result of impaired chondrocyte proliferation (Miyaki *et al.* 2010, Nakamura *et al.* 2011). Recently, Swingler et al found that miR-455-3p was expressed in developing long bones during chick development, restricted to cartilage and perichondrium, and in mouse embryos, where expression was selective in long bones and joints (Swingler *et al.* 2011).

These studies emphasize the importance of the miRNA pathway in skeletal development and revealed that some miRNAs are expressed with precise tissue and developmental stage specificity. Intensive research will uncover a complete spectrum of skeletally associated miRNAs as well as elucidate their biological function.

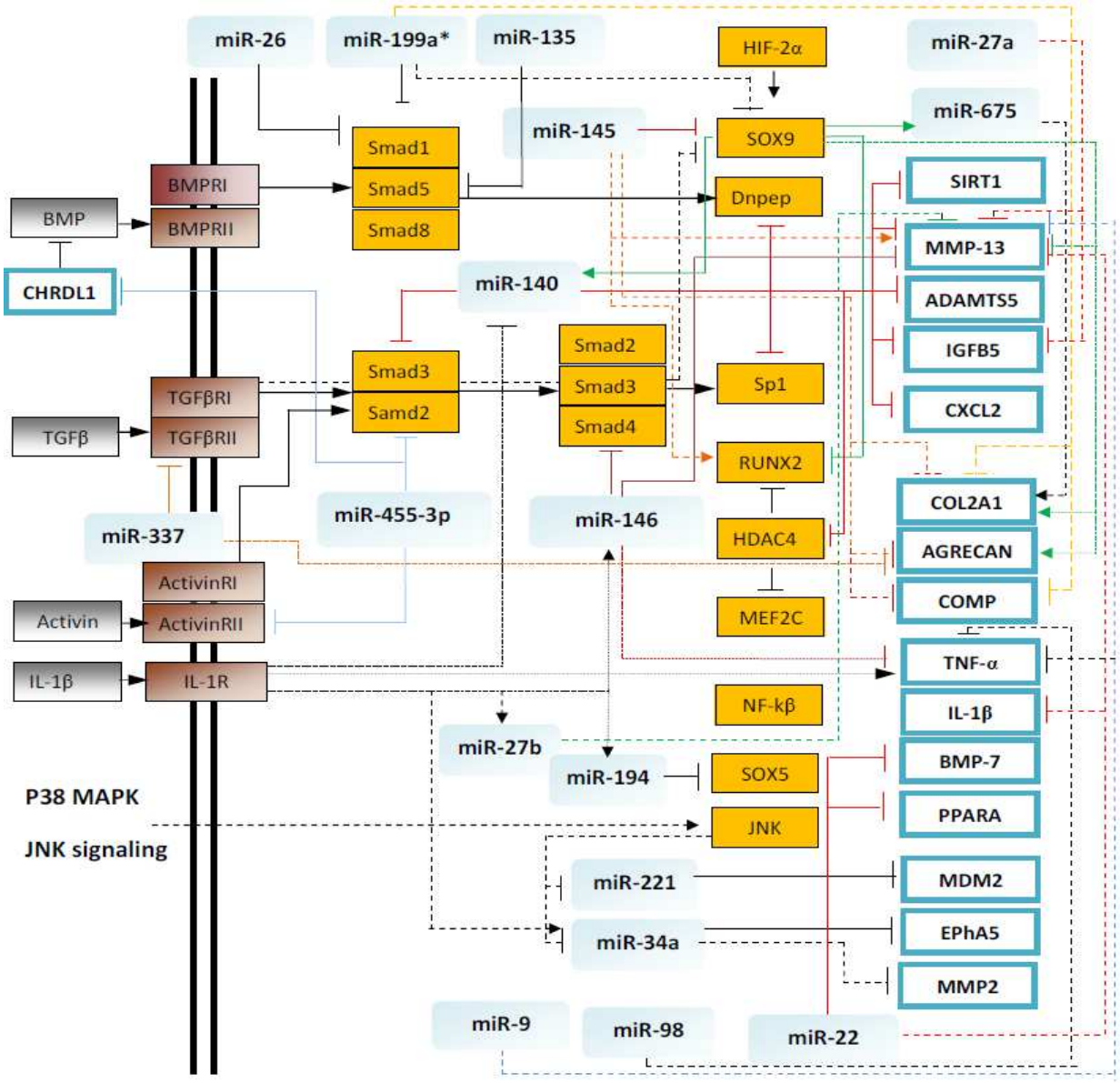

Figure 1.7: An overview of miRNAs involved in chondrogenesis, osteoarthritis and their direct and indirect targets

1.3.3. MicroRNAs in mechanotransduction

Articular cartilage has the unique capacity to resist significant mechanical loading during the lifetime of the organism (Guilak *et al.* 2001). The surface, middle and deep zones within articular cartilage are distinct domains, and they exhibit differential gene expression and attendant functional roles (Neu *et al.* 2007).

Mechano-responsive miRNAs are being identified in chondrocytes, the sole cell type of articular cartilage and evidence that specific miRNAs may impact on stress-related articular cartilage mechanotransduction has also been reported. MicroRNA-365 was the first identified mechanically responsive miRNA in chondrocytes, regulating chondrocyte differentiation through inhibiting HDAC4 (Guan *et al.* 2011). MicroRNA-221, miR-222 were postulated as potential regulators of the articular cartilage mechanotransduction pathway, since their expression patterns in bovine articular cartilage are higher in the weight-bearing anterior medial condyle as compared with the posterior non-weight-bearing medial condyle (Dunn *et al.* 2009). Recently, Li et al. reported that miR-146a was induced by joint instability resulting from medial collateral ligament transection and medial meniscal tear in the knee joints of an OA mouse model, suggesting that miR-146a might be a regulatory factor of the mechanical transduction process in articular cartilage (Li *et al.* 2012). All of these studies are useful for enriching the data on the regulatory mechanism for miRNAs in chondrocyte homeostasis.

1.3.4. MicroRNAs in chondrogenesis

Differential disruption of the Dicer gene in mice resulting in highly abnormal cartilage development suggests miRNAs play a significant role in chondrogenic differentiation. Furthermore, many studies profiled the expression of miRNAs to investigate their function in differentiating MSCs and showed that once they differentiate into chondrocytes, miRNA expression significantly altered (Sorrentino *et al.* 2008, Suomi et al. 2008, Lin *et al.* 2009, Miyaki *et al.* 2009, Karlsen *et al.* 2011, Lin *et al.* 2011, Yan *et al.* 2011, Yang *et al.* 2011) (Table1.2). However, there is no consensus expression signature of any miRNAs amongst these and we attribute this to the design of experiment including inducers of differentiation, cell types, numbers of detected miRNA probes and organism (Table1.2).

Table 1.2: Studies performing miRNA profile comparing between MSC and chondrocytes

	Sorrentino et al 2007	**Suomi et al 2008**	**Lin et al 2009**	**Miyaki et al 2009**	**Yang et al, 2010**	**Lin et al 2011**	**Yang et al 2011**	**Karlsen et al 2011**
Stimulators	-	TGF-β3	BMP-2	BMP-2 TGF-β3	TGF-β3	-	-	-
Cells	BM MSC	BM MSC	C12C2	BM MSC	BM MSC	DAC	BM MSC AC	DAC
Organisms	Human	Mice	-	Human	Mice	Human	Mice	Human
Probes	226	35	-	-	7,815	-	-	875
Cutoff(fold)	1.3	-	1.5	1.5	5	4	-	-
Platform	microarray	qPCR	microarray	microarray	microarray	microarray	microarray	microarray
miRNAs up-regulated	31 32 136 146 149 185 Pre-mir 192 199a-2-5 204 212 Pre-mir-212 Pre-miR-214	24 101 124a 199b 199a	199* 221 298 374 let-7e	15b 16 23b 27b 140 148 197 222 328 505	30a 81a-1 99a 125* 127 140 140* Let-7f	26a 140* 140 222 320a 320d 491* 547-5p 720 1308 let-7d let-7f let-7a	21 22 27b 27a 140 140* 152 291b* 330 431 433 455 let-7b let-7d let-7l	30d 140* 210 451 563
miRNAs down -regulated	10a 10b 21 23a 24-1-3p 24-2 26b 29b 30a-5p 34 100 103-2 107 130a 138-1 Pre-miR-143 145 181a-1 191-5p let-7a-1 let-7a-2 let-7a-3 let-7c let-7d	18 96	21 125a 125b 143 145 210		125b* 132 143 145 212	18a 27a 146a 193b 220b 342-5p 335 365 519e 548e 1248 1284	1 23a 23b 24 26b 99a 99b 99b* 125a-5p 143 144 145 146a 181a 181d 191 199a 199a* 210 320 355-5p 431 503 652 Let-7a Let-7c Let-7g Let-7f	15b 31 132 138 143 145 221 222 379 382 432 494 654* 1308 let-7e

AC: Articular chondrocytes; BM MSC: Bone marrow mesenchymal cells; DAC: dedifferentiated articular chondrocytes.

The regulation of chondrogenesis of murine MSCs in response to stimulation of TGF-β3 was investigated (Suomi et al. 2008, Yang et al. 2011) (Table1.2). Suomi et al compared the expression of 35 miRNAs in chondroblasts derived from MSCs, and found that miR-199a, miR-124a were strongly up-regulated while miR-96 was substantially suppressed (Suomi et al. 2008). They demonstrated how miRNAs and transcription factors could be capable of fine-tuning cellular differentiation by showing that miR-199a, miR-124a, miR-96 could target HIF-α, RFX1, Sox5, respectively (Suomi et al. 2008). Similarly, Yang et al , revealed eight significantly up-regulated and five down-regulated miRNAs (Yang et al. 2011) in this process. The miRNA clusters, miR-143/145 and miR-132/212 were down-regulated, with miR-132 the most down-regulated whilst miR-140* was the most up-regulated (Yang et al. 2011). Similar expression patterns of miR-145, miR-143 were also described in other studies (Lin et al. 2009, Karlsen et al. 2011, Lin et al. 2011, Yan et al. 2011). Corresponding targets of these differentially expressed miRNAs were predicted including: ADAMTS5 (miR-140*), ACVR1B (miR143/145), SMAD family members: SMAD1 (miR-30a), SMAD2 (miR-132/212), SMAD3 and SMAD5 (miR-145), Sox family members: Sox9 (miR-145); Sox6 (miR-143, miR-132/212), Runx2 (miR-30a and miR-140*) (Yang et al. 2011).

Further study has confirmed miR-145 as a key mediator which antagonizes early chondrogenic differentiation in mice via attenuating Sox9 at post-transcriptional level. (Yang *et al.* 2011). Interestingly, cells over-expressing miR-145 significantly decreased the expression of chondrogenic markers at the mRNA level including Col2a1, Agc1, COMP, Col9a2 and Col11a1. Consistent with this,, Martinez-Sanchez et al. reported miR-145 as a direct regulator of Sox9 in normal human articular chondrocytes though binding to a specific site in its 3'UTR, which is not conserved in mice (Martinez-Sanchez *et al.* 2012). Similarly, over-expression of miR-145 in articular cartilage chondrocytes reduced the levels of Sox9, the cartilage matrix components Col2a1 and Agc1 in combination with a significant increase of the hypertrophic markers Runx2 and MMP-13 (Martinez-Sanchez et al. 2012) (Figure 1.7).

This group also reported that miR-675, processed from H19, a non-coding RNA, was tightly regulated by Sox9 during chondrocyte differentiation. MicroRNA-675 could up-regulate expression of Col2a1, albeit indirectly, indicating its potential importance in

maintaining cartilage integrity and homeostasis. Forced over-expression of miR-675 rescued Col2a1 mRNA levels in either Sox9- or H19-depleted primary human articular chondrocytes (Dudek *et al.* 2010). Although its target mRNAs remain unknown, these data suggest that miR-675 may modulate cartilage homeostasis by suppressing a Col2a1 transcriptional repressor (Dudek et al. 2010) (Figure 1.7). Moreover, by performing miRNA expression profile during human primary chondrocyte dedifferentiation, Martinez-Sanchez found that 29 miRNAs were up-regulated more than two-fold and 18 miRNAs were down-regulated. Among these up-regulated miRNAs, miR-1247, transcribed from the DLK1-DIO3 locus, was of particular interest as its expression pattern still increased under hypoxia condition, together with miR-140. Also, miR-1247 level was found to correlate with cartilage-associated miR-675 across a range of 15 different mouse tissues (Martinez-Sanchez *et al.* 2013). Interestingly, SOX9, directly target of miR-1247 via coding sequence, inhibit this miRNA expression, suggesting a negative feedback loop between miR-1247 and its target SOX9 (Martinez-Sanchez and Murphy 2013).

Another study performed miRNA profiling to find expression signatures of nearly 380 miRNAs in C2C12 cells induced by BMP-2 for 24 hours and found that 5 miRNAs including miR-199a* and miR-221 were positively regulated while miR-125a, miR-210, miR-125b, miR-21, miR-145, miR-143 were repressed (Lin et al. 2009). Interestingly, using C3H10T1/2 cells, a well-established *in vitro* cell model of chondrogenesis, showed that miR-199a* expression was reduced significantly within several hours following BMP-2 treatment and then rose dramatically at 24 hours and remained higher thereafter, indicating that miR-199a* may function as a suppressor of the early steps of chondrogenic differentiation (Lin et al. 2009). Indeed, enforced miR-199a* expression in C3H10T1/2 cells or in the prechondrogenic cell line ATDC5, suppresses multiple markers of early chondrogenesis, including Col2a1 and COMP, whereas the antagomir blocking miR-199a* function has the opposite stimulatory effect (Lin et al. 2009). Consistent with these observations, Smad1, a positive downstream mediator of BMP-2 signalling, was shown to be a direct miR-199a* target. Moreover, miR-199a*, through its inhibition of the Smad pathway, is able to inhibit the expression of downstream genes such as p204 (Lin et al. 2009) (Figure 1.7).

The change in expression pattern of miRNAs across the dedifferentiation of chondrocytes also, adds to our understanding of the biology of *in vitro* human chondrogenesis (Karlsen

et al. 2011, Lin et al. 2011). MicroRNA-451, miR-140-3p, miR-210, miR-30d, and miR-563 were reported to be highly expressed on human primary articular chondrocytes at early passage compared with their dedifferentiated counterparts, suggesting their role as inhibitors of differentiation *in vitro* (Lin et al. 2011). Of these miRNAs, miR-140-3p had the highest expression. Conversely, 16 miRNAs were significantly up-regulated in dedifferentiated articular chondrocytes, reflecting their potential as modulators of the chondrogenenic process. Notably, miR-143, miR-145 also had similar expression patterns as previously reported (Lin et al. 2011). A second study also reported a group of 5 miRNAs: miR-451, miR140-3p, miR-210, miR-30d, and miR-563 upregulated on differentiation which may inhibit molecules participating in the dedifferentiation process whilst a further 16 miRNAs were downregulated and may potentially act conversely.

Recently, performing miRNA profiling across ATDC5 cell induced differentiation within 42 days to identify miRNAs with functions in cartilage development, we identified 7 cluster groups of miRNAs which may function cooperatively (Swingler et al. 2011). Among these, 39 miRNAs were found potentially co-regulated with miR-140 with expression increase during chondrogenic process (Swingler et al. 2011). Especially interesting is miR-455, located in an intron of the protein coding gene Col27a1, a cartilage-expressed collagen, which showed similar expression kinetics to collagen XXVII and to miR-140. Consistent with role for miR-140 in modulating TGFβ signalling, miR-455-3p was also found to directly target Smad2, ACVR2B and CHRDL1, again potentially attenuating the TGFβ pathway (Swingler et al. 2011) (Figure 1.7).

MicroRNA-140 shows a generally consistent expression pattern between studies. Indeed, cartilage miRNA research to date has focused heavily on miR-140 and has successfully shown the key roles of miR-140 in chondrocyte proliferation and differentiation. Miyaki et al compared gene expression profiling using miRNA microarrays and quantitative polymerase chain reaction in human articular chondrocytes and human mesenchymal stem cells. They demonstrated that miR-140 had the largest difference in expression between chondrocytes and MSCs (Miyaki et al. 2009), and this is in agreement with latter publications in human, rat and mice (Karlsen et al. 2011, Lin et al. 2011, Yan et al. 2011, Yang et al. 2011). MicroRNA-140 was first shown to target Hdac4, a known co-repressor of Runx2 and MEF2C transcription factors essential for chondrocyte hypertrophy and bone

development (Tuddenham et al. 2006). miR-140 also targets Cxcl12 (Nicolas *et al.* 2008) and Smad3 (Pais *et al.* 2010), both of which are implicated in chondrocyte differentiation. Interestingly, miR-140 is reported to suppress Dnpep, an aspartyl aminopeptidase, which has been suggested to antagonize BMP signalling downstream of Smad activation (Nakamura et al. 2011). Moreover, Sox9 a major transcription factor in maintaining cellular phenotype and preventing hypertrophy, particularly with L-Sox5 and Sox6, (Yamashita *et al.* 2012), is shown to control the expression of miR-140 (Yang *et al.* 2011, Nakamura *et al.* 2012).

The miR-194 is a key mediator during chondrogenic differentiation via suppression of the transcription factor Sox5 (Xu *et al.* 2012). The expression of miR-194 was significantly decreased in chondrogenic differentiation of adipose-derived stem cells (ASCs). Importantly, chondrogenic differentiation of ASCs could be achieved through controlling miR-194 expression (Xu et al. 2012) (Figure 1.7).

Using three rat models e.g. bone matrix gelatin-induced endochondral ossification, collagen-induced arthritis and pristane-induced arthritis, Zhong et al. further demonstrated that miR-337 was directly implicated with chondrogenesis. miR-337 acted as a repressor for TGFBR2 expression at the protein level (Zhong *et al.* 2012). Moreover, aggrecan was differentially expressed in both gain- or loss-of function of miR-337 experiments, providing evidence that miR-337 could influence cartilage specific gene expression in chondrocytes (Zhong et al. 2012) (Figure 1.7).

Kim et al. used chick as a model of chondrogenesis and focused on initiation, namely precartilage condensation, proliferation and migration. They reported that miR-221 and miR-34a, induced by c-Jun N-terminal kinase (JNK) signaling, played pivotal roles (Kim *et al.* 2010, Kim *et al.* 2011). Treatment of chick wing bud MSCs with a JNK inhibitor lead to the suppression of cell migration and stimulation of apoptosis with concurrent significant increase in expression of miR-221 and miR-34a (Kim et al. 2010, Kim et al. 2011). Notably, miR-221 may be involved in apoptosis, since treatment of MSCs with a miR-221 inhibitor increased cell proliferation and this could be rescued by the JNK inhibitor (Kim et al. 2010). MicroRNA-221 is reported to directly target Mdm2, which encodes for an oncoprotein with E3 ubiquitin ligase activity (Kim et al. 2010). Inhibition of Mdm2 expression via miR-221 suppresses ubiquitination leading to accumulation of

Slug protein, whose expression is associated with an increase in apoptosis (Kim et al. 2010). Conversely, miR-34a affects MSC migration, not proliferation (Kim et al. 2011). EphA5, a receptor in Eph/Ephrin signaling which mediates cell-to-cell interaction, has been proven to be a miR-34a target (Kim et al. 2011). Moreover, via regulating RhoA/Rac1 cross-talk, miR-34a negatively modulated reorganization of the actin cytoskeleton (Kim *et al.* 2012), one of the essential processes for establishing chondrocyte-specific morphology. MicroRNA-488 expression is up-regulated at the pre-condensation stage and then down-regulated at the post-condensation stage in chick limb chondrogenesis, suggested a key role in this process (Song *et al.* 2011). Interestingly, mir-488 could regulate cell–to-ECM interaction via modulation of focal adhesion activity by indirectly targeting MMP-2 (Song et al. 2011). More recently, this group reported that miR-142-3p was an important modulator in position-dependent chondrogenesis and was reported to regulate ADAM9 (Kim *et al.* 2011) (Figure 1.7).

1.3.5. MicroRNAs in osteoarthritis

The effects of miRNA deregulation on OA are evident through studies comparing the expression of miRNAs between OA tissues and their normal articular counterparts (Iliopoulos *et al.* 2008, Jones *et al.* 2009). Illopoulos et al. tested the expression of 365 miRNAs and identified a signature of 16 miRNAs, with 9 miRNAs significantly upregulated and 7 miRNAs downregulated in OA cartilage compared with normal controls. Some of these were postulated to be involved in obesity and inflammation (Iliopoulos et al. 2008). Interestingly, functional experiments implicated miR-9 in the regulation of MMP13 expression, as well as miR-9, miR-98 and miR-146 in the control of TNF-α expression, suggesting that these miRNAs may play a protective role in OA. Moreover, miR-22, whose expression correlated with body mass index, directly targets PPARA and BMP-7 at the mRNA and protein levels, respectively. Enforced miR-22 overexpression or siRNA-mediated suppression of either PPARA or BMP-7 resulted in increases in IL-1β and MMP-13 protein levels, again suggesting that miRNA deregulation can have effects on OA (Iliopoulos et al. 2008) (Figure 1.7).

Additionally, Jones et al. investigated the expression of 157 human miRNAs and identified 17 miRNAs whose expression varied by 4-fold or more when comparing normal versus

late-stage OA cartilage (Jones et al. 2009). Consistent with the Illopoulos data, the altered expression of miR-9, miR-98 and miR-146 in OA cartilage are highlighted. The over-expression of these miRNAs also reduced IL-1β-induced TNF-α production, whilst inhibition or over-expression of miR-9 modulated MMP-13 secretion (Jones et al. 2009) (Figure 1.7).

The miR-140 gene, located in an intron of the E3 ubiquitin protein ligase gene Wwp2 on murine chromosome 8 and the small arm of chromosome 16 in humans, is evolutionarily conserved among vertebrates. MicroRNA-140 expression in the cartilage of patients with OA was significantly lower than in normal cartilage (Miyaki et al. 2009, Tardif *et al.* 2009) and decreased miR-140 expression was reported also in OA chondrocytes (Tardif et al. 2009).

Deletion of miR-140 in mice predisposes to the development of age-related OA-like changes (Miyaki et al. 2010, Nakamura et al. 2011) and gives a significant increase in cartilage destruction in surgically induced OA. Conversely, in an antigen-induced arthritis model, transgenic over-expression of miR-140 in chondrocytes protects against cartilage damage (Miyaki *et al.* 2010). The ADAMTS5 gene has been shown to be a direct target of miR-140, whilst reciprocal regulation of ADAMTS5 in the in vivo models above suggests that suppression of OA may involve regulation of ADAMTS5 (Miyaki et al. 2010). Swingler et al. show that miR-140 is increased in expression in hip OA cartilage compared to fracture controls (Swingler et al. 2011), but ADAMTS5 expression is decreased in the former samples. As above, Nakamura et al. identified the aspartyl aminopeptidase Dnpep as a key target for miR-140 essential for skeletal defects in miR-140 null mice (Nakamura *et al.* 2011). Using functional interference, Tardif et al. confirmed IGFBP-5, whose expression in human chondrocytes was significantly higher in OA, as a direct target of miR-140 (Tardif et al. 2009). More recently, miR-140 was shown to directly mediate MMP13 expression *in vitro* by luciferase reporter assay (Liang *et al.* 2012) (Figure 1.7).

The human genome contains two miR-27 genes [mir-27a and miR-27b] on chromosomes 19 and 9, respectively, and their major products differ by only 1 nucleotide in the 3' region. MicroRNA-27a expression was shown to be decreased in OA compared to normal chondrocytes (Tardif et al. 2009). Down-regulation of miR-27a was proposed to be connected with adipose tissue dysregulation in obesity, a strong risk factor for OA. Tardif

et al. suggested that miR-27a may indirectly regulate the levels of both MMP-13 and IGFBP-5 by targeting upstream positive effectors of both genes (Tardif et al. 2009). Conversely, expression miR-27b was found to be significantly lower in OA cartilage samples compared with normal counterparts where it inversely correlated with MMP13, a direct target (Akhtar *et al.* 2010). This points to the possibility of novel avenues for OA therapeutic strategies (Figure 1.7).

MicroRNA-146a was strongly expressed in chondrocytes residing in the superficial layer of cartilage and in low-grade OA cartilage (Yamasaki *et al.* 2009, Li et al. 2012). Its expression level gradually decreased with progressive tissue degeneration. Interestingly, when miR-146 was highly expressed, the expression of MMP13 is low, suggesting that miR-146a has target genes that play a role in OA cartilage pathogenesis (Yamasaki et al. 2009). MicroRNA-146a has recently been implicated in the control of knee joint homeostasis and OA-associated algesia by balancing the inflammatory response in cartilage and synovium with pain-related factors in glial cells (Li *et al.* 2011). As such, it may be useful for the treatment of both cartilage regeneration and the pain symptoms caused by OA (Figure 1.7).

Park et al reported the miR-127-5p, an important mediator in OA whose expression was significant decreased in OA articular cartilage compared to the control counterpart, directly target MMP13. Noteworthy, pre-treatment with MAPK inhibitors and NFκβ inhibitor attenuated the inhibitory effects of IL-1 on miR-127-5p expression while overexpression of miR-127-5p significantly inhibited the phosphorylation of JNK, p38 and Iκβα in the human chondrocytes. These data suggest a reciprocal regulatory loop between NFκβ, MAP kinase, and IL-1β in controlling MMP13 expression (Park *et al.* 2013).

1.3.6. MicroRNAs in inflammation

Some miRNAs could be of importance in the inflammatory events of osteoarthritis. MicroRNA-140 was suppressed by IL-1β signaling, and transfection of human chondrocytes with miR-140 downregulated IL-1β driven induction of ADAMTS5 (Miyaki et al. 2009). However, contrary to this, Liang et al. reported that expression of miR-140

and MMP-13 was elevated in IL-1β-stimulated C28/I2 and expression of miR-140 was shown to be NF-κB-dependent (Liang *et al.* 2012) (Figure 1.7).

Expression of miR-34a was significantly induced by IL-1β while antagonism of miR-34a prevented IL-1β-induced chondrocyte apoptosis (Abouheif *et al.* 2010), as well as IL-1β-induced down regulation of type II collagen in rat chondrocytes (Abouheif et al. 2010). Other relevant miRNAs reported to be induced by IL-1β are miR-146a (Yamasaki et al. 2009, Li et al. 2012), miR-34a (Abouheif et al. 2010), miR-194 (Xu et al. 2012), miR-27b (Akhtar et al. 2010) (Figure 1.7).

1.3.7. Utility of microRNAs for diagnosis

It is evident that miRNAs in serum may become a powerful tool in the development of diagnostic biomarkers. MicroRNAs are relatively stable with enzymatic, freezing, thawing or extreme pH conditions (Mitchell *et al.* 2008, Link *et al.* 2010) due to lipid or lipoprotein complexes (Esau *et al.* 2006). Moreover, extracellular miRNAs are detectable in almost all body fluids and excretions including urine, faeces, saliva, tears, ascetic, pleural and amniotic fluid (Chen *et al.* 2008, Gilad *et al.* 2008). Interestingly, miRNAs in plasma have the capacity to interact with intact cells with some degree of specificity, and modify recipient cell gene expression and protein production via a miRNA-related mechanism (Arroyo *et al.* 2011). This opens up the possibility of genetic exchange between cells and the exogenous regulation of gene expression. MicroRNA-21 was the first serum miRNA biomarker to be discovered: patients with diffuse large B cell lymphoma had high serum levels of miR-21, which was associated with increased relapse-free survival (Lawrie *et al.* 2008). Subsequently, the usefulness of serum miRNAs for diagnosis and prognosis has been reported for solid cancers and leukemia (Ferracin *et al.* 2010, Kosaka *et al.* 2010, Wittmann *et al.* 2010). For OA, Murata et al. examined the potential of miRNA as diagnostic biomarkers and found a number of miRNA in plasma some of which were found at different levels between RA and OA patients (Murata *et al.* 2010). Recently, let-7e, miR-454, miR-886 were identified differentially expressed crilculating miRNAs in OA patient necessitating arthroplasty in a large, population – based cohort. Especially, let – 7e emerged as potential predictor for severe knee or hip OA (Beyer *et al.* 2014).

Besides the measurement of miRNAs in plasma, PBMCs could also be useful in developing a biomarker for OA. Circulating PBMCs such as macrophages and T cells accumulate in the synovium of OA patients, producing proinflammatory cytokines and proteinases associated with synovitis, linked to the early stages of OA progression. It has been demonstrated that the high expression of miR-146a, miR-155, miR-181a and miR-223 in PBMCs from OA patients versus normal controls may be related to the pathogenesis of OA (Okuhara *et al.* 2011). Interestingly, miR-146 and miR-223 are highly expressed in early-stage OA (Yamasaki et al. 2009), with expression gradually decreasing with OA progression with the promise for diagnosis of early OA is specificity can be demonstrated.

Taken together, there is growing evidence for future miRNA-based diagnostics. However, there is a requirement for detailed investigations directed at diagnostic performance (sensitivity, specificity, accuracy) of these promising novel biomarkers before the measurement of miRNAs can enter the clinic.

1.3.8. Utility of microRNAs in therapeutic treatment

Currently there is no disease-modifying therapeutics available for patients suffering from OA. Therapeutic options are limited to oral and intra-articularly injected analgesic medications, and joint replacement surgery (Wieland *et al.* 2005). OA patients often present with cartilage that already exhibits a damaged matrix, and in which repair/regeneration is. Although cartilage seems a relatively simple tissue type to engineer because of its single cell type and its lack of a blood, nerve or lymph system, regenerating cartilage in a form that can function effectively after implantation has proven difficult. Several approaches are currently being investigated to utilize a miRNA-based therapy to overcome these problems, and these may represent a novel therapeutic application for pharmacological control. Currently there are over 70 clinical trials worldwide based on miRNA manipulation to treat a range of conditions including various cancers and cardiovascular disease; however, none of these to date are for arthritis.

The targeting of miRNAs represents a novel therapeutic opportunity for OA treatment in which miRNA deficiencies could be corrected by either antagonizing (antagomirs) or

restoring (mimics) miRNA function. Poorly expressed miRNAs could be restored by over expression using stable vector transfection or transfection by double-stranded miRNA, whilst over-expressed miRNAs could be antagonized by modified DNA oligonucleotides. Particularly, it has been proven that the systematic administration of antagonist miRNAs modified with locked nucleic acids (LNA) could function without toxicity in non-human primates (Elmen *et al.* 2008). Evidence on efficacy was also demonstrated in mouse models using miR-122 antisense oligonucleotides, which resulted in a decrease in hepatic fatty acid and cholesterol synthesis (Esau et al. 2006). In man, when miR-143/miR-145 activity was restored in pancreatic cancer cells (in which their levels were repressed), the cell was no longer tumourigenic (Kent *et al.* 2010). Although this type of therapy has not been applied in OA, there is very promising evidence for therapeutic potential, e.g. the silencing of miR-34a by LNA-modified antisense oligonucleotides could effectively reduce rat chondrocyte apoptosis induced by IL-1β (Kongcharoensombat *et al.* 2010). This study revealed that silencing of miR-34a might be a novel intervention for OA treatment if this could be appropriately targeted.

Another approach is to combine miRNA technology with stem cell engineering. *In vivo* MSCs participate in chondrogenesis. MSCs can be conveniently obtained with less injury than primary cells and manipulated *in vitro* and hence they are promising cells in cartilage regeneration. At present, autologous MSCs have been transplanted in human injured or osteoarthritis knees for repair of articular cartilage defects. However, unexpected results from the ectopic transplantation of MSCs also have been reported, such as hypertrophy, mineralization, and vascularisation. Deciphering the role of miRNA regulation in the chondrogenesis of MSCs may open a new era of research and pave the way for the development of new treatments for OA

A growing body of evidence indicates that miRNAs convey a novel and efficient way for the regulation of gene expression, being involved in multiple aspects of cellular processes. Understanding their expression profile and dynamic regulation may be the key to enhancing chondrogenic differentiation, or maintaining phenotype in the treatment of OA. Recent advances in miRNA research have provided new perspectives on the regulation of OA and novel insight into the potential development of therapeutic treatments. Using miRNAs as therapeutic targets may well become a powerful tool in the development of

new therapeutic approaches. However, numerous questions including potential off-target effects and efficient and targeted delivery *in vivo* need to be solved before using miRNAs in therapeutics

SCOPE OF THE THESIS

OA is the most prevalent degenerative joint pathology leading to considerable problems with disability and pain in a huge number of people, especially the elderly population. As the population ages and with increased life expectancy, the burden of osteoarthritis will continue to rise. However, there is currently a lack of biomarkers and sensitive techniques for identifying and assessing patients with early changes. Also, clinical treatment for OA still remains unsatisfactory. Thus, deepening our understanding and gain further insights into the molecular mechanisms in OA would be very important for long term purpose of diagnosis and therapeutic treatment.

Several hundred miRNAs have been identified so far and initial studies have linked specific miRNAs to OA. However, there are no key miRNAs identified so far which functionally impact on early human OA onset and disease progression. Thus, I undertook this project to identify miRNAs mediating initiation and progression of OA and dissect their biological function in order to identify new signalling pathways involved in the pathogenesis of OA. The hypothesis and specific aims of the project were:

Hypothesis: The dysregulated expression of specific microRNAs contributes to the onset or progression of OA.

Specific aim 1: Profile miRNA and mRNA expressions in whole knee joint in DMM model to identify the potential miRNAs involved in the early stage of OA

Specific aim 2: Determine the involvement of the miRNA in human end stage OA cartilage, in murine injury model, in chondrogenesis.

Specific aim 3: Identify factors control the miRNA expression in articular cartilage

Specific aim 4: Identify miRNA direct targets to identify new signaling pathways involved in homeostasis of articular cartilage.

CHAPTER 2
MATERIALS AND METHODS

2.1.Materials

2.1.1. Murine models

2.1.1.1. Destabilization of the medial meniscus murine model (DMM model)

Induction of OA by destabilization of the medial meniscus (DMM) was kindly performed by Professor Tonia Vincent Kennedy Institute for Rheumatology, Oxford University, U.K. Protocols using C57Bl/6 mice were as described previously in (Burleigh *et al.* 2012, Chong *et al.* 2013).

Briefly, C57Bl/6 male mice were housed 3-5 per cage in 63x54x30 cm^3 standard individually vented cages and maintained with a 12h/12h light/dark cycle at an ambient temperature of 21ºC. Mice were fed a certified mouse diet (RM3 from Special Dietary Systems, Essex, UK) and water ad libitum. 10 week old mice were anaesthetized by intra-peritoneal injection of a 1:1:2 mixture of Hypnorm (0.315mg/ml fentanyl citrate and 10mg/ml fluanisone; VetaPharma Ltd, Leeds, UK), Hypnovol (5mg/ml midazolam; Roche), and sterile water for injection, at a dose of 10ml/kg body weight. The ventral portion of the right knee was shaved and swabbed with iodine to prepare a sterile surgical field. The medial meniscus was identified and the attachment of its anterior horn to the tibial plateau was cut. Care was taken to avoid injury to the anterior cruciate ligament and the cartilage surfaces. The mice were fully mobile within 2-4 hours after surgery. After 1, 3, 7 days after surgery, the mice were culled and knees harvested.

2.1.1.2. Murine hip avulsion injury model

The femoral caps of C57Bl/6 mice ages 4 weeks were avulsed using forceps as described in (Chong et al. 2013). After washing three times with sterile phosphate-buffered saline (PBS) (Life Technologies, 10010023), the femoral caps were immediately put in either 500µl Trizol® reagent (Invitrogen, 15569-026) (for time point 0) or in 24-well plate for (other time points e.g. 3, 6, 12, 48 hours). 200µl of Dulbecco's modified Eagle's medium (DMEM) (Life Technologies, 10566-016) containing 100 IU/ml penicillin and 100µg/ml

streptomycin (Sigma, P4333) was added to each well and the plate was incubated at 37ºC in 5% (v/v) CO_2. At the desired time points, the femoral caps were harvested (with Trizol reagent) and total RNA was isolated.

2.1.2. Human end stage OA specimens and normal counterparts

Ethical Committee approval for using discarded human tissue was received prior to the initiation of the studies. Full informed consent was obtained from all donors. Human articular cartilage was obtained from patients undergoing total hip/ knee replacement surgery at the Norfolk and Norwich University Hospital. In total, 8 hip and 7 knee OA cartilage samples were collected. 7 healthy articular cartilages were harvested from total hip replacement following fracture to the neck of femur. None of the healthy individuals had a clinical history of arthritis or other diseases affecting cartilage, no macroscopic lesions to the cartilage were seen.

2.1.3. Cell lines

All cell lines were maintained in DMEM high glucose, GlutaMAX supplement (Life Technologies, 10566-016) containing 10% (v/v) heat-inactivated fetal bovine serum (FCS) (PAA, UK), 100U/ml penicillin, and 100µg/ml streptomycin (Sigma, P4333) at 37ºC in 5% (v/v) CO_2.

2.1.3.1. Chondrosarcoma SW1353

The SW1353 cell line was initiated from a primary grade II chondrosarcoma of the right humerus obtained from a 72 year old female Caucasian. SW1353 cells were purchased from the American Type Culture Collection (ATCC) (no.HTB-94).

2.1.3.2. Chicken dermal fibroblasts DF1

DF-1 is a spontaneously immortalized chicken fibroblast cell line without viral or chemical treatment derived from 10 day old East Lansing Line (ELL-0) embryo. DF1 was a kind gift from Professor Andrea Munsterberg, University of East Anglia, U.K.

2.1.3.3. Dicer knockdown cell lines

DLD-1 Parental and DLD-1 Dicer null_cell lines were a kind gift from Professor Tamas Dalmay, University of East Anglia, U.K. These cell lines were originally purchased from Horizon Discovery (Cambridge, U.K.). Both cell lines were originally isolated from a colorectal adenocarcinoma.

2.2.Methods

2.2.1. Molecular biology- based methods

2.2.2.2. Human genomic DNA isolation

Buffer

Extraction Buffer: 10mM Tris-HCl pH 8 (Fisher Scientific, BP152-500), 5mM NaCl (Fisher Scientific, BP3581), 0.5% (w/v) SDS (Fisher Scientific, 10356463).

DNA extraction protocol

Human chondrosarcoma SW1353 cells were harvested from a 75cm^2 flask by trypsin-EDTA treatment (Life Technologies, 25200072) and pelleted by centrifugation at 17.3xg, 5 minutes.

The cell pellet was mixed well with 100µl nuclease-free water (Sigma, W4502), 400µl extraction buffer, 10µl Proteinase K (20mg/ml) (Sigma, P6556) and incubated at 50^{o}C, 2 hours.

500µl of PCI (phenol: chloroform: isoamyl alcohol 25:24:1) (Sigma, P2069) was added, mixed gently and centrifuged, 10 minutes at 130,000xg.

The top phase was transferred to a new tube, 1 ml of chloroform (Sigma, 288306) was added and after vortex, the mixture was again centrifuged at 130,000xg for 10 minutes.

The upper phase was transferred to a new tube and two volumes of 100% (v/v) ethanol (Sigma, 459844) were added, followed by centrifugation at 130,000xg for 5 minutes.

The DNA pellet was washed with 700µl of 70% (v/v) ethanol, and then centrifuged at 130,000xg for 1 minute. Discard the ethanol.

Finally, the pellet was dried at room temperature and dissolved in 100µl of nuclease-free water (Sigma, W4502).

2.2.2.3. PCR amplification for 3'UTR regions

3'UTR regions of all genes including *ADAMTS6, ADAMTS14, ADAMTS17, ADAMTS19, FZD3, FZD5, DVL3, FRAT2,* and *CK2A2* were downloaded from the Ensembl Genome Browser: http://www.ensembl.org/index.html. Primers were specifically designed to amplify a 1-2 kb region of 3'UTR of these genes including the miR-29 family binding sites. A restriction site of *Sac*I (5'GAGCTC3'), XbaI (5'TCTAGA3') or *Sal*I (5'GTCGAC3') are added to the 5' end of each primer. Primer sequences are listed in Appendix, Table 1.

All 3'UTR regions were amplified from human genomic DNA, isolated from the SW1353 cell line. 100ng genomic DNA was added together with 5µl 10X reaction buffer, 5 units accuTaq^{TM} LA DNA polymerase (Sigma, D8045), 0.5µl dNTP 10µM (Bioline, BIO-39044), 1µl forward primer 10µM (Sigma), 1µl reverse primer 10µM (Sigma) in a 50µl reaction volume. The reaction was run on a Veriti^{R} 96-well thermal cycler (Applied Biosystems, 4375786) at 98^{o}C, 30 seconds to denature DNA and follows by 32 cycles: 10 seconds at 98^{o}C, 20 seconds at annealing temperature (depending on each primer pair), 1-2 minutes at 68^{o}C. Finally, the reaction was left 2 minutes at 68^{o}C for final extension.

The PCR reaction was confirmed by loading 3µl PCR product on 1% (w/v) agarose gels, which were prepared by heating 1% (w/v) agarose (Sigma, A9639) in Tris-acetate-EDTA (TAE) buffer, and run at 120V. After staining in ethidium bromide solution (Sigma, E1510) for 20 minutes, the product was visualized under UV-light.

2.2.2.4. Phenol/chloroform clean up

Nuclease- free water (Sigma, W4502) was added to a PCR reaction to 200µl, followed by 200µl of phenol: chloroform: isoamyl alcohol (Sigma, P2069). The reaction was mixed well and centrifuged at 130,000xg for 10 minutes. The upper phase was collected to a fresh tube and a 2.5 volume of 100% (v/v) ethanol (Sigma, 459844) and 1/10 volume of 5M NaOAc (sodium acetate, Sigma, S2889) were added, followed by centrifugation at 130,000xg for 10 minutes. The DNA pellet was washed with 500µl of 70% (v/v) ethanol (Sigma, 459844), and centrifuged at 130,000xg for 10 minutes. Finally, the pellet was dried at room temperature for 5 minutes and dissolved in 27µl nuclease- free water (Sigma, W4502).

2.2.2.5. Plasmid isolation

A single colony from LB (Luria Bertani) agar plate supplemented with 100µg/ml ampicillin (Sigma, A0166) was inoculated into 5ml of LB broth medium also supplemented with 100µg/ml ampicillin incubated at 37°C, 180rpm overnight. The bacterial culture was pelleted by centrifugation at maximum speed for 5 minutes. Plasmids were isolated using the QIAprep Spin Miniprep Kit (Qiagen, 27104): The pellet was resuspended in 250µl of P1 buffer. 250µl of P2 buffer was added to the suspension which was then mixed thoroughly by vigorously inverting 4-6 times and incubated at room temperature for 5 minutes. After that, 50µl of P3 buffer was added and the mixture was inverted until a homogenous suspension containing a white flocculate was formed. The bacterial lysate was cleared by centrifugation at 130,000xg, 10 minutes and the supernatant was transferred to a spin column. The column was washed two times with 500µl of wash buffer. Finally, the plasmid was then eluted with 30µl nuclease free water (Sigma, W4502).

For preparation of large quantities of plasmid DNA, the QIAGEN Plasmid MIDI Kit was used (Qiagen, 12143): A single colony from LB ampicillin agar plate was inoculated into 100ml of LB medium supplemented with 100µg/ml ampicillin (Sigma, A0166), incubated at 37°C, 180rpm overnight and harvested by centrifugation at maximum speed for 10 minutes at 4°C. The bacterial pellet was resuspended in 4 ml of P1 buffer, followed by 4 ml of P2 buffer, and the suspension was thoroughly mixed by vigorously inverting the sealed tube 4-6 times and incubated at room temperature for 5 minutes. 4 ml of chilled P3 buffer was added, and the suspension was thoroughly mixed by vigorously inverting 4-6 times and incubated on ice for 15 min, followed by centrifugation at 130,000xg for 30 minutes at 4°C. The QIAGEN-tip was equilibrated by applying 3 ml of QBT buffer, and the column was allowed to empty by gravity flow. The supernatant (above) was applied to the QIAGEN-tip. The QIAGENtip was washed twice with 10ml of wash buffer. The DNA was eluted with 5 ml of elution buffer and precipitated by adding 5 ml of room temperature 100% (v/v) isopropanol (Sigma, 190764) to the eluted DNA, followed by centrifugation immediately at 130,000xg for 10 minutes at 4 °C. The supernatant was carefully decanted. The DNA pellet was washed with 2 ml of room temperature 70% (v/v) ethanol (Sigma, 459844), followed by centrifugation at 130,000xg for 5 minutes. The supernatant was carefully decanted without disturbing the pellet. The pellet was dried for

5-10 min. Finally, the plasmid pellet was dissolved in 500µl of nuclease free water and the plasmid concentration was determined using a Nanodrop spectrophotometer.

2.2.2.6. Digestion

2µg of plasmid pmiR-Glo or all PCR products after phenol/chloroform clean up was incubated with 1µl either *Sal*I (10 units/ µl) (Promega, R6061), *Sac*I (10 units/ µl) (Promega, R6051), or *Xba*I (Promega, R6181) in the recommended buffer in a final volume 20µl for 3 hours at 37ºC. The digestion reaction was terminated by heating at 75ºC for 15 minutes.

After digestion, the 5' phosphate of plasmid was removed to prevent self-ligating by incubating the digestion mix with 1µl Antarctic Phosphatase (5 units/µl) (NEB, M0289S) and 3µl Antarctic Phosphatase buffer 10X, in a final volume 30µl.The reaction was carried out at 37ºC for 15 minutes and followed 5 minutes at 70ºC to inactivate the enzyme.

2.2.2.7. Gel purification

The digestion mix was applied to 1% (w/v) SeaKem® LE Agarose (Lonza, 50002). DNA fragments were visualized by staining with ethidium bromide (Sigma, E1510). Under UV-light, the appropriate DNA band was excised from the gel with a clean scalpel and transferred into an Eppendorf tube. The Zymoclean Gel DNA Recovery Kit (Zymo Research, D4001) was used to purify DNA from the agarose gel. Briefly, 3 volumes of ADB were added to each volume of agarose excised from the gel and incubated at 37-55ºC for 5-10 minutes until the gel slice was completely dissolved. For DNA fragments higher than 8kb, 1 addition volume of water was also added to the agarose. The dissolved agarose solution was transferred to the Zymo-spin column and centrifuged for 30 seconds at full speed. The flow-though was discarded. The column was washed two times with 200µl DNA wash buffer and centrifuged at full speed at 30 seconds. The flow-though was discarded. DNA was eluted with 13µl nuclease-free water (Sigma, W4502) and quantified using a NanoDrop spectrophotometer.

2.2.2.8. Ligation

Ligation of DNA fragments was performed with a ratio of 1:3 of plasmid DNA: insert. The reaction mixture was incubated with 1µl of T4-DNA Ligase (1 unit/µl) (Life Technologies, 15224-017), 1µl of ligation buffer (10X) in a final volume of 10µl ddH2O. The reaction was left at 14^{o}C for 24hours.

2.2.2.9. Transformation

To 100µl of competent E.coli DH5α, either 50-100ng of plasmid DNA or 10 µl of ligation reaction were added and incubated for 20 minutes on ice. A heat shock at 42°C for 30 seconds was followed by incubation on ice for another 2 minutes. 500µl of LB medium was added to the bacteria and the bacterial suspension was shaken at 37°C and 180rpm for 60 minutes. The bacteria were then spread on LB-agar plates containing 100µg/ml ampicillin (Sigma, A9393). Plates were incubated at 37°C overnight.

2.2.2.10. MicroRNA 29 family binding site mutagenesis

QuikChange II XL site-directed mutagenesis kit (Agilent, 200521) was used to replace 5 nucleotides in the binding site of the miR-29 family to either *Xba*I (5'TCTAGA3'), *Sal*I (5'GTCGAC3'), *Sac*I (5'GAGCTC3') depending on which restriction enzymes were used in subcloning. The basic procedure utilizes PfuUltra high fidelity (HF) DNA polymerase for extending two mutagenic oligonucleotide primers which have desire mutations in the middle of their sequences and the rest of the sequence complementary to opposite strands of miR-GLO- 3'UTR. After cycling, PfuUltra HF DNA polymerase will generate a mutated plasmid containing staggered nicks (Figure 2.1). The product is then treated with *Dpn* I nuclease targeting sequence 5'-Gm^{6}ATC-3'. *Dpn* I, specific for methylated and hemimethylated DNA, will digest the parental DNA template and select for mutant-containing synthesized DNA. The nicked vector DNA incorporating the desire mutant of the miR-29 family binding site is then transformed into XL10 Gold ultracompetent cells (Figure 2.1).

Mutangenic primers were designed using Agilent's website: QuikChange primer design program: www.agilent.com/genomics/qcpd. The lists of primer mutants used are listed in Appendix, Table 2.

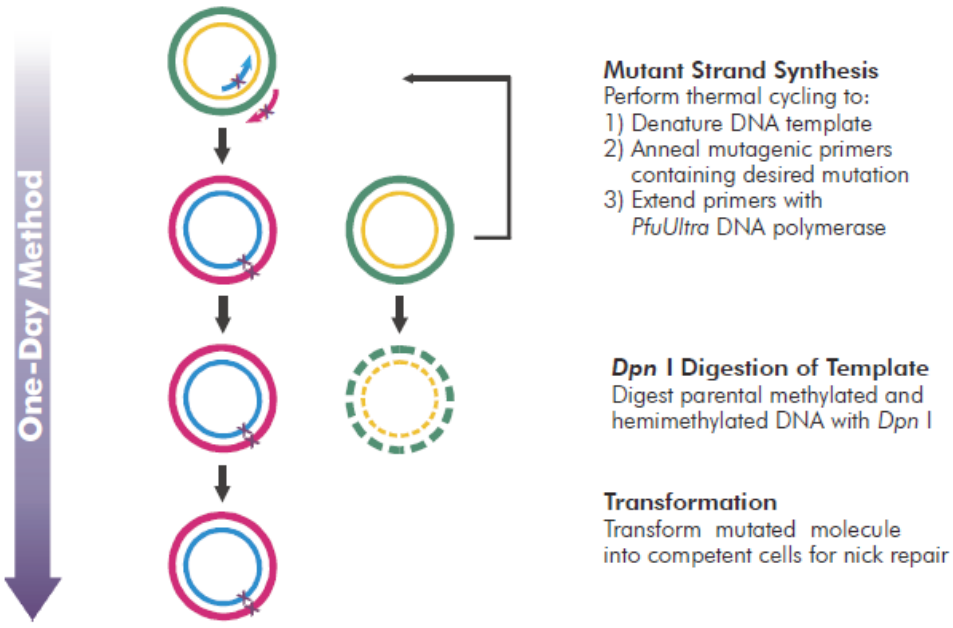

Figure 2.1: QuikChange II XL site-direct mutagenesis method

The reaction is prepared in a final volume of 50µl with 10ng of pmiR-Glo-3'UTR, 1.5µl primer mutant forward (100ng/µl), 1.5µl primer mutant reverse (100ng/µl), 1µl of dNTP mix (10mM), 5µl of reaction buffer (10X), 1µl of PfuUltra HP DNA polymerase (2.5 units/µl). The reaction is cycled at 1 minute at 95ºC, followed by 18 cycles at 95ºC 50 seconds, 68ºC 1 minute/1 kb plasmid length, and finally extension at 68ºC for 7 minutes. The amplification reaction was further incubated with 1µl of *Dpn*I restriction enzyme (10units/µl) at 37ºC for another 1 hour. To 50µl of XL10-Gold Ultracompetent cells, 5µl of *Dpn* I-treated DNA was added and the transformation protocol followed as above.

2.2.2.11. Sequencing

DNA Sequencing was performed by Source BioScience (http://www.lifesciences.sourcebioscience.com/). The sequencing signal was read by Chromas 2.4.

2.2.2.12. Total RNA isolation

2.2.2.12.1. Total RNA isolation from cultured cells

500ml of Trizol® reagent (Invitrogen, 15569-026) were added directly to adherent cells after removing the growth media from a 6-well plate. The cells were lysed by pipetting up and down several times. 250µl chloroform (Sigma, 288306) was added per 500µl Trizol®, vortexed for 15 seconds and incubated at room temperature for 10mins. The Trizol®/Chloroform mixture was centrifuged at 130,000xg, 10min, at 4°C and the aqueous layer recovered into a fresh tube. 500µl of 100% (v/v) isopropanol (Sigma, 190764) was added, mixed, left 10min at room temperature and centrifuged at 130,000xg, 10min, at 4°C then the supernatant was discarded. RNA pellets were washed with 75% (v/v) ethanol (Sigma, 459844), and centrifuged at 130,000xg, 2min, at 4°C. The supernatant was discarded, the pellet air dried and then suspended in 50µl RNase-free water and stored at -80°C until further use.

2.2.2.12.2. Total RNA isolation from murine whole knee joint

All materials used were RNase free. Whole knee joints were ground under liquid nitrogen using BioPulverizer (Biospec). Trizol® reagent (Invitrogen, 15569-026) were added immediately to ground samples (1.5ml/50mg samples) and mixed thoroughly for 5 minutes. Ground knee joints were pelleted at 130,000xg for 2min at 4°C and the supernatant recovered. 250µl chloroform (Sigma, 288306) was added per 500µl Trizol®, vortexed for 15 seconds and incubated at room temperature for 10mins. Samples were then treated as cultured cells above.

2.2.2.12.3. Total RNA isolated from murine hip or knee cartilage

Murine hip femoral caps were fully homogenized with 500µl Trizol® reagent (Invitrogen, 15569-026) using a disposable pestle. Then, 200µl chloroform (Sigma, 288306) was added, vortexed for 15 seconds, and left at room temperature for 10mins. The Trizol®/chloroform mixture was centrifuged at 130,000xg for 10 minutes at 4°C, and the aqueous layer collected into a fresh tube. The RNA purification step was performed using *mir*Vana™ miRNA Isolation Kit (AM1560, Life Technology) according to the manufactures recommendation for total RNA recovery. Briefly, 1.25x aqueous layer volume of 100% (v/v) RT ethanol was added to the aqueous phase and the samples were loaded onto

columns. The flow through was discarded after centrifuging 15 seconds at 130,000xg. Then three wash steps were followed by applying wash solution 1 (700µl), and then wash solution 2/3 (500µl) (twice) to the column. For each washing, the column was centrifuged at 130,000xg for 15 seconds followed by discarding the flow through. The columns was then placed in RNase-free collection tubes and 30µl of RNas-free water added. Columns were then left to stand for 2 minutes and centrifuged at 2 minutes, 13,000xg. RNA was then stored at -80^{o}C until used.

2.2.2.13. MicroRNA quantification and integrity

The concentration of RNA samples was determined by measuring the absorbance at 260nm using the NanoDrop spectrophotometer (NanoDrop Technologies). The purity of RNA is determined from the ratio A_{260}/A_{280} and A_{260}/A_{230}.

The integrity of total RNA was determined using the Experion^{TM} automated electrophoresis system (Bio-Rad, USA). This method measures fluorescence of a fluorophore bound to RNA. RNA integrity can be evaluated automatically by comparing the area of the peaks corresponding to the rRNAs. A 28S/18S rRNA ratio close to 2 indicates for intact RNA.

2.2.2.14. cDNA synthesis

2.2.2.14.1. SuperScript II reverse transcriptase cDNA synthesis

Total RNA was isolated from cells, whole knee joints, human or murine cartilages as above and reverse transcribed to cDNA using SuperScript II reverse transcriptase (Life Technologies, 18064-014). Briefly, in a total volume of 11µl in 96-well PCR plate, 1µg total RNA and 0.2µg random hexamer primer (Life Technologies, 48190-011) was mixed together and the plate was incubated at 70^{o}C for 10mins. Samples were chilled on ice, then, a master mix containing 1µl SuperScript II reverse transcriptase (200 units/µl) (Life Technologies, 18064-014), 4µl First Strand buffer (5X) (Life Technologies, 28028-013), 2µl 0.1M dithiothreitol (DTT) (Life Technologies, 18057-018), 2µl of 10mM dNTP mix (Bioline, BIO-39044), 1µl Recombinant RNasin Ribonuclease Inhibitor (20-40 units/µl) (Promega, N2511) was added to the randomly primed RNA to give a total volume of 20µl and incubated for 1 hour at 42^{o}C followed by a heat inactivation step at 70^{o}C, for 10mins.

cDNA was diluted to 0.5µg/ml in nuclease-free water (Sigma, W4502). 5µg cDNA was used for qRT-PCR analysis of genes of interest and 1µg cDNA was used for analysis of 18S rRNA. QRT-PCR is described in 2.2.2.15.

2.2.2.14.2. M-MLV reverse transcriptase cDNA synthesis

Moloney Murine Leukemia Virus (M-MLV) reverse transcriptase was used to perform cDNA synthesis straight from cell lysate without the need of purifying total RNA. This method was used for cell plated in 96-well plate where a number of cells are too small for RNA extraction.

Briefly, medium was removed and the cells in 96-well plate were washed with ice cold PBS (Life Technologies, 10010023). Then, 30µl cells to Cells-II-cDNA lysis buffer (Life Technologies, AM8723) was added to each well, providing a cell lysate which can immediately be reverse transcribed without the need for RNA isolation. Lysates were transferred to 96-well PCR plate and heated to 75ºC for 15 minutes to inactivate RNases. Lysates can be stored at -80ºC until reverse transcription. For genomic DNA digestion, 1µl DNase I 1 units/µl (Life Technologies, AM2222) and 3µl DNase I buffer (10X) were added per well. The plate was heated to 37ºC for 15 minutes, followed by an inactivation step at 75ºC for 5 minutes.

For reverse transcription, 8µl of DNase-treated samples were transferred to a new ice cold PCR plate. Following this, 3µl of 10mM dNTP mix (Bioline, BIO-39044) and 0.2µg random hexamer primers (50µM) (Life Technologies, 48190-011) were added per well and samples were heated to 70ºC for 5 minutes. Samples were chilled on ice and a master mix including 0.5µl Moloney Murine Leukemia Virus (M-MLV) reverse transcriptase 200 units/µl (Life Technologies, 28028-013), 4µl First Strand buffer (5X) (Life Technologies, 28028-013), 2µl 0.1M dithiothreitol (DTT) (Life Technologies, 18057-018), 0.5µl Recombinant RNasin Ribonuclease Inhibitor (20-40 units/µl) (Promega, N2511), 1µl nuclease-free water (Sigma, W4502) was added per well. Samples were then heated to 37ºC for 50 minutes, followed by an inactivation step of 75ºC for 15 minutes. After that, 30µl of nuclease-free water (Sigma, W4502) was added per sample. For quantitative real-time PCR (qRT-PCR) analysis of genes of interest, 5µl of each sample was used. For the

house keeping gene 18S rRNA, samples were diluted 1:10 and 5µl was used. QRT-PCR is described in 2.2.2.15.

2.2.2.14.3. miRCURY LNA™ Universal cDNA synthesis

MicroRNA cDNA was synthesized by the miRCURY LNA™ Universal cDNA synthesis kit (Exiqon, 203300). This step provides templates for all miRNA real-time PCR assays by one first-strand cDNA synthesis reaction. The basis principal is in Figure 2.2.

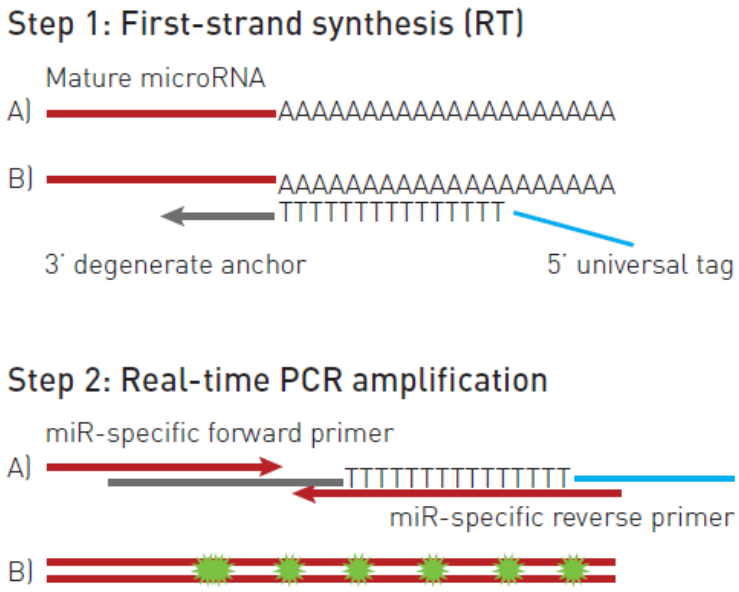

Figure 2.2: Outline of the miRCURY LNA Universal RT miRNAsynthesis.

A poly-A tail is added to the mature miRNA template (step 1A). cDNA was synthesized using a poly-T primer with a 3'degenerate anchor and a 5'universal tag (step1B). Then the cDNA template is amplified using miRNA-specific and LNA^{TM}-enhanced forward and reverse primers (step 2A). Sybr green is used for detection (step 2B). *Reprinted from miRCURY LNA^{TM} Universal RT microRNA PCR instruction manual (Exiqon).*

Total RNA was adjusted to 5ng/µl using nuclease-free water (Sigma, W4502). 10ng of RNA was transferred to an ice cold 96-well PCR plate. A master mix contained 2µl Reaction Buffer (5X) (Exiqon, 203300), 1µl enzyme mix was added to each well. The reaction was brought to 10µl with nuclease-free water and the plate was heated to 42^{o}C for 1 hour followed by a heat inactivation step at 95^{o}C for 5minutes. cDNA was then diluted to 12.5 pg/µl by nuclease free water (Sigma, W4502) and 50pg of cDNA was used for qRT-PCR analysis of miRNA of interest.

2.2.2.15. Real-time quantitative RT-PCR

2.2.2.15.1. Universal Probe Library Real-Time qRT-PCR

The Universal Probe Library (UPL) (Roche Diagnostics) enables extensive transcript coverage due to the short 8-9 nucleotide-long probes. Each probe has a fluorescein (FAM™) label at the 5' end and a dark quencher dye at the 3' end; shorter (typically 8-9 nucleotide) than conventional probe (25-35 nucleotides); locked nucleic acids (LNA™) are incorporated into it sequence. Each probe can detect ~7,000 transcripts and each transcript is detected by ~16 probes.

Primers were designed using the freely available ProbeFinder web-based software provided by Roche Applied Science in which the 'exon boundary spanning' option was selected. Primers were subjected to short sequence BLASTn search to confirm specificity. All the primers were purchased from Sigma and reconstituted in nuclease free water (Sigma, W4502) at 100nM. Primer sequences and UPL probe numbers are in Appendix, Table 3.

For quantitative RT-PCR using the universal primers and probes, the qRT-PCR was carried out using the ABI Prism 7900 HT Sequence Detector (Applied Biosystems) in a microAmp® optical 96-well plate (Life technologies, N8010560). When RNA quantity was known, the qRT-PCR was run using 5ng cDNA for genes of interest and 1ng cDNA for 18S rRNA. For M-MLV-reverse-transcribed- cDNA transcript samples, 5µl samples was used for gene of interest or diluted 1:10 and used 5µl for detecting 18S rRNA.

Each qRT-PCR reaction contained Kappa Fast Universal qPCR Master Mix (2X) (Kappa Biosystems, KK4703), a final concentration of 100nM of each of forward and reverse primers, 200nM of Universal Probe (Roche Diagnostics). The reaction was carried out in a final volume of 25µl. The plate was sealed with microAmp® optical adhesive film (Life Technologies, 4311971) and run with the following PCR cycles: 50°C 2 minutes, 95°C 10 minutes, 40 cycles for 95°C 15 seconds, 60°C 1 minute.

2.2.2.15.2. Standard probe-based Real-time qRT-PCR

The probe-based quantitative real-time PCR method was used to detect the expression of ADAMTS genes including *ADAMTS4, ADAMTS6, ADAMTS10, ADAMTS14, ADAMTS17, ADAMTS19*. These primer and probe sequences were described in (Davidson *et al.* 2006). Briefly, the primers and probes were designed by Primer Express® 1.0 software (Life Technologies, 4363991) and were closed to intron/exon boundaries to control amplification of genomic DNA. Where possible, the probes were designed to span two neighbouring exons. Specificity of primers and probes were validated thought BLASTn. Primer sequences and probe sequences are in Appendix, Table 4

The qRT-PCR reaction was also carried out in a final volume 25µl of Kappa Fast Universal qPCR Master Mix (2X) (Kappa Biosystems, KK4703), 100nM final concentration of each of forward and reverse primers, 200nM genes of interest-specific probe. Reaction set up and cycling conditions were as in 2.2.2.15.1.

2.2.2.15.3. SYBR® Green Real-time PCR

A combination of SYBR® green dye fluorescence with gene-of-interest specific primers enabled double stranded-DNA amplification measurement during PCR. SYBR® green real-time qRT-PCR was used to detect primary and pre sequences of the miR-29 family (which were described in (Eyholzer *et al.* 2010)) and other genes as below. Full primer sequences and list of genes detected by SYBR® green real-time PCR are listed in Appendix, Table 5. All primers were purchased from Sigma.

For SYBR® green qRT-PCR reaction, the amount of cDNA for genes of interest and 18S rRNA is as 2.2.2.15.1. The reaction contained 0.18µl SYBR® green I dye, Kappa Fast Universal qPCR Master Mix (2X) (Kappa Biosystems, KK4703), 100nM final concentration of each of forward and reverse primers. The PCR cycle conditions are as 2.2.2.15.1 followed by another dissociation step which produces the melting curve for the PCR amplification product.

2.2.2.15.4. SYBR® Green Real-time PCR for the mature miR-29 family detection

LNA primers for detecting miR-29 family mature sequence

All LNA primers were designed for optimal performance with the miRCURY LNA™ Universal cDNA synthesis kit. The LNA primers are Hsa-miR-29b-3p LNA™ PCR primer sets (Exiqon, 204679), Hsa-miR-29a-3p LNA™ PCR primer sets (Exiqon, 204698), Hsa-miR-29c-3p LNA™ PCR primer sets (Exiqon, 204729).

Real-time PCR protocol

The qRT-PCR reaction used SYBR® green I dye in combination with LNA™ PCR primer sets to quantify the original mature miR-29 family. The reactions contained 50pg of miRCURY-LNA™-Universal cDNAs for either the miR-29 family or U6. The PCR reaction mix contained 0.18µl SYBR® Green I dye, 5µl Kappa Fast Universal qPCR Master Mix (2X) (Kappa Biosystems, KK4703), and 1µl of forward and reverse primer mix (as recommend by the manufacture (Exiqon)) in a final volume of 10µl. PCR cycles: 10 minutes at 95°C, 40 cycles for 10 seconds at 95°C, 1 minute at 60°C and a dissociation step. The dissociation step produces a melting curve for the PCR amplification product and ensures there is only amplification of the target gene.

2.2.2.15.5. Quantitative RT-PCR Data analysis

2.2.2.15.5.1. Control genes

The constitutively expressed "housekeeping" 18S rRNA was used as the control for relative mRNA gene expression while U6 was used as endogenous control for relative miRNA gene expression.

2.2.2.15.5.2. Relative gene expression – comparative C_t method

Raw fluorescence data was analyzed by the 7000HT SDS 2.2 software to produce threshold cycle (C_t) values, which is the cycle number at which the signal is detectable above the baseline. The C_t values were transformed using the comparative C_t method to obtain relative quantification (RQ) of gene expression:

$$RQ=2^{-\Delta Ct}$$

Where: for mRNA expression: ΔC_t= target gene C_t - 18S C_t

Or for miRNA expression: ΔC_t= the miR-29 family C_t - U6 C_t

This method assumed that all primers and probe sets are working at the same efficiency.

2.2.2.15.6. Western Blot

Buffer and antibody

Radio immunoprecipitation assay (RIPA) buffer: The buffer was made (final concentration) with 50mM Tris base (Fisher Scientific, BP152-500) (which was adjusted to pH 7.6 with hydrochloric acid (Sigma, 258148)),150mM NaCl (Fisher Scientific, BP3581), 1% (v/v) Triton X-100 (Sigma, X100), 1% (w/v) sodium deoxycholate (Sigma, D6750), 0.1% (w/v) sodium dodecyl sulfate (SDS) (Fisher Scientific, 10356463), 10mM sodium fluoride (NaF) (Sigma, 201154), 2mM sodium orthovanadate (Na_3VO_4) (Sigma, S6508), 1X protease inhibitor cocktail (Fisher Scientific, PI-78410).

Resolving buffer: To make up 4X buffer: 91g Tris base (Fisher Scientific, BP152-500) was dissolved in Milli-Q Ultrapure water (Merck Millipore) and adjusted to pH 8.8 with hydrochloric acid (Sigma, 258148). The solution was then made up to 500ml. 2g SDS (Fisher Scientific, 10356463) was added and dissolved.

Staking buffer: To make up 4X buffer: 6.05g Tris base (Fisher Scientific, BP152-500) was dissolved in Milli-Q Ultrapure water and adjusted to pH 6.8 with hydrochloric acid (Sigma, 258148). Milli-Q water was added to 100ml volume. 0.4g SDS (Fisher Scientific, 10356463) was added and dissolved.

Running buffer: To make up 10X buffer: 30.2g Tris base (Fisher Scientific, BP152-500), 144g glycine (Fisher Scientific, 10467963), 10g SDS (Fisher Scientific, 10356463) were dissolved in Milli-Q water to a final volume 1L.

Transfer buffer: To make up 1X buffer: 5.8g Tris base (Fisher Scientific, BP152-500), 2.9g glycine (Fisher Scientific, 10467963), 0.37g SDS (Fisher Scientific, 10356463) were dissolved in Milli-Q water, 200ml 100% (v/v) methanol (Sigma, 322415) were added then Milli-Q water to a final volume of 1L.

Tris-buffered saline (TBS): To make up 10X buffer: 24.2g Tris base (Fisher Scientific, BP152-500), 80g NaCl (Fisher Scientific, BP3581) were dissolved in 900ml Milli-Q water and adjusted to pH 7.6 with hydrochloric acid (Sigma, 258148). Milli-Q water was added to 1L volume.

Blocking buffer: For 150ml, 15ml 10X TBS was diluted in 135ml Milli-Q water. 7,5g non-fat dry milk (OXOID, LP0031) was added and stirred to mix. Finally, 0.15ml Tween®-20 was added (Sigma, P5927).

Primary antibody dilution buffer: For 20 ml, 2 ml 10X TBS was diluted to 18 ml with Milli-Q water. 1.0 g BSA (Sigma, A9418) was added and dissolved by stirring. While stirring, 20µl Tween-20 (Sigma, P5927) was added.

Wash Buffer (TBST): TBS with a final concentration 0.1% (v/v) Tween-20 (Sigma, P5927).

Antibody: GAPDH antibody (Cell Signaling, #2118S), DVL3 antibody (Cell Signaling, #3218), FZD5 antibody (Cell Signaling, #3795)

Western blot protocol

SW1353 cells were plated in 6-well plates ($1.5x10^5$cells/well) and transfected with Syn-Hsa-miR-29b miScript miRNA mimic (Qiagen, MSY0000100) as referred in 2.2.2.7.2.5. At desired time post transfection, cells in each well of 6-well plate were washed twice with ice cold PBS (Life Technologies, 10010023) before adding 100µl RIPA buffer to each well and harvesting by scraping. The cell lysate was transferred to a fresh ice-cold 1.5ml tube and centrifuged at full speech in 10 minutes. The supernatant was collected and stored at -20^{o}C.

Protein was quantified using the Bio-Rad Protein Assay (Bio-Rad, #500-0006) which is based on the method of Bradford. Briefly, 200µl dye reagent concentrate was diluted 5 times with Milli-Q water before adding 20µl sample lysate. The mixture was incubated at room temperature for 10 minutes and absorbance measured at 595nm. Comparison of this value to a standard curve provided a relative concentration of solubilized protein. The

standard curve was created with five dilutions of proteins standards of bovine serum albumin (Bio-Rad, 500-0002) from 0.2 to 0.9 mg/ml.

Samples was adjusted to 20µg solubilized protein in a 30µl with nuclease-free water (Sigma, W4502), followed by adding 20ng/µl Bromophenol Blue (Sigma, 114391) and 1.2µl 1M DTT (Thermal Scientific, # R0861). The sample was gently mixed and heated to 95ºC for 5 minutes. Samples were then electrophoresed on 10% (w/v) polyacrylamide gels. The resolving gel was cast with the following components: 5ml 30% (w/v) Acrylamide/ Bis Acrylamide solution 37:5:1 (Bio-Rad, #161-0154), 3.75ml resolving buffer (4X), 6.25ml Milli-Q water, 50µl 10% (w/v) ammonium persulfate (APS) (Sigma, A3678), 10µl TEMED (Sigma, T9281). Resolving gels were topped with isopropanol (Sigma, 190764) until set. Then isopropanol was removed and the stacking gel was cast on top of the resolving gel and a comb was inserted. For 1 gel, the stacking gel was made with 0.71ml stacking buffer (4X), 0.41ml 30% (w/v) acrylamide/ bis acrylamide solution 37:5:1 (Bio-Rad, #161-0154), 1.91ml Milli-Q water, 16µl 10% (w/v) APS (Sigma, A3678), 3.2µl TEMED (Sigma, T9281). Samples were loaded on the gel and were electrophoresed at 50V until the bromophenol blue passed through the stacking gel and then 80V for 1.5 hours.

Immobilon®-FL PVDF membrane (Merck Millipore, IPFL00010) was incubated in 100% (v/v) methanol (Sigma, 322415) for 15 seconds and washed with Milli-Q water. Then, Immobilon®-FL PVDF membrane, gel, extra thick blotting paper (Bio-Rad, #170-3966) were incubated in transfer buffer for 5 minutes. The gel was plated on top of Immobilon®-FL PVDF membrane in Trans-blot® SD semi-Dry Electrophoretic transfer cell (Bio-Rad, #170-3940) with extra thick blotting paper underneath and on top and run for 25V for 30 minutes (for 2 gels,1 mm thick).

After transfer, the membranes were briefly washed with TBS and incubated in blocking buffer for 1 hour, with gently rocking at room temperature. Membranes were then washed in TBST three times for 5 minutes. Primary antibody and membrane was incubated with gentle agitation overnight at 4ºC. Membranes were then washed in TBST three times for 5 minutes and incubated with IRDye® 800CW goat polyclonal anti-rabbit IgG (Li-Cor, 926-32211) (50µg) for 1 hour at room temperature with gently rock. Membranes were washed

with TBST for another three times for 5 minutes. The membrane was visualized using a Li-Cor Odyssey InfraRed Scanner.

2.2.2.15.7. Whole mount *in situ* hybridization

Reagents and buffers

Sodium chloride (NaCl) (Fisher Scientific, BP3581), tri-sodium citrate (Fisher Scientific, 10637174), magnesium chloride hexahydrate ($MgCl_2.6.H_2O$) (Fisher Scientific, M35-500), potassium chloride (KCl) (Fisher Scientific, BP366-500), heparin (Sigma, H3393), yeast tRNA (Fisher Scientific, 10523043), paraformaldehyde (Sigma, P6148), normal goat serum (heat inactivated), Triton-X100 (Sigma, X100), Tween-20 (Sigma, P5927), BSA (Sigma, A9418)

Saline sodium citrate buffer (SSC): 20X SSC buffer was made up with 175.3 g of NaCl and 88.2 g of sodium citrate, pH 7, in a total volume of 1000ml.

Development solution (DS): The solution was made up with: 100 mM Tris-HCl pH9.5, 50mM magnesium chloride hexahydrate (MgCl2.6.H2O), 100mM sodium chloride (NaCl) + 0.1% (v/v)Tween 20.

Blocking solution: The solution was made up with: 2% (v/v) NGS, 2 mg/ml BSA, 0.1% (v/v) Triton X-100 + 0.05%)v/v) Tween 20 in PBS.

Hybridisation Buffer (HB): The buffer was made up with 50% (v/v) formamide, 5xSSC, 0.1% (v/v) Tween 20 + 10 mM citric acid pH6.0 + 50 µg/ml heparin + 100 µg/ml tRNA in PBS

Tris-buffered saline with Tween 20 (TBST): for 100ml (10X) buffer was made up with 8g NaCl, 25ml Tris-HCl pH7.5, 0.2g KCl, 10ml Tween 20

Phosphate-buffered saline with Tween 20 (PBST): PBS with 0.1% (v/v) Tween 20

Probe: miRCURY LNA™ miR-29b-3p detection probe, 250pmol, 5'-DIG and 3'-DIG labelled (Exiqon, 38131-15)

Fixation

Mouse embryos at desired stages were dissected and fixed in 4% PFA-PBS on a rolling platform overnight at 4^{o}C. Then next day, the embryos were washed 4 times with PBST and dehydrated through increasing MeOH concentration washes e.g. 25%, 50%, 75% and 100% MeOH on the gentle rocking platform. The embryos can then store in 100% MeOH at -20^{o}C until required.

In situ hybridization protocol

On a gently rocking platform, the embryos were washed with decreasing MeOH concentration i.e. 75% (v/v), 50% (v/v), 25% (v/v), 0 (v/v) % MeOH for 15 minutes each time to dehydrate. After that, the embryos were digested with Proteinase K (10µg/ml final concentration) for 30 minutes, followed by rinsing twice in PBST and fixing in 4% (v/v) PFA for 20 minutes. To get rid of the remaining PBST, the embryo was washed 4 times in PBST for 5-7 minutes. The embryo was prehybridized in hybridization buffer at 54^{o}C for 3 hours and the "nape" of the neck of embryo was pricked to facilitate the probe penetration. After prehybridisation step, the buffer was removed and replaced with fresh warm hybridisation buffer containing 20 pmol of the miR-29b LNA probe (Exiqon, 38131-15) and left at 54^{o}C overnight with gentle rocking. The probe hybridisation solution was removed followed by washes at 54^{o}C and 15 minutes each wash e.g. 75% HB: 25% 2xSSC, 50% HB:50% 2xSSC, 25% HB:75% 2xSSC, 2xSSC, 0.2xSSC. Following these washes, at room temperature, another 4 washes were carried on gently rocking platform, 10 minutes for each wash e.g. 75% 0.2xSSC:25% PBST, 50% 0.2xSSC:50% PBST, 25% 0.2xSSC:75% PBST, PBST. The embryo was then put in blocking solution for several hours at room temperature and incubated at 4°C O/N with the pre-absorbed antibody at a final dilution of 1:5000 in Blocking Solution. After that, the Blocking Solution was removed and washed throughout 2 or 3 days at RT in PBST with gentle rocking. To get rid of all remaining PBST, the embryos were washed twice with TBST and with development solution for 15 minutes each wash. Colour development was carried out at room temperature in 3.5ml development solution plus 15-50µl substrates.

The antibody was pre-adsorbed using previously fixed and dehydrated tissue that is not suitable for in situ hybridization. These tissues were dehydrated and washed 15 minutes in

blocking solution, followed by incubating with blocking solution containing the antibody at 1:1000 dilution for three hours.

2.2.2. Cell culture and cell-based assays

2.2.2.1. Human primary chondrocyte isolation

Human cartilage chips were incubated with digestion medium including DMEM GlutaMAX^{TM} (Life Technologies, 10566-016), 1mg/ml collagenase (Sigma, C1639), 0.4% (w/v) Hepes (Fisher Scientific, BP310-100), 100 IU/ml penicillin, 100µg/ml streptomycin (Sigma, P4333) at 37^{o}C, 180rpm overnight. The digestion mixture was then strained through a 70µm cell strainer. Cells were plated at 4x10^{4}cells/cm^{2} and grown to 80% confluence. Cells were used by passage 2.

2.2.2.2. Human de-differentiation assay

Human primary chondrocytes were isolated from human knee OA articular cartilage as described in 2.2.2.1. The cells were then subjected to serial subculture in monolayer. The de-differentiation assay was performed by Dr Natalie Crowe (Clark lab, University of East Anglia).

2.2.2.3. Chondrogenesis model

The human chondrogenesis model was performed by Dr Matthew Barter, Newcastle University. Briefly, human bone marrow stem cells (from seven donors, 18-25 years of age) were isolated from human bone marrow mononuclear cells (purchased from Lonza Biosciences) and resuspended in chondrogenic culture medium consisting of high glucose Dulbecco's modified Eagle's medium containing 100 µg/ml sodium pyruvate (Lonza), 10 ng/ml TGF-β3 (Peprotech), 100 nM dexamethasone, 1x ITS-1 premix, 40 µg/ml proline, and 25 µg/ml ascorbate-2-phosphate (Sigma). 5x10^{5} hMSC in 100µl medium were pipetted onto 6.5mm diameter, 0.4-µm pore size polycarbonate Transwell filters (Merck Millipore), centrifuged in a 24-well plate (200g, 5 minutes), then 0.5 ml of chondrogenic medium was added to the lower well as described. Media were replaced every 2 or 3 days up to 14 days.

The murine chondrogenesis model was performed by Dr Tracey Swingler, University of East Anglia. Briefly, ATDC5 cells were seeded at $6x10^4$/well of a 6-well plate in DMEM/Ham's F-12 medium (Life technologies, 11320-033) containing 5% (v/v) FCS (PAA), 2mM glutamine, 100 IU/ml penicillin, 100µm/ml streptomycin (Sigma, P4333), 5ng/ml sodium selenite, 10µg/ml human transferrin (Sigma, I3146), and 10µg/ml bovine pancreatic insulin at 37°C, in an atmosphere of 5% CO_2. Media was replaced every 2 days up to 42 days. After 21 days, the medium was replaced with α-minimal essential medium with the same supplements, and the atmosphere was changed to 3% CO_2.

2.2.2.4. Monolayer cell culture and storage

All cells were cultured at 37°C with 5% (v/v) CO_2. Cells were usually grown in Dulbecco's modified Eagle's medium (DMEM) High Glucose, GlutaMAX supplement (Life technologies, 10566-016) with 10% (v/v) heat-inactivated Fetal Calf Serum (FCS) (PAA) and 100 IU/ml penicillin and 100µg/ml streptomycin (Sigma, P4333). For maintenance, medium was refreshed at least three times weekly. Cells were passaged at around 80-90% confluence. Adherent cells were detached by washing x2 with HBSS (Life Technologies, 14025092) then treated with 2 ml of trypsin/EDTA (Life Technologies, 25200072) for 2-3 minutes at 37°C. After centrifugation (17.3xg, 5 minutes), the cell pellet was gently resuspended in fresh medium. Cells were replated at a ratio of 1: 20. For long term storage, cells were detached and pelleted by centrifugation at 17.3xg for 5 minutes. The pellets were resuspended in cryo-preservation medium including 90% (v/v) FCS (ATCC) and 10% (v/v) DMSO (Fisher, BP231-100), slowly frozen down at approximately 1°C/minute, and stored in liquid nitrogen.

2.2.2.5. Micromass culture

Media

Growth medium: Dulbecco's modified Eagle's medium (DMEM) High Glucose, GlutaMAX supplement (Life technologies, 10566-016) with 10% (v/v) heat-inactivated Fetal Calf Serum (FCS) (ATCC) and 100 IU/ml penicillin and 100µg/ml streptomycin (Sigma, P4333).

Different medium were prepared: the DMEM high glucose, GlutaMAX supplement (Life technologies, 10566-016) adding 1X Insulin- Transferrin-Selenium (ITS-G) (Life Technologies, 41400-045).

Micromass culture

The protocol was described in (Greco *et al.* 2011) with some modifications. Human primary chondrocytes was isolated from human OA knee cartilage as described in 2.2.2.1 and cultured in monolayer with growth medium. Whenever reaching confluence, the cells were passaged two times. Confluent passage 2 monolayer culture of human primary chondrocytes were released by trypsin/EDTA (Life Technologies, 25200072), and resuspended in growth media at a density of $2.5x10^7$ cells/ml. Micromass was obtained by pipetting 20µl of cell suspension into individual wells of 24 well-plates and leaving for 3 hours to attach without additional medium. Then, 1ml growth medium was gently added and the micromass was left for another 24 hours before stimulating with cytokines or growth factors.

2.2.2.6.Induction cells with regulatory factors: major cytokines and growth factors

Cytokines and growth factors:

Human recombinant TGFβ1 (R&D Systems, 240-B-002/CF) and **human recombinant TGFβ3** (R&D Systems, 243-B-002/CF) were reconstituted in sterile 4mM HCl (Sigma, 258148) containing 0.5% (w/v) bovine serum albumin (Sigma, A2058).

Human recombinant Wnt3a (R&D Systems, 5036-WN-010/CF) was reconstituted in sterile Phosphate Buffered Saline (PBS) (Life Technologies, 10010023).

Human Recombinant Interleukin-1β (IL-1β) (First Link, ILB4551) was reconstituted in sterile Phosphate Buffered Saline (PBS) containing 0.5% (w/v) bovine serum albumin (Sigma, A2058).

NFκB activation inhibitor II JSH-23 (Calbiochem, 481408) is a cell-permeable diamino compound that selectively blocks nuclear translocation of NF-κB p65 and its transcription activity without affecting IκB degradation.

Lipopolysaccharides (LPS) (Sigma, L3012) are components of the cell wall of gram negative bacteria. LPS are extracted from *E.coli* serotype O111:B4 and purified by gel filtration. LPS is reconstituted in sterile (PBS) (Life Technologies, 10010023).

P38 inhibitor SB203580 (Sigma, S8307) is a pyridinyl imidazole that suppresses the activation of MAPKAP kinase-2. The P38 inhibitor, therefore, inhibits the MAPKAP kinase-2 cascade which is activated by cellular stress, bacterial infection and pro-inflammatory cytokines. SB203580 was resuspended in DMSO (Fisher, BP231-100).

2.2.2.6.1. Stimulation of cells in monolayer with cytokines and growth factors

Human chondrosarcoma SW1353 and human primary chondrocytes were maintained as described above. For stimulation, either $5x10^3$ SW1353 cells or 10^4 human primary chondrocytes were seeded into each well of a 96-well plate with 100µl DMEM GlutaMax (Life Technologies, 10566-016) with 10% (v/v) FCS (ATCC) and 100 units/ml penicillin and 100µg/ml streptomycin (Sigma, P4333). Cells were serum starved for 14 hours and were stimulated with different cytokines and growth factors at final concentration: TGFβ1, TGFβ3 4ng/ml, IL-1 5ng/ml, Wnt3a 100ng/ml, LPS 1µg/ml at 4, 8, 12, 24, 48 hours. All treatments were performed in triplicate. At each time point, cells in each well were washed with ice cold PBS (Life Technologies, 10010023) and harvested with 30µl Cells-to-cDNA lysis buffer (Life Technologies, AM8723).

2.2.2.6.2. Stimulation of cells in micromass culture with cytokines and growth factors

After the micromass was rested in growth medium for 24 hours, the different medium with either TGFβ1 (10ng/ml), IL-1 (20ng/ml), Wnt3a (50ng/ml) or LPS (1µg/ml) was added. All treatments were performed in triplicate. After different time points as desired, some of micromasses were harvested for Alcian blue matrix staining and others for quantitative RT-PCR.

2.2.2.7. Mammalian cell transfection

2.2.2.7.1. Plasmids, constructs, siRNAs and microRNA mimic and inhibitor

Sox9 expression vector: The vector was kindly provided by Dr Simon Tew (University of Liverpool, UK). The vector was described in (Lefebvre *et al.* 1997). Briefly, an almost full-length coding sequence of human SOX9 which is from codon 27 (directly from the first ATG associated with the Kozak sequence) up to 39bp of 3'unstranslated region was subcloned into pCDNA-5'UT-FLAG. pCDNA-5'UT-FLAG is pCDNA 3.1 with a FLAG sequence.

The miR-29a/b1 promoter construct: The construct was kindly provided by Dr Anne Delany (University of Connecticut Health Center, US) and was described in (Kapinas *et al.* 2010). The 2kb region upstream from the transcriptional start site of the human miR-29a/b1 putative promoter (EU154353) was subcloned into the luciferase reporter pGL4.10 (Promega).

p(CAGA)$_{12}$-luc plasmid: The construct was a kind gift of Dr Andrew Chantry, University of East Anglia, UK and is described in (Pais *et al*. 2010). 12 binding sites of the complex Smad3/4 (GAGAC) was cloned upstream of the luciferase encoding gene in luciferase reporter pGL3 (Promega).

IκBα promoter reporter plasmid: The plasmid was a kind gift from Prof. Derek Mann, (Newcastle University, UK), (originally from Prof. Ronald Hay, University of Dundee, UK). The plasmid contains 5 binding sites of P65 cloned upstream of the luciferase gene.

TOPflash and FOPflash reporter plasmids: The TOPflash reporter is a kind gift from Prof. Andrea Munsterberg (University of East Anglia, UK), and was originally from Prof. Randall Moon (University of Washington, USA). The FOPflash vector is provided by Dr Sarah Snelling (University of Oxford, UK). TOPflash contains 7 binding sites of TCF/LEF (AGATCAAAGG) driving the expression of the firefly luciferase. The back bone is the pTA-luc vector. The FOPflash vector is the control of TOPflash where all 7 binding sites of TCF/LEF are mutated.

The miR-29 mimic:

- Syn-hsa-miR-29a-3p miScript miRNA mimic (Qiagen, MSY000086): 5'UAGCACCAUCUGAAAUCGGUUA
- Syn-hsa-miR-29b miScript miRNA mimic (Qiagen, MSY0000100): 5'UAGCACCAUUUGAAAUCAGUGUU
- Syn-hsa-miR-29c miScript miRNA mimic (Qiagen, MSY0000681) 5'UAGCACCAUUUGAAAUCGGUUA
- AllStars negative control siRNA (Qiagen, SI03650318)

The 29b inhibitor control

- Anti-hsa-miR-29b miScipt miRNA inhibitor (Qiagen, MIN000100)
- miScript Inhibitor negative control (Qiagen, 1027271)

siRNA

- SOX9 siRNA: Dharmacon siRNA SMARTpool® (Fisher Scientific)
- Control: non-targeting siRNA 2 (Dharmacon, 001210-02)

2.2.2.7.2. Transient transfection protocol

2.2.2.7.2.1. SOX9 overexpression

SW1353 cells were plated in a 96-well plate ($5x10^3$cells/well) in growth medium without antibiotics one day before transfection. The cells were 80% confluent at the time of transfection. Before addition of the transfection complexes, the growth medium was removed from the cells and the cells were covered with 50µl of fresh growth medium without antibiotics. For each transfection, two tubes are prepared as follows: **Tube 1:** 100ng SOX9 expression vector was diluted in 25µl DMEM GlutaMax (Life Technologies, 10566-016) without serum and antibiotics; **Tube 2:** 0.2µl transfection reagent Lipofectamine 2000 (Life Technologies, 11668027) was diluted in 25µl DMEM GlutaMax (Life technologies, 10566-016) no serum and antibiotics. After 5 min of incubation, the diluted DNA and the diluted transfection reagent were combined and incubated at room temperature for 20 min. Then, 50µl of complexes were added to each well. The plate was

gently rocked back and forth and incubated at 37°C in a CO_2 incubator. All transfection was performed in triplicate. The pcDNA3.1 vector was used as control. After 6 hours of transfection, transfection medium was replaced with fresh growth medium without antibiotics for another 24 hours. For harvesting, cells were washed with ice cold PBS (Life Technologies, 10010023) and harvested with 30µl Cells-to-cDNA lysis buffer (Life Technologies, AM8723).

2.2.2.7.2.2. SOX9 and miR-29a/b1 promoter cotransfection

To cotransfect SOX9 and the promoter miR-29a/b1, the SW1353 cells were prepared as described above one day before transfection. For each transfection, two tubes are prepared as follows: **Tube 1:** 100ng of 29a/b1 promoter, and either 100ng SOX9/200ng pcDNA3 or 300ng SOX9/100ng pcDNA3 was diluted in 25µl DMEM GlutaMax (Life Technologies, 10566-016) without serum and antibiotics; **Tube 2:** 0.2µl transfection reagent Lipofectamine 2000 (Life Technologies, 11668027) was diluted in 25µl DMEM GlutaMax (Life Technologies, 10566-016) no serum and antibiotics. The diluted DNA and the diluted transfection reagent were combined after 5 min of incubation and incubated at room temperature for another 20 min. Then, 50µl of complexes were added to each well. The plate was incubated at 37°C in a CO_2 incubator and transfection medium was changed with fresh medium without antibiotics for another 24 hours. Then, cells were washed with ice cold PBS (Life Technologies, 10010023) and a luciferase assay performed. All transfection were performed in triplicate.

2.2.2.7.2.3. Transfection of the miR-29a/b1 promoter with cytokines and growth factors

SW1353 cells were plated and transfected with 100ng miR-29a/b1 promoter as described above. Cells were incubated with the promoter for 24 hours. The medium was then removed and replaced with serum, antibiotic-free DMEM GlutaMAX medium (Life technologies, 10566-016), and cells were serum-starved overnight. Cells was stimulated for 6 hours with TGFβ1/3 (4ng/ml), IL-1 (5ng/ml), Wnt3a (100ng/ml), LPS (1µg/ml) in the presence or absence of 50nM NFκB inhibitor or 10nM p38 inhibitor (Sigma, S8307). Medium was removed 6 hours post stimulation and cells were washed twice with ice cold PBS (Life Technologies, 10010023) and then harvested for luciferase assay.

2.2.2.7.2.4. Short interfering RNA SOX9 mRNA knockdown

SW1353 cells were plated and transfected with either 100nM SOX9 siRNA (Dharmacon) or non-targeting siRNA 2 (Dharmacon, 001210-02) as section 2.2.2.7.2.1. To detect siRNA-mediated mRNA SOX9 knockdown, cells were incubated for 48 hours post transfection, then harvested in 30µl Cells-to-cDNA lysis buffer (Life Technologies, AM8723).

2.2.2.7.2.5. Human primary chondrocyte gain- and loss-of-function experiments

One day before transfection, human primary chondrocytes at passage 1 was plated in 6-well plate at $2x10^5$ cells/ wells in fresh growth medium without antibiotics so that the cells will be around 80% confluent. Complexes were prepared as followed for transfection: **Tube 1**: miR-29b mimic/ inhibitor/ AllStar negative control/ inhibitor negative control (50nM) was diluted in 250µl of serum, antibiotic-free DMEM GlutaMAX (Life Technologies, 10566-016). **Tube 2**: 5µl of Lipofectamine 2000 (Life Technologies, 11668027) was diluted in 250µl serum, antibiotic-free DMEM GlutaMax (Life technology, 10566-016). Time for incubation and transfection mixture was prepared similar to section 2.2.2.7.2.2. The original medium was aspirated from the wells, 500µl transfection mixture was added to each well and the final volume was made to 1ml with DMEM GlutaMAX with 10% (v/v) heat-inactivated FCS, without antibiotics. All transfections were performed in triplicated. Cells were incubated for 48 hours, then, supernatant was removed and cells was washed with ice cold PBS and 1ml Trizol reagent was added. Samples were stored at -20^{o}C until RNA extraction.

2.2.2.7.2.6. Transfection of human primary chondrocytes with miR-29 family mimics and treatment cytokines and growth factors

50nM either miR-29a/b/c mimics or AllStar negative control was transfected to human primary chondrocytes in 6-well plate as in section 2.2.2.7.2.5. After 24 hours, medium was removed from the wells and replaced with DMEM GlutaMAX with 0.5% (v/v) heat inactivated FCS overnight. Then, cells were stimulated with TGFβ1 (4ng/ml), IL-1 (5ng/ml), Wnt3a (100ng/ml). At desired times post stimulation as in Chapter 5, medium was removed, the cells were washed with ice cold PBS and harvested in 1ml Trizol reagent.

2.2.2.7.2.7. Transfection of the miR-29b mimic in micromass culture with cytokines and growth factors

Confluent passage 2 monolayer culture of human primary chondrocytes were released by trypsin/EDTA and plated in 175 cm^2 flask with growth medium with 10% (v/v) heat inactivated FCS, no antibiotics one day before transfection to give cells at 90-100% confluence. 100nM miR-29b mimic or non-targeting control was diluted in 500µl medium (tube1) and 4 µl Lipofectamine 2000 was also diluted in 500µl medium (tube 2). Transfection was carried out as in 2.2.2.7.2.2. The original medium from the flask was removed before adding 1ml transfection mixture and the flask was further covered with another 14ml growth medium with 10% (v/v) heat inactivated FCS. After incubating with miR-29b mimic for 48 hours, cells was detached by trypsin/EDTA and put in micromass culture as in 2.2.2.5. After 24 hours of resting, miR-29b transfected micromasses were treated with either TGFβ1 (10ng/ml), IL-1 (5ng/ml), Wnt3a (100ng/ml) in different media (referred in 2.2.2.5) with 10% (v/v) heat inactivated FCS without antibiotics. At desired time, micromasses were harvested in 500µl Trizol reagent.

2.2.2.7.2.8. Co-transfection of reporter vectors with the miR-29 family mimic/ miR-29b inhibitor and stimulation with cytokines and growth factors

SW1353 were seeded into 96-well plate 1 day before transfection as in 2.2.2.7.2.1 and transiently co-transfected with: (1)100ng of reporter plasmids of either $p(CAGAC)_{12}$- luc, $I\kappa B_3$-luc, TOPflash, FOPflash, (2) 10ng of renilla luciferase reporter, and (3) 50nM of either miR-29a/b/c mimic, AllStar non-targeting negative control, miR-29b inhibitor, or inhibitor negative control. The protocol for transfection is as in 2.2.2.7.2.5. After 24 hours of transfection, cells was serum starved overnight and were treated with recombinant human TGFβ1 (4ng/ml), IL-1β (5ng/ml), Wnt3a (100ng/ml) for 6 hours. After stimulation, cells were harvested and a luciferase assay performed as in 2.2.2.8.

2.2.2.7.2.9. Cotransfection of pmiR-Glo-3'UTR reporter with the miR-29 family mimic

Chicken fibroblasts DF1 were plated in a 96-well plate (10^4cells/well) in antibiotic free growth media with 10% (v/v) FCS overnight. 100ng of either pmiR-Glo-3'UTR wild type

or mutant constructs were co-transfected with 50nM miR-29a/b/c mimic using the non-targeting Allstars as control. The protocol for transfection was described in 2.2.2.7.2.5. After 24 hours post transfection. DF1 cells were harvested for luciferase assay as in 2.2.2.8.

2.2.2.8. Luciferase reporter assay

At desire times post transfection, the plate was removed from the incubator. Luminescence was detected using the Dual-Luciferase Reporter Assay system (Promega, E1980). Briefly, the medium on the cells was removed. The cells were washed twice with ice cold PBS and 70µl of cell lysis buffer provided in the kit (Promega, E1980) was added to each well. The plate was gently rocked back and forth for 30 minutes. Then, 10µl cell lysates were transferred to a 96- well white microplate. For measuring firefly luciferase activity, 50µl of Dual Luciferase Reagent was added to each well. The firefly luminescence was measured using a microplate reader. For measuring Renilla luciferase activity, 50 µl of Dual Stop & Glo Reagent was added to each well and mixed gently then the luminescence measured.

After measurement of the firefly luciferase luminescence and Renilla luciferase luminescence, the relative luciferase activity was calculated as the ratio of the firefly activity normalized to the Renilla luciferase activity.

2.2.3. MicroRNA and mRNA microarray

2.2.3.1. MicroRNA and mRNA microarray for destabilization of medial menicus (DMM) model

Whole knee joints from mice which underwent DMM surgery (e.g. DMM-operated right knee and unoperated left knee) were subjected to total RNA isolation and grouped as DMM left (referred to as control) or DMM right (referred as treatment). At each time point (1, 3, 7 days after surgery), equal amounts of total RNA from each sample in the same group was pooled together. The integrity of the new pooled samples was checked before sending to Exiqon Services (Denmark) or Source Bioscience (UK) to perform miRNA microarray or mRNA microarray, respectively.

The miRCURY LNA^{TM} microRNA Hi-Power Labelling Kit Hy3^{TM}/Hy5^{TM} was used for miRNA microarray in which the Hy3^{TM} labelled samples and Hy5^{TM} labelled samples

were mixed pair-wise and hybridized to capture probes targeting all miRNAs or human, mouse and rat registered in the miBASE 18.0. For whole genome array, Illumina's BeadArray-based technology was employed by using MouseWG-6 v2.0 Expression BeadChips whose feature content derived mainly from NCBI reference sequence (NCBI refseq), and simultaneously profiles more than 45,000 mouse transcripts. The BeadChips consists of oligonucleotides immobilized to bead held in microwells on the surface of any array substrate, and made up with 50-mer-gene-specific probe plus 29-mer address sequences. Especially, the chip has high level of bead type redundancy (average 30 beads per probe) to control the quality and reproducibility of the direct hybridization assay.

2.2.3.2. Whole genome array for miR-29b gain and loss-of-function experiment

Human primary chondrocytes were transiently transfected with either miR-29b mimic or miR-29b inhibitor for 48 hours in triplicate. Then, total RNA was isolated and equal amounts of total RNA of each sample in the triplicate was pooled together. After checking the quality and integrity, the new pooled samples were sent to Source Bioscience (UK) to perform human whole genome profile. Again, the Illumina's BeadArray-based technology was employed but using humanHT-12 V4.0 expression BeadChips. Similarly, the feature content derived mainly from NCBI reference sequence (NCBI refseq) which simultaneously profile more than 47,000 human transcripts.

2.2.4. Data analysis

2.2.4.1. Pre-processing microRNA array data

2.2.4.1.1. VST transformation and quantile normalization

It is necessary to do background correction to remove non-specific signal from total signal. However, the initial data-pre-processing in the Illumina GenomeStudio solfware provides users with bead summary data in the form of a single signal intensity value for each probe. This value is calculated by subtracting the local background from the signal intensity of each bead, then taking the means of all beads containing a given probe. This means BeadStudio output data has undergone background correction. Thus, no further background correction need to be done for the Bead summary data, received from Source Bioscience (UK).

To reliably detect changes in expression from the whole genome array, it is important to remove sources of variation of non-biological origin between arrays to make data comparable. There are two types of variations might be seen when comparing arrays e.g. interesting variation (biological differences), and obscuring variation. Sources of obscuring variation were introduced during the process of carrying out the experiments e.g. **during preparing the samples** including mRNA extraction and isolation, variation in introduction and incorporation of dye, effected by pipetting error, temperature fluctuations and reagent quality; **during manufacturing of the array** including variation in the amount of probe present at each feature or spot and variation in the hybridization efficiency of the probes for their mRNA targets; **during hybridization of the sample on the array** including variation in the amount of samples applied to the array and variation in the amount of target hybridized to the probe; and after array hybridization including variation in optical measurement and intensity computed from the scan image. So, comparisons between different biological samples can be made, it is important to remove these obscuring variations to ensure the values being analysed reflect the biology. For Beadchip array data, the two steps to achieve this are commonly referred to as between-array normalization, and transformation. Two popular methods that implement these steps are VST transformation and quantile normalization for the Lumi packages. Briefly, for analysing, bead summary array data was imported into R studio (http://www.rstudio.com/). Array data was then transformed and normalized using Lumi package.

2.2.4.1.2. Sequence data

The miR-29 family mature sequence data was retrieved from miRbase database (http://www.mirbase.org/). 3'UTR sequences were downloaded from UCSC (https://genome.ucsc.edu/) and Ensembl (http://www.ensembl.org/index.html). RefSeq IDs were used to map probe sets to UCSC database and Ensembl Gene IDs were used to map probesets to the Ensembl database.

2.2.4.1.3. The MicroRNA-29 family target prediction

Three types of seed matches in the 3'UTR were considered when predicting direct miRNA-29 targets e.g. **6-mer seed match** which is 6nt in length and was complementary

to nucleotides 2 to 7 in the miR-29 family; **7-mer seed match** which is 7nt length and is complementary to nucleotides 1–7 in the miRNA or nucleotides 2–7 in the miRNA with "A" at the first position; and **8-mer seed match** which is 8nt length, and matched nucleotides 1–8 in the miRNA or nucleotides 2–8 in the miRNA with an "A" at the first position. For searching these seed matches in the 3'UTR, 3'UTR sequences were imported and read in R studios using the "*readDNAStringSet*" function in Biostring package. Also, three types of miR-29 family seed matches were searched using "*vcountPattern*"function.

In line with using R studios, some miRNA target prediction programs available were also used to predict targets for miR-29 including TargetScan (http://www.targetscan.org/), miRNA body map (http://www.mirnabodymap.org/), miRDB (http://mirdb.org/miRDB/), DIANA (http://diana.cslab.ece.ntua.gr/), Pictar (http://pictar.mdc-berlin.de/), miRbase (http://www.mirbase.org/).

2.2.4.1.4. Functional pathway analysis

DAVID (Database for Annotation, Visualization and Integrated Discovery) functional annotation tool (http://david.abcc.ncifcrf.gov/) was used to perform functional analysis for particular gene groups.

2.2.4.1.5. Statistical analysis

Unless otherwise stated, for the whole thesis, Student's unpaired t-test (two-tail) was performed to compare difference between two groups. All values are given as mean values of replicates with error bar representing the standard error of the mean. The statistical analysis was carried using GraphPad Prism version 4.0 for Windows. Levels of statistical significant are represented as * $\leq$ 0.05, ** $\leq$ 0.01, *** $\leq$ 0.001.

CHAPTER III
IDENTIFICATION OF THE MIR-29 FAMILY IN CARTILAGE HOMEOSTASIS AND OSTEOARTHRITIS

3.1. Introduction

MicroRNAs are referred to as the master regulators for gene expression: they exert their suppressive functions on targeting genes at the post transcriptional level through a sequence-complementary mechanism (Bartel 2009). In human chondrocytes, many different miRNAs are found and each of them are shown to directly and/or indirectly regulate hundreds of target genes, implicating a complex gene regulatory network in which miRNAs are involved (Le *et al.* 2013). This means that miRNAs take a crucial part in controlling the balance of the mRNA network in cartilage homeostasis; and the dysregulation of miRNA expression could trigger OA onset by disrupting this regulatory network.

Indeed, an essential role of miRNAs has been reported in various aspects of cartilage development, cartilage homeostasis, and also in OA pathogenesis (Le et al. 2013). For instance, knockout of Dicer, the pre-miRNA processing enzyme, in a cartilage-specific manner resulted in skeletal growth defects, premature death of mice, reduction in growth plate chondrocytes, and an increase in hypertrophic chondrocytes (Kobayashi et al. 2008). Mutation of the Dnm3 locus, transcribing the miRNAs miR-199a, miR-199*, and miR-214, resulted in growth retardation including craniofacial hypoplasia (Watanabe *et al.* 2008). Universal knockout of miR-140, a cartilage and skeletal-restricted miRNA lead to: mild craniofacial deformities and dwarfism; early onset of age-related OA development; greater susceptibility to OA with accelerated proteoglycan loss and fibrillation of articular cartilage (Miyaki et al. 2010, Nakamura et al. 2011). Transgenic mice overexpressing miR-240 in cartilage were resistant to antigen-induced arthritis-associated loss of proteoglycan and type II collagen (Miyaki et al. 2010). Other specific miRNAs: miR-9, miR-98, and miR-146 were highlighted to be expressed differentially in miRNA profiles between human OA cartilage and its normal articular counterpart (Iliopoulos et al. 2008, Jones *et al.* 2009); miR-199a, miR-675, miR-145, miR-140, miR-455 have been proven to function in chondrogenesis and cartilage homeostasis (Lin *et al.* 2009, Miyaki *et al.* 2009, Dudek *et al.* 2010, Martinez-Sanchez *et al.* 2012, Swingler *et al.* 2012); miR-222 is

reported to play a potential role in the articular cartilage mechanotransduction pathway (Dunn *et al.* 2009); miR-146a and miR-146b, whose expression is regulated by NFκB, appear to be the key miRNAs in the inflammatory response (Taganov *et al.* 2006); miR-34a, miR-194, miR-27b were reported to be induced by IL-1β (Abouheif et al. 2010, Akhtar *et al.* 2010, Xu et al. 2012). All of these data reveal miRNAs as important modulators of various aspects of articular cartilage homeostasis and OA pathogenesis.

OA develops slowly with time and may not be symptomatic until significant joint damage has occurred. Currently, there is a lack of effective approaches to OA prevention or treatment. Available treatments are limited to pain management, and joint replacement surgery, this latter in the late phase of the disease. MicroRNAs, with the ability to fine-tune the expression of multiple genes, could be a promising tool for therapeutic applications for a complex disease like OA. The down regulation of gene expression by miRNAs is relatively modest, thus the approach of combining multiple miRNAs to simultaneously target OA pathogenesis-relevant networks may be needed. Furthermore, There is growing evidence for future miRNA-based diagnostics: a number of miRNA in plasma were found at different levels between RA and OA patients (Murata *et al.* 2010); let-7e, miR-454, miR-886 were identified as differentially expressed circulating miRNAs in OA patients necessitating arthroplasty, especially, let–7e emerged as potential predictor for severe knee or hip OA (Beyer et al. 2014). However, there is a requirement for detailed investigations directed at diagnostic performance (sensitivity, specificity, accuracy) of these promising novel biomarkers before the measurement of miRNAs can enter the clinic.

With all of the above information, the essential roles of miRNAs in cartilage homeostasis and OA are shown with potential for clinical application. The insights into the roles of miRNAs in chondrogenesis, articular cartilage homeostasis, and OA initiation and progression are, nevertheless, still insufficient. Thus, there is a continuing need to deepen our understanding of the molecular mechanisms miRNAs are involved in cartilage homeostasis and OA. Investigating the disease directly in man is challenging due to e.g. the inability to harvest articular tissue at an early stage; the slow disease progression; the absence of symptoms in the early stage of the disease; the variety of symptoms; the variety of causes and environmental influence. Animal models mimicking features of OA are, therefore, an important alternative solution.

In an effort to identify novel miRNAs important in the development of OA, the murine Destabilization of Medial Meniscus (DMM) model was used to identify miRNAs differentially expressed at 1, 3, 7 days (i.e. early stages) after the surgery. Performing miRNA and mRNA profiling followed with an integrated analysis highlighted miR-29b as a candidate miRNA participating in the early onset of OA in DMM model. Alongside the DMM model, the role of the miR-29 family in cartilage homeostasis and OA was also investigated in other human and mouse models e.g. human end-stage OA cartilage, the murine hip avulsion injury model, a human primary chondrocyte dedifferentiation model, a human chondrogenesis model, and murine limb development.

Aims

- Performing miRNA and mRNA profiling in DMM model at very early time points 1, 3, 7 days after surgery
- Identifying miRNA potentially involve in OA onset by bioinformatics analysis
- Investigating the regulation of the miR-29 family which is highlighted from bioinformatics analysis above in human end-stage OA cartilage
- Determining the expression pattern of the miR-29 family in injury model
- Establishing if the miR-29 family involving in chondrocyte phenotype
- Determining the role of miR-29 in human and murine chondrogenesis
- Investigating the involvement of miR-29 in murine limb development

3.2. Results

3.2.1. The microRNA profile in the DMM model at 1, 3, 7 days after surgery

As little is known about the involvement of miRNAs at the early stage of OA, identifying miRNAs modulated in OA initiation was a major aim. Since mRNA profiles have shown large changes in gene expression even at 24 hours post surgery, the DMM model was used to investigate this.

Alongside DMM mice (mice whose medial meniscal tibial ligament of the right knee was transected whilst the left knee was untouched), naïve mice (receiving no treatment), and sham-operated mice (mice whose right knees were operated to visualize the medial meniscal tibia ligament but not transected) were used. Total RNA was first isolated from the whole knee joints of DMM mice (both right and left knees) and their controls at 3 different time points i.e. 1, 3, 7 days after surgery, and subsequently checked for quality and integrity. Unfortunately, RNA from naïve mice was degraded and not further studied. For miRNA profiling, an equal amount of total RNA from individual in each triplicate in the DMM right knee and DMM left knee group at 1, 3, and 7 days after surgery was pooled and these pools were subsequently subjected to miRNA microarray using the miRCURY LNA^{TM} microRNA Hi-Power Labelling Kit Hy3^{TM}/Hy5^{TM}, containing probes targeting all human, mouse and rat miRNAs registered in the miRBase 18.0.

Clustering analysis showed that: the miRNA profiles of the DMM right or left knees were clustered quite closely to each other at day 1 and 3 but far apart at day 7 (Appendix, Figure 1), suggesting that more miRNAs were modulated at the later time point than the earlier. In line with this, calculating the number of miRNAs which changed expression at each time point revealed the same pattern: only small changes were observed until 7 days post-surgery (Figure 3.1). Using 1.5 fold-change (FC) as the cut off, only four miRNAs significantly increased expression at day 1 and 3 whilst more than 30 miRNAs were modulated at day 7. The list of miRNAs which changed expression is listed in Table 3.1.

To visualize the expression pattern of miRNAs across the time course of the DMM model, unsupervised hierarchical clustering analysis was carried out for miRNAs that met the filtering criteria e.g. absolute FC > 1.3 in each time point. Several clusters of miRNAs were identified comparing between DMM right and left knee i.e. (i) miRNAs which **increased** expression across the time course (cluster 1, 2, 3) (Figure 3.2a, b, c), (ii)

miRNAs which **decreased** expression across the time course (cluster 5, 6) (Figure 3.2.e, f), (iii) miRNAs **which decreased** expression across 3 days but **increased** at day 7 (cluster 4) (Figure 3.2d) and (iv) miRNAs which **increased** until 3 days but **decreased** at day 7 (cluster 7) (Figure 3.2.g).

A subset of miRNA differentially expressed by microarray analysis was selected for revalidating the array data by quantitative real-time RT-PCR. The result confirmed the miRNA array data since a similar expression pattern between the two platforms for miR-140, miR-455 (data not shown) and miR-29b (which will be discussed below) was observed.

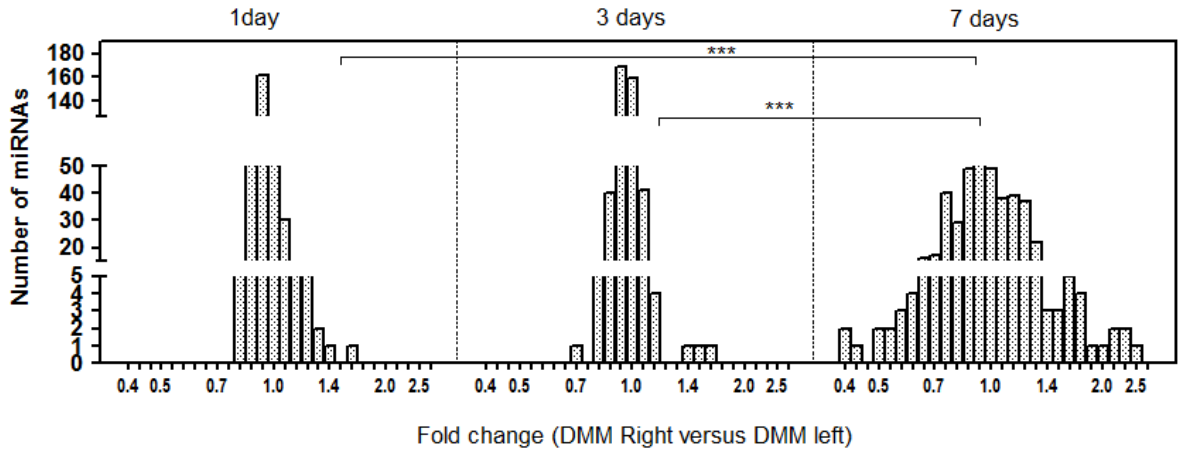

Figure 3.1: Modulation of miRNA expression across a 7 day time course

From the array data, for each miRNA, fold change (FC) was calculated by comparing its expression level in DMM right versus left knee. The number of regulated miRNAs were calculated for each of 0.05 interval of a (0.4, 2.5) range of FC. FC: > 1: increase expression; < 1: decrease expression. The difference in number of miRNAs modulated was calculated by unpaired two-tailed t test: * $p<0.05$, ** $p < 0.01$, *** $p<0.001$.

Day 1		Day 7	
miRNA	**FC**	**miRNA**	**FC**
miR-144-3p	1.7	miR-379-5p	2.6
miR-29b-3p	1.5	miR-127-3p	2.4
		miR-335-5p	2.4
		miR-370-5p	2.2
Day 3		miR-214-3p	2.2
miRNA	**FC**	miR-21-5p	2.1
miR-370-5p	1.7	miR-3073-3p	2.0
miR-21-5p	1.6	miR-199a-3p	1.9
		miR-214-5p	1.8
		miR-210-3p	1.8
		miR-455-3p	1.8
		miR-199a-5p	1.7
		miR-2137	1.7
		miR-199b-5p	1.7
		miR-136-5p	1.7
		miR-34a-5p	1.6
		miR-99b-5p	1.6
		miR-152-3p	1.5
		miR-34c-5p	1.5
		miR-144-3p	-1.5
		miR-3100-3p	-1.5
		miR-669c-3p	-1.6
		miR-378-3p	-1.6
		miR-3473b	-1.6
		miR-133a-5p	-1.6
		miR-3474	-1.7
		miR-378b	-1.7
		miR-133a-3p	-1.8
		miR-133b-3p	-1.8
		miR-1952	-1.9
		miR-491-3p	-1.9
		miR-1a-3p	-2.2
		miR-706	-2.3
		miR-3572	-2.3

Table 3.1: The list of miRNAs regulated in the DMM model with fold change higher than 1.5 (increase or decrease) at 1, 3, and 7 days after surgery.

Fold change (FC) was calculated by comparing between the DMM operated right and un-operated left knee. Down-regulated miRNAs are presented as negative FC.

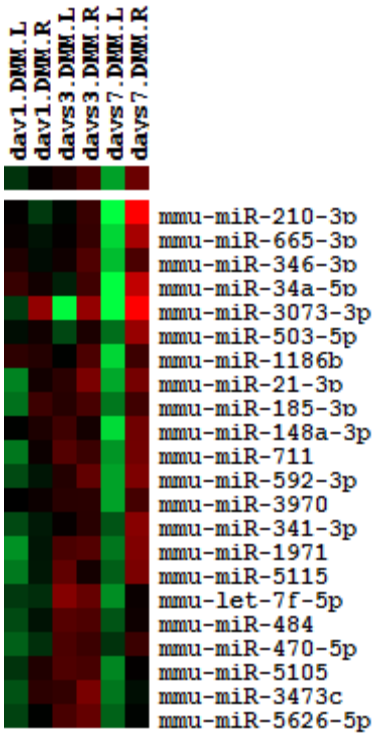
dav1.DMM.L
dav1.DMM.R
davs3.DMM.L
davs3.DMM.R
davs7.DMM.L
davs7.DMM.R
mmu-miR-210-3p
mmu-miR-665-3p
mmu-miR-346-3p
mmu-miR-34a-5p
mmu-miR-3073-3p
mmu-miR-503-5p
mmu-miR-1186b
mmu-miR-21-3p
mmu-miR-185-3p
mmu-miR-148a-3p
mmu-miR-711
mmu-miR-592-3p
mmu-miR-3970
mmu-miR-341-3p
mmu-miR-1971
mmu-miR-5115
mmu-let-7f-5p
mmu-miR-484
mmu-miR-470-5p
mmu-miR-5105
mmu-miR-3473c
mmu-miR-5626-5p

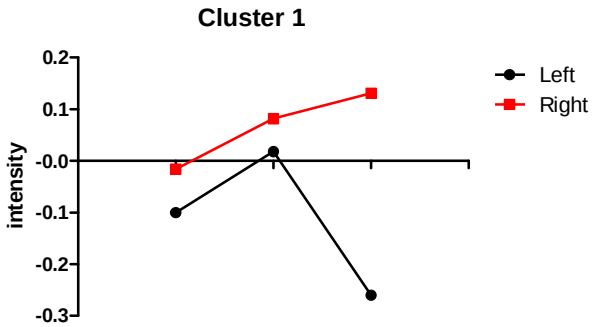
Cluster 1
intensity
0.2
0.1
-0.0
-0.1
-0.2
-0.3
Left
Right

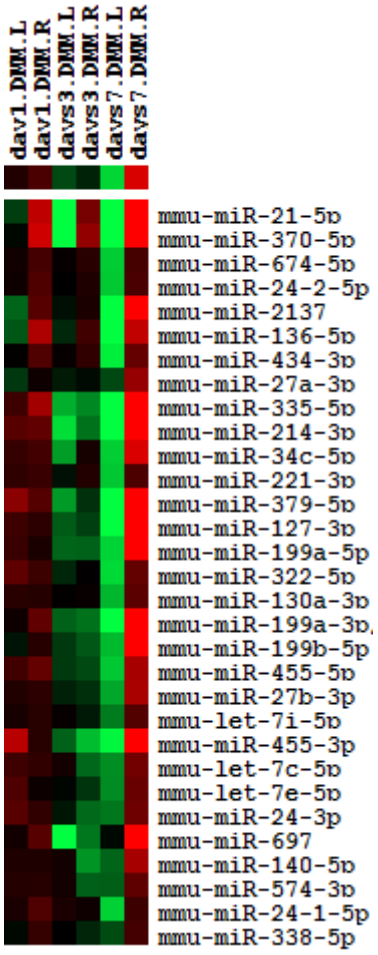
dav1.DMM.L
dav1.DMM.R
davs3.DMM.L
davs3.DMM.R
davs7.DMM.L
davs7.DMM.R
mmu-miR-21-5p
mmu-miR-370-5p
mmu-miR-674-5p
mmu-miR-24-2-5p
mmu-miR-2137
mmu-miR-136-5p
mmu-miR-434-3p
mmu-miR-27a-3p
mmu-miR-335-5p
mmu-miR-214-3p
mmu-miR-34c-5p
mmu-miR-221-3p
mmu-miR-379-5p
mmu-miR-127-3p
mmu-miR-199a-5p
mmu-miR-322-5p
mmu-miR-130a-3p
mmu-miR-199a-3p
mmu-miR-199b-5p
mmu-miR-455-5p
mmu-miR-27b-3p
mmu-let-7i-5p
mmu-miR-455-3p
mmu-let-7c-5p
mmu-let-7e-5p
mmu-miR-24-3p
mmu-miR-697
mmu-miR-140-5p
mmu-miR-574-3p
mmu-miR-24-1-5p
mmu-miR-338-5p

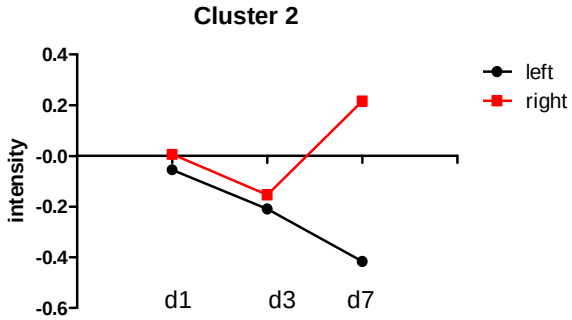
Cluster 2
intensity
0.4
0.2
-0.0
-0.2
-0.4
-0.6
d1
d3
d7
left
right

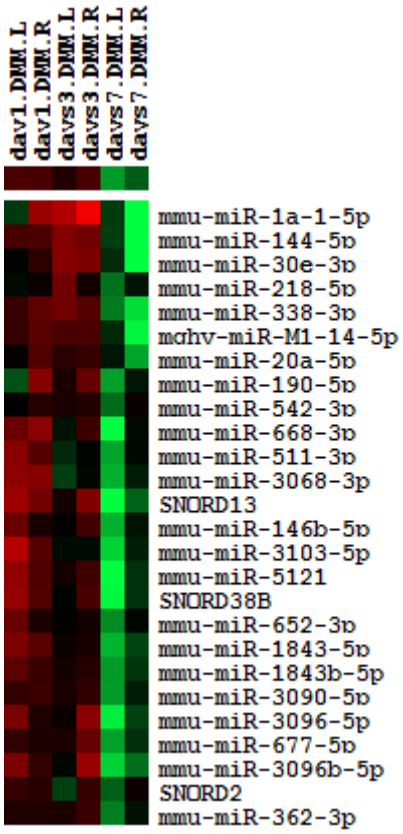
dav1.DMM.L
dav1.DMM.R
davs3.DMM.L
davs3.DMM.R
davs7.DMM.L
davs7.DMM.R
mmu-miR-1a-1-5p
mmu-miR-144-5p
mmu-miR-30e-3p
mmu-miR-218-5p
mmu-miR-338-3p
mghv-miR-M1-14-5p
mmu-miR-20a-5p
mmu-miR-190-5p
mmu-miR-542-3p
mmu-miR-668-3p
mmu-miR-511-3p
mmu-miR-3068-3p
SNORD13
mmu-miR-146b-5p
mmu-miR-3103-5p
mmu-miR-5121
SNORD38B
mmu-miR-652-3p
mmu-miR-1843-5p
mmu-miR-1843b-5p
mmu-miR-3090-5p
mmu-miR-3096-5p
mmu-miR-677-5p
mmu-miR-3096b-5p
SNORD2
mmu-miR-362-3p

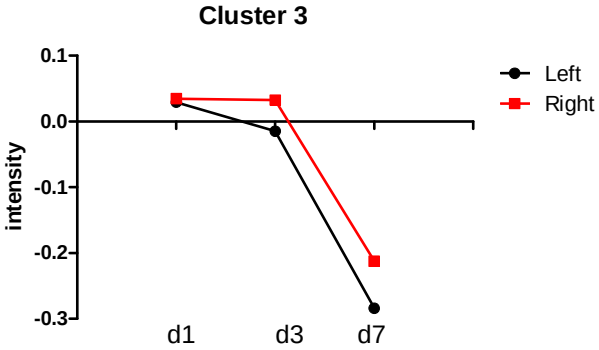
Cluster 3
0.1
0.0
-0.1
-0.2
-0.3
intensity
d1
d3
d7
Left
Right

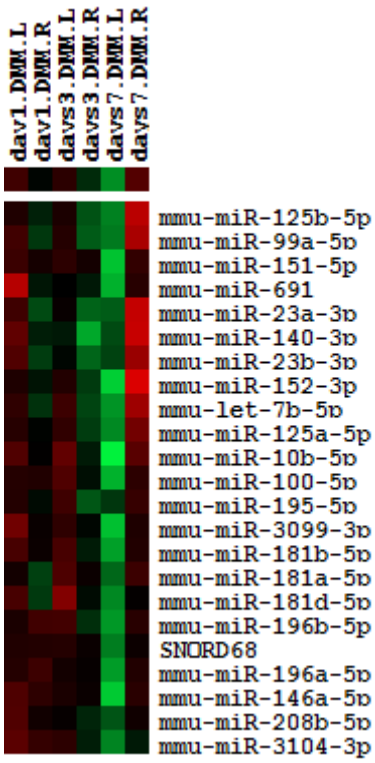
dav1.DMM.L
dav1.DMM.R
davs3.DMM.L
davs3.DMM.R
davs7.DMM.L
davs7.DMM.R
mmu-miR-125b-5p
mmu-miR-99a-5p
mmu-miR-151-5p
mmu-miR-691
mmu-miR-23a-3p
mmu-miR-140-3p
mmu-miR-23b-3p
mmu-miR-152-3p
mmu-let-7b-5p
mmu-miR-125a-5p
mmu-miR-10b-5p
mmu-miR-100-5p
mmu-miR-195-5p
mmu-miR-3099-3p
mmu-miR-181b-5p
mmu-miR-181a-5p
mmu-miR-181d-5p
mmu-miR-196b-5p
SNORD68
mmu-miR-196a-5p
mmu-miR-146a-5p
mmu-miR-208b-5p
mmu-miR-3104-3p

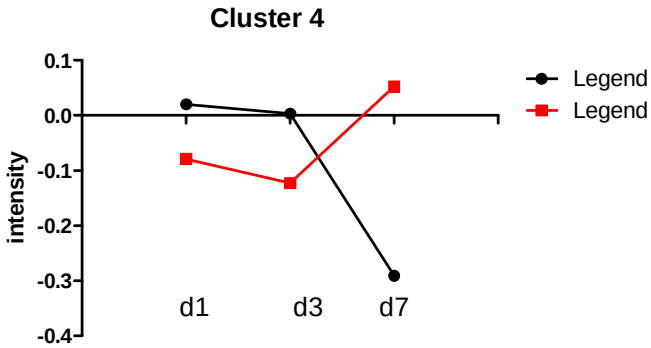
Cluster 4
0.1
0.0
-0.1
-0.2
-0.3
-0.4
intensity
d1
d3
d7
Legend
Legend

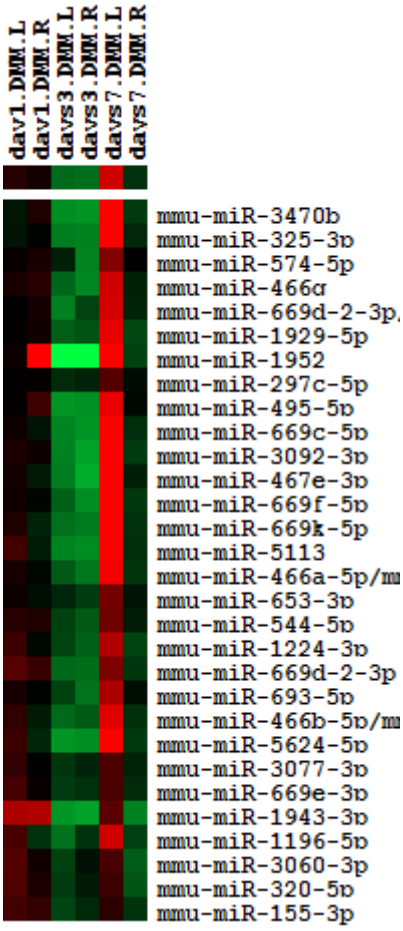
dav1.DMM.L
dav1.DMM.R
davs3.DMM.L
davs3.DMM.R
davs7.DMM.L
davs7.DMM.R
mmu-miR-3470b
mmu-miR-325-3p
mmu-miR-574-5p
mmu-miR-466a
mmu-miR-669d-2-3p
mmu-miR-1929-5p
mmu-miR-1952
mmu-miR-297c-5p
mmu-miR-495-5p
mmu-miR-669c-5p
mmu-miR-3092-3p
mmu-miR-467e-3p
mmu-miR-669f-5p
mmu-miR-669k-5p
mmu-miR-5113
mmu-miR-466a-5p/m
mmu-miR-653-3p
mmu-miR-544-5p
mmu-miR-1224-3p
mmu-miR-669d-2-3p
mmu-miR-693-5p
mmu-miR-466b-5p/m
mmu-miR-5624-5p
mmu-miR-3077-3p
mmu-miR-669e-3p
mmu-miR-1943-3p
mmu-miR-1196-5p
mmu-miR-3060-3p
mmu-miR-320-5p
mmu-miR-155-3p

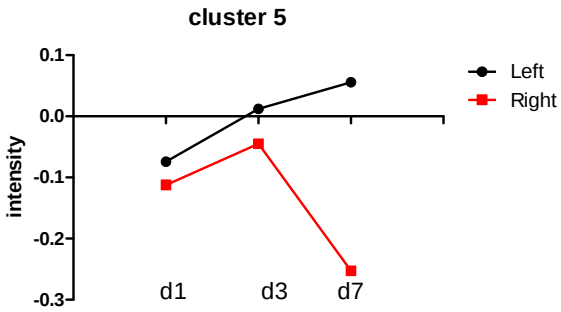
cluster 5
0.1
0.0
-0.1
-0.2
-0.3
intensity
d1
d3
d7
Left
Right

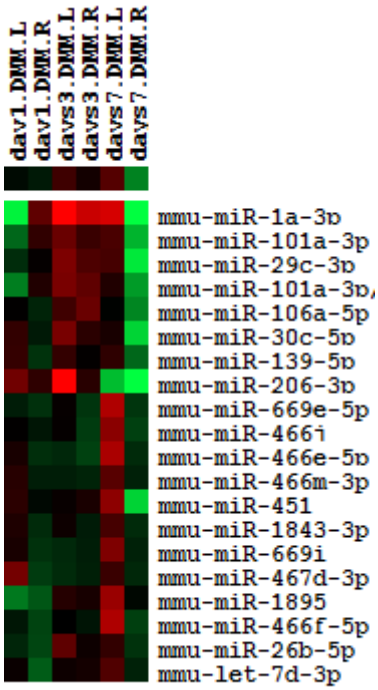
dav1.DMM.L
dav1.DMM.R
davs3.DMM.L
davs3.DMM.R
davs7.DMM.L
davs7.DMM.R
mmu-miR-1a-3p
mmu-miR-101a-3p
mmu-miR-29c-3p
mmu-miR-101a-3p
mmu-miR-106a-5p
mmu-miR-30c-5p
mmu-miR-139-5p
mmu-miR-206-3p
mmu-miR-669e-5p
mmu-miR-466i
mmu-miR-466e-5p
mmu-miR-466m-3p
mmu-miR-451
mmu-miR-1843-3p
mmu-miR-669i
mmu-miR-467d-3p
mmu-miR-1895
mmu-miR-466f-5p
mmu-miR-26b-5p
mmu-let-7d-3p

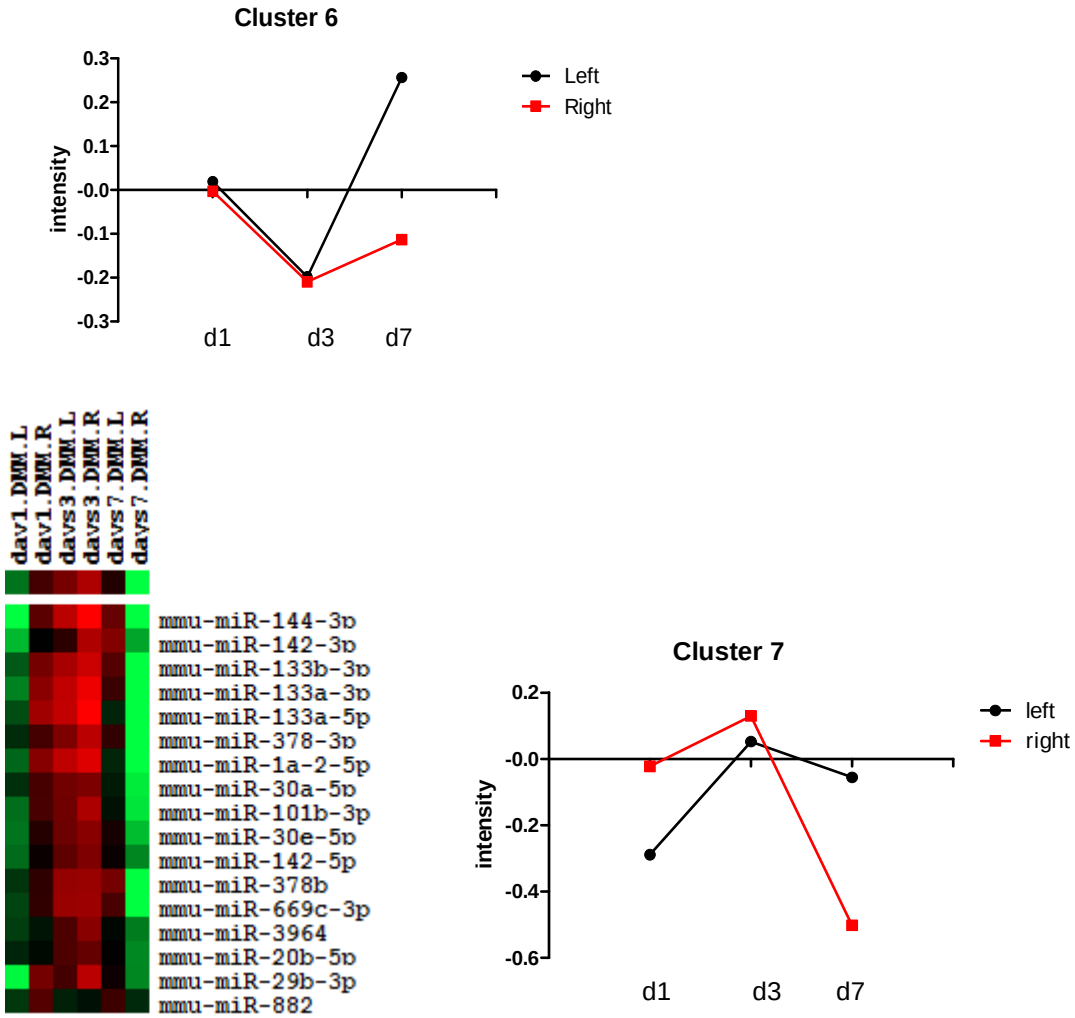

Figure 3.2: Unsupervised hierarchical clustering analysis for miRNAs with absolute fold change higher than 1.3.

Comparing DMM right versus left knee at 1, 3, 7 day time points: cluster 1, 2, 3: all the miRNAs induced expression; cluster 5, 6: all miRNAs decreased expression; cluster 4: miRNAs decreased across 3 days but increased at day 7; cluster 7: miRNAs increased across 3 days but decreased at day 7. Comparing between three time points: cluster 1: miRNAs increased across 7 days; cluster 2, 6: miRNAs decreased at day 3; cluster 3, 5: miRNAs decreased at day 7. SNORD: small nucleolar RNA.

3.2.2. Expression profile of mRNAs in DMM right and left knee

The microRNA microarray profiling revealed approximately 35 miRNAs modulated in the DMM model at 3 different time points, and whilst changes in expression are small, this may suggest that these miRNAs may have a role in regulating the onset of OA. For further filtering of miRNAs having important roles amongst these modulated miRNAs, examining the mRNA expression profile would be useful since miRNAs exert their function by directly targeting and subsequently inhibiting mRNA expression. Additionally, since no major modulation of miRNA expression level was observed until 7 days after DMM surgery, it was sufficient to profile mRNA expression for two time points i.e. 1 and 7 day following DMM surgery.

The Illumina BeadArray-based: MouseWG-6 v2.0 Expression BeadChip was used to profile more than 45,000 mouse transcripts in the pooled total RNA samples (DMM right and left knee), previously subjected to miRNA profiling. Consistent with the miRNA profile, mRNA array data also showed a similar expression pattern: no major change in mRNA expression level until day 7 when comparing between DMM right and left knee (Figure 3.3). If the absolute fold change cutoff is set at 1.5, only 30 mRNAs changed expression at day 1 whilst at day 7, more than 683 mRNAs were modulated. The full lists of mRNA which changed expression are in Appendix, Table 6, 7.

A subset of mRNA differentially expressed by microarray analysis was selected for revalidating the array data. Comparison of the expression levels between the mRNA microarray and quantitative real-time qRT-PCR demonstrated a similar expression pattern between the two platform for 4 genes i.e. *CCL2, IL6, SAA3, Arginase-1* (Appendix, Figure 2). These results confirmed the mRNA array data.

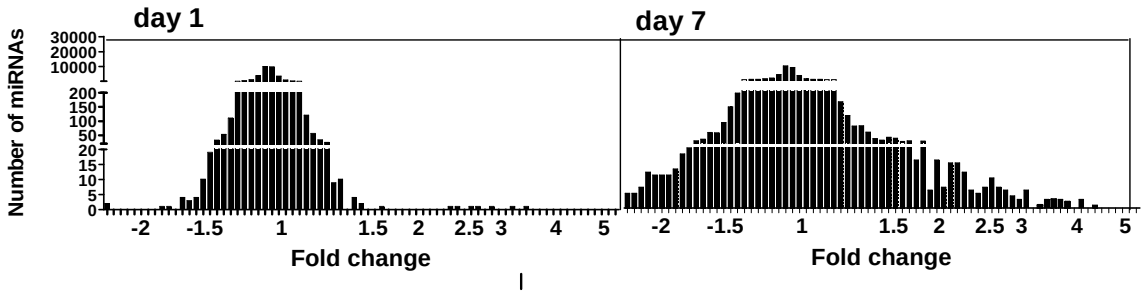

Figure 3.3 Total numbers of mRNAs at different fold change value at day 1 and day 7 following surgery in DMM model.

At each time point, Fold change = intensity value in DMM right - intensity value in DMM left. Numbers of mRNAs were calculated as fold change ranging from -3 to 7 for each increase of 0.05. Fold change: > 1: increase expression; < 1: decrease expression.

3.2.3. Integrated miRNA and mRNA expression profiles of the DMM model identify miR-29b as a miRNA associated with OA onset

To prioritize miRNAs which might have a role in OA onset in the DMM model, an integrated analysis between miRNA and mRNA profiles at 1 and 7 day of the DMM model was performed. This approach took advantage of inverse correlation analysis in which a miRNA was considered as a potential candidate if it was differentially expressed, and inversely correlated with the expression of its putative targets in the same biological samples.

Steps for the miRNA and mRNA profile integrating analysis include: (i) predicting miRNA putative targets by searching for 4 different types of seed sequences e.g. 6-, 7 match 8-, 7 A1-, and 8-mer seed sequences located in the 3' UTR; (ii) integrating expression levels at each time point in the DMM model for all miRNA targets; (iii) searching for a miRNA's putative target enrichment which is given more detail below.

If a miRNA has an impact in the pathological changes in the DMM model and could exert its suppressive function on variety of targets, then when it is down-regulated, there should be an enrichment of its predicted targets among up-regulated mRNA and vice versa. This means that for downregulated miRNAs, a greater percentage of upregulated mRNAs will be their targets and the inverse pattern will be observed for an upregulated miRNA. This should also be true when comparing between different time points, 1 and 7 days in the DMM model. For instance, if a miRNA was repressed across the 7 day time course, the percentage of its targets amongst up-regulated mRNA at day 7 should be higher than at day 1. Together with this, for a downregulated miRNA, an enrichment of miRNA targets in up-regulated mRNAs over unmodulated mRNAs should also be observed at each time point or across the time course.

Additionally, fold change threshold is another challenge faced in integrating analysis. In fact, it is almost impossible to choose the "right" cut off as the normal 1.5 fold change would be too stringent, and consequently, the power to detect potential miRNAs would be very low. To overcome this, in this study, all calculations were done for all fold change values greater than 1 at 0.05 fold intervals.

The integrating analysis for the miRNA and mRNA array data in the DMM model showed that amongst the differentially expressed miRNAs, miRNA-29b is the most interesting. Indeed, a substantial enrichment of miR-29b putative targets which was inversely correlated

with the miRNA expression level was observed at each time points (Figure 3.4, Figure 3.5). At day 1, when miR-29b increased expression, 6mer- and 7mer match 8- targets in the down-regulated section were dominant compared with the up-regulated section (Figure 3.4). Conversely, at day 7, when miR-29b decreased expression, there was a strong enrichment of targets with 4 different types of seed sites in the up-regulated section over the down-regulated (figure 3.4). Also at day 7, the ratio up-regulated targets/unchanged targets was substantially higher than the ratio down-regulated targets/unchanged targets (Figure 3.5).

The inverse correlation between miR-29b and its potential targets was also observed across the time course: whilst miR-29b level was down-regulated from day 1 to day 7, there was a substantial increase of miR-29 targets in the up-regulated mRNAs at day 7 compared with day 1. Consistent with this, the ratio up-regulated targets/unchanged targets showed an enrichment at day 7 (Figure 3.5). All of the data above suggest that miRNA-29b has a potential functional role in OA onset in the DMM model and was selected as the candidate miRNA for further functional studies.

From miRNA microarray data, miR-29b is the one on two miRNAs increased expression with 1.5 fold change at day 1 following DMM surgery. Real-time qRT-PCR was used to re-measure expression level of miR-29b in the DMM samples and sham surgery samples. The Real-time qRT-PCR data confirmed miRNA microarray data and showed a significant increase of miR-29b expression level in DMM right compared with left knee or sham surgery (Figure 3.6).

MicroRNA-29b is a member of the miR-29 family including miR-29a and miR-29c with the mature sequences differing at nucleotide positions 10, 18, 21, 22, or 23 but sharing a common seed sequence for target recognition. We hypothesized that not just miR-29b but all members of miR-29s may contribute to OA onset, as all miRNA-29s showed a downward trend at all 3 time points even though the difference did not reach statistical significance. Therefore, in this study, we investigated the link between all miR-29 members with OA rather than just miR-29b alone.

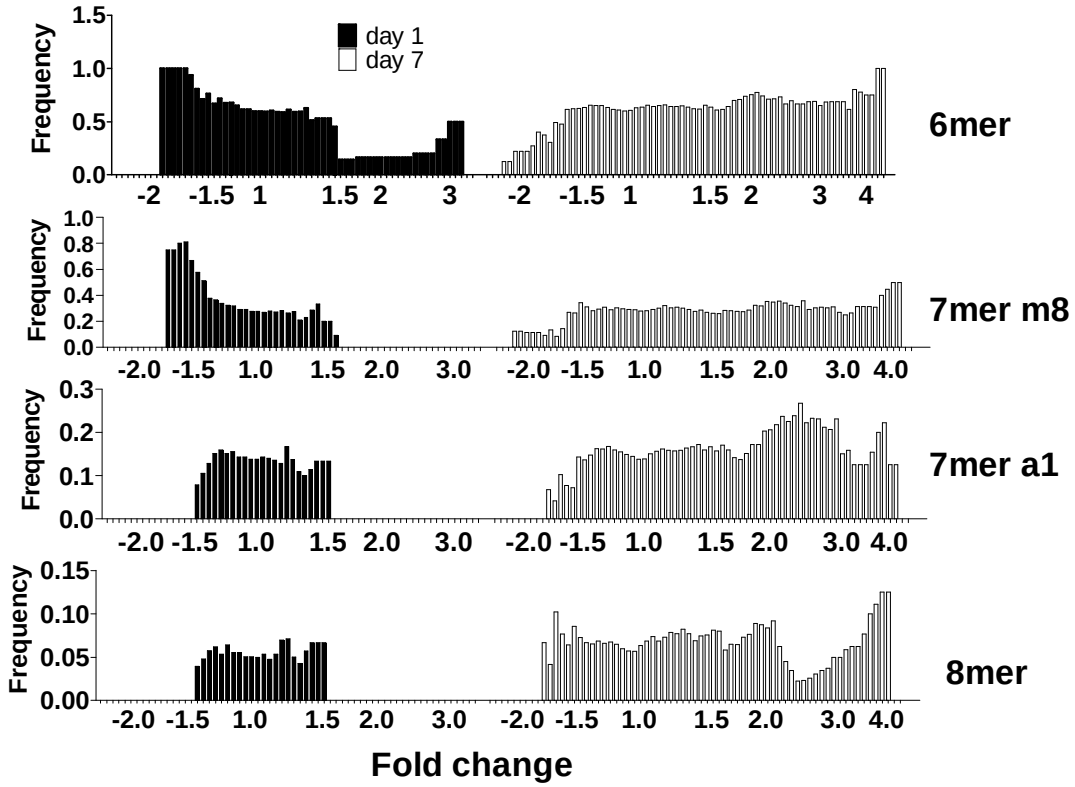

Figure 3.4 Percentage of miR-29 predicted targets in differentially expressed mRNA at day 1 and day 7 after surgery in DMM model.

The calculation was done for all the fold changes ± 0.05 from -2.5 to 4.0 and for each type of seed sequence e.g. 6mer, 7mer match 8, 7mer a1, 8mer. The mRNA having more than one binding site for each type of seed sequence was always assigned as 1. At k fold change, the percentage of 6mer-seed-site targets in modulated mRNAs was calculated: **a_6mer**= sum of mRNA having 6mer-seed site sequence in their 3'UTR with the fold change in the range (k, k+0.05); **b_k**= sum of mRNA with the fold change in the rank (k, k+0.05); **Freq= a_6mer/b_k**. The percentage of other seed site targets was calculated similarly. Day1: closed bar, day 7: opened bar.

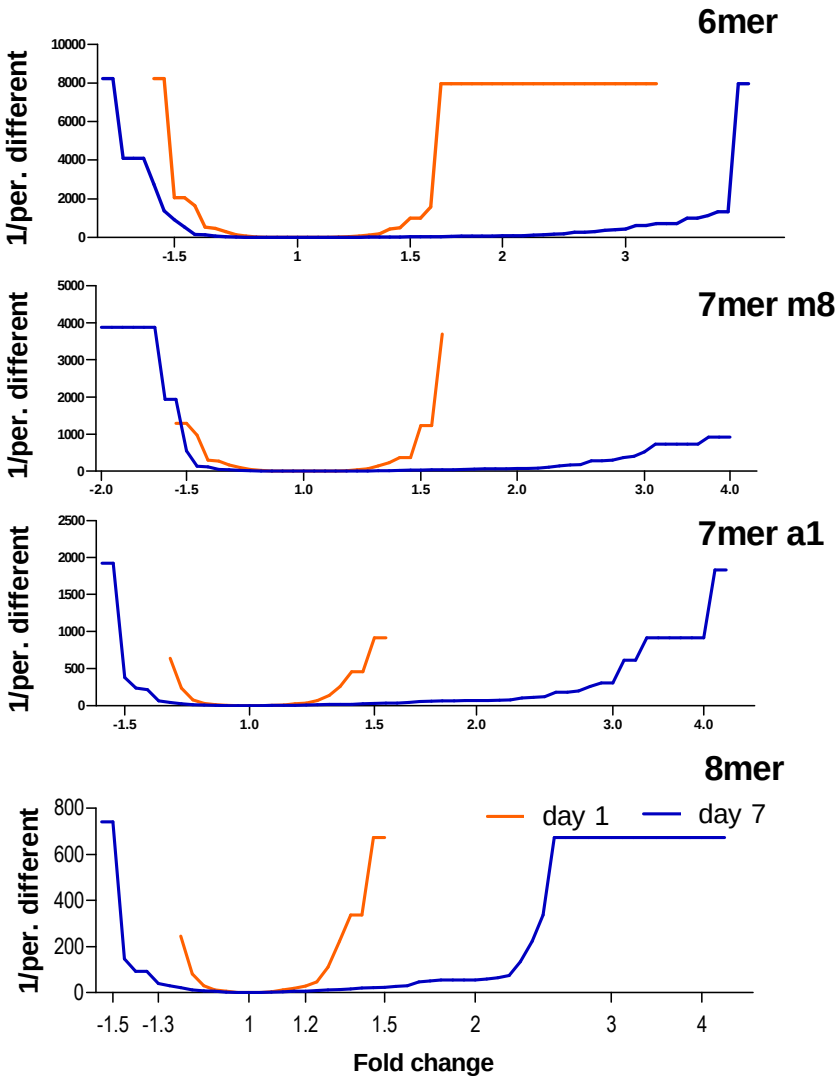

Figure 3.5 Percentage of miR-29 targets that changed expression compared to unchanged expression at day 1 and day 7 after surgery in DMM model.

The calculation was done for all the fold change (FC) ± 0.05 from each other from -2.5 to 4.0 and for each types of seed sequence e.g. 6mer, 7mer match 8, 7mer a1, 8mer. The mRNA having more than one binding site for each type of seed sequence was always assigned as 1. When FC=k, the percentage of 6mer-seed-site targets which increased or decreased expression was calculated: **6mer_changed** = sum of mRNA having 6mer-seed site sequence in their 3'UTR with FC in the range (k, FC max) if k >0, or (FC min, k) if k<0; **6mer_unchanged** = sum of mRNA having 6mer-seed site sequence in their 3'UTR with FC range in (0,k] if k>0, or (k, 0] if k< 0; **1/Per.different = 6mer_unchange/6mer_changed.** The percentage of other seed site targets was calculated similarly. Day1: red line, day 7: blue line.

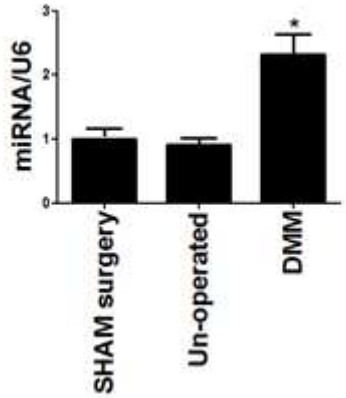

Figure 3.6: MicroRNA 29b was significantly induced in the DMM model at 1 day after surgery

Total RNA was reversed transcribed to cDNA and miR-29b expression was measured by real-time qRT-PCR in individual samples of sham right knee (sham surgery), DMM left knee (un-operated), and DMM right knee (DMM) at 1 day after surgery. U6 was used as endogenous control. Expression level of miR-29b in DMM and sham surgery was normalized to un-operated control. The data show mean +/- SEM, n=3. The expression of miR-29b between each group was analysed by unpaired two-tailed t test * $p<0.05$, ** $p < 0.01$, *** $p<0.001$.

3.2.4. Up-regulation of miR-29s in the murine hip avulsion injury model

Traumatic joint injury and joint magliment are linked to OA initiation. Patients with traumatic joint injury show an increased risk of OA, implicating the early events post-injury as important in the long term. To investigate the role of miR-29s in the onset of OA, a murine hip cartilage avulsion injury model, where the murine hip femoral cap cartilage was sub-cultured in serum-free media across a 48 hour-time course, was used. Total RNA was isolated from the explants using Trizol, reverse transcribed to cDNA by either SuperScript II reverse transcriptase (for mRNA detection) or miRCURY LNA^{TM} Universal cDNA synthesis (for miRNA detection). Expression levels were measured by real-time qRT-PCR.

The majority of the genes rapidly induced in murine joints following surgical destabilization (DMM model) were also regulated in murine hip cartilage explants upon injury (Chong et al. 2013). Interestingly, some genes such as *Dkk3, Ccl2, Il6* were significantly regulated after 3 hours in culture (Appendix, Figure 3) though likely regulating genes which are modulated at later time points. The expression pattern of the miR-29 family is similar to each other and tends to increase across the 48 hour time course (Figure 3.7): miR-29b and 29c significantly increased expression after 12 hours in culture; miR-29a significantly after 6 hours. This suggests that the regulation of the miR-29s may contribute to the molecular mechanism underlying the initiation of OA.

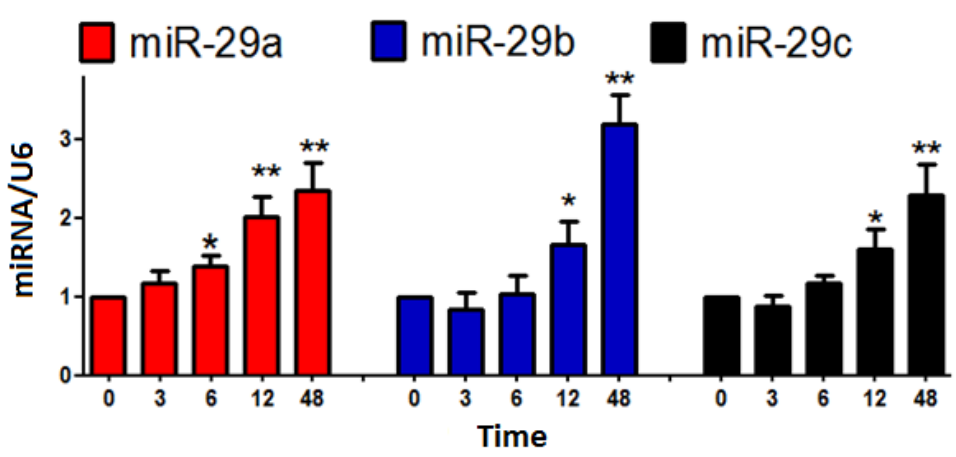

Figure 3.7: Expression of the miR-29 family in the hip avulsion injury model

The femoral caps of C57Bl/6 mice aged 4 weeks were avulsed and put in culture. At each of 3, 6, 12, 48 hour time points, the femoral caps were harvested. Total RNA was isolated using Trizol and reverse transcribed to cDNA. Expression of the mature miR-29 family was measured by real-time q-RTPCR where U6 was used as an endogenous control. At least triplicate samples were measured at each time. Means ± standard errors are presented, n=6. Difference in expression between each time point against control (t=0) was calculated by unpaired two-tailed t test. * $p<0.05$, ** $p < 0.01$, *** $p<0.001$.

3.2.5. Up-regulation of the miR-29 family in human end-stage OA cartilage

To determine whether the miR-29 family could play a role in human OA, its expression level was compared between hip / knee OA cartilage and non-disease tissue controls (hip cartilage followingfracture to the neck of femur).

Human articular cartilage samples (total: 8 hip and 7 knee OA cartilage, 7 healthy fracture to the neck of femur) were obtained from patients undergoing total hip/ knee replacement surgery at the Norfolk and Norwich University Hospital. Total RNA was isolated from all cartilage samples using Trizol and followed by a purification step through column using miRVana kit. The total RNA was reverse transcribed to cDNA using miRCURY LNA™ Universal cDNA synthesis. Expression of all miR-29 members was measured by real-time qRT-PCR with U6 as the endogenous control.

Data (Figure 3.8) showed an increase in miR-29 expression in hip OA but decrease in knee OA cartilage compared to fracture control. This reached significance, or close to significance in each case. Whilst there is no comparison with normal knee cartilage, these data show that the miR-29 family is regulated in human end-stage OA cartilage.

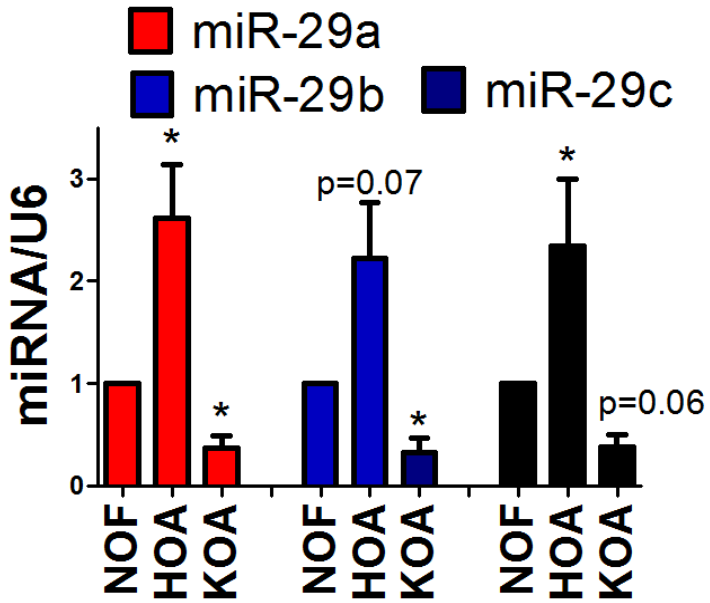

Figure 3.8: Expression of the miR-29 family in human OA cartilage

Total RNA was isolated from human articular cartilage of either end-stage OA patients or healthy controls and reverse transcribed to cDNA. Expression of the mature miR-29 family was measured by real-time qRT-PCR using U6 as an endogenous control. HOA (hip osteoarthritis cartilage, n=8), KOA (knee osteoarthritis, n=7), NOF (neck of the femur, n=7). Means ± standard errors are presented. Difference in expression between each time point against control (NOF) was calculated by unpaired two-tailed Student's t test. * $p<0.05$, ** $p < 0.01$, *** $p<0.001$.

3.2.6. The miR-29 family is regulated with chondrocyte phenotype

Dedifferentiation and the loss of phenotype is an obstacle in expanding human chondrocytes: the cells stop expressing aggrecan and collagen type II, and this limits capacity to form cartilage. In line with this, alteration chondrocyte phenotype is one of the characteristics of OA. As compared with normal articular cartilage, the chondrocytes embedded in different zones of OA cartilage were shown to express different markers of chondrocyte differentiation: chondrocytes in the middle zone re-expressing chondroprogenitor phenotype; cells in the upper middle zone expressing type III collagen (dedifferentiated phenotype) (Aigner *et al.* 1993). Assessing whether the miR-29 family is regulated with chondrocyte phenotype, therefore, would help to further determine the relevance of the miR-29 family in cartilage function.

This was investigated using human primary chondrocyte dedifferentiation model. After isolation from human knee OA cartilage by collagenase (collagenase-post digested HACs (PD)), primary chondrocytes were cultured in monolayer (primary culture HACs (P0), and three sequential passages were performed at 1: 3 dilution of cells (passage 1 to passage 3). Total RNA was isolated from cartilage, PD, P0 to P3 chondrocytes and reverse transcribed to cDNA. The expression level of all the miR-29 family was then measured by real-time qRT-PCR.

The expression of the miR-29 family was found to significantly decrease when HACs were passaged in monolayer (Figure 3.9), indicating the putative role of the miR-29 family in chondrocytic phenotype.

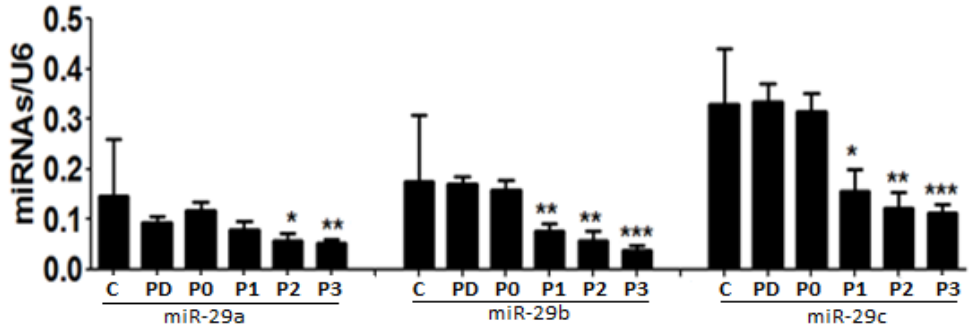

Figure 3.9: Expression of the miR-29 family in a chondrocyte dedifferentiation model

Human primary chondrocytes were isolated from the articular cartilage of 8 knee OA patients using collagenase digest. The cells were put in culture and passaged 3 times. Total RNA was isolated from either human articular cartilage (cart) or chondrocytes post digestion with collagenase (PD) or each passage 0, 1, 2, 3 (P0, P1, P2, P3). After reverse transcribing to cDNA, expression of the mature miR-29 family was measured by real-time qRT-PCR (U6 was used as an endogenous control). Mean ± standard errors are presented, n=8. Different in expression between was calculated by unpaired two-tailed t test. * $p<0.05$, ** $p < 0.01$, *** $p<0.001$.

3.2.7. MicroRNA-29s expression in chondrogenesis

Chondrogenesis is the earliest phase of skeletal development, occuring as a result of: mesenchymal cell condensation, chondroprogenitor cell differentiation, chondrocyte differentiation and maturation. Chondrogenesis results in the formation of cartilage and bone in the process of endochondral ossification (Goldring *et al.* 2006). It is pertinent to examine the role of miR-29 in chondrogenesis, particularly since the replay of this developmental process may contribute to osteoarthritis.

To determine the expression and therefore possible role of the miR-29 family in chondrogenesis both human and mouse chondrogenesis models were used. **Human chondrogenesis model**: human bone marrow stem cells were differentiated to form a cartilage disc (the model was kindly developed by Dr Matt J. Barter (Newcastle University, UK)); **Mouse chondrogenesis model**: the embryonic carcinoma cell line ATDC5 was stimulated to from chondrocytes using insulin for 42 days (this model was developed by Dr Tracey Swingler (University of East Anglia)). Total RNA was isolated, reverse transcribed to cDNA and used for measuring expression level of the miRNA by real-time qRT-PCR.

In the human chondrogenesis model, a significant down-regulation of the miR-29s after 3 days of differentiation was observed; after that, miR-29s return to the original expression levels (Figure 3.10). A similar expression pattern was also observed in the murine ATDC5 chondrocyte differentiation model: significantly decreased expression of all the miR-29 members after 14 days differentiation; with a return after 36 days, to the original level (Appendix, Figure 4). These data imply that miR-29 may be a negative regulator of the early stage of chondrogenesis.

Indeed, the miR-29 family was not the only miRNA regulated in either the human or murine chondrogenic process, many other miRNAs were strongly modulated e.g. (Barter et al, unpublished data) (Swingler et al. 2012). However, it can be postulated that the miRNA would have a functional role in chondrogenesis if it had affected on mRNA expression. To test this hypothesis, again an integrating analysis approachs (using mRNA expression profile data to analyse miR-29 putative target genes) was used. A substantial enrichment of miR-29 targets was inversely associated with the expression of miR-29s was observed (Data not shown). Together, these data suggest that the miR-29 family acts as the negative regulator of chondrogenesis, leading to an increase in mRNA to enable the process.

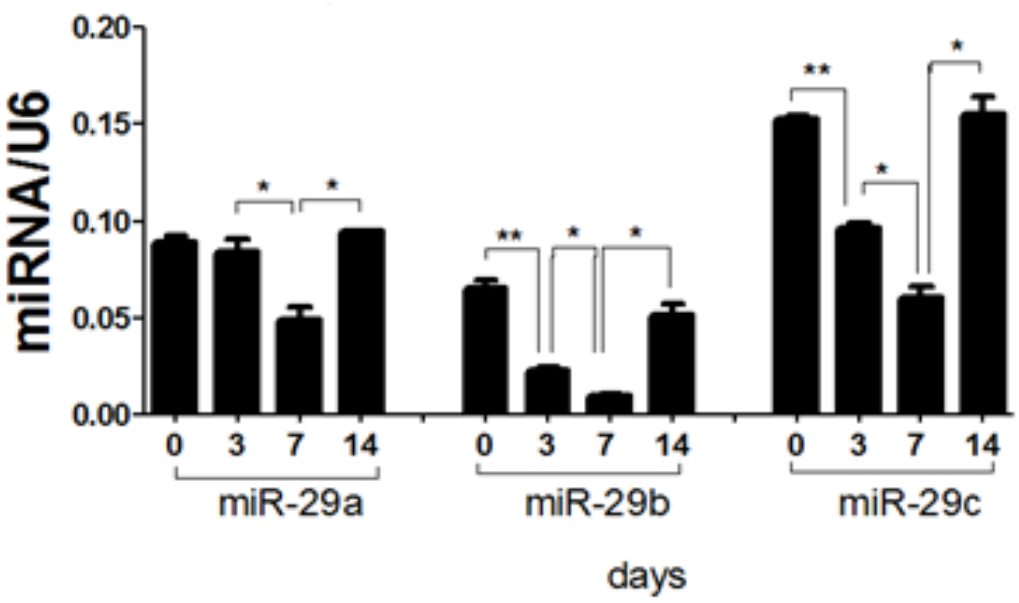

Figure 3.10: Expression of the miR-29 family in the human chondrogenesis model.

Human bone marrow stem cells (from 3 donors, 18-25 years of age, $5x10^5$ cells in 100µl growth medium) were put into polycarbonate Transwell filters and centrifuged in 24 well plates. 0.5ml chondrogenic culture medium containing 100µg/ml sodium pyruvate, 10ng/ml TGFβ3, 100nM dexamethasone, 1x ITS, 40µg/ml proline, and 25µg/ml ascorbate-2 phosphate was added to the lower well. Media were replaced every 2 or 3 days up to 14 days. At 0, 3, 7, 14 days, the cells were harvested and total RNA was extracted using Trizol. The RNA was then reverse transcribed to cDNA and was used for measuring the expression level of the mature miR-29 family by real-time qRT-PCR (U6 was used as an endogenous control). Assays were repeated 3 times. At least triplicate samples were in each time. Means ± standard errors are presented. Difference in expression between each time point was calculated by unpaired two-tailed t test. * $p<0.05$, ** $p < 0.01$, *** $p<0.001$.

3.2.8. The miR-29b is expressed in murine limb development

The formation of the skeleton first is initiated with the formation of a precartilage condensation (anlagen) which is followed by chondrogenesis triggered in the precartilage condensation and ultimately cartilage is formed. This process involves the cooperation of many cell activities e.g. migration, adhesion, intracellular signalling, and proliferation (Goldring et al. 2006). Given the likely involvement of the miR-29 family in chondrogenesis, it is pertinent to ask whether miR-29s are expressed in murine limb development. Additionally, the miR-29 family or its members have been shown to control cell proliferation and apoptosis in different tumour types. A murine model would thus be a useful model to study the role of the miR-29 family in cell proliferation and apoptosis limb development.

In mice, the forelimb starts to develop at stage E9.5 whilst the hindlimb starts behind by about half a day. Five days later, a miniature model of the adult limb is formed (E14.5 and E15 for fore and hindlimb, respectively). At stage E11, a distinct apical ectodermal ridge at the limb tip is formed in the forelimb and the handplate is beginning to form at E11.5. Similarly events happen in the hindlimb at half a day later (at E11.5 and E12) (Martin 1990).

Whole mount *in situ* hybridization was conducted using amiRCURY LNA^{TM} miR-29b-3p double-DIG labelled probe to detect the expression of miR-29b in the mouse embryo stage E11.5 and E15. The data showed that: at stage E11.5, miR29b was expressed in the cartilage of both fore and hindlimb; at stage E15 when the small scale the adult limb was formed, miR-29b was strongly expressed, implicating miR-29b playing a role in murine limb development. Besides limbs, miR-29b was also found on the brain and the spine of embryo stage E11.5 (Figure 3.11).

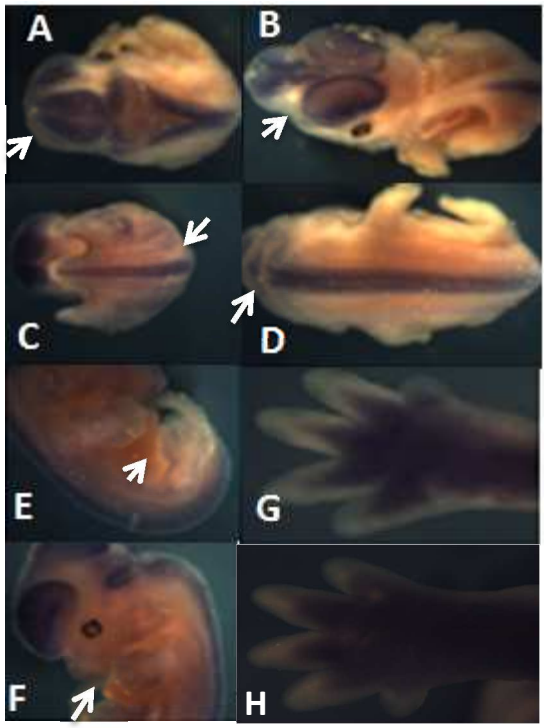

Figure 3.11: Whole mount *in situ* hybridization of miRNA-29b in murine embryo stage E11.5 and E.15.

Using a miRCURY LNA^{TM} double-DIG labelled miR-29b probe, miR-29b was found to be expressed: in the embryo stage E11.5 in the brain (A), mouth (B), spine (C-D), hindlimb (E), forelimb (F); in the embryo stage E15 in hindlimb (G) and forelimb (H).

3.3. DISCUSSION

The principal aim of this study was to begin to identify the miRNAs which were implicated in the early stages of OA and elucidate their function. Whilst there have been a number of studies on the role of miRNAs in OA pathogenesis, they have not focused on the disease onset. In the present study, for the first time, the miRNA expression profile was reported for the DMM mouse model at early time points e.g. 1, 3, 7 days following surgery. The fact that only a small number of miRNAs changed expression across the first three days after DMM surgery might indicate miRNAs mainly contribute in disease progression rather than initiation. However, there are some limitations of the study which prevent a firm conclusion about the role of miRNAs in the early stages of the disease. Total RNA for the miRNA microarray was isolated from whole knee joints of DMM mice. Thus, if a miRNA is expressed in a single tissue e.g. cartilage, bone, meniscus, ligament or synovium, pooling of tissues will reduce the signal to a lower level than in the individual tissue and that could be the explanation for the overall low levels of modulated miRNAs observed in the present study. Moreover, insufficient controls, e.g. naïve samples and genes responding to sham surgery in this study may also have been problematic. The DMM model does not completely recapitulate human OA pathogenesis, e.g. with more synovial involvement in the latter.

However, it remains unlikely that the miRNA microarray data acquired from the DMM model in this study is incorrect. The DMM left knee (no surgery) used as a control would show the consequence of surgery, even if it can't distinguish injury per se from early OA. Moreover, Burleigh et al (2012) reported a large and significant difference in expression levels of e.g. *Ccl2, Arg1e, Il6, Saa-3* in the same DMM model just 6 hours following surgery, which was interpreted as response to surgical destabilization rather than reaction to injury (Burleigh *et al.* 2012). In this study, such an increase in expression was also observed when comparing between the DMM right and DMM left, suggesting that the DMM left knee can act as a suitable control. Hence, it was expected that the changes in miRNA expression at early time points would be greater.

MicroRNA-29b, one of only two miRNAs significantly increased in expression at day one post-surgery and inversely correlated with expression of its putative targets, was investigated in detail. The miR-29b is encoded by two loci in the human genome e.g. the primary miR-29-a/b1 cluster in chromosome 7, and the primary miR-29b2/c cluster in chromosome 1.

Normally, clustered miRNAs in humans work in combination to accomplish their function. At the transcriptional level, at least one of the other miR-29 family members i.e. miR-29a or miR-29c will be co-transcribed with miR-29b. In addition, miR-29b is reported to have a short half-life (the time taken for the miRNA to fall to half of its original value) which is linked to the presence of uracil bases at positions 9-11, compared with miR-29a (more stable with a reported half-life of > 12 hours) (Zhang *et al.* 2011). Thus, in the DMM model at 1 day after surgery it would be expected that a significant increase in either miR-29a or miR-29c would accompany that of miR-29b. However, only miR-29b increased in expression (1.5 fold change in array data) but not any of the other miR-29 family members, perhaps implicating another post-transcriptional regulatory mechanism controlling miRNA processing. In line with the DMM model data, in a murine hip avulsion injury model, an increasing expression level was also observed for all miR-29 members post injury. Interestingly, a similar pattern of expression of some genes strongly induced in the DMM model at 6 hours after surgery (Burleigh et al. 2012) was seen in the injury model suggesting some molecular similarities between the two models. In line with this, Chong et al (2013) also observed a similar pattern when measuring the expression of the set of gene induced expression in DMM model 6 hours after surgery and in murine injury model in which the hip cartilages cultured for 6 hours (Chong et al. 2013). Since mechanical factors following traumatic joint injury may mediate OA onset, these data suggest for the first time an important role for the miR-29 family in the initiation of OA. The fact that the miR-29 family increased in expression in human OA end-stage cartilage supports a role for the miR-29s in the disease. In this study, human knee cartilage normal controls were not available, and the difference in hip and knee cartilage may explain in part why the miR-29 family levels increased in hip but decreased in knee OA cartilage compared to human hip fracture control. Also, in this project, the miR-29 family expression level is very variable across a human tissue panel e.g. heart, brain, lung, spleen (data not shown). In supporting these data, previous published data also demonstrated the different expression level of the miR-29 family in different tissues in zebrafish (Wienholds *et al.* 2005). These data suggest that the mechanisms controlling the miR-29 family expression in different tissues are not similar. The fact that miR-29 family expression was modulated in different mouse models and in human OA cartilage implies a role for the miR-29 family in cartilage, and suggest that the two pri-miR-29a/b1 and pri-miR-29b2/c clusters may be involved in both early and late stages of the disease. The direct mechanism

controlling miR-29 family expression and the extent to which each cluster contributes to OA remains unknown and is worthy of further investigation.

This study also provides evidence for the role of the miR-29 family in cartilage formation as its expression was regulated during human and mouse chondrogenesis and inversely correlated with its putative targets. In fact, such decreased expression level at an early stage of chondrogenesis is in line with published data e.g. Guerit et al (2013) showed the decreased expression of miR-29a is essential for chondrogenesis via its regulation of FOXO3a (Guerit *et al.* 2014); Sorentino et al (2008) found miR-29b was among miRNAs down-regulated when differentiating human MSCs through chondrogenesis (Sorrentino et al. 2008); Yan et al (2011) demonstrated that both miR-29a and miR-29b were significantly decreased in a chondrogenesis model where mouse MSC were grown on polyhydroxyalkanoates (Yan et al. 2011). However, I have demonstrated for the first time that all miR-29 family members are involved in chondrogenesis, stressing the important role of both miR-29 clusters in controlling cartilage homeostasis in human and mouse. In contrast to this data, there are others studies profiling the expression of miRNAs in murine and human chondrogenesis model (Suomi et al. 2008, Lin et al. 2009, Miyaki *et al.* 2009, Lin et al. 2011, Yang et al. 2011). The miR-29 family, nevertheless, was not amongst the miRNAs which had altered expression. This is not surprising and could be attributed to differing design of experiments including inducers of differentiation, cell type, numbers of detected miRNA probes and organism. In addition, despite of being a negative regulator of chondrogenesis, miR-29b was found to express in murine limb development. A number of published data report that the miR-29 family can act as oncogenes whose expression induces cell proliferation but inhibits apoptosis. Whether the miR-29 family is involved in murine limb development through inducing chondrocyte proliferation in the growth plate remains unknown. Therefore, examination of the role of miR-29 family in limb development in vivo will be a priority for future studies.

Another piece of data supporting the role of the miR-29 family in OA comes from the fact that expression of the miR-29 family is decreased during chondrocyte dedifferentiation. Again, other groups have profiled miRNAs in human dedifferentiation models (Karlsen et al. 2011, Lin et al. 2011) but the miR-29 family has not shown up in any of them. As mentioned above, this could be attributed to many different factors.

Taken together, all of these data show that the miR-29 family may modulate both cartilage homeostasis and OA and make a compelling case for further investigation. In this PhD thesis, for the first time, the whole miR-29 family is reported to be involved in OA although the increase of the miR-29b in OA had been shown (Moulin *et al.* 2012). Nevertheless, the miRNA-29 family has been implicated in many other areas of pathology. Many publications have reported the involvement of the miR-29 family in cancers where the miRNA family or a single member could serve as either a tumour suppressor or an oncogene. In rhabdomyosarcoma (Wang *et al.* 2008), nasopharyngeal carcinoma (Sengupta *et al.* 2008), hepatocellular carcinoma (Xiong *et al.* 2010), acute myeloid leukemia (Eyholzer et al. 2010) , multiple myeloma (Zhang *et al.* 2011, Amodio *et al.* 2012), chronic lymphocytic leukemia (Santanam *et al.* 2010), glioblastoma (Cortez *et al.* 2010), and lung (Fabbri *et al.* 2007) and pancreatic cancer (Muniyappa *et al.* 2009), miR-29 was described as a tumor suppressor whilst in acute myeloid leukemia , colorectal liver metastasis (Wang *et al.* 2012), and breast cancer (Chou *et al.* 2013) , miR-29 was shown to be as tumour promoter.

Besides cancers, the miR-29 family has been shown to participate in a number of physiological processes including (i) **muscle development** e.g. knockdown of miR-29b in vivo induced cardiac fibrosis in mice; miR-29a/b1 inhibition induced vascular smooth muscle cell calcification; miR-29 family expression was developmentally up-regulated in porcine skeletal muscle from fetal to adult, and this was also true in mice and human; the miR-29 family was found to be down-regulated in myotonic dystrophy type I and Duchenne muscular dystrophy (Wei *et al.* 2013), (ii) **bone formation** e.g. miR-29a increased bone mass, induced osteoblast differentiation, and inhibited osteoclast differentiation; reduced miR-29a expression was associated with low bone mass and poor skeletal microarchitecture in rats treated with glucocorticoids (Wang *et al.* 2013), (iii) **HIV virus infection** e.g. ectopic expression of miRNA-29a resulted in reduction of HIV virus levels, implicating this miRNA as a potential strategy in developing anti-HIV therapeutics (Ahluwalia *et al.* 2008), (iv) **aging** e.g. miR-29 family up-regulation was observed in a number of different organs e.g. liver, muscle, and brain of several aging models (Ugalde *et al.* 2011, Fenn *et al.* 2013, Hu *et al.* 2014), (v) **diabetes** e.g. the miR-29 family was up-regulated in diabetic rats and forced expression of miR-29 inhibited insulin induced glucose imported by 3T3-L1 adipocytes (He *et al.* 2007); reduced miR-29b in plasma samples of type 2 diabetes patients anticipated the

manifestation of the disease (Zampetaki *et al.* 2010); miR-29c was found up-regulated the kidney glomeruli from diabetic mice (Long *et al.* 2011); the continued expression of miR-29 isoforms in the pancreatic β-cell seems to be required for normal and selective stimulation of insulin secretion by glucose (Pullen *et al.* 2011); (vi) **fibrosis development**, the miR-29 family has been shown to be implicated in the development of fibrosis of many organs including heart, kidney, lung, liver, and systemic sclerosis; (vii) **Alzheimer disease,** the miR-29a/b1 cluster or miR-29a was significantly decreased in Alzheimer patients (Hebert *et al.* 2008, Shioya *et al.* 2010).

In conclusion, with all of the data above, the miR-29 family may play a key role in Osteoarthritis and of is worthy of further investigation. The mechanisms which control its expression together with its function in chondrocytes will be described in the next chapters.

CHAPTER IV
FACTORS THAT CONTROL EXPRESSION OF THE MICRORNA-29 FAMILY

4.1. Introduction

In the previous chapter, evidence for the involvement of the miR-29 family in cartilage homeostasis and OA was presented. The increased expression of the all family members is apparent in both early and late stages of OA. However, which factors or mechanisms are responsible for miR-29 induction or repression in chondrocytes remains unknown and is worthy of further investigation.

The miR-29 family is intergenic miRNAs and is encoded in two gene clusters e.g. one for the primary miR-29a/b1 on chr.7q32, and the other for the primary miR-29b2/c on chr.1q32.2 (Saini *et al.* 2007, Chang *et al.* 2008). The miR-29b1 and miR-29a precursors are processed from the pri-miR-29a/b1 last intron (Genbank accession EU154353) whist the miR-29b2 and miR-29c precursors are from the pri-miR-29b2/c last exon (Genbank accession EU154352 and EU154351) (Chang et al. 2008) (Figure 4.1). These precursors are all transcribed as polycistronic primary transcripts (Chang et al. 2008, Mott *et al.* 2010) upon which various transcriptional regulators e.g. NFκB (Liu *et al.* 2010, Mott et al. 2010), supressors (c-Myc (Mott et al. 2010, Parpart *et al.* 2014), Sp1(Liu et al. 2010, Amodio *et al.* 2012), Gli (Mott et al. 2010), Yin-Yang-1, Smad3 (Qin *et al.* 2011), Ezh, H3K27, HDAC1, HDAC3), or inducers (Gli, SRF, Mef2, TCF/LEF, GATA3 (Chou et al. 2013), CEBPA (Eyholzer et al. 2010)), and signalling pathways e.g, Wnt , TGFβ, TLR/NFκB, TNFα/NFκB, hedgehog signalling have been reported to be directly and/or indirectly involved. For instance, **both canonical and non-canonical Wnt signalling** was reported to induce the miR-29 family level in different cellular contexts: Wnt3a rapidly induces miR-29 levels in osteoblastic cells (Kapinas *et al.* 2009, Kapinas et al. 2010) or in muscle progenitor cells (MPCs) (Hu *et al.* 2014), respectively, at least in part through the two putative TCF/LEF-binding sites in the miR-29a promoter (Kapinas et al. 2010); non-canonical Wnt signalling through Wnt7a/Frizzled 9 resulted in increased expression of only the mature miR-29b but not miR-29a or c or any miR-29b primary or precursor forms in non-small lung cancer cell lines H661 and H15 (Avasarala *et al.* 2013). In addition, ERK5 and PPARγ, key effectors of the Wnt7a/Frizzled 9 pathway, were also observed to be strong inducers of miR-29b expression (Avasarala et al.

2013). In contrast to Wnt signalling, **TGFβ/Smad3 signalling** was shown to negatively regulate miR-29 family expression in different cell lines e.g. human aortic adventitial

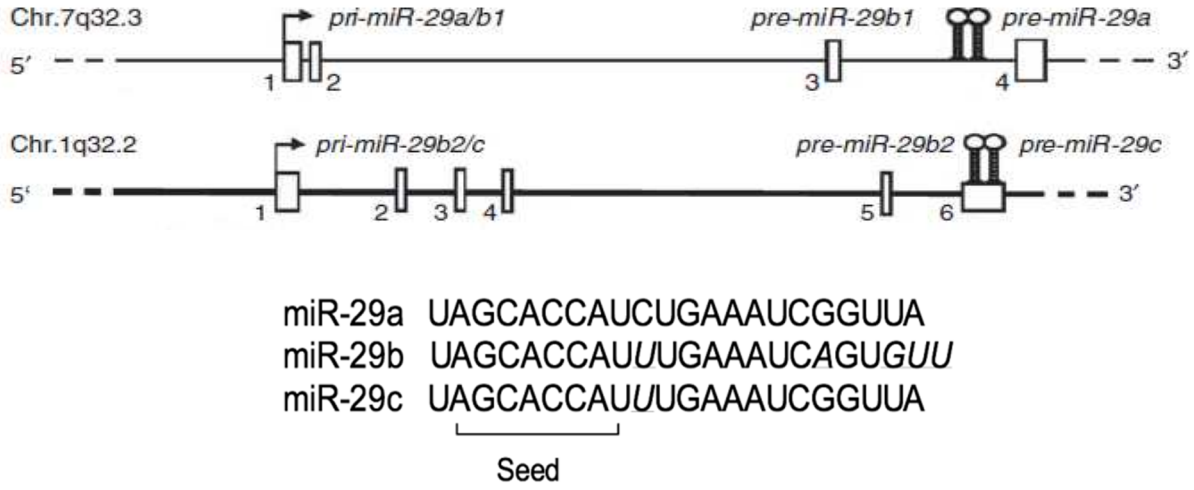

Figure 4.1: Genomic organization of the miR-29 family

The miR-29 family includes three members miR-29a, miR-29b and miR-29c. The primary pri-29a/b1 is located in chromosome 7 containing pre-29a and pre-29b1. The primary pri-29b2/c is located in chromosome 1 including pre-29b2 and pre-29c. The hairpins indicate the locations of the sequence encoding precursors of miR-29s. Pre-29a and pre-29c will process into mature miR-29a and miR-29c, respectively. Pre-29b1 and pre-29b2 will process into mature miR29b. The mature sequences of the miR-29 family members share identical seed regions. Nucleotides that differ among miR-29s are indicated in italics.

fibroblasts (Maegdefessel *et al.* 2012), renal fibrosis cells (Wang *et al.* 2012, Ramdas *et al.* 2013), murine hepatic stellate cells (Roderburg *et al.* 2011), rat hepatic stellate cells (Kwiecinski *et al.* 2011), human skin fibroblasts (Maurer *et al.* 2010), human tenon's fibroblast (Li *et al.* 2012), human lung fibroblast cell line (Cushing *et al.* 2011, Yang *et al.* 2013). The suppressive effect of TGFβ/Smad3 signalling on miR-29 expression was partly mediated through a Smad3 binding site in the highly conserved region around 22kb upstream of the miR-29b2/c promoter as showed by chromatin immunoprecipitation assay (Qin et al. 2011, Ramdas et al. 2013). Similar to TGFβ, **Toll-like receptor (TLR) signalling and TNFα signalling** have been shown to mediate suppressive effects on miR-29 family expression. In man, treating human cholangiocarcinoma cells with TLR ligands e.g. TLR3 (Poly (I:C)), TLR4 (LPS), TLR5 (flagellin), TLR6 (MALP-2) showed a significant decrease in the miR-29 level beginning after 4 hours of LPS treatment but increasing to 24 hours (Mott et al. 2010); treating human stellate cells with LPS strongly decreased all miR-29 family expression after 1 hour (Roderburg et al. 2011); treating C2C12 myoblasts with TNFα substantially reduced miR-29b and miR-29c expression (Wang et al. 2008); stimulating the choroidal-retinal pigment epithelial cell line ARPE-19 with TNFα resulted in significant down regulation of all miR-29s; conversely, transfecting with a synthetic NFκB decoy, (NFκB inhibitor), rescued the down regulation of miR-29 by TNFα (Χαι *εϖ αλ.* 2014). The activation of NFκB through TLR signalling with its three binding sites in the miR-29a/b1 cluster promoter (-561, -110, and +134) was proven to be the mechanism for the suppression of miR-29a/b1 promoter function (Mott et al. 2010). In mice, miR-29a and miR-29b significantly decreased expression in murine natural killer (NK) cells stimulated with the TLR3 ligand (Poly (I:C)) or phorbol ester (PMA) as well as in splenocytes, NK and T cells of mice infected with L. *monocytogenes* or *Mycobacterium bovis* bacillus Calmette-Guérin (Ma *et al.* 2011). Consistent with the human miRNA, a region about 25 kb upstream of the murine promoter of miR-29a/b1 contains two NFκB binding sites. The second binding site is more conserved between human and mouse and it has been shown to be key for suppression of the miR-29a/b1 promoter (Ma et al. 2011). Importantly, other transcriptional factors, co-operating with NFκB to suppress or induce miR-29 family expression, have also been reported e.g. YY1, Sp1, Ezh, H3K27, HDAC1, HADC3, Mef2, SFR. Forced expression of YY1 in C2C12 lead to a 2-fold decrease of miR-29b and miR-29c levels; similarly, siRNA knockdown of YY1 significantly enhanced expression of miRNA expression. ChIP analysis showed that YY1 did not bind to the miR-29b2/c locus in cells in the absence of NFκB,

suggesting that both pathways are necessarye for silencing the miR-29b2/c locus. Amongst 4 putative binding sites of YY1 in highly a conserved region ~20kb upstream of miR-29b2/c, only one site is bound by YY1 on ChIP assay whereas all 4 sites produced a binding complex with EMSAs using nucleus extract from C2C12. Notably, Ezh, H3K27, HDAC1, whose expression is associated with repression of muscle-specific genes, and recruited by YY1, was also detected by ChIP assay. In line of these transcription factors, Mef2 and SFR, well-known for activating muscle genes, were also found binding to the miR-29b2/c promoter. Again using luciferase reporter assay, a reporter containing a 4.5 kb fragment spanning YY1, Mef2, SFR binding sites was repressed by YY1 or loss of the YY1 binding site but stimulated with either YY1 knockdown or SRF or Mef2 (Wang et al. 2008). In addition, forced expression of Sp1 or NFκB (p65) reduced miR-29b expression; conversely, knockdown of Sp1 or NFκB (p65) by siRNAs resulted in induced miR-29b level (Liu et al. 2010). EMSA assay using probes spanning the -125/-75 miR-29b sequence yielded two major complexes, suggesting Sp1/NFκB acts as a repressive complex interacting with an element of the miR-29b enhancer (Liu et al. 2010). Interestingly, histone deacetylase (HDAC) 1 and 3 contribute to the repressor activity of Sp1/NFκB on miR-29b expression (Liu et al. 2010). Incubation of HDAC1/HDAC3 with ^{32}P-labelled probe from the miR-29a/b1 cluster region together with NFκB p50/p65 and Sp1 showed a delayed and more intense band; HDAC1/3 inhibitors increase miR-29b expression, supporting the interaction of HDAC1 and 3 and Sp1/NFκB with the miR-29b regulatory sequence (Liu et al. 2010). Similar to other signalling mentioned previously, **hedgehog signalling pathway** was also shown to repress miR-29 expression: cells treated with cyclopamine, an inhibitor of Smoothened (a hedgehog signalling component), or transfected with siRNA to knockdown Gli-3, the expression of miR-29b increased (Mott et al. 2010). Along with the transcription factors mentioned above, there are other transcriptional factors controlling miR-29 family expression. The serum alphafetoprotein (AFP), a membrane-secreted protein associated with poor patient outcome in hepatocellular carcinoma, was reported to inhibit miR-29a expression through facilitating c-MYC binding to the promoter of the pri-miR-29a/b. This conclusion was supported by: the inability of AFP to decrease the miR-29a level in the absence of c-MYC protein; c-MYC was abundantly bound to the miR-29a/b1 promoter in the presence of AFP, but did not bind without AFP (Parpart et al. 2014); c-MYC promoter binding protein (MBP), originally described to bind to and repress c-MYC promoter function, up-regulated miR-29b expression

by 6 fold in prostate cancer cells (Steele *et al.* 2010). The haematopoietic master transcription factor, CCAAT/enhancer-binding protein-α (CEBPA), was also reported to activate the expression of miR-29a and miR-29b. Forced expression of CEBPA in acute myeloid leukaemic cells lead to two-fold induced expression of the primary miR-29a/b1 and the mature miR-29a and miR-29b whereas the expression of miR-29b2/c primary transcript remained stable. Using luciferase reporter assays, the sequence, having the conserved region spanning -682 bp upstream to +296 bp downstream of the miR-29a/b1 transcriptional start site and containing 6 potential CEBPA sites, was also strongly induced with CEBPA. Among these binding sites, the one located at +15 to +29 bp was identified to be responsible for CEBPA-mediated activation of the pri-miR-29a/b1 promoter on ChIP assay (Eyholzer et al. 2010). Another transcriptional factor, GATA3, specifying and maintaining luminal epithelial cell differentiation in the mammary gland, was also found to induce miR-29 expression directly by binding to three GATA3 sites in the miR-29a/b1 promoter. Interestingly, GATA3 can induce miR-29s expression by inhibiting the TGFβ and NFκB signalling pathway. Additionally, STAT1 (signal transducer and activator of transcription) a transcription factor induced by interferon γ signalling, was reported to upregulate primary 29a/b1, the pre-29a, pre-29b1, and the mature miR-29a, miR-29b in melanoma cell and T cells (Schmitt *et al.* 2013).

With all the information above, it is likely that in different cellular contexts, the miR-29 family expression is controlled by different transcription factors and signalling pathways. Which factors control its expression in human chondrocytes remains unknown. The effects of a variety of anabolic and catabolic factors e.g. TGFβ, Wnt3a, IL-1, LPS on miR-29 family expression in human chondrocytes were thus investigated. Also, the effect of SOX9, a major specifier of chondrocyte phenotype was also investigated.

Aims:

- Analyse the promoter region (approximately 2kb upstream of the transcription starting site) of the miR-29 family for SOX9 binding sites. Experimentally validate the impact of SOX9 on miR-29 expression.
- Test major anabolic and catabolic cytokines controlling the miR-29 expression in chondocytes.

4.2. Results

4.2.1. The master regulator of chondrogenesis SOX9 suppresses expression of the miR-29 family

The master regulator for chondrogenesis SOX9 has a critical function in a number of development processes e.g. skeletal formation, sex determination, pre-B and T cell development. *SOX9* was found to be expressed in all chondroprogenitors and differentiated chondrocytes, but not in hypertrophic chondrocytes (Ng *et al.* 1997, Zhao *et al.* 1997). Importantly, SOX9 is considered as the critical transcriptional factor for chondrogenic differentiation, partly owing to the fact that its functions are required for differentiating chondrogenic mesenchymal condensations into chondrocytes, and for all stages of chondrocyte differentiation: in mouse chimera, *Sox9* knockout cells were excluded from all cartilage and no cartilage developed in teratomas derived from *Sox9* -/- embryonic stem cells (Bi *et al.* 1999); *Sox9* deletion from chondrocytes at later stages of development resulted in decrease in chondrocyte development, cartilage matrix gene transcriptional inhibition, and prematurely conversion from proliferating chondrocytes to hypertrophic chondrocytes (Akiyama *et al.* 2002). Considering the critical role of SOX9 in chondrocytes, I explored the connection between this factor and expression of the miR-29 family. Initial evidence suggested a link: in the DMM model mRNA profiling data, at 7 days after the surgery, *Sox9* expression was greatly induced (Appendix, Table 7) whilst the miR-29s expression was suppressed; in both human and mouse chondrogenesis models, the level of Sox9 was inversely correlated with the level of miR-29 expression (data not shown). Thus, SOX9 could be a miRNA-29 target or SOX9 could regulate miRNA-29 expression.

To test the postulate **that SOX9 is a miR-29 target**, the effect of the miR-29 members on SOX9 transcriptional expression was examined: after sub-cloning the *SOX9* 3'UTR downstream of the luciferase gene, this SOX9-3'UTR reporter vector was co-transfected with the miR-29 family into SW1353 cells; 24 hours after transfection, luciferase activity was measured. Luciferase activity showed that miR-29 family have no effect on the *SOX9* 3'UTR even though bioinformatics analysis found one 6-mer seed site for miR-29 in the *SOX9* 3'UTR (data not shown), suggesting that SOX9 is not a miR-29 family direct target. Also, whether SOX9 is a miR-29 indirect target was also determined: relative expression of SOX9 was checked in human primary chondrocytes transfected with miR-29 family for 48 hours. Quantitative RT-PCR confirmed that the SOX9 level was not changed with miR-29

transfection in chondrocytes (data not shown). Thus, SOX9 is not a direct or indirect target of miR-29s at least at the transcriptional level.

For testing the second hypothesis **SOX9 is a suppressor of miR-29 expression**, the effect of overexpression or knockdown of SOX9 on miR-29 expression was studied: a SOX9 expression construct or siRNA was transiently transfected into the human chondrosarcoma SW1353, 48 hours after transfection, the level of the mature miR-29 family was measured by quantitative RT-PCR. The data (Figure 4.2) show that SOX9 suppressed miR-29 transcription: the miR-29 family levels were significantly reduced when SOX9 was overexpressed (Figure 4.2.a,c) but induced when SOX9 was knocked down (Figure 4.2.b,c).

To further explore the regulatory mechanism by which SOX9 suppressed miR-29 expression, the 2kb region upstream from the primary miR-29a/b1 and miR-29b2/c transcription start sites were analysed by searching for the SOX9 DNA-binding motif ([A/T][A/T]CAA[A/T]). This analysis revealed 5 putative binding sites for SOX9 in the promoter regions of pri-miR-29a/b1 and pri-miR-29b2/c, respectively (Figure 4.3.a). A reporter construct with the primary miR-29a/b1 2kb promoter, kindly provided by Dr Anne Delany (University of Connecticut, USA) was used to further validate the direct effect of SOX9: the reporter was co-transfected with increasing amounts of SOX9-expression plasmid into SW1353 cells and luciferase activity measured after 24 hours of transfection. Luciferase activity in SW1353 cells significantly decreased in a dose-dependent manner (Figure 4.3.b) showing that SOX9 directly regulated the primary miR-29a/b1 promoter.

The data above demonstrate that SOX9 is a miR-29 family suppressor.

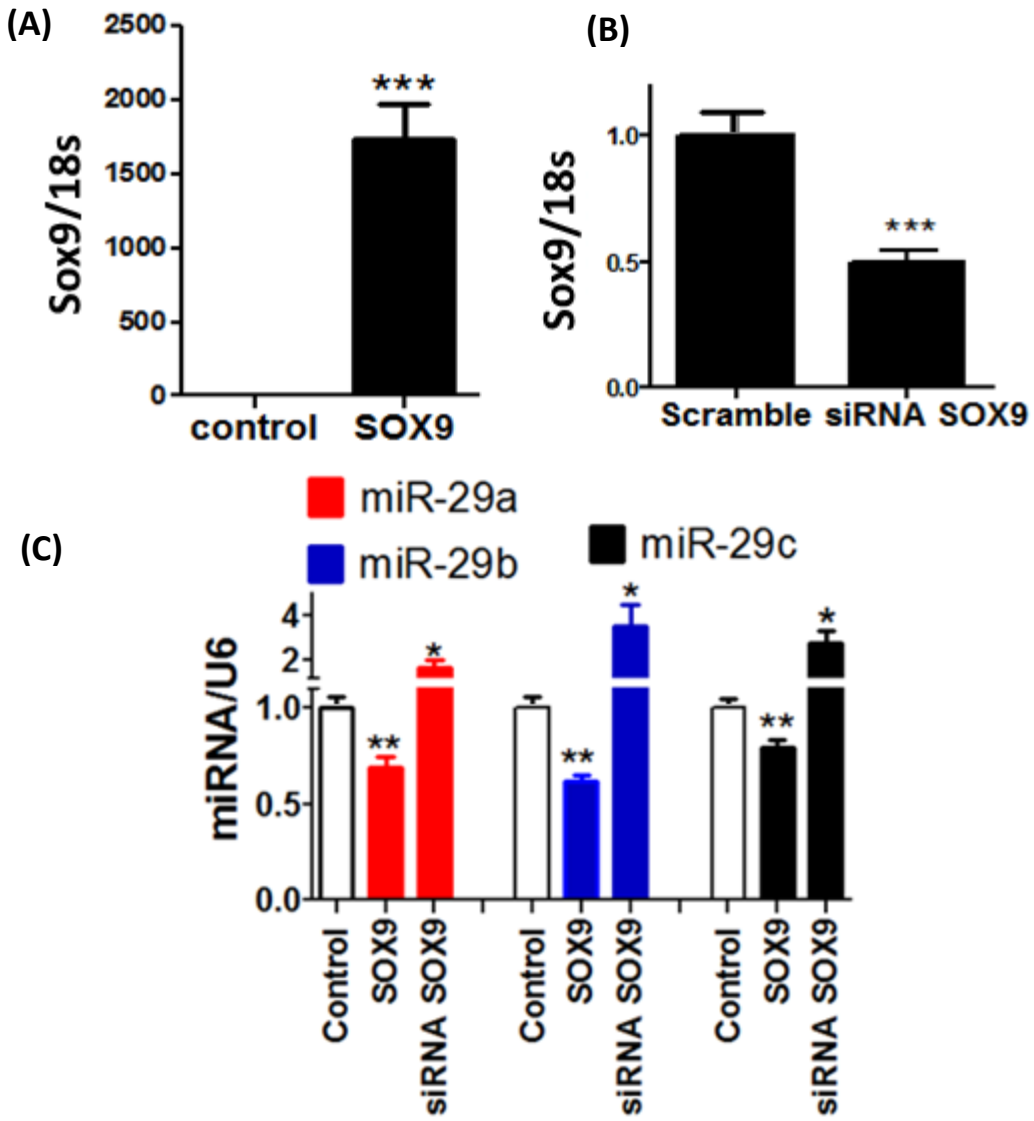

Figure 4.2: **Sox9 suppresses miR-29 family expression**.

(A) SOX9 gain-of-function: transiently transfection of a SOX9-expression vector or pcDNA3 empty vector (control) into SW1353 cells; (B) SOX9 loss-of-function: transiently transfection of SOX9 siRNA or a non-targeting control into SW1353 cells. Relative expression of SOX9 in (A) and (B) was measured 48 hours after transfection by quantitative RT-PCR using18S as the endogenous control; (C) The miR-29 family expression levels after overexpression or knockdown of SOX9 in SW1353 cells was measured by quantitative RT-PCR. Using U6 as the endogenous control. Red bar: miR-29a, green bar: miR-29b, black bar: miR-29c, open bar: control. Means ± standard errors are presented. Difference in expression was analysed by unpaired two-tailed Student's t test. * $p<0.05$, ** $p < 0.01$, *** $p<0.001$, n=3.

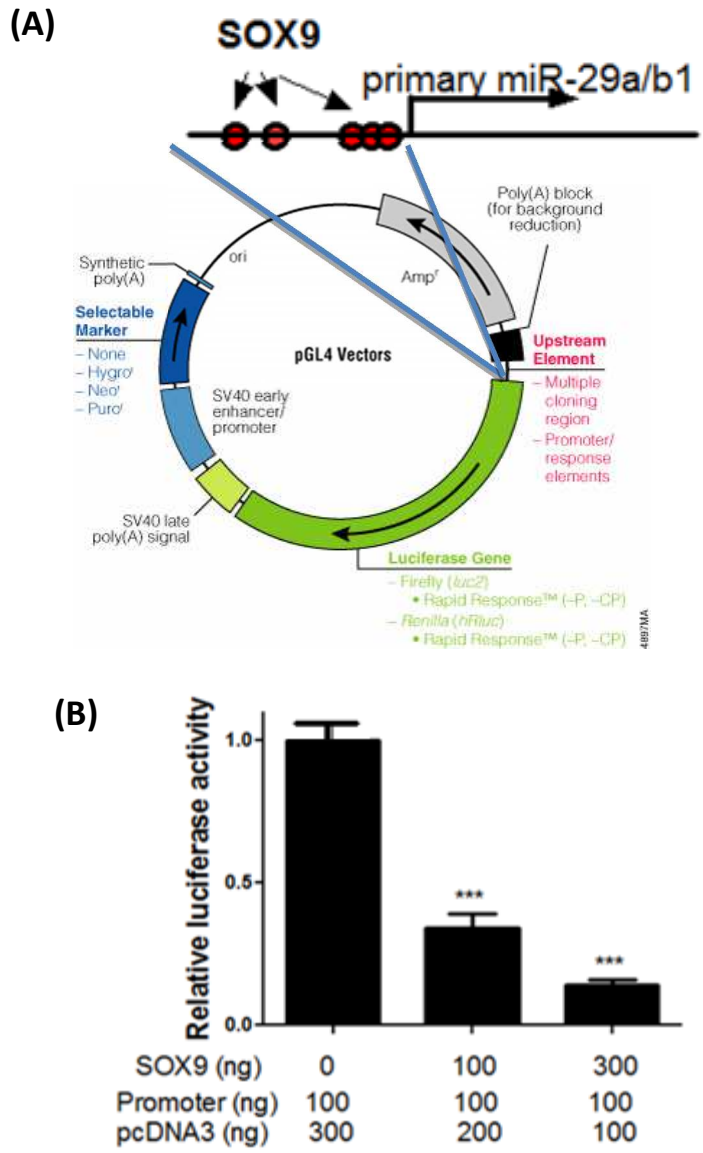

Figure 4.3: **Sox9 suppresses primary miR-29a/b1 transcription by directly binding to the proximal miR-29a/b1 promoter.**

(A) Structure of the miR-29a/b1 promoter reporter: 5 putative binding sites of SOX9 were identified by analysing the 2kb region upstream of the transcription start site of miR-29a/b1 by JASPAR. This 2kb region was sub-cloned upstream of the luciferase gene in a pGL4 vector.
(B) Suppressive effect of SOX9 on the primary miR-29a/b1 promoter reporter: transiently co-transfection of primary miR-29a/b1 promoter (100ng) with increasing amount of SOX9-expression vector (0, 100, 300ng) or pcDNA.3 to equalise DNA into SW1353. A constitutively expressed Renilla lucierase was used as a control for transfection efficiency. Luciferase activity was measured 24 hours after transfection. Means ± standard errors are presented. The difference in luciferase activity was analysed by unpaired two-tailed Student's t test. * $p<0.05$, ** $p < 0.01$, *** $p<0.001$, n=6.

4.2.2. TGFβ1 inhibits expression of the miR-29 family

TGFβ signalling has many important roles in chondrocytes and articular cartilage: TGFβ induces extracellular matrix formation; stimulates chondrocyte proliferation; inhibits the terminal differentiation of chondrocytes; retains chondrocytes in the pre hypertrophic stage; increases total glycosaminoglycan synthesis; maintains the matrix component in immature cartilage (Li *et al.* 2005). Animal studies showed that: transgenic mice overexpressing a cytoplasmically truncated, dominant-negative form of the TβRII in cartilage, resulted in a joint disease similar to human osteoarthritis (Serra *et al.* 1997); Smad3 deficient mice showed premature chondrocyte maturation with increased length of the hypertrophic region, disorganization of the chondrocyte columns, early expression of collagen type X in the growth plate; and null mice gradually developed an end-stage OA phenotype (Li et al. 2005). These essential roles of TGFβ signalling in chondrocytes suggest the necessity of examining whether the miR-29 family is regulated by TGFβ signalling in human chondrocytes. Moreover, a number of published data show that TGFβ signalling negatively regulates miR-29 family expression in different human fibroses e.g. renal, lung, liver fibrosis. The impact of TGFβ signalling in human chondrocytes on the miR-29 family was thus checked.

To address the above question, expression of the miR-29 family with TGFβ1 treatment in human primary chondrocytes was compared both in monolayer and micromass culture. **In monolayer culture**: HACs were put in high glucose media containing 10% (v/v) FCS until the cells reached 90% confluence; medium was replaced with that containing 0.5% (v/v) FCS) prior to stimulating with 4ng/ml TGFβ or vehicle control (4mM HCl with 0.5% (w/v) BSA). **In micromass culture**: HACs were put in high glucose media containing 10% (v/v) FCS in monolayer following two sequential passages to increase cell number; the micromass ($2.5x10^7$cells/ml) was cultured in high glucose media with 10% (v/v) FCS for 24 hours before treating with 10ng/ml TGFβ or vehicle control (4mM HCl with 0.5% (w/v) BSA). Cells were harvested for qRT-PCR after 24 hours or 48 hours treatment in monolayer or micromass cultures, respectively. Quantitative RT-PCR primers for measuring the miR-29 family were described before. For the primary transcripts: two primer pairs specific for exon 1 and exon 3 were used; for the precursor transcripts: primers directly bind to the precursor sequence (Appendix, Table 5); the mature transcripts were measure by LNA-primers.

The qRT-PCR data show that expression of the miR-29 family was suppressed by TGFβ signalling (Figure 4.4). However, each culture system gave a different response. The pri-29b2/c transcript was significantly decreased after stimulating HACs for 24 hours with TGFβ1 in monolayer culture, whilst the pri-29a/b1 transcript was unchanged (Figure 4.4 a); the pri-29a/b1 transcript was significantly decreased in micromass culture after 48 hours with TGFβ1 whilst the pri-29b2/c transcript was unchanged or even increased (Figure 4.4 b). Notably, the levels of all mature forms of miR-29 were significantly decreased by TGFβ1 in both systems. These data suggest a hypothesis that the primary and the precursor miRNAs may be rapidly regulated and then processed into mature miRNAs. In order to test this hypothesis, SW1353 cells were treated with TGFβ1 (4ng/ml) in monolayer in a time course. Since the expression levels of the primary and pre miRNAs modulated by TGFβ1 in human primary chondrocyte were similar and ahead the mature miRNAs, it might be sufficient to measure only the pre-miRNA rather than both the primary and precursor sequences. Consistent with above data, qRT-PCR showed that TGFβ1 suppressed miR-29 family expression in SW1353 cells (Figure 4.5). Interestingly, significantly suppressive effects of TGFβ1 on precursor miRNAs were observed after 4 hours till the end of the time course (Figure 4.5.a) whilst significant change in the mature miRNAs was only seen after 12 hour treatment (Figure 4.5.b). This data, thus, confirms the hypothesis above. Together with TGFβ1, the effect of TGFβ3 on the miR-29 family expression also checked on SW1353 in monolayer across the time course. Quantitative RT-PCR data (Figure 4.5) showed that TGFβ3 also strongly supressed the expression of the miR-29s. However, the TGFβ3 significant decrease the precursor and the mature miRNAs were observed at 12 hour time point though at 4 hours a

The suppressive effect of TGFβ on expression of the miR-29 family was also investigated on the proximal promoter of the primary miR-29a/b1 gene. The promoter-reporter was transfected into SW1353 cells, cells were serum starved for 24 hours and treated with TGFβ1 (4ng/ml) for another 6 hours before performing the luciferase assay. In line with the expression data, TGFβ1 significantly suppressed the promoter activity of pri-miR-29a/b1 (Figure 4.6).

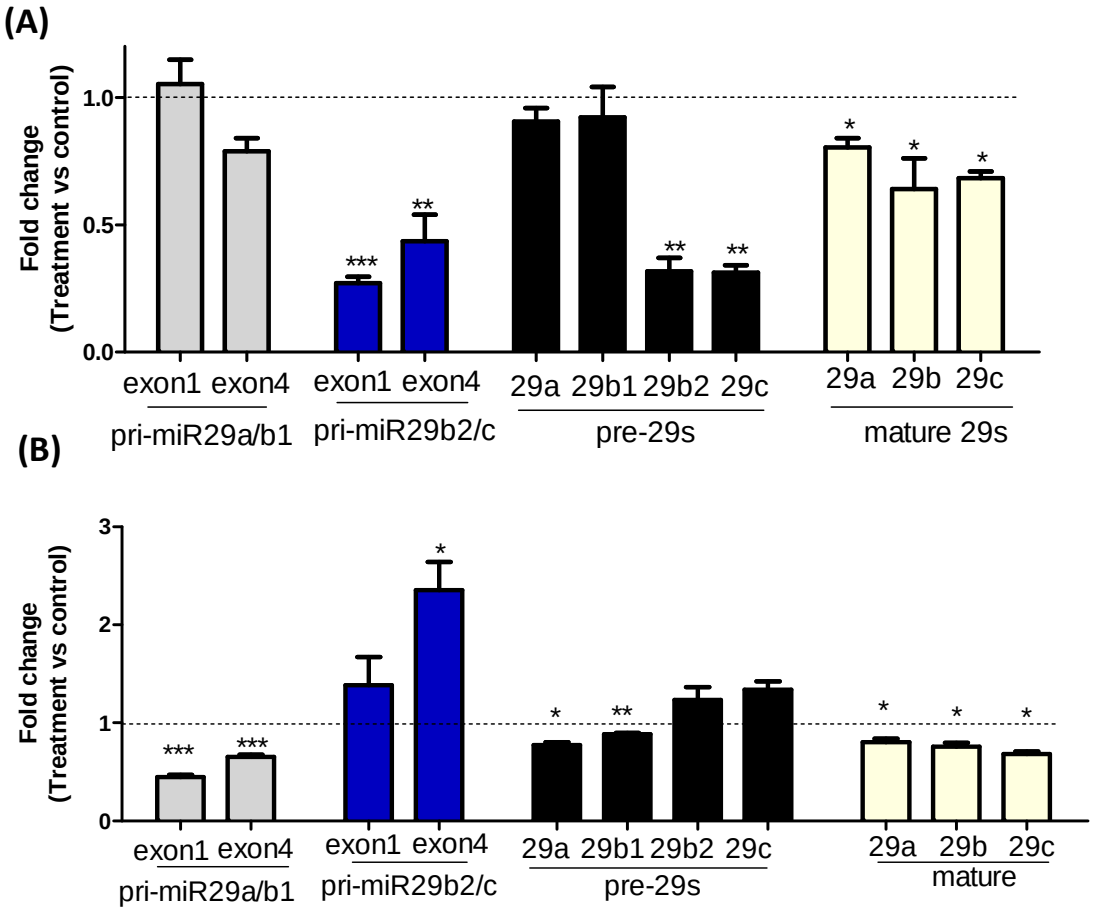

Figure 4.4 TGFβ1 suppresses expression of the miR-29 family in human primary chondrocyte

(A) TGFβ1suppresses expression of the miR-29 family in monolayer culture: Human primary chondrocytes were cultured in high glucose media with 10% (v/v) FCS in monolayer until 90% confluence. Cells were switched to high glucose media with 0.5% (v/v) FCS for 24 hours before treating with TGFβ1 (4ng/ml) or vehicle (4mM HCl+0.5% (w/v) BSA) for another 24 hours.

(B) TGFβ1suppresses expression of the miR-29 family in micromass culture: Human primary chondrocytes were cultured in high glucose media with 10% (v/v) FCS in monolayer. After 2 sequential passages, cells were put in micromass culture ($2.5x10^7$cells/ml) in high glucose media with 10% (v/v) FCS. After 24 hours in micromass, cells were stimulated for 48 hours with TGFβ (10ng/ml) or vehicle (4mM HCl+0.5% (w/v) BSA) in 10% (v/v) FCS media.

Relative expression of the primary miR-29a/b1, -29b2/c, precursor miR-29a, -29b1, -29b2, -29c, the mature miR-29a, b, c were measured by quantitative RT-PCR. 18S rRNA was the endogenous control for measuring primary and precursor transcripts; U6 was the endogenous control for measuring miR-29 mature transcripts. The horizontal line at 1 represents the mean of the vehicle control. Brown bar, pri-miR-29a/b1 transcripts; blue bar, pri-miR-29b2/c transcripts; black bar, precursor transcripts; yellow bar, mature transcripts. Means ± standard errors are presented. The difference between the treatment and the control was analysed by unpaired two-tailed t test. * $p<0.05$, ** $p < 0.01$, *** $p<0.001$, n=3.

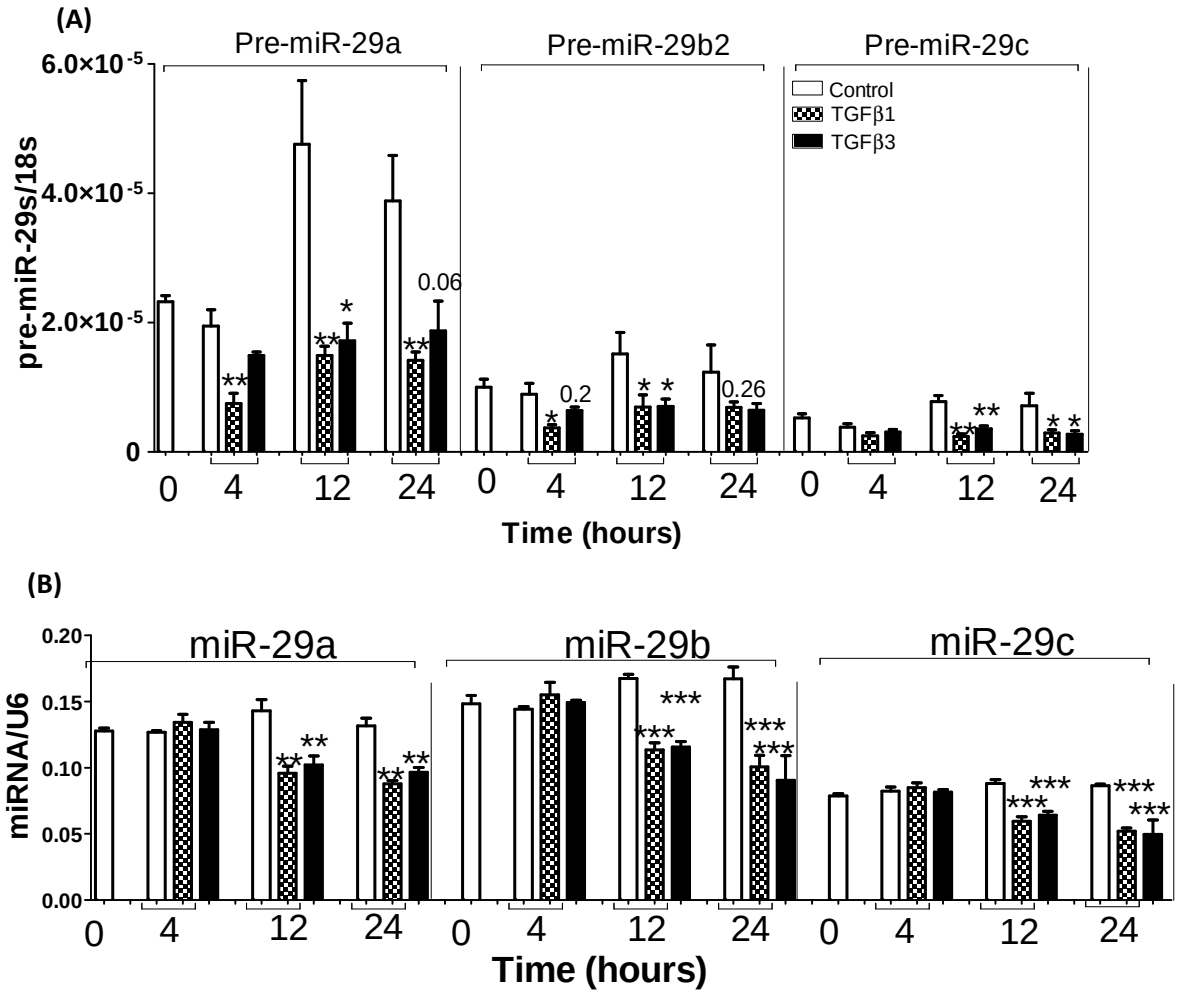

Figure 4.5 TGFβ1/3 suppresses expression of the miR-29 family in SW1353 cells

SW1353 cells were cultured in high glucose media with 10% (v/v) FCS in monolayer until 90% confluence. Cells were serum starved for 24 hours before treating with TGFβ1or TGFβ3 (4ng/ml) or vehicle (4mM HCl+0.5% (w/v) BSA) across 24 hour course.

Relative expression of the precursor miR-29a, -29b2, -29c, the mature miR-29a, b, c were measured by quantitative RT-PCR. 18S rRNA was the endogenous control for measuring the precursor transcripts; U6 was the endogenous control for measuring miR-29 mature transcripts. Open bar, control; brick bar, TGFβ1; close bar, TGFβ3. (A) Expression level of pre-miR-29a, 29b2, 29c. (B) Expression level of mature miR-29a, b, c. Means ± standard errors are presented. The difference between the treatment and the control was analysed by unpaired two-tailed t test. * $p<0.05$, ** $p < 0.01$, *** $p<0.001$, n=3.

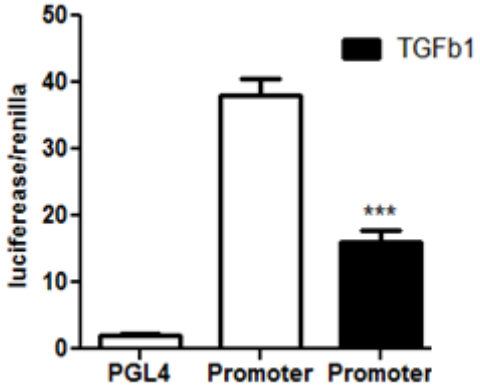

Figure 4.6: TGFβ1decreases expression from the primary miR-29a/b1 promoter

The pri-miR-29a/b1 promoter-reporter (100ng) or the empty vector pGL4 (control, 100ng) were transfected into SW1353 cells. After transfection, cells were serum starved for 24 hours, followed by stimulating for another 6 hours with TGFβ1 (4ng/ml), or vehicle (4mM HCl+0.5% BSA) before measuring luciferase activity. Renilla was use as endogenous control. Open bar: vehicle, black bar: TGFβ1. Means ± standard errors are presented. The difference of luciferase activity was analysed by unpaired two-tailed Student's t test. * $p<0.05$, ** $p < 0.01$, *** $p<0.001$, n=6.

4.2.3. Expression of the miR-29 family is not regulated by canonical Wnt signalling

As shown in the section above, the TGFβ signalling pathway, stimulated by TGFβ1 (or TGFβ3, data not shown), negatively regulated the expression of themiR-29 family. Signalling cross talk between TGFβ and Wnt signalling pathways has been previously reported, e.g. after TGFβ stimulation, Smad3 interacts with LEF1 to activate target gene transcription independently of β-catenin (Letamendia *et al.* 2001); TGFβ was shown to up-regulate the expression of many Wnt ligands e.g. Wnt2, 4, 5a, 7a, 10a, and Wnt co-receptors e.g. LRP5 (Zhou *et al.* 2004); TGFβ was found to increase nuclear accumulation and stability of β-catenin; interestingly, working synergistically with Wnt signalling pathways, TGFβ was reported to stimulate chondrocyte differentiation from mesenchymal cell (Zhou et al. 2004). Wnt signalling is also known to have a key role in cartilage homeostasis and osteoarthritis (Zhu et al. 2008, Zhu et al. 2009). Thus, it was pertinent to investigate the effect of Wnt signalling onexpression of the miR-29 family in chondrocytes, and then potential synergy with TGFβ signalling.

The effect of canonical Wnt signalling stimulated by Wnt3a (50 or 100ng/ml) on the miR-29 family was investigated in HACs cultured in monolayer or micromass after 24 hours or 48 hours, respectively; or in SW1353 cells in monolayer culture across a 24 hour time course. In addition, the effect of Wnt3a on the proximal pri-miR-29a/b1 promoter was also examined after 6 hour treatment with Wnt3a (50 or 100ng/ml). Quantitative RT-PCR data for all transcripts of miR-29 family and luciferase assay data for the miR-29a/b1 promoter showed canonical Wnt signalling did not regulate expression of the miR-29 family (Appendix, Figure 5). Wnt3a did regulate Axin2 expression in the same experiments, showing induction of the canonical Wnt pathway (Appendix, Figure 6).

4.2.4. IL-1 induces expression of the miR-29 family in part via the p38 signalling pathway.

IL-1 is a catabolic and anti-anabolic cytokines, it down regulates the expression of cartilage matrix components e.g. aggrecan and type II collagen and induces expression of matrix degrading enzymes e.g. MMP-3, MMP-13, ADAMTS4 (Koshy *et al.* 2002). *Il-1β*, or Il-1β-converting enzyme knockout mice showed the accelerated development of OA lesions in response to OA surgical induced in compared with wide type mice (Clements et al. 2003). It is considered to be a major cytokine driving the pathology of OA (Goldring *et al.* 2004). Thus, it was pertinent to examine whether IL-1 controls the expression of the miR-29 family in human chondrocytes.

The effect of IL-1 on the expression of the miR-29 family was first measured in IL-1-treated SW1353 for 48 hour time course in monolayer culture: SW1353 cells were cultured in high glucose media with 10% (v/v) FCS until reach confluence and followed by serum starved for 24 hours before treating with 5ng/ml IL-1 or vehicle (0.5% (w/v) BSA) for 48 hour time course. Relative expressions of the precursor and mature miRNA-29 transcripts were measured by qRT-PCR. Data (Figure 4.7) showed that IL-1 induced the expression of miR-29 family: the biggest induction on miR-29 precursors was observed at 4 hours; at later time point, the level of miR-29a precursors was decreased as compare with 4 hours (pre-29a) whilst other precursors did not change expression (Figure 4.7a); the induction of mature miR-29s were only observed significantly after 48 hours (Figure 4.7b). These data suggested that the increase in expression after IL-1 treatment of the miR-29 derivatives is time-dependent. The induction of IL-1 on the miR-29 family was again checked on the HACs in micromass culture: The micromass containing ($2.5x10^7$cells/ml) of passage 2 HAC was cultured in high glucose media with 10% (v/v) FCS for 48 hours before treating with 20ng/ml IL-1 or vehicle control (0.5% (w/v) BSA). Quantitative RT-PCR primers for measuring the miR-29 family were described before (Appendix, Table 5). Real-time RT-PCR data (Figure 4.8) showed that IL-1 strongly induced expression of the miR-29 family, with all processed transcripts significantly up-regulated by IL-1. The fold increase was highest for the pri-miR-29a/b1 locus in which the primary miR-29a/b1 and pre-miR29a and b1 were increased with 9 and 5 fold, respectively.

The molecular pathways induced by IL-1 can be the three classical MAPK-signalling pathways i.e. ERK, p38, JNK and through NFκB (Aigner *et al.* 2006, Fan *et al.* 2007). The

signalling pathway through which IL-1 regulated miR-29 family expression was investigated. SW1353 cells were stimulated with IL-1 together with an NFκB inhibitor (10μM) or a p38 inhibitor (SB203580) (10μM) or 6 hours in monolayer and the relative expression of the precursor miRNAs were again measured. The data showed that inhibition of the NFκB pathway further induced expression of the pre-miR-29a and b1 (Figure 4.9). Inhibition of p38 suppressed IL-1 induction of pre-miR-29a and b1, with a similar pattern for pre-miR-29b2 and c (Figure 4.10), suggesting that IL-1 induces expression of the miR-29 family at least in part through p38 MAPK signalling.

Furthermore, the effect of IL-1 on the promoter of pri-miR-29a/b1 was also examined by luciferase assay. The pri-miR-29a/b1 promoter-reporter was transfected into SW1353 cells for 24 hours before stimulation with IL-1 (5ng/ml) with or without the NFκB inhibitor (10nM) or p38 inhibitor (10μM) for another 6 hours. Luciferase data showed that the activity of the pri-miR-29a/b1 promoter was significantly decreased by IL-1 and that this effect was abolished by treatment with the NFκB inhibitor (Figure 4.11). However, the p38 inhibitor had no effect on the suppressive effect of IL-1 on the promoter of pri-miR-29a/b1 (data not shown).

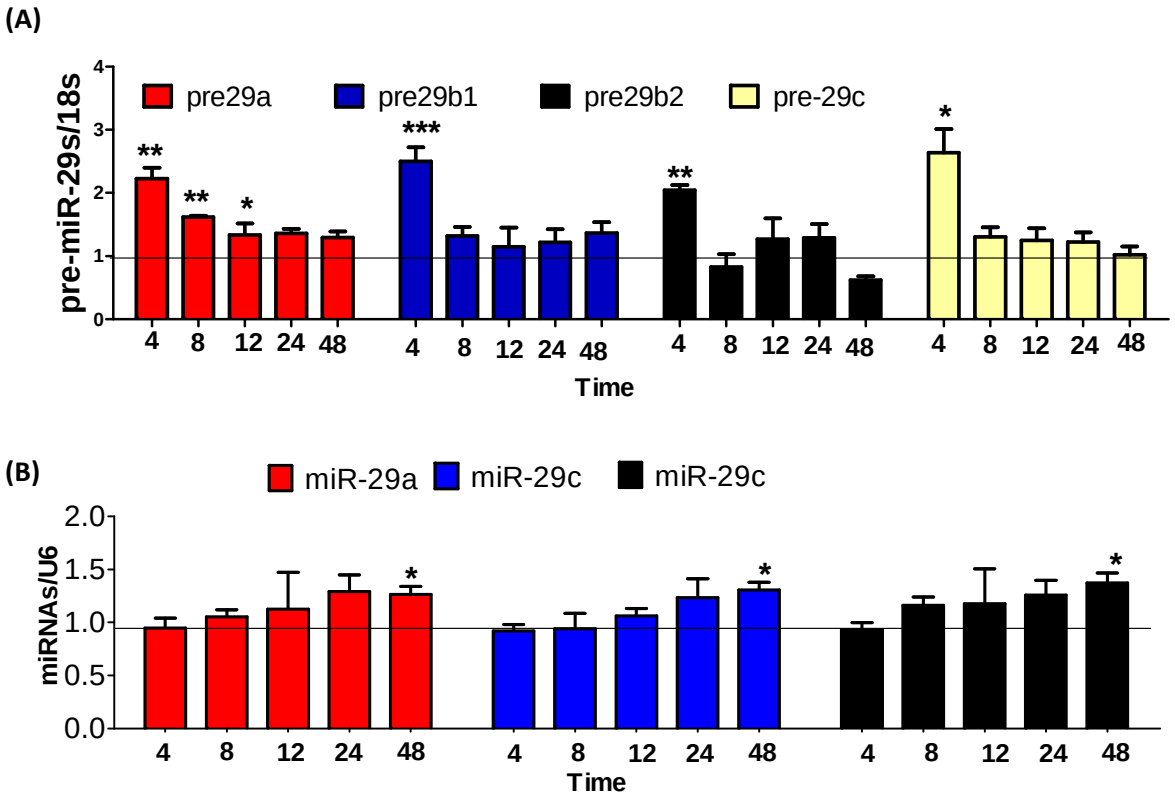

Figure 4.7: IL-1 induces expression of the miR-29 family in SW1353 in monolayer culture

SW1353 cells were cultured in high glucose media with 10% (v/v) FCS in monolayer until 90% confluence. Cells were serum starved for 24 hours before treating with IL-1 (5ng/ml) or vehicle (0.5% (w/v) BSA) across 48 hour course.
Relative expression of the precursor miR-29a, -b1, -b2, -c, the mature miR-29a, b, c were measured by quantitative RT-PCR. 18S rRNA was the endogenous control for measuring the precursor transcripts; U6 was the endogenous control for measuring miR-29 mature transcripts. The horizontal line at 1 serves as the vehicle control.
(A) Expression level of pre-miR-29a, 29b2, 29c. Red bar, pre-miR-29a; blue bar, pre-miR-29b1; black bar, pre-miR-29b2; yellow bar, pre-miR-29c
(B) Expression level of mature miR-29a, b, c. Red bar, miR-29a; blue bar, miR-29b; black bar, miR-29c
Means ± standard errors are presented. The difference between the treatment and the control was analysed by unpaired two-tailed t test. * $p<0.05$, ** $p < 0.01$, *** $p<0.001$, n=3.

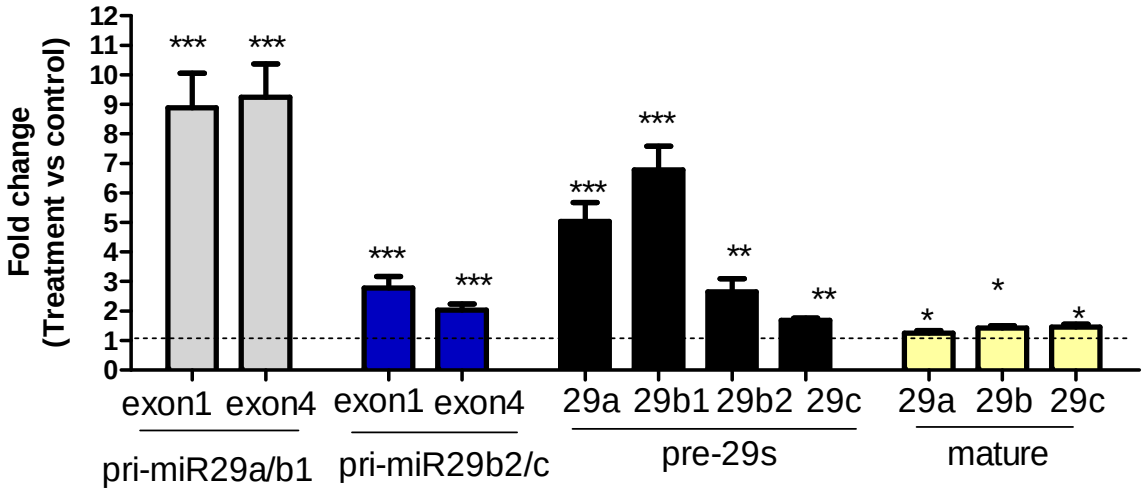

Figure 4.8: IL-1 induces expression of the miR-29 family in human primary chondrocyte in micromass culture

Human primary chondrocytes were cultured in high glucose media with 10% (v/v) FCS in monolayer. After 2 sequential passages, cells were put in micromass culture ($2.5x10^7$cells/ml) in high glucose media with 10% (v/v) FCS. After 24 hours in micromass, cells were stimulated for 48 hours with IL-1β (10ng/ml) or vehicle (0.5% (w/v) BSA).
Relative expression of the primary miR-29a/b1, -29b2/c, precursor miR-29a, -29b1, -29b2, -29c, the mature miR-29a,- 29b, -29c were measured by quantitative RT-PCR. 18S rRNA was the endogenous control for measuring primary and precursor transcripts; U6 was the endogenous control for measuring miR-29 mature transcripts. The horizontal line at 1 serves as the vehicle control. Brown bar, pri-miR-29a/b1 transcripts; blue bar, pri-miR-29b2/c transcripts; black bar, precursor transcripts; yellow bar, mature transcripts. Means ± standard errors are presented. The difference between the treatment and the control was analysed by unpaired two-tailed Student's t test. * $p<0.05$, ** $p < 0.01$, *** $p<0.001$, n=3.

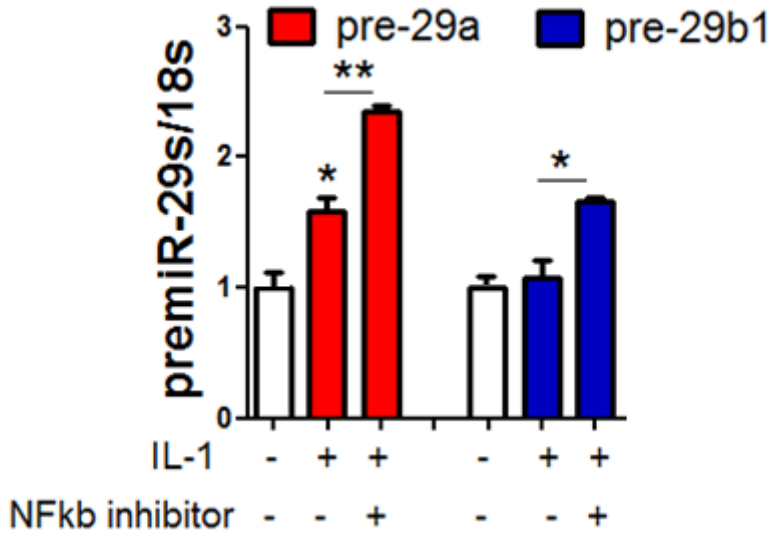

Figure 4.9 NFκB inhibition further increases the IL-1-induced expression of pre-miR-29a and pre-miR-29b1

SW1353 cells were plated in high glucose media with 10% (v/v) FCS in a 6 well-plate in monolayer and serum starved for 24 hours before treating with IL-1β (10ng/ml) in the presence or absence of NFκB inhibitor JSH-23 (10μM) for a further 8 hours. Cells were then harvested and the total RNA was isolated by Trizol. Relative expression of pre-miR-29a, -29b1 were measured by quantitative RT-PCR. 18S rRNA was the endogenous control. Red bar, pre-miR-29a; blue bar, pre-miR-29b1. Means ± standard errors are presented. The difference between the treatment and the control was analysed by unpaired two-tailed Student's t test * $p<0.05$, ** $p < 0.01$, *** $p<0.001$, n=6.

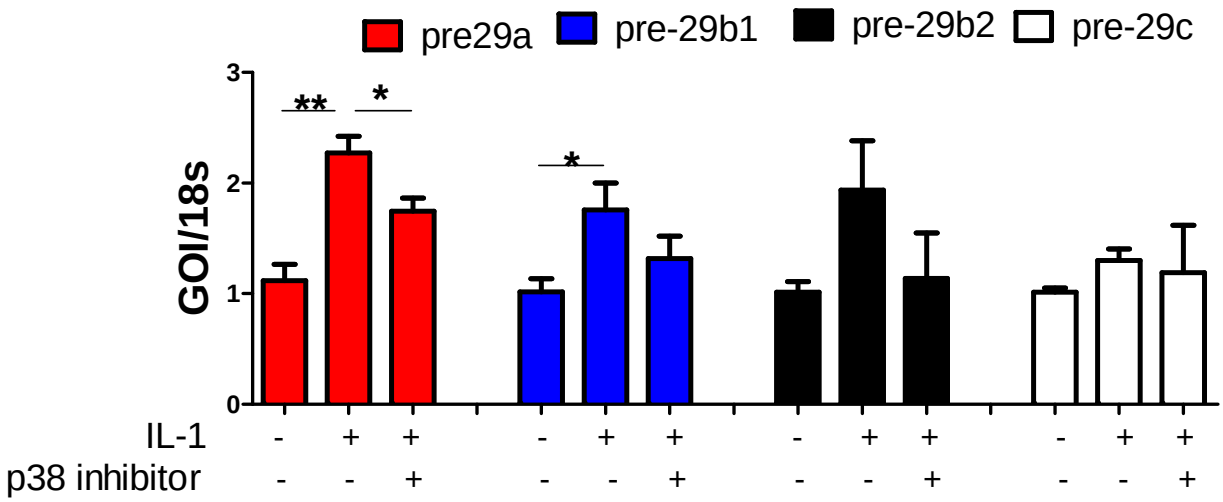

Figure 4.10 P38 inhibition suppresses the IL-1 induction of pre-miR-29s

SW1353 cells were plated in high glucose media with 10% (v/v) FCS in a 6 well-plate in monolayer and serum starved for 24 hours before treating with IL-1β (10ng/ml) in the presence or absence of p38 inhibitor SB203580 (10µM) for a further 8 hours. Cells were then harvested and the total RNA was isolated by Trizol. Relative expression of pre-miR-29a, -29b1, -29b2, -29c were measured by quantitative RT-PCR. 18S rRNA was the endogenous control. Red bar, pre-miR-29a; blue bar, pre-miR-29b1; black bar, pre-miR-29b2; white bar, pre-miR-29c. Means ± standard errors are presented. The difference between the treatment and the control was analysed by unpaired two-tailed Student's t test * $p<0.05$, ** $p < 0.01$, *** $p<0.001$, n=3.

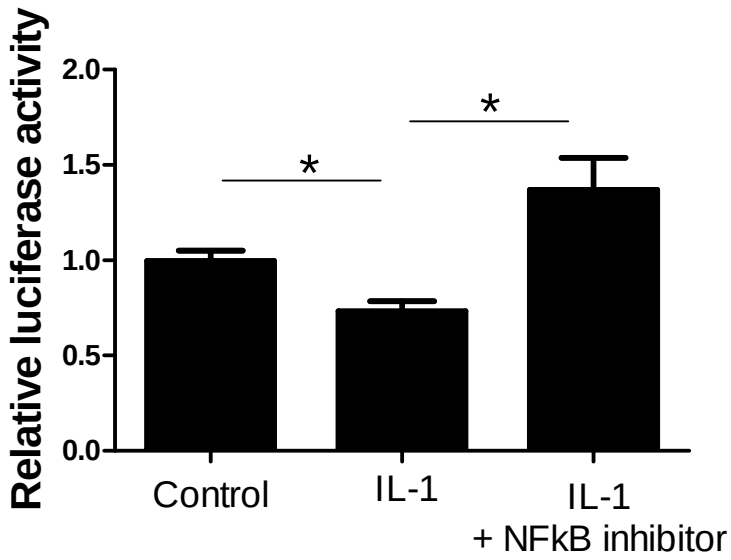

Figure 4.11: IL-1 suppresses the primary miR-29a/b1 promoter through NFκB

Pri-miR-29a/b1 promoter reporter (100ng) or pGL4 (control, 100ng) were transfected into SW1353 cells. After transfection, cells were serum starved for 24 hours, and followed by stimulating for another 6 hours with IL-1β (5ng/ml), IL-1β and NFκB inhibitor JSH-23 (10μM) or vehicle (0.5% (w/v) BSA) before measuring luciferase activity. Renilla was the endogenous control. Means ± standard errors are presented. The difference of luciferase activity was analysed by unpaired two-tailed Student's t test. * $p<0.05$, ** $p < 0.01$, *** $p<0.001$, n=6.

4.2.1. LPS suppressed the miR-29 family expression through NFκB signalling pathway

Toll-like receptors (TLRs) have important roles in activation of the innate and adaptive host defence against infections. TLR can bind to various damage-associated molecular patterns, which are endogenous danger signals or alarmins, leading to autoinflammatory conditions, and contributing to production of co-stimulatory signals necessary for adaptive immune reactions (Janeway *et al.* 2002). Lipopolysaccharide (endotoxin) (LPS) from bacteria is an example of a TLR-stimulating molecule. Chondrocytes are a potential source of several proinflammatory substances which may be TLR ligands: high-mobility group box 1, heat-shock proteins, and several components of the cartilage extracellular matrix (ECM) - e.g. low-molecular-weight hyaluronan, heparin sulphate, biglycan, and fibronectin fragments (Konttinen *et al.* 2012). From this point of view, OA could be considered as an autoinflammatory disease with the chondrocyte as its primary inflammatory cell (Konttinen et al. 2012). On this basis it was hypothesized that the activation of TLR-4, a receptor for LPS, may directly affect the biosynthetic activity of chondrocytes, including expression of the miR-29 family.

The level of miR-29 family expression was measured by qRT-PCR in HACs stimulated LPS (1µg/ml) in monolayer or micromass culture for a 24 hours or a 48 hour time course, respectively. Real-time PCR showed that the miR-29 family was significantly suppressed by LPS (Figure 4.12). Interesting, the levels of all processed miRNAs were strongly regulated by LPS in a time dependent manner: a significant decrease of the two miR-29 family clusters and their precursors were detected after 4 hours of treatment whilst decrease of the mature miRNAs was not detected until 24 hours. However, after 48 hours treating with LPS, all miR-29 family was tended to increase (Figure 4.12)

Again, the effect of LPS on the promoter of pri-miR-29a/b1 was also examined by luciferase assay. The pri-miR-29a/b1 promoter reporter was transfected into SW1353 cells for 24 hours before stimulation with LPS (1µg/ml) in the presence or absence of an NFκB inhibitor JSH-23 (10µM) for another 6 hours. Luciferase assay data showed that promoter activity of pri-miR-29a/b1 was significantly decreased by LPS and this effect was abolished with the NFκB inhibitor (Figure 4.13).

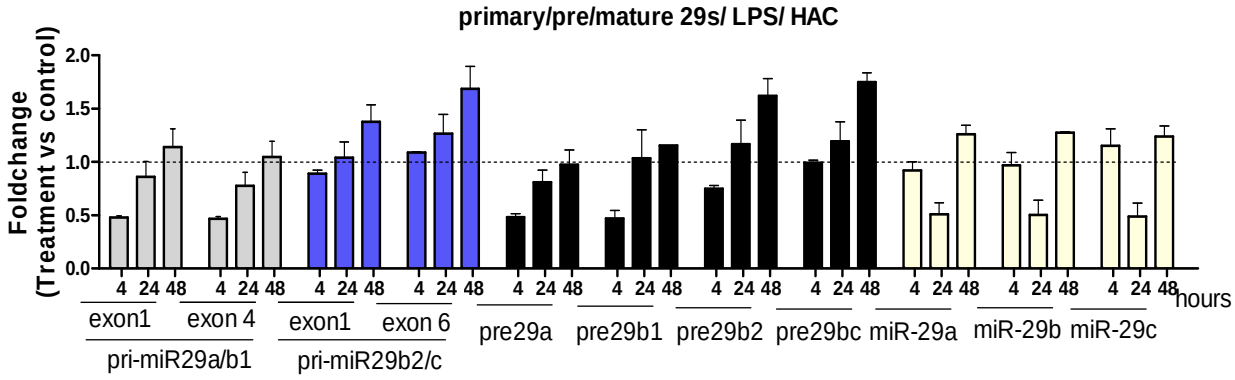

Figure 4.12: LPS suppresses expression of the miR-29 family

Human primary chondrocytes were cultured in high glucose media with 10% (v/v) FCS in monolayer. After 2 sequential passages, cells were put in micromass culture ($2.5x10^7$cells/ml) in high glucose media with 10% (v/v) FCS. After 24 hours in micromass, cells were stimulated for 4, 24, and 48 hours with LPS (1µg/ml) or vehicle (0.5% (w/v) BSA).
Relative expression of the primary miR-29a/b1, -29b2/c, precursor miR-29a, -29b1, -29b2, -29c, the mature miR-29a,- 29b, -29c was measured by quantitative RT-PCR. 18S rRNA was the endogenous control for measuring primary and precursor transcripts; U6 was the endogenous control for measuring miR-29 mature transcripts. The horizontal line at 1 serves as the vehicle control. Brown bar, pri-miR-29a/b1 transcripts; blue bar, pri-miR-29b2/c transcripts; black bar, pre-miR transcripts; yellow bar, mature miR transcripts. Means ± standard errors are presented. The difference between the treatment and the control was analysed by unpaired two-tailed Student's t test. * $p<0.05$, ** $p < 0.01$, *** $p<0.001$, n=3.

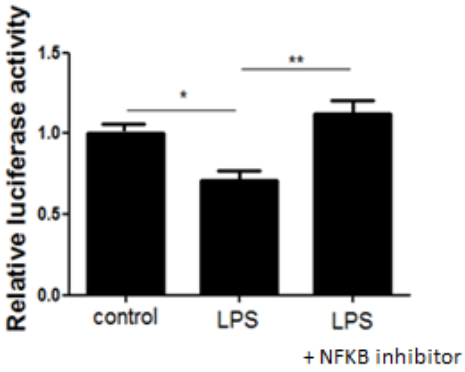

Figure 4.13: LPS suppresss the primary miR-29a/b1 promoter through NFκB

Pri-miR-29a/b1 promoter-reporter (100ng) or pGL4 (control, 100ng) was transfected into SW1353 cells. After transfection, cells were serum starved for 24 hours, followed by stimulatiion for another 6 hours with LPS (1µg/ml) in the absence or presence of an NFκB inhibitor JSH-23 (10µM) before measuring luciferase activity. Renilla was the endogenous control. Means ± standard errors are presented. The difference of luciferase activity was analysed by unpaired two-tailed Student's t test. * $p<0.05$, ** $p < 0.01$, *** $p<0.001$, n=6.

4.2.2. The microRNA-29 family targets Dicer giving a negative feedback loop for maturation of pre-miR-29

Previous data showed that expression of the miR-29 family was regulated by TGFβ, IL-1, LPS in which primary microRNA and precursor microRNA were modulated far ahead the mature microRNAs. In order to explain this, the 3'UTR regions of genes encoding for proteins involved in miRNA biogenesis were searched for putative binding site of the miR-29 family. Among these, of particular interest is the ribonuclease III enzyme Dicer, renowned for its central role in the biogenesis of microRNAs, converting the stem-loop pre-miRNA to mature miRNA (Bartel 2004). Bioinformatic analysis showed that there was a putative binding site of miR-29 in the *DICER* 3'UTR, suggesting the miR-29 family may regulate Dicer expression leading to the down-regulation of the Dicer level and as the consequence, the processing from precursors to mature miRNAs would potentially be slowed down. The 3'UTR region of *DICER* was therefore sub-cloned downstream of the firefly luciferase gene in the pmiR-GLO vector. The effect of the miR-29 family on the *DICER* 3'UTR was measured by luciferase assay after 24 hour co-transfection of the *DICER* 3'UTR- pmiR-GLO and the miR-29 family in SW1353 cells. Dual-luciferase reporter analysis showed the co-transfection of miR-29s significantly inhibited the wild type construct, whereas when the target site was mutated, the construct was not inhibited (Figure 4.14). This indicates that miR-29 may suppress expression of Dicer. The effect of the miR-29 family in *DICER* expression at transcriptional level was also investigated. Human primary chondrocyte was transfected with either miR-29b mimic (50nM) or non – targeting control (50nM). The transfected cells were then put in either monolayer or micromass culture for a further 48 hours. The expression of *DICER* was measured by qRT-PCR. Real-time qRT-PCR data showed that the expression of Dicer was not affected by miR-29s (data not shown), suggesting that the miR-29s does not control Dicer expression at mRNA level.

There is a growing body of work demonstrating that microRNAs can be processed independently of Dicer via Argonaute2 (Dueck *et al.* 2010). To evaluate whether or not miR-29s required Dicer to mature, the level of pre-miR-29s and mature miR-29s were measured in DLD, a Dicer-knockdown cell line. Data (Figure 4.15) showed that the levels of mature miR-29s were strongly reduced whilst the level of pre-miR-29s was not affected (Figure 4.15), demonstrating miR-29 processing is Dicer-dependent.

Taken together, these data show that the miR-29 family targets Dicer giving a negative feedback loop for its maturation.

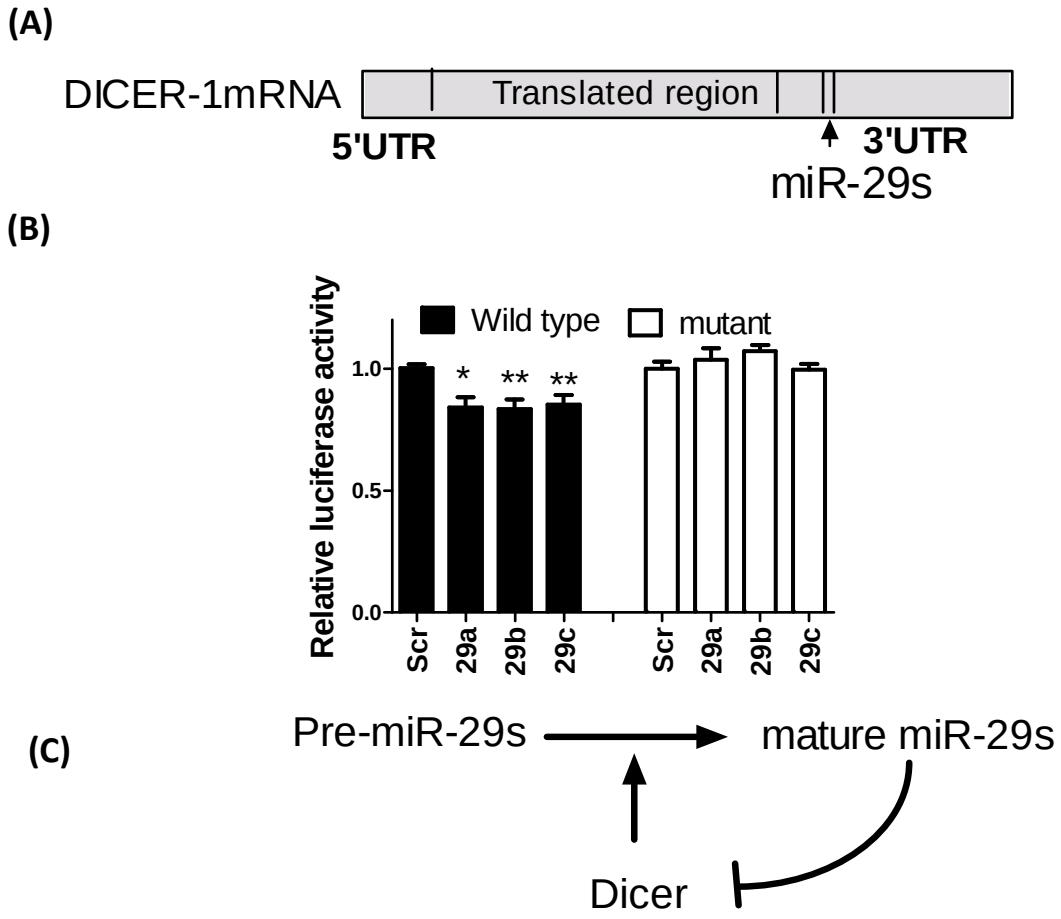

Figure 4.14: The miR-29 family targets Dicer

(A) Bioinformatic analysis reveals one binding site of the miR-29 family in the 3'UTR of Dicer. (B) miR-29 family targets Dicer: The Dicer 3'UTR containing the binding site of the miR-29 family (wild type) or a mutated, non-functional binding site for miR-29 family (mutant) were sub-cloned into the pmiR-GLO vector and were co-transfected with either miR-29a, -29b, -29c mimic (50nM) or non-targeting control (50nM) into SW1353 cells for 24 hours and luciferase activity was measured. Renilla was the endogenous control. (C) miR-29 targets Dicer giving a negative feedback loop for its maturation. Means ± standard errors are presented. The difference of luciferase activity was analysed by unpaired two-tailed Student's t test. * $p<0.05$, ** $p < 0.01$, *** $p<0.001$, n=6.

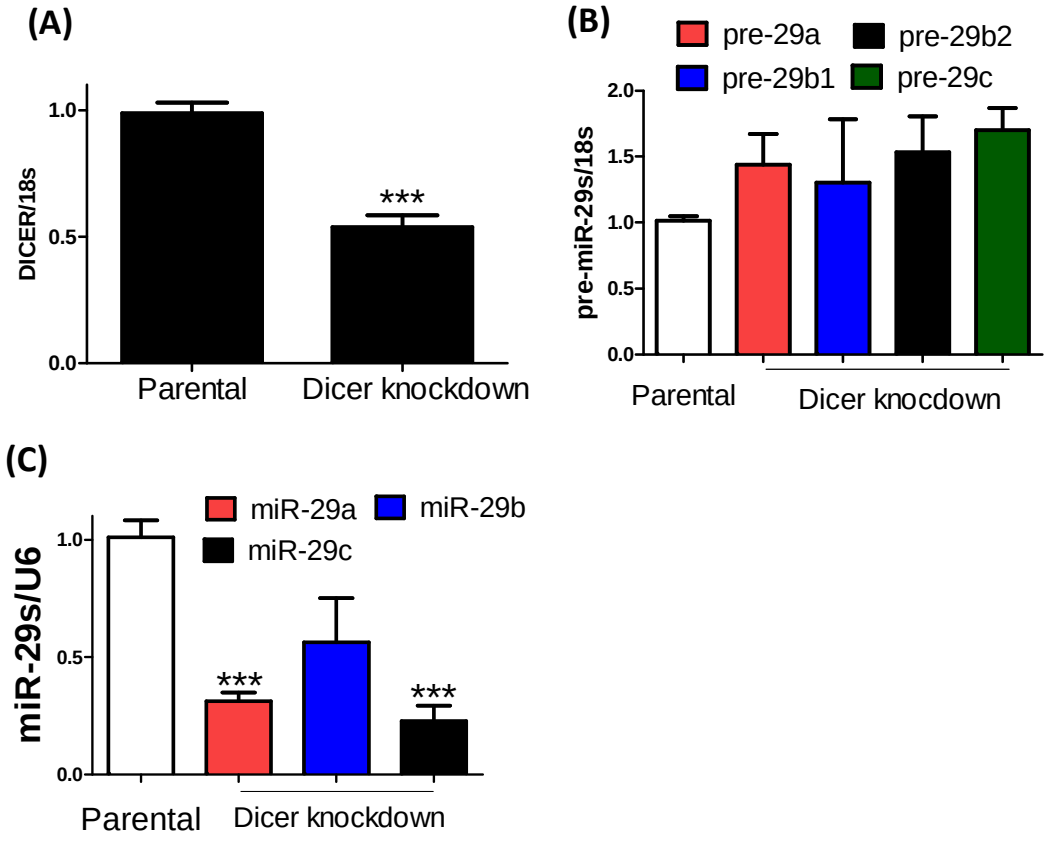

Figure 4.15: Dicer is required for the miR-29 family maturation

2

Level of Dicer, precursor and mature miR-29 were measured in DLD, Dicer knockdown cell line or parental control by quantitative RT-PCR. (A) Relative expression of Dicer; (B) Relative expression of precursor miR-29s (normalised to expression in parental control). 18S rRNA is endogenous control. Red, pre-29a; blue, pre-29b1; black, pre-29b2; green, pre-29c; white, levels of all precursors in control (set at 1); (C) Relative expression of mature miR-29 family (normalised to expression in parental control). U6 is endogenous control. Red, miR-29a; blue, miR-29b; black, miR-29c; white, levels of all mature miR-29 in control (set at 1). Means ± standard errors are presented. The difference of relative expression was analysed by unpaired two-tailed Student's t test. * $p<0.05$, ** $p < 0.01$, *** $p<0.001$, n=3.

4.3. Discussion

Since miRNAs have broad effects on cartilage homeostasis, and OA, it is particularly interesting to work out how miRNAs themselves are being regulated. Such data could provide crucial information for further understanding the mechanism underlying OA and for being able to manipulate these miRNAs in chondrocytes therapeutically. Generally, the expression of miRNAs can be regulated transcriptionally, epigenetically, or controlled by different stimuli e.g. cytokines and growth factors. In this study, just transcription factors, cytokines, and growth factors controlling the miR-29 family expression in chondrocytes were for the first time investigated. These studies were able to show that, in human chondrocytes, the master transcriptional regulator SOX9, TGFβ and LPS suppressed whilst IL-1 strongly induced the miRNA-29 family expression.

Several published data report the suppressive effect of SOX9 on the expression of individual members of the miR-29 family in other cellular contexts: in murine stem cells, overexpression of SOX9 or knockdown SOX9 in cell lines e.g. C3H10T1/2 or ATDC5 leads to suppression or induction of miR-29a and miR-29b expression (Yan et al. 2011), respectively; in human C-20/A4 chondrocytes, overexpression of SOX9 strongly down-regulated the level of miR-29a (Guerit et al. 2014). Herein, for the first time, suppressive effect of SOX9 on the expression of all members of the miR-29 family in primary human chondrocytes was shown. The effect was exerted, at least in part, through directly targeting the promoter of the miR-29a/b1 locus. In line with these data, Guerit et al (2014) reported that SOX9 can physically bind to at least 3 out of 4 putative binding sites within the proximal promoter of miR-29a/b1 cluster; also, another transcription factor YY1, was shown not to bind directly to the miR-29a/b1 promoter, but, physically interacted with SOX9 to suppress miR-29a/b1 expression (Guerit et al. 2014). The mechanism by which SOX9 negatively regulates the pri-miR-29b2/c cluster is still unknown. Several putative binding sites of SOX9 are found in the promoter of the pri-miR-29b2/c cluster, implicating a possible direct mechanism. However, this needs further investigation.

Alongside SOX9, other transcriptional regulatory mechanisms responsible for expression of the miR-29 family have also been reported: the pri-miR-29a/b1 locus was stimulated by the transcription factors CEBPA (Eyholzer et al, 2010), GATA3 (Chou et al. 2013), STAT1 (Schmitt et al, 2012) but suppressed by c-MYC (Mott et al. 2010, Parpart et al. 2014), NFκB

(Liu et al. 2010, Mott et al. 2010), Sp1(Liu et al. 2010, Amodio et al. 2012), HDAC1, HDAC3, and Gli (Mott et al. 2010); the pri-miR-29b2/c locus was inhibited by Smad3 (Qin et al. 2011), NFκB, YY1, Ezh2, H3K37, HDAC1 (Wang et al. 2008). Thus, it is likely that the transcriptional regulation of the miR-29a/b1 cluster is controlled by a combination of different transcription factors. Interestingly, in the chondrocyte context, miR-1247 together with miR-145 were reported to directly target and repress expression of SOX9 (Yang et al. 2011, Martinez-Sanchez and Murphy 2013), suggesting these miRNAs could contribute to the induction of the miR-29 family level in chondrocytes. Additionally, throughout the current project, the miR-29 family members exhibit different expression levels between the primary miR-29a/b1 and primary miR-29b2/c loci in different cellular contexts. This discrepancy could be explained in part by different transcription factor binding to each promoter.

Together with SOX9, TGFβ signalling was found to suppress the expression of all miR-29 family members in chondrocytes. Since TGFβ signalling induces SOX9 expression (Greco et al. 2011), the suppressive effect of TGFβ on the miR-29 family could be exerted through SOX9 and this TGFβ-SOX9 signalling could in part explain the down-regulation of the miR-29 family by TGFβ. The suppressive effect of TGFβ on the miR-29 family expression has also been observed in various cell types associated with fibrosis e.g. human aortic adventitial fibroblasts (Maegdefessel et al. 2012), renal fibrosis cells (Wang et al. 2012, Ramdas et al. 2013), murine hepatic stellate cells (Roderburg et al. 2011), rat hepatic stellate cells (Kwiecinski et al. 2011), human skin fibroblasts (Maurer et al. 2010), human tenon's fibroblast (Li et al. 2012), human lung fibroblast cell line (Cushing et al. 2011, Yang et al. 2013) in which either some members or the whole miR-29 family significantly decreased expression with TGFβ treatment. Apart from TGFβ-SOX9 signalling, the mechanism for the inhibition of TGFβ on the miR-29 family expression is currently unknown. There is some evidence that TGFβ inhibits miR-29 expression through SMAD3 signalling e.g. the inhibition effect of TGFβ on miR-29 expression was abolished when *Smad3* was knocked out in mouse embryonic fibroblast (Qin et al. 2011); SMAD3 could directly interact with at least two conserved SMAD3-binding sites in the promoter region of miR-29b2/c locus (Qin et al. 2011); activated TGFβ signalling induced SMAD3 translocate into nucleus and bind to miR-29b2/c promoter, resulting in the dissociation of MyoD and the stabilization of YY1 whose expression negatively regulated the miR-29b2/c expression through a conserved binding site

(Qin et al. 2011). However, this needs to be validated in chondrocytes. Besides the suppressive role, TGFβ also exerted an inductive effect on miR-29 expression at late time points. For instance, the primary miR-29b2/c locus was induced in human primary chondrocyte in micromass cultured with TGFβ1 for 48 hours (Figure 4.4b) though this increase did not reach significantly; the miR-29 family expression was increased at a late stage in the human chondrogenesis model with TGFβ3 as the major driver among others (Figure 3.12). That TGFβ induces miR-29 family expression suggests that there are may be several TGFβ-triggered signalling pathways, apart from TGFβ-SOX9, regulating the miRNA-29 expression. However, in this project, the molecular mechanisms by which TGFβ controls expression of the miR-29s are again not fully understood.

The TLR4 ligand, LPS, was found to repress the miR-29 family expression in chondrocytes. Importantly, this inhibition was facilitated by NFκB (p50/p65). Supporting the finding of this study, published data in cholangiocarcinoma cells and murine hepatic stellate cells also showed that LPS down-regulated expression of the miR-29 family (Mott et al. 2010, Roderburg et al. 2011) . Moreover, NFκB, activated by TLR ligands, was revealed to both directly or indirectly (cooperating with YY1) suppress the miR-29a/b1 or the miR-29b2/c locus, respectively (Wang et al. 2008, Mott et al. 2010). In contrast to LPS, it was surprising to find that IL-1β increased miR-29 expression and this stimulation was not NFκB but p38-dependent. However, the effect of inhibiting p38 signalling was only observed for miR-29a and miR-29b but not miR-29c, although all miR-29 family members were found strongly induced by IL-1β. Since IL-1β could activate the NFκB signalling pathway alongside p38 MAPK signalling (Aigner et al. 2006), the fact that an NFκB inhibitor further increased the IL-1 induction of the miR-29a/b1 locus implicates NFκB signalling in suppressing miR-29. It is likely that in human chondrocyte, for the period of time examined (48 hours), induction through 38 MAPK signalling was dominant over the NFκB, explaining why IL-1β induced (not suppressed) miR-29 expression. It therefore, made sense to expect a similar induction of the proximal promoter of miR-29a/b1 by IL-1β. However, a suppressive effect was observed. These data could be explained if the inductive p38-dependent transcription factors do not work through this 2kb proximal promoter of the miR-29a/b1, whilst several binding sites of NFκB in this promoter region are seen. This hypothesis needs experimental data to validate it. The mechanism responsible for the IL-1β induced miR-29b2/c cluster is still unclear and needed to be further explored. Notably, the IL-1β mRNA expression level was increased by

LPS/ TLR-4 and this is mediated by p38 MAP kinase in human chondrocytes (Bobacz *et al.* 2007). Therefore, that the miR-29 family expression was increased after 48 hours treatment with LPS could be explained in part by the accumulation of IL-1β which in turn up-regulated the miR-29 family expression.

This study also showed that the expression of all miR-29 members was not modulated by Wnt3a (β-catenin, canonical Wnt signalling), neither at the mRNA level by qRT-PCR or in the promoter assay. There are, several publications which have reported that either some members or the whole miR-29 family were Wnt3a-induced: In osteoblasts, Wnt3a positively modulates the expression of miR-29a and miR-29c though two T-cell factor/LEF-binding sites within the miR-29a/b1 promoter (Kapinas et al. 2009, Kapinas et al. 2010); in muscle progenitor cells (MPCs), Wnt3a treatment increased miR-29s expression in a time dependent manner (Hu et al. 2014); the promoter activities of both the miR-29a/b1 and miR-29b2/c cluster were strongly induced in MPCs where Wnt3a was overexpressed or added to media (Hu et al. 2014).Therefore, an interesting question that remains to be answered is why miR-29 expression is not modulated by Wnt3a in chondrocytes.

In contrast to the rapid change in expression of the pri-miR-29 or pre-miR-29 in response to stimuli, the modulation of the miR-29 family mature is quite slow. The posttranscriptional processing from the precursor to the mature form of the miR-29 family may be tightly controlled. Since the miR-29s has significant impact on a functional phenotype by regulating multiple genes that fall into the same or related pathways (which will be discussed more in Chapter 5), its expression must be regulated, potentially at more than one level. Interestingly, herein, Dicer was found to be the direct target of the miR29 family, suggesting a negative feedback loop for its maturation. In supporting this data, in T47D breast cancer cells, Dicer 1 was also reported as a miR-29a target (Cochrane *et al.* 2010). Apart from Dicer, other components of the microRNA precursor processing machinery e.g. Helicase, Exportin 4 and 5 are also predicted to be putative targets of the miR-29s as they have several binding sites in their 3'UTR regions (data not shown). Even though these have not been experimentally validated as the direct targets, this further supports the idea that miR-29 is involved in a negative feedback loop for its maturation.

In conclusion, the miR-29 family was found to be negatively regulated by the master regulator of chondrogensis SOX9, by TGFβ signalling and by LPS-NFκB signalling. It is

positively regulated by IL-1-p38 MAPK signalling. Interestingly, the canonical Wnt signalling pathway does not control expression of the miR-29 family. Furthermore, expression of the miR-29 family was tightly controlled at the level of posttranscriptional processing in which miR-29 directly targets Dicer, giving a negative feedback loop for its maturation.

CHAPTER 5
FUNCTIONS OF THE MICRORNA 29 FAMILY IN CHONDROCYTES

5.1 Introduction

The ability of a single miRNA to target multiple mRNAs especially those that function in the same intracellular pathways and/or diseases, adds an additional layer of regulation to gene expression. The aberrant expression of the miR-29 family has been found in multiple malignancies and fibroses, carcinogenesis. Also, an understanding of how miR-29 contributes to these processes has been revealed: miR-29 targets genes are involved in cellular proliferation, cell cycle, cell differentiation, and apoptosis at genetic and epigenetic levels. The following summarizes some functions of miR-29s in human disease.

In chondrogenesis or OA, around 30 miRNAs have been shown to have functions in cartilage homeostasis (Le et al, 2013), which is relatively small compared to the total number of miRNAs. Moreover, as mentioned in the previous chapter, for any potential miRNA therapeutic application, a combination of different miRNAs might be required for a complex disease like OA. Identifying novel miRNA targets and the cell signalling pathways and networks by which miRNAs exert their functions on disease phenotype are therefore, of particular importance both to have an insight into OA pathogenesis and also to ensure the specificity in any miRNA-based drug delivery method. Thus, this chapter places emphasis on identifying the function of the miR-29 family in chondrocytes including identifying the function of the miR-29 family in TGFβ/Smad, NFκB, and Wnt/β-catenin signalling pathways and novel targets of the miR-29s.

Aims:

- Investigate signalling pathways involved in chondrogenesis and osteoarthritis which are regulated by the miR-29 family
- Perform gain-and-loss of function of miR-29b experiments to identify potential targets of the miR-29 family
- Identify and validate novel direct targets of the miR-29 family

5.2 Results

5.2.1 The miR-29 family supress TGFβ/Smad signalling pathway

In articular cartilage, the canonical TGFβ/Smad signalling pathway has been shown to play a pivotal role in the maintenance of normal cartilage: it up-regulates the expression of several types of collagens and proteoglycan; and it down-regulates cartilage degrading enzymes. Importantly, disruption of the TGFβ pathway has been shown to lead to OA. Mice expressing a dominant negative TGFβRII exhibit articular cartilage degeneration similar to that observed in human OA with abnormal expression of type X collagen, an indicator of chondrocyte hypertrophy; mutant mice with targeted disruption of Smad3 (Smad3−/−) show a similar pathology in chondrocytes, including aberrant type X collagen expression in vivo; primary chondrocytes isolated from Smad3−/− mice demonstrate an accelerated differentiation process with up-regulated BMP signalling.

In Chapter 4, expression of the miR-29 family was found to be suppressed by TGFβ signalling. Here, I measure the impact of the miR-29 family on Smad signalling. The TGFβ/Smad signalling reporter (CAGA)12-luc (Figure 5.1a) containing 12 binding sites of the Smad2/3/4 (GAGAC) binding site upstream of the firefly luciferase-encoding gene was used. The principle of this experiment is based on the fact that: signals are transduced from TGFβ ligands to the Smad2/3/4 complex which subsequently regulates gene expression; the miR-29 family may change the expression or transcriptional activity of Smad2/3/4; thus altering luciferase levels. $(CAGA)_{12}$-luc (100ng) and Renilla (10ng) were co-transfected with either miR-29 mimic (50nM) or non-targeting control (50nM) into SW1353 cells for 24 hours and followed by serum starvation for another 24 hours. Cells were then treated with either TGFβ1 or TGFβ3 (4ng/ml) for another 6 hours before measuring the luciferase activity. Luciferase assay data (Figure 5.1b) showed that: stimulating cells with TGFβ1 strongly induced luciferase activity as compared with non-treatment control; pre-treatment with all members of the miR-29 family significantly decreased the luciferase activity at this 6 hour time point. A similar pattern was observed when treating cells with TGFβ3 (Appendix, Figure 7a). These data demonstrate that Smad signalling was successfully activated in SW1353 cells by TGFβ1or TGFβ3 and that the miR-29 family is a negative regulator of this signalling. As all miR-29 family members supressed the signalling, an experiment using only an inhibitor of miR-29b (50nM) was performed. Consistent with the mimic data above,

luciferase activity was significantly increased with the miR-29b inhibitor compared to control (Figure 5.1c and Appendix, Figure 7b).

The suppressive effect of the miR-29 family on the TGFβ signalling pathway was further confirmed by measuring the effect of the miR-29 family on a TGFβ responsive gene. ADAMTS4 was chosen since it is induced by TGFβ in chondrocytes, but was not a putative direct target of the miR-29 family. Human primary chondrocytes were transfected with miR-29 family mimics (50nM) in monolayer for 24 hours with 10% (v/v) FCS. The media was then replaced with media with 0.5% (v/v) FCS for another 24 hours before stimulating with TGFβ (4ng/ml) for a further 6 hours. The expression of ADAMTS4 was measured by qRT-PCR (Figure 5.2) showing that ADAMTS4 was strongly induced by TGFβ; the miR-29 mimics significantly decreased the expression of ADAMTS4 as compared with non-targeting control. These data again confirmed the suppressive effect of the miR-29 family on TGFβ signalling pathway.

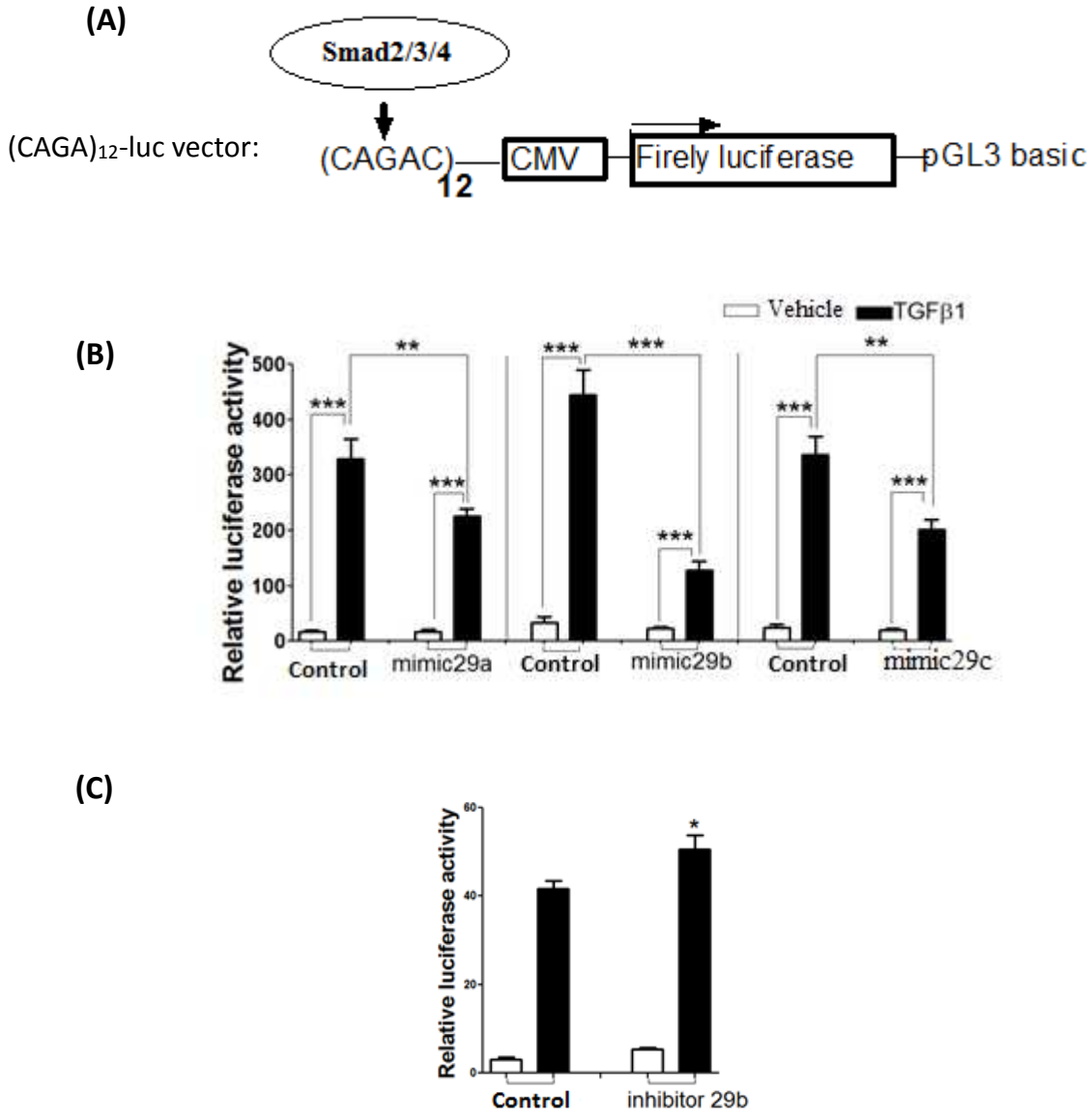

Figure 5.1 The miR-29 family suppress TGFβ signalling pathway

(A) The TGFβ signalling reporter ($CAGA_{12}$-luc) contains 12 binding sites of the Smad2/3/4 (GAGAC) binding consensus upstream of the firely luciferase-encoding gene in pGL3100ng $CAGA_{12}$-luc vector, and 10ng Renilla vector were co-transfected with either miR-29 family mimic (B) or miR-29b inhibitor (C) into SW1353 cells in monolayer. The non-targeting control (50nM) was also used as the negative control. 24 hours after transfection, cells were serum starved for another 24 hours, followed by treatment with TGFβ (4ng/ml) for another 6 hours before measuring luciferase activity. Renilla is the loading control for luciferase assay. Open bar: non – treatment control, close bar: TGFβ treatment. Means ± standard errors are presented, n=6. The difference of luciferase activity was analysed by Student's unpaired two-tailed t test. * $p<0.05$, ** $p < 0.01$, *** $p<0.001$

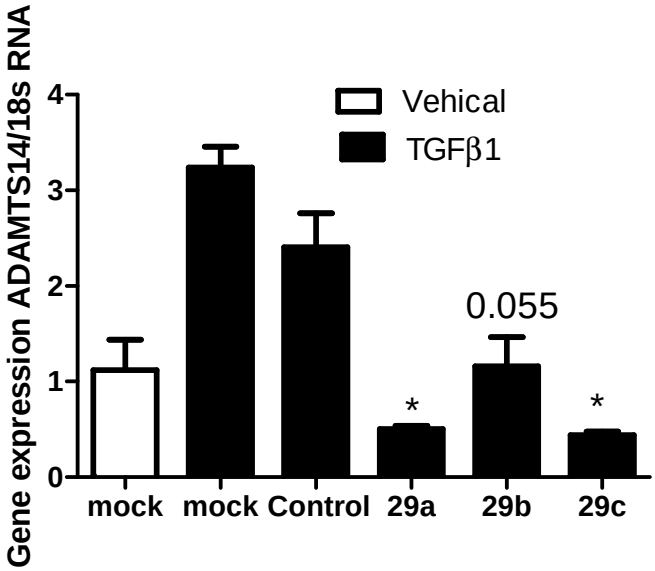

Figure 5.2 The miR-29 family suppresses the TGFβ induced gene ADAMTS4

Human primary chondrocytes were transfected with either miR-29 family mimics (50nM) or non – targeting control (50nM) for 24 hours. Cells were then changed into 0.5% (v/v) FCS for 24 hours and followed by stimulating with TGFβ1 (4ng/ml) for another 6 hours. Total RNA was isolated and the expression level of ADAMTS4 was measured by qRT-PCR. 18S rRNA was used as the endogenous control. Data were normalized to untreated, mock transfected cells. Open bar: non – treatment control, close bars: TGFβ treatment. Means ± standard errors are presented, n=3. The difference in expression level of ADAMTS was analysed by Student's unpaired two-tailed t test. * $p<0.05$, ** $p < 0.01$, *** $p<0.00$

5.2.2 The miR-29 family suppresses the NFκB signalling pathway

In Chapter 4, IL-1β was found to increase expression of the miR-29 family. It is, therefore, of importance to investigate how the miR-29 family regulates the signalling pathways triggered by IL-1β. There are at least three pathways triggered by IL-1β including NFκB, JNK, and p38 MAPK pathways. Nevertheless, in this project, just the interaction between the miR-29 family and NFκB signalling was investigated. The transcription factor NFκB is held in the cytoplasm in an inactive form associated with the inhibtory κB (IκB) protein. In response to IL-1β binding of the receptor, NFκB releases from IκB and the activated NFκB will then translocate to the nuclear, bind to DNA elements present in its target genes and facilitate their transcription.

Similar to the experiment for investigating the interacting between the miR-29 family and TGFβ signalling, the NFκB signalling reporter containing multiple binding sites for NFκB upstream of a luciferase-encoding gene was utilized (Figure 5.3a). The signal cascade from IL-1β will activate NFκB which consequently induces the transcription of the luciferase gene in the reporter and this may be modulated by the miR-29 family. The luciferase assay was set up similar to the experiment in 5.1.1 except the cells were treated with IL-1β (5ng/ml) instead of TGFβ1 (4ng/ml). Luciferase data (Figure 5.3b, c) showed that IL-1β strongly induced the luciferase activity of the κB reporter; all miR-29 family mimics significantly decreased activity (B) but the miR-29b inhibitor induced activity (C). These data show that NFκB signalling was successfully triggered in SW1353 cells by IL-1and that the miR-29 family is a negative regulator of the NFκB signalling pathway.

The suppressive effect of the miR-29 family on the NFκB signalling pathway was further confirmed by measuring the effect of the miR-29 family on an NFκB responsive gene. MMP3, which is induced expression by IL-1 and is not a putative direct target of the miR-29 family, was chosen. Again, the experiment was set up similar to the experiment in 5.1.1 except cells were stimulated with IL-1 (5ng/ml). The Taqman qRT-PCR (Figure 5.4) showed that MMP3 was strongly induced expression by IL-1β; the miR-29b and miR-29c mimics significantly decreased the expression of MMP3 as compared with non-targeting control, though the miR-29a mimic had no effect.

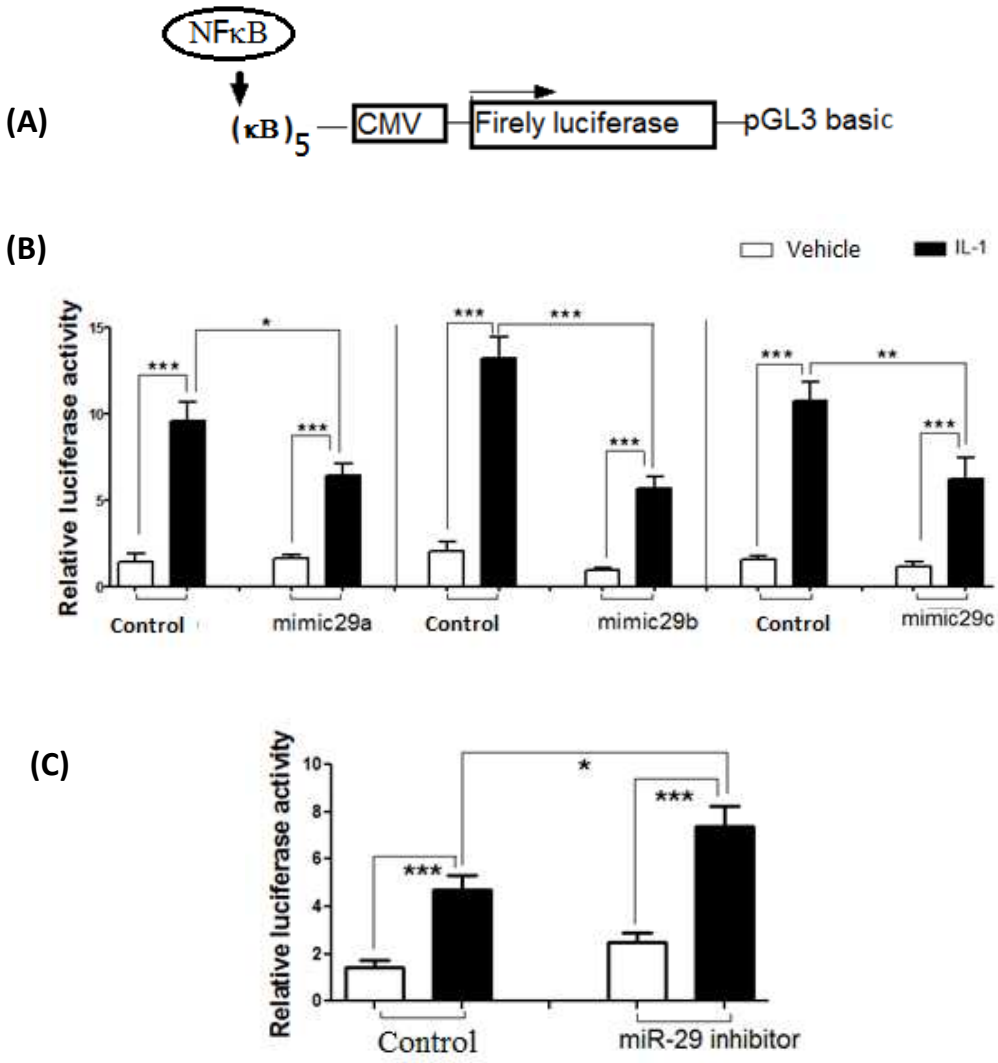

Figure 5.3 The miR-29 family suppresses NFκB signalling pathway

(A) The NFκB signalling reporter (κB vector) contains 5 binding sites of NFκB upstream of the firely luciferase-encoding gene in pGL3

100ng κB vector, and 10ng Renilla expression vector were co-transfected with either miR-29 family mimic (B) or miR-29b inhibitor (C) into SW1353 cells in monolayer. The non-targeting control (50nM) was also used as a negative control. 24 hours after transfection, cells were serum starved for further 24 hours, and followed by treating with IL-1 (5ng/ml) for another 6 hours before measuring luciferase activity. Renilla is the endogenous control for luciferase assay. Means ± standard errors are presented, n=6. The difference of luciferase activity was analysed by Student's unpaired two-tailed t test. * $p<0.05$, ** $p < 0.01$, *** $p<0.001$

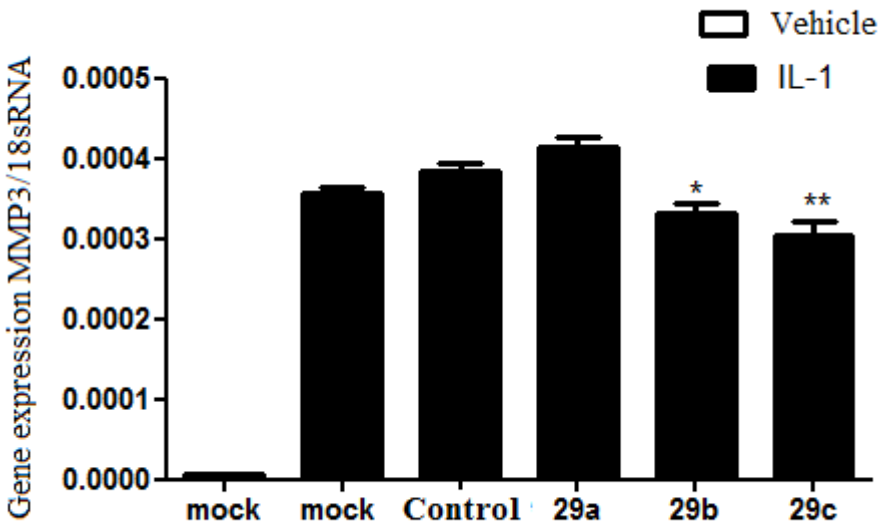

Figure 5.4 The miR-29 family suppresses expression of the IL-1-induced gene MMP3
Human primary chondrocytes were transfected with either miR-29 family mimic (50nM) or non – targeting control (50nM) for 24 hours. Cells were then changed into 0.5% (v/v) FCS for 24 hours, followed by stimulating with IL-1β (5ng/ml) for a further 6 hours. Total RNA was isolated and the expression of MMP3 was measured by qRT-PCR. 18S rRNA expression was used as the housekeeping gene. Open bar: non – treatment control, close bar: IL-1β treatment. Means ± standard errors are presented, n=3. The difference in expression level of IL-1β was analysed by unpaired two-tailed t test. * $p<0.05$, ** $p < 0.01$, *** $p<0.001$

5.2.3 The miR-29 family supresses the canonical Wnt signalling pathway

Even though expression of the miR-29 family is not regulated by Wnt3a in human chondrocyte, it is still of interest to investigate whether the WNT/β-catenin signalling is modulated by the miR-29 family because of the critical role of this signalling in OA development: balanced β-catenin levels are essential for maintaining homeostasis of articular cartilage and any factors impairing this balance could lead to pathological changes.

For investigating the interaction between the miR-29 family with the WNT/β-catenin signalling, the TOPFlash reporter (containing 7 binding sites of TCF/LEF driving the expression of the luciferase encoding gene) and FOPFlash reporter (control for TOPFlash where all the TCF/LEF binding sites are mutated) were used (Figure 5.5a). With the presence of e.g. Wnt3a, the signal transduced from the FZD receptor and LRP-5/6 co-receptor proteins will lead to the accumulation of β-catenin in the nucleus where it acts in concert with TCF/LEF transcription factors to generate a transcriptionally active complex inducing the expression of cognate genes and also therefore the TOPFlash reporter. Thus, any modulation of luciferase activity in the presence of the miR-29 family indicates that the miRNA family impacts on canonical signalling. Again the luciferase assay experiment was set up similarly to the assay in 5.1.1 but the TOPFlash (100ng) or FOPFlash (100ng) and Wnt3a (50ng/ml) were utilized. Luciferase assay data (Figure 5.5b, c) showed that Wnt3a strongly induced the luciferase activity from TOPFlash but not FOPFlash reporters; all members of the miR-29 family significantly decreased luciferase activity, whilst a miR-29b inhibitor increased the luciferase activity compared to control. These data show that the WNT/β-catenin pathway was induced in SW1353 cell with Wnt3a and that the miR-29 family is a negative regulator of this signalling.

The suppressive effect of the miR-29 family on the WNT/β-catenin signalling pathway was further confirmed by measuring the effect of the miR-29 family on the expression of *AXIN2*, a WNT/β-catenin responsive gene and not a putative direct target of the miR-29 family. The experiment was set up similarly to the experiment in 5.1.1 except cells were stimulated with Wnt3a (50ng/ml). The qRT-PCR data (Figure 5.6) showed that *AXIN2* expression was strongly induced by Wnt3a; the miR-29 family mimics significantly decreased the expression of *AXIN2* as compared with non-targeting control.

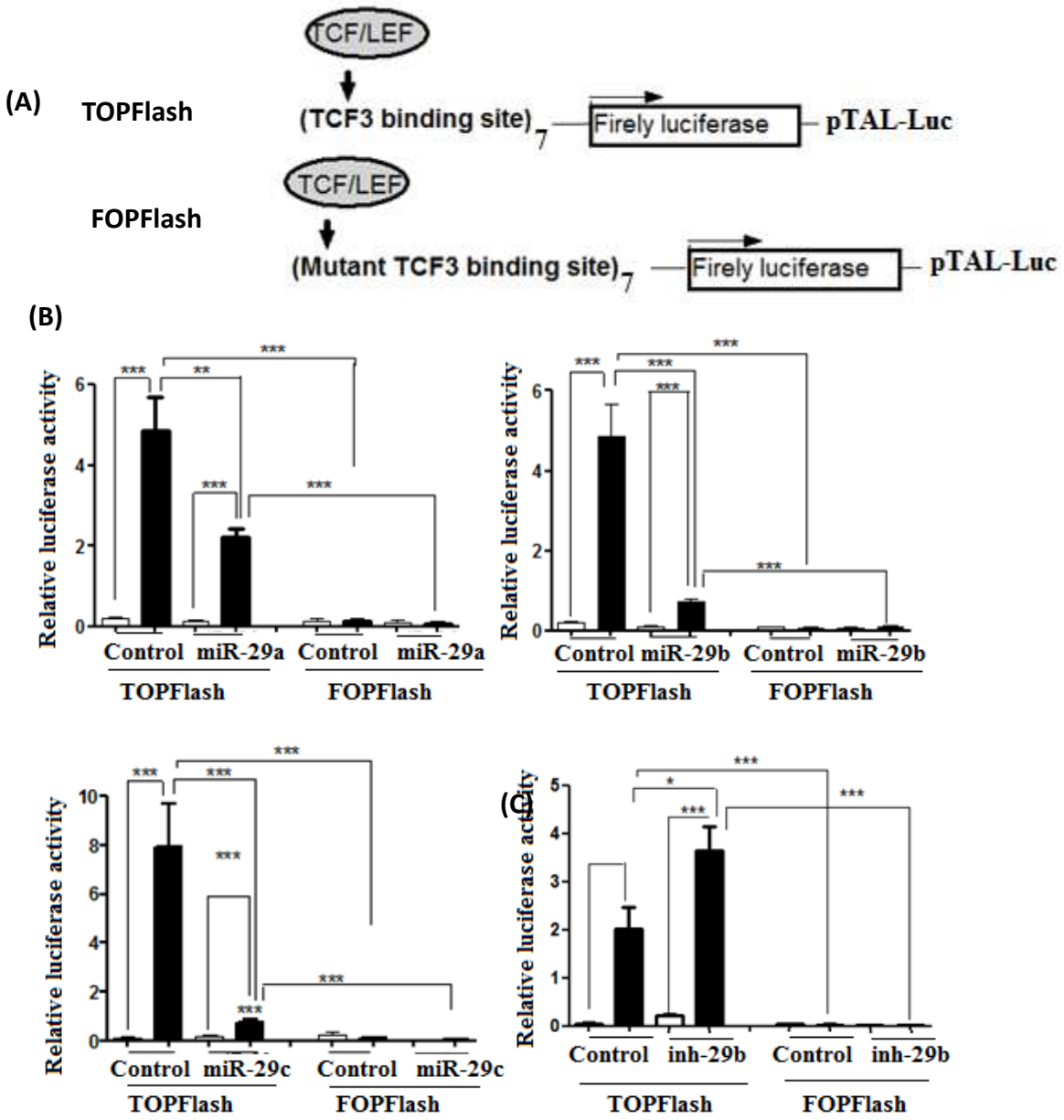

Figure 5.5 The miR-29 family suppresses the WNT/β-catenin signalling pathway

(A) The canonical WNT signalling reporter (TOPFlash vector) contains 7 binding sites of TCF/LEF upstream of the firely luciferase encoding gene in the pTAL-Luc vector. The FOPFlash vector is the control in which all binding sites of TCF/LEF are mutated.

100ng TOPFlash or FOPFlash vectors, and 10ng Renilla vector was co-transfected with either miR-29 family mimic (50nM) (B) or miR-29b inhibitor (50nM) (C) into SW1353 cells in monolayer. The non-targeting control (50nM) was also used as the control. 24 hours after transfection, cells were serum starved for another 24 hours, and followed by treatment with WNT3a (50ng/ml) for another 6 hours before measuring luciferase activity. Renilla is the endogenous control for luciferase assay. Means ± standard errors are presented, n=6. The difference of luciferase activity was analysed by Student's unpaired two-tailed t test. * $p<0.05$, ** $p < 0.01$, *** $p<0.001$

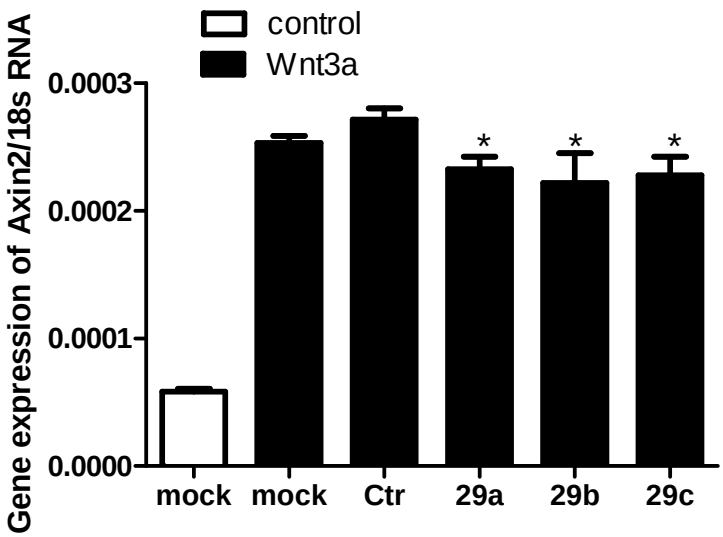

Figure 5.6 The miR-29 family suppresses expression of the WNT/β-catenin induced gene *AXIN2*

Human primary chondrocytes were transfected with either miR-29 family mimic (50nM) or non – targeting control (50nM) for 24 hours. Cells were then serum starved for 24 hours and followed by stimulating with Wnt3a (50ng/ml) for another 6 hours. The expression level of Axin2 was measured by qRT-PCR. 18S rRNA was used as the housekeeping gene. Open bar: non – treatment control, close bar: WNT3a treatment. Means ± standard errors are presented, n=3. The difference in expression level of *AXIN2* was analysed by unpaired two-tailed t test. * $p<0.05$, ** $p < 0.01$, *** $p<0.001$

5.2.4 Identification of miR-29 family targets

The miR-29 family was found to suppress the TGFβ/Smad, NFκB, and WNT/β-catenin signalling pathways. Nonetheless, it still remained unclear the direct mechanism by which the miR-29 family controlled these pathways. I therefore sought to identify novel targets of the miR-29 family to explain how the miR-29 family interacts with these pathways.

5.2.4.1 Gain- and loss- of function of miR-29b

For identifying new targets, a gain- and loss- of function experiment was performed. Since the miR-29 family shares the same seed binding site, it was deemed sufficient just to overexpress or silence miR-29b rather than all members of the family. Human primary chondrocytes were transiently transfected with miR-29b mimic or miR-29b inhibitor (50nM) and their non-targeting controls for 48 hours in triplicate and then total RNA was isolated. The transfection experiment was validated by measuring the miR-29b level by qRT-PCR. The data (data not shown) showed that the level of miR-29b strongly increased or decreased after transfection with either miR-29b mimic or inhibitor, respectively. These data suggest a good transfection efficiency into human chondrocytes. For performing a whole genome profile, an equal amount of total RNA from each sample in the triplicate was pooled together. These pooled samples were then subjected to whole genome array using Illumina human HT-12 V4.0 expression BeadChips to profile more than 47,000 human transcripts.

The global effect of the miR-29b mimic and inhibitor transfection on whole genome expression was first investigated by plotting the distribution of different expression values for all mRNAs in the miR-29b overexpression or knockdown experiments. Since the miRNA will exert its function by suppressing target gene expression, it was expected that the overexpression of miR-29b would significantly suppress target gene expression; conversely, a strong induction of target gene expression would be observed with the silencing of the miR-29b. Consistent with this hypothesis, data (Figure 5.7A) showed that in the miR-29b silencing experiment, the distribution of modulated genes was slightly skewed towards higher expression. Using an absolute 1.3 fold change (FC) as the cut off, there are 213 and 144 mRNA going up and down, respectively in this experiment (whilst just 9 and 10 mRNA going up and down respectively if the FC cut off was 1.5). Surprisingly, this pattern was also observed with the overexpression of the miR-29b (Figure 5.7B) with 703 and 518 mRNA

going up and down with 1.5 FC cut off, respectively. These data suggest that the miR-29b mimic has stronger effect than miR-29b inhibitor in chondrocytes and that the transfection with the miR-29b mimic strongly induced rather than supressed gene expression. Further analysis of the mRNAs strongly increased with miR-29b overexpression showed that the majority of these induced genes do not contain a binding site for the miR-29 family in their 3'UTR, suggesting that they are not direct targets of the miR-29 family. Indeed, a number of interferon responsive genes were strongly increased (Appendix, Table 7), suggesting a non-specific response to the synthetic oligonucleotide. This has been previously noted even for small RNAs (Karlsen et al. 2011). Interestingly, these genes were not modulated in the miR-29b silencing experiment, suggesting that a specific sequence in the miR-29b mimic is responsible.

The effect of the miR-29b mimic or inhibitor on whole genome expression was further analysed by examining the potential targets of the miR-29 family. The array data (Figure 5.8) revealed there were 12215 mRNAs in the intersection of the two experiments that increased in the miR-29b knockdown and decreased in miR-29b overexpression experiments. To further explore the effect of modulation of miR-29b on the transcriptome, the percentage of mRNAs containing seed sites (e.g. 6-mer, 7-mer, 8-mer) was calculated. It was a postulated that potential direct targets of miR-29s (those mRNA containing miR-29 seed sites) should be enriched in mRNA down-regulated by miR-29b and in mRNA up-regulated by miRNA-29b silencing. Particularly, this enrichment should be highest in genes that are decreased by miR-29b mimic and increased by miR-29b inhibitor. Data (Figure 5.8) showed that regardless of the length of the seed sequence, the percentage of mRNAs with seed sites is higher in the mRNAs which are decreased on overexpression or increased on silencing of miR-29b than in total mRNA. The percentage of mRNAs with seed sites is the highest in the intersection of the two experiments. These data confirm the hypothesis that taking the intersection containing mRNAs which decrease with the overexpression and increase with silencing of miR-29b is an effective way to filter the relevant miRNA targets.

Also, a subset of mRNA which was differentially expressed in the microarray analysis was selected for validating using RT-qPCR. Comparison of the expression levels between the microarray and RT-PCR results demonstrated a similar expression pattern between the two platforms (data not shown). These results confirmed the mRNA array data.

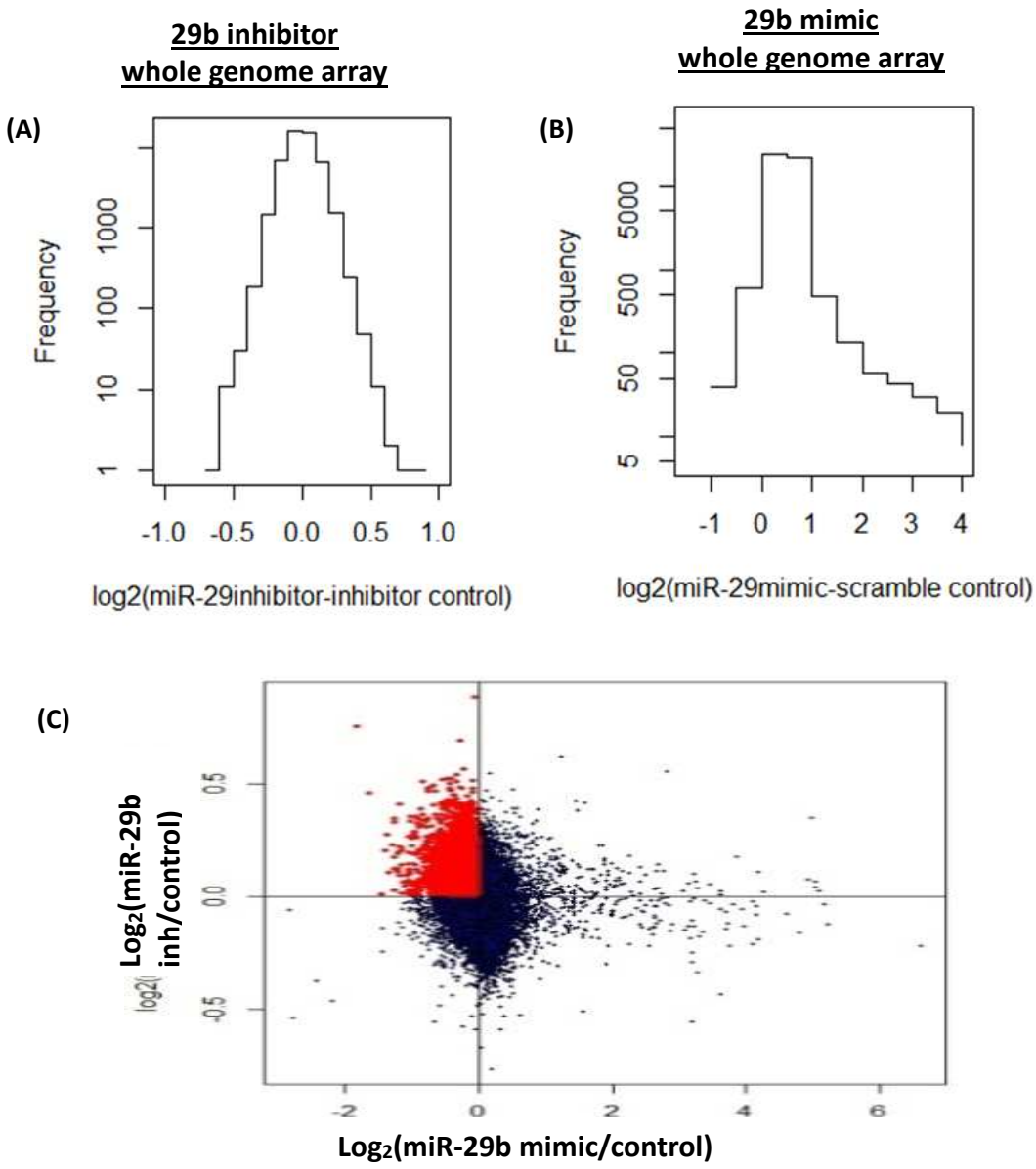

Figure 5.7 Gain- and loss- of function of miR-29b experiments

Human primary chondrocytes were cultured in high glucose media with 10% (v/v) FCS in monolayer until reaching 90% confluence. Cells were transfected with miR-29b mimic (50nM), miR-29b inhibitor (50nM), or non – targeting control (50nM) for 48 hours in triplicate. Cells were then harvested and total RNA was isolated from each sample. An equal amount of total RNA from each sample was pooled together. Pooled samples were subjected to whole genome array using Illumina humanHT-12 V4.0 expression BeadChip array. The Global effect of the miR-29b overexpression or silencing on whole genome expression was presented in (A) for the miR-29b silencing experiment and in (B) for the miR-29b overexpression experiment. Both datasets were plotted together on the same chart (C). The mRNAs which decreased in the miR-29 overexpression and increased in the miR-29b silencing experiment are highlighted in red.

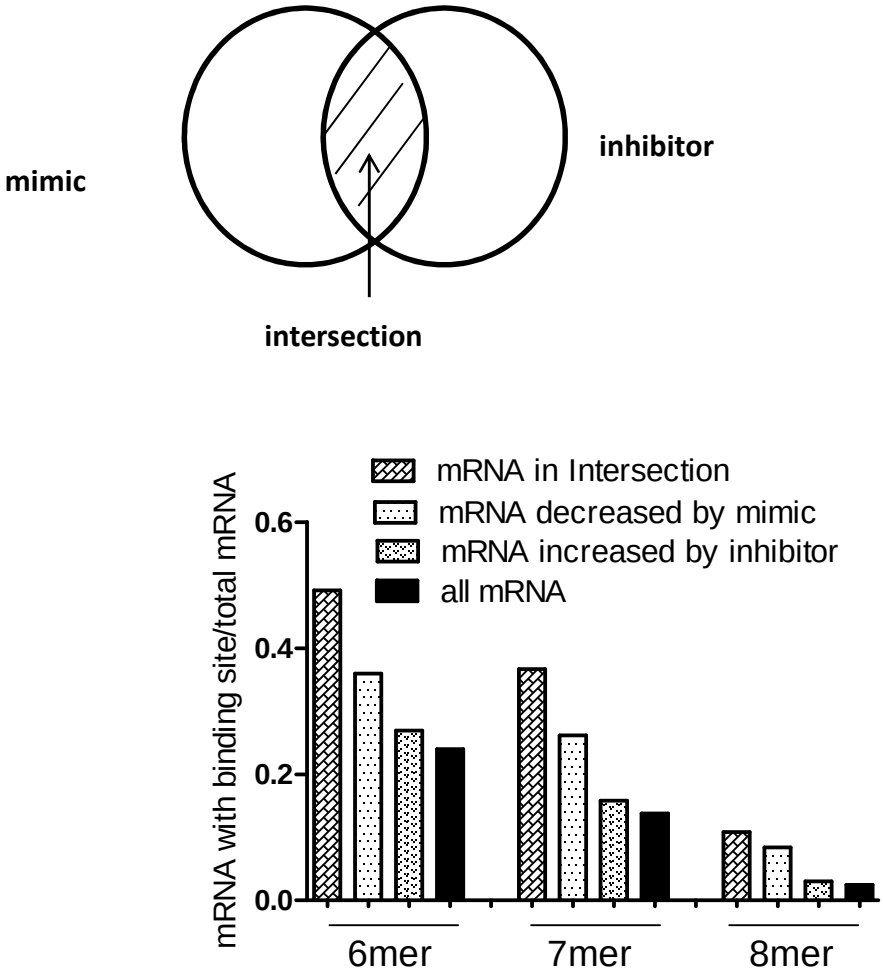

Figure 5.8: Enrichment of miR-29 putative direct targets in miR-29b gain – and loss – of function experiment.

From whole genome array data, the percentage of miR-29 putative direct targets was calculated for (i) mRNA decreased by the miR-29b mimic ; (ii) mRNA increased by the miR-29b inhibitor ; (iii) mRNA in the intersection of the two (decreased by miRN-29b mimic and increased by inhibitor) (iv) all the mRNAs detected from the whole genome array. The calculation was performed for the range of fold change (FC) and for each types of seed sequence e.g. 6-mer, 7-mer, 8-mer. The mRNA having more than one binding site for each type of seed sequence was always assigned as 1. When FC=k, the percentage of 6mer-seed-site targets increasing or decreasing expression was calculated: **6mer** = sum of mRNA having 6mer-seed site sequence in the 3'UTR with FC in the range of (k, FC max) if k >0, or (FC min, k) if k<0; **Total mRNA** = sum of mRNA with FC in the range of (k, FC max) if k>0, or (FC min, k) if k< 0; **mRNA with binding site/ total mRNA = 6mer/total mRNA.** The percentage of other seed site targets was calculated similarly. Here, calculation for the absolute FC 1.3 is presented.

5.2.4.2 Known targets of the miR-29 family

The miR-29 family has emerged as an important miRNA in a number of pathologic settings by regulating multiple genes that fall into the same or related pathways.

In the whole genome array of the overexpression and silencing of the miR-29b, a number of known direct targets of the miR-29 family were also identified in human chondrocytes (e.g. Table 5.1).

Gene	Binding sites				Fold change mimic (decrease)	Fold change inhibitor (increase)
	s6	s7m8	s7a1	s8		
COL1A1	**3**	**1**	**3**	**1**	**2.53**	**1.69**
COL1A2	**3**	**1**	**2**	**1**	**1.26**	**1.05**
COL2A1	**1**	**1**	**1**	**1**	**1.17**	**1.39**
COL3A1	**3**	**2**	**2**	**2**	**1.36**	**1.26**
COL4A1	**2**	**1**	**2**	**1**	**1.22**	**1.41**
COL5A1	**5**	**4**	**2**	**2**	**1.15**	**1.15**
COL5A2	**2**	**1**	**2**	**1**	**2.20**	**1.27**
COL6A1	**1**	**0**	**1**	**0**	**1.27**	**1.08**
COL6A2	**1**	**1**	**1**	**1**	**1.12**	**1.01**
COL6A3	**1**	**1**	**1**	**1**	**1.20**	**1.14**
COL8A1	**1**	**1**	**1**	**1**	**1.35**	**1.07**
COL11A1	**2**	**2**	**0**	**0**	**1.80**	**1.25**
COL15A1	**2**	**1**	**1**	**1**	**1.73**	**1.22**
COL16A1	**1**	**1**	**0**	**0**	**1.35**	**1.05**
COL20A1	**3**	**0**	**0**	**0**	**1.01**	**1.13**
ADAM19	**6**	**2**	**0**	**0**	**1.64**	**1.28**
CDK6	**3**	**2**	**1**	**0**	**1.61**	**1.07**

Table 5.1: Fold change expression of known targets of the miR-29 family in the miR-29b gain- and loss- of function experiment in human articular chondrocytes

5.2.4.3 Novel targets of the miR-29 family

5.2.4.3.1 The ADAMTS family

The miR-29 family is one example of the fact that a miRNA can regulate many functionally related genes. As shown above, a number of extracellular matrix-related genes were found to be direct targets of the miR-29 family. Since a miRNA can regulate the expression of several hundred genes, it was likely that the miR-29 family could directly target sets of novel genes within families. In chapter 4, TGFβ was found to suppress miR-29 family expression and the miR-29 family itself was also found to supress TGFβ signalling. These data suggest that the level of miR-29 and TGFβ-induced genes, may be inversely correlated and the miR-29 family might further inhibit the effect of TGFβ signalling on gene expression by exerting a second suppressive effect on the pathway through directly targeting inducible genes. This means that a number of TGFβ-inducible genes could potentially be direct targets of the miR-29 family. Herein, the ADAMTS family investigated as TGFβ inducible genes (except *ADAMTS 19*) (Figure 5.9) and genes which have roles in cartilage.

Human primary chondrocytes were stimulated with TGFβ1 for 24 hours in monolayer culture. The expression levels of members of the ADAMTS families were measured by qRT-PCR showing that *ADAMTS6*, *ADAMTS10*, *ADAMTS14* and *ADAMTS17* were significantly induced by TGFβ (Figure 5.9). Moreover, bioinformatic analysis found that there were a number of miR-29 binding sites in the 3'UTR regions of these ADAMTS genes (Table 5.2). Together with this, these TGFβ induced ADAMTS genes were predicted to be miR-29 potential direct targets by different bioinformatics algorithms e.g. Diana, Targetscan, Microcosm, miRDB, Picta (Table 5.2). Taken together, all of these data demonstrated that ADAMTS genes, including *ADAMTS6, ADAMTS10, ADAMTS14, ADAMTS17, ADAMTS19* are miR-29 potential direct targets.

In order to validate these ADAMTS genes as miR-29 direct targets, the expression levels of these genes were measured by qRT-PCR in human chondrocytes transfected with the miR-29b mimic for 48 hours. qRT-PCR (Figure 5.10) showed that the expression of these ADAMTS genes was significantly suppressed by overexpression of the miR-29b, again supporting that these genes are the miR-29 direct targets. To further validate these ADAMTS genes as miR-29 direct targets, the 3'UTR regions containing the miR-29 binding sties were

subcloned downstream of the luciferase encoding gene in pmiRGLO. These ADAMTS3'UTR-pmiRGLO reporter vectors (100ng) were co-transfected with the miR-29 family mimic (50nM) to DF1 cells. After 24 hours of transfection, the cells were harvested and luciferase assays were performed. Together with the ADAMTS 3'UTR-pmiRGLO reporter vectors, mutant vectors in which the miR-29 binding sites were mutated were constructed and tested. A 3'UTR was a direct target for the miR-29 family if the luciferase activity was suppressed with the overexpression of the miRNA in the wild-type construct and this effect was abolished when the miRNA binding sites were mutated. Luciferase assay data showed that *ADAMTS6* (Figure 5.14), *ADAMTS10* (Figure 5.15*), ADAMTS14* (Figure 5.11), *ADAMTS17* (Figure 5.12), *ADAMTS19* (Figure 5.13) were all direct targets of the miR-29 family.

Genes	8 -mer	7 -mer	6 -mer	Bioinformatic algorithm
ADAMTS6		2		Diana, Targetscan, Microcosm, miRDB,Picta
ADAMTS10		2		Diana, Microcosm, Picta
ADAMTS14		2	2	Diana, Picta
ADAMTS17		2	3	Targetscan, Microcosm, miRDB,Picta
ADAMTS19		2		Picta

Table 5.2: *ADAMTS6, ADAMTS10, ADAMTS14, ADAMTS17, ADAMTS19* are predicted to be miR-29 targets

A number of different binding sites for miR-29 were found in the 3'UTR regions of *ADAMTS6, ADAMTS10, ADAMTS14, ADAMTS17,* and *ADAMTS19*. These ADAMTSs were predicted to be miR-29 family targets by different bioinformatics algorithms.

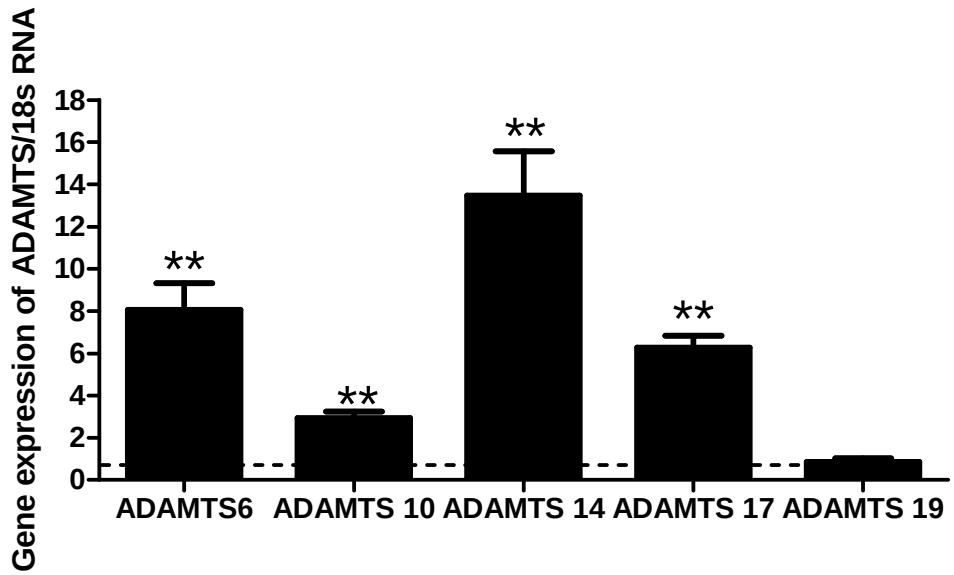

Figure 5.9 Members of ADAMTS family are TGFβ inducible genes

Human primary chondrocytes was cultured with 10% (v/v) FCS in monolayer until 90% confluence. Cells were switched to media with 0.5% (v/v) FCS for 24 hours before treating with TGFβ1 (4ng/ml) or vehicle (4mM HCl+0.5% (w/v) BSA) for another 24 hours. Cells were harvested and subjected to total RNA isolation. Relative expression of the ADAMTS genes was measured by quantitative RT-PCR. 18S rRNA was the housekeeping control. Relative expression value of each of the ADAMTSs in TGFβ stimulated cells was normalized to the vehicle control. The horizontal line at 1 serves as the vehicle control. Closed bar: TGFβ treatment, open bar: vehicle. Means ± standard errors are presented, n=3. The difference between the treatment and the control was analysed by Student's unpaired two-tailed t test. * $p<0.05$, ** $p < 0.01$, ***, $p<0.001$.

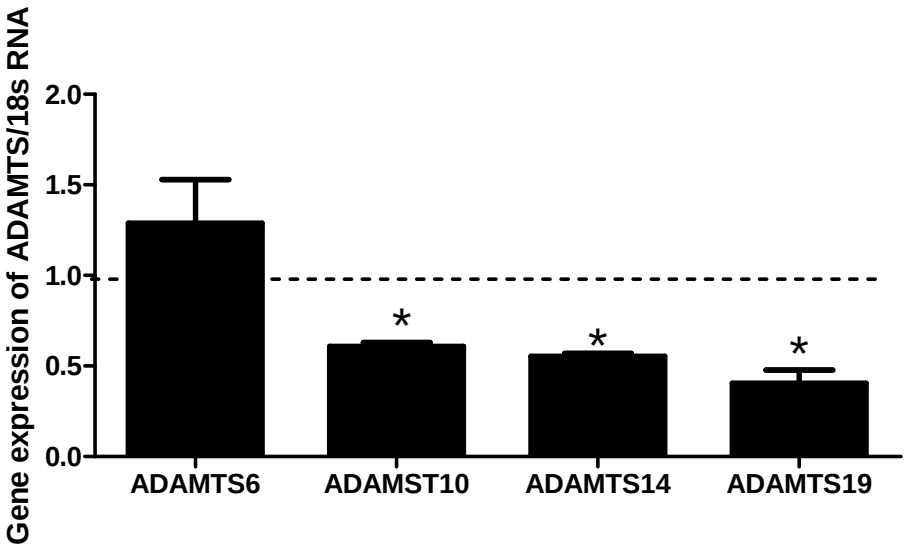

Figure 5.10 The expressions of members of the ADAMTS family were suppressed by miR-29b mimic

Human primary chondrocytes was cultured in media with 10% (v/v) FCS in monolayer until 90% confluence. Cells were then transfected with either miR-29b mimic (50nM) or non – targeting control (50nM) for 48 hours. Total RNA was isolated and the expression levels of the ADAMTS genes were measured by qRT-PCR. 18S rRNA was the housekeeping control. Relative expression value of each of the ADAMTS genes was normalized to non – targeting control. The horizontal line at 1 serves as the non-targeting control. Means ± standard errors are presented, n=3. The difference in expression between miR-29b overexpression and non – targeting control was analysed by Student's unpaired two-tailed t test. * $p<0.05$, ** $p < 0.01$, ***, $p<0.001$

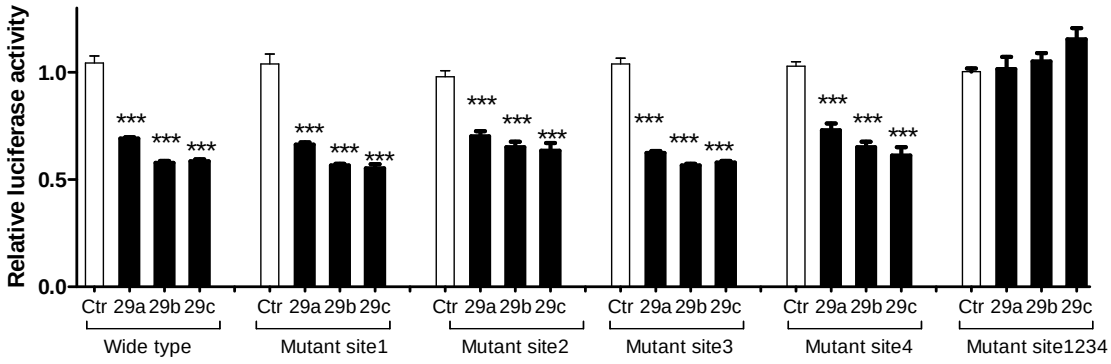

Figure 5.11: ADAMTS14 is a direct target of the miR-29 family

The ADAMTS14 3'UTR region containing 4 binding sites of the miR-29 family was subcloned downstream of the luciferase encoding gene in the pmiRGLO vector to create the ADAMTS14 3'UTR-pmiRGLO wide type (WT) vector. The mutant vectors were created from WT vector in which just single or quadruplicate binding sites of the miR-29 family were mutated. Either the WT or the mutants vectors (100ng) were co-transfected into chicken fibroblast DF1 cells with either miR-29b mimic (50nM) or non – targeting control (50nM). Luciferase assays were performed 24 hours after transfection. The relative luciferase value was normalised to the non-targetting control Open bar: non-targetting control, closed bar: miR-29 family mimic. Means ± standard errors are presented, n=6. The difference of luciferase activity was analysed by Student's unpaired two-tailed t test. * $p<0.05$, ** $p < 0.01$, *** $p<0.001$, Ctr, non-targetting control, 29a, 29b, 29c: miR-29a,-b,-c mimic.

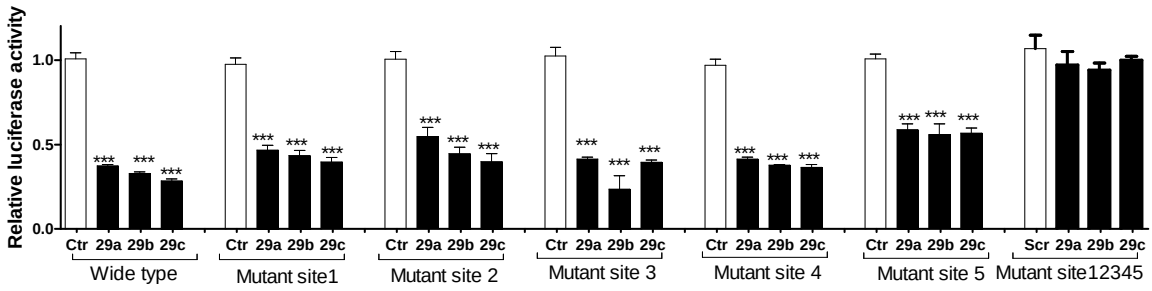

Figure 5.12: ADAMTS17 is a direct target of the miR-29 family

The ADAMTS17 3'UTR region containing 5 binding sites of the miR-29 family was subcloned downstream of the luciferase encoding gene in the pmiRGLO vector to create the ADAMTS17 3'UTR-pmiRGLO wide type (WT) vector. The mutant vectors were created from WT vector in which just single or quadruplicate binding sites of the miR-29 family were mutated. Either the WT or the mutants vectors (100ng) were co-transfected into chicken fibroblast DF1 cells with either miR-29b mimic (50nM) or non – targeting control (50nM). Luciferase assays were performed 24 hours after transfection. The relative luciferase value was normalised to the non-targetting control Open bar: non-targetting control, closed bar: miR-29 family mimic. Means ± standard errors are presented, n=6. The difference of luciferase activity was analysed by Student's unpaired two-tailed t test. * $p<0.05$, ** $p < 0.01$, *** $p<0.001$, Ctr, non-targetting control, 29a, 29b, 29c: miR-29a,-b,-c mimic.

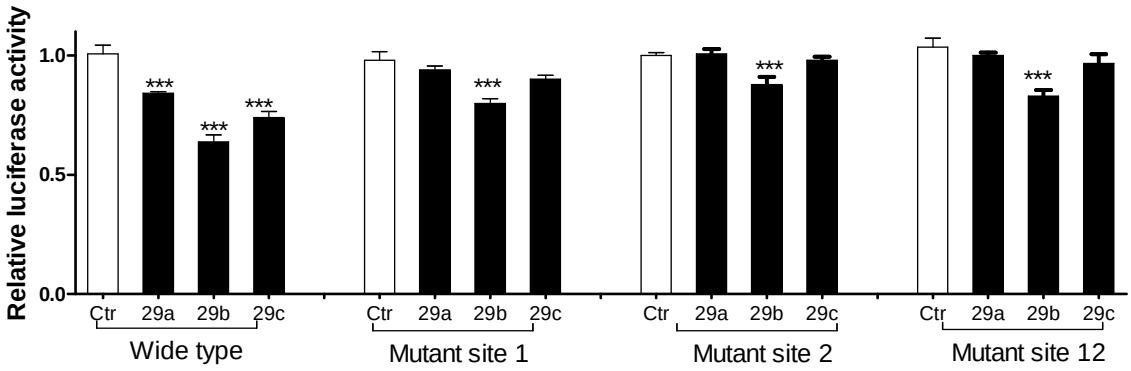

Figure 5.13: ADAMTS19 is a direct target of the miR-29 family

The ADAMTS19 3'UTR region containing 2 binding sites of the miR-29 family was subcloned downstream of the luciferase encoding gene in the pmiRGLO vector to create the ADAMTS19 3'UTR-pmiRGLO wide type (WT) vector. The mutant vectors were created from WT vector in which just single or duplicate binding sites of the miR-29 family were mutated. Either the WT or the mutants vectors (100ng) were co-transfected into chicken fibroblast DF1 cells with either miR-29b mimic (50nM) or non – targeting control (50nM). Luciferase assays were performed 24 hours after transfection. The relative luciferase value was normalised to the non-targetting control Open bar: non-targetting control, closed bar:

miR-29 family mimic. Means ± standard errors are presented, n=6. The difference of luciferase activity was analysed by Student's unpaired two-tailed t test. * $p<0.05$, ** $p < 0.01$, *** $p<0.001$, Ctr, non-targetting control, 29a, 29b, 29c: miR-29a,-b,-c mimic.

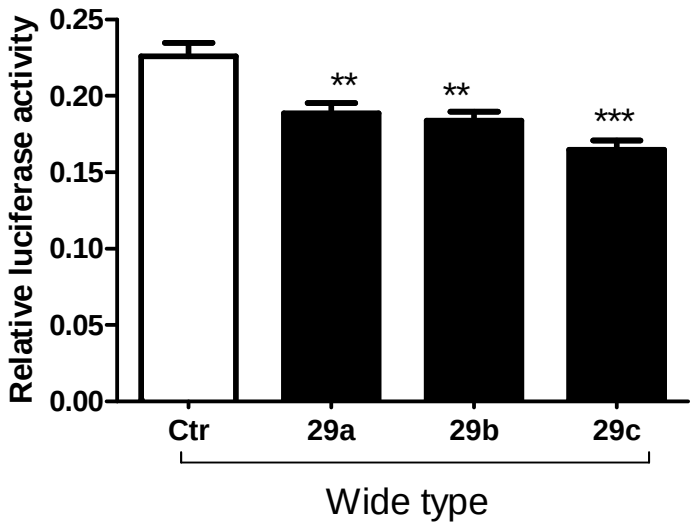

Figure 5.14: ADAMTS6 is a direct target of the miR-29 family

The ADAMTS6 3'UTR region containing 2 binding sites of the miR-29 family was subcloned downstream of the luciferase encoding gene in the pmiRGLO vector to create the ADAMTS6 3'UTR-pmiRGLO wide type (WT) vector. The WT vector (100ng) was co-transfected into chicken fibroblast DF1 cells with either miR-29b mimic (50nM) or non – targeting control (50nM). Luciferase assays were performed 24 hours after transfection. The relative luciferase value was normalised to the non-targeting control Open bar: non-targeting control, closed bar: miR-29 family mimic. Means ± standard errors are presented, n=6. The difference of luciferase activity was analysed by Student's unpaired two-tailed t test. * $p<0.05$, ** $p < 0.01$, *** $p<0.001$, Ctr, non-targeting control, 29a, 29b, 29c: miR-29a,-b,-c mimic.

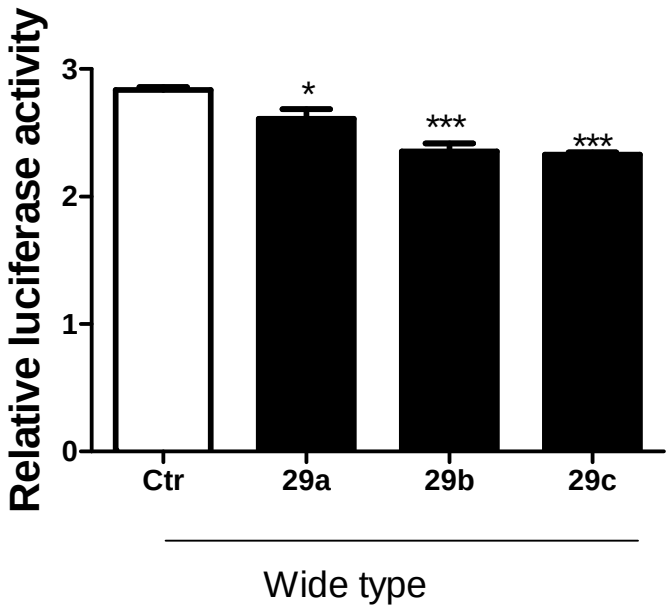

Figure 5.15: ADAMTS10 is a direct target of the miR-29 family
The ADAMTS10 3'UTR region containing 2 binding sites of the miR-29 family was subcloned downstream of the luciferase encoding gene in the pmiRGLO vector to create the ADAMTS10 3'UTR-pmiRGLO wide type (WT) vector. The WT vector (100ng) was co-transfected into chicken fibroblast DF1 cells with either miR-29b mimic (50nM) or non – targeting control (50nM). Luciferase assays were performed 24 hours after transfection. The relative luciferase value was normalised to the non-targeting control Open bar: non-targeting control, closed bar: miR-29 family mimic. Means ± standard errors are presented, n=6. The difference of luciferase activity was analysed by Student's unpaired two-tailed t test. * $p<0.05$, ** $p < 0.01$, *** $p<0.001$, Ctr, non-targeting control, 29a, 29b, 29c: miR-29a,-b,-c mimic.

5.2.4.3.2 WNT signalling pathway related genes

As shown previously, the miR-29 family was found to negatively regulate the TGFβ, NFκB, and WNT/β-catenin signalling pathways. The remaining question is how the miR-29 family supress these signalling pathways.

The whole genome array from the miR-29b gain – and loss – of function experiment found 12215 mRNAs that were the miR-29 putative targets. These consisted of 6925 mRNAs containing at least one 6-mer, 3400 mRNAs containing 7-mer, and 728 mRNAs containing 8-mer binding sites in their 3'UTR. Those mRNAs with miR-29 binding sites were considered as putative direct targets of the miR-29 family; the others without the miR-29 binding site were considered as indirect targets.

The miR-29 family suppression of TGFβ, NFκB, and WNT/β-catenin signalling pathways could be through a direct mechanism by targeting the mRNAs in the signalling cascade. In order to verify how miR-29 suppresses these signalling pathways, both putative miRNA-29 indirect and direct targets were analysed with DAVID functional analysis (web address) software to identify the most represented gene ontology (GO) categories. Analysing the miR-29 direct target sections found the enrichment for the Wnt signalling pathway together with MAPK kinase signalling pathway, apoptosis pathways, P53 signalling pathways. Since, NFκB and TGFβ pathways did not come up in this analysis, the miR-29 indirect targets were further analysed. However, neither NFκB nor TGFβ signalling pathways were enriched. In the scope of this project, the mechanisms by which the miR-29 suppressed these two signalling pathways remains unclear and need to be further explored.

All the miR-29 putative direct targets were selected regardless of the fold change cut off. In this manner, the Wnt signalling-related direct targets e.g. Dishevelled 3 (DVL3), casein kinase 2 alpha 2 polypeptide (CSNK2A2), GSK-3 binding protein frat2 (FRAT2), Frizzled family receptor 3 (FZD3), and Frizzled family receptor 5 (FZD5) were only modulated with a small fold change in the array (Fold change between 1 to 1.2). The expression of these mRNAs were measured by qRT-PCR, however in triplicate samples these data showed that the modulation of these genes under the control of the miR-29b did not reach statistical significance (Appendix, Figure 8).

Even though expression of these Wnt-related genes was not significantly modulated at the mRNA level, the genes were explored as miR-29 direct targets since miR-29 might exert its functions on these genes at the protein level. To verify these genes as the miR-29 direct targets, 3'UTR regions containing miR-29 binding sites of these genes were subcloned downstream of a luciferase encoding gene in the pmiRGLO vector. Constructs in which the miR-29 binding sites were mutated were also created. Either the 3'UTR-pmiRGLO vectors or the mutant 3'UTR-pmiRGLO vectors were co-transfected with the miR-29 family mimic (50nM) into DF1 cells for 24 hours. Then cells were harvested and the luciferase assays were performed. Luciferase assay data showed that FZD3 (Figure 5.19), FZD5 (Figure 5.18), FRAT2 (Figure 5.17), CK2A2 (Figure 5.16), DVL3 (Figure 5.15) were the direct targets of the miR-29 family since the luciferase activities were significantly decreased with the miR-29 family mimics and this effects were abolished when the miR-29 binding sites were mutated.

As mentioned above, qRT-PCR showed that the expression levels of these WNT signalling related genes were not significantly modulated with the miR-29b mimic at the mRNA level. However, the luciferase assay showed that miR-29 family could directly bind to the 3'UTR regions of these genes. It was postulated that the miR-29 family could directly target these genes at the protein level. Since all members of the miR-29 family directly targeted these genes, it was sufficient to check the effect of the miR-29b mimic on these genes at the protein level. In order to test this hypothesis, SW1353 cells were transfected with miR-29b mimic for 72 hours. Cells were then harvested and subjected to western blot. Time limitations meant that only expression levels of DVL3 were examined. Western blot data (Figure 5.15) showed that miR-29b supressed DVL3 expression level to 50% as compared to the non – targeting control, again confirming DVL3 is a direct target of miR-29 family.

Taken together, all of these data provide good evidence that the miR-29 family can inhibit the Wnt signalling, at least in part, via repression of these targets. Interestingly, DVL3, CSNK2A2 and FRAT2 were decreased in expression in hip OA cartilage compared to fracture controls, where the miR-29 family were increased in expression. Fzd3 expression however, was higher in expression in hip OA (Figure 5.20).

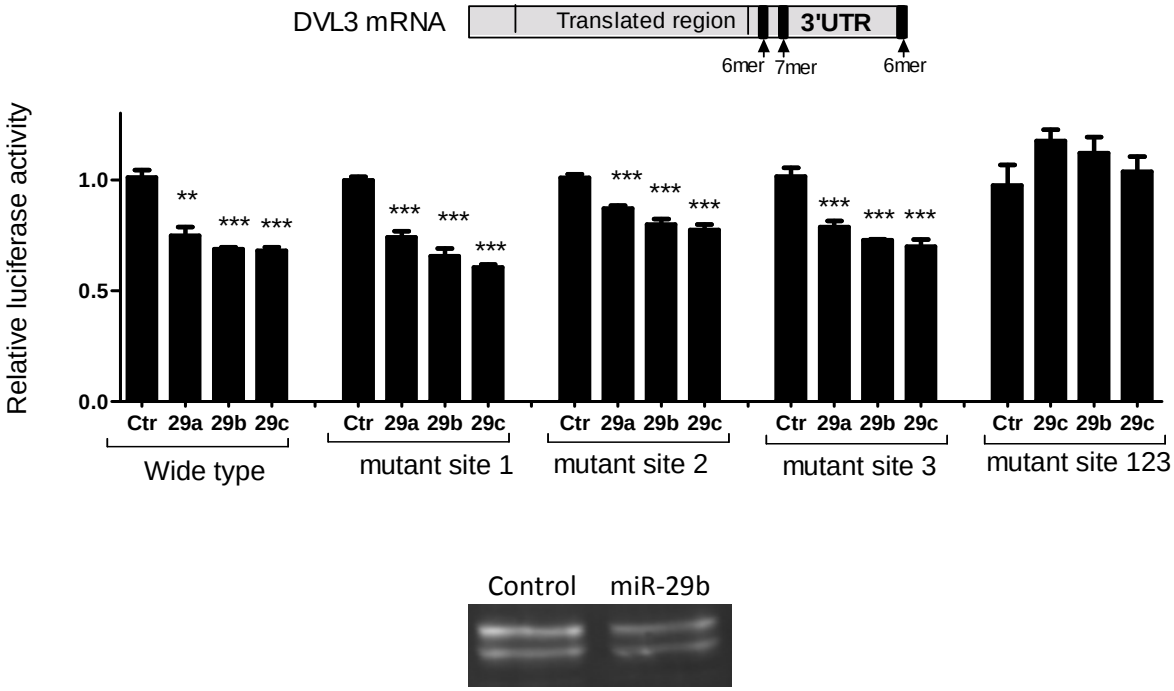

Figure 5.16: DVL3 is a direct target of the miR-29 family

(A) The DVL3 3'UTR region containing 3 binding sites of the miR-29 family was subcloned downstream of the luciferase encoding gene in the pmiRGLO vector to create the DVL3 3'UTR-pmiRGLO wide type (WT) vector. The mutant vectors were created from WT vector in which just single or triplicate binding sites of the miR-29 family were mutated. Either the WT or the mutants vectors (100ng) were co-transfected into chicken fibroblast DF1 cells with either miR-29b mimic (50nM) or non – targeting control (50nM). Luciferase assays were performed 24 hours after transfection. The relative luciferase value was normalised to the non-targetting control. Means ± standard errors are presented, n=6. The difference of luciferase activity was analysed by Student's unpaired two-tailed t test. * $p<0.05$, ** $p < 0.01$, *** $p<0.001$, Ctr, non-targetting control, 29a, 29b, 29c: miR-29a,-b,-c mimic.

(B) SW1353 was transfected with a miR-29b mimic (50nM) or non-targeting control (50nM) for 3 days. Protein was extracted and separated on 10 (w/v) SDS-PAGE, blotted onto PVDF and probed with an anti DVL3 antibody. The blot was stripped and re-probed with a GAPDH antibody to assess loading, n=2.

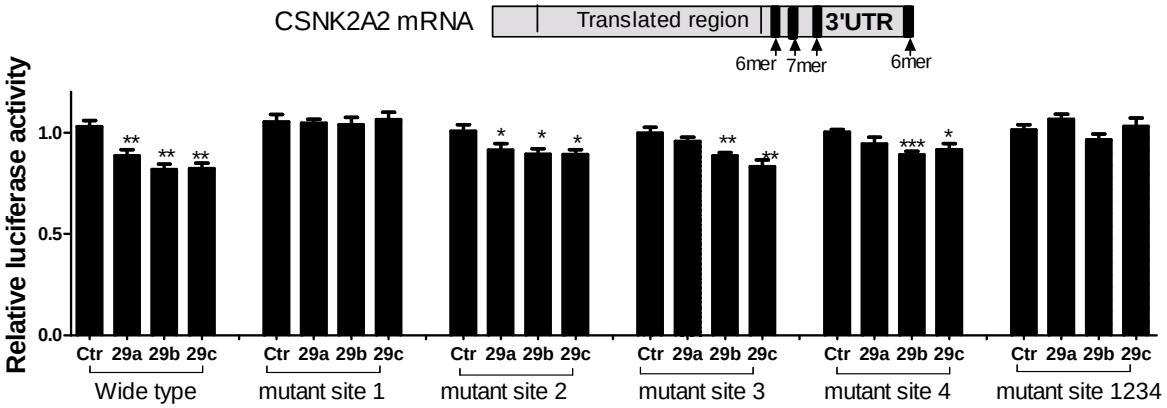

Figure 5.17: CK2A2 is a direct target of the miR-29 family

The CK2A2 3'UTR region containing 4 binding sites of the miR-29 family was subcloned downstream of the luciferase encoding gene in the pmiRGLO vector to create the CK2A2 3'UTR-pmiRGLO wide type (WT) vector. The mutant vectors were created from WT vector in which just single or quadruplicate binding sites of the miR-29 family were mutated. Either the WT or the mutants vectors (100ng) were co-transfected into chicken fibroblast DF1 cells with either miR-29b mimic (50nM) or non – targeting control (50nM). Luciferase assays were performed 24 hours after transfection. The relative luciferase value was normalised to the non-targeting control. Means ± standard errors are presented, n=6. The difference of luciferase activity was analysed by Student's unpaired two-tailed t test. * $p<0.05$, ** $p < 0.01$, *** $p<0.001$, Ctr, non-targeting control, 29a, 29b, 29c: miR-29a,-b,-c mimic.

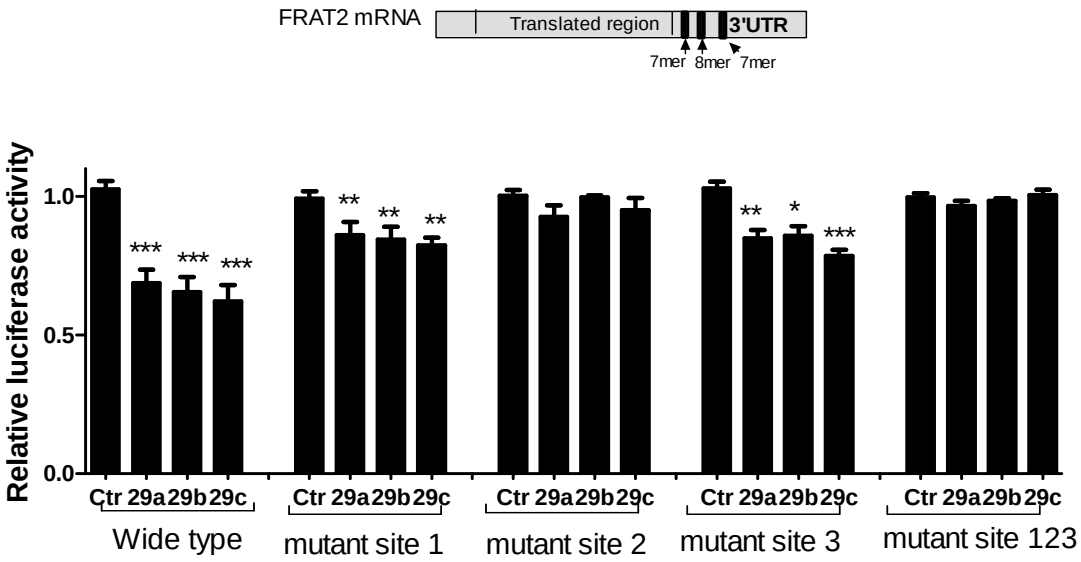

Figure 5.18: *FRAT2* is a direct target of the miR-29 family

The *FRAT2* 3'UTR region containing 4 binding sites of the miR-29 family was subcloned downstream of the luciferase encoding gene in the pmiRGLO vector to create the *FRAT2* 3'UTR-pmiRGLO wide type (WT) vector. The mutant vectors were created from WT vector in which just single or triplicate binding sites of the miR-29 family were mutated. Either the WT or the mutants vectors (100ng) were co-transfected into chicken fibroblast DF1 cells with either miR-29b mimic (50nM) or non – targeting control (50nM). Luciferase assays were performed 24 hours after transfection. The relative luciferase value was normalised to the non-targeting control. Means ± standard errors are presented, n=6. The difference of luciferase activity was analysed by Student's unpaired two-tailed t test. * $p<0.05$, ** $p < 0.01$, *** $p<0.001$, Ctr, non-targeting control, 29a, 29b, 29c: miR-29a,-b,-c mimic.

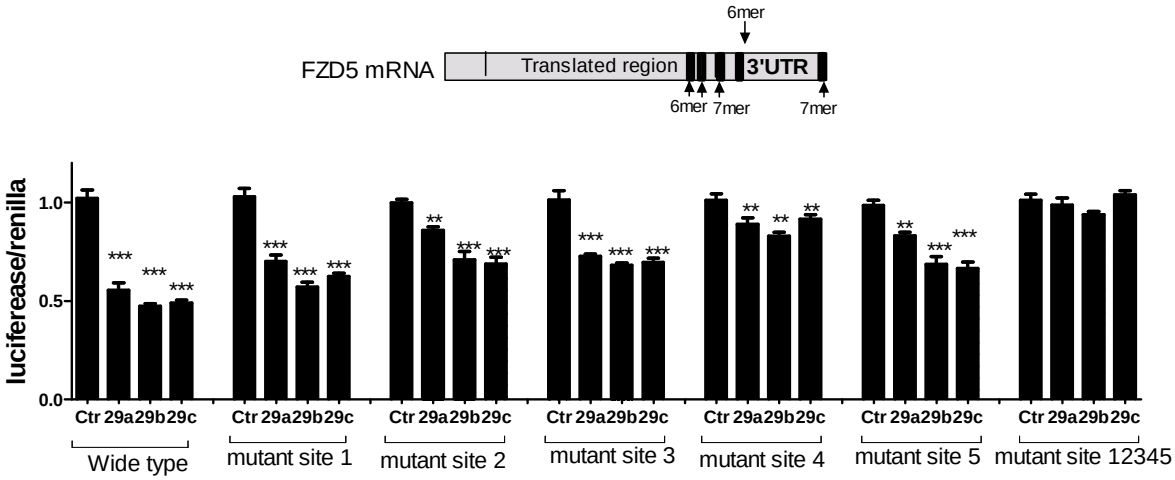

Figure 5.19: *FZD5* is a direct target of the miR-29 family

The *FZD5* 3'UTR region containing 5 binding sites of the miR-29 family was subcloned downstream of the luciferase encoding gene in the pmiRGLO vector to create the *FZD5* 3'UTR-pmiRGLO wide type (WT) vector. The mutant vectors were created from WT vector in which just single or quintuplicate binding sites of the miR-29 family were mutated. Either the WT or the mutants vectors (100ng) were co-transfected into chicken fibroblast DF1 cells with either miR-29b mimic (50nM) or non – targeting control (50nM). Luciferase assays were performed 24 hours after transfection. The relative luciferase value was normalised to the non-targeting control. Means ± standard errors are presented, n=6. The difference of luciferase activity was analysed by Student's unpaired two-tailed t test. * $p<0.05$, ** $p < 0.01$, *** $p<0.001$, Ctr, non-targeting control, 29a, 29b, 29c: miR-29a,-b,-c mimic.

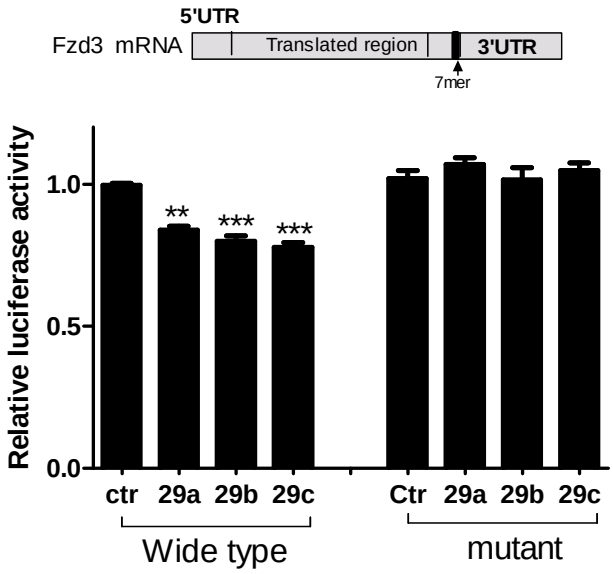

Figure 5.20: *FZD3* is a direct target of the miR-29 family

The *FZD3* 3'UTR region containing 1 binding sites of the miR-29 family was subcloned downstream of the luciferase encoding gene in the pmiRGLO vector to create the *FZD3* 3'UTR-pmiRGLO wide type (WT) vector. The mutant vectors were created from WT vector in which binding site of the miR-29 family were mutated. Either the WT or the mutants vectors (100ng) were co-transfected into chicken fibroblast DF1 cells with either miR-29b mimic (50nM) or non – targeting control (50nM). Luciferase assays were performed 24 hours after transfection. The relative luciferase value was normalised to the non-targeting control. Means ± standard errors are presented, n=6. The difference of luciferase activity was analysed by Student's unpaired two-tailed t test. * $p<0.05$, ** $p < 0.01$, *** $p<0.001$, Ctr, non-targeting control, 29a, 29b, 29c: miR-29a,-b,-c mimic.

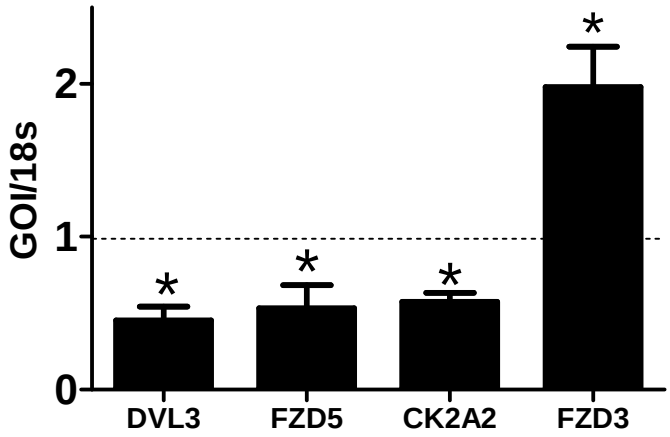

Figure 5.21: Expression of *FZD3, FZD5, DVL3,* and *CK2A2* in human cartilage

Total RNA was isolated from human hip articular cartilage of either end-stage OA patients or fracture controls and reverse transcribed to cDNA. Relative expressions of *FZD3, FZD5, DVL3,* and *CK2A2* were measured by real-time PCR where 18S rRNA was used as housekeeping control in hip osteoarthritis cartilage (HOA, n=8) and fracture to the neck of the femur (NOF, n=7). The horizontal line at 1 is the expression of these genes in NOF. Means ± standard errors are presented. Different in expression between HOA and control NOF was calculated by Student's unpaired two-tailed t test. * $p<0.05$, ** $p < 0.01$, *** $p<0.001$

5.3 Discussion

Previously, the miR-29 family has been shown to negatively interact with TGFβ signalling in several pathologic settings in which fibrosis development was the outcome of the disease such as liver, cardiac, renal fibrosis (van Rooij *et al.* 2008, Kwiecinski et al. 2011, Qin et al. 2011). In line with these studies, in the present study, the miR-29 family was also found to suppress the TGFβ signalling pathway in human chondrocytes. Noteworthy, miR-29 is one downstream mediator of TGFβ signalling in which the miRNA blocks the effect of the growth factor on gene expression. However, the direct mechanism by which miR-29 interferes with TGFβ signalling remains unclear in human chondrocytes. In fact, Smad3 was demonstrated to be a direct target of miR-29 in thyroid cells (Leone *et al.* 2012). In human chondrocytes, nevertheless, with transfection of miR-29 family mimics, the Smad3 mRNA level was not changed (data not shown); similarly, any decrease in luciferase activity when co-transfecting a Smad3-3'UTR reporter with miR-29 mimics was not statistically significant (data not shown), suggesting that Smad3 is not the target of miR-29 in the context of the chondrocyte. In addition, no obvious components of TGFβ signalling were regulated in the miR-29b gain- and loss-of function experiment with the whole genome array. This leads to the hypotheses that miR-29 may directly targets TGFβ signalling components at the protein level rather than mRNA level (similar to miR-140 (Pais et al. 2010)) or that the inhibition of miR-29 on TGFβ signalling is the consequence of the direct suppression of other factors inducing TGFβ signalling. To test this hypothesis, it may be best to perform miR-29b gain- and loss-of function experiment together with a proteomic assay. It may also be instructive to perform array experiments in the presence or absence of TGFβ itself

It has been shown that in the development and progression of OA, NFκB plays an active role e.g. mediating articular chondrocyte responses to proinflammatory cytokines (IL-1, TNF-α); inducing MMPs (e.g. MMP-1, MMP-3, MMP-13), cytokines (e,g, IL-6, IL-8) and chemokine expression (Marcu *et al.* 2010). Thus, NFκB is an attractive target for the treatment of OA. In this project, for the first time, NFκB signalling was confirmed as negatively regulated by the miR-29 family and miR-29 is also likely to serve as a downstream inhibitor of the signalling. Similar to TGFβ signalling, it is still not clear the direct mechanism by which miR-29 regulates NFκB signalling pathway. However, it suggests a potential therapeutic strategy for targeting NFκB signalling using miR-29. Further studies are needed to dissect the direct mechanism by which miR-29 interferes with NFκB signalling.

In this project, the miR-29 family was found to suppress the Wnt/β-catenin signalling pathway. In line with my data, the negative effect of the miR-29 on this signalling pathway is also reported. In human non-small-cell lung cancer cells, miR-29 directly targets DNMTs which in turn inhibited the methylation of Wnt inhibitory factor-1 (WIF-1) promoter; accordingly, miR-29 over-expression down-regulated β-catenin expression (Tan *et al.* 2013). In human colorectal cancer cells, miR-29b negatively regulated Wnt signalling and targeted B-cell CLL/lymphoma 9-like (BCL9L), thus decreasing its expression with a consequent decrease in nuclear translocation of β-catenin (Subramanian *et al.* 2014). In contrast to these studies, published data reports that the miR-29 family positively regulated canonical Wnt signalling by directly targeting its inhibitors in human embryonic kidney cells (Liu *et al.* 2011) and human fetal osteoblastic cells (Kapinas et al. 2010). This contradiction is not surprising as many miRNAs are known to act in a context-dependent manner depending on the relative availability of their targets in any cell type and this discordance could be a reflection of the differences in the miR-29 family regulatory networks in different cell lines.

Besides exerting function on several crucial signalling pathways implicated on chondrogenesis and OA, the crucial role of the miR-29 family was clearly shown through their target genes. In this project, miR-29b gain- and loss-of-function was applied to find miR-29 potential targets. Together with some novel and known targets which will be discussed later, the liposome – mediated transient transfection of the miR-29b-3p mimic surprisingly induced the expression of a number of immune genes which are not the miRNA targets. The Qiagen miR-29b-3p mimic used in the present study is double-stranded, 23 nucleotides in length with sequence identical to the sequence of the mature endogenous miRNA-29b-3p and does not contain any chemical modifications or overhangs, which makes it unlikely for any sequence difference between endogenous miRNA and Qiagen mimic to be responsible for the immune response. Moreover, the lack of immune response against the controls and the miR-29b inhibitor confirms that the immune response was specific and not due to a general response to small RNA. Indeed, it is likely that some specific GU- rich 4-mer sequences e.g. AUUU, UUGA, UGUU in the miR-29b-3p mature sequence (5'UAGCACCAUUUGAAAUCAGUGUU3') might be important for the immune gene up-regulation since these sequences have been shown to be potent immunostimulatory motifs mediated through TLR7 or TLR7/8 (Forsbach *et al.* 2008). Especially, it has been shown that the main effects induced upon activation of TLR7 in human immune cells are IFN- dependent

effects, proinflammatory cytokines and chemokines from cell expression only TLR7 or both TLR7 and 8 (Hertzog *et al.* 2003). Also, it is possible that this up-regulation of the immune genes could be attributed to the liposome alone besides the sequence of the synthetic miRNA since the levels of the immune genes were higher than the levels obtained for electroporation, and those observed in un-transfected controls (Karlsen *et al.* 2013). The explanation for this could be because liposomes fuse with the plasma membrane, which may trigger membrane – associated lipid receptors and/or distort the actin cytoskeleton which in turn up-regulates immune genes. However, it may depend on cellular context since electroporation could strongly trigger the increase of the immune genes in some cell types.

This study identifies FZD3, FZD5, FRAT2, CK2A2 and DVL3 as the critical targets of the miR-29 family in the Wnt signalling pathway. These genes have important roles in both canonical and/or non-canonical Wnt signalling pathways. **FZD3** and **FZD5** belong to the Frizzled proteins, which are the receptors for Wnt ligands. Wnt3a, Wnt5a, and Wnt2 can bind to FZD3 which in turn can activate both canonical and non-canonical WNT signalling pathways: Wnt3a activates the TOPFlash reporter in HEK293 cells overexpressing Wnt3a/FZD3/LRP6 (Lu *et al.* 2004) whist Wnt5a binding to FZD3 triggers downstream pathways independent of β-catenin (Hansen *et al.* 2009); Wnt2 can interact with FZD3 in human cumulus cells, but it is not known which downstream signalling pathways are activated after this binding interaction (Wang *et al.* 2009). **FZD5** functions as the receptor for Wnt5a, Wnt9b, and Wnt7a. Co-injection of hFZD5 and XWnt-5a induced the formation of dorsal axis duplication in *X. laevis* embryos; this axis duplication was suppressed after co-injection of RNA for human GSK-3β, suggesting the involvement β-catenin-dependent signalling in this receptor – ligand combination (He *et al.* 1997). Wnt9b was found in HEK293 cells as a binding partner for FZD5 to activate the TOPFlash reporter (Liu *et al.* 2008). Wnt7a was found to bind to FZD5 to activate the β-catenin signalling pathway and increase the proliferation of epithelial cells in the endometrium (Carmon *et al.* 2008). By targeting these two Frizzled proteins, miR-29 can interfere with Wnt signalling pathways. However, it will depend on the cellular context, whichWnt ligands are available to partner with, which will determine outcome. In line with these Frizzled proteins, another novel target of the miR-29 family, DVL3 (Disheveled 3), belonging to the Disheveled family including DVL1, 2 and 3, is a central component in mediating downstream events of both canonical and non-canonical Wnt signalling. Wnt ligands binding to Frizzled protein recruit Disheveled to the plasma membrane which leads to activation of downstream pathways. Disheveleds

includes DIX, PD2, and DEP domains: DIX and PDZ domains function together in canonical Wnt signalling to stabilize β-catenin; the DIX domain binds with Axin and results in inhibition of the β-catenin degradation complex in canonical Wnt signalling; PDZ and DEP domains cooperate in different subpathways of noncanonical Wnt signalling. Moreover, the other two targets FRAT2 and CSNK2A2 are potent activators of canonical Wnt signalling. **FRAT2** (Frequently rearranged in advanced T-cell lymphomas -2) belongs to the FRAT family including FRAT 1, 2, 3. By binding to GSK3, Frat prevents the phosphorylation and concomitant degradation of β – catenin (van Amerongen *et al.* 2005). **CSNK2A2** encodes for the subunit CK2α' of casein kinase 2 (CK2). CK2 has been shown to act as a positive modulator of WNT/β-catenin pathway, suppressing β-catenin degradation and β-catenin binding to APC (Price 2006). Several keys components of the WNT/β-catenin signalling are known substrates of CK2 in vitro including DVL (Willert *et al.* 1997), TEF/TCF (Homma *et al.* 2002, Miravet *et al.* 2002, Hammerlein *et al.* 2005), and β-catenin (Song *et al.* 2003). Taken together, it is likely that by directly targeting FZD3, FZD5, DVL3, FRAT2 and CSNK2A2, miR-29 could in part or in specific contexts, suppress the Wnt signalling pathway. Interestingly, in human cartilage, the expression levels of FZD5, CSNK2A2, and DLV3 were found to be down regulated in human OA, inversely correlating with the miR-29 expression level, suggesting a direct mechanism in which the suppression of these genes are controlled by miR-29 in human OA cartilage. However, FZD3 expression level was up-regulated in human OA cartilage which could be explained by the fact that there are many other factors which are involved in controlling gene expression together with miRNAs. Since the dys-regulation (either up-regulation or down-regulation) of the canonical Wnt signalling pathway can both lead to OA, there is a possible explanation for the disease development: the excessive amount of the miR-29 down-regulates the expression levels of a number of Wnt signalling related genes which consequently suppress the Wnt signalling pathway. Nevertheless, whether miR-29 targets all of these genes at the same time and the level at which the suppression of each gene contributing to the disease are still not explained in this project.

MicroRNA 29 has been suggested to serve as a master regulator in complex regulatory networks through fine-tuning a large set of functionally related genes, probably best illustrated by its extracellular matrix-related targets, whereby at least 16 ECM related genes are experimentally validated including collagen isoforms (van Rooij et al. 2008, Luna *et al.*

2009, Kwiecinski et al. 2011, Qin et al. 2011, Wang et al. 2012), laminin γ1 (Luna et al. 2009, Nishikawa *et al.* 2014), fibrillin 1, elastin (van Rooij et al. 2008), integrin β1 (Cushing et al. 2011). In line with these data, in this project, a number of ECM- related genes were highlighted as the direct targets of the miR-29 in human OA chondrocytes. However, there is not complete overlap since there are a number of genes that have been experimentally validated as direct targets of miR29 but not regulated when miR-29b was overexpressed or inhibited in human chondrocytes. For example, validated miR-29 direct target genes include DNMT3A, DNMT3B (Fabbri et al. 2007, Garzon *et al.* 2009, Amodio et al. 2012, Morita *et al.* 2013, Tan et al. 2013, Parpart et al. 2014), MMP2 (Liu et al. 2010, Steele et al. 2010, Fang *et al.* 2011), MMP9, ADAM12, ADAM19 (Luna et al. 2009, Ramdas et al. 2013), ADAMTS9 (Cushing et al. 2011). Nonetheless, in human chondrocyte, the expression levels of these genes were not modulated by the miR-29 family. The precise explanation for this difference is still not clear.

In this PhD thesis, members of ADAMTS family including *ADAMTS6, ADAMTS10 ADAMTS14, ADAMTS17, ADAMTS19* have been confirmed as novel direct targets of the miR-29 family. Interestingly, the miR-29 family is suppressed by TGFβ whist its direct targets, the ADAMTS family are strongly induced by TGFβ. However, except ADAMTS14 described as a procollagen N-propeptidase for pro-collagen type I, type II, and type III, the functions of ADAMTS 6, -17, and-19 remain unknown. Thus, further investigating the suppressive effect of miR-29 family on these ADAMTS becomes difficult both in vitro and in vivo. Moreover, ADAMTS14 and ADAMTS17 levels were reported to largely increase in hip OA cartilage and hip OA synovium, respectively (Davidson et al. 2006); the rs4747096 nsSNP in ADAMTS14 was over-represented in women requiring joint replacement because of knee OA and in patients with symptomatic hand OA (Rodriguez-Lopez *et al.* 2009, Poonpet *et al.* 2013), implicating the involvement of these ADAMTS on OA. The microRNA 29 family is, nevertheless, found to increase expression in hip OA cartilage in our sample set. Again, this could be explained in part by the fact that in cellular context, a miRNA is just one factor amongst others e.g. transcription, epigenetic silencing, differential biosynthesis, and extracellular stimuli controlling gene expression.

In summary, the miR-29 family was found to suppress the TGFβ/Smad3, NFκB, and Wnt/β-catenin signalling pathways. Gene expression profiles of gain- and-loss-of-function revealed the regulation of a large number of previously recognised extracellular matrix-associated

genes as well as an additional subset of protease and Wnt signalling pathway-related genes. Among these genes, the ADAMTS family e.g. *ADAMTS6, ADAMTS10, ADAMTS14, ADAMTS17, ADAMTS19,* and Wnt signalling related genes e.g. *FZD3, FZD5, DVL3, FRAT2, CK2A2* were validated as direct targets of the miR-29 family.

CHAPTER 6
GENERAL DISCUSSION

6.1 Summary

This project has identified the miR-29 family as important miRNAs involved in both cartilage homeostasis and OA (Chapter 3). In the murine DMM model of OA at 1, 3, and 7 days after surgery, miRNA profile data from total RNA isolated from the whole knee joints showed that miR-29b was significantly increased at day 1 and showed a trend to decrease at day 3 and 7 after surgery. Integrating analysis between the mRNA profiling and miRNA profiling data from the DMM model strongly highlighted the role of the miR-29 family since the expression of its putative targets inversely correlated with its expression across the time course. In human end-stage hip OA cartilage, the miR-29 family was increased compared with the facture to neck of femur controls. Furthermore, in a murine hip injury model, the expression of the miR-29 family was increased across a 48 hour time course. The miR-29 family was also found to be involved in chondrocyte phenotype since the expression of all members of the miR-29 family decreased across dedifferentiation of human chondrocytes. In chondrogenesis, the miR-29 family was found to significantly decrease at an early stage, suggesting a negative role in this phase of chondrogenesis in both human and murine models. The miR-29 family was also found to be expressed in murine limb development.

The factors controlling miR-29 family expression are another important finding of this project (Chapter 4). The master regulator of chondrogenesis SOX9 was found to negatively regulate miR-29 expression, at least in part through directly binding to the promoter region of miR-29a/b1. A number of growth factors and cytokines were identified which regulate expression of the miR-29 family in both human primary chondrocytes and SW1353 cell line: TGFβ supressed miR-29 family expression; IL-1 strongly increased the miRNA expression through the p38 MAPK signalling pathway; treatment with LPS for less than 24 hours decreased expression of miR-29 through NFκB signalling whilst treatment with LPS for longer times increased miR-29 expression. Interestingly, in response to cytokines and growth factors, the miR-29 primary and precursor transcripts were regulated ahead the mature transcripts. This was explained in part by the fact that several components taking part in the miRNA precursor processing were possibly the miR-29 targets. Among these, Dicer-1 was proven as a miR-29 direct target.

Crucially, the functions of the miR-29 family in chondrocyte were also revealed in which miR-29 served as the negative regulator of the TGFβ/SMAD, NFκB and WNT/β-catenin signalling pathways. A number of novel direct targets of the miR-29 family have been found e.g. the ADAMTS family (*ADAMTS6, -10, -14, -17, -19*) and components of the Wnt signalling pathway (*FZD3, -5, FRAT2, CK2A2, DVL3*) (Chapter 5).

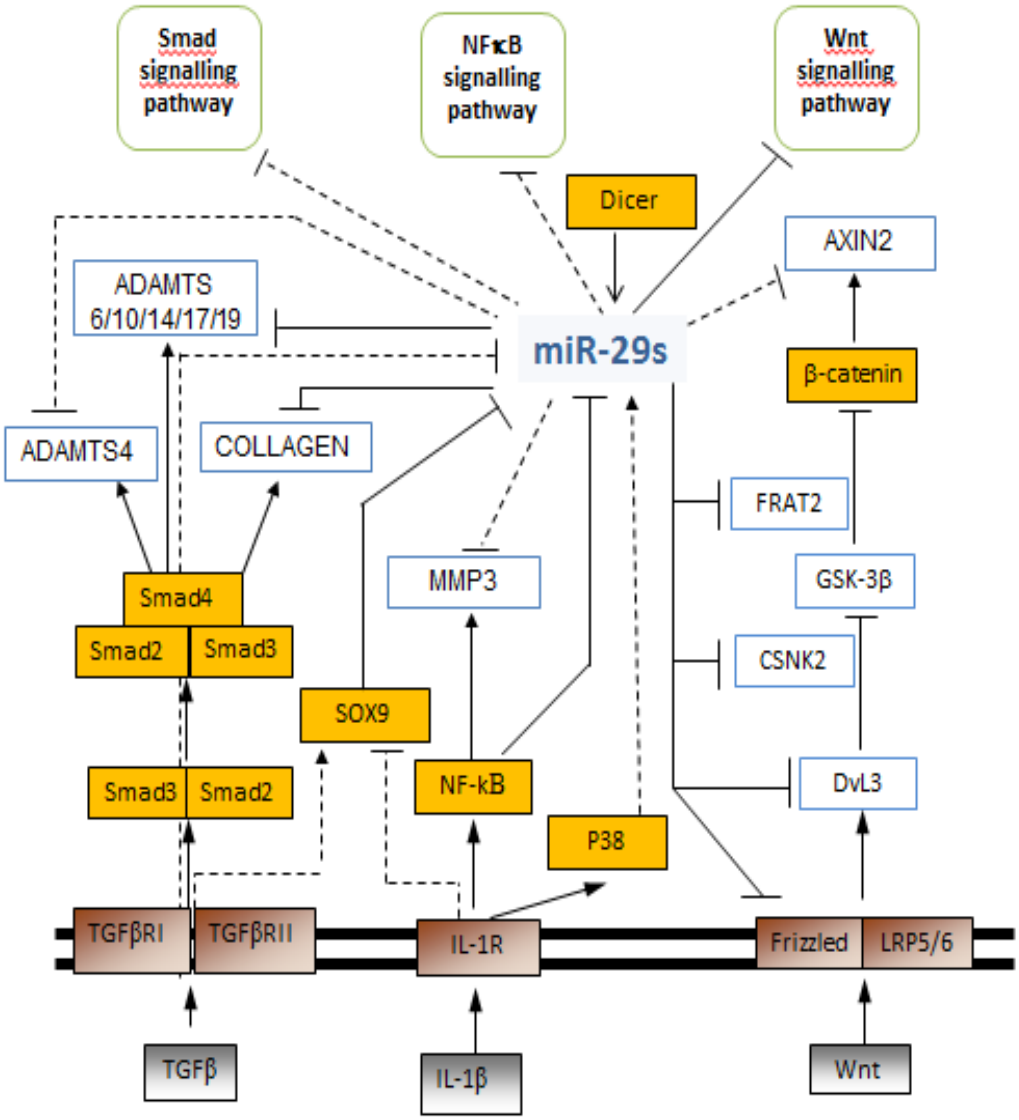

Figure 6.1. Summary of the role of the miR-29 family in chondrocytes

6.2 General discussion

6.2.1 Increased expression of the miR-29 family may contribute to the onset or progression of OA

The tight regulation of miRNA expression is crucial for cartilage homeostasis since the dysregulation of miRNAs may lead to OA. Especially, it has been shown that the aberrant expression of a single miRNA could have a profound effect on cartilage i.e. miR-140, with absence of miR-140 leading to premature OA (Miyaki et al. 2010). In the present study, all members of the miR-29 family have been implicated in cartilage homeostasis and OA. In both early and late stages of OA, an increase level of the miR-29 family was observed, suggesting that miR-29 may be involved in the onset of the disease. Moreover, in this study, the molecular mechanisms controlling this increased expression of miR-29 and the mechanisms by which increased miR-29 expression may lead to OA have been investigated: the miR-29 expression was up-regulated by IL-1, which is induced in both early and end stage OA, consequently suppressing both TGFβ and WNT/β-catenin signalling pathways. Since alteration of these two signalling pathways has been shown to be involved in OA development (Verrecchia et al. 2001, Verrecchia and Mauviel 2002, Zhu et al. 2008, Zhu et al. 2009), the increased expression level of the miR-29 family may contribute to this. In line with this, the miR-29 family was found to strongly suppress a number of ECM-related genes, especially collagens. Aggrecan was also found to be indirectly decreased by miR-29 (data not shown). However, more evidence is required to support this premise. If the increased expression level of miR-29 is a common observation in different OA models, this may also suggest that circulating miR-29 could be a biomarker for detecting early stage OA and also offers the possibility of using a miR-29 inhibitor as a novel treatment for OA. We are investigating the expression of the miR-29 family in the Str/ort model in collaboration with Dr Blandine Poulet (University College London, UK) and Professor Andy Pitsillides (Royal Veterinary College, London, UK).

The increased level of the miR-29 family may not be the only microRNA underlying the development of OA. In this project, miRNA profiling in the DMM model at 1, 3, and 7 days after surgery found a number of miRNAs modulated apart from miR-29s, suggesting these may also contribute to the pathogenesis of OA. Also, a number of miRNAs have been identified as differently expressed in human end stage OA cartilage as compared to the control counterparts. It is clear that in order to maintain cartilage homeostasis, miRNAs will interact with each other and mRNAs in a complex network that is tightly regulated. Thus, the up-regulation of miR-29 might be either the reason or the consequence of the deregulation of other networks of miRNAs. The question is how the other miRNAs interact with miR-29 and the effect of the increase expression of miR-29 on the miRNA/mRNA network in OA. This requires a computer modelling approach to resolve.

6.2.2 The signalling cascade IL-1/p38, IL-1/NFκB and the miR-29 family

Interestingly, in this study, it was found that whist IL-1 induced miR-29 expression through p38/MAPK, the NFκB pathway appears suppressive to miR-29 expression. In addition, the miRNA itself was found to suppress NFκB signalling. These data suggest that in response to the signalling cascade triggered by IL-1, the miR-29 expression level was induced through (i) induced expression of p38 MAPK and (ii) escape from the suppressive effect of NFκB through inhibiting the NFκB signalling pathway. However, the mechanism by which miR-29 suppressed NFκB signalling was not fully understood since the miR-29b gain- and loss- of function mRNA profiling experiment in human primary chondrocytes did not identify any potential targets related to the NFκB signalling pathway. It is a hypothesis that this suppressive effect could be an indirect effect or some potential targets could alter only at the protein level. Also, the direct mechanism through which p38 induced the miR-29 expression is not clear, even though in the promoter of miR-29a/b1 there are several binding sites for AP1 (data not shown). Interestingly, it is reported that p38 activation was found to induce NFκB activity in a dual way: by reducing IκB levels and by potentiating the translocation of p65/p50 (Baeza-Raja *et al.* 2004). Though evidence for this activation in human chondrocytes was not clear, the network controlling miR-29 expression in response to IL-1 becomes more complicated if this interaction is true in chondrocytes. Moreover, in this study, miR-29 was found to inhibit the pre-miRNA processing machinery to target Dicer and may also directly target other pre-miRNA processing genes, suggesting another regulatory layer for tightly

controlling the level of miR-29 in human chondrocytes. This could partly explain that the excessive amount of the miRNA in chondrocytes may lead to OA. Multiple regulatory layers are therefore needed for controlling miR-29 levels, clearly showed when the level of the primary miR-29 family was induced ahead of the level of mature miR-29 in chondrocytes stimulated with IL-1, TGFβ, and LPS. In the DMM model, miR-29 expression was induced 1 day after surgery together with the IL-1β expression level though this latter was not significant (data not shown), suggesting one possible explanation for the increase level of miR-29. However, it is unlikely that miR-29 was solely induced by IL-1 in the DMM model since the IL-1 level would have to be induced very early in order to then stimulate miR-29 expression. In line with this, mRNA profiling of DMM model 6 hours after surgery did not find a strongly induced expression of IL-1 (Burleigh et al. 2012). Similarly, in the murine hip injury model, the miR-29 expression level was also found to increase across the time course (reaching significance at 12 hours in culture). The precise mechanism for the increase expression of miR-29s in both DMM model and murine hip injury model are not clear and require further investigation.

6.2.3 The signalling cascade TGFβ/ Smad3 signalling pathway and the miR-29 family

In contrast with IL-1, TGFβ suppresses miR-29 expression. Since the miR-29 family directly targets a number of ECM-related genes, the suppressive effect TGFβ exerted on the miR-29 family is consistent with the well described protective effect of TGFβ in chondrocytes (Li et al. 2005). Interestingly, the miRNA itself gave a negative feedback loop on the TGFβ/Smad signalling pathway. This could be explained as an attempt to maintain miR-29 at homeostatic levels as TGFβ signalling becomes aberrant. This may also in part support the fact that an excessive amount of the miR-29 family could lead to OA: through suppressing Smad signalling and directly inhibiting responsive genes e.g. ECM related genes, the up-regulation of the miR-29s could strongly diminish the function of TGFβ in chondrocytes.

The precise mechanism by which TGFβ suppressed miR-29 expression and the mechanism by which miR-29 inhibited the TGFβ/Smad signalling were unclear. The miR-29b gain- and loss- of function mRNA profiling did not identify any TGFβ related potential targets, suggesting that this may also be at the protein level. Moreover, regarding the cellular context, when both IL-1 and TGFβ may be present, the cross talk between the two cytokines as well

as with other cytokines and growth factors in controlling the miR-29s expression levels are still unclear.

6.2.4 The canonical Wnt signalling and the miR-29 family

In this project, expression of the miR-29 family was not controlled by Wnt3a in chondrocytes. Since Wnt3a could trigger both canonical Wnt/β-catenin and CaMKII signalling pathways (Nalesso et al. 2011), it is likely that these two signalling pathways do not modulate the miR-29 levels in chondrocyte. However, expression ofmiR-29 was found to be induced by WNT3a in osteoblasts, suggesting a different mechanism controlling the miRNA-29 expression in the two cells types. The answer to this difference remains unknown and needs further investigation.

The canonical Wnt/β-catenin signalling pathway was inhibited by the miR-29 family in which some Wnt signalling related genes were validated as direct targets of the miRNA. Both over-activation and inhibition of Wnt signalling can lead to skeletal deformities and an early onset OA (Zhu et al. 2008, Zhu et al. 2009), illustrating that Wnt signalling needs to be tightly regulated in cartilage homeostasis. However, whether the decreasing of these direct targets is the mechanism for inhibition of the Wnt/β-catenin signalling pathway has not been confirmed in this study. This could be facilitated by utilizing siRNA to suppress the expression of each of these genes and measure this effect on the signalling though TOPFlash reporter.

6.2.5 Therapeautic applications for treating OA by targeting the miR-29 family

MicroRNAs have many advantages as a therapeutic modality. The mature miRNA sequences are short and often completely conserved across species. These characteristics make miRNAs relatively easy to target therapeutically and allow for using the same miRNA-modulating compound in preclinical efficacy and safety studies as well as in clinical trials. Moreover, miRNAs have typically many targets within cellular networks, which, in turn, enable modulation of entire pathways in a disease state via therapeutic targeting of disease – associated miRNAs.

The increase of the miR-29 family in OA potentially opens the door to develop a novel therapeutic strategy for OA. The therapeutic approach using **miRNA sponges** (transgenic

overexpression of RNA molecules harbouring complementary binding sites to a miRNA) or **miRNA-29 antagonists** to block the function of the endogenous miRNA-29s may have great promise as a novel treatment. The miRNA sponges have been proved to be successful in vivo whist the antagonists might have greater promise from a therapeutic perspective.

However, detailed examination of the miRNA therapy should be conducted before clinical use. Especially, the antagonists should have high binding affinity, and bio-stability. Indeed, this could be facilitated by chemically modifying them to increase the duplex melting temperature and improving nuclease resistance. Sugar modifications e.g. the 2'-O-methyl (2'-O-Me), 2'-O-Methoxyethyl (2'-MOE) 2'-fluoro and the bicyclic locked nucleic acid (LNA) modification are commonly used. Among these, the LNA exhibits the highest affinity toward complementary RNA with an increase in Tm of +2-8^{o}C per introduced LNA modification. In addition, by substituting the phosphodiester (PO) backbone linkages with phosphorothioate (PS) linkages in the antagonist oligonucleotides or by using peptide nucleic acid (PNA) or morpholino oligomers, respectively, their nuclease resistance properties might increase. Apart from nuclease resistance, PS backbone modifications also enhance binding to plasma proteins, leading to reduced clearance by glomerular filtration and urinary excretion. PNA oligomers are uncharged oligonucleotide analogues, in which the sugar-phosphate backbone has been replaced by a peptide-like backbone consisting of N-(2-aminoethyl)-glycine units. Polylysine-conjugated and nanoparticle-encapsulated PNA antimiRs have been shown to efficiently inhibit miRNA function in cultured cells and in mice (van Rooij *et al.* 2014). Morpholinos are uncharged and with slightly increased binding affinity to complementary miRNAs.

An effective way to deliver the miRNA-29 inhibitor to the arthritis joint to inhibit the endogenous miRNA-29 is needed. In particular, it is likely that the uptake of a synthetic antagonist into chondrocytes surrounded by the abundant matrix would be difficult in the treatment of damaged cartilage. The main challenge for development of miRNA - based therapeutics is efficient and safe delivery. Two strategies have been utilized to enhance in vivo delivery of antagonists: cholesterol conjugation and modification of the phosphate backbone with PS linkages. The 3' cholesterol conjugated, 2'-O-Me-modified antagonists have become a well-validated experimental tool for in vivo inhibition of miRNAs. PS backbone linkages can be employed to enhance the pharmacokinetic properties of antisense

oligonucleotides. The antagonist approach contains 2 PS modifications at the 5' end and 4 at the 3' end, which have been shown to be important for their in vivo activity, whereas complete replacement of the PO backbone by PS linkages decreased the antagonist efficiency. An increasing number of reports have described silencing of miRNA in vivo by unconjugated LNA-modified antagonists ranging from 8nt to 16nt in length as described in previous section. Administration of such antimiRs is either by intraperitoneal or subcutaneous injection resulted in antimiR uptake in the tissue of interest, which led to inhibition of miRNA function and derepression of direct target mRNAs. However, the mechanism of cellular uptake and distribution are still poorly understood. Directing uptake to cartilage is likely still to be difficult, and delivery by injection not pragmatic in OA.

6.3 Future direction

6.3.1 The modulation of the miR-29 family in OA

The miR-29 family was found to modulate expression in different animal models e.g. the DMM model, hip avulsion injury model, as well as human end stage OA cartilage. These data suggest that the increase in expression of the miR-29 family could be a common event in both early onset and end stage OA. However, care must be applied to conclude the up-regulation of miR-29s will lead to OA, with the expression level of miR-29s during OA progression remaining unclear. Thus, it is of importance to examine miR-29 expression in naturally occurring OA models too.

The miR-29 expression pattern increased in the hip avulsion injury across the time course in this study. Nonetheless, whether miR-29 potential targets were inversely correlated with the miR-29 expression level in this model has not been proven. Thus, we are performing mRNA profiling in the same samples in which the miR-29 expression was found to increase. This may also reveal additional mechanisms which lead to the increased expression of miR-29.

6.3.2 Biological functions of the miR-29 family in chondrocytes

The miR-29 family was found to suppress TGFβ/Smad, NFκB, and Wnt/β-catenin signalling pathways through using the reporters of these pathways together with measuring expression level of the responsive genes. However, whether interfering with the miR-29 effect on these signalling will lead to alter chondrocyte phenotype remains unclear. Overexpression and

knockdown of the miR-29 family in HACs in micromass culture in combination with measurement of chondrocyte markers e.g. *MMP13, COL2A1, SOX9, ADAMTS5* will help to address this.

From the miR-29b gain- and loss- of function mRNA data, apart from the Wnt signalling pathway, enrichment of some miR-29 potential targets which are related to MAPK signalling and apoptosis pathways was evident. Thus, validating these genes as the direct targets of the miR-29s is a priority in the future. It is now clear that miRNAs regulate gene expression at both mRNAs and protein levels. Also, the direct mechanisms the miR-29 supressing the two TGFβ and NFκB signalling pathways are unclear. Therefore, there is a need for proteomic analysis of the miR-29b gain- and loss- of function in HACs, likely in micromass culture. In addition, performing miR-29b gain – and loss - of function together with treatment with IL-1 and TGFβ could greatly help to find the mechanism miR-29 family interfering with NFκB and Smad signalling pathways. All of these experiments will give more information about biological functions of miR-29 in chondrocyte and the complex regulatory network the miR-29 is within.

A key step in understanding the biological functions of the miR-29 family in cartilage homeostasis and OA will be the development of multiple in vivo molecular tools to access gain – of – functions or loss – of – function in mouse models: A number of gain- of –function where the miR-29 family members are overexpressed through a transgenic model, such as the B cell – specific overexpression of the miR-29a/b1 cluster (Santanam et al. 2010), a viral transfection model such as the retroviral transfection of bone-marrow stem cells with miR-29a (Han *et al.* 2010) or systemic delivery of miR-29a have been reported (Wang *et al.* 2012). Also, loss-of-function models have been developed as a Cre-Lox-inducible knockout of the miR-29a/b-1 cluster or the expression of the miR-29 “sponge” sequence (either by transgene or lentivirus) (Ma et al. 2011). However, there is no information whether gain – and loss- of function of the miR-29s lead to OA in these models. Therefore, future studies in which these mice put on OA models e.g. DMM will provide more detail about the function of the miR-29 family.

6.3.3 The involvement of the miR-29 family expression in chick limb bud development and Zebrafish cartilage development.

The miR-29 family was suggested to be a negative regulator of early stage of chondrogenesis in both human and murine chondrogenesis models in this study. Nearly 16 collagen genes were validated as miR-29 direct targets in this study and others. Also, this miRNA was also expressed in murine limb development. It is likely that miR-29 would have a crucial role in cartilage and limb bud development and it is worthy of further investigation. This could be facilitated by again using the gain- and loss- of function of all members of the miR-29 family: a 500bp region around the mature sequence of the miR-29s or a sequence complementary to miR-29 can be subcloned and injected into the chicken limb. However, the involvement of the miR-29 family in chick limb development by in situ hybridization might be required to determine the stage in which miR-29 was expressed in the development process. In addition, ADAMTS14, a pro-collagen pro-peptidase, was validated as the miR-29 direct target. Overexpression or knockdown of the miR-29 family in chick limb could help to further investigate the functional outcome of the suppressive effect of the miR-29s on ADAMTS14 though the ADAMTS14 will need to be verified to be expressed in the chick limb first. This method could be useful for investigating the functional outcome of the interaction between miR-29 and other novel targets.

Interesting, the miR-29 family was found to be express in the cartilage of zebrafish (Wienholds et al. 2005). Thus, zebrafish might be a useful model for investigating the role of the miR-29s in cartilage development. Overexpression and knockdown of the miR-29 family could greatly help for answering this question.

6.3.4 The miR-29 family as the biomarker for OA

MicroRNAs exist in human body fluids such as plasma, urine, and saliva in a stable form which has the potential to be a novel diagnostic and prognostic biomarker. OA can be difficult to diagnose, but it is important to diagnose OA early and start treatment to prevent joint destruction in which the miR-29 based therapy could be an option. Indeed, there is growing evidence for future miRNA-based diagnostics: a number of miRNA in plasma were found at different levels between RA and OA patients. For examples, let-7e, miR-454, miR-886 were identified as differentially expressed circulating miRNAs in OA patients who underwent arthroplasty especially, let–7e emerged as potential predictor for severe knee or hip OA (Beyer et al. 2014). Since the miR-29 family was modulated at an early stage in DMM model, it could be a useful biomarker for OA in clinical use. Thus the expression level

of the miR-29 family in plasma should be determined to have an overview expression pattern of the miRNA.

REFERENCES

Abouheif, M., T. Nakasa, H. Shibuya, T. Niimoto, W. Kongcharoensombat and M. Ochi (2010). "Silencing microRNA-34a inhibits chondrocyte apoptosis in a rat osteoarthritis model in vitro." Rheumatology (Oxford, England) **49**(11): 2054-2060.

Abrahante, J., A. Daul, M. Li, M. Volk, J. Tennessen, E. Miller and A. Rougvie (2003). "The Caenorhabditis elegans hunchback-like Gene lin-57/hbl-1 Controls Developmental Time and Is Regulated by MicroRNAs." Developmental Cell **4**(5): 625-637.

Ahluwalia, J. K., S. Z. Khan, K. Soni, P. Rawat, A. Gupta, M. Hariharan, V. Scaria, M. Lalwani, B. Pillai, D. Mitra and S. K. Brahmachari (2008). "Human cellular microRNA hsa-miR-29a interferes with viral nef protein expression and HIV-1 replication." Retrovirology **5**: 117.

Aigner, T., W. Bertling, H. Stoss, G. Weseloh and K. von der Mark (1993). "Independent expression of fibril-forming collagens I, II, and III in chondrocytes of human osteoarthritic cartilage." J Clin Invest **91**(3): 829-837.

Aigner, T., A. Sachse, P. M. Gebhard and H. I. Roach (2006). "Osteoarthritis: pathobiology-targets and ways for therapeutic intervention." Adv Drug Deliv Rev **58**(2): 128-149.

Aigner, T., S. Soeder and J. Haag (2006). "IL-1beta and BMPs--interactive players of cartilage matrix degradation and regeneration." Eur Cell Mater **12**: 49-56; discussion 56.

Akhtar, N., Z. Rasheed, S. Ramamurthy, A. Anbazhagan, F. Voss and T. Haqqi (2010). "MicroRNA-27b regulates the expression of matrix metalloproteinase 13 in human osteoarthritis chondrocytes." Arthritis & Rheumatism **62**(5): 1361-1371.

(2010). "MicroRNA-27b regulates the expression of matrix metalloproteinase 13 in human osteoarthritis chondrocytes." Arthritis and rheumatism **62**(5): 1361-1371.

Akiyama, H., M. C. Chaboissier, J. F. Martin, A. Schedl and B. de Crombrugghe (2002). "The transcription factor Sox9 has essential roles in successive steps of the chondrocyte differentiation pathway and is required for expression of Sox5 and Sox6." Genes Dev **16**(21): 2813-2828.

Amarilio, R., S. V. Viukov, A. Sharir, I. Eshkar-Oren, R. S. Johnson and E. Zelzer (2007). "HIF1alpha regulation of Sox9 is necessary to maintain differentiation of hypoxic prechondrogenic cells during early skeletogenesis." Development **134**(21): 3917-3928.

Ambros, V. (2004). "The functions of animal microRNAs." Nature **431**(7006): 350-355.

Amodio, N., M. T. Di Martino, U. Foresta, E. Leone, M. Lionetti, M. Leotta, A. M. Gulla, M. R. Pitari, F. Conforti, M. Rossi, V. Agosti, M. Fulciniti, G. Misso, F. Morabito, M. Ferrarini, A. Neri, M. Caraglia, N. C. Munshi, K. C. Anderson, P. Tagliaferri and P. Tassone (2012). "miR-29b sensitizes multiple myeloma cells to bortezomib-induced apoptosis through the activation of a feedback loop with the transcription factor Sp1." Cell Death Dis **3**: e436.

Amodio, N., M. Leotta, D. Bellizzi, M. T. Di Martino, P. D'Aquila, M. Lionetti, F. Fabiani, E. Leone, A. M. Gulla, G. Passarino, M. Caraglia, M. Negrini, A. Neri, A. Giordano, P. Tagliaferri and P. Tassone (2012). "DNA-demethylating and anti-tumor activity of synthetic miR-29b mimics in multiple myeloma." Oncotarget **3**(10): 1246-1258.

Amos, N., S. Lauder, A. Evans, M. Feldmann and J. Bondeson (2006). "Adenoviral gene transfer into osteoarthritis synovial cells using the endogenous inhibitor IkappaBalpha reveals that most, but not all, inflammatory and destructive mediators are NFkappaB dependent." Rheumatology (Oxford) **45**(10): 1201-1209.

Arner, E. C. (2002). "Aggrecanase-mediated cartilage degradation." Curr Opin Pharmacol **2**(3): 322-329.

Arroyo, J., J. Chevillet, E. Kroh, I. Ruf, C. Pritchard, D. Gibson, P. Mitchell, C. Bennett, E. Pogosova-Agadjanyan, D. Stirewalt, J. Tait and M. Tewari (2011). "Argonaute2 complexes carry a

population of circulating microRNAs independent of vesicles in human plasma." Proceedings of the National Academy of Sciences **108**(12): 5003-5008.
Avasarala, S., M. Van Scoyk, J. Wang, M. Sechler, K. Vandervest, C. Brzezinski, C. Weekes, M. G. Edwards, J. Arcaroli, R. E. Davis, R. K. Bikkavilli and R. A. Winn (2013). "hsa-miR29b, a critical downstream target of non-canonical Wnt signaling, plays an anti-proliferative role in non-small cell lung cancer cells via targeting MDM2 expression." Biol Open **2**(7): 675-685.
Baeza-Raja, B. and P. Munoz-Canoves (2004). "p38 MAPK-induced nuclear factor-kappaB activity is required for skeletal muscle differentiation: role of interleukin-6." Mol Biol Cell **15**(4): 2013-2026.
Baker-Lepain, J. C., J. A. Lynch, N. Parimi, C. E. McCulloch, M. C. Nevitt, M. Corr and N. E. Lane (2012). "Variant alleles of the Wnt antagonist FRZB are determinants of hip shape and modify the relationship between hip shape and osteoarthritis." Arthritis Rheum **64**(5): 1457-1465.
Bartel, D. (2004). "MicroRNAs: genomics, biogenesis, mechanism, and function." Cell **116**(2): 281-297.
(2009). "MicroRNAs: target recognition and regulatory functions." Cell **136**(2): 215-233.
Benito, M. J., D. J. Veale, O. FitzGerald, W. B. van den Berg and B. Bresnihan (2005). "Synovial tissue inflammation in early and late osteoarthritis." Ann Rheum Dis **64**(9): 1263-1267.
Berezikov, E., W.-J. Chung, J. Willis, E. Cuppen and E. Lai (2007). "Mammalian mirtron genes." Mol Cell **28**(2): 328-336.
Beyer, C., A. Zampetaki, N. Y. Lin, A. Kleyer, C. Perricone, A. Iagnocco, A. Distler, S. R. Langley, K. Gelse, S. Sesselmann, R. Lorenzini, A. Niemeier, B. Swoboda, J. H. Distler, P. Santer, G. Egger, J. Willeit, M. Mayr, G. Schett and S. Kiechl (2014). "Signature of circulating microRNAs in osteoarthritis." Ann Rheum Dis.
Bi, W., J. M. Deng, Z. Zhang, R. R. Behringer and B. de Crombrugghe (1999). "Sox9 is required for cartilage formation." Nat Genet **22**(1): 85-89.
Billinghurst, R. C., L. Dahlberg, M. Ionescu, A. Reiner, R. Bourne, C. Rorabeck, P. Mitchell, J. Hambor, O. Diekmann, H. Tschesche, J. Chen, H. Van Wart and A. R. Poole (1997). "Enhanced cleavage of type II collagen by collagenases in osteoarthritic articular cartilage." J Clin Invest **99**(7): 1534-1545.
Blom, A. B., S. M. Brockbank, P. L. van Lent, H. M. van Beuningen, J. Geurts, N. Takahashi, P. M. van der Kraan, F. A. van de Loo, B. W. Schreurs, K. Clements, P. Newham and W. B. van den Berg (2009). "Involvement of the Wnt signaling pathway in experimental and human osteoarthritis: prominent role of Wnt-induced signaling protein 1." Arthritis Rheum **60**(2): 501-512.
Bobacz, K., I. G. Sunk, J. G. Hofstaetter, L. Amoyo, C. D. Toma, S. Akira, T. Weichhart, M. Saemann and J. S. Smolen (2007). "Toll-like receptors and chondrocytes: the lipopolysaccharide-induced decrease in cartilage matrix synthesis is dependent on the presence of toll-like receptor 4 and antagonized by bone morphogenetic protein 7." Arthritis Rheum **56**(6): 1880-1893.
Bohnsack, M., K. Czaplinski and D. Gorlich (2004). "Exportin 5 is a RanGTP-dependent dsRNA-binding protein that mediates nuclear export of pre-miRNAs." RNA (New York, N.Y.) **10**(2): 185-191.
Bondeson, J., A. B. Blom, S. Wainwright, C. Hughes, B. Caterson and W. B. van den Berg (2010). "The role of synovial macrophages and macrophage-produced mediators in driving inflammatory and destructive responses in osteoarthritis." Arthritis Rheum **62**(3): 647-657.
Bondeson, J., S. Lauder, S. Wainwright, N. Amos, A. Evans, C. Hughes, M. Feldmann and B. Caterson (2007). "Adenoviral gene transfer of the endogenous inhibitor IkappaBalpha into human osteoarthritis synovial fibroblasts demonstrates that several matrix metalloproteinases and aggrecanases are nuclear factor-kappaB-dependent." J Rheumatol **34**(3): 523-533.
Bossé, G. and M. Simard (2010). "A new twist in the microRNA pathway: Not Dicer but Argonaute is required for a microRNA production." Cell Res **20**(7): 735-737.

Brennecke, J., A. Stark, R. Russell and S. Cohen (2005). "Principles of MicroRNA–Target Recognition." PLoS Biol **3**(3): e85.

Brunner, A. M., C. M. Henn, E. I. Drewniak, A. Lesieur-Brooks, J. Machan, J. J. Crisco and M. G. Ehrlich (2012). "High dietary fat and the development of osteoarthritis in a rabbit model." Osteoarthritis Cartilage **20**(6): 584-592.

Buckwalter, J. A., H. J. Mankin and A. J. Grodzinsky (2005). "Articular cartilage and osteoarthritis." Instr Course Lect **54**: 465-480.

Burleigh, A., A. Chanalaris, M. Gardiner, C. Driscoll, O. Boruc, J. Saklatvala and T. Vincent (2012). "Joint immobilisation prevents murine osteoarthritis, and reveals the highly mechanosensitive nature of protease expression in vivo." Arthritis Rheum: n/a-n/a.

Burleigh, A., A. Chanalaris, M. D. Gardiner, C. Driscoll, O. Boruc, J. Saklatvala and T. L. Vincent (2012). "Joint immobilization prevents murine osteoarthritis and reveals the highly mechanosensitive nature of protease expression in vivo." Arthritis Rheum **64**(7): 2278-2288.

Burrage, P. S., K. S. Mix and C. E. Brinckerhoff (2006). "Matrix metalloproteinases: role in arthritis." Front Biosci **11**: 529-543.

Caetano-Lopes, J., H. Canhao and J. E. Fonseca (2007). "Osteoblasts and bone formation." Acta Reumatol Port **32**(2): 103-110.

Cai, J., G. Yin, B. Lin, X. Wang, X. Liu, X. Chen, D. Yan, G. Shan, J. Qu and S. Wu (2014). "Roles of NFkappaB-miR-29s-MMP-2 circuitry in experimental choroidal neovascularization." J Neuroinflammation **11**: 88.

Cai, X., C. Hagedorn and B. Cullen (2004). "Human microRNAs are processed from capped, polyadenylated transcripts that can also function as mRNAs." RNA (New York, N.Y.) **10**(12): 1957-1966.

Carmon, K. S. and D. S. Loose (2008). "Secreted frizzled-related protein 4 regulates two Wnt7a signaling pathways and inhibits proliferation in endometrial cancer cells." Mol Cancer Res **6**(6): 1017-1028.

Chalfie, M. (1981). "Mutations that lead to reiterations in the cell lineages of C. elegans." Cell **24**(1): 59-69.

Chang, T. C., D. Yu, Y. S. Lee, E. A. Wentzel, D. E. Arking, K. M. West, C. V. Dang, A. Thomas-Tikhonenko and J. T. Mendell (2008). "Widespread microRNA repression by Myc contributes to tumorigenesis." Nat Genet **40**(1): 43-50.

Chen, C., D. Ridzon, A. Broomer, Z. Zhou, D. Lee, J. Nguyen, M. Barbisin, N. Xu, V. Mahuvakar, M. Andersen, K. Lao, K. Livak and K. Guegler (2005). "Real-time quantification of microRNAs by stem–loop RT–PCR." Nucleic Acids Res **33**(20): e179-e179.

Chen, L. X., L. Lin, H. J. Wang, X. L. Wei, X. Fu, J. Y. Zhang and C. L. Yu (2008). "Suppression of early experimental osteoarthritis by in vivo delivery of the adenoviral vector-mediated NF-kappaBp65-specific siRNA." Osteoarthritis Cartilage **16**(2): 174-184.

Chen, X., Y. Ba, L. Ma, X. Cai, Y. Yin, K. Wang, J. Guo, Y. Zhang, J. Chen, X. Guo, Q. Li, X. Li, W. Wang, Y. Zhang, J. Wang, X. Jiang, Y. Xiang, C. Xu, P. Zheng, J. Zhang, R. Li, H. Zhang, X. Shang, T. Gong, G. Ning, J. Wang, K. Zen, J. Zhang and C.-Y. Zhang (2008). "Characterization of microRNAs in serum: a novel class of biomarkers for diagnosis of cancer and other diseases." Cell Res **18**(10): 997-1006.

Chendrimada, T., R. Gregory, E. Kumaraswamy, J. Norman, N. Cooch, K. Nishikura and R. Shiekhattar (2005). "TRBP recruits the Dicer complex to Ago2 for microRNA processing and gene silencing." Nature **436**(7051): 740-744.

Chong, K. W., A. Chanalaris, A. Burleigh, H. Jin, F. E. Watt, J. Saklatvala and T. L. Vincent (2013). "Fibroblast growth factor 2 drives changes in gene expression following injury to murine cartilage in vitro and in vivo." Arthritis Rheum **65**(9): 2346-2355.

Chou, J., J. H. Lin, A. Brenot, J. W. Kim, S. Provot and Z. Werb (2013). "GATA3 suppresses metastasis and modulates the tumour microenvironment by regulating microRNA-29b expression." Nat Cell Biol **15**(2): 201-213.

Clements, K. M., J. S. Price, M. G. Chambers, D. M. Visco, A. R. Poole and R. M. Mason (2003). "Gene deletion of either interleukin-1beta, interleukin-1beta-converting enzyme, inducible nitric oxide synthase, or stromelysin 1 accelerates the development of knee osteoarthritis in mice after surgical transection of the medial collateral ligament and partial medial meniscectomy." Arthritis Rheum **48**(12): 3452-3463.

Clevers, H. (2006). "Wnt/beta-catenin signaling in development and disease." Cell **127**(3): 469-480.

Cochrane, D. R., D. M. Cittelly, E. N. Howe, N. S. Spoelstra, E. L. McKinsey, K. LaPara, A. Elias, D. Yee and J. K. Richer (2010). "MicroRNAs link estrogen receptor alpha status and Dicer levels in breast cancer." Horm Cancer **1**(6): 306-319.

Colige, A., I. Vandenberghe, M. Thiry, C. A. Lambert, J. Van Beeumen, S. W. Li, D. J. Prockop, C. M. Lapiere and B. V. Nusgens (2002). "Cloning and characterization of ADAMTS-14, a novel ADAMTS displaying high homology with ADAMTS-2 and ADAMTS-3." J Biol Chem **277**(8): 5756-5766.

Cortez, M. A., M. S. Nicoloso, M. Shimizu, S. Rossi, G. Gopisetty, J. R. Molina, C. Carlotti, Jr., D. Tirapelli, L. Neder, M. S. Brassesco, C. A. Scrideli, L. G. Tone, M. M. Georgescu, W. Zhang, V. Puduvalli and G. A. Calin (2010). "miR-29b and miR-125a regulate podoplanin and suppress invasion in glioblastoma." Genes Chromosomes Cancer **49**(11): 981-990.

Cushing, L., P. P. Kuang, J. Qian, F. Shao, J. Wu, F. Little, V. J. Thannickal, W. V. Cardoso and J. Lu (2011). "miR-29 is a major regulator of genes associated with pulmonary fibrosis." Am J Respir Cell Mol Biol **45**(2): 287-294.

Davidson, R. K., J. G. Waters, L. Kevorkian, C. Darrah, A. Cooper, S. T. Donell and I. M. Clark (2006). "Expression profiling of metalloproteinases and their inhibitors in synovium and cartilage." Arthritis Res Ther **8**(4): R124.

DeLise, A. M., L. Fischer and R. S. Tuan (2000). "Cellular interactions and signaling in cartilage development." Osteoarthritis Cartilage **8**(5): 309-334.

Dell'accio, F., C. De Bari, N. M. Eltawil, P. Vanhummelen and C. Pitzalis (2008). "Identification of the molecular response of articular cartilage to injury, by microarray screening: Wnt-16 expression and signaling after injury and in osteoarthritis." Arthritis Rheum **58**(5): 1410-1421.

Diarra, D., M. Stolina, K. Polzer, J. Zwerina, M. S. Ominsky, D. Dwyer, A. Korb, J. Smolen, M. Hoffmann, C. Scheinecker, D. van der Heide, R. Landewe, D. Lacey, W. G. Richards and G. Schett (2007). "Dickkopf-1 is a master regulator of joint remodeling." Nat Med **13**(2): 156-163.

Dudek, K., J. Lafont, A. Martinez-Sanchez and C. Murphy (2010). "Type II collagen expression is regulated by tissue-specific miR-675 in human articular chondrocytes." The Journal of biological chemistry **285**(32): 24381-24387.

(2010). "Type II collagen expression is regulated by tissue-specific miR-675 in human articular chondrocytes." Journal of Biological Chemistry **285**(32): 24381-24387.

Dudhia, J. (2005). "Aggrecan, aging and assembly in articular cartilage." Cell Mol Life Sci **62**(19-20): 2241-2256.

Dueck, A. and G. Meister (2010). "MicroRNA processing without Dicer." Genome Biol **11**(6): 123.

Dunn, W., G. DuRaine and H. Reddi (2009). "Profiling microRNA expression in bovine articular cartilage and implications for mechanotransduction." Arthritis & Rheumatism **60**(8): 2333-2339.

(2009). "Profiling microRNA expression in bovine articular cartilage and implications for mechanotransduction." Arthritis and rheumatism **60**(8): 2333-2339.

Elmen, J., M. Lindow, S. Schutz, M. Lawrence, A. Petri, S. Obad, M. Lindholm, M. Hedtjarn, H. Hansen, U. Berger, S. Gullans, P. Kearney, P. Sarnow, E. Straarup and S. Kauppinen (2008). "LNA-mediated microRNA silencing in non-human primates." Nature **452**(7189): 896-899.

Esau, C., S. Davis, S. Murray, X. X. Yu, S. Pandey, M. Pear, L. Watts, S. Booten, M. Graham, R. McKay, A. Subramaniam, S. Propp, B. Lollo, S. Freier, F. Bennett, S. Bhanot and B. Monia (2006). "miR-122 regulation of lipid metabolism revealed by in vivo antisense targeting." Cell Metabolism **3**(2): 87-98.

Eyholzer, M., S. Schmid, L. Wilkens, B. U. Mueller and T. Pabst (2010). "The tumour-suppressive miR-29a/b1 cluster is regulated by CEBPA and blocked in human AML." Br J Cancer **103**(2): 275-284.

Fabbri, M., R. Garzon, A. Cimmino, Z. Liu, N. Zanesi, E. Callegari, S. Liu, H. Alder, S. Costinean, C. Fernandez-Cymering, S. Volinia, G. Guler, C. D. Morrison, K. K. Chan, G. Marcucci, G. A. Calin, K. Huebner and C. M. Croce (2007). "MicroRNA-29 family reverts aberrant methylation in lung cancer by targeting DNA methyltransferases 3A and 3B." Proc Natl Acad Sci U S A **104**(40): 15805-15810.

Fan, Z., S. Soder, S. Oehler, K. Fundel and T. Aigner (2007). "Activation of interleukin-1 signaling cascades in normal and osteoarthritic articular cartilage." Am J Pathol **171**(3): 938-946.

Fang, J. H., H. C. Zhou, C. Zeng, J. Yang, Y. Liu, X. Huang, J. P. Zhang, X. Y. Guan and S. M. Zhuang (2011). "MicroRNA-29b suppresses tumor angiogenesis, invasion, and metastasis by regulating matrix metalloproteinase 2 expression." Hepatology **54**(5): 1729-1740.

Fell, H. B. (1978). "Synoviocytes." J Clin Pathol Suppl (R Coll Pathol) **12**: 14-24.

Fenn, A. M., K. M. Smith, A. E. Lovett-Racke, M. Guerau-de-Arellano, C. C. Whitacre and J. P. Godbout (2013). "Increased micro-RNA 29b in the aged brain correlates with the reduction of insulin-like growth factor-1 and fractalkine ligand." Neurobiol Aging **34**(12): 2748-2758.

Fernandes, R. J., S. Hirohata, J. M. Engle, A. Colige, D. H. Cohn, D. R. Eyre and S. S. Apte (2001). "Procollagen II amino propeptide processing by ADAMTS-3. Insights on dermatosparaxis." J Biol Chem **276**(34): 31502-31509.

Ferracin, M., A. Veronese and M. Negrini (2010). "Micromarkers: miRNAs in cancer diagnosis and prognosis." Expert review of Molecular Diagnostics **10**(3): 297-308.

Forsbach, A., J. G. Nemorin, C. Montino, C. Muller, U. Samulowitz, A. P. Vicari, M. Jurk, G. K. Mutwiri, A. M. Krieg, G. B. Lipford and J. Vollmer (2008). "Identification of RNA sequence motifs stimulating sequence-specific TLR8-dependent immune responses." J Immunol **180**(6): 3729-3738.

Friedman, R., K. Farh, C. Burge and D. Bartel (2009). "Most mammalian mRNAs are conserved targets of microRNAs." Genome Res **19**(1): 92-105.

Frisbie, D. D., S. C. Ghivizzani, P. D. Robbins, C. H. Evans and C. W. McIlwraith (2002). "Treatment of experimental equine osteoarthritis by in vivo delivery of the equine interleukin-1 receptor antagonist gene." Gene Ther **9**(1): 12-20.

Garzon, R., C. E. Heaphy, V. Havelange, M. Fabbri, S. Volinia, T. Tsao, N. Zanesi, S. M. Kornblau, G. Marcucci, G. A. Calin, M. Andreeff and C. M. Croce (2009). "MicroRNA 29b functions in acute myeloid leukemia." Blood **114**(26): 5331-5341.

Gierman, L. M., F. van der Ham, A. Koudijs, P. Y. Wielinga, R. Kleemann, T. Kooistra, R. Stoop, M. Kloppenburg, G. J. van Osch, V. Stojanovic-Susulic, T. W. Huizinga and A. M. Zuurmond (2012). "Metabolic stress-induced inflammation plays a major role in the development of osteoarthritis in mice." Arthritis Rheum **64**(4): 1172-1181.

Gilad, S., E. Meiri, Y. Yogev, S. Benjamin, D. Lebanony, N. Yerushalmi, H. Benjamin, M. Kushnir, H. Cholakh, N. Melamed, Z. Bentwich, M. Hod, Y. Goren and A. Chajut (2008). "Serum MicroRNAs Are Promising Novel Biomarkers." PLoS One **3**(9): e3148.

Girkontaite, I., S. Frischholz, P. Lammi, K. Wagner, B. Swoboda, T. Aigner and K. Von der Mark (1996). "Immunolocalization of type X collagen in normal fetal and adult osteoarthritic cartilage with monoclonal antibodies." Matrix Biol **15**(4): 231-238.

Glasson, S. S., R. Askew, B. Sheppard, B. Carito, T. Blanchet, H. L. Ma, C. R. Flannery, D. Peluso, K. Kanki, Z. Yang, M. K. Majumdar and E. A. Morris (2005). "Deletion of active ADAMTS5 prevents cartilage degradation in a murine model of osteoarthritis." Nature **434**(7033): 644-648.

Goldring, M., K. Tsuchimochi and K. Ijiri (2006). "The control of chondrogenesis." J Cell Biochem **97**(1): 33-44.

Goldring, M. B. (2000). "Osteoarthritis and cartilage: the role of cytokines." Curr Rheumatol Rep **2**(6): 459-465.

(2012). "Chondrogenesis, chondrocyte differentiation, and articular cartilage metabolism in health and osteoarthritis." Ther Adv Musculoskelet Dis **4**(4): 269-285.

Goldring, M. B., J. Birkhead, L. J. Sandell, T. Kimura and S. M. Krane (1988). "Interleukin 1 suppresses expression of cartilage-specific types II and IX collagens and increases types I and III collagens in human chondrocytes." J Clin Invest **82**(6): 2026-2037.

Goldring, M. B. and S. R. Goldring (2007). "Osteoarthritis." J Cell Physiol **213**(3): 626-634.

Goldring, M. B., K. Tsuchimochi and K. Ijiri (2006). "The control of chondrogenesis." J Cell Biochem **97**(1): 33-44.

Goldring, S. R. and M. B. Goldring (2004). "The role of cytokines in cartilage matrix degeneration in osteoarthritis." Clin Orthop Relat Res(427 Suppl): S27-36.

Greco, K. V., A. J. Iqbal, L. Rattazzi, G. Nalesso, N. Moradi-Bidhendi, A. R. Moore, M. B. Goldring, F. Dell'Accio and M. Perretti (2011). "High density micromass cultures of a human chondrocyte cell line: a reliable assay system to reveal the modulatory functions of pharmacological agents." Biochem Pharmacol **82**(12): 1919-1929.

Griffin, T. M., J. L. Huebner, V. B. Kraus and F. Guilak (2009). "Extreme obesity due to impaired leptin signaling in mice does not cause knee osteoarthritis." Arthritis Rheum **60**(10): 2935-2944.

Grishok, A., A. E. Pasquinelli, D. Conte, N. Li, S. Parrish, I. Ha, D. L. Baillie, A. Fire, G. Ruvkun and C. C. Mello (2001). "Genes and mechanisms related to RNA interference regulate expression of the small temporal RNAs that control C. elegans developmental timing." Cell **106**(1): 23-34.

Grotle, M., K. B. Hagen, B. Natvig, F. A. Dahl and T. K. Kvien (2008). "Obesity and osteoarthritis in knee, hip and/or hand: an epidemiological study in the general population with 10 years follow-up." BMC Musculoskelet Disord **9**: 132.

Guan, Y.-J., X. Yang, L. Wei and Q. Chen (2011). "MiR-365: a mechanosensitive microRNA stimulates chondrocyte differentiation through targeting histone deacetylase 4." FASEB Journal **25**(12): 4457-4466.

Guerit, D., J. M. Brondello, P. Chuchana, D. Philipot, K. Toupet, C. Bony, C. Jorgensen and D. Noel (2014). "FoxO3a regulation by miRNA-29a controls chondrogenic differentiation of mesenchymal stem cells and cartilage formation." Stem Cells Dev.

Guilak, F., D. L. Butler and S. A. Goldstein (2001). "Functional tissue engineering: the role of biomechanics in articular cartilage repair." Clin Orthop Relat Res(391 Suppl).

Hammerlein, A., J. Weiske and O. Huber (2005). "A second protein kinase CK1-mediated step negatively regulates Wnt signalling by disrupting the lymphocyte enhancer factor-1/beta-catenin complex." Cell Mol Life Sci **62**(5): 606-618.

Hammond, S. M., E. Bernstein, D. Beach and G. J. Hannon (2000). "An RNA-directed nuclease mediates post-transcriptional gene silencing in Drosophila cells." Nature **404**(6775): 293-296.

Han, J., Y. Lee, K.-H. Yeom, Y.-K. Kim, H. Jin and N. Kim (2004). "The Drosha-DGCR8 complex in primary microRNA processing." Genes Dev **18**(24): 3016-3027.

Han, Y. C., C. Y. Park, G. Bhagat, J. Zhang, Y. Wang, J. B. Fan, M. Liu, Y. Zou, I. L. Weissman and H. Gu (2010). "microRNA-29a induces aberrant self-renewal capacity in hematopoietic progenitors, biased myeloid development, and acute myeloid leukemia." J Exp Med **207**(3): 475-489.

Hansen, C., J. Howlin, A. Tengholm, O. Dyachok, W. F. Vogel, A. C. Nairn, P. Greengard and T. Andersson (2009). "Wnt-5a-induced phosphorylation of DARPP-32 inhibits breast cancer cell migration in a CREB-dependent manner." J Biol Chem **284**(40): 27533-27543.

Harfe, B., M. McManus, J. Mansfield, E. Hornstein and C. Tabin (2005). "The RNaseIII enzyme Dicer is required for morphogenesis but not patterning of the vertebrate limb." Proc Natl Acad Sci U S A **102**(31): 10898-10903.

He, A., L. Zhu, N. Gupta, Y. Chang and F. Fang (2007). "Overexpression of micro ribonucleic acid 29, highly up-regulated in diabetic rats, leads to insulin resistance in 3T3-L1 adipocytes." Mol Endocrinol **21**(11): 2785-2794.

He, X., J. P. Saint-Jeannet, Y. Wang, J. Nathans, I. Dawid and H. Varmus (1997). "A member of the Frizzled protein family mediating axis induction by Wnt-5A." Science **275**(5306): 1652-1654.

Hebert, S. S., K. Horre, L. Nicolai, A. S. Papadopoulou, W. Mandemakers, A. N. Silahtaroglu, S. Kauppinen, A. Delacourte and B. De Strooper (2008). "Loss of microRNA cluster miR-29a/b-1 in sporadic Alzheimer's disease correlates with increased BACE1/beta-secretase expression." Proc Natl Acad Sci U S A **105**(17): 6415-6420.

Heimberg, A., L. Sempere, V. Moy, P. Donoghue and K. Peterson (2008). "MicroRNAs and the advent of vertebrate morphological complexity." Proceedings of the National Academy of Sciences **105**(8): 2946-2950.

Heinegard, D. and T. Saxne (2011). "The role of the cartilage matrix in osteoarthritis." Nat Rev Rheumatol **7**(1): 50-56.

Hertzog, P. J., L. A. O'Neill and J. A. Hamilton (2003). "The interferon in TLR signaling: more than just antiviral." Trends Immunol **24**(10): 534-539.

Homma, M. K., D. Li, E. G. Krebs, Y. Yuasa and Y. Homma (2002). "Association and regulation of casein kinase 2 activity by adenomatous polyposis coli protein." Proc Natl Acad Sci U S A **99**(9): 5959-5964.

Houard, X., M. B. Goldring and F. Berenbaum (2013). "Homeostatic mechanisms in articular cartilage and role of inflammation in osteoarthritis." Curr Rheumatol Rep **15**(11): 375.

Hu, Z., J. D. Klein, W. E. Mitch, L. Zhang, I. Martinez and X. H. Wang (2014). "MicroRNA-29 induces cellular senescence in aging muscle through multiple signaling pathways." AGING **6**(3): 15.

Hu, Z., J. D. Klein, W. E. Mitch, L. Zhang, I. Martinez and X. H. Wang (2014). "MicroRNA-29 induces cellular senescence in aging muscle through multiple signaling pathways." Aging (Albany NY) **6**(3): 160-175.

Hui, W., G. J. Litherland, M. S. Elias, G. I. Kitson, T. E. Cawston, A. D. Rowan and D. A. Young (2012). "Leptin produced by joint white adipose tissue induces cartilage degradation via upregulation and activation of matrix metalloproteinases." Ann Rheum Dis **71**(3): 455-462.

Hutvagner, G. (2005). "Small RNA asymmetry in RNAi: function in RISC assembly and gene regulation." FEBS Lett **579**(26): 5850-5857.

Hutvágner, G., J. McLachlan, A. Pasquinelli, É. Bálint, T. Tuschl and P. Zamore (2001). "A Cellular Function for the RNA-Interference Enzyme Dicer in the Maturation of the let-7 Small Temporal RNA." Science **293**(5531): 834-838.

Hutvagner, G. and M. Simard (2008). "Argonaute proteins: key players in RNA silencing." Nature Reviews. Molecular Cell Biology **9**(1): 22-32.

Iliopoulos, D., K. Malizos, P. Oikonomou and A. Tsezou (2008). "Integrative microRNA and proteomic approaches identify novel osteoarthritis genes and their collaborative metabolic and inflammatory networks." PLoS One **3**(11): e3740.

Inui, M., G. Martello and S. Piccolo (2010). "MicroRNA control of signal transduction." Nature Reviews. Molecular Cell Biology **11**(4): 252-263.

Janeway, C. A., Jr. and R. Medzhitov (2002). "Innate immune recognition." Annu Rev Immunol **20**: 197-216.

Jones, S. W., G. Watkins, N. Le Good, S. Roberts, C. L. Murphy, S. M. Brockbank, M. R. Needham, S. J. Read and P. Newham (2009). "The identification of differentially expressed microRNA in osteoarthritic tissue that modulate the production of TNF-alpha and MMP13." Osteoarthritis and Cartilage **17**(4): 464-472.

(2009). "The identification of differentially expressed microRNA in osteoarthritic tissue that modulate the production of TNF-alpha and MMP13." Osteoarthritis and cartilage / OARS, Osteoarthritis Research Society **17**(4): 464-472.

Kadler, K. E., D. F. Holmes, J. A. Trotter and J. A. Chapman (1996). "Collagen fibril formation." Biochem J **316 (Pt 1)**: 1-11.

Kapinas, K., C. Kessler and A. Delany (2009). "miR-29 suppression of osteonectin in osteoblasts: regulation during differentiation and by canonical Wnt signaling." J Cell Biochem **108**(1): 216-224.

Kapinas, K., C. Kessler, T. Ricks, G. Gronowicz and A. M. Delany (2010). "miR-29 modulates Wnt signaling in human osteoblasts through a positive feedback loop." J Biol Chem **285**(33): 25221-25231.

Karlsen, T., A. Shahdadfar and J. Brinchmann (2011). "Human primary articular chondrocytes, chondroblasts-like cells, and dedifferentiated chondrocytes: differences in gene, microRNA, and protein expression and phenotype." Tissue engineering. Part C, Methods **17**(2): 219-227.

Karlsen, T. A. and J. E. Brinchmann (2013). "Liposome delivery of microRNA-145 to mesenchymal stem cells leads to immunological off-target effects mediated by RIG-I." Mol Ther **21**(6): 1169-1181.

Karsdal, M. A., A. C. Bay-Jensen, R. J. Lories, S. Abramson, T. Spector, P. Pastoureau, C. Christiansen, M. Attur, K. Henriksen, S. R. Goldring and V. Kraus (2014). "The coupling of bone and cartilage turnover in osteoarthritis: opportunities for bone antiresorptives and anabolics as potential treatments?" Ann Rheum Dis **73**(2): 336-348.

Kawano, Y. and R. Kypta (2003). "Secreted antagonists of the Wnt signalling pathway." J Cell Sci **116**(Pt 13): 2627-2634.

Kent, O., R. Chivukula, M. Mullendore, E. Wentzel, G. Feldmann, K. Lee, S. Liu, S. Leach, A. Maitra and J. Mendell (2010). "Repression of the miR-143/145 cluster by oncogenic Ras initiates a tumor-promoting feed-forward pathway." Genes Dev **24**(24): 2754-2759.

Kerkhof, H. J., R. J. Lories, I. Meulenbelt, I. Jonsdottir, A. M. Valdes, P. Arp, T. Ingvarsson, M. Jhamai, H. Jonsson, L. Stolk, G. Thorleifsson, G. Zhai, F. Zhang, Y. Zhu, R. van der Breggen, A. Carr, M. Doherty, S. Doherty, D. T. Felson, A. Gonzalez, B. V. Halldorsson, D. J. Hart, V. B. Hauksson, A. Hofman, J. P. Ioannidis, M. Kloppenburg, N. E. Lane, J. Loughlin, F. P. Luyten, M. C. Nevitt, N. Parimi, H. A. Pols, F. Rivadeneira, E. P. Slagboom, U. Styrkarsdottir, A. Tsezou, T. van de Putte, J. Zmuda, T. D. Spector, K. Stefansson, A. G. Uitterlinden and J. B. van Meurs (2010). "A genome-wide association study identifies an osteoarthritis susceptibility locus on chromosome 7q22." Arthritis Rheum **62**(2): 499-510.

Ketting, R. F., S. E. Fischer, E. Bernstein, T. Sijen, G. J. Hannon and R. H. Plasterk (2001). "Dicer functions in RNA interference and in synthesis of small RNA involved in developmental timing in C. elegans." Genes Dev **15**(20): 2654-2659.

Khvorova, A., A. Reynolds and S. Jayasena (2003). "Functional siRNAs and miRNAs exhibit strand bias." Cell **115**(2): 209-216.

Kiani, C., L. Chen, Y. J. Wu, A. J. Yee and B. B. Yang (2002). "Structure and function of aggrecan." Cell Res **12**(1): 19-32.

Kim, D., J. Song and E.-J. Jin (2010). "MicroRNA-221 Regulates Chondrogenic Differentiation through Promoting Proteosomal Degradation of Slug by Targeting Mdm2." Journal of Biological Chemistry **285**(35): 26900-26907.
Kim, D., J. Song, S. Kim, C.-H. Chun and E.-J. Jin (2011). "MicroRNA-34a regulates migration of chondroblast and IL-1β-induced degeneration of chondrocytes by targeting EphA5." Biochem Biophys Res Commun **415**(4): 551-557.
Kim, D., J. Song, S. Kim, C.-H. Chun, J. Sonn and E.-J. Jin (2012). "MicroRNA-34a modulates cytoskeletal dynamics through regulating RhoA/Rac1 crosstalk in chondroblasts." The Journal of biological chemistry.
Kim, D., J. Song, S. Kim, S.-S. Kang and E.-J. Jin (2011). "MicroRNA-142-3p regulates TGF-β3-mediated region-dependent chondrogenesis by regulating ADAM9." Biochem Biophys Res Commun **414**(4): 653-659.
Kim, N. (2005). "MicroRNA biogenesis: coordinated cropping and dicing." Nature Reviews. Molecular Cell Biology **6**(5): 376-385.
Kim, N., J. Han and M. Siomi (2009). "Biogenesis of small RNAs in animals." Nature reviews. Molecular cell biology **10**(2): 126-139.
Kiriakidou, M., G. Tan, S. Lamprinaki, M. De Planell-Saguer, P. Nelson and Z. Mourelatos (2007). "An mRNA m7G cap binding-like motif within human Ago2 represses translation." Cell **129**(6): 1141-1151.
Knauper, V., C. Lopez-Otin, B. Smith, G. Knight and G. Murphy (1996). "Biochemical characterization of human collagenase-3." J Biol Chem **271**(3): 1544-1550.
Kobayashi, M., G. R. Squires, A. Mousa, M. Tanzer, D. J. Zukor, J. Antoniou, U. Feige and A. R. Poole (2005). "Role of interleukin-1 and tumor necrosis factor alpha in matrix degradation of human osteoarthritic cartilage." Arthritis Rheum **52**(1): 128-135.
Kobayashi, T., J. Lu, B. Cobb, S. Rodda, A. McMahon, E. Schipani, M. Merkenschlager and H. Kronenberg (2008). "Dicer-dependent pathways regulate chondrocyte proliferation and differentiation." Proc Natl Acad Sci U S A **105**(6): 1949-1954.
Kongcharoensombat, W., T. Nakasa, M. Ishikawa, A. Nakamae, M. Deie, N. Adachi, A. Mohamed and M. Ochi (2010). "The effect of microRNA-21 on proliferation and matrix synthesis of chondrocytes embedded in atelocollagen gel." Knee Surgery, Sports Traumatology, Arthroscopy **18**(12): 1679-1684.
Konttinen, Y. T., T. Sillat, G. Barreto, M. Ainola and D. C. Nordstrom (2012). "Osteoarthritis as an autoinflammatory disease caused by chondrocyte-mediated inflammatory responses." Arthritis Rheum **64**(3): 613-616.
Kosaka, N., H. Iguchi and T. Ochiya (2010). "Circulating microRNA in body fluid: a new potential biomarker for cancer diagnosis and prognosis." Cancer Sci **101**(10): 2087-2092.
Koshy, P. J., C. J. Lundy, A. D. Rowan, S. Porter, D. R. Edwards, A. Hogan, I. M. Clark and T. E. Cawston (2002). "The modulation of matrix metalloproteinase and ADAM gene expression in human chondrocytes by interleukin-1 and oncostatin M: a time-course study using real-time quantitative reverse transcription-polymerase chain reaction." Arthritis Rheum **46**(4): 961-967.
Kozomara, A. and S. Griffiths-Jones (2011). "miRBase: integrating microRNA annotation and deep-sequencing data." Nucleic Acids Research **39**(Database issue): D152-D157.
Kwiecinski, M., A. Noetel, N. Elfimova, J. Trebicka, S. Schievenbusch, I. Strack, L. Molnar, M. von Brandenstein, U. Tox, R. Nischt, O. Coutelle, H. P. Dienes and M. Odenthal (2011). "Hepatocyte growth factor (HGF) inhibits collagen I and IV synthesis in hepatic stellate cells by miRNA-29 induction." PLoS One **6**(9): e24568.
Lagos-Quintana, M., R. Rauhut, W. Lendeckel and T. Tuschl (2001). "Identification of novel genes coding for small expressed RNAs." Science (New York, N.Y.) **294**(5543): 853-858.

Lai, E. (2002). "Micro RNAs are complementary to 3' UTR sequence motifs that mediate negative post-transcriptional regulation." Nat Genet **30**(4): 363-364.
Lane, L. B., A. Villacin and P. G. Bullough (1977). "The vascularity and remodelling of subchondrial bone and calcified cartilage in adult human femoral and humeral heads. An age- and stress-related phenomenon." J Bone Joint Surg Br **59**(3): 272-278.
Lane, N. E., K. Lian, M. C. Nevitt, J. M. Zmuda, L. Lui, J. Li, J. Wang, M. Fontecha, N. Umblas, M. Rosenbach, P. de Leon and M. Corr (2006). "Frizzled-related protein variants are risk factors for hip osteoarthritis." Arthritis Rheum **54**(4): 1246-1254.
Lapiere, C. M., A. Lenaers and L. D. Kohn (1971). "Procollagen peptidase: an enzyme excising the coordination peptides of procollagen." Proc Natl Acad Sci U S A **68**(12): 3054-3058.
Lau, N. C., L. P. Lim, E. G. Weinstein and D. P. Bartel (2001). "An abundant class of tiny RNAs with probable regulatory roles in Caenorhabditis elegans." Science (New York, N.Y.) **294**(5543): 858-862.
Lau, P.-W. and I. MacRae (2009). "The molecular machines that mediate microRNA maturation." J Cell Mol Med **13**(1): 54-60.
Lawrie, C., S. Gal, H. Dunlop, B. Pushkaran, A. Liggins, K. Pulford, A. Banham, F. Pezzella, J. Boultwood, J. Wainscoat, C. Hatton and A. Harris (2008). "Detection of elevated levels of tumour-associated microRNAs in serum of patients with diffuse large B-cell lymphoma." Br J Haematol **141**(5): 672-675.
Le, L. T., T. E. Swingler and I. M. Clark (2013). "Review: the role of microRNAs in osteoarthritis and chondrogenesis." Arthritis Rheum **65**(8): 1963-1974.
Lee, D. A., G. Bentley and C. W. Archer (1993). "The control of cell division in articular chondrocytes." Osteoarthritis Cartilage **1**(2): 137-146.
Lee, I., S. Ajay, J. I. Yook, H. S. Kim, S. H. Hong, N. H. Kim, S. Dhanasekaran, A. Chinnaiyan and B. Athey (2009). "New class of microRNA targets containing simultaneous 5'-UTR and 3'-UTR interaction sites." Genome Res **19**(7): 1175-1183.
Lee, J. H., T. Ort, K. Ma, K. Picha, J. Carton, P. A. Marsters, L. S. Lohmander, F. Baribaud, X. Y. Song and S. Blake (2009). "Resistin is elevated following traumatic joint injury and causes matrix degradation and release of inflammatory cytokines from articular cartilage in vitro." Osteoarthritis Cartilage **17**(5): 613-620.
Lee, R. and V. Ambros (2001). "An Extensive Class of Small RNAs in Caenorhabditis elegans." Science **294**(5543): 862-864.
Lee, R. C., R. L. Feinbaum and V. Ambros (1993). "The C. elegans heterochronic gene lin-4 encodes small RNAs with antisense complementarity to lin-14." Cell **75**(5): 843-854.
Lee, Y., C. Ahn, J. Han, H. Choi, J. Kim, J. Yim, J. Lee, P. Provost, O. Radmark, S. Kim and N. Kim (2003). "The nuclear RNase III Drosha initiates microRNA processing." Nature **425**(6956): 415-419.
Lee, Y., K. Jeon, J.-T. Lee, S. Kim and N. Kim (2002). "MicroRNA maturation: stepwise processing and subcellular localization." The EMBO Journal **21**(17): 4663-4670.
Lee, Y., M. Kim, J. Han, K.-H. Yeom, S. Lee, S. Baek and N. Kim (2004). "MicroRNA genes are transcribed by RNA polymerase II." The EMBO Journal **23**(20): 4051-4060.
Lefebvre, V., W. Huang, V. R. Harley, P. N. Goodfellow and B. de Crombrugghe (1997). "SOX9 is a potent activator of the chondrocyte-specific enhancer of the pro alpha1(II) collagen gene." Mol Cell Biol **17**(4): 2336-2346.
Lefebvre, V., C. Peeters-Joris and G. Vaes (1990). "Modulation by interleukin 1 and tumor necrosis factor alpha of production of collagenase, tissue inhibitor of metalloproteinases and collagen types in differentiated and dedifferentiated articular chondrocytes." Biochim Biophys Acta **1052**(3): 366-378.

Leone, V., D. D'Angelo, P. Pallante, C. M. Croce and A. Fusco (2012). "Thyrotropin regulates thyroid cell proliferation by up-regulating miR-23b and miR-29b that target SMAD3." J Clin Endocrinol Metab **97**(9): 3292-3301.

Letamendia, A., E. Labbe and L. Attisano (2001). "Transcriptional regulation by Smads: crosstalk between the TGF-beta and Wnt pathways." J Bone Joint Surg Am **83-A Suppl 1**(Pt 1): S31-39.

Lewis, B., C. Burge and D. Bartel (2005). "Conserved Seed Pairing, Often Flanked by Adenosines, Indicates that Thousands of Human Genes are MicroRNA Targets." Cell **120**(1): 15-20.

Li, G., J. Yin, J. Gao, T. S. Cheng, N. J. Pavlos, C. Zhang and M. H. Zheng (2013). "Subchondral bone in osteoarthritis: insight into risk factors and microstructural changes." Arthritis Res Ther **15**(6): 223.

Li, H., H. Xie, W. Liu, R. Hu, B. Huang, Y.-F. Tan, K. Xu, Z.-F. Sheng, H.-D. Zhou, X.-P. Wu and X.-H. Luo (2009). "A novel microRNA targeting HDAC5 regulates osteoblast differentiation in mice and contributes to primary osteoporosis in humans." The Journal of clinical investigation **119**(12): 3666-3677.

Li, J., J. Huang, L. Dai, D. Yu, Q. Chen, X. Zhang and K. Dai (2012). "MiR-146a, an interleukin-1beta responsive microRNA, induces vascular endothelial growth factor and chondrocyte apoptosis by targeting Smad4." Arthritis Res Ther **14**(2): R75.

Li, N., J. Cui, X. Duan, H. Chen and F. Fan (2012). "Suppression of type I collagen expression by miR-29b via PI3K, Akt, and Sp1 pathway in human Tenon's fibroblasts." Invest Ophthalmol Vis Sci **53**(3): 1670-1678.

Li, T. F., R. J. O'Keefe and D. Chen (2005). "TGF-beta signaling in chondrocytes." Front Biosci **10**: 681-688.

Li, X., G. Gibson, J.-S. Kim, J. Kroin, S. Xu, A. van Wijnen and H.-J. Im (2011). "MicroRNA-146a is linked to pain-related pathophysiology of osteoarthritis." Gene **480**(1-2): 34-41.

Liang, Z.-J., H. Zhuang, G.-X. Wang, Z. Li, H.-T. Zhang, T.-Q. Yu and B.-D. Zhang (2012). "MiRNA-140 is a negative feedback regulator of MMP-13 in IL-1β-stimulated human articular chondrocyte C28/I2 cells." Inflammation Research **61**(5): 503-509.

(2012). "MiRNA-140 is a negative feedback regulator of MMP-13 in IL-1β-stimulated human articular chondrocyte C28/I2 cells." Inflammation research: 1-7.

Lim, L., N. Lau, P. Garrett-Engele, A. Grimson, J. Schelter, J. Castle, D. Bartel, P. Linsley and J. Johnson (2005). "Microarray analysis shows that some microRNAs downregulate large numbers of target mRNAs." Nature **433**(7027): 769-773.

Lin, E., L. Kong, X.-H. Bai, Y. Luan and C.-J. Liu (2009). "miR-199a, a bone morphogenic protein 2-responsive MicroRNA, regulates chondrogenesis via direct targeting to Smad1." The Journal of biological chemistry **284**(17): 11326-11335.

(2009). "miR-199a, a bone morphogenic protein 2-responsive MicroRNA, regulates chondrogenesis via direct targeting to Smad1." Journal of Biological Chemistry **284**(17): 11326-11335.

Lin, L., Q. Shen, C. Zhang, L. Chen and C. Yu (2011). "Assessment of the profiling microRNA expression of differentiated and dedifferentiated human adult articular chondrocytes." Journal of Orthopaedic Research **29**(10): 1578-1584.

Lin, S.-Y., S. Johnson, M. Abraham, M. Vella, A. Pasquinelli, C. Gamberi, E. Gottlieb and F. Slack (2003). "The C elegans hunchback homolog, hbl-1, controls temporal patterning and is a probable microRNA target." Developmental Cell **4**(5): 639-650.

Link, A., F. Balaguer, Y. Shen, T. Nagasaka, J. J. Lozano, R. Boland and A. Goel (2010). "Fecal MicroRNAs as novel biomarkers for colon cancer screening." Cancer Epidemiol Biomarkers Prev **19**(7): 1766-1774.

Liu, C., Y. Wang, P. M. Smallwood and J. Nathans (2008). "An essential role for Frizzled5 in neuronal survival in the parafascicular nucleus of the thalamus." J Neurosci **28**(22): 5641-5653.

Liu, S., L. C. Wu, J. Pang, R. Santhanam, S. Schwind, Y. Z. Wu, C. J. Hickey, J. Yu, H. Becker, K. Maharry, M. D. Radmacher, C. Li, S. P. Whitman, A. Mishra, N. Stauffer, A. M. Eiring, R. Briesewitz, R. A.

Baiocchi, K. K. Chan, P. Paschka, M. A. Caligiuri, J. C. Byrd, C. M. Croce, C. D. Bloomfield, D. Perrotti, R. Garzon and G. Marcucci (2010). "Sp1/NFkappaB/HDAC/miR-29b regulatory network in KIT-driven myeloid leukemia." Cancer Cell **17**(4): 333-347.

Liu, Y., T. Huang, X. Zhao and L. Cheng (2011). "MicroRNAs modulate the Wnt signaling pathway through targeting its inhibitors." Biochem Biophys Res Commun **408**(2): 259-264.

Lodewyckx, L., F. P. Luyten and R. J. Lories (2012). "Genetic deletion of low-density lipoprotein receptor-related protein 5 increases cartilage degradation in instability-induced osteoarthritis." Rheumatology (Oxford) **51**(11): 1973-1978.

Loeser, R., S. Goldring, C. Scanzello and M. Goldring (2012). "Osteoarthritis: A disease of the joint as an organ." Arthritis & Rheumatism: n/a-n/a.

Loeser, R. F., S. R. Goldring, C. R. Scanzello and M. B. Goldring (2012). "Osteoarthritis: a disease of the joint as an organ." Arthritis Rheum **64**(6): 1697-1707.

Long, J., Y. Wang, W. Wang, B. H. Chang and F. R. Danesh (2011). "MicroRNA-29c is a signature microRNA under high glucose conditions that targets Sprouty homolog 1, and its in vivo knockdown prevents progression of diabetic nephropathy." J Biol Chem **286**(13): 11837-11848.

Lories, R. J., J. Peeters, A. Bakker, P. Tylzanowski, I. Derese, J. Schrooten, J. T. Thomas and F. P. Luyten (2007). "Articular cartilage and biomechanical properties of the long bones in Frzb-knockout mice." Arthritis Rheum **56**(12): 4095-4103.

Loughlin, J., B. Dowling, K. Chapman, L. Marcelline, Z. Mustafa, L. Southam, A. Ferreira, C. Ciesielski, D. A. Carson and M. Corr (2004). "Functional variants within the secreted frizzled-related protein 3 gene are associated with hip osteoarthritis in females." Proc Natl Acad Sci U S A **101**(26): 9757-9762.

Lu, D., Y. Zhao, R. Tawatao, H. B. Cottam, M. Sen, L. M. Leoni, T. J. Kipps, M. Corr and D. A. Carson (2004). "Activation of the Wnt signaling pathway in chronic lymphocytic leukemia." Proc Natl Acad Sci U S A **101**(9): 3118-3123.

Luna, C., G. Li, J. Qiu, D. L. Epstein and P. Gonzalez (2009). "Role of miR-29b on the regulation of the extracellular matrix in human trabecular meshwork cells under chronic oxidative stress." Mol Vis **15**: 2488-2497.

Lund, E., S. Güttinger, A. Calado, J. Dahlberg and U. Kutay (2004). "Nuclear Export of MicroRNA Precursors." Science **303**(5654): 95-98.

Lytle, R., T. Yario and J. Steitz (2007). "Target mRNAs are repressed as efficiently by microRNA-binding sites in the 5′ UTR as in the 3′ UTR." Proceedings of the National Academy of Sciences **104**(23): 9667-9672.

Ma, F., S. Xu, X. Liu, Q. Zhang, X. Xu, M. Liu, M. Hua, N. Li, H. Yao and X. Cao (2011). "The microRNA miR-29 controls innate and adaptive immune responses to intracellular bacterial infection by targeting interferon-gamma." Nat Immunol **12**(9): 861-869.

Maegdefessel, L., J. Azuma, R. Toh, D. R. Merk, A. Deng, J. T. Chin, U. Raaz, A. M. Schoelmerich, A. Raiesdana, N. J. Leeper, M. V. McConnell, R. L. Dalman, J. M. Spin and P. S. Tsao (2012). "Inhibition of microRNA-29b reduces murine abdominal aortic aneurysm development." J Clin Invest **122**(2): 497-506.

Marcu, K. B., M. Otero, E. Olivotto, R. M. Borzi and M. B. Goldring (2010). "NF-kappaB signaling: multiple angles to target OA." Curr Drug Targets **11**(5): 599-613.

Martel-Pelletier, J., C. Boileau, J. P. Pelletier and P. J. Roughley (2008). "Cartilage in normal and osteoarthritis conditions." Best Pract Res Clin Rheumatol **22**(2): 351-384.

Martin, P. (1990). "Tissue patterning in the developing mouse limb." Int J Dev Biol **34**(3): 323-336.

Martinez-Sanchez, A., K. Dudek and C. Murphy (2012). "Regulation of human chondrocyte function through direct inhibition of cartilage master regulator SOX9 by microRNA-145 (miRNA-145)." Journal of Biological Chemistry **287**(2): 916-924.

(2012). "Regulation of human chondrocyte function through direct inhibition of cartilage master regulator SOX9 by microRNA-145 (miRNA-145)." The Journal of biological chemistry **287**(2): 916-924.
Martinez-Sanchez, A. and C. L. Murphy (2013). "miR-1247 functions by targeting cartilage transcription factor SOX9." J Biol Chem **288**(43): 30802-30814.
Martinez, J., A. Patkaniowska, H. Urlaub, R. Lührmann and T. Tuschl (2002). "Single-stranded antisense siRNAs guide target RNA cleavage in RNAi." Cell **110**(5): 563-574.
Matyas, J. R., L. J. Sandell and M. E. Adams (1997). "Gene expression of type II collagens in chondro-osteophytes in experimental osteoarthritis." Osteoarthritis Cartilage **5**(2): 99-105.
Maurer, B., J. Stanczyk, A. Jungel, A. Akhmetshina, M. Trenkmann, M. Brock, O. Kowal-Bielecka, R. E. Gay, B. A. Michel, J. H. Distler, S. Gay and O. Distler (2010). "MicroRNA-29, a key regulator of collagen expression in systemic sclerosis." Arthritis Rheum **62**(6): 1733-1743.
Meachim, G. and D. H. Collins (1962). "Cell counts of normal and osteoarthritic articular cartilage in relation to the uptake of sulphate (35SO4) in vitro." Ann Rheum Dis **21**: 45-50.
Messier, S. P., D. J. Gutekunst, C. Davis and P. DeVita (2005). "Weight loss reduces knee-joint loads in overweight and obese older adults with knee osteoarthritis." Arthritis Rheum **52**(7): 2026-2032.
Miravet, S., J. Piedra, F. Miro, E. Itarte, A. Garcia de Herreros and M. Dunach (2002). "The transcriptional factor Tcf-4 contains different binding sites for beta-catenin and plakoglobin." J Biol Chem **277**(3): 1884-1891.
Mitchell, P., R. Parkin, E. Kroh, B. Fritz, S. Wyman, E. Pogosova-Agadjanyan, A. Peterson, J. Noteboom, K. O'Briant, A. Allen, D. Lin, N. Urban, C. Drescher, B. Knudsen, D. Stirewalt, R. Gentleman, R. Vessella, P. Nelson, D. Martin and M. Tewari (2008). "Circulating microRNAs as stable blood-based markers for cancer detection." Proceedings of the National Academy of Sciences **105**(30): 10513-10518.
Miyaki, S., T. Nakasa, S. Otsuki, S. Grogan, R. Higashiyama, A. Inoue, Y. Kato, T. Sato, M. Lotz and H. Asahara (2009). "MicroRNA-140 is expressed in differentiated human articular chondrocytes and modulates interleukin-1 responses." Arthritis & Rheumatism **60**(9): 2723-2730.
(2009). "MicroRNA-140 is expressed in differentiated human articular chondrocytes and modulates interleukin-1 responses." Arthritis and rheumatism **60**(9): 2723-2730.
Miyaki, S., T. Nakasa, S. Otsuki, S. P. Grogan, R. Higashiyama, A. Inoue, Y. Kato, T. Sato, M. K. Lotz and H. Asahara (2009). "MicroRNA-140 is expressed in differentiated human articular chondrocytes and modulates interleukin-1 responses." Arthritis Rheum **60**(9): 2723-2730.
Miyaki, S., T. Sato, A. Inoue, S. Otsuki, Y. Ito, S. Yokoyama, Y. Kato, F. Takemoto, T. Nakasa, S. Yamashita, S. Takada, M. Lotz, H. Ueno-Kudo and H. Asahara (2010). "MicroRNA-140 plays dual roles in both cartilage development and homeostasis." Genes Dev **24**(11): 1173-1185.
Miyaki, S., T. Sato, A. Inoue, S. Otsuki, Y. Ito, S. Yokoyama, Y. Kato, F. Takemoto, T. Nakasa, S. Yamashita, S. Takada, M. K. Lotz, H. Ueno-Kudo and H. Asahara (2010). "MicroRNA-140 plays dual roles in both cartilage development and homeostasis." Genes Dev **24**(11): 1173-1185.
Miyazawa, K., M. Shinozaki, T. Hara, T. Furuya and K. Miyazono (2002). "Two major Smad pathways in TGF-beta superfamily signalling." Genes Cells **7**(12): 1191-1204.
Mooney, R. A., E. R. Sampson, J. Lerea, R. N. Rosier and M. J. Zuscik (2011). "High-fat diet accelerates progression of osteoarthritis after meniscal/ligamentous injury." Arthritis Res Ther **13**(6): R198.
Morita, S., T. Horii, M. Kimura, T. Ochiya, S. Tajima and I. Hatada (2013). "miR-29 represses the activities of DNA methyltransferases and DNA demethylases." Int J Mol Sci **14**(7): 14647-14658.
Mott, J. L., S. Kurita, S. C. Cazanave, S. F. Bronk, N. W. Werneburg and M. E. Fernandez-Zapico (2010). "Transcriptional suppression of mir-29b-1/mir-29a promoter by c-Myc, hedgehog, and NF-kappaB." J Cell Biochem **110**(5): 1155-1164.

Moulin, D., V. Salone, M. Koufany, T. Clement, P. Netter, I. Behm-Ansmant, B. Charpentier, C. Branlant and J.-Y. Jouzeau (2012). "miR-29b is overexpressed in osteoarthritic patients and targets type II collagen." Osteoarthritis and Cartilage **20**: S139 - S140.

Muniyappa, M. K., P. Dowling, M. Henry, P. Meleady, P. Doolan, P. Gammell, M. Clynes and N. Barron (2009). "MiRNA-29a regulates the expression of numerous proteins and reduces the invasiveness and proliferation of human carcinoma cell lines." Eur J Cancer **45**(17): 3104-3118.

Murata, K., H. Yoshitomi, S. Tanida, M. Ishikawa, K. Nishitani, H. Ito and T. Nakamura (2010). "Plasma and synovial fluid microRNAs as potential biomarkers of rheumatoid arthritis and osteoarthritis." Arthritis Res Ther **12**(3): R86.

Murata, K., H. Yoshitomi, S. Tanida, M. Ishikawa, K. Nishitani, H. Ito and T. Nakamura (2010). "Plasma and synovial fluid microRNAs as potential biomarkers of rheumatoid arthritis and osteoarthritis." Arthritis Res Ther **12**(3): R86.

Nah, S. S., I. Y. Choi, B. Yoo, Y. G. Kim, H. B. Moon and C. K. Lee (2007). "Advanced glycation end products increases matrix metalloproteinase-1, -3, and -13, and TNF-alpha in human osteoarthritic chondrocytes." FEBS Lett **581**(9): 1928-1932.

Nakamura, Y., X. He, H. Kato, S. Wakitani, T. Kobayashi, S. Watanabe, A. Iida, H. Tahara, M. L. Warman, R. Watanapokasin and J. H. Postlethwait (2012). "Sox9 is upstream of microRNA-140 in cartilage." Appl Biochem Biotechnol **166**(1): 64-71.

Nakamura, Y., J. Inloes, T. Katagiri and T. Kobayashi (2011). "Chondrocyte-specific microRNA-140 regulates endochondral bone development and targets Dnpep to modulate bone morphogenetic protein signaling." Mol Cell Biol **31**(14): 3019-3028.

Nakamura, Y., J. B. Inloes, T. Katagiri and T. Kobayashi (2011). "Chondrocyte-specific microRNA-140 regulates endochondral bone development and targets Dnpep to modulate bone morphogenetic protein signaling." Mol Cell Biol **31**(14): 3019-3028.

Nalesso, G., J. Sherwood, J. Bertrand, T. Pap, M. Ramachandran, C. De Bari, C. Pitzalis and F. Dell'accio (2011). "WNT-3A modulates articular chondrocyte phenotype by activating both canonical and noncanonical pathways." J Cell Biol **193**(3): 551-564.

Neu, C., A. Khalafi, K. Komvopoulos, T. Schmid and H. Reddi (2007). "Mechanotransduction of bovine articular cartilage superficial zone protein by transforming growth factor β signaling." Arthritis & Rheumatism **56**(11): 3706-3714.

Ng, L. J., S. Wheatley, G. E. Muscat, J. Conway-Campbell, J. Bowles, E. Wright, D. M. Bell, P. P. Tam, K. S. Cheah and P. Koopman (1997). "SOX9 binds DNA, activates transcription, and coexpresses with type II collagen during chondrogenesis in the mouse." Dev Biol **183**(1): 108-121.

Nicolas, F. E., H. Pais, F. Schwach, M. Lindow, S. Kauppinen, V. Moulton and T. Dalmay (2008). "Experimental identification of microRNA-140 targets by silencing and overexpressing miR-140." RNA (New York, N.Y.) **14**(12): 2513-2520.

Nishikawa, R., Y. Goto, S. Kojima, H. Enokida, T. Chiyomaru, T. Kinoshita, S. Sakamoto, M. Fuse, M. Nakagawa, Y. Naya, T. Ichikawa and N. Seki (2014). "Tumor-suppressive microRNA-29s inhibit cancer cell migration and invasion via targeting LAMC1 in prostate cancer." Int J Oncol **45**(1): 401-410.

Okamura, K., J. Hagen, H. Duan, D. Tyler and E. Lai (2007). "The mirtron pathway generates microRNA-class regulatory RNAs in Drosophila." Cell **130**(1): 89-100.

Okuhara, A., T. Nakasa, H. Shibuya, T. Niimoto, N. Adachi, M. Deie and M. Ochi (2011). "Changes in microRNA expression in peripheral mononuclear cells according to the progression of osteoarthritis." Modern rheumatology / the Japan Rheumatism Association: 1-12.

Pais, H., E. Francisco, S. Soond, T. Swingler, I. Clark, A. Chantry, V. Moulton and T. Dalmay (2010). "Analyzing mRNA expression identifies Smad3 as a microRNA-140 target regulated only at protein level." RNA **16**(3): 489-494.

Pais, H., F. E. Nicolas, S. M. Soond, T. E. Swingler, I. M. Clark, A. Chantry, V. Moulton and T. Dalmay (2010). "Analyzing mRNA expression identifies Smad3 as a microRNA-140 target regulated only at protein level." RNA **16**(3): 489-494.

Park, S. J., E. J. Cheon, M. H. Lee and H. A. Kim (2013). "MicroRNA-127-5p regulates matrix metalloproteinase 13 expression and interleukin-1beta-induced catabolic effects in human chondrocytes." Arthritis Rheum **65**(12): 3141-3152.

Parpart, S., S. Roessler, F. Dong, V. Rao, A. Takai, J. Ji, L. X. Qin, Q. H. Ye, H. L. Jia, Z. Y. Tang and X. W. Wang (2014). "Modulation of miR-29 expression by alpha-fetoprotein is linked to the hepatocellular carcinoma epigenome." Hepatology **60**(3): 872-883.

Pearle, A. D., C. R. Scanzello, S. George, L. A. Mandl, E. F. DiCarlo, M. Peterson, T. P. Sculco and M. K. Crow (2007). "Elevated high-sensitivity C-reactive protein levels are associated with local inflammatory findings in patients with osteoarthritis." Osteoarthritis Cartilage **15**(5): 516-523.

Pearle, A. D., R. F. Warren and S. A. Rodeo (2005). "Basic science of articular cartilage and osteoarthritis." Clin Sports Med **24**(1): 1-12.

Pelletier, J. P., J. P. Caron, C. Evans, P. D. Robbins, H. I. Georgescu, D. Jovanovic, J. C. Fernandes and J. Martel-Pelletier (1997). "In vivo suppression of early experimental osteoarthritis by interleukin-1 receptor antagonist using gene therapy." Arthritis Rheum **40**(6): 1012-1019.

Petersen, C., M.-E. Bordeleau, J. Pelletier and P. Sharp (2006). "Short RNAs repress translation after initiation in mammalian cells." Mol Cell **21**(4): 533-542.

Petrovich, O. n., S. L. llyich and M. S. Pavlovich (2014). "Connectic tissue: Histophysiology, Biochemistry, Molecular Biology ".

Pfander, D., T. Cramer, E. Schipani and R. S. Johnson (2003). "HIF-1alpha controls extracellular matrix synthesis by epiphyseal chondrocytes." J Cell Sci **116**(Pt 9): 1819-1826.

Poonpet, T., S. Honsawek, N. Tammachote, S. Kanitnate and R. Tammachote (2013). "ADAMTS14 gene polymorphism associated with knee osteoarthritis in Thai women." Genet Mol Res **12**(4): 5301-5309.

Presle, N., P. Pottie, H. Dumond, C. Guillaume, F. Lapicque, S. Pallu, D. Mainard, P. Netter and B. Terlain (2006). "Differential distribution of adipokines between serum and synovial fluid in patients with osteoarthritis. Contribution of joint tissues to their articular production." Osteoarthritis Cartilage **14**(7): 690-695.

Price, M. A. (2006). "CKI, there's more than one: casein kinase I family members in Wnt and Hedgehog signaling." Genes Dev **20**(4): 399-410.

Pujol, J.-P., C. Chadjichristos, F. Legendre, C. Bauge, G. Beauchef, R. Andriamanalijaona, P. Galera and K. Boumediene (2008). "Interleukin-1 and transforming growth factor-beta 1 as crucial factors in osteoarthritic cartilage metabolism." Connect Tissue Res **49**(3): 293-297.

Pullen, T. J., G. da Silva Xavier, G. Kelsey and G. A. Rutter (2011). "miR-29a and miR-29b contribute to pancreatic beta-cell-specific silencing of monocarboxylate transporter 1 (Mct1)." Mol Cell Biol **31**(15): 3182-3194.

Qin, W., A. C. Chung, X. R. Huang, X. M. Meng, D. S. Hui, C. M. Yu, J. J. Sung and H. Y. Lan (2011). "TGF-beta/Smad3 signaling promotes renal fibrosis by inhibiting miR-29." J Am Soc Nephrol **22**(8): 1462-1474.

Ramdas, V., M. McBride, L. Denby and A. H. Baker (2013). "Canonical transforming growth factor-beta signaling regulates disintegrin metalloprotease expression in experimental renal fibrosis via miR-29." Am J Pathol **183**(6): 1885-1896.

Reinhart, B. J., F. J. Slack, M. Basson, A. E. Pasquinelli, J. C. Bettinger, A. E. Rougvie, H. R. Horvitz and G. Ruvkun (2000). "The 21-nucleotide let-7 RNA regulates developmental timing in Caenorhabditis elegans." Nature **403**(6772): 901-906.

Riordan, E. A., C. Little and D. Hunter (2014). "Pathogenesis of post-traumatic OA with a view to intervention." Best Pract Res Clin Rheumatol **28**(1): 17-30.

Ro, S., C. Park, D. Young, K. Sanders and W. Yan (2007). "Tissue-dependent paired expression of miRNAs." Nucleic Acids Res **35**(17): 5944-5953.
Roderburg, C., G. W. Urban, K. Bettermann, M. Vucur, H. Zimmermann, S. Schmidt, J. Janssen, C. Koppe, P. Knolle, M. Castoldi, F. Tacke, C. Trautwein and T. Luedde (2011). "Micro-RNA profiling reveals a role for miR-29 in human and murine liver fibrosis." Hepatology **53**(1): 209-218.
Rodriguez-Lopez, J., M. Pombo-Suarez, J. Loughlin, A. Tsezou, F. J. Blanco, I. Meulenbelt, P. E. Slagboom, A. M. Valdes, T. D. Spector, J. J. Gomez-Reino and A. Gonzalez (2009). "Association of a nsSNP in ADAMTS14 to some osteoarthritis phenotypes." Osteoarthritis Cartilage **17**(3): 321-327.
Rodriguez, A., S. Griffiths-Jones, J. Ashurst and A. Bradley (2004). "Identification of mammalian microRNA host genes and transcription units." Genome Res **14**(10A): 1902-1910.
Roodman, G. D. (1999). "Cell biology of the osteoclast." Exp Hematol **27**(8): 1229-1241.
Rothwell, A. G. and G. Bentley (1973). "Chondrocyte multiplication in osteoarthritic articular cartilage." J Bone Joint Surg Br **55**(3): 588-594.
Ruby, G., C. Jan and D. Bartel (2007). "Intronic microRNA precursors that bypass Drosha processing." Nature **448**(7149): 83-86.
Sætrom, P., B. Heale, O. Snøve, L. Aagaard, J. Alluin and J. Rossi (2007). "Distance constraints between microRNA target sites dictate efficacy and cooperativity." Nucleic Acids Res **35**(7): 2333-2342.
Saini, H. K., S. Griffiths-Jones and A. J. Enright (2007). "Genomic analysis of human microRNA transcripts." Proc Natl Acad Sci U S A **104**(45): 17719-17724.
Sandell, L. J. and T. Aigner (2001). "Articular cartilage and changes in arthritis. An introduction: cell biology of osteoarthritis." Arthritis Res **3**(2): 107-113.
Sandell, L. J., N. Morris, J. R. Robbins and M. B. Goldring (1991). "Alternatively spliced type II procollagen mRNAs define distinct populations of cells during vertebral development: differential expression of the amino-propeptide." J Cell Biol **114**(6): 1307-1319.
Santanam, U., N. Zanesi, A. Efanov, S. Costinean, A. Palamarchuk, J. P. Hagan, S. Volinia, H. Alder, L. Rassenti, T. Kipps, C. M. Croce and Y. Pekarsky (2010). "Chronic lymphocytic leukemia modeled in mouse by targeted miR-29 expression." Proc Natl Acad Sci U S A **107**(27): 12210-12215.
Scanzello, C. R. and S. R. Goldring (2012). "The role of synovitis in osteoarthritis pathogenesis." Bone **51**(2): 249-257.
Schipani, E., H. E. Ryan, S. Didrickson, T. Kobayashi, M. Knight and R. S. Johnson (2001). "Hypoxia in cartilage: HIF-1alpha is essential for chondrocyte growth arrest and survival." Genes Dev **15**(21): 2865-2876.
Schmid, T. M. and T. F. Linsenmayer (1985). "Developmental acquisition of type X collagen in the embryonic chick tibiotarsus." Dev Biol **107**(2): 373-381.
Schmitt, M. J., C. Margue, I. Behrmann and S. Kreis (2013). "MiRNA-29: a microRNA family with tumor-suppressing and immune-modulating properties." Curr Mol Med **13**(4): 572-585.
Schwarz, D., G. Hutvágner, T. Du, Z. Xu, N. Aronin and P. Zamore (2003). "Asymmetry in the assembly of the RNAi enzyme complex." Cell **115**(2): 199-208.
Sengupta, S., J. A. den Boon, I. H. Chen, M. A. Newton, S. A. Stanhope, Y. J. Cheng, C. J. Chen, A. Hildesheim, B. Sugden and P. Ahlquist (2008). "MicroRNA 29c is down-regulated in nasopharyngeal carcinomas, up-regulating mRNAs encoding extracellular matrix proteins." Proc Natl Acad Sci U S A **105**(15): 5874-5878.
Serra, R., M. Johnson, E. H. Filvaroff, J. LaBorde, D. M. Sheehan, R. Derynck and H. L. Moses (1997). "Expression of a truncated, kinase-defective TGF-beta type II receptor in mouse skeletal

tissue promotes terminal chondrocyte differentiation and osteoarthritis." J Cell Biol **139**(2): 541-552.
Shioya, M., S. Obayashi, H. Tabunoki, K. Arima, Y. Saito, T. Ishida and J. Satoh (2010). "Aberrant microRNA expression in the brains of neurodegenerative diseases: miR-29a decreased in Alzheimer disease brains targets neurone navigator 3." Neuropathol Appl Neurobiol **36**(4): 320-330.
Sibley, C., Y. Seow, S. Saayman, K. Dijkstra, S. El Andaloussi, M. Weinberg and M. Wood (2012). "The biogenesis and characterization of mammalian microRNAs of mirtron origin." Nucleic Acids Res **40**(1): 438-448.
Silver, I. A. (1975). "Measurement of pH and ionic composition of pericellular sites." Philos Trans R Soc Lond B Biol Sci **271**(912): 261-272.
Smith, M. D., E. Barg, H. Weedon, V. Papengelis, T. Smeets, P. P. Tak, M. Kraan, M. Coleman and M. J. Ahern (2003). "Microarchitecture and protective mechanisms in synovial tissue from clinically and arthroscopically normal knee joints." Ann Rheum Dis **62**(4): 303-307.
Song, D. H., I. Dominguez, J. Mizuno, M. Kaut, S. C. Mohr and D. C. Seldin (2003). "CK2 phosphorylation of the armadillo repeat region of beta-catenin potentiates Wnt signaling." J Biol Chem **278**(26): 24018-24025.
Song, J., D. Kim and E.-J. Jin (2011). "MicroRNA-488 suppresses cell migration through modulation of the focal adhesion activity during chondrogenic differentiation of chick limb mesenchymal cells." Cell Biology International **35**(2): 179-185.
Song, R. H., M. D. Tortorella, A. M. Malfait, J. T. Alston, Z. Yang, E. C. Arner and D. W. Griggs (2007). "Aggrecan degradation in human articular cartilage explants is mediated by both ADAMTS-4 and ADAMTS-5." Arthritis Rheum **56**(2): 575-585.
Sorrentino, A., M. Ferracin, G. Castelli, M. Biffoni, G. Tomaselli, M. Baiocchi, A. Fatica, M. Negrini, C. Peschle and M. Valtieri (2008). "Isolation and characterization of CD146+ multipotent mesenchymal stromal cells." Exp Hematol **36**(8): 1035-1046.
Stanton, H., F. M. Rogerson, C. J. East, S. B. Golub, K. E. Lawlor, C. T. Meeker, C. B. Little, K. Last, P. J. Farmer, I. K. Campbell, A. M. Fourie and A. J. Fosang (2005). "ADAMTS5 is the major aggrecanase in mouse cartilage in vivo and in vitro." Nature **434**(7033): 648-652.
Steele, R., J. L. Mott and R. B. Ray (2010). "MBP-1 upregulates miR-29b that represses Mcl-1, collagens, and matrix-metalloproteinase-2 in prostate cancer cells." Genes Cancer **1**(4): 381-387.
Subramanian, M., S. R. Rao, P. Thacker, S. Chatterjee and D. Karunagaran (2014). "MiR-29b downregulates canonical Wnt signaling by suppressing coactivators of beta-catenin in human colorectal cancer cells." J Cell Biochem **115**(11): 1974-1984.
Sulzbacher, I. (2013). "Osteoarthritis: histology and pathogenesis." Wien Med Wochenschr **163**(9-10): 212-219.
Suomi, S., H. Taipaleenmäki, A. Seppänen, T. Ripatti, K. Väänänen, T. Hentunen, A.-M. Säämänen and T. Laitala-Leinonen (2008). "MicroRNAs regulate osteogenesis and chondrogenesis of mouse bone marrow stromal cells." Gene Regulation and Systems Biology **2**: 177-191.
Swingler, T., G. Wheeler, V. Carmont, H. Elliott, M. Barter, M. Abu-Elmagd, S. Donell, R. Boot-Handford, M. Hajihosseini, A. Münsterberg, T. Dalmay, D. Young and I. Clark (2011). "The expression and function of microRNAs in chondrogenesis and osteoarthritis." Arthritis & Rheumatism: n/a-n/a.
(2012). "The expression and function of microRNAs in chondrogenesis and osteoarthritis." Arthritis & Rheumatism **64**: 1909-1919.
Taganov, K., M. Boldin, K.-J. Chang and D. Baltimore (2006). "NF-kappaB-dependent induction of microRNA miR-146, an inhibitor targeted to signaling proteins of innate immune responses." Proc Natl Acad Sci U S A **103**(33): 12481-12486.

Tan, M., J. Wu and Y. Cai (2013). "Suppression of Wnt signaling by the miR-29 family is mediated by demethylation of WIF-1 in non-small-cell lung cancer." Biochem Biophys Res Commun **438**(4): 673-679.

Tardif, G., D. Hum, J.-P. Pelletier, N. Duval and J. Martel-Pelletier (2009). "Regulation of the IGFBP-5 and MMP-13 genes by the microRNAs miR-140 and miR-27a in human osteoarthritic chondrocytes." BMC Musculoskelet Disord **10**: 148.

Tetlow, L., D. Adlam and D. Woolley (2001). "Matrix metalloproteinase and proinflammatory cytokine production by chondrocytes of human osteoarthritic cartilage: Associations with degenerative changes." Arthritis & Rheumatism **44**(3): 585-594.

Tortorella, M. D., A. M. Malfait, C. Deccico and E. Arner (2001). "The role of ADAM-TS4 (aggrecanase-1) and ADAM-TS5 (aggrecanase-2) in a model of cartilage degradation." Osteoarthritis Cartilage **9**(6): 539-552.

Tuddenham, L., G. Wheeler, S. Ntounia-Fousara, J. Waters, M. Hajihosseini, I. Clark and T. Dalmay (2006). "The cartilage specific microRNA-140 targets histone deacetylase 4 in mouse cells." FEBS Lett **580**(17): 4214-4217.

Ugalde, A. P., A. J. Ramsay, J. de la Rosa, I. Varela, G. Marino, J. Cadinanos, J. Lu, J. M. Freije and C. Lopez-Otin (2011). "Aging and chronic DNA damage response activate a regulatory pathway involving miR-29 and p53." EMBO J **30**(11): 2219-2232.

Umlauf, D., S. Frank, T. Pap and J. Bertrand (2010). "Cartilage biology, pathology, and repair." Cellular and Molecular Life Sciences **67**(24): 4197-4211.

van Amerongen, R. and A. Berns (2005). "Re-evaluating the role of Frat in Wnt-signal transduction." Cell Cycle **4**(8): 1065-1072.

van Beuningen, H. M., H. L. Glansbeek, P. M. van der Kraan and W. B. van den Berg (1998). "Differential effects of local application of BMP-2 or TGF-beta 1 on both articular cartilage composition and osteophyte formation." Osteoarthritis Cartilage **6**(5): 306-317.

van der Kraan, P. M. and W. B. van den Berg (2007). "Osteophytes: relevance and biology." Osteoarthritis Cartilage **15**(3): 237-244.

van Rooij, E. and S. Kauppinen (2014). "Development of microRNA therapeutics is coming of age." EMBO Mol Med **6**(7): 851-864.

van Rooij, E., L. B. Sutherland, J. E. Thatcher, J. M. DiMaio, R. H. Naseem, W. S. Marshall, J. A. Hill and E. N. Olson (2008). "Dysregulation of microRNAs after myocardial infarction reveals a role of miR-29 in cardiac fibrosis." Proc Natl Acad Sci U S A **105**(35): 13027-13032.

Vasudevan, S. and J. Steitz (2007). "AU-rich-element-mediated upregulation of translation by FXR1 and Argonaute 2." Cell **128**(6): 1105-1118.

Vasudevan, S., Y. Tong and J. Steitz (2007). "Switching from repression to activation: microRNAs can up-regulate translation." Science (New York, N.Y.) **318**(5858): 1931-1934.

Ventura, A., A. Young, M. Winslow, L. Lintault, A. Meissner, S. Erkeland, J. Newman, R. Bronson, D. Crowley, J. Stone, R. Jaenisch, P. Sharp and T. Jacks (2008). "Targeted deletion reveals essential and overlapping functions of the miR-17 through 92 family of miRNA clusters." Cell **132**(5): 875-886.

Verrecchia, F., M. L. Chu and A. Mauviel (2001). "Identification of novel TGF-beta /Smad gene targets in dermal fibroblasts using a combined cDNA microarray/promoter transactivation approach." J Biol Chem **276**(20): 17058-17062.

Verrecchia, F. and A. Mauviel (2002). "Transforming growth factor-beta signaling through the Smad pathway: role in extracellular matrix gene expression and regulation." J Invest Dermatol **118**(2): 211-215.

Wang, B., R. Komers, R. Carew, C. E. Winbanks, B. Xu, M. Herman-Edelstein, P. Koh, M. Thomas, K. Jandeleit-Dahm, P. Gregorevic, M. E. Cooper and P. Kantharidis (2012). "Suppression of

microRNA-29 expression by TGF-beta1 promotes collagen expression and renal fibrosis." J Am Soc Nephrol **23**(2): 252-265.
Wang, F. S., P. C. Chuang, C. L. Lin, M. W. Chen, H. J. Ke, Y. H. Chang, Y. S. Chen, S. L. Wu and J. Y. Ko (2013). "MicroRNA-29a protects against glucocorticoid-induced bone loss and fragility in rats by orchestrating bone acquisition and resorption." Arthritis Rheum **65**(6): 1530-1540.
Wang, H., R. Garzon, H. Sun, K. J. Ladner, R. Singh, J. Dahlman, A. Cheng, B. M. Hall, S. J. Qualman, D. S. Chandler, C. M. Croce and D. C. Guttridge (2008). "NF-kappaB-YY1-miR-29 regulatory circuitry in skeletal myogenesis and rhabdomyosarcoma." Cancer Cell **14**(5): 369-381.
Wang, H. X., F. R. Tekpetey and G. M. Kidder (2009). "Identification of WNT/beta-CATENIN signaling pathway components in human cumulus cells." Mol Hum Reprod **15**(1): 11-17.
Wang, L., L. Zhou, P. Jiang, L. Lu, X. Chen, H. Lan, D. C. Guttridge, H. Sun and H. Wang (2012). "Loss of miR-29 in myoblasts contributes to dystrophic muscle pathogenesis." Mol Ther **20**(6): 1222-1233.
Wang, L. G. and J. Gu (2012). "Serum microRNA-29a is a promising novel marker for early detection of colorectal liver metastasis." Cancer Epidemiol **36**(1): e61-67.
Watanabe, T., T. Sato, T. Amano, Y. Kawamura, N. Kawamura, H. Kawaguchi, N. Yamashita, H. Kurihara and T. Nakaoka (2008). "Dnm3os, a non-coding RNA, is required for normal growth and skeletal development in mice." Dev Dyn **237**(12): 3738-3748.
Wei, W., H. B. He, W. Y. Zhang, H. X. Zhang, J. B. Bai, H. Z. Liu, J. H. Cao, K. C. Chang, X. Y. Li and S. H. Zhao (2013). "miR-29 targets Akt3 to reduce proliferation and facilitate differentiation of myoblasts in skeletal muscle development." Cell Death Dis **4**: e668.
Weng, L. H., C. J. Wang, J. Y. Ko, Y. C. Sun and F. S. Wang (2010). "Control of Dkk-1 ameliorates chondrocyte apoptosis, cartilage destruction, and subchondral bone deterioration in osteoarthritic knees." Arthritis Rheum **62**(5): 1393-1402.
Wermter, C., M. Howel, V. Hintze, B. Bombosch, K. Aufenvenne, I. Yiallouros and W. Stocker (2007). "The protease domain of procollagen C-proteinase (BMP1) lacks substrate selectivity, which is conferred by non-proteolytic domains." Biol Chem **388**(5): 513-521.
Westholm, J. and E. Lai (2011). "Mirtrons: microRNA biogenesis via splicing." Biochimie **93**(11): 1897-1904.
Wieland, H., M. Michaelis, B. Kirschbaum and K. Rudolphi (2005). "Osteoarthritis — an untreatable disease?" Nature Reviews Drug Discovery **4**(4): 331-344.
Wienholds, E., W. P. Kloosterman, E. Miska, E. Alvarez-Saavedra, E. Berezikov, E. de Bruijn, H. R. Horvitz, S. Kauppinen and R. H. Plasterk (2005). "MicroRNA expression in zebrafish embryonic development." Science **309**(5732): 310-311.
Wienholds, E., M. Koudijs, F. van Eeden, E. Cuppen and R. Plasterk (2003). "The microRNA-producing enzyme Dicer1 is essential for zebrafish development." Nat Genet **35**(3): 217-218.
Wightman, B., I. Ha and G. Ruvkun (1993). "Posttranscriptional regulation of the heterochronic gene lin-14 by lin-4 mediates temporal pattern formation in C. elegans." Cell **75**(5): 855-862.
Willert, K., M. Brink, A. Wodarz, H. Varmus and R. Nusse (1997). "Casein kinase 2 associates with and phosphorylates dishevelled." EMBO J **16**(11): 3089-3096.
Willert, K. and K. A. Jones (2006). "Wnt signaling: is the party in the nucleus?" Genes Dev **20**(11): 1394-1404.
Wittmann, J. and H.-M. Jäck (2010). "Serum microRNAs as powerful cancer biomarkers." Biochim Biophys Acta **1806**(2): 200-207.
Xiong, Y., J. H. Fang, J. P. Yun, J. Yang, Y. Zhang, W. H. Jia and S. M. Zhuang (2010). "Effects of microRNA-29 on apoptosis, tumorigenicity, and prognosis of hepatocellular carcinoma." Hepatology **51**(3): 836-845.
Xu, J., Y. Kang, W.-m. Liao and L. Yu (2012). "MiR-194 Regulates Chondrogenic Differentiation of Human Adipose-Derived Stem Cells by Targeting Sox5." PLoS One **7**(3): e31861.

Yamasaki, K., T. Nakasa, S. Miyaki, M. Ishikawa, M. Deie, N. Adachi, Y. Yasunaga, H. Asahara and M. Ochi (2009). "Expression of MicroRNA-146a in osteoarthritis cartilage." Arthritis and rheumatism **60**(4): 1035-1041.

Yamashita, S., S. Miyaki, Y. Kato, S. Yokoyama, T. Sato, F. Barrionuevo, H. Akiyama, G. Scherer, S. Takada and H. Asahara (2012). "L-Sox5 and Sox6 enhance chondrogenic miR-140 expression by strengthening dimeric Sox9 activity." Journal of Biological Chemistry.

Yan, C., Y. Wang, X.-Y. Shen, G. Yang, J. Jian, H.-S. Wang, G.-Q. Chen and Q. Wu (2011). "MicroRNA regulation associated chondrogenesis of mouse MSCs grown on polyhydroxyalkanoates." Biomaterials **32**(27): 6435-6444.

Yang, B., H. Guo, Y. Zhang, L. Chen, D. Ying and S. Dong (2011). "MicroRNA-145 Regulates Chondrogenic Differentiation of Mesenchymal Stem Cells by Targeting Sox9." PLoS One **6**(7): e21679.

Yang, B., H. Guo, Y. Zhang, S. Dong and D. Ying (2011). "The microRNA expression profiles of mouse mesenchymal stem cell during chondrogenic differentiation." BMB Reports **44**(1): 28-33.

Yang, J., S. Qin, C. Yi, G. Ma, H. Zhu, W. Zhou, Y. Xiong, X. Zhu, Y. Wang, L. He and X. Guo (2011). "MiR-140 is co-expressed with Wwp2-C transcript and activated by Sox9 to target Sp1 in maintaining the chondrocyte proliferation." FEBS Lett **585**(19): 2992-2997.

Yang, T., Y. Liang, Q. Lin, J. Liu, F. Luo, X. Li, H. Zhou, S. Zhuang and H. Zhang (2013). "miR-29 mediates TGFbeta1-induced extracellular matrix synthesis through activation of PI3K-AKT pathway in human lung fibroblasts." J Cell Biochem **114**(6): 1336-1342.

Yi, R., Y. Qin, I. Macara and B. Cullen (2003). "Exportin-5 mediates the nuclear export of pre-microRNAs and short hairpin RNAs." Genes Dev **17**(24): 3011-3016.

Zamli, Z. and M. Sharif (2011). "Chondrocyte apoptosis: a cause or consequence of osteoarthritis?" Int J Rheum Dis **14**(2): 159-166.

Zampetaki, A., S. Kiechl, I. Drozdov, P. Willeit, U. Mayr, M. Prokopi, A. Mayr, S. Weger, F. Oberhollenzer, E. Bonora, A. Shah, J. Willeit and M. Mayr (2010). "Plasma microRNA profiling reveals loss of endothelial miR-126 and other microRNAs in type 2 diabetes." Circ Res **107**(6): 810-817.

Zeng, Y. and B. Cullen (2004). "Structural requirements for pre-microRNA binding and nuclear export by Exportin 5." Nucleic Acids Res **32**(16): 4776-4785.

Zhang, Y. K., H. Wang, Y. Leng, Z. L. Li, Y. F. Yang, F. J. Xiao, Q. F. Li, X. Q. Chen and L. S. Wang (2011). "Overexpression of microRNA-29b induces apoptosis of multiple myeloma cells through down regulating Mcl-1." Biochem Biophys Res Commun **414**(1): 233-239.

Zhang, Z., J. Zou, G. K. Wang, J. T. Zhang, S. Huang, Y. W. Qin and Q. Jing (2011). "Uracils at nucleotide position 9-11 are required for the rapid turnover of miR-29 family." Nucleic Acids Res **39**(10): 4387-4395.

Zhao, Q., H. Eberspaecher, V. Lefebvre and B. De Crombrugghe (1997). "Parallel expression of Sox9 and Col2a1 in cells undergoing chondrogenesis." Dev Dyn **209**(4): 377-386.

Zhong, N., J. Sun, Z. Min, W. Zhao, R. Zhang, W. Wang, J. Tian, L. Tian, J. Ma, D. Li, Y. Han and S. Lu (2012). "MicroRNA-337 is associated with chondrogenesis through regulating TGFBR2 expression." Osteoarthritis and Cartilage.

Zhou, S., K. Eid and J. Glowacki (2004). "Cooperation between TGF-beta and Wnt pathways during chondrocyte and adipocyte differentiation of human marrow stromal cells." J Bone Miner Res **19**(3): 463-470.

Zhu, M., M. Chen, M. Zuscik, Q. Wu, Y. J. Wang, R. N. Rosier, R. J. O'Keefe and D. Chen (2008). "Inhibition of beta-catenin signaling in articular chondrocytes results in articular cartilage destruction." Arthritis Rheum **58**(7): 2053-2064.

Zhu, M., D. Tang, Q. Wu, S. Hao, M. Chen, C. Xie, R. N. Rosier, R. J. O'Keefe, M. Zuscik and D. Chen (2009). "Activation of beta-catenin signaling in articular chondrocytes leads to osteoarthritis-

like phenotype in adult beta-catenin conditional activation mice." J Bone Miner Res **24**(1): 12-21.

ENDICES

Genes	Accession number	Sequences (5'->3')
ADAMTS6	ENSG00000049192	Forward: ACGTGAGCTCTCTCATCGTCATGGTTCTGC Reverse: ACGTGAGCTCCAAGCAGGAGAATGAATGTAGG
ADAMTS14	ENSG00000138316	Forward: GAGCTCGCTGTGCCCTGCCATC GAGCTCGGGTCCAATGGCGATGTTA
ADAMTS17	ENSG00000140470	Forward: ACGTTCTAGAAACATGAGCGTGGACTTGG Reverse: ACGTTCTAGATGTAATGCAAGTTAACGAATGG
ADAMTS19	ENSG00000145808	Forward: ACGTGAGCTCAATCACAGCTCCAGGTAATC Reverse: ACGTGAGCTCCCAAGAGACATACTATCTTCCAAGG
FZD3	ENSG00000104290	Forward: ATGCGTCGACTATTAGATGCCCAGCCTTTCTC Reverse: ATGCGTCGACATGCCTACCAAGAGGATAACATTC
FZD5	ENSG00000163251	Forward: ATGCGTCGACGGCATCGGCTACAACCTGAC Reverse: ATGCGTCGACAGACCACACAGTTCAAAGA AACCTG
FRAT2	ENSG00000181274	Forward: ATGCGTCGACCAACAGCGTCCAGTTCCTAC Reverse: ATGCGTCGACGCCGTCAAGTTTCATACAGC
CK2A2	ENSG00000070770	Forward: ATGCGTCGACATGCAGGTACTAGAGTTGTGTGG Reverse: ATGCGTCGACAATAAGTTTGCTTGTTTCTGTGG
DVL3	ENSG00000161202	Forward: ATGCGTCGACGCTGCGTTCCTCTCTCCATC Reverse: ATGCGTCGACTACCATTTATTGAGCACCTACTCTACTG TG

Table 1: Primer sequences for PCR amplification 3'UTR region of potential targets of the miR-29 family. For subcloning purpose, restriction sites (bases underlined) were added to the 5'P of the primers. *Sac*I (GAGCTC), *Sal*I (GTCGAC), *Xba*I (TCTAGA).

Genes	Mutant	Primer sequence (5'->3')
ADAMTS6	Site 1	Forward: TATGTGATGCACTGACATGTAATTTAAGAAGCTTATGATGGAATCAAGTCAAACATGCTGTTTAACTGAAAG Reverse: CTTTCAGTTAAACAGCATGTTTGACTTGATTCCATCATAAGCTTCTTAAATTACATGTCAGTGCATCACATA
	Site 2	Forward: TATTTATTTCACCAGGGCACATTAAGCTTAAGTTAACTGTTCTTTGAAAAGGCGCAAGGGAATTCAGT Reverse: ACTGAATTCCCTTGCGCCTTTTCAAAGAACAGTTAACTTAAGCTTAATGTGCCCTGGTGAAATAAATA
ADAMTS10	Site 1	Forward: GGGGACACAGACCCGTTTGTAAGCTTACCCCTTGTCGATGGTGTGCG Reverse: CGCACACCATCGACAAGGGGTAAGCTTACAAACGGGTCTGTGTCCCC
	Site 2	Forward: GCTCGGTCCGGGCCAAGCTTATGACGATGAGAGATGCATTAATCGGTCC Reverse: GGACCGATTAATGCATCTCTCATCGTCATAAGCTTGGCCCGGACCGAGC
ADAMTS14	Site 1	Forward: GTTTGTCTTTGCTGGCCAGAAGAGTCGACTCATGGCCATACTCTGGCCTTG Reverse: CAAGGCCAGAGTATGGCCATGAGTCGACTCTTCTGGCCAGCAAAGAC
	Site 2	Forward: GGGTGCCAGCCCCTGGCCGTCGACTGGAGTGGGGAAGACAC Reverse: GTGTCTTCCCCACTCCAGTCGACGGCCAGGGGCTGGCACCC
	Site 3	Forward: CTAAACTCCTGCCAGGTGATAGAGAGCTCTCTCACTTCTTCCTTCCCCAAGGC

		Reverse: GCCTTGGGGAAGGAAGAAGTGAGAGAGCTCTCTATCACCTGGCAGGAGTTTAG
	Site 4	Forward: CTAAACTCCTGCCAGGTGATAGAGAGCTCTCTCACTTCTTCCTTCCCCAAGGC Reverse: GCCTTGGGGAAGGAAGAAGTGAGAGAGCTCTCTATCACCTGGCAGGAGTTTAG
ADAMTS17	Site 1	Forward: GCAATTACCGTTTCTTATGTCACAGTCGACTGAAGAGAGGCCCTTCTGTTTCCC Reverse: GGGAAACAGAAGGGCCTCTCTTCAGTCGACTGTGACATAAGAAACGGTAATTGC
	Site 2	Forward: CACCAACTTGGTGGGCATTTCATGTCGACTTATGTTCTAGGACTTTACCGTA Reverse: TACGGTAAAGTCCTAGAACATAAGTCGACATGAAATGCCCACCAAGTTGGTG
	Site 3	Forward: TAACAAAACAAAACACAGAAACACAGTCGACATAAATCAAGAAGCACAGGGAGATGATCCCATGG Reverse: CCATGGGATCATCTCCCTGTGCTTCTTGATTTATGTCGACTGTGTTTCTGTGTTTTGTTTTGTTA
	Site 4	Forward: GAAGTGTTGAGAAACTTCCGTGTCGACTCTGTGGAAAGAACCGAGGGT Reverse: ACCCTCGGTTCTTTCCACAGAGTCGACACGGAAGTTTCTCAACACTTC
	Site 5	Forward: CCAGAGTCTCACGACCCTACGGTCGCCTTTTTATTGGTGCAAAATTAAACC Reverse: GGTTTAATTTTGCACCAATAAAAAGGCGACCGTAGGGTCGTGAGACTCTGG
ADAMTS	Site 1	Forward: ATCAAATTAATTTATTTTTTTGCCTGCCAAACATCCAATGGTCGACTTGTTTTGGTTACACAAACATTTTGATTTATACTATATG

19		Reverse: CATATAGTATAAATCAAAATGTTTGTGTAACCAAAACAAGTCGACCATTGGATGTTTGGCAGGCAAAAAAATAAATTAATTTGAT
	Site 2	Forward: GTTGTTTGTTAGGGCTATCTCTAAGTCGACCCTCTCTCCCCACCAATAACATTGAATTATC Reverse: ATAATTCAATGTTATTGGTGGGGAGAGAGGGTCGACTTAGAGATAGCCCTAACAAACAACG
FZD3		Forward: GGATTTAGTCTAACTCACAGCTAAGGTAGAAAAGTACTCTGATGGCAAGAGAATGTCCAGACTAATATTTTC Reverse: GAAAATATTAGTCTGGACATTCTCTTGCCATCAGAGTACTTTTCTACCTTAGCTGTGAGTTAGACTAAATCC
FZD5	Site 1	Forward: CGGCGTCGCGGCCCAAGCTTGGGAGGCGGTCGCAG Reverse: CTGCGACCGCCTCCCAAGCTTGGGCCGCGACGCCG
	Site 2	Forward: GTGGACGTGGAGATGAAGCACAAGCTTGACCACAGGCCTATCCAGAAGG Reverse: CCTTCTGGATAGGCCTGTGGTCAAGCTTGTGCTTCATCTCCACGTCCAC
	Site 3	Forward: GCCCACCAGCAGGTAGAAGCTTAGCGGGCCCAGCACGAAGCC Reverse: GGCTTCGTGCTGGGCCCGCTAAGCTTCTACCTGCTGGTGGGC
	Site 4	Forward: CACATGAAGTACTTGAGCATGAAGCTTCAGTACTCGGGCTTGGCGCGCG Reverse: CGCGCGCCAAGCCCGAGTACTGAAGCTTCATGCTCAAGTACTTCATGTG
	Site 5	Forward: CGGGAGGGGGCAACAAGCTTATGAAGGTAAACGGAAGTGACCTTGGCA Reverse: TGCCAAGGTCACTTCCGTTTACCTTCATAAGCTTGTTGCCCCCTCCCG
FRAT2	Site 1	Forward: GCGTGGAGAAATGTATGCGCCAGAAGCTTTCCGTGGGGCATGAG

		AATTTCC Reverse: GGAAATTCTCATGCCCCACGGAAAGCTTCTGGCGCATACATTTCTCCACGC
	Site 2	Forward: CTTATTTTCTGGTGGAGGAGCTTAGTAAGTAAGCTTACAATTGCTGTGCAAAGAAATTCCAGAGG-3' Reverse: CCTCTGGAATTTCTTTGCACAGCAATTGTAAGCTTACTTACTAAGCTCCTCCACCAGAAAATAAG
	Site 3	Forward: GGGAGACTCCAAGCGGTGGTAAAAGCTTAACAGGGCTCTTCTTGGAGCAAG Reverse: CTTGCTCCAAGAAGAGCCCTGTTAAGCTTTTACCACCGCTTGGAGTCTCCC
CK2A2	Site 1	Forward: AGAGGAATATACAAGGGGCTTGGGGAAGAAAATAAGCTTCCCGGAGCAAGTGTTG Reverse: CAACACTTGCTCCGGGAAGCTTATTTTCTTCCCCAAGCCCCTTGTATATTCCTCT
	Site 2	Forward: TCTCCTCTAATCTATCAGTCTGAGAAGCTTTTCCTCTCTGCAAGGGAACACATTTGC Reverse: GCAAATGTGTTCCCTTGCAGAGAGGAAAAGCTTCTCAGACTGATAGATTAGAGGAGA
	Site 3	Forward: GCGCCTGACTCGAGAAGCTTACCTTTCAGTCCACTGGGACCAATCCA Reverse: TGGATTGGTCCCAGTGGACTGAAAGGTAAGCTTCTCGAGTCAGGCGC
	Site 4	Forward: CTGCTTCCATCCTTATCAACAGAAGCTTTGGGAGAACCTAAGTCATTTCCCTGAG Reverse: TCAGGGAAATGACTTAGGTTCTCCCAAAGCTTCTGTTGATAAGGATGGAAGCAG
DVL3	Site 1	Forward: GTGCGCTAACTGCTCGCAGAAGCTTGCGAGGGTGGGGTGCACC

		Reverse: GGTGCACCCCACCCTCGCAAGCTTCTGCGAGCAGTTAGCGCAC
	Site 2	Forward: CCCTTTTGTCTCTGGGACCAGACTTGTTAAGCTTACCCCTTACTCCCCTCTGC Reverse: GCAGAGGGGAGTAAGGGGTAAGCTTAACAAGTCTGGTCCCAGAGACAAAAGGG
	Site 3	Forward: GCACAGTGCCTGGCACACAGTAGAGTAAAGCTTCAATAAATGGTAGTCGACC Reverse: GGTCGACTACCATTTATTGAAGCTTTACTCTACTGTGTGCCAGGCACTGTGC
DICER		Forward: ACGTGAGCTCGTGTGCAGTAGTGCCAGTCC Reverse: ACGTGAGCTCTGCAATCACAGGAACACAGG

Table 2: Primers for mutating the binding sites of the miR-29 family

Genes	Accession number	Primer sequence (5'->3')	Probe
Arginase-1	ENSMUST00000020161	Forward: CCTGAAGGAACTGAAAGGAAAG Reverse: TTGGCAGATATGCAGGGAGT	2
IL-6	ENSMUST00000026845	Forward: TGATGGATGCTACCAAACTGG Reverse: TTCATGTACTCCAGGTAGCTATGG	6
SAA3	ENAMUST00000006956	Forward: GCTCGGGGGAACTATGATG Reverse: AACTTCTGAACAGCCTCTCTGG	26
Axin2		Forward: GCTGACGGATGATTCCATGT Reverse: ACTGCCCACACGATAAGGAG	56
SOX9	ENST00000245479	Forward: TACCCGCACTTGCACAAC Reverse: TCTCGCTCTCGTTCAGAAGTC	61
FZD3	NM_017412	Forward: ACAGCAAAGTGAGCAGCTACC Reverse: CTGTAACTGCAGGGCGTGTA	75
FZD5	NM_003468	Forward:ACCCCAGGGGAGAGAAACT Reverse: TGCAAATTGGGGGAAGTAAG	83
DVL3	NM_004423	Forward:CCCTGAGCACCATCACCT Reverse: GGATGGACAAGTGGAAGTCG	17
FRAT2		Forward: GTTCAAGGTCACGGTTTGCT Reverse: GAAAAGACTCCGGGGTGAGT	14
CK2A2	NM_001896	Forward: CCATGGAGCACCCATACTTC Reverse: CACAGCATTGTCTGCACAAG	68

Table 3: Primer sequence and the Universal Probe Library probe for gene of interest

Genes	Accession number	Primer sequence (5'-3')
ADAMTS4	MM_005099	Forward: CAAGGTCCCATGTGCAACGT Reverse: CATCTGCCACCACCAGTGTCT Probe: FAM-CCGAAGAGCCAAGCGCTTTGCTTC-TAMRA
ADAMTS6	NM_014273	Forward: GGCTGAATGACACATCCACTGTT Reverse: CAAACCGTTCAATGCTCACTGA Probe: FAM-AAGCGCTTCCGCCTCTGCAACC-TAMRA
ADAMTS10	NM_030957	Forward: AGAGAACGGTGTGGCTAACCA Reverse: TCTCTCGCGCTCACACATTC Probe: FAM-CAGTGCTCATCACACGCTATGACATCTGC-TAMRA
ADAMTS14	AF366351	Forward: CGCTGGATGGGACTGAGTGT Reverse: CGCGAACATGACCCAAACTT Probe: FAM-CCCGGCAAGTGGTGCTTCAAAGGT-TAMRA
ADAMTS17	NM_139057	Forward: GGTCTCAATTTGGCCTTTACCAT Reverse: GACCTGCCAGCGGCAAGAT Probe: FAM-CCACAACTTGGGCATGAACCACGA-TAMRA
ADAMTS19	AJ311904	Forward: GGTGTAAGGCTGGAGAATGTACCA Reverse: TGCGCTCTCGACTGCTGAT Probe: FAM-CCTCAGCACCTGAACATCTGGCCG-TAMRA
MMP3	NM002422	Forward: TTCCGCCTGTCTCAAGATGATAT Reverse: AAAGGACAAAGCAGGATCACAGTT Probe: FAM-TCAGTCCCTCTATGGACCTCCCCCTGAC-TAMRA

Table 4: Primer pairs and probe for gene of interest

Genes	Primer sequences (5'->3')
Pri-miR-29a/b1exon 1	Forward: TACTGAACTGTCACGGCAGA Reverse: TGTAGTTAGCGACCTCTGCT
Pri-miR-29a/b1Exon4	Forward: TTGCACCCTCACGACATGCT Reverse: TGACTCTCAGCAGGCCTCA
Pri-miR-29b2/c exon 1	Forward: ACTTCTTTAGGGGTGTGCGTA Reverse: ACCCATCTCCCTAGCATTCT
Pri-miR-29b2/c Exon6	Forward: TCAGACTTGCCACCTGGACT Reverse: AGTTGGCATGAGGCTTCGA
Pre-29a	Forward: CTGATTTCTTTTGGTGTTCAG Reverse: AACCGATTTCAGATGGTGC
Pre-29b1	Forward: CATATGGTGGTTTAGATTT Reverse: AACACTGATTTCAAATGGTG
Pre-29b2	Forward: GCTGGTTTCACATGGTGGC Reverse: AACACTGATTTCAAATGGTG
Pre-29c	Forward: CGATTTCTCCTGGTGTTCA Reverse: ACCGATTTCAAATGGTGC

Table 5: Primers for detecting the primary and the premature sequence of the miR-29 family

Names	24_DMM_R	24_DMM_L	log2 Fold change	Fold change
CYP2E1	9.0	10.2	-1.2	2.3
CES3	8.1	9.3	-1.2	2.3
TMEM45B	7.9	8.6	-0.8	1.7
CFD	12.9	13.6	-0.7	1.6
SCD1	10.1	10.7	-0.6	1.6
IGFBP6	8.9	9.6	-0.6	1.5
CHAD	12.4	13.0	-0.6	1.5
LOC100045005	9.6	10.2	-0.6	1.5
TENS1	8.5	9.1	-0.6	1.5
C130045I22RIK	8.2	8.8	-0.6	1.5
LOC667337	9.4	9.9	-0.6	1.5
CXCL1	9.1	7.3	1.9	3.6
CCL7	9.2	7.5	1.8	3.4
SAA3	8.9	7.3	1.6	3.1
TIMP1	12.0	10.5	1.5	2.9
SERPINA3N	11.2	9.7	1.5	2.8
GP38	10.8	9.4	1.4	2.6
MMP3	8.9	7.6	1.3	2.5
ARG1	8.0	7.1	0.8	1.8
CXCL14	9.4	8.8	0.7	1.6
MB	11.9	11.2	0.7	1.6
ANGPTL4	9.5	8.9	0.6	1.6
MT1	13.5	12.9	0.6	1.6
ANKRD23	9.5	8.9	0.6	1.5
MS4A6D	9.9	9.3	0.6	1.5
LOC386330	9.9	9.4	0.5	1.5
LOC270589	8.9	8.4	0.5	1.5
CCL9	11.2	10.6	0.5	1.5
CKM	12.3	11.8	0.5	1.5
LOC386144	9.6	9.1	0.5	1.4

Table 6: List genes changed expression at day 1 in DMM model

GENES	7_DMM_R	7_DMM_L	log2 Fold change	Fold change
MYL3	9.8	11.0	-1.2	2.3
ATP1A2	9.0	10.1	-1.2	2.3
NDRG2	10.0	11.2	-1.2	2.3
CKMT2	11.7	12.8	-1.2	2.2
ANKRD23	10.2	11.4	-1.2	2.2
2310003M01RIK	9.5	10.6	-1.1	2.2
ACTN2	11.1	12.2	-1.1	2.2
2310042D19RIK	9.2	10.3	-1.1	2.2
MYH2	11.0	12.1	-1.1	2.2
PFKM	11.5	12.6	-1.1	2.2
ABRA	8.6	9.7	-1.1	2.1
COX7A1	11.4	12.5	-1.1	2.1
ANKRD2	8.0	9.1	-1.1	2.1
COX8B	11.8	12.8	-1.1	2.1
MB	12.0	13.1	-1.1	2.1
ENO3	12.9	14.0	-1.1	2.1
DUSP26	8.1	9.2	-1.1	2.1
RTN2	10.0	11.1	-1.0	2.1
PKIA	10.4	11.5	-1.0	2.1
TCAP	12.5	13.6	-1.0	2.1
MYOZ1	10.4	11.5	-1.0	2.0
MYOM1	9.9	10.9	-1.0	2.0
ACTN3	11.3	12.3	-1.0	2.0
2310002L09RIK	8.6	9.6	-1.0	2.0
HRC	10.3	11.3	-1.0	2.0
MYOM2	9.1	10.1	-1.0	2.0
CKM	13.0	14.0	-1.0	2.0
CSRP3	8.5	9.5	-1.0	2.0
TMEM38A	9.3	10.3	-1.0	2.0
1110012N22RIK	9.2	10.2	-1.0	2.0
TPM2	11.3	12.3	-1.0	2.0
RYR1	10.1	11.1	-1.0	2.0
MLF1	9.5	10.5	-1.0	2.0
TTN	9.7	10.7	-1.0	2.0
TMOD4	10.7	11.7	-1.0	2.0
DYSFIP1	8.7	9.7	-1.0	2.0
NRAP	9.1	10.1	-1.0	2.0
CMYA5	10.8	11.8	-1.0	2.0
SMTNL2	8.5	9.5	-1.0	1.9
MYLK2	9.2	10.2	-1.0	1.9

MYL2	9.3	10.3	-0.9	1.9
LOC669660	8.6	9.6	-0.9	1.9
KBTBD10	9.8	10.7	-0.9	1.9
ASB2	10.6	11.5	-0.9	1.9
A530098C11RIK	8.7	9.6	-0.9	1.9
F730003H07RIK	9.3	10.3	-0.9	1.9
ZMYND17	8.5	9.4	-0.9	1.9
CPT1B	8.3	9.2	-0.9	1.9
2310079P10RIK	8.5	9.4	-0.9	1.9
EEF1A2	10.7	11.6	-0.9	1.9
YIPF7	8.5	9.4	-0.9	1.9
SCL0003151.1_1374	8.9	9.8	-0.9	1.9
INMT	7.6	8.5	-0.9	1.9
CES3	8.8	9.7	-0.9	1.9
PYGM	9.2	10.1	-0.9	1.8
MYBPC2	11.6	12.5	-0.9	1.8
8030451F13RIK	8.6	9.5	-0.9	1.8
FABP3	10.6	11.4	-0.9	1.8
NEURL	9.5	10.4	-0.9	1.8
PDLIM3	10.4	11.3	-0.9	1.8
SYPL2	9.6	10.5	-0.9	1.8
4833419K08RIK	9.0	9.9	-0.9	1.8
AMPD1	11.1	12.0	-0.8	1.8
CACNA1S	8.6	9.5	-0.8	1.8
SCL0002069.1_48	8.1	9.0	-0.8	1.8
C130073O12RIK	9.0	9.9	-0.8	1.8
GM1157	7.8	8.6	-0.8	1.8
MYH1	9.2	10.1	-0.8	1.8
SLC25A37	11.8	12.6	-0.8	1.8
LOC638935	8.1	9.0	-0.8	1.8
LOC386360	10.4	11.2	-0.8	1.8
BC030476	9.0	9.8	-0.8	1.8
MYH4	10.0	10.8	-0.8	1.7
SCL000959.1_2	13.3	14.1	-0.8	1.7
RPL3L	12.2	13.0	-0.8	1.7
COX6A2	12.7	13.5	-0.8	1.7
MTDNA_ND4L	8.7	9.5	-0.8	1.7
TNNT3	13.1	13.9	-0.8	1.7
AK1	9.8	10.6	-0.8	1.7
DES	11.1	11.9	-0.8	1.7
A2BP1	8.4	9.2	-0.8	1.7
KY	9.1	9.8	-0.8	1.7

UNC45B	8.4	9.2	-0.8	1.7
AI595366	8.7	9.4	-0.8	1.7
D830037I21RIK	7.3	8.1	-0.8	1.7
PGM2	12.0	12.8	-0.8	1.7
4933421G18RIK	9.7	10.4	-0.8	1.7
MYF6	8.3	9.0	-0.8	1.7
SCN4B	8.3	9.1	-0.8	1.7
ALPK3	8.5	9.3	-0.8	1.7
PGAM2	12.3	13.1	-0.8	1.7
ITGA2B	8.9	9.7	-0.8	1.7
CRYAB	9.8	10.6	-0.7	1.7
LOC386144	9.1	9.8	-0.7	1.7
LOC100047934	10.8	11.6	-0.7	1.7
SRL	9.3	10.0	-0.7	1.7
PHKG1	8.8	9.5	-0.7	1.7
ATP1B1	9.5	10.2	-0.7	1.7
HSPB7	8.2	8.9	-0.7	1.7
TNNC1	8.3	9.0	-0.7	1.6
CHCHD10	12.4	13.1	-0.7	1.6
GMPR	9.0	9.7	-0.7	1.6
S3-12	9.3	10.0	-0.7	1.6
9930004G02RIK	9.4	10.1	-0.7	1.6
TCEA3	10.3	11.0	-0.7	1.6
PPP1R3C	10.7	11.4	-0.7	1.6
TRIM54	9.0	9.7	-0.7	1.6
FBP2	8.3	9.0	-0.7	1.6
COQ10A	8.8	9.5	-0.7	1.6
TXLNB	7.8	8.5	-0.7	1.6
XIRP2	8.4	9.1	-0.7	1.6
FSD2	8.6	9.3	-0.7	1.6
PDE4DIP	9.9	10.6	-0.7	1.6
NDUFC1	10.9	11.6	-0.7	1.6
MSCP	11.9	12.6	-0.7	1.6
EG433229	9.2	9.9	-0.7	1.6
SMARCD3	8.2	8.9	-0.7	1.6
SCL0003073.1_164	8.2	8.8	-0.7	1.6
HHATL	8.6	9.3	-0.7	1.6
DNAJC7	8.9	9.6	-0.7	1.6
USP13	7.9	8.6	-0.7	1.6
ADSSL1	11.5	12.2	-0.7	1.6
ACADM	11.2	11.9	-0.7	1.6
MT-ATP6	11.3	12.0	-0.7	1.6
6430573H23RIK	8.2	8.9	-0.7	1.6
TUBA8	8.6	9.3	-0.7	1.6

DEDD2	9.8	10.4	-0.7	1.6
LOC100041835	12.3	12.9	-0.7	1.6
1300013J15RIK	7.9	8.6	-0.7	1.6
MACROD1	9.1	9.8	-0.7	1.6
ALDOA	13.2	13.9	-0.7	1.6
LOC667034	8.5	9.2	-0.7	1.6
MDH2	10.0	10.6	-0.7	1.6
PDK4	9.3	10.0	-0.7	1.6
ART5	7.7	8.4	-0.7	1.6
JSRP1	7.9	8.6	-0.7	1.6
PPM1L	8.4	9.0	-0.7	1.6
MFN2	10.1	10.8	-0.7	1.6
RILPL1	8.8	9.4	-0.6	1.6
EHBP1L1	8.8	9.4	-0.6	1.6
NDUFA5	10.3	10.9	-0.6	1.6
MTDNA_ND2	11.5	12.2	-0.6	1.6
MTDNA_ND5	11.5	12.2	-0.6	1.6
TRIM72	9.7	10.4	-0.6	1.6
B930008G03RIK	10.0	10.7	-0.6	1.6
2310040G24RIK	7.9	8.5	-0.6	1.6
ALAD	12.0	12.7	-0.6	1.6
SGCA	8.4	9.0	-0.6	1.5
LOC385959	8.3	8.9	-0.6	1.5
LOC547380	8.3	8.9	-0.6	1.5
NDUFS7	11.8	12.4	-0.6	1.5
1300017J02RIK	8.9	9.5	-0.6	1.5
LOC381792	7.7	8.3	-0.6	1.5
FLNC	8.5	9.1	-0.6	1.5
DHRS7C	8.1	8.7	-0.6	1.5
ART1	8.0	8.6	-0.6	1.5
EG245190	8.8	9.5	-0.6	1.5
A530020A01RIK	7.9	8.5	-0.6	1.5
PRKAA2	7.8	8.4	-0.6	1.5
VLDLR	8.7	9.3	-0.6	1.5
1110002E22RIK	8.1	8.7	-0.6	1.5
NDUFB9	7.8	8.4	-0.6	1.5
MYO18B	8.1	8.7	-0.6	1.5
ITGB1BP3	8.3	8.9	-0.6	1.5
PHLDA3	9.4	10.0	-0.6	1.5
GPT2	8.5	9.1	-0.6	1.5
LOC386256	7.9	8.5	-0.6	1.5
TSC22D3	9.4	10.0	-0.6	1.5
NDUFA4	12.4	13.0	-0.6	1.5

4CYTL1	9.4	10.0	-0.6	1.5
PTP4A3	9.0	9.6	-0.6	1.5
FBXO32	7.9	8.5	-0.6	1.5
CNKSR1	7.7	8.3	-0.6	1.5
ZXDA	9.0	9.6	-0.6	1.5
LOC100044934	8.4	9.0	-0.6	1.5
KBTBD5	7.8	8.4	-0.6	1.5
SRR	11.0	11.6	-0.6	1.5
CACNG1	8.1	8.7	-0.6	1.5
SCL0002124.1_39	7.7	8.3	-0.6	1.5
DEB1	11.0	11.6	-0.6	1.5
LMOD3	7.9	8.5	-0.6	1.5
9830134C10RIK	8.2	8.8	-0.6	1.5
TYKI	9.3	9.9	-0.6	1.5
UFSP1	8.6	9.2	-0.6	1.5
SMPX	7.7	8.2	-0.6	1.5
LOC100047214	9.1	9.7	-0.6	1.5
VGLL2	7.6	8.2	-0.6	1.5
CAR3	10.3	10.9	-0.6	1.5
SLC25A12	9.1	9.7	-0.6	1.5
EG622339	13.4	14.0	-0.6	1.5
CIB2	9.4	9.9	-0.6	1.5
A630006E02RIK	9.5	10.1	-0.6	1.5
UGP2	9.4	10.0	-0.6	1.5
4933428A15RIK	8.6	9.2	-0.6	1.5
CHKA	9.4	10.0	-0.6	1.5
SNTA1	8.5	9.0	-0.6	1.5
SLC6A9	9.3	9.9	-0.6	1.5
2410076I21RIK	8.4	8.9	-0.6	1.5
TPI1	12.1	12.6	-0.6	1.5
SMTNL1	7.9	8.4	-0.6	1.5
TMOD1	8.7	9.3	-0.6	1.5
TSPAN8	8.5	9.1	-0.6	1.5
MTDNA_COXII	12.8	13.4	-0.6	1.5
NDUFS2	8.7	9.3	-0.6	1.5
SLC2A4	8.1	8.7	-0.6	1.5
MYOT	7.8	8.4	-0.6	1.5
A230005G17RIK	8.3	8.9	-0.6	1.5
TNNT1	8.9	9.4	-0.6	1.5
FHL1	11.6	12.1	-0.6	1.5
SPNB1	9.5	10.0	-0.6	1.5
5830496L11RIK	9.1	9.6	-0.6	1.5
ENSMUSG00000054212	9.5	10.1	-0.6	1.5

5430434G16RIK	8.9	9.4	-0.6	1.5
IDH3A	8.9	9.4	-0.6	1.5
SLC38A5	11.1	11.7	-0.6	1.5
LDB3	8.1	8.6	-0.6	1.5
E430039I23RIK	11.1	11.6	-0.6	1.5
KEL	10.5	11.0	-0.6	1.5
2310039E09RIK	8.2	8.7	-0.6	1.5
D530007E13RIK	8.9	9.4	-0.6	1.5
1110018J23RIK	7.9	8.5	-0.6	1.5
TMEM45B	8.2	8.7	-0.6	1.5
BC022224	10.2	10.7	-0.6	1.5
RBM38	9.9	10.5	-0.6	1.5
2810484G07RIK	10.9	11.5	-0.5	1.5
ACO2	10.8	11.4	-0.5	1.5
1700021F05RIK	10.3	10.8	-0.5	1.5
VEGFB	9.8	10.4	-0.5	1.5
STXBP3	8.2	8.7	-0.5	1.5
AGL	9.3	9.8	-0.5	1.5
TAL1	9.3	9.8	-0.5	1.5
MYOZ2	7.7	8.2	-0.5	1.5
NCTC1	7.8	8.3	-0.5	1.5
ABCA7	9.4	10.0	-0.5	1.5
SAR1B	10.3	10.9	-0.5	1.5
3632431M01RIK	8.6	9.1	-0.5	1.5
FCHO1	10.0	10.5	-0.5	1.5
P2RY1	8.8	9.3	-0.5	1.5
B230387C07RIK	9.1	9.7	-0.5	1.5
TRIM63	7.5	8.0	-0.5	1.5
1810020D17RIK	9.5	10.0	-0.5	1.4
FYCO1	8.1	8.6	-0.5	1.4
RABGEF1	10.3	10.8	-0.5	1.4
ITGB1BP2	8.2	8.8	-0.5	1.4
IFT140	9.1	9.6	-0.5	1.4
SAMD11	8.2	8.7	-0.5	1.4
ABCB10	8.2	8.8	-0.5	1.4
LOC100046690	9.0	9.5	-0.5	1.4
PFN2	8.9	9.5	-0.5	1.4
C1QTNF3	11.0	7.5	3.5	11.3
LRRC15	10.6	8.4	2.2	4.7
ANGPTL1	9.7	7.6	2.1	4.4
MFAP5	10.2	8.1	2.1	4.4
THBS2	11.8	9.7	2.1	4.3
FSTL1	11.1	9.0	2.0	4.1

COL6A2	10.4	8.4	2.0	4.1
MMP2	13.7	11.7	2.0	3.9
COL6A1	12.4	10.4	2.0	3.9
CAPN6	9.7	7.7	2.0	3.9
COL3A1	9.8	7.9	1.9	3.8
MMP3	9.3	7.4	1.9	3.8
TIMP1	11.8	9.9	1.9	3.8
COL5A1	12.6	10.7	1.9	3.7
CTHRC1	9.5	7.6	1.9	3.7
AEBP1	10.9	9.1	1.9	3.6
COL18A1	9.8	8.0	1.8	3.5
DKK3	10.2	8.5	1.7	3.4
COL14A1	9.3	7.6	1.7	3.3
E430002G05RIK	9.9	8.1	1.7	3.3
PCOLCE	10.9	9.2	1.7	3.3
LUM	12.2	10.5	1.7	3.3
DPT	10.3	8.6	1.7	3.2
MMP14	11.9	10.2	1.7	3.2
GP38	11.0	9.3	1.7	3.2
FCRLS	9.9	8.2	1.6	3.1
MFAP4	9.2	7.6	1.6	3.1
CSRP2	11.0	9.4	1.6	3.1
LOX	11.4	9.8	1.6	3.1
SPON2	11.2	9.6	1.6	3.0
ITM2A	9.8	8.2	1.6	3.0
LY6A	12.8	11.3	1.6	3.0
DDAH1	9.3	7.7	1.6	3.0
MUP2	9.7	8.2	1.6	3.0
GPNMB	9.5	8.0	1.6	3.0
CD248	9.9	8.3	1.5	2.9
ANTXR1	9.9	8.3	1.5	2.9
6330406I15RIK	9.7	8.1	1.5	2.9
LOXL1	10.8	9.2	1.5	2.9
MUP1	9.2	7.7	1.5	2.9
NBL1	10.3	8.8	1.5	2.9
MFAP2	9.2	7.7	1.5	2.8
CCL21A	10.6	9.1	1.5	2.8
FN1	10.4	8.9	1.5	2.8
MEST	8.8	7.3	1.5	2.8
MRGPRF	9.5	8.0	1.5	2.8
CCL21C	10.0	8.5	1.5	2.8
SAA3	8.7	7.2	1.5	2.8
LOC100048554	9.2	7.7	1.5	2.8
THY1	10.0	8.5	1.5	2.7

HTRA1	10.5	9.1	1.5	2.7
OSR2	9.3	7.8	1.5	2.7
LOC100041504	9.9	8.4	1.4	2.7
GPX7	9.8	8.4	1.4	2.7
KDELR3	10.4	8.9	1.4	2.7
H19	11.4	10.0	1.4	2.7
PDLIM4	10.3	8.9	1.4	2.6
C1QTNF2	9.3	7.9	1.4	2.6
COL6A3	11.3	9.9	1.4	2.6
FBLN2	9.4	8.0	1.4	2.6
MXRA8	10.5	9.1	1.4	2.6
SCL0001849.1_2273	9.0	7.6	1.4	2.6
VKORC1	11.1	9.7	1.3	2.5
PPIC	12.3	11.0	1.3	2.5
ITGBL1	9.6	8.3	1.3	2.5
EMP1	12.7	11.4	1.3	2.5
KNSL5	11.8	10.5	1.3	2.5
SERPINH1	12.8	11.5	1.3	2.5
2310016C16RIK	10.3	9.0	1.3	2.5
WISP2	10.4	9.1	1.3	2.5
MAGED1	11.6	10.3	1.3	2.5
COL16A1	11.6	10.3	1.3	2.5
LEPREL2	9.2	7.9	1.3	2.4
GPX8	10.7	9.4	1.3	2.4
BGN	14.3	13.0	1.3	2.4
SRPX2	10.2	8.9	1.3	2.4
ITGA11	9.9	8.6	1.3	2.4
CCDC80	11.0	9.7	1.3	2.4
CLEC11A	10.4	9.2	1.3	2.4
SMOC1	9.7	8.5	1.2	2.4
OGN	10.3	9.0	1.2	2.4
CRTAP	10.1	8.9	1.2	2.4
VIM	11.1	9.8	1.2	2.3
COL4A2	11.3	10.0	1.2	2.3
FKBP11	10.0	8.7	1.2	2.3
CD276	9.3	8.1	1.2	2.3
PRKCDBP	10.1	8.9	1.2	2.3
CCL7	8.4	7.2	1.2	2.3
NFATC4	9.4	8.1	1.2	2.3
ECM1	10.8	9.6	1.2	2.3
COL15A1	9.4	8.2	1.2	2.3
2610027C15RIK	10.0	8.8	1.2	2.3

PRELP	13.1	11.9	1.2	2.3
TIMP2	12.6	11.4	1.2	2.3
GRB10	9.4	8.2	1.2	2.3
FBN1	9.6	8.4	1.2	2.3
COPZ2	10.0	8.8	1.2	2.3
SCARF2	12.0	10.8	1.2	2.3
ENPP1	9.6	8.4	1.2	2.3
COL4A1	11.7	10.5	1.2	2.3
IGF1	9.6	8.4	1.2	2.2
SULF2	9.2	8.0	1.2	2.2
SERPINA3N	10.2	9.0	1.2	2.2
FKBP9	11.1	9.9	1.2	2.2
RNASE4	9.8	8.6	1.2	2.2
COMP	12.8	11.6	1.2	2.2
MS4A6D	9.8	8.6	1.2	2.2
CPXM1	9.3	8.2	1.1	2.2
DAB2	9.7	8.5	1.1	2.2
EFEMP2	10.0	8.9	1.1	2.2
LOC100047053	8.4	7.3	1.1	2.2
COL8A1	9.5	8.4	1.1	2.2
SERPING1	11.9	10.7	1.1	2.2
ANGPTL4	10.2	9.1	1.1	2.2
THBS3	8.7	7.6	1.1	2.1
HSPG2	10.5	9.4	1.1	2.1
PTN	8.9	7.8	1.1	2.1
GM22	9.3	8.2	1.1	2.1
NNMT	9.6	8.6	1.1	2.1
LGMN	10.9	9.8	1.1	2.1
4930533K18RIK	9.8	8.7	1.1	2.1
VASN	10.9	9.8	1.1	2.1
ELN	8.5	7.5	1.1	2.1
FMOD	10.2	9.1	1.1	2.1
LOC100046883	10.8	9.8	1.1	2.1
CLEC4N	8.6	7.6	1.1	2.1
NDN	10.0	8.9	1.1	2.1
ACAN	9.7	8.6	1.1	2.1
OLFML1	8.8	7.8	1.1	2.1
C1QTNF1	8.7	7.6	1.1	2.1
SOCS3	9.3	8.3	1.0	2.1
1500015O10RIK	11.9	10.8	1.0	2.0
FKBP10	9.7	8.7	1.0	2.0
TREM2	9.4	8.4	1.0	2.0
MGP	13.5	12.5	1.0	2.0
COL10A1	10.7	9.6	1.0	2.0

ADAMTS12	8.7	7.7	1.0	2.0
CRLF1	8.5	7.5	1.0	2.0
HTRA3	9.6	8.6	1.0	2.0
P4HA2	9.0	8.0	1.0	2.0
FSCN1	9.0	8.1	1.0	2.0
NUPR1	12.0	11.0	1.0	2.0
SCARA3	11.9	10.9	1.0	2.0
SYNPO	10.1	9.1	1.0	2.0
NID2	8.8	7.8	1.0	2.0
TSPAN6	8.9	7.9	1.0	2.0
LGALS1	12.5	11.5	1.0	2.0
IGFBP7	10.5	9.5	1.0	2.0
TMEM119	9.7	8.7	1.0	2.0
COL2A1	13.6	12.6	1.0	2.0
MS4A7	8.8	7.8	1.0	2.0
ANXA5	12.4	11.4	1.0	2.0
RAMP2	10.0	9.1	1.0	2.0
MMP23	9.5	8.5	1.0	1.9
SLC1A4	8.5	7.6	1.0	1.9
LOC100047856	9.1	8.2	1.0	1.9
AHNAK2	9.1	8.2	1.0	1.9
CDKN1C	11.0	10.0	1.0	1.9
APOE	11.0	10.0	1.0	1.9
SPARC	13.1	12.1	1.0	1.9
BC020108	8.5	7.5	0.9	1.9
C1QB	11.5	10.5	0.9	1.9
FNDC3B	10.2	9.3	0.9	1.9
IGSF10	8.8	7.9	0.9	1.9
COL12A1	9.1	8.2	0.9	1.9
9030024J15RIK	9.7	8.7	0.9	1.9
1110036O03RIK	8.9	8.0	0.9	1.9
LRIG3	9.4	8.5	0.9	1.9
FAM129B	10.2	9.3	0.9	1.9
EDNRA	9.5	8.5	0.9	1.9
IL33	8.3	7.4	0.9	1.9
IGFBP6	10.0	9.0	0.9	1.9
LGALS3BP	10.8	9.9	0.9	1.9
OLFML3	11.5	10.6	0.9	1.9
COL1A2	11.1	10.2	0.9	1.9
GPR176	8.4	7.5	0.9	1.9
CERCAM	9.9	9.0	0.9	1.9
CNRIP1	9.7	8.8	0.9	1.9
GALNTL1	8.5	7.7	0.9	1.9

KERA	8.2	7.3	0.9	1.9
PRG4	12.7	11.8	0.9	1.9
IGKV3-2_X16954_IG_KAPPA_VARIABLE_3-2_18	9.0	8.1	0.9	1.9
LOC676136	9.5	8.6	0.9	1.9
ABI3BP	8.6	7.7	0.9	1.9
PKD2	8.9	8.0	0.9	1.8
COL1A1	13.2	12.3	0.9	1.8
SCX	8.6	7.7	0.9	1.8
IGF2	10.3	9.4	0.9	1.8
SFRP1	8.3	7.4	0.9	1.8
KCTD17	9.1	8.2	0.9	1.8
IGFBP4	12.0	11.2	0.9	1.8
MFGE8	12.3	11.5	0.9	1.8
EFS	9.2	8.4	0.9	1.8
BC064033	8.4	7.6	0.9	1.8
LOC243431	9.8	9.0	0.9	1.8
MAGED2	11.1	10.2	0.9	1.8
DPYSL3	9.3	8.4	0.9	1.8
ANPEP	8.4	7.6	0.9	1.8
A430110N23RIK	8.2	7.4	0.9	1.8
CXCL1	8.1	7.2	0.8	1.8
LTBP3	9.0	8.2	0.8	1.8
LRRC17	8.3	7.4	0.8	1.8
LOC100047583	9.3	8.5	0.8	1.8
UTS2R	8.3	7.4	0.8	1.8
TNN	8.3	7.5	0.8	1.8
CALU	10.0	9.2	0.8	1.8
BMP1	9.9	9.1	0.8	1.8
SCARA5	9.7	8.9	0.8	1.8
TXNDC5	10.7	9.9	0.8	1.8
SDC2	10.4	9.6	0.8	1.8
IFITM2	12.1	11.3	0.8	1.8
PRDX4	11.0	10.1	0.8	1.8
DLK1	8.2	7.3	0.8	1.8
0610007N19RIK	9.4	8.6	0.8	1.8
TPST1	9.9	9.0	0.8	1.8
NT5DC2	9.1	8.3	0.8	1.8
SULF1	8.9	8.1	0.8	1.8
HTRA4	9.0	8.2	0.8	1.8
AKR1B8	8.3	7.4	0.8	1.8
SRPX	8.8	8.0	0.8	1.8

MARCKS	11.2	10.4	0.8	1.8
PARVA	9.6	8.8	0.8	1.7
TGFB3	8.8	8.0	0.8	1.7
LOC232060	8.7	7.9	0.8	1.7
WISP1	9.5	8.7	0.8	1.7
LXN	10.0	9.2	0.8	1.7
D14ERTD449E	9.2	8.5	0.8	1.7
MDK	8.6	7.8	0.8	1.7
TGFBI	11.3	10.5	0.8	1.7
SH3PXD2B	9.4	8.6	0.8	1.7
EMP2	9.0	8.2	0.8	1.7
IGHG	9.7	9.0	0.8	1.7
RIN2	9.1	8.3	0.8	1.7
1700023M03RIK	9.9	9.2	0.8	1.7
WBP5	10.9	10.1	0.8	1.7
CD68	10.3	9.5	0.8	1.7
1200009O22RIK	8.6	7.8	0.8	1.7
IL1RL1	8.1	7.3	0.8	1.7
ADAMTS2	11.0	10.2	0.8	1.7
A730054J21RIK	8.3	7.5	0.8	1.7
4732462B05RIK	10.0	9.3	0.8	1.7
LBP	9.9	9.1	0.8	1.7
IL13RA1	8.7	7.9	0.8	1.7
FER1L3	8.4	7.6	0.8	1.7
C4A	10.0	9.2	0.8	1.7
SOX9	9.8	9.0	0.8	1.7
1810055G02RIK	10.2	9.4	0.8	1.7
PANX3	10.7	10.0	0.8	1.7
FKBP14	8.5	7.7	0.8	1.7
SERPINF1	12.8	12.1	0.8	1.7
TUBB6	9.9	9.2	0.8	1.7
C1QC	10.8	10.0	0.8	1.7
OLFML2B	11.5	10.7	0.8	1.7
TCEAL8	9.9	9.2	0.8	1.7
PDGFRA	9.4	8.6	0.8	1.7
NOX4	8.3	7.5	0.8	1.7
SFRP2	8.1	7.3	0.7	1.7
6720469N11RIK	10.1	9.3	0.7	1.7
LOC380799	8.7	8.0	0.7	1.7
CSTB	12.6	11.8	0.7	1.7
CYB561	8.7	8.0	0.7	1.7
LHFPL2	9.7	9.0	0.7	1.7
LOC98434	10.3	9.5	0.7	1.7

CD14	8.5	7.7	0.7	1.7
PMP22	9.4	8.7	0.7	1.7
RBP1	8.6	7.8	0.7	1.7
2310008M10RIK	11.4	10.6	0.7	1.7
MT1	13.4	12.7	0.7	1.7
EXT1	9.9	9.2	0.7	1.7
LIMA1	9.0	8.3	0.7	1.7
MATN4	8.3	7.5	0.7	1.7
EDG5	9.3	8.6	0.7	1.7
SPSB1	8.7	8.0	0.7	1.7
ARMCX2	9.4	8.7	0.7	1.7
SVEP1	8.3	7.6	0.7	1.7
HMGN3	10.5	9.8	0.7	1.6
GPR23	8.7	8.0	0.7	1.6
FOLR2	8.6	7.8	0.7	1.6
UBE2E2	9.3	8.6	0.7	1.6
RHOJ	9.4	8.7	0.7	1.6
PROS1	9.9	9.2	0.7	1.6
STAB1	9.6	8.9	0.7	1.6
LOC637227	9.6	8.8	0.7	1.6
MYADM	10.8	10.1	0.7	1.6
ANXA8	8.4	7.7	0.7	1.6
PLOD1	8.3	7.6	0.7	1.6
MEOX2	8.9	8.2	0.7	1.6
LOC381629	10.7	10.0	0.7	1.6
LOC384413	9.4	8.7	0.7	1.6
TAX1BP3	10.5	9.8	0.7	1.6
6330404C01RIK	9.3	8.6	0.7	1.6
FRMD6	9.8	9.1	0.7	1.6
COL9A2	10.6	9.9	0.7	1.6
NT5E	9.0	8.3	0.7	1.6
MYO1E	9.0	8.3	0.7	1.6
LMAN1	9.5	8.8	0.7	1.6
GRN	12.1	11.4	0.7	1.6
LOC669053	9.3	8.6	0.7	1.6
CUL7	9.5	8.8	0.7	1.6
P4HB	13.1	12.4	0.7	1.6
TWSG1	10.1	9.4	0.7	1.6
D4BWG0951E	8.3	7.7	0.7	1.6
BICC1	9.6	8.9	0.7	1.6
WTIP	9.3	8.6	0.7	1.6
IL11RA1	11.3	10.7	0.7	1.6
LOC636944	9.9	9.3	0.7	1.6
PLVAP	10.2	9.5	0.7	1.6

EGFR	8.5	7.8	0.7	1.6
RFTN2	8.6	8.0	0.7	1.6
TMED3	9.9	9.2	0.7	1.6
TUBB2B	8.7	8.1	0.7	1.6
C130021I20	7.9	7.3	0.7	1.6
CXCL16	8.2	7.5	0.7	1.6
CDON	8.2	7.6	0.7	1.6
SDC3	11.1	10.5	0.7	1.6
5430435G22RIK	8.4	7.8	0.7	1.6
ADRA2A	8.6	7.9	0.7	1.6
C1QA	9.3	8.7	0.7	1.6
PRRC1	9.8	9.2	0.7	1.6
TPBG	8.3	7.7	0.6	1.6
BOK	8.5	7.8	0.6	1.6
NID1	8.8	8.1	0.6	1.6
FXYD6	11.3	10.7	0.6	1.6
TGFBR2	9.8	9.2	0.6	1.6
LAMC1	9.2	8.5	0.6	1.6
ZFP521	8.4	7.7	0.6	1.6
GPR125	9.4	8.8	0.6	1.6
COL5A2	8.0	7.4	0.6	1.6
PAPSS2	9.2	8.6	0.6	1.6
BDH2	9.5	8.9	0.6	1.6
MIA1	10.1	9.4	0.6	1.6
SOCS2	9.9	9.2	0.6	1.6
GLT8D1	9.4	8.8	0.6	1.6
PLOD2	8.5	7.9	0.6	1.6
FSTL	8.0	7.4	0.6	1.6
IGFBP3	8.1	7.5	0.6	1.5
2410146L05RIK	8.0	7.3	0.6	1.5
GSTM2	10.2	9.5	0.6	1.5
ISLR	8.0	7.4	0.6	1.5
PPIB	11.3	10.7	0.6	1.5
PDGFRB	8.6	7.9	0.6	1.5
DLG5	9.5	8.9	0.6	1.5
CAV1	10.4	9.8	0.6	1.5
CCL4	8.2	7.6	0.6	1.5
TMEM176B	10.1	9.4	0.6	1.5
RAB34	8.4	7.7	0.6	1.5
CDKN1A	8.7	8.1	0.6	1.5
CYB5R3	9.6	9.0	0.6	1.5
SEPN1	10.2	9.6	0.6	1.5
LOC630253	8.2	7.6	0.6	1.5

PRRX2	8.1	7.5	0.6	1.5
RHOC	8.4	7.8	0.6	1.5
PRSS35	8.8	8.2	0.6	1.5
GPRC5B	8.4	7.8	0.6	1.5
PDIA5	8.1	7.5	0.6	1.5
PMEPA1	8.2	7.6	0.6	1.5
ADAMTS4	7.9	7.3	0.6	1.5
RRBP1	9.3	8.7	0.6	1.5
FAM171B	8.4	7.8	0.6	1.5
SERTAD4	8.1	7.5	0.6	1.5
CRABP2	7.8	7.2	0.6	1.5
5430433G21RIK	9.4	8.9	0.6	1.5
RAB11FIP5	9.3	8.7	0.6	1.5
4933421H10RIK	8.7	8.1	0.6	1.5
DCN	12.3	11.7	0.6	1.5
2610009E16RIK	9.1	8.5	0.6	1.5
3110079O15RIK	12.8	12.2	0.6	1.5
VAT1	9.6	9.1	0.6	1.5
COL8A2	8.2	7.6	0.6	1.5
LOC100047162	9.9	9.4	0.6	1.5
HOXC6	9.1	8.5	0.6	1.5
ZFYVE21	10.3	9.7	0.6	1.5
BGLAP-RS1	13.8	13.2	0.6	1.5
9430028L06RIK	7.9	7.3	0.6	1.5
ACTA2	10.3	9.7	0.6	1.5
GLT25D1	10.7	10.1	0.6	1.5
RCN3	8.3	7.7	0.6	1.5
CLEC3B	8.2	7.6	0.6	1.5
GMDS	8.8	8.2	0.6	1.5
BMPER	8.3	7.7	0.6	1.5
2300002D11RIK	8.0	7.4	0.6	1.5
PLAT	8.0	7.4	0.6	1.5
TWIST1	8.4	7.8	0.6	1.5
6230400G14RIK	8.8	8.2	0.6	1.5
PLOD3	10.2	9.7	0.6	1.5
CAPG	10.0	9.5	0.6	1.5
LOC626583	8.1	7.5	0.6	1.5
ALG14	8.9	8.4	0.6	1.5
MMP12	7.8	7.2	0.6	1.5
TNXB	8.5	7.9	0.6	1.5
TUBA1A	9.4	8.9	0.6	1.5
CD81	12.8	12.2	0.6	1.5
TMEM86A	9.9	9.4	0.6	1.5
C1QTNF5	7.9	7.3	0.6	1.5

ERGIC1	9.4	8.8	0.6	1.5
5031439A09RIK	8.9	8.4	0.6	1.5
S100A10	9.2	8.6	0.6	1.5
CBR2	9.1	8.6	0.6	1.5
FBLN7	7.8	7.3	0.6	1.5
B9D1	8.3	7.7	0.6	1.5
ALG5	9.6	9.1	0.6	1.5
RRAS	9.9	9.3	0.6	1.5
CHMP4B	10.4	9.8	0.6	1.5
GNS	10.9	10.4	0.6	1.5
H47	10.8	10.3	0.6	1.5
IFITM5	9.2	8.7	0.6	1.5
WWTR1	8.8	8.2	0.5	1.5
CRIP2	11.0	10.4	0.5	1.5
ANXA2	13.6	13.1	0.5	1.5
A730017D01RIK	8.5	7.9	0.5	1.5
PRRX1	8.1	7.6	0.5	1.5
COL22A1	10.4	9.9	0.5	1.5
MANBAL	10.3	9.8	0.5	1.5
POFUT2	8.1	7.6	0.5	1.5
APLNR	8.3	7.7	0.5	1.5
FBLIM1	8.7	8.2	0.5	1.5
LMNA	10.4	9.9	0.5	1.5
PLCD1	8.7	8.1	0.5	1.5
RHBDF1	9.9	9.4	0.5	1.5
LOC100039175	8.8	8.2	0.5	1.5
EBPL	8.8	8.3	0.5	1.5
KDELR2	8.5	8.0	0.5	1.5
FAH	8.9	8.3	0.5	1.5
PDIA3	11.7	11.1	0.5	1.5
PLA1A	8.1	7.6	0.5	1.5
GAS6	11.3	10.8	0.5	1.5
BC065085	8.3	7.8	0.5	1.5
D10ERTD610E	8.6	8.1	0.5	1.4
IFIT3	8.5	8.0	0.5	1.4
PDGFRL	7.9	7.4	0.5	1.4
3632451O06RIK	8.0	7.5	0.5	1.4
TPM4	11.3	10.8	0.5	1.4
PLP2	10.0	9.5	0.5	1.4
C4B	8.7	8.1	0.5	1.4

Table 7: Genes changed expression in DMM model at day 7

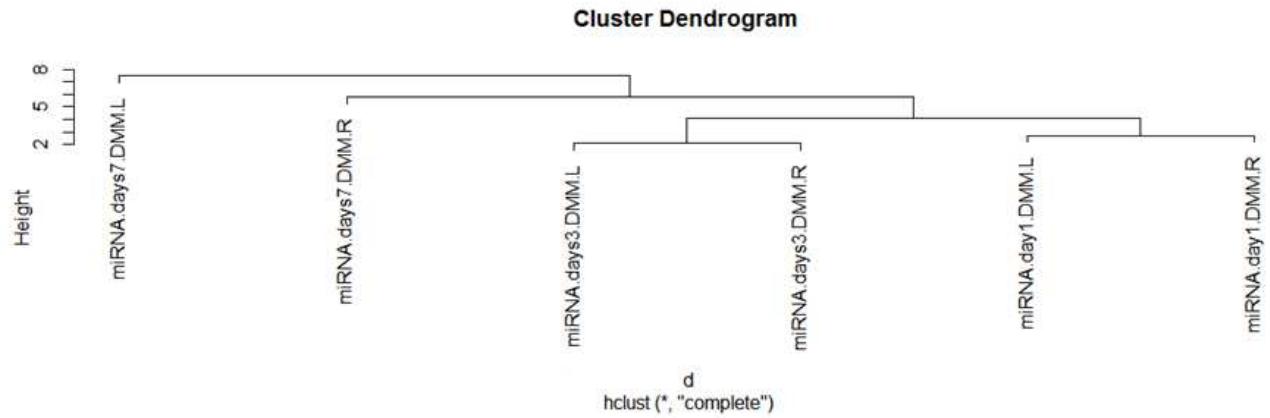

Figure 1: Hierarchical cluster analysis for DMM models at 1, 3, and 7 days after surgery

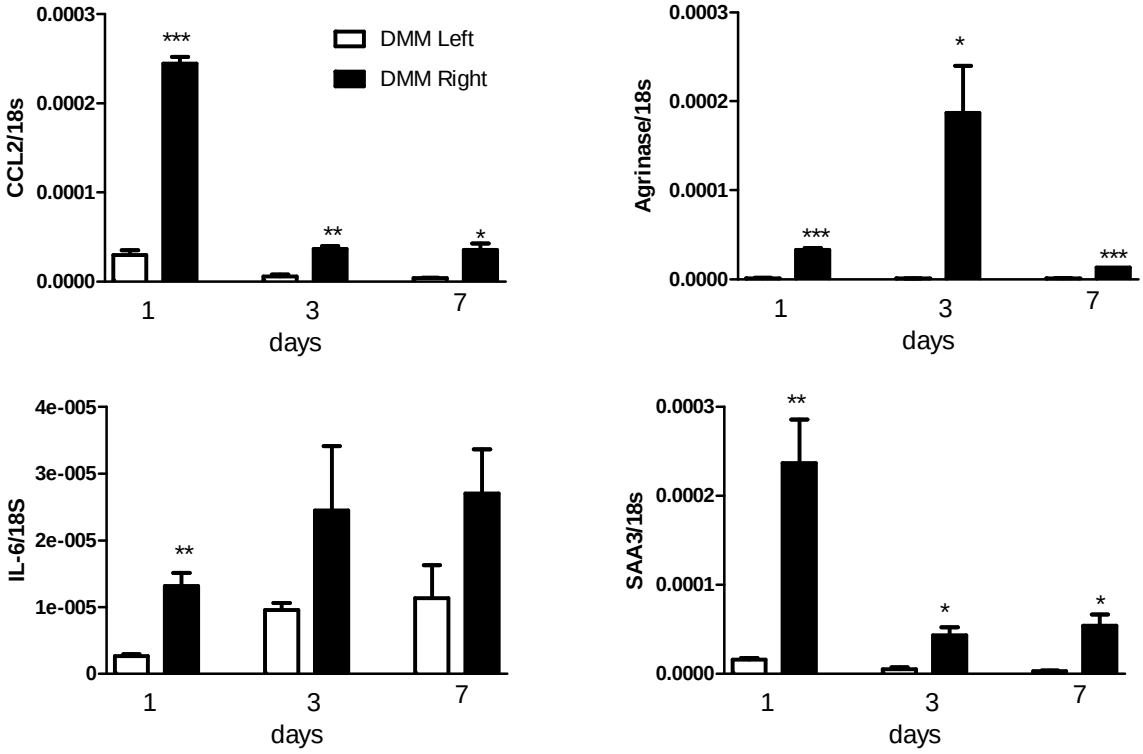

Figure 2: CCL2, Agrinase, IL-6 and SAA-3 were significantly induced expression in DMM model at 1, 3, and 7 days after surgery

Total RNA was reversed transcribed to cDNA and gene expression was measured by real-time qRT-PCR in individual samples of DMM left knee (un-operated, open bar), and DMM right knee (DMM, close bar). 18S was used as endogenous control. The data show mean +/- SEM, n=3. The expression of genes of interest between each group was analysed by unpaired two-tailed t test * $p<0.05$, ** $p < 0.01$, *** $p<0.001$.

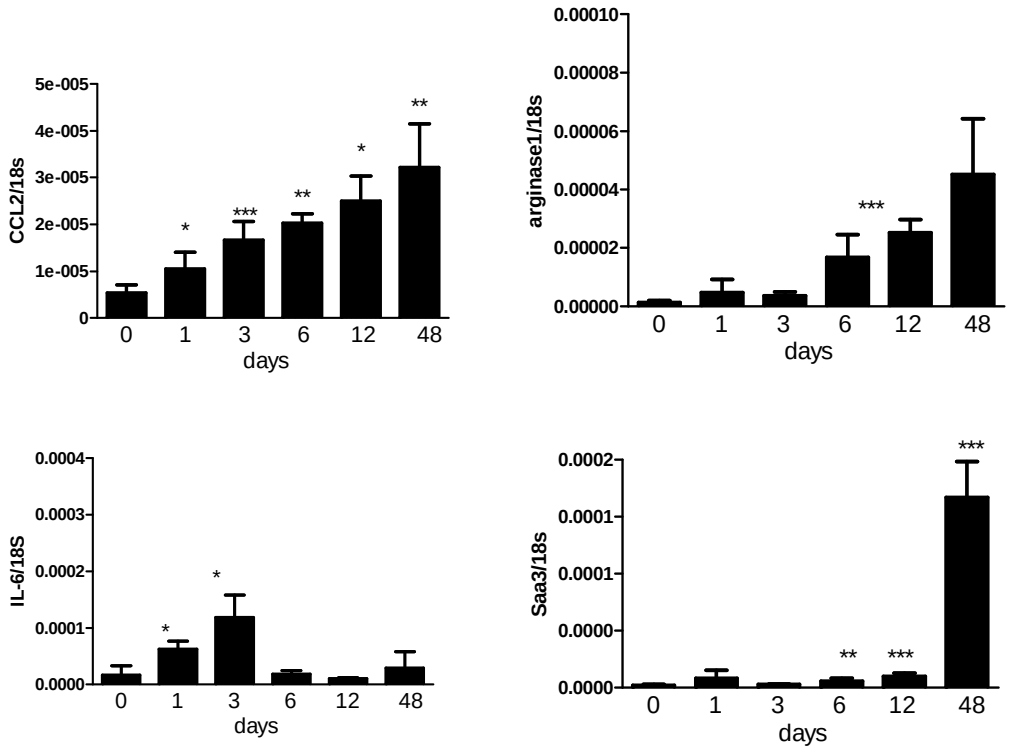

Figure 3: Gene expression in hip avulsion injury model

The femoral caps of C57Bl/6 mice aged 4 weeks were avulsed and put in culture. At each of 3, 6, 12, 48 hour time points, the femoral caps were harvested. Total RNA was isolated using Trizol and reverse transcribed to cDNA. Gene expression was measured by real-time qRT-PCR where 18S was used as an endogenous control. Assays were repeated 3 times. At least triplicate samples were measured at each time. Means ± standard errors are presented. Difference in expression between each time point against control (t=0) was calculated by unpaired two-tailed t test. * $p<0.05$, ** $p < 0.01$, *** $p<0.001$.

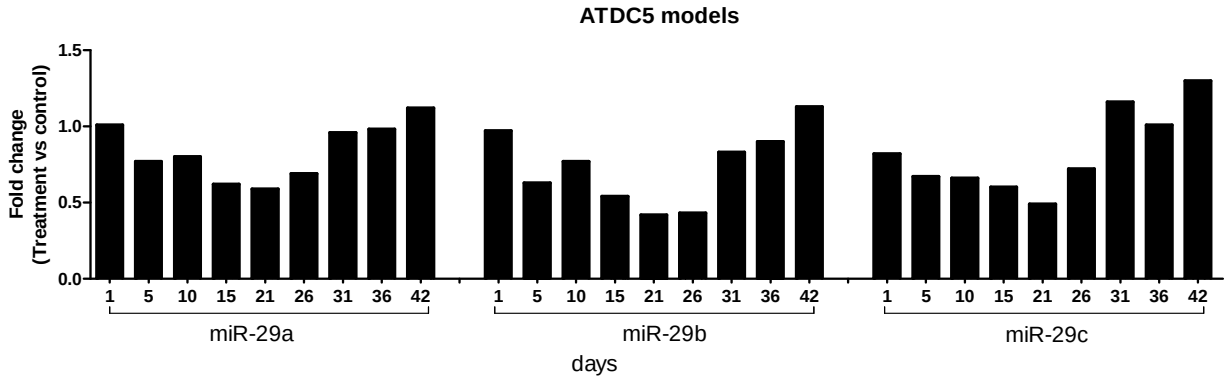

Figure 4: The expression of the miR-29 family in ATDC5 model

The embryonic carcinoma cell line ATDC5 was stimulated to from chondrocytes using insulin for 42 days. Total RNA was isolated, reverse transcribed to cDNA and used for miRNA microarray.

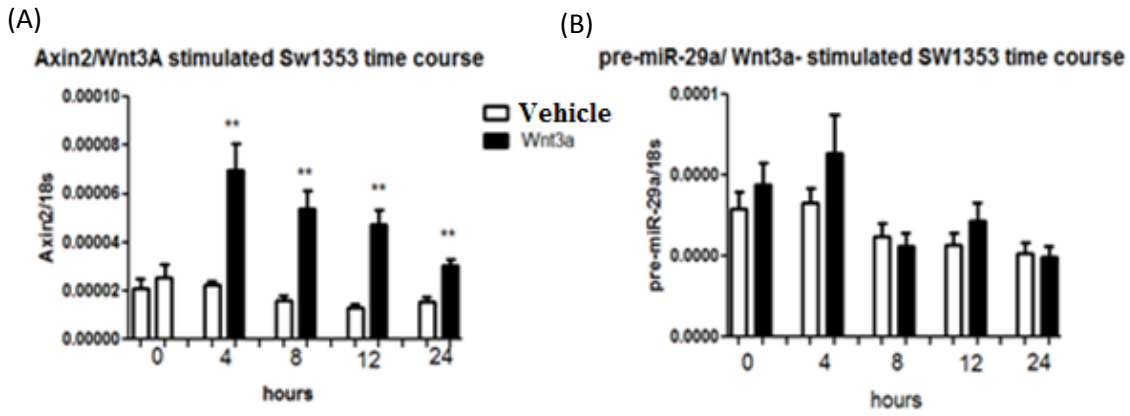

Figure 5: Expression of the miR-29 family was not controlled by Wnt3a

SW1353 cells were cultured in high glucose media with 10% (v/v) FCS in monolayer until 90% confluence. Cells were serum starved for 24 hours before treating with Wnt3a or vehicle (0.5% (w/v) BSA) across 24 hour course.

Relative expression of the precursor miR-29a and axin2 was measured by quantitative RT-PCR. 18S rRNA was the endogenous control for measuring the precursor transcripts. Open bar, control; close bar, WNT3a. (A) Expression level of axin2. (B) Expression level of precursor miR-29a. Means ± standard errors are presented. The difference between the treatment and the control was analysed by unpaired two-tailed t test. * $p<0.05$, ** $p < 0.01$, *** $p<0.001$, n=3.

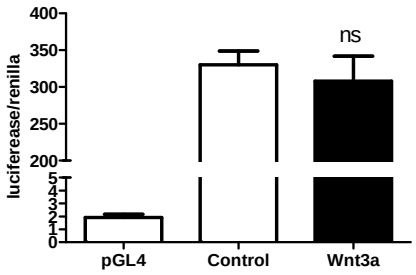

Figure 6: Wnt3a does not control the expression from the primary miR-29a/b1 promoter

The pri-miR-29a/b1 promoter-reporter (100ng) or the empty vector pGL4 (control, 100ng) were transfected into SW1353 cells. After transfection, cells were serum starved for 24 hours, followed by stimulating for another 6 hours with WNT3a (100ng/ml), or vehicle (0.5% BSA) before measuring luciferase activity. Renilla was use as endogenous control. Open bar: vehicle, black bar: Wnt3a. Means ± standard errors are presented, n=3. The difference of luciferase activity was analysed by unpaired two-tailed Student's t test. * $p<0.05$, ** $p < 0.01$, *** $p<0.00$.

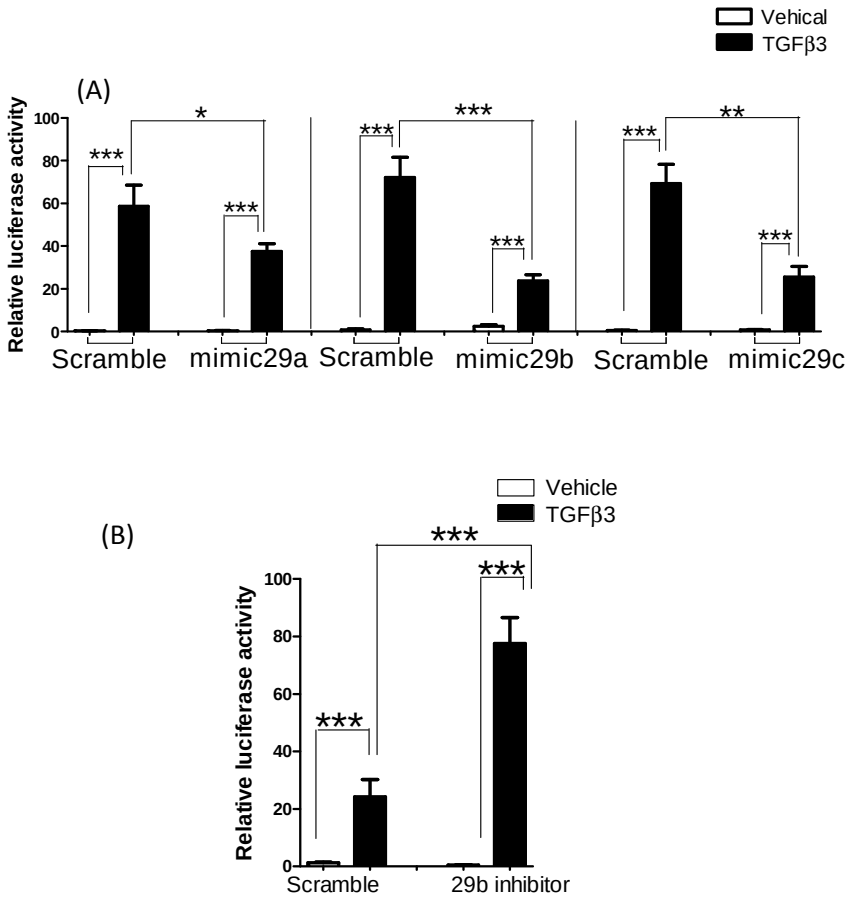

Figure 7 The miR-29 family suppress TGFβ signalling pathway

(A) The TGFβ signalling reporter ($CAGA_{12}$-luc) contains 12 binding sites of the Smad2/3/4 (GAGAC) binding consensus upstream of the firely luciferase-encoding gene in pGL3100ng $CAGA_{12}$-luc vector, and 10ng Renilla vector were co-transfected with either miR-29 family mimic (B) or miR-29b inhibitor (C) into SW1353 cells in monolayer. The non-targeting control (50nM) was also used as the negative control. 24 hours after transfection, cells were serum starved for another 24 hours, followed by treatment with TGFβ3 (4ng/ml) for another 6 hours before measuring luciferase activity. Renilla is the loading control for luciferase assay. Open bar: non – treatment control, close bar: TGFβ3 treatment. Means ± standard errors are presented, n=6. The difference of luciferase activity was analysed by Student's unpaired two-tailed t test. * $p<0.05$, ** $p < 0.01$, *** $p<0.001$

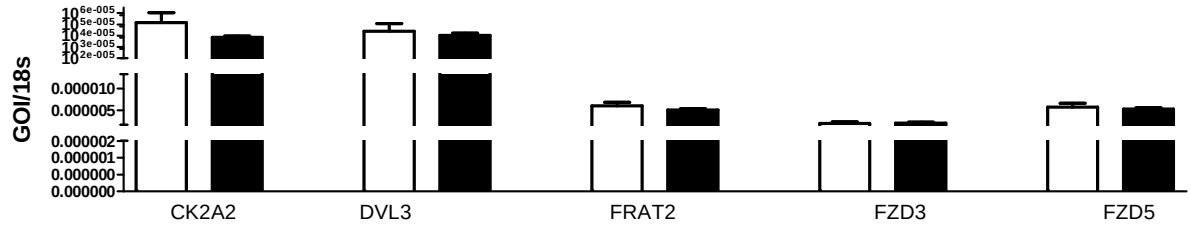

Figure 8 The miR-29 family does not target some of its putative targets at mRNA level Human primary chondrocytes was cultured in media with 10% (v/v) FCS in monolayer until 90% confluence. Cells were then transfected with either miR-29b mimic (50nM) or non – targeting control (50nM) for 48 hours. Total RNA was isolated and the expression levels of GOI were measured by qRT-PCR. 18S rRNA was the housekeeping control. Relative expression value of each of these genes was normalized to non – targeting control. Means ± standard errors are presented, n=3. The difference in expression between miR-29b overexpression and non – targeting control was analysed by Student's unpaired two-tailed t test. * $p<0.05$, ** $p < 0.01$, ***, $p<0.001$

THE ROLES OF THE MICRORNA 29 FAMILY IN CARTILAGE HOMEOSTASIS AND OSTEOARTHRITIS

LE THI TRUC LINH

THESIS SUBMITTED FOR THE DEGREE OF DOCTOR OF PHILOSOPHY

University of East Anglia

School of biological Sciences

Norwich, United Kingdom

December, 2014

DEDICATION

I would like to dedicate this thesis to my family

my parents

Mr Le Hung Son,

Mrs Le Thi Khanh Hong

my brother

Mr Le Hung Phong

for their constant love, friendship, support and encouragement throughout my life

ABSTRACT

MicroRNAs are short endogenous non-coding RNA molecules, typically 19-25 nucleotides in length, which negatively regulate gene expression. In osteoarthritis (OA), several genes necessary for cartilage homeostasis are aberrantly expressed, with a number of miRNAs implicated in this process. However, our knowledge of the earliest stages of OA, prior to the onset of irreversible changes, remains limited. The purpose of this study was to identify miRNAs involved across the time-course of OA using both a murine model and human cartilage, and to define their function.

Expression profile of miRNAs (Exiqon) and mRNAs (Illumina) on total RNA purified from whole knee joints taken from mice which underwent destabilisation of the medial meniscus (DMM) surgery at day 1, 3 and 7 post-surgery showed: the miRNA expression in whole mouse joints post DMM surgery increased over 7 days; at day 1 and 3, the expression of only 4 miRNAs altered significantly; at day 7, 19 miRNAs were upregulated and 15 downregulated. Among the modulated miRNAs, the miR-29b was the most interesting and was chosen to further investigate since integrating analysis of the miRNA and mRNA expression array data showed the inverse correlation between miR-29b and its potential targets. In end-stage human OA cartilage and in murine injury model, the miR-29 family was found to increase expression. Moreover, the miR-29 family was found to be the negative regulator in both human and murine chondrogenesis, and was also found to involve in murine limb development. Expression of the miR-29 family was found to suppress by SOX9 at least in part through directly binding to the promoter of the primary miR-29a/b1. Also, TGFβ1/3 decreased expression of the miR-29 family whilst Wnt3a did not have any effect. Lipopolysaccharide suppressed the miR-29 family expression in part through NFκB signalling pathway while the IL-1 strongly induced its expression partly through P38 MAKP signalling. Using luciferase reporter assay, the miR-29 family was showed to suppress the TGFβ, NFκB, and WNT/β-catenin signalling pathways. Gene expression profiles of gain- and-loss-of-function revealed regulation of a large number of previously recognised extracellular matrix-associated genes as well as an additional subset of protease and Wnt signalling pathway-related genes. Among these genes, *ADAMTS6, ADAMTS10, ADAMTS14, ADAMTS17, ADAMTS19, FZD3, DVL3, FRAT2, CK2A2* were experimentally validated as direct targets of the miR-29 family.

CONTENTS

LISTS OF TABLES

LISTS OF FIGURES

LISTS OF APPENDICES

Paper: Le et al, 2013

ACKOWNLEGMENTS

I would like to express my special appreciation and thanks to my primary supervisor Professor Ian Clark. I thank him for giving me the opportunity to become a Clark laboratory member and for allowing me to growth as a research scientist as I am now. I deeply appreciate the change to work and study from a great scientist and an honourable person like him. Without his time, support, guidance and encouragement, my PhD project is impossible.

I would also like to thank my second supervisor Professor Andrea Munsterberg for her comments, and suggestion which really helped me to refine my project. I am also in debted to Dr Tracey Swingler, my third supervisor. Her brilliant lab work skills, experiences, and knowledge tremendously help me go through all the obstacles and finish the study. Her time and her availability for all of my constant string of questions during the last 3 years are invaluable.

I am very thankful for all the past and current members of Clark laboratory for helping me on my research and make my PhD journey enjoyable. Special thank you to Dr Natalie Crowe for sharing with me her human osteoarthritis and normal articular cartilage samples, her dedifferentiation model which will take me a lot of time to do it myself. Thanks to Dr Rosemary Davidson for letting me including her DVL3 expression data in my thesis and for her knowledge, advice, support, and encouragement during my PhD. I would like to acknowledge Jonathan Green, Sarah Garner, Yvette Wormstone for their expertise and kind help in mouse injury model, human primary chondrocyte isolation, and cloning.

I would especially thank to Dr Guy Wheeler in Dalmay laboratory, Dr Geoffrey Mok, and Camille Viaut in Munsterberg laboratory for sharing their knowledge and help me through my whole mount in situ hybridization experiment. Thank you to Dr Eleanor Jones in Riley laboratory for kindly sharing with me her data and for her constantly help during my PhD. In addition, a thank you to Dr Helio Pais, who introduced me to bioinformatics analysis using R. His instruction about how to look for miRNA targets in big data set has become priceless to me. I would especially thank to Dr Mathew Barter in David Young laboratory, Newcastle University, members in Professor Tonia Vincent laboratory, Oxford University,

members of Dr Anne Delany laboratory, University of Connecticut, USA for kindly sharing with me their MSCs model, DMM samples, and vectors.

Great thanks to all of my friends for the time they shared with me throughout my PhD journey. I am grateful their incredible friendship which makes the journey to achieve my goal more enjoyable.

Finally, I would like to acknowledge Vietnam Ministry of Education and Training (project 322), University of Each Anglia scholarship for international student for giving me the opportunity to do PhD in the UK. I also deeply thank Arthritis Research UK (program grant #19424, Tracey Swingler, Ian Clark) for supporting my project. Due to the currency exchange rates and the international fees, there are minimal funds from my Vietnam Government Scholarship for laboratory consumables. Thus, my PhD project is impossible without the support from Arthritis Research UK. I also acknowledge the John and Pamela Salter Trust for supporting me with the LNA probe for miR-29b used in my project.

CHAPTER 1
INTRODUCTION

1.1. Synovial joints

In mammals, joints are functionally classified into 3 categories: synarthroses (immovable joints), amphiarthroses (slightly movable joints), and diarthroses (freely movable joints). Most of the main joints of the appendicular skeleton are synovial joints, suggesting this type of joint has a crucial role in the body. The main component of synovial joints includes **the hyaline cartilage**, also known as articular cartilage, covering the bone of the synovial joint providing the cartilage lubricating and shock absorbing characteristics; **a capsule** enclosing the joint in line with **synovial membrane** which contains synovial membrane-resident cells secreting synovial fluid into the synovial cavity helping reduce friction, enabling free movement; **bones**, further held together by **ligaments**. The characteristics of some important components of the synovial joint relevant to this PhD thesis are described below.

1.1.1. Articular cartilage biology

Articular cartilage, a highly specialized tissue with unique mechanical behaviour, consists of **(i) chondrocytes,** the only cells, responsible for the homeostasis of extracellular matrix (ECM), and **(ii) a dense layer of ECM** composed primarily of water, collagen and proteoglycan.

1.1.1.1 Cartilage structural organization

Healthy articular cartilage comprises four different areas: the superficial, intermediate, radial or deep, and calcified zones (Buckwalter *et al.* 2005, Dudhia 2005, Pearle *et al.* 2005, Aigner *et al.* 2006, Martel-Pelletier *et al.* 2008, Umlauf *et al.* 2010, Houard *et al.* 2013) **(Figure 1.0)**. Each is characterized by a particular chondrocyte phenotype, and by distinctive extracellular matrix organization and composition (Buckwalter et al. 2005).

The superficial zone, the articulating surface and the thinnest of the four, makes up 10%-20% of articular cartilage thickness (Buckwalter et al. 2005, Pearle et al. 2005). This

region contains a high amount of collagen (primary type II, and IX) but very low amount of proteoglycan. The collagen fibrils are densely packed and aligned paralleled to the articular surface. Chondrocytes in this layer are characterized by an elongated appearance (Pearle et al. 2005), express many proteins having lubricating and protective functions (e.g. lubricin) but relatively little proteoglycan. This zone is in contact with synovial fluid, and is responsible for most of the tensile properties of cartilage that enable cartilage to resist shear and the tensile and compressive forces imposed by the movement of the articulation (Martel-Pelletier et al. 2008).

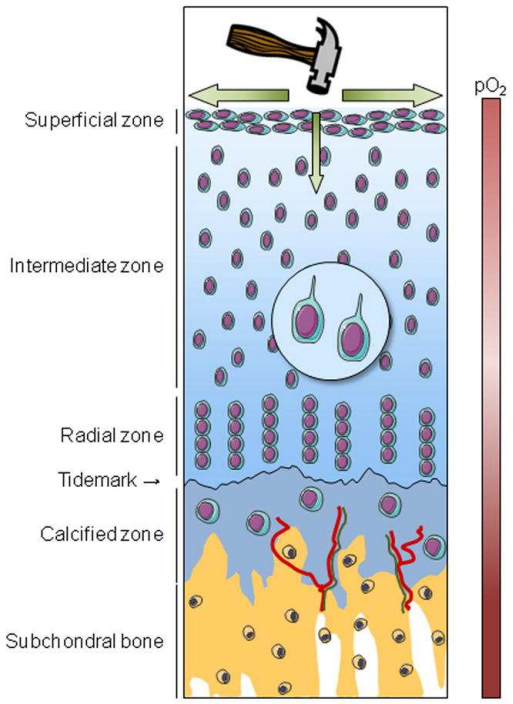

Figure 1.0: Histology of a healthy cartilage structural

The articular cartilage is organized into superficial, intermediate, radial, and calcified zones. Each zone can be distinguished by the difference in chondrocyte morphologies and components of collagen, proteoglycan, mineral and water

The intermediate and the radial zones contain large diameter collagen fibrils oriented perpendicular to the articular surface. These regions also have high amount of proteoglycan which is mainly aggrecan, a large chondroitin sulphate proteoglycan. Chondrocytes in the middle zone are more round than in the superficial zone. In the radial zone, the cells are arranged in columnar fashion (Buckwalter et al. 2005).

The tide mark, a thin line revealed after hematoxylin staining, marks the mineralization front between the calcified and non-calcified articular cartilage (Houard et al. 2013). In **the calcified cartilage zone**, the cell population is very scarce and chondrocytes are hypertrophic (Pearle et al. 2005, Martel-Pelletier et al. 2008). With aging, bloods vessels and nerves can be seen in calcified cartilage arising from the subchondral bones (Lane *et al.* 1977). The main function of this zone seems to be to anchor the cartilage to the bone as collagen fibrils from the radial zone penetrate into the calcified cartilage.

Furthermore, it is noteworthy to know that for mechanical protection purposes, in articular cartilage, the chondrocyte is surrounded by a pericellular matrix and a territorial cartilage matrix forming a capsule-like structure around the cells. Whilst the pericellular matrix is made of a thin layer of non-fibrillar material, which most likely represents the synthetic products of the chondrocytes, such as proteoglycans and glycoproteins, the pericellular matrix also contains a dense meshwork of thin collagen fibers (see below) (Dudhia 2005, Aigner et al. 2006, Martel-Pelletier et al. 2008, Heinegard *et al.* 2011).

1.1.1.2 Biology of chondrocytes

As mention above, chondrocytes are the only cellular components of articular cartilage, make up 5% of the wet weight of articular cartilage, and are surrounded by a pericellular matrix containing type VI collagen, microfibrils, hyaluronic acid, biglycan, and decorin but little or no type II collagen (Buckwalter et al. 2005, Dudhia 2005, Heinegard and Saxne 2011). The arrangement of chondrocytes and articular cartilage specific organisation result from a complex development process called endochondral ossification including four steps e.g. chondrogenesis, chondrocyte differentiation and hypertrophy, mineralization and invasion of bone cells, and finally the formation of bone (DeLise *et al.* 2000, Goldring *et al.* 2006, Goldring 2012). Chondrocytes arise from mesenchymal progenitors as a result of chondrogenesis started with the condensation of mesenchymal stem cell (expressing collagens I, III and V), and followed by the differentiation of chondroprogenitor cell (expressing cartilage-specific collagens II, IX and XI) (Goldring et al. 2006). After chondrogenesis, the chondrocytes remain as resting cells to form the articular cartilage or undergo proliferation, terminal differentiation to chondrocyte hypertrophy, and apoptosis.

There are no blood vessels in articular cartilage, thus the cells rely on diffusion from articular surface or subchondral bone for nutrients and metabolites. Importantly, the oxygen level in the cartilage matrix is quite low, ranging from 10% at the surface to less than 1% in the deep zone (Silver 1975), suggesting the cells have to adapt to this low oxygen level. The mechanisms of this adaption remain unclear but some published data reported the involvement of hypoxia inducible factor -1 alpha (HF-1α) (Schipani *et al.* 2001, Pfander *et al.* 2003). Hipoxia via HIF-1α can stimulate chondrocytes to express a number of genes associated with cartilage anabolism and chondrocyte differentiation like SOX9, TGFβ (Amarilio *et al.* 2007).

1.1.1.3 Biology of cartilage extracellular matrix

Together with chondrocytes, extracellular matrix (ECM) produced by these cells is among the main components of articular cartilage and its integrity is critical for the cartilage biochemical properties and joint physical function.

About structure, the ECM in articular cartilage is organized into pericellular, territorial, interterritorial zones, each of which is represented at specific distance from the chondrocytes (Dudhia 2005, Heinegard and Saxne 2011) (**Figure 1.1**).

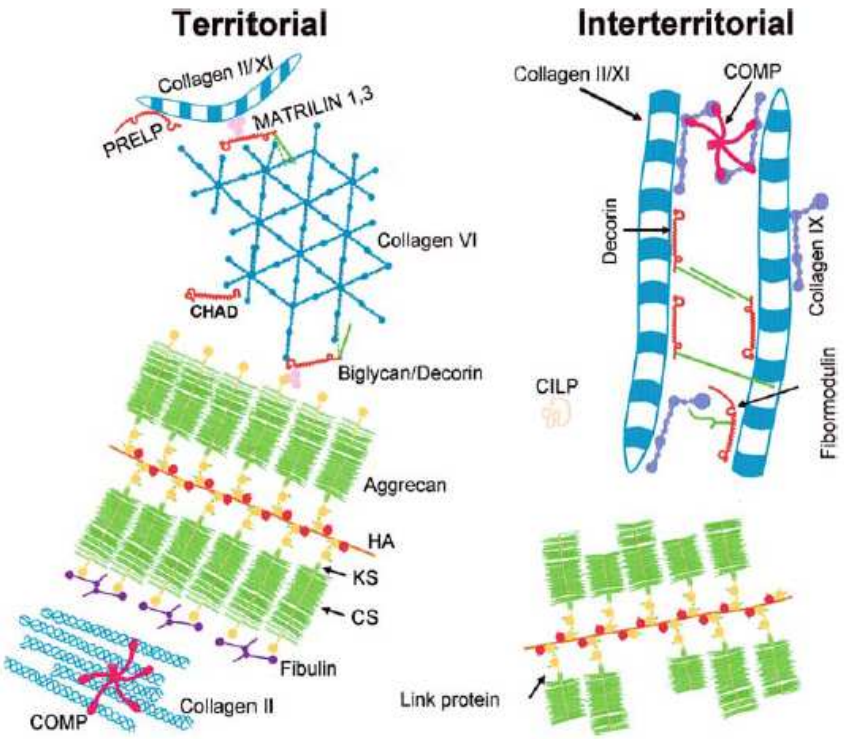

Figure 1.1: **Molecular organisation of normal articular cartilage.**

The cartilage matrix surrounding chondrocytes in healthy articular cartilage is arranged into zones defined by their distance from the cell. Pericellular matrix lies immediately around the cell and is the zone where molecules that interact with cell surface receptors are located. Next to the pericellular matrix, slightly further from the cell, lies the territorial matrix. At largest distance from the cell is the interterritorial matrix (adapted from Heinegard et al, 2011) (Heinegard and Saxne 2011)

Biochemically, of the ECM, approximately 70% is water (Pearle et al. 2005) , and 30% left is solid, of which 5-6% are inorganic compounds (hydroxyapatite), and the remaining 25% are organic compounds. Of the organic components, type II collagen constitutes 68% and the 32% left is formed by proteoglycan (mainly aggrecan) (Martel-Pelletier et al. 2008). The biology of aggrecan and collagen and their functions in articular cartilage are described as below.

1.1.1.3.1 Aggrecan

Molecules made up of a core protein attached to glycosaminoglycan chain are referred as proteoglycan. In articular cartilage, the most abundant proteoglycan is aggrecan, composed of chondroitin sulphate chains and keratan sulphate chains with N- and O-linked oligosaccharides. Aggrecan has three globular domains (G1, G2 and G3) and three extended domains (IGD, KS and CS). The N-terminal G1 domain, responsible for aggrecan-hyaluronan interaction, is followed after the signal peptide. The inter-globular (IGD) connects G1 and G2 domains, whose functions are unclear. Keratan sulphate binding (KS) and chondroitin sulphate (CS) domain lie between G2 and G3 domains (Kiani *et al.* 2002, Dudhia 2005, Martel-Pelletier et al. 2008, Heinegard and Saxne 2011) (Figure 1.2).

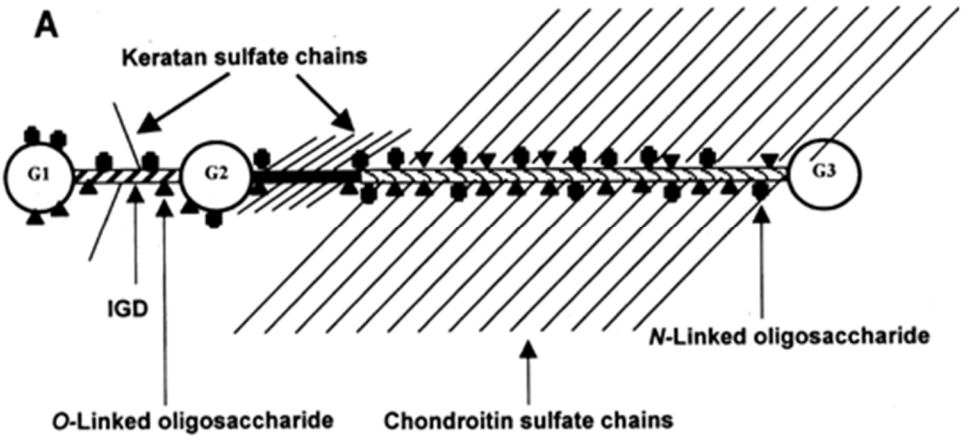

Figure 1.2: Aggrecan structure.

Aggrecan consists of 3 globular domains (G1, G2, and G3) and an attached GAG chain structure. The GAG attachment region is separated into keratin sulphate binding (KS) domain and chondroitin sulphate (CS) domain (Adapted from Kiani et al, 2002) (Kiani et al. 2002).

The chondroitin sulphate domain is the largest domain of aggrecan and is composed of around 100 chondroitin sulphate chains (typically around 2kDa each). Each chain is made up of some 50 disaccharides of glucuronic acid and N-acetylgalactosamine, with a sulphate group in the 4- or 6- position. The negatively-charge chondroitin sulphate chain accounts for the major function of aggrecan as a structural proteoglycan. The function of the keratan sulphate domain is not very clear but may be involved in the tissue distribution of aggrecan. There are about 30 KS chains, usually of small size (5-15 kDa), attached to the mature aggrecan molecule.

Chondroitin sulphate, keratan sulphate, and the interaction of aggrecan and hyaluronic acid are responsible for retaining water the cartilage. The interaction between aggrecan and collagen fibrils makes the ECM highly hydrophilic, leading to high resistance to compressive mechanical loads (Dudhia 2005, Martel-Pelletier et al. 2008).

1.1.1.3.2 Collagen

Collagen fibrils are composed of a protein macromolecular providing cartilage with resistance to tension. Collagen type II constitutes 85% total collagen content in the ECM of articular cartilage. Apart from type II Collagen, ECM also contains other collagens called minor collagens since their concentration is low in comparison with the type II collagen. A list of these collagens is provided in Table 1.1.

All fibril collagens are synthesized in the form of three polypeptide α-chains as a procollagen in which each chain has an N-terminal extension and a C-terminal extension. The three chains are covalently linked via disulphide bridges in the C-terminal propeptide. Following or during secretion of procollagens into the extracellular matrix, the terminal propeptides are cleaved off by specific proteinases e.g. ADAMTS-2, ADAMTS-3, ADAMTS-14 (cleaves the N-terminal) (Lapiere *et al.* 1971, Fernandes *et al.* 2001, Colige *et al.* 2002), and BMP-1 (cleaves the C terminal) (Wermter *et al.* 2007) to produce the mature collagen molecules. The mature collagens then spontaneously self-assemble into

cross-striated fibrils in the extracellular matrix. The fibrils are stabilized by covalent cross-linking (Figure 1.3)

Collagen molecules then associate on a core of two homologous collagen XI and two collagen II molecules to form an outer shell of 10 collagen II molecules of the micro fibril. In addition to collagen type II, fibers contain other collagens, particular collagen type IX. The collagen network is then stabilized by the formation of covalent crosslinks that link the collagen II chains. The links formed are both intra- and inter-molecules, for example, between the chains of collagen XI, between collagens e.g. collagen II and collagen IX.

Many other proteins also have a high affinity for collagens including thrombospondins, leucine-rich repeat proteins (biglycan, decorin, fibromodulin, lumican), matrillins, and fibronectin. Some of these interactions support fibre formation while others modify the collagen fibre surface to provide sites for interactions with neighbouring structures (Heinegard and Saxne 2011).

Collagen types	Characteristics
Type IX	Located on the surface of type II collagen fibrils; promotes the binding of the fibrils to other components of the matrix and to each other; carries a glycosaminoglycan chain.
Type XI	Forms the core of the same fibrosis. Regulates the formation and the diameter of the fibrils
Type V	Sometimes replaces the type XI collagen in cartilage; included in type I collagen fibrils in other tissues. Data on the composition and structure of the third a-chain are contradictory
Type III	Small amount are covalently bound to type II collagen
Type XII	Very small amounts are present on the surface of type II collagen
Type XIV	Very small amounts are present on the surface of type II collagen
Type VI	As in other tissue, forms a network of microfibrils. Concentrated mainly in the pericellular areas, provides a connection between the chondrocytes and the matrix
Type X	Expressed only by hypertrophic chondrocytes in cartilage areas undergoing ossification
Type XXVII	Expressed in cartilage tissue

Table 1.1 Minor collagen of cartilage tissue (adapt from Omelyanenko et al, 2014)(Petrovich *et al.* 2014)

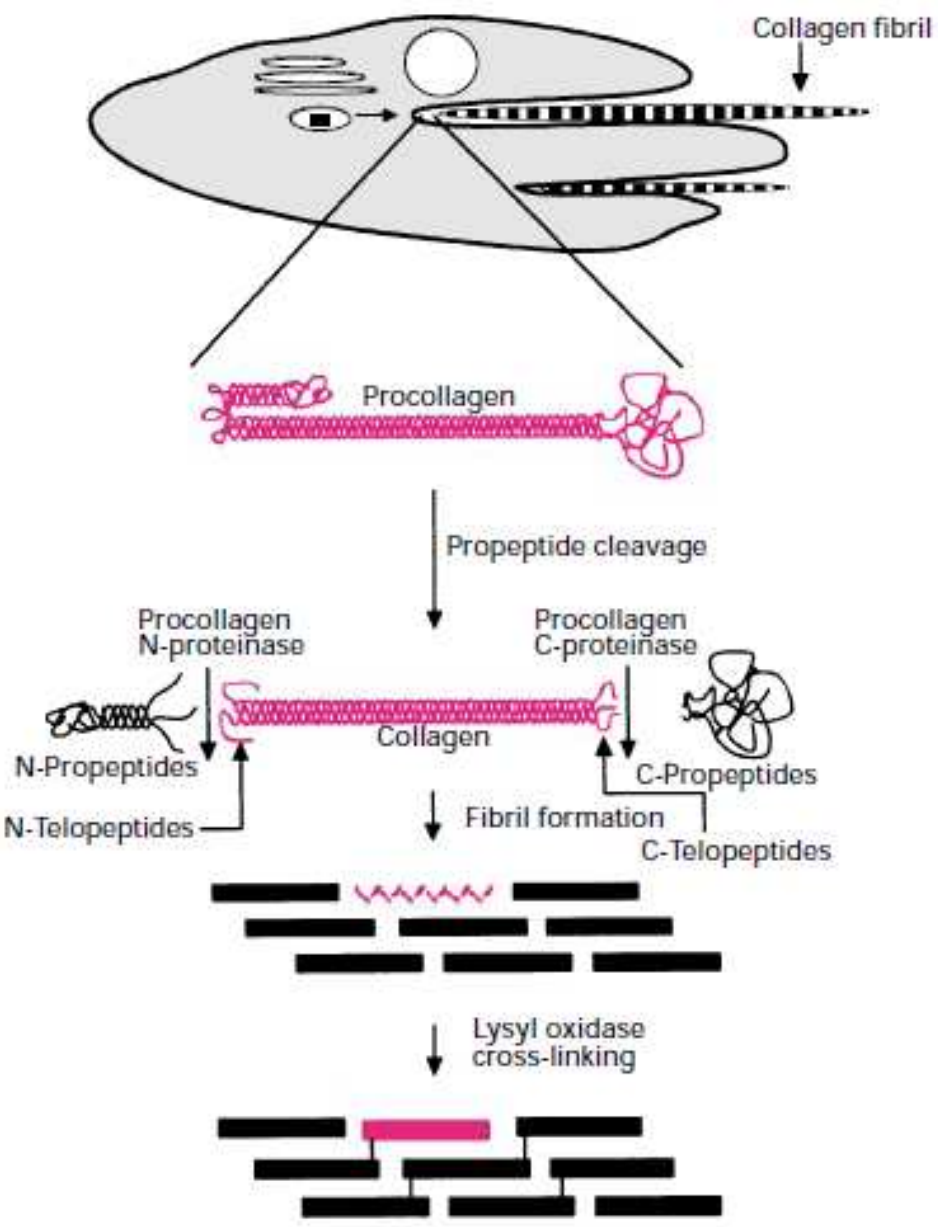

Figure 1.3: The formation of the fibrillar collagens

Procollagen is secreted from cells and converted into collagen by removal of the N- and C-propeptids by pro-collagen metalloproteinases. This produces mature collagen that spontaneously self-assembles into cross-striated fibrils which are stabilized by covalent cross-linking. Taken from (Kadler et al, 1996)(Kadler *et al.* 1996).

1.1.2. Synovium

Synovium is a thin tissue only a few cell layers thick (Fell 1978). The synovium acts as the controller for the environment within the joint where nutrients for chondrocytes can pass into the synovial cavity. Also, the synovium gives the joint its mechanical properties. The synovium can be divided into two compartments e.g. the synovial lining and the sub-lining. The synovial lining contains two cell types e.g. **type A (macrophage-like cells)** clearing all excess materials and potential pathogens from the joint, producing and secreting a number of enzymes and cytokines and chemokines that mediate tissue damage and inflammation in disease; **type B synoviocytes**, **fibroblast like cells**, producing the main component of synovial fluid, hyaluronan. The synovial sublining consists of connective tissue containing blood vessels, fibroblasts, adipocytes, and a limited number of resident immune cells, such as macrophage and mast cells (Smith *et al.* 2003). The synovial fluid has crucial role for lubrication of the joint and for transporting nutrients and oxygen to the cartilage.

1.1.3. Bone

Periarticular bone can be separated into distinct anatomic entities e.g. the subchondral bone plate, the subchondral trabecular bone, and the bone at the joint margins. The subchondral bone plate consists of cortical bone, which is relatively nonporous and poorly vascularized. It is separated from the overlying articular cartilage by the zone of calcified cartilage.

Bone is a very dynamic tissue with constantly undergoing remodelling in which bone resorption is normally followed by new bone formation. The primary cell responsible for bone resorption is the **osteoclast**, a specialized multinucleated cell of hemopoietic origin (Roodman 1999). Bone resorption takes place under a specialized area of the osteoclast cell membrane called “ruffled border,” which comprises a sealed lysosomal compartment where the acidic pH solubilizes the mineral and proteolytic enzymes digest the matrix. On the contrary, **osteoblasts**, the bone forming cells, originally from MSCs committed to osteoblastic lineage. Osteoblasts synthesize and secrete most of the proteins of the bone matrix, including type I collagen and non-collagenous proteins (Caetano-Lopes *et al.* 2007). In normal physiological condition, the amount of bone removed during the resorption and formation phases is balanced such that bone mass is maintained.

1.2. Osteoarthritis

Osteoarthritis (OA) is defined by the American College of Rheumatology as a "heterogeneous group of conditions that lead to joint symptoms and signs which are associated with defective integrity of articular cartilage, in addition to related changes in the underlying bone at the joint margins''.

There are more than 100 types of arthritis. However, OA or degenerative joint disease is the most common type. From a clinical point of view, OA can be classified into two categories e.g. **primary** which refers to its occurrence not related to any prior condition or event which is also referred as idiopathic, and **secondary** which refers to the development of the disease after trauma or pre-existing condition.

The disease most commonly affects the middle-age and elderly, although it may begin earlier as result of injury, obesity or congenitally. As a greater proportion of the population is old aged and with increasing obesity, OA will have a great impact on society in the future with enormous socioeconomic costs.

1.2.1. Osteoarthritis pathology

It is now considered that OA is a disease of the whole joint as an organ resulting in "joint failure" where all major components of the joint e.g. the cartilage, the synovium, and the underlying bone are affected (Loeser *et al.* 2012). The pathologic changes seen in OA include cartilage destruction, fibrosis of the synovial capsule, hyperplasia of the synovial membrane, osteophyte formation, the subchondral bone thickening (**Figure 1.4**) (Aigner et al. 2006, Loeser et al. 2012). These changes result from an incompletely understood series of functional events.

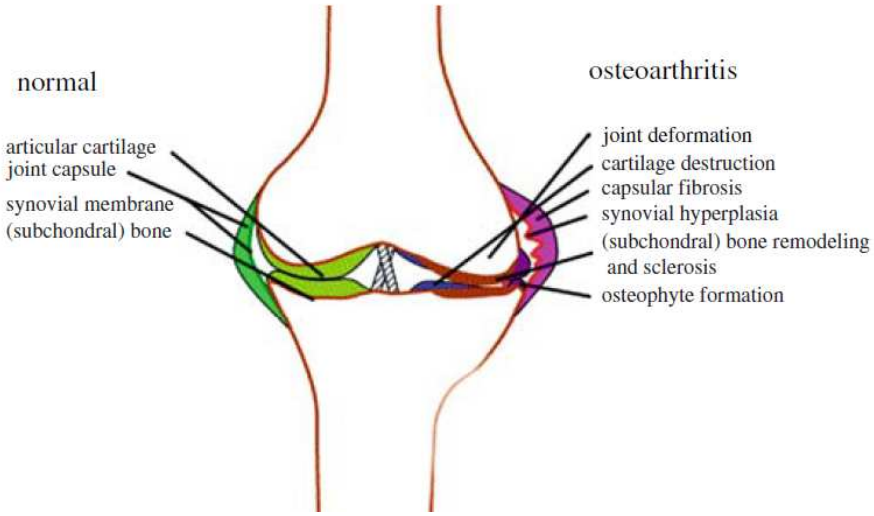

Figure 1.4: Overview of the pathologic changes associated with OA.

In a normal joint, the subchondral bone is covered by a thick layer of articular cartilage and the joint is enclosed in a capsule where the synovial membrane lies. In an OA joint, articular cartilage is destroyed, the subchondral bone is remodelled (thickens), the synovial capsule is fibrosed and osteophytes are formed (reprinted from Aigner et al, 2006) (Aigner et al. 2006)

1.2.1.1.Articular cartilage destruction in osteoarthritis

Biochemical, genetic factors, and mechanical stress contribute to the OA lesion in cartilage, leading to articular cartilage degradation, and chondrocyte metabolism disorders as a consequence. Articular cartilage degeneration is a two phase process controlled mainly by chondrocytes e.g. a short biosynthesis phase where the cells attempt to repair the damaged ECM, followed by the degenerative phase, where the cells destroy the articular cartilage by increasing the synthesis of matrix degradating proteinases and decreasing their synthesis of matrix components, in particular of aggrecan. Besides changes in synthesis and degradation, other aberrant behaviours in cell proliferation and death, and phenotypic modulation are also observed in OA chondrocytes (Sandell *et al.* 2001).

Contrary to normal chondrocytes with no proliferative activity, OA chondrocytes have a low proliferative activity (Meachim *et al.* 1962, Rothwell *et al.* 1973, Lee *et al.* 1993), explained in part due to the better access to proliferation factors from the synovial fluid as well as due to the damage of the ECM (Meachim and Collins 1962, Lee et al. 1993), subsequently causing chondrocyte clustering, a characteristic feature of OA cartilage. Chondrocyte death, caused by apoptosis, necrosis, or other cell death mechanisms such as chondroptosis, is another known feature of OA. Many studies have demonstrated the significant correlations between chondrocyte death and severity of OA and aging. These changes are associated with the production of reactive oxygen species, a lack of growth factors, release of glycosaminoglycan and mechanical injury. However, which of these types of cell death predominate in OA is debatable. The detection of specific form of cell death in articular cartilage is difficult in which current gold standard for detecting chondrocyte death is electron microscopy which suggests that the morphological changes of chondrocytes in OA cartilage are attributed to apoptosis and / or chondroptosis. Chondrocyte death by apoptosis has been reported play an important role: normal cartilage explants or chondrocyte culture exposed to nitric oxide, collagenase, anti CD-59, or mechanical factors e.g. shear strain, loading strain induced apoptosis; cartilage from equine joints have shown that chondrocyte apoptosis is positively correlated with early stages of OA and severity of cartilage damage (Zamli *et al.* 2011).

When the damage occurs, the chondrocytes attempt to repair the damaged matrix by increasing their anabolic activity to enhance ECM synthesis. However, a net loss of ECM content is one of the hallmarks of all stages of OA, suggesting the dominance of ECM degradation over the synthesis. This is characterized by the increase in expression and activation of matrix-degrading enzymes e.g. matrix metalloproteinase (MMPs) and aggrecanases (from the ADAMTS family) (Buckwalter et al. 2005, Pearle et al. 2005, Aigner et al. 2006, Umlauf et al. 2010, Loeser *et al.* 2012). **The MMPs,** belonging to a family of zinc-dependent proteases, show activation correlating with cartilage degradation. Among these, the groups of collagenases 1, 2, 3 (MMP-1, MMP-8, and MMP-13, respectively), stromelysins (MMP-3, MMP-10, MMP-11) and gelatinases (MMP-2, MMP-9) have the highest impact on OA cartilage breakdown (Burrage *et al.* 2006). The MMP-1, MMP-8 and MMP-13 which cleave native fibrillar collagen, contribute to the pathological cleavage of collagen fibrils in OA (Burrage et al. 2006). Of the collagenase group, MMP-13 is deemed to be responsible for most of the collagen II breakdown whilst MMP-1 cleaves type II collagen stronger than MMP-8 (Billinghurst *et al.* 1997) has a pivotal role for collagen cleavage in OA (Knauper *et al.* 1996). In addition to collagenases, others MMPs degrading non-collagen have also been shown to be elevated in OA cartilage e.g. the gelatinases (which cleave denatured collagen, gelatin, type V collagen) and the stromelysins (having substrate preference for proteoglycans, elastin, laminin, fibronectin) (Umlauf et al. 2010) **The aggrecanases** (the ADAMTS family), are also of particular importance in cartilage turnover, and have activity against the proteoglycan aggrecan. Of all ADAMTS members, ADAMTS-4 and ADAMTS-5 are most active against aggrecan (Arner 2002). ADAMTS-5 is constitutively expressed in chondrocytes whereas ADAMTS-4 expression is stimulated by proinflammatory cytokines IL-1β, and TNF-α (Umlauf et al. 2010) (Tortorella *et al.* 2001). In vitro studies with human cartilage show that both ADAMTS-4 and ADAMTS-5 contribute to ECM breakdown during the disease progression even though human recombinant ADAMTS-5 has higher rate of aggrecan cleavage than ADAMTS-4 (Song *et al.* 2007). In mice, ADAMTS-5 has been shown to be the major aggrecanase, by studies with ADAMTS-4 and ADAMTS-5 knockout mice in which only ADAMTS-5 deficiency prevented the mice from cartilage degradation in both inflammatory and a joint-instability model of arthritis (Glasson *et al.* 2005, Stanton *et al.* 2005) .

As mentioned above, despite the attempt at repairing the ECM, the damage to the cartilage becomes irreversible because the adult chondrocytes fail in regenerating the normal cartilage matrix structure. This failure could be, in part, attributed to the phenotypic alteration of chondrocytes. Chondrocyte phenotypes are categorized largely by subtyping collagen expression e.g. chondroprogenitor cells express type IIA procollagen. The alternative splice variant) (Sandell *et al.* 1991), mature chondrocytes are marked by expressing type IIB procollagen, IX, and XI, aggrecan and link protein (Sandell and Aigner 2001), and hypertrophic chondrocytes express type X collagen (Schmid *et al.* 1985). In OA cartilage degeneration, an important proportion of adult articular cartilage chondrocytes, found mostly in the middle zone, re-expressed type IIA procollagen (chondroprogenitor cells) in both early and late OA stages (Sandell and Aigner 2001). Cells in the upper middle zone mainly express type III collagen which is a fibroblast-like phenotype. This phenotype is normally observed in vitro, where the chondrocyte phenotypes are modulated through so-called "dedifferentiation" process by several factors like retinoic acid or IL-1. Dedifferentiated chondrocytes are still very active, express collagen types I, III and V but stop expressing aggrecan and collagen type II (Sandell and Aigner 2001). In the deepest zone of OA cartilage, the cells start to express type X collagen, specific marker for hypertrophy of growth-plate chondrocytes (Girkontaite *et al.* 1996). Indeed, the hypertrophic chondrocytes in OA cartilage and in the growth-plate share similarities and the subsequent functional event associated with hypertrophic differentiation is cartilage mineralization which is also a feature of OA. However, the mechanism involved in pathological cartilage calcification during OA is not completely understood.

1.2.1.2. Synovium in osteoarthritis

Inflammation of the synovial membrane (synovitis) is identified in many OA patients despite lower severity and greater variability as compared to rheumatoid arthritis. It is reported that synovitis can occur even in early stages of the disease (Benito *et al.* 2005). Synovitis is associated with symptoms such as pain, the degree of joint dysfunction, the rapid degeneration of cartilage, and is characterized by the thickening of the synovial lining layer, leukocyte infiltration, and thickening of the sub-lining stroma. The

mechanisms underlying the development of synovitis in OA remain unclear. It is however well known that this inflammatory process is triggered by ECM degradation products, which engage Toll-like receptors and the complement cascade (Scanzello *et al.* 2012). Noteworthy, the synovial reaction may produce a variety of cytokines and chemokines, in turn affecting catabolism of chondrocytes (Scanzello and Goldring 2012).

Of all cell types in the inflamed OA synovium, the macrophages are among the most abundant and depletion of synovial macrophages has been shown to result in decreased osteophyte formation, and IL-1, TNF-α, IL-6, IL-8, MMP-1, MMP-3 production (Bondeson *et al.* 2010). Natural killer cells and dendritic cells are also reported to present in synovial tissue. However, the role of both of them in OA pathogenesis has not yet been elucidated in detail.

1.2.1.3. Subchondral bone in osteoarthritis

Articular cartilage helps to distribute load across the whole joint surface. Any alteration in the properties of cartilage leads to alter load experience by the underlying bone and probably causes a tissue remodelling response. The properties of bone might also modulate how the overlying cartilage reacts to load.

Although OA is often characterized as a disease of articular cartilage, the alteration of bone metabolism is increasingly recognised as a mediator of pain and OA progression. Subchondral bone consists of a dome-like subchondral plate and underlying trabeculae, having a close biomechanical and biochemical relationship with the overlying cartilage. Strong evidence associates subchondral bone alterations with cartilage damage and loss in OA (Karsdal *et al.* 2014). However, there is still an incomplete understanding of the mechanisms for the numerous pathophysiological alterations detected in subchondral bone with OA.

The pathological cascade may be started when the normal subchondral bone suffers from a non-physiological strain. In early-stage OA, the subchondral plate becomes thinner and more porous, together with initial cartilage degeneration. Subchondral trabecular bone also deteriorates, with increased separation and thinner trabeculae. At the same time, microdamage begins to appear in both calcified cartilage and subchondral bone, which will persist throughout the whole pathological process. In late-stage OA, calcified cartilage and the subchondral plate become thicker, with duplicated tidemarks and progressive non-calcified cartilage damage. Subchondral trabecular bone becomes sclerotic (Li *et al.* 2013).

The sclerosis of periarticular mineralized tissues may be a biomechanical compensational adaption to the widespread cysts and microdamage in subchondral bone, which render subchondral bone structure more fragile (Figure 1.5).

Despite increased bone volume density in the sclerotic subchondral bone, its mineralization is reduced and lower than in normal joints. Although collagen synthesis is elevated in subchondral bone, the deposited collagen is hypomineralized and has a markedly reduced calcium-to-collagen ratio [42].

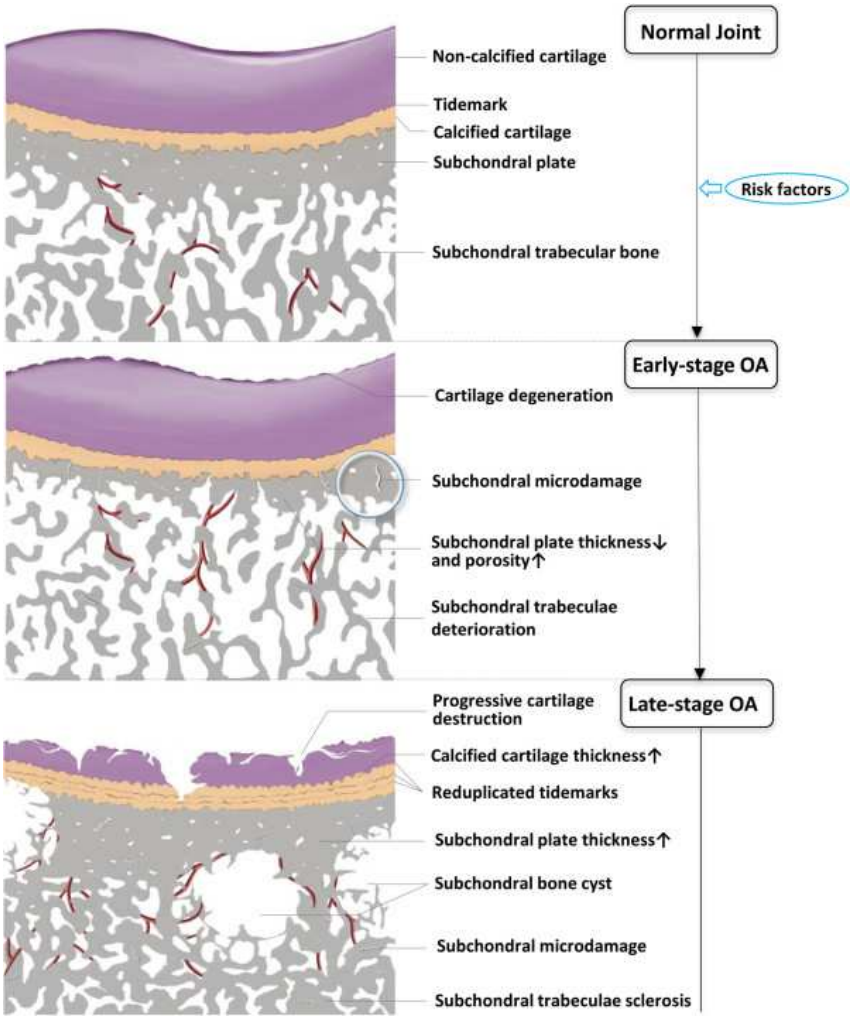

Figure 1.5: Alteration in subchonral bone in Osteoarthritis

In early stage of OA, subchondral microdamage occurs, the subchondral plate is thinner with increased porosity, and subchondral trabeculae are deteriorated. At OA later stage, the calcified cartilage and subchondral plate is thicker, with reduplicated tidemarks. Subchondral trabecular bone becomes sclerotic (adapted from Li et al, 2013)(Li et al. 2013)

1.2.1.4. Osteophytes

Osteophytes, considered as an adaptation to the altered biomechanics, are non-neoplastic osteo-cartilaginous protrusions growing at the margins of OA joints, and represent areas of new cartilage and bone formation. Osteophytes limit joint movement, represent a source of joint pain, and are a radiographic hallmark of OA. However, it is noteworthy that when osteophytes appear in the absence of other bony changes, e.g. subchondral cysts or subchondral sclerosis, they may be a manifestation of aging, rather than of OA.

Osteophytes derive from precursor cells within periosteal or synovial tissue (van der Kraan *et al.* 2007) but the initial stimuli for osteophyte formation remains unclear, probably involving both mechanical and humoral factors as repeated injections of mouse joints with TGFβ or BMP induced or enhanced osteophyte formation in animals with experimentally induced OA (van Beuningen *et al.* 1998).

Osteophytes are composed of cells that express type I procollagen mRNA, mesenchymal prechondrocytes that express type IIA procollagen mRNA, and maturing chondrocytes that express type IIB procollagen mRNA. Based on the spatial pattern of gene expression and cytomorphology, the neochondrogenesis associated with osteophyte formation closely resembles that of healing fracture callus (Matyas *et al.* 1997) and is also similar to the growth plate. Thus, osteophytes may represent an excellent *in vivo* model for induced cartilage repair processes.

1.2.2. Anabolic and catabolic signalling in OA

Anabolic and catabolic activation are largely the result of exposing cells to various cytokines and growth factors e.g. TGFβ, BMPs, IGF-1, TNF-α, IL-1β, Wnt3a. In OA cartilage, the catabolic and anabolic equilibrium is broken and favours the activation of catabolic pathways or mechanisms leading to matrix degradation.

1.2.2.1.Anabolic signalling in OA

As previously mentioned, the early phase of the response to mechanical injury is characterized by the attempt to repair the damage matrix by increasing the anabolic activity of chondrocytes, enhancing synthesis of extracellular matrix components. This is facilitated by enhancing levels of anabolic factors e.g. TGFβ, FGF, and BMPs, and Wnt.

1.2.2.1.1. TGFβ signalling

The TGFβ family, consisting of over 35 members including TGFβ and BMPs, has been widely known to play a crucial role in the development and homeostasis of various tissues. Activated TGFβ (TGFβ-1, -2, -3) binds to their two receptor complex, TGFβ-R1 and TGFβ-RII and phosphorylates members of the receptor-specific Smad family, Smad2 and Smad3. Upon phosphorylation, Smad2/3 subsequently forms a complex with the common mediator Smad4. This complex then translocates into the nucleus where it can act as a transcription factor. Unlike TGFβ-1, -2, -3 which signal via Smad2/3/4, BMPs transduce their signal through Smad-1, -5 and -8 (Miyazawa *et al.* 2002, Verrecchia *et al.* 2002).

Members of the TGFβ family are considered potent mediators of cartilage matrix synthesis, in which they up-regulate the expression of several types of collagens and proteoglycan but down-regulate cartilage degrading enzymes (Verrecchia *et al.* 2001, Verrecchia and Mauviel 2002). Despite such promising data, therapeutic studies with TGFβ revealed major side effects e.g. injection or adenovirus–mediated delivery of TGFβ1 into normal murine knee joint resulted in joint fibrosis and osteophyte formation (van Beuningen et al. 1998) .

1.2.2.1.2. Wnt signalling

The human Wnt family includes 19 members which mostly exert their function by binding to Frizzled (FZD) receptor proteins and LRP-5/6 co-receptor proteins, in turn activating several signal transduction pathways e.g. canonical, and non-canonical signalling pathways. In the canonical Wnt pathway, most β-catenin in the cytoplasm is sequestered and targeted for proteasome-mediated degradation within a multi-protein complex of casein kinase, axin, the adenomatous polyposis coli tumour suppressor protein (APC) and glycogen synthase kinase 3β (GSK3β). With the presence of appropriate Wnt ligands, signalling through the Frizzled receptors inhibits this degradation process, and thereby leads to β-catenin accumulation and translocation into the nucleus (Clevers 2006). Within the nucleus, it acts in concert with Tcf/Lef transcription factors to generate a transcriptionally active complex that regulates a number of genes e.g. MYC, cyclin D1, MMP3 and CD44, E-cadherin, MMP7, MMP26(Dell'accio *et al.* 2008, Umlauf et al. 2010). In contrast to the canonical pathway, non-canonical Wnt signalling is mostly a β-catenin independent mechanism like the Wnt/calcium and Wnt/JNK pathways in vertebrates and the Wnt/planar cell polarity pathway (PCP) in flies (Willert *et al.* 2006). In addition, there

are some natural extracellular inhibitory factors for Wnt signalling. One of the best characterized families is the Dickkopf (Dkk) family which bind to LRP-5/6 and antagonize the canonical pathway. Other antagonists are the secreted frizzled-related protein (sFRP) family which bind directly to Wnt ligands and inhibiting both canonical and non-canonical Wnt pathways (Kawano *et al.* 2003).

A number of published data provide evidence of the critical role of Wnt signalling in OA development. Direct evidences come from animal model studies where β-catenin is conditionally activated or inhibited in articular cartilage chondrocyte of adult mice (Zhu *et al.* 2008, Zhu *et al.* 2009). Mice with β-catenin activated had OA-like cartilage degradation, osteophyte formation, associated with accelerated chondrocyte maturation and MMP13 expression (Zhu et al. 2009). Similarly, selective suppression of β-catenin signalling in Col2a1-ICAT (inhibitor of β-catenin and TCF) transgenic mice also causes OA-like cartilage degradation(Zhu et al. 2008). In line with these reports, in vitro culture of human primary chondrocyte, either activation or blockade of β-catenin signalling all resulted in cartilage loss (Nalesso *et al.* 2011). These data suggest that balanced β-catenin levels are essential for maintaining homeostasis of articular chondrocytes and that any factors impairing this balance could lead to pathological changes. Moreover, LRP5 is located in chromosome 11q12-13, which is thought to be an OA susceptibility locus. LRP5-/- mice displayed increased cartilage degradation, probably due to low bone mass density (Lodewyckx *et al.* 2012). Another study in a mouse OA model also demonstrated that control of Dkk1 expression, a negative regulator of β-catenin/Wnt signalling, prevents joint cartilage deterioration in OA knees through attenuating the apoptosis regulator Bax, MMP3 and RANKL (Weng *et al.* 2010). Also, the inhibition of Dkk1, has been reported to be able to reverse the bone-destructive characteristics of rheumatoid arthritis to the bone-forming characteristics of OA (Diarra *et al.* 2007). This evidence further supports the crucial role of β-catenin/Wnt signalling in OA. Wnt signalling is also reported to function as an OA initiation factor e.g. a down-regulation of Wnt antagonist FRZB and an up-regulation of the ligand Wnt16 and target genes encoding β-catenin, Axin-2, C-JUN and LEF-1 was observed in mouse model of mechanical injury, a major cause of OA; expression of WNT1-inducible signalling protein (WISP-1) was also increased twofold in cartilage lesions compared to healthy intact cartilage (Blom *et al.* 2009).

Human studies also observed the critical role of WNT signalling in OA development. A loss-of-function allelic Arg200Trp and Arg324Gly Frzb variants, encoding sFRP-3, a β-catenin/Wnt signalling inhibitor, contributed to genetic susceptibility of women to hip OA (Loughlin *et al.* 2004, Lane *et al.* 2006). Given the close relationship between bone shape and OA development, Baker-Lepain et al proposed that SNPs in Frzb are associated with the shape of proximal femur and further contribute to hip OA development (Baker-Lepain *et al.* 2012). Moreover, the Frzb knockout mice increased articular cartilage loss during arthritis triggered and this damage was associated with increased WNT signalling and MMP-3 expression and activity. Also, the FRZB deficiency resulted in the cortical bone thickness and density with stiffer bones (Lories *et al.* 2007).

1.2.2.2. Catabolic signalling in OA

Opposing the anabolic effects of growth factors are pro-inflammatory cytokines and a variety of mediators associated with inflammation e.g. NO, prostaglandins, IL-1β, TNF-α, IL-6, IL-8 These factors are first produced by the synovial membrane and diffuse into the cartilage through synovial fluid, together with activate chondrocytes which also have the capacity to produce a variety of cytokines and mediators, responsible for functional alterations in the synovium, the cartilage, and the subchondral bone. Their role in OA has attracted considerable attention.

Of pro-inflammatory cytokines, IL-1β, TNF-α seem prominent and of major importance to cartilage destruction. The biologic activation of cells by IL-1 is mediated through the association with its specific receptors e.g. type I and II IL-1R. Especially, the type I IL-1R, responsible for signal transduction, was found to increase in OA chondrocytes and synovial fibroblasts. IL-1β is a critical mediator, and stimulation of chondrocytes by IL-1β causes gene expression patterns similar to those in OA cartilage (Goldring *et al.* 1988, Lefebvre *et al.* 1990). IL-1β localizes to the site of cartilage degradation in OA joints, providing evidence of its key role in the pathogenesis of OA (Tetlow *et al.* 2001, Pujol *et al.* 2008). IL-1β was reported to suppress aggrecan and collagen and up-regulate the proteolytic enzymes e.g. ADAMTS4 and MMP13 (Goldring 2000, Kobayashi *et al.* 2005). In addition, *IL-1β*, or IL-1β-converting enzyme knockout mice showed the accelerated development of OA lesions in response to OA surgical induced compared to wild type mice (Clements *et al.* 2003). The blocking effects of IL-1β by IL-1 receptor antagonist

(IL-1ra), which is the natural inhibitor of IL-1β by competing with IL-1β for occupancy of the IL-1β cell surface receptors but cannot initiate cellular signals protect against the development of experimentally induced OA lesions in animal models e.g. dogs, horses (Pelletier *et al.* 1997, Frisbie *et al.* 2002). Interestingly, it was reported that the IL-1β concentration is low in inflamed joints and a level from 10-1000 fold excess of IL-1ra over IL-1β was required to efficiency block all of the available IL-1β receptors enough to inhibit joint degradation (Pelletier et al. 1997).

1.2.2.2.1. NFκB Signalling

The transcription factor NFκB is the master regulator of expression of a number of genes critical to innate and adaptive immunity, cell proliferation, and inflammation. NFκB is held in the cytoplasm in an inactive form associated with the inhibitory κB (IκB) protein. A broad range of stimuli, including TNF-α, IL-1β, bacteria and viruses trigger a cascade of signalling, leading to release of NFκB from IκB. The activated NFκB will then translocate to the nucleus, bind to DNA elements present in its target genes and facilitate their transcription.

Numerous published data support the central role of NFκB signalling in cartilage metabolism and development of OA e.g. IκB overexpression in human OA synovial fibroblasts resulted in a decrease in expression of IL-6, IL-8, MPC-1/CCL-2, and MMPs (Amos *et al.* 2006) as well as abolishing the IL-1β-induced effect on expression of ADAMTS-4 (Bondeson *et al.* 2007); In a mouse surgically induced OA model, siRNA inhibiting NFκB/p65 resulted in reducing the amount of IL-1βand TNF-α in synovial fluid, reducing the level of inflammation in the synovium, and decreasing cartilage damage (Chen *et al.* 2008).

1.2.3. Risk factors for Osteoarthritis

The pathogenesis of OA is complex and poorly understood but involves the interaction of multiple factors ranging from genetic predisposition to mechanical and environmental components. Studies are in progress to define the molecular mechanisms involved in initiation and progression of OA.

1.2.3.1.Trauma and altered mechanical load

Mechanical factors and trauma have a central role in the initiation and propagation of OA: Excessive load and trauma which lead to injury of the menisci or ligaments predispose to

the development of the disease; the level and nature of the load experienced might also influence the progression of joint damage: an acute trauma leading to rupture of the meniscus or the cruciate ligaments might precipitate the development of OA. However, the differing contributions to this effect of the initial trauma and the ensuing mechanical instability have not been clearly delineated; also, in immobilized joints, there is lack of OA: further supporting the importance of mechanical triggers in the disease process (Riordan *et al.* 2014).

After joint trauma, the onset and progression of clinical symptoms differs even among groups with the same type of injury and physical activity profile, pointing to the involvement of other factors apart from the trauma.

1.2.3.2. Inflammation

Histologically, the disease was denominated osteoarthrosis, a term that implied the absence of inflammation. However, data acquired using high-sensitivity assays for inflammatory markers (such as C-reactive protein) demonstrate that low-grade inflammation is present (Pearle *et al.* 2007). Numerous inflammatory cytokines are found at increased levels in joint tissues during the acute post-injury phase, including IL-1, IL-6, IL-17, and TNFα (Lee *et al.* 2009). Inflammation seems to be a very early event in OA since the increase of CRP levels precedes the release of other OA indicators or molecular markers of matrix breakdown, and is observed well before clinical disease.

Inflammatory might be of particular importance to the onset and propagation of the primary and secondary OA. However, why the inflammation triggered in OA remains controversial. It was hypothesized that it was caused by traumatic joint injury or an age – related process. Joint injury leads to cartilage degradation and tissue damage. Once degraded, cartilage fragments accumulate in the joint and contact the synovium. Considered foreign bodies, synovial cells react by producing inflammatory mediators, found in synovial fluid. These mediators can activate chondrocytes present in the superficial layer of cartilage, which leads to metalloproteinase synthesis and, eventually, increase cartilage degradation. Published data support for the hypothesis that inflammation was triggered by aging process: advance glycation endproducts (AGEs), produced by a non-enzymatic process in aging tissue, weaken cartilage by modifying its mechanical properties triggering chondrocyte activation by binding to specific receptors present at the

surface of the chondrocytes, called RAGE (receptor for AGEs) lead to an overproduction of proinflammatory cytokines and MMPs (Nah *et al.* 2007); or after a period of vigorous proliferation, chondrocyte division rate declines but has high capacity to synthesize soluble mediators which in turn induces several inflammatory and pro-degradative mediators.

1.2.3.3. Obesity

Obesity is a well known risk factor for the initiation and progression of OA. This association is obvious because any overload on a weight – bearing joint would provoke tear and wear at the surface of the cartilage.

The molecular mechanisms explaining why obesity is one of the major risk factors for OA (Messier *et al.* 2005) is not exactly known. It is possible that the excess weight increases the load borne by all parts of the joint. However, the association between overweight and OA is not simply a question of increased mechanical load because obesity acts as a risk factor for developing hand OA (Grotle *et al.* 2008). Together with this, published data from animal studies: knee cartilage from rabbits fed a high – fat diet showed lower glycosaminoglycan content and aggrecan-1 than cartilage from rabbits fed a normal – fat diet independently of animal weight (Brunner *et al.* 2012); OA surgical induced mice fed a high – fat diet from 4 weeks of age showed higher OA cartilage degeneration at 8 weeks after surgery than those fed a normal diet (Mooney *et al.* 2011); in mice transgenic for human C – reactive protein (CRP) on a high – fat diet, there is a lack of correlation between OA severity and body weight (Gierman *et al.* 2012).

Many studies suggest that systemic inflammatory mediators contribute to the increased risk of OA with obesity. Adipose tissue, especially from the abdomen, is a rich source of pro-inflammatory cytokines, which are often referred to as adipokines. Many adipokines elevated with obesity have also been shown to mediate synovial tissue inflammation. For example, leptin is a 16-kd polypeptide hormone encoded by the obese (*ob*) gene and is primarily secreted by adipocytes. Female C57BL/6J mice with impaired leptin signalling are protected from obesity – induced OA, suggesting elevated body fat in the absence of leptin signalling is insufficient to induce systemic inflammation and OA (Griffin *et al.* 2009). Leptin has been found to exist at higher concentrations in the synovial fluid compared to serum (Presle *et al.* 2006). Leptin, alone or in synergy with IL-1, induced collagen release from bovine cartilage explants and upregulated MMP-1 and MMP-13 expression in bovine chondrocytes(Hui *et al.* 2012).

1.2.3.4. Aging

Aging is the most important risk factor for OA. After 40 year old, many people will appear to have some damage to their joints which may lead to OA, and approximately 50% of individuals greater than the age of 65 suffer from OA. The incidence of the disease through age has been observed: the prevalence of OA rises from 4% in people under the age of 24 to as high as 85% for those at 75-79 years of age. The common justification is the long-term effect of mechanical load on all joint components. Also, the regenerative capability of cartilage is reduced and cellular apoptosis is enhanced with age (Goldring *et al.* 2007).

1.2.3.5.Genetic factors

Evidence from family clustering and twin studies indicates that the risk of OA has an inherited component. Genetic factors may influence between 39% and 65% in radiographic OA of the hand and knee in OA, about 60% in OA of the hip, and about 70% in OA of the spine. Mutations to genes that play a role in the ECM, proteases and inhibitors, cytokines, and growth factors have been found to affect one's susceptibility to develop of OA (Sulzbacher 2013). However, the individual effects are relatively small. For example, a genome – wide association study showing that the C allele of rs3815148 on chr 7q22 was associated with a 1.14- fold increased prevalence of knee and/ or hand OA(Kerkhof *et al.* 2010).

1.3. MicroRNAs in osteoarthritis

1.3.1. The basic biology of miRNA

miRNAs are an abundant class of evolutionarily conserved, short (~22nt long), single – stranded RNA molecules that have emerged as important post transcriptional regulators of gene expression by binding to specific sequences within a target mRNA (Ambros 2004, Bartel 2004). To date, 1424 miRNAs have been identified in human cells and each is predicted to regulate several target genes (Lim *et al.* 2005, Kozomara *et al.* 2011). Computational predictions indicate that more than 50% of all human protein – coding genes are potentially regulated by miRNAs (Lewis *et al.* 2005, Friedman *et al.* 2009). The abundance of mature miRNAs varies extensively from as few as ten to more than 80,000 copies in a single cell, which provides a high degree of flexibility in the regulation of gene expression (Chen *et al.* 2005, Suomi *et al.* 2008). The regulation exerted by miRNAs is

reversible, as feedback/forward regulatory loops have been shown to exert modifying effects during translation (Inui *et al.* 2010) .

1.3.1.1. MicroRNA discovery

In 1981, the first miRNA: *lin-4* was discovered in *Caenorhabditis elegans* (Chalfie 1981). In the early 1990s, Ambros and Ruvkun revealed that *lin-4* controlled a specific step in developmental timing in *C.elegans* by downregulating *lin-14* (a conventional protein – coding gene) (Chalfie 1981, Lee *et al.* 1993, Wightman *et al.* 1993). They recognized that the *lin-14* 3'UTR harbours multiple sites of imperfect complementarity to *lin-4* and proposed that *lin-4* binds to these sites and blocks *lin-14* translation.

Forward genetics also discovered a second miRNA in *C.elegans,* known as *let-7* (Reinhart *et al.* 2000) which targets *lin-41* and *hbl-1* (Abrahante *et al.* 2003, Lin *et al.* 2003). The concept of miRNAs then jumped from worms to higher species, since *let-7* had well-known homologues even in human and fly. In 2001, the term "microRNA" was coined for this class of non-coding gene regulators (Lagos-Quintana *et al.* 2001, Lau *et al.* 2001, Lee *et al.* 2001). The discovery of miRNAs had crossed over to human, and finding miRNA targets became a high priority.

1.3.1.2. MicroRNA biogenesis

Most of the currently known miRNA sequences are located in introns of protein coding genes; a lower percentage of miRNAs originate from exons or non-coding mRNA-like regions (Rodriguez *et al.* 2004). In addition, a significant number of miRNA are found in polycistronic units that encode more than one miRNA. The miRNAs within clusters are often functionally related (Lagos-Quintana et al. 2001, Lau et al. 2001).

Despite the obvious differences between the biology of miRNAs and mRNAs, all available evidence suggests that these transcripts share common mechanisms of transcriptional regulation. Generally, the generation of a miRNA is a multi-step process that starts in the nucleus and finishes in the cytoplasm (Lee *et al.* 2002). First, miRNAs are transcribed by the RNA polymerase II complex (Lee *et al.* 2004) and subsequently capped, polyadenylated, and spliced (Cai *et al.* 2004). Transcription results in a primary miRNA transcript (pri-miRNA) that harbors a hairpin structure (Lee et al. 2002, Kim 2005). Within

the nucleus, the RNAse II–type molecule Drosha and its cofactor DGCR8 process the pri-miRNAs into 70- to 100-nt-long pre-miRNA structures (Lee *et al.* 2003, Han *et al.* 2004), which in turn are exported to the cytoplasm through the nuclear pores by Exportin-5 (Yi *et al.* 2003, Bohnsack *et al.* 2004, Lund *et al.* 2004, Zeng *et al.* 2004). Subsequently, the RNAse III-type protein Dicer generates a double stranded short RNA in the cytoplasm that consists of the leading – strand miRNA and its complementary sequence (Grishok *et al.* 2001, Hutvágner *et al.* 2001, Ketting *et al.* 2001, Chendrimada *et al.* 2005). This duplex miRNA is unwound by a helicase into a single stranded short RNA in the cytoplasm and the leading strand is incorporated into the argonaute protein (Ago 2)-containing ribonucleoprotein complex known as the miRNA-induced silencing complex, mRISC (Hammond *et al.* 2000, Hutvagner *et al.* 2008, Bossé *et al.* 2010). During this process, one strand of the miRNA duplex is selected as the guide miRNA and remains stably associated with mRISC, while the other strand, known as the passenger strand is rapidly removed and degraded (Martinez *et al.* 2002) (Figure 1.5). Selection of the appropriate strand is primarily determined by the strength of base pairing at the ends of the miRNA duplex. The strand with less-stable base pairing at its 5' end is usually destined to become the mature miRNA (Khvorova *et al.* 2003, Schwarz *et al.* 2003, Hutvagner 2005). However, some miRNA passenger strands are thought themselves to negatively regulate gene expression. One hypothesis is that both strands could be used differently in response to extracellular or intracellular cues, to regulate a more diverse set of protein –coding genes as needed, or strand selection could be tissue specific (Ro *et al.* 2007). The mature miRNA guides the RISC complex to the 3'UTR of its target miRNA (Lai 2002, Bartel 2009) . The seed sequence, comprising nucleotides 2-8 at 5'-end of the mature miRNA, is important for binding of the miRNA to its target site in the mRNA (Lewis et al. 2005). Association of miRNA with its target results in mRNA cleavage (if sequence complementarity is high) or more usually in higher eukaryotes, blockade of translation (Zeng and Cullen 2004) (see below).

In an alternative pathway for miRNA biogenesis, short hairpin introns termed mirtrons are spliced and debranched to generate pre-miRNA hairpin mimics (Berezikov *et al.* 2007, Okamura *et al.* 2007, Ruby *et al.* 2007, Westholm *et al.* 2011, Sibley *et al.* 2012). These are then cleaved by Dicer in the cytoplasm and incorporated into typical miRNA silencing

complexes (Berezikov et al. 2007, Okamura et al. 2007, Ruby et al. 2007, Westholm and Lai 2011, Sibley et al. 2012). The presence of mirtrons may be an evolutionary strategy to diversify miRNA-based gene silencing (Lau *et al.* 2009).

1.3.1.3. Mechanisms of action of miRNAs

Mammalian miRNAs often have several isoforms encoded from one or more chromosome, suggesting that they are functionally redundant (Heimberg *et al.* 2008, Kim *et al.* 2009). They may exert variable roles *in vivo* via differences in their expression pattern and 3'-end binding (Ventura *et al.* 2008).

Regulation is mainly exerted by the binding of the miRNA to the 3'UTR of the target mRNA, but binding to other positions on the target mRNA, e.g. in 5'UTR or coding sequence has also been reported (Lytle *et al.* 2007, Lee *et al.* 2009, Li *et al.* 2009). Interestingly, miRNA binding sites within the coding region of a transcript are reported as less effective at mediating translational repression. Aside from the location of miRNA binding sites, factors including the sequence context of the miRNA binding site, the number of target sites within the mRNA, the focal RNA structure, the distance between target sites, all contribute to the efficacy of repression mediated by miRNAs (Brennecke *et al.* 2005, Sætrom *et al.* 2007).

The degree of base pairing between the miRNA and its target in the mRISC complex determines the fate of the transcript. If there is perfect binding between the miRNA and target, the mRNA target is cleaved by Ago2 at the annealing site, with subsequent degradation of the mRNA. In contrast, in cases where the miRNA is only partially complementary to its corresponding 3'UTR, inhibition of target mRNA translation occurs via Ago1. Repression may be exerted either at the initiation step of mRNA translation in which Ago competes with eIF4E or at some stage subsequent to initiation (Kiriakidou *et al.* 2007) (Figure 1.6). This is because miRNA-mRISC complex can bind to actively translating mRNAs, reducing translational elongation and/ or enhancing termination, concomitant with a reduction in ribosome initiation and nascent peptide destablilization (Petersen *et al.* 2006).

Interestingly, besides generally promoting mRNA cleavage or translational repression, miRNA binding to 3'UTR can also induce translation of some target mRNAs. MicroRNAs have been identified which activate translation on cell cycle arrest by directing AGO-containing protein complexes to AU-rich elements in the 3'UTR (Vasudevan *et al.* 2007, Vasudevan *et al.* 2007)

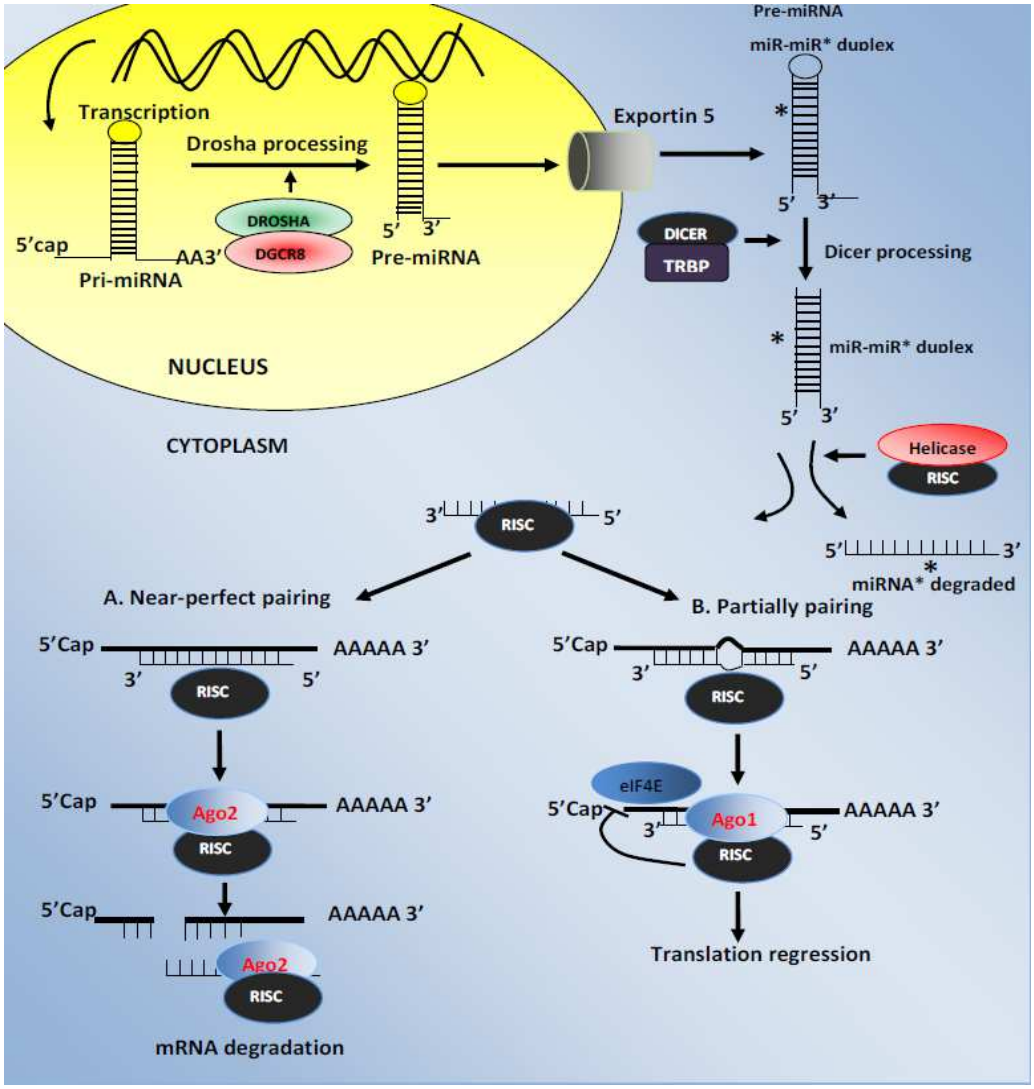

Figure 1.6: Biogenesis of miRNAs.

MicroRNAs are transcribed as RNA precursor molecules (pri-miRNA), which are processed by Drosha and its cofactor DGCR8 into short hairpin structure (pre-miRNA). These are exported into the cytoplasm by Exportin 5, where they are further processed by Dicer and TRBP (Dicer-TAR RNA binding protein) into a miRNA duplex. The duplex is unwound by a helicase and the "guide" strand is incorporated into the RNA–induced silencing complex (RISC) whilst the "passenger" strand undergoes degradation. This miRNA-RISC complex acts by two possible mechanisms: (A) Degradation of target mRNA occurs when miRNA is near-perfectly complementary with 3' untranslated region of target mRNA; (B) Translation inhibition occurs when miRNA is only partially complementary to its target mRNA.

1.3.2. MicroRNAs in skeletal development

It is evident that miRNAs are essential for skeletal development, however, our current knowledge of expression and function of specific miRNAs is still limited. Experimentally removing the majority of miRNAs by a block in miRNA biogenesis through mutating or deleting Dicer, reveals that the miRNA pathway plays a prominent role in skeletal development. An excellent example is the conditional knockout of Dicer in limb mesenchyme at the early stages of embryonic development, which leads to the formation of a much smaller limb. Dicer-null growth plates display a pronounced lack of chondrocyte proliferation in conjunction with enhanced differentiation to postmiototic hypertrophic chondrocytes; this latter may be explained by Dicer having distinct functional effects at different stages of chondrocyte development (Harfe *et al.* 2005). Recently, Kobayashi et al. reported that mice null for Dicer in chondrocytes resulted in skeletal growth defects and premature death (Kobayashi *et al.* 2008), again pointing to essential role of miRNAs in skeletal development.

Further evidence of the important role of miRNAs in skeletogenesis is that some miRNAs were found to exhibit bone-specific and cartilage-specific expression in late development. Wienholds et al. first provided evidence for miR-140 specifically expressed in cartilage of the jaw, head, and fins in zebrafish cartilage during embryonic development (Wienholds *et al.* 2003). Later, Tuddenham et al found that miR-140 is specifically expressed in cartilage tissues during mouse embryonic development (Tuddenham *et al.* 2006). Importantly, Miyaki et al and then Nakamura et al reported that universal knockout of miR-140 lead to mild dwarfism, probably as a result of impaired chondrocyte proliferation (Miyaki *et al.* 2010, Nakamura *et al.* 2011). Recently, Swingler et al found that miR-455-3p was expressed in developing long bones during chick development, restricted to cartilage and perichondrium, and in mouse embryos, where expression was selective in long bones and joints (Swingler *et al.* 2011).

These studies emphasize the importance of the miRNA pathway in skeletal development and revealed that some miRNAs are expressed with precise tissue and developmental stage specificity. Intensive research will uncover a complete spectrum of skeletally associated miRNAs as well as elucidate their biological function.

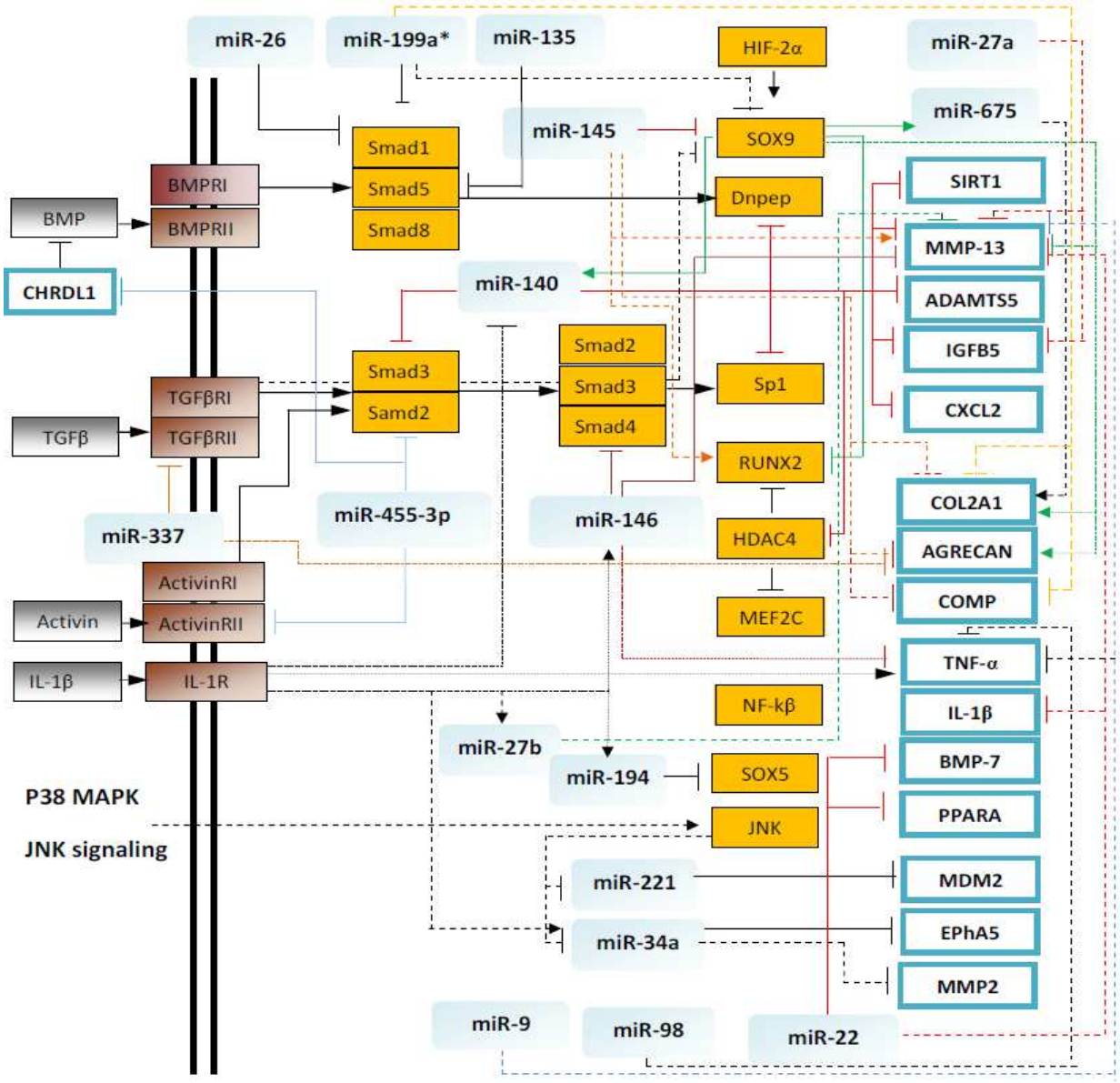

Figure 1.7: An overview of miRNAs involved in chondrogenesis, osteoarthritis and their direct and indirect targets

1.3.3. MicroRNAs in mechanotransduction

Articular cartilage has the unique capacity to resist significant mechanical loading during the lifetime of the organism (Guilak *et al.* 2001). The surface, middle and deep zones within articular cartilage are distinct domains, and they exhibit differential gene expression and attendant functional roles (Neu *et al.* 2007).

Mechano-responsive miRNAs are being identified in chondrocytes, the sole cell type of articular cartilage and evidence that specific miRNAs may impact on stress-related articular cartilage mechanotransduction has also been reported. MicroRNA-365 was the first identified mechanically responsive miRNA in chondrocytes, regulating chondrocyte differentiation through inhibiting HDAC4 (Guan *et al.* 2011). MicroRNA-221, miR-222 were postulated as potential regulators of the articular cartilage mechanotransduction pathway, since their expression patterns in bovine articular cartilage are higher in the weight-bearing anterior medial condyle as compared with the posterior non-weight-bearing medial condyle (Dunn *et al.* 2009). Recently, Li et al. reported that miR-146a was induced by joint instability resulting from medial collateral ligament transection and medial meniscal tear in the knee joints of an OA mouse model, suggesting that miR-146a might be a regulatory factor of the mechanical transduction process in articular cartilage (Li *et al.* 2012). All of these studies are useful for enriching the data on the regulatory mechanism for miRNAs in chondrocyte homeostasis.

1.3.4. MicroRNAs in chondrogenesis

Differential disruption of the Dicer gene in mice resulting in highly abnormal cartilage development suggests miRNAs play a significant role in chondrogenic differentiation. Furthermore, many studies profiled the expression of miRNAs to investigate their function in differentiating MSCs and showed that once they differentiate into chondrocytes, miRNA expression significantly altered (Sorrentino *et al.* 2008, Suomi et al. 2008, Lin *et al.* 2009, Miyaki *et al.* 2009, Karlsen *et al.* 2011, Lin *et al.* 2011, Yan *et al.* 2011, Yang *et al.* 2011) (Table1.2). However, there is no consensus expression signature of any miRNAs amongst these and we attribute this to the design of experiment including inducers of differentiation, cell types, numbers of detected miRNA probes and organism (Table1.2).

Table 1.2: Studies performing miRNA profile comparing between MSC and chondrocytes

	Sorrentino et al 2007	**Suomi et al 2008**	**Lin et al 2009**	**Miyaki et al 2009**	**Yang et al, 2010**	**Lin et al 2011**	**Yang et al 2011**	**Karlsen et al 2011**
Stimulators	-	TGF-β3	BMP-2	BMP-2 TGF-β3	TGF-β3	-	-	-
Cells	BM MSC	BM MSC	C12C2	BM MSC	BM MSC	DAC	BM MSC AC	DAC
Organisms	Human	Mice	-	Human	Mice	Human	Mice	Human
Probes	226	35	-	-	7,815	-	-	875
Cutoff(fold)	1.3	-	1.5	1.5	5	4	-	-
Platform	microarray	qPCR	microarray	microarray	microarray	microarray	microarray	microarray
miRNAs up-regulated	31 32 136 146 149 185 Pre-mir 192 199a-2-5 204 212 Pre-mir-212 Pre-miR-214	24 101 124a 199b 199a	199* 221 298 374 let-7e	15b 16 23b 27b 140 148 197 222 328 505	30a 81a-1 99a 125* 127 140 140* Let-7f	26a 140* 140 222 320a 320d 491* 547-5p 720 1308 let-7d let-7f let-7a	21 22 27b 27a 140 140* 152 291b* 330 431 433 455 let-7b let-7d let-7l	30d 140* 210 451 563
miRNAs down -regulated	10a 10b 21 23a 24-1-3p 24-2 26b 29b 30a-5p 34 100 103-2 107 130a 138-1 Pre-miR-143 145 181a-1 191-5p let-7a-1 let-7a-2 let-7a-3 let-7c let-7d	18 96	21 125a 125b 143 145 210		125b* 132 143 145 212	18a 27a 146a 193b 220b 342-5p 335 365 519e 548e 1248 1284	1 23a 23b 24 26b 99a 99b 99b* 125a-5p 143 144 145 146a 181a 181d 191 199a 199a* 210 320 355-5p 431 503 652 Let-7a Let-7c Let-7g Let-7f	15b 31 132 138 143 145 221 222 379 382 432 494 654* 1308 let-7e

AC: Articular chondrocytes; BM MSC: Bone marrow mesenchymal cells; DAC: dedifferentiated articular chondrocytes.

The regulation of chondrogenesis of murine MSCs in response to stimulation of TGF-β3 was investigated (Suomi et al. 2008, Yang et al. 2011) (Table1.2). Suomi et al compared the expression of 35 miRNAs in chondroblasts derived from MSCs, and found that miR-199a, miR-124a were strongly up-regulated while miR-96 was substantially suppressed (Suomi et al. 2008). They demonstrated how miRNAs and transcription factors could be capable of fine-tuning cellular differentiation by showing that miR-199a, miR-124a, miR-96 could target HIF-α, RFX1, Sox5, respectively (Suomi et al. 2008). Similarly, Yang et al , revealed eight significantly up-regulated and five down-regulated miRNAs (Yang et al. 2011) in this process. The miRNA clusters, miR-143/145 and miR-132/212 were down-regulated, with miR-132 the most down-regulated whilst miR-140* was the most up-regulated (Yang et al. 2011). Similar expression patterns of miR-145, miR-143 were also described in other studies (Lin et al. 2009, Karlsen et al. 2011, Lin et al. 2011, Yan et al. 2011). Corresponding targets of these differentially expressed miRNAs were predicted including: ADAMTS5 (miR-140*), ACVR1B (miR143/145), SMAD family members: SMAD1 (miR-30a), SMAD2 (miR-132/212), SMAD3 and SMAD5 (miR-145), Sox family members: Sox9 (miR-145); Sox6 (miR-143, miR-132/212), Runx2 (miR-30a and miR-140*) (Yang et al. 2011).

Further study has confirmed miR-145 as a key mediator which antagonizes early chondrogenic differentiation in mice via attenuating Sox9 at post-transcriptional level. (Yang *et al.* 2011). Interestingly, cells over-expressing miR-145 significantly decreased the expression of chondrogenic markers at the mRNA level including Col2a1, Agc1, COMP, Col9a2 and Col11a1. Consistent with this,, Martinez-Sanchez et al. reported miR-145 as a direct regulator of Sox9 in normal human articular chondrocytes though binding to a specific site in its 3'UTR, which is not conserved in mice (Martinez-Sanchez *et al.* 2012). Similarly, over-expression of miR-145 in articular cartilage chondrocytes reduced the levels of Sox9, the cartilage matrix components Col2a1 and Agc1 in combination with a significant increase of the hypertrophic markers Runx2 and MMP-13 (Martinez-Sanchez et al. 2012) (Figure 1.7).

This group also reported that miR-675, processed from H19, a non-coding RNA, was tightly regulated by Sox9 during chondrocyte differentiation. MicroRNA-675 could up-regulate expression of Col2a1, albeit indirectly, indicating its potential importance in

maintaining cartilage integrity and homeostasis. Forced over-expression of miR-675 rescued Col2a1 mRNA levels in either Sox9- or H19-depleted primary human articular chondrocytes (Dudek *et al.* 2010). Although its target mRNAs remain unknown, these data suggest that miR-675 may modulate cartilage homeostasis by suppressing a Col2a1 transcriptional repressor (Dudek et al. 2010) (Figure 1.7). Moreover, by performing miRNA expression profile during human primary chondrocyte dedifferentiation, Martinez-Sanchez found that 29 miRNAs were up-regulated more than two-fold and 18 miRNAs were down-regulated. Among these up-regulated miRNAs, miR-1247, transcribed from the DLK1-DIO3 locus, was of particular interest as its expression pattern still increased under hypoxia condition, together with miR-140. Also, miR-1247 level was found to correlate with cartilage-associated miR-675 across a range of 15 different mouse tissues (Martinez-Sanchez *et al.* 2013). Interestingly, SOX9, directly target of miR-1247 via coding sequence, inhibit this miRNA expression, suggesting a negative feedback loop between miR-1247 and its target SOX9 (Martinez-Sanchez and Murphy 2013).

Another study performed miRNA profiling to find expression signatures of nearly 380 miRNAs in C2C12 cells induced by BMP-2 for 24 hours and found that 5 miRNAs including miR-199a* and miR-221 were positively regulated while miR-125a, miR-210, miR-125b, miR-21, miR-145, miR-143 were repressed (Lin et al. 2009). Interestingly, using C3H10T1/2 cells, a well-established *in vitro* cell model of chondrogenesis, showed that miR-199a* expression was reduced significantly within several hours following BMP-2 treatment and then rose dramatically at 24 hours and remained higher thereafter, indicating that miR-199a* may function as a suppressor of the early steps of chondrogenic differentiation (Lin et al. 2009). Indeed, enforced miR-199a* expression in C3H10T1/2 cells or in the prechondrogenic cell line ATDC5, suppresses multiple markers of early chondrogenesis, including Col2a1 and COMP, whereas the antagomir blocking miR-199a* function has the opposite stimulatory effect (Lin et al. 2009). Consistent with these observations, Smad1, a positive downstream mediator of BMP-2 signalling, was shown to be a direct miR-199a* target. Moreover, miR-199a*, through its inhibition of the Smad pathway, is able to inhibit the expression of downstream genes such as p204 (Lin et al. 2009) (Figure 1.7).

The change in expression pattern of miRNAs across the dedifferentiation of chondrocytes also, adds to our understanding of the biology of *in vitro* human chondrogenesis (Karlsen

et al. 2011, Lin et al. 2011). MicroRNA-451, miR-140-3p, miR-210, miR-30d, and miR-563 were reported to be highly expressed on human primary articular chondrocytes at early passage compared with their dedifferentiated counterparts, suggesting their role as inhibitors of differentiation *in vitro* (Lin et al. 2011). Of these miRNAs, miR-140-3p had the highest expression. Conversely, 16 miRNAs were significantly up-regulated in dedifferentiated articular chondrocytes, reflecting their potential as modulators of the chondrogenenic process. Notably, miR-143, miR-145 also had similar expression patterns as previously reported (Lin et al. 2011). A second study also reported a group of 5 miRNAs: miR-451, miR140-3p, miR-210, miR-30d, and miR-563 upregulated on differentiation which may inhibit molecules participating in the dedifferentiation process whilst a further 16 miRNAs were downregulated and may potentially act conversely.

Recently, performing miRNA profiling across ATDC5 cell induced differentiation within 42 days to identify miRNAs with functions in cartilage development, we identified 7 cluster groups of miRNAs which may function cooperatively (Swingler et al. 2011). Among these, 39 miRNAs were found potentially co-regulated with miR-140 with expression increase during chondrogenic process (Swingler et al. 2011). Especially interesting is miR-455, located in an intron of the protein coding gene Col27a1, a cartilage-expressed collagen, which showed similar expression kinetics to collagen XXVII and to miR-140. Consistent with role for miR-140 in modulating TGFβ signalling, miR-455-3p was also found to directly target Smad2, ACVR2B and CHRDL1, again potentially attenuating the TGFβ pathway (Swingler et al. 2011) (Figure 1.7).

MicroRNA-140 shows a generally consistent expression pattern between studies. Indeed, cartilage miRNA research to date has focused heavily on miR-140 and has successfully shown the key roles of miR-140 in chondrocyte proliferation and differentiation. Miyaki et al compared gene expression profiling using miRNA microarrays and quantitative polymerase chain reaction in human articular chondrocytes and human mesenchymal stem cells. They demonstrated that miR-140 had the largest difference in expression between chondrocytes and MSCs (Miyaki et al. 2009), and this is in agreement with latter publications in human, rat and mice (Karlsen et al. 2011, Lin et al. 2011, Yan et al. 2011, Yang et al. 2011). MicroRNA-140 was first shown to target Hdac4, a known co-repressor of Runx2 and MEF2C transcription factors essential for chondrocyte hypertrophy and bone

development (Tuddenham et al. 2006). miR-140 also targets Cxcl12 (Nicolas *et al.* 2008) and Smad3 (Pais *et al.* 2010), both of which are implicated in chondrocyte differentiation. Interestingly, miR-140 is reported to suppress Dnpep, an aspartyl aminopeptidase, which has been suggested to antagonize BMP signalling downstream of Smad activation (Nakamura et al. 2011). Moreover, Sox9 a major transcription factor in maintaining cellular phenotype and preventing hypertrophy, particularly with L-Sox5 and Sox6, (Yamashita *et al.* 2012), is shown to control the expression of miR-140 (Yang *et al.* 2011, Nakamura *et al.* 2012).

The miR-194 is a key mediator during chondrogenic differentiation via suppression of the transcription factor Sox5 (Xu *et al.* 2012). The expression of miR-194 was significantly decreased in chondrogenic differentiation of adipose-derived stem cells (ASCs). Importantly, chondrogenic differentiation of ASCs could be achieved through controlling miR-194 expression (Xu et al. 2012) (Figure 1.7).

Using three rat models e.g. bone matrix gelatin-induced endochondral ossification, collagen-induced arthritis and pristane-induced arthritis, Zhong et al. further demonstrated that miR-337 was directly implicated with chondrogenesis. miR-337 acted as a repressor for TGFBR2 expression at the protein level (Zhong *et al.* 2012). Moreover, aggrecan was differentially expressed in both gain- or loss-of function of miR-337 experiments, providing evidence that miR-337 could influence cartilage specific gene expression in chondrocytes (Zhong et al. 2012) (Figure 1.7).

Kim et al. used chick as a model of chondrogenesis and focused on initiation, namely precartilage condensation, proliferation and migration. They reported that miR-221 and miR-34a, induced by c-Jun N-terminal kinase (JNK) signaling, played pivotal roles (Kim *et al.* 2010, Kim *et al.* 2011). Treatment of chick wing bud MSCs with a JNK inhibitor lead to the suppression of cell migration and stimulation of apoptosis with concurrent significant increase in expression of miR-221 and miR-34a (Kim et al. 2010, Kim et al. 2011). Notably, miR-221 may be involved in apoptosis, since treatment of MSCs with a miR-221 inhibitor increased cell proliferation and this could be rescued by the JNK inhibitor (Kim et al. 2010). MicroRNA-221 is reported to directly target Mdm2, which encodes for an oncoprotein with E3 ubiquitin ligase activity (Kim et al. 2010). Inhibition of Mdm2 expression via miR-221 suppresses ubiquitination leading to accumulation of

Slug protein, whose expression is associated with an increase in apoptosis (Kim et al. 2010). Conversely, miR-34a affects MSC migration, not proliferation (Kim et al. 2011). EphA5, a receptor in Eph/Ephrin signaling which mediates cell-to-cell interaction, has been proven to be a miR-34a target (Kim et al. 2011). Moreover, via regulating RhoA/Rac1 cross-talk, miR-34a negatively modulated reorganization of the actin cytoskeleton (Kim *et al.* 2012), one of the essential processes for establishing chondrocyte-specific morphology. MicroRNA-488 expression is up-regulated at the pre-condensation stage and then down-regulated at the post-condensation stage in chick limb chondrogenesis, suggested a key role in this process (Song *et al.* 2011). Interestingly, mir-488 could regulate cell–to-ECM interaction via modulation of focal adhesion activity by indirectly targeting MMP-2 (Song et al. 2011). More recently, this group reported that miR-142-3p was an important modulator in position-dependent chondrogenesis and was reported to regulate ADAM9 (Kim *et al.* 2011) (Figure 1.7).

1.3.5. MicroRNAs in osteoarthritis

The effects of miRNA deregulation on OA are evident through studies comparing the expression of miRNAs between OA tissues and their normal articular counterparts (Iliopoulos *et al.* 2008, Jones *et al.* 2009). Illopoulos et al. tested the expression of 365 miRNAs and identified a signature of 16 miRNAs, with 9 miRNAs significantly upregulated and 7 miRNAs downregulated in OA cartilage compared with normal controls. Some of these were postulated to be involved in obesity and inflammation (Iliopoulos et al. 2008). Interestingly, functional experiments implicated miR-9 in the regulation of MMP13 expression, as well as miR-9, miR-98 and miR-146 in the control of TNF-α expression, suggesting that these miRNAs may play a protective role in OA. Moreover, miR-22, whose expression correlated with body mass index, directly targets PPARA and BMP-7 at the mRNA and protein levels, respectively. Enforced miR-22 overexpression or siRNA-mediated suppression of either PPARA or BMP-7 resulted in increases in IL-1β and MMP-13 protein levels, again suggesting that miRNA deregulation can have effects on OA (Iliopoulos et al. 2008) (Figure 1.7).

Additionally, Jones et al. investigated the expression of 157 human miRNAs and identified 17 miRNAs whose expression varied by 4-fold or more when comparing normal versus

late-stage OA cartilage (Jones et al. 2009). Consistent with the Illopoulos data, the altered expression of miR-9, miR-98 and miR-146 in OA cartilage are highlighted. The over-expression of these miRNAs also reduced IL-1β-induced TNF-α production, whilst inhibition or over-expression of miR-9 modulated MMP-13 secretion (Jones et al. 2009) (Figure 1.7).

The miR-140 gene, located in an intron of the E3 ubiquitin protein ligase gene Wwp2 on murine chromosome 8 and the small arm of chromosome 16 in humans, is evolutionarily conserved among vertebrates. MicroRNA-140 expression in the cartilage of patients with OA was significantly lower than in normal cartilage (Miyaki et al. 2009, Tardif *et al.* 2009) and decreased miR-140 expression was reported also in OA chondrocytes (Tardif et al. 2009).

Deletion of miR-140 in mice predisposes to the development of age-related OA-like changes (Miyaki et al. 2010, Nakamura et al. 2011) and gives a significant increase in cartilage destruction in surgically induced OA. Conversely, in an antigen-induced arthritis model, transgenic over-expression of miR-140 in chondrocytes protects against cartilage damage (Miyaki *et al.* 2010). The ADAMTS5 gene has been shown to be a direct target of miR-140, whilst reciprocal regulation of ADAMTS5 in the in vivo models above suggests that suppression of OA may involve regulation of ADAMTS5 (Miyaki et al. 2010). Swingler et al. show that miR-140 is increased in expression in hip OA cartilage compared to fracture controls (Swingler et al. 2011), but ADAMTS5 expression is decreased in the former samples. As above, Nakamura et al. identified the aspartyl aminopeptidase Dnpep as a key target for miR-140 essential for skeletal defects in miR-140 null mice (Nakamura *et al.* 2011). Using functional interference, Tardif et al. confirmed IGFBP-5, whose expression in human chondrocytes was significantly higher in OA, as a direct target of miR-140 (Tardif et al. 2009). More recently, miR-140 was shown to directly mediate MMP13 expression *in vitro* by luciferase reporter assay (Liang *et al.* 2012) (Figure 1.7).

The human genome contains two miR-27 genes [mir-27a and miR-27b] on chromosomes 19 and 9, respectively, and their major products differ by only 1 nucleotide in the 3' region. MicroRNA-27a expression was shown to be decreased in OA compared to normal chondrocytes (Tardif et al. 2009). Down-regulation of miR-27a was proposed to be connected with adipose tissue dysregulation in obesity, a strong risk factor for OA. Tardif

et al. suggested that miR-27a may indirectly regulate the levels of both MMP-13 and IGFBP-5 by targeting upstream positive effectors of both genes (Tardif et al. 2009). Conversely, expression miR-27b was found to be significantly lower in OA cartilage samples compared with normal counterparts where it inversely correlated with MMP13, a direct target (Akhtar *et al.* 2010). This points to the possibility of novel avenues for OA therapeutic strategies (Figure 1.7).

MicroRNA-146a was strongly expressed in chondrocytes residing in the superficial layer of cartilage and in low-grade OA cartilage (Yamasaki *et al.* 2009, Li et al. 2012). Its expression level gradually decreased with progressive tissue degeneration. Interestingly, when miR-146 was highly expressed, the expression of MMP13 is low, suggesting that miR-146a has target genes that play a role in OA cartilage pathogenesis (Yamasaki et al. 2009). MicroRNA-146a has recently been implicated in the control of knee joint homeostasis and OA-associated algesia by balancing the inflammatory response in cartilage and synovium with pain-related factors in glial cells (Li *et al.* 2011). As such, it may be useful for the treatment of both cartilage regeneration and the pain symptoms caused by OA (Figure 1.7).

Park et al reported the miR-127-5p, an important mediator in OA whose expression was significant decreased in OA articular cartilage compared to the control counterpart, directly target MMP13. Noteworthy, pre-treatment with MAPK inhibitors and NFκβ inhibitor attenuated the inhibitory effects of IL-1 on miR-127-5p expression while overexpression of miR-127-5p significantly inhibited the phosphorylation of JNK, p38 and Iκβα in the human chondrocytes. These data suggest a reciprocal regulatory loop between NFκβ, MAP kinase, and IL-1β in controlling MMP13 expression (Park *et al.* 2013).

1.3.6. MicroRNAs in inflammation

Some miRNAs could be of importance in the inflammatory events of osteoarthritis. MicroRNA-140 was suppressed by IL-1β signaling, and transfection of human chondrocytes with miR-140 downregulated IL-1β driven induction of ADAMTS5 (Miyaki et al. 2009). However, contrary to this, Liang et al. reported that expression of miR-140

and MMP-13 was elevated in IL-1β-stimulated C28/I2 and expression of miR-140 was shown to be NF-κB-dependent (Liang *et al.* 2012) (Figure 1.7).

Expression of miR-34a was significantly induced by IL-1β while antagonism of miR-34a prevented IL-1β-induced chondrocyte apoptosis (Abouheif *et al.* 2010), as well as IL-1β-induced down regulation of type II collagen in rat chondrocytes (Abouheif et al. 2010). Other relevant miRNAs reported to be induced by IL-1β are miR-146a (Yamasaki et al. 2009, Li et al. 2012), miR-34a (Abouheif et al. 2010), miR-194 (Xu et al. 2012), miR-27b (Akhtar et al. 2010) (Figure 1.7).

1.3.7. Utility of microRNAs for diagnosis

It is evident that miRNAs in serum may become a powerful tool in the development of diagnostic biomarkers. MicroRNAs are relatively stable with enzymatic, freezing, thawing or extreme pH conditions (Mitchell *et al.* 2008, Link *et al.* 2010) due to lipid or lipoprotein complexes (Esau *et al.* 2006). Moreover, extracellular miRNAs are detectable in almost all body fluids and excretions including urine, faeces, saliva, tears, ascetic, pleural and amniotic fluid (Chen *et al.* 2008, Gilad *et al.* 2008). Interestingly, miRNAs in plasma have the capacity to interact with intact cells with some degree of specificity, and modify recipient cell gene expression and protein production via a miRNA-related mechanism (Arroyo *et al.* 2011). This opens up the possibility of genetic exchange between cells and the exogenous regulation of gene expression. MicroRNA-21 was the first serum miRNA biomarker to be discovered: patients with diffuse large B cell lymphoma had high serum levels of miR-21, which was associated with increased relapse-free survival (Lawrie *et al.* 2008). Subsequently, the usefulness of serum miRNAs for diagnosis and prognosis has been reported for solid cancers and leukemia (Ferracin *et al.* 2010, Kosaka *et al.* 2010, Wittmann *et al.* 2010). For OA, Murata et al. examined the potential of miRNA as diagnostic biomarkers and found a number of miRNA in plasma some of which were found at different levels between RA and OA patients (Murata *et al.* 2010). Recently, let-7e, miR-454, miR-886 were identified differentially expressed crilculating miRNAs in OA patient necessitating arthroplasty in a large, population – based cohort. Especially, let – 7e emerged as potential predictor for severe knee or hip OA (Beyer *et al.* 2014).

Besides the measurement of miRNAs in plasma, PBMCs could also be useful in developing a biomarker for OA. Circulating PBMCs such as macrophages and T cells accumulate in the synovium of OA patients, producing proinflammatory cytokines and proteinases associated with synovitis, linked to the early stages of OA progression. It has been demonstrated that the high expression of miR-146a, miR-155, miR-181a and miR-223 in PBMCs from OA patients versus normal controls may be related to the pathogenesis of OA (Okuhara *et al.* 2011). Interestingly, miR-146 and miR-223 are highly expressed in early-stage OA (Yamasaki et al. 2009), with expression gradually decreasing with OA progression with the promise for diagnosis of early OA is specificity can be demonstrated.

Taken together, there is growing evidence for future miRNA-based diagnostics. However, there is a requirement for detailed investigations directed at diagnostic performance (sensitivity, specificity, accuracy) of these promising novel biomarkers before the measurement of miRNAs can enter the clinic.

1.3.8. Utility of microRNAs in therapeutic treatment

Currently there is no disease-modifying therapeutics available for patients suffering from OA. Therapeutic options are limited to oral and intra-articularly injected analgesic medications, and joint replacement surgery (Wieland *et al.* 2005). OA patients often present with cartilage that already exhibits a damaged matrix, and in which repair/regeneration is. Although cartilage seems a relatively simple tissue type to engineer because of its single cell type and its lack of a blood, nerve or lymph system, regenerating cartilage in a form that can function effectively after implantation has proven difficult. Several approaches are currently being investigated to utilize a miRNA-based therapy to overcome these problems, and these may represent a novel therapeutic application for pharmacological control. Currently there are over 70 clinical trials worldwide based on miRNA manipulation to treat a range of conditions including various cancers and cardiovascular disease; however, none of these to date are for arthritis.

The targeting of miRNAs represents a novel therapeutic opportunity for OA treatment in which miRNA deficiencies could be corrected by either antagonizing (antagomirs) or

restoring (mimics) miRNA function. Poorly expressed miRNAs could be restored by over expression using stable vector transfection or transfection by double-stranded miRNA, whilst over-expressed miRNAs could be antagonized by modified DNA oligonucleotides. Particularly, it has been proven that the systematic administration of antagonist miRNAs modified with locked nucleic acids (LNA) could function without toxicity in non-human primates (Elmen *et al.* 2008). Evidence on efficacy was also demonstrated in mouse models using miR-122 antisense oligonucleotides, which resulted in a decrease in hepatic fatty acid and cholesterol synthesis (Esau et al. 2006). In man, when miR-143/miR-145 activity was restored in pancreatic cancer cells (in which their levels were repressed), the cell was no longer tumourigenic (Kent *et al.* 2010). Although this type of therapy has not been applied in OA, there is very promising evidence for therapeutic potential, e.g. the silencing of miR-34a by LNA-modified antisense oligonucleotides could effectively reduce rat chondrocyte apoptosis induced by IL-1β (Kongcharoensombat *et al.* 2010). This study revealed that silencing of miR-34a might be a novel intervention for OA treatment if this could be appropriately targeted.

Another approach is to combine miRNA technology with stem cell engineering. *In vivo* MSCs participate in chondrogenesis. MSCs can be conveniently obtained with less injury than primary cells and manipulated *in vitro* and hence they are promising cells in cartilage regeneration. At present, autologous MSCs have been transplanted in human injured or osteoarthritis knees for repair of articular cartilage defects. However, unexpected results from the ectopic transplantation of MSCs also have been reported, such as hypertrophy, mineralization, and vascularisation. Deciphering the role of miRNA regulation in the chondrogenesis of MSCs may open a new era of research and pave the way for the development of new treatments for OA

A growing body of evidence indicates that miRNAs convey a novel and efficient way for the regulation of gene expression, being involved in multiple aspects of cellular processes. Understanding their expression profile and dynamic regulation may be the key to enhancing chondrogenic differentiation, or maintaining phenotype in the treatment of OA. Recent advances in miRNA research have provided new perspectives on the regulation of OA and novel insight into the potential development of therapeutic treatments. Using miRNAs as therapeutic targets may well become a powerful tool in the development of

new therapeutic approaches. However, numerous questions including potential off-target effects and efficient and targeted delivery *in vivo* need to be solved before using miRNAs in therapeutics

SCOPE OF THE THESIS

OA is the most prevalent degenerative joint pathology leading to considerable problems with disability and pain in a huge number of people, especially the elderly population. As the population ages and with increased life expectancy, the burden of osteoarthritis will continue to rise. However, there is currently a lack of biomarkers and sensitive techniques for identifying and assessing patients with early changes. Also, clinical treatment for OA still remains unsatisfactory. Thus, deepening our understanding and gain further insights into the molecular mechanisms in OA would be very important for long term purpose of diagnosis and therapeutic treatment.

Several hundred miRNAs have been identified so far and initial studies have linked specific miRNAs to OA. However, there are no key miRNAs identified so far which functionally impact on early human OA onset and disease progression. Thus, I undertook this project to identify miRNAs mediating initiation and progression of OA and dissect their biological function in order to identify new signalling pathways involved in the pathogenesis of OA. The hypothesis and specific aims of the project were:

Hypothesis: The dysregulated expression of specific microRNAs contributes to the onset or progression of OA.

Specific aim 1: Profile miRNA and mRNA expressions in whole knee joint in DMM model to identify the potential miRNAs involved in the early stage of OA

Specific aim 2: Determine the involvement of the miRNA in human end stage OA cartilage, in murine injury model, in chondrogenesis.

Specific aim 3: Identify factors control the miRNA expression in articular cartilage

Specific aim 4: Identify miRNA direct targets to identify new signaling pathways involved in homeostasis of articular cartilage.

CHAPTER 2
MATERIALS AND METHODS

2.1.Materials

2.1.1. Murine models

2.1.1.1. Destabilization of the medial meniscus murine model (DMM model)

Induction of OA by destabilization of the medial meniscus (DMM) was kindly performed by Professor Tonia Vincent Kennedy Institute for Rheumatology, Oxford University, U.K. Protocols using C57Bl/6 mice were as described previously in (Burleigh *et al.* 2012, Chong *et al.* 2013).

Briefly, C57Bl/6 male mice were housed 3-5 per cage in 63x54x30 cm^3 standard individually vented cages and maintained with a 12h/12h light/dark cycle at an ambient temperature of 21ºC. Mice were fed a certified mouse diet (RM3 from Special Dietary Systems, Essex, UK) and water ad libitum. 10 week old mice were anaesthetized by intra-peritoneal injection of a 1:1:2 mixture of Hypnorm (0.315mg/ml fentanyl citrate and 10mg/ml fluanisone; VetaPharma Ltd, Leeds, UK), Hypnovol (5mg/ml midazolam; Roche), and sterile water for injection, at a dose of 10ml/kg body weight. The ventral portion of the right knee was shaved and swabbed with iodine to prepare a sterile surgical field. The medial meniscus was identified and the attachment of its anterior horn to the tibial plateau was cut. Care was taken to avoid injury to the anterior cruciate ligament and the cartilage surfaces. The mice were fully mobile within 2-4 hours after surgery. After 1, 3, 7 days after surgery, the mice were culled and knees harvested.

2.1.1.2. Murine hip avulsion injury model

The femoral caps of C57Bl/6 mice ages 4 weeks were avulsed using forceps as described in (Chong et al. 2013). After washing three times with sterile phosphate-buffered saline (PBS) (Life Technologies, 10010023), the femoral caps were immediately put in either 500µl Trizol® reagent (Invitrogen, 15569-026) (for time point 0) or in 24-well plate for (other time points e.g. 3, 6, 12, 48 hours). 200µl of Dulbecco's modified Eagle's medium (DMEM) (Life Technologies, 10566-016) containing 100 IU/ml penicillin and 100µg/ml

streptomycin (Sigma, P4333) was added to each well and the plate was incubated at 37ºC in 5% (v/v) CO_2. At the desired time points, the femoral caps were harvested (with Trizol reagent) and total RNA was isolated.

2.1.2. Human end stage OA specimens and normal counterparts

Ethical Committee approval for using discarded human tissue was received prior to the initiation of the studies. Full informed consent was obtained from all donors. Human articular cartilage was obtained from patients undergoing total hip/ knee replacement surgery at the Norfolk and Norwich University Hospital. In total, 8 hip and 7 knee OA cartilage samples were collected. 7 healthy articular cartilages were harvested from total hip replacement following fracture to the neck of femur. None of the healthy individuals had a clinical history of arthritis or other diseases affecting cartilage, no macroscopic lesions to the cartilage were seen.

2.1.3. Cell lines

All cell lines were maintained in DMEM high glucose, GlutaMAX supplement (Life Technologies, 10566-016) containing 10% (v/v) heat-inactivated fetal bovine serum (FCS) (PAA, UK), 100U/ml penicillin, and 100µg/ml streptomycin (Sigma, P4333) at 37ºC in 5% (v/v) CO_2.

2.1.3.1. Chondrosarcoma SW1353

The SW1353 cell line was initiated from a primary grade II chondrosarcoma of the right humerus obtained from a 72 year old female Caucasian. SW1353 cells were purchased from the American Type Culture Collection (ATCC) (no.HTB-94).

2.1.3.2. Chicken dermal fibroblasts DF1

DF-1 is a spontaneously immortalized chicken fibroblast cell line without viral or chemical treatment derived from 10 day old East Lansing Line (ELL-0) embryo. DF1 was a kind gift from Professor Andrea Munsterberg, University of East Anglia, U.K.

2.1.3.3. Dicer knockdown cell lines

DLD-1 Parental and DLD-1 Dicer null_cell lines were a kind gift from Professor Tamas Dalmay, University of East Anglia, U.K. These cell lines were originally purchased from Horizon Discovery (Cambridge, U.K.). Both cell lines were originally isolated from a colorectal adenocarcinoma.

2.2.Methods

2.2.1. Molecular biology- based methods

2.2.2.2. Human genomic DNA isolation

Buffer

Extraction Buffer: 10mM Tris-HCl pH 8 (Fisher Scientific, BP152-500), 5mM NaCl (Fisher Scientific, BP3581), 0.5% (w/v) SDS (Fisher Scientific, 10356463).

DNA extraction protocol

Human chondrosarcoma SW1353 cells were harvested from a 75cm^2 flask by trypsin-EDTA treatment (Life Technologies, 25200072) and pelleted by centrifugation at 17.3xg, 5 minutes.

The cell pellet was mixed well with 100µl nuclease-free water (Sigma, W4502), 400µl extraction buffer, 10µl Proteinase K (20mg/ml) (Sigma, P6556) and incubated at 50^{o}C, 2 hours.

500µl of PCI (phenol: chloroform: isoamyl alcohol 25:24:1) (Sigma, P2069) was added, mixed gently and centrifuged, 10 minutes at 130,000xg.

The top phase was transferred to a new tube, 1 ml of chloroform (Sigma, 288306) was added and after vortex, the mixture was again centrifuged at 130,000xg for 10 minutes.

The upper phase was transferred to a new tube and two volumes of 100% (v/v) ethanol (Sigma, 459844) were added, followed by centrifugation at 130,000xg for 5 minutes.

The DNA pellet was washed with 700µl of 70% (v/v) ethanol, and then centrifuged at 130,000xg for 1 minute. Discard the ethanol.

Finally, the pellet was dried at room temperature and dissolved in 100µl of nuclease-free water (Sigma, W4502).

2.2.2.3. PCR amplification for 3'UTR regions

3'UTR regions of all genes including *ADAMTS6, ADAMTS14, ADAMTS17, ADAMTS19, FZD3, FZD5, DVL3, FRAT2,* and *CK2A2* were downloaded from the Ensembl Genome Browser: http://www.ensembl.org/index.html. Primers were specifically designed to amplify a 1-2 kb region of 3'UTR of these genes including the miR-29 family binding sites. A restriction site of *Sac*I (5'GAGCTC3'), XbaI (5'TCTAGA3') or *Sal*I (5'GTCGAC3') are added to the 5' end of each primer. Primer sequences are listed in Appendix, Table 1.

All 3'UTR regions were amplified from human genomic DNA, isolated from the SW1353 cell line. 100ng genomic DNA was added together with 5µl 10X reaction buffer, 5 units accuTaq^{TM} LA DNA polymerase (Sigma, D8045), 0.5µl dNTP 10µM (Bioline, BIO-39044), 1µl forward primer 10µM (Sigma), 1µl reverse primer 10µM (Sigma) in a 50µl reaction volume. The reaction was run on a Veriti^{R} 96-well thermal cycler (Applied Biosystems, 4375786) at 98^{o}C, 30 seconds to denature DNA and follows by 32 cycles: 10 seconds at 98^{o}C, 20 seconds at annealing temperature (depending on each primer pair), 1-2 minutes at 68^{o}C. Finally, the reaction was left 2 minutes at 68^{o}C for final extension.

The PCR reaction was confirmed by loading 3µl PCR product on 1% (w/v) agarose gels, which were prepared by heating 1% (w/v) agarose (Sigma, A9639) in Tris-acetate-EDTA (TAE) buffer, and run at 120V. After staining in ethidium bromide solution (Sigma, E1510) for 20 minutes, the product was visualized under UV-light.

2.2.2.4. Phenol/chloroform clean up

Nuclease- free water (Sigma, W4502) was added to a PCR reaction to 200µl, followed by 200µl of phenol: chloroform: isoamyl alcohol (Sigma, P2069). The reaction was mixed well and centrifuged at 130,000xg for 10 minutes. The upper phase was collected to a fresh tube and a 2.5 volume of 100% (v/v) ethanol (Sigma, 459844) and 1/10 volume of 5M NaOAc (sodium acetate, Sigma, S2889) were added, followed by centrifugation at 130,000xg for 10 minutes. The DNA pellet was washed with 500µl of 70% (v/v) ethanol (Sigma, 459844), and centrifuged at 130,000xg for 10 minutes. Finally, the pellet was dried at room temperature for 5 minutes and dissolved in 27µl nuclease- free water (Sigma, W4502).

2.2.2.5. Plasmid isolation

A single colony from LB (Luria Bertani) agar plate supplemented with 100µg/ml ampicillin (Sigma, A0166) was inoculated into 5ml of LB broth medium also supplemented with 100µg/ml ampicillin incubated at 37°C, 180rpm overnight. The bacterial culture was pelleted by centrifugation at maximum speed for 5 minutes. Plasmids were isolated using the QIAprep Spin Miniprep Kit (Qiagen, 27104): The pellet was resuspended in 250µl of P1 buffer. 250µl of P2 buffer was added to the suspension which was then mixed thoroughly by vigorously inverting 4-6 times and incubated at room temperature for 5 minutes. After that, 50µl of P3 buffer was added and the mixture was inverted until a homogenous suspension containing a white flocculate was formed. The bacterial lysate was cleared by centrifugation at 130,000xg, 10 minutes and the supernatant was transferred to a spin column. The column was washed two times with 500µl of wash buffer. Finally, the plasmid was then eluted with 30µl nuclease free water (Sigma, W4502).

For preparation of large quantities of plasmid DNA, the QIAGEN Plasmid MIDI Kit was used (Qiagen, 12143): A single colony from LB ampicillin agar plate was inoculated into 100ml of LB medium supplemented with 100µg/ml ampicillin (Sigma, A0166), incubated at 37°C, 180rpm overnight and harvested by centrifugation at maximum speed for 10 minutes at 4°C. The bacterial pellet was resuspended in 4 ml of P1 buffer, followed by 4 ml of P2 buffer, and the suspension was thoroughly mixed by vigorously inverting the sealed tube 4-6 times and incubated at room temperature for 5 minutes. 4 ml of chilled P3 buffer was added, and the suspension was thoroughly mixed by vigorously inverting 4-6 times and incubated on ice for 15 min, followed by centrifugation at 130,000xg for 30 minutes at 4°C. The QIAGEN-tip was equilibrated by applying 3 ml of QBT buffer, and the column was allowed to empty by gravity flow. The supernatant (above) was applied to the QIAGEN-tip. The QIAGENtip was washed twice with 10ml of wash buffer. The DNA was eluted with 5 ml of elution buffer and precipitated by adding 5 ml of room temperature 100% (v/v) isopropanol (Sigma, 190764) to the eluted DNA, followed by centrifugation immediately at 130,000xg for 10 minutes at 4 °C. The supernatant was carefully decanted. The DNA pellet was washed with 2 ml of room temperature 70% (v/v) ethanol (Sigma, 459844), followed by centrifugation at 130,000xg for 5 minutes. The supernatant was carefully decanted without disturbing the pellet. The pellet was dried for

5-10 min. Finally, the plasmid pellet was dissolved in 500µl of nuclease free water and the plasmid concentration was determined using a Nanodrop spectrophotometer.

2.2.2.6. Digestion

2µg of plasmid pmiR-Glo or all PCR products after phenol/chloroform clean up was incubated with 1µl either *Sal*I (10 units/ µl) (Promega, R6061), *Sac*I (10 units/ µl) (Promega, R6051), or *Xba*I (Promega, R6181) in the recommended buffer in a final volume 20µl for 3 hours at 37ºC. The digestion reaction was terminated by heating at 75ºC for 15 minutes.

After digestion, the 5' phosphate of plasmid was removed to prevent self-ligating by incubating the digestion mix with 1µl Antarctic Phosphatase (5 units/µl) (NEB, M0289S) and 3µl Antarctic Phosphatase buffer 10X, in a final volume 30µl.The reaction was carried out at 37ºC for 15 minutes and followed 5 minutes at 70ºC to inactivate the enzyme.

2.2.2.7. Gel purification

The digestion mix was applied to 1% (w/v) SeaKem® LE Agarose (Lonza, 50002). DNA fragments were visualized by staining with ethidium bromide (Sigma, E1510). Under UV-light, the appropriate DNA band was excised from the gel with a clean scalpel and transferred into an Eppendorf tube. The Zymoclean Gel DNA Recovery Kit (Zymo Research, D4001) was used to purify DNA from the agarose gel. Briefly, 3 volumes of ADB were added to each volume of agarose excised from the gel and incubated at 37-55ºC for 5-10 minutes until the gel slice was completely dissolved. For DNA fragments higher than 8kb, 1 addition volume of water was also added to the agarose. The dissolved agarose solution was transferred to the Zymo-spin column and centrifuged for 30 seconds at full speed. The flow-though was discarded. The column was washed two times with 200µl DNA wash buffer and centrifuged at full speed at 30 seconds. The flow-though was discarded. DNA was eluted with 13µl nuclease-free water (Sigma, W4502) and quantified using a NanoDrop spectrophotometer.

2.2.2.8. Ligation

Ligation of DNA fragments was performed with a ratio of 1:3 of plasmid DNA: insert. The reaction mixture was incubated with 1µl of T4-DNA Ligase (1 unit/µl) (Life Technologies, 15224-017), 1µl of ligation buffer (10X) in a final volume of 10µl ddH2O. The reaction was left at 14^{o}C for 24hours.

2.2.2.9. Transformation

To 100µl of competent E.coli DH5α, either 50-100ng of plasmid DNA or 10 µl of ligation reaction were added and incubated for 20 minutes on ice. A heat shock at 42°C for 30 seconds was followed by incubation on ice for another 2 minutes. 500µl of LB medium was added to the bacteria and the bacterial suspension was shaken at 37°C and 180rpm for 60 minutes. The bacteria were then spread on LB-agar plates containing 100µg/ml ampicillin (Sigma, A9393). Plates were incubated at 37°C overnight.

2.2.2.10. MicroRNA 29 family binding site mutagenesis

QuikChange II XL site-directed mutagenesis kit (Agilent, 200521) was used to replace 5 nucleotides in the binding site of the miR-29 family to either *Xba*I (5'TCTAGA3'), *Sal*I (5'GTCGAC3'), *Sac*I (5'GAGCTC3') depending on which restriction enzymes were used in subcloning. The basic procedure utilizes PfuUltra high fidelity (HF) DNA polymerase for extending two mutagenic oligonucleotide primers which have desire mutations in the middle of their sequences and the rest of the sequence complementary to opposite strands of miR-GLO- 3'UTR. After cycling, PfuUltra HF DNA polymerase will generate a mutated plasmid containing staggered nicks (Figure 2.1). The product is then treated with *Dpn* I nuclease targeting sequence 5'-Gm^{6}ATC-3'. *Dpn* I, specific for methylated and hemimethylated DNA, will digest the parental DNA template and select for mutant-containing synthesized DNA. The nicked vector DNA incorporating the desire mutant of the miR-29 family binding site is then transformed into XL10 Gold ultracompetent cells (Figure 2.1).

Mutangenic primers were designed using Agilent's website: QuikChange primer design program: www.agilent.com/genomics/qcpd. The lists of primer mutants used are listed in Appendix, Table 2.

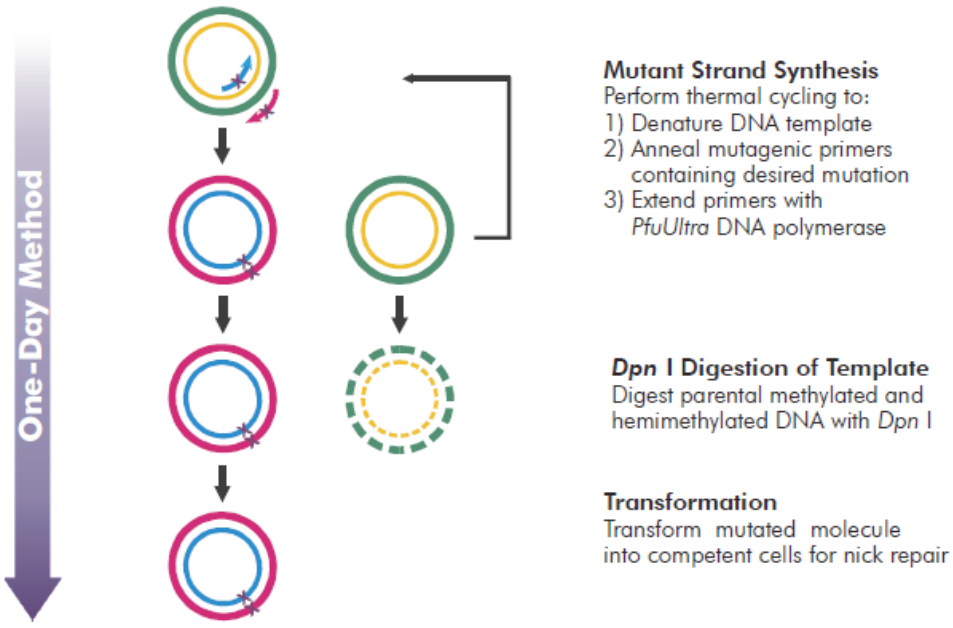

Figure 2.1: QuikChange II XL site-direct mutagenesis method

The reaction is prepared in a final volume of 50µl with 10ng of pmiR-Glo-3'UTR, 1.5µl primer mutant forward (100ng/µl), 1.5µl primer mutant reverse (100ng/µl), 1µl of dNTP mix (10mM), 5µl of reaction buffer (10X), 1µl of PfuUltra HP DNA polymerase (2.5 units/µl). The reaction is cycled at 1 minute at 95ºC, followed by 18 cycles at 95ºC 50 seconds, 68ºC 1 minute/1 kb plasmid length, and finally extension at 68ºC for 7 minutes. The amplification reaction was further incubated with 1µl of *Dpn*I restriction enzyme (10units/µl) at 37ºC for another 1 hour. To 50µl of XL10-Gold Ultracompetent cells, 5µl of *Dpn* I-treated DNA was added and the transformation protocol followed as above.

2.2.2.11. Sequencing

DNA Sequencing was performed by Source BioScience (http://www.lifesciences.sourcebioscience.com/). The sequencing signal was read by Chromas 2.4.

2.2.2.12. Total RNA isolation

2.2.2.12.1. Total RNA isolation from cultured cells

500ml of Trizol® reagent (Invitrogen, 15569-026) were added directly to adherent cells after removing the growth media from a 6-well plate. The cells were lysed by pipetting up and down several times. 250µl chloroform (Sigma, 288306) was added per 500µl Trizol®, vortexed for 15 seconds and incubated at room temperature for 10mins. The Trizol®/Chloroform mixture was centrifuged at 130,000xg, 10min, at 4°C and the aqueous layer recovered into a fresh tube. 500µl of 100% (v/v) isopropanol (Sigma, 190764) was added, mixed, left 10min at room temperature and centrifuged at 130,000xg, 10min, at 4°C then the supernatant was discarded. RNA pellets were washed with 75% (v/v) ethanol (Sigma, 459844), and centrifuged at 130,000xg, 2min, at 4°C. The supernatant was discarded, the pellet air dried and then suspended in 50µl RNase-free water and stored at -80°C until further use.

2.2.2.12.2. Total RNA isolation from murine whole knee joint

All materials used were RNase free. Whole knee joints were ground under liquid nitrogen using BioPulverizer (Biospec). Trizol® reagent (Invitrogen, 15569-026) were added immediately to ground samples (1.5ml/50mg samples) and mixed thoroughly for 5 minutes. Ground knee joints were pelleted at 130,000xg for 2min at 4°C and the supernatant recovered. 250µl chloroform (Sigma, 288306) was added per 500µl Trizol®, vortexed for 15 seconds and incubated at room temperature for 10mins. Samples were then treated as cultured cells above.

2.2.2.12.3. Total RNA isolated from murine hip or knee cartilage

Murine hip femoral caps were fully homogenized with 500µl Trizol® reagent (Invitrogen, 15569-026) using a disposable pestle. Then, 200µl chloroform (Sigma, 288306) was added, vortexed for 15 seconds, and left at room temperature for 10mins. The Trizol®/chloroform mixture was centrifuged at 130,000xg for 10 minutes at 4°C, and the aqueous layer collected into a fresh tube. The RNA purification step was performed using *mir*Vana™ miRNA Isolation Kit (AM1560, Life Technology) according to the manufactures recommendation for total RNA recovery. Briefly, 1.25x aqueous layer volume of 100% (v/v) RT ethanol was added to the aqueous phase and the samples were loaded onto

columns. The flow through was discarded after centrifuging 15 seconds at 130,000xg. Then three wash steps were followed by applying wash solution 1 (700µl), and then wash solution 2/3 (500µl) (twice) to the column. For each washing, the column was centrifuged at 130,000xg for 15 seconds followed by discarding the flow through. The columns was then placed in RNase-free collection tubes and 30µl of RNas-free water added. Columns were then left to stand for 2 minutes and centrifuged at 2 minutes, 13,000xg. RNA was then stored at -80^{o}C until used.

2.2.2.13. MicroRNA quantification and integrity

The concentration of RNA samples was determined by measuring the absorbance at 260nm using the NanoDrop spectrophotometer (NanoDrop Technologies). The purity of RNA is determined from the ratio A_{260}/A_{280} and A_{260}/A_{230}.

The integrity of total RNA was determined using the Experion^{TM} automated electrophoresis system (Bio-Rad, USA). This method measures fluorescence of a fluorophore bound to RNA. RNA integrity can be evaluated automatically by comparing the area of the peaks corresponding to the rRNAs. A 28S/18S rRNA ratio close to 2 indicates for intact RNA.

2.2.2.14. cDNA synthesis

2.2.2.14.1. SuperScript II reverse transcriptase cDNA synthesis

Total RNA was isolated from cells, whole knee joints, human or murine cartilages as above and reverse transcribed to cDNA using SuperScript II reverse transcriptase (Life Technologies, 18064-014). Briefly, in a total volume of 11µl in 96-well PCR plate, 1µg total RNA and 0.2µg random hexamer primer (Life Technologies, 48190-011) was mixed together and the plate was incubated at 70^{o}C for 10mins. Samples were chilled on ice, then, a master mix containing 1µl SuperScript II reverse transcriptase (200 units/µl) (Life Technologies, 18064-014), 4µl First Strand buffer (5X) (Life Technologies, 28028-013), 2µl 0.1M dithiothreitol (DTT) (Life Technologies, 18057-018), 2µl of 10mM dNTP mix (Bioline, BIO-39044), 1µl Recombinant RNasin Ribonuclease Inhibitor (20-40 units/µl) (Promega, N2511) was added to the randomly primed RNA to give a total volume of 20µl and incubated for 1 hour at 42^{o}C followed by a heat inactivation step at 70^{o}C, for 10mins.

cDNA was diluted to 0.5µg/ml in nuclease-free water (Sigma, W4502). 5µg cDNA was used for qRT-PCR analysis of genes of interest and 1µg cDNA was used for analysis of 18S rRNA. QRT-PCR is described in 2.2.2.15.

2.2.2.14.2. M-MLV reverse transcriptase cDNA synthesis

Moloney Murine Leukemia Virus (M-MLV) reverse transcriptase was used to perform cDNA synthesis straight from cell lysate without the need of purifying total RNA. This method was used for cell plated in 96-well plate where a number of cells are too small for RNA extraction.

Briefly, medium was removed and the cells in 96-well plate were washed with ice cold PBS (Life Technologies, 10010023). Then, 30µl cells to Cells-II-cDNA lysis buffer (Life Technologies, AM8723) was added to each well, providing a cell lysate which can immediately be reverse transcribed without the need for RNA isolation. Lysates were transferred to 96-well PCR plate and heated to 75ºC for 15 minutes to inactivate RNases. Lysates can be stored at -80ºC until reverse transcription. For genomic DNA digestion, 1µl DNase I 1 units/µl (Life Technologies, AM2222) and 3µl DNase I buffer (10X) were added per well. The plate was heated to 37ºC for 15 minutes, followed by an inactivation step at 75ºC for 5 minutes.

For reverse transcription, 8µl of DNase-treated samples were transferred to a new ice cold PCR plate. Following this, 3µl of 10mM dNTP mix (Bioline, BIO-39044) and 0.2µg random hexamer primers (50µM) (Life Technologies, 48190-011) were added per well and samples were heated to 70ºC for 5 minutes. Samples were chilled on ice and a master mix including 0.5µl Moloney Murine Leukemia Virus (M-MLV) reverse transcriptase 200 units/µl (Life Technologies, 28028-013), 4µl First Strand buffer (5X) (Life Technologies, 28028-013), 2µl 0.1M dithiothreitol (DTT) (Life Technologies, 18057-018), 0.5µl Recombinant RNasin Ribonuclease Inhibitor (20-40 units/µl) (Promega, N2511), 1µl nuclease-free water (Sigma, W4502) was added per well. Samples were then heated to 37ºC for 50 minutes, followed by an inactivation step of 75ºC for 15 minutes. After that, 30µl of nuclease-free water (Sigma, W4502) was added per sample. For quantitative real-time PCR (qRT-PCR) analysis of genes of interest, 5µl of each sample was used. For the

house keeping gene 18S rRNA, samples were diluted 1:10 and 5µl was used. QRT-PCR is described in 2.2.2.15.

2.2.2.14.3. miRCURY LNA™ Universal cDNA synthesis

MicroRNA cDNA was synthesized by the miRCURY LNA™ Universal cDNA synthesis kit (Exiqon, 203300). This step provides templates for all miRNA real-time PCR assays by one first-strand cDNA synthesis reaction. The basis principal is in Figure 2.2.

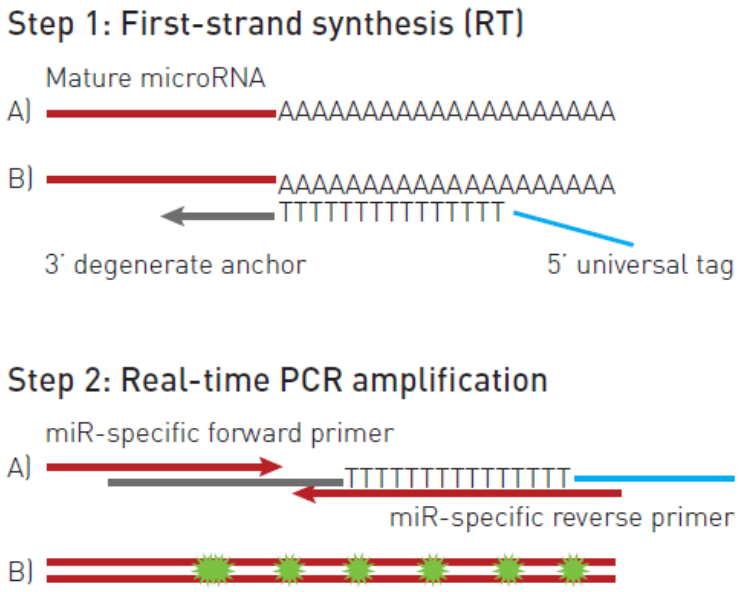

Figure 2.2: Outline of the miRCURY LNA Universal RT miRNAsynthesis.

A poly-A tail is added to the mature miRNA template (step 1A). cDNA was synthesized using a poly-T primer with a 3'degenerate anchor and a 5'universal tag (step1B). Then the cDNA template is amplified using miRNA-specific and LNA^{TM}-enhanced forward and reverse primers (step 2A). Sybr green is used for detection (step 2B). *Reprinted from miRCURY LNA^{TM} Universal RT microRNA PCR instruction manual (Exiqon).*

Total RNA was adjusted to 5ng/µl using nuclease-free water (Sigma, W4502). 10ng of RNA was transferred to an ice cold 96-well PCR plate. A master mix contained 2µl Reaction Buffer (5X) (Exiqon, 203300), 1µl enzyme mix was added to each well. The reaction was brought to 10µl with nuclease-free water and the plate was heated to 42^{o}C for 1 hour followed by a heat inactivation step at 95^{o}C for 5minutes. cDNA was then diluted to 12.5 pg/µl by nuclease free water (Sigma, W4502) and 50pg of cDNA was used for qRT-PCR analysis of miRNA of interest.

2.2.2.15. Real-time quantitative RT-PCR

2.2.2.15.1. Universal Probe Library Real-Time qRT-PCR

The Universal Probe Library (UPL) (Roche Diagnostics) enables extensive transcript coverage due to the short 8-9 nucleotide-long probes. Each probe has a fluorescein (FAM™) label at the 5' end and a dark quencher dye at the 3' end; shorter (typically 8-9 nucleotide) than conventional probe (25-35 nucleotides); locked nucleic acids (LNA™) are incorporated into it sequence. Each probe can detect ~7,000 transcripts and each transcript is detected by ~16 probes.

Primers were designed using the freely available ProbeFinder web-based software provided by Roche Applied Science in which the 'exon boundary spanning' option was selected. Primers were subjected to short sequence BLASTn search to confirm specificity. All the primers were purchased from Sigma and reconstituted in nuclease free water (Sigma, W4502) at 100nM. Primer sequences and UPL probe numbers are in Appendix, Table 3.

For quantitative RT-PCR using the universal primers and probes, the qRT-PCR was carried out using the ABI Prism 7900 HT Sequence Detector (Applied Biosystems) in a microAmp® optical 96-well plate (Life technologies, N8010560). When RNA quantity was known, the qRT-PCR was run using 5ng cDNA for genes of interest and 1ng cDNA for 18S rRNA. For M-MLV-reverse-transcribed- cDNA transcript samples, 5µl samples was used for gene of interest or diluted 1:10 and used 5µl for detecting 18S rRNA.

Each qRT-PCR reaction contained Kappa Fast Universal qPCR Master Mix (2X) (Kappa Biosystems, KK4703), a final concentration of 100nM of each of forward and reverse primers, 200nM of Universal Probe (Roche Diagnostics). The reaction was carried out in a final volume of 25µl. The plate was sealed with microAmp® optical adhesive film (Life Technologies, 4311971) and run with the following PCR cycles: 50°C 2 minutes, 95°C 10 minutes, 40 cycles for 95°C 15 seconds, 60°C 1 minute.

2.2.2.15.2. Standard probe-based Real-time qRT-PCR

The probe-based quantitative real-time PCR method was used to detect the expression of ADAMTS genes including *ADAMTS4, ADAMTS6, ADAMTS10, ADAMTS14, ADAMTS17, ADAMTS19*. These primer and probe sequences were described in (Davidson *et al.* 2006). Briefly, the primers and probes were designed by Primer Express® 1.0 software (Life Technologies, 4363991) and were closed to intron/exon boundaries to control amplification of genomic DNA. Where possible, the probes were designed to span two neighbouring exons. Specificity of primers and probes were validated thought BLASTn. Primer sequences and probe sequences are in Appendix, Table 4

The qRT-PCR reaction was also carried out in a final volume 25µl of Kappa Fast Universal qPCR Master Mix (2X) (Kappa Biosystems, KK4703), 100nM final concentration of each of forward and reverse primers, 200nM genes of interest-specific probe. Reaction set up and cycling conditions were as in 2.2.2.15.1.

2.2.2.15.3. SYBR® Green Real-time PCR

A combination of SYBR® green dye fluorescence with gene-of-interest specific primers enabled double stranded-DNA amplification measurement during PCR. SYBR® green real-time qRT-PCR was used to detect primary and pre sequences of the miR-29 family (which were described in (Eyholzer *et al.* 2010)) and other genes as below. Full primer sequences and list of genes detected by SYBR® green real-time PCR are listed in Appendix, Table 5. All primers were purchased from Sigma.

For SYBR® green qRT-PCR reaction, the amount of cDNA for genes of interest and 18S rRNA is as 2.2.2.15.1. The reaction contained 0.18µl SYBR® green I dye, Kappa Fast Universal qPCR Master Mix (2X) (Kappa Biosystems, KK4703), 100nM final concentration of each of forward and reverse primers. The PCR cycle conditions are as 2.2.2.15.1 followed by another dissociation step which produces the melting curve for the PCR amplification product.

2.2.2.15.4. SYBR® Green Real-time PCR for the mature miR-29 family detection

LNA primers for detecting miR-29 family mature sequence

All LNA primers were designed for optimal performance with the miRCURY LNA™ Universal cDNA synthesis kit. The LNA primers are Hsa-miR-29b-3p LNA™ PCR primer sets (Exiqon, 204679), Hsa-miR-29a-3p LNA™ PCR primer sets (Exiqon, 204698), Hsa-miR-29c-3p LNA™ PCR primer sets (Exiqon, 204729).

Real-time PCR protocol

The qRT-PCR reaction used SYBR® green I dye in combination with LNA™ PCR primer sets to quantify the original mature miR-29 family. The reactions contained 50pg of miRCURY-LNA™-Universal cDNAs for either the miR-29 family or U6. The PCR reaction mix contained 0.18µl SYBR® Green I dye, 5µl Kappa Fast Universal qPCR Master Mix (2X) (Kappa Biosystems, KK4703), and 1µl of forward and reverse primer mix (as recommend by the manufacture (Exiqon)) in a final volume of 10µl. PCR cycles: 10 minutes at 95°C, 40 cycles for 10 seconds at 95°C, 1 minute at 60°C and a dissociation step. The dissociation step produces a melting curve for the PCR amplification product and ensures there is only amplification of the target gene.

2.2.2.15.5. Quantitative RT-PCR Data analysis

2.2.2.15.5.1. Control genes

The constitutively expressed "housekeeping" 18S rRNA was used as the control for relative mRNA gene expression while U6 was used as endogenous control for relative miRNA gene expression.

2.2.2.15.5.2. Relative gene expression – comparative C_t method

Raw fluorescence data was analyzed by the 7000HT SDS 2.2 software to produce threshold cycle (C_t) values, which is the cycle number at which the signal is detectable above the baseline. The C_t values were transformed using the comparative C_t method to obtain relative quantification (RQ) of gene expression:

$$RQ=2^{-\Delta Ct}$$

Where: for mRNA expression: ΔC_t= target gene C_t - 18S C_t

Or for miRNA expression: ΔC_t= the miR-29 family C_t - U6 C_t

This method assumed that all primers and probe sets are working at the same efficiency.

2.2.2.15.6. Western Blot

Buffer and antibody

Radio immunoprecipitation assay (RIPA) buffer: The buffer was made (final concentration) with 50mM Tris base (Fisher Scientific, BP152-500) (which was adjusted to pH 7.6 with hydrochloric acid (Sigma, 258148)),150mM NaCl (Fisher Scientific, BP3581), 1% (v/v) Triton X-100 (Sigma, X100), 1% (w/v) sodium deoxycholate (Sigma, D6750), 0.1% (w/v) sodium dodecyl sulfate (SDS) (Fisher Scientific, 10356463), 10mM sodium fluoride (NaF) (Sigma, 201154), 2mM sodium orthovanadate (Na_3VO_4) (Sigma, S6508), 1X protease inhibitor cocktail (Fisher Scientific, PI-78410).

Resolving buffer: To make up 4X buffer: 91g Tris base (Fisher Scientific, BP152-500) was dissolved in Milli-Q Ultrapure water (Merck Millipore) and adjusted to pH 8.8 with hydrochloric acid (Sigma, 258148). The solution was then made up to 500ml. 2g SDS (Fisher Scientific, 10356463) was added and dissolved.

Staking buffer: To make up 4X buffer: 6.05g Tris base (Fisher Scientific, BP152-500) was dissolved in Milli-Q Ultrapure water and adjusted to pH 6.8 with hydrochloric acid (Sigma, 258148). Milli-Q water was added to 100ml volume. 0.4g SDS (Fisher Scientific, 10356463) was added and dissolved.

Running buffer: To make up 10X buffer: 30.2g Tris base (Fisher Scientific, BP152-500), 144g glycine (Fisher Scientific, 10467963), 10g SDS (Fisher Scientific, 10356463) were dissolved in Milli-Q water to a final volume 1L.

Transfer buffer: To make up 1X buffer: 5.8g Tris base (Fisher Scientific, BP152-500), 2.9g glycine (Fisher Scientific, 10467963), 0.37g SDS (Fisher Scientific, 10356463) were dissolved in Milli-Q water, 200ml 100% (v/v) methanol (Sigma, 322415) were added then Milli-Q water to a final volume of 1L.

Tris-buffered saline (TBS): To make up 10X buffer: 24.2g Tris base (Fisher Scientific, BP152-500), 80g NaCl (Fisher Scientific, BP3581) were dissolved in 900ml Milli-Q water and adjusted to pH 7.6 with hydrochloric acid (Sigma, 258148). Milli-Q water was added to 1L volume.

Blocking buffer: For 150ml, 15ml 10X TBS was diluted in 135ml Milli-Q water. 7,5g non-fat dry milk (OXOID, LP0031) was added and stirred to mix. Finally, 0.15ml Tween®-20 was added (Sigma, P5927).

Primary antibody dilution buffer: For 20 ml, 2 ml 10X TBS was diluted to 18 ml with Milli-Q water. 1.0 g BSA (Sigma, A9418) was added and dissolved by stirring. While stirring, 20µl Tween-20 (Sigma, P5927) was added.

Wash Buffer (TBST): TBS with a final concentration 0.1% (v/v) Tween-20 (Sigma, P5927).

Antibody: GAPDH antibody (Cell Signaling, #2118S), DVL3 antibody (Cell Signaling, #3218), FZD5 antibody (Cell Signaling, #3795)

Western blot protocol

SW1353 cells were plated in 6-well plates ($1.5x10^5$cells/well) and transfected with Syn-Hsa-miR-29b miScript miRNA mimic (Qiagen, MSY0000100) as referred in 2.2.2.7.2.5. At desired time post transfection, cells in each well of 6-well plate were washed twice with ice cold PBS (Life Technologies, 10010023) before adding 100µl RIPA buffer to each well and harvesting by scraping. The cell lysate was transferred to a fresh ice-cold 1.5ml tube and centrifuged at full speech in 10 minutes. The supernatant was collected and stored at -20^{o}C.

Protein was quantified using the Bio-Rad Protein Assay (Bio-Rad, #500-0006) which is based on the method of Bradford. Briefly, 200µl dye reagent concentrate was diluted 5 times with Milli-Q water before adding 20µl sample lysate. The mixture was incubated at room temperature for 10 minutes and absorbance measured at 595nm. Comparison of this value to a standard curve provided a relative concentration of solubilized protein. The

standard curve was created with five dilutions of proteins standards of bovine serum albumin (Bio-Rad, 500-0002) from 0.2 to 0.9 mg/ml.

Samples was adjusted to 20µg solubilized protein in a 30µl with nuclease-free water (Sigma, W4502), followed by adding 20ng/µl Bromophenol Blue (Sigma, 114391) and 1.2µl 1M DTT (Thermal Scientific, # R0861). The sample was gently mixed and heated to 95ºC for 5 minutes. Samples were then electrophoresed on 10% (w/v) polyacrylamide gels. The resolving gel was cast with the following components: 5ml 30% (w/v) Acrylamide/ Bis Acrylamide solution 37:5:1 (Bio-Rad, #161-0154), 3.75ml resolving buffer (4X), 6.25ml Milli-Q water, 50µl 10% (w/v) ammonium persulfate (APS) (Sigma, A3678), 10µl TEMED (Sigma, T9281). Resolving gels were topped with isopropanol (Sigma, 190764) until set. Then isopropanol was removed and the stacking gel was cast on top of the resolving gel and a comb was inserted. For 1 gel, the stacking gel was made with 0.71ml stacking buffer (4X), 0.41ml 30% (w/v) acrylamide/ bis acrylamide solution 37:5:1 (Bio-Rad, #161-0154), 1.91ml Milli-Q water, 16µl 10% (w/v) APS (Sigma, A3678), 3.2µl TEMED (Sigma, T9281). Samples were loaded on the gel and were electrophoresed at 50V until the bromophenol blue passed through the stacking gel and then 80V for 1.5 hours.

Immobilon®-FL PVDF membrane (Merck Millipore, IPFL00010) was incubated in 100% (v/v) methanol (Sigma, 322415) for 15 seconds and washed with Milli-Q water. Then, Immobilon®-FL PVDF membrane, gel, extra thick blotting paper (Bio-Rad, #170-3966) were incubated in transfer buffer for 5 minutes. The gel was plated on top of Immobilon®-FL PVDF membrane in Trans-blot® SD semi-Dry Electrophoretic transfer cell (Bio-Rad, #170-3940) with extra thick blotting paper underneath and on top and run for 25V for 30 minutes (for 2 gels,1 mm thick).

After transfer, the membranes were briefly washed with TBS and incubated in blocking buffer for 1 hour, with gently rocking at room temperature. Membranes were then washed in TBST three times for 5 minutes. Primary antibody and membrane was incubated with gentle agitation overnight at 4ºC. Membranes were then washed in TBST three times for 5 minutes and incubated with IRDye® 800CW goat polyclonal anti-rabbit IgG (Li-Cor, 926-32211) (50µg) for 1 hour at room temperature with gently rock. Membranes were washed

with TBST for another three times for 5 minutes. The membrane was visualized using a Li-Cor Odyssey InfraRed Scanner.

2.2.2.15.7. Whole mount *in situ* hybridization

Reagents and buffers

Sodium chloride (NaCl) (Fisher Scientific, BP3581), tri-sodium citrate (Fisher Scientific, 10637174), magnesium chloride hexahydrate ($MgCl_2.6.H_2O$) (Fisher Scientific, M35-500), potassium chloride (KCl) (Fisher Scientific, BP366-500), heparin (Sigma, H3393), yeast tRNA (Fisher Scientific, 10523043), paraformaldehyde (Sigma, P6148), normal goat serum (heat inactivated), Triton-X100 (Sigma, X100), Tween-20 (Sigma, P5927), BSA (Sigma, A9418)

Saline sodium citrate buffer (SSC): 20X SSC buffer was made up with 175.3 g of NaCl and 88.2 g of sodium citrate, pH 7, in a total volume of 1000ml.

Development solution (DS): The solution was made up with: 100 mM Tris-HCl pH9.5, 50mM magnesium chloride hexahydrate (MgCl2.6.H2O), 100mM sodium chloride (NaCl) + 0.1% (v/v)Tween 20.

Blocking solution: The solution was made up with: 2% (v/v) NGS, 2 mg/ml BSA, 0.1% (v/v) Triton X-100 + 0.05%)v/v) Tween 20 in PBS.

Hybridisation Buffer (HB): The buffer was made up with 50% (v/v) formamide, 5xSSC, 0.1% (v/v) Tween 20 + 10 mM citric acid pH6.0 + 50 µg/ml heparin + 100 µg/ml tRNA in PBS

Tris-buffered saline with Tween 20 (TBST): for 100ml (10X) buffer was made up with 8g NaCl, 25ml Tris-HCl pH7.5, 0.2g KCl, 10ml Tween 20

Phosphate-buffered saline with Tween 20 (PBST): PBS with 0.1% (v/v) Tween 20

Probe: miRCURY LNA™ miR-29b-3p detection probe, 250pmol, 5'-DIG and 3'-DIG labelled (Exiqon, 38131-15)

Fixation

Mouse embryos at desired stages were dissected and fixed in 4% PFA-PBS on a rolling platform overnight at 4^{o}C. Then next day, the embryos were washed 4 times with PBST and dehydrated through increasing MeOH concentration washes e.g. 25%, 50%, 75% and 100% MeOH on the gentle rocking platform. The embryos can then store in 100% MeOH at -20^{o}C until required.

In situ hybridization protocol

On a gently rocking platform, the embryos were washed with decreasing MeOH concentration i.e. 75% (v/v), 50% (v/v), 25% (v/v), 0 (v/v) % MeOH for 15 minutes each time to dehydrate. After that, the embryos were digested with Proteinase K (10µg/ml final concentration) for 30 minutes, followed by rinsing twice in PBST and fixing in 4% (v/v) PFA for 20 minutes. To get rid of the remaining PBST, the embryo was washed 4 times in PBST for 5-7 minutes. The embryo was prehybridized in hybridization buffer at 54^{o}C for 3 hours and the "nape" of the neck of embryo was pricked to facilitate the probe penetration. After prehybridisation step, the buffer was removed and replaced with fresh warm hybridisation buffer containing 20 pmol of the miR-29b LNA probe (Exiqon, 38131-15) and left at 54^{o}C overnight with gentle rocking. The probe hybridisation solution was removed followed by washes at 54^{o}C and 15 minutes each wash e.g. 75% HB: 25% 2xSSC, 50% HB:50% 2xSSC, 25% HB:75% 2xSSC, 2xSSC, 0.2xSSC. Following these washes, at room temperature, another 4 washes were carried on gently rocking platform, 10 minutes for each wash e.g. 75% 0.2xSSC:25% PBST, 50% 0.2xSSC:50% PBST, 25% 0.2xSSC:75% PBST, PBST. The embryo was then put in blocking solution for several hours at room temperature and incubated at 4°C O/N with the pre-absorbed antibody at a final dilution of 1:5000 in Blocking Solution. After that, the Blocking Solution was removed and washed throughout 2 or 3 days at RT in PBST with gentle rocking. To get rid of all remaining PBST, the embryos were washed twice with TBST and with development solution for 15 minutes each wash. Colour development was carried out at room temperature in 3.5ml development solution plus 15-50µl substrates.

The antibody was pre-adsorbed using previously fixed and dehydrated tissue that is not suitable for in situ hybridization. These tissues were dehydrated and washed 15 minutes in

blocking solution, followed by incubating with blocking solution containing the antibody at 1:1000 dilution for three hours.

2.2.2. Cell culture and cell-based assays

2.2.2.1. Human primary chondrocyte isolation

Human cartilage chips were incubated with digestion medium including DMEM GlutaMAX^{TM} (Life Technologies, 10566-016), 1mg/ml collagenase (Sigma, C1639), 0.4% (w/v) Hepes (Fisher Scientific, BP310-100), 100 IU/ml penicillin, 100µg/ml streptomycin (Sigma, P4333) at 37^{o}C, 180rpm overnight. The digestion mixture was then strained through a 70µm cell strainer. Cells were plated at 4x10^{4}cells/cm^{2} and grown to 80% confluence. Cells were used by passage 2.

2.2.2.2. Human de-differentiation assay

Human primary chondrocytes were isolated from human knee OA articular cartilage as described in 2.2.2.1. The cells were then subjected to serial subculture in monolayer. The de-differentiation assay was performed by Dr Natalie Crowe (Clark lab, University of East Anglia).

2.2.2.3. Chondrogenesis model

The human chondrogenesis model was performed by Dr Matthew Barter, Newcastle University. Briefly, human bone marrow stem cells (from seven donors, 18-25 years of age) were isolated from human bone marrow mononuclear cells (purchased from Lonza Biosciences) and resuspended in chondrogenic culture medium consisting of high glucose Dulbecco's modified Eagle's medium containing 100 µg/ml sodium pyruvate (Lonza), 10 ng/ml TGF-β3 (Peprotech), 100 nM dexamethasone, 1x ITS-1 premix, 40 µg/ml proline, and 25 µg/ml ascorbate-2-phosphate (Sigma). 5x10^{5} hMSC in 100µl medium were pipetted onto 6.5mm diameter, 0.4-µm pore size polycarbonate Transwell filters (Merck Millipore), centrifuged in a 24-well plate (200g, 5 minutes), then 0.5 ml of chondrogenic medium was added to the lower well as described. Media were replaced every 2 or 3 days up to 14 days.

The murine chondrogenesis model was performed by Dr Tracey Swingler, University of East Anglia. Briefly, ATDC5 cells were seeded at $6x10^4$/well of a 6-well plate in DMEM/Ham's F-12 medium (Life technologies, 11320-033) containing 5% (v/v) FCS (PAA), 2mM glutamine, 100 IU/ml penicillin, 100µm/ml streptomycin (Sigma, P4333), 5ng/ml sodium selenite, 10µg/ml human transferrin (Sigma, I3146), and 10µg/ml bovine pancreatic insulin at 37°C, in an atmosphere of 5% CO_2. Media was replaced every 2 days up to 42 days. After 21 days, the medium was replaced with α-minimal essential medium with the same supplements, and the atmosphere was changed to 3% CO_2.

2.2.2.4. Monolayer cell culture and storage

All cells were cultured at 37°C with 5% (v/v) CO_2. Cells were usually grown in Dulbecco's modified Eagle's medium (DMEM) High Glucose, GlutaMAX supplement (Life technologies, 10566-016) with 10% (v/v) heat-inactivated Fetal Calf Serum (FCS) (PAA) and 100 IU/ml penicillin and 100µg/ml streptomycin (Sigma, P4333). For maintenance, medium was refreshed at least three times weekly. Cells were passaged at around 80-90% confluence. Adherent cells were detached by washing x2 with HBSS (Life Technologies, 14025092) then treated with 2 ml of trypsin/EDTA (Life Technologies, 25200072) for 2-3 minutes at 37°C. After centrifugation (17.3xg, 5 minutes), the cell pellet was gently resuspended in fresh medium. Cells were replated at a ratio of 1: 20. For long term storage, cells were detached and pelleted by centrifugation at 17.3xg for 5 minutes. The pellets were resuspended in cryo-preservation medium including 90% (v/v) FCS (ATCC) and 10% (v/v) DMSO (Fisher, BP231-100), slowly frozen down at approximately 1°C/minute, and stored in liquid nitrogen.

2.2.2.5. Micromass culture

Media

Growth medium: Dulbecco's modified Eagle's medium (DMEM) High Glucose, GlutaMAX supplement (Life technologies, 10566-016) with 10% (v/v) heat-inactivated Fetal Calf Serum (FCS) (ATCC) and 100 IU/ml penicillin and 100µg/ml streptomycin (Sigma, P4333).

Different medium were prepared: the DMEM high glucose, GlutaMAX supplement (Life technologies, 10566-016) adding 1X Insulin- Transferrin-Selenium (ITS-G) (Life Technologies, 41400-045).

Micromass culture

The protocol was described in (Greco *et al.* 2011) with some modifications. Human primary chondrocytes was isolated from human OA knee cartilage as described in 2.2.2.1 and cultured in monolayer with growth medium. Whenever reaching confluence, the cells were passaged two times. Confluent passage 2 monolayer culture of human primary chondrocytes were released by trypsin/EDTA (Life Technologies, 25200072), and resuspended in growth media at a density of $2.5x10^7$ cells/ml. Micromass was obtained by pipetting 20µl of cell suspension into individual wells of 24 well-plates and leaving for 3 hours to attach without additional medium. Then, 1ml growth medium was gently added and the micromass was left for another 24 hours before stimulating with cytokines or growth factors.

2.2.2.6.Induction cells with regulatory factors: major cytokines and growth factors

Cytokines and growth factors:

Human recombinant TGFβ1 (R&D Systems, 240-B-002/CF) and **human recombinant TGFβ3** (R&D Systems, 243-B-002/CF) were reconstituted in sterile 4mM HCl (Sigma, 258148) containing 0.5% (w/v) bovine serum albumin (Sigma, A2058).

Human recombinant Wnt3a (R&D Systems, 5036-WN-010/CF) was reconstituted in sterile Phosphate Buffered Saline (PBS) (Life Technologies, 10010023).

Human Recombinant Interleukin-1β (IL-1β) (First Link, ILB4551) was reconstituted in sterile Phosphate Buffered Saline (PBS) containing 0.5% (w/v) bovine serum albumin (Sigma, A2058).

NFκB activation inhibitor II JSH-23 (Calbiochem, 481408) is a cell-permeable diamino compound that selectively blocks nuclear translocation of NF-κB p65 and its transcription activity without affecting IκB degradation.

Lipopolysaccharides (LPS) (Sigma, L3012) are components of the cell wall of gram negative bacteria. LPS are extracted from *E.coli* serotype O111:B4 and purified by gel filtration. LPS is reconstituted in sterile (PBS) (Life Technologies, 10010023).

P38 inhibitor SB203580 (Sigma, S8307) is a pyridinyl imidazole that suppresses the activation of MAPKAP kinase-2. The P38 inhibitor, therefore, inhibits the MAPKAP kinase-2 cascade which is activated by cellular stress, bacterial infection and pro-inflammatory cytokines. SB203580 was resuspended in DMSO (Fisher, BP231-100).

2.2.2.6.1. Stimulation of cells in monolayer with cytokines and growth factors

Human chondrosarcoma SW1353 and human primary chondrocytes were maintained as described above. For stimulation, either $5x10^3$ SW1353 cells or 10^4 human primary chondrocytes were seeded into each well of a 96-well plate with 100µl DMEM GlutaMax (Life Technologies, 10566-016) with 10% (v/v) FCS (ATCC) and 100 units/ml penicillin and 100µg/ml streptomycin (Sigma, P4333). Cells were serum starved for 14 hours and were stimulated with different cytokines and growth factors at final concentration: TGFβ1, TGFβ3 4ng/ml, IL-1 5ng/ml, Wnt3a 100ng/ml, LPS 1µg/ml at 4, 8, 12, 24, 48 hours. All treatments were performed in triplicate. At each time point, cells in each well were washed with ice cold PBS (Life Technologies, 10010023) and harvested with 30µl Cells-to-cDNA lysis buffer (Life Technologies, AM8723).

2.2.2.6.2. Stimulation of cells in micromass culture with cytokines and growth factors

After the micromass was rested in growth medium for 24 hours, the different medium with either TGFβ1 (10ng/ml), IL-1 (20ng/ml), Wnt3a (50ng/ml) or LPS (1µg/ml) was added. All treatments were performed in triplicate. After different time points as desired, some of micromasses were harvested for Alcian blue matrix staining and others for quantitative RT-PCR.

2.2.2.7. Mammalian cell transfection

2.2.2.7.1. Plasmids, constructs, siRNAs and microRNA mimic and inhibitor

Sox9 expression vector: The vector was kindly provided by Dr Simon Tew (University of Liverpool, UK). The vector was described in (Lefebvre *et al.* 1997). Briefly, an almost full-length coding sequence of human SOX9 which is from codon 27 (directly from the first ATG associated with the Kozak sequence) up to 39bp of 3'unstranslated region was subcloned into pCDNA-5'UT-FLAG. pCDNA-5'UT-FLAG is pCDNA 3.1 with a FLAG sequence.

The miR-29a/b1 promoter construct: The construct was kindly provided by Dr Anne Delany (University of Connecticut Health Center, US) and was described in (Kapinas *et al.* 2010). The 2kb region upstream from the transcriptional start site of the human miR-29a/b1 putative promoter (EU154353) was subcloned into the luciferase reporter pGL4.10 (Promega).

p(CAGA)$_{12}$-luc plasmid: The construct was a kind gift of Dr Andrew Chantry, University of East Anglia, UK and is described in (Pais *et al*. 2010). 12 binding sites of the complex Smad3/4 (GAGAC) was cloned upstream of the luciferase encoding gene in luciferase reporter pGL3 (Promega).

IκBα promoter reporter plasmid: The plasmid was a kind gift from Prof. Derek Mann, (Newcastle University, UK), (originally from Prof. Ronald Hay, University of Dundee, UK). The plasmid contains 5 binding sites of P65 cloned upstream of the luciferase gene.

TOPflash and FOPflash reporter plasmids: The TOPflash reporter is a kind gift from Prof. Andrea Munsterberg (University of East Anglia, UK), and was originally from Prof. Randall Moon (University of Washington, USA). The FOPflash vector is provided by Dr Sarah Snelling (University of Oxford, UK). TOPflash contains 7 binding sites of TCF/LEF (AGATCAAAGG) driving the expression of the firefly luciferase. The back bone is the pTA-luc vector. The FOPflash vector is the control of TOPflash where all 7 binding sites of TCF/LEF are mutated.

The miR-29 mimic:

- Syn-hsa-miR-29a-3p miScript miRNA mimic (Qiagen, MSY000086): 5'UAGCACCAUCUGAAAUCGGUUA
- Syn-hsa-miR-29b miScript miRNA mimic (Qiagen, MSY0000100): 5'UAGCACCAUUUGAAAUCAGUGUU
- Syn-hsa-miR-29c miScript miRNA mimic (Qiagen, MSY0000681) 5'UAGCACCAUUUGAAAUCGGUUA
- AllStars negative control siRNA (Qiagen, SI03650318)

The 29b inhibitor control

- Anti-hsa-miR-29b miScipt miRNA inhibitor (Qiagen, MIN000100)
- miScript Inhibitor negative control (Qiagen, 1027271)

siRNA

- SOX9 siRNA: Dharmacon siRNA SMARTpool® (Fisher Scientific)
- Control: non-targeting siRNA 2 (Dharmacon, 001210-02)

2.2.2.7.2. Transient transfection protocol

2.2.2.7.2.1. SOX9 overexpression

SW1353 cells were plated in a 96-well plate ($5x10^3$cells/well) in growth medium without antibiotics one day before transfection. The cells were 80% confluent at the time of transfection. Before addition of the transfection complexes, the growth medium was removed from the cells and the cells were covered with 50µl of fresh growth medium without antibiotics. For each transfection, two tubes are prepared as follows: **Tube 1:** 100ng SOX9 expression vector was diluted in 25µl DMEM GlutaMax (Life Technologies, 10566-016) without serum and antibiotics; **Tube 2:** 0.2µl transfection reagent Lipofectamine 2000 (Life Technologies, 11668027) was diluted in 25µl DMEM GlutaMax (Life technologies, 10566-016) no serum and antibiotics. After 5 min of incubation, the diluted DNA and the diluted transfection reagent were combined and incubated at room temperature for 20 min. Then, 50µl of complexes were added to each well. The plate was

gently rocked back and forth and incubated at 37°C in a CO_2 incubator. All transfection was performed in triplicate. The pcDNA3.1 vector was used as control. After 6 hours of transfection, transfection medium was replaced with fresh growth medium without antibiotics for another 24 hours. For harvesting, cells were washed with ice cold PBS (Life Technologies, 10010023) and harvested with 30µl Cells-to-cDNA lysis buffer (Life Technologies, AM8723).

2.2.2.7.2.2. SOX9 and miR-29a/b1 promoter cotransfection

To cotransfect SOX9 and the promoter miR-29a/b1, the SW1353 cells were prepared as described above one day before transfection. For each transfection, two tubes are prepared as follows: **Tube 1:** 100ng of 29a/b1 promoter, and either 100ng SOX9/200ng pcDNA3 or 300ng SOX9/100ng pcDNA3 was diluted in 25µl DMEM GlutaMax (Life Technologies, 10566-016) without serum and antibiotics; **Tube 2:** 0.2µl transfection reagent Lipofectamine 2000 (Life Technologies, 11668027) was diluted in 25µl DMEM GlutaMax (Life Technologies, 10566-016) no serum and antibiotics. The diluted DNA and the diluted transfection reagent were combined after 5 min of incubation and incubated at room temperature for another 20 min. Then, 50µl of complexes were added to each well. The plate was incubated at 37°C in a CO_2 incubator and transfection medium was changed with fresh medium without antibiotics for another 24 hours. Then, cells were washed with ice cold PBS (Life Technologies, 10010023) and a luciferase assay performed. All transfection were performed in triplicate.

2.2.2.7.2.3. Transfection of the miR-29a/b1 promoter with cytokines and growth factors

SW1353 cells were plated and transfected with 100ng miR-29a/b1 promoter as described above. Cells were incubated with the promoter for 24 hours. The medium was then removed and replaced with serum, antibiotic-free DMEM GlutaMAX medium (Life technologies, 10566-016), and cells were serum-starved overnight. Cells was stimulated for 6 hours with TGFβ1/3 (4ng/ml), IL-1 (5ng/ml), Wnt3a (100ng/ml), LPS (1µg/ml) in the presence or absence of 50nM NFκB inhibitor or 10nM p38 inhibitor (Sigma, S8307). Medium was removed 6 hours post stimulation and cells were washed twice with ice cold PBS (Life Technologies, 10010023) and then harvested for luciferase assay.

2.2.2.7.2.4. Short interfering RNA SOX9 mRNA knockdown

SW1353 cells were plated and transfected with either 100nM SOX9 siRNA (Dharmacon) or non-targeting siRNA 2 (Dharmacon, 001210-02) as section 2.2.2.7.2.1. To detect siRNA-mediated mRNA SOX9 knockdown, cells were incubated for 48 hours post transfection, then harvested in 30µl Cells-to-cDNA lysis buffer (Life Technologies, AM8723).

2.2.2.7.2.5. Human primary chondrocyte gain- and loss-of-function experiments

One day before transfection, human primary chondrocytes at passage 1 was plated in 6-well plate at $2x10^5$ cells/ wells in fresh growth medium without antibiotics so that the cells will be around 80% confluent. Complexes were prepared as followed for transfection: **Tube 1**: miR-29b mimic/ inhibitor/ AllStar negative control/ inhibitor negative control (50nM) was diluted in 250µl of serum, antibiotic-free DMEM GlutaMAX (Life Technologies, 10566-016). **Tube 2**: 5µl of Lipofectamine 2000 (Life Technologies, 11668027) was diluted in 250µl serum, antibiotic-free DMEM GlutaMax (Life technology, 10566-016). Time for incubation and transfection mixture was prepared similar to section 2.2.2.7.2.2. The original medium was aspirated from the wells, 500µl transfection mixture was added to each well and the final volume was made to 1ml with DMEM GlutaMAX with 10% (v/v) heat-inactivated FCS, without antibiotics. All transfections were performed in triplicated. Cells were incubated for 48 hours, then, supernatant was removed and cells was washed with ice cold PBS and 1ml Trizol reagent was added. Samples were stored at -20^{o}C until RNA extraction.

2.2.2.7.2.6. Transfection of human primary chondrocytes with miR-29 family mimics and treatment cytokines and growth factors

50nM either miR-29a/b/c mimics or AllStar negative control was transfected to human primary chondrocytes in 6-well plate as in section 2.2.2.7.2.5. After 24 hours, medium was removed from the wells and replaced with DMEM GlutaMAX with 0.5% (v/v) heat inactivated FCS overnight. Then, cells were stimulated with TGFβ1 (4ng/ml), IL-1 (5ng/ml), Wnt3a (100ng/ml). At desired times post stimulation as in Chapter 5, medium was removed, the cells were washed with ice cold PBS and harvested in 1ml Trizol reagent.

2.2.2.7.2.7. Transfection of the miR-29b mimic in micromass culture with cytokines and growth factors

Confluent passage 2 monolayer culture of human primary chondrocytes were released by trypsin/EDTA and plated in 175 cm^2 flask with growth medium with 10% (v/v) heat inactivated FCS, no antibiotics one day before transfection to give cells at 90-100% confluence. 100nM miR-29b mimic or non-targeting control was diluted in 500µl medium (tube1) and 4 µl Lipofectamine 2000 was also diluted in 500µl medium (tube 2). Transfection was carried out as in 2.2.2.7.2.2. The original medium from the flask was removed before adding 1ml transfection mixture and the flask was further covered with another 14ml growth medium with 10% (v/v) heat inactivated FCS. After incubating with miR-29b mimic for 48 hours, cells was detached by trypsin/EDTA and put in micromass culture as in 2.2.2.5. After 24 hours of resting, miR-29b transfected micromasses were treated with either TGFβ1 (10ng/ml), IL-1 (5ng/ml), Wnt3a (100ng/ml) in different media (referred in 2.2.2.5) with 10% (v/v) heat inactivated FCS without antibiotics. At desired time, micromasses were harvested in 500µl Trizol reagent.

2.2.2.7.2.8. Co-transfection of reporter vectors with the miR-29 family mimic/ miR-29b inhibitor and stimulation with cytokines and growth factors

SW1353 were seeded into 96-well plate 1 day before transfection as in 2.2.2.7.2.1 and transiently co-transfected with: (1)100ng of reporter plasmids of either $p(CAGAC)_{12}$- luc, $I\kappa B_3$-luc, TOPflash, FOPflash, (2) 10ng of renilla luciferase reporter, and (3) 50nM of either miR-29a/b/c mimic, AllStar non-targeting negative control, miR-29b inhibitor, or inhibitor negative control. The protocol for transfection is as in 2.2.2.7.2.5. After 24 hours of transfection, cells was serum starved overnight and were treated with recombinant human TGFβ1 (4ng/ml), IL-1β (5ng/ml), Wnt3a (100ng/ml) for 6 hours. After stimulation, cells were harvested and a luciferase assay performed as in 2.2.2.8.

2.2.2.7.2.9. Cotransfection of pmiR-Glo-3'UTR reporter with the miR-29 family mimic

Chicken fibroblasts DF1 were plated in a 96-well plate (10^4cells/well) in antibiotic free growth media with 10% (v/v) FCS overnight. 100ng of either pmiR-Glo-3'UTR wild type

or mutant constructs were co-transfected with 50nM miR-29a/b/c mimic using the non-targeting Allstars as control. The protocol for transfection was described in 2.2.2.7.2.5. After 24 hours post transfection. DF1 cells were harvested for luciferase assay as in 2.2.2.8.

2.2.2.8. Luciferase reporter assay

At desire times post transfection, the plate was removed from the incubator. Luminescence was detected using the Dual-Luciferase Reporter Assay system (Promega, E1980). Briefly, the medium on the cells was removed. The cells were washed twice with ice cold PBS and 70µl of cell lysis buffer provided in the kit (Promega, E1980) was added to each well. The plate was gently rocked back and forth for 30 minutes. Then, 10µl cell lysates were transferred to a 96- well white microplate. For measuring firefly luciferase activity, 50µl of Dual Luciferase Reagent was added to each well. The firefly luminescence was measured using a microplate reader. For measuring Renilla luciferase activity, 50 µl of Dual Stop & Glo Reagent was added to each well and mixed gently then the luminescence measured.

After measurement of the firefly luciferase luminescence and Renilla luciferase luminescence, the relative luciferase activity was calculated as the ratio of the firefly activity normalized to the Renilla luciferase activity.

2.2.3. MicroRNA and mRNA microarray

2.2.3.1. MicroRNA and mRNA microarray for destabilization of medial menicus (DMM) model

Whole knee joints from mice which underwent DMM surgery (e.g. DMM-operated right knee and unoperated left knee) were subjected to total RNA isolation and grouped as DMM left (referred to as control) or DMM right (referred as treatment). At each time point (1, 3, 7 days after surgery), equal amounts of total RNA from each sample in the same group was pooled together. The integrity of the new pooled samples was checked before sending to Exiqon Services (Denmark) or Source Bioscience (UK) to perform miRNA microarray or mRNA microarray, respectively.

The miRCURY LNA^{TM} microRNA Hi-Power Labelling Kit Hy3^{TM}/Hy5^{TM} was used for miRNA microarray in which the Hy3^{TM} labelled samples and Hy5^{TM} labelled samples

were mixed pair-wise and hybridized to capture probes targeting all miRNAs or human, mouse and rat registered in the miBASE 18.0. For whole genome array, Illumina's BeadArray-based technology was employed by using MouseWG-6 v2.0 Expression BeadChips whose feature content derived mainly from NCBI reference sequence (NCBI refseq), and simultaneously profiles more than 45,000 mouse transcripts. The BeadChips consists of oligonucleotides immobilized to bead held in microwells on the surface of any array substrate, and made up with 50-mer-gene-specific probe plus 29-mer address sequences. Especially, the chip has high level of bead type redundancy (average 30 beads per probe) to control the quality and reproducibility of the direct hybridization assay.

2.2.3.2. Whole genome array for miR-29b gain and loss-of-function experiment

Human primary chondrocytes were transiently transfected with either miR-29b mimic or miR-29b inhibitor for 48 hours in triplicate. Then, total RNA was isolated and equal amounts of total RNA of each sample in the triplicate was pooled together. After checking the quality and integrity, the new pooled samples were sent to Source Bioscience (UK) to perform human whole genome profile. Again, the Illumina's BeadArray-based technology was employed but using humanHT-12 V4.0 expression BeadChips. Similarly, the feature content derived mainly from NCBI reference sequence (NCBI refseq) which simultaneously profile more than 47,000 human transcripts.

2.2.4. Data analysis

2.2.4.1. Pre-processing microRNA array data

2.2.4.1.1. VST transformation and quantile normalization

It is necessary to do background correction to remove non-specific signal from total signal. However, the initial data-pre-processing in the Illumina GenomeStudio solfware provides users with bead summary data in the form of a single signal intensity value for each probe. This value is calculated by subtracting the local background from the signal intensity of each bead, then taking the means of all beads containing a given probe. This means BeadStudio output data has undergone background correction. Thus, no further background correction need to be done for the Bead summary data, received from Source Bioscience (UK).

To reliably detect changes in expression from the whole genome array, it is important to remove sources of variation of non-biological origin between arrays to make data comparable. There are two types of variations might be seen when comparing arrays e.g. interesting variation (biological differences), and obscuring variation. Sources of obscuring variation were introduced during the process of carrying out the experiments e.g. **during preparing the samples** including mRNA extraction and isolation, variation in introduction and incorporation of dye, effected by pipetting error, temperature fluctuations and reagent quality; **during manufacturing of the array** including variation in the amount of probe present at each feature or spot and variation in the hybridization efficiency of the probes for their mRNA targets; **during hybridization of the sample on the array** including variation in the amount of samples applied to the array and variation in the amount of target hybridized to the probe; and after array hybridization including variation in optical measurement and intensity computed from the scan image. So, comparisons between different biological samples can be made, it is important to remove these obscuring variations to ensure the values being analysed reflect the biology. For Beadchip array data, the two steps to achieve this are commonly referred to as between-array normalization, and transformation. Two popular methods that implement these steps are VST transformation and quantile normalization for the Lumi packages. Briefly, for analysing, bead summary array data was imported into R studio (http://www.rstudio.com/). Array data was then transformed and normalized using Lumi package.

2.2.4.1.2. Sequence data

The miR-29 family mature sequence data was retrieved from miRbase database (http://www.mirbase.org/). 3'UTR sequences were downloaded from UCSC (https://genome.ucsc.edu/) and Ensembl (http://www.ensembl.org/index.html). RefSeq IDs were used to map probe sets to UCSC database and Ensembl Gene IDs were used to map probesets to the Ensembl database.

2.2.4.1.3. The MicroRNA-29 family target prediction

Three types of seed matches in the 3'UTR were considered when predicting direct miRNA-29 targets e.g. **6-mer seed match** which is 6nt in length and was complementary

to nucleotides 2 to 7 in the miR-29 family; **7-mer seed match** which is 7nt length and is complementary to nucleotides 1–7 in the miRNA or nucleotides 2–7 in the miRNA with "A" at the first position; and **8-mer seed match** which is 8nt length, and matched nucleotides 1–8 in the miRNA or nucleotides 2–8 in the miRNA with an "A" at the first position. For searching these seed matches in the 3'UTR, 3'UTR sequences were imported and read in R studios using the "*readDNAStringSet*" function in Biostring package. Also, three types of miR-29 family seed matches were searched using "*vcountPattern*"function.

In line with using R studios, some miRNA target prediction programs available were also used to predict targets for miR-29 including TargetScan (http://www.targetscan.org/), miRNA body map (http://www.mirnabodymap.org/), miRDB (http://mirdb.org/miRDB/), DIANA (http://diana.cslab.ece.ntua.gr/), Pictar (http://pictar.mdc-berlin.de/), miRbase (http://www.mirbase.org/).

2.2.4.1.4. Functional pathway analysis

DAVID (Database for Annotation, Visualization and Integrated Discovery) functional annotation tool (http://david.abcc.ncifcrf.gov/) was used to perform functional analysis for particular gene groups.

2.2.4.1.5. Statistical analysis

Unless otherwise stated, for the whole thesis, Student's unpaired t-test (two-tail) was performed to compare difference between two groups. All values are given as mean values of replicates with error bar representing the standard error of the mean. The statistical analysis was carried using GraphPad Prism version 4.0 for Windows. Levels of statistical significant are represented as * $\leq$ 0.05, ** $\leq$ 0.01, *** $\leq$ 0.001.

CHAPTER III
IDENTIFICATION OF THE MIR-29 FAMILY IN CARTILAGE HOMEOSTASIS AND OSTEOARTHRITIS

3.1. Introduction

MicroRNAs are referred to as the master regulators for gene expression: they exert their suppressive functions on targeting genes at the post transcriptional level through a sequence-complementary mechanism (Bartel 2009). In human chondrocytes, many different miRNAs are found and each of them are shown to directly and/or indirectly regulate hundreds of target genes, implicating a complex gene regulatory network in which miRNAs are involved (Le *et al.* 2013). This means that miRNAs take a crucial part in controlling the balance of the mRNA network in cartilage homeostasis; and the dysregulation of miRNA expression could trigger OA onset by disrupting this regulatory network.

Indeed, an essential role of miRNAs has been reported in various aspects of cartilage development, cartilage homeostasis, and also in OA pathogenesis (Le et al. 2013). For instance, knockout of Dicer, the pre-miRNA processing enzyme, in a cartilage-specific manner resulted in skeletal growth defects, premature death of mice, reduction in growth plate chondrocytes, and an increase in hypertrophic chondrocytes (Kobayashi et al. 2008). Mutation of the Dnm3 locus, transcribing the miRNAs miR-199a, miR-199*, and miR-214, resulted in growth retardation including craniofacial hypoplasia (Watanabe *et al.* 2008). Universal knockout of miR-140, a cartilage and skeletal-restricted miRNA lead to: mild craniofacial deformities and dwarfism; early onset of age-related OA development; greater susceptibility to OA with accelerated proteoglycan loss and fibrillation of articular cartilage (Miyaki et al. 2010, Nakamura et al. 2011). Transgenic mice overexpressing miR-240 in cartilage were resistant to antigen-induced arthritis-associated loss of proteoglycan and type II collagen (Miyaki et al. 2010). Other specific miRNAs: miR-9, miR-98, and miR-146 were highlighted to be expressed differentially in miRNA profiles between human OA cartilage and its normal articular counterpart (Iliopoulos et al. 2008, Jones *et al.* 2009); miR-199a, miR-675, miR-145, miR-140, miR-455 have been proven to function in chondrogenesis and cartilage homeostasis (Lin *et al.* 2009, Miyaki *et al.* 2009, Dudek *et al.* 2010, Martinez-Sanchez *et al.* 2012, Swingler *et al.* 2012); miR-222 is

reported to play a potential role in the articular cartilage mechanotransduction pathway (Dunn *et al.* 2009); miR-146a and miR-146b, whose expression is regulated by NFκB, appear to be the key miRNAs in the inflammatory response (Taganov *et al.* 2006); miR-34a, miR-194, miR-27b were reported to be induced by IL-1β (Abouheif et al. 2010, Akhtar *et al.* 2010, Xu et al. 2012). All of these data reveal miRNAs as important modulators of various aspects of articular cartilage homeostasis and OA pathogenesis.

OA develops slowly with time and may not be symptomatic until significant joint damage has occurred. Currently, there is a lack of effective approaches to OA prevention or treatment. Available treatments are limited to pain management, and joint replacement surgery, this latter in the late phase of the disease. MicroRNAs, with the ability to fine-tune the expression of multiple genes, could be a promising tool for therapeutic applications for a complex disease like OA. The down regulation of gene expression by miRNAs is relatively modest, thus the approach of combining multiple miRNAs to simultaneously target OA pathogenesis-relevant networks may be needed. Furthermore, There is growing evidence for future miRNA-based diagnostics: a number of miRNA in plasma were found at different levels between RA and OA patients (Murata *et al.* 2010); let-7e, miR-454, miR-886 were identified as differentially expressed circulating miRNAs in OA patients necessitating arthroplasty, especially, let–7e emerged as potential predictor for severe knee or hip OA (Beyer et al. 2014). However, there is a requirement for detailed investigations directed at diagnostic performance (sensitivity, specificity, accuracy) of these promising novel biomarkers before the measurement of miRNAs can enter the clinic.

With all of the above information, the essential roles of miRNAs in cartilage homeostasis and OA are shown with potential for clinical application. The insights into the roles of miRNAs in chondrogenesis, articular cartilage homeostasis, and OA initiation and progression are, nevertheless, still insufficient. Thus, there is a continuing need to deepen our understanding of the molecular mechanisms miRNAs are involved in cartilage homeostasis and OA. Investigating the disease directly in man is challenging due to e.g. the inability to harvest articular tissue at an early stage; the slow disease progression; the absence of symptoms in the early stage of the disease; the variety of symptoms; the variety of causes and environmental influence. Animal models mimicking features of OA are, therefore, an important alternative solution.

In an effort to identify novel miRNAs important in the development of OA, the murine Destabilization of Medial Meniscus (DMM) model was used to identify miRNAs differentially expressed at 1, 3, 7 days (i.e. early stages) after the surgery. Performing miRNA and mRNA profiling followed with an integrated analysis highlighted miR-29b as a candidate miRNA participating in the early onset of OA in DMM model. Alongside the DMM model, the role of the miR-29 family in cartilage homeostasis and OA was also investigated in other human and mouse models e.g. human end-stage OA cartilage, the murine hip avulsion injury model, a human primary chondrocyte dedifferentiation model, a human chondrogenesis model, and murine limb development.

Aims

- Performing miRNA and mRNA profiling in DMM model at very early time points 1, 3, 7 days after surgery
- Identifying miRNA potentially involve in OA onset by bioinformatics analysis
- Investigating the regulation of the miR-29 family which is highlighted from bioinformatics analysis above in human end-stage OA cartilage
- Determining the expression pattern of the miR-29 family in injury model
- Establishing if the miR-29 family involving in chondrocyte phenotype
- Determining the role of miR-29 in human and murine chondrogenesis
- Investigating the involvement of miR-29 in murine limb development

3.2. Results

3.2.1. The microRNA profile in the DMM model at 1, 3, 7 days after surgery

As little is known about the involvement of miRNAs at the early stage of OA, identifying miRNAs modulated in OA initiation was a major aim. Since mRNA profiles have shown large changes in gene expression even at 24 hours post surgery, the DMM model was used to investigate this.

Alongside DMM mice (mice whose medial meniscal tibial ligament of the right knee was transected whilst the left knee was untouched), naïve mice (receiving no treatment), and sham-operated mice (mice whose right knees were operated to visualize the medial meniscal tibia ligament but not transected) were used. Total RNA was first isolated from the whole knee joints of DMM mice (both right and left knees) and their controls at 3 different time points i.e. 1, 3, 7 days after surgery, and subsequently checked for quality and integrity. Unfortunately, RNA from naïve mice was degraded and not further studied. For miRNA profiling, an equal amount of total RNA from individual in each triplicate in the DMM right knee and DMM left knee group at 1, 3, and 7 days after surgery was pooled and these pools were subsequently subjected to miRNA microarray using the miRCURY LNA^{TM} microRNA Hi-Power Labelling Kit Hy3^{TM}/Hy5^{TM}, containing probes targeting all human, mouse and rat miRNAs registered in the miRBase 18.0.

Clustering analysis showed that: the miRNA profiles of the DMM right or left knees were clustered quite closely to each other at day 1 and 3 but far apart at day 7 (Appendix, Figure 1), suggesting that more miRNAs were modulated at the later time point than the earlier. In line with this, calculating the number of miRNAs which changed expression at each time point revealed the same pattern: only small changes were observed until 7 days post-surgery (Figure 3.1). Using 1.5 fold-change (FC) as the cut off, only four miRNAs significantly increased expression at day 1 and 3 whilst more than 30 miRNAs were modulated at day 7. The list of miRNAs which changed expression is listed in Table 3.1.

To visualize the expression pattern of miRNAs across the time course of the DMM model, unsupervised hierarchical clustering analysis was carried out for miRNAs that met the filtering criteria e.g. absolute FC > 1.3 in each time point. Several clusters of miRNAs were identified comparing between DMM right and left knee i.e. (i) miRNAs which **increased** expression across the time course (cluster 1, 2, 3) (Figure 3.2a, b, c), (ii)

miRNAs which **decreased** expression across the time course (cluster 5, 6) (Figure 3.2.e, f), (iii) miRNAs **which decreased** expression across 3 days but **increased** at day 7 (cluster 4) (Figure 3.2d) and (iv) miRNAs which **increased** until 3 days but **decreased** at day 7 (cluster 7) (Figure 3.2.g).

A subset of miRNA differentially expressed by microarray analysis was selected for revalidating the array data by quantitative real-time RT-PCR. The result confirmed the miRNA array data since a similar expression pattern between the two platforms for miR-140, miR-455 (data not shown) and miR-29b (which will be discussed below) was observed.

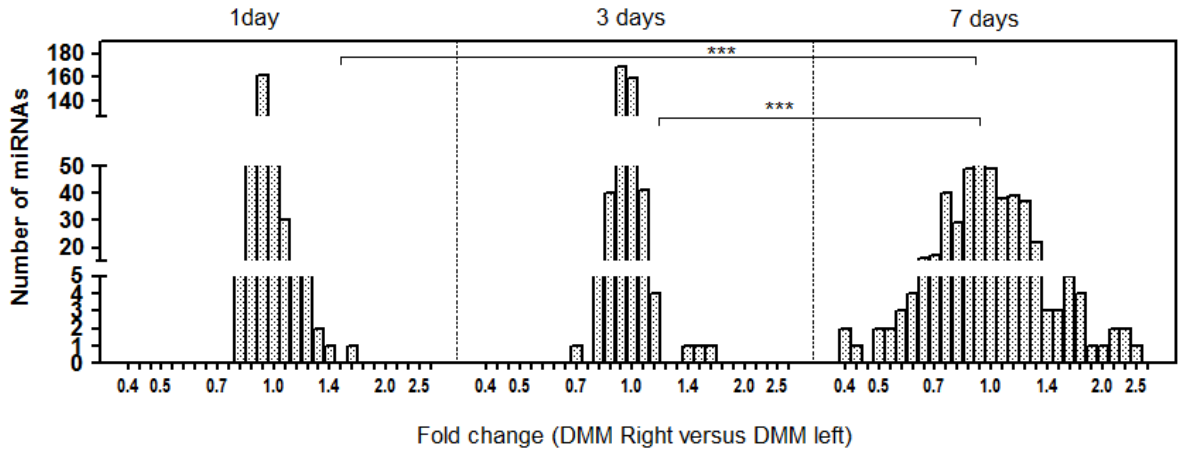

Figure 3.1: Modulation of miRNA expression across a 7 day time course

From the array data, for each miRNA, fold change (FC) was calculated by comparing its expression level in DMM right versus left knee. The number of regulated miRNAs were calculated for each of 0.05 interval of a (0.4, 2.5) range of FC. FC: > 1: increase expression; < 1: decrease expression. The difference in number of miRNAs modulated was calculated by unpaired two-tailed t test: * $p<0.05$, ** $p < 0.01$, *** $p<0.001$.

Day 1		Day 7	
miRNA	**FC**	**miRNA**	**FC**
miR-144-3p	1.7	miR-379-5p	2.6
miR-29b-3p	1.5	miR-127-3p	2.4
		miR-335-5p	2.4
		miR-370-5p	2.2
Day 3		miR-214-3p	2.2
miRNA	**FC**	miR-21-5p	2.1
miR-370-5p	1.7	miR-3073-3p	2.0
miR-21-5p	1.6	miR-199a-3p	1.9
		miR-214-5p	1.8
		miR-210-3p	1.8
		miR-455-3p	1.8
		miR-199a-5p	1.7
		miR-2137	1.7
		miR-199b-5p	1.7
		miR-136-5p	1.7
		miR-34a-5p	1.6
		miR-99b-5p	1.6
		miR-152-3p	1.5
		miR-34c-5p	1.5
		miR-144-3p	-1.5
		miR-3100-3p	-1.5
		miR-669c-3p	-1.6
		miR-378-3p	-1.6
		miR-3473b	-1.6
		miR-133a-5p	-1.6
		miR-3474	-1.7
		miR-378b	-1.7
		miR-133a-3p	-1.8
		miR-133b-3p	-1.8
		miR-1952	-1.9
		miR-491-3p	-1.9
		miR-1a-3p	-2.2
		miR-706	-2.3
		miR-3572	-2.3

Table 3.1: The list of miRNAs regulated in the DMM model with fold change higher than 1.5 (increase or decrease) at 1, 3, and 7 days after surgery.

Fold change (FC) was calculated by comparing between the DMM operated right and un-operated left knee. Down-regulated miRNAs are presented as negative FC.

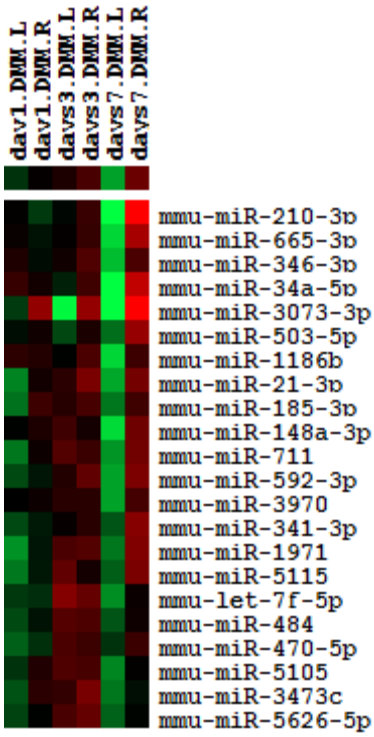
dav1.DMM.L
dav1.DMM.R
davs3.DMM.L
davs3.DMM.R
davs7.DMM.L
davs7.DMM.R
mmu-miR-210-3p
mmu-miR-665-3p
mmu-miR-346-3p
mmu-miR-34a-5p
mmu-miR-3073-3p
mmu-miR-503-5p
mmu-miR-1186b
mmu-miR-21-3p
mmu-miR-185-3p
mmu-miR-148a-3p
mmu-miR-711
mmu-miR-592-3p
mmu-miR-3970
mmu-miR-341-3p
mmu-miR-1971
mmu-miR-5115
mmu-let-7f-5p
mmu-miR-484
mmu-miR-470-5p
mmu-miR-5105
mmu-miR-3473c
mmu-miR-5626-5p

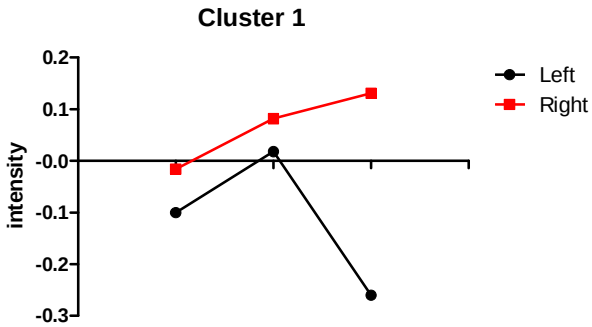
Cluster 1
intensity
0.2
0.1
-0.0
-0.1
-0.2
-0.3
Left
Right

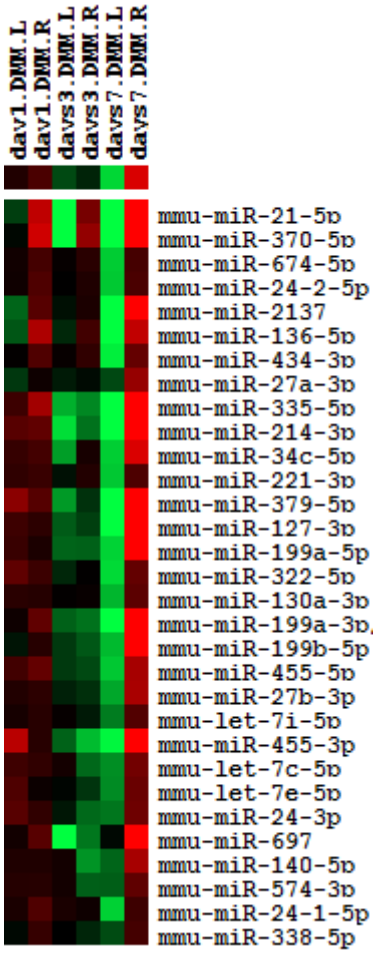
dav1.DMM.L
dav1.DMM.R
davs3.DMM.L
davs3.DMM.R
davs7.DMM.L
davs7.DMM.R
mmu-miR-21-5p
mmu-miR-370-5p
mmu-miR-674-5p
mmu-miR-24-2-5p
mmu-miR-2137
mmu-miR-136-5p
mmu-miR-434-3p
mmu-miR-27a-3p
mmu-miR-335-5p
mmu-miR-214-3p
mmu-miR-34c-5p
mmu-miR-221-3p
mmu-miR-379-5p
mmu-miR-127-3p
mmu-miR-199a-5p
mmu-miR-322-5p
mmu-miR-130a-3p
mmu-miR-199a-3p
mmu-miR-199b-5p
mmu-miR-455-5p
mmu-miR-27b-3p
mmu-let-7i-5p
mmu-miR-455-3p
mmu-let-7c-5p
mmu-let-7e-5p
mmu-miR-24-3p
mmu-miR-697
mmu-miR-140-5p
mmu-miR-574-3p
mmu-miR-24-1-5p
mmu-miR-338-5p

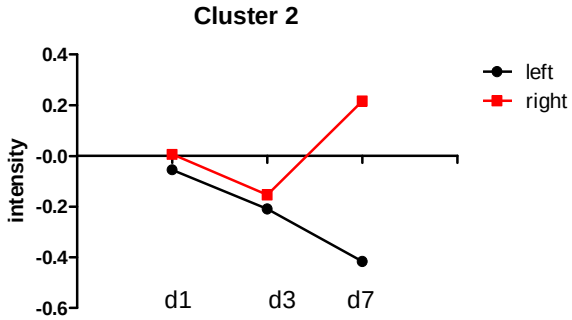
Cluster 2
intensity
0.4
0.2
-0.0
-0.2
-0.4
-0.6
d1
d3
d7
left
right

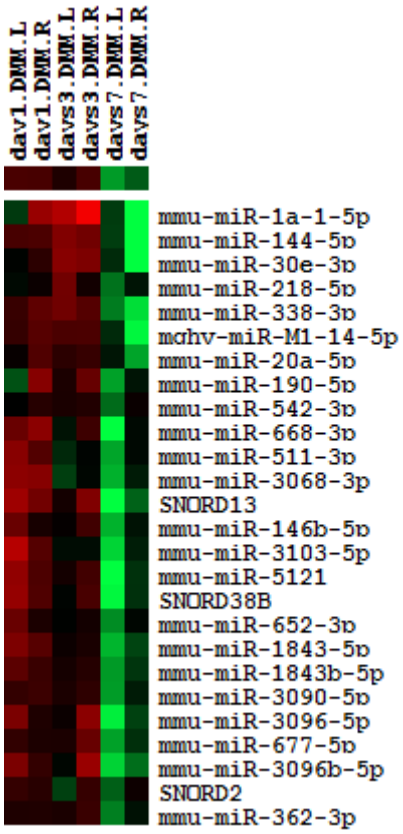
dav1.DMM.L
dav1.DMM.R
davs3.DMM.L
davs3.DMM.R
davs7.DMM.L
davs7.DMM.R
mmu-miR-1a-1-5p
mmu-miR-144-5p
mmu-miR-30e-3p
mmu-miR-218-5p
mmu-miR-338-3p
mghv-miR-M1-14-5p
mmu-miR-20a-5p
mmu-miR-190-5p
mmu-miR-542-3p
mmu-miR-668-3p
mmu-miR-511-3p
mmu-miR-3068-3p
SNORD13
mmu-miR-146b-5p
mmu-miR-3103-5p
mmu-miR-5121
SNORD38B
mmu-miR-652-3p
mmu-miR-1843-5p
mmu-miR-1843b-5p
mmu-miR-3090-5p
mmu-miR-3096-5p
mmu-miR-677-5p
mmu-miR-3096b-5p
SNORD2
mmu-miR-362-3p

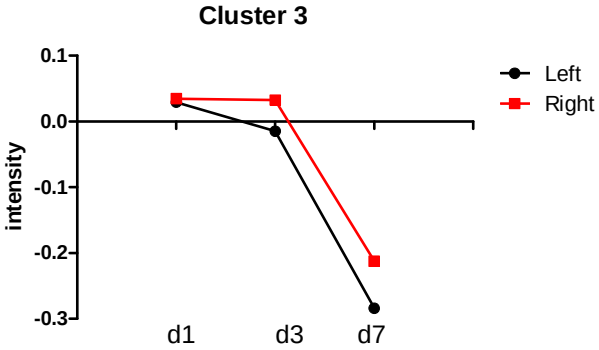
Cluster 3
0.1
0.0
-0.1
-0.2
-0.3
intensity
d1
d3
d7
Left
Right

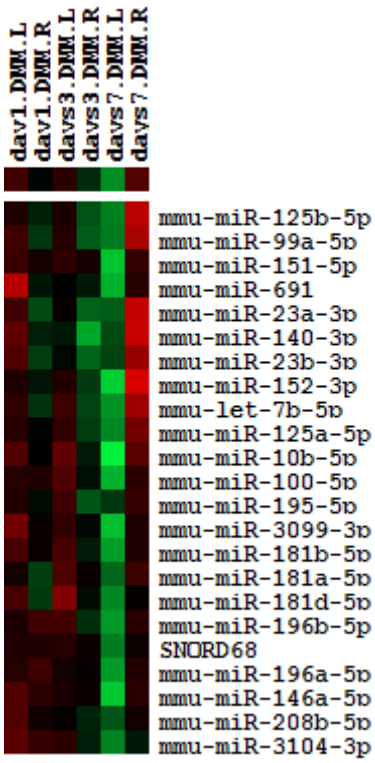
dav1.DMM.L
dav1.DMM.R
davs3.DMM.L
davs3.DMM.R
davs7.DMM.L
davs7.DMM.R
mmu-miR-125b-5p
mmu-miR-99a-5p
mmu-miR-151-5p
mmu-miR-691
mmu-miR-23a-3p
mmu-miR-140-3p
mmu-miR-23b-3p
mmu-miR-152-3p
mmu-let-7b-5p
mmu-miR-125a-5p
mmu-miR-10b-5p
mmu-miR-100-5p
mmu-miR-195-5p
mmu-miR-3099-3p
mmu-miR-181b-5p
mmu-miR-181a-5p
mmu-miR-181d-5p
mmu-miR-196b-5p
SNORD68
mmu-miR-196a-5p
mmu-miR-146a-5p
mmu-miR-208b-5p
mmu-miR-3104-3p

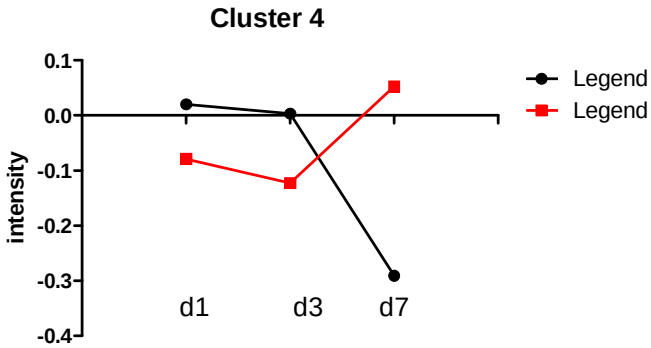
Cluster 4
0.1
0.0
-0.1
-0.2
-0.3
-0.4
intensity
d1
d3
d7
Legend
Legend

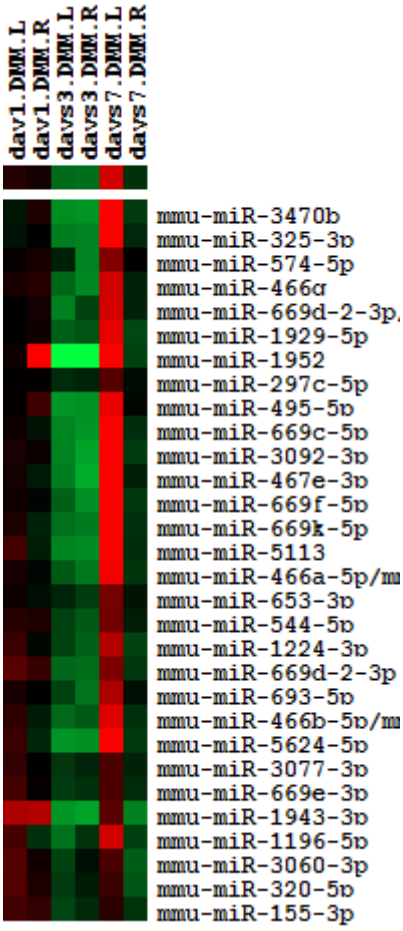
dav1.DMM.L
dav1.DMM.R
davs3.DMM.L
davs3.DMM.R
davs7.DMM.L
davs7.DMM.R
mmu-miR-3470b
mmu-miR-325-3p
mmu-miR-574-5p
mmu-miR-466a
mmu-miR-669d-2-3p
mmu-miR-1929-5p
mmu-miR-1952
mmu-miR-297c-5p
mmu-miR-495-5p
mmu-miR-669c-5p
mmu-miR-3092-3p
mmu-miR-467e-3p
mmu-miR-669f-5p
mmu-miR-669k-5p
mmu-miR-5113
mmu-miR-466a-5p/m
mmu-miR-653-3p
mmu-miR-544-5p
mmu-miR-1224-3p
mmu-miR-669d-2-3p
mmu-miR-693-5p
mmu-miR-466b-5p/m
mmu-miR-5624-5p
mmu-miR-3077-3p
mmu-miR-669e-3p
mmu-miR-1943-3p
mmu-miR-1196-5p
mmu-miR-3060-3p
mmu-miR-320-5p
mmu-miR-155-3p

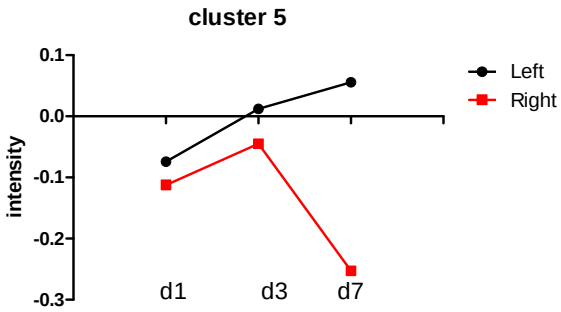
cluster 5
0.1
0.0
-0.1
-0.2
-0.3
intensity
d1
d3
d7
Left
Right

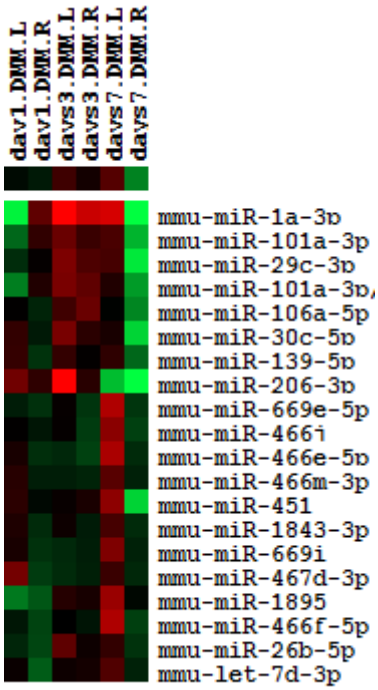
dav1.DMM.L
dav1.DMM.R
davs3.DMM.L
davs3.DMM.R
davs7.DMM.L
davs7.DMM.R
mmu-miR-1a-3p
mmu-miR-101a-3p
mmu-miR-29c-3p
mmu-miR-101a-3p
mmu-miR-106a-5p
mmu-miR-30c-5p
mmu-miR-139-5p
mmu-miR-206-3p
mmu-miR-669e-5p
mmu-miR-466i
mmu-miR-466e-5p
mmu-miR-466m-3p
mmu-miR-451
mmu-miR-1843-3p
mmu-miR-669i
mmu-miR-467d-3p
mmu-miR-1895
mmu-miR-466f-5p
mmu-miR-26b-5p
mmu-let-7d-3p

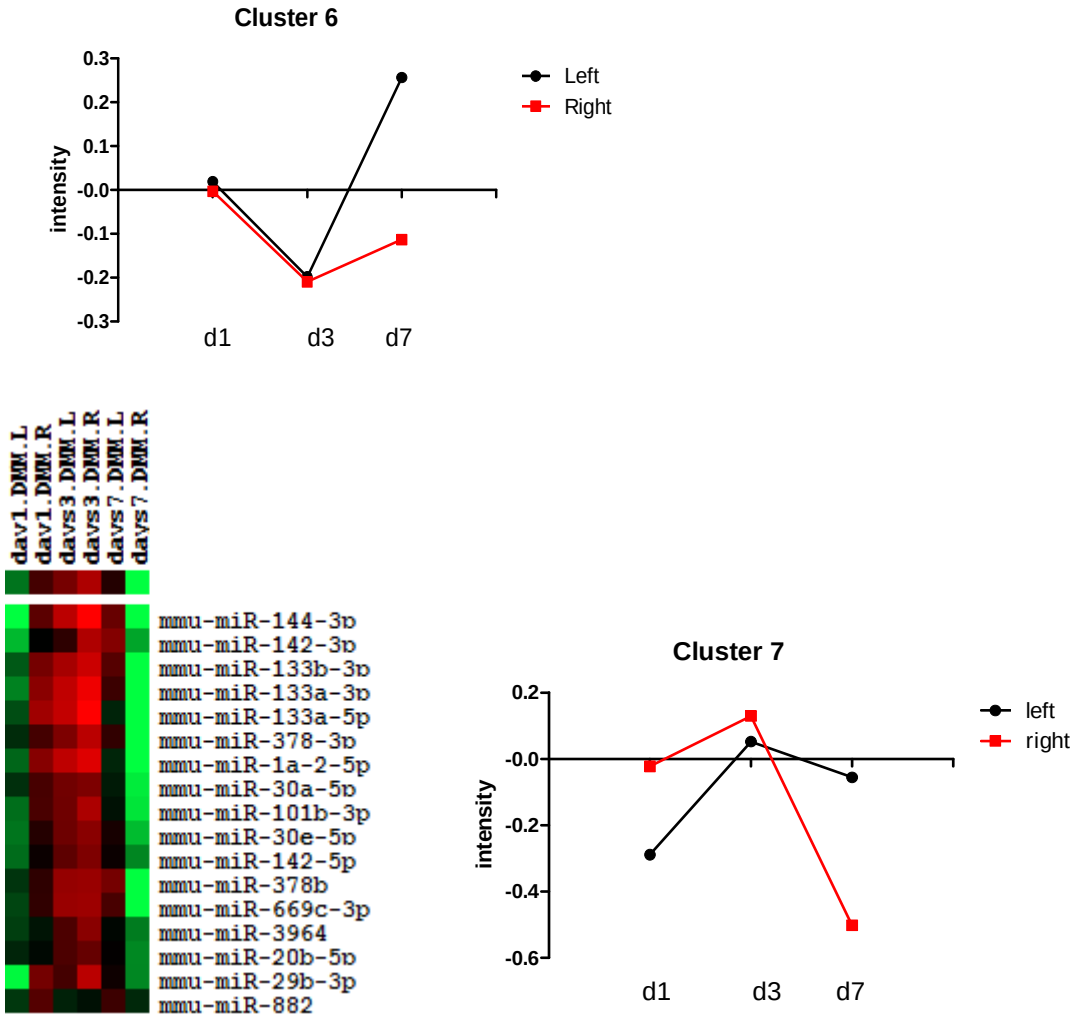

Figure 3.2: Unsupervised hierarchical clustering analysis for miRNAs with absolute fold change higher than 1.3.

Comparing DMM right versus left knee at 1, 3, 7 day time points: cluster 1, 2, 3: all the miRNAs induced expression; cluster 5, 6: all miRNAs decreased expression; cluster 4: miRNAs decreased across 3 days but increased at day 7; cluster 7: miRNAs increased across 3 days but decreased at day 7. Comparing between three time points: cluster 1: miRNAs increased across 7 days; cluster 2, 6: miRNAs decreased at day 3; cluster 3, 5: miRNAs decreased at day 7. SNORD: small nucleolar RNA.

3.2.2. Expression profile of mRNAs in DMM right and left knee

The microRNA microarray profiling revealed approximately 35 miRNAs modulated in the DMM model at 3 different time points, and whilst changes in expression are small, this may suggest that these miRNAs may have a role in regulating the onset of OA. For further filtering of miRNAs having important roles amongst these modulated miRNAs, examining the mRNA expression profile would be useful since miRNAs exert their function by directly targeting and subsequently inhibiting mRNA expression. Additionally, since no major modulation of miRNA expression level was observed until 7 days after DMM surgery, it was sufficient to profile mRNA expression for two time points i.e. 1 and 7 day following DMM surgery.

The Illumina BeadArray-based: MouseWG-6 v2.0 Expression BeadChip was used to profile more than 45,000 mouse transcripts in the pooled total RNA samples (DMM right and left knee), previously subjected to miRNA profiling. Consistent with the miRNA profile, mRNA array data also showed a similar expression pattern: no major change in mRNA expression level until day 7 when comparing between DMM right and left knee (Figure 3.3). If the absolute fold change cutoff is set at 1.5, only 30 mRNAs changed expression at day 1 whilst at day 7, more than 683 mRNAs were modulated. The full lists of mRNA which changed expression are in Appendix, Table 6, 7.

A subset of mRNA differentially expressed by microarray analysis was selected for revalidating the array data. Comparison of the expression levels between the mRNA microarray and quantitative real-time qRT-PCR demonstrated a similar expression pattern between the two platform for 4 genes i.e. *CCL2, IL6, SAA3, Arginase-1* (Appendix, Figure 2). These results confirmed the mRNA array data.

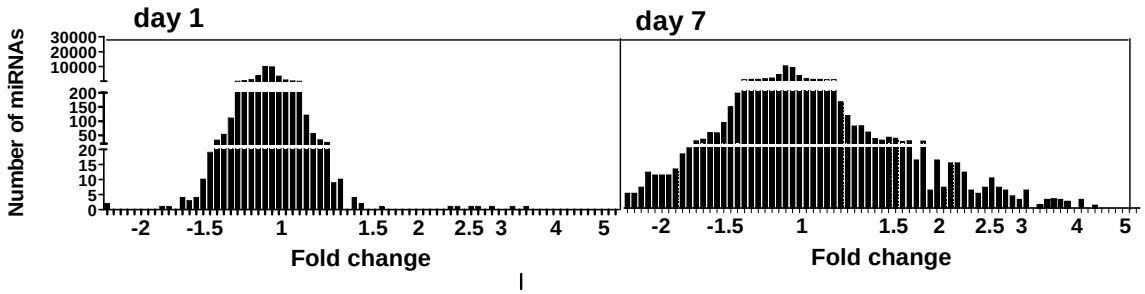

Figure 3.3 Total numbers of mRNAs at different fold change value at day 1 and day 7 following surgery in DMM model.

At each time point, Fold change = intensity value in DMM right - intensity value in DMM left. Numbers of mRNAs were calculated as fold change ranging from -3 to 7 for each increase of 0.05. Fold change: > 1: increase expression; < 1: decrease expression.

3.2.3. Integrated miRNA and mRNA expression profiles of the DMM model identify miR-29b as a miRNA associated with OA onset

To prioritize miRNAs which might have a role in OA onset in the DMM model, an integrated analysis between miRNA and mRNA profiles at 1 and 7 day of the DMM model was performed. This approach took advantage of inverse correlation analysis in which a miRNA was considered as a potential candidate if it was differentially expressed, and inversely correlated with the expression of its putative targets in the same biological samples.

Steps for the miRNA and mRNA profile integrating analysis include: (i) predicting miRNA putative targets by searching for 4 different types of seed sequences e.g. 6-, 7 match 8-, 7 A1-, and 8-mer seed sequences located in the 3' UTR; (ii) integrating expression levels at each time point in the DMM model for all miRNA targets; (iii) searching for a miRNA's putative target enrichment which is given more detail below.

If a miRNA has an impact in the pathological changes in the DMM model and could exert its suppressive function on variety of targets, then when it is down-regulated, there should be an enrichment of its predicted targets among up-regulated mRNA and vice versa. This means that for downregulated miRNAs, a greater percentage of upregulated mRNAs will be their targets and the inverse pattern will be observed for an upregulated miRNA. This should also be true when comparing between different time points, 1 and 7 days in the DMM model. For instance, if a miRNA was repressed across the 7 day time course, the percentage of its targets amongst up-regulated mRNA at day 7 should be higher than at day 1. Together with this, for a downregulated miRNA, an enrichment of miRNA targets in up-regulated mRNAs over unmodulated mRNAs should also be observed at each time point or across the time course.

Additionally, fold change threshold is another challenge faced in integrating analysis. In fact, it is almost impossible to choose the "right" cut off as the normal 1.5 fold change would be too stringent, and consequently, the power to detect potential miRNAs would be very low. To overcome this, in this study, all calculations were done for all fold change values greater than 1 at 0.05 fold intervals.

The integrating analysis for the miRNA and mRNA array data in the DMM model showed that amongst the differentially expressed miRNAs, miRNA-29b is the most interesting. Indeed, a substantial enrichment of miR-29b putative targets which was inversely correlated

with the miRNA expression level was observed at each time points (Figure 3.4, Figure 3.5). At day 1, when miR-29b increased expression, 6mer- and 7mer match 8- targets in the down-regulated section were dominant compared with the up-regulated section (Figure 3.4). Conversely, at day 7, when miR-29b decreased expression, there was a strong enrichment of targets with 4 different types of seed sites in the up-regulated section over the down-regulated (figure 3.4). Also at day 7, the ratio up-regulated targets/unchanged targets was substantially higher than the ratio down-regulated targets/unchanged targets (Figure 3.5).

The inverse correlation between miR-29b and its potential targets was also observed across the time course: whilst miR-29b level was down-regulated from day 1 to day 7, there was a substantial increase of miR-29 targets in the up-regulated mRNAs at day 7 compared with day 1. Consistent with this, the ratio up-regulated targets/unchanged targets showed an enrichment at day 7 (Figure 3.5). All of the data above suggest that miRNA-29b has a potential functional role in OA onset in the DMM model and was selected as the candidate miRNA for further functional studies.

From miRNA microarray data, miR-29b is the one on two miRNAs increased expression with 1.5 fold change at day 1 following DMM surgery. Real-time qRT-PCR was used to re-measure expression level of miR-29b in the DMM samples and sham surgery samples. The Real-time qRT-PCR data confirmed miRNA microarray data and showed a significant increase of miR-29b expression level in DMM right compared with left knee or sham surgery (Figure 3.6).

MicroRNA-29b is a member of the miR-29 family including miR-29a and miR-29c with the mature sequences differing at nucleotide positions 10, 18, 21, 22, or 23 but sharing a common seed sequence for target recognition. We hypothesized that not just miR-29b but all members of miR-29s may contribute to OA onset, as all miRNA-29s showed a downward trend at all 3 time points even though the difference did not reach statistical significance. Therefore, in this study, we investigated the link between all miR-29 members with OA rather than just miR-29b alone.

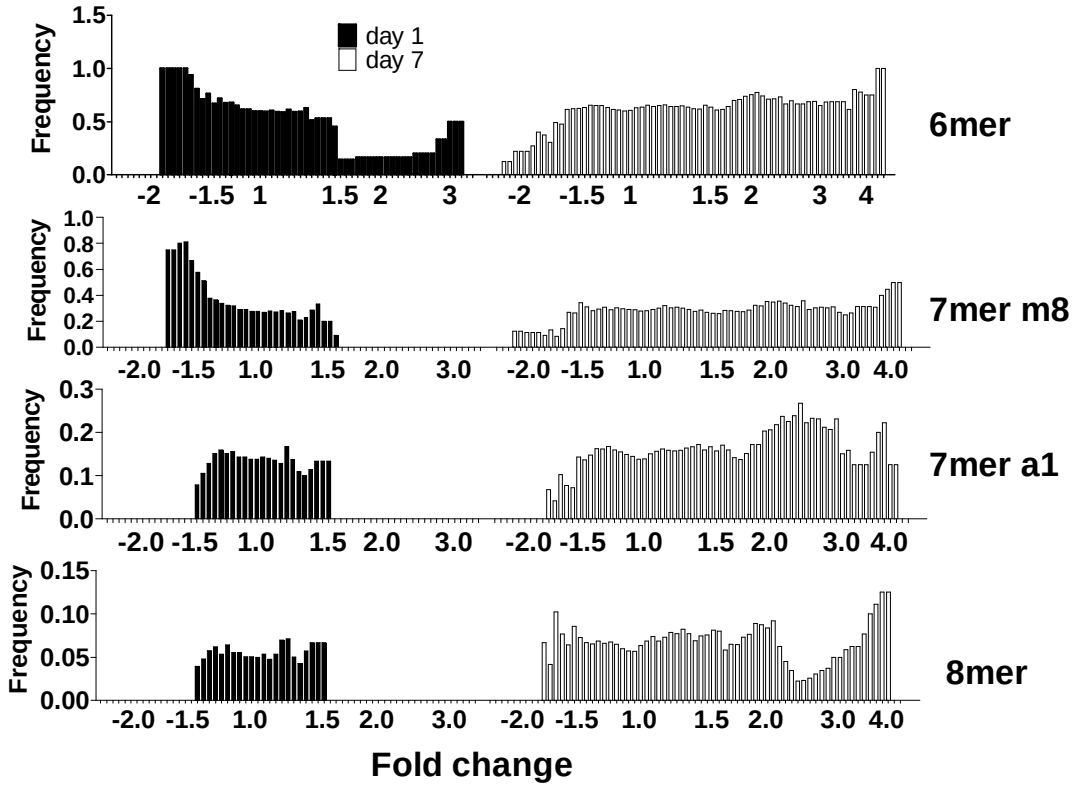

Figure 3.4 Percentage of miR-29 predicted targets in differentially expressed mRNA at day 1 and day 7 after surgery in DMM model.

The calculation was done for all the fold changes ± 0.05 from -2.5 to 4.0 and for each type of seed sequence e.g. 6mer, 7mer match 8, 7mer a1, 8mer. The mRNA having more than one binding site for each type of seed sequence was always assigned as 1. At k fold change, the percentage of 6mer-seed-site targets in modulated mRNAs was calculated: **a_6mer**= sum of mRNA having 6mer-seed site sequence in their 3'UTR with the fold change in the range (k, k+0.05); **b_k**= sum of mRNA with the fold change in the rank (k, k+0.05); **Freq= a_6mer/b_k**. The percentage of other seed site targets was calculated similarly. Day1: closed bar, day 7: opened bar.

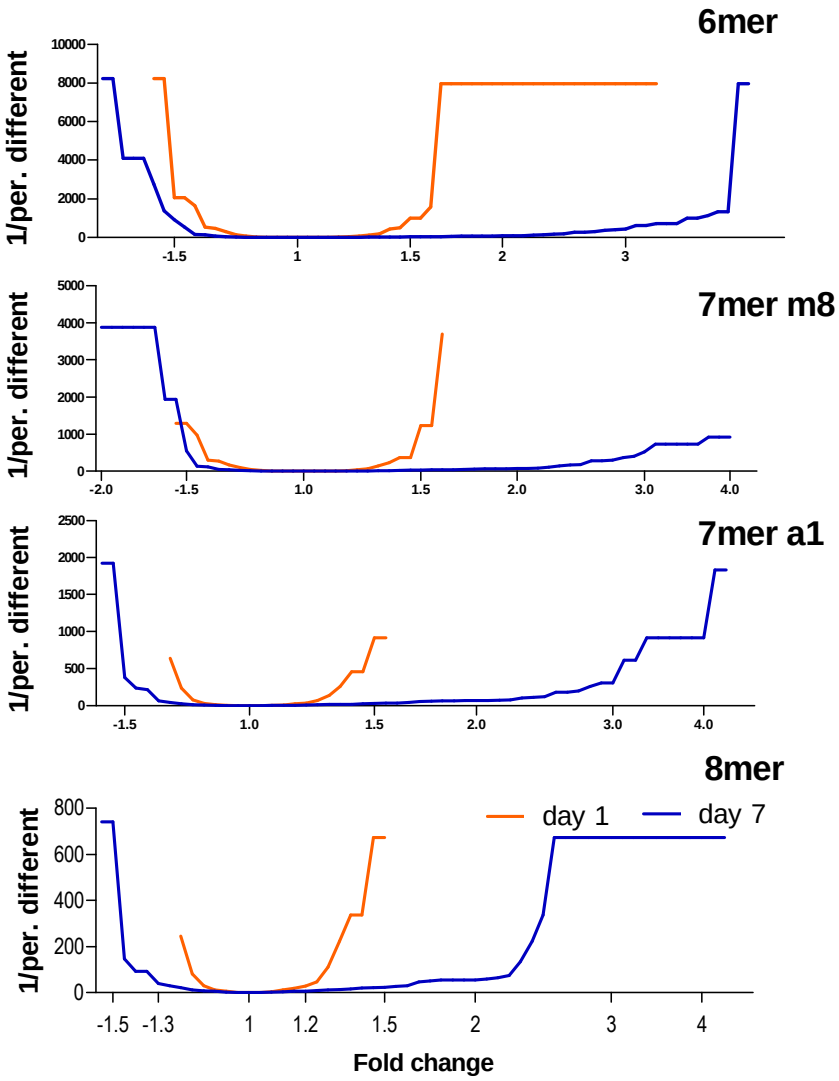

Figure 3.5 Percentage of miR-29 targets that changed expression compared to unchanged expression at day 1 and day 7 after surgery in DMM model.

The calculation was done for all the fold change (FC) ± 0.05 from each other from -2.5 to 4.0 and for each types of seed sequence e.g. 6mer, 7mer match 8, 7mer a1, 8mer. The mRNA having more than one binding site for each type of seed sequence was always assigned as 1. When FC=k, the percentage of 6mer-seed-site targets which increased or decreased expression was calculated: **6mer_changed** = sum of mRNA having 6mer-seed site sequence in their 3'UTR with FC in the range (k, FC max) if k >0, or (FC min, k) if k<0; **6mer_unchanged** = sum of mRNA having 6mer-seed site sequence in their 3'UTR with FC range in (0,k] if k>0, or (k, 0] if k< 0; **1/Per.different = 6mer_unchange/6mer_changed.** The percentage of other seed site targets was calculated similarly. Day1: red line, day 7: blue line.

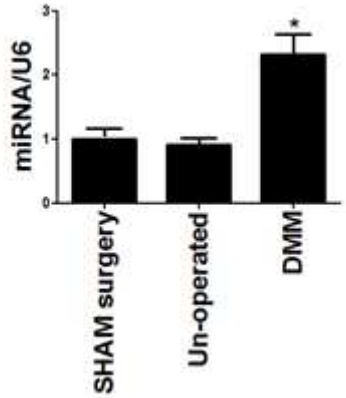

Figure 3.6: MicroRNA 29b was significantly induced in the DMM model at 1 day after surgery

Total RNA was reversed transcribed to cDNA and miR-29b expression was measured by real-time qRT-PCR in individual samples of sham right knee (sham surgery), DMM left knee (un-operated), and DMM right knee (DMM) at 1 day after surgery. U6 was used as endogenous control. Expression level of miR-29b in DMM and sham surgery was normalized to un-operated control. The data show mean +/- SEM, n=3. The expression of miR-29b between each group was analysed by unpaired two-tailed t test * $p<0.05$, ** $p < 0.01$, *** $p<0.001$.

3.2.4. Up-regulation of miR-29s in the murine hip avulsion injury model

Traumatic joint injury and joint magliment are linked to OA initiation. Patients with traumatic joint injury show an increased risk of OA, implicating the early events post-injury as important in the long term. To investigate the role of miR-29s in the onset of OA, a murine hip cartilage avulsion injury model, where the murine hip femoral cap cartilage was sub-cultured in serum-free media across a 48 hour-time course, was used. Total RNA was isolated from the explants using Trizol, reverse transcribed to cDNA by either SuperScript II reverse transcriptase (for mRNA detection) or miRCURY LNA^{TM} Universal cDNA synthesis (for miRNA detection). Expression levels were measured by real-time qRT-PCR.

The majority of the genes rapidly induced in murine joints following surgical destabilization (DMM model) were also regulated in murine hip cartilage explants upon injury (Chong et al. 2013). Interestingly, some genes such as *Dkk3, Ccl2, Il6* were significantly regulated after 3 hours in culture (Appendix, Figure 3) though likely regulating genes which are modulated at later time points. The expression pattern of the miR-29 family is similar to each other and tends to increase across the 48 hour time course (Figure 3.7): miR-29b and 29c significantly increased expression after 12 hours in culture; miR-29a significantly after 6 hours. This suggests that the regulation of the miR-29s may contribute to the molecular mechanism underlying the initiation of OA.

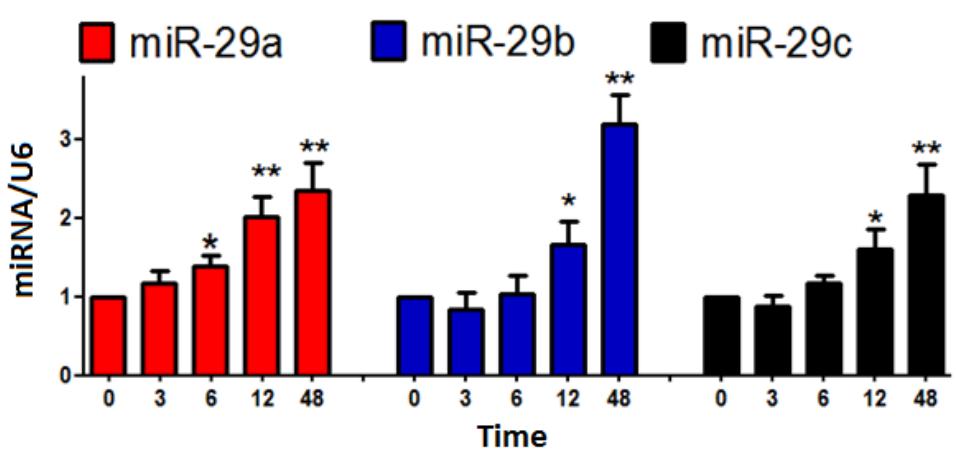

Figure 3.7: Expression of the miR-29 family in the hip avulsion injury model

The femoral caps of C57Bl/6 mice aged 4 weeks were avulsed and put in culture. At each of 3, 6, 12, 48 hour time points, the femoral caps were harvested. Total RNA was isolated using Trizol and reverse transcribed to cDNA. Expression of the mature miR-29 family was measured by real-time q-RTPCR where U6 was used as an endogenous control. At least triplicate samples were measured at each time. Means ± standard errors are presented, n=6. Difference in expression between each time point against control (t=0) was calculated by unpaired two-tailed t test. * $p<0.05$, ** $p < 0.01$, *** $p<0.001$.

3.2.5. Up-regulation of the miR-29 family in human end-stage OA cartilage

To determine whether the miR-29 family could play a role in human OA, its expression level was compared between hip / knee OA cartilage and non-disease tissue controls (hip cartilage followingfracture to the neck of femur).

Human articular cartilage samples (total: 8 hip and 7 knee OA cartilage, 7 healthy fracture to the neck of femur) were obtained from patients undergoing total hip/ knee replacement surgery at the Norfolk and Norwich University Hospital. Total RNA was isolated from all cartilage samples using Trizol and followed by a purification step through column using miRVana kit. The total RNA was reverse transcribed to cDNA using miRCURY LNA™ Universal cDNA synthesis. Expression of all miR-29 members was measured by real-time qRT-PCR with U6 as the endogenous control.

Data (Figure 3.8) showed an increase in miR-29 expression in hip OA but decrease in knee OA cartilage compared to fracture control. This reached significance, or close to significance in each case. Whilst there is no comparison with normal knee cartilage, these data show that the miR-29 family is regulated in human end-stage OA cartilage.

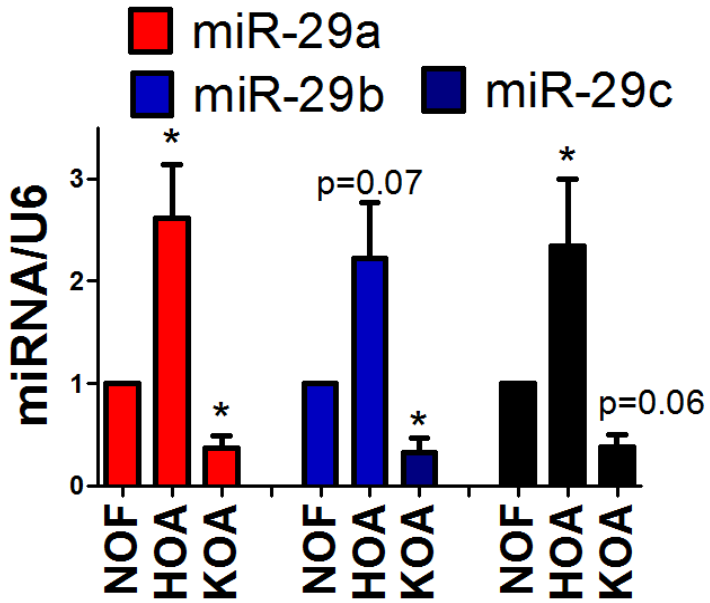

Figure 3.8: Expression of the miR-29 family in human OA cartilage

Total RNA was isolated from human articular cartilage of either end-stage OA patients or healthy controls and reverse transcribed to cDNA. Expression of the mature miR-29 family was measured by real-time qRT-PCR using U6 as an endogenous control. HOA (hip osteoarthritis cartilage, n=8), KOA (knee osteoarthritis, n=7), NOF (neck of the femur, n=7). Means ± standard errors are presented. Difference in expression between each time point against control (NOF) was calculated by unpaired two-tailed Student's t test. * $p<0.05$, ** $p < 0.01$, *** $p<0.001$.

3.2.6. The miR-29 family is regulated with chondrocyte phenotype

Dedifferentiation and the loss of phenotype is an obstacle in expanding human chondrocytes: the cells stop expressing aggrecan and collagen type II, and this limits capacity to form cartilage. In line with this, alteration chondrocyte phenotype is one of the characteristics of OA. As compared with normal articular cartilage, the chondrocytes embedded in different zones of OA cartilage were shown to express different markers of chondrocyte differentiation: chondrocytes in the middle zone re-expressing chondroprogenitor phenotype; cells in the upper middle zone expressing type III collagen (dedifferentiated phenotype) (Aigner *et al.* 1993). Assessing whether the miR-29 family is regulated with chondrocyte phenotype, therefore, would help to further determine the relevance of the miR-29 family in cartilage function.

This was investigated using human primary chondrocyte dedifferentiation model. After isolation from human knee OA cartilage by collagenase (collagenase-post digested HACs (PD)), primary chondrocytes were cultured in monolayer (primary culture HACs (P0), and three sequential passages were performed at 1: 3 dilution of cells (passage 1 to passage 3). Total RNA was isolated from cartilage, PD, P0 to P3 chondrocytes and reverse transcribed to cDNA. The expression level of all the miR-29 family was then measured by real-time qRT-PCR.

The expression of the miR-29 family was found to significantly decrease when HACs were passaged in monolayer (Figure 3.9), indicating the putative role of the miR-29 family in chondrocytic phenotype.

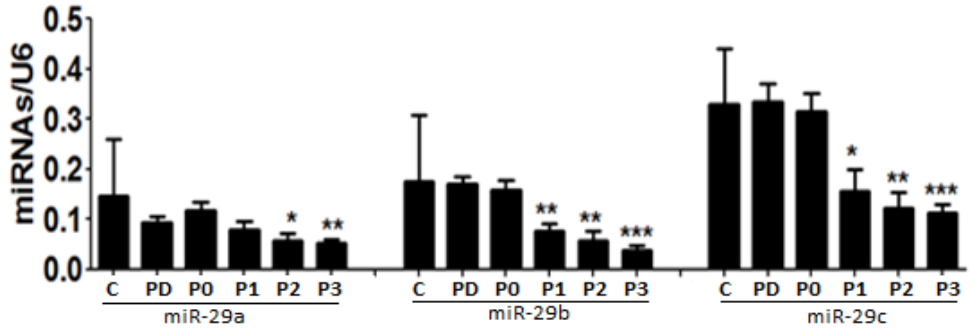

Figure 3.9: Expression of the miR-29 family in a chondrocyte dedifferentiation model

Human primary chondrocytes were isolated from the articular cartilage of 8 knee OA patients using collagenase digest. The cells were put in culture and passaged 3 times. Total RNA was isolated from either human articular cartilage (cart) or chondrocytes post digestion with collagenase (PD) or each passage 0, 1, 2, 3 (P0, P1, P2, P3). After reverse transcribing to cDNA, expression of the mature miR-29 family was measured by real-time qRT-PCR (U6 was used as an endogenous control). Mean ± standard errors are presented, n=8. Different in expression between was calculated by unpaired two-tailed t test. * $p<0.05$, ** $p < 0.01$, *** $p<0.001$.

3.2.7. MicroRNA-29s expression in chondrogenesis

Chondrogenesis is the earliest phase of skeletal development, occuring as a result of: mesenchymal cell condensation, chondroprogenitor cell differentiation, chondrocyte differentiation and maturation. Chondrogenesis results in the formation of cartilage and bone in the process of endochondral ossification (Goldring *et al.* 2006). It is pertinent to examine the role of miR-29 in chondrogenesis, particularly since the replay of this developmental process may contribute to osteoarthritis.

To determine the expression and therefore possible role of the miR-29 family in chondrogenesis both human and mouse chondrogenesis models were used. **Human chondrogenesis model**: human bone marrow stem cells were differentiated to form a cartilage disc (the model was kindly developed by Dr Matt J. Barter (Newcastle University, UK)); **Mouse chondrogenesis model**: the embryonic carcinoma cell line ATDC5 was stimulated to from chondrocytes using insulin for 42 days (this model was developed by Dr Tracey Swingler (University of East Anglia)). Total RNA was isolated, reverse transcribed to cDNA and used for measuring expression level of the miRNA by real-time qRT-PCR.

In the human chondrogenesis model, a significant down-regulation of the miR-29s after 3 days of differentiation was observed; after that, miR-29s return to the original expression levels (Figure 3.10). A similar expression pattern was also observed in the murine ATDC5 chondrocyte differentiation model: significantly decreased expression of all the miR-29 members after 14 days differentiation; with a return after 36 days, to the original level (Appendix, Figure 4). These data imply that miR-29 may be a negative regulator of the early stage of chondrogenesis.

Indeed, the miR-29 family was not the only miRNA regulated in either the human or murine chondrogenic process, many other miRNAs were strongly modulated e.g. (Barter et al, unpublished data) (Swingler et al. 2012). However, it can be postulated that the miRNA would have a functional role in chondrogenesis if it had affected on mRNA expression. To test this hypothesis, again an integrating analysis approachs (using mRNA expression profile data to analyse miR-29 putative target genes) was used. A substantial enrichment of miR-29 targets was inversely associated with the expression of miR-29s was observed (Data not shown). Together, these data suggest that the miR-29 family acts as the negative regulator of chondrogenesis, leading to an increase in mRNA to enable the process.

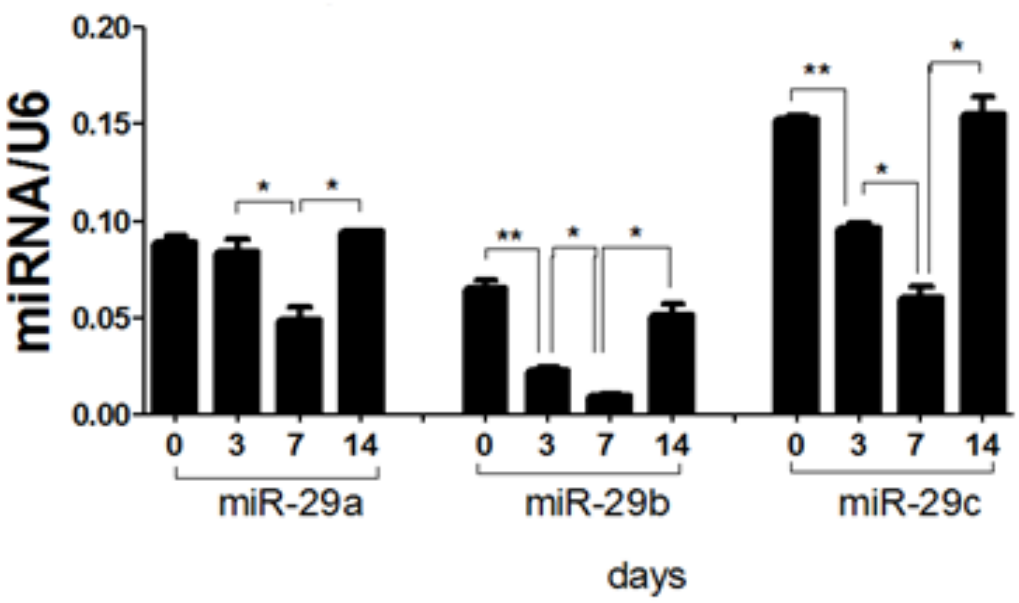

Figure 3.10: Expression of the miR-29 family in the human chondrogenesis model.

Human bone marrow stem cells (from 3 donors, 18-25 years of age, $5x10^5$ cells in 100µl growth medium) were put into polycarbonate Transwell filters and centrifuged in 24 well plates. 0.5ml chondrogenic culture medium containing 100µg/ml sodium pyruvate, 10ng/ml TGFβ3, 100nM dexamethasone, 1x ITS, 40µg/ml proline, and 25µg/ml ascorbate-2 phosphate was added to the lower well. Media were replaced every 2 or 3 days up to 14 days. At 0, 3, 7, 14 days, the cells were harvested and total RNA was extracted using Trizol. The RNA was then reverse transcribed to cDNA and was used for measuring the expression level of the mature miR-29 family by real-time qRT-PCR (U6 was used as an endogenous control). Assays were repeated 3 times. At least triplicate samples were in each time. Means ± standard errors are presented. Difference in expression between each time point was calculated by unpaired two-tailed t test. * $p<0.05$, ** $p < 0.01$, *** $p<0.001$.

3.2.8. The miR-29b is expressed in murine limb development

The formation of the skeleton first is initiated with the formation of a precartilage condensation (anlagen) which is followed by chondrogenesis triggered in the precartilage condensation and ultimately cartilage is formed. This process involves the cooperation of many cell activities e.g. migration, adhesion, intracellular signalling, and proliferation (Goldring et al. 2006). Given the likely involvement of the miR-29 family in chondrogenesis, it is pertinent to ask whether miR-29s are expressed in murine limb development. Additionally, the miR-29 family or its members have been shown to control cell proliferation and apoptosis in different tumour types. A murine model would thus be a useful model to study the role of the miR-29 family in cell proliferation and apoptosis limb development.

In mice, the forelimb starts to develop at stage E9.5 whilst the hindlimb starts behind by about half a day. Five days later, a miniature model of the adult limb is formed (E14.5 and E15 for fore and hindlimb, respectively). At stage E11, a distinct apical ectodermal ridge at the limb tip is formed in the forelimb and the handplate is beginning to form at E11.5. Similarly events happen in the hindlimb at half a day later (at E11.5 and E12) (Martin 1990).

Whole mount *in situ* hybridization was conducted using amiRCURY LNA^{TM} miR-29b-3p double-DIG labelled probe to detect the expression of miR-29b in the mouse embryo stage E11.5 and E15. The data showed that: at stage E11.5, miR29b was expressed in the cartilage of both fore and hindlimb; at stage E15 when the small scale the adult limb was formed, miR-29b was strongly expressed, implicating miR-29b playing a role in murine limb development. Besides limbs, miR-29b was also found on the brain and the spine of embryo stage E11.5 (Figure 3.11).

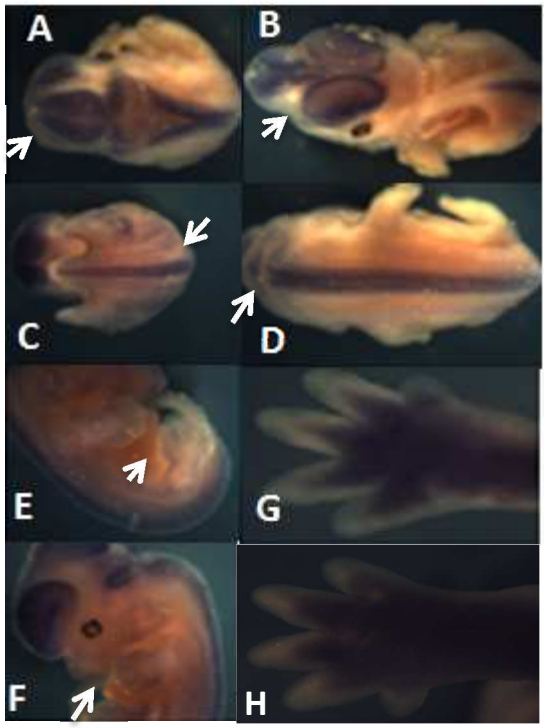

Figure 3.11: Whole mount *in situ* hybridization of miRNA-29b in murine embryo stage E11.5 and E.15.

Using a miRCURY LNA^{TM} double-DIG labelled miR-29b probe, miR-29b was found to be expressed: in the embryo stage E11.5 in the brain (A), mouth (B), spine (C-D), hindlimb (E), forelimb (F); in the embryo stage E15 in hindlimb (G) and forelimb (H).

3.3. DISCUSSION

The principal aim of this study was to begin to identify the miRNAs which were implicated in the early stages of OA and elucidate their function. Whilst there have been a number of studies on the role of miRNAs in OA pathogenesis, they have not focused on the disease onset. In the present study, for the first time, the miRNA expression profile was reported for the DMM mouse model at early time points e.g. 1, 3, 7 days following surgery. The fact that only a small number of miRNAs changed expression across the first three days after DMM surgery might indicate miRNAs mainly contribute in disease progression rather than initiation. However, there are some limitations of the study which prevent a firm conclusion about the role of miRNAs in the early stages of the disease. Total RNA for the miRNA microarray was isolated from whole knee joints of DMM mice. Thus, if a miRNA is expressed in a single tissue e.g. cartilage, bone, meniscus, ligament or synovium, pooling of tissues will reduce the signal to a lower level than in the individual tissue and that could be the explanation for the overall low levels of modulated miRNAs observed in the present study. Moreover, insufficient controls, e.g. naïve samples and genes responding to sham surgery in this study may also have been problematic. The DMM model does not completely recapitulate human OA pathogenesis, e.g. with more synovial involvement in the latter.

However, it remains unlikely that the miRNA microarray data acquired from the DMM model in this study is incorrect. The DMM left knee (no surgery) used as a control would show the consequence of surgery, even if it can't distinguish injury per se from early OA. Moreover, Burleigh et al (2012) reported a large and significant difference in expression levels of e.g. *Ccl2, Arg1e, Il6, Saa-3* in the same DMM model just 6 hours following surgery, which was interpreted as response to surgical destabilization rather than reaction to injury (Burleigh *et al.* 2012). In this study, such an increase in expression was also observed when comparing between the DMM right and DMM left, suggesting that the DMM left knee can act as a suitable control. Hence, it was expected that the changes in miRNA expression at early time points would be greater.

MicroRNA-29b, one of only two miRNAs significantly increased in expression at day one post-surgery and inversely correlated with expression of its putative targets, was investigated in detail. The miR-29b is encoded by two loci in the human genome e.g. the primary miR-29-a/b1 cluster in chromosome 7, and the primary miR-29b2/c cluster in chromosome 1.

Normally, clustered miRNAs in humans work in combination to accomplish their function. At the transcriptional level, at least one of the other miR-29 family members i.e. miR-29a or miR-29c will be co-transcribed with miR-29b. In addition, miR-29b is reported to have a short half-life (the time taken for the miRNA to fall to half of its original value) which is linked to the presence of uracil bases at positions 9-11, compared with miR-29a (more stable with a reported half-life of > 12 hours) (Zhang *et al.* 2011). Thus, in the DMM model at 1 day after surgery it would be expected that a significant increase in either miR-29a or miR-29c would accompany that of miR-29b. However, only miR-29b increased in expression (1.5 fold change in array data) but not any of the other miR-29 family members, perhaps implicating another post-transcriptional regulatory mechanism controlling miRNA processing. In line with the DMM model data, in a murine hip avulsion injury model, an increasing expression level was also observed for all miR-29 members post injury. Interestingly, a similar pattern of expression of some genes strongly induced in the DMM model at 6 hours after surgery (Burleigh et al. 2012) was seen in the injury model suggesting some molecular similarities between the two models. In line with this, Chong et al (2013) also observed a similar pattern when measuring the expression of the set of gene induced expression in DMM model 6 hours after surgery and in murine injury model in which the hip cartilages cultured for 6 hours (Chong et al. 2013). Since mechanical factors following traumatic joint injury may mediate OA onset, these data suggest for the first time an important role for the miR-29 family in the initiation of OA. The fact that the miR-29 family increased in expression in human OA end-stage cartilage supports a role for the miR-29s in the disease. In this study, human knee cartilage normal controls were not available, and the difference in hip and knee cartilage may explain in part why the miR-29 family levels increased in hip but decreased in knee OA cartilage compared to human hip fracture control. Also, in this project, the miR-29 family expression level is very variable across a human tissue panel e.g. heart, brain, lung, spleen (data not shown). In supporting these data, previous published data also demonstrated the different expression level of the miR-29 family in different tissues in zebrafish (Wienholds *et al.* 2005). These data suggest that the mechanisms controlling the miR-29 family expression in different tissues are not similar. The fact that miR-29 family expression was modulated in different mouse models and in human OA cartilage implies a role for the miR-29 family in cartilage, and suggest that the two pri-miR-29a/b1 and pri-miR-29b2/c clusters may be involved in both early and late stages of the disease. The direct mechanism

controlling miR-29 family expression and the extent to which each cluster contributes to OA remains unknown and is worthy of further investigation.

This study also provides evidence for the role of the miR-29 family in cartilage formation as its expression was regulated during human and mouse chondrogenesis and inversely correlated with its putative targets. In fact, such decreased expression level at an early stage of chondrogenesis is in line with published data e.g. Guerit et al (2013) showed the decreased expression of miR-29a is essential for chondrogenesis via its regulation of FOXO3a (Guerit *et al.* 2014); Sorentino et al (2008) found miR-29b was among miRNAs down-regulated when differentiating human MSCs through chondrogenesis (Sorrentino et al. 2008); Yan et al (2011) demonstrated that both miR-29a and miR-29b were significantly decreased in a chondrogenesis model where mouse MSC were grown on polyhydroxyalkanoates (Yan et al. 2011). However, I have demonstrated for the first time that all miR-29 family members are involved in chondrogenesis, stressing the important role of both miR-29 clusters in controlling cartilage homeostasis in human and mouse. In contrast to this data, there are others studies profiling the expression of miRNAs in murine and human chondrogenesis model (Suomi et al. 2008, Lin et al. 2009, Miyaki *et al.* 2009, Lin et al. 2011, Yang et al. 2011). The miR-29 family, nevertheless, was not amongst the miRNAs which had altered expression. This is not surprising and could be attributed to differing design of experiments including inducers of differentiation, cell type, numbers of detected miRNA probes and organism. In addition, despite of being a negative regulator of chondrogenesis, miR-29b was found to express in murine limb development. A number of published data report that the miR-29 family can act as oncogenes whose expression induces cell proliferation but inhibits apoptosis. Whether the miR-29 family is involved in murine limb development through inducing chondrocyte proliferation in the growth plate remains unknown. Therefore, examination of the role of miR-29 family in limb development in vivo will be a priority for future studies.

Another piece of data supporting the role of the miR-29 family in OA comes from the fact that expression of the miR-29 family is decreased during chondrocyte dedifferentiation. Again, other groups have profiled miRNAs in human dedifferentiation models (Karlsen et al. 2011, Lin et al. 2011) but the miR-29 family has not shown up in any of them. As mentioned above, this could be attributed to many different factors.

Taken together, all of these data show that the miR-29 family may modulate both cartilage homeostasis and OA and make a compelling case for further investigation. In this PhD thesis, for the first time, the whole miR-29 family is reported to be involved in OA although the increase of the miR-29b in OA had been shown (Moulin *et al.* 2012). Nevertheless, the miRNA-29 family has been implicated in many other areas of pathology. Many publications have reported the involvement of the miR-29 family in cancers where the miRNA family or a single member could serve as either a tumour suppressor or an oncogene. In rhabdomyosarcoma (Wang *et al.* 2008), nasopharyngeal carcinoma (Sengupta *et al.* 2008), hepatocellular carcinoma (Xiong *et al.* 2010), acute myeloid leukemia (Eyholzer et al. 2010) , multiple myeloma (Zhang *et al.* 2011, Amodio *et al.* 2012), chronic lymphocytic leukemia (Santanam *et al.* 2010), glioblastoma (Cortez *et al.* 2010), and lung (Fabbri *et al.* 2007) and pancreatic cancer (Muniyappa *et al.* 2009), miR-29 was described as a tumor suppressor whilst in acute myeloid leukemia , colorectal liver metastasis (Wang *et al.* 2012), and breast cancer (Chou *et al.* 2013) , miR-29 was shown to be as tumour promoter.

Besides cancers, the miR-29 family has been shown to participate in a number of physiological processes including (i) **muscle development** e.g. knockdown of miR-29b in vivo induced cardiac fibrosis in mice; miR-29a/b1 inhibition induced vascular smooth muscle cell calcification; miR-29 family expression was developmentally up-regulated in porcine skeletal muscle from fetal to adult, and this was also true in mice and human; the miR-29 family was found to be down-regulated in myotonic dystrophy type I and Duchenne muscular dystrophy (Wei *et al.* 2013), (ii) **bone formation** e.g. miR-29a increased bone mass, induced osteoblast differentiation, and inhibited osteoclast differentiation; reduced miR-29a expression was associated with low bone mass and poor skeletal microarchitecture in rats treated with glucocorticoids (Wang *et al.* 2013), (iii) **HIV virus infection** e.g. ectopic expression of miRNA-29a resulted in reduction of HIV virus levels, implicating this miRNA as a potential strategy in developing anti-HIV therapeutics (Ahluwalia *et al.* 2008), (iv) **aging** e.g. miR-29 family up-regulation was observed in a number of different organs e.g. liver, muscle, and brain of several aging models (Ugalde *et al.* 2011, Fenn *et al.* 2013, Hu *et al.* 2014), (v) **diabetes** e.g. the miR-29 family was up-regulated in diabetic rats and forced expression of miR-29 inhibited insulin induced glucose imported by 3T3-L1 adipocytes (He *et al.* 2007); reduced miR-29b in plasma samples of type 2 diabetes patients anticipated the

manifestation of the disease (Zampetaki *et al.* 2010); miR-29c was found up-regulated the kidney glomeruli from diabetic mice (Long *et al.* 2011); the continued expression of miR-29 isoforms in the pancreatic β-cell seems to be required for normal and selective stimulation of insulin secretion by glucose (Pullen *et al.* 2011); (vi) **fibrosis development**, the miR-29 family has been shown to be implicated in the development of fibrosis of many organs including heart, kidney, lung, liver, and systemic sclerosis; (vii) **Alzheimer disease,** the miR-29a/b1 cluster or miR-29a was significantly decreased in Alzheimer patients (Hebert *et al.* 2008, Shioya *et al.* 2010).

In conclusion, with all of the data above, the miR-29 family may play a key role in Osteoarthritis and of is worthy of further investigation. The mechanisms which control its expression together with its function in chondrocytes will be described in the next chapters.

CHAPTER IV
FACTORS THAT CONTROL EXPRESSION OF THE MICRORNA-29 FAMILY

4.1. Introduction

In the previous chapter, evidence for the involvement of the miR-29 family in cartilage homeostasis and OA was presented. The increased expression of the all family members is apparent in both early and late stages of OA. However, which factors or mechanisms are responsible for miR-29 induction or repression in chondrocytes remains unknown and is worthy of further investigation.

The miR-29 family is intergenic miRNAs and is encoded in two gene clusters e.g. one for the primary miR-29a/b1 on chr.7q32, and the other for the primary miR-29b2/c on chr.1q32.2 (Saini *et al.* 2007, Chang *et al.* 2008). The miR-29b1 and miR-29a precursors are processed from the pri-miR-29a/b1 last intron (Genbank accession EU154353) whist the miR-29b2 and miR-29c precursors are from the pri-miR-29b2/c last exon (Genbank accession EU154352 and EU154351) (Chang et al. 2008) (Figure 4.1). These precursors are all transcribed as polycistronic primary transcripts (Chang et al. 2008, Mott *et al.* 2010) upon which various transcriptional regulators e.g. NFκB (Liu *et al.* 2010, Mott et al. 2010), supressors (c-Myc (Mott et al. 2010, Parpart *et al.* 2014), Sp1(Liu et al. 2010, Amodio *et al.* 2012), Gli (Mott et al. 2010), Yin-Yang-1, Smad3 (Qin *et al.* 2011), Ezh, H3K27, HDAC1, HDAC3), or inducers (Gli, SRF, Mef2, TCF/LEF, GATA3 (Chou et al. 2013), CEBPA (Eyholzer et al. 2010)), and signalling pathways e.g, Wnt , TGFβ, TLR/NFκB, TNFα/NFκB, hedgehog signalling have been reported to be directly and/or indirectly involved. For instance, **both canonical and non-canonical Wnt signalling** was reported to induce the miR-29 family level in different cellular contexts: Wnt3a rapidly induces miR-29 levels in osteoblastic cells (Kapinas *et al.* 2009, Kapinas et al. 2010) or in muscle progenitor cells (MPCs) (Hu *et al.* 2014), respectively, at least in part through the two putative TCF/LEF-binding sites in the miR-29a promoter (Kapinas et al. 2010); non-canonical Wnt signalling through Wnt7a/Frizzled 9 resulted in increased expression of only the mature miR-29b but not miR-29a or c or any miR-29b primary or precursor forms in non-small lung cancer cell lines H661 and H15 (Avasarala *et al.* 2013). In addition, ERK5 and PPARγ, key effectors of the Wnt7a/Frizzled 9 pathway, were also observed to be strong inducers of miR-29b expression (Avasarala et al.

2013). In contrast to Wnt signalling, **TGFβ/Smad3 signalling** was shown to negatively regulate miR-29 family expression in different cell lines e.g. human aortic adventitial

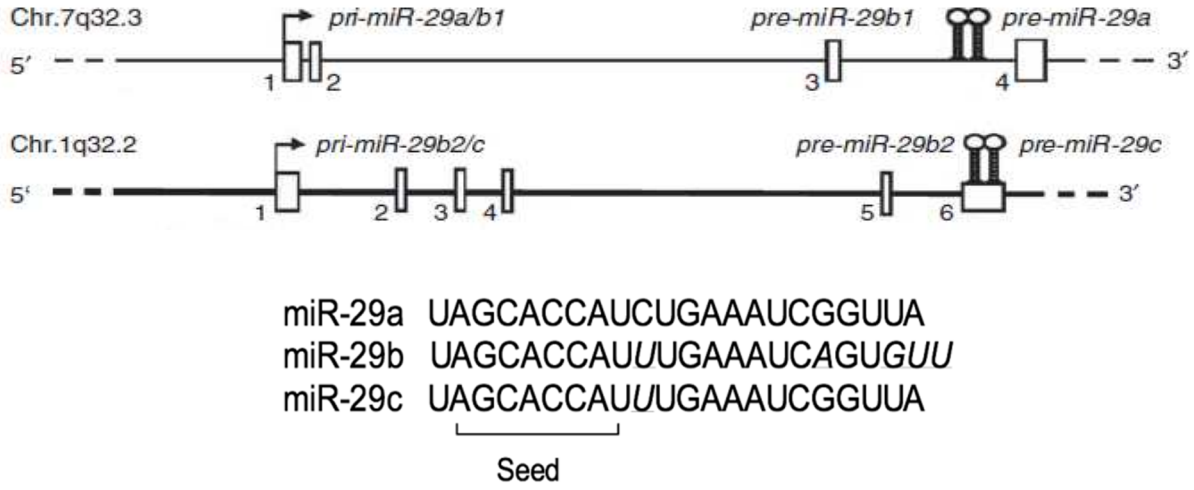

Figure 4.1: Genomic organization of the miR-29 family

The miR-29 family includes three members miR-29a, miR-29b and miR-29c. The primary pri-29a/b1 is located in chromosome 7 containing pre-29a and pre-29b1. The primary pri-29b2/c is located in chromosome 1 including pre-29b2 and pre-29c. The hairpins indicate the locations of the sequence encoding precursors of miR-29s. Pre-29a and pre-29c will process into mature miR-29a and miR-29c, respectively. Pre-29b1 and pre-29b2 will process into mature miR29b. The mature sequences of the miR-29 family members share identical seed regions. Nucleotides that differ among miR-29s are indicated in italics.

fibroblasts (Maegdefessel *et al.* 2012), renal fibrosis cells (Wang *et al.* 2012, Ramdas *et al.* 2013), murine hepatic stellate cells (Roderburg *et al.* 2011), rat hepatic stellate cells (Kwiecinski *et al.* 2011), human skin fibroblasts (Maurer *et al.* 2010), human tenon's fibroblast (Li *et al.* 2012), human lung fibroblast cell line (Cushing *et al.* 2011, Yang *et al.* 2013). The suppressive effect of TGFβ/Smad3 signalling on miR-29 expression was partly mediated through a Smad3 binding site in the highly conserved region around 22kb upstream of the miR-29b2/c promoter as showed by chromatin immunoprecipitation assay (Qin et al. 2011, Ramdas et al. 2013). Similar to TGFβ, **Toll-like receptor (TLR) signalling and TNFα signalling** have been shown to mediate suppressive effects on miR-29 family expression. In man, treating human cholangiocarcinoma cells with TLR ligands e.g. TLR3 (Poly (I:C)), TLR4 (LPS), TLR5 (flagellin), TLR6 (MALP-2) showed a significant decrease in the miR-29 level beginning after 4 hours of LPS treatment but increasing to 24 hours (Mott et al. 2010); treating human stellate cells with LPS strongly decreased all miR-29 family expression after 1 hour (Roderburg et al. 2011); treating C2C12 myoblasts with TNFα substantially reduced miR-29b and miR-29c expression (Wang et al. 2008); stimulating the choroidal-retinal pigment epithelial cell line ARPE-19 with TNFα resulted in significant down regulation of all miR-29s; conversely, transfecting with a synthetic NFκB decoy, (NFκB inhibitor), rescued the down regulation of miR-29 by TNFα (Χαι *εϖ αλ.* 2014). The activation of NFκB through TLR signalling with its three binding sites in the miR-29a/b1 cluster promoter (-561, -110, and +134) was proven to be the mechanism for the suppression of miR-29a/b1 promoter function (Mott et al. 2010). In mice, miR-29a and miR-29b significantly decreased expression in murine natural killer (NK) cells stimulated with the TLR3 ligand (Poly (I:C)) or phorbol ester (PMA) as well as in splenocytes, NK and T cells of mice infected with L. *monocytogenes* or *Mycobacterium bovis* bacillus Calmette-Guérin (Ma *et al.* 2011). Consistent with the human miRNA, a region about 25 kb upstream of the murine promoter of miR-29a/b1 contains two NFκB binding sites. The second binding site is more conserved between human and mouse and it has been shown to be key for suppression of the miR-29a/b1 promoter (Ma et al. 2011). Importantly, other transcriptional factors, co-operating with NFκB to suppress or induce miR-29 family expression, have also been reported e.g. YY1, Sp1, Ezh, H3K27, HDAC1, HADC3, Mef2, SFR. Forced expression of YY1 in C2C12 lead to a 2-fold decrease of miR-29b and miR-29c levels; similarly, siRNA knockdown of YY1 significantly enhanced expression of miRNA expression. ChIP analysis showed that YY1 did not bind to the miR-29b2/c locus in cells in the absence of NFκB,

suggesting that both pathways are necessarye for silencing the miR-29b2/c locus. Amongst 4 putative binding sites of YY1 in highly a conserved region ~20kb upstream of miR-29b2/c, only one site is bound by YY1 on ChIP assay whereas all 4 sites produced a binding complex with EMSAs using nucleus extract from C2C12. Notably, Ezh, H3K27, HDAC1, whose expression is associated with repression of muscle-specific genes, and recruited by YY1, was also detected by ChIP assay. In line of these transcription factors, Mef2 and SFR, well-known for activating muscle genes, were also found binding to the miR-29b2/c promoter. Again using luciferase reporter assay, a reporter containing a 4.5 kb fragment spanning YY1, Mef2, SFR binding sites was repressed by YY1 or loss of the YY1 binding site but stimulated with either YY1 knockdown or SRF or Mef2 (Wang et al. 2008). In addition, forced expression of Sp1 or NFκB (p65) reduced miR-29b expression; conversely, knockdown of Sp1 or NFκB (p65) by siRNAs resulted in induced miR-29b level (Liu et al. 2010). EMSA assay using probes spanning the -125/-75 miR-29b sequence yielded two major complexes, suggesting Sp1/NFκB acts as a repressive complex interacting with an element of the miR-29b enhancer (Liu et al. 2010). Interestingly, histone deacetylase (HDAC) 1 and 3 contribute to the repressor activity of Sp1/NFκB on miR-29b expression (Liu et al. 2010). Incubation of HDAC1/HDAC3 with ^{32}P-labelled probe from the miR-29a/b1 cluster region together with NFκB p50/p65 and Sp1 showed a delayed and more intense band; HDAC1/3 inhibitors increase miR-29b expression, supporting the interaction of HDAC1 and 3 and Sp1/NFκB with the miR-29b regulatory sequence (Liu et al. 2010). Similar to other signalling mentioned previously, **hedgehog signalling pathway** was also shown to repress miR-29 expression: cells treated with cyclopamine, an inhibitor of Smoothened (a hedgehog signalling component), or transfected with siRNA to knockdown Gli-3, the expression of miR-29b increased (Mott et al. 2010). Along with the transcription factors mentioned above, there are other transcriptional factors controlling miR-29 family expression. The serum alphafetoprotein (AFP), a membrane-secreted protein associated with poor patient outcome in hepatocellular carcinoma, was reported to inhibit miR-29a expression through facilitating c-MYC binding to the promoter of the pri-miR-29a/b. This conclusion was supported by: the inability of AFP to decrease the miR-29a level in the absence of c-MYC protein; c-MYC was abundantly bound to the miR-29a/b1 promoter in the presence of AFP, but did not bind without AFP (Parpart et al. 2014); c-MYC promoter binding protein (MBP), originally described to bind to and repress c-MYC promoter function, up-regulated miR-29b expression

by 6 fold in prostate cancer cells (Steele *et al.* 2010). The haematopoietic master transcription factor, CCAAT/enhancer-binding protein-α (CEBPA), was also reported to activate the expression of miR-29a and miR-29b. Forced expression of CEBPA in acute myeloid leukaemic cells lead to two-fold induced expression of the primary miR-29a/b1 and the mature miR-29a and miR-29b whereas the expression of miR-29b2/c primary transcript remained stable. Using luciferase reporter assays, the sequence, having the conserved region spanning -682 bp upstream to +296 bp downstream of the miR-29a/b1 transcriptional start site and containing 6 potential CEBPA sites, was also strongly induced with CEBPA. Among these binding sites, the one located at +15 to +29 bp was identified to be responsible for CEBPA-mediated activation of the pri-miR-29a/b1 promoter on ChIP assay (Eyholzer et al. 2010). Another transcriptional factor, GATA3, specifying and maintaining luminal epithelial cell differentiation in the mammary gland, was also found to induce miR-29 expression directly by binding to three GATA3 sites in the miR-29a/b1 promoter. Interestingly, GATA3 can induce miR-29s expression by inhibiting the TGFβ and NFκB signalling pathway. Additionally, STAT1 (signal transducer and activator of transcription) a transcription factor induced by interferon γ signalling, was reported to upregulate primary 29a/b1, the pre-29a, pre-29b1, and the mature miR-29a, miR-29b in melanoma cell and T cells (Schmitt *et al.* 2013).

With all the information above, it is likely that in different cellular contexts, the miR-29 family expression is controlled by different transcription factors and signalling pathways. Which factors control its expression in human chondrocytes remains unknown. The effects of a variety of anabolic and catabolic factors e.g. TGFβ, Wnt3a, IL-1, LPS on miR-29 family expression in human chondrocytes were thus investigated. Also, the effect of SOX9, a major specifier of chondrocyte phenotype was also investigated.

Aims:

- Analyse the promoter region (approximately 2kb upstream of the transcription starting site) of the miR-29 family for SOX9 binding sites. Experimentally validate the impact of SOX9 on miR-29 expression.
- Test major anabolic and catabolic cytokines controlling the miR-29 expression in chondocytes.

4.2. Results

4.2.1. The master regulator of chondrogenesis SOX9 suppresses expression of the miR-29 family

The master regulator for chondrogenesis SOX9 has a critical function in a number of development processes e.g. skeletal formation, sex determination, pre-B and T cell development. *SOX9* was found to be expressed in all chondroprogenitors and differentiated chondrocytes, but not in hypertrophic chondrocytes (Ng *et al.* 1997, Zhao *et al.* 1997). Importantly, SOX9 is considered as the critical transcriptional factor for chondrogenic differentiation, partly owing to the fact that its functions are required for differentiating chondrogenic mesenchymal condensations into chondrocytes, and for all stages of chondrocyte differentiation: in mouse chimera, *Sox9* knockout cells were excluded from all cartilage and no cartilage developed in teratomas derived from *Sox9* -/- embryonic stem cells (Bi *et al.* 1999); *Sox9* deletion from chondrocytes at later stages of development resulted in decrease in chondrocyte development, cartilage matrix gene transcriptional inhibition, and prematurely conversion from proliferating chondrocytes to hypertrophic chondrocytes (Akiyama *et al.* 2002). Considering the critical role of SOX9 in chondrocytes, I explored the connection between this factor and expression of the miR-29 family. Initial evidence suggested a link: in the DMM model mRNA profiling data, at 7 days after the surgery, *Sox9* expression was greatly induced (Appendix, Table 7) whilst the miR-29s expression was suppressed; in both human and mouse chondrogenesis models, the level of Sox9 was inversely correlated with the level of miR-29 expression (data not shown). Thus, SOX9 could be a miRNA-29 target or SOX9 could regulate miRNA-29 expression.

To test the postulate **that SOX9 is a miR-29 target**, the effect of the miR-29 members on SOX9 transcriptional expression was examined: after sub-cloning the *SOX9* 3'UTR downstream of the luciferase gene, this SOX9-3'UTR reporter vector was co-transfected with the miR-29 family into SW1353 cells; 24 hours after transfection, luciferase activity was measured. Luciferase activity showed that miR-29 family have no effect on the *SOX9* 3'UTR even though bioinformatics analysis found one 6-mer seed site for miR-29 in the *SOX9* 3'UTR (data not shown), suggesting that SOX9 is not a miR-29 family direct target. Also, whether SOX9 is a miR-29 indirect target was also determined: relative expression of SOX9 was checked in human primary chondrocytes transfected with miR-29 family for 48 hours. Quantitative RT-PCR confirmed that the SOX9 level was not changed with miR-29

transfection in chondrocytes (data not shown). Thus, SOX9 is not a direct or indirect target of miR-29s at least at the transcriptional level.

For testing the second hypothesis **SOX9 is a suppressor of miR-29 expression**, the effect of overexpression or knockdown of SOX9 on miR-29 expression was studied: a SOX9 expression construct or siRNA was transiently transfected into the human chondrosarcoma SW1353, 48 hours after transfection, the level of the mature miR-29 family was measured by quantitative RT-PCR. The data (Figure 4.2) show that SOX9 suppressed miR-29 transcription: the miR-29 family levels were significantly reduced when SOX9 was overexpressed (Figure 4.2.a,c) but induced when SOX9 was knocked down (Figure 4.2.b,c).

To further explore the regulatory mechanism by which SOX9 suppressed miR-29 expression, the 2kb region upstream from the primary miR-29a/b1 and miR-29b2/c transcription start sites were analysed by searching for the SOX9 DNA-binding motif ([A/T][A/T]CAA[A/T]). This analysis revealed 5 putative binding sites for SOX9 in the promoter regions of pri-miR-29a/b1 and pri-miR-29b2/c, respectively (Figure 4.3.a). A reporter construct with the primary miR-29a/b1 2kb promoter, kindly provided by Dr Anne Delany (University of Connecticut, USA) was used to further validate the direct effect of SOX9: the reporter was co-transfected with increasing amounts of SOX9-expression plasmid into SW1353 cells and luciferase activity measured after 24 hours of transfection. Luciferase activity in SW1353 cells significantly decreased in a dose-dependent manner (Figure 4.3.b) showing that SOX9 directly regulated the primary miR-29a/b1 promoter.

The data above demonstrate that SOX9 is a miR-29 family suppressor.

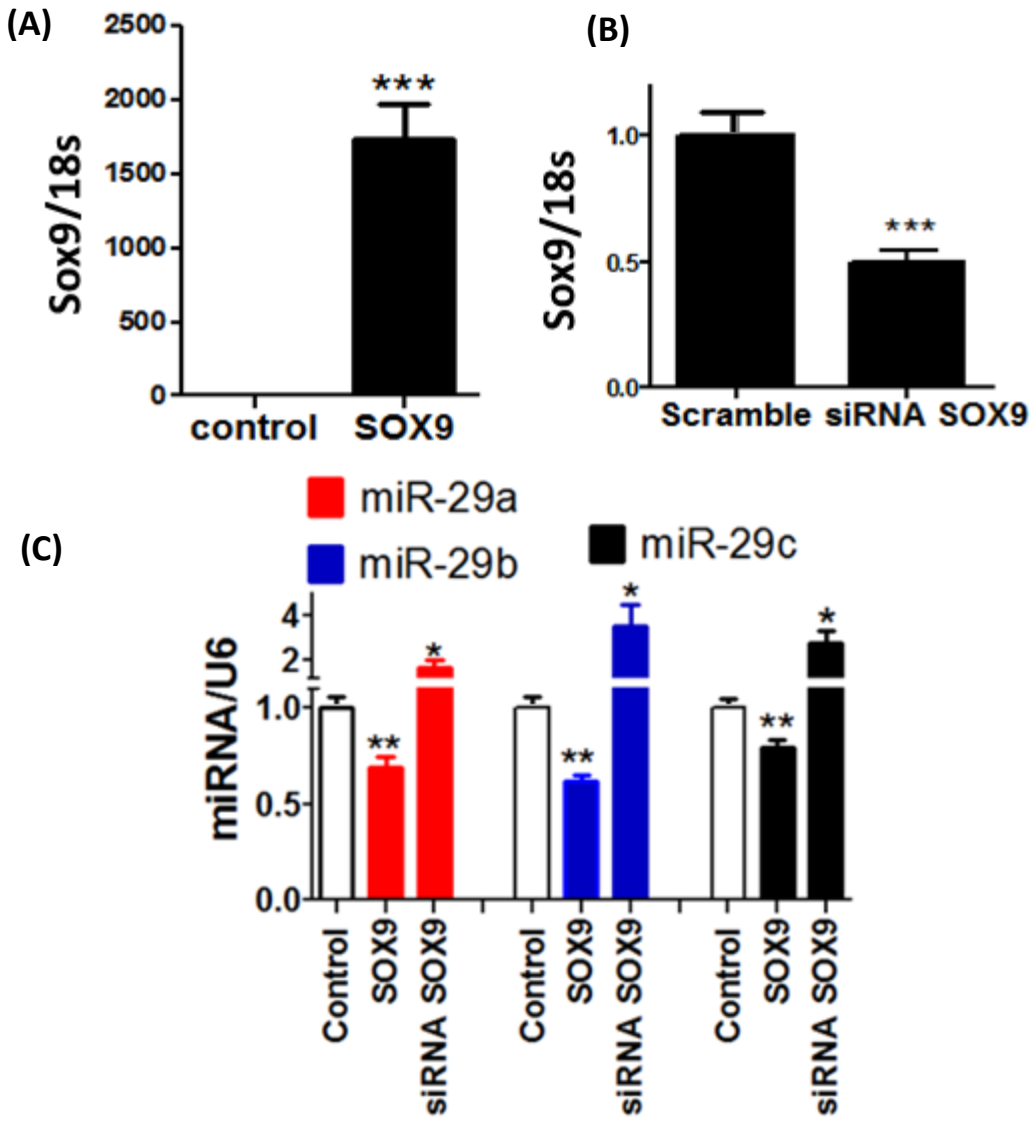

Figure 4.2: **Sox9 suppresses miR-29 family expression**.

(A) SOX9 gain-of-function: transiently transfection of a SOX9-expression vector or pcDNA3 empty vector (control) into SW1353 cells; (B) SOX9 loss-of-function: transiently transfection of SOX9 siRNA or a non-targeting control into SW1353 cells. Relative expression of SOX9 in (A) and (B) was measured 48 hours after transfection by quantitative RT-PCR using18S as the endogenous control; (C) The miR-29 family expression levels after overexpression or knockdown of SOX9 in SW1353 cells was measured by quantitative RT-PCR. Using U6 as the endogenous control. Red bar: miR-29a, green bar: miR-29b, black bar: miR-29c, open bar: control. Means ± standard errors are presented. Difference in expression was analysed by unpaired two-tailed Student's t test. * $p<0.05$, ** $p < 0.01$, *** $p<0.001$, n=3.

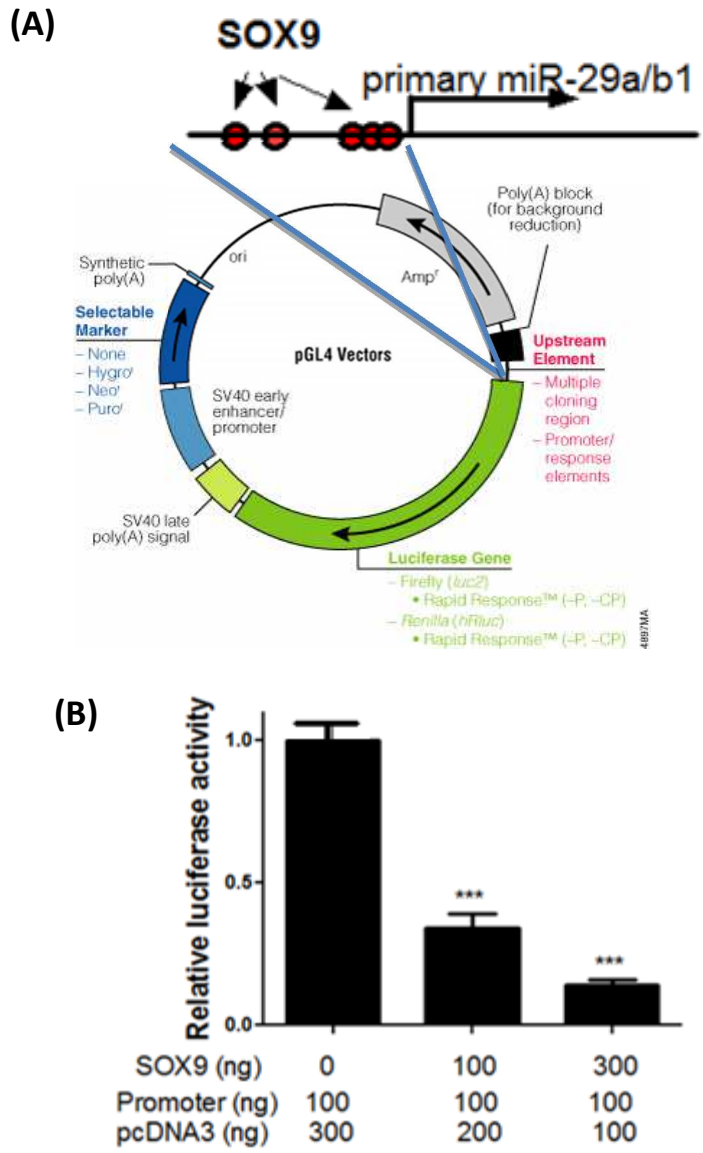

Figure 4.3: **Sox9 suppresses primary miR-29a/b1 transcription by directly binding to the proximal miR-29a/b1 promoter.**

(A) Structure of the miR-29a/b1 promoter reporter: 5 putative binding sites of SOX9 were identified by analysing the 2kb region upstream of the transcription start site of miR-29a/b1 by JASPAR. This 2kb region was sub-cloned upstream of the luciferase gene in a pGL4 vector.
(B) Suppressive effect of SOX9 on the primary miR-29a/b1 promoter reporter: transiently co-transfection of primary miR-29a/b1 promoter (100ng) with increasing amount of SOX9-expression vector (0, 100, 300ng) or pcDNA.3 to equalise DNA into SW1353. A constitutively expressed Renilla lucierase was used as a control for transfection efficiency. Luciferase activity was measured 24 hours after transfection. Means ± standard errors are presented. The difference in luciferase activity was analysed by unpaired two-tailed Student's t test. * $p<0.05$, ** $p < 0.01$, *** $p<0.001$, n=6.

4.2.2. TGFβ1 inhibits expression of the miR-29 family

TGFβ signalling has many important roles in chondrocytes and articular cartilage: TGFβ induces extracellular matrix formation; stimulates chondrocyte proliferation; inhibits the terminal differentiation of chondrocytes; retains chondrocytes in the pre hypertrophic stage; increases total glycosaminoglycan synthesis; maintains the matrix component in immature cartilage (Li *et al.* 2005). Animal studies showed that: transgenic mice overexpressing a cytoplasmically truncated, dominant-negative form of the TβRII in cartilage, resulted in a joint disease similar to human osteoarthritis (Serra *et al.* 1997); Smad3 deficient mice showed premature chondrocyte maturation with increased length of the hypertrophic region, disorganization of the chondrocyte columns, early expression of collagen type X in the growth plate; and null mice gradually developed an end-stage OA phenotype (Li et al. 2005). These essential roles of TGFβ signalling in chondrocytes suggest the necessity of examining whether the miR-29 family is regulated by TGFβ signalling in human chondrocytes. Moreover, a number of published data show that TGFβ signalling negatively regulates miR-29 family expression in different human fibroses e.g. renal, lung, liver fibrosis. The impact of TGFβ signalling in human chondrocytes on the miR-29 family was thus checked.

To address the above question, expression of the miR-29 family with TGFβ1 treatment in human primary chondrocytes was compared both in monolayer and micromass culture. **In monolayer culture**: HACs were put in high glucose media containing 10% (v/v) FCS until the cells reached 90% confluence; medium was replaced with that containing 0.5% (v/v) FCS) prior to stimulating with 4ng/ml TGFβ or vehicle control (4mM HCl with 0.5% (w/v) BSA). **In micromass culture**: HACs were put in high glucose media containing 10% (v/v) FCS in monolayer following two sequential passages to increase cell number; the micromass ($2.5x10^7$cells/ml) was cultured in high glucose media with 10% (v/v) FCS for 24 hours before treating with 10ng/ml TGFβ or vehicle control (4mM HCl with 0.5% (w/v) BSA). Cells were harvested for qRT-PCR after 24 hours or 48 hours treatment in monolayer or micromass cultures, respectively. Quantitative RT-PCR primers for measuring the miR-29 family were described before. For the primary transcripts: two primer pairs specific for exon 1 and exon 3 were used; for the precursor transcripts: primers directly bind to the precursor sequence (Appendix, Table 5); the mature transcripts were measure by LNA-primers.

The qRT-PCR data show that expression of the miR-29 family was suppressed by TGFβ signalling (Figure 4.4). However, each culture system gave a different response. The pri-29b2/c transcript was significantly decreased after stimulating HACs for 24 hours with TGFβ1 in monolayer culture, whilst the pri-29a/b1 transcript was unchanged (Figure 4.4 a); the pri-29a/b1 transcript was significantly decreased in micromass culture after 48 hours with TGFβ1 whilst the pri-29b2/c transcript was unchanged or even increased (Figure 4.4 b). Notably, the levels of all mature forms of miR-29 were significantly decreased by TGFβ1 in both systems. These data suggest a hypothesis that the primary and the precursor miRNAs may be rapidly regulated and then processed into mature miRNAs. In order to test this hypothesis, SW1353 cells were treated with TGFβ1 (4ng/ml) in monolayer in a time course. Since the expression levels of the primary and pre miRNAs modulated by TGFβ1 in human primary chondrocyte were similar and ahead the mature miRNAs, it might be sufficient to measure only the pre-miRNA rather than both the primary and precursor sequences. Consistent with above data, qRT-PCR showed that TGFβ1 suppressed miR-29 family expression in SW1353 cells (Figure 4.5). Interestingly, significantly suppressive effects of TGFβ1 on precursor miRNAs were observed after 4 hours till the end of the time course (Figure 4.5.a) whilst significant change in the mature miRNAs was only seen after 12 hour treatment (Figure 4.5.b). This data, thus, confirms the hypothesis above. Together with TGFβ1, the effect of TGFβ3 on the miR-29 family expression also checked on SW1353 in monolayer across the time course. Quantitative RT-PCR data (Figure 4.5) showed that TGFβ3 also strongly supressed the expression of the miR-29s. However, the TGFβ3 significant decrease the precursor and the mature miRNAs were observed at 12 hour time point though at 4 hours a

The suppressive effect of TGFβ on expression of the miR-29 family was also investigated on the proximal promoter of the primary miR-29a/b1 gene. The promoter-reporter was transfected into SW1353 cells, cells were serum starved for 24 hours and treated with TGFβ1 (4ng/ml) for another 6 hours before performing the luciferase assay. In line with the expression data, TGFβ1 significantly suppressed the promoter activity of pri-miR-29a/b1 (Figure 4.6).

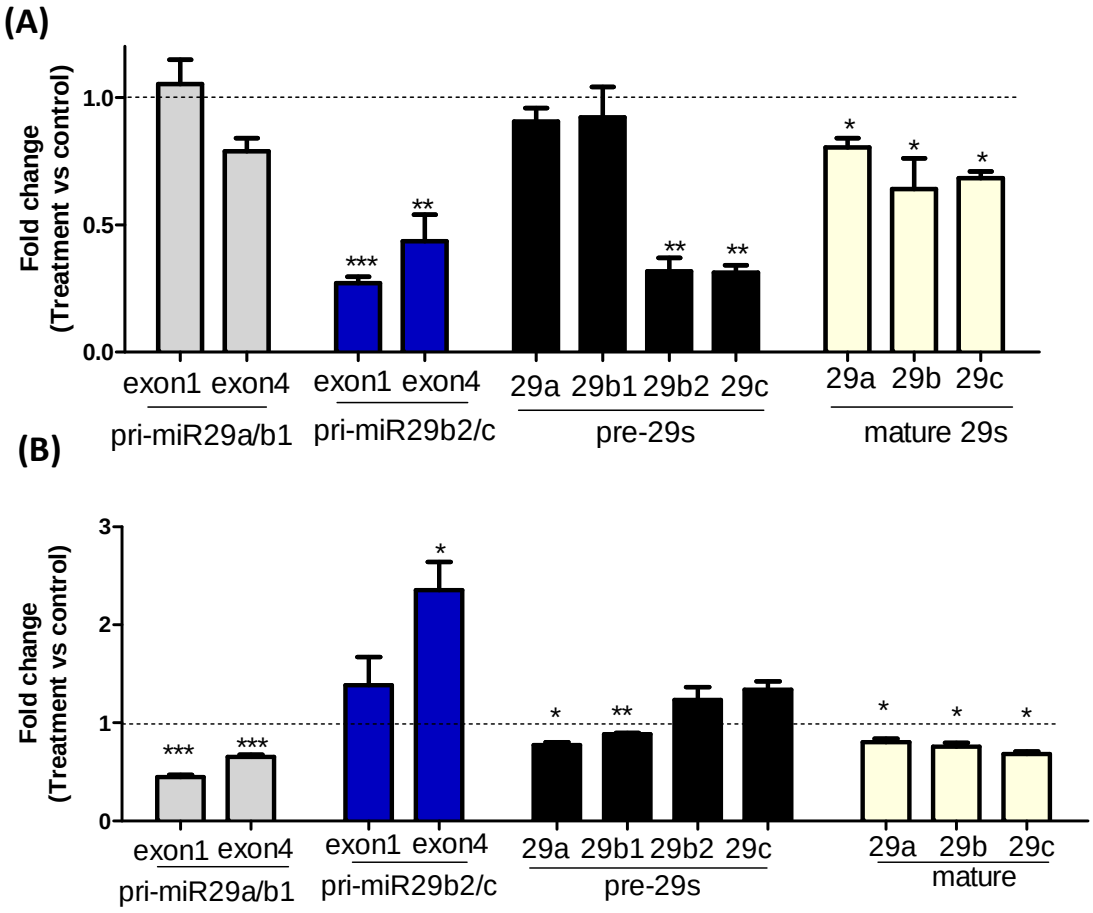

Figure 4.4 TGFβ1 suppresses expression of the miR-29 family in human primary chondrocyte

(A) TGFβ1suppresses expression of the miR-29 family in monolayer culture: Human primary chondrocytes were cultured in high glucose media with 10% (v/v) FCS in monolayer until 90% confluence. Cells were switched to high glucose media with 0.5% (v/v) FCS for 24 hours before treating with TGFβ1 (4ng/ml) or vehicle (4mM HCl+0.5% (w/v) BSA) for another 24 hours.

(B) TGFβ1suppresses expression of the miR-29 family in micromass culture: Human primary chondrocytes were cultured in high glucose media with 10% (v/v) FCS in monolayer. After 2 sequential passages, cells were put in micromass culture ($2.5x10^7$cells/ml) in high glucose media with 10% (v/v) FCS. After 24 hours in micromass, cells were stimulated for 48 hours with TGFβ (10ng/ml) or vehicle (4mM HCl+0.5% (w/v) BSA) in 10% (v/v) FCS media.

Relative expression of the primary miR-29a/b1, -29b2/c, precursor miR-29a, -29b1, -29b2, -29c, the mature miR-29a, b, c were measured by quantitative RT-PCR. 18S rRNA was the endogenous control for measuring primary and precursor transcripts; U6 was the endogenous control for measuring miR-29 mature transcripts. The horizontal line at 1 represents the mean of the vehicle control. Brown bar, pri-miR-29a/b1 transcripts; blue bar, pri-miR-29b2/c transcripts; black bar, precursor transcripts; yellow bar, mature transcripts. Means ± standard errors are presented. The difference between the treatment and the control was analysed by unpaired two-tailed t test. * $p<0.05$, ** $p < 0.01$, *** $p<0.001$, n=3.

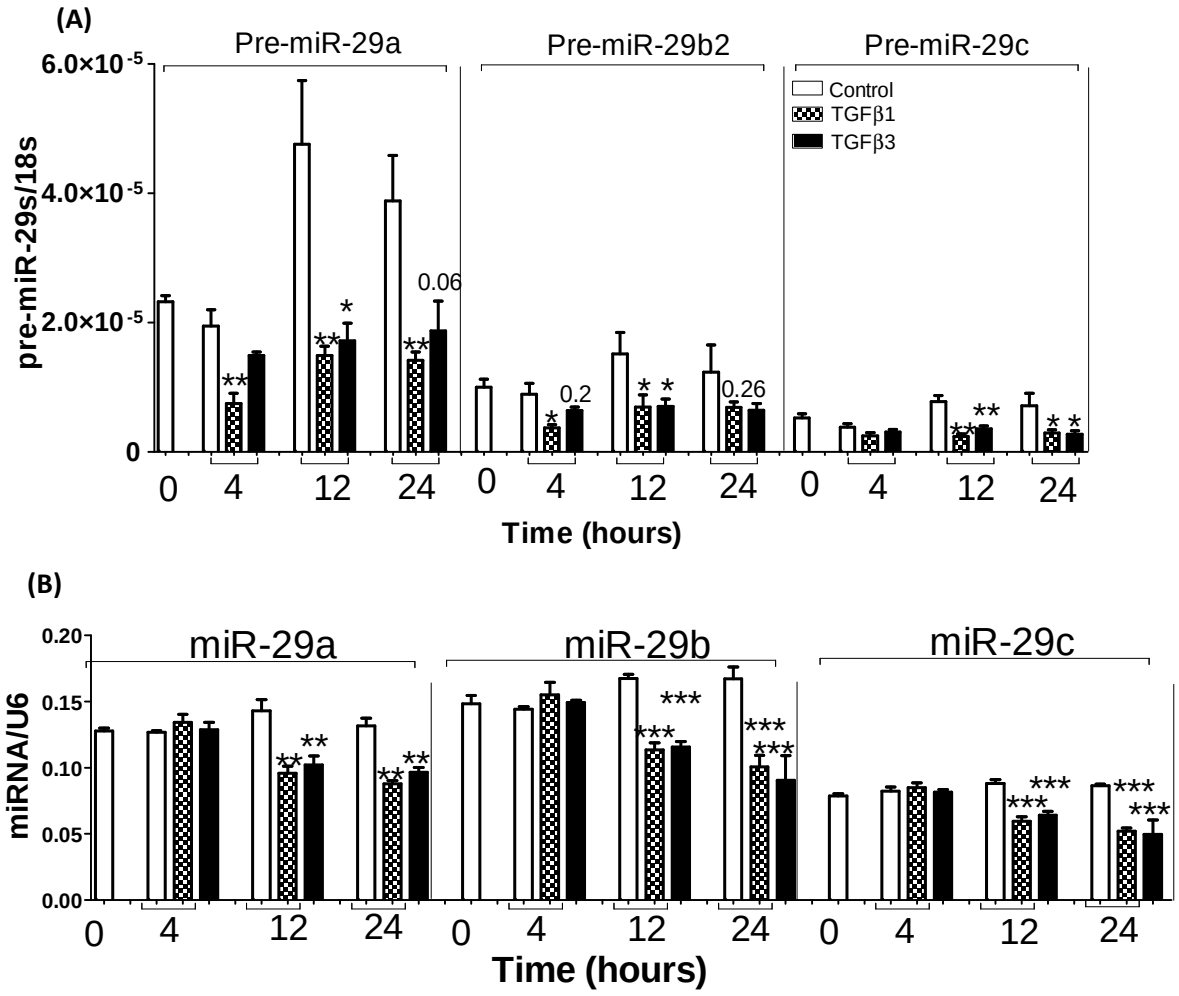

Figure 4.5 TGFβ1/3 suppresses expression of the miR-29 family in SW1353 cells

SW1353 cells were cultured in high glucose media with 10% (v/v) FCS in monolayer until 90% confluence. Cells were serum starved for 24 hours before treating with TGFβ1or TGFβ3 (4ng/ml) or vehicle (4mM HCl+0.5% (w/v) BSA) across 24 hour course.

Relative expression of the precursor miR-29a, -29b2, -29c, the mature miR-29a, b, c were measured by quantitative RT-PCR. 18S rRNA was the endogenous control for measuring the precursor transcripts; U6 was the endogenous control for measuring miR-29 mature transcripts. Open bar, control; brick bar, TGFβ1; close bar, TGFβ3. (A) Expression level of pre-miR-29a, 29b2, 29c. (B) Expression level of mature miR-29a, b, c. Means ± standard errors are presented. The difference between the treatment and the control was analysed by unpaired two-tailed t test. * $p<0.05$, ** $p < 0.01$, *** $p<0.001$, n=3.

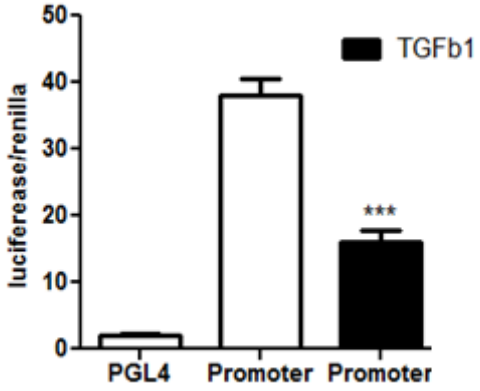

Figure 4.6: TGFβ1decreases expression from the primary miR-29a/b1 promoter

The pri-miR-29a/b1 promoter-reporter (100ng) or the empty vector pGL4 (control, 100ng) were transfected into SW1353 cells. After transfection, cells were serum starved for 24 hours, followed by stimulating for another 6 hours with TGFβ1 (4ng/ml), or vehicle (4mM HCl+0.5% BSA) before measuring luciferase activity. Renilla was use as endogenous control. Open bar: vehicle, black bar: TGFβ1. Means ± standard errors are presented. The difference of luciferase activity was analysed by unpaired two-tailed Student's t test. * $p<0.05$, ** $p < 0.01$, *** $p<0.001$, n=6.

4.2.3. Expression of the miR-29 family is not regulated by canonical Wnt signalling

As shown in the section above, the TGFβ signalling pathway, stimulated by TGFβ1 (or TGFβ3, data not shown), negatively regulated the expression of themiR-29 family. Signalling cross talk between TGFβ and Wnt signalling pathways has been previously reported, e.g. after TGFβ stimulation, Smad3 interacts with LEF1 to activate target gene transcription independently of β-catenin (Letamendia *et al.* 2001); TGFβ was shown to up-regulate the expression of many Wnt ligands e.g. Wnt2, 4, 5a, 7a, 10a, and Wnt co-receptors e.g. LRP5 (Zhou *et al.* 2004); TGFβ was found to increase nuclear accumulation and stability of β-catenin; interestingly, working synergistically with Wnt signalling pathways, TGFβ was reported to stimulate chondrocyte differentiation from mesenchymal cell (Zhou et al. 2004). Wnt signalling is also known to have a key role in cartilage homeostasis and osteoarthritis (Zhu et al. 2008, Zhu et al. 2009). Thus, it was pertinent to investigate the effect of Wnt signalling onexpression of the miR-29 family in chondrocytes, and then potential synergy with TGFβ signalling.

The effect of canonical Wnt signalling stimulated by Wnt3a (50 or 100ng/ml) on the miR-29 family was investigated in HACs cultured in monolayer or micromass after 24 hours or 48 hours, respectively; or in SW1353 cells in monolayer culture across a 24 hour time course. In addition, the effect of Wnt3a on the proximal pri-miR-29a/b1 promoter was also examined after 6 hour treatment with Wnt3a (50 or 100ng/ml). Quantitative RT-PCR data for all transcripts of miR-29 family and luciferase assay data for the miR-29a/b1 promoter showed canonical Wnt signalling did not regulate expression of the miR-29 family (Appendix, Figure 5). Wnt3a did regulate Axin2 expression in the same experiments, showing induction of the canonical Wnt pathway (Appendix, Figure 6).

4.2.4. IL-1 induces expression of the miR-29 family in part via the p38 signalling pathway.

IL-1 is a catabolic and anti-anabolic cytokines, it down regulates the expression of cartilage matrix components e.g. aggrecan and type II collagen and induces expression of matrix degrading enzymes e.g. MMP-3, MMP-13, ADAMTS4 (Koshy *et al.* 2002). *Il-1β*, or Il-1β-converting enzyme knockout mice showed the accelerated development of OA lesions in response to OA surgical induced in compared with wide type mice (Clements et al. 2003). It is considered to be a major cytokine driving the pathology of OA (Goldring *et al.* 2004). Thus, it was pertinent to examine whether IL-1 controls the expression of the miR-29 family in human chondrocytes.

The effect of IL-1 on the expression of the miR-29 family was first measured in IL-1-treated SW1353 for 48 hour time course in monolayer culture: SW1353 cells were cultured in high glucose media with 10% (v/v) FCS until reach confluence and followed by serum starved for 24 hours before treating with 5ng/ml IL-1 or vehicle (0.5% (w/v) BSA) for 48 hour time course. Relative expressions of the precursor and mature miRNA-29 transcripts were measured by qRT-PCR. Data (Figure 4.7) showed that IL-1 induced the expression of miR-29 family: the biggest induction on miR-29 precursors was observed at 4 hours; at later time point, the level of miR-29a precursors was decreased as compare with 4 hours (pre-29a) whilst other precursors did not change expression (Figure 4.7a); the induction of mature miR-29s were only observed significantly after 48 hours (Figure 4.7b). These data suggested that the increase in expression after IL-1 treatment of the miR-29 derivatives is time-dependent. The induction of IL-1 on the miR-29 family was again checked on the HACs in micromass culture: The micromass containing ($2.5x10^7$cells/ml) of passage 2 HAC was cultured in high glucose media with 10% (v/v) FCS for 48 hours before treating with 20ng/ml IL-1 or vehicle control (0.5% (w/v) BSA). Quantitative RT-PCR primers for measuring the miR-29 family were described before (Appendix, Table 5). Real-time RT-PCR data (Figure 4.8) showed that IL-1 strongly induced expression of the miR-29 family, with all processed transcripts significantly up-regulated by IL-1. The fold increase was highest for the pri-miR-29a/b1 locus in which the primary miR-29a/b1 and pre-miR29a and b1 were increased with 9 and 5 fold, respectively.

The molecular pathways induced by IL-1 can be the three classical MAPK-signalling pathways i.e. ERK, p38, JNK and through NFκB (Aigner *et al.* 2006, Fan *et al.* 2007). The

signalling pathway through which IL-1 regulated miR-29 family expression was investigated. SW1353 cells were stimulated with IL-1 together with an NFκB inhibitor (10μM) or a p38 inhibitor (SB203580) (10μM) or 6 hours in monolayer and the relative expression of the precursor miRNAs were again measured. The data showed that inhibition of the NFκB pathway further induced expression of the pre-miR-29a and b1 (Figure 4.9). Inhibition of p38 suppressed IL-1 induction of pre-miR-29a and b1, with a similar pattern for pre-miR-29b2 and c (Figure 4.10), suggesting that IL-1 induces expression of the miR-29 family at least in part through p38 MAPK signalling.

Furthermore, the effect of IL-1 on the promoter of pri-miR-29a/b1 was also examined by luciferase assay. The pri-miR-29a/b1 promoter-reporter was transfected into SW1353 cells for 24 hours before stimulation with IL-1 (5ng/ml) with or without the NFκB inhibitor (10nM) or p38 inhibitor (10μM) for another 6 hours. Luciferase data showed that the activity of the pri-miR-29a/b1 promoter was significantly decreased by IL-1 and that this effect was abolished by treatment with the NFκB inhibitor (Figure 4.11). However, the p38 inhibitor had no effect on the suppressive effect of IL-1 on the promoter of pri-miR-29a/b1 (data not shown).

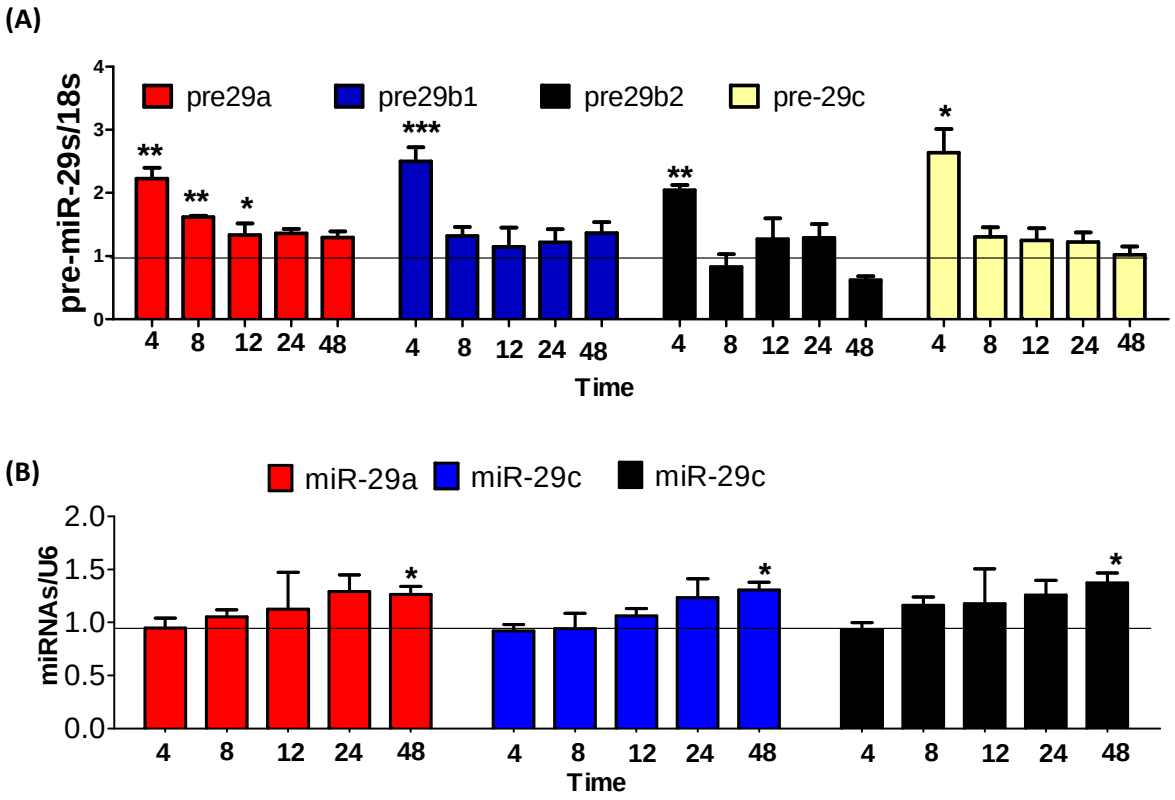

Figure 4.7: IL-1 induces expression of the miR-29 family in SW1353 in monolayer culture

SW1353 cells were cultured in high glucose media with 10% (v/v) FCS in monolayer until 90% confluence. Cells were serum starved for 24 hours before treating with IL-1 (5ng/ml) or vehicle (0.5% (w/v) BSA) across 48 hour course.
Relative expression of the precursor miR-29a, -b1, -b2, -c, the mature miR-29a, b, c were measured by quantitative RT-PCR. 18S rRNA was the endogenous control for measuring the precursor transcripts; U6 was the endogenous control for measuring miR-29 mature transcripts. The horizontal line at 1 serves as the vehicle control.
(A) Expression level of pre-miR-29a, 29b2, 29c. Red bar, pre-miR-29a; blue bar, pre-miR-29b1; black bar, pre-miR-29b2; yellow bar, pre-miR-29c
(B) Expression level of mature miR-29a, b, c. Red bar, miR-29a; blue bar, miR-29b; black bar, miR-29c
Means ± standard errors are presented. The difference between the treatment and the control was analysed by unpaired two-tailed t test. * $p<0.05$, ** $p < 0.01$, *** $p<0.001$, n=3.

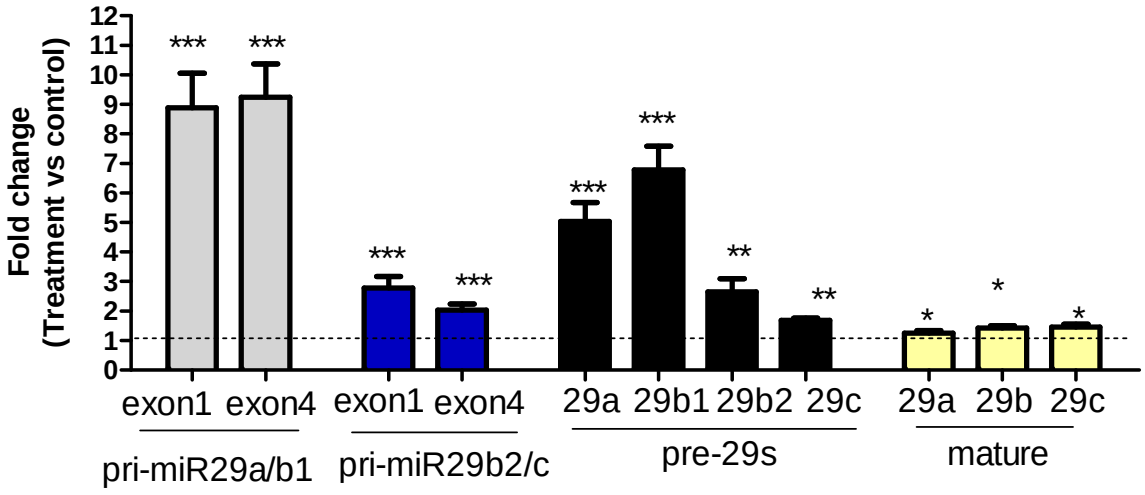

Figure 4.8: IL-1 induces expression of the miR-29 family in human primary chondrocyte in micromass culture

Human primary chondrocytes were cultured in high glucose media with 10% (v/v) FCS in monolayer. After 2 sequential passages, cells were put in micromass culture ($2.5x10^7$cells/ml) in high glucose media with 10% (v/v) FCS. After 24 hours in micromass, cells were stimulated for 48 hours with IL-1β (10ng/ml) or vehicle (0.5% (w/v) BSA).
Relative expression of the primary miR-29a/b1, -29b2/c, precursor miR-29a, -29b1, -29b2, -29c, the mature miR-29a,- 29b, -29c were measured by quantitative RT-PCR. 18S rRNA was the endogenous control for measuring primary and precursor transcripts; U6 was the endogenous control for measuring miR-29 mature transcripts. The horizontal line at 1 serves as the vehicle control. Brown bar, pri-miR-29a/b1 transcripts; blue bar, pri-miR-29b2/c transcripts; black bar, precursor transcripts; yellow bar, mature transcripts. Means ± standard errors are presented. The difference between the treatment and the control was analysed by unpaired two-tailed Student's t test. * $p<0.05$, ** $p < 0.01$, *** $p<0.001$, n=3.

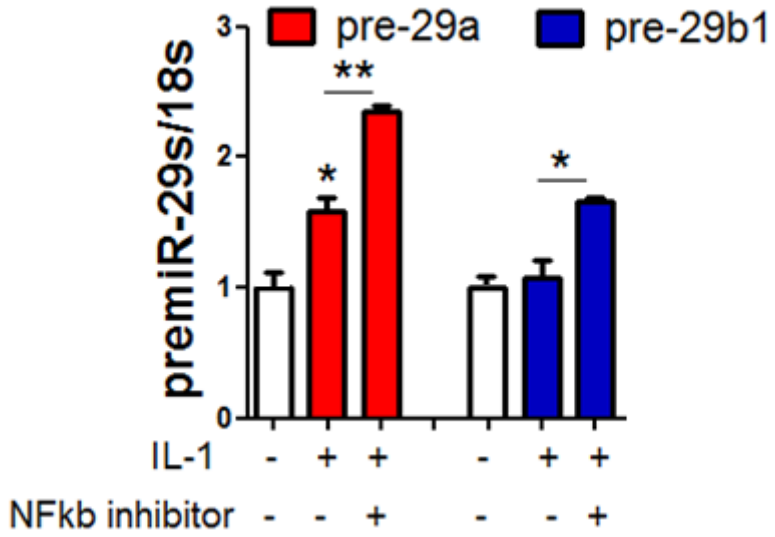

Figure 4.9 NFκB inhibition further increases the IL-1-induced expression of pre-miR-29a and pre-miR-29b1

SW1353 cells were plated in high glucose media with 10% (v/v) FCS in a 6 well-plate in monolayer and serum starved for 24 hours before treating with IL-1β (10ng/ml) in the presence or absence of NFκB inhibitor JSH-23 (10μM) for a further 8 hours. Cells were then harvested and the total RNA was isolated by Trizol. Relative expression of pre-miR-29a, -29b1 were measured by quantitative RT-PCR. 18S rRNA was the endogenous control. Red bar, pre-miR-29a; blue bar, pre-miR-29b1. Means ± standard errors are presented. The difference between the treatment and the control was analysed by unpaired two-tailed Student's t test * $p<0.05$, ** $p < 0.01$, *** $p<0.001$, n=6.

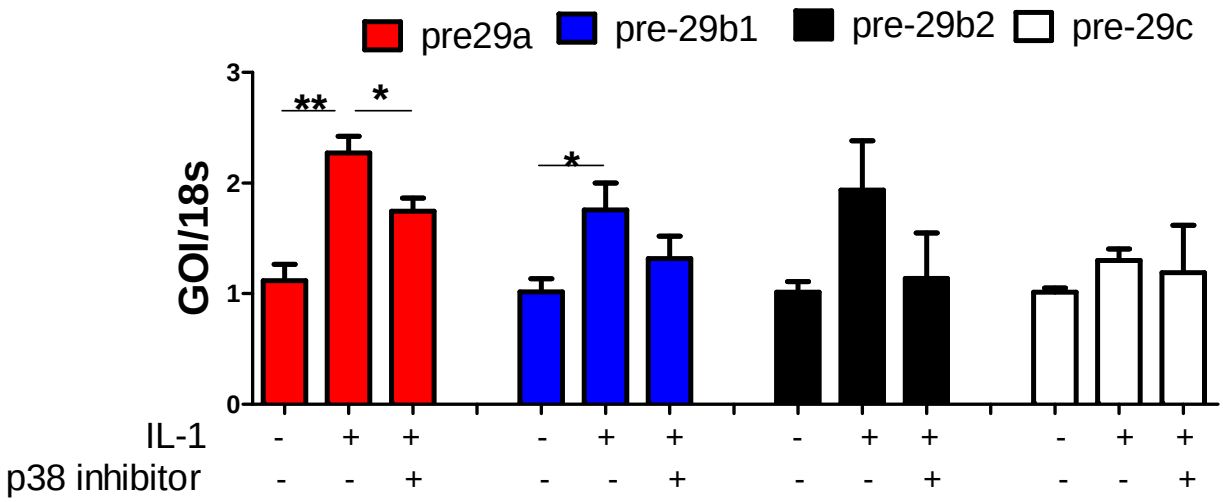

Figure 4.10 P38 inhibition suppresses the IL-1 induction of pre-miR-29s

SW1353 cells were plated in high glucose media with 10% (v/v) FCS in a 6 well-plate in monolayer and serum starved for 24 hours before treating with IL-1β (10ng/ml) in the presence or absence of p38 inhibitor SB203580 (10µM) for a further 8 hours. Cells were then harvested and the total RNA was isolated by Trizol. Relative expression of pre-miR-29a, -29b1, -29b2, -29c were measured by quantitative RT-PCR. 18S rRNA was the endogenous control. Red bar, pre-miR-29a; blue bar, pre-miR-29b1; black bar, pre-miR-29b2; white bar, pre-miR-29c. Means ± standard errors are presented. The difference between the treatment and the control was analysed by unpaired two-tailed Student's t test * $p<0.05$, ** $p < 0.01$, *** $p<0.001$, n=3.

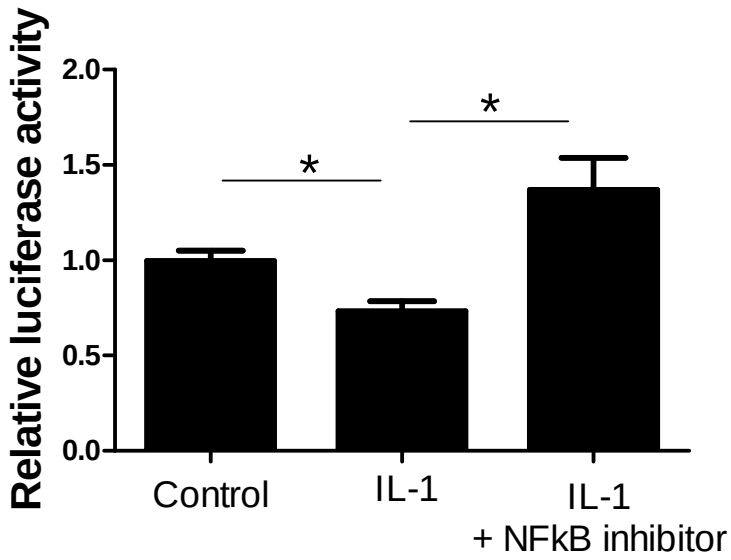

Figure 4.11: IL-1 suppresses the primary miR-29a/b1 promoter through NFκB

Pri-miR-29a/b1 promoter reporter (100ng) or pGL4 (control, 100ng) were transfected into SW1353 cells. After transfection, cells were serum starved for 24 hours, and followed by stimulating for another 6 hours with IL-1β (5ng/ml), IL-1β and NFκB inhibitor JSH-23 (10μM) or vehicle (0.5% (w/v) BSA) before measuring luciferase activity. Renilla was the endogenous control. Means ± standard errors are presented. The difference of luciferase activity was analysed by unpaired two-tailed Student's t test. * $p<0.05$, ** $p < 0.01$, *** $p<0.001$, n=6.

4.2.1. LPS suppressed the miR-29 family expression through NFκB signalling pathway

Toll-like receptors (TLRs) have important roles in activation of the innate and adaptive host defence against infections. TLR can bind to various damage-associated molecular patterns, which are endogenous danger signals or alarmins, leading to autoinflammatory conditions, and contributing to production of co-stimulatory signals necessary for adaptive immune reactions (Janeway *et al.* 2002). Lipopolysaccharide (endotoxin) (LPS) from bacteria is an example of a TLR-stimulating molecule. Chondrocytes are a potential source of several proinflammatory substances which may be TLR ligands: high-mobility group box 1, heat-shock proteins, and several components of the cartilage extracellular matrix (ECM) - e.g. low-molecular-weight hyaluronan, heparin sulphate, biglycan, and fibronectin fragments (Konttinen *et al.* 2012). From this point of view, OA could be considered as an autoinflammatory disease with the chondrocyte as its primary inflammatory cell (Konttinen et al. 2012). On this basis it was hypothesized that the activation of TLR-4, a receptor for LPS, may directly affect the biosynthetic activity of chondrocytes, including expression of the miR-29 family.

The level of miR-29 family expression was measured by qRT-PCR in HACs stimulated LPS (1µg/ml) in monolayer or micromass culture for a 24 hours or a 48 hour time course, respectively. Real-time PCR showed that the miR-29 family was significantly suppressed by LPS (Figure 4.12). Interesting, the levels of all processed miRNAs were strongly regulated by LPS in a time dependent manner: a significant decrease of the two miR-29 family clusters and their precursors were detected after 4 hours of treatment whilst decrease of the mature miRNAs was not detected until 24 hours. However, after 48 hours treating with LPS, all miR-29 family was tended to increase (Figure 4.12)

Again, the effect of LPS on the promoter of pri-miR-29a/b1 was also examined by luciferase assay. The pri-miR-29a/b1 promoter reporter was transfected into SW1353 cells for 24 hours before stimulation with LPS (1µg/ml) in the presence or absence of an NFκB inhibitor JSH-23 (10µM) for another 6 hours. Luciferase assay data showed that promoter activity of pri-miR-29a/b1 was significantly decreased by LPS and this effect was abolished with the NFκB inhibitor (Figure 4.13).

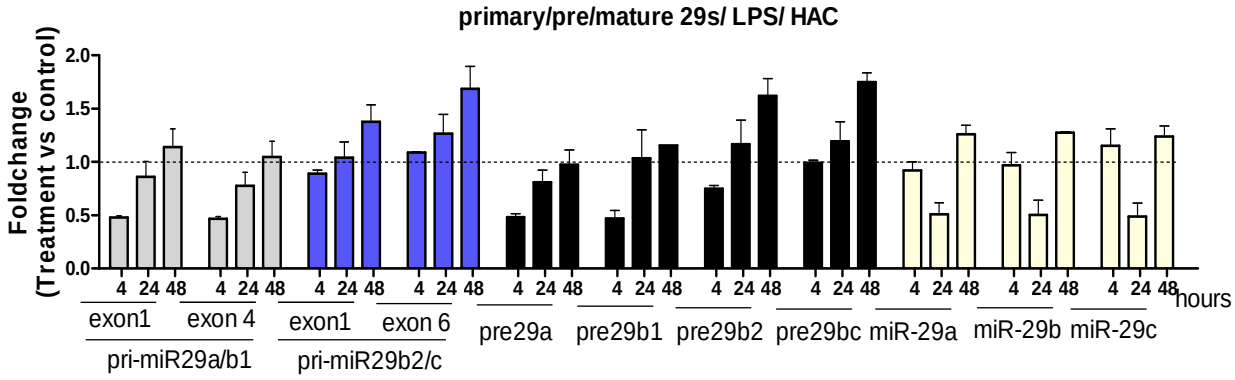

Figure 4.12: LPS suppresses expression of the miR-29 family

Human primary chondrocytes were cultured in high glucose media with 10% (v/v) FCS in monolayer. After 2 sequential passages, cells were put in micromass culture ($2.5x10^7$cells/ml) in high glucose media with 10% (v/v) FCS. After 24 hours in micromass, cells were stimulated for 4, 24, and 48 hours with LPS (1µg/ml) or vehicle (0.5% (w/v) BSA).
Relative expression of the primary miR-29a/b1, -29b2/c, precursor miR-29a, -29b1, -29b2, -29c, the mature miR-29a,- 29b, -29c was measured by quantitative RT-PCR. 18S rRNA was the endogenous control for measuring primary and precursor transcripts; U6 was the endogenous control for measuring miR-29 mature transcripts. The horizontal line at 1 serves as the vehicle control. Brown bar, pri-miR-29a/b1 transcripts; blue bar, pri-miR-29b2/c transcripts; black bar, pre-miR transcripts; yellow bar, mature miR transcripts. Means ± standard errors are presented. The difference between the treatment and the control was analysed by unpaired two-tailed Student's t test. * $p<0.05$, ** $p < 0.01$, *** $p<0.001$, n=3.

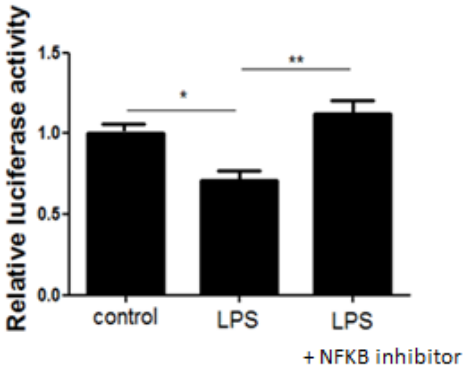

Figure 4.13: LPS suppresss the primary miR-29a/b1 promoter through NFκB

Pri-miR-29a/b1 promoter-reporter (100ng) or pGL4 (control, 100ng) was transfected into SW1353 cells. After transfection, cells were serum starved for 24 hours, followed by stimulatiion for another 6 hours with LPS (1µg/ml) in the absence or presence of an NFκB inhibitor JSH-23 (10µM) before measuring luciferase activity. Renilla was the endogenous control. Means ± standard errors are presented. The difference of luciferase activity was analysed by unpaired two-tailed Student's t test. * $p<0.05$, ** $p < 0.01$, *** $p<0.001$, n=6.

4.2.2. The microRNA-29 family targets Dicer giving a negative feedback loop for maturation of pre-miR-29

Previous data showed that expression of the miR-29 family was regulated by TGFβ, IL-1, LPS in which primary microRNA and precursor microRNA were modulated far ahead the mature microRNAs. In order to explain this, the 3'UTR regions of genes encoding for proteins involved in miRNA biogenesis were searched for putative binding site of the miR-29 family. Among these, of particular interest is the ribonuclease III enzyme Dicer, renowned for its central role in the biogenesis of microRNAs, converting the stem-loop pre-miRNA to mature miRNA (Bartel 2004). Bioinformatic analysis showed that there was a putative binding site of miR-29 in the *DICER* 3'UTR, suggesting the miR-29 family may regulate Dicer expression leading to the down-regulation of the Dicer level and as the consequence, the processing from precursors to mature miRNAs would potentially be slowed down. The 3'UTR region of *DICER* was therefore sub-cloned downstream of the firefly luciferase gene in the pmiR-GLO vector. The effect of the miR-29 family on the *DICER* 3'UTR was measured by luciferase assay after 24 hour co-transfection of the *DICER* 3'UTR- pmiR-GLO and the miR-29 family in SW1353 cells. Dual-luciferase reporter analysis showed the co-transfection of miR-29s significantly inhibited the wild type construct, whereas when the target site was mutated, the construct was not inhibited (Figure 4.14). This indicates that miR-29 may suppress expression of Dicer. The effect of the miR-29 family in *DICER* expression at transcriptional level was also investigated. Human primary chondrocyte was transfected with either miR-29b mimic (50nM) or non – targeting control (50nM). The transfected cells were then put in either monolayer or micromass culture for a further 48 hours. The expression of *DICER* was measured by qRT-PCR. Real-time qRT-PCR data showed that the expression of Dicer was not affected by miR-29s (data not shown), suggesting that the miR-29s does not control Dicer expression at mRNA level.

There is a growing body of work demonstrating that microRNAs can be processed independently of Dicer via Argonaute2 (Dueck *et al.* 2010). To evaluate whether or not miR-29s required Dicer to mature, the level of pre-miR-29s and mature miR-29s were measured in DLD, a Dicer-knockdown cell line. Data (Figure 4.15) showed that the levels of mature miR-29s were strongly reduced whilst the level of pre-miR-29s was not affected (Figure 4.15), demonstrating miR-29 processing is Dicer-dependent.

Taken together, these data show that the miR-29 family targets Dicer giving a negative feedback loop for its maturation.

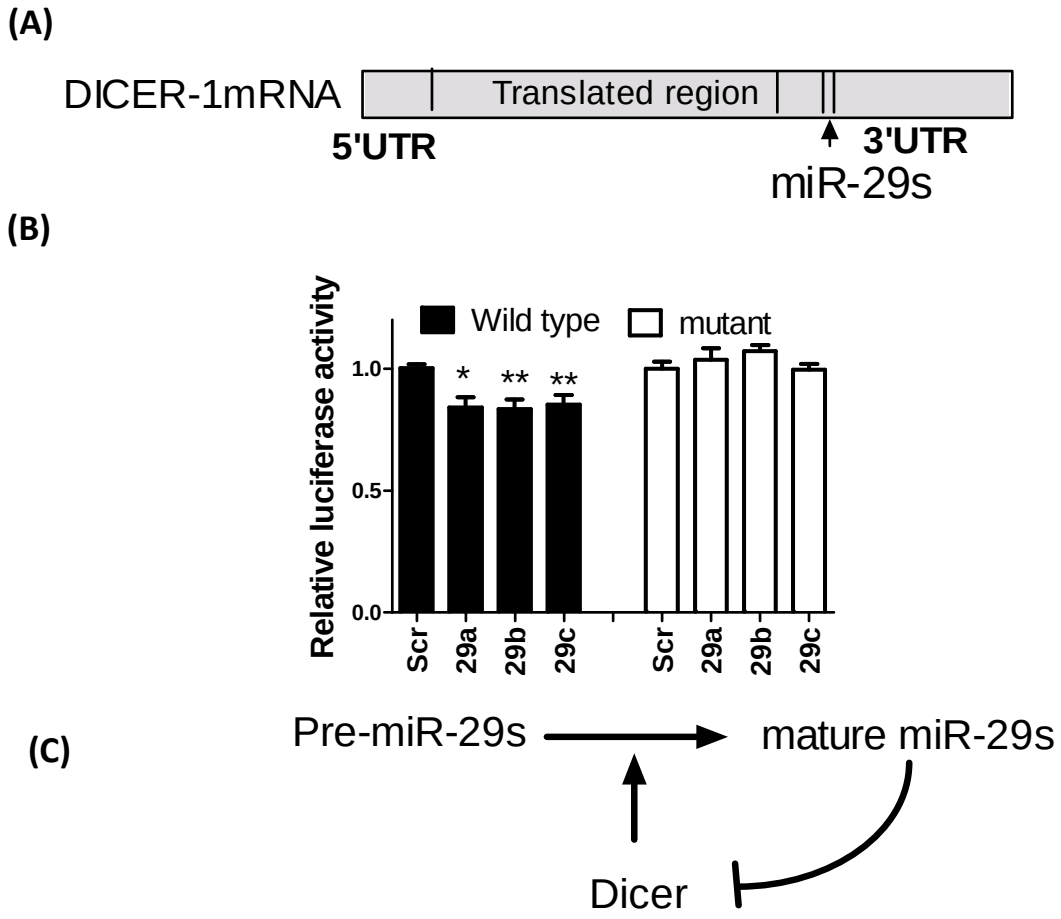

Figure 4.14: The miR-29 family targets Dicer

(A) Bioinformatic analysis reveals one binding site of the miR-29 family in the 3'UTR of Dicer. (B) miR-29 family targets Dicer: The Dicer 3'UTR containing the binding site of the miR-29 family (wild type) or a mutated, non-functional binding site for miR-29 family (mutant) were sub-cloned into the pmiR-GLO vector and were co-transfected with either miR-29a, -29b, -29c mimic (50nM) or non-targeting control (50nM) into SW1353 cells for 24 hours and luciferase activity was measured. Renilla was the endogenous control. (C) miR-29 targets Dicer giving a negative feedback loop for its maturation. Means ± standard errors are presented. The difference of luciferase activity was analysed by unpaired two-tailed Student's t test. * $p<0.05$, ** $p < 0.01$, *** $p<0.001$, n=6.

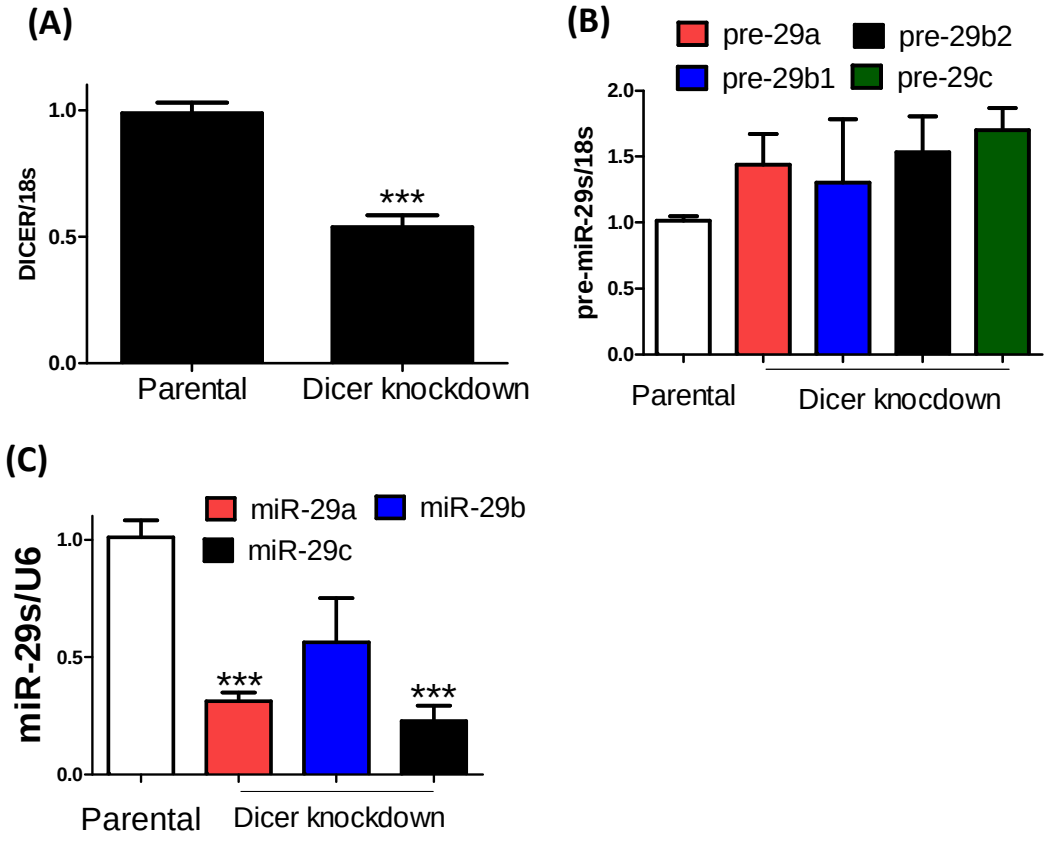

Figure 4.15: Dicer is required for the miR-29 family maturation

2

Level of Dicer, precursor and mature miR-29 were measured in DLD, Dicer knockdown cell line or parental control by quantitative RT-PCR. (A) Relative expression of Dicer; (B) Relative expression of precursor miR-29s (normalised to expression in parental control). 18S rRNA is endogenous control. Red, pre-29a; blue, pre-29b1; black, pre-29b2; green, pre-29c; white, levels of all precursors in control (set at 1); (C) Relative expression of mature miR-29 family (normalised to expression in parental control). U6 is endogenous control. Red, miR-29a; blue, miR-29b; black, miR-29c; white, levels of all mature miR-29 in control (set at 1). Means ± standard errors are presented. The difference of relative expression was analysed by unpaired two-tailed Student's t test. * $p<0.05$, ** $p < 0.01$, *** $p<0.001$, n=3.

4.3. Discussion

Since miRNAs have broad effects on cartilage homeostasis, and OA, it is particularly interesting to work out how miRNAs themselves are being regulated. Such data could provide crucial information for further understanding the mechanism underlying OA and for being able to manipulate these miRNAs in chondrocytes therapeutically. Generally, the expression of miRNAs can be regulated transcriptionally, epigenetically, or controlled by different stimuli e.g. cytokines and growth factors. In this study, just transcription factors, cytokines, and growth factors controlling the miR-29 family expression in chondrocytes were for the first time investigated. These studies were able to show that, in human chondrocytes, the master transcriptional regulator SOX9, TGFβ and LPS suppressed whilst IL-1 strongly induced the miRNA-29 family expression.

Several published data report the suppressive effect of SOX9 on the expression of individual members of the miR-29 family in other cellular contexts: in murine stem cells, overexpression of SOX9 or knockdown SOX9 in cell lines e.g. C3H10T1/2 or ATDC5 leads to suppression or induction of miR-29a and miR-29b expression (Yan et al. 2011), respectively; in human C-20/A4 chondrocytes, overexpression of SOX9 strongly down-regulated the level of miR-29a (Guerit et al. 2014). Herein, for the first time, suppressive effect of SOX9 on the expression of all members of the miR-29 family in primary human chondrocytes was shown. The effect was exerted, at least in part, through directly targeting the promoter of the miR-29a/b1 locus. In line with these data, Guerit et al (2014) reported that SOX9 can physically bind to at least 3 out of 4 putative binding sites within the proximal promoter of miR-29a/b1 cluster; also, another transcription factor YY1, was shown not to bind directly to the miR-29a/b1 promoter, but, physically interacted with SOX9 to suppress miR-29a/b1 expression (Guerit et al. 2014). The mechanism by which SOX9 negatively regulates the pri-miR-29b2/c cluster is still unknown. Several putative binding sites of SOX9 are found in the promoter of the pri-miR-29b2/c cluster, implicating a possible direct mechanism. However, this needs further investigation.

Alongside SOX9, other transcriptional regulatory mechanisms responsible for expression of the miR-29 family have also been reported: the pri-miR-29a/b1 locus was stimulated by the transcription factors CEBPA (Eyholzer et al, 2010), GATA3 (Chou et al. 2013), STAT1 (Schmitt et al, 2012) but suppressed by c-MYC (Mott et al. 2010, Parpart et al. 2014), NFκB

(Liu et al. 2010, Mott et al. 2010), Sp1(Liu et al. 2010, Amodio et al. 2012), HDAC1, HDAC3, and Gli (Mott et al. 2010); the pri-miR-29b2/c locus was inhibited by Smad3 (Qin et al. 2011), NFκB, YY1, Ezh2, H3K37, HDAC1 (Wang et al. 2008). Thus, it is likely that the transcriptional regulation of the miR-29a/b1 cluster is controlled by a combination of different transcription factors. Interestingly, in the chondrocyte context, miR-1247 together with miR-145 were reported to directly target and repress expression of SOX9 (Yang et al. 2011, Martinez-Sanchez and Murphy 2013), suggesting these miRNAs could contribute to the induction of the miR-29 family level in chondrocytes. Additionally, throughout the current project, the miR-29 family members exhibit different expression levels between the primary miR-29a/b1 and primary miR-29b2/c loci in different cellular contexts. This discrepancy could be explained in part by different transcription factor binding to each promoter.

Together with SOX9, TGFβ signalling was found to suppress the expression of all miR-29 family members in chondrocytes. Since TGFβ signalling induces SOX9 expression (Greco et al. 2011), the suppressive effect of TGFβ on the miR-29 family could be exerted through SOX9 and this TGFβ-SOX9 signalling could in part explain the down-regulation of the miR-29 family by TGFβ. The suppressive effect of TGFβ on the miR-29 family expression has also been observed in various cell types associated with fibrosis e.g. human aortic adventitial fibroblasts (Maegdefessel et al. 2012), renal fibrosis cells (Wang et al. 2012, Ramdas et al. 2013), murine hepatic stellate cells (Roderburg et al. 2011), rat hepatic stellate cells (Kwiecinski et al. 2011), human skin fibroblasts (Maurer et al. 2010), human tenon's fibroblast (Li et al. 2012), human lung fibroblast cell line (Cushing et al. 2011, Yang et al. 2013) in which either some members or the whole miR-29 family significantly decreased expression with TGFβ treatment. Apart from TGFβ-SOX9 signalling, the mechanism for the inhibition of TGFβ on the miR-29 family expression is currently unknown. There is some evidence that TGFβ inhibits miR-29 expression through SMAD3 signalling e.g. the inhibition effect of TGFβ on miR-29 expression was abolished when *Smad3* was knocked out in mouse embryonic fibroblast (Qin et al. 2011); SMAD3 could directly interact with at least two conserved SMAD3-binding sites in the promoter region of miR-29b2/c locus (Qin et al. 2011); activated TGFβ signalling induced SMAD3 translocate into nucleus and bind to miR-29b2/c promoter, resulting in the dissociation of MyoD and the stabilization of YY1 whose expression negatively regulated the miR-29b2/c expression through a conserved binding site

(Qin et al. 2011). However, this needs to be validated in chondrocytes. Besides the suppressive role, TGFβ also exerted an inductive effect on miR-29 expression at late time points. For instance, the primary miR-29b2/c locus was induced in human primary chondrocyte in micromass cultured with TGFβ1 for 48 hours (Figure 4.4b) though this increase did not reach significantly; the miR-29 family expression was increased at a late stage in the human chondrogenesis model with TGFβ3 as the major driver among others (Figure 3.12). That TGFβ induces miR-29 family expression suggests that there are may be several TGFβ-triggered signalling pathways, apart from TGFβ-SOX9, regulating the miRNA-29 expression. However, in this project, the molecular mechanisms by which TGFβ controls expression of the miR-29s are again not fully understood.

The TLR4 ligand, LPS, was found to repress the miR-29 family expression in chondrocytes. Importantly, this inhibition was facilitated by NFκB (p50/p65). Supporting the finding of this study, published data in cholangiocarcinoma cells and murine hepatic stellate cells also showed that LPS down-regulated expression of the miR-29 family (Mott et al. 2010, Roderburg et al. 2011) . Moreover, NFκB, activated by TLR ligands, was revealed to both directly or indirectly (cooperating with YY1) suppress the miR-29a/b1 or the miR-29b2/c locus, respectively (Wang et al. 2008, Mott et al. 2010). In contrast to LPS, it was surprising to find that IL-1β increased miR-29 expression and this stimulation was not NFκB but p38-dependent. However, the effect of inhibiting p38 signalling was only observed for miR-29a and miR-29b but not miR-29c, although all miR-29 family members were found strongly induced by IL-1β. Since IL-1β could activate the NFκB signalling pathway alongside p38 MAPK signalling (Aigner et al. 2006), the fact that an NFκB inhibitor further increased the IL-1 induction of the miR-29a/b1 locus implicates NFκB signalling in suppressing miR-29. It is likely that in human chondrocyte, for the period of time examined (48 hours), induction through 38 MAPK signalling was dominant over the NFκB, explaining why IL-1β induced (not suppressed) miR-29 expression. It therefore, made sense to expect a similar induction of the proximal promoter of miR-29a/b1 by IL-1β. However, a suppressive effect was observed. These data could be explained if the inductive p38-dependent transcription factors do not work through this 2kb proximal promoter of the miR-29a/b1, whilst several binding sites of NFκB in this promoter region are seen. This hypothesis needs experimental data to validate it. The mechanism responsible for the IL-1β induced miR-29b2/c cluster is still unclear and needed to be further explored. Notably, the IL-1β mRNA expression level was increased by

LPS/ TLR-4 and this is mediated by p38 MAP kinase in human chondrocytes (Bobacz *et al.* 2007). Therefore, that the miR-29 family expression was increased after 48 hours treatment with LPS could be explained in part by the accumulation of IL-1β which in turn up-regulated the miR-29 family expression.

This study also showed that the expression of all miR-29 members was not modulated by Wnt3a (β-catenin, canonical Wnt signalling), neither at the mRNA level by qRT-PCR or in the promoter assay. There are, several publications which have reported that either some members or the whole miR-29 family were Wnt3a-induced: In osteoblasts, Wnt3a positively modulates the expression of miR-29a and miR-29c though two T-cell factor/LEF-binding sites within the miR-29a/b1 promoter (Kapinas et al. 2009, Kapinas et al. 2010); in muscle progenitor cells (MPCs), Wnt3a treatment increased miR-29s expression in a time dependent manner (Hu et al. 2014); the promoter activities of both the miR-29a/b1 and miR-29b2/c cluster were strongly induced in MPCs where Wnt3a was overexpressed or added to media (Hu et al. 2014).Therefore, an interesting question that remains to be answered is why miR-29 expression is not modulated by Wnt3a in chondrocytes.

In contrast to the rapid change in expression of the pri-miR-29 or pre-miR-29 in response to stimuli, the modulation of the miR-29 family mature is quite slow. The posttranscriptional processing from the precursor to the mature form of the miR-29 family may be tightly controlled. Since the miR-29s has significant impact on a functional phenotype by regulating multiple genes that fall into the same or related pathways (which will be discussed more in Chapter 5), its expression must be regulated, potentially at more than one level. Interestingly, herein, Dicer was found to be the direct target of the miR29 family, suggesting a negative feedback loop for its maturation. In supporting this data, in T47D breast cancer cells, Dicer 1 was also reported as a miR-29a target (Cochrane *et al.* 2010). Apart from Dicer, other components of the microRNA precursor processing machinery e.g. Helicase, Exportin 4 and 5 are also predicted to be putative targets of the miR-29s as they have several binding sites in their 3'UTR regions (data not shown). Even though these have not been experimentally validated as the direct targets, this further supports the idea that miR-29 is involved in a negative feedback loop for its maturation.

In conclusion, the miR-29 family was found to be negatively regulated by the master regulator of chondrogensis SOX9, by TGFβ signalling and by LPS-NFκB signalling. It is

positively regulated by IL-1-p38 MAPK signalling. Interestingly, the canonical Wnt signalling pathway does not control expression of the miR-29 family. Furthermore, expression of the miR-29 family was tightly controlled at the level of posttranscriptional processing in which miR-29 directly targets Dicer, giving a negative feedback loop for its maturation.

CHAPTER 5
FUNCTIONS OF THE MICRORNA 29 FAMILY IN CHONDROCYTES

5.1 Introduction

The ability of a single miRNA to target multiple mRNAs especially those that function in the same intracellular pathways and/or diseases, adds an additional layer of regulation to gene expression. The aberrant expression of the miR-29 family has been found in multiple malignancies and fibroses, carcinogenesis. Also, an understanding of how miR-29 contributes to these processes has been revealed: miR-29 targets genes are involved in cellular proliferation, cell cycle, cell differentiation, and apoptosis at genetic and epigenetic levels. The following summarizes some functions of miR-29s in human disease.

In chondrogenesis or OA, around 30 miRNAs have been shown to have functions in cartilage homeostasis (Le et al, 2013), which is relatively small compared to the total number of miRNAs. Moreover, as mentioned in the previous chapter, for any potential miRNA therapeutic application, a combination of different miRNAs might be required for a complex disease like OA. Identifying novel miRNA targets and the cell signalling pathways and networks by which miRNAs exert their functions on disease phenotype are therefore, of particular importance both to have an insight into OA pathogenesis and also to ensure the specificity in any miRNA-based drug delivery method. Thus, this chapter places emphasis on identifying the function of the miR-29 family in chondrocytes including identifying the function of the miR-29 family in TGFβ/Smad, NFκB, and Wnt/β-catenin signalling pathways and novel targets of the miR-29s.

Aims:

- Investigate signalling pathways involved in chondrogenesis and osteoarthritis which are regulated by the miR-29 family
- Perform gain-and-loss of function of miR-29b experiments to identify potential targets of the miR-29 family
- Identify and validate novel direct targets of the miR-29 family

5.2 Results

5.2.1 The miR-29 family supress TGFβ/Smad signalling pathway

In articular cartilage, the canonical TGFβ/Smad signalling pathway has been shown to play a pivotal role in the maintenance of normal cartilage: it up-regulates the expression of several types of collagens and proteoglycan; and it down-regulates cartilage degrading enzymes. Importantly, disruption of the TGFβ pathway has been shown to lead to OA. Mice expressing a dominant negative TGFβRII exhibit articular cartilage degeneration similar to that observed in human OA with abnormal expression of type X collagen, an indicator of chondrocyte hypertrophy; mutant mice with targeted disruption of Smad3 (Smad3−/−) show a similar pathology in chondrocytes, including aberrant type X collagen expression in vivo; primary chondrocytes isolated from Smad3−/− mice demonstrate an accelerated differentiation process with up-regulated BMP signalling.

In Chapter 4, expression of the miR-29 family was found to be suppressed by TGFβ signalling. Here, I measure the impact of the miR-29 family on Smad signalling. The TGFβ/Smad signalling reporter (CAGA)12-luc (Figure 5.1a) containing 12 binding sites of the Smad2/3/4 (GAGAC) binding site upstream of the firefly luciferase-encoding gene was used. The principle of this experiment is based on the fact that: signals are transduced from TGFβ ligands to the Smad2/3/4 complex which subsequently regulates gene expression; the miR-29 family may change the expression or transcriptional activity of Smad2/3/4; thus altering luciferase levels. $(CAGA)_{12}$-luc (100ng) and Renilla (10ng) were co-transfected with either miR-29 mimic (50nM) or non-targeting control (50nM) into SW1353 cells for 24 hours and followed by serum starvation for another 24 hours. Cells were then treated with either TGFβ1 or TGFβ3 (4ng/ml) for another 6 hours before measuring the luciferase activity. Luciferase assay data (Figure 5.1b) showed that: stimulating cells with TGFβ1 strongly induced luciferase activity as compared with non-treatment control; pre-treatment with all members of the miR-29 family significantly decreased the luciferase activity at this 6 hour time point. A similar pattern was observed when treating cells with TGFβ3 (Appendix, Figure 7a). These data demonstrate that Smad signalling was successfully activated in SW1353 cells by TGFβ1or TGFβ3 and that the miR-29 family is a negative regulator of this signalling. As all miR-29 family members supressed the signalling, an experiment using only an inhibitor of miR-29b (50nM) was performed. Consistent with the mimic data above,

luciferase activity was significantly increased with the miR-29b inhibitor compared to control (Figure 5.1c and Appendix, Figure 7b).

The suppressive effect of the miR-29 family on the TGFβ signalling pathway was further confirmed by measuring the effect of the miR-29 family on a TGFβ responsive gene. ADAMTS4 was chosen since it is induced by TGFβ in chondrocytes, but was not a putative direct target of the miR-29 family. Human primary chondrocytes were transfected with miR-29 family mimics (50nM) in monolayer for 24 hours with 10% (v/v) FCS. The media was then replaced with media with 0.5% (v/v) FCS for another 24 hours before stimulating with TGFβ (4ng/ml) for a further 6 hours. The expression of ADAMTS4 was measured by qRT-PCR (Figure 5.2) showing that ADAMTS4 was strongly induced by TGFβ; the miR-29 mimics significantly decreased the expression of ADAMTS4 as compared with non-targeting control. These data again confirmed the suppressive effect of the miR-29 family on TGFβ signalling pathway.

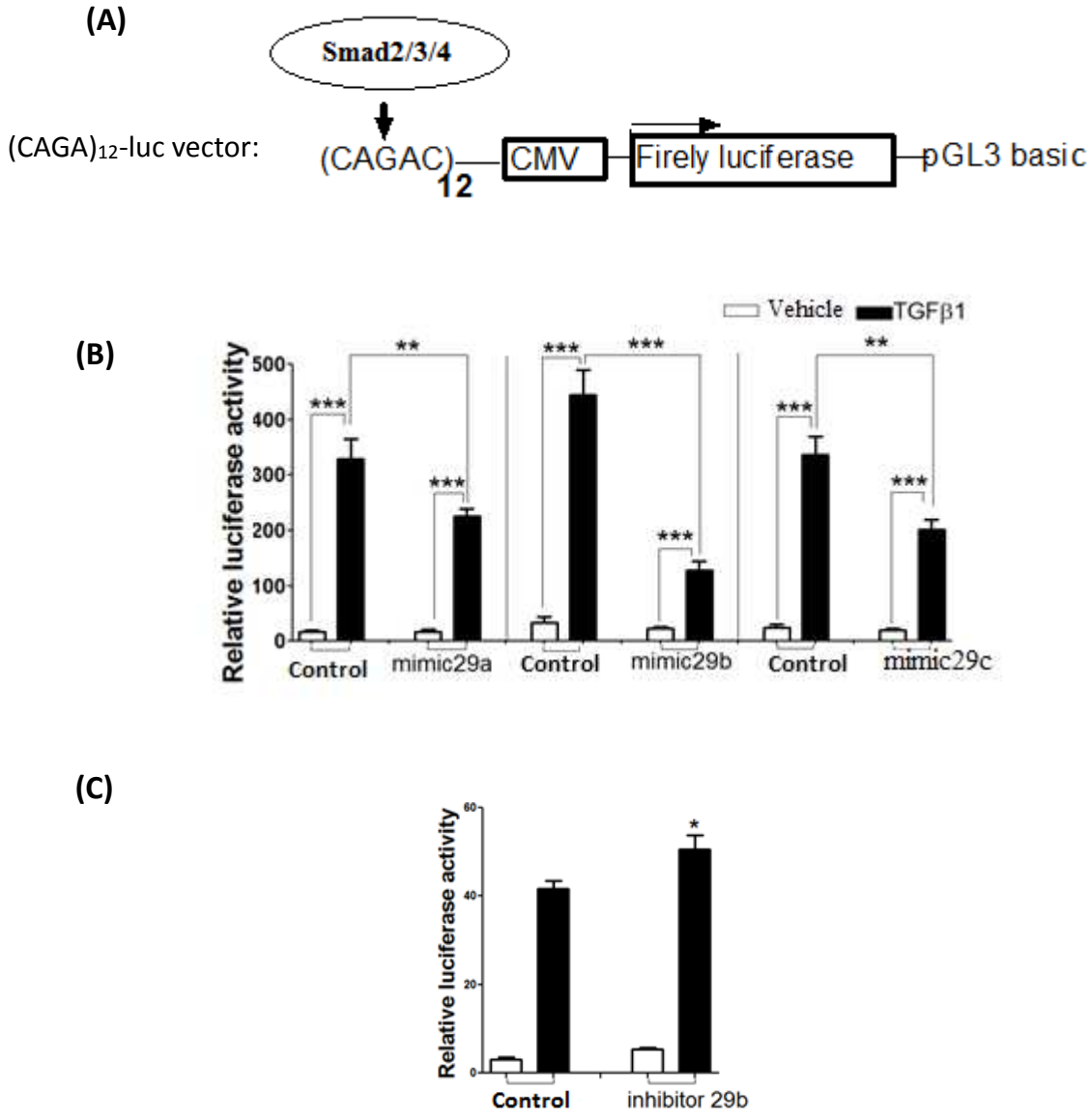

Figure 5.1 The miR-29 family suppress TGFβ signalling pathway

(A) The TGFβ signalling reporter ($CAGA_{12}$-luc) contains 12 binding sites of the Smad2/3/4 (GAGAC) binding consensus upstream of the firely luciferase-encoding gene in pGL3100ng $CAGA_{12}$-luc vector, and 10ng Renilla vector were co-transfected with either miR-29 family mimic (B) or miR-29b inhibitor (C) into SW1353 cells in monolayer. The non-targeting control (50nM) was also used as the negative control. 24 hours after transfection, cells were serum starved for another 24 hours, followed by treatment with TGFβ (4ng/ml) for another 6 hours before measuring luciferase activity. Renilla is the loading control for luciferase assay. Open bar: non – treatment control, close bar: TGFβ treatment. Means ± standard errors are presented, n=6. The difference of luciferase activity was analysed by Student's unpaired two-tailed t test. * $p<0.05$, ** $p < 0.01$, *** $p<0.001$

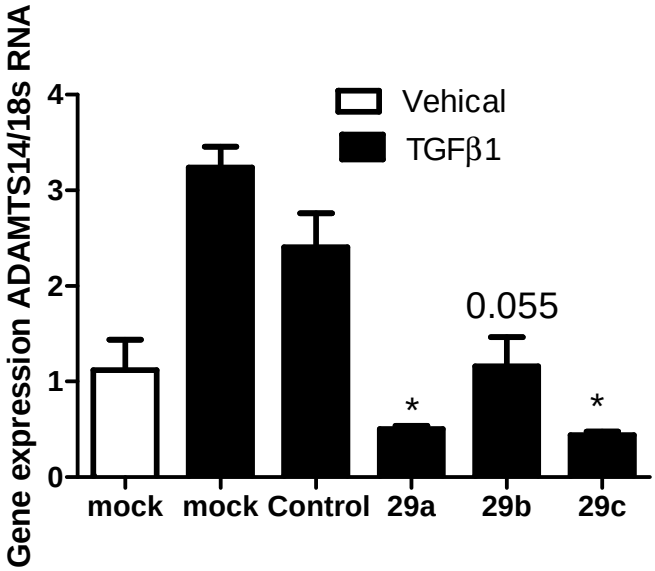

Figure 5.2 The miR-29 family suppresses the TGFβ induced gene ADAMTS4

Human primary chondrocytes were transfected with either miR-29 family mimics (50nM) or non – targeting control (50nM) for 24 hours. Cells were then changed into 0.5% (v/v) FCS for 24 hours and followed by stimulating with TGFβ1 (4ng/ml) for another 6 hours. Total RNA was isolated and the expression level of ADAMTS4 was measured by qRT-PCR. 18S rRNA was used as the endogenous control. Data were normalized to untreated, mock transfected cells. Open bar: non – treatment control, close bars: TGFβ treatment. Means ± standard errors are presented, n=3. The difference in expression level of ADAMTS was analysed by Student's unpaired two-tailed t test. * $p<0.05$, ** $p < 0.01$, *** $p<0.00$

5.2.2 The miR-29 family suppresses the NFκB signalling pathway

In Chapter 4, IL-1β was found to increase expression of the miR-29 family. It is, therefore, of importance to investigate how the miR-29 family regulates the signalling pathways triggered by IL-1β. There are at least three pathways triggered by IL-1β including NFκB, JNK, and p38 MAPK pathways. Nevertheless, in this project, just the interaction between the miR-29 family and NFκB signalling was investigated. The transcription factor NFκB is held in the cytoplasm in an inactive form associated with the inhibtory κB (IκB) protein. In response to IL-1β binding of the receptor, NFκB releases from IκB and the activated NFκB will then translocate to the nuclear, bind to DNA elements present in its target genes and facilitate their transcription.

Similar to the experiment for investigating the interacting between the miR-29 family and TGFβ signalling, the NFκB signalling reporter containing multiple binding sites for NFκB upstream of a luciferase-encoding gene was utilized (Figure 5.3a). The signal cascade from IL-1β will activate NFκB which consequently induces the transcription of the luciferase gene in the reporter and this may be modulated by the miR-29 family. The luciferase assay was set up similar to the experiment in 5.1.1 except the cells were treated with IL-1β (5ng/ml) instead of TGFβ1 (4ng/ml). Luciferase data (Figure 5.3b, c) showed that IL-1β strongly induced the luciferase activity of the κB reporter; all miR-29 family mimics significantly decreased activity (B) but the miR-29b inhibitor induced activity (C). These data show that NFκB signalling was successfully triggered in SW1353 cells by IL-1and that the miR-29 family is a negative regulator of the NFκB signalling pathway.

The suppressive effect of the miR-29 family on the NFκB signalling pathway was further confirmed by measuring the effect of the miR-29 family on an NFκB responsive gene. MMP3, which is induced expression by IL-1 and is not a putative direct target of the miR-29 family, was chosen. Again, the experiment was set up similar to the experiment in 5.1.1 except cells were stimulated with IL-1 (5ng/ml). The Taqman qRT-PCR (Figure 5.4) showed that MMP3 was strongly induced expression by IL-1β; the miR-29b and miR-29c mimics significantly decreased the expression of MMP3 as compared with non-targeting control, though the miR-29a mimic had no effect.

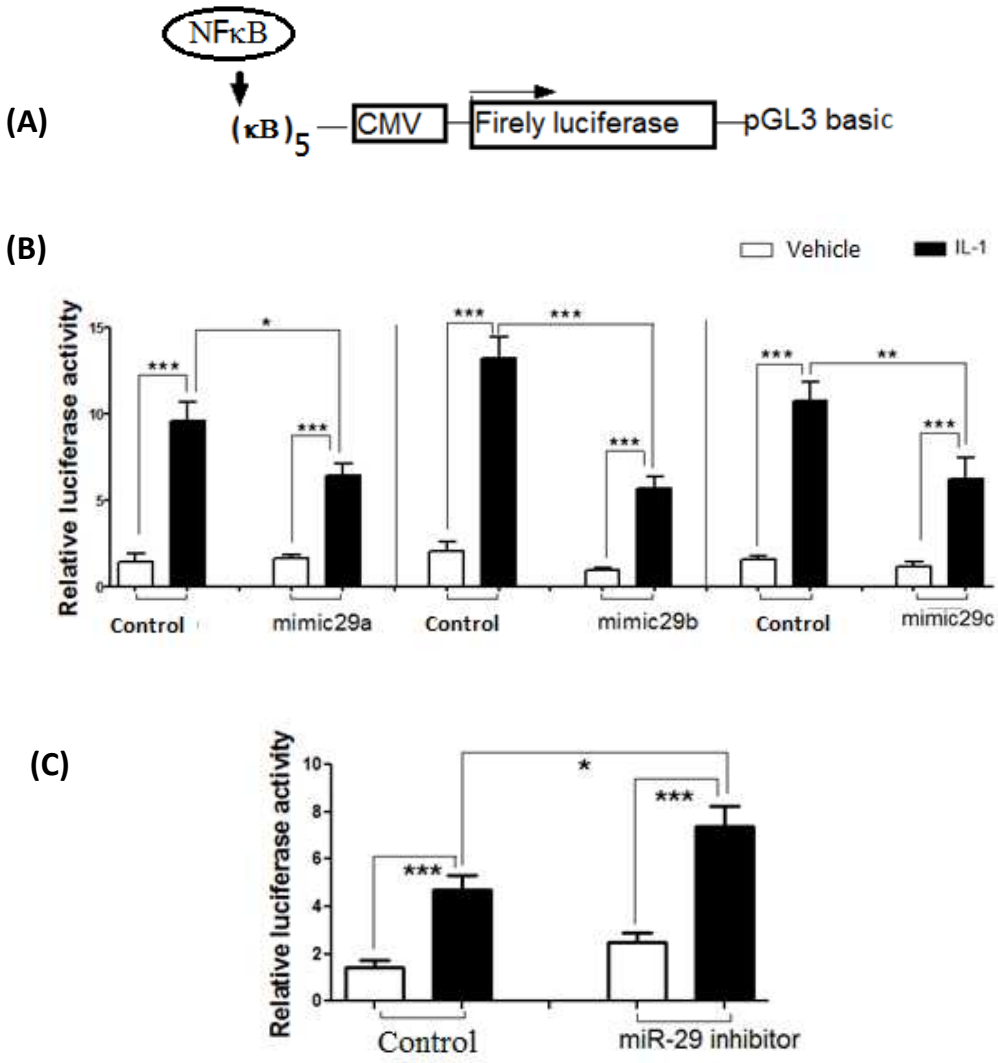

Figure 5.3 The miR-29 family suppresses NFκB signalling pathway

(A) The NFκB signalling reporter (κB vector) contains 5 binding sites of NFκB upstream of the firely luciferase-encoding gene in pGL3

100ng κB vector, and 10ng Renilla expression vector were co-transfected with either miR-29 family mimic (B) or miR-29b inhibitor (C) into SW1353 cells in monolayer. The non-targeting control (50nM) was also used as a negative control. 24 hours after transfection, cells were serum starved for further 24 hours, and followed by treating with IL-1 (5ng/ml) for another 6 hours before measuring luciferase activity. Renilla is the endogenous control for luciferase assay. Means ± standard errors are presented, n=6. The difference of luciferase activity was analysed by Student's unpaired two-tailed t test. * $p<0.05$, ** $p < 0.01$, *** $p<0.001$

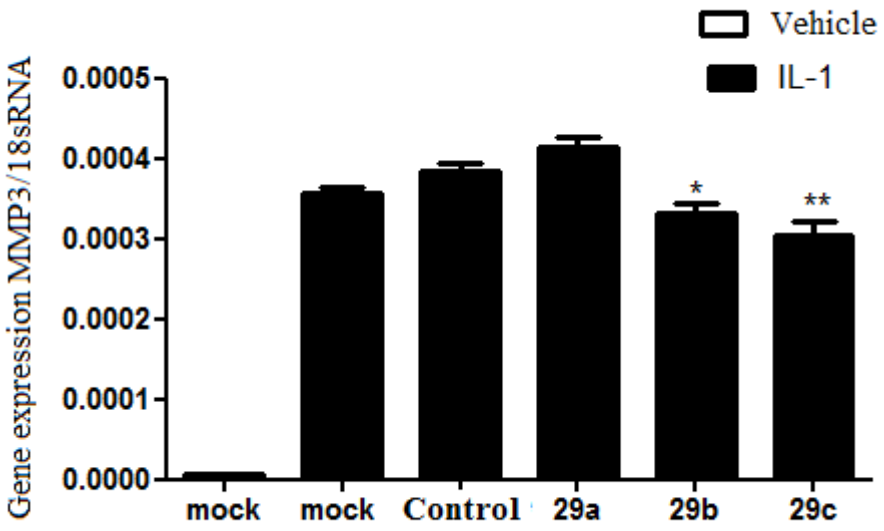

Figure 5.4 The miR-29 family suppresses expression of the IL-1-induced gene MMP3
Human primary chondrocytes were transfected with either miR-29 family mimic (50nM) or non – targeting control (50nM) for 24 hours. Cells were then changed into 0.5% (v/v) FCS for 24 hours, followed by stimulating with IL-1β (5ng/ml) for a further 6 hours. Total RNA was isolated and the expression of MMP3 was measured by qRT-PCR. 18S rRNA expression was used as the housekeeping gene. Open bar: non – treatment control, close bar: IL-1β treatment. Means ± standard errors are presented, n=3. The difference in expression level of IL-1β was analysed by unpaired two-tailed t test. * $p<0.05$, ** $p < 0.01$, *** $p<0.001$

5.2.3 The miR-29 family supresses the canonical Wnt signalling pathway

Even though expression of the miR-29 family is not regulated by Wnt3a in human chondrocyte, it is still of interest to investigate whether the WNT/β-catenin signalling is modulated by the miR-29 family because of the critical role of this signalling in OA development: balanced β-catenin levels are essential for maintaining homeostasis of articular cartilage and any factors impairing this balance could lead to pathological changes.

For investigating the interaction between the miR-29 family with the WNT/β-catenin signalling, the TOPFlash reporter (containing 7 binding sites of TCF/LEF driving the expression of the luciferase encoding gene) and FOPFlash reporter (control for TOPFlash where all the TCF/LEF binding sites are mutated) were used (Figure 5.5a). With the presence of e.g. Wnt3a, the signal transduced from the FZD receptor and LRP-5/6 co-receptor proteins will lead to the accumulation of β-catenin in the nucleus where it acts in concert with TCF/LEF transcription factors to generate a transcriptionally active complex inducing the expression of cognate genes and also therefore the TOPFlash reporter. Thus, any modulation of luciferase activity in the presence of the miR-29 family indicates that the miRNA family impacts on canonical signalling. Again the luciferase assay experiment was set up similarly to the assay in 5.1.1 but the TOPFlash (100ng) or FOPFlash (100ng) and Wnt3a (50ng/ml) were utilized. Luciferase assay data (Figure 5.5b, c) showed that Wnt3a strongly induced the luciferase activity from TOPFlash but not FOPFlash reporters; all members of the miR-29 family significantly decreased luciferase activity, whilst a miR-29b inhibitor increased the luciferase activity compared to control. These data show that the WNT/β-catenin pathway was induced in SW1353 cell with Wnt3a and that the miR-29 family is a negative regulator of this signalling.

The suppressive effect of the miR-29 family on the WNT/β-catenin signalling pathway was further confirmed by measuring the effect of the miR-29 family on the expression of *AXIN2*, a WNT/β-catenin responsive gene and not a putative direct target of the miR-29 family. The experiment was set up similarly to the experiment in 5.1.1 except cells were stimulated with Wnt3a (50ng/ml). The qRT-PCR data (Figure 5.6) showed that *AXIN2* expression was strongly induced by Wnt3a; the miR-29 family mimics significantly decreased the expression of *AXIN2* as compared with non-targeting control.

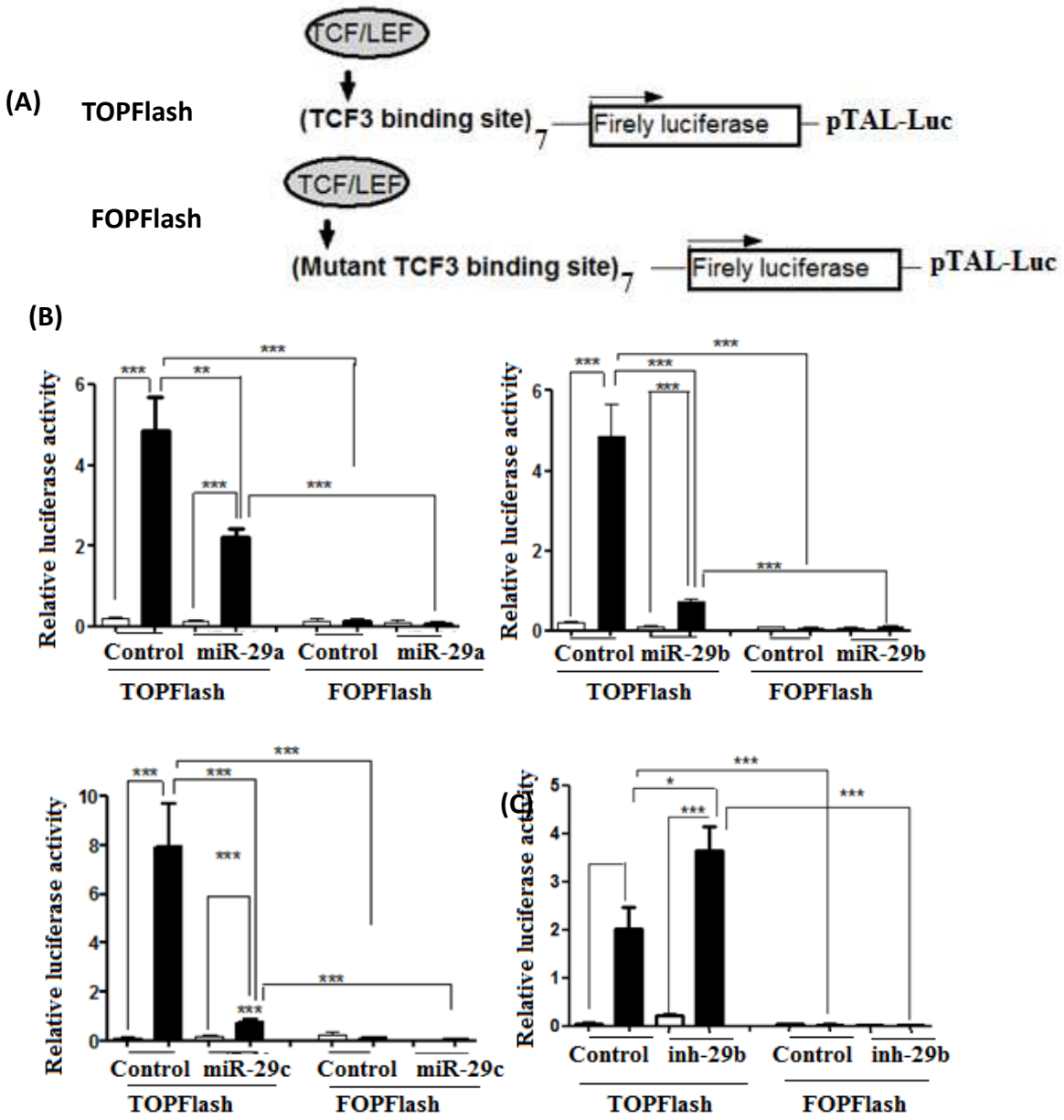

Figure 5.5 The miR-29 family suppresses the WNT/β-catenin signalling pathway

(A) The canonical WNT signalling reporter (TOPFlash vector) contains 7 binding sites of TCF/LEF upstream of the firely luciferase encoding gene in the pTAL-Luc vector. The FOPFlash vector is the control in which all binding sites of TCF/LEF are mutated.

100ng TOPFlash or FOPFlash vectors, and 10ng Renilla vector was co-transfected with either miR-29 family mimic (50nM) (B) or miR-29b inhibitor (50nM) (C) into SW1353 cells in monolayer. The non-targeting control (50nM) was also used as the control. 24 hours after transfection, cells were serum starved for another 24 hours, and followed by treatment with WNT3a (50ng/ml) for another 6 hours before measuring luciferase activity. Renilla is the endogenous control for luciferase assay. Means ± standard errors are presented, n=6. The difference of luciferase activity was analysed by Student's unpaired two-tailed t test. * $p<0.05$, ** $p < 0.01$, *** $p<0.001$

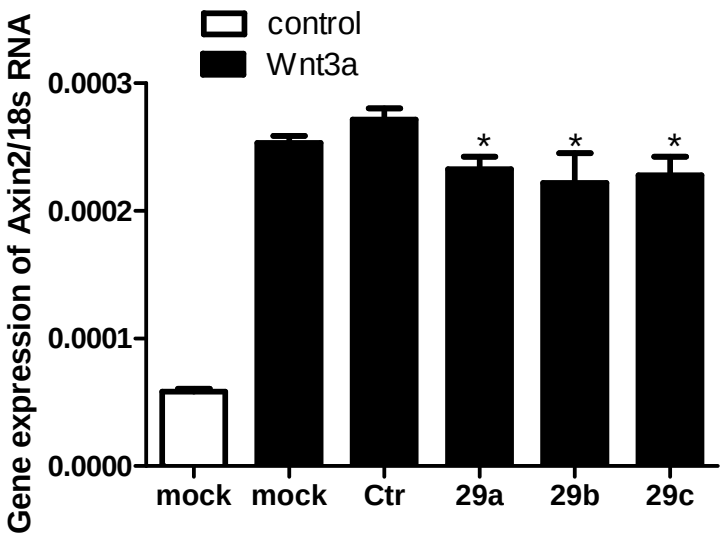

Figure 5.6 The miR-29 family suppresses expression of the WNT/β-catenin induced gene *AXIN2*

Human primary chondrocytes were transfected with either miR-29 family mimic (50nM) or non – targeting control (50nM) for 24 hours. Cells were then serum starved for 24 hours and followed by stimulating with Wnt3a (50ng/ml) for another 6 hours. The expression level of Axin2 was measured by qRT-PCR. 18S rRNA was used as the housekeeping gene. Open bar: non – treatment control, close bar: WNT3a treatment. Means ± standard errors are presented, n=3. The difference in expression level of *AXIN2* was analysed by unpaired two-tailed t test. * $p<0.05$, ** $p < 0.01$, *** $p<0.001$

5.2.4 Identification of miR-29 family targets

The miR-29 family was found to suppress the TGFβ/Smad, NFκB, and WNT/β-catenin signalling pathways. Nonetheless, it still remained unclear the direct mechanism by which the miR-29 family controlled these pathways. I therefore sought to identify novel targets of the miR-29 family to explain how the miR-29 family interacts with these pathways.

5.2.4.1 Gain- and loss- of function of miR-29b

For identifying new targets, a gain- and loss- of function experiment was performed. Since the miR-29 family shares the same seed binding site, it was deemed sufficient just to overexpress or silence miR-29b rather than all members of the family. Human primary chondrocytes were transiently transfected with miR-29b mimic or miR-29b inhibitor (50nM) and their non-targeting controls for 48 hours in triplicate and then total RNA was isolated. The transfection experiment was validated by measuring the miR-29b level by qRT-PCR. The data (data not shown) showed that the level of miR-29b strongly increased or decreased after transfection with either miR-29b mimic or inhibitor, respectively. These data suggest a good transfection efficiency into human chondrocytes. For performing a whole genome profile, an equal amount of total RNA from each sample in the triplicate was pooled together. These pooled samples were then subjected to whole genome array using Illumina human HT-12 V4.0 expression BeadChips to profile more than 47,000 human transcripts.

The global effect of the miR-29b mimic and inhibitor transfection on whole genome expression was first investigated by plotting the distribution of different expression values for all mRNAs in the miR-29b overexpression or knockdown experiments. Since the miRNA will exert its function by suppressing target gene expression, it was expected that the overexpression of miR-29b would significantly suppress target gene expression; conversely, a strong induction of target gene expression would be observed with the silencing of the miR-29b. Consistent with this hypothesis, data (Figure 5.7A) showed that in the miR-29b silencing experiment, the distribution of modulated genes was slightly skewed towards higher expression. Using an absolute 1.3 fold change (FC) as the cut off, there are 213 and 144 mRNA going up and down, respectively in this experiment (whilst just 9 and 10 mRNA going up and down respectively if the FC cut off was 1.5). Surprisingly, this pattern was also observed with the overexpression of the miR-29b (Figure 5.7B) with 703 and 518 mRNA

going up and down with 1.5 FC cut off, respectively. These data suggest that the miR-29b mimic has stronger effect than miR-29b inhibitor in chondrocytes and that the transfection with the miR-29b mimic strongly induced rather than supressed gene expression. Further analysis of the mRNAs strongly increased with miR-29b overexpression showed that the majority of these induced genes do not contain a binding site for the miR-29 family in their 3'UTR, suggesting that they are not direct targets of the miR-29 family. Indeed, a number of interferon responsive genes were strongly increased (Appendix, Table 7), suggesting a non-specific response to the synthetic oligonucleotide. This has been previously noted even for small RNAs (Karlsen et al. 2011). Interestingly, these genes were not modulated in the miR-29b silencing experiment, suggesting that a specific sequence in the miR-29b mimic is responsible.

The effect of the miR-29b mimic or inhibitor on whole genome expression was further analysed by examining the potential targets of the miR-29 family. The array data (Figure 5.8) revealed there were 12215 mRNAs in the intersection of the two experiments that increased in the miR-29b knockdown and decreased in miR-29b overexpression experiments. To further explore the effect of modulation of miR-29b on the transcriptome, the percentage of mRNAs containing seed sites (e.g. 6-mer, 7-mer, 8-mer) was calculated. It was a postulated that potential direct targets of miR-29s (those mRNA containing miR-29 seed sites) should be enriched in mRNA down-regulated by miR-29b and in mRNA up-regulated by miRNA-29b silencing. Particularly, this enrichment should be highest in genes that are decreased by miR-29b mimic and increased by miR-29b inhibitor. Data (Figure 5.8) showed that regardless of the length of the seed sequence, the percentage of mRNAs with seed sites is higher in the mRNAs which are decreased on overexpression or increased on silencing of miR-29b than in total mRNA. The percentage of mRNAs with seed sites is the highest in the intersection of the two experiments. These data confirm the hypothesis that taking the intersection containing mRNAs which decrease with the overexpression and increase with silencing of miR-29b is an effective way to filter the relevant miRNA targets.

Also, a subset of mRNA which was differentially expressed in the microarray analysis was selected for validating using RT-qPCR. Comparison of the expression levels between the microarray and RT-PCR results demonstrated a similar expression pattern between the two platforms (data not shown). These results confirmed the mRNA array data.

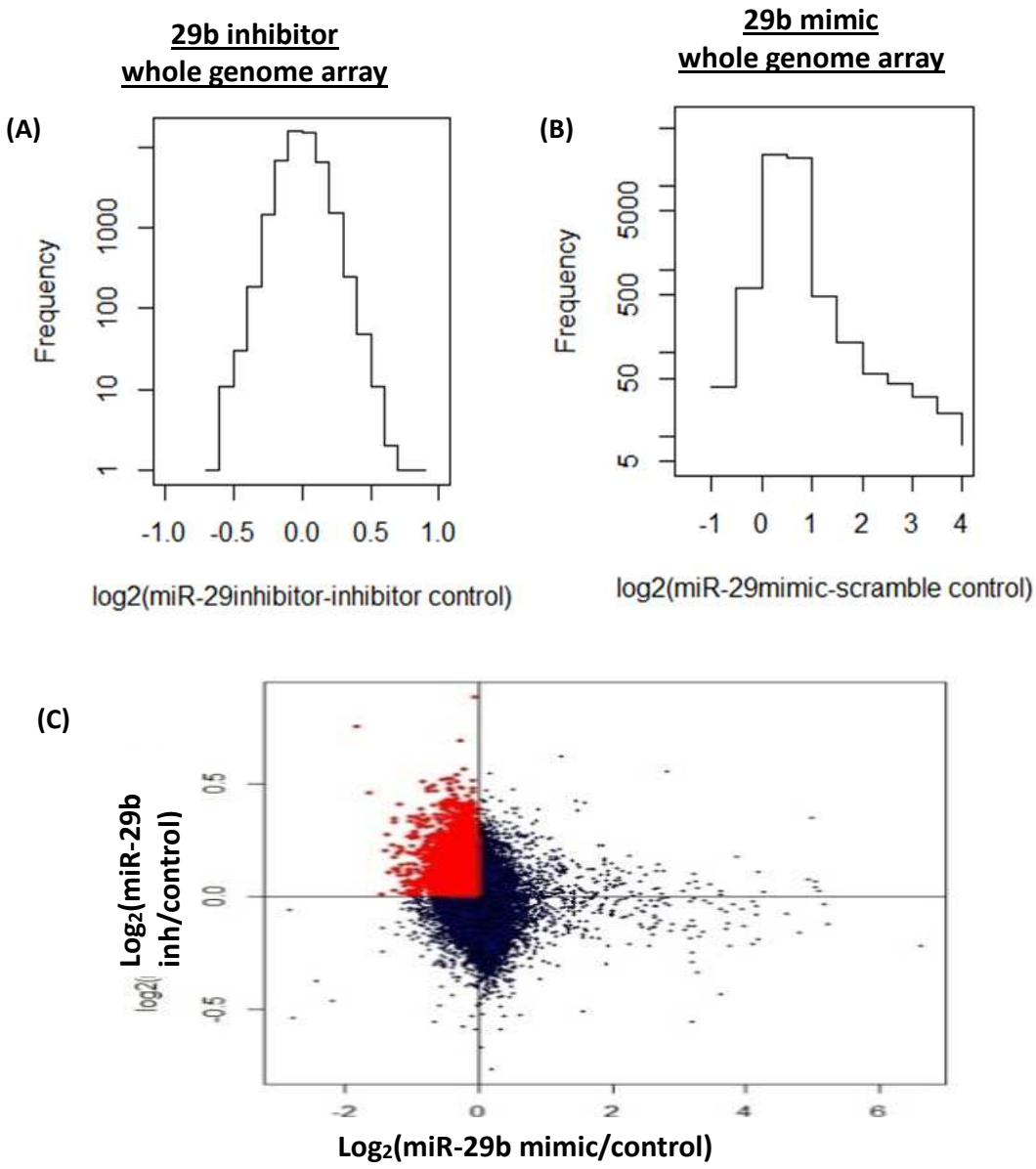

Figure 5.7 Gain- and loss- of function of miR-29b experiments

Human primary chondrocytes were cultured in high glucose media with 10% (v/v) FCS in monolayer until reaching 90% confluence. Cells were transfected with miR-29b mimic (50nM), miR-29b inhibitor (50nM), or non – targeting control (50nM) for 48 hours in triplicate. Cells were then harvested and total RNA was isolated from each sample. An equal amount of total RNA from each sample was pooled together. Pooled samples were subjected to whole genome array using Illumina humanHT-12 V4.0 expression BeadChip array. The Global effect of the miR-29b overexpression or silencing on whole genome expression was presented in (A) for the miR-29b silencing experiment and in (B) for the miR-29b overexpression experiment. Both datasets were plotted together on the same chart (C). The mRNAs which decreased in the miR-29 overexpression and increased in the miR-29b silencing experiment are highlighted in red.

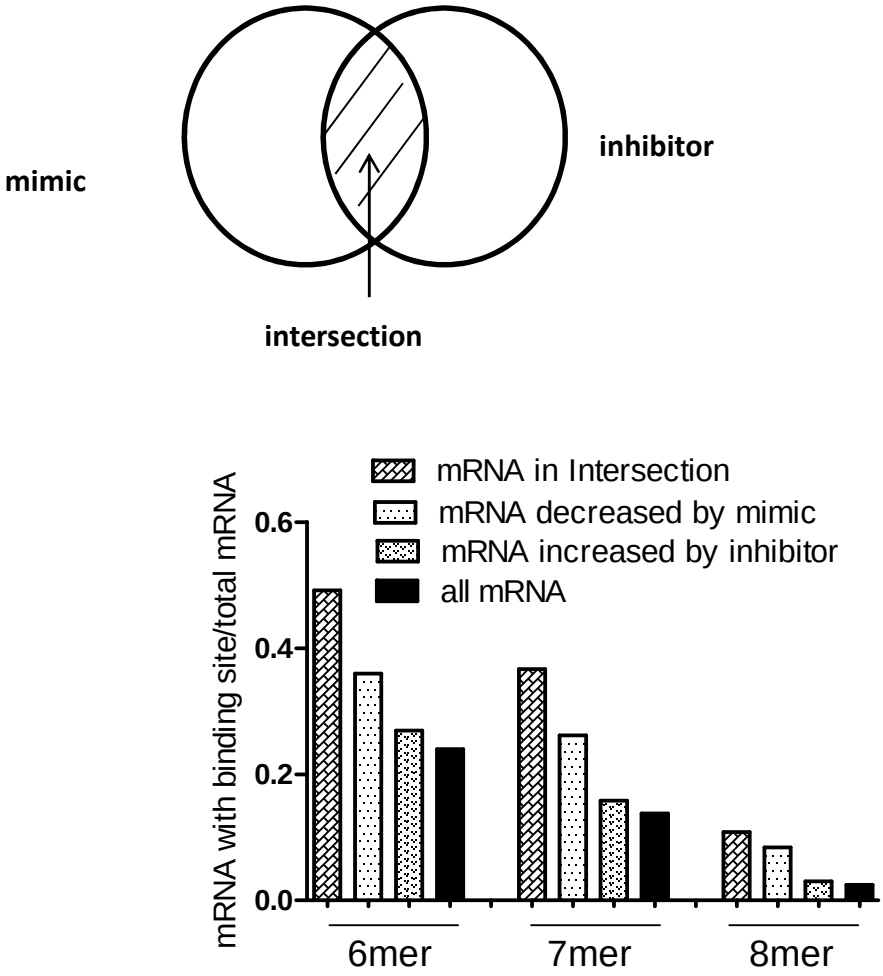

Figure 5.8: Enrichment of miR-29 putative direct targets in miR-29b gain – and loss – of function experiment.

From whole genome array data, the percentage of miR-29 putative direct targets was calculated for (i) mRNA decreased by the miR-29b mimic ; (ii) mRNA increased by the miR-29b inhibitor ; (iii) mRNA in the intersection of the two (decreased by miRN-29b mimic and increased by inhibitor) (iv) all the mRNAs detected from the whole genome array. The calculation was performed for the range of fold change (FC) and for each types of seed sequence e.g. 6-mer, 7-mer, 8-mer. The mRNA having more than one binding site for each type of seed sequence was always assigned as 1. When FC=k, the percentage of 6mer-seed-site targets increasing or decreasing expression was calculated: **6mer** = sum of mRNA having 6mer-seed site sequence in the 3'UTR with FC in the range of (k, FC max) if k >0, or (FC min, k) if k<0; **Total mRNA** = sum of mRNA with FC in the range of (k, FC max) if k>0, or (FC min, k) if k< 0; **mRNA with binding site/ total mRNA = 6mer/total mRNA.** The percentage of other seed site targets was calculated similarly. Here, calculation for the absolute FC 1.3 is presented.

5.2.4.2 Known targets of the miR-29 family

The miR-29 family has emerged as an important miRNA in a number of pathologic settings by regulating multiple genes that fall into the same or related pathways.

In the whole genome array of the overexpression and silencing of the miR-29b, a number of known direct targets of the miR-29 family were also identified in human chondrocytes (e.g. Table 5.1).

Gene	Binding sites				Fold change mimic (decrease)	Fold change inhibitor (increase)
	s6	s7m8	s7a1	s8		
COL1A1	**3**	**1**	**3**	**1**	**2.53**	**1.69**
COL1A2	**3**	**1**	**2**	**1**	**1.26**	**1.05**
COL2A1	**1**	**1**	**1**	**1**	**1.17**	**1.39**
COL3A1	**3**	**2**	**2**	**2**	**1.36**	**1.26**
COL4A1	**2**	**1**	**2**	**1**	**1.22**	**1.41**
COL5A1	**5**	**4**	**2**	**2**	**1.15**	**1.15**
COL5A2	**2**	**1**	**2**	**1**	**2.20**	**1.27**
COL6A1	**1**	**0**	**1**	**0**	**1.27**	**1.08**
COL6A2	**1**	**1**	**1**	**1**	**1.12**	**1.01**
COL6A3	**1**	**1**	**1**	**1**	**1.20**	**1.14**
COL8A1	**1**	**1**	**1**	**1**	**1.35**	**1.07**
COL11A1	**2**	**2**	**0**	**0**	**1.80**	**1.25**
COL15A1	**2**	**1**	**1**	**1**	**1.73**	**1.22**
COL16A1	**1**	**1**	**0**	**0**	**1.35**	**1.05**
COL20A1	**3**	**0**	**0**	**0**	**1.01**	**1.13**
ADAM19	**6**	**2**	**0**	**0**	**1.64**	**1.28**
CDK6	**3**	**2**	**1**	**0**	**1.61**	**1.07**

Table 5.1: Fold change expression of known targets of the miR-29 family in the miR-29b gain- and loss- of function experiment in human articular chondrocytes

5.2.4.3 Novel targets of the miR-29 family

5.2.4.3.1 The ADAMTS family

The miR-29 family is one example of the fact that a miRNA can regulate many functionally related genes. As shown above, a number of extracellular matrix-related genes were found to be direct targets of the miR-29 family. Since a miRNA can regulate the expression of several hundred genes, it was likely that the miR-29 family could directly target sets of novel genes within families. In chapter 4, TGFβ was found to suppress miR-29 family expression and the miR-29 family itself was also found to supress TGFβ signalling. These data suggest that the level of miR-29 and TGFβ-induced genes, may be inversely correlated and the miR-29 family might further inhibit the effect of TGFβ signalling on gene expression by exerting a second suppressive effect on the pathway through directly targeting inducible genes. This means that a number of TGFβ-inducible genes could potentially be direct targets of the miR-29 family. Herein, the ADAMTS family investigated as TGFβ inducible genes (except *ADAMTS 19*) (Figure 5.9) and genes which have roles in cartilage.

Human primary chondrocytes were stimulated with TGFβ1 for 24 hours in monolayer culture. The expression levels of members of the ADAMTS families were measured by qRT-PCR showing that *ADAMTS6*, *ADAMTS10*, *ADAMTS14* and *ADAMTS17* were significantly induced by TGFβ (Figure 5.9). Moreover, bioinformatic analysis found that there were a number of miR-29 binding sites in the 3'UTR regions of these ADAMTS genes (Table 5.2). Together with this, these TGFβ induced ADAMTS genes were predicted to be miR-29 potential direct targets by different bioinformatics algorithms e.g. Diana, Targetscan, Microcosm, miRDB, Picta (Table 5.2). Taken together, all of these data demonstrated that ADAMTS genes, including *ADAMTS6, ADAMTS10, ADAMTS14, ADAMTS17, ADAMTS19* are miR-29 potential direct targets.

In order to validate these ADAMTS genes as miR-29 direct targets, the expression levels of these genes were measured by qRT-PCR in human chondrocytes transfected with the miR-29b mimic for 48 hours. qRT-PCR (Figure 5.10) showed that the expression of these ADAMTS genes was significantly suppressed by overexpression of the miR-29b, again supporting that these genes are the miR-29 direct targets. To further validate these ADAMTS genes as miR-29 direct targets, the 3'UTR regions containing the miR-29 binding sties were

subcloned downstream of the luciferase encoding gene in pmiRGLO. These ADAMTS3'UTR-pmiRGLO reporter vectors (100ng) were co-transfected with the miR-29 family mimic (50nM) to DF1 cells. After 24 hours of transfection, the cells were harvested and luciferase assays were performed. Together with the ADAMTS 3'UTR-pmiRGLO reporter vectors, mutant vectors in which the miR-29 binding sites were mutated were constructed and tested. A 3'UTR was a direct target for the miR-29 family if the luciferase activity was suppressed with the overexpression of the miRNA in the wild-type construct and this effect was abolished when the miRNA binding sites were mutated. Luciferase assay data showed that *ADAMTS6* (Figure 5.14), *ADAMTS10* (Figure 5.15*), ADAMTS14* (Figure 5.11), *ADAMTS17* (Figure 5.12), *ADAMTS19* (Figure 5.13) were all direct targets of the miR-29 family.

Genes	8 -mer	7 -mer	6 -mer	Bioinformatic algorithm
ADAMTS6		2		Diana, Targetscan, Microcosm, miRDB,Picta
ADAMTS10		2		Diana, Microcosm, Picta
ADAMTS14		2	2	Diana, Picta
ADAMTS17		2	3	Targetscan, Microcosm, miRDB,Picta
ADAMTS19		2		Picta

Table 5.2: *ADAMTS6, ADAMTS10, ADAMTS14, ADAMTS17, ADAMTS19* are predicted to be miR-29 targets

A number of different binding sites for miR-29 were found in the 3'UTR regions of *ADAMTS6, ADAMTS10, ADAMTS14, ADAMTS17,* and *ADAMTS19*. These ADAMTSs were predicted to be miR-29 family targets by different bioinformatics algorithms.

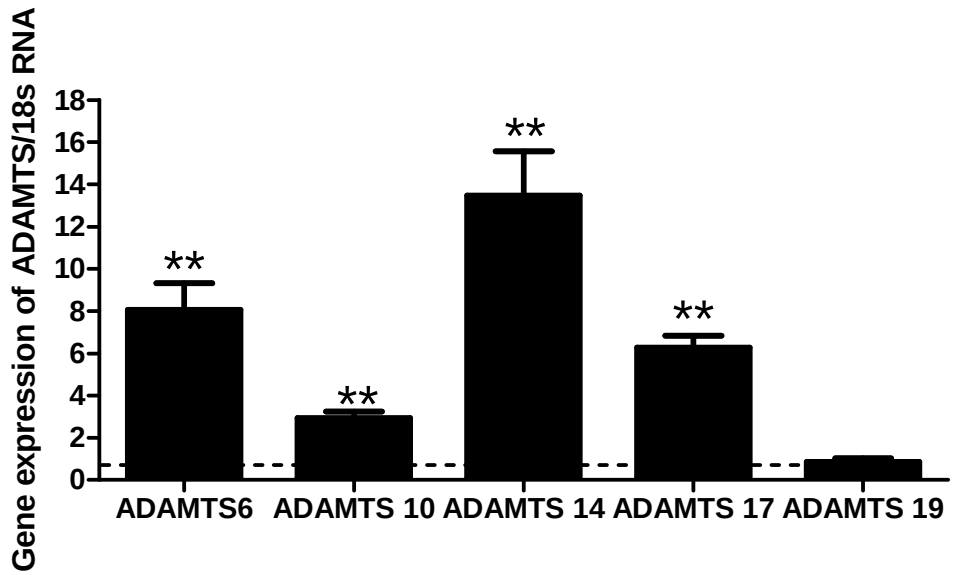

Figure 5.9 Members of ADAMTS family are TGFβ inducible genes

Human primary chondrocytes was cultured with 10% (v/v) FCS in monolayer until 90% confluence. Cells were switched to media with 0.5% (v/v) FCS for 24 hours before treating with TGFβ1 (4ng/ml) or vehicle (4mM HCl+0.5% (w/v) BSA) for another 24 hours. Cells were harvested and subjected to total RNA isolation. Relative expression of the ADAMTS genes was measured by quantitative RT-PCR. 18S rRNA was the housekeeping control. Relative expression value of each of the ADAMTSs in TGFβ stimulated cells was normalized to the vehicle control. The horizontal line at 1 serves as the vehicle control. Closed bar: TGFβ treatment, open bar: vehicle. Means ± standard errors are presented, n=3. The difference between the treatment and the control was analysed by Student's unpaired two-tailed t test. * $p<0.05$, ** $p < 0.01$, ***, $p<0.001$.

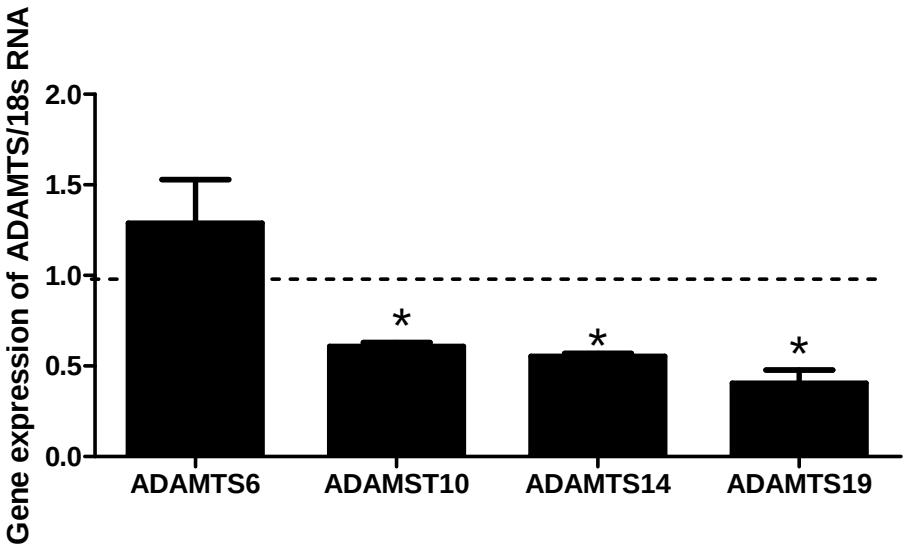

Figure 5.10 The expressions of members of the ADAMTS family were suppressed by miR-29b mimic

Human primary chondrocytes was cultured in media with 10% (v/v) FCS in monolayer until 90% confluence. Cells were then transfected with either miR-29b mimic (50nM) or non – targeting control (50nM) for 48 hours. Total RNA was isolated and the expression levels of the ADAMTS genes were measured by qRT-PCR. 18S rRNA was the housekeeping control. Relative expression value of each of the ADAMTS genes was normalized to non – targeting control. The horizontal line at 1 serves as the non-targeting control. Means ± standard errors are presented, n=3. The difference in expression between miR-29b overexpression and non – targeting control was analysed by Student's unpaired two-tailed t test. * $p<0.05$, ** $p < 0.01$, ***, $p<0.001$

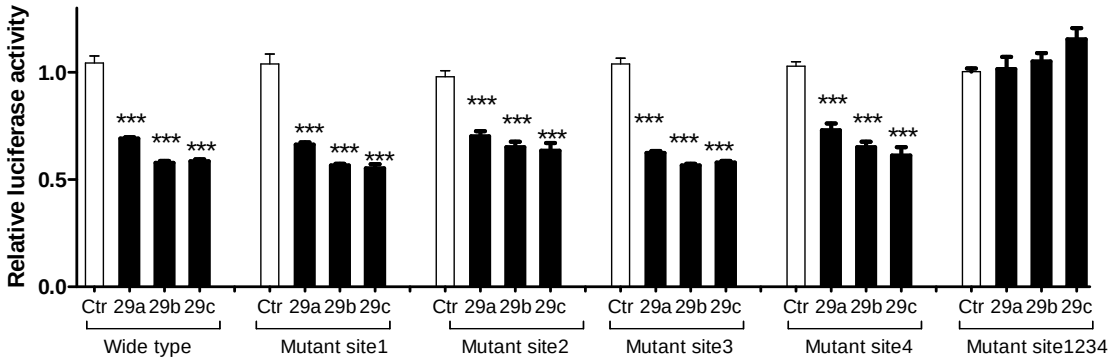

Figure 5.11: ADAMTS14 is a direct target of the miR-29 family

The ADAMTS14 3'UTR region containing 4 binding sites of the miR-29 family was subcloned downstream of the luciferase encoding gene in the pmiRGLO vector to create the ADAMTS14 3'UTR-pmiRGLO wide type (WT) vector. The mutant vectors were created from WT vector in which just single or quadruplicate binding sites of the miR-29 family were mutated. Either the WT or the mutants vectors (100ng) were co-transfected into chicken fibroblast DF1 cells with either miR-29b mimic (50nM) or non – targeting control (50nM). Luciferase assays were performed 24 hours after transfection. The relative luciferase value was normalised to the non-targetting control Open bar: non-targetting control, closed bar: miR-29 family mimic. Means ± standard errors are presented, n=6. The difference of luciferase activity was analysed by Student's unpaired two-tailed t test. * $p<0.05$, ** $p < 0.01$, *** $p<0.001$, Ctr, non-targetting control, 29a, 29b, 29c: miR-29a,-b,-c mimic.

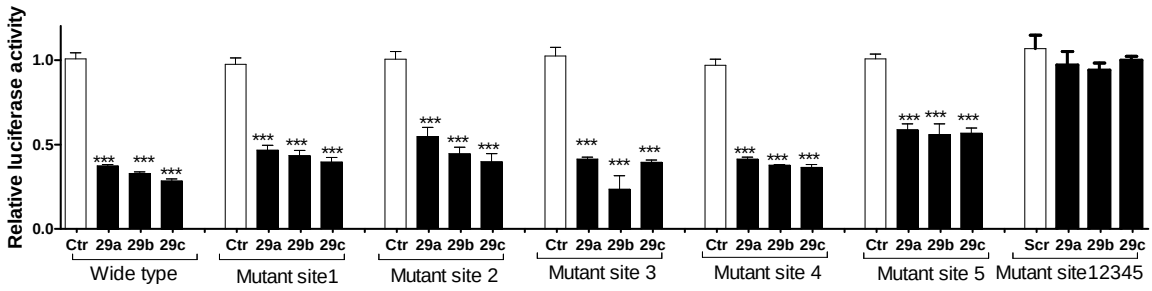

Figure 5.12: ADAMTS17 is a direct target of the miR-29 family

The ADAMTS17 3'UTR region containing 5 binding sites of the miR-29 family was subcloned downstream of the luciferase encoding gene in the pmiRGLO vector to create the ADAMTS17 3'UTR-pmiRGLO wide type (WT) vector. The mutant vectors were created from WT vector in which just single or quadruplicate binding sites of the miR-29 family were mutated. Either the WT or the mutants vectors (100ng) were co-transfected into chicken fibroblast DF1 cells with either miR-29b mimic (50nM) or non – targeting control (50nM). Luciferase assays were performed 24 hours after transfection. The relative luciferase value was normalised to the non-targetting control Open bar: non-targetting control, closed bar: miR-29 family mimic. Means ± standard errors are presented, n=6. The difference of luciferase activity was analysed by Student's unpaired two-tailed t test. * $p<0.05$, ** $p < 0.01$, *** $p<0.001$, Ctr, non-targetting control, 29a, 29b, 29c: miR-29a,-b,-c mimic.

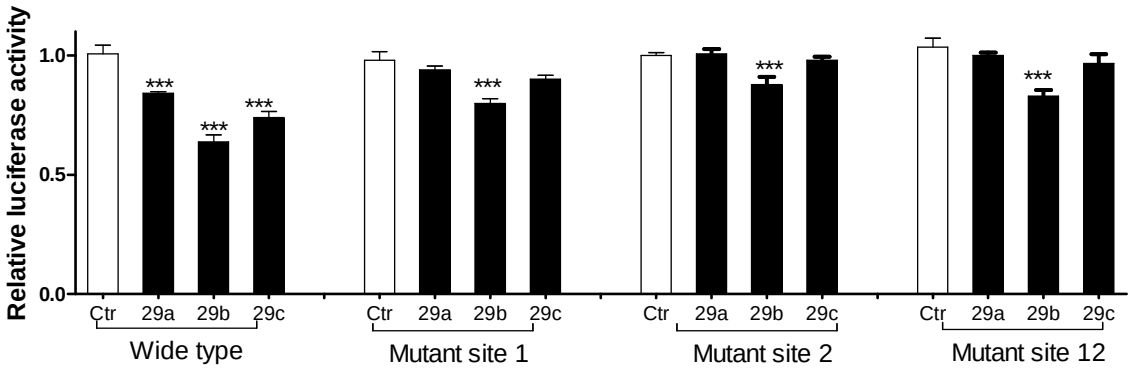

Figure 5.13: ADAMTS19 is a direct target of the miR-29 family

The ADAMTS19 3'UTR region containing 2 binding sites of the miR-29 family was subcloned downstream of the luciferase encoding gene in the pmiRGLO vector to create the ADAMTS19 3'UTR-pmiRGLO wide type (WT) vector. The mutant vectors were created from WT vector in which just single or duplicate binding sites of the miR-29 family were mutated. Either the WT or the mutants vectors (100ng) were co-transfected into chicken fibroblast DF1 cells with either miR-29b mimic (50nM) or non – targeting control (50nM). Luciferase assays were performed 24 hours after transfection. The relative luciferase value was normalised to the non-targetting control Open bar: non-targetting control, closed bar:

miR-29 family mimic. Means ± standard errors are presented, n=6. The difference of luciferase activity was analysed by Student's unpaired two-tailed t test. * $p<0.05$, ** $p < 0.01$, *** $p<0.001$, Ctr, non-targetting control, 29a, 29b, 29c: miR-29a,-b,-c mimic.

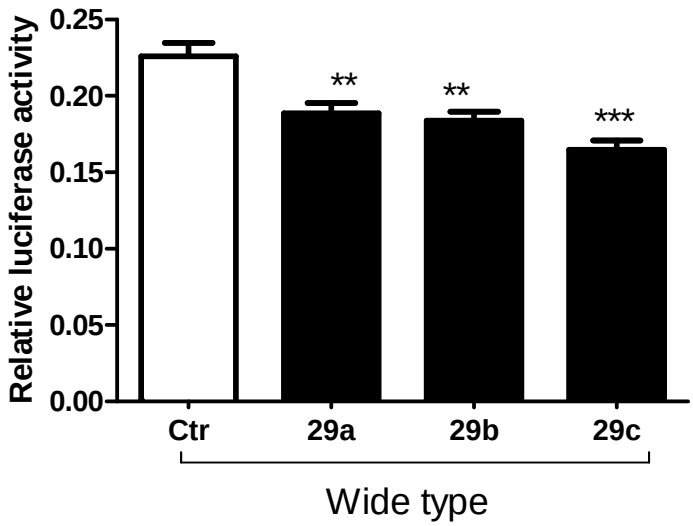

Figure 5.14: ADAMTS6 is a direct target of the miR-29 family

The ADAMTS6 3'UTR region containing 2 binding sites of the miR-29 family was subcloned downstream of the luciferase encoding gene in the pmiRGLO vector to create the ADAMTS6 3'UTR-pmiRGLO wide type (WT) vector. The WT vector (100ng) was co-transfected into chicken fibroblast DF1 cells with either miR-29b mimic (50nM) or non – targeting control (50nM). Luciferase assays were performed 24 hours after transfection. The relative luciferase value was normalised to the non-targeting control Open bar: non-targeting control, closed bar: miR-29 family mimic. Means ± standard errors are presented, n=6. The difference of luciferase activity was analysed by Student's unpaired two-tailed t test. * $p<0.05$, ** $p < 0.01$, *** $p<0.001$, Ctr, non-targeting control, 29a, 29b, 29c: miR-29a,-b,-c mimic.

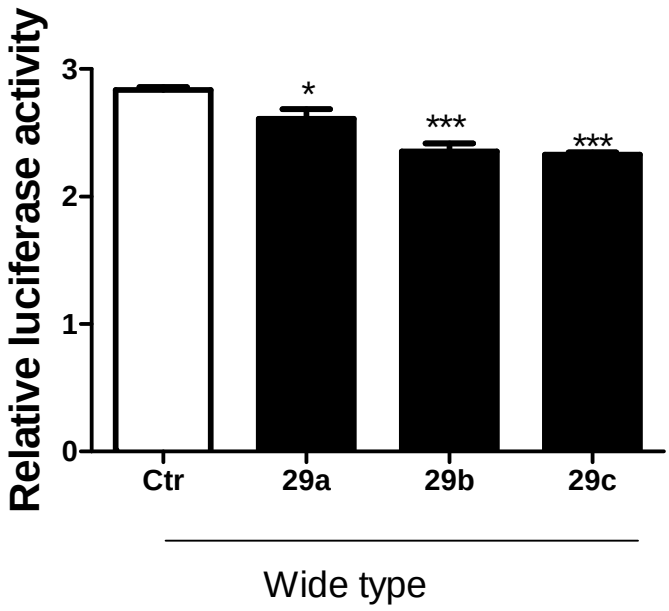

Figure 5.15: ADAMTS10 is a direct target of the miR-29 family
The ADAMTS10 3'UTR region containing 2 binding sites of the miR-29 family was subcloned downstream of the luciferase encoding gene in the pmiRGLO vector to create the ADAMTS10 3'UTR-pmiRGLO wide type (WT) vector. The WT vector (100ng) was co-transfected into chicken fibroblast DF1 cells with either miR-29b mimic (50nM) or non – targeting control (50nM). Luciferase assays were performed 24 hours after transfection. The relative luciferase value was normalised to the non-targeting control Open bar: non-targeting control, closed bar: miR-29 family mimic. Means ± standard errors are presented, n=6. The difference of luciferase activity was analysed by Student's unpaired two-tailed t test. * $p<0.05$, ** $p < 0.01$, *** $p<0.001$, Ctr, non-targeting control, 29a, 29b, 29c: miR-29a,-b,-c mimic.

5.2.4.3.2 WNT signalling pathway related genes

As shown previously, the miR-29 family was found to negatively regulate the TGFβ, NFκB, and WNT/β-catenin signalling pathways. The remaining question is how the miR-29 family supress these signalling pathways.

The whole genome array from the miR-29b gain – and loss – of function experiment found 12215 mRNAs that were the miR-29 putative targets. These consisted of 6925 mRNAs containing at least one 6-mer, 3400 mRNAs containing 7-mer, and 728 mRNAs containing 8-mer binding sites in their 3'UTR. Those mRNAs with miR-29 binding sites were considered as putative direct targets of the miR-29 family; the others without the miR-29 binding site were considered as indirect targets.

The miR-29 family suppression of TGFβ, NFκB, and WNT/β-catenin signalling pathways could be through a direct mechanism by targeting the mRNAs in the signalling cascade. In order to verify how miR-29 suppresses these signalling pathways, both putative miRNA-29 indirect and direct targets were analysed with DAVID functional analysis (web address) software to identify the most represented gene ontology (GO) categories. Analysing the miR-29 direct target sections found the enrichment for the Wnt signalling pathway together with MAPK kinase signalling pathway, apoptosis pathways, P53 signalling pathways. Since, NFκB and TGFβ pathways did not come up in this analysis, the miR-29 indirect targets were further analysed. However, neither NFκB nor TGFβ signalling pathways were enriched. In the scope of this project, the mechanisms by which the miR-29 suppressed these two signalling pathways remains unclear and need to be further explored.

All the miR-29 putative direct targets were selected regardless of the fold change cut off. In this manner, the Wnt signalling-related direct targets e.g. Dishevelled 3 (DVL3), casein kinase 2 alpha 2 polypeptide (CSNK2A2), GSK-3 binding protein frat2 (FRAT2), Frizzled family receptor 3 (FZD3), and Frizzled family receptor 5 (FZD5) were only modulated with a small fold change in the array (Fold change between 1 to 1.2). The expression of these mRNAs were measured by qRT-PCR, however in triplicate samples these data showed that the modulation of these genes under the control of the miR-29b did not reach statistical significance (Appendix, Figure 8).

Even though expression of these Wnt-related genes was not significantly modulated at the mRNA level, the genes were explored as miR-29 direct targets since miR-29 might exert its functions on these genes at the protein level. To verify these genes as the miR-29 direct targets, 3'UTR regions containing miR-29 binding sites of these genes were subcloned downstream of a luciferase encoding gene in the pmiRGLO vector. Constructs in which the miR-29 binding sites were mutated were also created. Either the 3'UTR-pmiRGLO vectors or the mutant 3'UTR-pmiRGLO vectors were co-transfected with the miR-29 family mimic (50nM) into DF1 cells for 24 hours. Then cells were harvested and the luciferase assays were performed. Luciferase assay data showed that FZD3 (Figure 5.19), FZD5 (Figure 5.18), FRAT2 (Figure 5.17), CK2A2 (Figure 5.16), DVL3 (Figure 5.15) were the direct targets of the miR-29 family since the luciferase activities were significantly decreased with the miR-29 family mimics and this effects were abolished when the miR-29 binding sites were mutated.

As mentioned above, qRT-PCR showed that the expression levels of these WNT signalling related genes were not significantly modulated with the miR-29b mimic at the mRNA level. However, the luciferase assay showed that miR-29 family could directly bind to the 3'UTR regions of these genes. It was postulated that the miR-29 family could directly target these genes at the protein level. Since all members of the miR-29 family directly targeted these genes, it was sufficient to check the effect of the miR-29b mimic on these genes at the protein level. In order to test this hypothesis, SW1353 cells were transfected with miR-29b mimic for 72 hours. Cells were then harvested and subjected to western blot. Time limitations meant that only expression levels of DVL3 were examined. Western blot data (Figure 5.15) showed that miR-29b supressed DVL3 expression level to 50% as compared to the non – targeting control, again confirming DVL3 is a direct target of miR-29 family.

Taken together, all of these data provide good evidence that the miR-29 family can inhibit the Wnt signalling, at least in part, via repression of these targets. Interestingly, DVL3, CSNK2A2 and FRAT2 were decreased in expression in hip OA cartilage compared to fracture controls, where the miR-29 family were increased in expression. Fzd3 expression however, was higher in expression in hip OA (Figure 5.20).

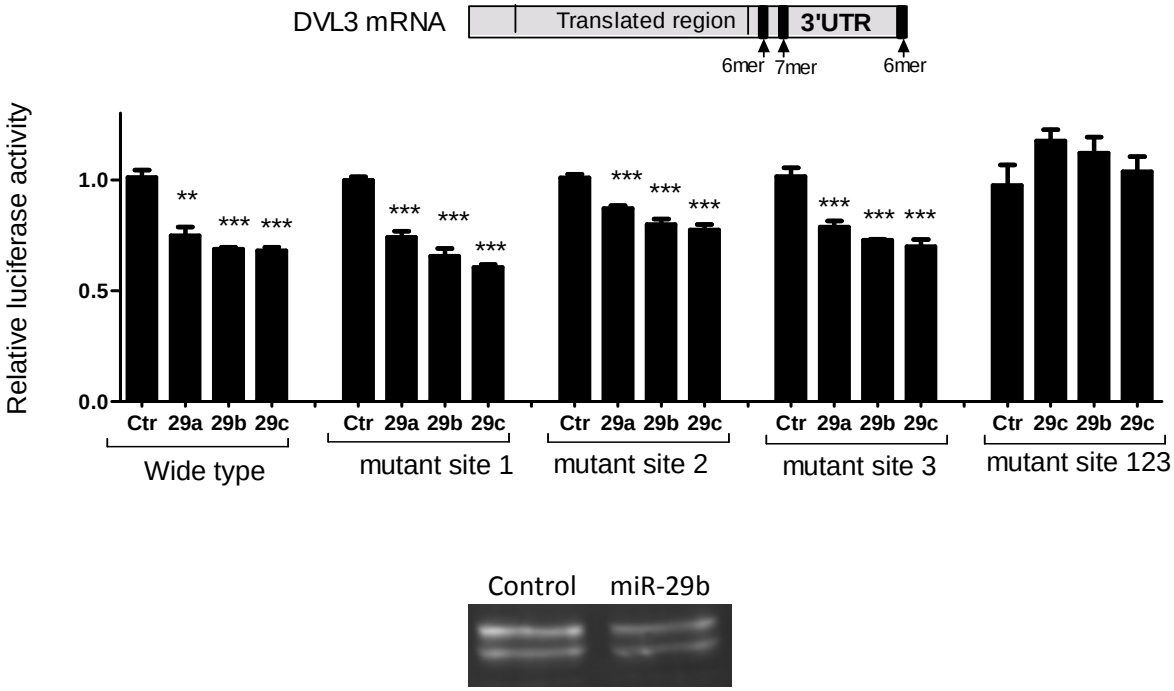

Figure 5.16: DVL3 is a direct target of the miR-29 family

(A) The DVL3 3'UTR region containing 3 binding sites of the miR-29 family was subcloned downstream of the luciferase encoding gene in the pmiRGLO vector to create the DVL3 3'UTR-pmiRGLO wide type (WT) vector. The mutant vectors were created from WT vector in which just single or triplicate binding sites of the miR-29 family were mutated. Either the WT or the mutants vectors (100ng) were co-transfected into chicken fibroblast DF1 cells with either miR-29b mimic (50nM) or non – targeting control (50nM). Luciferase assays were performed 24 hours after transfection. The relative luciferase value was normalised to the non-targetting control. Means ± standard errors are presented, n=6. The difference of luciferase activity was analysed by Student's unpaired two-tailed t test. * $p<0.05$, ** $p < 0.01$, *** $p<0.001$, Ctr, non-targetting control, 29a, 29b, 29c: miR-29a,-b,-c mimic.

(B) SW1353 was transfected with a miR-29b mimic (50nM) or non-targeting control (50nM) for 3 days. Protein was extracted and separated on 10 (w/v) SDS-PAGE, blotted onto PVDF and probed with an anti DVL3 antibody. The blot was stripped and re-probed with a GAPDH antibody to assess loading, n=2.

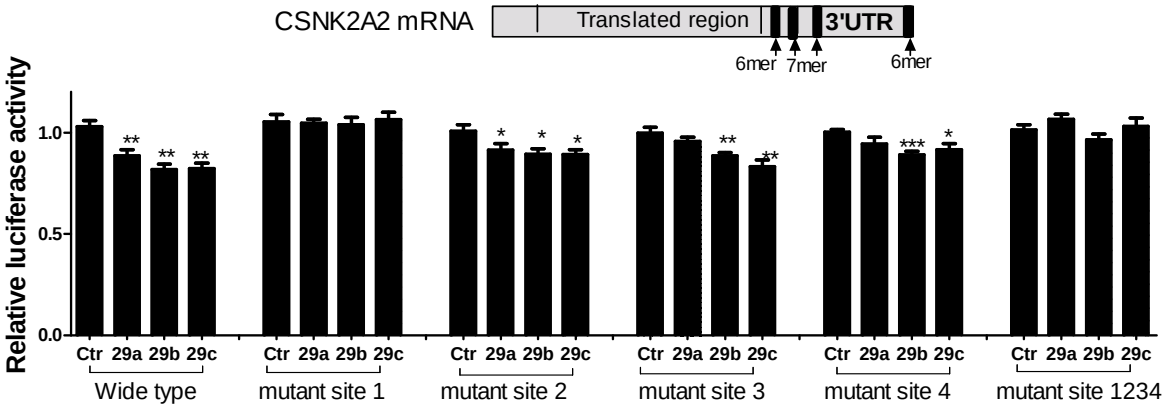

Figure 5.17: CK2A2 is a direct target of the miR-29 family

The CK2A2 3'UTR region containing 4 binding sites of the miR-29 family was subcloned downstream of the luciferase encoding gene in the pmiRGLO vector to create the CK2A2 3'UTR-pmiRGLO wide type (WT) vector. The mutant vectors were created from WT vector in which just single or quadruplicate binding sites of the miR-29 family were mutated. Either the WT or the mutants vectors (100ng) were co-transfected into chicken fibroblast DF1 cells with either miR-29b mimic (50nM) or non – targeting control (50nM). Luciferase assays were performed 24 hours after transfection. The relative luciferase value was normalised to the non-targeting control. Means ± standard errors are presented, n=6. The difference of luciferase activity was analysed by Student's unpaired two-tailed t test. * $p<0.05$, ** $p < 0.01$, *** $p<0.001$, Ctr, non-targeting control, 29a, 29b, 29c: miR-29a,-b,-c mimic.

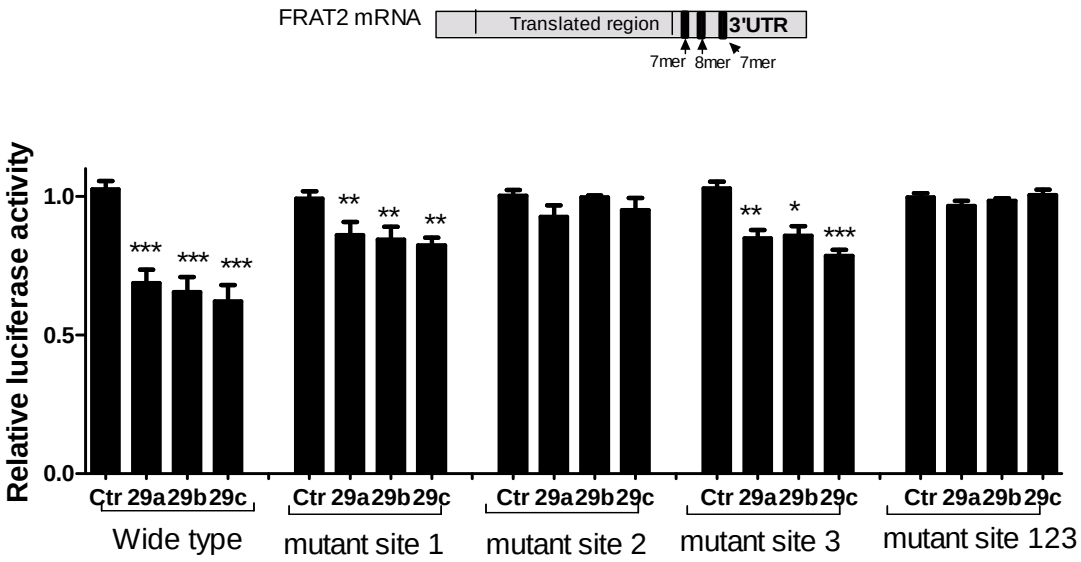

Figure 5.18: *FRAT2* is a direct target of the miR-29 family

The *FRAT2* 3'UTR region containing 4 binding sites of the miR-29 family was subcloned downstream of the luciferase encoding gene in the pmiRGLO vector to create the *FRAT2* 3'UTR-pmiRGLO wide type (WT) vector. The mutant vectors were created from WT vector in which just single or triplicate binding sites of the miR-29 family were mutated. Either the WT or the mutants vectors (100ng) were co-transfected into chicken fibroblast DF1 cells with either miR-29b mimic (50nM) or non – targeting control (50nM). Luciferase assays were performed 24 hours after transfection. The relative luciferase value was normalised to the non-targeting control. Means ± standard errors are presented, n=6. The difference of luciferase activity was analysed by Student's unpaired two-tailed t test. * $p<0.05$, ** $p < 0.01$, *** $p<0.001$, Ctr, non-targeting control, 29a, 29b, 29c: miR-29a,-b,-c mimic.

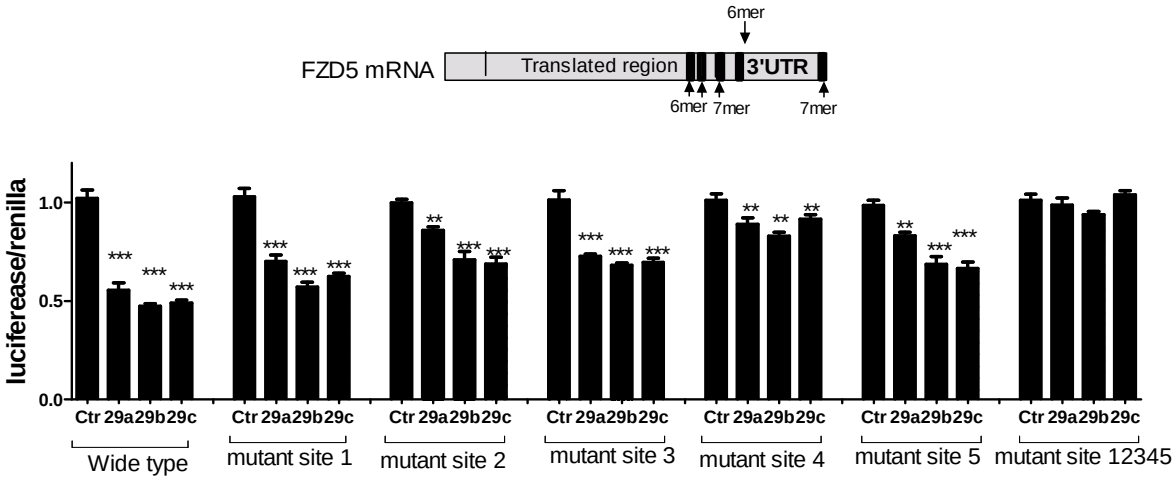

Figure 5.19: *FZD5* is a direct target of the miR-29 family

The *FZD5* 3'UTR region containing 5 binding sites of the miR-29 family was subcloned downstream of the luciferase encoding gene in the pmiRGLO vector to create the *FZD5* 3'UTR-pmiRGLO wide type (WT) vector. The mutant vectors were created from WT vector in which just single or quintuplicate binding sites of the miR-29 family were mutated. Either the WT or the mutants vectors (100ng) were co-transfected into chicken fibroblast DF1 cells with either miR-29b mimic (50nM) or non – targeting control (50nM). Luciferase assays were performed 24 hours after transfection. The relative luciferase value was normalised to the non-targeting control. Means ± standard errors are presented, n=6. The difference of luciferase activity was analysed by Student's unpaired two-tailed t test. * $p<0.05$, ** $p < 0.01$, *** $p<0.001$, Ctr, non-targeting control, 29a, 29b, 29c: miR-29a,-b,-c mimic.

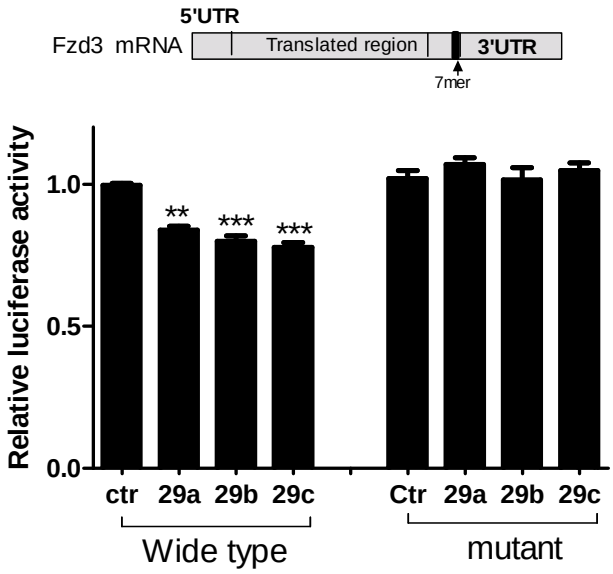

Figure 5.20: *FZD3* is a direct target of the miR-29 family

The *FZD3* 3'UTR region containing 1 binding sites of the miR-29 family was subcloned downstream of the luciferase encoding gene in the pmiRGLO vector to create the *FZD3* 3'UTR-pmiRGLO wide type (WT) vector. The mutant vectors were created from WT vector in which binding site of the miR-29 family were mutated. Either the WT or the mutants vectors (100ng) were co-transfected into chicken fibroblast DF1 cells with either miR-29b mimic (50nM) or non – targeting control (50nM). Luciferase assays were performed 24 hours after transfection. The relative luciferase value was normalised to the non-targeting control. Means ± standard errors are presented, n=6. The difference of luciferase activity was analysed by Student's unpaired two-tailed t test. * $p<0.05$, ** $p < 0.01$, *** $p<0.001$, Ctr, non-targeting control, 29a, 29b, 29c: miR-29a,-b,-c mimic.

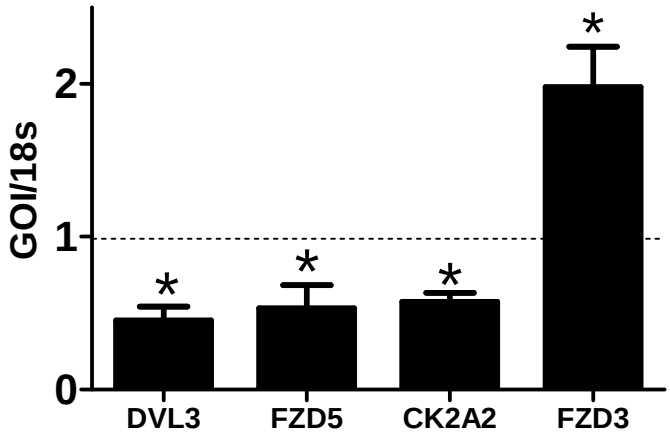

Figure 5.21: Expression of *FZD3, FZD5, DVL3,* and *CK2A2* in human cartilage

Total RNA was isolated from human hip articular cartilage of either end-stage OA patients or fracture controls and reverse transcribed to cDNA. Relative expressions of *FZD3, FZD5, DVL3,* and *CK2A2* were measured by real-time PCR where 18S rRNA was used as housekeeping control in hip osteoarthritis cartilage (HOA, n=8) and fracture to the neck of the femur (NOF, n=7). The horizontal line at 1 is the expression of these genes in NOF. Means ± standard errors are presented. Different in expression between HOA and control NOF was calculated by Student's unpaired two-tailed t test. * $p<0.05$, ** $p < 0.01$, *** $p<0.001$

5.3 Discussion

Previously, the miR-29 family has been shown to negatively interact with TGFβ signalling in several pathologic settings in which fibrosis development was the outcome of the disease such as liver, cardiac, renal fibrosis (van Rooij *et al.* 2008, Kwiecinski et al. 2011, Qin et al. 2011). In line with these studies, in the present study, the miR-29 family was also found to suppress the TGFβ signalling pathway in human chondrocytes. Noteworthy, miR-29 is one downstream mediator of TGFβ signalling in which the miRNA blocks the effect of the growth factor on gene expression. However, the direct mechanism by which miR-29 interferes with TGFβ signalling remains unclear in human chondrocytes. In fact, Smad3 was demonstrated to be a direct target of miR-29 in thyroid cells (Leone *et al.* 2012). In human chondrocytes, nevertheless, with transfection of miR-29 family mimics, the Smad3 mRNA level was not changed (data not shown); similarly, any decrease in luciferase activity when co-transfecting a Smad3-3'UTR reporter with miR-29 mimics was not statistically significant (data not shown), suggesting that Smad3 is not the target of miR-29 in the context of the chondrocyte. In addition, no obvious components of TGFβ signalling were regulated in the miR-29b gain- and loss-of function experiment with the whole genome array. This leads to the hypotheses that miR-29 may directly targets TGFβ signalling components at the protein level rather than mRNA level (similar to miR-140 (Pais et al. 2010)) or that the inhibition of miR-29 on TGFβ signalling is the consequence of the direct suppression of other factors inducing TGFβ signalling. To test this hypothesis, it may be best to perform miR-29b gain- and loss-of function experiment together with a proteomic assay. It may also be instructive to perform array experiments in the presence or absence of TGFβ itself

It has been shown that in the development and progression of OA, NFκB plays an active role e.g. mediating articular chondrocyte responses to proinflammatory cytokines (IL-1, TNF-α); inducing MMPs (e.g. MMP-1, MMP-3, MMP-13), cytokines (e,g, IL-6, IL-8) and chemokine expression (Marcu *et al.* 2010). Thus, NFκB is an attractive target for the treatment of OA. In this project, for the first time, NFκB signalling was confirmed as negatively regulated by the miR-29 family and miR-29 is also likely to serve as a downstream inhibitor of the signalling. Similar to TGFβ signalling, it is still not clear the direct mechanism by which miR-29 regulates NFκB signalling pathway. However, it suggests a potential therapeutic strategy for targeting NFκB signalling using miR-29. Further studies are needed to dissect the direct mechanism by which miR-29 interferes with NFκB signalling.

In this project, the miR-29 family was found to suppress the Wnt/β-catenin signalling pathway. In line with my data, the negative effect of the miR-29 on this signalling pathway is also reported. In human non-small-cell lung cancer cells, miR-29 directly targets DNMTs which in turn inhibited the methylation of Wnt inhibitory factor-1 (WIF-1) promoter; accordingly, miR-29 over-expression down-regulated β-catenin expression (Tan *et al.* 2013). In human colorectal cancer cells, miR-29b negatively regulated Wnt signalling and targeted B-cell CLL/lymphoma 9-like (BCL9L), thus decreasing its expression with a consequent decrease in nuclear translocation of β-catenin (Subramanian *et al.* 2014). In contrast to these studies, published data reports that the miR-29 family positively regulated canonical Wnt signalling by directly targeting its inhibitors in human embryonic kidney cells (Liu *et al.* 2011) and human fetal osteoblastic cells (Kapinas et al. 2010). This contradiction is not surprising as many miRNAs are known to act in a context-dependent manner depending on the relative availability of their targets in any cell type and this discordance could be a reflection of the differences in the miR-29 family regulatory networks in different cell lines.

Besides exerting function on several crucial signalling pathways implicated on chondrogenesis and OA, the crucial role of the miR-29 family was clearly shown through their target genes. In this project, miR-29b gain- and loss-of-function was applied to find miR-29 potential targets. Together with some novel and known targets which will be discussed later, the liposome – mediated transient transfection of the miR-29b-3p mimic surprisingly induced the expression of a number of immune genes which are not the miRNA targets. The Qiagen miR-29b-3p mimic used in the present study is double-stranded, 23 nucleotides in length with sequence identical to the sequence of the mature endogenous miRNA-29b-3p and does not contain any chemical modifications or overhangs, which makes it unlikely for any sequence difference between endogenous miRNA and Qiagen mimic to be responsible for the immune response. Moreover, the lack of immune response against the controls and the miR-29b inhibitor confirms that the immune response was specific and not due to a general response to small RNA. Indeed, it is likely that some specific GU- rich 4-mer sequences e.g. AUUU, UUGA, UGUU in the miR-29b-3p mature sequence (5'UAGCACCAUUUGAAAUCAGUGUU3') might be important for the immune gene up-regulation since these sequences have been shown to be potent immunostimulatory motifs mediated through TLR7 or TLR7/8 (Forsbach *et al.* 2008). Especially, it has been shown that the main effects induced upon activation of TLR7 in human immune cells are IFN- dependent

effects, proinflammatory cytokines and chemokines from cell expression only TLR7 or both TLR7 and 8 (Hertzog *et al.* 2003). Also, it is possible that this up-regulation of the immune genes could be attributed to the liposome alone besides the sequence of the synthetic miRNA since the levels of the immune genes were higher than the levels obtained for electroporation, and those observed in un-transfected controls (Karlsen *et al.* 2013). The explanation for this could be because liposomes fuse with the plasma membrane, which may trigger membrane – associated lipid receptors and/or distort the actin cytoskeleton which in turn up-regulates immune genes. However, it may depend on cellular context since electroporation could strongly trigger the increase of the immune genes in some cell types.

This study identifies FZD3, FZD5, FRAT2, CK2A2 and DVL3 as the critical targets of the miR-29 family in the Wnt signalling pathway. These genes have important roles in both canonical and/or non-canonical Wnt signalling pathways. **FZD3** and **FZD5** belong to the Frizzled proteins, which are the receptors for Wnt ligands. Wnt3a, Wnt5a, and Wnt2 can bind to FZD3 which in turn can activate both canonical and non-canonical WNT signalling pathways: Wnt3a activates the TOPFlash reporter in HEK293 cells overexpressing Wnt3a/FZD3/LRP6 (Lu *et al.* 2004) whist Wnt5a binding to FZD3 triggers downstream pathways independent of β-catenin (Hansen *et al.* 2009); Wnt2 can interact with FZD3 in human cumulus cells, but it is not known which downstream signalling pathways are activated after this binding interaction (Wang *et al.* 2009). **FZD5** functions as the receptor for Wnt5a, Wnt9b, and Wnt7a. Co-injection of hFZD5 and XWnt-5a induced the formation of dorsal axis duplication in *X. laevis* embryos; this axis duplication was suppressed after co-injection of RNA for human GSK-3β, suggesting the involvement β-catenin-dependent signalling in this receptor – ligand combination (He *et al.* 1997). Wnt9b was found in HEK293 cells as a binding partner for FZD5 to activate the TOPFlash reporter (Liu *et al.* 2008). Wnt7a was found to bind to FZD5 to activate the β-catenin signalling pathway and increase the proliferation of epithelial cells in the endometrium (Carmon *et al.* 2008). By targeting these two Frizzled proteins, miR-29 can interfere with Wnt signalling pathways. However, it will depend on the cellular context, whichWnt ligands are available to partner with, which will determine outcome. In line with these Frizzled proteins, another novel target of the miR-29 family, DVL3 (Disheveled 3), belonging to the Disheveled family including DVL1, 2 and 3, is a central component in mediating downstream events of both canonical and non-canonical Wnt signalling. Wnt ligands binding to Frizzled protein recruit Disheveled to the plasma membrane which leads to activation of downstream pathways. Disheveleds

includes DIX, PD2, and DEP domains: DIX and PDZ domains function together in canonical Wnt signalling to stabilize β-catenin; the DIX domain binds with Axin and results in inhibition of the β-catenin degradation complex in canonical Wnt signalling; PDZ and DEP domains cooperate in different subpathways of noncanonical Wnt signalling. Moreover, the other two targets FRAT2 and CSNK2A2 are potent activators of canonical Wnt signalling. **FRAT2** (Frequently rearranged in advanced T-cell lymphomas -2) belongs to the FRAT family including FRAT 1, 2, 3. By binding to GSK3, Frat prevents the phosphorylation and concomitant degradation of β – catenin (van Amerongen *et al.* 2005). **CSNK2A2** encodes for the subunit CK2α' of casein kinase 2 (CK2). CK2 has been shown to act as a positive modulator of WNT/β-catenin pathway, suppressing β-catenin degradation and β-catenin binding to APC (Price 2006). Several keys components of the WNT/β-catenin signalling are known substrates of CK2 in vitro including DVL (Willert *et al.* 1997), TEF/TCF (Homma *et al.* 2002, Miravet *et al.* 2002, Hammerlein *et al.* 2005), and β-catenin (Song *et al.* 2003). Taken together, it is likely that by directly targeting FZD3, FZD5, DVL3, FRAT2 and CSNK2A2, miR-29 could in part or in specific contexts, suppress the Wnt signalling pathway. Interestingly, in human cartilage, the expression levels of FZD5, CSNK2A2, and DLV3 were found to be down regulated in human OA, inversely correlating with the miR-29 expression level, suggesting a direct mechanism in which the suppression of these genes are controlled by miR-29 in human OA cartilage. However, FZD3 expression level was up-regulated in human OA cartilage which could be explained by the fact that there are many other factors which are involved in controlling gene expression together with miRNAs. Since the dys-regulation (either up-regulation or down-regulation) of the canonical Wnt signalling pathway can both lead to OA, there is a possible explanation for the disease development: the excessive amount of the miR-29 down-regulates the expression levels of a number of Wnt signalling related genes which consequently suppress the Wnt signalling pathway. Nevertheless, whether miR-29 targets all of these genes at the same time and the level at which the suppression of each gene contributing to the disease are still not explained in this project.

MicroRNA 29 has been suggested to serve as a master regulator in complex regulatory networks through fine-tuning a large set of functionally related genes, probably best illustrated by its extracellular matrix-related targets, whereby at least 16 ECM related genes are experimentally validated including collagen isoforms (van Rooij et al. 2008, Luna *et al.*

2009, Kwiecinski et al. 2011, Qin et al. 2011, Wang et al. 2012), laminin γ1 (Luna et al. 2009, Nishikawa *et al.* 2014), fibrillin 1, elastin (van Rooij et al. 2008), integrin β1 (Cushing et al. 2011). In line with these data, in this project, a number of ECM- related genes were highlighted as the direct targets of the miR-29 in human OA chondrocytes. However, there is not complete overlap since there are a number of genes that have been experimentally validated as direct targets of miR29 but not regulated when miR-29b was overexpressed or inhibited in human chondrocytes. For example, validated miR-29 direct target genes include DNMT3A, DNMT3B (Fabbri et al. 2007, Garzon *et al.* 2009, Amodio et al. 2012, Morita *et al.* 2013, Tan et al. 2013, Parpart et al. 2014), MMP2 (Liu et al. 2010, Steele et al. 2010, Fang *et al.* 2011), MMP9, ADAM12, ADAM19 (Luna et al. 2009, Ramdas et al. 2013), ADAMTS9 (Cushing et al. 2011). Nonetheless, in human chondrocyte, the expression levels of these genes were not modulated by the miR-29 family. The precise explanation for this difference is still not clear.

In this PhD thesis, members of ADAMTS family including *ADAMTS6, ADAMTS10 ADAMTS14, ADAMTS17, ADAMTS19* have been confirmed as novel direct targets of the miR-29 family. Interestingly, the miR-29 family is suppressed by TGFβ whist its direct targets, the ADAMTS family are strongly induced by TGFβ. However, except ADAMTS14 described as a procollagen N-propeptidase for pro-collagen type I, type II, and type III, the functions of ADAMTS 6, -17, and-19 remain unknown. Thus, further investigating the suppressive effect of miR-29 family on these ADAMTS becomes difficult both in vitro and in vivo. Moreover, ADAMTS14 and ADAMTS17 levels were reported to largely increase in hip OA cartilage and hip OA synovium, respectively (Davidson et al. 2006); the rs4747096 nsSNP in ADAMTS14 was over-represented in women requiring joint replacement because of knee OA and in patients with symptomatic hand OA (Rodriguez-Lopez *et al.* 2009, Poonpet *et al.* 2013), implicating the involvement of these ADAMTS on OA. The microRNA 29 family is, nevertheless, found to increase expression in hip OA cartilage in our sample set. Again, this could be explained in part by the fact that in cellular context, a miRNA is just one factor amongst others e.g. transcription, epigenetic silencing, differential biosynthesis, and extracellular stimuli controlling gene expression.

In summary, the miR-29 family was found to suppress the TGFβ/Smad3, NFκB, and Wnt/β-catenin signalling pathways. Gene expression profiles of gain- and-loss-of-function revealed the regulation of a large number of previously recognised extracellular matrix-associated

genes as well as an additional subset of protease and Wnt signalling pathway-related genes. Among these genes, the ADAMTS family e.g. *ADAMTS6, ADAMTS10, ADAMTS14, ADAMTS17, ADAMTS19,* and Wnt signalling related genes e.g. *FZD3, FZD5, DVL3, FRAT2, CK2A2* were validated as direct targets of the miR-29 family.

CHAPTER 6
GENERAL DISCUSSION

6.1 Summary

This project has identified the miR-29 family as important miRNAs involved in both cartilage homeostasis and OA (Chapter 3). In the murine DMM model of OA at 1, 3, and 7 days after surgery, miRNA profile data from total RNA isolated from the whole knee joints showed that miR-29b was significantly increased at day 1 and showed a trend to decrease at day 3 and 7 after surgery. Integrating analysis between the mRNA profiling and miRNA profiling data from the DMM model strongly highlighted the role of the miR-29 family since the expression of its putative targets inversely correlated with its expression across the time course. In human end-stage hip OA cartilage, the miR-29 family was increased compared with the facture to neck of femur controls. Furthermore, in a murine hip injury model, the expression of the miR-29 family was increased across a 48 hour time course. The miR-29 family was also found to be involved in chondrocyte phenotype since the expression of all members of the miR-29 family decreased across dedifferentiation of human chondrocytes. In chondrogenesis, the miR-29 family was found to significantly decrease at an early stage, suggesting a negative role in this phase of chondrogenesis in both human and murine models. The miR-29 family was also found to be expressed in murine limb development.

The factors controlling miR-29 family expression are another important finding of this project (Chapter 4). The master regulator of chondrogenesis SOX9 was found to negatively regulate miR-29 expression, at least in part through directly binding to the promoter region of miR-29a/b1. A number of growth factors and cytokines were identified which regulate expression of the miR-29 family in both human primary chondrocytes and SW1353 cell line: TGFβ supressed miR-29 family expression; IL-1 strongly increased the miRNA expression through the p38 MAPK signalling pathway; treatment with LPS for less than 24 hours decreased expression of miR-29 through NFκB signalling whilst treatment with LPS for longer times increased miR-29 expression. Interestingly, in response to cytokines and growth factors, the miR-29 primary and precursor transcripts were regulated ahead the mature transcripts. This was explained in part by the fact that several components taking part in the miRNA precursor processing were possibly the miR-29 targets. Among these, Dicer-1 was proven as a miR-29 direct target.

Crucially, the functions of the miR-29 family in chondrocyte were also revealed in which miR-29 served as the negative regulator of the TGFβ/SMAD, NFκB and WNT/β-catenin signalling pathways. A number of novel direct targets of the miR-29 family have been found e.g. the ADAMTS family (*ADAMTS6, -10, -14, -17, -19*) and components of the Wnt signalling pathway (*FZD3, -5, FRAT2, CK2A2, DVL3*) (Chapter 5).

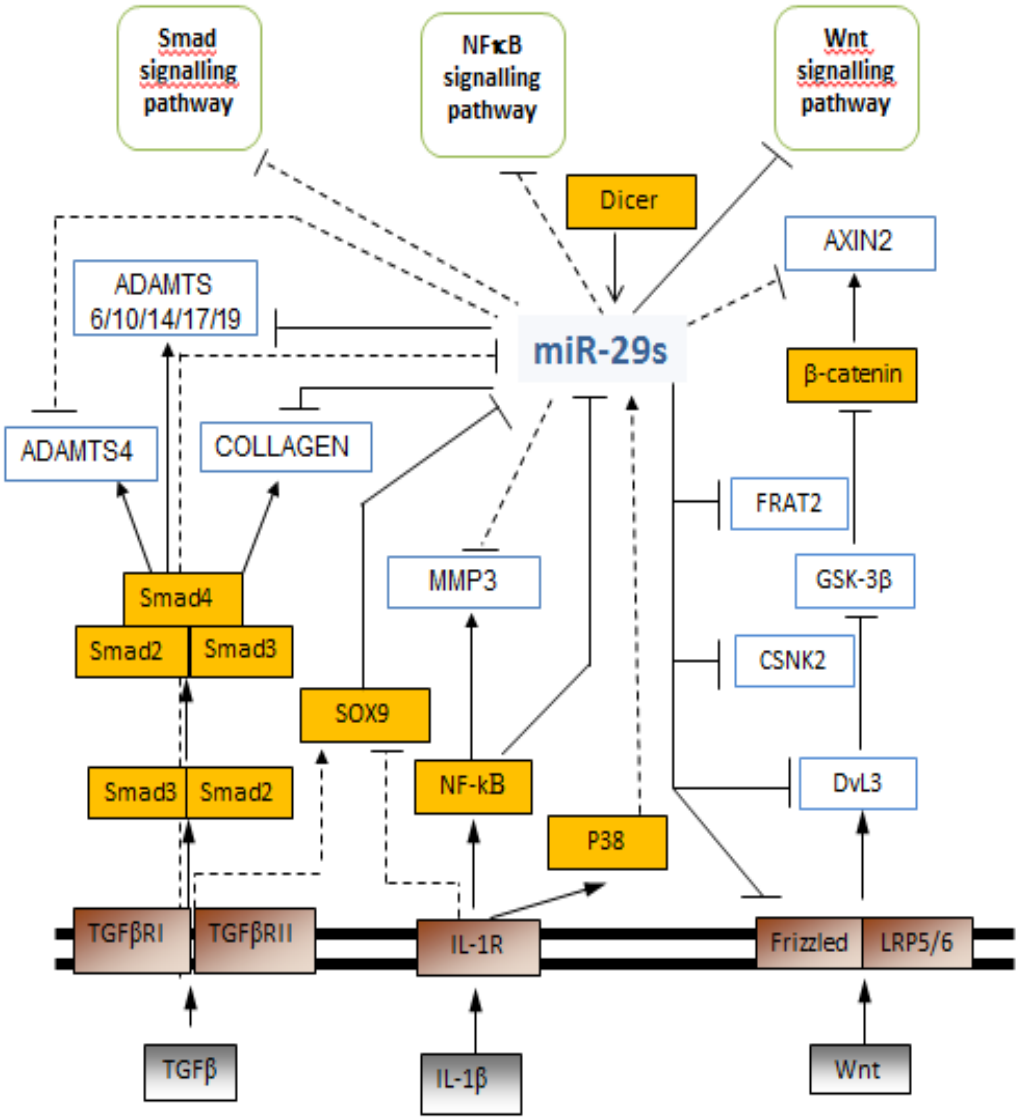

Figure 6.1. Summary of the role of the miR-29 family in chondrocytes

6.2 General discussion

6.2.1 Increased expression of the miR-29 family may contribute to the onset or progression of OA

The tight regulation of miRNA expression is crucial for cartilage homeostasis since the dysregulation of miRNAs may lead to OA. Especially, it has been shown that the aberrant expression of a single miRNA could have a profound effect on cartilage i.e. miR-140, with absence of miR-140 leading to premature OA (Miyaki et al. 2010). In the present study, all members of the miR-29 family have been implicated in cartilage homeostasis and OA. In both early and late stages of OA, an increase level of the miR-29 family was observed, suggesting that miR-29 may be involved in the onset of the disease. Moreover, in this study, the molecular mechanisms controlling this increased expression of miR-29 and the mechanisms by which increased miR-29 expression may lead to OA have been investigated: the miR-29 expression was up-regulated by IL-1, which is induced in both early and end stage OA, consequently suppressing both TGFβ and WNT/β-catenin signalling pathways. Since alteration of these two signalling pathways has been shown to be involved in OA development (Verrecchia et al. 2001, Verrecchia and Mauviel 2002, Zhu et al. 2008, Zhu et al. 2009), the increased expression level of the miR-29 family may contribute to this. In line with this, the miR-29 family was found to strongly suppress a number of ECM-related genes, especially collagens. Aggrecan was also found to be indirectly decreased by miR-29 (data not shown). However, more evidence is required to support this premise. If the increased expression level of miR-29 is a common observation in different OA models, this may also suggest that circulating miR-29 could be a biomarker for detecting early stage OA and also offers the possibility of using a miR-29 inhibitor as a novel treatment for OA. We are investigating the expression of the miR-29 family in the Str/ort model in collaboration with Dr Blandine Poulet (University College London, UK) and Professor Andy Pitsillides (Royal Veterinary College, London, UK).

The increased level of the miR-29 family may not be the only microRNA underlying the development of OA. In this project, miRNA profiling in the DMM model at 1, 3, and 7 days after surgery found a number of miRNAs modulated apart from miR-29s, suggesting these may also contribute to the pathogenesis of OA. Also, a number of miRNAs have been identified as differently expressed in human end stage OA cartilage as compared to the control counterparts. It is clear that in order to maintain cartilage homeostasis, miRNAs will interact with each other and mRNAs in a complex network that is tightly regulated. Thus, the up-regulation of miR-29 might be either the reason or the consequence of the deregulation of other networks of miRNAs. The question is how the other miRNAs interact with miR-29 and the effect of the increase expression of miR-29 on the miRNA/mRNA network in OA. This requires a computer modelling approach to resolve.

6.2.2 The signalling cascade IL-1/p38, IL-1/NFκB and the miR-29 family

Interestingly, in this study, it was found that whist IL-1 induced miR-29 expression through p38/MAPK, the NFκB pathway appears suppressive to miR-29 expression. In addition, the miRNA itself was found to suppress NFκB signalling. These data suggest that in response to the signalling cascade triggered by IL-1, the miR-29 expression level was induced through (i) induced expression of p38 MAPK and (ii) escape from the suppressive effect of NFκB through inhibiting the NFκB signalling pathway. However, the mechanism by which miR-29 suppressed NFκB signalling was not fully understood since the miR-29b gain- and loss- of function mRNA profiling experiment in human primary chondrocytes did not identify any potential targets related to the NFκB signalling pathway. It is a hypothesis that this suppressive effect could be an indirect effect or some potential targets could alter only at the protein level. Also, the direct mechanism through which p38 induced the miR-29 expression is not clear, even though in the promoter of miR-29a/b1 there are several binding sites for AP1 (data not shown). Interestingly, it is reported that p38 activation was found to induce NFκB activity in a dual way: by reducing IκB levels and by potentiating the translocation of p65/p50 (Baeza-Raja *et al.* 2004). Though evidence for this activation in human chondrocytes was not clear, the network controlling miR-29 expression in response to IL-1 becomes more complicated if this interaction is true in chondrocytes. Moreover, in this study, miR-29 was found to inhibit the pre-miRNA processing machinery to target Dicer and may also directly target other pre-miRNA processing genes, suggesting another regulatory layer for tightly

controlling the level of miR-29 in human chondrocytes. This could partly explain that the excessive amount of the miRNA in chondrocytes may lead to OA. Multiple regulatory layers are therefore needed for controlling miR-29 levels, clearly showed when the level of the primary miR-29 family was induced ahead of the level of mature miR-29 in chondrocytes stimulated with IL-1, TGFβ, and LPS. In the DMM model, miR-29 expression was induced 1 day after surgery together with the IL-1β expression level though this latter was not significant (data not shown), suggesting one possible explanation for the increase level of miR-29. However, it is unlikely that miR-29 was solely induced by IL-1 in the DMM model since the IL-1 level would have to be induced very early in order to then stimulate miR-29 expression. In line with this, mRNA profiling of DMM model 6 hours after surgery did not find a strongly induced expression of IL-1 (Burleigh et al. 2012). Similarly, in the murine hip injury model, the miR-29 expression level was also found to increase across the time course (reaching significance at 12 hours in culture). The precise mechanism for the increase expression of miR-29s in both DMM model and murine hip injury model are not clear and require further investigation.

6.2.3 The signalling cascade TGFβ/ Smad3 signalling pathway and the miR-29 family

In contrast with IL-1, TGFβ suppresses miR-29 expression. Since the miR-29 family directly targets a number of ECM-related genes, the suppressive effect TGFβ exerted on the miR-29 family is consistent with the well described protective effect of TGFβ in chondrocytes (Li et al. 2005). Interestingly, the miRNA itself gave a negative feedback loop on the TGFβ/Smad signalling pathway. This could be explained as an attempt to maintain miR-29 at homeostatic levels as TGFβ signalling becomes aberrant. This may also in part support the fact that an excessive amount of the miR-29 family could lead to OA: through suppressing Smad signalling and directly inhibiting responsive genes e.g. ECM related genes, the up-regulation of the miR-29s could strongly diminish the function of TGFβ in chondrocytes.

The precise mechanism by which TGFβ suppressed miR-29 expression and the mechanism by which miR-29 inhibited the TGFβ/Smad signalling were unclear. The miR-29b gain- and loss- of function mRNA profiling did not identify any TGFβ related potential targets, suggesting that this may also be at the protein level. Moreover, regarding the cellular context, when both IL-1 and TGFβ may be present, the cross talk between the two cytokines as well

as with other cytokines and growth factors in controlling the miR-29s expression levels are still unclear.

6.2.4 The canonical Wnt signalling and the miR-29 family

In this project, expression of the miR-29 family was not controlled by Wnt3a in chondrocytes. Since Wnt3a could trigger both canonical Wnt/β-catenin and CaMKII signalling pathways (Nalesso et al. 2011), it is likely that these two signalling pathways do not modulate the miR-29 levels in chondrocyte. However, expression ofmiR-29 was found to be induced by WNT3a in osteoblasts, suggesting a different mechanism controlling the miRNA-29 expression in the two cells types. The answer to this difference remains unknown and needs further investigation.

The canonical Wnt/β-catenin signalling pathway was inhibited by the miR-29 family in which some Wnt signalling related genes were validated as direct targets of the miRNA. Both over-activation and inhibition of Wnt signalling can lead to skeletal deformities and an early onset OA (Zhu et al. 2008, Zhu et al. 2009), illustrating that Wnt signalling needs to be tightly regulated in cartilage homeostasis. However, whether the decreasing of these direct targets is the mechanism for inhibition of the Wnt/β-catenin signalling pathway has not been confirmed in this study. This could be facilitated by utilizing siRNA to suppress the expression of each of these genes and measure this effect on the signalling though TOPFlash reporter.

6.2.5 Therapeautic applications for treating OA by targeting the miR-29 family

MicroRNAs have many advantages as a therapeutic modality. The mature miRNA sequences are short and often completely conserved across species. These characteristics make miRNAs relatively easy to target therapeutically and allow for using the same miRNA-modulating compound in preclinical efficacy and safety studies as well as in clinical trials. Moreover, miRNAs have typically many targets within cellular networks, which, in turn, enable modulation of entire pathways in a disease state via therapeutic targeting of disease – associated miRNAs.

The increase of the miR-29 family in OA potentially opens the door to develop a novel therapeutic strategy for OA. The therapeutic approach using **miRNA sponges** (transgenic

overexpression of RNA molecules harbouring complementary binding sites to a miRNA) or **miRNA-29 antagonists** to block the function of the endogenous miRNA-29s may have great promise as a novel treatment. The miRNA sponges have been proved to be successful in vivo whist the antagonists might have greater promise from a therapeutic perspective.

However, detailed examination of the miRNA therapy should be conducted before clinical use. Especially, the antagonists should have high binding affinity, and bio-stability. Indeed, this could be facilitated by chemically modifying them to increase the duplex melting temperature and improving nuclease resistance. Sugar modifications e.g. the 2'-O-methyl (2'-O-Me), 2'-O-Methoxyethyl (2'-MOE) 2'-fluoro and the bicyclic locked nucleic acid (LNA) modification are commonly used. Among these, the LNA exhibits the highest affinity toward complementary RNA with an increase in Tm of +2-8^{o}C per introduced LNA modification. In addition, by substituting the phosphodiester (PO) backbone linkages with phosphorothioate (PS) linkages in the antagonist oligonucleotides or by using peptide nucleic acid (PNA) or morpholino oligomers, respectively, their nuclease resistance properties might increase. Apart from nuclease resistance, PS backbone modifications also enhance binding to plasma proteins, leading to reduced clearance by glomerular filtration and urinary excretion. PNA oligomers are uncharged oligonucleotide analogues, in which the sugar-phosphate backbone has been replaced by a peptide-like backbone consisting of N-(2-aminoethyl)-glycine units. Polylysine-conjugated and nanoparticle-encapsulated PNA antimiRs have been shown to efficiently inhibit miRNA function in cultured cells and in mice (van Rooij *et al.* 2014). Morpholinos are uncharged and with slightly increased binding affinity to complementary miRNAs.

An effective way to deliver the miRNA-29 inhibitor to the arthritis joint to inhibit the endogenous miRNA-29 is needed. In particular, it is likely that the uptake of a synthetic antagonist into chondrocytes surrounded by the abundant matrix would be difficult in the treatment of damaged cartilage. The main challenge for development of miRNA - based therapeutics is efficient and safe delivery. Two strategies have been utilized to enhance in vivo delivery of antagonists: cholesterol conjugation and modification of the phosphate backbone with PS linkages. The 3' cholesterol conjugated, 2'-O-Me-modified antagonists have become a well-validated experimental tool for in vivo inhibition of miRNAs. PS backbone linkages can be employed to enhance the pharmacokinetic properties of antisense

oligonucleotides. The antagonist approach contains 2 PS modifications at the 5' end and 4 at the 3' end, which have been shown to be important for their in vivo activity, whereas complete replacement of the PO backbone by PS linkages decreased the antagonist efficiency. An increasing number of reports have described silencing of miRNA in vivo by unconjugated LNA-modified antagonists ranging from 8nt to 16nt in length as described in previous section. Administration of such antimiRs is either by intraperitoneal or subcutaneous injection resulted in antimiR uptake in the tissue of interest, which led to inhibition of miRNA function and derepression of direct target mRNAs. However, the mechanism of cellular uptake and distribution are still poorly understood. Directing uptake to cartilage is likely still to be difficult, and delivery by injection not pragmatic in OA.

6.3 Future direction

6.3.1 The modulation of the miR-29 family in OA

The miR-29 family was found to modulate expression in different animal models e.g. the DMM model, hip avulsion injury model, as well as human end stage OA cartilage. These data suggest that the increase in expression of the miR-29 family could be a common event in both early onset and end stage OA. However, care must be applied to conclude the up-regulation of miR-29s will lead to OA, with the expression level of miR-29s during OA progression remaining unclear. Thus, it is of importance to examine miR-29 expression in naturally occurring OA models too.

The miR-29 expression pattern increased in the hip avulsion injury across the time course in this study. Nonetheless, whether miR-29 potential targets were inversely correlated with the miR-29 expression level in this model has not been proven. Thus, we are performing mRNA profiling in the same samples in which the miR-29 expression was found to increase. This may also reveal additional mechanisms which lead to the increased expression of miR-29.

6.3.2 Biological functions of the miR-29 family in chondrocytes

The miR-29 family was found to suppress TGFβ/Smad, NFκB, and Wnt/β-catenin signalling pathways through using the reporters of these pathways together with measuring expression level of the responsive genes. However, whether interfering with the miR-29 effect on these signalling will lead to alter chondrocyte phenotype remains unclear. Overexpression and

knockdown of the miR-29 family in HACs in micromass culture in combination with measurement of chondrocyte markers e.g. *MMP13, COL2A1, SOX9, ADAMTS5* will help to address this.

From the miR-29b gain- and loss- of function mRNA data, apart from the Wnt signalling pathway, enrichment of some miR-29 potential targets which are related to MAPK signalling and apoptosis pathways was evident. Thus, validating these genes as the direct targets of the miR-29s is a priority in the future. It is now clear that miRNAs regulate gene expression at both mRNAs and protein levels. Also, the direct mechanisms the miR-29 supressing the two TGFβ and NFκB signalling pathways are unclear. Therefore, there is a need for proteomic analysis of the miR-29b gain- and loss- of function in HACs, likely in micromass culture. In addition, performing miR-29b gain – and loss - of function together with treatment with IL-1 and TGFβ could greatly help to find the mechanism miR-29 family interfering with NFκB and Smad signalling pathways. All of these experiments will give more information about biological functions of miR-29 in chondrocyte and the complex regulatory network the miR-29 is within.

A key step in understanding the biological functions of the miR-29 family in cartilage homeostasis and OA will be the development of multiple in vivo molecular tools to access gain – of – functions or loss – of – function in mouse models: A number of gain- of –function where the miR-29 family members are overexpressed through a transgenic model, such as the B cell – specific overexpression of the miR-29a/b1 cluster (Santanam et al. 2010), a viral transfection model such as the retroviral transfection of bone-marrow stem cells with miR-29a (Han *et al.* 2010) or systemic delivery of miR-29a have been reported (Wang *et al.* 2012). Also, loss-of-function models have been developed as a Cre-Lox-inducible knockout of the miR-29a/b-1 cluster or the expression of the miR-29 “sponge” sequence (either by transgene or lentivirus) (Ma et al. 2011). However, there is no information whether gain – and loss- of function of the miR-29s lead to OA in these models. Therefore, future studies in which these mice put on OA models e.g. DMM will provide more detail about the function of the miR-29 family.

6.3.3 The involvement of the miR-29 family expression in chick limb bud development and Zebrafish cartilage development.

The miR-29 family was suggested to be a negative regulator of early stage of chondrogenesis in both human and murine chondrogenesis models in this study. Nearly 16 collagen genes were validated as miR-29 direct targets in this study and others. Also, this miRNA was also expressed in murine limb development. It is likely that miR-29 would have a crucial role in cartilage and limb bud development and it is worthy of further investigation. This could be facilitated by again using the gain- and loss- of function of all members of the miR-29 family: a 500bp region around the mature sequence of the miR-29s or a sequence complementary to miR-29 can be subcloned and injected into the chicken limb. However, the involvement of the miR-29 family in chick limb development by in situ hybridization might be required to determine the stage in which miR-29 was expressed in the development process. In addition, ADAMTS14, a pro-collagen pro-peptidase, was validated as the miR-29 direct target. Overexpression or knockdown of the miR-29 family in chick limb could help to further investigate the functional outcome of the suppressive effect of the miR-29s on ADAMTS14 though the ADAMTS14 will need to be verified to be expressed in the chick limb first. This method could be useful for investigating the functional outcome of the interaction between miR-29 and other novel targets.

Interesting, the miR-29 family was found to be express in the cartilage of zebrafish (Wienholds et al. 2005). Thus, zebrafish might be a useful model for investigating the role of the miR-29s in cartilage development. Overexpression and knockdown of the miR-29 family could greatly help for answering this question.

6.3.4 The miR-29 family as the biomarker for OA

MicroRNAs exist in human body fluids such as plasma, urine, and saliva in a stable form which has the potential to be a novel diagnostic and prognostic biomarker. OA can be difficult to diagnose, but it is important to diagnose OA early and start treatment to prevent joint destruction in which the miR-29 based therapy could be an option. Indeed, there is growing evidence for future miRNA-based diagnostics: a number of miRNA in plasma were found at different levels between RA and OA patients. For examples, let-7e, miR-454, miR-886 were identified as differentially expressed circulating miRNAs in OA patients who underwent arthroplasty especially, let–7e emerged as potential predictor for severe knee or hip OA (Beyer et al. 2014). Since the miR-29 family was modulated at an early stage in DMM model, it could be a useful biomarker for OA in clinical use. Thus the expression level

of the miR-29 family in plasma should be determined to have an overview expression pattern of the miRNA.

REFERENCES

Abouheif, M., T. Nakasa, H. Shibuya, T. Niimoto, W. Kongcharoensombat and M. Ochi (2010). "Silencing microRNA-34a inhibits chondrocyte apoptosis in a rat osteoarthritis model in vitro." Rheumatology (Oxford, England) **49**(11): 2054-2060.

Abrahante, J., A. Daul, M. Li, M. Volk, J. Tennessen, E. Miller and A. Rougvie (2003). "The Caenorhabditis elegans hunchback-like Gene lin-57/hbl-1 Controls Developmental Time and Is Regulated by MicroRNAs." Developmental Cell **4**(5): 625-637.

Ahluwalia, J. K., S. Z. Khan, K. Soni, P. Rawat, A. Gupta, M. Hariharan, V. Scaria, M. Lalwani, B. Pillai, D. Mitra and S. K. Brahmachari (2008). "Human cellular microRNA hsa-miR-29a interferes with viral nef protein expression and HIV-1 replication." Retrovirology **5**: 117.

Aigner, T., W. Bertling, H. Stoss, G. Weseloh and K. von der Mark (1993). "Independent expression of fibril-forming collagens I, II, and III in chondrocytes of human osteoarthritic cartilage." J Clin Invest **91**(3): 829-837.

Aigner, T., A. Sachse, P. M. Gebhard and H. I. Roach (2006). "Osteoarthritis: pathobiology-targets and ways for therapeutic intervention." Adv Drug Deliv Rev **58**(2): 128-149.

Aigner, T., S. Soeder and J. Haag (2006). "IL-1beta and BMPs--interactive players of cartilage matrix degradation and regeneration." Eur Cell Mater **12**: 49-56; discussion 56.

Akhtar, N., Z. Rasheed, S. Ramamurthy, A. Anbazhagan, F. Voss and T. Haqqi (2010). "MicroRNA-27b regulates the expression of matrix metalloproteinase 13 in human osteoarthritis chondrocytes." Arthritis & Rheumatism **62**(5): 1361-1371.

(2010). "MicroRNA-27b regulates the expression of matrix metalloproteinase 13 in human osteoarthritis chondrocytes." Arthritis and rheumatism **62**(5): 1361-1371.

Akiyama, H., M. C. Chaboissier, J. F. Martin, A. Schedl and B. de Crombrugghe (2002). "The transcription factor Sox9 has essential roles in successive steps of the chondrocyte differentiation pathway and is required for expression of Sox5 and Sox6." Genes Dev **16**(21): 2813-2828.

Amarilio, R., S. V. Viukov, A. Sharir, I. Eshkar-Oren, R. S. Johnson and E. Zelzer (2007). "HIF1alpha regulation of Sox9 is necessary to maintain differentiation of hypoxic prechondrogenic cells during early skeletogenesis." Development **134**(21): 3917-3928.

Ambros, V. (2004). "The functions of animal microRNAs." Nature **431**(7006): 350-355.

Amodio, N., M. T. Di Martino, U. Foresta, E. Leone, M. Lionetti, M. Leotta, A. M. Gulla, M. R. Pitari, F. Conforti, M. Rossi, V. Agosti, M. Fulciniti, G. Misso, F. Morabito, M. Ferrarini, A. Neri, M. Caraglia, N. C. Munshi, K. C. Anderson, P. Tagliaferri and P. Tassone (2012). "miR-29b sensitizes multiple myeloma cells to bortezomib-induced apoptosis through the activation of a feedback loop with the transcription factor Sp1." Cell Death Dis **3**: e436.

Amodio, N., M. Leotta, D. Bellizzi, M. T. Di Martino, P. D'Aquila, M. Lionetti, F. Fabiani, E. Leone, A. M. Gulla, G. Passarino, M. Caraglia, M. Negrini, A. Neri, A. Giordano, P. Tagliaferri and P. Tassone (2012). "DNA-demethylating and anti-tumor activity of synthetic miR-29b mimics in multiple myeloma." Oncotarget **3**(10): 1246-1258.

Amos, N., S. Lauder, A. Evans, M. Feldmann and J. Bondeson (2006). "Adenoviral gene transfer into osteoarthritis synovial cells using the endogenous inhibitor IkappaBalpha reveals that most, but not all, inflammatory and destructive mediators are NFkappaB dependent." Rheumatology (Oxford) **45**(10): 1201-1209.

Arner, E. C. (2002). "Aggrecanase-mediated cartilage degradation." Curr Opin Pharmacol **2**(3): 322-329.

Arroyo, J., J. Chevillet, E. Kroh, I. Ruf, C. Pritchard, D. Gibson, P. Mitchell, C. Bennett, E. Pogosova-Agadjanyan, D. Stirewalt, J. Tait and M. Tewari (2011). "Argonaute2 complexes carry a

population of circulating microRNAs independent of vesicles in human plasma." Proceedings of the National Academy of Sciences **108**(12): 5003-5008.
Avasarala, S., M. Van Scoyk, J. Wang, M. Sechler, K. Vandervest, C. Brzezinski, C. Weekes, M. G. Edwards, J. Arcaroli, R. E. Davis, R. K. Bikkavilli and R. A. Winn (2013). "hsa-miR29b, a critical downstream target of non-canonical Wnt signaling, plays an anti-proliferative role in non-small cell lung cancer cells via targeting MDM2 expression." Biol Open **2**(7): 675-685.
Baeza-Raja, B. and P. Munoz-Canoves (2004). "p38 MAPK-induced nuclear factor-kappaB activity is required for skeletal muscle differentiation: role of interleukin-6." Mol Biol Cell **15**(4): 2013-2026.
Baker-Lepain, J. C., J. A. Lynch, N. Parimi, C. E. McCulloch, M. C. Nevitt, M. Corr and N. E. Lane (2012). "Variant alleles of the Wnt antagonist FRZB are determinants of hip shape and modify the relationship between hip shape and osteoarthritis." Arthritis Rheum **64**(5): 1457-1465.
Bartel, D. (2004). "MicroRNAs: genomics, biogenesis, mechanism, and function." Cell **116**(2): 281-297.
(2009). "MicroRNAs: target recognition and regulatory functions." Cell **136**(2): 215-233.
Benito, M. J., D. J. Veale, O. FitzGerald, W. B. van den Berg and B. Bresnihan (2005). "Synovial tissue inflammation in early and late osteoarthritis." Ann Rheum Dis **64**(9): 1263-1267.
Berezikov, E., W.-J. Chung, J. Willis, E. Cuppen and E. Lai (2007). "Mammalian mirtron genes." Mol Cell **28**(2): 328-336.
Beyer, C., A. Zampetaki, N. Y. Lin, A. Kleyer, C. Perricone, A. Iagnocco, A. Distler, S. R. Langley, K. Gelse, S. Sesselmann, R. Lorenzini, A. Niemeier, B. Swoboda, J. H. Distler, P. Santer, G. Egger, J. Willeit, M. Mayr, G. Schett and S. Kiechl (2014). "Signature of circulating microRNAs in osteoarthritis." Ann Rheum Dis.
Bi, W., J. M. Deng, Z. Zhang, R. R. Behringer and B. de Crombrugghe (1999). "Sox9 is required for cartilage formation." Nat Genet **22**(1): 85-89.
Billinghurst, R. C., L. Dahlberg, M. Ionescu, A. Reiner, R. Bourne, C. Rorabeck, P. Mitchell, J. Hambor, O. Diekmann, H. Tschesche, J. Chen, H. Van Wart and A. R. Poole (1997). "Enhanced cleavage of type II collagen by collagenases in osteoarthritic articular cartilage." J Clin Invest **99**(7): 1534-1545.
Blom, A. B., S. M. Brockbank, P. L. van Lent, H. M. van Beuningen, J. Geurts, N. Takahashi, P. M. van der Kraan, F. A. van de Loo, B. W. Schreurs, K. Clements, P. Newham and W. B. van den Berg (2009). "Involvement of the Wnt signaling pathway in experimental and human osteoarthritis: prominent role of Wnt-induced signaling protein 1." Arthritis Rheum **60**(2): 501-512.
Bobacz, K., I. G. Sunk, J. G. Hofstaetter, L. Amoyo, C. D. Toma, S. Akira, T. Weichhart, M. Saemann and J. S. Smolen (2007). "Toll-like receptors and chondrocytes: the lipopolysaccharide-induced decrease in cartilage matrix synthesis is dependent on the presence of toll-like receptor 4 and antagonized by bone morphogenetic protein 7." Arthritis Rheum **56**(6): 1880-1893.
Bohnsack, M., K. Czaplinski and D. Gorlich (2004). "Exportin 5 is a RanGTP-dependent dsRNA-binding protein that mediates nuclear export of pre-miRNAs." RNA (New York, N.Y.) **10**(2): 185-191.
Bondeson, J., A. B. Blom, S. Wainwright, C. Hughes, B. Caterson and W. B. van den Berg (2010). "The role of synovial macrophages and macrophage-produced mediators in driving inflammatory and destructive responses in osteoarthritis." Arthritis Rheum **62**(3): 647-657.
Bondeson, J., S. Lauder, S. Wainwright, N. Amos, A. Evans, C. Hughes, M. Feldmann and B. Caterson (2007). "Adenoviral gene transfer of the endogenous inhibitor IkappaBalpha into human osteoarthritis synovial fibroblasts demonstrates that several matrix metalloproteinases and aggrecanases are nuclear factor-kappaB-dependent." J Rheumatol **34**(3): 523-533.
Bossé, G. and M. Simard (2010). "A new twist in the microRNA pathway: Not Dicer but Argonaute is required for a microRNA production." Cell Res **20**(7): 735-737.

Brennecke, J., A. Stark, R. Russell and S. Cohen (2005). "Principles of MicroRNA–Target Recognition." PLoS Biol **3**(3): e85.

Brunner, A. M., C. M. Henn, E. I. Drewniak, A. Lesieur-Brooks, J. Machan, J. J. Crisco and M. G. Ehrlich (2012). "High dietary fat and the development of osteoarthritis in a rabbit model." Osteoarthritis Cartilage **20**(6): 584-592.

Buckwalter, J. A., H. J. Mankin and A. J. Grodzinsky (2005). "Articular cartilage and osteoarthritis." Instr Course Lect **54**: 465-480.

Burleigh, A., A. Chanalaris, M. Gardiner, C. Driscoll, O. Boruc, J. Saklatvala and T. Vincent (2012). "Joint immobilisation prevents murine osteoarthritis, and reveals the highly mechanosensitive nature of protease expression in vivo." Arthritis Rheum: n/a-n/a.

Burleigh, A., A. Chanalaris, M. D. Gardiner, C. Driscoll, O. Boruc, J. Saklatvala and T. L. Vincent (2012). "Joint immobilization prevents murine osteoarthritis and reveals the highly mechanosensitive nature of protease expression in vivo." Arthritis Rheum **64**(7): 2278-2288.

Burrage, P. S., K. S. Mix and C. E. Brinckerhoff (2006). "Matrix metalloproteinases: role in arthritis." Front Biosci **11**: 529-543.

Caetano-Lopes, J., H. Canhao and J. E. Fonseca (2007). "Osteoblasts and bone formation." Acta Reumatol Port **32**(2): 103-110.

Cai, J., G. Yin, B. Lin, X. Wang, X. Liu, X. Chen, D. Yan, G. Shan, J. Qu and S. Wu (2014). "Roles of NFkappaB-miR-29s-MMP-2 circuitry in experimental choroidal neovascularization." J Neuroinflammation **11**: 88.

Cai, X., C. Hagedorn and B. Cullen (2004). "Human microRNAs are processed from capped, polyadenylated transcripts that can also function as mRNAs." RNA (New York, N.Y.) **10**(12): 1957-1966.

Carmon, K. S. and D. S. Loose (2008). "Secreted frizzled-related protein 4 regulates two Wnt7a signaling pathways and inhibits proliferation in endometrial cancer cells." Mol Cancer Res **6**(6): 1017-1028.

Chalfie, M. (1981). "Mutations that lead to reiterations in the cell lineages of C. elegans." Cell **24**(1): 59-69.

Chang, T. C., D. Yu, Y. S. Lee, E. A. Wentzel, D. E. Arking, K. M. West, C. V. Dang, A. Thomas-Tikhonenko and J. T. Mendell (2008). "Widespread microRNA repression by Myc contributes to tumorigenesis." Nat Genet **40**(1): 43-50.

Chen, C., D. Ridzon, A. Broomer, Z. Zhou, D. Lee, J. Nguyen, M. Barbisin, N. Xu, V. Mahuvakar, M. Andersen, K. Lao, K. Livak and K. Guegler (2005). "Real-time quantification of microRNAs by stem–loop RT–PCR." Nucleic Acids Res **33**(20): e179-e179.

Chen, L. X., L. Lin, H. J. Wang, X. L. Wei, X. Fu, J. Y. Zhang and C. L. Yu (2008). "Suppression of early experimental osteoarthritis by in vivo delivery of the adenoviral vector-mediated NF-kappaBp65-specific siRNA." Osteoarthritis Cartilage **16**(2): 174-184.

Chen, X., Y. Ba, L. Ma, X. Cai, Y. Yin, K. Wang, J. Guo, Y. Zhang, J. Chen, X. Guo, Q. Li, X. Li, W. Wang, Y. Zhang, J. Wang, X. Jiang, Y. Xiang, C. Xu, P. Zheng, J. Zhang, R. Li, H. Zhang, X. Shang, T. Gong, G. Ning, J. Wang, K. Zen, J. Zhang and C.-Y. Zhang (2008). "Characterization of microRNAs in serum: a novel class of biomarkers for diagnosis of cancer and other diseases." Cell Res **18**(10): 997-1006.

Chendrimada, T., R. Gregory, E. Kumaraswamy, J. Norman, N. Cooch, K. Nishikura and R. Shiekhattar (2005). "TRBP recruits the Dicer complex to Ago2 for microRNA processing and gene silencing." Nature **436**(7051): 740-744.

Chong, K. W., A. Chanalaris, A. Burleigh, H. Jin, F. E. Watt, J. Saklatvala and T. L. Vincent (2013). "Fibroblast growth factor 2 drives changes in gene expression following injury to murine cartilage in vitro and in vivo." Arthritis Rheum **65**(9): 2346-2355.

Chou, J., J. H. Lin, A. Brenot, J. W. Kim, S. Provot and Z. Werb (2013). "GATA3 suppresses metastasis and modulates the tumour microenvironment by regulating microRNA-29b expression." Nat Cell Biol **15**(2): 201-213.

Clements, K. M., J. S. Price, M. G. Chambers, D. M. Visco, A. R. Poole and R. M. Mason (2003). "Gene deletion of either interleukin-1beta, interleukin-1beta-converting enzyme, inducible nitric oxide synthase, or stromelysin 1 accelerates the development of knee osteoarthritis in mice after surgical transection of the medial collateral ligament and partial medial meniscectomy." Arthritis Rheum **48**(12): 3452-3463.

Clevers, H. (2006). "Wnt/beta-catenin signaling in development and disease." Cell **127**(3): 469-480.

Cochrane, D. R., D. M. Cittelly, E. N. Howe, N. S. Spoelstra, E. L. McKinsey, K. LaPara, A. Elias, D. Yee and J. K. Richer (2010). "MicroRNAs link estrogen receptor alpha status and Dicer levels in breast cancer." Horm Cancer **1**(6): 306-319.

Colige, A., I. Vandenberghe, M. Thiry, C. A. Lambert, J. Van Beeumen, S. W. Li, D. J. Prockop, C. M. Lapiere and B. V. Nusgens (2002). "Cloning and characterization of ADAMTS-14, a novel ADAMTS displaying high homology with ADAMTS-2 and ADAMTS-3." J Biol Chem **277**(8): 5756-5766.

Cortez, M. A., M. S. Nicoloso, M. Shimizu, S. Rossi, G. Gopisetty, J. R. Molina, C. Carlotti, Jr., D. Tirapelli, L. Neder, M. S. Brassesco, C. A. Scrideli, L. G. Tone, M. M. Georgescu, W. Zhang, V. Puduvalli and G. A. Calin (2010). "miR-29b and miR-125a regulate podoplanin and suppress invasion in glioblastoma." Genes Chromosomes Cancer **49**(11): 981-990.

Cushing, L., P. P. Kuang, J. Qian, F. Shao, J. Wu, F. Little, V. J. Thannickal, W. V. Cardoso and J. Lu (2011). "miR-29 is a major regulator of genes associated with pulmonary fibrosis." Am J Respir Cell Mol Biol **45**(2): 287-294.

Davidson, R. K., J. G. Waters, L. Kevorkian, C. Darrah, A. Cooper, S. T. Donell and I. M. Clark (2006). "Expression profiling of metalloproteinases and their inhibitors in synovium and cartilage." Arthritis Res Ther **8**(4): R124.

DeLise, A. M., L. Fischer and R. S. Tuan (2000). "Cellular interactions and signaling in cartilage development." Osteoarthritis Cartilage **8**(5): 309-334.

Dell'accio, F., C. De Bari, N. M. Eltawil, P. Vanhummelen and C. Pitzalis (2008). "Identification of the molecular response of articular cartilage to injury, by microarray screening: Wnt-16 expression and signaling after injury and in osteoarthritis." Arthritis Rheum **58**(5): 1410-1421.

Diarra, D., M. Stolina, K. Polzer, J. Zwerina, M. S. Ominsky, D. Dwyer, A. Korb, J. Smolen, M. Hoffmann, C. Scheinecker, D. van der Heide, R. Landewe, D. Lacey, W. G. Richards and G. Schett (2007). "Dickkopf-1 is a master regulator of joint remodeling." Nat Med **13**(2): 156-163.

Dudek, K., J. Lafont, A. Martinez-Sanchez and C. Murphy (2010). "Type II collagen expression is regulated by tissue-specific miR-675 in human articular chondrocytes." The Journal of biological chemistry **285**(32): 24381-24387.

(2010). "Type II collagen expression is regulated by tissue-specific miR-675 in human articular chondrocytes." Journal of Biological Chemistry **285**(32): 24381-24387.

Dudhia, J. (2005). "Aggrecan, aging and assembly in articular cartilage." Cell Mol Life Sci **62**(19-20): 2241-2256.

Dueck, A. and G. Meister (2010). "MicroRNA processing without Dicer." Genome Biol **11**(6): 123.

Dunn, W., G. DuRaine and H. Reddi (2009). "Profiling microRNA expression in bovine articular cartilage and implications for mechanotransduction." Arthritis & Rheumatism **60**(8): 2333-2339.

(2009). "Profiling microRNA expression in bovine articular cartilage and implications for mechanotransduction." Arthritis and rheumatism **60**(8): 2333-2339.

Elmen, J., M. Lindow, S. Schutz, M. Lawrence, A. Petri, S. Obad, M. Lindholm, M. Hedtjarn, H. Hansen, U. Berger, S. Gullans, P. Kearney, P. Sarnow, E. Straarup and S. Kauppinen (2008). "LNA-mediated microRNA silencing in non-human primates." Nature **452**(7189): 896-899.

Esau, C., S. Davis, S. Murray, X. X. Yu, S. Pandey, M. Pear, L. Watts, S. Booten, M. Graham, R. McKay, A. Subramaniam, S. Propp, B. Lollo, S. Freier, F. Bennett, S. Bhanot and B. Monia (2006). "miR-122 regulation of lipid metabolism revealed by in vivo antisense targeting." Cell Metabolism **3**(2): 87-98.

Eyholzer, M., S. Schmid, L. Wilkens, B. U. Mueller and T. Pabst (2010). "The tumour-suppressive miR-29a/b1 cluster is regulated by CEBPA and blocked in human AML." Br J Cancer **103**(2): 275-284.

Fabbri, M., R. Garzon, A. Cimmino, Z. Liu, N. Zanesi, E. Callegari, S. Liu, H. Alder, S. Costinean, C. Fernandez-Cymering, S. Volinia, G. Guler, C. D. Morrison, K. K. Chan, G. Marcucci, G. A. Calin, K. Huebner and C. M. Croce (2007). "MicroRNA-29 family reverts aberrant methylation in lung cancer by targeting DNA methyltransferases 3A and 3B." Proc Natl Acad Sci U S A **104**(40): 15805-15810.

Fan, Z., S. Soder, S. Oehler, K. Fundel and T. Aigner (2007). "Activation of interleukin-1 signaling cascades in normal and osteoarthritic articular cartilage." Am J Pathol **171**(3): 938-946.

Fang, J. H., H. C. Zhou, C. Zeng, J. Yang, Y. Liu, X. Huang, J. P. Zhang, X. Y. Guan and S. M. Zhuang (2011). "MicroRNA-29b suppresses tumor angiogenesis, invasion, and metastasis by regulating matrix metalloproteinase 2 expression." Hepatology **54**(5): 1729-1740.

Fell, H. B. (1978). "Synoviocytes." J Clin Pathol Suppl (R Coll Pathol) **12**: 14-24.

Fenn, A. M., K. M. Smith, A. E. Lovett-Racke, M. Guerau-de-Arellano, C. C. Whitacre and J. P. Godbout (2013). "Increased micro-RNA 29b in the aged brain correlates with the reduction of insulin-like growth factor-1 and fractalkine ligand." Neurobiol Aging **34**(12): 2748-2758.

Fernandes, R. J., S. Hirohata, J. M. Engle, A. Colige, D. H. Cohn, D. R. Eyre and S. S. Apte (2001). "Procollagen II amino propeptide processing by ADAMTS-3. Insights on dermatosparaxis." J Biol Chem **276**(34): 31502-31509.

Ferracin, M., A. Veronese and M. Negrini (2010). "Micromarkers: miRNAs in cancer diagnosis and prognosis." Expert review of Molecular Diagnostics **10**(3): 297-308.

Forsbach, A., J. G. Nemorin, C. Montino, C. Muller, U. Samulowitz, A. P. Vicari, M. Jurk, G. K. Mutwiri, A. M. Krieg, G. B. Lipford and J. Vollmer (2008). "Identification of RNA sequence motifs stimulating sequence-specific TLR8-dependent immune responses." J Immunol **180**(6): 3729-3738.

Friedman, R., K. Farh, C. Burge and D. Bartel (2009). "Most mammalian mRNAs are conserved targets of microRNAs." Genome Res **19**(1): 92-105.

Frisbie, D. D., S. C. Ghivizzani, P. D. Robbins, C. H. Evans and C. W. McIlwraith (2002). "Treatment of experimental equine osteoarthritis by in vivo delivery of the equine interleukin-1 receptor antagonist gene." Gene Ther **9**(1): 12-20.

Garzon, R., C. E. Heaphy, V. Havelange, M. Fabbri, S. Volinia, T. Tsao, N. Zanesi, S. M. Kornblau, G. Marcucci, G. A. Calin, M. Andreeff and C. M. Croce (2009). "MicroRNA 29b functions in acute myeloid leukemia." Blood **114**(26): 5331-5341.

Gierman, L. M., F. van der Ham, A. Koudijs, P. Y. Wielinga, R. Kleemann, T. Kooistra, R. Stoop, M. Kloppenburg, G. J. van Osch, V. Stojanovic-Susulic, T. W. Huizinga and A. M. Zuurmond (2012). "Metabolic stress-induced inflammation plays a major role in the development of osteoarthritis in mice." Arthritis Rheum **64**(4): 1172-1181.

Gilad, S., E. Meiri, Y. Yogev, S. Benjamin, D. Lebanony, N. Yerushalmi, H. Benjamin, M. Kushnir, H. Cholakh, N. Melamed, Z. Bentwich, M. Hod, Y. Goren and A. Chajut (2008). "Serum MicroRNAs Are Promising Novel Biomarkers." PLoS One **3**(9): e3148.

Girkontaite, I., S. Frischholz, P. Lammi, K. Wagner, B. Swoboda, T. Aigner and K. Von der Mark (1996). "Immunolocalization of type X collagen in normal fetal and adult osteoarthritic cartilage with monoclonal antibodies." Matrix Biol **15**(4): 231-238.

Glasson, S. S., R. Askew, B. Sheppard, B. Carito, T. Blanchet, H. L. Ma, C. R. Flannery, D. Peluso, K. Kanki, Z. Yang, M. K. Majumdar and E. A. Morris (2005). "Deletion of active ADAMTS5 prevents cartilage degradation in a murine model of osteoarthritis." Nature **434**(7033): 644-648.

Goldring, M., K. Tsuchimochi and K. Ijiri (2006). "The control of chondrogenesis." J Cell Biochem **97**(1): 33-44.

Goldring, M. B. (2000). "Osteoarthritis and cartilage: the role of cytokines." Curr Rheumatol Rep **2**(6): 459-465.

(2012). "Chondrogenesis, chondrocyte differentiation, and articular cartilage metabolism in health and osteoarthritis." Ther Adv Musculoskelet Dis **4**(4): 269-285.

Goldring, M. B., J. Birkhead, L. J. Sandell, T. Kimura and S. M. Krane (1988). "Interleukin 1 suppresses expression of cartilage-specific types II and IX collagens and increases types I and III collagens in human chondrocytes." J Clin Invest **82**(6): 2026-2037.

Goldring, M. B. and S. R. Goldring (2007). "Osteoarthritis." J Cell Physiol **213**(3): 626-634.

Goldring, M. B., K. Tsuchimochi and K. Ijiri (2006). "The control of chondrogenesis." J Cell Biochem **97**(1): 33-44.

Goldring, S. R. and M. B. Goldring (2004). "The role of cytokines in cartilage matrix degeneration in osteoarthritis." Clin Orthop Relat Res(427 Suppl): S27-36.

Greco, K. V., A. J. Iqbal, L. Rattazzi, G. Nalesso, N. Moradi-Bidhendi, A. R. Moore, M. B. Goldring, F. Dell'Accio and M. Perretti (2011). "High density micromass cultures of a human chondrocyte cell line: a reliable assay system to reveal the modulatory functions of pharmacological agents." Biochem Pharmacol **82**(12): 1919-1929.

Griffin, T. M., J. L. Huebner, V. B. Kraus and F. Guilak (2009). "Extreme obesity due to impaired leptin signaling in mice does not cause knee osteoarthritis." Arthritis Rheum **60**(10): 2935-2944.

Grishok, A., A. E. Pasquinelli, D. Conte, N. Li, S. Parrish, I. Ha, D. L. Baillie, A. Fire, G. Ruvkun and C. C. Mello (2001). "Genes and mechanisms related to RNA interference regulate expression of the small temporal RNAs that control C. elegans developmental timing." Cell **106**(1): 23-34.

Grotle, M., K. B. Hagen, B. Natvig, F. A. Dahl and T. K. Kvien (2008). "Obesity and osteoarthritis in knee, hip and/or hand: an epidemiological study in the general population with 10 years follow-up." BMC Musculoskelet Disord **9**: 132.

Guan, Y.-J., X. Yang, L. Wei and Q. Chen (2011). "MiR-365: a mechanosensitive microRNA stimulates chondrocyte differentiation through targeting histone deacetylase 4." FASEB Journal **25**(12): 4457-4466.

Guerit, D., J. M. Brondello, P. Chuchana, D. Philipot, K. Toupet, C. Bony, C. Jorgensen and D. Noel (2014). "FoxO3a regulation by miRNA-29a controls chondrogenic differentiation of mesenchymal stem cells and cartilage formation." Stem Cells Dev.

Guilak, F., D. L. Butler and S. A. Goldstein (2001). "Functional tissue engineering: the role of biomechanics in articular cartilage repair." Clin Orthop Relat Res(391 Suppl).

Hammerlein, A., J. Weiske and O. Huber (2005). "A second protein kinase CK1-mediated step negatively regulates Wnt signalling by disrupting the lymphocyte enhancer factor-1/beta-catenin complex." Cell Mol Life Sci **62**(5): 606-618.

Hammond, S. M., E. Bernstein, D. Beach and G. J. Hannon (2000). "An RNA-directed nuclease mediates post-transcriptional gene silencing in Drosophila cells." Nature **404**(6775): 293-296.

Han, J., Y. Lee, K.-H. Yeom, Y.-K. Kim, H. Jin and N. Kim (2004). "The Drosha-DGCR8 complex in primary microRNA processing." Genes Dev **18**(24): 3016-3027.

Han, Y. C., C. Y. Park, G. Bhagat, J. Zhang, Y. Wang, J. B. Fan, M. Liu, Y. Zou, I. L. Weissman and H. Gu (2010). "microRNA-29a induces aberrant self-renewal capacity in hematopoietic progenitors, biased myeloid development, and acute myeloid leukemia." J Exp Med **207**(3): 475-489.

Hansen, C., J. Howlin, A. Tengholm, O. Dyachok, W. F. Vogel, A. C. Nairn, P. Greengard and T. Andersson (2009). "Wnt-5a-induced phosphorylation of DARPP-32 inhibits breast cancer cell migration in a CREB-dependent manner." J Biol Chem **284**(40): 27533-27543.

Harfe, B., M. McManus, J. Mansfield, E. Hornstein and C. Tabin (2005). "The RNaseIII enzyme Dicer is required for morphogenesis but not patterning of the vertebrate limb." Proc Natl Acad Sci U S A **102**(31): 10898-10903.

He, A., L. Zhu, N. Gupta, Y. Chang and F. Fang (2007). "Overexpression of micro ribonucleic acid 29, highly up-regulated in diabetic rats, leads to insulin resistance in 3T3-L1 adipocytes." Mol Endocrinol **21**(11): 2785-2794.

He, X., J. P. Saint-Jeannet, Y. Wang, J. Nathans, I. Dawid and H. Varmus (1997). "A member of the Frizzled protein family mediating axis induction by Wnt-5A." Science **275**(5306): 1652-1654.

Hebert, S. S., K. Horre, L. Nicolai, A. S. Papadopoulou, W. Mandemakers, A. N. Silahtaroglu, S. Kauppinen, A. Delacourte and B. De Strooper (2008). "Loss of microRNA cluster miR-29a/b-1 in sporadic Alzheimer's disease correlates with increased BACE1/beta-secretase expression." Proc Natl Acad Sci U S A **105**(17): 6415-6420.

Heimberg, A., L. Sempere, V. Moy, P. Donoghue and K. Peterson (2008). "MicroRNAs and the advent of vertebrate morphological complexity." Proceedings of the National Academy of Sciences **105**(8): 2946-2950.

Heinegard, D. and T. Saxne (2011). "The role of the cartilage matrix in osteoarthritis." Nat Rev Rheumatol **7**(1): 50-56.

Hertzog, P. J., L. A. O'Neill and J. A. Hamilton (2003). "The interferon in TLR signaling: more than just antiviral." Trends Immunol **24**(10): 534-539.

Homma, M. K., D. Li, E. G. Krebs, Y. Yuasa and Y. Homma (2002). "Association and regulation of casein kinase 2 activity by adenomatous polyposis coli protein." Proc Natl Acad Sci U S A **99**(9): 5959-5964.

Houard, X., M. B. Goldring and F. Berenbaum (2013). "Homeostatic mechanisms in articular cartilage and role of inflammation in osteoarthritis." Curr Rheumatol Rep **15**(11): 375.

Hu, Z., J. D. Klein, W. E. Mitch, L. Zhang, I. Martinez and X. H. Wang (2014). "MicroRNA-29 induces cellular senescence in aging muscle through multiple signaling pathways." AGING **6**(3): 15.

Hu, Z., J. D. Klein, W. E. Mitch, L. Zhang, I. Martinez and X. H. Wang (2014). "MicroRNA-29 induces cellular senescence in aging muscle through multiple signaling pathways." Aging (Albany NY) **6**(3): 160-175.

Hui, W., G. J. Litherland, M. S. Elias, G. I. Kitson, T. E. Cawston, A. D. Rowan and D. A. Young (2012). "Leptin produced by joint white adipose tissue induces cartilage degradation via upregulation and activation of matrix metalloproteinases." Ann Rheum Dis **71**(3): 455-462.

Hutvagner, G. (2005). "Small RNA asymmetry in RNAi: function in RISC assembly and gene regulation." FEBS Lett **579**(26): 5850-5857.

Hutvágner, G., J. McLachlan, A. Pasquinelli, É. Bálint, T. Tuschl and P. Zamore (2001). "A Cellular Function for the RNA-Interference Enzyme Dicer in the Maturation of the let-7 Small Temporal RNA." Science **293**(5531): 834-838.

Hutvagner, G. and M. Simard (2008). "Argonaute proteins: key players in RNA silencing." Nature Reviews. Molecular Cell Biology **9**(1): 22-32.

Iliopoulos, D., K. Malizos, P. Oikonomou and A. Tsezou (2008). "Integrative microRNA and proteomic approaches identify novel osteoarthritis genes and their collaborative metabolic and inflammatory networks." PLoS One **3**(11): e3740.

Inui, M., G. Martello and S. Piccolo (2010). "MicroRNA control of signal transduction." Nature Reviews. Molecular Cell Biology **11**(4): 252-263.

Janeway, C. A., Jr. and R. Medzhitov (2002). "Innate immune recognition." Annu Rev Immunol **20**: 197-216.

Jones, S. W., G. Watkins, N. Le Good, S. Roberts, C. L. Murphy, S. M. Brockbank, M. R. Needham, S. J. Read and P. Newham (2009). "The identification of differentially expressed microRNA in osteoarthritic tissue that modulate the production of TNF-alpha and MMP13." Osteoarthritis and Cartilage **17**(4): 464-472.

(2009). "The identification of differentially expressed microRNA in osteoarthritic tissue that modulate the production of TNF-alpha and MMP13." Osteoarthritis and cartilage / OARS, Osteoarthritis Research Society **17**(4): 464-472.

Kadler, K. E., D. F. Holmes, J. A. Trotter and J. A. Chapman (1996). "Collagen fibril formation." Biochem J **316 (Pt 1)**: 1-11.

Kapinas, K., C. Kessler and A. Delany (2009). "miR-29 suppression of osteonectin in osteoblasts: regulation during differentiation and by canonical Wnt signaling." J Cell Biochem **108**(1): 216-224.

Kapinas, K., C. Kessler, T. Ricks, G. Gronowicz and A. M. Delany (2010). "miR-29 modulates Wnt signaling in human osteoblasts through a positive feedback loop." J Biol Chem **285**(33): 25221-25231.

Karlsen, T., A. Shahdadfar and J. Brinchmann (2011). "Human primary articular chondrocytes, chondroblasts-like cells, and dedifferentiated chondrocytes: differences in gene, microRNA, and protein expression and phenotype." Tissue engineering. Part C, Methods **17**(2): 219-227.

Karlsen, T. A. and J. E. Brinchmann (2013). "Liposome delivery of microRNA-145 to mesenchymal stem cells leads to immunological off-target effects mediated by RIG-I." Mol Ther **21**(6): 1169-1181.

Karsdal, M. A., A. C. Bay-Jensen, R. J. Lories, S. Abramson, T. Spector, P. Pastoureau, C. Christiansen, M. Attur, K. Henriksen, S. R. Goldring and V. Kraus (2014). "The coupling of bone and cartilage turnover in osteoarthritis: opportunities for bone antiresorptives and anabolics as potential treatments?" Ann Rheum Dis **73**(2): 336-348.

Kawano, Y. and R. Kypta (2003). "Secreted antagonists of the Wnt signalling pathway." J Cell Sci **116**(Pt 13): 2627-2634.

Kent, O., R. Chivukula, M. Mullendore, E. Wentzel, G. Feldmann, K. Lee, S. Liu, S. Leach, A. Maitra and J. Mendell (2010). "Repression of the miR-143/145 cluster by oncogenic Ras initiates a tumor-promoting feed-forward pathway." Genes Dev **24**(24): 2754-2759.

Kerkhof, H. J., R. J. Lories, I. Meulenbelt, I. Jonsdottir, A. M. Valdes, P. Arp, T. Ingvarsson, M. Jhamai, H. Jonsson, L. Stolk, G. Thorleifsson, G. Zhai, F. Zhang, Y. Zhu, R. van der Breggen, A. Carr, M. Doherty, S. Doherty, D. T. Felson, A. Gonzalez, B. V. Halldorsson, D. J. Hart, V. B. Hauksson, A. Hofman, J. P. Ioannidis, M. Kloppenburg, N. E. Lane, J. Loughlin, F. P. Luyten, M. C. Nevitt, N. Parimi, H. A. Pols, F. Rivadeneira, E. P. Slagboom, U. Styrkarsdottir, A. Tsezou, T. van de Putte, J. Zmuda, T. D. Spector, K. Stefansson, A. G. Uitterlinden and J. B. van Meurs (2010). "A genome-wide association study identifies an osteoarthritis susceptibility locus on chromosome 7q22." Arthritis Rheum **62**(2): 499-510.

Ketting, R. F., S. E. Fischer, E. Bernstein, T. Sijen, G. J. Hannon and R. H. Plasterk (2001). "Dicer functions in RNA interference and in synthesis of small RNA involved in developmental timing in C. elegans." Genes Dev **15**(20): 2654-2659.

Khvorova, A., A. Reynolds and S. Jayasena (2003). "Functional siRNAs and miRNAs exhibit strand bias." Cell **115**(2): 209-216.

Kiani, C., L. Chen, Y. J. Wu, A. J. Yee and B. B. Yang (2002). "Structure and function of aggrecan." Cell Res **12**(1): 19-32.

Kim, D., J. Song and E.-J. Jin (2010). "MicroRNA-221 Regulates Chondrogenic Differentiation through Promoting Proteosomal Degradation of Slug by Targeting Mdm2." Journal of Biological Chemistry **285**(35): 26900-26907.
Kim, D., J. Song, S. Kim, C.-H. Chun and E.-J. Jin (2011). "MicroRNA-34a regulates migration of chondroblast and IL-1β-induced degeneration of chondrocytes by targeting EphA5." Biochem Biophys Res Commun **415**(4): 551-557.
Kim, D., J. Song, S. Kim, C.-H. Chun, J. Sonn and E.-J. Jin (2012). "MicroRNA-34a modulates cytoskeletal dynamics through regulating RhoA/Rac1 crosstalk in chondroblasts." The Journal of biological chemistry.
Kim, D., J. Song, S. Kim, S.-S. Kang and E.-J. Jin (2011). "MicroRNA-142-3p regulates TGF-β3-mediated region-dependent chondrogenesis by regulating ADAM9." Biochem Biophys Res Commun **414**(4): 653-659.
Kim, N. (2005). "MicroRNA biogenesis: coordinated cropping and dicing." Nature Reviews. Molecular Cell Biology **6**(5): 376-385.
Kim, N., J. Han and M. Siomi (2009). "Biogenesis of small RNAs in animals." Nature reviews. Molecular cell biology **10**(2): 126-139.
Kiriakidou, M., G. Tan, S. Lamprinaki, M. De Planell-Saguer, P. Nelson and Z. Mourelatos (2007). "An mRNA m7G cap binding-like motif within human Ago2 represses translation." Cell **129**(6): 1141-1151.
Knauper, V., C. Lopez-Otin, B. Smith, G. Knight and G. Murphy (1996). "Biochemical characterization of human collagenase-3." J Biol Chem **271**(3): 1544-1550.
Kobayashi, M., G. R. Squires, A. Mousa, M. Tanzer, D. J. Zukor, J. Antoniou, U. Feige and A. R. Poole (2005). "Role of interleukin-1 and tumor necrosis factor alpha in matrix degradation of human osteoarthritic cartilage." Arthritis Rheum **52**(1): 128-135.
Kobayashi, T., J. Lu, B. Cobb, S. Rodda, A. McMahon, E. Schipani, M. Merkenschlager and H. Kronenberg (2008). "Dicer-dependent pathways regulate chondrocyte proliferation and differentiation." Proc Natl Acad Sci U S A **105**(6): 1949-1954.
Kongcharoensombat, W., T. Nakasa, M. Ishikawa, A. Nakamae, M. Deie, N. Adachi, A. Mohamed and M. Ochi (2010). "The effect of microRNA-21 on proliferation and matrix synthesis of chondrocytes embedded in atelocollagen gel." Knee Surgery, Sports Traumatology, Arthroscopy **18**(12): 1679-1684.
Konttinen, Y. T., T. Sillat, G. Barreto, M. Ainola and D. C. Nordstrom (2012). "Osteoarthritis as an autoinflammatory disease caused by chondrocyte-mediated inflammatory responses." Arthritis Rheum **64**(3): 613-616.
Kosaka, N., H. Iguchi and T. Ochiya (2010). "Circulating microRNA in body fluid: a new potential biomarker for cancer diagnosis and prognosis." Cancer Sci **101**(10): 2087-2092.
Koshy, P. J., C. J. Lundy, A. D. Rowan, S. Porter, D. R. Edwards, A. Hogan, I. M. Clark and T. E. Cawston (2002). "The modulation of matrix metalloproteinase and ADAM gene expression in human chondrocytes by interleukin-1 and oncostatin M: a time-course study using real-time quantitative reverse transcription-polymerase chain reaction." Arthritis Rheum **46**(4): 961-967.
Kozomara, A. and S. Griffiths-Jones (2011). "miRBase: integrating microRNA annotation and deep-sequencing data." Nucleic Acids Research **39**(Database issue): D152-D157.
Kwiecinski, M., A. Noetel, N. Elfimova, J. Trebicka, S. Schievenbusch, I. Strack, L. Molnar, M. von Brandenstein, U. Tox, R. Nischt, O. Coutelle, H. P. Dienes and M. Odenthal (2011). "Hepatocyte growth factor (HGF) inhibits collagen I and IV synthesis in hepatic stellate cells by miRNA-29 induction." PLoS One **6**(9): e24568.
Lagos-Quintana, M., R. Rauhut, W. Lendeckel and T. Tuschl (2001). "Identification of novel genes coding for small expressed RNAs." Science (New York, N.Y.) **294**(5543): 853-858.

Lai, E. (2002). "Micro RNAs are complementary to 3' UTR sequence motifs that mediate negative post-transcriptional regulation." Nat Genet **30**(4): 363-364.
Lane, L. B., A. Villacin and P. G. Bullough (1977). "The vascularity and remodelling of subchondrial bone and calcified cartilage in adult human femoral and humeral heads. An age- and stress-related phenomenon." J Bone Joint Surg Br **59**(3): 272-278.
Lane, N. E., K. Lian, M. C. Nevitt, J. M. Zmuda, L. Lui, J. Li, J. Wang, M. Fontecha, N. Umblas, M. Rosenbach, P. de Leon and M. Corr (2006). "Frizzled-related protein variants are risk factors for hip osteoarthritis." Arthritis Rheum **54**(4): 1246-1254.
Lapiere, C. M., A. Lenaers and L. D. Kohn (1971). "Procollagen peptidase: an enzyme excising the coordination peptides of procollagen." Proc Natl Acad Sci U S A **68**(12): 3054-3058.
Lau, N. C., L. P. Lim, E. G. Weinstein and D. P. Bartel (2001). "An abundant class of tiny RNAs with probable regulatory roles in Caenorhabditis elegans." Science (New York, N.Y.) **294**(5543): 858-862.
Lau, P.-W. and I. MacRae (2009). "The molecular machines that mediate microRNA maturation." J Cell Mol Med **13**(1): 54-60.
Lawrie, C., S. Gal, H. Dunlop, B. Pushkaran, A. Liggins, K. Pulford, A. Banham, F. Pezzella, J. Boultwood, J. Wainscoat, C. Hatton and A. Harris (2008). "Detection of elevated levels of tumour-associated microRNAs in serum of patients with diffuse large B-cell lymphoma." Br J Haematol **141**(5): 672-675.
Le, L. T., T. E. Swingler and I. M. Clark (2013). "Review: the role of microRNAs in osteoarthritis and chondrogenesis." Arthritis Rheum **65**(8): 1963-1974.
Lee, D. A., G. Bentley and C. W. Archer (1993). "The control of cell division in articular chondrocytes." Osteoarthritis Cartilage **1**(2): 137-146.
Lee, I., S. Ajay, J. I. Yook, H. S. Kim, S. H. Hong, N. H. Kim, S. Dhanasekaran, A. Chinnaiyan and B. Athey (2009). "New class of microRNA targets containing simultaneous 5'-UTR and 3'-UTR interaction sites." Genome Res **19**(7): 1175-1183.
Lee, J. H., T. Ort, K. Ma, K. Picha, J. Carton, P. A. Marsters, L. S. Lohmander, F. Baribaud, X. Y. Song and S. Blake (2009). "Resistin is elevated following traumatic joint injury and causes matrix degradation and release of inflammatory cytokines from articular cartilage in vitro." Osteoarthritis Cartilage **17**(5): 613-620.
Lee, R. and V. Ambros (2001). "An Extensive Class of Small RNAs in Caenorhabditis elegans." Science **294**(5543): 862-864.
Lee, R. C., R. L. Feinbaum and V. Ambros (1993). "The C. elegans heterochronic gene lin-4 encodes small RNAs with antisense complementarity to lin-14." Cell **75**(5): 843-854.
Lee, Y., C. Ahn, J. Han, H. Choi, J. Kim, J. Yim, J. Lee, P. Provost, O. Radmark, S. Kim and N. Kim (2003). "The nuclear RNase III Drosha initiates microRNA processing." Nature **425**(6956): 415-419.
Lee, Y., K. Jeon, J.-T. Lee, S. Kim and N. Kim (2002). "MicroRNA maturation: stepwise processing and subcellular localization." The EMBO Journal **21**(17): 4663-4670.
Lee, Y., M. Kim, J. Han, K.-H. Yeom, S. Lee, S. Baek and N. Kim (2004). "MicroRNA genes are transcribed by RNA polymerase II." The EMBO Journal **23**(20): 4051-4060.
Lefebvre, V., W. Huang, V. R. Harley, P. N. Goodfellow and B. de Crombrugghe (1997). "SOX9 is a potent activator of the chondrocyte-specific enhancer of the pro alpha1(II) collagen gene." Mol Cell Biol **17**(4): 2336-2346.
Lefebvre, V., C. Peeters-Joris and G. Vaes (1990). "Modulation by interleukin 1 and tumor necrosis factor alpha of production of collagenase, tissue inhibitor of metalloproteinases and collagen types in differentiated and dedifferentiated articular chondrocytes." Biochim Biophys Acta **1052**(3): 366-378.

Leone, V., D. D'Angelo, P. Pallante, C. M. Croce and A. Fusco (2012). "Thyrotropin regulates thyroid cell proliferation by up-regulating miR-23b and miR-29b that target SMAD3." J Clin Endocrinol Metab **97**(9): 3292-3301.

Letamendia, A., E. Labbe and L. Attisano (2001). "Transcriptional regulation by Smads: crosstalk between the TGF-beta and Wnt pathways." J Bone Joint Surg Am **83-A Suppl 1**(Pt 1): S31-39.

Lewis, B., C. Burge and D. Bartel (2005). "Conserved Seed Pairing, Often Flanked by Adenosines, Indicates that Thousands of Human Genes are MicroRNA Targets." Cell **120**(1): 15-20.

Li, G., J. Yin, J. Gao, T. S. Cheng, N. J. Pavlos, C. Zhang and M. H. Zheng (2013). "Subchondral bone in osteoarthritis: insight into risk factors and microstructural changes." Arthritis Res Ther **15**(6): 223.

Li, H., H. Xie, W. Liu, R. Hu, B. Huang, Y.-F. Tan, K. Xu, Z.-F. Sheng, H.-D. Zhou, X.-P. Wu and X.-H. Luo (2009). "A novel microRNA targeting HDAC5 regulates osteoblast differentiation in mice and contributes to primary osteoporosis in humans." The Journal of clinical investigation **119**(12): 3666-3677.

Li, J., J. Huang, L. Dai, D. Yu, Q. Chen, X. Zhang and K. Dai (2012). "MiR-146a, an interleukin-1beta responsive microRNA, induces vascular endothelial growth factor and chondrocyte apoptosis by targeting Smad4." Arthritis Res Ther **14**(2): R75.

Li, N., J. Cui, X. Duan, H. Chen and F. Fan (2012). "Suppression of type I collagen expression by miR-29b via PI3K, Akt, and Sp1 pathway in human Tenon's fibroblasts." Invest Ophthalmol Vis Sci **53**(3): 1670-1678.

Li, T. F., R. J. O'Keefe and D. Chen (2005). "TGF-beta signaling in chondrocytes." Front Biosci **10**: 681-688.

Li, X., G. Gibson, J.-S. Kim, J. Kroin, S. Xu, A. van Wijnen and H.-J. Im (2011). "MicroRNA-146a is linked to pain-related pathophysiology of osteoarthritis." Gene **480**(1-2): 34-41.

Liang, Z.-J., H. Zhuang, G.-X. Wang, Z. Li, H.-T. Zhang, T.-Q. Yu and B.-D. Zhang (2012). "MiRNA-140 is a negative feedback regulator of MMP-13 in IL-1β-stimulated human articular chondrocyte C28/I2 cells." Inflammation Research **61**(5): 503-509.

(2012). "MiRNA-140 is a negative feedback regulator of MMP-13 in IL-1β-stimulated human articular chondrocyte C28/I2 cells." Inflammation research: 1-7.

Lim, L., N. Lau, P. Garrett-Engele, A. Grimson, J. Schelter, J. Castle, D. Bartel, P. Linsley and J. Johnson (2005). "Microarray analysis shows that some microRNAs downregulate large numbers of target mRNAs." Nature **433**(7027): 769-773.

Lin, E., L. Kong, X.-H. Bai, Y. Luan and C.-J. Liu (2009). "miR-199a, a bone morphogenic protein 2-responsive MicroRNA, regulates chondrogenesis via direct targeting to Smad1." The Journal of biological chemistry **284**(17): 11326-11335.

(2009). "miR-199a, a bone morphogenic protein 2-responsive MicroRNA, regulates chondrogenesis via direct targeting to Smad1." Journal of Biological Chemistry **284**(17): 11326-11335.

Lin, L., Q. Shen, C. Zhang, L. Chen and C. Yu (2011). "Assessment of the profiling microRNA expression of differentiated and dedifferentiated human adult articular chondrocytes." Journal of Orthopaedic Research **29**(10): 1578-1584.

Lin, S.-Y., S. Johnson, M. Abraham, M. Vella, A. Pasquinelli, C. Gamberi, E. Gottlieb and F. Slack (2003). "The C elegans hunchback homolog, hbl-1, controls temporal patterning and is a probable microRNA target." Developmental Cell **4**(5): 639-650.

Link, A., F. Balaguer, Y. Shen, T. Nagasaka, J. J. Lozano, R. Boland and A. Goel (2010). "Fecal MicroRNAs as novel biomarkers for colon cancer screening." Cancer Epidemiol Biomarkers Prev **19**(7): 1766-1774.

Liu, C., Y. Wang, P. M. Smallwood and J. Nathans (2008). "An essential role for Frizzled5 in neuronal survival in the parafascicular nucleus of the thalamus." J Neurosci **28**(22): 5641-5653.

Liu, S., L. C. Wu, J. Pang, R. Santhanam, S. Schwind, Y. Z. Wu, C. J. Hickey, J. Yu, H. Becker, K. Maharry, M. D. Radmacher, C. Li, S. P. Whitman, A. Mishra, N. Stauffer, A. M. Eiring, R. Briesewitz, R. A.

Baiocchi, K. K. Chan, P. Paschka, M. A. Caligiuri, J. C. Byrd, C. M. Croce, C. D. Bloomfield, D. Perrotti, R. Garzon and G. Marcucci (2010). "Sp1/NFkappaB/HDAC/miR-29b regulatory network in KIT-driven myeloid leukemia." Cancer Cell **17**(4): 333-347.

Liu, Y., T. Huang, X. Zhao and L. Cheng (2011). "MicroRNAs modulate the Wnt signaling pathway through targeting its inhibitors." Biochem Biophys Res Commun **408**(2): 259-264.

Lodewyckx, L., F. P. Luyten and R. J. Lories (2012). "Genetic deletion of low-density lipoprotein receptor-related protein 5 increases cartilage degradation in instability-induced osteoarthritis." Rheumatology (Oxford) **51**(11): 1973-1978.

Loeser, R., S. Goldring, C. Scanzello and M. Goldring (2012). "Osteoarthritis: A disease of the joint as an organ." Arthritis & Rheumatism: n/a-n/a.

Loeser, R. F., S. R. Goldring, C. R. Scanzello and M. B. Goldring (2012). "Osteoarthritis: a disease of the joint as an organ." Arthritis Rheum **64**(6): 1697-1707.

Long, J., Y. Wang, W. Wang, B. H. Chang and F. R. Danesh (2011). "MicroRNA-29c is a signature microRNA under high glucose conditions that targets Sprouty homolog 1, and its in vivo knockdown prevents progression of diabetic nephropathy." J Biol Chem **286**(13): 11837-11848.

Lories, R. J., J. Peeters, A. Bakker, P. Tylzanowski, I. Derese, J. Schrooten, J. T. Thomas and F. P. Luyten (2007). "Articular cartilage and biomechanical properties of the long bones in Frzb-knockout mice." Arthritis Rheum **56**(12): 4095-4103.

Loughlin, J., B. Dowling, K. Chapman, L. Marcelline, Z. Mustafa, L. Southam, A. Ferreira, C. Ciesielski, D. A. Carson and M. Corr (2004). "Functional variants within the secreted frizzled-related protein 3 gene are associated with hip osteoarthritis in females." Proc Natl Acad Sci U S A **101**(26): 9757-9762.

Lu, D., Y. Zhao, R. Tawatao, H. B. Cottam, M. Sen, L. M. Leoni, T. J. Kipps, M. Corr and D. A. Carson (2004). "Activation of the Wnt signaling pathway in chronic lymphocytic leukemia." Proc Natl Acad Sci U S A **101**(9): 3118-3123.

Luna, C., G. Li, J. Qiu, D. L. Epstein and P. Gonzalez (2009). "Role of miR-29b on the regulation of the extracellular matrix in human trabecular meshwork cells under chronic oxidative stress." Mol Vis **15**: 2488-2497.

Lund, E., S. Güttinger, A. Calado, J. Dahlberg and U. Kutay (2004). "Nuclear Export of MicroRNA Precursors." Science **303**(5654): 95-98.

Lytle, R., T. Yario and J. Steitz (2007). "Target mRNAs are repressed as efficiently by microRNA-binding sites in the 5′ UTR as in the 3′ UTR." Proceedings of the National Academy of Sciences **104**(23): 9667-9672.

Ma, F., S. Xu, X. Liu, Q. Zhang, X. Xu, M. Liu, M. Hua, N. Li, H. Yao and X. Cao (2011). "The microRNA miR-29 controls innate and adaptive immune responses to intracellular bacterial infection by targeting interferon-gamma." Nat Immunol **12**(9): 861-869.

Maegdefessel, L., J. Azuma, R. Toh, D. R. Merk, A. Deng, J. T. Chin, U. Raaz, A. M. Schoelmerich, A. Raiesdana, N. J. Leeper, M. V. McConnell, R. L. Dalman, J. M. Spin and P. S. Tsao (2012). "Inhibition of microRNA-29b reduces murine abdominal aortic aneurysm development." J Clin Invest **122**(2): 497-506.

Marcu, K. B., M. Otero, E. Olivotto, R. M. Borzi and M. B. Goldring (2010). "NF-kappaB signaling: multiple angles to target OA." Curr Drug Targets **11**(5): 599-613.

Martel-Pelletier, J., C. Boileau, J. P. Pelletier and P. J. Roughley (2008). "Cartilage in normal and osteoarthritis conditions." Best Pract Res Clin Rheumatol **22**(2): 351-384.

Martin, P. (1990). "Tissue patterning in the developing mouse limb." Int J Dev Biol **34**(3): 323-336.

Martinez-Sanchez, A., K. Dudek and C. Murphy (2012). "Regulation of human chondrocyte function through direct inhibition of cartilage master regulator SOX9 by microRNA-145 (miRNA-145)." Journal of Biological Chemistry **287**(2): 916-924.

(2012). "Regulation of human chondrocyte function through direct inhibition of cartilage master regulator SOX9 by microRNA-145 (miRNA-145)." The Journal of biological chemistry **287**(2): 916-924.
Martinez-Sanchez, A. and C. L. Murphy (2013). "miR-1247 functions by targeting cartilage transcription factor SOX9." J Biol Chem **288**(43): 30802-30814.
Martinez, J., A. Patkaniowska, H. Urlaub, R. Lührmann and T. Tuschl (2002). "Single-stranded antisense siRNAs guide target RNA cleavage in RNAi." Cell **110**(5): 563-574.
Matyas, J. R., L. J. Sandell and M. E. Adams (1997). "Gene expression of type II collagens in chondro-osteophytes in experimental osteoarthritis." Osteoarthritis Cartilage **5**(2): 99-105.
Maurer, B., J. Stanczyk, A. Jungel, A. Akhmetshina, M. Trenkmann, M. Brock, O. Kowal-Bielecka, R. E. Gay, B. A. Michel, J. H. Distler, S. Gay and O. Distler (2010). "MicroRNA-29, a key regulator of collagen expression in systemic sclerosis." Arthritis Rheum **62**(6): 1733-1743.
Meachim, G. and D. H. Collins (1962). "Cell counts of normal and osteoarthritic articular cartilage in relation to the uptake of sulphate (35SO4) in vitro." Ann Rheum Dis **21**: 45-50.
Messier, S. P., D. J. Gutekunst, C. Davis and P. DeVita (2005). "Weight loss reduces knee-joint loads in overweight and obese older adults with knee osteoarthritis." Arthritis Rheum **52**(7): 2026-2032.
Miravet, S., J. Piedra, F. Miro, E. Itarte, A. Garcia de Herreros and M. Dunach (2002). "The transcriptional factor Tcf-4 contains different binding sites for beta-catenin and plakoglobin." J Biol Chem **277**(3): 1884-1891.
Mitchell, P., R. Parkin, E. Kroh, B. Fritz, S. Wyman, E. Pogosova-Agadjanyan, A. Peterson, J. Noteboom, K. O'Briant, A. Allen, D. Lin, N. Urban, C. Drescher, B. Knudsen, D. Stirewalt, R. Gentleman, R. Vessella, P. Nelson, D. Martin and M. Tewari (2008). "Circulating microRNAs as stable blood-based markers for cancer detection." Proceedings of the National Academy of Sciences **105**(30): 10513-10518.
Miyaki, S., T. Nakasa, S. Otsuki, S. Grogan, R. Higashiyama, A. Inoue, Y. Kato, T. Sato, M. Lotz and H. Asahara (2009). "MicroRNA-140 is expressed in differentiated human articular chondrocytes and modulates interleukin-1 responses." Arthritis & Rheumatism **60**(9): 2723-2730.
(2009). "MicroRNA-140 is expressed in differentiated human articular chondrocytes and modulates interleukin-1 responses." Arthritis and rheumatism **60**(9): 2723-2730.
Miyaki, S., T. Nakasa, S. Otsuki, S. P. Grogan, R. Higashiyama, A. Inoue, Y. Kato, T. Sato, M. K. Lotz and H. Asahara (2009). "MicroRNA-140 is expressed in differentiated human articular chondrocytes and modulates interleukin-1 responses." Arthritis Rheum **60**(9): 2723-2730.
Miyaki, S., T. Sato, A. Inoue, S. Otsuki, Y. Ito, S. Yokoyama, Y. Kato, F. Takemoto, T. Nakasa, S. Yamashita, S. Takada, M. Lotz, H. Ueno-Kudo and H. Asahara (2010). "MicroRNA-140 plays dual roles in both cartilage development and homeostasis." Genes Dev **24**(11): 1173-1185.
Miyaki, S., T. Sato, A. Inoue, S. Otsuki, Y. Ito, S. Yokoyama, Y. Kato, F. Takemoto, T. Nakasa, S. Yamashita, S. Takada, M. K. Lotz, H. Ueno-Kudo and H. Asahara (2010). "MicroRNA-140 plays dual roles in both cartilage development and homeostasis." Genes Dev **24**(11): 1173-1185.
Miyazawa, K., M. Shinozaki, T. Hara, T. Furuya and K. Miyazono (2002). "Two major Smad pathways in TGF-beta superfamily signalling." Genes Cells **7**(12): 1191-1204.
Mooney, R. A., E. R. Sampson, J. Lerea, R. N. Rosier and M. J. Zuscik (2011). "High-fat diet accelerates progression of osteoarthritis after meniscal/ligamentous injury." Arthritis Res Ther **13**(6): R198.
Morita, S., T. Horii, M. Kimura, T. Ochiya, S. Tajima and I. Hatada (2013). "miR-29 represses the activities of DNA methyltransferases and DNA demethylases." Int J Mol Sci **14**(7): 14647-14658.
Mott, J. L., S. Kurita, S. C. Cazanave, S. F. Bronk, N. W. Werneburg and M. E. Fernandez-Zapico (2010). "Transcriptional suppression of mir-29b-1/mir-29a promoter by c-Myc, hedgehog, and NF-kappaB." J Cell Biochem **110**(5): 1155-1164.

Moulin, D., V. Salone, M. Koufany, T. Clement, P. Netter, I. Behm-Ansmant, B. Charpentier, C. Branlant and J.-Y. Jouzeau (2012). "miR-29b is overexpressed in osteoarthritic patients and targets type II collagen." Osteoarthritis and Cartilage **20**: S139 - S140.

Muniyappa, M. K., P. Dowling, M. Henry, P. Meleady, P. Doolan, P. Gammell, M. Clynes and N. Barron (2009). "MiRNA-29a regulates the expression of numerous proteins and reduces the invasiveness and proliferation of human carcinoma cell lines." Eur J Cancer **45**(17): 3104-3118.

Murata, K., H. Yoshitomi, S. Tanida, M. Ishikawa, K. Nishitani, H. Ito and T. Nakamura (2010). "Plasma and synovial fluid microRNAs as potential biomarkers of rheumatoid arthritis and osteoarthritis." Arthritis Res Ther **12**(3): R86.

Murata, K., H. Yoshitomi, S. Tanida, M. Ishikawa, K. Nishitani, H. Ito and T. Nakamura (2010). "Plasma and synovial fluid microRNAs as potential biomarkers of rheumatoid arthritis and osteoarthritis." Arthritis Res Ther **12**(3): R86.

Nah, S. S., I. Y. Choi, B. Yoo, Y. G. Kim, H. B. Moon and C. K. Lee (2007). "Advanced glycation end products increases matrix metalloproteinase-1, -3, and -13, and TNF-alpha in human osteoarthritic chondrocytes." FEBS Lett **581**(9): 1928-1932.

Nakamura, Y., X. He, H. Kato, S. Wakitani, T. Kobayashi, S. Watanabe, A. Iida, H. Tahara, M. L. Warman, R. Watanapokasin and J. H. Postlethwait (2012). "Sox9 is upstream of microRNA-140 in cartilage." Appl Biochem Biotechnol **166**(1): 64-71.

Nakamura, Y., J. Inloes, T. Katagiri and T. Kobayashi (2011). "Chondrocyte-specific microRNA-140 regulates endochondral bone development and targets Dnpep to modulate bone morphogenetic protein signaling." Mol Cell Biol **31**(14): 3019-3028.

Nakamura, Y., J. B. Inloes, T. Katagiri and T. Kobayashi (2011). "Chondrocyte-specific microRNA-140 regulates endochondral bone development and targets Dnpep to modulate bone morphogenetic protein signaling." Mol Cell Biol **31**(14): 3019-3028.

Nalesso, G., J. Sherwood, J. Bertrand, T. Pap, M. Ramachandran, C. De Bari, C. Pitzalis and F. Dell'accio (2011). "WNT-3A modulates articular chondrocyte phenotype by activating both canonical and noncanonical pathways." J Cell Biol **193**(3): 551-564.

Neu, C., A. Khalafi, K. Komvopoulos, T. Schmid and H. Reddi (2007). "Mechanotransduction of bovine articular cartilage superficial zone protein by transforming growth factor β signaling." Arthritis & Rheumatism **56**(11): 3706-3714.

Ng, L. J., S. Wheatley, G. E. Muscat, J. Conway-Campbell, J. Bowles, E. Wright, D. M. Bell, P. P. Tam, K. S. Cheah and P. Koopman (1997). "SOX9 binds DNA, activates transcription, and coexpresses with type II collagen during chondrogenesis in the mouse." Dev Biol **183**(1): 108-121.

Nicolas, F. E., H. Pais, F. Schwach, M. Lindow, S. Kauppinen, V. Moulton and T. Dalmay (2008). "Experimental identification of microRNA-140 targets by silencing and overexpressing miR-140." RNA (New York, N.Y.) **14**(12): 2513-2520.

Nishikawa, R., Y. Goto, S. Kojima, H. Enokida, T. Chiyomaru, T. Kinoshita, S. Sakamoto, M. Fuse, M. Nakagawa, Y. Naya, T. Ichikawa and N. Seki (2014). "Tumor-suppressive microRNA-29s inhibit cancer cell migration and invasion via targeting LAMC1 in prostate cancer." Int J Oncol **45**(1): 401-410.

Okamura, K., J. Hagen, H. Duan, D. Tyler and E. Lai (2007). "The mirtron pathway generates microRNA-class regulatory RNAs in Drosophila." Cell **130**(1): 89-100.

Okuhara, A., T. Nakasa, H. Shibuya, T. Niimoto, N. Adachi, M. Deie and M. Ochi (2011). "Changes in microRNA expression in peripheral mononuclear cells according to the progression of osteoarthritis." Modern rheumatology / the Japan Rheumatism Association: 1-12.

Pais, H., E. Francisco, S. Soond, T. Swingler, I. Clark, A. Chantry, V. Moulton and T. Dalmay (2010). "Analyzing mRNA expression identifies Smad3 as a microRNA-140 target regulated only at protein level." RNA **16**(3): 489-494.

Pais, H., F. E. Nicolas, S. M. Soond, T. E. Swingler, I. M. Clark, A. Chantry, V. Moulton and T. Dalmay (2010). "Analyzing mRNA expression identifies Smad3 as a microRNA-140 target regulated only at protein level." RNA **16**(3): 489-494.

Park, S. J., E. J. Cheon, M. H. Lee and H. A. Kim (2013). "MicroRNA-127-5p regulates matrix metalloproteinase 13 expression and interleukin-1beta-induced catabolic effects in human chondrocytes." Arthritis Rheum **65**(12): 3141-3152.

Parpart, S., S. Roessler, F. Dong, V. Rao, A. Takai, J. Ji, L. X. Qin, Q. H. Ye, H. L. Jia, Z. Y. Tang and X. W. Wang (2014). "Modulation of miR-29 expression by alpha-fetoprotein is linked to the hepatocellular carcinoma epigenome." Hepatology **60**(3): 872-883.

Pearle, A. D., C. R. Scanzello, S. George, L. A. Mandl, E. F. DiCarlo, M. Peterson, T. P. Sculco and M. K. Crow (2007). "Elevated high-sensitivity C-reactive protein levels are associated with local inflammatory findings in patients with osteoarthritis." Osteoarthritis Cartilage **15**(5): 516-523.

Pearle, A. D., R. F. Warren and S. A. Rodeo (2005). "Basic science of articular cartilage and osteoarthritis." Clin Sports Med **24**(1): 1-12.

Pelletier, J. P., J. P. Caron, C. Evans, P. D. Robbins, H. I. Georgescu, D. Jovanovic, J. C. Fernandes and J. Martel-Pelletier (1997). "In vivo suppression of early experimental osteoarthritis by interleukin-1 receptor antagonist using gene therapy." Arthritis Rheum **40**(6): 1012-1019.

Petersen, C., M.-E. Bordeleau, J. Pelletier and P. Sharp (2006). "Short RNAs repress translation after initiation in mammalian cells." Mol Cell **21**(4): 533-542.

Petrovich, O. n., S. L. llyich and M. S. Pavlovich (2014). "Connectic tissue: Histophysiology, Biochemistry, Molecular Biology ".

Pfander, D., T. Cramer, E. Schipani and R. S. Johnson (2003). "HIF-1alpha controls extracellular matrix synthesis by epiphyseal chondrocytes." J Cell Sci **116**(Pt 9): 1819-1826.

Poonpet, T., S. Honsawek, N. Tammachote, S. Kanitnate and R. Tammachote (2013). "ADAMTS14 gene polymorphism associated with knee osteoarthritis in Thai women." Genet Mol Res **12**(4): 5301-5309.

Presle, N., P. Pottie, H. Dumond, C. Guillaume, F. Lapicque, S. Pallu, D. Mainard, P. Netter and B. Terlain (2006). "Differential distribution of adipokines between serum and synovial fluid in patients with osteoarthritis. Contribution of joint tissues to their articular production." Osteoarthritis Cartilage **14**(7): 690-695.

Price, M. A. (2006). "CKI, there's more than one: casein kinase I family members in Wnt and Hedgehog signaling." Genes Dev **20**(4): 399-410.

Pujol, J.-P., C. Chadjichristos, F. Legendre, C. Bauge, G. Beauchef, R. Andriamanalijaona, P. Galera and K. Boumediene (2008). "Interleukin-1 and transforming growth factor-beta 1 as crucial factors in osteoarthritic cartilage metabolism." Connect Tissue Res **49**(3): 293-297.

Pullen, T. J., G. da Silva Xavier, G. Kelsey and G. A. Rutter (2011). "miR-29a and miR-29b contribute to pancreatic beta-cell-specific silencing of monocarboxylate transporter 1 (Mct1)." Mol Cell Biol **31**(15): 3182-3194.

Qin, W., A. C. Chung, X. R. Huang, X. M. Meng, D. S. Hui, C. M. Yu, J. J. Sung and H. Y. Lan (2011). "TGF-beta/Smad3 signaling promotes renal fibrosis by inhibiting miR-29." J Am Soc Nephrol **22**(8): 1462-1474.

Ramdas, V., M. McBride, L. Denby and A. H. Baker (2013). "Canonical transforming growth factor-beta signaling regulates disintegrin metalloprotease expression in experimental renal fibrosis via miR-29." Am J Pathol **183**(6): 1885-1896.

Reinhart, B. J., F. J. Slack, M. Basson, A. E. Pasquinelli, J. C. Bettinger, A. E. Rougvie, H. R. Horvitz and G. Ruvkun (2000). "The 21-nucleotide let-7 RNA regulates developmental timing in Caenorhabditis elegans." Nature **403**(6772): 901-906.

Riordan, E. A., C. Little and D. Hunter (2014). "Pathogenesis of post-traumatic OA with a view to intervention." Best Pract Res Clin Rheumatol **28**(1): 17-30.

Ro, S., C. Park, D. Young, K. Sanders and W. Yan (2007). "Tissue-dependent paired expression of miRNAs." Nucleic Acids Res **35**(17): 5944-5953.
Roderburg, C., G. W. Urban, K. Bettermann, M. Vucur, H. Zimmermann, S. Schmidt, J. Janssen, C. Koppe, P. Knolle, M. Castoldi, F. Tacke, C. Trautwein and T. Luedde (2011). "Micro-RNA profiling reveals a role for miR-29 in human and murine liver fibrosis." Hepatology **53**(1): 209-218.
Rodriguez-Lopez, J., M. Pombo-Suarez, J. Loughlin, A. Tsezou, F. J. Blanco, I. Meulenbelt, P. E. Slagboom, A. M. Valdes, T. D. Spector, J. J. Gomez-Reino and A. Gonzalez (2009). "Association of a nsSNP in ADAMTS14 to some osteoarthritis phenotypes." Osteoarthritis Cartilage **17**(3): 321-327.
Rodriguez, A., S. Griffiths-Jones, J. Ashurst and A. Bradley (2004). "Identification of mammalian microRNA host genes and transcription units." Genome Res **14**(10A): 1902-1910.
Roodman, G. D. (1999). "Cell biology of the osteoclast." Exp Hematol **27**(8): 1229-1241.
Rothwell, A. G. and G. Bentley (1973). "Chondrocyte multiplication in osteoarthritic articular cartilage." J Bone Joint Surg Br **55**(3): 588-594.
Ruby, G., C. Jan and D. Bartel (2007). "Intronic microRNA precursors that bypass Drosha processing." Nature **448**(7149): 83-86.
Sætrom, P., B. Heale, O. Snøve, L. Aagaard, J. Alluin and J. Rossi (2007). "Distance constraints between microRNA target sites dictate efficacy and cooperativity." Nucleic Acids Res **35**(7): 2333-2342.
Saini, H. K., S. Griffiths-Jones and A. J. Enright (2007). "Genomic analysis of human microRNA transcripts." Proc Natl Acad Sci U S A **104**(45): 17719-17724.
Sandell, L. J. and T. Aigner (2001). "Articular cartilage and changes in arthritis. An introduction: cell biology of osteoarthritis." Arthritis Res **3**(2): 107-113.
Sandell, L. J., N. Morris, J. R. Robbins and M. B. Goldring (1991). "Alternatively spliced type II procollagen mRNAs define distinct populations of cells during vertebral development: differential expression of the amino-propeptide." J Cell Biol **114**(6): 1307-1319.
Santanam, U., N. Zanesi, A. Efanov, S. Costinean, A. Palamarchuk, J. P. Hagan, S. Volinia, H. Alder, L. Rassenti, T. Kipps, C. M. Croce and Y. Pekarsky (2010). "Chronic lymphocytic leukemia modeled in mouse by targeted miR-29 expression." Proc Natl Acad Sci U S A **107**(27): 12210-12215.
Scanzello, C. R. and S. R. Goldring (2012). "The role of synovitis in osteoarthritis pathogenesis." Bone **51**(2): 249-257.
Schipani, E., H. E. Ryan, S. Didrickson, T. Kobayashi, M. Knight and R. S. Johnson (2001). "Hypoxia in cartilage: HIF-1alpha is essential for chondrocyte growth arrest and survival." Genes Dev **15**(21): 2865-2876.
Schmid, T. M. and T. F. Linsenmayer (1985). "Developmental acquisition of type X collagen in the embryonic chick tibiotarsus." Dev Biol **107**(2): 373-381.
Schmitt, M. J., C. Margue, I. Behrmann and S. Kreis (2013). "MiRNA-29: a microRNA family with tumor-suppressing and immune-modulating properties." Curr Mol Med **13**(4): 572-585.
Schwarz, D., G. Hutvágner, T. Du, Z. Xu, N. Aronin and P. Zamore (2003). "Asymmetry in the assembly of the RNAi enzyme complex." Cell **115**(2): 199-208.
Sengupta, S., J. A. den Boon, I. H. Chen, M. A. Newton, S. A. Stanhope, Y. J. Cheng, C. J. Chen, A. Hildesheim, B. Sugden and P. Ahlquist (2008). "MicroRNA 29c is down-regulated in nasopharyngeal carcinomas, up-regulating mRNAs encoding extracellular matrix proteins." Proc Natl Acad Sci U S A **105**(15): 5874-5878.
Serra, R., M. Johnson, E. H. Filvaroff, J. LaBorde, D. M. Sheehan, R. Derynck and H. L. Moses (1997). "Expression of a truncated, kinase-defective TGF-beta type II receptor in mouse skeletal

tissue promotes terminal chondrocyte differentiation and osteoarthritis." J Cell Biol **139**(2): 541-552.
Shioya, M., S. Obayashi, H. Tabunoki, K. Arima, Y. Saito, T. Ishida and J. Satoh (2010). "Aberrant microRNA expression in the brains of neurodegenerative diseases: miR-29a decreased in Alzheimer disease brains targets neurone navigator 3." Neuropathol Appl Neurobiol **36**(4): 320-330.
Sibley, C., Y. Seow, S. Saayman, K. Dijkstra, S. El Andaloussi, M. Weinberg and M. Wood (2012). "The biogenesis and characterization of mammalian microRNAs of mirtron origin." Nucleic Acids Res **40**(1): 438-448.
Silver, I. A. (1975). "Measurement of pH and ionic composition of pericellular sites." Philos Trans R Soc Lond B Biol Sci **271**(912): 261-272.
Smith, M. D., E. Barg, H. Weedon, V. Papengelis, T. Smeets, P. P. Tak, M. Kraan, M. Coleman and M. J. Ahern (2003). "Microarchitecture and protective mechanisms in synovial tissue from clinically and arthroscopically normal knee joints." Ann Rheum Dis **62**(4): 303-307.
Song, D. H., I. Dominguez, J. Mizuno, M. Kaut, S. C. Mohr and D. C. Seldin (2003). "CK2 phosphorylation of the armadillo repeat region of beta-catenin potentiates Wnt signaling." J Biol Chem **278**(26): 24018-24025.
Song, J., D. Kim and E.-J. Jin (2011). "MicroRNA-488 suppresses cell migration through modulation of the focal adhesion activity during chondrogenic differentiation of chick limb mesenchymal cells." Cell Biology International **35**(2): 179-185.
Song, R. H., M. D. Tortorella, A. M. Malfait, J. T. Alston, Z. Yang, E. C. Arner and D. W. Griggs (2007). "Aggrecan degradation in human articular cartilage explants is mediated by both ADAMTS-4 and ADAMTS-5." Arthritis Rheum **56**(2): 575-585.
Sorrentino, A., M. Ferracin, G. Castelli, M. Biffoni, G. Tomaselli, M. Baiocchi, A. Fatica, M. Negrini, C. Peschle and M. Valtieri (2008). "Isolation and characterization of CD146+ multipotent mesenchymal stromal cells." Exp Hematol **36**(8): 1035-1046.
Stanton, H., F. M. Rogerson, C. J. East, S. B. Golub, K. E. Lawlor, C. T. Meeker, C. B. Little, K. Last, P. J. Farmer, I. K. Campbell, A. M. Fourie and A. J. Fosang (2005). "ADAMTS5 is the major aggrecanase in mouse cartilage in vivo and in vitro." Nature **434**(7033): 648-652.
Steele, R., J. L. Mott and R. B. Ray (2010). "MBP-1 upregulates miR-29b that represses Mcl-1, collagens, and matrix-metalloproteinase-2 in prostate cancer cells." Genes Cancer **1**(4): 381-387.
Subramanian, M., S. R. Rao, P. Thacker, S. Chatterjee and D. Karunagaran (2014). "MiR-29b downregulates canonical Wnt signaling by suppressing coactivators of beta-catenin in human colorectal cancer cells." J Cell Biochem **115**(11): 1974-1984.
Sulzbacher, I. (2013). "Osteoarthritis: histology and pathogenesis." Wien Med Wochenschr **163**(9-10): 212-219.
Suomi, S., H. Taipaleenmäki, A. Seppänen, T. Ripatti, K. Väänänen, T. Hentunen, A.-M. Säämänen and T. Laitala-Leinonen (2008). "MicroRNAs regulate osteogenesis and chondrogenesis of mouse bone marrow stromal cells." Gene Regulation and Systems Biology **2**: 177-191.
Swingler, T., G. Wheeler, V. Carmont, H. Elliott, M. Barter, M. Abu-Elmagd, S. Donell, R. Boot-Handford, M. Hajihosseini, A. Münsterberg, T. Dalmay, D. Young and I. Clark (2011). "The expression and function of microRNAs in chondrogenesis and osteoarthritis." Arthritis & Rheumatism: n/a-n/a.
(2012). "The expression and function of microRNAs in chondrogenesis and osteoarthritis." Arthritis & Rheumatism **64**: 1909-1919.
Taganov, K., M. Boldin, K.-J. Chang and D. Baltimore (2006). "NF-kappaB-dependent induction of microRNA miR-146, an inhibitor targeted to signaling proteins of innate immune responses." Proc Natl Acad Sci U S A **103**(33): 12481-12486.

Tan, M., J. Wu and Y. Cai (2013). "Suppression of Wnt signaling by the miR-29 family is mediated by demethylation of WIF-1 in non-small-cell lung cancer." Biochem Biophys Res Commun **438**(4): 673-679.

Tardif, G., D. Hum, J.-P. Pelletier, N. Duval and J. Martel-Pelletier (2009). "Regulation of the IGFBP-5 and MMP-13 genes by the microRNAs miR-140 and miR-27a in human osteoarthritic chondrocytes." BMC Musculoskelet Disord **10**: 148.

Tetlow, L., D. Adlam and D. Woolley (2001). "Matrix metalloproteinase and proinflammatory cytokine production by chondrocytes of human osteoarthritic cartilage: Associations with degenerative changes." Arthritis & Rheumatism **44**(3): 585-594.

Tortorella, M. D., A. M. Malfait, C. Deccico and E. Arner (2001). "The role of ADAM-TS4 (aggrecanase-1) and ADAM-TS5 (aggrecanase-2) in a model of cartilage degradation." Osteoarthritis Cartilage **9**(6): 539-552.

Tuddenham, L., G. Wheeler, S. Ntounia-Fousara, J. Waters, M. Hajihosseini, I. Clark and T. Dalmay (2006). "The cartilage specific microRNA-140 targets histone deacetylase 4 in mouse cells." FEBS Lett **580**(17): 4214-4217.

Ugalde, A. P., A. J. Ramsay, J. de la Rosa, I. Varela, G. Marino, J. Cadinanos, J. Lu, J. M. Freije and C. Lopez-Otin (2011). "Aging and chronic DNA damage response activate a regulatory pathway involving miR-29 and p53." EMBO J **30**(11): 2219-2232.

Umlauf, D., S. Frank, T. Pap and J. Bertrand (2010). "Cartilage biology, pathology, and repair." Cellular and Molecular Life Sciences **67**(24): 4197-4211.

van Amerongen, R. and A. Berns (2005). "Re-evaluating the role of Frat in Wnt-signal transduction." Cell Cycle **4**(8): 1065-1072.

van Beuningen, H. M., H. L. Glansbeek, P. M. van der Kraan and W. B. van den Berg (1998). "Differential effects of local application of BMP-2 or TGF-beta 1 on both articular cartilage composition and osteophyte formation." Osteoarthritis Cartilage **6**(5): 306-317.

van der Kraan, P. M. and W. B. van den Berg (2007). "Osteophytes: relevance and biology." Osteoarthritis Cartilage **15**(3): 237-244.

van Rooij, E. and S. Kauppinen (2014). "Development of microRNA therapeutics is coming of age." EMBO Mol Med **6**(7): 851-864.

van Rooij, E., L. B. Sutherland, J. E. Thatcher, J. M. DiMaio, R. H. Naseem, W. S. Marshall, J. A. Hill and E. N. Olson (2008). "Dysregulation of microRNAs after myocardial infarction reveals a role of miR-29 in cardiac fibrosis." Proc Natl Acad Sci U S A **105**(35): 13027-13032.

Vasudevan, S. and J. Steitz (2007). "AU-rich-element-mediated upregulation of translation by FXR1 and Argonaute 2." Cell **128**(6): 1105-1118.

Vasudevan, S., Y. Tong and J. Steitz (2007). "Switching from repression to activation: microRNAs can up-regulate translation." Science (New York, N.Y.) **318**(5858): 1931-1934.

Ventura, A., A. Young, M. Winslow, L. Lintault, A. Meissner, S. Erkeland, J. Newman, R. Bronson, D. Crowley, J. Stone, R. Jaenisch, P. Sharp and T. Jacks (2008). "Targeted deletion reveals essential and overlapping functions of the miR-17 through 92 family of miRNA clusters." Cell **132**(5): 875-886.

Verrecchia, F., M. L. Chu and A. Mauviel (2001). "Identification of novel TGF-beta /Smad gene targets in dermal fibroblasts using a combined cDNA microarray/promoter transactivation approach." J Biol Chem **276**(20): 17058-17062.

Verrecchia, F. and A. Mauviel (2002). "Transforming growth factor-beta signaling through the Smad pathway: role in extracellular matrix gene expression and regulation." J Invest Dermatol **118**(2): 211-215.

Wang, B., R. Komers, R. Carew, C. E. Winbanks, B. Xu, M. Herman-Edelstein, P. Koh, M. Thomas, K. Jandeleit-Dahm, P. Gregorevic, M. E. Cooper and P. Kantharidis (2012). "Suppression of

microRNA-29 expression by TGF-beta1 promotes collagen expression and renal fibrosis." J Am Soc Nephrol **23**(2): 252-265.
Wang, F. S., P. C. Chuang, C. L. Lin, M. W. Chen, H. J. Ke, Y. H. Chang, Y. S. Chen, S. L. Wu and J. Y. Ko (2013). "MicroRNA-29a protects against glucocorticoid-induced bone loss and fragility in rats by orchestrating bone acquisition and resorption." Arthritis Rheum **65**(6): 1530-1540.
Wang, H., R. Garzon, H. Sun, K. J. Ladner, R. Singh, J. Dahlman, A. Cheng, B. M. Hall, S. J. Qualman, D. S. Chandler, C. M. Croce and D. C. Guttridge (2008). "NF-kappaB-YY1-miR-29 regulatory circuitry in skeletal myogenesis and rhabdomyosarcoma." Cancer Cell **14**(5): 369-381.
Wang, H. X., F. R. Tekpetey and G. M. Kidder (2009). "Identification of WNT/beta-CATENIN signaling pathway components in human cumulus cells." Mol Hum Reprod **15**(1): 11-17.
Wang, L., L. Zhou, P. Jiang, L. Lu, X. Chen, H. Lan, D. C. Guttridge, H. Sun and H. Wang (2012). "Loss of miR-29 in myoblasts contributes to dystrophic muscle pathogenesis." Mol Ther **20**(6): 1222-1233.
Wang, L. G. and J. Gu (2012). "Serum microRNA-29a is a promising novel marker for early detection of colorectal liver metastasis." Cancer Epidemiol **36**(1): e61-67.
Watanabe, T., T. Sato, T. Amano, Y. Kawamura, N. Kawamura, H. Kawaguchi, N. Yamashita, H. Kurihara and T. Nakaoka (2008). "Dnm3os, a non-coding RNA, is required for normal growth and skeletal development in mice." Dev Dyn **237**(12): 3738-3748.
Wei, W., H. B. He, W. Y. Zhang, H. X. Zhang, J. B. Bai, H. Z. Liu, J. H. Cao, K. C. Chang, X. Y. Li and S. H. Zhao (2013). "miR-29 targets Akt3 to reduce proliferation and facilitate differentiation of myoblasts in skeletal muscle development." Cell Death Dis **4**: e668.
Weng, L. H., C. J. Wang, J. Y. Ko, Y. C. Sun and F. S. Wang (2010). "Control of Dkk-1 ameliorates chondrocyte apoptosis, cartilage destruction, and subchondral bone deterioration in osteoarthritic knees." Arthritis Rheum **62**(5): 1393-1402.
Wermter, C., M. Howel, V. Hintze, B. Bombosch, K. Aufenvenne, I. Yiallouros and W. Stocker (2007). "The protease domain of procollagen C-proteinase (BMP1) lacks substrate selectivity, which is conferred by non-proteolytic domains." Biol Chem **388**(5): 513-521.
Westholm, J. and E. Lai (2011). "Mirtrons: microRNA biogenesis via splicing." Biochimie **93**(11): 1897-1904.
Wieland, H., M. Michaelis, B. Kirschbaum and K. Rudolphi (2005). "Osteoarthritis — an untreatable disease?" Nature Reviews Drug Discovery **4**(4): 331-344.
Wienholds, E., W. P. Kloosterman, E. Miska, E. Alvarez-Saavedra, E. Berezikov, E. de Bruijn, H. R. Horvitz, S. Kauppinen and R. H. Plasterk (2005). "MicroRNA expression in zebrafish embryonic development." Science **309**(5732): 310-311.
Wienholds, E., M. Koudijs, F. van Eeden, E. Cuppen and R. Plasterk (2003). "The microRNA-producing enzyme Dicer1 is essential for zebrafish development." Nat Genet **35**(3): 217-218.
Wightman, B., I. Ha and G. Ruvkun (1993). "Posttranscriptional regulation of the heterochronic gene lin-14 by lin-4 mediates temporal pattern formation in C. elegans." Cell **75**(5): 855-862.
Willert, K., M. Brink, A. Wodarz, H. Varmus and R. Nusse (1997). "Casein kinase 2 associates with and phosphorylates dishevelled." EMBO J **16**(11): 3089-3096.
Willert, K. and K. A. Jones (2006). "Wnt signaling: is the party in the nucleus?" Genes Dev **20**(11): 1394-1404.
Wittmann, J. and H.-M. Jäck (2010). "Serum microRNAs as powerful cancer biomarkers." Biochim Biophys Acta **1806**(2): 200-207.
Xiong, Y., J. H. Fang, J. P. Yun, J. Yang, Y. Zhang, W. H. Jia and S. M. Zhuang (2010). "Effects of microRNA-29 on apoptosis, tumorigenicity, and prognosis of hepatocellular carcinoma." Hepatology **51**(3): 836-845.
Xu, J., Y. Kang, W.-m. Liao and L. Yu (2012). "MiR-194 Regulates Chondrogenic Differentiation of Human Adipose-Derived Stem Cells by Targeting Sox5." PLoS One **7**(3): e31861.

Yamasaki, K., T. Nakasa, S. Miyaki, M. Ishikawa, M. Deie, N. Adachi, Y. Yasunaga, H. Asahara and M. Ochi (2009). "Expression of MicroRNA-146a in osteoarthritis cartilage." Arthritis and rheumatism **60**(4): 1035-1041.

Yamashita, S., S. Miyaki, Y. Kato, S. Yokoyama, T. Sato, F. Barrionuevo, H. Akiyama, G. Scherer, S. Takada and H. Asahara (2012). "L-Sox5 and Sox6 enhance chondrogenic miR-140 expression by strengthening dimeric Sox9 activity." Journal of Biological Chemistry.

Yan, C., Y. Wang, X.-Y. Shen, G. Yang, J. Jian, H.-S. Wang, G.-Q. Chen and Q. Wu (2011). "MicroRNA regulation associated chondrogenesis of mouse MSCs grown on polyhydroxyalkanoates." Biomaterials **32**(27): 6435-6444.

Yang, B., H. Guo, Y. Zhang, L. Chen, D. Ying and S. Dong (2011). "MicroRNA-145 Regulates Chondrogenic Differentiation of Mesenchymal Stem Cells by Targeting Sox9." PLoS One **6**(7): e21679.

Yang, B., H. Guo, Y. Zhang, S. Dong and D. Ying (2011). "The microRNA expression profiles of mouse mesenchymal stem cell during chondrogenic differentiation." BMB Reports **44**(1): 28-33.

Yang, J., S. Qin, C. Yi, G. Ma, H. Zhu, W. Zhou, Y. Xiong, X. Zhu, Y. Wang, L. He and X. Guo (2011). "MiR-140 is co-expressed with Wwp2-C transcript and activated by Sox9 to target Sp1 in maintaining the chondrocyte proliferation." FEBS Lett **585**(19): 2992-2997.

Yang, T., Y. Liang, Q. Lin, J. Liu, F. Luo, X. Li, H. Zhou, S. Zhuang and H. Zhang (2013). "miR-29 mediates TGFbeta1-induced extracellular matrix synthesis through activation of PI3K-AKT pathway in human lung fibroblasts." J Cell Biochem **114**(6): 1336-1342.

Yi, R., Y. Qin, I. Macara and B. Cullen (2003). "Exportin-5 mediates the nuclear export of pre-microRNAs and short hairpin RNAs." Genes Dev **17**(24): 3011-3016.

Zamli, Z. and M. Sharif (2011). "Chondrocyte apoptosis: a cause or consequence of osteoarthritis?" Int J Rheum Dis **14**(2): 159-166.

Zampetaki, A., S. Kiechl, I. Drozdov, P. Willeit, U. Mayr, M. Prokopi, A. Mayr, S. Weger, F. Oberhollenzer, E. Bonora, A. Shah, J. Willeit and M. Mayr (2010). "Plasma microRNA profiling reveals loss of endothelial miR-126 and other microRNAs in type 2 diabetes." Circ Res **107**(6): 810-817.

Zeng, Y. and B. Cullen (2004). "Structural requirements for pre-microRNA binding and nuclear export by Exportin 5." Nucleic Acids Res **32**(16): 4776-4785.

Zhang, Y. K., H. Wang, Y. Leng, Z. L. Li, Y. F. Yang, F. J. Xiao, Q. F. Li, X. Q. Chen and L. S. Wang (2011). "Overexpression of microRNA-29b induces apoptosis of multiple myeloma cells through down regulating Mcl-1." Biochem Biophys Res Commun **414**(1): 233-239.

Zhang, Z., J. Zou, G. K. Wang, J. T. Zhang, S. Huang, Y. W. Qin and Q. Jing (2011). "Uracils at nucleotide position 9-11 are required for the rapid turnover of miR-29 family." Nucleic Acids Res **39**(10): 4387-4395.

Zhao, Q., H. Eberspaecher, V. Lefebvre and B. De Crombrugghe (1997). "Parallel expression of Sox9 and Col2a1 in cells undergoing chondrogenesis." Dev Dyn **209**(4): 377-386.

Zhong, N., J. Sun, Z. Min, W. Zhao, R. Zhang, W. Wang, J. Tian, L. Tian, J. Ma, D. Li, Y. Han and S. Lu (2012). "MicroRNA-337 is associated with chondrogenesis through regulating TGFBR2 expression." Osteoarthritis and Cartilage.

Zhou, S., K. Eid and J. Glowacki (2004). "Cooperation between TGF-beta and Wnt pathways during chondrocyte and adipocyte differentiation of human marrow stromal cells." J Bone Miner Res **19**(3): 463-470.

Zhu, M., M. Chen, M. Zuscik, Q. Wu, Y. J. Wang, R. N. Rosier, R. J. O'Keefe and D. Chen (2008). "Inhibition of beta-catenin signaling in articular chondrocytes results in articular cartilage destruction." Arthritis Rheum **58**(7): 2053-2064.

Zhu, M., D. Tang, Q. Wu, S. Hao, M. Chen, C. Xie, R. N. Rosier, R. J. O'Keefe, M. Zuscik and D. Chen (2009). "Activation of beta-catenin signaling in articular chondrocytes leads to osteoarthritis-

like phenotype in adult beta-catenin conditional activation mice." J Bone Miner Res **24**(1): 12-21.

ENDICES

Genes	Accession number	Sequences (5'->3')
ADAMTS6	ENSG00000049192	Forward: ACGTGAGCTCTCTCATCGTCATGGTTCTGC Reverse: ACGTGAGCTCCAAGCAGGAGAATGAATGTAGG
ADAMTS14	ENSG00000138316	Forward: GAGCTCGCTGTGCCCTGCCATC GAGCTCGGGTCCAATGGCGATGTTA
ADAMTS17	ENSG00000140470	Forward: ACGTTCTAGAAACATGAGCGTGGACTTGG Reverse: ACGTTCTAGATGTAATGCAAGTTAACGAATGG
ADAMTS19	ENSG00000145808	Forward: ACGTGAGCTCAATCACAGCTCCAGGTAATC Reverse: ACGTGAGCTCCCAAGAGACATACTATCTTCCAAGG
FZD3	ENSG00000104290	Forward: ATGCGTCGACTATTAGATGCCCAGCCTTTCTC Reverse: ATGCGTCGACATGCCTACCAAGAGGATAACATTC
FZD5	ENSG00000163251	Forward: ATGCGTCGACGGCATCGGCTACAACCTGAC Reverse: ATGCGTCGACAGACCACACAGTTCAAAGA AACCTG
FRAT2	ENSG00000181274	Forward: ATGCGTCGACCAACAGCGTCCAGTTCCTAC Reverse: ATGCGTCGACGCCGTCAAGTTTCATACAGC
CK2A2	ENSG00000070770	Forward: ATGCGTCGACATGCAGGTACTAGAGTTGTGTGG Reverse: ATGCGTCGACAATAAGTTTGCTTGTTTCTGTGG
DVL3	ENSG00000161202	Forward: ATGCGTCGACGCTGCGTTCCTCTCTCCATC Reverse: ATGCGTCGACTACCATTTATTGAGCACCTACTCTACTG TG

Table 1: Primer sequences for PCR amplification 3'UTR region of potential targets of the miR-29 family. For subcloning purpose, restriction sites (bases underlined) were added to the 5'P of the primers. *Sac*I (GAGCTC), *Sal*I (GTCGAC), *Xba*I (TCTAGA).

Genes	Mutant	Primer sequence (5'->3')
ADAMTS6	Site 1	Forward: TATGTGATGCACTGACATGTAATTTAAGAAGCTTATGATGGAATCAAGTCAAACATGCTGTTTAACTGAAAG Reverse: CTTTCAGTTAAACAGCATGTTTGACTTGATTCCATCATAAGCTTCTTAAATTACATGTCAGTGCATCACATA
	Site 2	Forward: TATTTATTTCACCAGGGCACATTAAGCTTAAGTTAACTGTTCTTTGAAAAGGCGCAAGGGAATTCAGT Reverse: ACTGAATTCCCTTGCGCCTTTTCAAAGAACAGTTAACTTAAGCTTAATGTGCCCTGGTGAAATAAATA
ADAMTS10	Site 1	Forward: GGGGACACAGACCCGTTTGTAAGCTTACCCCTTGTCGATGGTGTGCG Reverse: CGCACACCATCGACAAGGGGTAAGCTTACAAACGGGTCTGTGTCCCC
	Site 2	Forward: GCTCGGTCCGGGCCAAGCTTATGACGATGAGAGATGCATTAATCGGTCC Reverse: GGACCGATTAATGCATCTCTCATCGTCATAAGCTTGGCCCGGACCGAGC
ADAMTS14	Site 1	Forward: GTTTGTCTTTGCTGGCCAGAAGAGTCGACTCATGGCCATACTCTGGCCTTG Reverse: CAAGGCCAGAGTATGGCCATGAGTCGACTCTTCTGGCCAGCAAAGAC
	Site 2	Forward: GGGTGCCAGCCCCTGGCCGTCGACTGGAGTGGGGAAGACAC Reverse: GTGTCTTCCCCACTCCAGTCGACGGCCAGGGGCTGGCACCC
	Site 3	Forward: CTAAACTCCTGCCAGGTGATAGAGAGCTCTCTCACTTCTTCCTTCCCCAAGGC

		Reverse: GCCTTGGGGAAGGAAGAAGTGAGAGAGCTCTCTATCACCTGGCAGGAGTTTAG
	Site 4	Forward: CTAAACTCCTGCCAGGTGATAGAGAGCTCTCTCACTTCTTCCTTCCCCAAGGC Reverse: GCCTTGGGGAAGGAAGAAGTGAGAGAGCTCTCTATCACCTGGCAGGAGTTTAG
ADAMTS17	Site 1	Forward: GCAATTACCGTTTCTTATGTCACAGTCGACTGAAGAGAGGCCCTTCTGTTTCCC Reverse: GGGAAACAGAAGGGCCTCTCTTCAGTCGACTGTGACATAAGAAACGGTAATTGC
	Site 2	Forward: CACCAACTTGGTGGGCATTTCATGTCGACTTATGTTCTAGGACTTTACCGTA Reverse: TACGGTAAAGTCCTAGAACATAAGTCGACATGAAATGCCCACCAAGTTGGTG
	Site 3	Forward: TAACAAAACAAAACACAGAAACACAGTCGACATAAATCAAGAAGCACAGGGAGATGATCCCATGG Reverse: CCATGGGATCATCTCCCTGTGCTTCTTGATTTATGTCGACTGTGTTTCTGTGTTTTGTTTTGTTA
	Site 4	Forward: GAAGTGTTGAGAAACTTCCGTGTCGACTCTGTGGAAAGAACCGAGGGT Reverse: ACCCTCGGTTCTTTCCACAGAGTCGACACGGAAGTTTCTCAACACTTC
	Site 5	Forward: CCAGAGTCTCACGACCCTACGGTCGCCTTTTTATTGGTGCAAAATTAAACC Reverse: GGTTTAATTTTGCACCAATAAAAAGGCGACCGTAGGGTCGTGAGACTCTGG
ADAMTS	Site 1	Forward: ATCAAATTAATTTATTTTTTTGCCTGCCAAACATCCAATGGTCGACTTGTTTTGGTTACACAAACATTTTGATTTATACTATATG

19		Reverse: CATATAGTATAAATCAAAATGTTTGTGTAACCAAAACAAGTCGACCATTGGATGTTTGGCAGGCAAAAAAATAAATTAATTTGAT
	Site 2	Forward: GTTGTTTGTTAGGGCTATCTCTAAGTCGACCCTCTCTCCCCACCAATAACATTGAATTATC Reverse: ATAATTCAATGTTATTGGTGGGGAGAGAGGGTCGACTTAGAGATAGCCCTAACAAACAACG
FZD3		Forward: GGATTTAGTCTAACTCACAGCTAAGGTAGAAAAGTACTCTGATGGCAAGAGAATGTCCAGACTAATATTTTC Reverse: GAAAATATTAGTCTGGACATTCTCTTGCCATCAGAGTACTTTTCTACCTTAGCTGTGAGTTAGACTAAATCC
FZD5	Site 1	Forward: CGGCGTCGCGGCCCAAGCTTGGGAGGCGGTCGCAG Reverse: CTGCGACCGCCTCCCAAGCTTGGGCCGCGACGCCG
	Site 2	Forward: GTGGACGTGGAGATGAAGCACAAGCTTGACCACAGGCCTATCCAGAAGG Reverse: CCTTCTGGATAGGCCTGTGGTCAAGCTTGTGCTTCATCTCCACGTCCAC
	Site 3	Forward: GCCCACCAGCAGGTAGAAGCTTAGCGGGCCCAGCACGAAGCC Reverse: GGCTTCGTGCTGGGCCCGCTAAGCTTCTACCTGCTGGTGGGC
	Site 4	Forward: CACATGAAGTACTTGAGCATGAAGCTTCAGTACTCGGGCTTGGCGCGCG Reverse: CGCGCGCCAAGCCCGAGTACTGAAGCTTCATGCTCAAGTACTTCATGTG
	Site 5	Forward: CGGGAGGGGGCAACAAGCTTATGAAGGTAAACGGAAGTGACCTTGGCA Reverse: TGCCAAGGTCACTTCCGTTTACCTTCATAAGCTTGTTGCCCCCTCCCG
FRAT2	Site 1	Forward: GCGTGGAGAAATGTATGCGCCAGAAGCTTTCCGTGGGGCATGAG

		AATTTCC Reverse: GGAAATTCTCATGCCCCACGGAAAGCTTCTGGCGCATACATTTCTCCACGC
	Site 2	Forward: CTTATTTTCTGGTGGAGGAGCTTAGTAAGTAAGCTTACAATTGCTGTGCAAAGAAATTCCAGAGG-3' Reverse: CCTCTGGAATTTCTTTGCACAGCAATTGTAAGCTTACTTACTAAGCTCCTCCACCAGAAAATAAG
	Site 3	Forward: GGGAGACTCCAAGCGGTGGTAAAAGCTTAACAGGGCTCTTCTTGGAGCAAG Reverse: CTTGCTCCAAGAAGAGCCCTGTTAAGCTTTTACCACCGCTTGGAGTCTCCC
CK2A2	Site 1	Forward: AGAGGAATATACAAGGGGCTTGGGGAAGAAAATAAGCTTCCCGGAGCAAGTGTTG Reverse: CAACACTTGCTCCGGGAAGCTTATTTTCTTCCCCAAGCCCCTTGTATATTCCTCT
	Site 2	Forward: TCTCCTCTAATCTATCAGTCTGAGAAGCTTTTCCTCTCTGCAAGGGAACACATTTGC Reverse: GCAAATGTGTTCCCTTGCAGAGAGGAAAAGCTTCTCAGACTGATAGATTAGAGGAGA
	Site 3	Forward: GCGCCTGACTCGAGAAGCTTACCTTTCAGTCCACTGGGACCAATCCA Reverse: TGGATTGGTCCCAGTGGACTGAAAGGTAAGCTTCTCGAGTCAGGCGC
	Site 4	Forward: CTGCTTCCATCCTTATCAACAGAAGCTTTGGGAGAACCTAAGTCATTTCCCTGAG Reverse: TCAGGGAAATGACTTAGGTTCTCCCAAAGCTTCTGTTGATAAGGATGGAAGCAG
DVL3	Site 1	Forward: GTGCGCTAACTGCTCGCAGAAGCTTGCGAGGGTGGGGTGCACC

		Reverse: GGTGCACCCCACCCTCGCAAGCTTCTGCGAGCAGTTAGCGCAC
	Site 2	Forward: CCCTTTTGTCTCTGGGACCAGACTTGTTAAGCTTACCCCTTACTCCCCTCTGC Reverse: GCAGAGGGGAGTAAGGGGTAAGCTTAACAAGTCTGGTCCCAGAGACAAAAGGG
	Site 3	Forward: GCACAGTGCCTGGCACACAGTAGAGTAAAGCTTCAATAAATGGTAGTCGACC Reverse: GGTCGACTACCATTTATTGAAGCTTTACTCTACTGTGTGCCAGGCACTGTGC
DICER		Forward: ACGTGAGCTCGTGTGCAGTAGTGCCAGTCC Reverse: ACGTGAGCTCTGCAATCACAGGAACACAGG

Table 2: Primers for mutating the binding sites of the miR-29 family

Genes	Accession number	Primer sequence (5'->3')	Probe
Arginase-1	ENSMUST00000020161	Forward: CCTGAAGGAACTGAAAGGAAAG Reverse: TTGGCAGATATGCAGGGAGT	2
IL-6	ENSMUST00000026845	Forward: TGATGGATGCTACCAAACTGG Reverse: TTCATGTACTCCAGGTAGCTATGG	6
SAA3	ENAMUST00000006956	Forward: GCTCGGGGGAACTATGATG Reverse: AACTTCTGAACAGCCTCTCTGG	26
Axin2		Forward: GCTGACGGATGATTCCATGT Reverse: ACTGCCCACACGATAAGGAG	56
SOX9	ENST00000245479	Forward: TACCCGCACTTGCACAAC Reverse: TCTCGCTCTCGTTCAGAAGTC	61
FZD3	NM_017412	Forward: ACAGCAAAGTGAGCAGCTACC Reverse: CTGTAACTGCAGGGCGTGTA	75
FZD5	NM_003468	Forward:ACCCCAGGGGAGAGAAACT Reverse: TGCAAATTGGGGGAAGTAAG	83
DVL3	NM_004423	Forward:CCCTGAGCACCATCACCT Reverse: GGATGGACAAGTGGAAGTCG	17
FRAT2		Forward: GTTCAAGGTCACGGTTTGCT Reverse: GAAAAGACTCCGGGGTGAGT	14
CK2A2	NM_001896	Forward: CCATGGAGCACCCATACTTC Reverse: CACAGCATTGTCTGCACAAG	68

Table 3: Primer sequence and the Universal Probe Library probe for gene of interest

Genes	Accession number	Primer sequence (5'-3')
ADAMTS4	MM_005099	Forward: CAAGGTCCCATGTGCAACGT Reverse: CATCTGCCACCACCAGTGTCT Probe: FAM-CCGAAGAGCCAAGCGCTTTGCTTC-TAMRA
ADAMTS6	NM_014273	Forward: GGCTGAATGACACATCCACTGTT Reverse: CAAACCGTTCAATGCTCACTGA Probe: FAM-AAGCGCTTCCGCCTCTGCAACC-TAMRA
ADAMTS10	NM_030957	Forward: AGAGAACGGTGTGGCTAACCA Reverse: TCTCTCGCGCTCACACATTC Probe: FAM-CAGTGCTCATCACACGCTATGACATCTGC-TAMRA
ADAMTS14	AF366351	Forward: CGCTGGATGGGACTGAGTGT Reverse: CGCGAACATGACCCAAACTT Probe: FAM-CCCGGCAAGTGGTGCTTCAAAGGT-TAMRA
ADAMTS17	NM_139057	Forward: GGTCTCAATTTGGCCTTTACCAT Reverse: GACCTGCCAGCGGCAAGAT Probe: FAM-CCACAACTTGGGCATGAACCACGA-TAMRA
ADAMTS19	AJ311904	Forward: GGTGTAAGGCTGGAGAATGTACCA Reverse: TGCGCTCTCGACTGCTGAT Probe: FAM-CCTCAGCACCTGAACATCTGGCCG-TAMRA
MMP3	NM002422	Forward: TTCCGCCTGTCTCAAGATGATAT Reverse: AAAGGACAAAGCAGGATCACAGTT Probe: FAM-TCAGTCCCTCTATGGACCTCCCCCTGAC-TAMRA

Table 4: Primer pairs and probe for gene of interest

Genes	Primer sequences (5'->3')
Pri-miR-29a/b1exon 1	Forward: TACTGAACTGTCACGGCAGA Reverse: TGTAGTTAGCGACCTCTGCT
Pri-miR-29a/b1Exon4	Forward: TTGCACCCTCACGACATGCT Reverse: TGACTCTCAGCAGGCCTCA
Pri-miR-29b2/c exon 1	Forward: ACTTCTTTAGGGGTGTGCGTA Reverse: ACCCATCTCCCTAGCATTCT
Pri-miR-29b2/c Exon6	Forward: TCAGACTTGCCACCTGGACT Reverse: AGTTGGCATGAGGCTTCGA
Pre-29a	Forward: CTGATTTCTTTTGGTGTTCAG Reverse: AACCGATTTCAGATGGTGC
Pre-29b1	Forward: CATATGGTGGTTTAGATTT Reverse: AACACTGATTTCAAATGGTG
Pre-29b2	Forward: GCTGGTTTCACATGGTGGC Reverse: AACACTGATTTCAAATGGTG
Pre-29c	Forward: CGATTTCTCCTGGTGTTCA Reverse: ACCGATTTCAAATGGTGC

Table 5: Primers for detecting the primary and the premature sequence of the miR-29 family

Names	24_DMM_R	24_DMM_L	log2 Fold change	Fold change
CYP2E1	9.0	10.2	-1.2	2.3
CES3	8.1	9.3	-1.2	2.3
TMEM45B	7.9	8.6	-0.8	1.7
CFD	12.9	13.6	-0.7	1.6
SCD1	10.1	10.7	-0.6	1.6
IGFBP6	8.9	9.6	-0.6	1.5
CHAD	12.4	13.0	-0.6	1.5
LOC100045005	9.6	10.2	-0.6	1.5
TENS1	8.5	9.1	-0.6	1.5
C130045I22RIK	8.2	8.8	-0.6	1.5
LOC667337	9.4	9.9	-0.6	1.5
CXCL1	9.1	7.3	1.9	3.6
CCL7	9.2	7.5	1.8	3.4
SAA3	8.9	7.3	1.6	3.1
TIMP1	12.0	10.5	1.5	2.9
SERPINA3N	11.2	9.7	1.5	2.8
GP38	10.8	9.4	1.4	2.6
MMP3	8.9	7.6	1.3	2.5
ARG1	8.0	7.1	0.8	1.8
CXCL14	9.4	8.8	0.7	1.6
MB	11.9	11.2	0.7	1.6
ANGPTL4	9.5	8.9	0.6	1.6
MT1	13.5	12.9	0.6	1.6
ANKRD23	9.5	8.9	0.6	1.5
MS4A6D	9.9	9.3	0.6	1.5
LOC386330	9.9	9.4	0.5	1.5
LOC270589	8.9	8.4	0.5	1.5
CCL9	11.2	10.6	0.5	1.5
CKM	12.3	11.8	0.5	1.5
LOC386144	9.6	9.1	0.5	1.4

Table 6: List genes changed expression at day 1 in DMM model

GENES	7_DMM_R	7_DMM_L	log2 Fold change	Fold change
MYL3	9.8	11.0	-1.2	2.3
ATP1A2	9.0	10.1	-1.2	2.3
NDRG2	10.0	11.2	-1.2	2.3
CKMT2	11.7	12.8	-1.2	2.2
ANKRD23	10.2	11.4	-1.2	2.2
2310003M01RIK	9.5	10.6	-1.1	2.2
ACTN2	11.1	12.2	-1.1	2.2
2310042D19RIK	9.2	10.3	-1.1	2.2
MYH2	11.0	12.1	-1.1	2.2
PFKM	11.5	12.6	-1.1	2.2
ABRA	8.6	9.7	-1.1	2.1
COX7A1	11.4	12.5	-1.1	2.1
ANKRD2	8.0	9.1	-1.1	2.1
COX8B	11.8	12.8	-1.1	2.1
MB	12.0	13.1	-1.1	2.1
ENO3	12.9	14.0	-1.1	2.1
DUSP26	8.1	9.2	-1.1	2.1
RTN2	10.0	11.1	-1.0	2.1
PKIA	10.4	11.5	-1.0	2.1
TCAP	12.5	13.6	-1.0	2.1
MYOZ1	10.4	11.5	-1.0	2.0
MYOM1	9.9	10.9	-1.0	2.0
ACTN3	11.3	12.3	-1.0	2.0
2310002L09RIK	8.6	9.6	-1.0	2.0
HRC	10.3	11.3	-1.0	2.0
MYOM2	9.1	10.1	-1.0	2.0
CKM	13.0	14.0	-1.0	2.0
CSRP3	8.5	9.5	-1.0	2.0
TMEM38A	9.3	10.3	-1.0	2.0
1110012N22RIK	9.2	10.2	-1.0	2.0
TPM2	11.3	12.3	-1.0	2.0
RYR1	10.1	11.1	-1.0	2.0
MLF1	9.5	10.5	-1.0	2.0
TTN	9.7	10.7	-1.0	2.0
TMOD4	10.7	11.7	-1.0	2.0
DYSFIP1	8.7	9.7	-1.0	2.0
NRAP	9.1	10.1	-1.0	2.0
CMYA5	10.8	11.8	-1.0	2.0
SMTNL2	8.5	9.5	-1.0	1.9
MYLK2	9.2	10.2	-1.0	1.9

MYL2	9.3	10.3	-0.9	1.9
LOC669660	8.6	9.6	-0.9	1.9
KBTBD10	9.8	10.7	-0.9	1.9
ASB2	10.6	11.5	-0.9	1.9
A530098C11RIK	8.7	9.6	-0.9	1.9
F730003H07RIK	9.3	10.3	-0.9	1.9
ZMYND17	8.5	9.4	-0.9	1.9
CPT1B	8.3	9.2	-0.9	1.9
2310079P10RIK	8.5	9.4	-0.9	1.9
EEF1A2	10.7	11.6	-0.9	1.9
YIPF7	8.5	9.4	-0.9	1.9
SCL0003151.1_1374	8.9	9.8	-0.9	1.9
INMT	7.6	8.5	-0.9	1.9
CES3	8.8	9.7	-0.9	1.9
PYGM	9.2	10.1	-0.9	1.8
MYBPC2	11.6	12.5	-0.9	1.8
8030451F13RIK	8.6	9.5	-0.9	1.8
FABP3	10.6	11.4	-0.9	1.8
NEURL	9.5	10.4	-0.9	1.8
PDLIM3	10.4	11.3	-0.9	1.8
SYPL2	9.6	10.5	-0.9	1.8
4833419K08RIK	9.0	9.9	-0.9	1.8
AMPD1	11.1	12.0	-0.8	1.8
CACNA1S	8.6	9.5	-0.8	1.8
SCL0002069.1_48	8.1	9.0	-0.8	1.8
C130073O12RIK	9.0	9.9	-0.8	1.8
GM1157	7.8	8.6	-0.8	1.8
MYH1	9.2	10.1	-0.8	1.8
SLC25A37	11.8	12.6	-0.8	1.8
LOC638935	8.1	9.0	-0.8	1.8
LOC386360	10.4	11.2	-0.8	1.8
BC030476	9.0	9.8	-0.8	1.8
MYH4	10.0	10.8	-0.8	1.7
SCL000959.1_2	13.3	14.1	-0.8	1.7
RPL3L	12.2	13.0	-0.8	1.7
COX6A2	12.7	13.5	-0.8	1.7
MTDNA_ND4L	8.7	9.5	-0.8	1.7
TNNT3	13.1	13.9	-0.8	1.7
AK1	9.8	10.6	-0.8	1.7
DES	11.1	11.9	-0.8	1.7
A2BP1	8.4	9.2	-0.8	1.7
KY	9.1	9.8	-0.8	1.7

UNC45B	8.4	9.2	-0.8	1.7
AI595366	8.7	9.4	-0.8	1.7
D830037I21RIK	7.3	8.1	-0.8	1.7
PGM2	12.0	12.8	-0.8	1.7
4933421G18RIK	9.7	10.4	-0.8	1.7
MYF6	8.3	9.0	-0.8	1.7
SCN4B	8.3	9.1	-0.8	1.7
ALPK3	8.5	9.3	-0.8	1.7
PGAM2	12.3	13.1	-0.8	1.7
ITGA2B	8.9	9.7	-0.8	1.7
CRYAB	9.8	10.6	-0.7	1.7
LOC386144	9.1	9.8	-0.7	1.7
LOC100047934	10.8	11.6	-0.7	1.7
SRL	9.3	10.0	-0.7	1.7
PHKG1	8.8	9.5	-0.7	1.7
ATP1B1	9.5	10.2	-0.7	1.7
HSPB7	8.2	8.9	-0.7	1.7
TNNC1	8.3	9.0	-0.7	1.6
CHCHD10	12.4	13.1	-0.7	1.6
GMPR	9.0	9.7	-0.7	1.6
S3-12	9.3	10.0	-0.7	1.6
9930004G02RIK	9.4	10.1	-0.7	1.6
TCEA3	10.3	11.0	-0.7	1.6
PPP1R3C	10.7	11.4	-0.7	1.6
TRIM54	9.0	9.7	-0.7	1.6
FBP2	8.3	9.0	-0.7	1.6
COQ10A	8.8	9.5	-0.7	1.6
TXLNB	7.8	8.5	-0.7	1.6
XIRP2	8.4	9.1	-0.7	1.6
FSD2	8.6	9.3	-0.7	1.6
PDE4DIP	9.9	10.6	-0.7	1.6
NDUFC1	10.9	11.6	-0.7	1.6
MSCP	11.9	12.6	-0.7	1.6
EG433229	9.2	9.9	-0.7	1.6
SMARCD3	8.2	8.9	-0.7	1.6
SCL0003073.1_164	8.2	8.8	-0.7	1.6
HHATL	8.6	9.3	-0.7	1.6
DNAJC7	8.9	9.6	-0.7	1.6
USP13	7.9	8.6	-0.7	1.6
ADSSL1	11.5	12.2	-0.7	1.6
ACADM	11.2	11.9	-0.7	1.6
MT-ATP6	11.3	12.0	-0.7	1.6
6430573H23RIK	8.2	8.9	-0.7	1.6
TUBA8	8.6	9.3	-0.7	1.6

DEDD2	9.8	10.4	-0.7	1.6
LOC100041835	12.3	12.9	-0.7	1.6
1300013J15RIK	7.9	8.6	-0.7	1.6
MACROD1	9.1	9.8	-0.7	1.6
ALDOA	13.2	13.9	-0.7	1.6
LOC667034	8.5	9.2	-0.7	1.6
MDH2	10.0	10.6	-0.7	1.6
PDK4	9.3	10.0	-0.7	1.6
ART5	7.7	8.4	-0.7	1.6
JSRP1	7.9	8.6	-0.7	1.6
PPM1L	8.4	9.0	-0.7	1.6
MFN2	10.1	10.8	-0.7	1.6
RILPL1	8.8	9.4	-0.6	1.6
EHBP1L1	8.8	9.4	-0.6	1.6
NDUFA5	10.3	10.9	-0.6	1.6
MTDNA_ND2	11.5	12.2	-0.6	1.6
MTDNA_ND5	11.5	12.2	-0.6	1.6
TRIM72	9.7	10.4	-0.6	1.6
B930008G03RIK	10.0	10.7	-0.6	1.6
2310040G24RIK	7.9	8.5	-0.6	1.6
ALAD	12.0	12.7	-0.6	1.6
SGCA	8.4	9.0	-0.6	1.5
LOC385959	8.3	8.9	-0.6	1.5
LOC547380	8.3	8.9	-0.6	1.5
NDUFS7	11.8	12.4	-0.6	1.5
1300017J02RIK	8.9	9.5	-0.6	1.5
LOC381792	7.7	8.3	-0.6	1.5
FLNC	8.5	9.1	-0.6	1.5
DHRS7C	8.1	8.7	-0.6	1.5
ART1	8.0	8.6	-0.6	1.5
EG245190	8.8	9.5	-0.6	1.5
A530020A01RIK	7.9	8.5	-0.6	1.5
PRKAA2	7.8	8.4	-0.6	1.5
VLDLR	8.7	9.3	-0.6	1.5
1110002E22RIK	8.1	8.7	-0.6	1.5
NDUFB9	7.8	8.4	-0.6	1.5
MYO18B	8.1	8.7	-0.6	1.5
ITGB1BP3	8.3	8.9	-0.6	1.5
PHLDA3	9.4	10.0	-0.6	1.5
GPT2	8.5	9.1	-0.6	1.5
LOC386256	7.9	8.5	-0.6	1.5
TSC22D3	9.4	10.0	-0.6	1.5
NDUFA4	12.4	13.0	-0.6	1.5

4CYTL1	9.4	10.0	-0.6	1.5
PTP4A3	9.0	9.6	-0.6	1.5
FBXO32	7.9	8.5	-0.6	1.5
CNKSR1	7.7	8.3	-0.6	1.5
ZXDA	9.0	9.6	-0.6	1.5
LOC100044934	8.4	9.0	-0.6	1.5
KBTBD5	7.8	8.4	-0.6	1.5
SRR	11.0	11.6	-0.6	1.5
CACNG1	8.1	8.7	-0.6	1.5
SCL0002124.1_39	7.7	8.3	-0.6	1.5
DEB1	11.0	11.6	-0.6	1.5
LMOD3	7.9	8.5	-0.6	1.5
9830134C10RIK	8.2	8.8	-0.6	1.5
TYKI	9.3	9.9	-0.6	1.5
UFSP1	8.6	9.2	-0.6	1.5
SMPX	7.7	8.2	-0.6	1.5
LOC100047214	9.1	9.7	-0.6	1.5
VGLL2	7.6	8.2	-0.6	1.5
CAR3	10.3	10.9	-0.6	1.5
SLC25A12	9.1	9.7	-0.6	1.5
EG622339	13.4	14.0	-0.6	1.5
CIB2	9.4	9.9	-0.6	1.5
A630006E02RIK	9.5	10.1	-0.6	1.5
UGP2	9.4	10.0	-0.6	1.5
4933428A15RIK	8.6	9.2	-0.6	1.5
CHKA	9.4	10.0	-0.6	1.5
SNTA1	8.5	9.0	-0.6	1.5
SLC6A9	9.3	9.9	-0.6	1.5
2410076I21RIK	8.4	8.9	-0.6	1.5
TPI1	12.1	12.6	-0.6	1.5
SMTNL1	7.9	8.4	-0.6	1.5
TMOD1	8.7	9.3	-0.6	1.5
TSPAN8	8.5	9.1	-0.6	1.5
MTDNA_COXII	12.8	13.4	-0.6	1.5
NDUFS2	8.7	9.3	-0.6	1.5
SLC2A4	8.1	8.7	-0.6	1.5
MYOT	7.8	8.4	-0.6	1.5
A230005G17RIK	8.3	8.9	-0.6	1.5
TNNT1	8.9	9.4	-0.6	1.5
FHL1	11.6	12.1	-0.6	1.5
SPNB1	9.5	10.0	-0.6	1.5
5830496L11RIK	9.1	9.6	-0.6	1.5
ENSMUSG00000054212	9.5	10.1	-0.6	1.5

5430434G16RIK	8.9	9.4	-0.6	1.5
IDH3A	8.9	9.4	-0.6	1.5
SLC38A5	11.1	11.7	-0.6	1.5
LDB3	8.1	8.6	-0.6	1.5
E430039I23RIK	11.1	11.6	-0.6	1.5
KEL	10.5	11.0	-0.6	1.5
2310039E09RIK	8.2	8.7	-0.6	1.5
D530007E13RIK	8.9	9.4	-0.6	1.5
1110018J23RIK	7.9	8.5	-0.6	1.5
TMEM45B	8.2	8.7	-0.6	1.5
BC022224	10.2	10.7	-0.6	1.5
RBM38	9.9	10.5	-0.6	1.5
2810484G07RIK	10.9	11.5	-0.5	1.5
ACO2	10.8	11.4	-0.5	1.5
1700021F05RIK	10.3	10.8	-0.5	1.5
VEGFB	9.8	10.4	-0.5	1.5
STXBP3	8.2	8.7	-0.5	1.5
AGL	9.3	9.8	-0.5	1.5
TAL1	9.3	9.8	-0.5	1.5
MYOZ2	7.7	8.2	-0.5	1.5
NCTC1	7.8	8.3	-0.5	1.5
ABCA7	9.4	10.0	-0.5	1.5
SAR1B	10.3	10.9	-0.5	1.5
3632431M01RIK	8.6	9.1	-0.5	1.5
FCHO1	10.0	10.5	-0.5	1.5
P2RY1	8.8	9.3	-0.5	1.5
B230387C07RIK	9.1	9.7	-0.5	1.5
TRIM63	7.5	8.0	-0.5	1.5
1810020D17RIK	9.5	10.0	-0.5	1.4
FYCO1	8.1	8.6	-0.5	1.4
RABGEF1	10.3	10.8	-0.5	1.4
ITGB1BP2	8.2	8.8	-0.5	1.4
IFT140	9.1	9.6	-0.5	1.4
SAMD11	8.2	8.7	-0.5	1.4
ABCB10	8.2	8.8	-0.5	1.4
LOC100046690	9.0	9.5	-0.5	1.4
PFN2	8.9	9.5	-0.5	1.4
C1QTNF3	11.0	7.5	3.5	11.3
LRRC15	10.6	8.4	2.2	4.7
ANGPTL1	9.7	7.6	2.1	4.4
MFAP5	10.2	8.1	2.1	4.4
THBS2	11.8	9.7	2.1	4.3
FSTL1	11.1	9.0	2.0	4.1

COL6A2	10.4	8.4	2.0	4.1
MMP2	13.7	11.7	2.0	3.9
COL6A1	12.4	10.4	2.0	3.9
CAPN6	9.7	7.7	2.0	3.9
COL3A1	9.8	7.9	1.9	3.8
MMP3	9.3	7.4	1.9	3.8
TIMP1	11.8	9.9	1.9	3.8
COL5A1	12.6	10.7	1.9	3.7
CTHRC1	9.5	7.6	1.9	3.7
AEBP1	10.9	9.1	1.9	3.6
COL18A1	9.8	8.0	1.8	3.5
DKK3	10.2	8.5	1.7	3.4
COL14A1	9.3	7.6	1.7	3.3
E430002G05RIK	9.9	8.1	1.7	3.3
PCOLCE	10.9	9.2	1.7	3.3
LUM	12.2	10.5	1.7	3.3
DPT	10.3	8.6	1.7	3.2
MMP14	11.9	10.2	1.7	3.2
GP38	11.0	9.3	1.7	3.2
FCRLS	9.9	8.2	1.6	3.1
MFAP4	9.2	7.6	1.6	3.1
CSRP2	11.0	9.4	1.6	3.1
LOX	11.4	9.8	1.6	3.1
SPON2	11.2	9.6	1.6	3.0
ITM2A	9.8	8.2	1.6	3.0
LY6A	12.8	11.3	1.6	3.0
DDAH1	9.3	7.7	1.6	3.0
MUP2	9.7	8.2	1.6	3.0
GPNMB	9.5	8.0	1.6	3.0
CD248	9.9	8.3	1.5	2.9
ANTXR1	9.9	8.3	1.5	2.9
6330406I15RIK	9.7	8.1	1.5	2.9
LOXL1	10.8	9.2	1.5	2.9
MUP1	9.2	7.7	1.5	2.9
NBL1	10.3	8.8	1.5	2.9
MFAP2	9.2	7.7	1.5	2.8
CCL21A	10.6	9.1	1.5	2.8
FN1	10.4	8.9	1.5	2.8
MEST	8.8	7.3	1.5	2.8
MRGPRF	9.5	8.0	1.5	2.8
CCL21C	10.0	8.5	1.5	2.8
SAA3	8.7	7.2	1.5	2.8
LOC100048554	9.2	7.7	1.5	2.8
THY1	10.0	8.5	1.5	2.7

HTRA1	10.5	9.1	1.5	2.7
OSR2	9.3	7.8	1.5	2.7
LOC100041504	9.9	8.4	1.4	2.7
GPX7	9.8	8.4	1.4	2.7
KDELR3	10.4	8.9	1.4	2.7
H19	11.4	10.0	1.4	2.7
PDLIM4	10.3	8.9	1.4	2.6
C1QTNF2	9.3	7.9	1.4	2.6
COL6A3	11.3	9.9	1.4	2.6
FBLN2	9.4	8.0	1.4	2.6
MXRA8	10.5	9.1	1.4	2.6
SCL0001849.1_2273	9.0	7.6	1.4	2.6
VKORC1	11.1	9.7	1.3	2.5
PPIC	12.3	11.0	1.3	2.5
ITGBL1	9.6	8.3	1.3	2.5
EMP1	12.7	11.4	1.3	2.5
KNSL5	11.8	10.5	1.3	2.5
SERPINH1	12.8	11.5	1.3	2.5
2310016C16RIK	10.3	9.0	1.3	2.5
WISP2	10.4	9.1	1.3	2.5
MAGED1	11.6	10.3	1.3	2.5
COL16A1	11.6	10.3	1.3	2.5
LEPREL2	9.2	7.9	1.3	2.4
GPX8	10.7	9.4	1.3	2.4
BGN	14.3	13.0	1.3	2.4
SRPX2	10.2	8.9	1.3	2.4
ITGA11	9.9	8.6	1.3	2.4
CCDC80	11.0	9.7	1.3	2.4
CLEC11A	10.4	9.2	1.3	2.4
SMOC1	9.7	8.5	1.2	2.4
OGN	10.3	9.0	1.2	2.4
CRTAP	10.1	8.9	1.2	2.4
VIM	11.1	9.8	1.2	2.3
COL4A2	11.3	10.0	1.2	2.3
FKBP11	10.0	8.7	1.2	2.3
CD276	9.3	8.1	1.2	2.3
PRKCDBP	10.1	8.9	1.2	2.3
CCL7	8.4	7.2	1.2	2.3
NFATC4	9.4	8.1	1.2	2.3
ECM1	10.8	9.6	1.2	2.3
COL15A1	9.4	8.2	1.2	2.3
2610027C15RIK	10.0	8.8	1.2	2.3

PRELP	13.1	11.9	1.2	2.3
TIMP2	12.6	11.4	1.2	2.3
GRB10	9.4	8.2	1.2	2.3
FBN1	9.6	8.4	1.2	2.3
COPZ2	10.0	8.8	1.2	2.3
SCARF2	12.0	10.8	1.2	2.3
ENPP1	9.6	8.4	1.2	2.3
COL4A1	11.7	10.5	1.2	2.3
IGF1	9.6	8.4	1.2	2.2
SULF2	9.2	8.0	1.2	2.2
SERPINA3N	10.2	9.0	1.2	2.2
FKBP9	11.1	9.9	1.2	2.2
RNASE4	9.8	8.6	1.2	2.2
COMP	12.8	11.6	1.2	2.2
MS4A6D	9.8	8.6	1.2	2.2
CPXM1	9.3	8.2	1.1	2.2
DAB2	9.7	8.5	1.1	2.2
EFEMP2	10.0	8.9	1.1	2.2
LOC100047053	8.4	7.3	1.1	2.2
COL8A1	9.5	8.4	1.1	2.2
SERPING1	11.9	10.7	1.1	2.2
ANGPTL4	10.2	9.1	1.1	2.2
THBS3	8.7	7.6	1.1	2.1
HSPG2	10.5	9.4	1.1	2.1
PTN	8.9	7.8	1.1	2.1
GM22	9.3	8.2	1.1	2.1
NNMT	9.6	8.6	1.1	2.1
LGMN	10.9	9.8	1.1	2.1
4930533K18RIK	9.8	8.7	1.1	2.1
VASN	10.9	9.8	1.1	2.1
ELN	8.5	7.5	1.1	2.1
FMOD	10.2	9.1	1.1	2.1
LOC100046883	10.8	9.8	1.1	2.1
CLEC4N	8.6	7.6	1.1	2.1
NDN	10.0	8.9	1.1	2.1
ACAN	9.7	8.6	1.1	2.1
OLFML1	8.8	7.8	1.1	2.1
C1QTNF1	8.7	7.6	1.1	2.1
SOCS3	9.3	8.3	1.0	2.1
1500015O10RIK	11.9	10.8	1.0	2.0
FKBP10	9.7	8.7	1.0	2.0
TREM2	9.4	8.4	1.0	2.0
MGP	13.5	12.5	1.0	2.0
COL10A1	10.7	9.6	1.0	2.0

ADAMTS12	8.7	7.7	1.0	2.0
CRLF1	8.5	7.5	1.0	2.0
HTRA3	9.6	8.6	1.0	2.0
P4HA2	9.0	8.0	1.0	2.0
FSCN1	9.0	8.1	1.0	2.0
NUPR1	12.0	11.0	1.0	2.0
SCARA3	11.9	10.9	1.0	2.0
SYNPO	10.1	9.1	1.0	2.0
NID2	8.8	7.8	1.0	2.0
TSPAN6	8.9	7.9	1.0	2.0
LGALS1	12.5	11.5	1.0	2.0
IGFBP7	10.5	9.5	1.0	2.0
TMEM119	9.7	8.7	1.0	2.0
COL2A1	13.6	12.6	1.0	2.0
MS4A7	8.8	7.8	1.0	2.0
ANXA5	12.4	11.4	1.0	2.0
RAMP2	10.0	9.1	1.0	2.0
MMP23	9.5	8.5	1.0	1.9
SLC1A4	8.5	7.6	1.0	1.9
LOC100047856	9.1	8.2	1.0	1.9
AHNAK2	9.1	8.2	1.0	1.9
CDKN1C	11.0	10.0	1.0	1.9
APOE	11.0	10.0	1.0	1.9
SPARC	13.1	12.1	1.0	1.9
BC020108	8.5	7.5	0.9	1.9
C1QB	11.5	10.5	0.9	1.9
FNDC3B	10.2	9.3	0.9	1.9
IGSF10	8.8	7.9	0.9	1.9
COL12A1	9.1	8.2	0.9	1.9
9030024J15RIK	9.7	8.7	0.9	1.9
1110036O03RIK	8.9	8.0	0.9	1.9
LRIG3	9.4	8.5	0.9	1.9
FAM129B	10.2	9.3	0.9	1.9
EDNRA	9.5	8.5	0.9	1.9
IL33	8.3	7.4	0.9	1.9
IGFBP6	10.0	9.0	0.9	1.9
LGALS3BP	10.8	9.9	0.9	1.9
OLFML3	11.5	10.6	0.9	1.9
COL1A2	11.1	10.2	0.9	1.9
GPR176	8.4	7.5	0.9	1.9
CERCAM	9.9	9.0	0.9	1.9
CNRIP1	9.7	8.8	0.9	1.9
GALNTL1	8.5	7.7	0.9	1.9

KERA	8.2	7.3	0.9	1.9
PRG4	12.7	11.8	0.9	1.9
IGKV3-2_X16954_IG_KAPPA_VARIABLE_3-2_18	9.0	8.1	0.9	1.9
LOC676136	9.5	8.6	0.9	1.9
ABI3BP	8.6	7.7	0.9	1.9
PKD2	8.9	8.0	0.9	1.8
COL1A1	13.2	12.3	0.9	1.8
SCX	8.6	7.7	0.9	1.8
IGF2	10.3	9.4	0.9	1.8
SFRP1	8.3	7.4	0.9	1.8
KCTD17	9.1	8.2	0.9	1.8
IGFBP4	12.0	11.2	0.9	1.8
MFGE8	12.3	11.5	0.9	1.8
EFS	9.2	8.4	0.9	1.8
BC064033	8.4	7.6	0.9	1.8
LOC243431	9.8	9.0	0.9	1.8
MAGED2	11.1	10.2	0.9	1.8
DPYSL3	9.3	8.4	0.9	1.8
ANPEP	8.4	7.6	0.9	1.8
A430110N23RIK	8.2	7.4	0.9	1.8
CXCL1	8.1	7.2	0.8	1.8
LTBP3	9.0	8.2	0.8	1.8
LRRC17	8.3	7.4	0.8	1.8
LOC100047583	9.3	8.5	0.8	1.8
UTS2R	8.3	7.4	0.8	1.8
TNN	8.3	7.5	0.8	1.8
CALU	10.0	9.2	0.8	1.8
BMP1	9.9	9.1	0.8	1.8
SCARA5	9.7	8.9	0.8	1.8
TXNDC5	10.7	9.9	0.8	1.8
SDC2	10.4	9.6	0.8	1.8
IFITM2	12.1	11.3	0.8	1.8
PRDX4	11.0	10.1	0.8	1.8
DLK1	8.2	7.3	0.8	1.8
0610007N19RIK	9.4	8.6	0.8	1.8
TPST1	9.9	9.0	0.8	1.8
NT5DC2	9.1	8.3	0.8	1.8
SULF1	8.9	8.1	0.8	1.8
HTRA4	9.0	8.2	0.8	1.8
AKR1B8	8.3	7.4	0.8	1.8
SRPX	8.8	8.0	0.8	1.8

MARCKS	11.2	10.4	0.8	1.8
PARVA	9.6	8.8	0.8	1.7
TGFB3	8.8	8.0	0.8	1.7
LOC232060	8.7	7.9	0.8	1.7
WISP1	9.5	8.7	0.8	1.7
LXN	10.0	9.2	0.8	1.7
D14ERTD449E	9.2	8.5	0.8	1.7
MDK	8.6	7.8	0.8	1.7
TGFBI	11.3	10.5	0.8	1.7
SH3PXD2B	9.4	8.6	0.8	1.7
EMP2	9.0	8.2	0.8	1.7
IGHG	9.7	9.0	0.8	1.7
RIN2	9.1	8.3	0.8	1.7
1700023M03RIK	9.9	9.2	0.8	1.7
WBP5	10.9	10.1	0.8	1.7
CD68	10.3	9.5	0.8	1.7
1200009O22RIK	8.6	7.8	0.8	1.7
IL1RL1	8.1	7.3	0.8	1.7
ADAMTS2	11.0	10.2	0.8	1.7
A730054J21RIK	8.3	7.5	0.8	1.7
4732462B05RIK	10.0	9.3	0.8	1.7
LBP	9.9	9.1	0.8	1.7
IL13RA1	8.7	7.9	0.8	1.7
FER1L3	8.4	7.6	0.8	1.7
C4A	10.0	9.2	0.8	1.7
SOX9	9.8	9.0	0.8	1.7
1810055G02RIK	10.2	9.4	0.8	1.7
PANX3	10.7	10.0	0.8	1.7
FKBP14	8.5	7.7	0.8	1.7
SERPINF1	12.8	12.1	0.8	1.7
TUBB6	9.9	9.2	0.8	1.7
C1QC	10.8	10.0	0.8	1.7
OLFML2B	11.5	10.7	0.8	1.7
TCEAL8	9.9	9.2	0.8	1.7
PDGFRA	9.4	8.6	0.8	1.7
NOX4	8.3	7.5	0.8	1.7
SFRP2	8.1	7.3	0.7	1.7
6720469N11RIK	10.1	9.3	0.7	1.7
LOC380799	8.7	8.0	0.7	1.7
CSTB	12.6	11.8	0.7	1.7
CYB561	8.7	8.0	0.7	1.7
LHFPL2	9.7	9.0	0.7	1.7
LOC98434	10.3	9.5	0.7	1.7

CD14	8.5	7.7	0.7	1.7
PMP22	9.4	8.7	0.7	1.7
RBP1	8.6	7.8	0.7	1.7
2310008M10RIK	11.4	10.6	0.7	1.7
MT1	13.4	12.7	0.7	1.7
EXT1	9.9	9.2	0.7	1.7
LIMA1	9.0	8.3	0.7	1.7
MATN4	8.3	7.5	0.7	1.7
EDG5	9.3	8.6	0.7	1.7
SPSB1	8.7	8.0	0.7	1.7
ARMCX2	9.4	8.7	0.7	1.7
SVEP1	8.3	7.6	0.7	1.7
HMGN3	10.5	9.8	0.7	1.6
GPR23	8.7	8.0	0.7	1.6
FOLR2	8.6	7.8	0.7	1.6
UBE2E2	9.3	8.6	0.7	1.6
RHOJ	9.4	8.7	0.7	1.6
PROS1	9.9	9.2	0.7	1.6
STAB1	9.6	8.9	0.7	1.6
LOC637227	9.6	8.8	0.7	1.6
MYADM	10.8	10.1	0.7	1.6
ANXA8	8.4	7.7	0.7	1.6
PLOD1	8.3	7.6	0.7	1.6
MEOX2	8.9	8.2	0.7	1.6
LOC381629	10.7	10.0	0.7	1.6
LOC384413	9.4	8.7	0.7	1.6
TAX1BP3	10.5	9.8	0.7	1.6
6330404C01RIK	9.3	8.6	0.7	1.6
FRMD6	9.8	9.1	0.7	1.6
COL9A2	10.6	9.9	0.7	1.6
NT5E	9.0	8.3	0.7	1.6
MYO1E	9.0	8.3	0.7	1.6
LMAN1	9.5	8.8	0.7	1.6
GRN	12.1	11.4	0.7	1.6
LOC669053	9.3	8.6	0.7	1.6
CUL7	9.5	8.8	0.7	1.6
P4HB	13.1	12.4	0.7	1.6
TWSG1	10.1	9.4	0.7	1.6
D4BWG0951E	8.3	7.7	0.7	1.6
BICC1	9.6	8.9	0.7	1.6
WTIP	9.3	8.6	0.7	1.6
IL11RA1	11.3	10.7	0.7	1.6
LOC636944	9.9	9.3	0.7	1.6
PLVAP	10.2	9.5	0.7	1.6

EGFR	8.5	7.8	0.7	1.6
RFTN2	8.6	8.0	0.7	1.6
TMED3	9.9	9.2	0.7	1.6
TUBB2B	8.7	8.1	0.7	1.6
C130021I20	7.9	7.3	0.7	1.6
CXCL16	8.2	7.5	0.7	1.6
CDON	8.2	7.6	0.7	1.6
SDC3	11.1	10.5	0.7	1.6
5430435G22RIK	8.4	7.8	0.7	1.6
ADRA2A	8.6	7.9	0.7	1.6
C1QA	9.3	8.7	0.7	1.6
PRRC1	9.8	9.2	0.7	1.6
TPBG	8.3	7.7	0.6	1.6
BOK	8.5	7.8	0.6	1.6
NID1	8.8	8.1	0.6	1.6
FXYD6	11.3	10.7	0.6	1.6
TGFBR2	9.8	9.2	0.6	1.6
LAMC1	9.2	8.5	0.6	1.6
ZFP521	8.4	7.7	0.6	1.6
GPR125	9.4	8.8	0.6	1.6
COL5A2	8.0	7.4	0.6	1.6
PAPSS2	9.2	8.6	0.6	1.6
BDH2	9.5	8.9	0.6	1.6
MIA1	10.1	9.4	0.6	1.6
SOCS2	9.9	9.2	0.6	1.6
GLT8D1	9.4	8.8	0.6	1.6
PLOD2	8.5	7.9	0.6	1.6
FSTL	8.0	7.4	0.6	1.6
IGFBP3	8.1	7.5	0.6	1.5
2410146L05RIK	8.0	7.3	0.6	1.5
GSTM2	10.2	9.5	0.6	1.5
ISLR	8.0	7.4	0.6	1.5
PPIB	11.3	10.7	0.6	1.5
PDGFRB	8.6	7.9	0.6	1.5
DLG5	9.5	8.9	0.6	1.5
CAV1	10.4	9.8	0.6	1.5
CCL4	8.2	7.6	0.6	1.5
TMEM176B	10.1	9.4	0.6	1.5
RAB34	8.4	7.7	0.6	1.5
CDKN1A	8.7	8.1	0.6	1.5
CYB5R3	9.6	9.0	0.6	1.5
SEPN1	10.2	9.6	0.6	1.5
LOC630253	8.2	7.6	0.6	1.5

PRRX2	8.1	7.5	0.6	1.5
RHOC	8.4	7.8	0.6	1.5
PRSS35	8.8	8.2	0.6	1.5
GPRC5B	8.4	7.8	0.6	1.5
PDIA5	8.1	7.5	0.6	1.5
PMEPA1	8.2	7.6	0.6	1.5
ADAMTS4	7.9	7.3	0.6	1.5
RRBP1	9.3	8.7	0.6	1.5
FAM171B	8.4	7.8	0.6	1.5
SERTAD4	8.1	7.5	0.6	1.5
CRABP2	7.8	7.2	0.6	1.5
5430433G21RIK	9.4	8.9	0.6	1.5
RAB11FIP5	9.3	8.7	0.6	1.5
4933421H10RIK	8.7	8.1	0.6	1.5
DCN	12.3	11.7	0.6	1.5
2610009E16RIK	9.1	8.5	0.6	1.5
3110079O15RIK	12.8	12.2	0.6	1.5
VAT1	9.6	9.1	0.6	1.5
COL8A2	8.2	7.6	0.6	1.5
LOC100047162	9.9	9.4	0.6	1.5
HOXC6	9.1	8.5	0.6	1.5
ZFYVE21	10.3	9.7	0.6	1.5
BGLAP-RS1	13.8	13.2	0.6	1.5
9430028L06RIK	7.9	7.3	0.6	1.5
ACTA2	10.3	9.7	0.6	1.5
GLT25D1	10.7	10.1	0.6	1.5
RCN3	8.3	7.7	0.6	1.5
CLEC3B	8.2	7.6	0.6	1.5
GMDS	8.8	8.2	0.6	1.5
BMPER	8.3	7.7	0.6	1.5
2300002D11RIK	8.0	7.4	0.6	1.5
PLAT	8.0	7.4	0.6	1.5
TWIST1	8.4	7.8	0.6	1.5
6230400G14RIK	8.8	8.2	0.6	1.5
PLOD3	10.2	9.7	0.6	1.5
CAPG	10.0	9.5	0.6	1.5
LOC626583	8.1	7.5	0.6	1.5
ALG14	8.9	8.4	0.6	1.5
MMP12	7.8	7.2	0.6	1.5
TNXB	8.5	7.9	0.6	1.5
TUBA1A	9.4	8.9	0.6	1.5
CD81	12.8	12.2	0.6	1.5
TMEM86A	9.9	9.4	0.6	1.5
C1QTNF5	7.9	7.3	0.6	1.5

ERGIC1	9.4	8.8	0.6	1.5
5031439A09RIK	8.9	8.4	0.6	1.5
S100A10	9.2	8.6	0.6	1.5
CBR2	9.1	8.6	0.6	1.5
FBLN7	7.8	7.3	0.6	1.5
B9D1	8.3	7.7	0.6	1.5
ALG5	9.6	9.1	0.6	1.5
RRAS	9.9	9.3	0.6	1.5
CHMP4B	10.4	9.8	0.6	1.5
GNS	10.9	10.4	0.6	1.5
H47	10.8	10.3	0.6	1.5
IFITM5	9.2	8.7	0.6	1.5
WWTR1	8.8	8.2	0.5	1.5
CRIP2	11.0	10.4	0.5	1.5
ANXA2	13.6	13.1	0.5	1.5
A730017D01RIK	8.5	7.9	0.5	1.5
PRRX1	8.1	7.6	0.5	1.5
COL22A1	10.4	9.9	0.5	1.5
MANBAL	10.3	9.8	0.5	1.5
POFUT2	8.1	7.6	0.5	1.5
APLNR	8.3	7.7	0.5	1.5
FBLIM1	8.7	8.2	0.5	1.5
LMNA	10.4	9.9	0.5	1.5
PLCD1	8.7	8.1	0.5	1.5
RHBDF1	9.9	9.4	0.5	1.5
LOC100039175	8.8	8.2	0.5	1.5
EBPL	8.8	8.3	0.5	1.5
KDELR2	8.5	8.0	0.5	1.5
FAH	8.9	8.3	0.5	1.5
PDIA3	11.7	11.1	0.5	1.5
PLA1A	8.1	7.6	0.5	1.5
GAS6	11.3	10.8	0.5	1.5
BC065085	8.3	7.8	0.5	1.5
D10ERTD610E	8.6	8.1	0.5	1.4
IFIT3	8.5	8.0	0.5	1.4
PDGFRL	7.9	7.4	0.5	1.4
3632451O06RIK	8.0	7.5	0.5	1.4
TPM4	11.3	10.8	0.5	1.4
PLP2	10.0	9.5	0.5	1.4
C4B	8.7	8.1	0.5	1.4

Table 7: Genes changed expression in DMM model at day 7

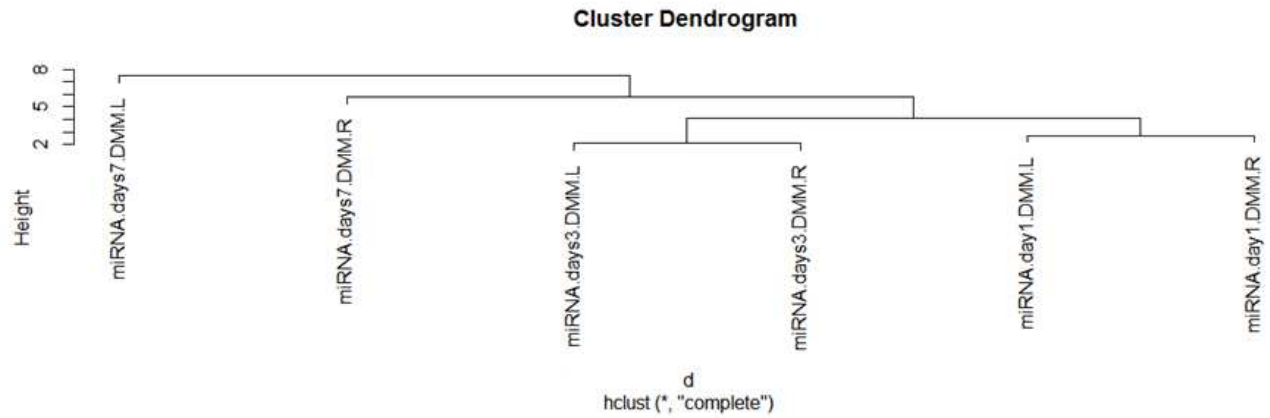

Figure 1: Hierarchical cluster analysis for DMM models at 1, 3, and 7 days after surgery

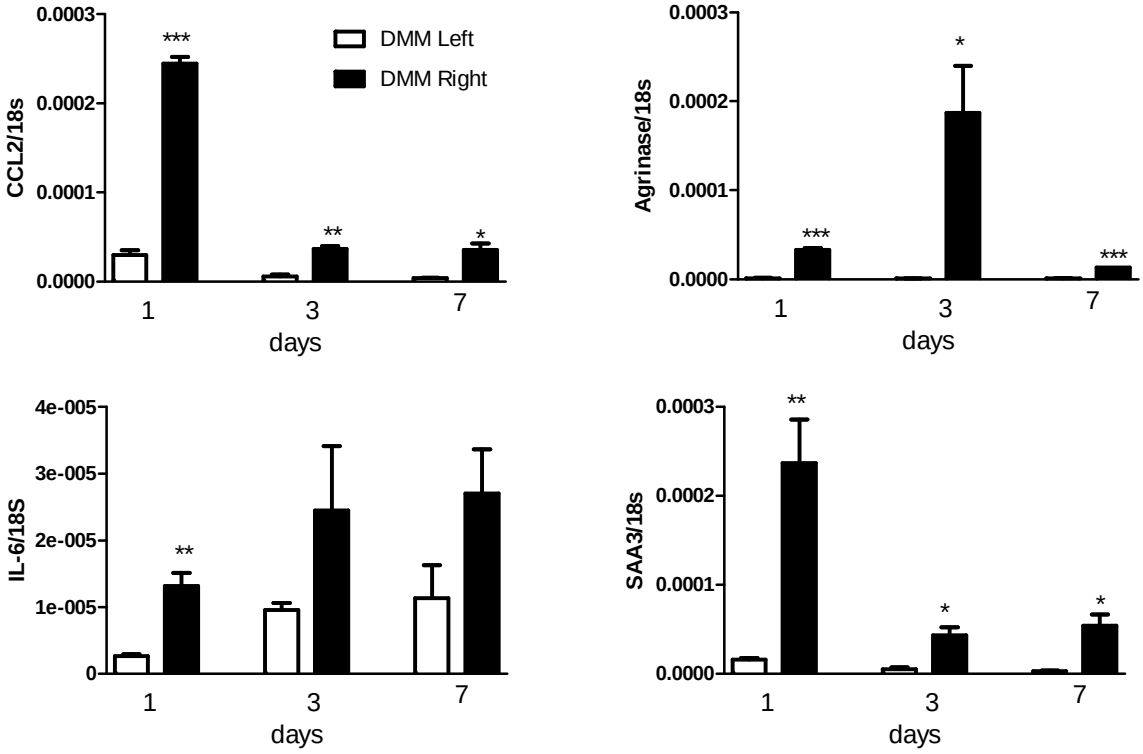

Figure 2: CCL2, Agrinase, IL-6 and SAA-3 were significantly induced expression in DMM model at 1, 3, and 7 days after surgery

Total RNA was reversed transcribed to cDNA and gene expression was measured by real-time qRT-PCR in individual samples of DMM left knee (un-operated, open bar), and DMM right knee (DMM, close bar). 18S was used as endogenous control. The data show mean +/- SEM, n=3. The expression of genes of interest between each group was analysed by unpaired two-tailed t test * $p<0.05$, ** $p < 0.01$, *** $p<0.001$.

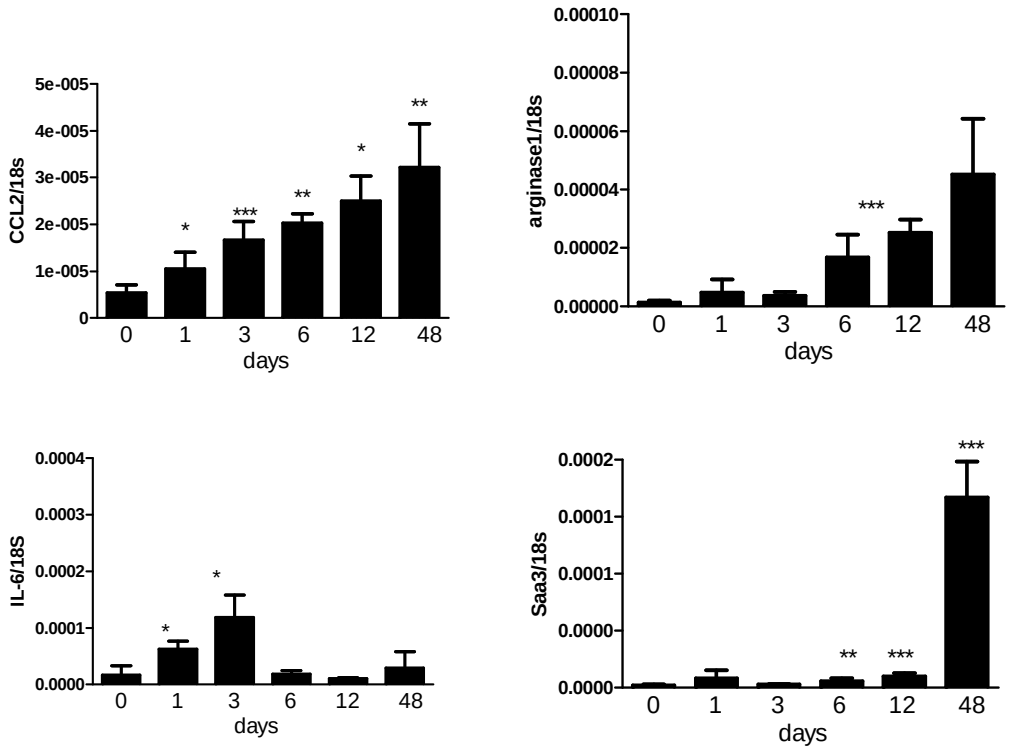

Figure 3: Gene expression in hip avulsion injury model

The femoral caps of C57Bl/6 mice aged 4 weeks were avulsed and put in culture. At each of 3, 6, 12, 48 hour time points, the femoral caps were harvested. Total RNA was isolated using Trizol and reverse transcribed to cDNA. Gene expression was measured by real-time qRT-PCR where 18S was used as an endogenous control. Assays were repeated 3 times. At least triplicate samples were measured at each time. Means ± standard errors are presented. Difference in expression between each time point against control (t=0) was calculated by unpaired two-tailed t test. * $p<0.05$, ** $p < 0.01$, *** $p<0.001$.

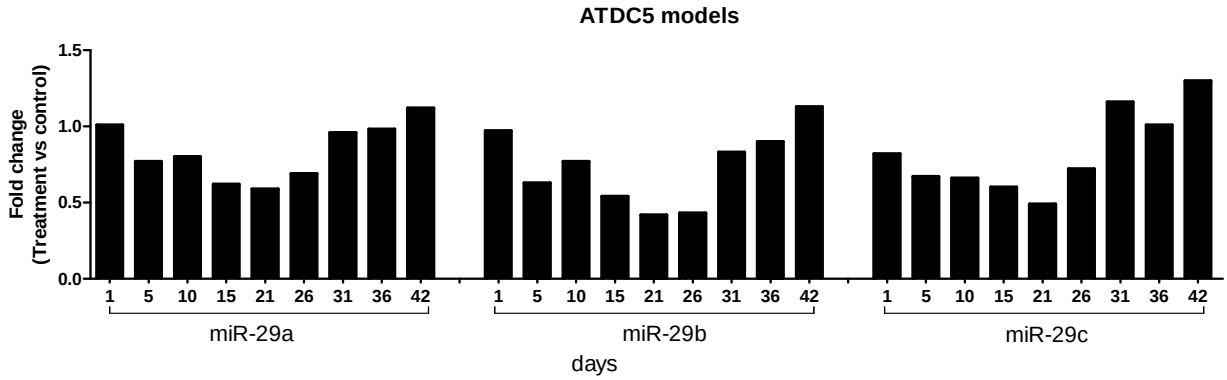

Figure 4: The expression of the miR-29 family in ATDC5 model

The embryonic carcinoma cell line ATDC5 was stimulated to from chondrocytes using insulin for 42 days. Total RNA was isolated, reverse transcribed to cDNA and used for miRNA microarray.

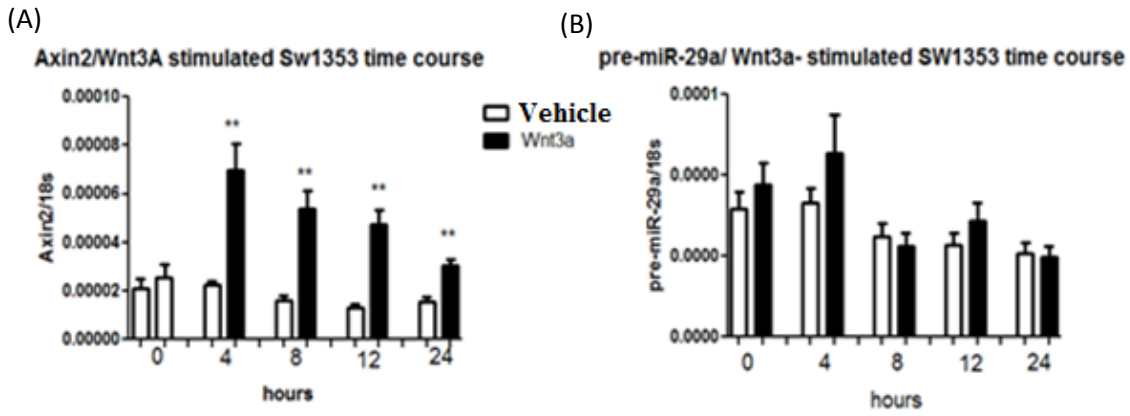

Figure 5: Expression of the miR-29 family was not controlled by Wnt3a

SW1353 cells were cultured in high glucose media with 10% (v/v) FCS in monolayer until 90% confluence. Cells were serum starved for 24 hours before treating with Wnt3a or vehicle (0.5% (w/v) BSA) across 24 hour course.

Relative expression of the precursor miR-29a and axin2 was measured by quantitative RT-PCR. 18S rRNA was the endogenous control for measuring the precursor transcripts. Open bar, control; close bar, WNT3a. (A) Expression level of axin2. (B) Expression level of precursor miR-29a. Means ± standard errors are presented. The difference between the treatment and the control was analysed by unpaired two-tailed t test. * $p<0.05$, ** $p < 0.01$, *** $p<0.001$, n=3.

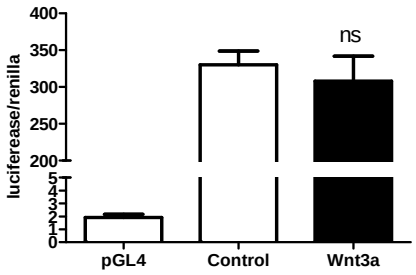

Figure 6: Wnt3a does not control the expression from the primary miR-29a/b1 promoter

The pri-miR-29a/b1 promoter-reporter (100ng) or the empty vector pGL4 (control, 100ng) were transfected into SW1353 cells. After transfection, cells were serum starved for 24 hours, followed by stimulating for another 6 hours with WNT3a (100ng/ml), or vehicle (0.5% BSA) before measuring luciferase activity. Renilla was use as endogenous control. Open bar: vehicle, black bar: Wnt3a. Means ± standard errors are presented, n=3. The difference of luciferase activity was analysed by unpaired two-tailed Student's t test. * $p<0.05$, ** $p < 0.01$, *** $p<0.00$.

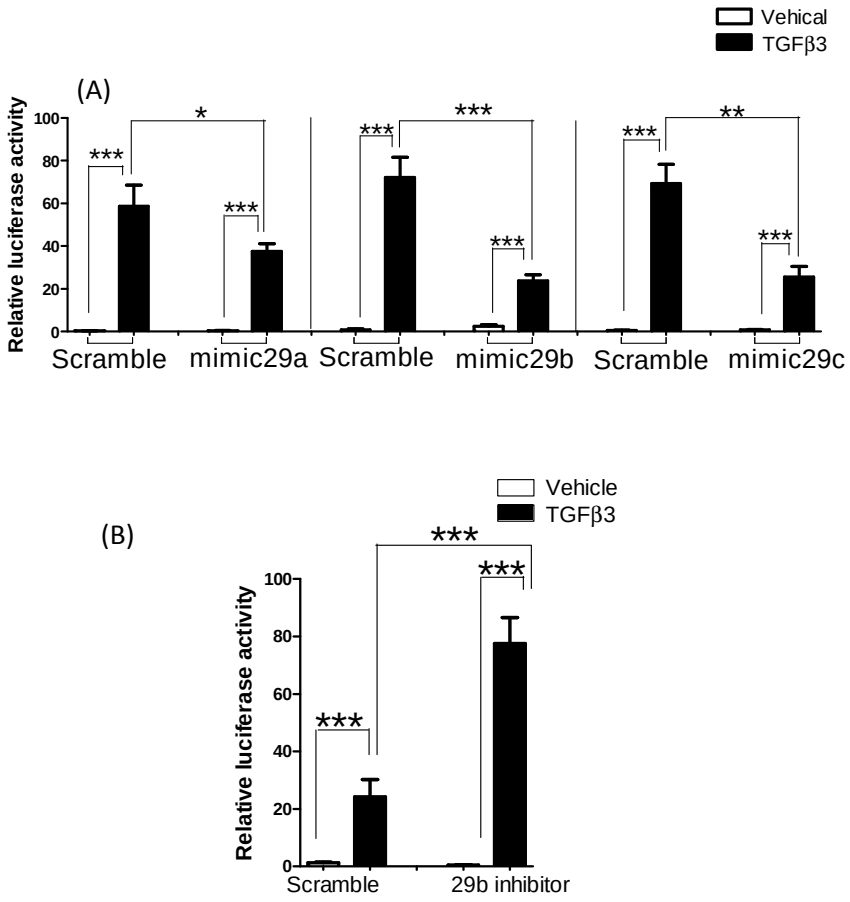

Figure 7 The miR-29 family suppress TGFβ signalling pathway

(A) The TGFβ signalling reporter ($CAGA_{12}$-luc) contains 12 binding sites of the Smad2/3/4 (GAGAC) binding consensus upstream of the firely luciferase-encoding gene in pGL3100ng $CAGA_{12}$-luc vector, and 10ng Renilla vector were co-transfected with either miR-29 family mimic (B) or miR-29b inhibitor (C) into SW1353 cells in monolayer. The non-targeting control (50nM) was also used as the negative control. 24 hours after transfection, cells were serum starved for another 24 hours, followed by treatment with TGFβ3 (4ng/ml) for another 6 hours before measuring luciferase activity. Renilla is the loading control for luciferase assay. Open bar: non – treatment control, close bar: TGFβ3 treatment. Means ± standard errors are presented, n=6. The difference of luciferase activity was analysed by Student's unpaired two-tailed t test. * $p<0.05$, ** $p < 0.01$, *** $p<0.001$

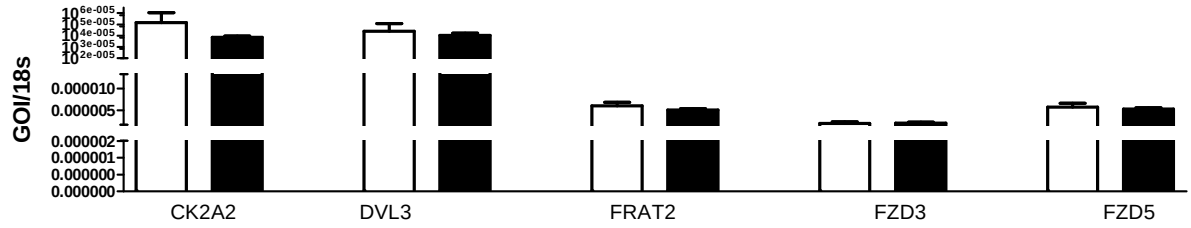

Figure 8 The miR-29 family does not target some of its putative targets at mRNA level Human primary chondrocytes was cultured in media with 10% (v/v) FCS in monolayer until 90% confluence. Cells were then transfected with either miR-29b mimic (50nM) or non – targeting control (50nM) for 48 hours. Total RNA was isolated and the expression levels of GOI were measured by qRT-PCR. 18S rRNA was the housekeeping control. Relative expression value of each of these genes was normalized to non – targeting control. Means ± standard errors are presented, n=3. The difference in expression between miR-29b overexpression and non – targeting control was analysed by Student's unpaired two-tailed t test. * $p<0.05$, ** $p < 0.01$, ***, $p<0.001$

THE ROLES OF THE MICRORNA 29 FAMILY IN CARTILAGE HOMEOSTASIS AND OSTEOARTHRITIS

LE THI TRUC LINH

THESIS SUBMITTED FOR THE DEGREE OF DOCTOR OF PHILOSOPHY

University of East Anglia

School of biological Sciences

Norwich, United Kingdom

December, 2014

DEDICATION

I would like to dedicate this thesis to my family

my parents

Mr Le Hung Son,

Mrs Le Thi Khanh Hong

my brother

Mr Le Hung Phong

for their constant love, friendship, support and encouragement throughout my life

ABSTRACT

MicroRNAs are short endogenous non-coding RNA molecules, typically 19-25 nucleotides in length, which negatively regulate gene expression. In osteoarthritis (OA), several genes necessary for cartilage homeostasis are aberrantly expressed, with a number of miRNAs implicated in this process. However, our knowledge of the earliest stages of OA, prior to the onset of irreversible changes, remains limited. The purpose of this study was to identify miRNAs involved across the time-course of OA using both a murine model and human cartilage, and to define their function.

Expression profile of miRNAs (Exiqon) and mRNAs (Illumina) on total RNA purified from whole knee joints taken from mice which underwent destabilisation of the medial meniscus (DMM) surgery at day 1, 3 and 7 post-surgery showed: the miRNA expression in whole mouse joints post DMM surgery increased over 7 days; at day 1 and 3, the expression of only 4 miRNAs altered significantly; at day 7, 19 miRNAs were upregulated and 15 downregulated. Among the modulated miRNAs, the miR-29b was the most interesting and was chosen to further investigate since integrating analysis of the miRNA and mRNA expression array data showed the inverse correlation between miR-29b and its potential targets. In end-stage human OA cartilage and in murine injury model, the miR-29 family was found to increase expression. Moreover, the miR-29 family was found to be the negative regulator in both human and murine chondrogenesis, and was also found to involve in murine limb development. Expression of the miR-29 family was found to suppress by SOX9 at least in part through directly binding to the promoter of the primary miR-29a/b1. Also, TGFβ1/3 decreased expression of the miR-29 family whilst Wnt3a did not have any effect. Lipopolysaccharide suppressed the miR-29 family expression in part through NFκB signalling pathway while the IL-1 strongly induced its expression partly through P38 MAKP signalling. Using luciferase reporter assay, the miR-29 family was showed to suppress the TGFβ, NFκB, and WNT/β-catenin signalling pathways. Gene expression profiles of gain- and-loss-of-function revealed regulation of a large number of previously recognised extracellular matrix-associated genes as well as an additional subset of protease and Wnt signalling pathway-related genes. Among these genes, *ADAMTS6, ADAMTS10, ADAMTS14, ADAMTS17, ADAMTS19, FZD3, DVL3, FRAT2, CK2A2* were experimentally validated as direct targets of the miR-29 family.

CONTENTS

LISTS OF TABLES

LISTS OF FIGURES

LISTS OF APPENDICES

Paper: Le et al, 2013

ACKOWNLEGMENTS

I would like to express my special appreciation and thanks to my primary supervisor Professor Ian Clark. I thank him for giving me the opportunity to become a Clark laboratory member and for allowing me to growth as a research scientist as I am now. I deeply appreciate the change to work and study from a great scientist and an honourable person like him. Without his time, support, guidance and encouragement, my PhD project is impossible.

I would also like to thank my second supervisor Professor Andrea Munsterberg for her comments, and suggestion which really helped me to refine my project. I am also in debted to Dr Tracey Swingler, my third supervisor. Her brilliant lab work skills, experiences, and knowledge tremendously help me go through all the obstacles and finish the study. Her time and her availability for all of my constant string of questions during the last 3 years are invaluable.

I am very thankful for all the past and current members of Clark laboratory for helping me on my research and make my PhD journey enjoyable. Special thank you to Dr Natalie Crowe for sharing with me her human osteoarthritis and normal articular cartilage samples, her dedifferentiation model which will take me a lot of time to do it myself. Thanks to Dr Rosemary Davidson for letting me including her DVL3 expression data in my thesis and for her knowledge, advice, support, and encouragement during my PhD. I would like to acknowledge Jonathan Green, Sarah Garner, Yvette Wormstone for their expertise and kind help in mouse injury model, human primary chondrocyte isolation, and cloning.

I would especially thank to Dr Guy Wheeler in Dalmay laboratory, Dr Geoffrey Mok, and Camille Viaut in Munsterberg laboratory for sharing their knowledge and help me through my whole mount in situ hybridization experiment. Thank you to Dr Eleanor Jones in Riley laboratory for kindly sharing with me her data and for her constantly help during my PhD. In addition, a thank you to Dr Helio Pais, who introduced me to bioinformatics analysis using R. His instruction about how to look for miRNA targets in big data set has become priceless to me. I would especially thank to Dr Mathew Barter in David Young laboratory, Newcastle University, members in Professor Tonia Vincent laboratory, Oxford University,

members of Dr Anne Delany laboratory, University of Connecticut, USA for kindly sharing with me their MSCs model, DMM samples, and vectors.

Great thanks to all of my friends for the time they shared with me throughout my PhD journey. I am grateful their incredible friendship which makes the journey to achieve my goal more enjoyable.

Finally, I would like to acknowledge Vietnam Ministry of Education and Training (project 322), University of Each Anglia scholarship for international student for giving me the opportunity to do PhD in the UK. I also deeply thank Arthritis Research UK (program grant #19424, Tracey Swingler, Ian Clark) for supporting my project. Due to the currency exchange rates and the international fees, there are minimal funds from my Vietnam Government Scholarship for laboratory consumables. Thus, my PhD project is impossible without the support from Arthritis Research UK. I also acknowledge the John and Pamela Salter Trust for supporting me with the LNA probe for miR-29b used in my project.

CHAPTER 1
INTRODUCTION

1.1. Synovial joints

In mammals, joints are functionally classified into 3 categories: synarthroses (immovable joints), amphiarthroses (slightly movable joints), and diarthroses (freely movable joints). Most of the main joints of the appendicular skeleton are synovial joints, suggesting this type of joint has a crucial role in the body. The main component of synovial joints includes **the hyaline cartilage**, also known as articular cartilage, covering the bone of the synovial joint providing the cartilage lubricating and shock absorbing characteristics; **a capsule** enclosing the joint in line with **synovial membrane** which contains synovial membrane-resident cells secreting synovial fluid into the synovial cavity helping reduce friction, enabling free movement; **bones**, further held together by **ligaments**. The characteristics of some important components of the synovial joint relevant to this PhD thesis are described below.

1.1.1. Articular cartilage biology

Articular cartilage, a highly specialized tissue with unique mechanical behaviour, consists of **(i) chondrocytes,** the only cells, responsible for the homeostasis of extracellular matrix (ECM), and **(ii) a dense layer of ECM** composed primarily of water, collagen and proteoglycan.

1.1.1.1 Cartilage structural organization

Healthy articular cartilage comprises four different areas: the superficial, intermediate, radial or deep, and calcified zones (Buckwalter *et al.* 2005, Dudhia 2005, Pearle *et al.* 2005, Aigner *et al.* 2006, Martel-Pelletier *et al.* 2008, Umlauf *et al.* 2010, Houard *et al.* 2013) **(Figure 1.0)**. Each is characterized by a particular chondrocyte phenotype, and by distinctive extracellular matrix organization and composition (Buckwalter et al. 2005).

The superficial zone, the articulating surface and the thinnest of the four, makes up 10%-20% of articular cartilage thickness (Buckwalter et al. 2005, Pearle et al. 2005). This

region contains a high amount of collagen (primary type II, and IX) but very low amount of proteoglycan. The collagen fibrils are densely packed and aligned paralleled to the articular surface. Chondrocytes in this layer are characterized by an elongated appearance (Pearle et al. 2005), express many proteins having lubricating and protective functions (e.g. lubricin) but relatively little proteoglycan. This zone is in contact with synovial fluid, and is responsible for most of the tensile properties of cartilage that enable cartilage to resist shear and the tensile and compressive forces imposed by the movement of the articulation (Martel-Pelletier et al. 2008).

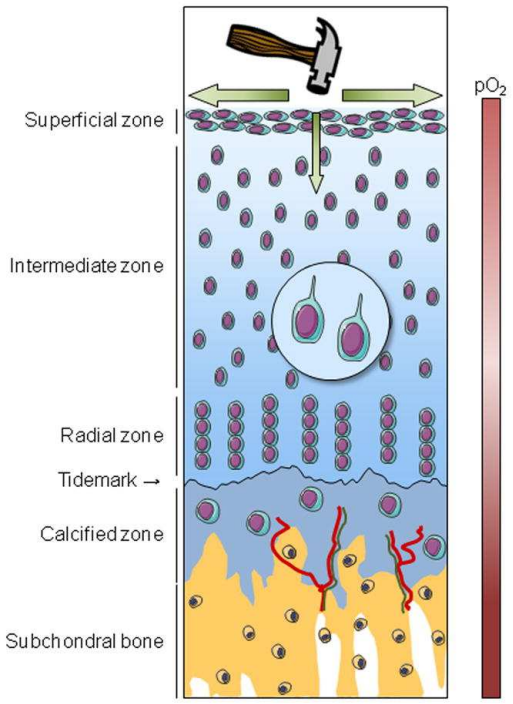

Figure 1.0: Histology of a healthy cartilage structural

The articular cartilage is organized into superficial, intermediate, radial, and calcified zones. Each zone can be distinguished by the difference in chondrocyte morphologies and components of collagen, proteoglycan, mineral and water

The intermediate and the radial zones contain large diameter collagen fibrils oriented perpendicular to the articular surface. These regions also have high amount of proteoglycan which is mainly aggrecan, a large chondroitin sulphate proteoglycan. Chondrocytes in the middle zone are more round than in the superficial zone. In the radial zone, the cells are arranged in columnar fashion (Buckwalter et al. 2005).

The tide mark, a thin line revealed after hematoxylin staining, marks the mineralization front between the calcified and non-calcified articular cartilage (Houard et al. 2013). In **the calcified cartilage zone**, the cell population is very scarce and chondrocytes are hypertrophic (Pearle et al. 2005, Martel-Pelletier et al. 2008). With aging, bloods vessels and nerves can be seen in calcified cartilage arising from the subchondral bones (Lane *et al.* 1977). The main function of this zone seems to be to anchor the cartilage to the bone as collagen fibrils from the radial zone penetrate into the calcified cartilage.

Furthermore, it is noteworthy to know that for mechanical protection purposes, in articular cartilage, the chondrocyte is surrounded by a pericellular matrix and a territorial cartilage matrix forming a capsule-like structure around the cells. Whilst the pericellular matrix is made of a thin layer of non-fibrillar material, which most likely represents the synthetic products of the chondrocytes, such as proteoglycans and glycoproteins, the pericellular matrix also contains a dense meshwork of thin collagen fibers (see below) (Dudhia 2005, Aigner et al. 2006, Martel-Pelletier et al. 2008, Heinegard *et al.* 2011).

1.1.1.2 Biology of chondrocytes

As mention above, chondrocytes are the only cellular components of articular cartilage, make up 5% of the wet weight of articular cartilage, and are surrounded by a pericellular matrix containing type VI collagen, microfibrils, hyaluronic acid, biglycan, and decorin but little or no type II collagen (Buckwalter et al. 2005, Dudhia 2005, Heinegard and Saxne 2011). The arrangement of chondrocytes and articular cartilage specific organisation result from a complex development process called endochondral ossification including four steps e.g. chondrogenesis, chondrocyte differentiation and hypertrophy, mineralization and invasion of bone cells, and finally the formation of bone (DeLise *et al.* 2000, Goldring *et al.* 2006, Goldring 2012). Chondrocytes arise from mesenchymal progenitors as a result of chondrogenesis started with the condensation of mesenchymal stem cell (expressing collagens I, III and V), and followed by the differentiation of chondroprogenitor cell (expressing cartilage-specific collagens II, IX and XI) (Goldring et al. 2006). After chondrogenesis, the chondrocytes remain as resting cells to form the articular cartilage or undergo proliferation, terminal differentiation to chondrocyte hypertrophy, and apoptosis.

There are no blood vessels in articular cartilage, thus the cells rely on diffusion from articular surface or subchondral bone for nutrients and metabolites. Importantly, the oxygen level in the cartilage matrix is quite low, ranging from 10% at the surface to less than 1% in the deep zone (Silver 1975), suggesting the cells have to adapt to this low oxygen level. The mechanisms of this adaption remain unclear but some published data reported the involvement of hypoxia inducible factor -1 alpha (HF-1α) (Schipani *et al.* 2001, Pfander *et al.* 2003). Hipoxia via HIF-1α can stimulate chondrocytes to express a number of genes associated with cartilage anabolism and chondrocyte differentiation like SOX9, TGFβ (Amarilio *et al.* 2007).

1.1.1.3 Biology of cartilage extracellular matrix

Together with chondrocytes, extracellular matrix (ECM) produced by these cells is among the main components of articular cartilage and its integrity is critical for the cartilage biochemical properties and joint physical function.

About structure, the ECM in articular cartilage is organized into pericellular, territorial, interterritorial zones, each of which is represented at specific distance from the chondrocytes (Dudhia 2005, Heinegard and Saxne 2011) (**Figure 1.1**).

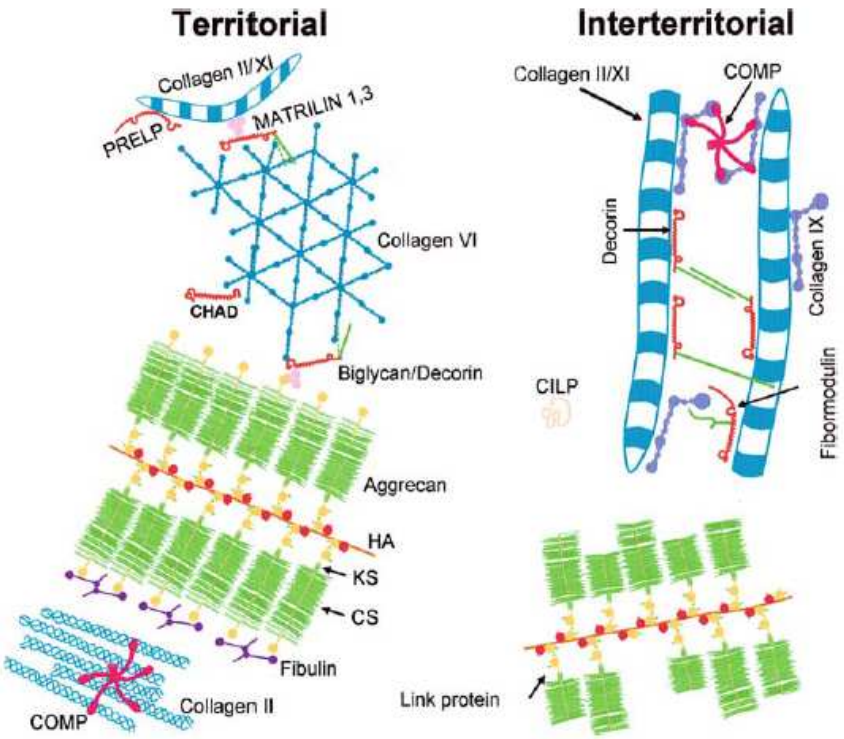

Figure 1.1: **Molecular organisation of normal articular cartilage.**

The cartilage matrix surrounding chondrocytes in healthy articular cartilage is arranged into zones defined by their distance from the cell. Pericellular matrix lies immediately around the cell and is the zone where molecules that interact with cell surface receptors are located. Next to the pericellular matrix, slightly further from the cell, lies the territorial matrix. At largest distance from the cell is the interterritorial matrix (adapted from Heinegard et al, 2011) (Heinegard and Saxne 2011)

Biochemically, of the ECM, approximately 70% is water (Pearle et al. 2005) , and 30% left is solid, of which 5-6% are inorganic compounds (hydroxyapatite), and the remaining 25% are organic compounds. Of the organic components, type II collagen constitutes 68% and the 32% left is formed by proteoglycan (mainly aggrecan) (Martel-Pelletier et al. 2008). The biology of aggrecan and collagen and their functions in articular cartilage are described as below.

1.1.1.3.1 Aggrecan

Molecules made up of a core protein attached to glycosaminoglycan chain are referred as proteoglycan. In articular cartilage, the most abundant proteoglycan is aggrecan, composed of chondroitin sulphate chains and keratan sulphate chains with N- and O-linked oligosaccharides. Aggrecan has three globular domains (G1, G2 and G3) and three extended domains (IGD, KS and CS). The N-terminal G1 domain, responsible for aggrecan-hyaluronan interaction, is followed after the signal peptide. The inter-globular (IGD) connects G1 and G2 domains, whose functions are unclear. Keratan sulphate binding (KS) and chondroitin sulphate (CS) domain lie between G2 and G3 domains (Kiani *et al.* 2002, Dudhia 2005, Martel-Pelletier et al. 2008, Heinegard and Saxne 2011) (Figure 1.2).

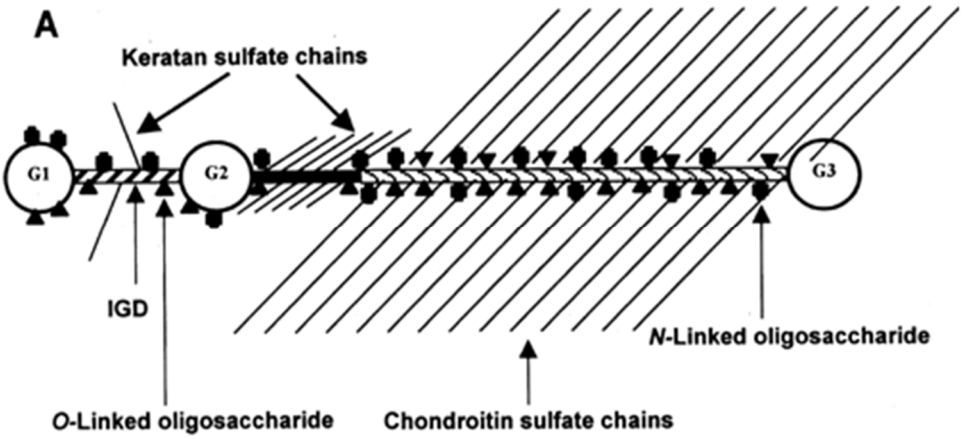

Figure 1.2: Aggrecan structure.

Aggrecan consists of 3 globular domains (G1, G2, and G3) and an attached GAG chain structure. The GAG attachment region is separated into keratin sulphate binding (KS) domain and chondroitin sulphate (CS) domain (Adapted from Kiani et al, 2002) (Kiani et al. 2002).

The chondroitin sulphate domain is the largest domain of aggrecan and is composed of around 100 chondroitin sulphate chains (typically around 2kDa each). Each chain is made up of some 50 disaccharides of glucuronic acid and N-acetylgalactosamine, with a sulphate group in the 4- or 6- position. The negatively-charge chondroitin sulphate chain accounts for the major function of aggrecan as a structural proteoglycan. The function of the keratan sulphate domain is not very clear but may be involved in the tissue distribution of aggrecan. There are about 30 KS chains, usually of small size (5-15 kDa), attached to the mature aggrecan molecule.

Chondroitin sulphate, keratan sulphate, and the interaction of aggrecan and hyaluronic acid are responsible for retaining water the cartilage. The interaction between aggrecan and collagen fibrils makes the ECM highly hydrophilic, leading to high resistance to compressive mechanical loads (Dudhia 2005, Martel-Pelletier et al. 2008).

1.1.1.3.2 Collagen

Collagen fibrils are composed of a protein macromolecular providing cartilage with resistance to tension. Collagen type II constitutes 85% total collagen content in the ECM of articular cartilage. Apart from type II Collagen, ECM also contains other collagens called minor collagens since their concentration is low in comparison with the type II collagen. A list of these collagens is provided in Table 1.1.

All fibril collagens are synthesized in the form of three polypeptide α-chains as a procollagen in which each chain has an N-terminal extension and a C-terminal extension. The three chains are covalently linked via disulphide bridges in the C-terminal propeptide. Following or during secretion of procollagens into the extracellular matrix, the terminal propeptides are cleaved off by specific proteinases e.g. ADAMTS-2, ADAMTS-3, ADAMTS-14 (cleaves the N-terminal) (Lapiere *et al.* 1971, Fernandes *et al.* 2001, Colige *et al.* 2002), and BMP-1 (cleaves the C terminal) (Wermter *et al.* 2007) to produce the mature collagen molecules. The mature collagens then spontaneously self-assemble into

cross-striated fibrils in the extracellular matrix. The fibrils are stabilized by covalent cross-linking (Figure 1.3)

Collagen molecules then associate on a core of two homologous collagen XI and two collagen II molecules to form an outer shell of 10 collagen II molecules of the micro fibril. In addition to collagen type II, fibers contain other collagens, particular collagen type IX. The collagen network is then stabilized by the formation of covalent crosslinks that link the collagen II chains. The links formed are both intra- and inter-molecules, for example, between the chains of collagen XI, between collagens e.g. collagen II and collagen IX.

Many other proteins also have a high affinity for collagens including thrombospondins, leucine-rich repeat proteins (biglycan, decorin, fibromodulin, lumican), matrillins, and fibronectin. Some of these interactions support fibre formation while others modify the collagen fibre surface to provide sites for interactions with neighbouring structures (Heinegard and Saxne 2011).

Collagen types	Characteristics
Type IX	Located on the surface of type II collagen fibrils; promotes the binding of the fibrils to other components of the matrix and to each other; carries a glycosaminoglycan chain.
Type XI	Forms the core of the same fibrosis. Regulates the formation and the diameter of the fibrils
Type V	Sometimes replaces the type XI collagen in cartilage; included in type I collagen fibrils in other tissues. Data on the composition and structure of the third a-chain are contradictory
Type III	Small amount are covalently bound to type II collagen
Type XII	Very small amounts are present on the surface of type II collagen
Type XIV	Very small amounts are present on the surface of type II collagen
Type VI	As in other tissue, forms a network of microfibrils. Concentrated mainly in the pericellular areas, provides a connection between the chondrocytes and the matrix
Type X	Expressed only by hypertrophic chondrocytes in cartilage areas undergoing ossification
Type XXVII	Expressed in cartilage tissue

Table 1.1 Minor collagen of cartilage tissue (adapt from Omelyanenko et al, 2014)(Petrovich *et al.* 2014)

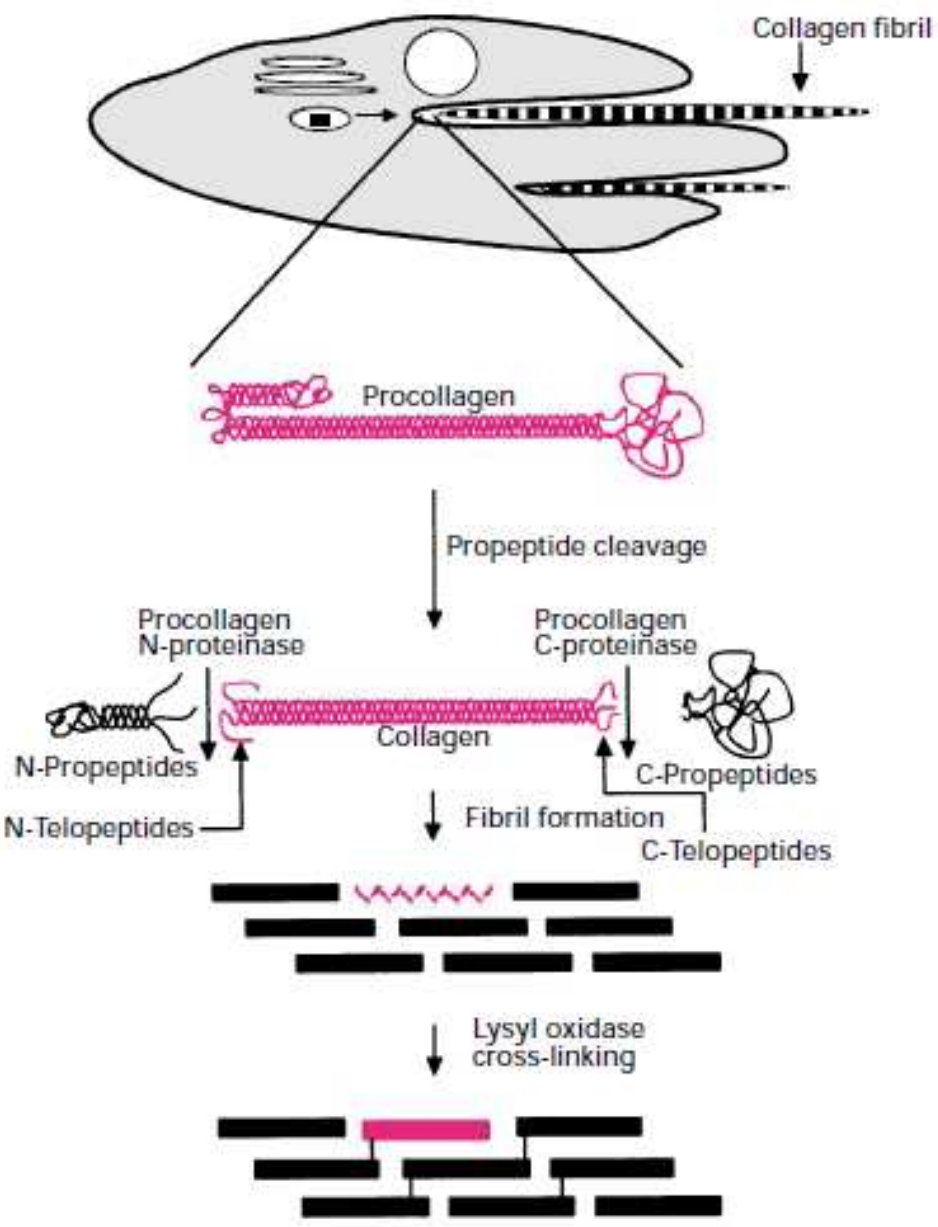

Figure 1.3: The formation of the fibrillar collagens

Procollagen is secreted from cells and converted into collagen by removal of the N- and C-propeptids by pro-collagen metalloproteinases. This produces mature collagen that spontaneously self-assembles into cross-striated fibrils which are stabilized by covalent cross-linking. Taken from (Kadler et al, 1996)(Kadler *et al.* 1996).

1.1.2. Synovium

Synovium is a thin tissue only a few cell layers thick (Fell 1978). The synovium acts as the controller for the environment within the joint where nutrients for chondrocytes can pass into the synovial cavity. Also, the synovium gives the joint its mechanical properties. The synovium can be divided into two compartments e.g. the synovial lining and the sub-lining. The synovial lining contains two cell types e.g. **type A (macrophage-like cells)** clearing all excess materials and potential pathogens from the joint, producing and secreting a number of enzymes and cytokines and chemokines that mediate tissue damage and inflammation in disease; **type B synoviocytes**, **fibroblast like cells**, producing the main component of synovial fluid, hyaluronan. The synovial sublining consists of connective tissue containing blood vessels, fibroblasts, adipocytes, and a limited number of resident immune cells, such as macrophage and mast cells (Smith *et al.* 2003). The synovial fluid has crucial role for lubrication of the joint and for transporting nutrients and oxygen to the cartilage.

1.1.3. Bone

Periarticular bone can be separated into distinct anatomic entities e.g. the subchondral bone plate, the subchondral trabecular bone, and the bone at the joint margins. The subchondral bone plate consists of cortical bone, which is relatively nonporous and poorly vascularized. It is separated from the overlying articular cartilage by the zone of calcified cartilage.

Bone is a very dynamic tissue with constantly undergoing remodelling in which bone resorption is normally followed by new bone formation. The primary cell responsible for bone resorption is the **osteoclast**, a specialized multinucleated cell of hemopoietic origin (Roodman 1999). Bone resorption takes place under a specialized area of the osteoclast cell membrane called “ruffled border,” which comprises a sealed lysosomal compartment where the acidic pH solubilizes the mineral and proteolytic enzymes digest the matrix. On the contrary, **osteoblasts**, the bone forming cells, originally from MSCs committed to osteoblastic lineage. Osteoblasts synthesize and secrete most of the proteins of the bone matrix, including type I collagen and non-collagenous proteins (Caetano-Lopes *et al.* 2007). In normal physiological condition, the amount of bone removed during the resorption and formation phases is balanced such that bone mass is maintained.

1.2. Osteoarthritis

Osteoarthritis (OA) is defined by the American College of Rheumatology as a "heterogeneous group of conditions that lead to joint symptoms and signs which are associated with defective integrity of articular cartilage, in addition to related changes in the underlying bone at the joint margins''.

There are more than 100 types of arthritis. However, OA or degenerative joint disease is the most common type. From a clinical point of view, OA can be classified into two categories e.g. **primary** which refers to its occurrence not related to any prior condition or event which is also referred as idiopathic, and **secondary** which refers to the development of the disease after trauma or pre-existing condition.

The disease most commonly affects the middle-age and elderly, although it may begin earlier as result of injury, obesity or congenitally. As a greater proportion of the population is old aged and with increasing obesity, OA will have a great impact on society in the future with enormous socioeconomic costs.

1.2.1. Osteoarthritis pathology

It is now considered that OA is a disease of the whole joint as an organ resulting in "joint failure" where all major components of the joint e.g. the cartilage, the synovium, and the underlying bone are affected (Loeser *et al.* 2012). The pathologic changes seen in OA include cartilage destruction, fibrosis of the synovial capsule, hyperplasia of the synovial membrane, osteophyte formation, the subchondral bone thickening (**Figure 1.4**) (Aigner et al. 2006, Loeser et al. 2012). These changes result from an incompletely understood series of functional events.

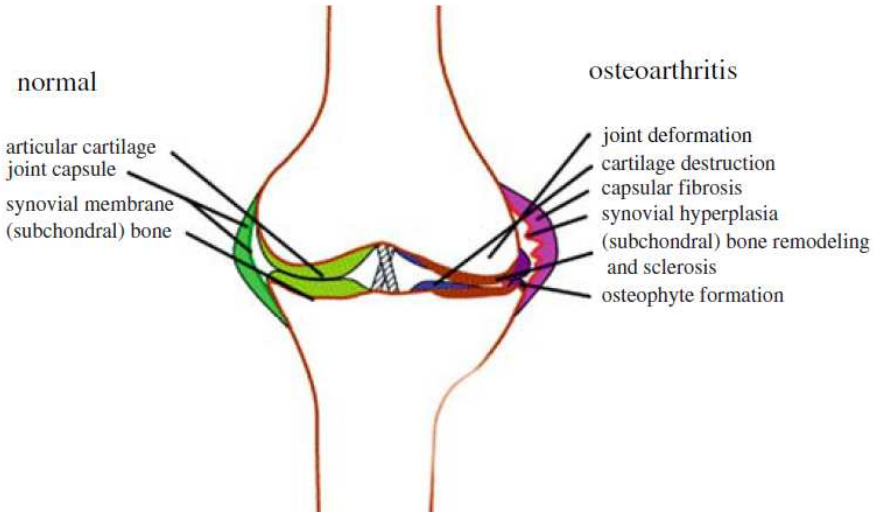

Figure 1.4: Overview of the pathologic changes associated with OA.

In a normal joint, the subchondral bone is covered by a thick layer of articular cartilage and the joint is enclosed in a capsule where the synovial membrane lies. In an OA joint, articular cartilage is destroyed, the subchondral bone is remodelled (thickens), the synovial capsule is fibrosed and osteophytes are formed (reprinted from Aigner et al, 2006) (Aigner et al. 2006)

1.2.1.1.Articular cartilage destruction in osteoarthritis

Biochemical, genetic factors, and mechanical stress contribute to the OA lesion in cartilage, leading to articular cartilage degradation, and chondrocyte metabolism disorders as a consequence. Articular cartilage degeneration is a two phase process controlled mainly by chondrocytes e.g. a short biosynthesis phase where the cells attempt to repair the damaged ECM, followed by the degenerative phase, where the cells destroy the articular cartilage by increasing the synthesis of matrix degradating proteinases and decreasing their synthesis of matrix components, in particular of aggrecan. Besides changes in synthesis and degradation, other aberrant behaviours in cell proliferation and death, and phenotypic modulation are also observed in OA chondrocytes (Sandell *et al.* 2001).

Contrary to normal chondrocytes with no proliferative activity, OA chondrocytes have a low proliferative activity (Meachim *et al.* 1962, Rothwell *et al.* 1973, Lee *et al.* 1993), explained in part due to the better access to proliferation factors from the synovial fluid as well as due to the damage of the ECM (Meachim and Collins 1962, Lee et al. 1993), subsequently causing chondrocyte clustering, a characteristic feature of OA cartilage. Chondrocyte death, caused by apoptosis, necrosis, or other cell death mechanisms such as chondroptosis, is another known feature of OA. Many studies have demonstrated the significant correlations between chondrocyte death and severity of OA and aging. These changes are associated with the production of reactive oxygen species, a lack of growth factors, release of glycosaminoglycan and mechanical injury. However, which of these types of cell death predominate in OA is debatable. The detection of specific form of cell death in articular cartilage is difficult in which current gold standard for detecting chondrocyte death is electron microscopy which suggests that the morphological changes of chondrocytes in OA cartilage are attributed to apoptosis and / or chondroptosis. Chondrocyte death by apoptosis has been reported play an important role: normal cartilage explants or chondrocyte culture exposed to nitric oxide, collagenase, anti CD-59, or mechanical factors e.g. shear strain, loading strain induced apoptosis; cartilage from equine joints have shown that chondrocyte apoptosis is positively correlated with early stages of OA and severity of cartilage damage (Zamli *et al.* 2011).

When the damage occurs, the chondrocytes attempt to repair the damaged matrix by increasing their anabolic activity to enhance ECM synthesis. However, a net loss of ECM content is one of the hallmarks of all stages of OA, suggesting the dominance of ECM degradation over the synthesis. This is characterized by the increase in expression and activation of matrix-degrading enzymes e.g. matrix metalloproteinase (MMPs) and aggrecanases (from the ADAMTS family) (Buckwalter et al. 2005, Pearle et al. 2005, Aigner et al. 2006, Umlauf et al. 2010, Loeser *et al.* 2012). **The MMPs,** belonging to a family of zinc-dependent proteases, show activation correlating with cartilage degradation. Among these, the groups of collagenases 1, 2, 3 (MMP-1, MMP-8, and MMP-13, respectively), stromelysins (MMP-3, MMP-10, MMP-11) and gelatinases (MMP-2, MMP-9) have the highest impact on OA cartilage breakdown (Burrage *et al.* 2006). The MMP-1, MMP-8 and MMP-13 which cleave native fibrillar collagen, contribute to the pathological cleavage of collagen fibrils in OA (Burrage et al. 2006). Of the collagenase group, MMP-13 is deemed to be responsible for most of the collagen II breakdown whilst MMP-1 cleaves type II collagen stronger than MMP-8 (Billinghurst *et al.* 1997) has a pivotal role for collagen cleavage in OA (Knauper *et al.* 1996). In addition to collagenases, others MMPs degrading non-collagen have also been shown to be elevated in OA cartilage e.g. the gelatinases (which cleave denatured collagen, gelatin, type V collagen) and the stromelysins (having substrate preference for proteoglycans, elastin, laminin, fibronectin) (Umlauf et al. 2010) **The aggrecanases** (the ADAMTS family), are also of particular importance in cartilage turnover, and have activity against the proteoglycan aggrecan. Of all ADAMTS members, ADAMTS-4 and ADAMTS-5 are most active against aggrecan (Arner 2002). ADAMTS-5 is constitutively expressed in chondrocytes whereas ADAMTS-4 expression is stimulated by proinflammatory cytokines IL-1β, and TNF-α (Umlauf et al. 2010) (Tortorella *et al.* 2001). In vitro studies with human cartilage show that both ADAMTS-4 and ADAMTS-5 contribute to ECM breakdown during the disease progression even though human recombinant ADAMTS-5 has higher rate of aggrecan cleavage than ADAMTS-4 (Song *et al.* 2007). In mice, ADAMTS-5 has been shown to be the major aggrecanase, by studies with ADAMTS-4 and ADAMTS-5 knockout mice in which only ADAMTS-5 deficiency prevented the mice from cartilage degradation in both inflammatory and a joint-instability model of arthritis (Glasson *et al.* 2005, Stanton *et al.* 2005) .

As mentioned above, despite the attempt at repairing the ECM, the damage to the cartilage becomes irreversible because the adult chondrocytes fail in regenerating the normal cartilage matrix structure. This failure could be, in part, attributed to the phenotypic alteration of chondrocytes. Chondrocyte phenotypes are categorized largely by subtyping collagen expression e.g. chondroprogenitor cells express type IIA procollagen. The alternative splice variant) (Sandell *et al.* 1991), mature chondrocytes are marked by expressing type IIB procollagen, IX, and XI, aggrecan and link protein (Sandell and Aigner 2001), and hypertrophic chondrocytes express type X collagen (Schmid *et al.* 1985). In OA cartilage degeneration, an important proportion of adult articular cartilage chondrocytes, found mostly in the middle zone, re-expressed type IIA procollagen (chondroprogenitor cells) in both early and late OA stages (Sandell and Aigner 2001). Cells in the upper middle zone mainly express type III collagen which is a fibroblast-like phenotype. This phenotype is normally observed in vitro, where the chondrocyte phenotypes are modulated through so-called "dedifferentiation" process by several factors like retinoic acid or IL-1. Dedifferentiated chondrocytes are still very active, express collagen types I, III and V but stop expressing aggrecan and collagen type II (Sandell and Aigner 2001). In the deepest zone of OA cartilage, the cells start to express type X collagen, specific marker for hypertrophy of growth-plate chondrocytes (Girkontaite *et al.* 1996). Indeed, the hypertrophic chondrocytes in OA cartilage and in the growth-plate share similarities and the subsequent functional event associated with hypertrophic differentiation is cartilage mineralization which is also a feature of OA. However, the mechanism involved in pathological cartilage calcification during OA is not completely understood.

1.2.1.2. Synovium in osteoarthritis

Inflammation of the synovial membrane (synovitis) is identified in many OA patients despite lower severity and greater variability as compared to rheumatoid arthritis. It is reported that synovitis can occur even in early stages of the disease (Benito *et al.* 2005). Synovitis is associated with symptoms such as pain, the degree of joint dysfunction, the rapid degeneration of cartilage, and is characterized by the thickening of the synovial lining layer, leukocyte infiltration, and thickening of the sub-lining stroma. The

mechanisms underlying the development of synovitis in OA remain unclear. It is however well known that this inflammatory process is triggered by ECM degradation products, which engage Toll-like receptors and the complement cascade (Scanzello *et al.* 2012). Noteworthy, the synovial reaction may produce a variety of cytokines and chemokines, in turn affecting catabolism of chondrocytes (Scanzello and Goldring 2012).

Of all cell types in the inflamed OA synovium, the macrophages are among the most abundant and depletion of synovial macrophages has been shown to result in decreased osteophyte formation, and IL-1, TNF-α, IL-6, IL-8, MMP-1, MMP-3 production (Bondeson *et al.* 2010). Natural killer cells and dendritic cells are also reported to present in synovial tissue. However, the role of both of them in OA pathogenesis has not yet been elucidated in detail.

1.2.1.3. Subchondral bone in osteoarthritis

Articular cartilage helps to distribute load across the whole joint surface. Any alteration in the properties of cartilage leads to alter load experience by the underlying bone and probably causes a tissue remodelling response. The properties of bone might also modulate how the overlying cartilage reacts to load.

Although OA is often characterized as a disease of articular cartilage, the alteration of bone metabolism is increasingly recognised as a mediator of pain and OA progression. Subchondral bone consists of a dome-like subchondral plate and underlying trabeculae, having a close biomechanical and biochemical relationship with the overlying cartilage. Strong evidence associates subchondral bone alterations with cartilage damage and loss in OA (Karsdal *et al.* 2014). However, there is still an incomplete understanding of the mechanisms for the numerous pathophysiological alterations detected in subchondral bone with OA.

The pathological cascade may be started when the normal subchondral bone suffers from a non-physiological strain. In early-stage OA, the subchondral plate becomes thinner and more porous, together with initial cartilage degeneration. Subchondral trabecular bone also deteriorates, with increased separation and thinner trabeculae. At the same time, microdamage begins to appear in both calcified cartilage and subchondral bone, which will persist throughout the whole pathological process. In late-stage OA, calcified cartilage and the subchondral plate become thicker, with duplicated tidemarks and progressive non-calcified cartilage damage. Subchondral trabecular bone becomes sclerotic (Li *et al.* 2013).

The sclerosis of periarticular mineralized tissues may be a biomechanical compensational adaption to the widespread cysts and microdamage in subchondral bone, which render subchondral bone structure more fragile (Figure 1.5).

Despite increased bone volume density in the sclerotic subchondral bone, its mineralization is reduced and lower than in normal joints. Although collagen synthesis is elevated in subchondral bone, the deposited collagen is hypomineralized and has a markedly reduced calcium-to-collagen ratio [42].

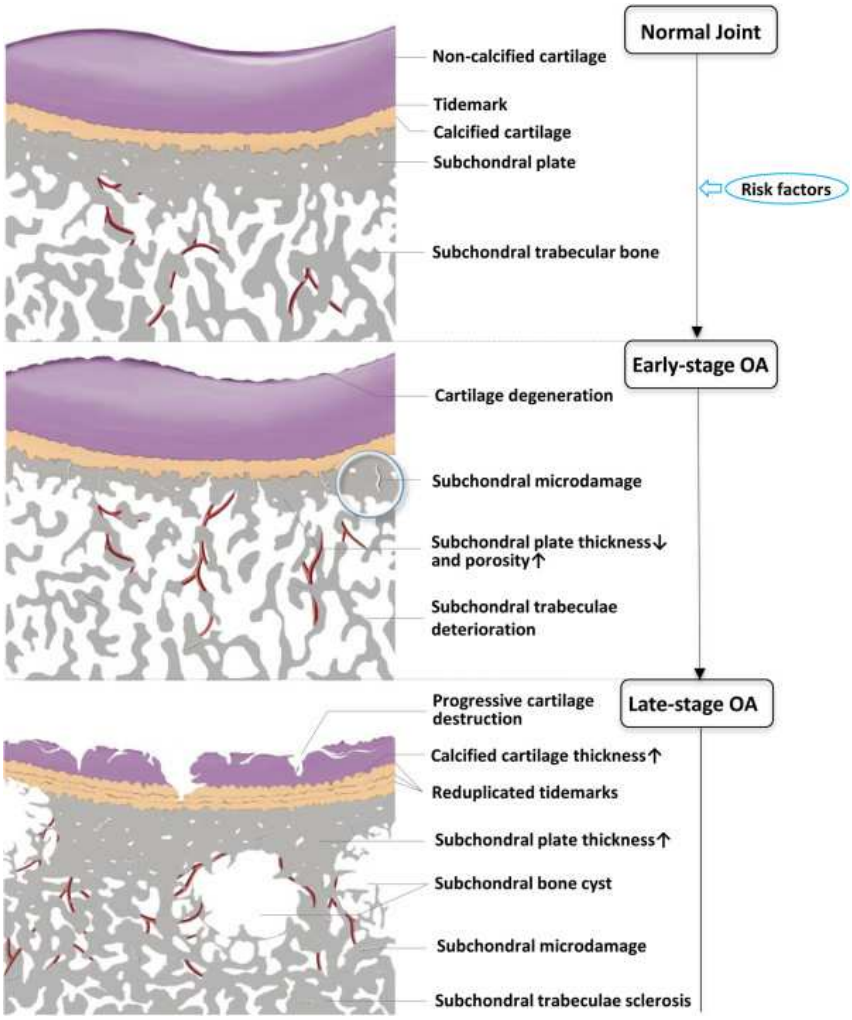

Figure 1.5: Alteration in subchonral bone in Osteoarthritis

In early stage of OA, subchondral microdamage occurs, the subchondral plate is thinner with increased porosity, and subchondral trabeculae are deteriorated. At OA later stage, the calcified cartilage and subchondral plate is thicker, with reduplicated tidemarks. Subchondral trabecular bone becomes sclerotic (adapted from Li et al, 2013)(Li et al. 2013)

1.2.1.4. Osteophytes

Osteophytes, considered as an adaptation to the altered biomechanics, are non-neoplastic osteo-cartilaginous protrusions growing at the margins of OA joints, and represent areas of new cartilage and bone formation. Osteophytes limit joint movement, represent a source of joint pain, and are a radiographic hallmark of OA. However, it is noteworthy that when osteophytes appear in the absence of other bony changes, e.g. subchondral cysts or subchondral sclerosis, they may be a manifestation of aging, rather than of OA.

Osteophytes derive from precursor cells within periosteal or synovial tissue (van der Kraan *et al.* 2007) but the initial stimuli for osteophyte formation remains unclear, probably involving both mechanical and humoral factors as repeated injections of mouse joints with TGFβ or BMP induced or enhanced osteophyte formation in animals with experimentally induced OA (van Beuningen *et al.* 1998).

Osteophytes are composed of cells that express type I procollagen mRNA, mesenchymal prechondrocytes that express type IIA procollagen mRNA, and maturing chondrocytes that express type IIB procollagen mRNA. Based on the spatial pattern of gene expression and cytomorphology, the neochondrogenesis associated with osteophyte formation closely resembles that of healing fracture callus (Matyas *et al.* 1997) and is also similar to the growth plate. Thus, osteophytes may represent an excellent *in vivo* model for induced cartilage repair processes.

1.2.2. Anabolic and catabolic signalling in OA

Anabolic and catabolic activation are largely the result of exposing cells to various cytokines and growth factors e.g. TGFβ, BMPs, IGF-1, TNF-α, IL-1β, Wnt3a. In OA cartilage, the catabolic and anabolic equilibrium is broken and favours the activation of catabolic pathways or mechanisms leading to matrix degradation.

1.2.2.1.Anabolic signalling in OA

As previously mentioned, the early phase of the response to mechanical injury is characterized by the attempt to repair the damage matrix by increasing the anabolic activity of chondrocytes, enhancing synthesis of extracellular matrix components. This is facilitated by enhancing levels of anabolic factors e.g. TGFβ, FGF, and BMPs, and Wnt.

1.2.2.1.1. TGFβ signalling

The TGFβ family, consisting of over 35 members including TGFβ and BMPs, has been widely known to play a crucial role in the development and homeostasis of various tissues. Activated TGFβ (TGFβ-1, -2, -3) binds to their two receptor complex, TGFβ-R1 and TGFβ-RII and phosphorylates members of the receptor-specific Smad family, Smad2 and Smad3. Upon phosphorylation, Smad2/3 subsequently forms a complex with the common mediator Smad4. This complex then translocates into the nucleus where it can act as a transcription factor. Unlike TGFβ-1, -2, -3 which signal via Smad2/3/4, BMPs transduce their signal through Smad-1, -5 and -8 (Miyazawa *et al.* 2002, Verrecchia *et al.* 2002).

Members of the TGFβ family are considered potent mediators of cartilage matrix synthesis, in which they up-regulate the expression of several types of collagens and proteoglycan but down-regulate cartilage degrading enzymes (Verrecchia *et al.* 2001, Verrecchia and Mauviel 2002). Despite such promising data, therapeutic studies with TGFβ revealed major side effects e.g. injection or adenovirus–mediated delivery of TGFβ1 into normal murine knee joint resulted in joint fibrosis and osteophyte formation (van Beuningen et al. 1998) .

1.2.2.1.2. Wnt signalling

The human Wnt family includes 19 members which mostly exert their function by binding to Frizzled (FZD) receptor proteins and LRP-5/6 co-receptor proteins, in turn activating several signal transduction pathways e.g. canonical, and non-canonical signalling pathways. In the canonical Wnt pathway, most β-catenin in the cytoplasm is sequestered and targeted for proteasome-mediated degradation within a multi-protein complex of casein kinase, axin, the adenomatous polyposis coli tumour suppressor protein (APC) and glycogen synthase kinase 3β (GSK3β). With the presence of appropriate Wnt ligands, signalling through the Frizzled receptors inhibits this degradation process, and thereby leads to β-catenin accumulation and translocation into the nucleus (Clevers 2006). Within the nucleus, it acts in concert with Tcf/Lef transcription factors to generate a transcriptionally active complex that regulates a number of genes e.g. MYC, cyclin D1, MMP3 and CD44, E-cadherin, MMP7, MMP26(Dell'accio *et al.* 2008, Umlauf et al. 2010). In contrast to the canonical pathway, non-canonical Wnt signalling is mostly a β-catenin independent mechanism like the Wnt/calcium and Wnt/JNK pathways in vertebrates and the Wnt/planar cell polarity pathway (PCP) in flies (Willert *et al.* 2006). In addition, there

are some natural extracellular inhibitory factors for Wnt signalling. One of the best characterized families is the Dickkopf (Dkk) family which bind to LRP-5/6 and antagonize the canonical pathway. Other antagonists are the secreted frizzled-related protein (sFRP) family which bind directly to Wnt ligands and inhibiting both canonical and non-canonical Wnt pathways (Kawano *et al.* 2003).

A number of published data provide evidence of the critical role of Wnt signalling in OA development. Direct evidences come from animal model studies where β-catenin is conditionally activated or inhibited in articular cartilage chondrocyte of adult mice (Zhu *et al.* 2008, Zhu *et al.* 2009). Mice with β-catenin activated had OA-like cartilage degradation, osteophyte formation, associated with accelerated chondrocyte maturation and MMP13 expression (Zhu et al. 2009). Similarly, selective suppression of β-catenin signalling in Col2a1-ICAT (inhibitor of β-catenin and TCF) transgenic mice also causes OA-like cartilage degradation(Zhu et al. 2008). In line with these reports, in vitro culture of human primary chondrocyte, either activation or blockade of β-catenin signalling all resulted in cartilage loss (Nalesso *et al.* 2011). These data suggest that balanced β-catenin levels are essential for maintaining homeostasis of articular chondrocytes and that any factors impairing this balance could lead to pathological changes. Moreover, LRP5 is located in chromosome 11q12-13, which is thought to be an OA susceptibility locus. LRP5-/- mice displayed increased cartilage degradation, probably due to low bone mass density (Lodewyckx *et al.* 2012). Another study in a mouse OA model also demonstrated that control of Dkk1 expression, a negative regulator of β-catenin/Wnt signalling, prevents joint cartilage deterioration in OA knees through attenuating the apoptosis regulator Bax, MMP3 and RANKL (Weng *et al.* 2010). Also, the inhibition of Dkk1, has been reported to be able to reverse the bone-destructive characteristics of rheumatoid arthritis to the bone-forming characteristics of OA (Diarra *et al.* 2007). This evidence further supports the crucial role of β-catenin/Wnt signalling in OA. Wnt signalling is also reported to function as an OA initiation factor e.g. a down-regulation of Wnt antagonist FRZB and an up-regulation of the ligand Wnt16 and target genes encoding β-catenin, Axin-2, C-JUN and LEF-1 was observed in mouse model of mechanical injury, a major cause of OA; expression of WNT1-inducible signalling protein (WISP-1) was also increased twofold in cartilage lesions compared to healthy intact cartilage (Blom *et al.* 2009).

Human studies also observed the critical role of WNT signalling in OA development. A loss-of-function allelic Arg200Trp and Arg324Gly Frzb variants, encoding sFRP-3, a β-catenin/Wnt signalling inhibitor, contributed to genetic susceptibility of women to hip OA (Loughlin *et al.* 2004, Lane *et al.* 2006). Given the close relationship between bone shape and OA development, Baker-Lepain et al proposed that SNPs in Frzb are associated with the shape of proximal femur and further contribute to hip OA development (Baker-Lepain *et al.* 2012). Moreover, the Frzb knockout mice increased articular cartilage loss during arthritis triggered and this damage was associated with increased WNT signalling and MMP-3 expression and activity. Also, the FRZB deficiency resulted in the cortical bone thickness and density with stiffer bones (Lories *et al.* 2007).

1.2.2.2. Catabolic signalling in OA

Opposing the anabolic effects of growth factors are pro-inflammatory cytokines and a variety of mediators associated with inflammation e.g. NO, prostaglandins, IL-1β, TNF-α, IL-6, IL-8 These factors are first produced by the synovial membrane and diffuse into the cartilage through synovial fluid, together with activate chondrocytes which also have the capacity to produce a variety of cytokines and mediators, responsible for functional alterations in the synovium, the cartilage, and the subchondral bone. Their role in OA has attracted considerable attention.

Of pro-inflammatory cytokines, IL-1β, TNF-α seem prominent and of major importance to cartilage destruction. The biologic activation of cells by IL-1 is mediated through the association with its specific receptors e.g. type I and II IL-1R. Especially, the type I IL-1R, responsible for signal transduction, was found to increase in OA chondrocytes and synovial fibroblasts. IL-1β is a critical mediator, and stimulation of chondrocytes by IL-1β causes gene expression patterns similar to those in OA cartilage (Goldring *et al.* 1988, Lefebvre *et al.* 1990). IL-1β localizes to the site of cartilage degradation in OA joints, providing evidence of its key role in the pathogenesis of OA (Tetlow *et al.* 2001, Pujol *et al.* 2008). IL-1β was reported to suppress aggrecan and collagen and up-regulate the proteolytic enzymes e.g. ADAMTS4 and MMP13 (Goldring 2000, Kobayashi *et al.* 2005). In addition, *IL-1β*, or IL-1β-converting enzyme knockout mice showed the accelerated development of OA lesions in response to OA surgical induced compared to wild type mice (Clements *et al.* 2003). The blocking effects of IL-1β by IL-1 receptor antagonist

(IL-1ra), which is the natural inhibitor of IL-1β by competing with IL-1β for occupancy of the IL-1β cell surface receptors but cannot initiate cellular signals protect against the development of experimentally induced OA lesions in animal models e.g. dogs, horses (Pelletier *et al.* 1997, Frisbie *et al.* 2002). Interestingly, it was reported that the IL-1β concentration is low in inflamed joints and a level from 10-1000 fold excess of IL-1ra over IL-1β was required to efficiency block all of the available IL-1β receptors enough to inhibit joint degradation (Pelletier et al. 1997).

1.2.2.2.1. NFκB Signalling

The transcription factor NFκB is the master regulator of expression of a number of genes critical to innate and adaptive immunity, cell proliferation, and inflammation. NFκB is held in the cytoplasm in an inactive form associated with the inhibitory κB (IκB) protein. A broad range of stimuli, including TNF-α, IL-1β, bacteria and viruses trigger a cascade of signalling, leading to release of NFκB from IκB. The activated NFκB will then translocate to the nucleus, bind to DNA elements present in its target genes and facilitate their transcription.

Numerous published data support the central role of NFκB signalling in cartilage metabolism and development of OA e.g. IκB overexpression in human OA synovial fibroblasts resulted in a decrease in expression of IL-6, IL-8, MPC-1/CCL-2, and MMPs (Amos *et al.* 2006) as well as abolishing the IL-1β-induced effect on expression of ADAMTS-4 (Bondeson *et al.* 2007); In a mouse surgically induced OA model, siRNA inhibiting NFκB/p65 resulted in reducing the amount of IL-1βand TNF-α in synovial fluid, reducing the level of inflammation in the synovium, and decreasing cartilage damage (Chen *et al.* 2008).

1.2.3. Risk factors for Osteoarthritis

The pathogenesis of OA is complex and poorly understood but involves the interaction of multiple factors ranging from genetic predisposition to mechanical and environmental components. Studies are in progress to define the molecular mechanisms involved in initiation and progression of OA.

1.2.3.1.Trauma and altered mechanical load

Mechanical factors and trauma have a central role in the initiation and propagation of OA: Excessive load and trauma which lead to injury of the menisci or ligaments predispose to

the development of the disease; the level and nature of the load experienced might also influence the progression of joint damage: an acute trauma leading to rupture of the meniscus or the cruciate ligaments might precipitate the development of OA. However, the differing contributions to this effect of the initial trauma and the ensuing mechanical instability have not been clearly delineated; also, in immobilized joints, there is lack of OA: further supporting the importance of mechanical triggers in the disease process (Riordan *et al.* 2014).

After joint trauma, the onset and progression of clinical symptoms differs even among groups with the same type of injury and physical activity profile, pointing to the involvement of other factors apart from the trauma.

1.2.3.2. Inflammation

Histologically, the disease was denominated osteoarthrosis, a term that implied the absence of inflammation. However, data acquired using high-sensitivity assays for inflammatory markers (such as C-reactive protein) demonstrate that low-grade inflammation is present (Pearle *et al.* 2007). Numerous inflammatory cytokines are found at increased levels in joint tissues during the acute post-injury phase, including IL-1, IL-6, IL-17, and TNFα (Lee *et al.* 2009). Inflammation seems to be a very early event in OA since the increase of CRP levels precedes the release of other OA indicators or molecular markers of matrix breakdown, and is observed well before clinical disease.

Inflammatory might be of particular importance to the onset and propagation of the primary and secondary OA. However, why the inflammation triggered in OA remains controversial. It was hypothesized that it was caused by traumatic joint injury or an age – related process. Joint injury leads to cartilage degradation and tissue damage. Once degraded, cartilage fragments accumulate in the joint and contact the synovium. Considered foreign bodies, synovial cells react by producing inflammatory mediators, found in synovial fluid. These mediators can activate chondrocytes present in the superficial layer of cartilage, which leads to metalloproteinase synthesis and, eventually, increase cartilage degradation. Published data support for the hypothesis that inflammation was triggered by aging process: advance glycation endproducts (AGEs), produced by a non-enzymatic process in aging tissue, weaken cartilage by modifying its mechanical properties triggering chondrocyte activation by binding to specific receptors present at the

surface of the chondrocytes, called RAGE (receptor for AGEs) lead to an overproduction of proinflammatory cytokines and MMPs (Nah *et al.* 2007); or after a period of vigorous proliferation, chondrocyte division rate declines but has high capacity to synthesize soluble mediators which in turn induces several inflammatory and pro-degradative mediators.

1.2.3.3. Obesity

Obesity is a well known risk factor for the initiation and progression of OA. This association is obvious because any overload on a weight – bearing joint would provoke tear and wear at the surface of the cartilage.

The molecular mechanisms explaining why obesity is one of the major risk factors for OA (Messier *et al.* 2005) is not exactly known. It is possible that the excess weight increases the load borne by all parts of the joint. However, the association between overweight and OA is not simply a question of increased mechanical load because obesity acts as a risk factor for developing hand OA (Grotle *et al.* 2008). Together with this, published data from animal studies: knee cartilage from rabbits fed a high – fat diet showed lower glycosaminoglycan content and aggrecan-1 than cartilage from rabbits fed a normal – fat diet independently of animal weight (Brunner *et al.* 2012); OA surgical induced mice fed a high – fat diet from 4 weeks of age showed higher OA cartilage degeneration at 8 weeks after surgery than those fed a normal diet (Mooney *et al.* 2011); in mice transgenic for human C – reactive protein (CRP) on a high – fat diet, there is a lack of correlation between OA severity and body weight (Gierman *et al.* 2012).

Many studies suggest that systemic inflammatory mediators contribute to the increased risk of OA with obesity. Adipose tissue, especially from the abdomen, is a rich source of pro-inflammatory cytokines, which are often referred to as adipokines. Many adipokines elevated with obesity have also been shown to mediate synovial tissue inflammation. For example, leptin is a 16-kd polypeptide hormone encoded by the obese (*ob*) gene and is primarily secreted by adipocytes. Female C57BL/6J mice with impaired leptin signalling are protected from obesity – induced OA, suggesting elevated body fat in the absence of leptin signalling is insufficient to induce systemic inflammation and OA (Griffin *et al.* 2009). Leptin has been found to exist at higher concentrations in the synovial fluid compared to serum (Presle *et al.* 2006). Leptin, alone or in synergy with IL-1, induced collagen release from bovine cartilage explants and upregulated MMP-1 and MMP-13 expression in bovine chondrocytes(Hui *et al.* 2012).

1.2.3.4. Aging

Aging is the most important risk factor for OA. After 40 year old, many people will appear to have some damage to their joints which may lead to OA, and approximately 50% of individuals greater than the age of 65 suffer from OA. The incidence of the disease through age has been observed: the prevalence of OA rises from 4% in people under the age of 24 to as high as 85% for those at 75-79 years of age. The common justification is the long-term effect of mechanical load on all joint components. Also, the regenerative capability of cartilage is reduced and cellular apoptosis is enhanced with age (Goldring *et al.* 2007).

1.2.3.5.Genetic factors

Evidence from family clustering and twin studies indicates that the risk of OA has an inherited component. Genetic factors may influence between 39% and 65% in radiographic OA of the hand and knee in OA, about 60% in OA of the hip, and about 70% in OA of the spine. Mutations to genes that play a role in the ECM, proteases and inhibitors, cytokines, and growth factors have been found to affect one's susceptibility to develop of OA (Sulzbacher 2013). However, the individual effects are relatively small. For example, a genome – wide association study showing that the C allele of rs3815148 on chr 7q22 was associated with a 1.14- fold increased prevalence of knee and/ or hand OA(Kerkhof *et al.* 2010).

1.3. MicroRNAs in osteoarthritis

1.3.1. The basic biology of miRNA

miRNAs are an abundant class of evolutionarily conserved, short (~22nt long), single – stranded RNA molecules that have emerged as important post transcriptional regulators of gene expression by binding to specific sequences within a target mRNA (Ambros 2004, Bartel 2004). To date, 1424 miRNAs have been identified in human cells and each is predicted to regulate several target genes (Lim *et al.* 2005, Kozomara *et al.* 2011). Computational predictions indicate that more than 50% of all human protein – coding genes are potentially regulated by miRNAs (Lewis *et al.* 2005, Friedman *et al.* 2009). The abundance of mature miRNAs varies extensively from as few as ten to more than 80,000 copies in a single cell, which provides a high degree of flexibility in the regulation of gene expression (Chen *et al.* 2005, Suomi *et al.* 2008). The regulation exerted by miRNAs is

reversible, as feedback/forward regulatory loops have been shown to exert modifying effects during translation (Inui *et al.* 2010) .

1.3.1.1. MicroRNA discovery

In 1981, the first miRNA: *lin-4* was discovered in *Caenorhabditis elegans* (Chalfie 1981). In the early 1990s, Ambros and Ruvkun revealed that *lin-4* controlled a specific step in developmental timing in *C.elegans* by downregulating *lin-14* (a conventional protein – coding gene) (Chalfie 1981, Lee *et al.* 1993, Wightman *et al.* 1993). They recognized that the *lin-14* 3'UTR harbours multiple sites of imperfect complementarity to *lin-4* and proposed that *lin-4* binds to these sites and blocks *lin-14* translation.

Forward genetics also discovered a second miRNA in *C.elegans,* known as *let-7* (Reinhart *et al.* 2000) which targets *lin-41* and *hbl-1* (Abrahante *et al.* 2003, Lin *et al.* 2003). The concept of miRNAs then jumped from worms to higher species, since *let-7* had well-known homologues even in human and fly. In 2001, the term "microRNA" was coined for this class of non-coding gene regulators (Lagos-Quintana *et al.* 2001, Lau *et al.* 2001, Lee *et al.* 2001). The discovery of miRNAs had crossed over to human, and finding miRNA targets became a high priority.

1.3.1.2. MicroRNA biogenesis

Most of the currently known miRNA sequences are located in introns of protein coding genes; a lower percentage of miRNAs originate from exons or non-coding mRNA-like regions (Rodriguez *et al.* 2004). In addition, a significant number of miRNA are found in polycistronic units that encode more than one miRNA. The miRNAs within clusters are often functionally related (Lagos-Quintana et al. 2001, Lau et al. 2001).

Despite the obvious differences between the biology of miRNAs and mRNAs, all available evidence suggests that these transcripts share common mechanisms of transcriptional regulation. Generally, the generation of a miRNA is a multi-step process that starts in the nucleus and finishes in the cytoplasm (Lee *et al.* 2002). First, miRNAs are transcribed by the RNA polymerase II complex (Lee *et al.* 2004) and subsequently capped, polyadenylated, and spliced (Cai *et al.* 2004). Transcription results in a primary miRNA transcript (pri-miRNA) that harbors a hairpin structure (Lee et al. 2002, Kim 2005). Within

the nucleus, the RNAse II–type molecule Drosha and its cofactor DGCR8 process the pri-miRNAs into 70- to 100-nt-long pre-miRNA structures (Lee *et al.* 2003, Han *et al.* 2004), which in turn are exported to the cytoplasm through the nuclear pores by Exportin-5 (Yi *et al.* 2003, Bohnsack *et al.* 2004, Lund *et al.* 2004, Zeng *et al.* 2004). Subsequently, the RNAse III-type protein Dicer generates a double stranded short RNA in the cytoplasm that consists of the leading – strand miRNA and its complementary sequence (Grishok *et al.* 2001, Hutvágner *et al.* 2001, Ketting *et al.* 2001, Chendrimada *et al.* 2005). This duplex miRNA is unwound by a helicase into a single stranded short RNA in the cytoplasm and the leading strand is incorporated into the argonaute protein (Ago 2)-containing ribonucleoprotein complex known as the miRNA-induced silencing complex, mRISC (Hammond *et al.* 2000, Hutvagner *et al.* 2008, Bossé *et al.* 2010). During this process, one strand of the miRNA duplex is selected as the guide miRNA and remains stably associated with mRISC, while the other strand, known as the passenger strand is rapidly removed and degraded (Martinez *et al.* 2002) (Figure 1.5). Selection of the appropriate strand is primarily determined by the strength of base pairing at the ends of the miRNA duplex. The strand with less-stable base pairing at its 5' end is usually destined to become the mature miRNA (Khvorova *et al.* 2003, Schwarz *et al.* 2003, Hutvagner 2005). However, some miRNA passenger strands are thought themselves to negatively regulate gene expression. One hypothesis is that both strands could be used differently in response to extracellular or intracellular cues, to regulate a more diverse set of protein –coding genes as needed, or strand selection could be tissue specific (Ro *et al.* 2007). The mature miRNA guides the RISC complex to the 3'UTR of its target miRNA (Lai 2002, Bartel 2009) . The seed sequence, comprising nucleotides 2-8 at 5'-end of the mature miRNA, is important for binding of the miRNA to its target site in the mRNA (Lewis et al. 2005). Association of miRNA with its target results in mRNA cleavage (if sequence complementarity is high) or more usually in higher eukaryotes, blockade of translation (Zeng and Cullen 2004) (see below).

In an alternative pathway for miRNA biogenesis, short hairpin introns termed mirtrons are spliced and debranched to generate pre-miRNA hairpin mimics (Berezikov *et al.* 2007, Okamura *et al.* 2007, Ruby *et al.* 2007, Westholm *et al.* 2011, Sibley *et al.* 2012). These are then cleaved by Dicer in the cytoplasm and incorporated into typical miRNA silencing

complexes (Berezikov et al. 2007, Okamura et al. 2007, Ruby et al. 2007, Westholm and Lai 2011, Sibley et al. 2012). The presence of mirtrons may be an evolutionary strategy to diversify miRNA-based gene silencing (Lau *et al.* 2009).

1.3.1.3. Mechanisms of action of miRNAs

Mammalian miRNAs often have several isoforms encoded from one or more chromosome, suggesting that they are functionally redundant (Heimberg *et al.* 2008, Kim *et al.* 2009). They may exert variable roles *in vivo* via differences in their expression pattern and 3'-end binding (Ventura *et al.* 2008).

Regulation is mainly exerted by the binding of the miRNA to the 3'UTR of the target mRNA, but binding to other positions on the target mRNA, e.g. in 5'UTR or coding sequence has also been reported (Lytle *et al.* 2007, Lee *et al.* 2009, Li *et al.* 2009). Interestingly, miRNA binding sites within the coding region of a transcript are reported as less effective at mediating translational repression. Aside from the location of miRNA binding sites, factors including the sequence context of the miRNA binding site, the number of target sites within the mRNA, the focal RNA structure, the distance between target sites, all contribute to the efficacy of repression mediated by miRNAs (Brennecke *et al.* 2005, Sætrom *et al.* 2007).

The degree of base pairing between the miRNA and its target in the mRISC complex determines the fate of the transcript. If there is perfect binding between the miRNA and target, the mRNA target is cleaved by Ago2 at the annealing site, with subsequent degradation of the mRNA. In contrast, in cases where the miRNA is only partially complementary to its corresponding 3'UTR, inhibition of target mRNA translation occurs via Ago1. Repression may be exerted either at the initiation step of mRNA translation in which Ago competes with eIF4E or at some stage subsequent to initiation (Kiriakidou *et al.* 2007) (Figure 1.6). This is because miRNA-mRISC complex can bind to actively translating mRNAs, reducing translational elongation and/ or enhancing termination, concomitant with a reduction in ribosome initiation and nascent peptide destablilization (Petersen *et al.* 2006).

Interestingly, besides generally promoting mRNA cleavage or translational repression, miRNA binding to 3'UTR can also induce translation of some target mRNAs. MicroRNAs have been identified which activate translation on cell cycle arrest by directing AGO-containing protein complexes to AU-rich elements in the 3'UTR (Vasudevan *et al.* 2007, Vasudevan *et al.* 2007)

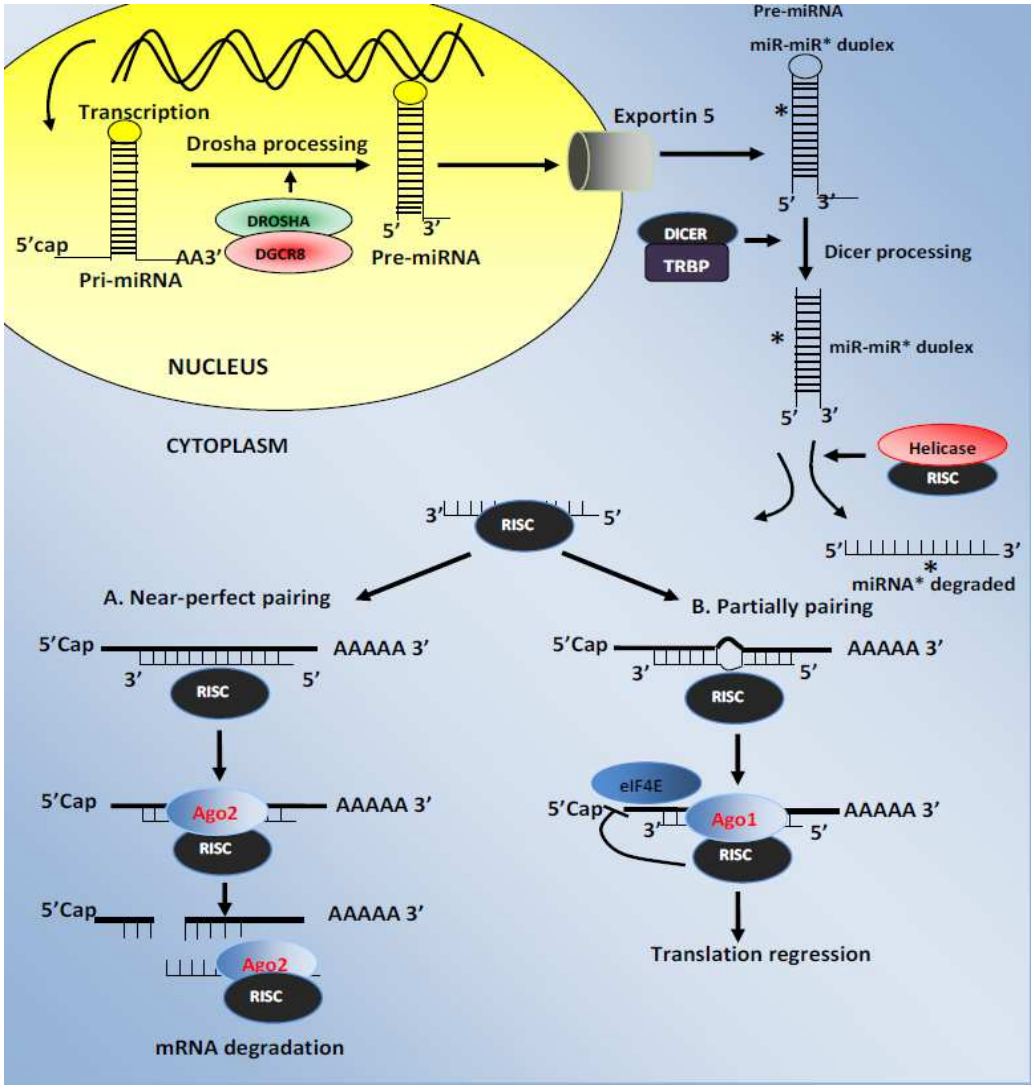

Figure 1.6: Biogenesis of miRNAs.

MicroRNAs are transcribed as RNA precursor molecules (pri-miRNA), which are processed by Drosha and its cofactor DGCR8 into short hairpin structure (pre-miRNA). These are exported into the cytoplasm by Exportin 5, where they are further processed by Dicer and TRBP (Dicer-TAR RNA binding protein) into a miRNA duplex. The duplex is unwound by a helicase and the "guide" strand is incorporated into the RNA–induced silencing complex (RISC) whilst the "passenger" strand undergoes degradation. This miRNA-RISC complex acts by two possible mechanisms: (A) Degradation of target mRNA occurs when miRNA is near-perfectly complementary with 3' untranslated region of target mRNA; (B) Translation inhibition occurs when miRNA is only partially complementary to its target mRNA.

1.3.2. MicroRNAs in skeletal development

It is evident that miRNAs are essential for skeletal development, however, our current knowledge of expression and function of specific miRNAs is still limited. Experimentally removing the majority of miRNAs by a block in miRNA biogenesis through mutating or deleting Dicer, reveals that the miRNA pathway plays a prominent role in skeletal development. An excellent example is the conditional knockout of Dicer in limb mesenchyme at the early stages of embryonic development, which leads to the formation of a much smaller limb. Dicer-null growth plates display a pronounced lack of chondrocyte proliferation in conjunction with enhanced differentiation to postmiototic hypertrophic chondrocytes; this latter may be explained by Dicer having distinct functional effects at different stages of chondrocyte development (Harfe *et al.* 2005). Recently, Kobayashi et al. reported that mice null for Dicer in chondrocytes resulted in skeletal growth defects and premature death (Kobayashi *et al.* 2008), again pointing to essential role of miRNAs in skeletal development.

Further evidence of the important role of miRNAs in skeletogenesis is that some miRNAs were found to exhibit bone-specific and cartilage-specific expression in late development. Wienholds et al. first provided evidence for miR-140 specifically expressed in cartilage of the jaw, head, and fins in zebrafish cartilage during embryonic development (Wienholds *et al.* 2003). Later, Tuddenham et al found that miR-140 is specifically expressed in cartilage tissues during mouse embryonic development (Tuddenham *et al.* 2006). Importantly, Miyaki et al and then Nakamura et al reported that universal knockout of miR-140 lead to mild dwarfism, probably as a result of impaired chondrocyte proliferation (Miyaki *et al.* 2010, Nakamura *et al.* 2011). Recently, Swingler et al found that miR-455-3p was expressed in developing long bones during chick development, restricted to cartilage and perichondrium, and in mouse embryos, where expression was selective in long bones and joints (Swingler *et al.* 2011).

These studies emphasize the importance of the miRNA pathway in skeletal development and revealed that some miRNAs are expressed with precise tissue and developmental stage specificity. Intensive research will uncover a complete spectrum of skeletally associated miRNAs as well as elucidate their biological function.

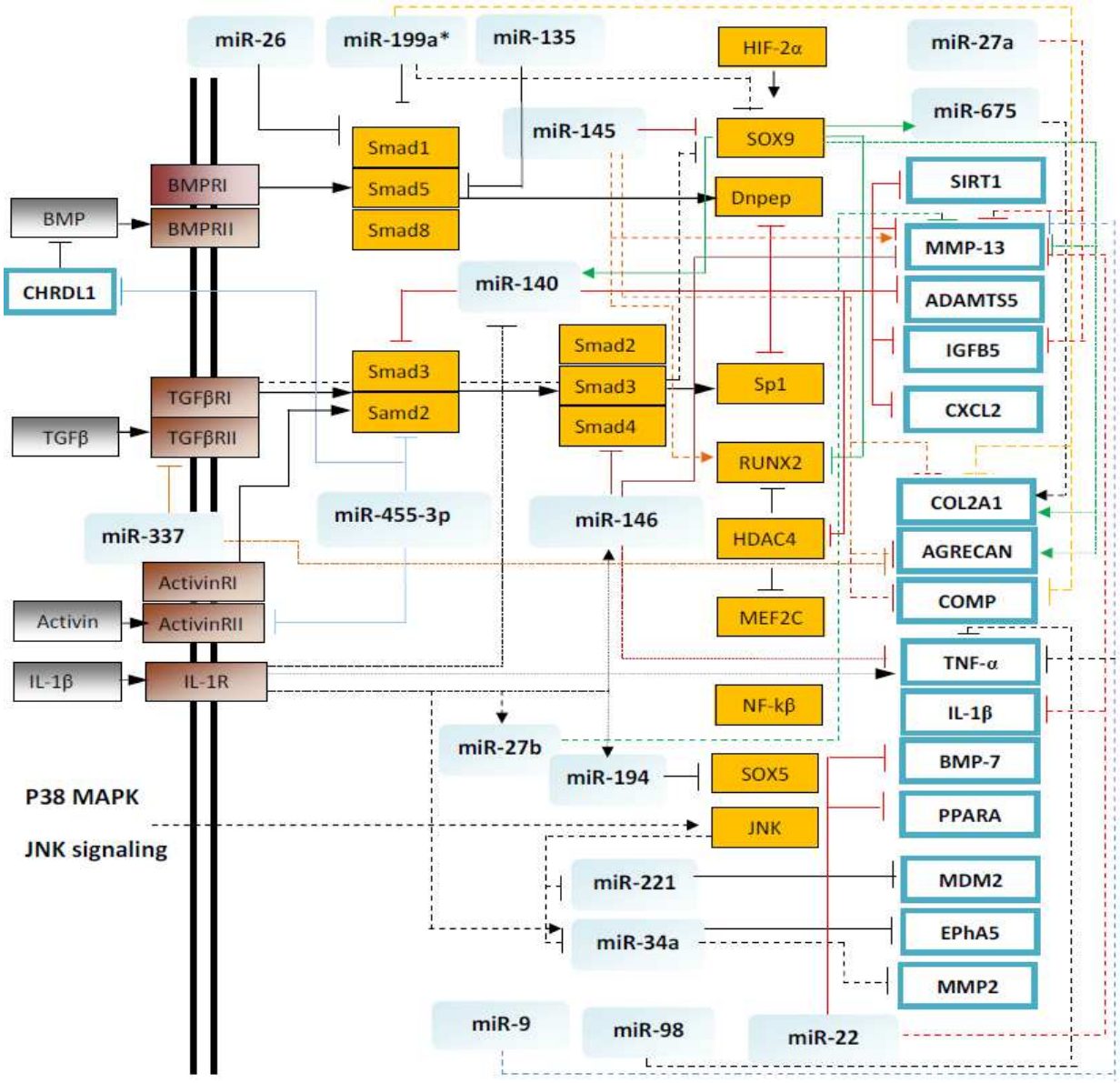

Figure 1.7: An overview of miRNAs involved in chondrogenesis, osteoarthritis and their direct and indirect targets

1.3.3. MicroRNAs in mechanotransduction

Articular cartilage has the unique capacity to resist significant mechanical loading during the lifetime of the organism (Guilak *et al.* 2001). The surface, middle and deep zones within articular cartilage are distinct domains, and they exhibit differential gene expression and attendant functional roles (Neu *et al.* 2007).

Mechano-responsive miRNAs are being identified in chondrocytes, the sole cell type of articular cartilage and evidence that specific miRNAs may impact on stress-related articular cartilage mechanotransduction has also been reported. MicroRNA-365 was the first identified mechanically responsive miRNA in chondrocytes, regulating chondrocyte differentiation through inhibiting HDAC4 (Guan *et al.* 2011). MicroRNA-221, miR-222 were postulated as potential regulators of the articular cartilage mechanotransduction pathway, since their expression patterns in bovine articular cartilage are higher in the weight-bearing anterior medial condyle as compared with the posterior non-weight-bearing medial condyle (Dunn *et al.* 2009). Recently, Li et al. reported that miR-146a was induced by joint instability resulting from medial collateral ligament transection and medial meniscal tear in the knee joints of an OA mouse model, suggesting that miR-146a might be a regulatory factor of the mechanical transduction process in articular cartilage (Li *et al.* 2012). All of these studies are useful for enriching the data on the regulatory mechanism for miRNAs in chondrocyte homeostasis.

1.3.4. MicroRNAs in chondrogenesis

Differential disruption of the Dicer gene in mice resulting in highly abnormal cartilage development suggests miRNAs play a significant role in chondrogenic differentiation. Furthermore, many studies profiled the expression of miRNAs to investigate their function in differentiating MSCs and showed that once they differentiate into chondrocytes, miRNA expression significantly altered (Sorrentino *et al.* 2008, Suomi et al. 2008, Lin *et al.* 2009, Miyaki *et al.* 2009, Karlsen *et al.* 2011, Lin *et al.* 2011, Yan *et al.* 2011, Yang *et al.* 2011) (Table1.2). However, there is no consensus expression signature of any miRNAs amongst these and we attribute this to the design of experiment including inducers of differentiation, cell types, numbers of detected miRNA probes and organism (Table1.2).

Table 1.2: Studies performing miRNA profile comparing between MSC and chondrocytes

	Sorrentino et al 2007	**Suomi et al 2008**	**Lin et al 2009**	**Miyaki et al 2009**	**Yang et al, 2010**	**Lin et al 2011**	**Yang et al 2011**	**Karlsen et al 2011**
Stimulators	-	TGF-β3	BMP-2	BMP-2 TGF-β3	TGF-β3	-	-	-
Cells	BM MSC	BM MSC	C12C2	BM MSC	BM MSC	DAC	BM MSC AC	DAC
Organisms	Human	Mice	-	Human	Mice	Human	Mice	Human
Probes	226	35	-	-	7,815	-	-	875
Cutoff(fold)	1.3	-	1.5	1.5	5	4	-	-
Platform	microarray	qPCR	microarray	microarray	microarray	microarray	microarray	microarray
miRNAs up-regulated	31 32 136 146 149 185 Pre-mir 192 199a-2-5 204 212 Pre-mir-212 Pre-miR-214	24 101 124a 199b 199a	199* 221 298 374 let-7e	15b 16 23b 27b 140 148 197 222 328 505	30a 81a-1 99a 125* 127 140 140* Let-7f	26a 140* 140 222 320a 320d 491* 547-5p 720 1308 let-7d let-7f let-7a	21 22 27b 27a 140 140* 152 291b* 330 431 433 455 let-7b let-7d let-7l	30d 140* 210 451 563
miRNAs down -regulated	10a 10b 21 23a 24-1-3p 24-2 26b 29b 30a-5p 34 100 103-2 107 130a 138-1 Pre-miR-143 145 181a-1 191-5p let-7a-1 let-7a-2 let-7a-3 let-7c let-7d	18 96	21 125a 125b 143 145 210		125b* 132 143 145 212	18a 27a 146a 193b 220b 342-5p 335 365 519e 548e 1248 1284	1 23a 23b 24 26b 99a 99b 99b* 125a-5p 143 144 145 146a 181a 181d 191 199a 199a* 210 320 355-5p 431 503 652 Let-7a Let-7c Let-7g Let-7f	15b 31 132 138 143 145 221 222 379 382 432 494 654* 1308 let-7e

AC: Articular chondrocytes; BM MSC: Bone marrow mesenchymal cells; DAC: dedifferentiated articular chondrocytes.

The regulation of chondrogenesis of murine MSCs in response to stimulation of TGF-β3 was investigated (Suomi et al. 2008, Yang et al. 2011) (Table1.2). Suomi et al compared the expression of 35 miRNAs in chondroblasts derived from MSCs, and found that miR-199a, miR-124a were strongly up-regulated while miR-96 was substantially suppressed (Suomi et al. 2008). They demonstrated how miRNAs and transcription factors could be capable of fine-tuning cellular differentiation by showing that miR-199a, miR-124a, miR-96 could target HIF-α, RFX1, Sox5, respectively (Suomi et al. 2008). Similarly, Yang et al , revealed eight significantly up-regulated and five down-regulated miRNAs (Yang et al. 2011) in this process. The miRNA clusters, miR-143/145 and miR-132/212 were down-regulated, with miR-132 the most down-regulated whilst miR-140* was the most up-regulated (Yang et al. 2011). Similar expression patterns of miR-145, miR-143 were also described in other studies (Lin et al. 2009, Karlsen et al. 2011, Lin et al. 2011, Yan et al. 2011). Corresponding targets of these differentially expressed miRNAs were predicted including: ADAMTS5 (miR-140*), ACVR1B (miR143/145), SMAD family members: SMAD1 (miR-30a), SMAD2 (miR-132/212), SMAD3 and SMAD5 (miR-145), Sox family members: Sox9 (miR-145); Sox6 (miR-143, miR-132/212), Runx2 (miR-30a and miR-140*) (Yang et al. 2011).

Further study has confirmed miR-145 as a key mediator which antagonizes early chondrogenic differentiation in mice via attenuating Sox9 at post-transcriptional level. (Yang *et al.* 2011). Interestingly, cells over-expressing miR-145 significantly decreased the expression of chondrogenic markers at the mRNA level including Col2a1, Agc1, COMP, Col9a2 and Col11a1. Consistent with this,, Martinez-Sanchez et al. reported miR-145 as a direct regulator of Sox9 in normal human articular chondrocytes though binding to a specific site in its 3'UTR, which is not conserved in mice (Martinez-Sanchez *et al.* 2012). Similarly, over-expression of miR-145 in articular cartilage chondrocytes reduced the levels of Sox9, the cartilage matrix components Col2a1 and Agc1 in combination with a significant increase of the hypertrophic markers Runx2 and MMP-13 (Martinez-Sanchez et al. 2012) (Figure 1.7).

This group also reported that miR-675, processed from H19, a non-coding RNA, was tightly regulated by Sox9 during chondrocyte differentiation. MicroRNA-675 could up-regulate expression of Col2a1, albeit indirectly, indicating its potential importance in

maintaining cartilage integrity and homeostasis. Forced over-expression of miR-675 rescued Col2a1 mRNA levels in either Sox9- or H19-depleted primary human articular chondrocytes (Dudek *et al.* 2010). Although its target mRNAs remain unknown, these data suggest that miR-675 may modulate cartilage homeostasis by suppressing a Col2a1 transcriptional repressor (Dudek et al. 2010) (Figure 1.7). Moreover, by performing miRNA expression profile during human primary chondrocyte dedifferentiation, Martinez-Sanchez found that 29 miRNAs were up-regulated more than two-fold and 18 miRNAs were down-regulated. Among these up-regulated miRNAs, miR-1247, transcribed from the DLK1-DIO3 locus, was of particular interest as its expression pattern still increased under hypoxia condition, together with miR-140. Also, miR-1247 level was found to correlate with cartilage-associated miR-675 across a range of 15 different mouse tissues (Martinez-Sanchez *et al.* 2013). Interestingly, SOX9, directly target of miR-1247 via coding sequence, inhibit this miRNA expression, suggesting a negative feedback loop between miR-1247 and its target SOX9 (Martinez-Sanchez and Murphy 2013).

Another study performed miRNA profiling to find expression signatures of nearly 380 miRNAs in C2C12 cells induced by BMP-2 for 24 hours and found that 5 miRNAs including miR-199a* and miR-221 were positively regulated while miR-125a, miR-210, miR-125b, miR-21, miR-145, miR-143 were repressed (Lin et al. 2009). Interestingly, using C3H10T1/2 cells, a well-established *in vitro* cell model of chondrogenesis, showed that miR-199a* expression was reduced significantly within several hours following BMP-2 treatment and then rose dramatically at 24 hours and remained higher thereafter, indicating that miR-199a* may function as a suppressor of the early steps of chondrogenic differentiation (Lin et al. 2009). Indeed, enforced miR-199a* expression in C3H10T1/2 cells or in the prechondrogenic cell line ATDC5, suppresses multiple markers of early chondrogenesis, including Col2a1 and COMP, whereas the antagomir blocking miR-199a* function has the opposite stimulatory effect (Lin et al. 2009). Consistent with these observations, Smad1, a positive downstream mediator of BMP-2 signalling, was shown to be a direct miR-199a* target. Moreover, miR-199a*, through its inhibition of the Smad pathway, is able to inhibit the expression of downstream genes such as p204 (Lin et al. 2009) (Figure 1.7).

The change in expression pattern of miRNAs across the dedifferentiation of chondrocytes also, adds to our understanding of the biology of *in vitro* human chondrogenesis (Karlsen

et al. 2011, Lin et al. 2011). MicroRNA-451, miR-140-3p, miR-210, miR-30d, and miR-563 were reported to be highly expressed on human primary articular chondrocytes at early passage compared with their dedifferentiated counterparts, suggesting their role as inhibitors of differentiation *in vitro* (Lin et al. 2011). Of these miRNAs, miR-140-3p had the highest expression. Conversely, 16 miRNAs were significantly up-regulated in dedifferentiated articular chondrocytes, reflecting their potential as modulators of the chondrogenenic process. Notably, miR-143, miR-145 also had similar expression patterns as previously reported (Lin et al. 2011). A second study also reported a group of 5 miRNAs: miR-451, miR140-3p, miR-210, miR-30d, and miR-563 upregulated on differentiation which may inhibit molecules participating in the dedifferentiation process whilst a further 16 miRNAs were downregulated and may potentially act conversely.

Recently, performing miRNA profiling across ATDC5 cell induced differentiation within 42 days to identify miRNAs with functions in cartilage development, we identified 7 cluster groups of miRNAs which may function cooperatively (Swingler et al. 2011). Among these, 39 miRNAs were found potentially co-regulated with miR-140 with expression increase during chondrogenic process (Swingler et al. 2011). Especially interesting is miR-455, located in an intron of the protein coding gene Col27a1, a cartilage-expressed collagen, which showed similar expression kinetics to collagen XXVII and to miR-140. Consistent with role for miR-140 in modulating TGFβ signalling, miR-455-3p was also found to directly target Smad2, ACVR2B and CHRDL1, again potentially attenuating the TGFβ pathway (Swingler et al. 2011) (Figure 1.7).

MicroRNA-140 shows a generally consistent expression pattern between studies. Indeed, cartilage miRNA research to date has focused heavily on miR-140 and has successfully shown the key roles of miR-140 in chondrocyte proliferation and differentiation. Miyaki et al compared gene expression profiling using miRNA microarrays and quantitative polymerase chain reaction in human articular chondrocytes and human mesenchymal stem cells. They demonstrated that miR-140 had the largest difference in expression between chondrocytes and MSCs (Miyaki et al. 2009), and this is in agreement with latter publications in human, rat and mice (Karlsen et al. 2011, Lin et al. 2011, Yan et al. 2011, Yang et al. 2011). MicroRNA-140 was first shown to target Hdac4, a known co-repressor of Runx2 and MEF2C transcription factors essential for chondrocyte hypertrophy and bone

development (Tuddenham et al. 2006). miR-140 also targets Cxcl12 (Nicolas *et al.* 2008) and Smad3 (Pais *et al.* 2010), both of which are implicated in chondrocyte differentiation. Interestingly, miR-140 is reported to suppress Dnpep, an aspartyl aminopeptidase, which has been suggested to antagonize BMP signalling downstream of Smad activation (Nakamura et al. 2011). Moreover, Sox9 a major transcription factor in maintaining cellular phenotype and preventing hypertrophy, particularly with L-Sox5 and Sox6, (Yamashita *et al.* 2012), is shown to control the expression of miR-140 (Yang *et al.* 2011, Nakamura *et al.* 2012).

The miR-194 is a key mediator during chondrogenic differentiation via suppression of the transcription factor Sox5 (Xu *et al.* 2012). The expression of miR-194 was significantly decreased in chondrogenic differentiation of adipose-derived stem cells (ASCs). Importantly, chondrogenic differentiation of ASCs could be achieved through controlling miR-194 expression (Xu et al. 2012) (Figure 1.7).

Using three rat models e.g. bone matrix gelatin-induced endochondral ossification, collagen-induced arthritis and pristane-induced arthritis, Zhong et al. further demonstrated that miR-337 was directly implicated with chondrogenesis. miR-337 acted as a repressor for TGFBR2 expression at the protein level (Zhong *et al.* 2012). Moreover, aggrecan was differentially expressed in both gain- or loss-of function of miR-337 experiments, providing evidence that miR-337 could influence cartilage specific gene expression in chondrocytes (Zhong et al. 2012) (Figure 1.7).

Kim et al. used chick as a model of chondrogenesis and focused on initiation, namely precartilage condensation, proliferation and migration. They reported that miR-221 and miR-34a, induced by c-Jun N-terminal kinase (JNK) signaling, played pivotal roles (Kim *et al.* 2010, Kim *et al.* 2011). Treatment of chick wing bud MSCs with a JNK inhibitor lead to the suppression of cell migration and stimulation of apoptosis with concurrent significant increase in expression of miR-221 and miR-34a (Kim et al. 2010, Kim et al. 2011). Notably, miR-221 may be involved in apoptosis, since treatment of MSCs with a miR-221 inhibitor increased cell proliferation and this could be rescued by the JNK inhibitor (Kim et al. 2010). MicroRNA-221 is reported to directly target Mdm2, which encodes for an oncoprotein with E3 ubiquitin ligase activity (Kim et al. 2010). Inhibition of Mdm2 expression via miR-221 suppresses ubiquitination leading to accumulation of

Slug protein, whose expression is associated with an increase in apoptosis (Kim et al. 2010). Conversely, miR-34a affects MSC migration, not proliferation (Kim et al. 2011). EphA5, a receptor in Eph/Ephrin signaling which mediates cell-to-cell interaction, has been proven to be a miR-34a target (Kim et al. 2011). Moreover, via regulating RhoA/Rac1 cross-talk, miR-34a negatively modulated reorganization of the actin cytoskeleton (Kim *et al.* 2012), one of the essential processes for establishing chondrocyte-specific morphology. MicroRNA-488 expression is up-regulated at the pre-condensation stage and then down-regulated at the post-condensation stage in chick limb chondrogenesis, suggested a key role in this process (Song *et al.* 2011). Interestingly, mir-488 could regulate cell–to-ECM interaction via modulation of focal adhesion activity by indirectly targeting MMP-2 (Song et al. 2011). More recently, this group reported that miR-142-3p was an important modulator in position-dependent chondrogenesis and was reported to regulate ADAM9 (Kim *et al.* 2011) (Figure 1.7).

1.3.5. MicroRNAs in osteoarthritis

The effects of miRNA deregulation on OA are evident through studies comparing the expression of miRNAs between OA tissues and their normal articular counterparts (Iliopoulos *et al.* 2008, Jones *et al.* 2009). Illopoulos et al. tested the expression of 365 miRNAs and identified a signature of 16 miRNAs, with 9 miRNAs significantly upregulated and 7 miRNAs downregulated in OA cartilage compared with normal controls. Some of these were postulated to be involved in obesity and inflammation (Iliopoulos et al. 2008). Interestingly, functional experiments implicated miR-9 in the regulation of MMP13 expression, as well as miR-9, miR-98 and miR-146 in the control of TNF-α expression, suggesting that these miRNAs may play a protective role in OA. Moreover, miR-22, whose expression correlated with body mass index, directly targets PPARA and BMP-7 at the mRNA and protein levels, respectively. Enforced miR-22 overexpression or siRNA-mediated suppression of either PPARA or BMP-7 resulted in increases in IL-1β and MMP-13 protein levels, again suggesting that miRNA deregulation can have effects on OA (Iliopoulos et al. 2008) (Figure 1.7).

Additionally, Jones et al. investigated the expression of 157 human miRNAs and identified 17 miRNAs whose expression varied by 4-fold or more when comparing normal versus

late-stage OA cartilage (Jones et al. 2009). Consistent with the Illopoulos data, the altered expression of miR-9, miR-98 and miR-146 in OA cartilage are highlighted. The over-expression of these miRNAs also reduced IL-1β-induced TNF-α production, whilst inhibition or over-expression of miR-9 modulated MMP-13 secretion (Jones et al. 2009) (Figure 1.7).

The miR-140 gene, located in an intron of the E3 ubiquitin protein ligase gene Wwp2 on murine chromosome 8 and the small arm of chromosome 16 in humans, is evolutionarily conserved among vertebrates. MicroRNA-140 expression in the cartilage of patients with OA was significantly lower than in normal cartilage (Miyaki et al. 2009, Tardif *et al.* 2009) and decreased miR-140 expression was reported also in OA chondrocytes (Tardif et al. 2009).

Deletion of miR-140 in mice predisposes to the development of age-related OA-like changes (Miyaki et al. 2010, Nakamura et al. 2011) and gives a significant increase in cartilage destruction in surgically induced OA. Conversely, in an antigen-induced arthritis model, transgenic over-expression of miR-140 in chondrocytes protects against cartilage damage (Miyaki *et al.* 2010). The ADAMTS5 gene has been shown to be a direct target of miR-140, whilst reciprocal regulation of ADAMTS5 in the in vivo models above suggests that suppression of OA may involve regulation of ADAMTS5 (Miyaki et al. 2010). Swingler et al. show that miR-140 is increased in expression in hip OA cartilage compared to fracture controls (Swingler et al. 2011), but ADAMTS5 expression is decreased in the former samples. As above, Nakamura et al. identified the aspartyl aminopeptidase Dnpep as a key target for miR-140 essential for skeletal defects in miR-140 null mice (Nakamura *et al.* 2011). Using functional interference, Tardif et al. confirmed IGFBP-5, whose expression in human chondrocytes was significantly higher in OA, as a direct target of miR-140 (Tardif et al. 2009). More recently, miR-140 was shown to directly mediate MMP13 expression *in vitro* by luciferase reporter assay (Liang *et al.* 2012) (Figure 1.7).

The human genome contains two miR-27 genes [mir-27a and miR-27b] on chromosomes 19 and 9, respectively, and their major products differ by only 1 nucleotide in the 3' region. MicroRNA-27a expression was shown to be decreased in OA compared to normal chondrocytes (Tardif et al. 2009). Down-regulation of miR-27a was proposed to be connected with adipose tissue dysregulation in obesity, a strong risk factor for OA. Tardif

et al. suggested that miR-27a may indirectly regulate the levels of both MMP-13 and IGFBP-5 by targeting upstream positive effectors of both genes (Tardif et al. 2009). Conversely, expression miR-27b was found to be significantly lower in OA cartilage samples compared with normal counterparts where it inversely correlated with MMP13, a direct target (Akhtar *et al.* 2010). This points to the possibility of novel avenues for OA therapeutic strategies (Figure 1.7).

MicroRNA-146a was strongly expressed in chondrocytes residing in the superficial layer of cartilage and in low-grade OA cartilage (Yamasaki *et al.* 2009, Li et al. 2012). Its expression level gradually decreased with progressive tissue degeneration. Interestingly, when miR-146 was highly expressed, the expression of MMP13 is low, suggesting that miR-146a has target genes that play a role in OA cartilage pathogenesis (Yamasaki et al. 2009). MicroRNA-146a has recently been implicated in the control of knee joint homeostasis and OA-associated algesia by balancing the inflammatory response in cartilage and synovium with pain-related factors in glial cells (Li *et al.* 2011). As such, it may be useful for the treatment of both cartilage regeneration and the pain symptoms caused by OA (Figure 1.7).

Park et al reported the miR-127-5p, an important mediator in OA whose expression was significant decreased in OA articular cartilage compared to the control counterpart, directly target MMP13. Noteworthy, pre-treatment with MAPK inhibitors and NFκβ inhibitor attenuated the inhibitory effects of IL-1 on miR-127-5p expression while overexpression of miR-127-5p significantly inhibited the phosphorylation of JNK, p38 and Iκβα in the human chondrocytes. These data suggest a reciprocal regulatory loop between NFκβ, MAP kinase, and IL-1β in controlling MMP13 expression (Park *et al.* 2013).

1.3.6. MicroRNAs in inflammation

Some miRNAs could be of importance in the inflammatory events of osteoarthritis. MicroRNA-140 was suppressed by IL-1β signaling, and transfection of human chondrocytes with miR-140 downregulated IL-1β driven induction of ADAMTS5 (Miyaki et al. 2009). However, contrary to this, Liang et al. reported that expression of miR-140

and MMP-13 was elevated in IL-1β-stimulated C28/I2 and expression of miR-140 was shown to be NF-κB-dependent (Liang *et al.* 2012) (Figure 1.7).

Expression of miR-34a was significantly induced by IL-1β while antagonism of miR-34a prevented IL-1β-induced chondrocyte apoptosis (Abouheif *et al.* 2010), as well as IL-1β-induced down regulation of type II collagen in rat chondrocytes (Abouheif et al. 2010). Other relevant miRNAs reported to be induced by IL-1β are miR-146a (Yamasaki et al. 2009, Li et al. 2012), miR-34a (Abouheif et al. 2010), miR-194 (Xu et al. 2012), miR-27b (Akhtar et al. 2010) (Figure 1.7).

1.3.7. Utility of microRNAs for diagnosis

It is evident that miRNAs in serum may become a powerful tool in the development of diagnostic biomarkers. MicroRNAs are relatively stable with enzymatic, freezing, thawing or extreme pH conditions (Mitchell *et al.* 2008, Link *et al.* 2010) due to lipid or lipoprotein complexes (Esau *et al.* 2006). Moreover, extracellular miRNAs are detectable in almost all body fluids and excretions including urine, faeces, saliva, tears, ascetic, pleural and amniotic fluid (Chen *et al.* 2008, Gilad *et al.* 2008). Interestingly, miRNAs in plasma have the capacity to interact with intact cells with some degree of specificity, and modify recipient cell gene expression and protein production via a miRNA-related mechanism (Arroyo *et al.* 2011). This opens up the possibility of genetic exchange between cells and the exogenous regulation of gene expression. MicroRNA-21 was the first serum miRNA biomarker to be discovered: patients with diffuse large B cell lymphoma had high serum levels of miR-21, which was associated with increased relapse-free survival (Lawrie *et al.* 2008). Subsequently, the usefulness of serum miRNAs for diagnosis and prognosis has been reported for solid cancers and leukemia (Ferracin *et al.* 2010, Kosaka *et al.* 2010, Wittmann *et al.* 2010). For OA, Murata et al. examined the potential of miRNA as diagnostic biomarkers and found a number of miRNA in plasma some of which were found at different levels between RA and OA patients (Murata *et al.* 2010). Recently, let-7e, miR-454, miR-886 were identified differentially expressed crilculating miRNAs in OA patient necessitating arthroplasty in a large, population – based cohort. Especially, let – 7e emerged as potential predictor for severe knee or hip OA (Beyer *et al.* 2014).

Besides the measurement of miRNAs in plasma, PBMCs could also be useful in developing a biomarker for OA. Circulating PBMCs such as macrophages and T cells accumulate in the synovium of OA patients, producing proinflammatory cytokines and proteinases associated with synovitis, linked to the early stages of OA progression. It has been demonstrated that the high expression of miR-146a, miR-155, miR-181a and miR-223 in PBMCs from OA patients versus normal controls may be related to the pathogenesis of OA (Okuhara *et al.* 2011). Interestingly, miR-146 and miR-223 are highly expressed in early-stage OA (Yamasaki et al. 2009), with expression gradually decreasing with OA progression with the promise for diagnosis of early OA is specificity can be demonstrated.

Taken together, there is growing evidence for future miRNA-based diagnostics. However, there is a requirement for detailed investigations directed at diagnostic performance (sensitivity, specificity, accuracy) of these promising novel biomarkers before the measurement of miRNAs can enter the clinic.

1.3.8. Utility of microRNAs in therapeutic treatment

Currently there is no disease-modifying therapeutics available for patients suffering from OA. Therapeutic options are limited to oral and intra-articularly injected analgesic medications, and joint replacement surgery (Wieland *et al.* 2005). OA patients often present with cartilage that already exhibits a damaged matrix, and in which repair/regeneration is. Although cartilage seems a relatively simple tissue type to engineer because of its single cell type and its lack of a blood, nerve or lymph system, regenerating cartilage in a form that can function effectively after implantation has proven difficult. Several approaches are currently being investigated to utilize a miRNA-based therapy to overcome these problems, and these may represent a novel therapeutic application for pharmacological control. Currently there are over 70 clinical trials worldwide based on miRNA manipulation to treat a range of conditions including various cancers and cardiovascular disease; however, none of these to date are for arthritis.

The targeting of miRNAs represents a novel therapeutic opportunity for OA treatment in which miRNA deficiencies could be corrected by either antagonizing (antagomirs) or

restoring (mimics) miRNA function. Poorly expressed miRNAs could be restored by over expression using stable vector transfection or transfection by double-stranded miRNA, whilst over-expressed miRNAs could be antagonized by modified DNA oligonucleotides. Particularly, it has been proven that the systematic administration of antagonist miRNAs modified with locked nucleic acids (LNA) could function without toxicity in non-human primates (Elmen *et al.* 2008). Evidence on efficacy was also demonstrated in mouse models using miR-122 antisense oligonucleotides, which resulted in a decrease in hepatic fatty acid and cholesterol synthesis (Esau et al. 2006). In man, when miR-143/miR-145 activity was restored in pancreatic cancer cells (in which their levels were repressed), the cell was no longer tumourigenic (Kent *et al.* 2010). Although this type of therapy has not been applied in OA, there is very promising evidence for therapeutic potential, e.g. the silencing of miR-34a by LNA-modified antisense oligonucleotides could effectively reduce rat chondrocyte apoptosis induced by IL-1β (Kongcharoensombat *et al.* 2010). This study revealed that silencing of miR-34a might be a novel intervention for OA treatment if this could be appropriately targeted.

Another approach is to combine miRNA technology with stem cell engineering. *In vivo* MSCs participate in chondrogenesis. MSCs can be conveniently obtained with less injury than primary cells and manipulated *in vitro* and hence they are promising cells in cartilage regeneration. At present, autologous MSCs have been transplanted in human injured or osteoarthritis knees for repair of articular cartilage defects. However, unexpected results from the ectopic transplantation of MSCs also have been reported, such as hypertrophy, mineralization, and vascularisation. Deciphering the role of miRNA regulation in the chondrogenesis of MSCs may open a new era of research and pave the way for the development of new treatments for OA

A growing body of evidence indicates that miRNAs convey a novel and efficient way for the regulation of gene expression, being involved in multiple aspects of cellular processes. Understanding their expression profile and dynamic regulation may be the key to enhancing chondrogenic differentiation, or maintaining phenotype in the treatment of OA. Recent advances in miRNA research have provided new perspectives on the regulation of OA and novel insight into the potential development of therapeutic treatments. Using miRNAs as therapeutic targets may well become a powerful tool in the development of

new therapeutic approaches. However, numerous questions including potential off-target effects and efficient and targeted delivery *in vivo* need to be solved before using miRNAs in therapeutics

SCOPE OF THE THESIS

OA is the most prevalent degenerative joint pathology leading to considerable problems with disability and pain in a huge number of people, especially the elderly population. As the population ages and with increased life expectancy, the burden of osteoarthritis will continue to rise. However, there is currently a lack of biomarkers and sensitive techniques for identifying and assessing patients with early changes. Also, clinical treatment for OA still remains unsatisfactory. Thus, deepening our understanding and gain further insights into the molecular mechanisms in OA would be very important for long term purpose of diagnosis and therapeutic treatment.

Several hundred miRNAs have been identified so far and initial studies have linked specific miRNAs to OA. However, there are no key miRNAs identified so far which functionally impact on early human OA onset and disease progression. Thus, I undertook this project to identify miRNAs mediating initiation and progression of OA and dissect their biological function in order to identify new signalling pathways involved in the pathogenesis of OA. The hypothesis and specific aims of the project were:

Hypothesis: The dysregulated expression of specific microRNAs contributes to the onset or progression of OA.

Specific aim 1: Profile miRNA and mRNA expressions in whole knee joint in DMM model to identify the potential miRNAs involved in the early stage of OA

Specific aim 2: Determine the involvement of the miRNA in human end stage OA cartilage, in murine injury model, in chondrogenesis.

Specific aim 3: Identify factors control the miRNA expression in articular cartilage

Specific aim 4: Identify miRNA direct targets to identify new signaling pathways involved in homeostasis of articular cartilage.

CHAPTER 2
MATERIALS AND METHODS

2.1.Materials

2.1.1. Murine models

2.1.1.1. Destabilization of the medial meniscus murine model (DMM model)

Induction of OA by destabilization of the medial meniscus (DMM) was kindly performed by Professor Tonia Vincent Kennedy Institute for Rheumatology, Oxford University, U.K. Protocols using C57Bl/6 mice were as described previously in (Burleigh *et al.* 2012, Chong *et al.* 2013).

Briefly, C57Bl/6 male mice were housed 3-5 per cage in 63x54x30 cm^3 standard individually vented cages and maintained with a 12h/12h light/dark cycle at an ambient temperature of 21ºC. Mice were fed a certified mouse diet (RM3 from Special Dietary Systems, Essex, UK) and water ad libitum. 10 week old mice were anaesthetized by intra-peritoneal injection of a 1:1:2 mixture of Hypnorm (0.315mg/ml fentanyl citrate and 10mg/ml fluanisone; VetaPharma Ltd, Leeds, UK), Hypnovol (5mg/ml midazolam; Roche), and sterile water for injection, at a dose of 10ml/kg body weight. The ventral portion of the right knee was shaved and swabbed with iodine to prepare a sterile surgical field. The medial meniscus was identified and the attachment of its anterior horn to the tibial plateau was cut. Care was taken to avoid injury to the anterior cruciate ligament and the cartilage surfaces. The mice were fully mobile within 2-4 hours after surgery. After 1, 3, 7 days after surgery, the mice were culled and knees harvested.

2.1.1.2. Murine hip avulsion injury model

The femoral caps of C57Bl/6 mice ages 4 weeks were avulsed using forceps as described in (Chong et al. 2013). After washing three times with sterile phosphate-buffered saline (PBS) (Life Technologies, 10010023), the femoral caps were immediately put in either 500µl Trizol® reagent (Invitrogen, 15569-026) (for time point 0) or in 24-well plate for (other time points e.g. 3, 6, 12, 48 hours). 200µl of Dulbecco's modified Eagle's medium (DMEM) (Life Technologies, 10566-016) containing 100 IU/ml penicillin and 100µg/ml

streptomycin (Sigma, P4333) was added to each well and the plate was incubated at 37ºC in 5% (v/v) CO_2. At the desired time points, the femoral caps were harvested (with Trizol reagent) and total RNA was isolated.

2.1.2. Human end stage OA specimens and normal counterparts

Ethical Committee approval for using discarded human tissue was received prior to the initiation of the studies. Full informed consent was obtained from all donors. Human articular cartilage was obtained from patients undergoing total hip/ knee replacement surgery at the Norfolk and Norwich University Hospital. In total, 8 hip and 7 knee OA cartilage samples were collected. 7 healthy articular cartilages were harvested from total hip replacement following fracture to the neck of femur. None of the healthy individuals had a clinical history of arthritis or other diseases affecting cartilage, no macroscopic lesions to the cartilage were seen.

2.1.3. Cell lines

All cell lines were maintained in DMEM high glucose, GlutaMAX supplement (Life Technologies, 10566-016) containing 10% (v/v) heat-inactivated fetal bovine serum (FCS) (PAA, UK), 100U/ml penicillin, and 100µg/ml streptomycin (Sigma, P4333) at 37ºC in 5% (v/v) CO_2.

2.1.3.1. Chondrosarcoma SW1353

The SW1353 cell line was initiated from a primary grade II chondrosarcoma of the right humerus obtained from a 72 year old female Caucasian. SW1353 cells were purchased from the American Type Culture Collection (ATCC) (no.HTB-94).

2.1.3.2. Chicken dermal fibroblasts DF1

DF-1 is a spontaneously immortalized chicken fibroblast cell line without viral or chemical treatment derived from 10 day old East Lansing Line (ELL-0) embryo. DF1 was a kind gift from Professor Andrea Munsterberg, University of East Anglia, U.K.

2.1.3.3. Dicer knockdown cell lines

DLD-1 Parental and DLD-1 Dicer null_cell lines were a kind gift from Professor Tamas Dalmay, University of East Anglia, U.K. These cell lines were originally purchased from Horizon Discovery (Cambridge, U.K.). Both cell lines were originally isolated from a colorectal adenocarcinoma.

2.2.Methods

2.2.1. Molecular biology- based methods

2.2.2.2. Human genomic DNA isolation

Buffer

Extraction Buffer: 10mM Tris-HCl pH 8 (Fisher Scientific, BP152-500), 5mM NaCl (Fisher Scientific, BP3581), 0.5% (w/v) SDS (Fisher Scientific, 10356463).

DNA extraction protocol

Human chondrosarcoma SW1353 cells were harvested from a 75cm^2 flask by trypsin-EDTA treatment (Life Technologies, 25200072) and pelleted by centrifugation at 17.3xg, 5 minutes.

The cell pellet was mixed well with 100µl nuclease-free water (Sigma, W4502), 400µl extraction buffer, 10µl Proteinase K (20mg/ml) (Sigma, P6556) and incubated at 50^{o}C, 2 hours.

500µl of PCI (phenol: chloroform: isoamyl alcohol 25:24:1) (Sigma, P2069) was added, mixed gently and centrifuged, 10 minutes at 130,000xg.

The top phase was transferred to a new tube, 1 ml of chloroform (Sigma, 288306) was added and after vortex, the mixture was again centrifuged at 130,000xg for 10 minutes.

The upper phase was transferred to a new tube and two volumes of 100% (v/v) ethanol (Sigma, 459844) were added, followed by centrifugation at 130,000xg for 5 minutes.

The DNA pellet was washed with 700µl of 70% (v/v) ethanol, and then centrifuged at 130,000xg for 1 minute. Discard the ethanol.

Finally, the pellet was dried at room temperature and dissolved in 100µl of nuclease-free water (Sigma, W4502).

2.2.2.3. PCR amplification for 3'UTR regions

3'UTR regions of all genes including *ADAMTS6, ADAMTS14, ADAMTS17, ADAMTS19, FZD3, FZD5, DVL3, FRAT2,* and *CK2A2* were downloaded from the Ensembl Genome Browser: http://www.ensembl.org/index.html. Primers were specifically designed to amplify a 1-2 kb region of 3'UTR of these genes including the miR-29 family binding sites. A restriction site of *Sac*I (5'GAGCTC3'), XbaI (5'TCTAGA3') or *Sal*I (5'GTCGAC3') are added to the 5' end of each primer. Primer sequences are listed in Appendix, Table 1.

All 3'UTR regions were amplified from human genomic DNA, isolated from the SW1353 cell line. 100ng genomic DNA was added together with 5µl 10X reaction buffer, 5 units accuTaq^{TM} LA DNA polymerase (Sigma, D8045), 0.5µl dNTP 10µM (Bioline, BIO-39044), 1µl forward primer 10µM (Sigma), 1µl reverse primer 10µM (Sigma) in a 50µl reaction volume. The reaction was run on a Veriti^{R} 96-well thermal cycler (Applied Biosystems, 4375786) at 98^{o}C, 30 seconds to denature DNA and follows by 32 cycles: 10 seconds at 98^{o}C, 20 seconds at annealing temperature (depending on each primer pair), 1-2 minutes at 68^{o}C. Finally, the reaction was left 2 minutes at 68^{o}C for final extension.

The PCR reaction was confirmed by loading 3µl PCR product on 1% (w/v) agarose gels, which were prepared by heating 1% (w/v) agarose (Sigma, A9639) in Tris-acetate-EDTA (TAE) buffer, and run at 120V. After staining in ethidium bromide solution (Sigma, E1510) for 20 minutes, the product was visualized under UV-light.

2.2.2.4. Phenol/chloroform clean up

Nuclease- free water (Sigma, W4502) was added to a PCR reaction to 200µl, followed by 200µl of phenol: chloroform: isoamyl alcohol (Sigma, P2069). The reaction was mixed well and centrifuged at 130,000xg for 10 minutes. The upper phase was collected to a fresh tube and a 2.5 volume of 100% (v/v) ethanol (Sigma, 459844) and 1/10 volume of 5M NaOAc (sodium acetate, Sigma, S2889) were added, followed by centrifugation at 130,000xg for 10 minutes. The DNA pellet was washed with 500µl of 70% (v/v) ethanol (Sigma, 459844), and centrifuged at 130,000xg for 10 minutes. Finally, the pellet was dried at room temperature for 5 minutes and dissolved in 27µl nuclease- free water (Sigma, W4502).

2.2.2.5. Plasmid isolation

A single colony from LB (Luria Bertani) agar plate supplemented with 100µg/ml ampicillin (Sigma, A0166) was inoculated into 5ml of LB broth medium also supplemented with 100µg/ml ampicillin incubated at 37°C, 180rpm overnight. The bacterial culture was pelleted by centrifugation at maximum speed for 5 minutes. Plasmids were isolated using the QIAprep Spin Miniprep Kit (Qiagen, 27104): The pellet was resuspended in 250µl of P1 buffer. 250µl of P2 buffer was added to the suspension which was then mixed thoroughly by vigorously inverting 4-6 times and incubated at room temperature for 5 minutes. After that, 50µl of P3 buffer was added and the mixture was inverted until a homogenous suspension containing a white flocculate was formed. The bacterial lysate was cleared by centrifugation at 130,000xg, 10 minutes and the supernatant was transferred to a spin column. The column was washed two times with 500µl of wash buffer. Finally, the plasmid was then eluted with 30µl nuclease free water (Sigma, W4502).

For preparation of large quantities of plasmid DNA, the QIAGEN Plasmid MIDI Kit was used (Qiagen, 12143): A single colony from LB ampicillin agar plate was inoculated into 100ml of LB medium supplemented with 100µg/ml ampicillin (Sigma, A0166), incubated at 37°C, 180rpm overnight and harvested by centrifugation at maximum speed for 10 minutes at 4°C. The bacterial pellet was resuspended in 4 ml of P1 buffer, followed by 4 ml of P2 buffer, and the suspension was thoroughly mixed by vigorously inverting the sealed tube 4-6 times and incubated at room temperature for 5 minutes. 4 ml of chilled P3 buffer was added, and the suspension was thoroughly mixed by vigorously inverting 4-6 times and incubated on ice for 15 min, followed by centrifugation at 130,000xg for 30 minutes at 4°C. The QIAGEN-tip was equilibrated by applying 3 ml of QBT buffer, and the column was allowed to empty by gravity flow. The supernatant (above) was applied to the QIAGEN-tip. The QIAGENtip was washed twice with 10ml of wash buffer. The DNA was eluted with 5 ml of elution buffer and precipitated by adding 5 ml of room temperature 100% (v/v) isopropanol (Sigma, 190764) to the eluted DNA, followed by centrifugation immediately at 130,000xg for 10 minutes at 4 °C. The supernatant was carefully decanted. The DNA pellet was washed with 2 ml of room temperature 70% (v/v) ethanol (Sigma, 459844), followed by centrifugation at 130,000xg for 5 minutes. The supernatant was carefully decanted without disturbing the pellet. The pellet was dried for

5-10 min. Finally, the plasmid pellet was dissolved in 500µl of nuclease free water and the plasmid concentration was determined using a Nanodrop spectrophotometer.

2.2.2.6. Digestion

2µg of plasmid pmiR-Glo or all PCR products after phenol/chloroform clean up was incubated with 1µl either *Sal*I (10 units/ µl) (Promega, R6061), *Sac*I (10 units/ µl) (Promega, R6051), or *Xba*I (Promega, R6181) in the recommended buffer in a final volume 20µl for 3 hours at 37ºC. The digestion reaction was terminated by heating at 75ºC for 15 minutes.

After digestion, the 5' phosphate of plasmid was removed to prevent self-ligating by incubating the digestion mix with 1µl Antarctic Phosphatase (5 units/µl) (NEB, M0289S) and 3µl Antarctic Phosphatase buffer 10X, in a final volume 30µl.The reaction was carried out at 37ºC for 15 minutes and followed 5 minutes at 70ºC to inactivate the enzyme.

2.2.2.7. Gel purification

The digestion mix was applied to 1% (w/v) SeaKem® LE Agarose (Lonza, 50002). DNA fragments were visualized by staining with ethidium bromide (Sigma, E1510). Under UV-light, the appropriate DNA band was excised from the gel with a clean scalpel and transferred into an Eppendorf tube. The Zymoclean Gel DNA Recovery Kit (Zymo Research, D4001) was used to purify DNA from the agarose gel. Briefly, 3 volumes of ADB were added to each volume of agarose excised from the gel and incubated at 37-55ºC for 5-10 minutes until the gel slice was completely dissolved. For DNA fragments higher than 8kb, 1 addition volume of water was also added to the agarose. The dissolved agarose solution was transferred to the Zymo-spin column and centrifuged for 30 seconds at full speed. The flow-though was discarded. The column was washed two times with 200µl DNA wash buffer and centrifuged at full speed at 30 seconds. The flow-though was discarded. DNA was eluted with 13µl nuclease-free water (Sigma, W4502) and quantified using a NanoDrop spectrophotometer.

2.2.2.8. Ligation

Ligation of DNA fragments was performed with a ratio of 1:3 of plasmid DNA: insert. The reaction mixture was incubated with 1µl of T4-DNA Ligase (1 unit/µl) (Life Technologies, 15224-017), 1µl of ligation buffer (10X) in a final volume of 10µl ddH2O. The reaction was left at 14^{o}C for 24hours.

2.2.2.9. Transformation

To 100µl of competent E.coli DH5α, either 50-100ng of plasmid DNA or 10 µl of ligation reaction were added and incubated for 20 minutes on ice. A heat shock at 42°C for 30 seconds was followed by incubation on ice for another 2 minutes. 500µl of LB medium was added to the bacteria and the bacterial suspension was shaken at 37°C and 180rpm for 60 minutes. The bacteria were then spread on LB-agar plates containing 100µg/ml ampicillin (Sigma, A9393). Plates were incubated at 37°C overnight.

2.2.2.10. MicroRNA 29 family binding site mutagenesis

QuikChange II XL site-directed mutagenesis kit (Agilent, 200521) was used to replace 5 nucleotides in the binding site of the miR-29 family to either *Xba*I (5'TCTAGA3'), *Sal*I (5'GTCGAC3'), *Sac*I (5'GAGCTC3') depending on which restriction enzymes were used in subcloning. The basic procedure utilizes PfuUltra high fidelity (HF) DNA polymerase for extending two mutagenic oligonucleotide primers which have desire mutations in the middle of their sequences and the rest of the sequence complementary to opposite strands of miR-GLO- 3'UTR. After cycling, PfuUltra HF DNA polymerase will generate a mutated plasmid containing staggered nicks (Figure 2.1). The product is then treated with *Dpn* I nuclease targeting sequence 5'-Gm^{6}ATC-3'. *Dpn* I, specific for methylated and hemimethylated DNA, will digest the parental DNA template and select for mutant-containing synthesized DNA. The nicked vector DNA incorporating the desire mutant of the miR-29 family binding site is then transformed into XL10 Gold ultracompetent cells (Figure 2.1).

Mutangenic primers were designed using Agilent's website: QuikChange primer design program: www.agilent.com/genomics/qcpd. The lists of primer mutants used are listed in Appendix, Table 2.

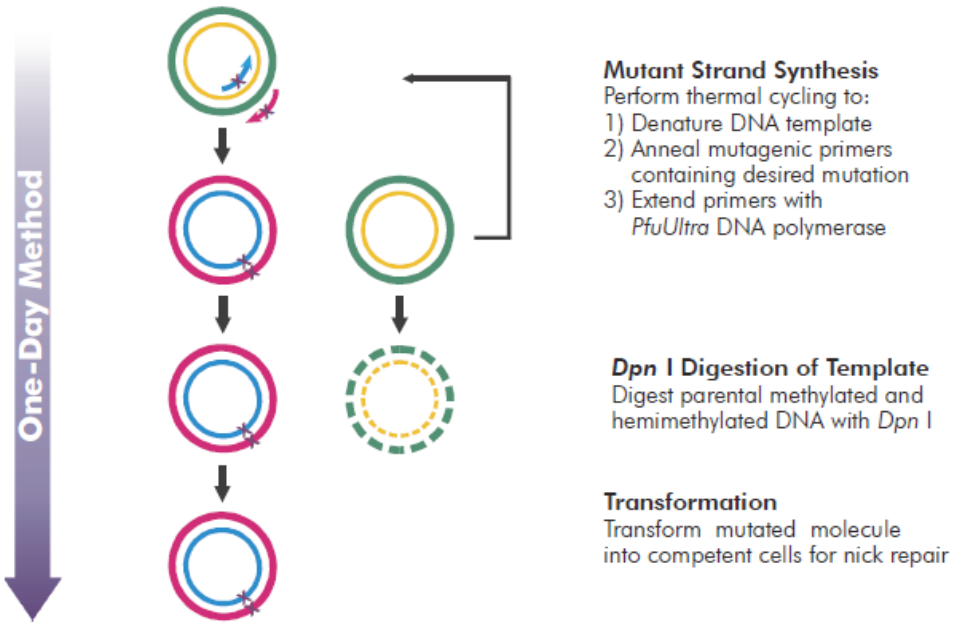

Figure 2.1: QuikChange II XL site-direct mutagenesis method

The reaction is prepared in a final volume of 50µl with 10ng of pmiR-Glo-3'UTR, 1.5µl primer mutant forward (100ng/µl), 1.5µl primer mutant reverse (100ng/µl), 1µl of dNTP mix (10mM), 5µl of reaction buffer (10X), 1µl of PfuUltra HP DNA polymerase (2.5 units/µl). The reaction is cycled at 1 minute at 95ºC, followed by 18 cycles at 95ºC 50 seconds, 68ºC 1 minute/1 kb plasmid length, and finally extension at 68ºC for 7 minutes. The amplification reaction was further incubated with 1µl of *Dpn*I restriction enzyme (10units/µl) at 37ºC for another 1 hour. To 50µl of XL10-Gold Ultracompetent cells, 5µl of *Dpn* I-treated DNA was added and the transformation protocol followed as above.

2.2.2.11. Sequencing

DNA Sequencing was performed by Source BioScience (http://www.lifesciences.sourcebioscience.com/). The sequencing signal was read by Chromas 2.4.

2.2.2.12. Total RNA isolation

2.2.2.12.1. Total RNA isolation from cultured cells

500ml of Trizol® reagent (Invitrogen, 15569-026) were added directly to adherent cells after removing the growth media from a 6-well plate. The cells were lysed by pipetting up and down several times. 250µl chloroform (Sigma, 288306) was added per 500µl Trizol®, vortexed for 15 seconds and incubated at room temperature for 10mins. The Trizol®/Chloroform mixture was centrifuged at 130,000xg, 10min, at 4°C and the aqueous layer recovered into a fresh tube. 500µl of 100% (v/v) isopropanol (Sigma, 190764) was added, mixed, left 10min at room temperature and centrifuged at 130,000xg, 10min, at 4°C then the supernatant was discarded. RNA pellets were washed with 75% (v/v) ethanol (Sigma, 459844), and centrifuged at 130,000xg, 2min, at 4°C. The supernatant was discarded, the pellet air dried and then suspended in 50µl RNase-free water and stored at -80°C until further use.

2.2.2.12.2. Total RNA isolation from murine whole knee joint

All materials used were RNase free. Whole knee joints were ground under liquid nitrogen using BioPulverizer (Biospec). Trizol® reagent (Invitrogen, 15569-026) were added immediately to ground samples (1.5ml/50mg samples) and mixed thoroughly for 5 minutes. Ground knee joints were pelleted at 130,000xg for 2min at 4°C and the supernatant recovered. 250µl chloroform (Sigma, 288306) was added per 500µl Trizol®, vortexed for 15 seconds and incubated at room temperature for 10mins. Samples were then treated as cultured cells above.

2.2.2.12.3. Total RNA isolated from murine hip or knee cartilage

Murine hip femoral caps were fully homogenized with 500µl Trizol® reagent (Invitrogen, 15569-026) using a disposable pestle. Then, 200µl chloroform (Sigma, 288306) was added, vortexed for 15 seconds, and left at room temperature for 10mins. The Trizol®/chloroform mixture was centrifuged at 130,000xg for 10 minutes at 4°C, and the aqueous layer collected into a fresh tube. The RNA purification step was performed using *mir*Vana™ miRNA Isolation Kit (AM1560, Life Technology) according to the manufactures recommendation for total RNA recovery. Briefly, 1.25x aqueous layer volume of 100% (v/v) RT ethanol was added to the aqueous phase and the samples were loaded onto

columns. The flow through was discarded after centrifuging 15 seconds at 130,000xg. Then three wash steps were followed by applying wash solution 1 (700µl), and then wash solution 2/3 (500µl) (twice) to the column. For each washing, the column was centrifuged at 130,000xg for 15 seconds followed by discarding the flow through. The columns was then placed in RNase-free collection tubes and 30µl of RNas-free water added. Columns were then left to stand for 2 minutes and centrifuged at 2 minutes, 13,000xg. RNA was then stored at -80^{o}C until used.

2.2.2.13. MicroRNA quantification and integrity

The concentration of RNA samples was determined by measuring the absorbance at 260nm using the NanoDrop spectrophotometer (NanoDrop Technologies). The purity of RNA is determined from the ratio A_{260}/A_{280} and A_{260}/A_{230}.

The integrity of total RNA was determined using the Experion^{TM} automated electrophoresis system (Bio-Rad, USA). This method measures fluorescence of a fluorophore bound to RNA. RNA integrity can be evaluated automatically by comparing the area of the peaks corresponding to the rRNAs. A 28S/18S rRNA ratio close to 2 indicates for intact RNA.

2.2.2.14. cDNA synthesis

2.2.2.14.1. SuperScript II reverse transcriptase cDNA synthesis

Total RNA was isolated from cells, whole knee joints, human or murine cartilages as above and reverse transcribed to cDNA using SuperScript II reverse transcriptase (Life Technologies, 18064-014). Briefly, in a total volume of 11µl in 96-well PCR plate, 1µg total RNA and 0.2µg random hexamer primer (Life Technologies, 48190-011) was mixed together and the plate was incubated at 70^{o}C for 10mins. Samples were chilled on ice, then, a master mix containing 1µl SuperScript II reverse transcriptase (200 units/µl) (Life Technologies, 18064-014), 4µl First Strand buffer (5X) (Life Technologies, 28028-013), 2µl 0.1M dithiothreitol (DTT) (Life Technologies, 18057-018), 2µl of 10mM dNTP mix (Bioline, BIO-39044), 1µl Recombinant RNasin Ribonuclease Inhibitor (20-40 units/µl) (Promega, N2511) was added to the randomly primed RNA to give a total volume of 20µl and incubated for 1 hour at 42^{o}C followed by a heat inactivation step at 70^{o}C, for 10mins.

cDNA was diluted to 0.5µg/ml in nuclease-free water (Sigma, W4502). 5µg cDNA was used for qRT-PCR analysis of genes of interest and 1µg cDNA was used for analysis of 18S rRNA. QRT-PCR is described in 2.2.2.15.

2.2.2.14.2. M-MLV reverse transcriptase cDNA synthesis

Moloney Murine Leukemia Virus (M-MLV) reverse transcriptase was used to perform cDNA synthesis straight from cell lysate without the need of purifying total RNA. This method was used for cell plated in 96-well plate where a number of cells are too small for RNA extraction.

Briefly, medium was removed and the cells in 96-well plate were washed with ice cold PBS (Life Technologies, 10010023). Then, 30µl cells to Cells-II-cDNA lysis buffer (Life Technologies, AM8723) was added to each well, providing a cell lysate which can immediately be reverse transcribed without the need for RNA isolation. Lysates were transferred to 96-well PCR plate and heated to 75ºC for 15 minutes to inactivate RNases. Lysates can be stored at -80ºC until reverse transcription. For genomic DNA digestion, 1µl DNase I 1 units/µl (Life Technologies, AM2222) and 3µl DNase I buffer (10X) were added per well. The plate was heated to 37ºC for 15 minutes, followed by an inactivation step at 75ºC for 5 minutes.

For reverse transcription, 8µl of DNase-treated samples were transferred to a new ice cold PCR plate. Following this, 3µl of 10mM dNTP mix (Bioline, BIO-39044) and 0.2µg random hexamer primers (50µM) (Life Technologies, 48190-011) were added per well and samples were heated to 70ºC for 5 minutes. Samples were chilled on ice and a master mix including 0.5µl Moloney Murine Leukemia Virus (M-MLV) reverse transcriptase 200 units/µl (Life Technologies, 28028-013), 4µl First Strand buffer (5X) (Life Technologies, 28028-013), 2µl 0.1M dithiothreitol (DTT) (Life Technologies, 18057-018), 0.5µl Recombinant RNasin Ribonuclease Inhibitor (20-40 units/µl) (Promega, N2511), 1µl nuclease-free water (Sigma, W4502) was added per well. Samples were then heated to 37ºC for 50 minutes, followed by an inactivation step of 75ºC for 15 minutes. After that, 30µl of nuclease-free water (Sigma, W4502) was added per sample. For quantitative real-time PCR (qRT-PCR) analysis of genes of interest, 5µl of each sample was used. For the

house keeping gene 18S rRNA, samples were diluted 1:10 and 5µl was used. QRT-PCR is described in 2.2.2.15.

2.2.2.14.3. miRCURY LNA™ Universal cDNA synthesis

MicroRNA cDNA was synthesized by the miRCURY LNA™ Universal cDNA synthesis kit (Exiqon, 203300). This step provides templates for all miRNA real-time PCR assays by one first-strand cDNA synthesis reaction. The basis principal is in Figure 2.2.

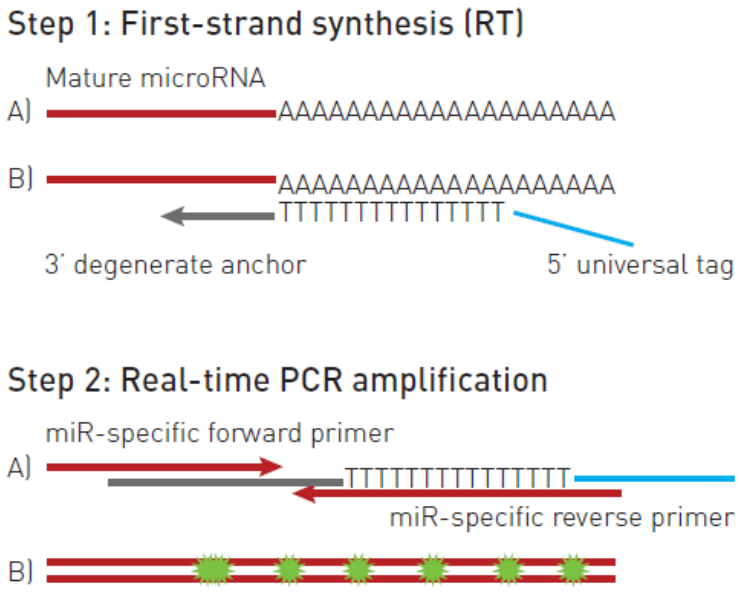

Figure 2.2: Outline of the miRCURY LNA Universal RT miRNAsynthesis.

A poly-A tail is added to the mature miRNA template (step 1A). cDNA was synthesized using a poly-T primer with a 3'degenerate anchor and a 5'universal tag (step1B). Then the cDNA template is amplified using miRNA-specific and LNA^{TM}-enhanced forward and reverse primers (step 2A). Sybr green is used for detection (step 2B). *Reprinted from miRCURY LNA^{TM} Universal RT microRNA PCR instruction manual (Exiqon).*

Total RNA was adjusted to 5ng/µl using nuclease-free water (Sigma, W4502). 10ng of RNA was transferred to an ice cold 96-well PCR plate. A master mix contained 2µl Reaction Buffer (5X) (Exiqon, 203300), 1µl enzyme mix was added to each well. The reaction was brought to 10µl with nuclease-free water and the plate was heated to 42^{o}C for 1 hour followed by a heat inactivation step at 95^{o}C for 5minutes. cDNA was then diluted to 12.5 pg/µl by nuclease free water (Sigma, W4502) and 50pg of cDNA was used for qRT-PCR analysis of miRNA of interest.

2.2.2.15. Real-time quantitative RT-PCR

2.2.2.15.1. Universal Probe Library Real-Time qRT-PCR

The Universal Probe Library (UPL) (Roche Diagnostics) enables extensive transcript coverage due to the short 8-9 nucleotide-long probes. Each probe has a fluorescein (FAM™) label at the 5' end and a dark quencher dye at the 3' end; shorter (typically 8-9 nucleotide) than conventional probe (25-35 nucleotides); locked nucleic acids (LNA™) are incorporated into it sequence. Each probe can detect ~7,000 transcripts and each transcript is detected by ~16 probes.

Primers were designed using the freely available ProbeFinder web-based software provided by Roche Applied Science in which the 'exon boundary spanning' option was selected. Primers were subjected to short sequence BLASTn search to confirm specificity. All the primers were purchased from Sigma and reconstituted in nuclease free water (Sigma, W4502) at 100nM. Primer sequences and UPL probe numbers are in Appendix, Table 3.

For quantitative RT-PCR using the universal primers and probes, the qRT-PCR was carried out using the ABI Prism 7900 HT Sequence Detector (Applied Biosystems) in a microAmp® optical 96-well plate (Life technologies, N8010560). When RNA quantity was known, the qRT-PCR was run using 5ng cDNA for genes of interest and 1ng cDNA for 18S rRNA. For M-MLV-reverse-transcribed- cDNA transcript samples, 5µl samples was used for gene of interest or diluted 1:10 and used 5µl for detecting 18S rRNA.

Each qRT-PCR reaction contained Kappa Fast Universal qPCR Master Mix (2X) (Kappa Biosystems, KK4703), a final concentration of 100nM of each of forward and reverse primers, 200nM of Universal Probe (Roche Diagnostics). The reaction was carried out in a final volume of 25µl. The plate was sealed with microAmp® optical adhesive film (Life Technologies, 4311971) and run with the following PCR cycles: 50°C 2 minutes, 95°C 10 minutes, 40 cycles for 95°C 15 seconds, 60°C 1 minute.

2.2.2.15.2. Standard probe-based Real-time qRT-PCR

The probe-based quantitative real-time PCR method was used to detect the expression of ADAMTS genes including *ADAMTS4, ADAMTS6, ADAMTS10, ADAMTS14, ADAMTS17, ADAMTS19*. These primer and probe sequences were described in (Davidson *et al.* 2006). Briefly, the primers and probes were designed by Primer Express® 1.0 software (Life Technologies, 4363991) and were closed to intron/exon boundaries to control amplification of genomic DNA. Where possible, the probes were designed to span two neighbouring exons. Specificity of primers and probes were validated thought BLASTn. Primer sequences and probe sequences are in Appendix, Table 4

The qRT-PCR reaction was also carried out in a final volume 25µl of Kappa Fast Universal qPCR Master Mix (2X) (Kappa Biosystems, KK4703), 100nM final concentration of each of forward and reverse primers, 200nM genes of interest-specific probe. Reaction set up and cycling conditions were as in 2.2.2.15.1.

2.2.2.15.3. SYBR® Green Real-time PCR

A combination of SYBR® green dye fluorescence with gene-of-interest specific primers enabled double stranded-DNA amplification measurement during PCR. SYBR® green real-time qRT-PCR was used to detect primary and pre sequences of the miR-29 family (which were described in (Eyholzer *et al.* 2010)) and other genes as below. Full primer sequences and list of genes detected by SYBR® green real-time PCR are listed in Appendix, Table 5. All primers were purchased from Sigma.

For SYBR® green qRT-PCR reaction, the amount of cDNA for genes of interest and 18S rRNA is as 2.2.2.15.1. The reaction contained 0.18µl SYBR® green I dye, Kappa Fast Universal qPCR Master Mix (2X) (Kappa Biosystems, KK4703), 100nM final concentration of each of forward and reverse primers. The PCR cycle conditions are as 2.2.2.15.1 followed by another dissociation step which produces the melting curve for the PCR amplification product.

2.2.2.15.4. SYBR® Green Real-time PCR for the mature miR-29 family detection

LNA primers for detecting miR-29 family mature sequence

All LNA primers were designed for optimal performance with the miRCURY LNA™ Universal cDNA synthesis kit. The LNA primers are Hsa-miR-29b-3p LNA™ PCR primer sets (Exiqon, 204679), Hsa-miR-29a-3p LNA™ PCR primer sets (Exiqon, 204698), Hsa-miR-29c-3p LNA™ PCR primer sets (Exiqon, 204729).

Real-time PCR protocol

The qRT-PCR reaction used SYBR® green I dye in combination with LNA™ PCR primer sets to quantify the original mature miR-29 family. The reactions contained 50pg of miRCURY-LNA™-Universal cDNAs for either the miR-29 family or U6. The PCR reaction mix contained 0.18µl SYBR® Green I dye, 5µl Kappa Fast Universal qPCR Master Mix (2X) (Kappa Biosystems, KK4703), and 1µl of forward and reverse primer mix (as recommend by the manufacture (Exiqon)) in a final volume of 10µl. PCR cycles: 10 minutes at 95°C, 40 cycles for 10 seconds at 95°C, 1 minute at 60°C and a dissociation step. The dissociation step produces a melting curve for the PCR amplification product and ensures there is only amplification of the target gene.

2.2.2.15.5. Quantitative RT-PCR Data analysis

2.2.2.15.5.1. Control genes

The constitutively expressed "housekeeping" 18S rRNA was used as the control for relative mRNA gene expression while U6 was used as endogenous control for relative miRNA gene expression.

2.2.2.15.5.2. Relative gene expression – comparative C_t method

Raw fluorescence data was analyzed by the 7000HT SDS 2.2 software to produce threshold cycle (C_t) values, which is the cycle number at which the signal is detectable above the baseline. The C_t values were transformed using the comparative C_t method to obtain relative quantification (RQ) of gene expression:

$$RQ=2^{-\Delta Ct}$$

Where: for mRNA expression: ΔC_t= target gene C_t - 18S C_t

Or for miRNA expression: ΔC_t= the miR-29 family C_t - U6 C_t

This method assumed that all primers and probe sets are working at the same efficiency.

2.2.2.15.6. Western Blot

Buffer and antibody

Radio immunoprecipitation assay (RIPA) buffer: The buffer was made (final concentration) with 50mM Tris base (Fisher Scientific, BP152-500) (which was adjusted to pH 7.6 with hydrochloric acid (Sigma, 258148)),150mM NaCl (Fisher Scientific, BP3581), 1% (v/v) Triton X-100 (Sigma, X100), 1% (w/v) sodium deoxycholate (Sigma, D6750), 0.1% (w/v) sodium dodecyl sulfate (SDS) (Fisher Scientific, 10356463), 10mM sodium fluoride (NaF) (Sigma, 201154), 2mM sodium orthovanadate (Na_3VO_4) (Sigma, S6508), 1X protease inhibitor cocktail (Fisher Scientific, PI-78410).

Resolving buffer: To make up 4X buffer: 91g Tris base (Fisher Scientific, BP152-500) was dissolved in Milli-Q Ultrapure water (Merck Millipore) and adjusted to pH 8.8 with hydrochloric acid (Sigma, 258148). The solution was then made up to 500ml. 2g SDS (Fisher Scientific, 10356463) was added and dissolved.

Staking buffer: To make up 4X buffer: 6.05g Tris base (Fisher Scientific, BP152-500) was dissolved in Milli-Q Ultrapure water and adjusted to pH 6.8 with hydrochloric acid (Sigma, 258148). Milli-Q water was added to 100ml volume. 0.4g SDS (Fisher Scientific, 10356463) was added and dissolved.

Running buffer: To make up 10X buffer: 30.2g Tris base (Fisher Scientific, BP152-500), 144g glycine (Fisher Scientific, 10467963), 10g SDS (Fisher Scientific, 10356463) were dissolved in Milli-Q water to a final volume 1L.

Transfer buffer: To make up 1X buffer: 5.8g Tris base (Fisher Scientific, BP152-500), 2.9g glycine (Fisher Scientific, 10467963), 0.37g SDS (Fisher Scientific, 10356463) were dissolved in Milli-Q water, 200ml 100% (v/v) methanol (Sigma, 322415) were added then Milli-Q water to a final volume of 1L.

Tris-buffered saline (TBS): To make up 10X buffer: 24.2g Tris base (Fisher Scientific, BP152-500), 80g NaCl (Fisher Scientific, BP3581) were dissolved in 900ml Milli-Q water and adjusted to pH 7.6 with hydrochloric acid (Sigma, 258148). Milli-Q water was added to 1L volume.

Blocking buffer: For 150ml, 15ml 10X TBS was diluted in 135ml Milli-Q water. 7,5g non-fat dry milk (OXOID, LP0031) was added and stirred to mix. Finally, 0.15ml Tween®-20 was added (Sigma, P5927).

Primary antibody dilution buffer: For 20 ml, 2 ml 10X TBS was diluted to 18 ml with Milli-Q water. 1.0 g BSA (Sigma, A9418) was added and dissolved by stirring. While stirring, 20µl Tween-20 (Sigma, P5927) was added.

Wash Buffer (TBST): TBS with a final concentration 0.1% (v/v) Tween-20 (Sigma, P5927).

Antibody: GAPDH antibody (Cell Signaling, #2118S), DVL3 antibody (Cell Signaling, #3218), FZD5 antibody (Cell Signaling, #3795)

Western blot protocol

SW1353 cells were plated in 6-well plates ($1.5x10^5$cells/well) and transfected with Syn-Hsa-miR-29b miScript miRNA mimic (Qiagen, MSY0000100) as referred in 2.2.2.7.2.5. At desired time post transfection, cells in each well of 6-well plate were washed twice with ice cold PBS (Life Technologies, 10010023) before adding 100µl RIPA buffer to each well and harvesting by scraping. The cell lysate was transferred to a fresh ice-cold 1.5ml tube and centrifuged at full speech in 10 minutes. The supernatant was collected and stored at -20^{o}C.

Protein was quantified using the Bio-Rad Protein Assay (Bio-Rad, #500-0006) which is based on the method of Bradford. Briefly, 200µl dye reagent concentrate was diluted 5 times with Milli-Q water before adding 20µl sample lysate. The mixture was incubated at room temperature for 10 minutes and absorbance measured at 595nm. Comparison of this value to a standard curve provided a relative concentration of solubilized protein. The

standard curve was created with five dilutions of proteins standards of bovine serum albumin (Bio-Rad, 500-0002) from 0.2 to 0.9 mg/ml.

Samples was adjusted to 20µg solubilized protein in a 30µl with nuclease-free water (Sigma, W4502), followed by adding 20ng/µl Bromophenol Blue (Sigma, 114391) and 1.2µl 1M DTT (Thermal Scientific, # R0861). The sample was gently mixed and heated to 95ºC for 5 minutes. Samples were then electrophoresed on 10% (w/v) polyacrylamide gels. The resolving gel was cast with the following components: 5ml 30% (w/v) Acrylamide/ Bis Acrylamide solution 37:5:1 (Bio-Rad, #161-0154), 3.75ml resolving buffer (4X), 6.25ml Milli-Q water, 50µl 10% (w/v) ammonium persulfate (APS) (Sigma, A3678), 10µl TEMED (Sigma, T9281). Resolving gels were topped with isopropanol (Sigma, 190764) until set. Then isopropanol was removed and the stacking gel was cast on top of the resolving gel and a comb was inserted. For 1 gel, the stacking gel was made with 0.71ml stacking buffer (4X), 0.41ml 30% (w/v) acrylamide/ bis acrylamide solution 37:5:1 (Bio-Rad, #161-0154), 1.91ml Milli-Q water, 16µl 10% (w/v) APS (Sigma, A3678), 3.2µl TEMED (Sigma, T9281). Samples were loaded on the gel and were electrophoresed at 50V until the bromophenol blue passed through the stacking gel and then 80V for 1.5 hours.

Immobilon®-FL PVDF membrane (Merck Millipore, IPFL00010) was incubated in 100% (v/v) methanol (Sigma, 322415) for 15 seconds and washed with Milli-Q water. Then, Immobilon®-FL PVDF membrane, gel, extra thick blotting paper (Bio-Rad, #170-3966) were incubated in transfer buffer for 5 minutes. The gel was plated on top of Immobilon®-FL PVDF membrane in Trans-blot® SD semi-Dry Electrophoretic transfer cell (Bio-Rad, #170-3940) with extra thick blotting paper underneath and on top and run for 25V for 30 minutes (for 2 gels,1 mm thick).

After transfer, the membranes were briefly washed with TBS and incubated in blocking buffer for 1 hour, with gently rocking at room temperature. Membranes were then washed in TBST three times for 5 minutes. Primary antibody and membrane was incubated with gentle agitation overnight at 4ºC. Membranes were then washed in TBST three times for 5 minutes and incubated with IRDye® 800CW goat polyclonal anti-rabbit IgG (Li-Cor, 926-32211) (50µg) for 1 hour at room temperature with gently rock. Membranes were washed

with TBST for another three times for 5 minutes. The membrane was visualized using a Li-Cor Odyssey InfraRed Scanner.

2.2.2.15.7. Whole mount *in situ* hybridization

Reagents and buffers

Sodium chloride (NaCl) (Fisher Scientific, BP3581), tri-sodium citrate (Fisher Scientific, 10637174), magnesium chloride hexahydrate ($MgCl_2.6.H_2O$) (Fisher Scientific, M35-500), potassium chloride (KCl) (Fisher Scientific, BP366-500), heparin (Sigma, H3393), yeast tRNA (Fisher Scientific, 10523043), paraformaldehyde (Sigma, P6148), normal goat serum (heat inactivated), Triton-X100 (Sigma, X100), Tween-20 (Sigma, P5927), BSA (Sigma, A9418)

Saline sodium citrate buffer (SSC): 20X SSC buffer was made up with 175.3 g of NaCl and 88.2 g of sodium citrate, pH 7, in a total volume of 1000ml.

Development solution (DS): The solution was made up with: 100 mM Tris-HCl pH9.5, 50mM magnesium chloride hexahydrate (MgCl2.6.H2O), 100mM sodium chloride (NaCl) + 0.1% (v/v)Tween 20.

Blocking solution: The solution was made up with: 2% (v/v) NGS, 2 mg/ml BSA, 0.1% (v/v) Triton X-100 + 0.05%)v/v) Tween 20 in PBS.

Hybridisation Buffer (HB): The buffer was made up with 50% (v/v) formamide, 5xSSC, 0.1% (v/v) Tween 20 + 10 mM citric acid pH6.0 + 50 µg/ml heparin + 100 µg/ml tRNA in PBS

Tris-buffered saline with Tween 20 (TBST): for 100ml (10X) buffer was made up with 8g NaCl, 25ml Tris-HCl pH7.5, 0.2g KCl, 10ml Tween 20

Phosphate-buffered saline with Tween 20 (PBST): PBS with 0.1% (v/v) Tween 20

Probe: miRCURY LNA™ miR-29b-3p detection probe, 250pmol, 5'-DIG and 3'-DIG labelled (Exiqon, 38131-15)

Fixation

Mouse embryos at desired stages were dissected and fixed in 4% PFA-PBS on a rolling platform overnight at 4^{o}C. Then next day, the embryos were washed 4 times with PBST and dehydrated through increasing MeOH concentration washes e.g. 25%, 50%, 75% and 100% MeOH on the gentle rocking platform. The embryos can then store in 100% MeOH at -20^{o}C until required.

In situ hybridization protocol

On a gently rocking platform, the embryos were washed with decreasing MeOH concentration i.e. 75% (v/v), 50% (v/v), 25% (v/v), 0 (v/v) % MeOH for 15 minutes each time to dehydrate. After that, the embryos were digested with Proteinase K (10µg/ml final concentration) for 30 minutes, followed by rinsing twice in PBST and fixing in 4% (v/v) PFA for 20 minutes. To get rid of the remaining PBST, the embryo was washed 4 times in PBST for 5-7 minutes. The embryo was prehybridized in hybridization buffer at 54^{o}C for 3 hours and the "nape" of the neck of embryo was pricked to facilitate the probe penetration. After prehybridisation step, the buffer was removed and replaced with fresh warm hybridisation buffer containing 20 pmol of the miR-29b LNA probe (Exiqon, 38131-15) and left at 54^{o}C overnight with gentle rocking. The probe hybridisation solution was removed followed by washes at 54^{o}C and 15 minutes each wash e.g. 75% HB: 25% 2xSSC, 50% HB:50% 2xSSC, 25% HB:75% 2xSSC, 2xSSC, 0.2xSSC. Following these washes, at room temperature, another 4 washes were carried on gently rocking platform, 10 minutes for each wash e.g. 75% 0.2xSSC:25% PBST, 50% 0.2xSSC:50% PBST, 25% 0.2xSSC:75% PBST, PBST. The embryo was then put in blocking solution for several hours at room temperature and incubated at 4°C O/N with the pre-absorbed antibody at a final dilution of 1:5000 in Blocking Solution. After that, the Blocking Solution was removed and washed throughout 2 or 3 days at RT in PBST with gentle rocking. To get rid of all remaining PBST, the embryos were washed twice with TBST and with development solution for 15 minutes each wash. Colour development was carried out at room temperature in 3.5ml development solution plus 15-50µl substrates.

The antibody was pre-adsorbed using previously fixed and dehydrated tissue that is not suitable for in situ hybridization. These tissues were dehydrated and washed 15 minutes in

blocking solution, followed by incubating with blocking solution containing the antibody at 1:1000 dilution for three hours.

2.2.2. Cell culture and cell-based assays

2.2.2.1. Human primary chondrocyte isolation

Human cartilage chips were incubated with digestion medium including DMEM GlutaMAX^{TM} (Life Technologies, 10566-016), 1mg/ml collagenase (Sigma, C1639), 0.4% (w/v) Hepes (Fisher Scientific, BP310-100), 100 IU/ml penicillin, 100µg/ml streptomycin (Sigma, P4333) at 37^{o}C, 180rpm overnight. The digestion mixture was then strained through a 70µm cell strainer. Cells were plated at 4x10^{4}cells/cm^{2} and grown to 80% confluence. Cells were used by passage 2.

2.2.2.2. Human de-differentiation assay

Human primary chondrocytes were isolated from human knee OA articular cartilage as described in 2.2.2.1. The cells were then subjected to serial subculture in monolayer. The de-differentiation assay was performed by Dr Natalie Crowe (Clark lab, University of East Anglia).

2.2.2.3. Chondrogenesis model

The human chondrogenesis model was performed by Dr Matthew Barter, Newcastle University. Briefly, human bone marrow stem cells (from seven donors, 18-25 years of age) were isolated from human bone marrow mononuclear cells (purchased from Lonza Biosciences) and resuspended in chondrogenic culture medium consisting of high glucose Dulbecco's modified Eagle's medium containing 100 µg/ml sodium pyruvate (Lonza), 10 ng/ml TGF-β3 (Peprotech), 100 nM dexamethasone, 1x ITS-1 premix, 40 µg/ml proline, and 25 µg/ml ascorbate-2-phosphate (Sigma). 5x10^{5} hMSC in 100µl medium were pipetted onto 6.5mm diameter, 0.4-µm pore size polycarbonate Transwell filters (Merck Millipore), centrifuged in a 24-well plate (200g, 5 minutes), then 0.5 ml of chondrogenic medium was added to the lower well as described. Media were replaced every 2 or 3 days up to 14 days.

The murine chondrogenesis model was performed by Dr Tracey Swingler, University of East Anglia. Briefly, ATDC5 cells were seeded at $6x10^4$/well of a 6-well plate in DMEM/Ham's F-12 medium (Life technologies, 11320-033) containing 5% (v/v) FCS (PAA), 2mM glutamine, 100 IU/ml penicillin, 100µm/ml streptomycin (Sigma, P4333), 5ng/ml sodium selenite, 10µg/ml human transferrin (Sigma, I3146), and 10µg/ml bovine pancreatic insulin at 37°C, in an atmosphere of 5% CO_2. Media was replaced every 2 days up to 42 days. After 21 days, the medium was replaced with α-minimal essential medium with the same supplements, and the atmosphere was changed to 3% CO_2.

2.2.2.4. Monolayer cell culture and storage

All cells were cultured at 37°C with 5% (v/v) CO_2. Cells were usually grown in Dulbecco's modified Eagle's medium (DMEM) High Glucose, GlutaMAX supplement (Life technologies, 10566-016) with 10% (v/v) heat-inactivated Fetal Calf Serum (FCS) (PAA) and 100 IU/ml penicillin and 100µg/ml streptomycin (Sigma, P4333). For maintenance, medium was refreshed at least three times weekly. Cells were passaged at around 80-90% confluence. Adherent cells were detached by washing x2 with HBSS (Life Technologies, 14025092) then treated with 2 ml of trypsin/EDTA (Life Technologies, 25200072) for 2-3 minutes at 37°C. After centrifugation (17.3xg, 5 minutes), the cell pellet was gently resuspended in fresh medium. Cells were replated at a ratio of 1: 20. For long term storage, cells were detached and pelleted by centrifugation at 17.3xg for 5 minutes. The pellets were resuspended in cryo-preservation medium including 90% (v/v) FCS (ATCC) and 10% (v/v) DMSO (Fisher, BP231-100), slowly frozen down at approximately 1°C/minute, and stored in liquid nitrogen.

2.2.2.5. Micromass culture

Media

Growth medium: Dulbecco's modified Eagle's medium (DMEM) High Glucose, GlutaMAX supplement (Life technologies, 10566-016) with 10% (v/v) heat-inactivated Fetal Calf Serum (FCS) (ATCC) and 100 IU/ml penicillin and 100µg/ml streptomycin (Sigma, P4333).

Different medium were prepared: the DMEM high glucose, GlutaMAX supplement (Life technologies, 10566-016) adding 1X Insulin- Transferrin-Selenium (ITS-G) (Life Technologies, 41400-045).

Micromass culture

The protocol was described in (Greco *et al.* 2011) with some modifications. Human primary chondrocytes was isolated from human OA knee cartilage as described in 2.2.2.1 and cultured in monolayer with growth medium. Whenever reaching confluence, the cells were passaged two times. Confluent passage 2 monolayer culture of human primary chondrocytes were released by trypsin/EDTA (Life Technologies, 25200072), and resuspended in growth media at a density of $2.5x10^7$ cells/ml. Micromass was obtained by pipetting 20µl of cell suspension into individual wells of 24 well-plates and leaving for 3 hours to attach without additional medium. Then, 1ml growth medium was gently added and the micromass was left for another 24 hours before stimulating with cytokines or growth factors.

2.2.2.6.Induction cells with regulatory factors: major cytokines and growth factors

Cytokines and growth factors:

Human recombinant TGFβ1 (R&D Systems, 240-B-002/CF) and **human recombinant TGFβ3** (R&D Systems, 243-B-002/CF) were reconstituted in sterile 4mM HCl (Sigma, 258148) containing 0.5% (w/v) bovine serum albumin (Sigma, A2058).

Human recombinant Wnt3a (R&D Systems, 5036-WN-010/CF) was reconstituted in sterile Phosphate Buffered Saline (PBS) (Life Technologies, 10010023).

Human Recombinant Interleukin-1β (IL-1β) (First Link, ILB4551) was reconstituted in sterile Phosphate Buffered Saline (PBS) containing 0.5% (w/v) bovine serum albumin (Sigma, A2058).

NFκB activation inhibitor II JSH-23 (Calbiochem, 481408) is a cell-permeable diamino compound that selectively blocks nuclear translocation of NF-κB p65 and its transcription activity without affecting IκB degradation.

Lipopolysaccharides (LPS) (Sigma, L3012) are components of the cell wall of gram negative bacteria. LPS are extracted from *E.coli* serotype O111:B4 and purified by gel filtration. LPS is reconstituted in sterile (PBS) (Life Technologies, 10010023).

P38 inhibitor SB203580 (Sigma, S8307) is a pyridinyl imidazole that suppresses the activation of MAPKAP kinase-2. The P38 inhibitor, therefore, inhibits the MAPKAP kinase-2 cascade which is activated by cellular stress, bacterial infection and pro-inflammatory cytokines. SB203580 was resuspended in DMSO (Fisher, BP231-100).

2.2.2.6.1. Stimulation of cells in monolayer with cytokines and growth factors

Human chondrosarcoma SW1353 and human primary chondrocytes were maintained as described above. For stimulation, either $5x10^3$ SW1353 cells or 10^4 human primary chondrocytes were seeded into each well of a 96-well plate with 100µl DMEM GlutaMax (Life Technologies, 10566-016) with 10% (v/v) FCS (ATCC) and 100 units/ml penicillin and 100µg/ml streptomycin (Sigma, P4333). Cells were serum starved for 14 hours and were stimulated with different cytokines and growth factors at final concentration: TGFβ1, TGFβ3 4ng/ml, IL-1 5ng/ml, Wnt3a 100ng/ml, LPS 1µg/ml at 4, 8, 12, 24, 48 hours. All treatments were performed in triplicate. At each time point, cells in each well were washed with ice cold PBS (Life Technologies, 10010023) and harvested with 30µl Cells-to-cDNA lysis buffer (Life Technologies, AM8723).

2.2.2.6.2. Stimulation of cells in micromass culture with cytokines and growth factors

After the micromass was rested in growth medium for 24 hours, the different medium with either TGFβ1 (10ng/ml), IL-1 (20ng/ml), Wnt3a (50ng/ml) or LPS (1µg/ml) was added. All treatments were performed in triplicate. After different time points as desired, some of micromasses were harvested for Alcian blue matrix staining and others for quantitative RT-PCR.

2.2.2.7. Mammalian cell transfection

2.2.2.7.1. Plasmids, constructs, siRNAs and microRNA mimic and inhibitor

Sox9 expression vector: The vector was kindly provided by Dr Simon Tew (University of Liverpool, UK). The vector was described in (Lefebvre *et al.* 1997). Briefly, an almost full-length coding sequence of human SOX9 which is from codon 27 (directly from the first ATG associated with the Kozak sequence) up to 39bp of 3'unstranslated region was subcloned into pCDNA-5'UT-FLAG. pCDNA-5'UT-FLAG is pCDNA 3.1 with a FLAG sequence.

The miR-29a/b1 promoter construct: The construct was kindly provided by Dr Anne Delany (University of Connecticut Health Center, US) and was described in (Kapinas *et al.* 2010). The 2kb region upstream from the transcriptional start site of the human miR-29a/b1 putative promoter (EU154353) was subcloned into the luciferase reporter pGL4.10 (Promega).

p(CAGA)$_{12}$-luc plasmid: The construct was a kind gift of Dr Andrew Chantry, University of East Anglia, UK and is described in (Pais *et al*. 2010). 12 binding sites of the complex Smad3/4 (GAGAC) was cloned upstream of the luciferase encoding gene in luciferase reporter pGL3 (Promega).

IκBα promoter reporter plasmid: The plasmid was a kind gift from Prof. Derek Mann, (Newcastle University, UK), (originally from Prof. Ronald Hay, University of Dundee, UK). The plasmid contains 5 binding sites of P65 cloned upstream of the luciferase gene.

TOPflash and FOPflash reporter plasmids: The TOPflash reporter is a kind gift from Prof. Andrea Munsterberg (University of East Anglia, UK), and was originally from Prof. Randall Moon (University of Washington, USA). The FOPflash vector is provided by Dr Sarah Snelling (University of Oxford, UK). TOPflash contains 7 binding sites of TCF/LEF (AGATCAAAGG) driving the expression of the firefly luciferase. The back bone is the pTA-luc vector. The FOPflash vector is the control of TOPflash where all 7 binding sites of TCF/LEF are mutated.

The miR-29 mimic:

- Syn-hsa-miR-29a-3p miScript miRNA mimic (Qiagen, MSY000086): 5'UAGCACCAUCUGAAAUCGGUUA
- Syn-hsa-miR-29b miScript miRNA mimic (Qiagen, MSY0000100): 5'UAGCACCAUUUGAAAUCAGUGUU
- Syn-hsa-miR-29c miScript miRNA mimic (Qiagen, MSY0000681) 5'UAGCACCAUUUGAAAUCGGUUA
- AllStars negative control siRNA (Qiagen, SI03650318)

The 29b inhibitor control

- Anti-hsa-miR-29b miScipt miRNA inhibitor (Qiagen, MIN000100)
- miScript Inhibitor negative control (Qiagen, 1027271)

siRNA

- SOX9 siRNA: Dharmacon siRNA SMARTpool® (Fisher Scientific)
- Control: non-targeting siRNA 2 (Dharmacon, 001210-02)

2.2.2.7.2. Transient transfection protocol

2.2.2.7.2.1. SOX9 overexpression

SW1353 cells were plated in a 96-well plate ($5x10^3$cells/well) in growth medium without antibiotics one day before transfection. The cells were 80% confluent at the time of transfection. Before addition of the transfection complexes, the growth medium was removed from the cells and the cells were covered with 50µl of fresh growth medium without antibiotics. For each transfection, two tubes are prepared as follows: **Tube 1:** 100ng SOX9 expression vector was diluted in 25µl DMEM GlutaMax (Life Technologies, 10566-016) without serum and antibiotics; **Tube 2:** 0.2µl transfection reagent Lipofectamine 2000 (Life Technologies, 11668027) was diluted in 25µl DMEM GlutaMax (Life technologies, 10566-016) no serum and antibiotics. After 5 min of incubation, the diluted DNA and the diluted transfection reagent were combined and incubated at room temperature for 20 min. Then, 50µl of complexes were added to each well. The plate was

gently rocked back and forth and incubated at 37°C in a CO_2 incubator. All transfection was performed in triplicate. The pcDNA3.1 vector was used as control. After 6 hours of transfection, transfection medium was replaced with fresh growth medium without antibiotics for another 24 hours. For harvesting, cells were washed with ice cold PBS (Life Technologies, 10010023) and harvested with 30µl Cells-to-cDNA lysis buffer (Life Technologies, AM8723).

2.2.2.7.2.2. SOX9 and miR-29a/b1 promoter cotransfection

To cotransfect SOX9 and the promoter miR-29a/b1, the SW1353 cells were prepared as described above one day before transfection. For each transfection, two tubes are prepared as follows: **Tube 1:** 100ng of 29a/b1 promoter, and either 100ng SOX9/200ng pcDNA3 or 300ng SOX9/100ng pcDNA3 was diluted in 25µl DMEM GlutaMax (Life Technologies, 10566-016) without serum and antibiotics; **Tube 2:** 0.2µl transfection reagent Lipofectamine 2000 (Life Technologies, 11668027) was diluted in 25µl DMEM GlutaMax (Life Technologies, 10566-016) no serum and antibiotics. The diluted DNA and the diluted transfection reagent were combined after 5 min of incubation and incubated at room temperature for another 20 min. Then, 50µl of complexes were added to each well. The plate was incubated at 37°C in a CO_2 incubator and transfection medium was changed with fresh medium without antibiotics for another 24 hours. Then, cells were washed with ice cold PBS (Life Technologies, 10010023) and a luciferase assay performed. All transfection were performed in triplicate.

2.2.2.7.2.3. Transfection of the miR-29a/b1 promoter with cytokines and growth factors

SW1353 cells were plated and transfected with 100ng miR-29a/b1 promoter as described above. Cells were incubated with the promoter for 24 hours. The medium was then removed and replaced with serum, antibiotic-free DMEM GlutaMAX medium (Life technologies, 10566-016), and cells were serum-starved overnight. Cells was stimulated for 6 hours with TGFβ1/3 (4ng/ml), IL-1 (5ng/ml), Wnt3a (100ng/ml), LPS (1µg/ml) in the presence or absence of 50nM NFκB inhibitor or 10nM p38 inhibitor (Sigma, S8307). Medium was removed 6 hours post stimulation and cells were washed twice with ice cold PBS (Life Technologies, 10010023) and then harvested for luciferase assay.

2.2.2.7.2.4. Short interfering RNA SOX9 mRNA knockdown

SW1353 cells were plated and transfected with either 100nM SOX9 siRNA (Dharmacon) or non-targeting siRNA 2 (Dharmacon, 001210-02) as section 2.2.2.7.2.1. To detect siRNA-mediated mRNA SOX9 knockdown, cells were incubated for 48 hours post transfection, then harvested in 30µl Cells-to-cDNA lysis buffer (Life Technologies, AM8723).

2.2.2.7.2.5. Human primary chondrocyte gain- and loss-of-function experiments

One day before transfection, human primary chondrocytes at passage 1 was plated in 6-well plate at $2x10^5$ cells/ wells in fresh growth medium without antibiotics so that the cells will be around 80% confluent. Complexes were prepared as followed for transfection: **Tube 1**: miR-29b mimic/ inhibitor/ AllStar negative control/ inhibitor negative control (50nM) was diluted in 250µl of serum, antibiotic-free DMEM GlutaMAX (Life Technologies, 10566-016). **Tube 2**: 5µl of Lipofectamine 2000 (Life Technologies, 11668027) was diluted in 250µl serum, antibiotic-free DMEM GlutaMax (Life technology, 10566-016). Time for incubation and transfection mixture was prepared similar to section 2.2.2.7.2.2. The original medium was aspirated from the wells, 500µl transfection mixture was added to each well and the final volume was made to 1ml with DMEM GlutaMAX with 10% (v/v) heat-inactivated FCS, without antibiotics. All transfections were performed in triplicated. Cells were incubated for 48 hours, then, supernatant was removed and cells was washed with ice cold PBS and 1ml Trizol reagent was added. Samples were stored at -20^{o}C until RNA extraction.

2.2.2.7.2.6. Transfection of human primary chondrocytes with miR-29 family mimics and treatment cytokines and growth factors

50nM either miR-29a/b/c mimics or AllStar negative control was transfected to human primary chondrocytes in 6-well plate as in section 2.2.2.7.2.5. After 24 hours, medium was removed from the wells and replaced with DMEM GlutaMAX with 0.5% (v/v) heat inactivated FCS overnight. Then, cells were stimulated with TGFβ1 (4ng/ml), IL-1 (5ng/ml), Wnt3a (100ng/ml). At desired times post stimulation as in Chapter 5, medium was removed, the cells were washed with ice cold PBS and harvested in 1ml Trizol reagent.

2.2.2.7.2.7. Transfection of the miR-29b mimic in micromass culture with cytokines and growth factors

Confluent passage 2 monolayer culture of human primary chondrocytes were released by trypsin/EDTA and plated in 175 cm^2 flask with growth medium with 10% (v/v) heat inactivated FCS, no antibiotics one day before transfection to give cells at 90-100% confluence. 100nM miR-29b mimic or non-targeting control was diluted in 500µl medium (tube1) and 4 µl Lipofectamine 2000 was also diluted in 500µl medium (tube 2). Transfection was carried out as in 2.2.2.7.2.2. The original medium from the flask was removed before adding 1ml transfection mixture and the flask was further covered with another 14ml growth medium with 10% (v/v) heat inactivated FCS. After incubating with miR-29b mimic for 48 hours, cells was detached by trypsin/EDTA and put in micromass culture as in 2.2.2.5. After 24 hours of resting, miR-29b transfected micromasses were treated with either TGFβ1 (10ng/ml), IL-1 (5ng/ml), Wnt3a (100ng/ml) in different media (referred in 2.2.2.5) with 10% (v/v) heat inactivated FCS without antibiotics. At desired time, micromasses were harvested in 500µl Trizol reagent.

2.2.2.7.2.8. Co-transfection of reporter vectors with the miR-29 family mimic/ miR-29b inhibitor and stimulation with cytokines and growth factors

SW1353 were seeded into 96-well plate 1 day before transfection as in 2.2.2.7.2.1 and transiently co-transfected with: (1)100ng of reporter plasmids of either $p(CAGAC)_{12}$- luc, $I\kappa B_3$-luc, TOPflash, FOPflash, (2) 10ng of renilla luciferase reporter, and (3) 50nM of either miR-29a/b/c mimic, AllStar non-targeting negative control, miR-29b inhibitor, or inhibitor negative control. The protocol for transfection is as in 2.2.2.7.2.5. After 24 hours of transfection, cells was serum starved overnight and were treated with recombinant human TGFβ1 (4ng/ml), IL-1β (5ng/ml), Wnt3a (100ng/ml) for 6 hours. After stimulation, cells were harvested and a luciferase assay performed as in 2.2.2.8.

2.2.2.7.2.9. Cotransfection of pmiR-Glo-3'UTR reporter with the miR-29 family mimic

Chicken fibroblasts DF1 were plated in a 96-well plate (10^4cells/well) in antibiotic free growth media with 10% (v/v) FCS overnight. 100ng of either pmiR-Glo-3'UTR wild type

or mutant constructs were co-transfected with 50nM miR-29a/b/c mimic using the non-targeting Allstars as control. The protocol for transfection was described in 2.2.2.7.2.5. After 24 hours post transfection. DF1 cells were harvested for luciferase assay as in 2.2.2.8.

2.2.2.8. Luciferase reporter assay

At desire times post transfection, the plate was removed from the incubator. Luminescence was detected using the Dual-Luciferase Reporter Assay system (Promega, E1980). Briefly, the medium on the cells was removed. The cells were washed twice with ice cold PBS and 70µl of cell lysis buffer provided in the kit (Promega, E1980) was added to each well. The plate was gently rocked back and forth for 30 minutes. Then, 10µl cell lysates were transferred to a 96- well white microplate. For measuring firefly luciferase activity, 50µl of Dual Luciferase Reagent was added to each well. The firefly luminescence was measured using a microplate reader. For measuring Renilla luciferase activity, 50 µl of Dual Stop & Glo Reagent was added to each well and mixed gently then the luminescence measured.

After measurement of the firefly luciferase luminescence and Renilla luciferase luminescence, the relative luciferase activity was calculated as the ratio of the firefly activity normalized to the Renilla luciferase activity.

2.2.3. MicroRNA and mRNA microarray

2.2.3.1. MicroRNA and mRNA microarray for destabilization of medial menicus (DMM) model

Whole knee joints from mice which underwent DMM surgery (e.g. DMM-operated right knee and unoperated left knee) were subjected to total RNA isolation and grouped as DMM left (referred to as control) or DMM right (referred as treatment). At each time point (1, 3, 7 days after surgery), equal amounts of total RNA from each sample in the same group was pooled together. The integrity of the new pooled samples was checked before sending to Exiqon Services (Denmark) or Source Bioscience (UK) to perform miRNA microarray or mRNA microarray, respectively.

The miRCURY LNA^{TM} microRNA Hi-Power Labelling Kit Hy3^{TM}/Hy5^{TM} was used for miRNA microarray in which the Hy3^{TM} labelled samples and Hy5^{TM} labelled samples

were mixed pair-wise and hybridized to capture probes targeting all miRNAs or human, mouse and rat registered in the miBASE 18.0. For whole genome array, Illumina's BeadArray-based technology was employed by using MouseWG-6 v2.0 Expression BeadChips whose feature content derived mainly from NCBI reference sequence (NCBI refseq), and simultaneously profiles more than 45,000 mouse transcripts. The BeadChips consists of oligonucleotides immobilized to bead held in microwells on the surface of any array substrate, and made up with 50-mer-gene-specific probe plus 29-mer address sequences. Especially, the chip has high level of bead type redundancy (average 30 beads per probe) to control the quality and reproducibility of the direct hybridization assay.

2.2.3.2. Whole genome array for miR-29b gain and loss-of-function experiment

Human primary chondrocytes were transiently transfected with either miR-29b mimic or miR-29b inhibitor for 48 hours in triplicate. Then, total RNA was isolated and equal amounts of total RNA of each sample in the triplicate was pooled together. After checking the quality and integrity, the new pooled samples were sent to Source Bioscience (UK) to perform human whole genome profile. Again, the Illumina's BeadArray-based technology was employed but using humanHT-12 V4.0 expression BeadChips. Similarly, the feature content derived mainly from NCBI reference sequence (NCBI refseq) which simultaneously profile more than 47,000 human transcripts.

2.2.4. Data analysis

2.2.4.1. Pre-processing microRNA array data

2.2.4.1.1. VST transformation and quantile normalization

It is necessary to do background correction to remove non-specific signal from total signal. However, the initial data-pre-processing in the Illumina GenomeStudio solfware provides users with bead summary data in the form of a single signal intensity value for each probe. This value is calculated by subtracting the local background from the signal intensity of each bead, then taking the means of all beads containing a given probe. This means BeadStudio output data has undergone background correction. Thus, no further background correction need to be done for the Bead summary data, received from Source Bioscience (UK).

To reliably detect changes in expression from the whole genome array, it is important to remove sources of variation of non-biological origin between arrays to make data comparable. There are two types of variations might be seen when comparing arrays e.g. interesting variation (biological differences), and obscuring variation. Sources of obscuring variation were introduced during the process of carrying out the experiments e.g. **during preparing the samples** including mRNA extraction and isolation, variation in introduction and incorporation of dye, effected by pipetting error, temperature fluctuations and reagent quality; **during manufacturing of the array** including variation in the amount of probe present at each feature or spot and variation in the hybridization efficiency of the probes for their mRNA targets; **during hybridization of the sample on the array** including variation in the amount of samples applied to the array and variation in the amount of target hybridized to the probe; and after array hybridization including variation in optical measurement and intensity computed from the scan image. So, comparisons between different biological samples can be made, it is important to remove these obscuring variations to ensure the values being analysed reflect the biology. For Beadchip array data, the two steps to achieve this are commonly referred to as between-array normalization, and transformation. Two popular methods that implement these steps are VST transformation and quantile normalization for the Lumi packages. Briefly, for analysing, bead summary array data was imported into R studio (http://www.rstudio.com/). Array data was then transformed and normalized using Lumi package.

2.2.4.1.2. Sequence data

The miR-29 family mature sequence data was retrieved from miRbase database (http://www.mirbase.org/). 3'UTR sequences were downloaded from UCSC (https://genome.ucsc.edu/) and Ensembl (http://www.ensembl.org/index.html). RefSeq IDs were used to map probe sets to UCSC database and Ensembl Gene IDs were used to map probesets to the Ensembl database.

2.2.4.1.3. The MicroRNA-29 family target prediction

Three types of seed matches in the 3'UTR were considered when predicting direct miRNA-29 targets e.g. **6-mer seed match** which is 6nt in length and was complementary

to nucleotides 2 to 7 in the miR-29 family; **7-mer seed match** which is 7nt length and is complementary to nucleotides 1–7 in the miRNA or nucleotides 2–7 in the miRNA with "A" at the first position; and **8-mer seed match** which is 8nt length, and matched nucleotides 1–8 in the miRNA or nucleotides 2–8 in the miRNA with an "A" at the first position. For searching these seed matches in the 3'UTR, 3'UTR sequences were imported and read in R studios using the "*readDNAStringSet*" function in Biostring package. Also, three types of miR-29 family seed matches were searched using "*vcountPattern*"function.

In line with using R studios, some miRNA target prediction programs available were also used to predict targets for miR-29 including TargetScan (http://www.targetscan.org/), miRNA body map (http://www.mirnabodymap.org/), miRDB (http://mirdb.org/miRDB/), DIANA (http://diana.cslab.ece.ntua.gr/), Pictar (http://pictar.mdc-berlin.de/), miRbase (http://www.mirbase.org/).

2.2.4.1.4. Functional pathway analysis

DAVID (Database for Annotation, Visualization and Integrated Discovery) functional annotation tool (http://david.abcc.ncifcrf.gov/) was used to perform functional analysis for particular gene groups.

2.2.4.1.5. Statistical analysis

Unless otherwise stated, for the whole thesis, Student's unpaired t-test (two-tail) was performed to compare difference between two groups. All values are given as mean values of replicates with error bar representing the standard error of the mean. The statistical analysis was carried using GraphPad Prism version 4.0 for Windows. Levels of statistical significant are represented as * ≤ 0.05, ** ≤ 0.01, *** ≤ 0.001.

CHAPTER III
IDENTIFICATION OF THE MIR-29 FAMILY IN CARTILAGE HOMEOSTASIS AND OSTEOARTHRITIS

3.1. Introduction

MicroRNAs are referred to as the master regulators for gene expression: they exert their suppressive functions on targeting genes at the post transcriptional level through a sequence-complementary mechanism (Bartel 2009). In human chondrocytes, many different miRNAs are found and each of them are shown to directly and/or indirectly regulate hundreds of target genes, implicating a complex gene regulatory network in which miRNAs are involved (Le *et al.* 2013). This means that miRNAs take a crucial part in controlling the balance of the mRNA network in cartilage homeostasis; and the dysregulation of miRNA expression could trigger OA onset by disrupting this regulatory network.

Indeed, an essential role of miRNAs has been reported in various aspects of cartilage development, cartilage homeostasis, and also in OA pathogenesis (Le et al. 2013). For instance, knockout of Dicer, the pre-miRNA processing enzyme, in a cartilage-specific manner resulted in skeletal growth defects, premature death of mice, reduction in growth plate chondrocytes, and an increase in hypertrophic chondrocytes (Kobayashi et al. 2008). Mutation of the Dnm3 locus, transcribing the miRNAs miR-199a, miR-199*, and miR-214, resulted in growth retardation including craniofacial hypoplasia (Watanabe *et al.* 2008). Universal knockout of miR-140, a cartilage and skeletal-restricted miRNA lead to: mild craniofacial deformities and dwarfism; early onset of age-related OA development; greater susceptibility to OA with accelerated proteoglycan loss and fibrillation of articular cartilage (Miyaki et al. 2010, Nakamura et al. 2011). Transgenic mice overexpressing miR-240 in cartilage were resistant to antigen-induced arthritis-associated loss of proteoglycan and type II collagen (Miyaki et al. 2010). Other specific miRNAs: miR-9, miR-98, and miR-146 were highlighted to be expressed differentially in miRNA profiles between human OA cartilage and its normal articular counterpart (Iliopoulos et al. 2008, Jones *et al.* 2009); miR-199a, miR-675, miR-145, miR-140, miR-455 have been proven to function in chondrogenesis and cartilage homeostasis (Lin *et al.* 2009, Miyaki *et al.* 2009, Dudek *et al.* 2010, Martinez-Sanchez *et al.* 2012, Swingler *et al.* 2012); miR-222 is

reported to play a potential role in the articular cartilage mechanotransduction pathway (Dunn *et al.* 2009); miR-146a and miR-146b, whose expression is regulated by NFκB, appear to be the key miRNAs in the inflammatory response (Taganov *et al.* 2006); miR-34a, miR-194, miR-27b were reported to be induced by IL-1β (Abouheif et al. 2010, Akhtar *et al.* 2010, Xu et al. 2012). All of these data reveal miRNAs as important modulators of various aspects of articular cartilage homeostasis and OA pathogenesis.

OA develops slowly with time and may not be symptomatic until significant joint damage has occurred. Currently, there is a lack of effective approaches to OA prevention or treatment. Available treatments are limited to pain management, and joint replacement surgery, this latter in the late phase of the disease. MicroRNAs, with the ability to fine-tune the expression of multiple genes, could be a promising tool for therapeutic applications for a complex disease like OA. The down regulation of gene expression by miRNAs is relatively modest, thus the approach of combining multiple miRNAs to simultaneously target OA pathogenesis-relevant networks may be needed. Furthermore, There is growing evidence for future miRNA-based diagnostics: a number of miRNA in plasma were found at different levels between RA and OA patients (Murata *et al.* 2010); let-7e, miR-454, miR-886 were identified as differentially expressed circulating miRNAs in OA patients necessitating arthroplasty, especially, let–7e emerged as potential predictor for severe knee or hip OA (Beyer et al. 2014). However, there is a requirement for detailed investigations directed at diagnostic performance (sensitivity, specificity, accuracy) of these promising novel biomarkers before the measurement of miRNAs can enter the clinic.

With all of the above information, the essential roles of miRNAs in cartilage homeostasis and OA are shown with potential for clinical application. The insights into the roles of miRNAs in chondrogenesis, articular cartilage homeostasis, and OA initiation and progression are, nevertheless, still insufficient. Thus, there is a continuing need to deepen our understanding of the molecular mechanisms miRNAs are involved in cartilage homeostasis and OA. Investigating the disease directly in man is challenging due to e.g. the inability to harvest articular tissue at an early stage; the slow disease progression; the absence of symptoms in the early stage of the disease; the variety of symptoms; the variety of causes and environmental influence. Animal models mimicking features of OA are, therefore, an important alternative solution.

In an effort to identify novel miRNAs important in the development of OA, the murine Destabilization of Medial Meniscus (DMM) model was used to identify miRNAs differentially expressed at 1, 3, 7 days (i.e. early stages) after the surgery. Performing miRNA and mRNA profiling followed with an integrated analysis highlighted miR-29b as a candidate miRNA participating in the early onset of OA in DMM model. Alongside the DMM model, the role of the miR-29 family in cartilage homeostasis and OA was also investigated in other human and mouse models e.g. human end-stage OA cartilage, the murine hip avulsion injury model, a human primary chondrocyte dedifferentiation model, a human chondrogenesis model, and murine limb development.

Aims

- Performing miRNA and mRNA profiling in DMM model at very early time points 1, 3, 7 days after surgery
- Identifying miRNA potentially involve in OA onset by bioinformatics analysis
- Investigating the regulation of the miR-29 family which is highlighted from bioinformatics analysis above in human end-stage OA cartilage
- Determining the expression pattern of the miR-29 family in injury model
- Establishing if the miR-29 family involving in chondrocyte phenotype
- Determining the role of miR-29 in human and murine chondrogenesis
- Investigating the involvement of miR-29 in murine limb development

3.2. Results

3.2.1. The microRNA profile in the DMM model at 1, 3, 7 days after surgery

As little is known about the involvement of miRNAs at the early stage of OA, identifying miRNAs modulated in OA initiation was a major aim. Since mRNA profiles have shown large changes in gene expression even at 24 hours post surgery, the DMM model was used to investigate this.

Alongside DMM mice (mice whose medial meniscal tibial ligament of the right knee was transected whilst the left knee was untouched), naïve mice (receiving no treatment), and sham-operated mice (mice whose right knees were operated to visualize the medial meniscal tibia ligament but not transected) were used. Total RNA was first isolated from the whole knee joints of DMM mice (both right and left knees) and their controls at 3 different time points i.e. 1, 3, 7 days after surgery, and subsequently checked for quality and integrity. Unfortunately, RNA from naïve mice was degraded and not further studied. For miRNA profiling, an equal amount of total RNA from individual in each triplicate in the DMM right knee and DMM left knee group at 1, 3, and 7 days after surgery was pooled and these pools were subsequently subjected to miRNA microarray using the miRCURY LNA^{TM} microRNA Hi-Power Labelling Kit Hy3^{TM}/Hy5^{TM}, containing probes targeting all human, mouse and rat miRNAs registered in the miRBase 18.0.

Clustering analysis showed that: the miRNA profiles of the DMM right or left knees were clustered quite closely to each other at day 1 and 3 but far apart at day 7 (Appendix, Figure 1), suggesting that more miRNAs were modulated at the later time point than the earlier. In line with this, calculating the number of miRNAs which changed expression at each time point revealed the same pattern: only small changes were observed until 7 days post-surgery (Figure 3.1). Using 1.5 fold-change (FC) as the cut off, only four miRNAs significantly increased expression at day 1 and 3 whilst more than 30 miRNAs were modulated at day 7. The list of miRNAs which changed expression is listed in Table 3.1.

To visualize the expression pattern of miRNAs across the time course of the DMM model, unsupervised hierarchical clustering analysis was carried out for miRNAs that met the filtering criteria e.g. absolute FC > 1.3 in each time point. Several clusters of miRNAs were identified comparing between DMM right and left knee i.e. (i) miRNAs which **increased** expression across the time course (cluster 1, 2, 3) (Figure 3.2a, b, c), (ii)

miRNAs which **decreased** expression across the time course (cluster 5, 6) (Figure 3.2.e, f), (iii) miRNAs **which decreased** expression across 3 days but **increased** at day 7 (cluster 4) (Figure 3.2d) and (iv) miRNAs which **increased** until 3 days but **decreased** at day 7 (cluster 7) (Figure 3.2.g).

A subset of miRNA differentially expressed by microarray analysis was selected for revalidating the array data by quantitative real-time RT-PCR. The result confirmed the miRNA array data since a similar expression pattern between the two platforms for miR-140, miR-455 (data not shown) and miR-29b (which will be discussed below) was observed.

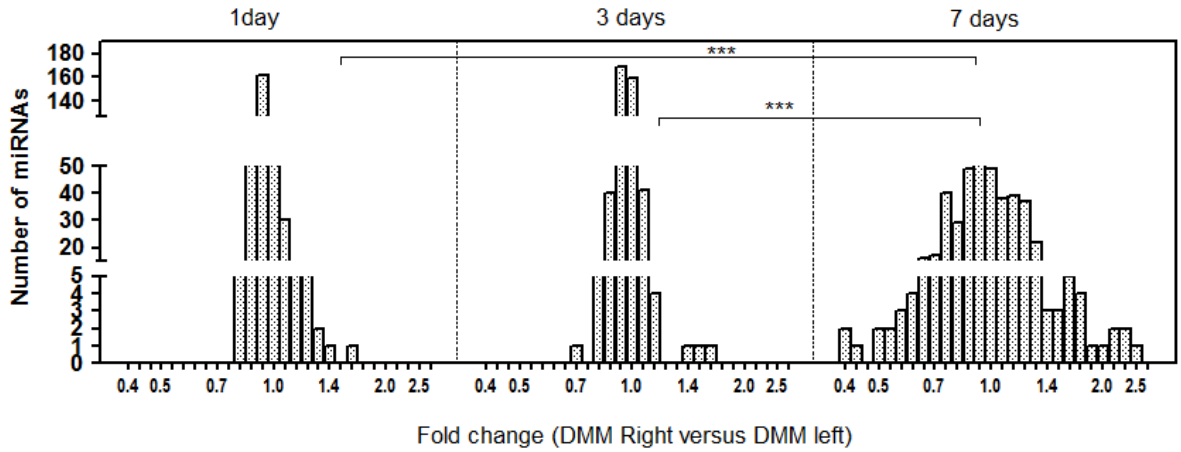

Figure 3.1: Modulation of miRNA expression across a 7 day time course

From the array data, for each miRNA, fold change (FC) was calculated by comparing its expression level in DMM right versus left knee. The number of regulated miRNAs were calculated for each of 0.05 interval of a (0.4, 2.5) range of FC. FC: > 1: increase expression; < 1: decrease expression. The difference in number of miRNAs modulated was calculated by unpaired two-tailed t test: * $p<0.05$, ** $p < 0.01$, *** $p<0.001$.

Day 1		Day 7	
miRNA	**FC**	**miRNA**	**FC**
miR-144-3p	1.7	miR-379-5p	2.6
miR-29b-3p	1.5	miR-127-3p	2.4
		miR-335-5p	2.4
		miR-370-5p	2.2
Day 3		miR-214-3p	2.2
miRNA	**FC**	miR-21-5p	2.1
miR-370-5p	1.7	miR-3073-3p	2.0
miR-21-5p	1.6	miR-199a-3p	1.9
		miR-214-5p	1.8
		miR-210-3p	1.8
		miR-455-3p	1.8
		miR-199a-5p	1.7
		miR-2137	1.7
		miR-199b-5p	1.7
		miR-136-5p	1.7
		miR-34a-5p	1.6
		miR-99b-5p	1.6
		miR-152-3p	1.5
		miR-34c-5p	1.5
		miR-144-3p	-1.5
		miR-3100-3p	-1.5
		miR-669c-3p	-1.6
		miR-378-3p	-1.6
		miR-3473b	-1.6
		miR-133a-5p	-1.6
		miR-3474	-1.7
		miR-378b	-1.7
		miR-133a-3p	-1.8
		miR-133b-3p	-1.8
		miR-1952	-1.9
		miR-491-3p	-1.9
		miR-1a-3p	-2.2
		miR-706	-2.3
		miR-3572	-2.3

Table 3.1: The list of miRNAs regulated in the DMM model with fold change higher than 1.5 (increase or decrease) at 1, 3, and 7 days after surgery.

Fold change (FC) was calculated by comparing between the DMM operated right and un-operated left knee. Down-regulated miRNAs are presented as negative FC.

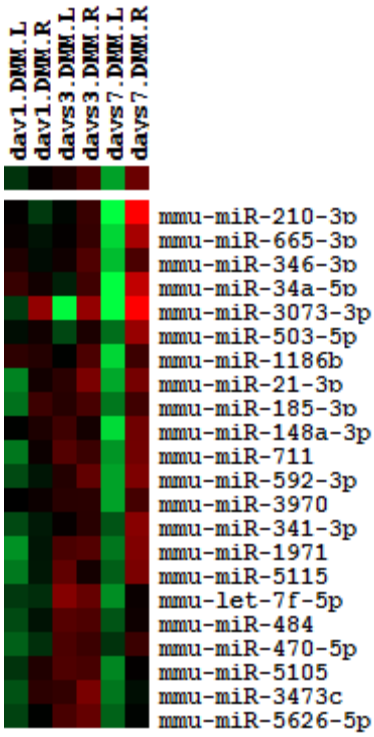
dav1.DMM.L
dav1.DMM.R
davs3.DMM.L
davs3.DMM.R
davs7.DMM.L
davs7.DMM.R
mmu-miR-210-3p
mmu-miR-665-3p
mmu-miR-346-3p
mmu-miR-34a-5p
mmu-miR-3073-3p
mmu-miR-503-5p
mmu-miR-1186b
mmu-miR-21-3p
mmu-miR-185-3p
mmu-miR-148a-3p
mmu-miR-711
mmu-miR-592-3p
mmu-miR-3970
mmu-miR-341-3p
mmu-miR-1971
mmu-miR-5115
mmu-let-7f-5p
mmu-miR-484
mmu-miR-470-5p
mmu-miR-5105
mmu-miR-3473c
mmu-miR-5626-5p

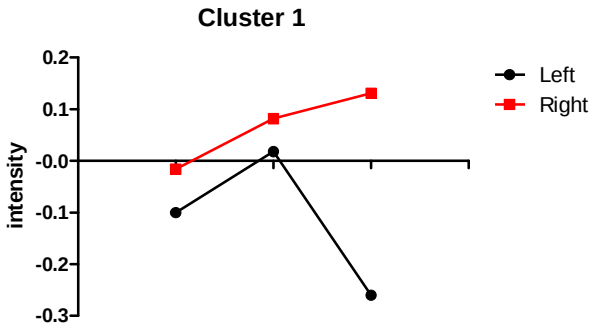
Cluster 1
intensity
0.2
0.1
-0.0
-0.1
-0.2
-0.3
Left
Right

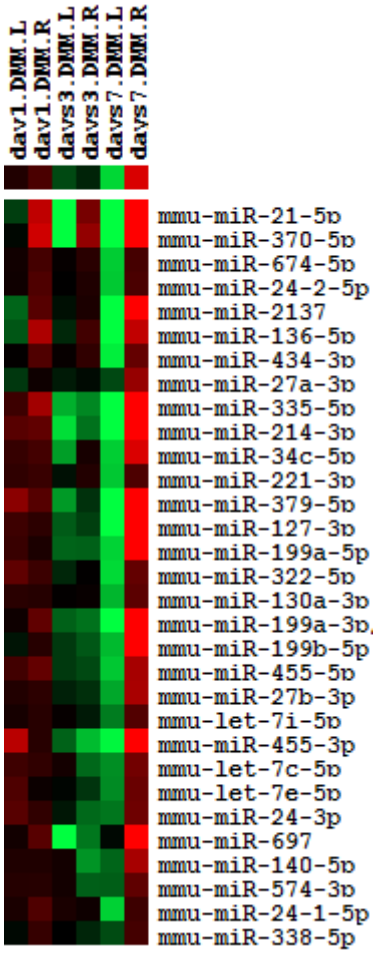
dav1.DMM.L
dav1.DMM.R
davs3.DMM.L
davs3.DMM.R
davs7.DMM.L
davs7.DMM.R
mmu-miR-21-5p
mmu-miR-370-5p
mmu-miR-674-5p
mmu-miR-24-2-5p
mmu-miR-2137
mmu-miR-136-5p
mmu-miR-434-3p
mmu-miR-27a-3p
mmu-miR-335-5p
mmu-miR-214-3p
mmu-miR-34c-5p
mmu-miR-221-3p
mmu-miR-379-5p
mmu-miR-127-3p
mmu-miR-199a-5p
mmu-miR-322-5p
mmu-miR-130a-3p
mmu-miR-199a-3p
mmu-miR-199b-5p
mmu-miR-455-5p
mmu-miR-27b-3p
mmu-let-7i-5p
mmu-miR-455-3p
mmu-let-7c-5p
mmu-let-7e-5p
mmu-miR-24-3p
mmu-miR-697
mmu-miR-140-5p
mmu-miR-574-3p
mmu-miR-24-1-5p
mmu-miR-338-5p

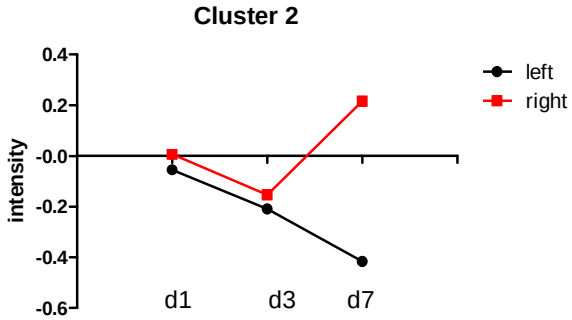
Cluster 2
intensity
0.4
0.2
-0.0
-0.2
-0.4
-0.6
d1
d3
d7
left
right

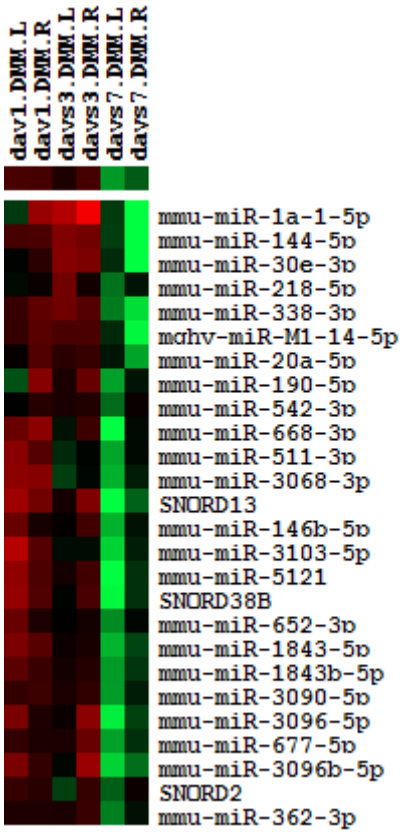
dav1.DMM.L
dav1.DMM.R
davs3.DMM.L
davs3.DMM.R
davs7.DMM.L
davs7.DMM.R
mmu-miR-1a-1-5p
mmu-miR-144-5p
mmu-miR-30e-3p
mmu-miR-218-5p
mmu-miR-338-3p
mghv-miR-M1-14-5p
mmu-miR-20a-5p
mmu-miR-190-5p
mmu-miR-542-3p
mmu-miR-668-3p
mmu-miR-511-3p
mmu-miR-3068-3p
SNORD13
mmu-miR-146b-5p
mmu-miR-3103-5p
mmu-miR-5121
SNORD38B
mmu-miR-652-3p
mmu-miR-1843-5p
mmu-miR-1843b-5p
mmu-miR-3090-5p
mmu-miR-3096-5p
mmu-miR-677-5p
mmu-miR-3096b-5p
SNORD2
mmu-miR-362-3p

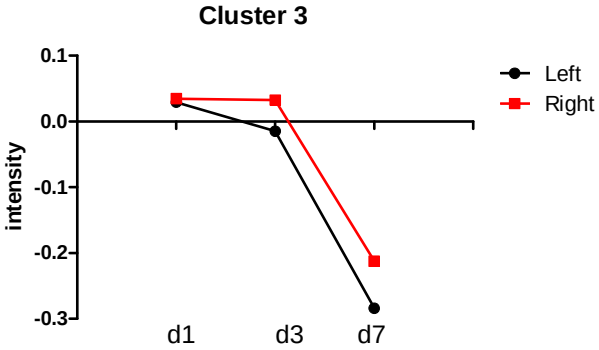
Cluster 3
0.1
0.0
-0.1
-0.2
-0.3
intensity
d1
d3
d7
Left
Right

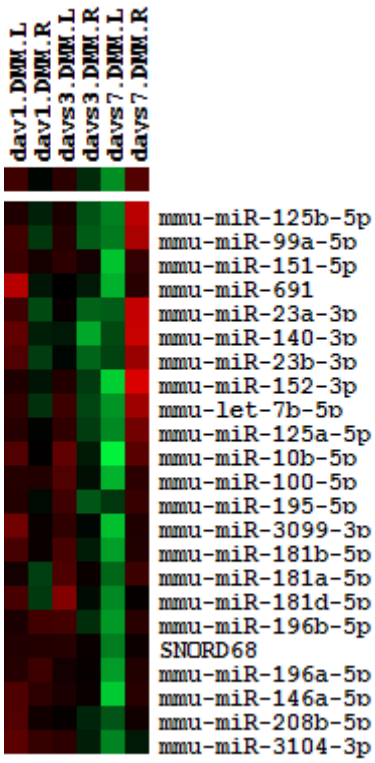
dav1.DMM.L
dav1.DMM.R
davs3.DMM.L
davs3.DMM.R
davs7.DMM.L
davs7.DMM.R
mmu-miR-125b-5p
mmu-miR-99a-5p
mmu-miR-151-5p
mmu-miR-691
mmu-miR-23a-3p
mmu-miR-140-3p
mmu-miR-23b-3p
mmu-miR-152-3p
mmu-let-7b-5p
mmu-miR-125a-5p
mmu-miR-10b-5p
mmu-miR-100-5p
mmu-miR-195-5p
mmu-miR-3099-3p
mmu-miR-181b-5p
mmu-miR-181a-5p
mmu-miR-181d-5p
mmu-miR-196b-5p
SNORD68
mmu-miR-196a-5p
mmu-miR-146a-5p
mmu-miR-208b-5p
mmu-miR-3104-3p

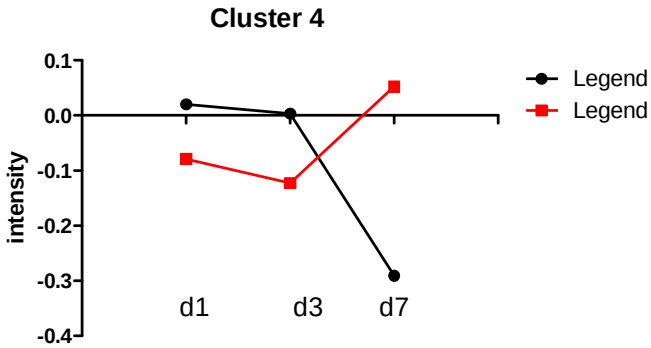
Cluster 4
0.1
0.0
-0.1
-0.2
-0.3
-0.4
intensity
d1
d3
d7
Legend
Legend

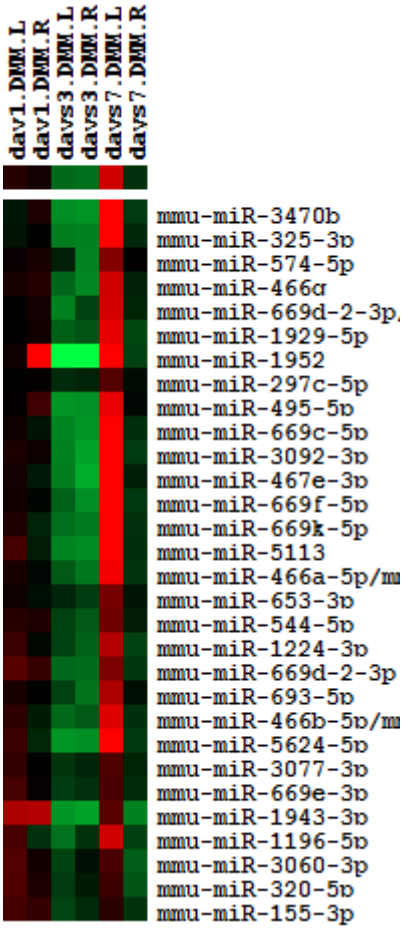
dav1.DMM.L
dav1.DMM.R
davs3.DMM.L
davs3.DMM.R
davs7.DMM.L
davs7.DMM.R
mmu-miR-3470b
mmu-miR-325-3p
mmu-miR-574-5p
mmu-miR-466a
mmu-miR-669d-2-3p
mmu-miR-1929-5p
mmu-miR-1952
mmu-miR-297c-5p
mmu-miR-495-5p
mmu-miR-669c-5p
mmu-miR-3092-3p
mmu-miR-467e-3p
mmu-miR-669f-5p
mmu-miR-669k-5p
mmu-miR-5113
mmu-miR-466a-5p/m
mmu-miR-653-3p
mmu-miR-544-5p
mmu-miR-1224-3p
mmu-miR-669d-2-3p
mmu-miR-693-5p
mmu-miR-466b-5p/m
mmu-miR-5624-5p
mmu-miR-3077-3p
mmu-miR-669e-3p
mmu-miR-1943-3p
mmu-miR-1196-5p
mmu-miR-3060-3p
mmu-miR-320-5p
mmu-miR-155-3p

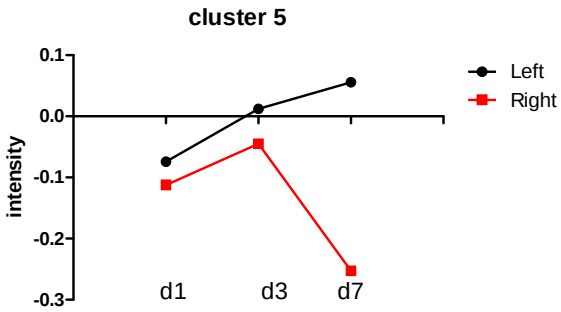
cluster 5
0.1
0.0
-0.1
-0.2
-0.3
intensity
d1
d3
d7
Left
Right

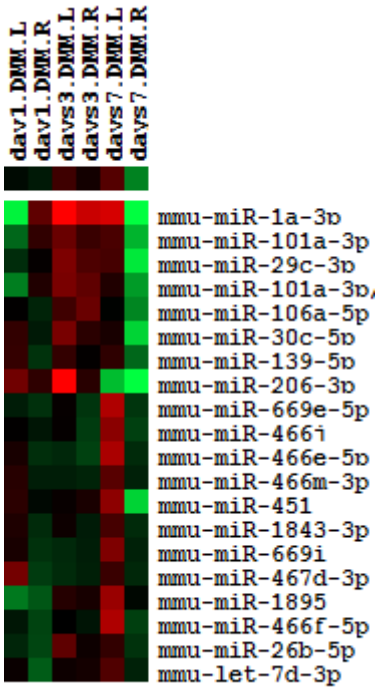
dav1.DMM.L
dav1.DMM.R
davs3.DMM.L
davs3.DMM.R
davs7.DMM.L
davs7.DMM.R
mmu-miR-1a-3p
mmu-miR-101a-3p
mmu-miR-29c-3p
mmu-miR-101a-3p
mmu-miR-106a-5p
mmu-miR-30c-5p
mmu-miR-139-5p
mmu-miR-206-3p
mmu-miR-669e-5p
mmu-miR-466i
mmu-miR-466e-5p
mmu-miR-466m-3p
mmu-miR-451
mmu-miR-1843-3p
mmu-miR-669i
mmu-miR-467d-3p
mmu-miR-1895
mmu-miR-466f-5p
mmu-miR-26b-5p
mmu-let-7d-3p

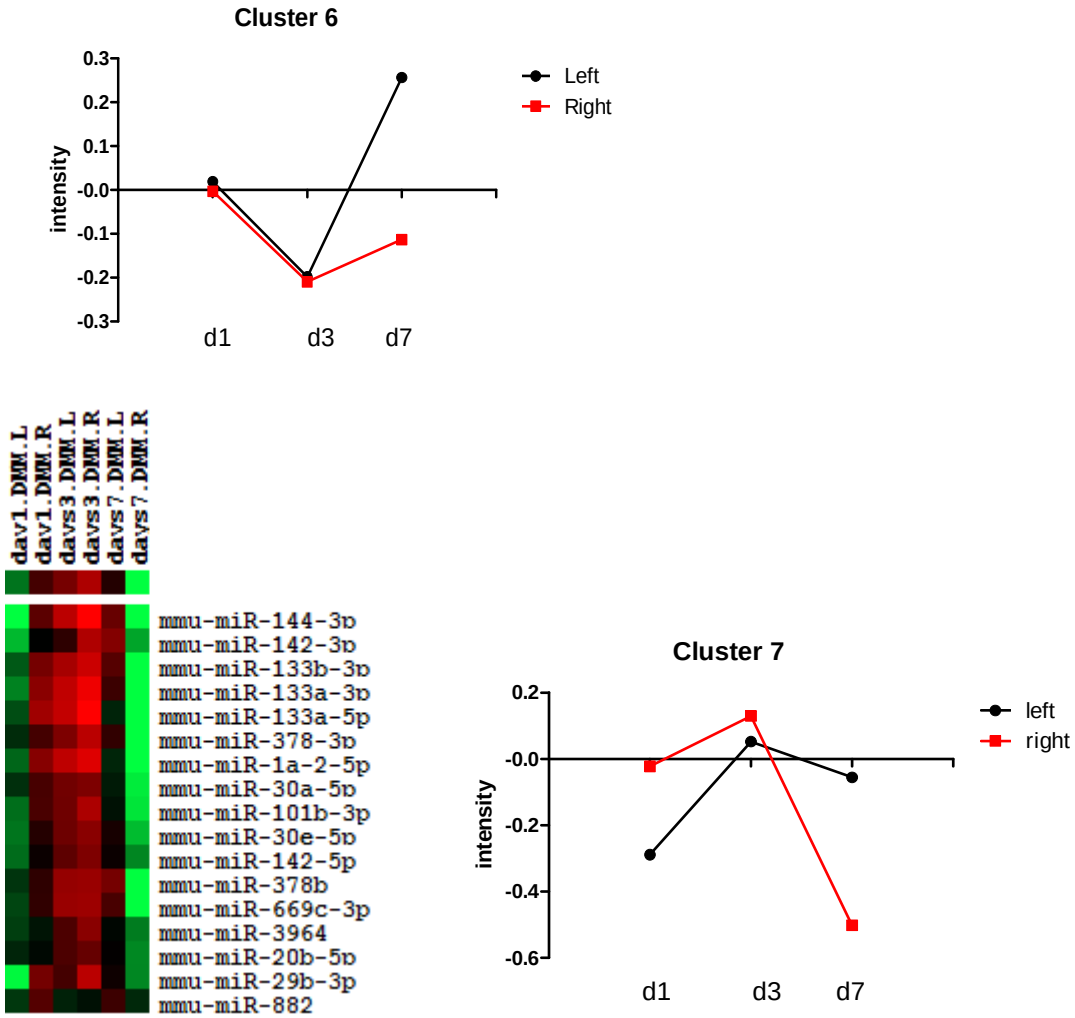

Figure 3.2: Unsupervised hierarchical clustering analysis for miRNAs with absolute fold change higher than 1.3.

Comparing DMM right versus left knee at 1, 3, 7 day time points: cluster 1, 2, 3: all the miRNAs induced expression; cluster 5, 6: all miRNAs decreased expression; cluster 4: miRNAs decreased across 3 days but increased at day 7; cluster 7: miRNAs increased across 3 days but decreased at day 7. Comparing between three time points: cluster 1: miRNAs increased across 7 days; cluster 2, 6: miRNAs decreased at day 3; cluster 3, 5: miRNAs decreased at day 7. SNORD: small nucleolar RNA.

3.2.2. Expression profile of mRNAs in DMM right and left knee

The microRNA microarray profiling revealed approximately 35 miRNAs modulated in the DMM model at 3 different time points, and whilst changes in expression are small, this may suggest that these miRNAs may have a role in regulating the onset of OA. For further filtering of miRNAs having important roles amongst these modulated miRNAs, examining the mRNA expression profile would be useful since miRNAs exert their function by directly targeting and subsequently inhibiting mRNA expression. Additionally, since no major modulation of miRNA expression level was observed until 7 days after DMM surgery, it was sufficient to profile mRNA expression for two time points i.e. 1 and 7 day following DMM surgery.

The Illumina BeadArray-based: MouseWG-6 v2.0 Expression BeadChip was used to profile more than 45,000 mouse transcripts in the pooled total RNA samples (DMM right and left knee), previously subjected to miRNA profiling. Consistent with the miRNA profile, mRNA array data also showed a similar expression pattern: no major change in mRNA expression level until day 7 when comparing between DMM right and left knee (Figure 3.3). If the absolute fold change cutoff is set at 1.5, only 30 mRNAs changed expression at day 1 whilst at day 7, more than 683 mRNAs were modulated. The full lists of mRNA which changed expression are in Appendix, Table 6, 7.

A subset of mRNA differentially expressed by microarray analysis was selected for revalidating the array data. Comparison of the expression levels between the mRNA microarray and quantitative real-time qRT-PCR demonstrated a similar expression pattern between the two platform for 4 genes i.e. *CCL2, IL6, SAA3, Arginase-1* (Appendix, Figure 2). These results confirmed the mRNA array data.

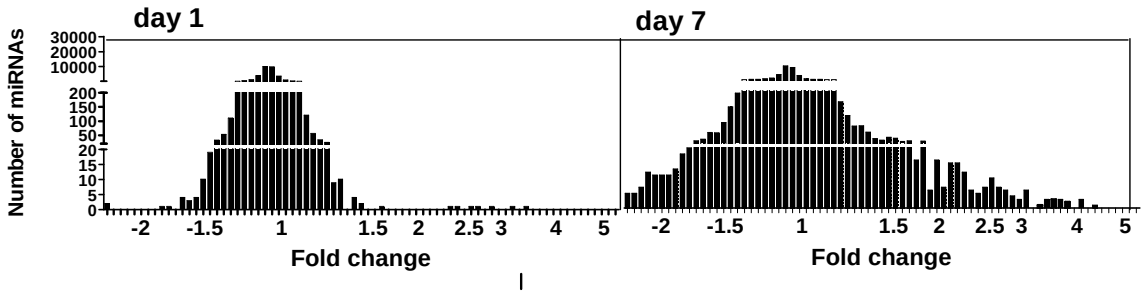

Figure 3.3 Total numbers of mRNAs at different fold change value at day 1 and day 7 following surgery in DMM model.

At each time point, Fold change = intensity value in DMM right - intensity value in DMM left. Numbers of mRNAs were calculated as fold change ranging from -3 to 7 for each increase of 0.05. Fold change: > 1: increase expression; < 1: decrease expression.

3.2.3. Integrated miRNA and mRNA expression profiles of the DMM model identify miR-29b as a miRNA associated with OA onset

To prioritize miRNAs which might have a role in OA onset in the DMM model, an integrated analysis between miRNA and mRNA profiles at 1 and 7 day of the DMM model was performed. This approach took advantage of inverse correlation analysis in which a miRNA was considered as a potential candidate if it was differentially expressed, and inversely correlated with the expression of its putative targets in the same biological samples.

Steps for the miRNA and mRNA profile integrating analysis include: (i) predicting miRNA putative targets by searching for 4 different types of seed sequences e.g. 6-, 7 match 8-, 7 A1-, and 8-mer seed sequences located in the 3' UTR; (ii) integrating expression levels at each time point in the DMM model for all miRNA targets; (iii) searching for a miRNA's putative target enrichment which is given more detail below.

If a miRNA has an impact in the pathological changes in the DMM model and could exert its suppressive function on variety of targets, then when it is down-regulated, there should be an enrichment of its predicted targets among up-regulated mRNA and vice versa. This means that for downregulated miRNAs, a greater percentage of upregulated mRNAs will be their targets and the inverse pattern will be observed for an upregulated miRNA. This should also be true when comparing between different time points, 1 and 7 days in the DMM model. For instance, if a miRNA was repressed across the 7 day time course, the percentage of its targets amongst up-regulated mRNA at day 7 should be higher than at day 1. Together with this, for a downregulated miRNA, an enrichment of miRNA targets in up-regulated mRNAs over unmodulated mRNAs should also be observed at each time point or across the time course.

Additionally, fold change threshold is another challenge faced in integrating analysis. In fact, it is almost impossible to choose the "right" cut off as the normal 1.5 fold change would be too stringent, and consequently, the power to detect potential miRNAs would be very low. To overcome this, in this study, all calculations were done for all fold change values greater than 1 at 0.05 fold intervals.

The integrating analysis for the miRNA and mRNA array data in the DMM model showed that amongst the differentially expressed miRNAs, miRNA-29b is the most interesting. Indeed, a substantial enrichment of miR-29b putative targets which was inversely correlated

with the miRNA expression level was observed at each time points (Figure 3.4, Figure 3.5). At day 1, when miR-29b increased expression, 6mer- and 7mer match 8- targets in the down-regulated section were dominant compared with the up-regulated section (Figure 3.4). Conversely, at day 7, when miR-29b decreased expression, there was a strong enrichment of targets with 4 different types of seed sites in the up-regulated section over the down-regulated (figure 3.4). Also at day 7, the ratio up-regulated targets/unchanged targets was substantially higher than the ratio down-regulated targets/unchanged targets (Figure 3.5).

The inverse correlation between miR-29b and its potential targets was also observed across the time course: whilst miR-29b level was down-regulated from day 1 to day 7, there was a substantial increase of miR-29 targets in the up-regulated mRNAs at day 7 compared with day 1. Consistent with this, the ratio up-regulated targets/unchanged targets showed an enrichment at day 7 (Figure 3.5). All of the data above suggest that miRNA-29b has a potential functional role in OA onset in the DMM model and was selected as the candidate miRNA for further functional studies.

From miRNA microarray data, miR-29b is the one on two miRNAs increased expression with 1.5 fold change at day 1 following DMM surgery. Real-time qRT-PCR was used to re-measure expression level of miR-29b in the DMM samples and sham surgery samples. The Real-time qRT-PCR data confirmed miRNA microarray data and showed a significant increase of miR-29b expression level in DMM right compared with left knee or sham surgery (Figure 3.6).

MicroRNA-29b is a member of the miR-29 family including miR-29a and miR-29c with the mature sequences differing at nucleotide positions 10, 18, 21, 22, or 23 but sharing a common seed sequence for target recognition. We hypothesized that not just miR-29b but all members of miR-29s may contribute to OA onset, as all miRNA-29s showed a downward trend at all 3 time points even though the difference did not reach statistical significance. Therefore, in this study, we investigated the link between all miR-29 members with OA rather than just miR-29b alone.

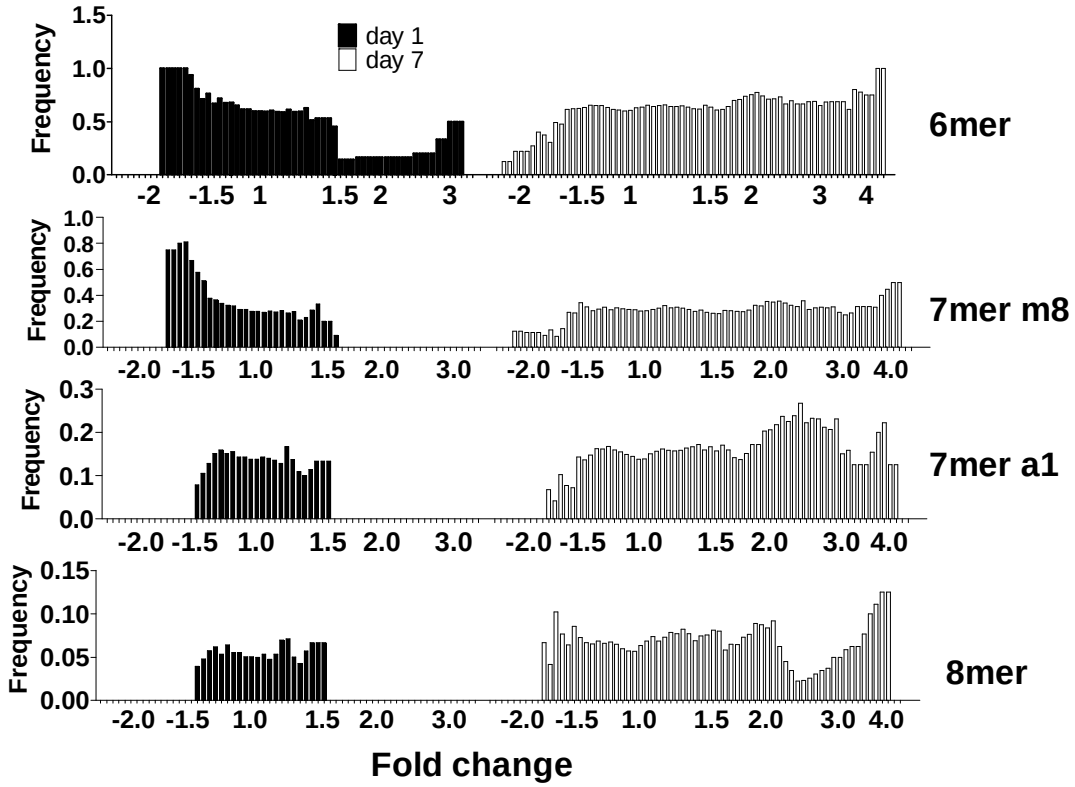

Figure 3.4 Percentage of miR-29 predicted targets in differentially expressed mRNA at day 1 and day 7 after surgery in DMM model.

The calculation was done for all the fold changes ± 0.05 from -2.5 to 4.0 and for each type of seed sequence e.g. 6mer, 7mer match 8, 7mer a1, 8mer. The mRNA having more than one binding site for each type of seed sequence was always assigned as 1. At k fold change, the percentage of 6mer-seed-site targets in modulated mRNAs was calculated: **a_6mer**= sum of mRNA having 6mer-seed site sequence in their 3'UTR with the fold change in the range (k, k+0.05); **b_k**= sum of mRNA with the fold change in the rank (k, k+0.05); **Freq= a_6mer/b_k**. The percentage of other seed site targets was calculated similarly. Day1: closed bar, day 7: opened bar.

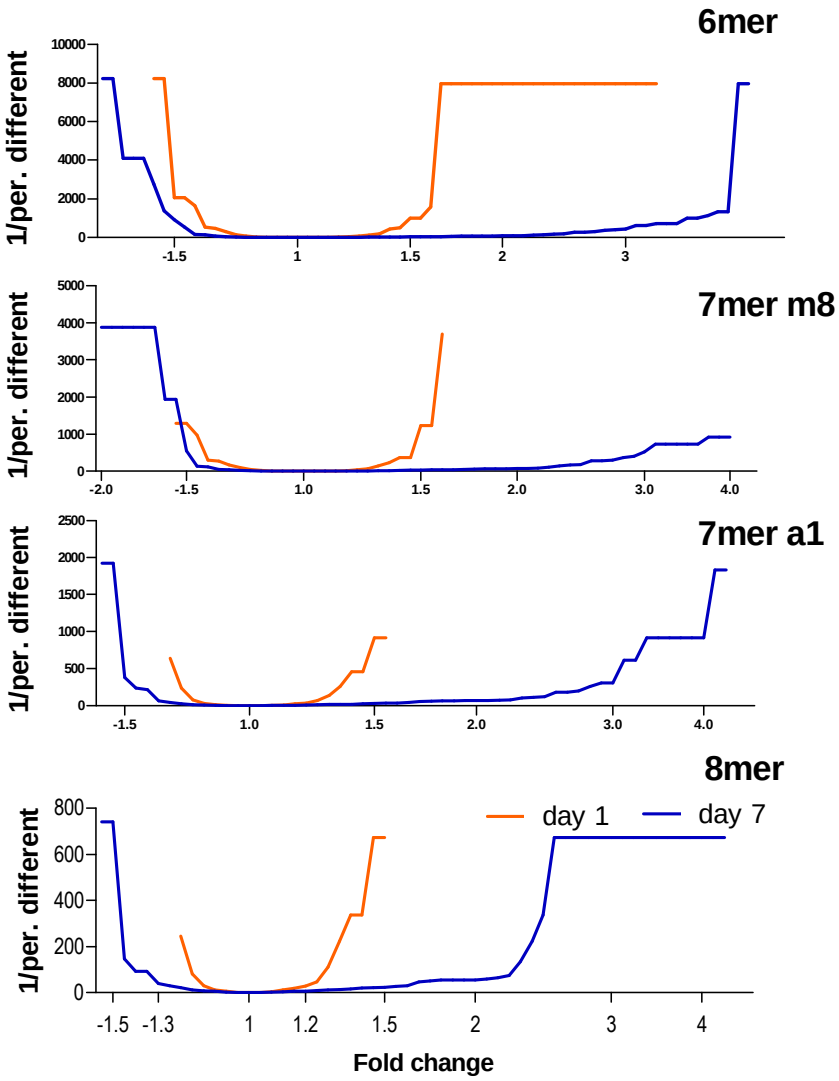

Figure 3.5 Percentage of miR-29 targets that changed expression compared to unchanged expression at day 1 and day 7 after surgery in DMM model.

The calculation was done for all the fold change (FC) ± 0.05 from each other from -2.5 to 4.0 and for each types of seed sequence e.g. 6mer, 7mer match 8, 7mer a1, 8mer. The mRNA having more than one binding site for each type of seed sequence was always assigned as 1. When FC=k, the percentage of 6mer-seed-site targets which increased or decreased expression was calculated: **6mer_changed** = sum of mRNA having 6mer-seed site sequence in their 3'UTR with FC in the range (k, FC max) if k >0, or (FC min, k) if k<0; **6mer_unchanged** = sum of mRNA having 6mer-seed site sequence in their 3'UTR with FC range in (0,k] if k>0, or (k, 0] if k< 0; **1/Per.different = 6mer_unchange/6mer_changed.** The percentage of other seed site targets was calculated similarly. Day1: red line, day 7: blue line.

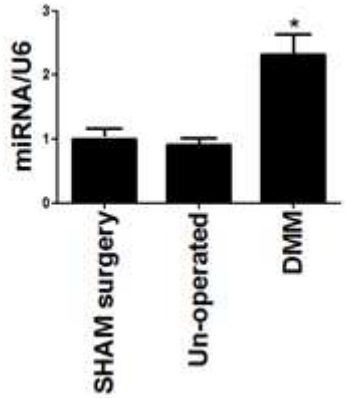

Figure 3.6: MicroRNA 29b was significantly induced in the DMM model at 1 day after surgery

Total RNA was reversed transcribed to cDNA and miR-29b expression was measured by real-time qRT-PCR in individual samples of sham right knee (sham surgery), DMM left knee (un-operated), and DMM right knee (DMM) at 1 day after surgery. U6 was used as endogenous control. Expression level of miR-29b in DMM and sham surgery was normalized to un-operated control. The data show mean +/- SEM, n=3. The expression of miR-29b between each group was analysed by unpaired two-tailed t test * $p<0.05$, ** $p < 0.01$, *** $p<0.001$.

3.2.4. Up-regulation of miR-29s in the murine hip avulsion injury model

Traumatic joint injury and joint magliment are linked to OA initiation. Patients with traumatic joint injury show an increased risk of OA, implicating the early events post-injury as important in the long term. To investigate the role of miR-29s in the onset of OA, a murine hip cartilage avulsion injury model, where the murine hip femoral cap cartilage was sub-cultured in serum-free media across a 48 hour-time course, was used. Total RNA was isolated from the explants using Trizol, reverse transcribed to cDNA by either SuperScript II reverse transcriptase (for mRNA detection) or miRCURY LNA^{TM} Universal cDNA synthesis (for miRNA detection). Expression levels were measured by real-time qRT-PCR.

The majority of the genes rapidly induced in murine joints following surgical destabilization (DMM model) were also regulated in murine hip cartilage explants upon injury (Chong et al. 2013). Interestingly, some genes such as *Dkk3, Ccl2, Il6* were significantly regulated after 3 hours in culture (Appendix, Figure 3) though likely regulating genes which are modulated at later time points. The expression pattern of the miR-29 family is similar to each other and tends to increase across the 48 hour time course (Figure 3.7): miR-29b and 29c significantly increased expression after 12 hours in culture; miR-29a significantly after 6 hours. This suggests that the regulation of the miR-29s may contribute to the molecular mechanism underlying the initiation of OA.

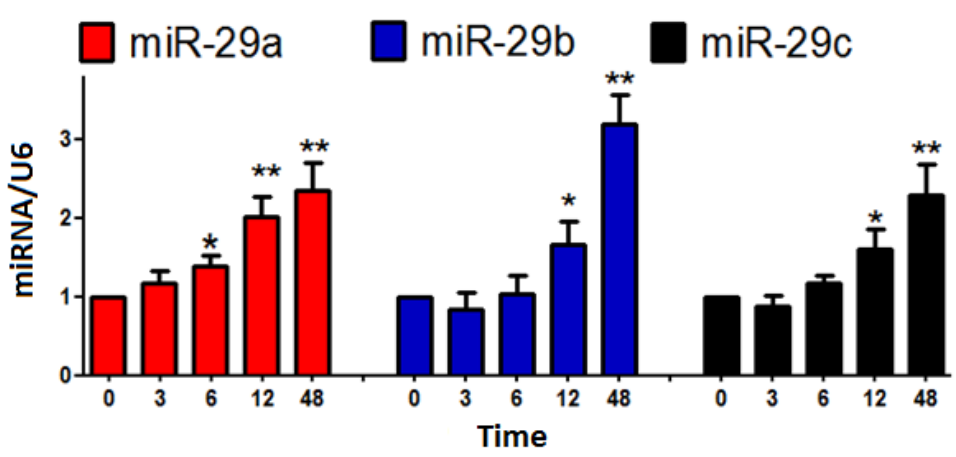

Figure 3.7: Expression of the miR-29 family in the hip avulsion injury model

The femoral caps of C57Bl/6 mice aged 4 weeks were avulsed and put in culture. At each of 3, 6, 12, 48 hour time points, the femoral caps were harvested. Total RNA was isolated using Trizol and reverse transcribed to cDNA. Expression of the mature miR-29 family was measured by real-time q-RTPCR where U6 was used as an endogenous control. At least triplicate samples were measured at each time. Means ± standard errors are presented, n=6. Difference in expression between each time point against control (t=0) was calculated by unpaired two-tailed t test. * $p<0.05$, ** $p < 0.01$, *** $p<0.001$.

3.2.5. Up-regulation of the miR-29 family in human end-stage OA cartilage

To determine whether the miR-29 family could play a role in human OA, its expression level was compared between hip / knee OA cartilage and non-disease tissue controls (hip cartilage followingfracture to the neck of femur).

Human articular cartilage samples (total: 8 hip and 7 knee OA cartilage, 7 healthy fracture to the neck of femur) were obtained from patients undergoing total hip/ knee replacement surgery at the Norfolk and Norwich University Hospital. Total RNA was isolated from all cartilage samples using Trizol and followed by a purification step through column using miRVana kit. The total RNA was reverse transcribed to cDNA using miRCURY LNA™ Universal cDNA synthesis. Expression of all miR-29 members was measured by real-time qRT-PCR with U6 as the endogenous control.

Data (Figure 3.8) showed an increase in miR-29 expression in hip OA but decrease in knee OA cartilage compared to fracture control. This reached significance, or close to significance in each case. Whilst there is no comparison with normal knee cartilage, these data show that the miR-29 family is regulated in human end-stage OA cartilage.

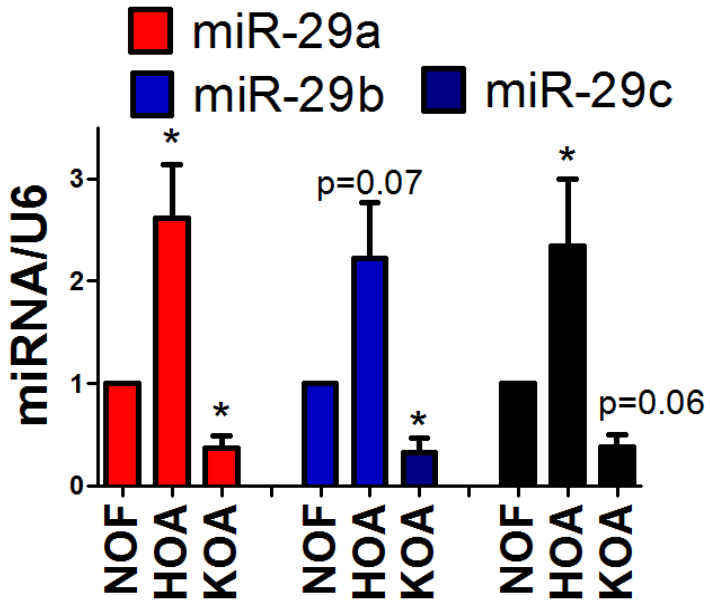

Figure 3.8: Expression of the miR-29 family in human OA cartilage

Total RNA was isolated from human articular cartilage of either end-stage OA patients or healthy controls and reverse transcribed to cDNA. Expression of the mature miR-29 family was measured by real-time qRT-PCR using U6 as an endogenous control. HOA (hip osteoarthritis cartilage, n=8), KOA (knee osteoarthritis, n=7), NOF (neck of the femur, n=7). Means ± standard errors are presented. Difference in expression between each time point against control (NOF) was calculated by unpaired two-tailed Student's t test. * $p<0.05$, ** $p < 0.01$, *** $p<0.001$.

3.2.6. The miR-29 family is regulated with chondrocyte phenotype

Dedifferentiation and the loss of phenotype is an obstacle in expanding human chondrocytes: the cells stop expressing aggrecan and collagen type II, and this limits capacity to form cartilage. In line with this, alteration chondrocyte phenotype is one of the characteristics of OA. As compared with normal articular cartilage, the chondrocytes embedded in different zones of OA cartilage were shown to express different markers of chondrocyte differentiation: chondrocytes in the middle zone re-expressing chondroprogenitor phenotype; cells in the upper middle zone expressing type III collagen (dedifferentiated phenotype) (Aigner *et al.* 1993). Assessing whether the miR-29 family is regulated with chondrocyte phenotype, therefore, would help to further determine the relevance of the miR-29 family in cartilage function.

This was investigated using human primary chondrocyte dedifferentiation model. After isolation from human knee OA cartilage by collagenase (collagenase-post digested HACs (PD)), primary chondrocytes were cultured in monolayer (primary culture HACs (P0), and three sequential passages were performed at 1: 3 dilution of cells (passage 1 to passage 3). Total RNA was isolated from cartilage, PD, P0 to P3 chondrocytes and reverse transcribed to cDNA. The expression level of all the miR-29 family was then measured by real-time qRT-PCR.

The expression of the miR-29 family was found to significantly decrease when HACs were passaged in monolayer (Figure 3.9), indicating the putative role of the miR-29 family in chondrocytic phenotype.

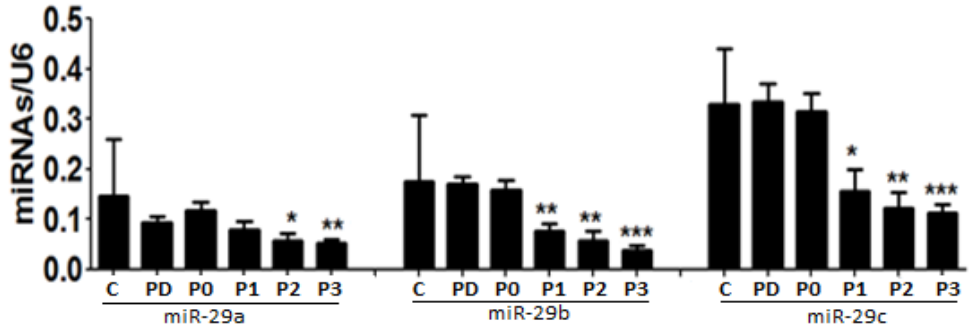

Figure 3.9: Expression of the miR-29 family in a chondrocyte dedifferentiation model

Human primary chondrocytes were isolated from the articular cartilage of 8 knee OA patients using collagenase digest. The cells were put in culture and passaged 3 times. Total RNA was isolated from either human articular cartilage (cart) or chondrocytes post digestion with collagenase (PD) or each passage 0, 1, 2, 3 (P0, P1, P2, P3). After reverse transcribing to cDNA, expression of the mature miR-29 family was measured by real-time qRT-PCR (U6 was used as an endogenous control). Mean ± standard errors are presented, n=8. Different in expression between was calculated by unpaired two-tailed t test. * $p<0.05$, ** $p < 0.01$, *** $p<0.001$.

3.2.7. MicroRNA-29s expression in chondrogenesis

Chondrogenesis is the earliest phase of skeletal development, occuring as a result of: mesenchymal cell condensation, chondroprogenitor cell differentiation, chondrocyte differentiation and maturation. Chondrogenesis results in the formation of cartilage and bone in the process of endochondral ossification (Goldring *et al.* 2006). It is pertinent to examine the role of miR-29 in chondrogenesis, particularly since the replay of this developmental process may contribute to osteoarthritis.

To determine the expression and therefore possible role of the miR-29 family in chondrogenesis both human and mouse chondrogenesis models were used. **Human chondrogenesis model**: human bone marrow stem cells were differentiated to form a cartilage disc (the model was kindly developed by Dr Matt J. Barter (Newcastle University, UK)); **Mouse chondrogenesis model**: the embryonic carcinoma cell line ATDC5 was stimulated to from chondrocytes using insulin for 42 days (this model was developed by Dr Tracey Swingler (University of East Anglia)). Total RNA was isolated, reverse transcribed to cDNA and used for measuring expression level of the miRNA by real-time qRT-PCR.

In the human chondrogenesis model, a significant down-regulation of the miR-29s after 3 days of differentiation was observed; after that, miR-29s return to the original expression levels (Figure 3.10). A similar expression pattern was also observed in the murine ATDC5 chondrocyte differentiation model: significantly decreased expression of all the miR-29 members after 14 days differentiation; with a return after 36 days, to the original level (Appendix, Figure 4). These data imply that miR-29 may be a negative regulator of the early stage of chondrogenesis.

Indeed, the miR-29 family was not the only miRNA regulated in either the human or murine chondrogenic process, many other miRNAs were strongly modulated e.g. (Barter et al, unpublished data) (Swingler et al. 2012). However, it can be postulated that the miRNA would have a functional role in chondrogenesis if it had affected on mRNA expression. To test this hypothesis, again an integrating analysis approachs (using mRNA expression profile data to analyse miR-29 putative target genes) was used. A substantial enrichment of miR-29 targets was inversely associated with the expression of miR-29s was observed (Data not shown). Together, these data suggest that the miR-29 family acts as the negative regulator of chondrogenesis, leading to an increase in mRNA to enable the process.

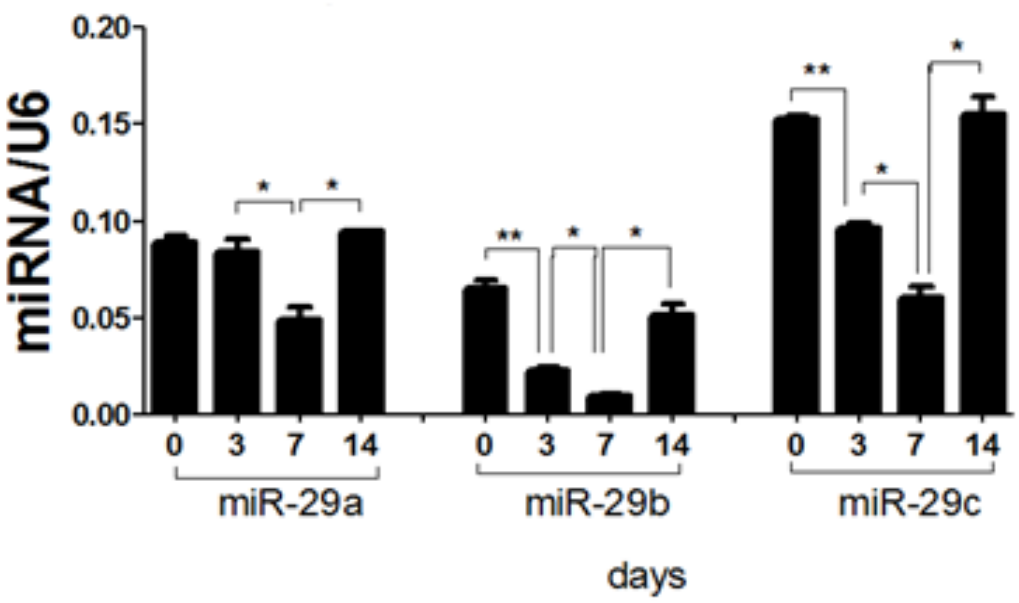

Figure 3.10: Expression of the miR-29 family in the human chondrogenesis model.

Human bone marrow stem cells (from 3 donors, 18-25 years of age, $5x10^5$ cells in 100µl growth medium) were put into polycarbonate Transwell filters and centrifuged in 24 well plates. 0.5ml chondrogenic culture medium containing 100µg/ml sodium pyruvate, 10ng/ml TGFβ3, 100nM dexamethasone, 1x ITS, 40µg/ml proline, and 25µg/ml ascorbate-2 phosphate was added to the lower well. Media were replaced every 2 or 3 days up to 14 days. At 0, 3, 7, 14 days, the cells were harvested and total RNA was extracted using Trizol. The RNA was then reverse transcribed to cDNA and was used for measuring the expression level of the mature miR-29 family by real-time qRT-PCR (U6 was used as an endogenous control). Assays were repeated 3 times. At least triplicate samples were in each time. Means ± standard errors are presented. Difference in expression between each time point was calculated by unpaired two-tailed t test. * $p<0.05$, ** $p < 0.01$, *** $p<0.001$.

3.2.8. The miR-29b is expressed in murine limb development

The formation of the skeleton first is initiated with the formation of a precartilage condensation (anlagen) which is followed by chondrogenesis triggered in the precartilage condensation and ultimately cartilage is formed. This process involves the cooperation of many cell activities e.g. migration, adhesion, intracellular signalling, and proliferation (Goldring et al. 2006). Given the likely involvement of the miR-29 family in chondrogenesis, it is pertinent to ask whether miR-29s are expressed in murine limb development. Additionally, the miR-29 family or its members have been shown to control cell proliferation and apoptosis in different tumour types. A murine model would thus be a useful model to study the role of the miR-29 family in cell proliferation and apoptosis limb development.

In mice, the forelimb starts to develop at stage E9.5 whilst the hindlimb starts behind by about half a day. Five days later, a miniature model of the adult limb is formed (E14.5 and E15 for fore and hindlimb, respectively). At stage E11, a distinct apical ectodermal ridge at the limb tip is formed in the forelimb and the handplate is beginning to form at E11.5. Similarly events happen in the hindlimb at half a day later (at E11.5 and E12) (Martin 1990).

Whole mount *in situ* hybridization was conducted using amiRCURY LNA^{TM} miR-29b-3p double-DIG labelled probe to detect the expression of miR-29b in the mouse embryo stage E11.5 and E15. The data showed that: at stage E11.5, miR29b was expressed in the cartilage of both fore and hindlimb; at stage E15 when the small scale the adult limb was formed, miR-29b was strongly expressed, implicating miR-29b playing a role in murine limb development. Besides limbs, miR-29b was also found on the brain and the spine of embryo stage E11.5 (Figure 3.11).

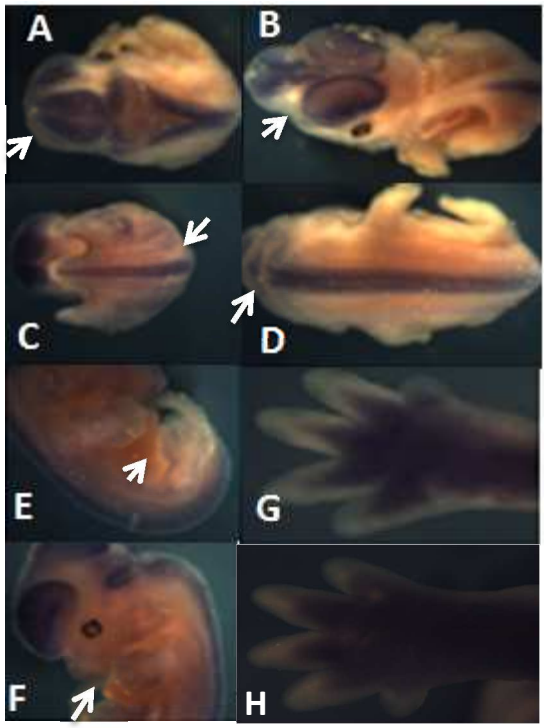

Figure 3.11: Whole mount *in situ* hybridization of miRNA-29b in murine embryo stage E11.5 and E.15.

Using a miRCURY LNA^{TM} double-DIG labelled miR-29b probe, miR-29b was found to be expressed: in the embryo stage E11.5 in the brain (A), mouth (B), spine (C-D), hindlimb (E), forelimb (F); in the embryo stage E15 in hindlimb (G) and forelimb (H).

3.3. DISCUSSION

The principal aim of this study was to begin to identify the miRNAs which were implicated in the early stages of OA and elucidate their function. Whilst there have been a number of studies on the role of miRNAs in OA pathogenesis, they have not focused on the disease onset. In the present study, for the first time, the miRNA expression profile was reported for the DMM mouse model at early time points e.g. 1, 3, 7 days following surgery. The fact that only a small number of miRNAs changed expression across the first three days after DMM surgery might indicate miRNAs mainly contribute in disease progression rather than initiation. However, there are some limitations of the study which prevent a firm conclusion about the role of miRNAs in the early stages of the disease. Total RNA for the miRNA microarray was isolated from whole knee joints of DMM mice. Thus, if a miRNA is expressed in a single tissue e.g. cartilage, bone, meniscus, ligament or synovium, pooling of tissues will reduce the signal to a lower level than in the individual tissue and that could be the explanation for the overall low levels of modulated miRNAs observed in the present study. Moreover, insufficient controls, e.g. naïve samples and genes responding to sham surgery in this study may also have been problematic. The DMM model does not completely recapitulate human OA pathogenesis, e.g. with more synovial involvement in the latter.

However, it remains unlikely that the miRNA microarray data acquired from the DMM model in this study is incorrect. The DMM left knee (no surgery) used as a control would show the consequence of surgery, even if it can't distinguish injury per se from early OA. Moreover, Burleigh et al (2012) reported a large and significant difference in expression levels of e.g. *Ccl2, Arg1e, Il6, Saa-3* in the same DMM model just 6 hours following surgery, which was interpreted as response to surgical destabilization rather than reaction to injury (Burleigh *et al.* 2012). In this study, such an increase in expression was also observed when comparing between the DMM right and DMM left, suggesting that the DMM left knee can act as a suitable control. Hence, it was expected that the changes in miRNA expression at early time points would be greater.

MicroRNA-29b, one of only two miRNAs significantly increased in expression at day one post-surgery and inversely correlated with expression of its putative targets, was investigated in detail. The miR-29b is encoded by two loci in the human genome e.g. the primary miR-29-a/b1 cluster in chromosome 7, and the primary miR-29b2/c cluster in chromosome 1.

Normally, clustered miRNAs in humans work in combination to accomplish their function. At the transcriptional level, at least one of the other miR-29 family members i.e. miR-29a or miR-29c will be co-transcribed with miR-29b. In addition, miR-29b is reported to have a short half-life (the time taken for the miRNA to fall to half of its original value) which is linked to the presence of uracil bases at positions 9-11, compared with miR-29a (more stable with a reported half-life of > 12 hours) (Zhang *et al.* 2011). Thus, in the DMM model at 1 day after surgery it would be expected that a significant increase in either miR-29a or miR-29c would accompany that of miR-29b. However, only miR-29b increased in expression (1.5 fold change in array data) but not any of the other miR-29 family members, perhaps implicating another post-transcriptional regulatory mechanism controlling miRNA processing. In line with the DMM model data, in a murine hip avulsion injury model, an increasing expression level was also observed for all miR-29 members post injury. Interestingly, a similar pattern of expression of some genes strongly induced in the DMM model at 6 hours after surgery (Burleigh et al. 2012) was seen in the injury model suggesting some molecular similarities between the two models. In line with this, Chong et al (2013) also observed a similar pattern when measuring the expression of the set of gene induced expression in DMM model 6 hours after surgery and in murine injury model in which the hip cartilages cultured for 6 hours (Chong et al. 2013). Since mechanical factors following traumatic joint injury may mediate OA onset, these data suggest for the first time an important role for the miR-29 family in the initiation of OA. The fact that the miR-29 family increased in expression in human OA end-stage cartilage supports a role for the miR-29s in the disease. In this study, human knee cartilage normal controls were not available, and the difference in hip and knee cartilage may explain in part why the miR-29 family levels increased in hip but decreased in knee OA cartilage compared to human hip fracture control. Also, in this project, the miR-29 family expression level is very variable across a human tissue panel e.g. heart, brain, lung, spleen (data not shown). In supporting these data, previous published data also demonstrated the different expression level of the miR-29 family in different tissues in zebrafish (Wienholds *et al.* 2005). These data suggest that the mechanisms controlling the miR-29 family expression in different tissues are not similar. The fact that miR-29 family expression was modulated in different mouse models and in human OA cartilage implies a role for the miR-29 family in cartilage, and suggest that the two pri-miR-29a/b1 and pri-miR-29b2/c clusters may be involved in both early and late stages of the disease. The direct mechanism

controlling miR-29 family expression and the extent to which each cluster contributes to OA remains unknown and is worthy of further investigation.

This study also provides evidence for the role of the miR-29 family in cartilage formation as its expression was regulated during human and mouse chondrogenesis and inversely correlated with its putative targets. In fact, such decreased expression level at an early stage of chondrogenesis is in line with published data e.g. Guerit et al (2013) showed the decreased expression of miR-29a is essential for chondrogenesis via its regulation of FOXO3a (Guerit *et al.* 2014); Sorentino et al (2008) found miR-29b was among miRNAs down-regulated when differentiating human MSCs through chondrogenesis (Sorrentino et al. 2008); Yan et al (2011) demonstrated that both miR-29a and miR-29b were significantly decreased in a chondrogenesis model where mouse MSC were grown on polyhydroxyalkanoates (Yan et al. 2011). However, I have demonstrated for the first time that all miR-29 family members are involved in chondrogenesis, stressing the important role of both miR-29 clusters in controlling cartilage homeostasis in human and mouse. In contrast to this data, there are others studies profiling the expression of miRNAs in murine and human chondrogenesis model (Suomi et al. 2008, Lin et al. 2009, Miyaki *et al.* 2009, Lin et al. 2011, Yang et al. 2011). The miR-29 family, nevertheless, was not amongst the miRNAs which had altered expression. This is not surprising and could be attributed to differing design of experiments including inducers of differentiation, cell type, numbers of detected miRNA probes and organism. In addition, despite of being a negative regulator of chondrogenesis, miR-29b was found to express in murine limb development. A number of published data report that the miR-29 family can act as oncogenes whose expression induces cell proliferation but inhibits apoptosis. Whether the miR-29 family is involved in murine limb development through inducing chondrocyte proliferation in the growth plate remains unknown. Therefore, examination of the role of miR-29 family in limb development in vivo will be a priority for future studies.

Another piece of data supporting the role of the miR-29 family in OA comes from the fact that expression of the miR-29 family is decreased during chondrocyte dedifferentiation. Again, other groups have profiled miRNAs in human dedifferentiation models (Karlsen et al. 2011, Lin et al. 2011) but the miR-29 family has not shown up in any of them. As mentioned above, this could be attributed to many different factors.

Taken together, all of these data show that the miR-29 family may modulate both cartilage homeostasis and OA and make a compelling case for further investigation. In this PhD thesis, for the first time, the whole miR-29 family is reported to be involved in OA although the increase of the miR-29b in OA had been shown (Moulin *et al.* 2012). Nevertheless, the miRNA-29 family has been implicated in many other areas of pathology. Many publications have reported the involvement of the miR-29 family in cancers where the miRNA family or a single member could serve as either a tumour suppressor or an oncogene. In rhabdomyosarcoma (Wang *et al.* 2008), nasopharyngeal carcinoma (Sengupta *et al.* 2008), hepatocellular carcinoma (Xiong *et al.* 2010), acute myeloid leukemia (Eyholzer et al. 2010) , multiple myeloma (Zhang *et al.* 2011, Amodio *et al.* 2012), chronic lymphocytic leukemia (Santanam *et al.* 2010), glioblastoma (Cortez *et al.* 2010), and lung (Fabbri *et al.* 2007) and pancreatic cancer (Muniyappa *et al.* 2009), miR-29 was described as a tumor suppressor whilst in acute myeloid leukemia , colorectal liver metastasis (Wang *et al.* 2012), and breast cancer (Chou *et al.* 2013) , miR-29 was shown to be as tumour promoter.

Besides cancers, the miR-29 family has been shown to participate in a number of physiological processes including (i) **muscle development** e.g. knockdown of miR-29b in vivo induced cardiac fibrosis in mice; miR-29a/b1 inhibition induced vascular smooth muscle cell calcification; miR-29 family expression was developmentally up-regulated in porcine skeletal muscle from fetal to adult, and this was also true in mice and human; the miR-29 family was found to be down-regulated in myotonic dystrophy type I and Duchenne muscular dystrophy (Wei *et al.* 2013), (ii) **bone formation** e.g. miR-29a increased bone mass, induced osteoblast differentiation, and inhibited osteoclast differentiation; reduced miR-29a expression was associated with low bone mass and poor skeletal microarchitecture in rats treated with glucocorticoids (Wang *et al.* 2013), (iii) **HIV virus infection** e.g. ectopic expression of miRNA-29a resulted in reduction of HIV virus levels, implicating this miRNA as a potential strategy in developing anti-HIV therapeutics (Ahluwalia *et al.* 2008), (iv) **aging** e.g. miR-29 family up-regulation was observed in a number of different organs e.g. liver, muscle, and brain of several aging models (Ugalde *et al.* 2011, Fenn *et al.* 2013, Hu *et al.* 2014), (v) **diabetes** e.g. the miR-29 family was up-regulated in diabetic rats and forced expression of miR-29 inhibited insulin induced glucose imported by 3T3-L1 adipocytes (He *et al.* 2007); reduced miR-29b in plasma samples of type 2 diabetes patients anticipated the

manifestation of the disease (Zampetaki *et al.* 2010); miR-29c was found up-regulated the kidney glomeruli from diabetic mice (Long *et al.* 2011); the continued expression of miR-29 isoforms in the pancreatic β-cell seems to be required for normal and selective stimulation of insulin secretion by glucose (Pullen *et al.* 2011); (vi) **fibrosis development**, the miR-29 family has been shown to be implicated in the development of fibrosis of many organs including heart, kidney, lung, liver, and systemic sclerosis; (vii) **Alzheimer disease,** the miR-29a/b1 cluster or miR-29a was significantly decreased in Alzheimer patients (Hebert *et al.* 2008, Shioya *et al.* 2010).

In conclusion, with all of the data above, the miR-29 family may play a key role in Osteoarthritis and of is worthy of further investigation. The mechanisms which control its expression together with its function in chondrocytes will be described in the next chapters.

CHAPTER IV
FACTORS THAT CONTROL EXPRESSION OF THE MICRORNA-29 FAMILY

4.1. Introduction

In the previous chapter, evidence for the involvement of the miR-29 family in cartilage homeostasis and OA was presented. The increased expression of the all family members is apparent in both early and late stages of OA. However, which factors or mechanisms are responsible for miR-29 induction or repression in chondrocytes remains unknown and is worthy of further investigation.

The miR-29 family is intergenic miRNAs and is encoded in two gene clusters e.g. one for the primary miR-29a/b1 on chr.7q32, and the other for the primary miR-29b2/c on chr.1q32.2 (Saini *et al.* 2007, Chang *et al.* 2008). The miR-29b1 and miR-29a precursors are processed from the pri-miR-29a/b1 last intron (Genbank accession EU154353) whist the miR-29b2 and miR-29c precursors are from the pri-miR-29b2/c last exon (Genbank accession EU154352 and EU154351) (Chang et al. 2008) (Figure 4.1). These precursors are all transcribed as polycistronic primary transcripts (Chang et al. 2008, Mott *et al.* 2010) upon which various transcriptional regulators e.g. NFκB (Liu *et al.* 2010, Mott et al. 2010), supressors (c-Myc (Mott et al. 2010, Parpart *et al.* 2014), Sp1(Liu et al. 2010, Amodio *et al.* 2012), Gli (Mott et al. 2010), Yin-Yang-1, Smad3 (Qin *et al.* 2011), Ezh, H3K27, HDAC1, HDAC3), or inducers (Gli, SRF, Mef2, TCF/LEF, GATA3 (Chou et al. 2013), CEBPA (Eyholzer et al. 2010)), and signalling pathways e.g, Wnt , TGFβ, TLR/NFκB, TNFα/NFκB, hedgehog signalling have been reported to be directly and/or indirectly involved. For instance, **both canonical and non-canonical Wnt signalling** was reported to induce the miR-29 family level in different cellular contexts: Wnt3a rapidly induces miR-29 levels in osteoblastic cells (Kapinas *et al.* 2009, Kapinas et al. 2010) or in muscle progenitor cells (MPCs) (Hu *et al.* 2014), respectively, at least in part through the two putative TCF/LEF-binding sites in the miR-29a promoter (Kapinas et al. 2010); non-canonical Wnt signalling through Wnt7a/Frizzled 9 resulted in increased expression of only the mature miR-29b but not miR-29a or c or any miR-29b primary or precursor forms in non-small lung cancer cell lines H661 and H15 (Avasarala *et al.* 2013). In addition, ERK5 and PPARγ, key effectors of the Wnt7a/Frizzled 9 pathway, were also observed to be strong inducers of miR-29b expression (Avasarala et al.

2013). In contrast to Wnt signalling, **TGFβ/Smad3 signalling** was shown to negatively regulate miR-29 family expression in different cell lines e.g. human aortic adventitial

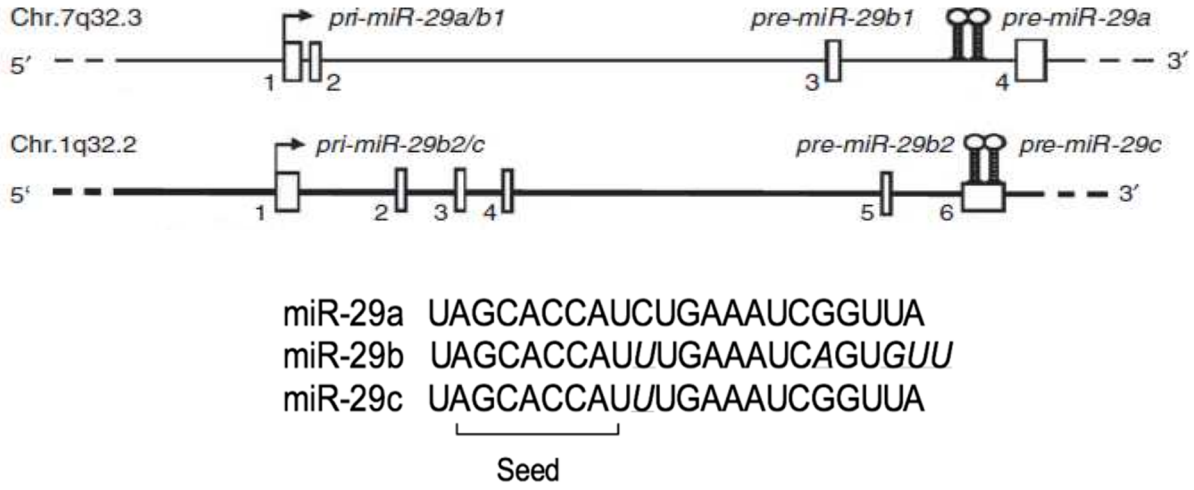

Figure 4.1: Genomic organization of the miR-29 family

The miR-29 family includes three members miR-29a, miR-29b and miR-29c. The primary pri-29a/b1 is located in chromosome 7 containing pre-29a and pre-29b1. The primary pri-29b2/c is located in chromosome 1 including pre-29b2 and pre-29c. The hairpins indicate the locations of the sequence encoding precursors of miR-29s. Pre-29a and pre-29c will process into mature miR-29a and miR-29c, respectively. Pre-29b1 and pre-29b2 will process into mature miR29b. The mature sequences of the miR-29 family members share identical seed regions. Nucleotides that differ among miR-29s are indicated in italics.

fibroblasts (Maegdefessel *et al.* 2012), renal fibrosis cells (Wang *et al.* 2012, Ramdas *et al.* 2013), murine hepatic stellate cells (Roderburg *et al.* 2011), rat hepatic stellate cells (Kwiecinski *et al.* 2011), human skin fibroblasts (Maurer *et al.* 2010), human tenon's fibroblast (Li *et al.* 2012), human lung fibroblast cell line (Cushing *et al.* 2011, Yang *et al.* 2013). The suppressive effect of TGFβ/Smad3 signalling on miR-29 expression was partly mediated through a Smad3 binding site in the highly conserved region around 22kb upstream of the miR-29b2/c promoter as showed by chromatin immunoprecipitation assay (Qin et al. 2011, Ramdas et al. 2013). Similar to TGFβ, **Toll-like receptor (TLR) signalling and TNFα signalling** have been shown to mediate suppressive effects on miR-29 family expression. In man, treating human cholangiocarcinoma cells with TLR ligands e.g. TLR3 (Poly (I:C)), TLR4 (LPS), TLR5 (flagellin), TLR6 (MALP-2) showed a significant decrease in the miR-29 level beginning after 4 hours of LPS treatment but increasing to 24 hours (Mott et al. 2010); treating human stellate cells with LPS strongly decreased all miR-29 family expression after 1 hour (Roderburg et al. 2011); treating C2C12 myoblasts with TNFα substantially reduced miR-29b and miR-29c expression (Wang et al. 2008); stimulating the choroidal-retinal pigment epithelial cell line ARPE-19 with TNFα resulted in significant down regulation of all miR-29s; conversely, transfecting with a synthetic NFκB decoy, (NFκB inhibitor), rescued the down regulation of miR-29 by TNFα (Χαι *εϖ αλ.* 2014). The activation of NFκB through TLR signalling with its three binding sites in the miR-29a/b1 cluster promoter (-561, -110, and +134) was proven to be the mechanism for the suppression of miR-29a/b1 promoter function (Mott et al. 2010). In mice, miR-29a and miR-29b significantly decreased expression in murine natural killer (NK) cells stimulated with the TLR3 ligand (Poly (I:C)) or phorbol ester (PMA) as well as in splenocytes, NK and T cells of mice infected with L. *monocytogenes* or *Mycobacterium bovis* bacillus Calmette-Guérin (Ma *et al.* 2011). Consistent with the human miRNA, a region about 25 kb upstream of the murine promoter of miR-29a/b1 contains two NFκB binding sites. The second binding site is more conserved between human and mouse and it has been shown to be key for suppression of the miR-29a/b1 promoter (Ma et al. 2011). Importantly, other transcriptional factors, co-operating with NFκB to suppress or induce miR-29 family expression, have also been reported e.g. YY1, Sp1, Ezh, H3K27, HDAC1, HADC3, Mef2, SFR. Forced expression of YY1 in C2C12 lead to a 2-fold decrease of miR-29b and miR-29c levels; similarly, siRNA knockdown of YY1 significantly enhanced expression of miRNA expression. ChIP analysis showed that YY1 did not bind to the miR-29b2/c locus in cells in the absence of NFκB,

suggesting that both pathways are necessarye for silencing the miR-29b2/c locus. Amongst 4 putative binding sites of YY1 in highly a conserved region ~20kb upstream of miR-29b2/c, only one site is bound by YY1 on ChIP assay whereas all 4 sites produced a binding complex with EMSAs using nucleus extract from C2C12. Notably, Ezh, H3K27, HDAC1, whose expression is associated with repression of muscle-specific genes, and recruited by YY1, was also detected by ChIP assay. In line of these transcription factors, Mef2 and SFR, well-known for activating muscle genes, were also found binding to the miR-29b2/c promoter. Again using luciferase reporter assay, a reporter containing a 4.5 kb fragment spanning YY1, Mef2, SFR binding sites was repressed by YY1 or loss of the YY1 binding site but stimulated with either YY1 knockdown or SRF or Mef2 (Wang et al. 2008). In addition, forced expression of Sp1 or NFκB (p65) reduced miR-29b expression; conversely, knockdown of Sp1 or NFκB (p65) by siRNAs resulted in induced miR-29b level (Liu et al. 2010). EMSA assay using probes spanning the -125/-75 miR-29b sequence yielded two major complexes, suggesting Sp1/NFκB acts as a repressive complex interacting with an element of the miR-29b enhancer (Liu et al. 2010). Interestingly, histone deacetylase (HDAC) 1 and 3 contribute to the repressor activity of Sp1/NFκB on miR-29b expression (Liu et al. 2010). Incubation of HDAC1/HDAC3 with ^{32}P-labelled probe from the miR-29a/b1 cluster region together with NFκB p50/p65 and Sp1 showed a delayed and more intense band; HDAC1/3 inhibitors increase miR-29b expression, supporting the interaction of HDAC1 and 3 and Sp1/NFκB with the miR-29b regulatory sequence (Liu et al. 2010). Similar to other signalling mentioned previously, **hedgehog signalling pathway** was also shown to repress miR-29 expression: cells treated with cyclopamine, an inhibitor of Smoothened (a hedgehog signalling component), or transfected with siRNA to knockdown Gli-3, the expression of miR-29b increased (Mott et al. 2010). Along with the transcription factors mentioned above, there are other transcriptional factors controlling miR-29 family expression. The serum alphafetoprotein (AFP), a membrane-secreted protein associated with poor patient outcome in hepatocellular carcinoma, was reported to inhibit miR-29a expression through facilitating c-MYC binding to the promoter of the pri-miR-29a/b. This conclusion was supported by: the inability of AFP to decrease the miR-29a level in the absence of c-MYC protein; c-MYC was abundantly bound to the miR-29a/b1 promoter in the presence of AFP, but did not bind without AFP (Parpart et al. 2014); c-MYC promoter binding protein (MBP), originally described to bind to and repress c-MYC promoter function, up-regulated miR-29b expression

by 6 fold in prostate cancer cells (Steele *et al.* 2010). The haematopoietic master transcription factor, CCAAT/enhancer-binding protein-α (CEBPA), was also reported to activate the expression of miR-29a and miR-29b. Forced expression of CEBPA in acute myeloid leukaemic cells lead to two-fold induced expression of the primary miR-29a/b1 and the mature miR-29a and miR-29b whereas the expression of miR-29b2/c primary transcript remained stable. Using luciferase reporter assays, the sequence, having the conserved region spanning -682 bp upstream to +296 bp downstream of the miR-29a/b1 transcriptional start site and containing 6 potential CEBPA sites, was also strongly induced with CEBPA. Among these binding sites, the one located at +15 to +29 bp was identified to be responsible for CEBPA-mediated activation of the pri-miR-29a/b1 promoter on ChIP assay (Eyholzer et al. 2010). Another transcriptional factor, GATA3, specifying and maintaining luminal epithelial cell differentiation in the mammary gland, was also found to induce miR-29 expression directly by binding to three GATA3 sites in the miR-29a/b1 promoter. Interestingly, GATA3 can induce miR-29s expression by inhibiting the TGFβ and NFκB signalling pathway. Additionally, STAT1 (signal transducer and activator of transcription) a transcription factor induced by interferon γ signalling, was reported to upregulate primary 29a/b1, the pre-29a, pre-29b1, and the mature miR-29a, miR-29b in melanoma cell and T cells (Schmitt *et al.* 2013).

With all the information above, it is likely that in different cellular contexts, the miR-29 family expression is controlled by different transcription factors and signalling pathways. Which factors control its expression in human chondrocytes remains unknown. The effects of a variety of anabolic and catabolic factors e.g. TGFβ, Wnt3a, IL-1, LPS on miR-29 family expression in human chondrocytes were thus investigated. Also, the effect of SOX9, a major specifier of chondrocyte phenotype was also investigated.

Aims:

- Analyse the promoter region (approximately 2kb upstream of the transcription starting site) of the miR-29 family for SOX9 binding sites. Experimentally validate the impact of SOX9 on miR-29 expression.
- Test major anabolic and catabolic cytokines controlling the miR-29 expression in chondocytes.

4.2. Results

4.2.1. The master regulator of chondrogenesis SOX9 suppresses expression of the miR-29 family

The master regulator for chondrogenesis SOX9 has a critical function in a number of development processes e.g. skeletal formation, sex determination, pre-B and T cell development. *SOX9* was found to be expressed in all chondroprogenitors and differentiated chondrocytes, but not in hypertrophic chondrocytes (Ng *et al.* 1997, Zhao *et al.* 1997). Importantly, SOX9 is considered as the critical transcriptional factor for chondrogenic differentiation, partly owing to the fact that its functions are required for differentiating chondrogenic mesenchymal condensations into chondrocytes, and for all stages of chondrocyte differentiation: in mouse chimera, *Sox9* knockout cells were excluded from all cartilage and no cartilage developed in teratomas derived from *Sox9* -/- embryonic stem cells (Bi *et al.* 1999); *Sox9* deletion from chondrocytes at later stages of development resulted in decrease in chondrocyte development, cartilage matrix gene transcriptional inhibition, and prematurely conversion from proliferating chondrocytes to hypertrophic chondrocytes (Akiyama *et al.* 2002). Considering the critical role of SOX9 in chondrocytes, I explored the connection between this factor and expression of the miR-29 family. Initial evidence suggested a link: in the DMM model mRNA profiling data, at 7 days after the surgery, *Sox9* expression was greatly induced (Appendix, Table 7) whilst the miR-29s expression was suppressed; in both human and mouse chondrogenesis models, the level of Sox9 was inversely correlated with the level of miR-29 expression (data not shown). Thus, SOX9 could be a miRNA-29 target or SOX9 could regulate miRNA-29 expression.

To test the postulate **that SOX9 is a miR-29 target**, the effect of the miR-29 members on SOX9 transcriptional expression was examined: after sub-cloning the *SOX9* 3'UTR downstream of the luciferase gene, this SOX9-3'UTR reporter vector was co-transfected with the miR-29 family into SW1353 cells; 24 hours after transfection, luciferase activity was measured. Luciferase activity showed that miR-29 family have no effect on the *SOX9* 3'UTR even though bioinformatics analysis found one 6-mer seed site for miR-29 in the *SOX9* 3'UTR (data not shown), suggesting that SOX9 is not a miR-29 family direct target. Also, whether SOX9 is a miR-29 indirect target was also determined: relative expression of SOX9 was checked in human primary chondrocytes transfected with miR-29 family for 48 hours. Quantitative RT-PCR confirmed that the SOX9 level was not changed with miR-29

transfection in chondrocytes (data not shown). Thus, SOX9 is not a direct or indirect target of miR-29s at least at the transcriptional level.

For testing the second hypothesis **SOX9 is a suppressor of miR-29 expression**, the effect of overexpression or knockdown of SOX9 on miR-29 expression was studied: a SOX9 expression construct or siRNA was transiently transfected into the human chondrosarcoma SW1353, 48 hours after transfection, the level of the mature miR-29 family was measured by quantitative RT-PCR. The data (Figure 4.2) show that SOX9 suppressed miR-29 transcription: the miR-29 family levels were significantly reduced when SOX9 was overexpressed (Figure 4.2.a,c) but induced when SOX9 was knocked down (Figure 4.2.b,c).

To further explore the regulatory mechanism by which SOX9 suppressed miR-29 expression, the 2kb region upstream from the primary miR-29a/b1 and miR-29b2/c transcription start sites were analysed by searching for the SOX9 DNA-binding motif ([A/T][A/T]CAA[A/T]). This analysis revealed 5 putative binding sites for SOX9 in the promoter regions of pri-miR-29a/b1 and pri-miR-29b2/c, respectively (Figure 4.3.a). A reporter construct with the primary miR-29a/b1 2kb promoter, kindly provided by Dr Anne Delany (University of Connecticut, USA) was used to further validate the direct effect of SOX9: the reporter was co-transfected with increasing amounts of SOX9-expression plasmid into SW1353 cells and luciferase activity measured after 24 hours of transfection. Luciferase activity in SW1353 cells significantly decreased in a dose-dependent manner (Figure 4.3.b) showing that SOX9 directly regulated the primary miR-29a/b1 promoter.

The data above demonstrate that SOX9 is a miR-29 family suppressor.

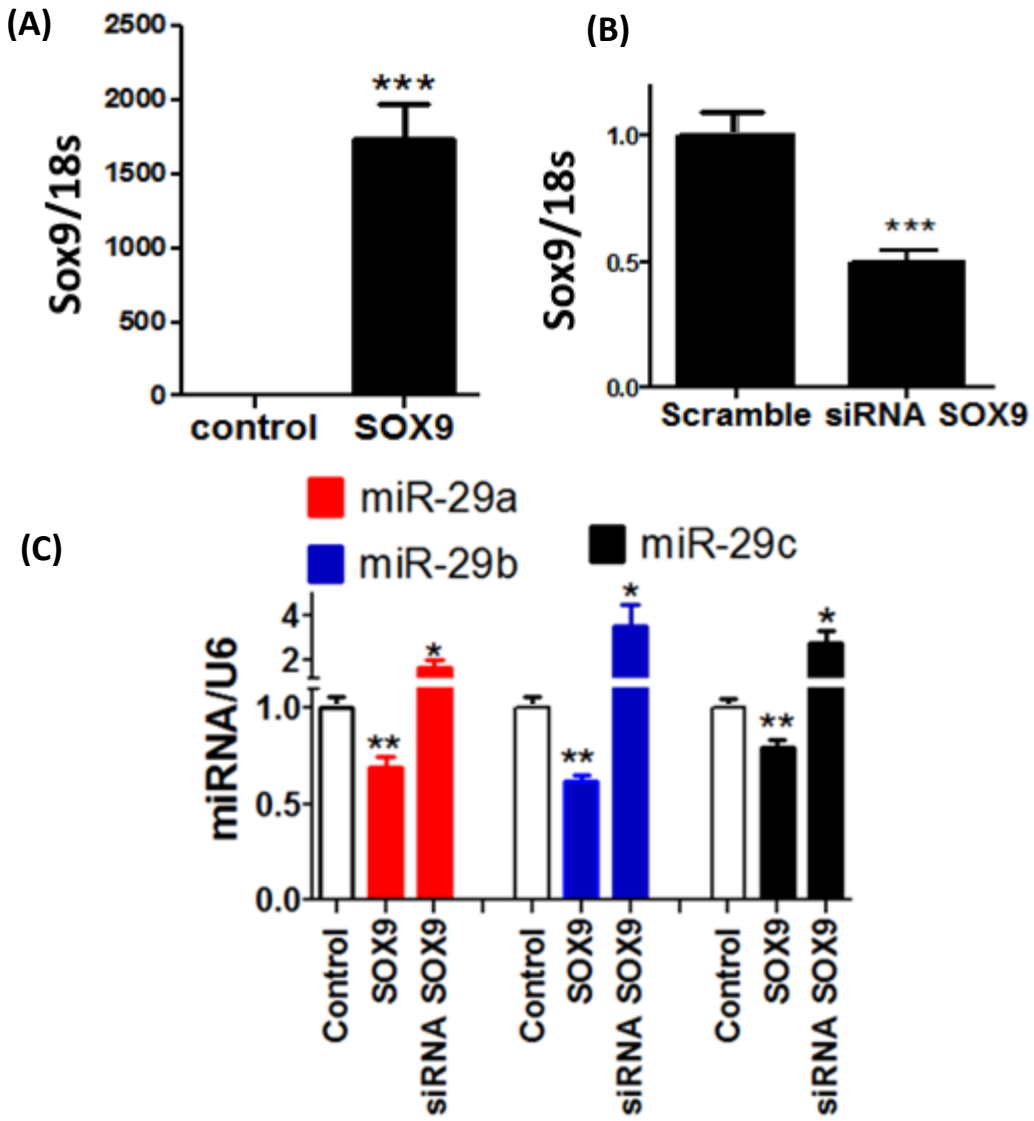

Figure 4.2: **Sox9 suppresses miR-29 family expression**.

(A) SOX9 gain-of-function: transiently transfection of a SOX9-expression vector or pcDNA3 empty vector (control) into SW1353 cells; (B) SOX9 loss-of-function: transiently transfection of SOX9 siRNA or a non-targeting control into SW1353 cells. Relative expression of SOX9 in (A) and (B) was measured 48 hours after transfection by quantitative RT-PCR using18S as the endogenous control; (C) The miR-29 family expression levels after overexpression or knockdown of SOX9 in SW1353 cells was measured by quantitative RT-PCR. Using U6 as the endogenous control. Red bar: miR-29a, green bar: miR-29b, black bar: miR-29c, open bar: control. Means ± standard errors are presented. Difference in expression was analysed by unpaired two-tailed Student's t test. * $p<0.05$, ** $p < 0.01$, *** $p<0.001$, n=3.

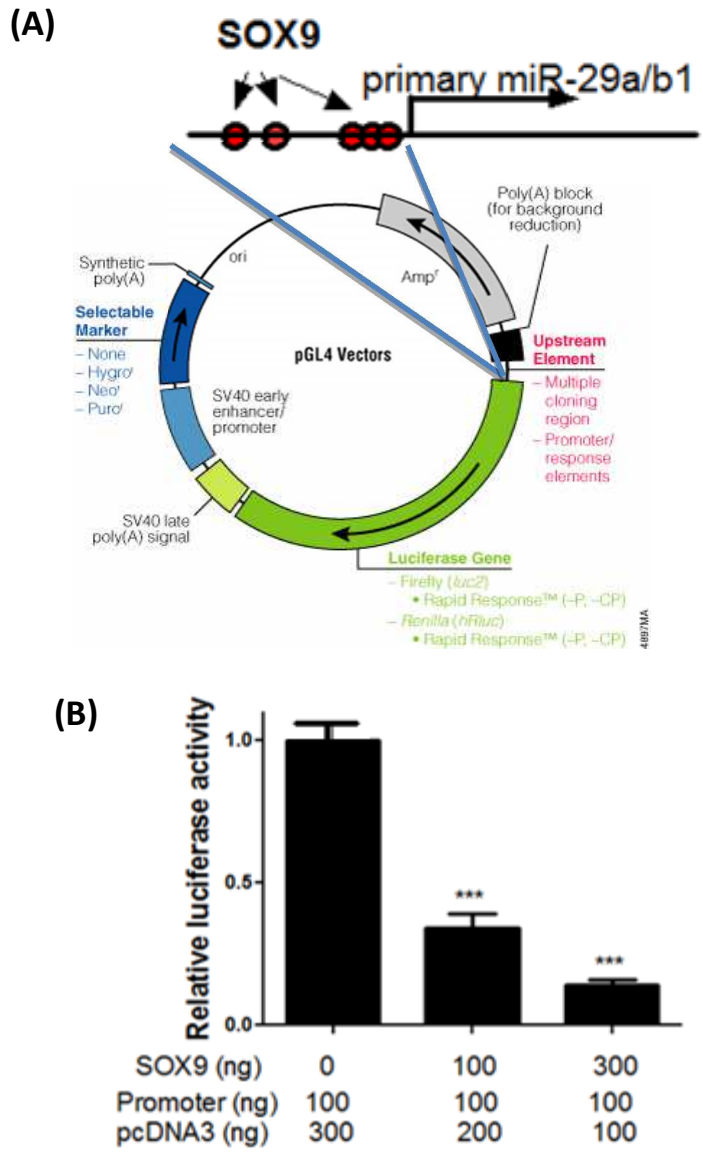

Figure 4.3: **Sox9 suppresses primary miR-29a/b1 transcription by directly binding to the proximal miR-29a/b1 promoter.**

(A) Structure of the miR-29a/b1 promoter reporter: 5 putative binding sites of SOX9 were identified by analysing the 2kb region upstream of the transcription start site of miR-29a/b1 by JASPAR. This 2kb region was sub-cloned upstream of the luciferase gene in a pGL4 vector.
(B) Suppressive effect of SOX9 on the primary miR-29a/b1 promoter reporter: transiently co-transfection of primary miR-29a/b1 promoter (100ng) with increasing amount of SOX9-expression vector (0, 100, 300ng) or pcDNA.3 to equalise DNA into SW1353. A constitutively expressed Renilla lucierase was used as a control for transfection efficiency. Luciferase activity was measured 24 hours after transfection. Means ± standard errors are presented. The difference in luciferase activity was analysed by unpaired two-tailed Student's t test. * $p<0.05$, ** $p < 0.01$, *** $p<0.001$, n=6.

4.2.2. TGFβ1 inhibits expression of the miR-29 family

TGFβ signalling has many important roles in chondrocytes and articular cartilage: TGFβ induces extracellular matrix formation; stimulates chondrocyte proliferation; inhibits the terminal differentiation of chondrocytes; retains chondrocytes in the pre hypertrophic stage; increases total glycosaminoglycan synthesis; maintains the matrix component in immature cartilage (Li *et al.* 2005). Animal studies showed that: transgenic mice overexpressing a cytoplasmically truncated, dominant-negative form of the TβRII in cartilage, resulted in a joint disease similar to human osteoarthritis (Serra *et al.* 1997); Smad3 deficient mice showed premature chondrocyte maturation with increased length of the hypertrophic region, disorganization of the chondrocyte columns, early expression of collagen type X in the growth plate; and null mice gradually developed an end-stage OA phenotype (Li et al. 2005). These essential roles of TGFβ signalling in chondrocytes suggest the necessity of examining whether the miR-29 family is regulated by TGFβ signalling in human chondrocytes. Moreover, a number of published data show that TGFβ signalling negatively regulates miR-29 family expression in different human fibroses e.g. renal, lung, liver fibrosis. The impact of TGFβ signalling in human chondrocytes on the miR-29 family was thus checked.

To address the above question, expression of the miR-29 family with TGFβ1 treatment in human primary chondrocytes was compared both in monolayer and micromass culture. **In monolayer culture**: HACs were put in high glucose media containing 10% (v/v) FCS until the cells reached 90% confluence; medium was replaced with that containing 0.5% (v/v) FCS) prior to stimulating with 4ng/ml TGFβ or vehicle control (4mM HCl with 0.5% (w/v) BSA). **In micromass culture**: HACs were put in high glucose media containing 10% (v/v) FCS in monolayer following two sequential passages to increase cell number; the micromass ($2.5x10^7$cells/ml) was cultured in high glucose media with 10% (v/v) FCS for 24 hours before treating with 10ng/ml TGFβ or vehicle control (4mM HCl with 0.5% (w/v) BSA). Cells were harvested for qRT-PCR after 24 hours or 48 hours treatment in monolayer or micromass cultures, respectively. Quantitative RT-PCR primers for measuring the miR-29 family were described before. For the primary transcripts: two primer pairs specific for exon 1 and exon 3 were used; for the precursor transcripts: primers directly bind to the precursor sequence (Appendix, Table 5); the mature transcripts were measure by LNA-primers.

The qRT-PCR data show that expression of the miR-29 family was suppressed by TGFβ signalling (Figure 4.4). However, each culture system gave a different response. The pri-29b2/c transcript was significantly decreased after stimulating HACs for 24 hours with TGFβ1 in monolayer culture, whilst the pri-29a/b1 transcript was unchanged (Figure 4.4 a); the pri-29a/b1 transcript was significantly decreased in micromass culture after 48 hours with TGFβ1 whilst the pri-29b2/c transcript was unchanged or even increased (Figure 4.4 b). Notably, the levels of all mature forms of miR-29 were significantly decreased by TGFβ1 in both systems. These data suggest a hypothesis that the primary and the precursor miRNAs may be rapidly regulated and then processed into mature miRNAs. In order to test this hypothesis, SW1353 cells were treated with TGFβ1 (4ng/ml) in monolayer in a time course. Since the expression levels of the primary and pre miRNAs modulated by TGFβ1 in human primary chondrocyte were similar and ahead the mature miRNAs, it might be sufficient to measure only the pre-miRNA rather than both the primary and precursor sequences. Consistent with above data, qRT-PCR showed that TGFβ1 suppressed miR-29 family expression in SW1353 cells (Figure 4.5). Interestingly, significantly suppressive effects of TGFβ1 on precursor miRNAs were observed after 4 hours till the end of the time course (Figure 4.5.a) whilst significant change in the mature miRNAs was only seen after 12 hour treatment (Figure 4.5.b). This data, thus, confirms the hypothesis above. Together with TGFβ1, the effect of TGFβ3 on the miR-29 family expression also checked on SW1353 in monolayer across the time course. Quantitative RT-PCR data (Figure 4.5) showed that TGFβ3 also strongly supressed the expression of the miR-29s. However, the TGFβ3 significant decrease the precursor and the mature miRNAs were observed at 12 hour time point though at 4 hours a

The suppressive effect of TGFβ on expression of the miR-29 family was also investigated on the proximal promoter of the primary miR-29a/b1 gene. The promoter-reporter was transfected into SW1353 cells, cells were serum starved for 24 hours and treated with TGFβ1 (4ng/ml) for another 6 hours before performing the luciferase assay. In line with the expression data, TGFβ1 significantly suppressed the promoter activity of pri-miR-29a/b1 (Figure 4.6).

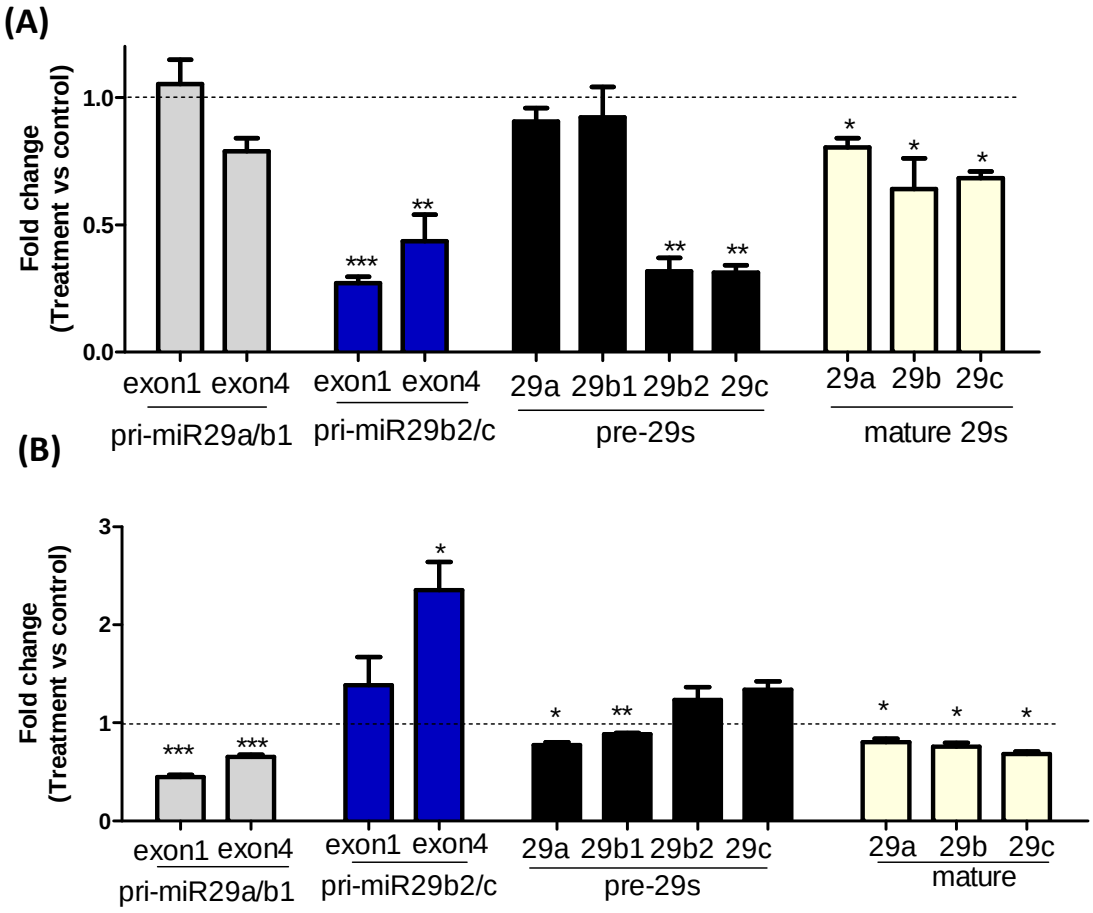

Figure 4.4 TGFβ1 suppresses expression of the miR-29 family in human primary chondrocyte

(A) TGFβ1suppresses expression of the miR-29 family in monolayer culture: Human primary chondrocytes were cultured in high glucose media with 10% (v/v) FCS in monolayer until 90% confluence. Cells were switched to high glucose media with 0.5% (v/v) FCS for 24 hours before treating with TGFβ1 (4ng/ml) or vehicle (4mM HCl+0.5% (w/v) BSA) for another 24 hours.

(B) TGFβ1suppresses expression of the miR-29 family in micromass culture: Human primary chondrocytes were cultured in high glucose media with 10% (v/v) FCS in monolayer. After 2 sequential passages, cells were put in micromass culture ($2.5x10^7$cells/ml) in high glucose media with 10% (v/v) FCS. After 24 hours in micromass, cells were stimulated for 48 hours with TGFβ (10ng/ml) or vehicle (4mM HCl+0.5% (w/v) BSA) in 10% (v/v) FCS media.

Relative expression of the primary miR-29a/b1, -29b2/c, precursor miR-29a, -29b1, -29b2, -29c, the mature miR-29a, b, c were measured by quantitative RT-PCR. 18S rRNA was the endogenous control for measuring primary and precursor transcripts; U6 was the endogenous control for measuring miR-29 mature transcripts. The horizontal line at 1 represents the mean of the vehicle control. Brown bar, pri-miR-29a/b1 transcripts; blue bar, pri-miR-29b2/c transcripts; black bar, precursor transcripts; yellow bar, mature transcripts. Means ± standard errors are presented. The difference between the treatment and the control was analysed by unpaired two-tailed t test. * $p<0.05$, ** $p < 0.01$, *** $p<0.001$, n=3.

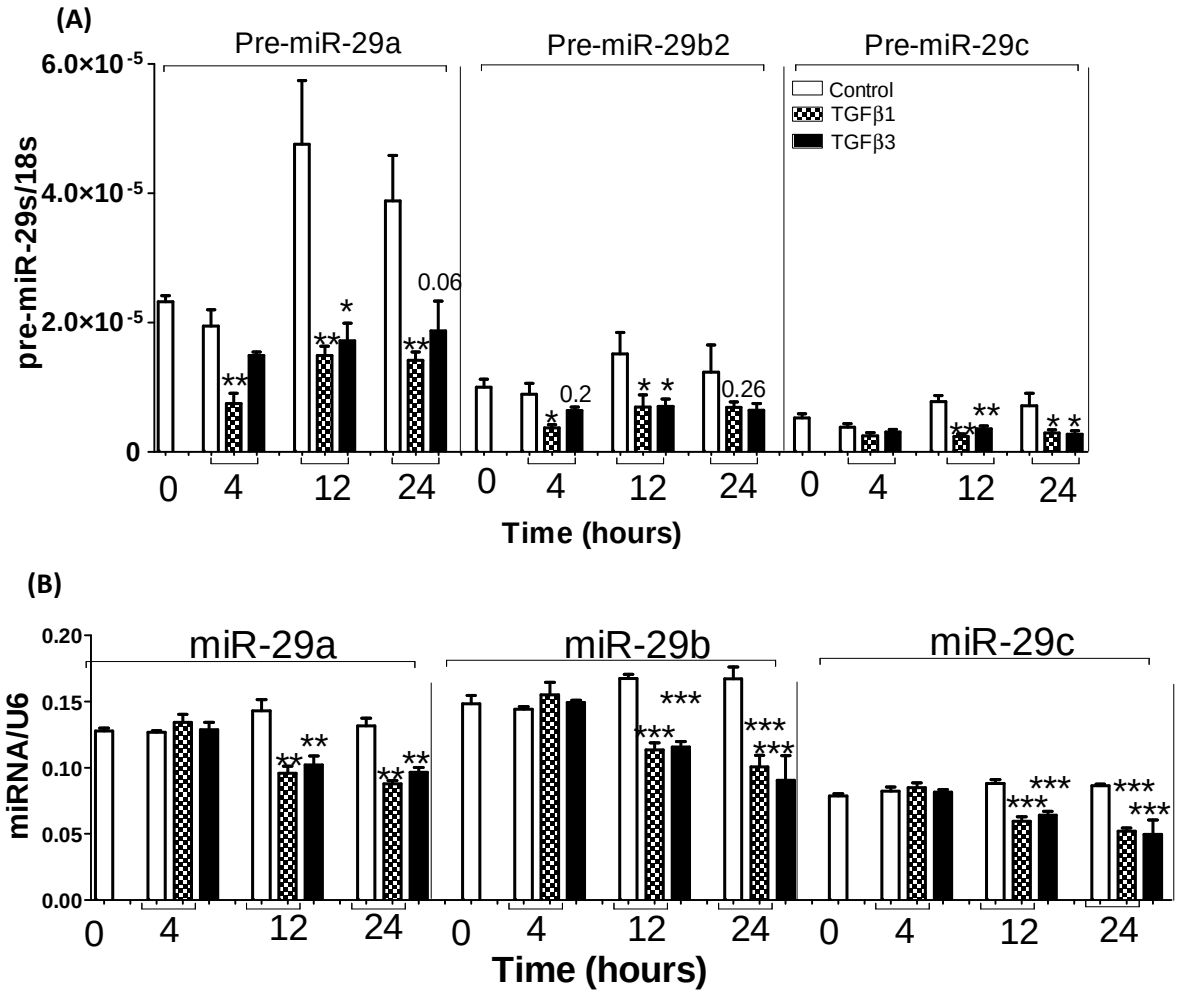

Figure 4.5 TGFβ1/3 suppresses expression of the miR-29 family in SW1353 cells

SW1353 cells were cultured in high glucose media with 10% (v/v) FCS in monolayer until 90% confluence. Cells were serum starved for 24 hours before treating with TGFβ1or TGFβ3 (4ng/ml) or vehicle (4mM HCl+0.5% (w/v) BSA) across 24 hour course.

Relative expression of the precursor miR-29a, -29b2, -29c, the mature miR-29a, b, c were measured by quantitative RT-PCR. 18S rRNA was the endogenous control for measuring the precursor transcripts; U6 was the endogenous control for measuring miR-29 mature transcripts. Open bar, control; brick bar, TGFβ1; close bar, TGFβ3. (A) Expression level of pre-miR-29a, 29b2, 29c. (B) Expression level of mature miR-29a, b, c. Means ± standard errors are presented. The difference between the treatment and the control was analysed by unpaired two-tailed t test. * $p<0.05$, ** $p < 0.01$, *** $p<0.001$, n=3.

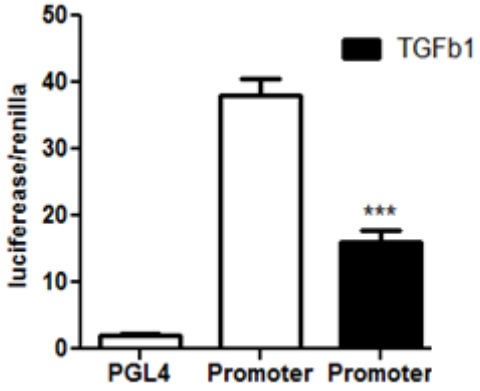

Figure 4.6: TGFβ1decreases expression from the primary miR-29a/b1 promoter

The pri-miR-29a/b1 promoter-reporter (100ng) or the empty vector pGL4 (control, 100ng) were transfected into SW1353 cells. After transfection, cells were serum starved for 24 hours, followed by stimulating for another 6 hours with TGFβ1 (4ng/ml), or vehicle (4mM HCl+0.5% BSA) before measuring luciferase activity. Renilla was use as endogenous control. Open bar: vehicle, black bar: TGFβ1. Means ± standard errors are presented. The difference of luciferase activity was analysed by unpaired two-tailed Student's t test. * $p<0.05$, ** $p < 0.01$, *** $p<0.001$, n=6.

4.2.3. Expression of the miR-29 family is not regulated by canonical Wnt signalling

As shown in the section above, the TGFβ signalling pathway, stimulated by TGFβ1 (or TGFβ3, data not shown), negatively regulated the expression of themiR-29 family. Signalling cross talk between TGFβ and Wnt signalling pathways has been previously reported, e.g. after TGFβ stimulation, Smad3 interacts with LEF1 to activate target gene transcription independently of β-catenin (Letamendia *et al.* 2001); TGFβ was shown to up-regulate the expression of many Wnt ligands e.g. Wnt2, 4, 5a, 7a, 10a, and Wnt co-receptors e.g. LRP5 (Zhou *et al.* 2004); TGFβ was found to increase nuclear accumulation and stability of β-catenin; interestingly, working synergistically with Wnt signalling pathways, TGFβ was reported to stimulate chondrocyte differentiation from mesenchymal cell (Zhou et al. 2004). Wnt signalling is also known to have a key role in cartilage homeostasis and osteoarthritis (Zhu et al. 2008, Zhu et al. 2009). Thus, it was pertinent to investigate the effect of Wnt signalling onexpression of the miR-29 family in chondrocytes, and then potential synergy with TGFβ signalling.

The effect of canonical Wnt signalling stimulated by Wnt3a (50 or 100ng/ml) on the miR-29 family was investigated in HACs cultured in monolayer or micromass after 24 hours or 48 hours, respectively; or in SW1353 cells in monolayer culture across a 24 hour time course. In addition, the effect of Wnt3a on the proximal pri-miR-29a/b1 promoter was also examined after 6 hour treatment with Wnt3a (50 or 100ng/ml). Quantitative RT-PCR data for all transcripts of miR-29 family and luciferase assay data for the miR-29a/b1 promoter showed canonical Wnt signalling did not regulate expression of the miR-29 family (Appendix, Figure 5). Wnt3a did regulate Axin2 expression in the same experiments, showing induction of the canonical Wnt pathway (Appendix, Figure 6).

4.2.4. IL-1 induces expression of the miR-29 family in part via the p38 signalling pathway.

IL-1 is a catabolic and anti-anabolic cytokines, it down regulates the expression of cartilage matrix components e.g. aggrecan and type II collagen and induces expression of matrix degrading enzymes e.g. MMP-3, MMP-13, ADAMTS4 (Koshy *et al.* 2002). *Il-1β*, or Il-1β-converting enzyme knockout mice showed the accelerated development of OA lesions in response to OA surgical induced in compared with wide type mice (Clements et al. 2003). It is considered to be a major cytokine driving the pathology of OA (Goldring *et al.* 2004). Thus, it was pertinent to examine whether IL-1 controls the expression of the miR-29 family in human chondrocytes.

The effect of IL-1 on the expression of the miR-29 family was first measured in IL-1-treated SW1353 for 48 hour time course in monolayer culture: SW1353 cells were cultured in high glucose media with 10% (v/v) FCS until reach confluence and followed by serum starved for 24 hours before treating with 5ng/ml IL-1 or vehicle (0.5% (w/v) BSA) for 48 hour time course. Relative expressions of the precursor and mature miRNA-29 transcripts were measured by qRT-PCR. Data (Figure 4.7) showed that IL-1 induced the expression of miR-29 family: the biggest induction on miR-29 precursors was observed at 4 hours; at later time point, the level of miR-29a precursors was decreased as compare with 4 hours (pre-29a) whilst other precursors did not change expression (Figure 4.7a); the induction of mature miR-29s were only observed significantly after 48 hours (Figure 4.7b). These data suggested that the increase in expression after IL-1 treatment of the miR-29 derivatives is time-dependent. The induction of IL-1 on the miR-29 family was again checked on the HACs in micromass culture: The micromass containing ($2.5x10^7$cells/ml) of passage 2 HAC was cultured in high glucose media with 10% (v/v) FCS for 48 hours before treating with 20ng/ml IL-1 or vehicle control (0.5% (w/v) BSA). Quantitative RT-PCR primers for measuring the miR-29 family were described before (Appendix, Table 5). Real-time RT-PCR data (Figure 4.8) showed that IL-1 strongly induced expression of the miR-29 family, with all processed transcripts significantly up-regulated by IL-1. The fold increase was highest for the pri-miR-29a/b1 locus in which the primary miR-29a/b1 and pre-miR29a and b1 were increased with 9 and 5 fold, respectively.

The molecular pathways induced by IL-1 can be the three classical MAPK-signalling pathways i.e. ERK, p38, JNK and through NFκB (Aigner *et al.* 2006, Fan *et al.* 2007). The

signalling pathway through which IL-1 regulated miR-29 family expression was investigated. SW1353 cells were stimulated with IL-1 together with an NFκB inhibitor (10μM) or a p38 inhibitor (SB203580) (10μM) or 6 hours in monolayer and the relative expression of the precursor miRNAs were again measured. The data showed that inhibition of the NFκB pathway further induced expression of the pre-miR-29a and b1 (Figure 4.9). Inhibition of p38 suppressed IL-1 induction of pre-miR-29a and b1, with a similar pattern for pre-miR-29b2 and c (Figure 4.10), suggesting that IL-1 induces expression of the miR-29 family at least in part through p38 MAPK signalling.

Furthermore, the effect of IL-1 on the promoter of pri-miR-29a/b1 was also examined by luciferase assay. The pri-miR-29a/b1 promoter-reporter was transfected into SW1353 cells for 24 hours before stimulation with IL-1 (5ng/ml) with or without the NFκB inhibitor (10nM) or p38 inhibitor (10μM) for another 6 hours. Luciferase data showed that the activity of the pri-miR-29a/b1 promoter was significantly decreased by IL-1 and that this effect was abolished by treatment with the NFκB inhibitor (Figure 4.11). However, the p38 inhibitor had no effect on the suppressive effect of IL-1 on the promoter of pri-miR-29a/b1 (data not shown).

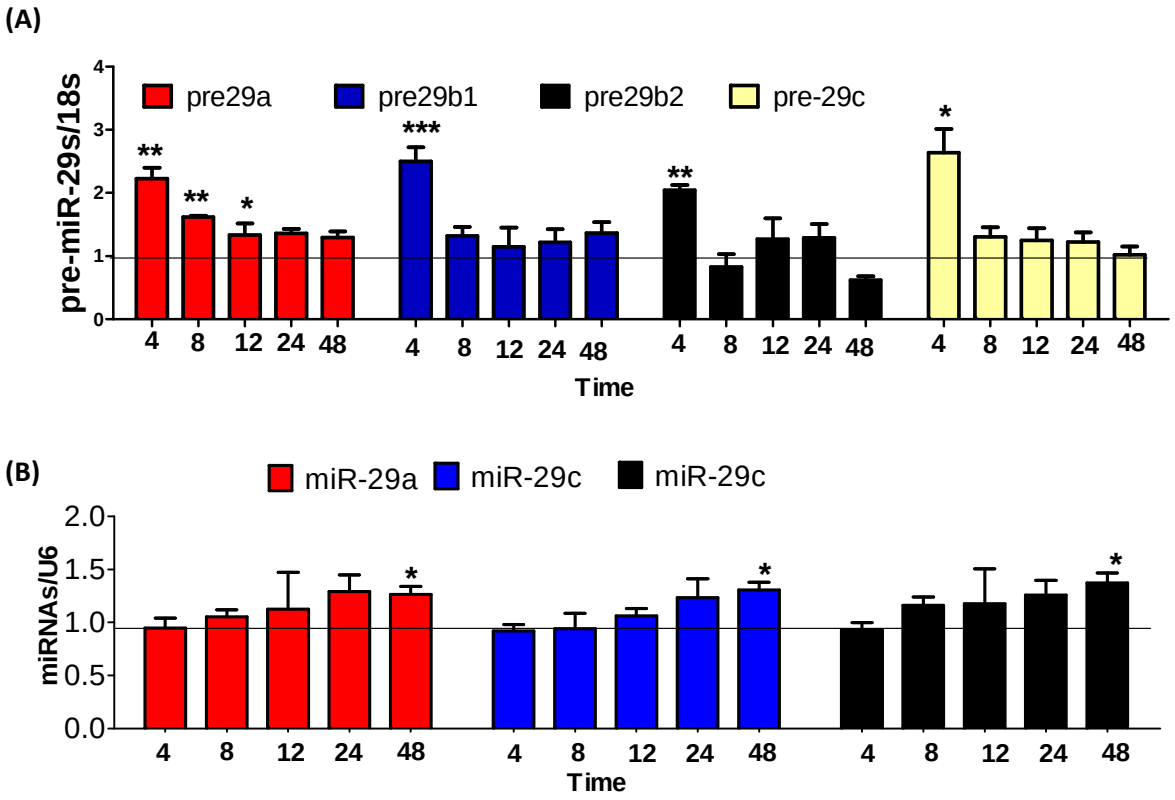

Figure 4.7: IL-1 induces expression of the miR-29 family in SW1353 in monolayer culture

SW1353 cells were cultured in high glucose media with 10% (v/v) FCS in monolayer until 90% confluence. Cells were serum starved for 24 hours before treating with IL-1 (5ng/ml) or vehicle (0.5% (w/v) BSA) across 48 hour course.
Relative expression of the precursor miR-29a, -b1, -b2, -c, the mature miR-29a, b, c were measured by quantitative RT-PCR. 18S rRNA was the endogenous control for measuring the precursor transcripts; U6 was the endogenous control for measuring miR-29 mature transcripts. The horizontal line at 1 serves as the vehicle control.
(A) Expression level of pre-miR-29a, 29b2, 29c. Red bar, pre-miR-29a; blue bar, pre-miR-29b1; black bar, pre-miR-29b2; yellow bar, pre-miR-29c
(B) Expression level of mature miR-29a, b, c. Red bar, miR-29a; blue bar, miR-29b; black bar, miR-29c
Means ± standard errors are presented. The difference between the treatment and the control was analysed by unpaired two-tailed t test. * $p<0.05$, ** $p < 0.01$, *** $p<0.001$, n=3.

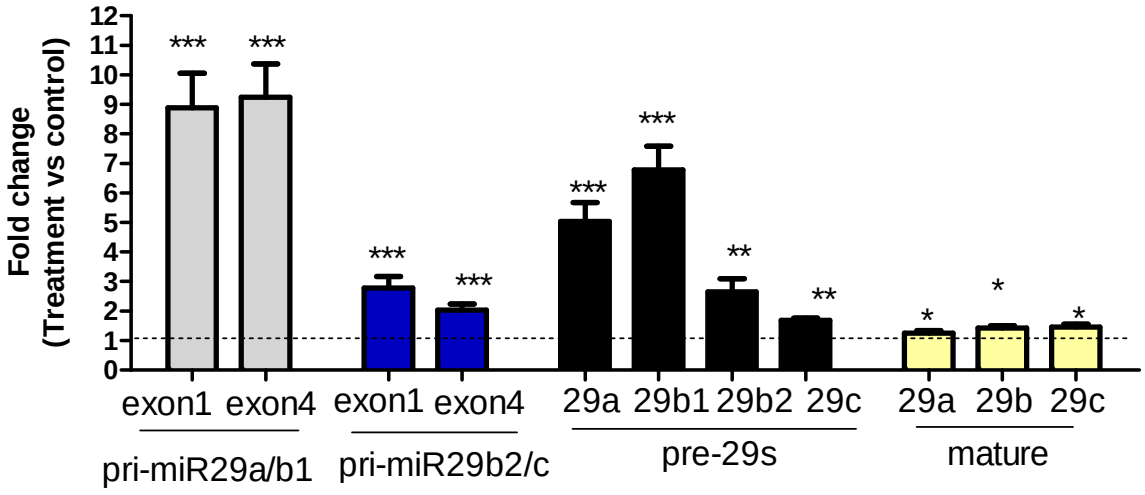

Figure 4.8: IL-1 induces expression of the miR-29 family in human primary chondrocyte in micromass culture

Human primary chondrocytes were cultured in high glucose media with 10% (v/v) FCS in monolayer. After 2 sequential passages, cells were put in micromass culture ($2.5x10^7$cells/ml) in high glucose media with 10% (v/v) FCS. After 24 hours in micromass, cells were stimulated for 48 hours with IL-1β (10ng/ml) or vehicle (0.5% (w/v) BSA).
Relative expression of the primary miR-29a/b1, -29b2/c, precursor miR-29a, -29b1, -29b2, -29c, the mature miR-29a,- 29b, -29c were measured by quantitative RT-PCR. 18S rRNA was the endogenous control for measuring primary and precursor transcripts; U6 was the endogenous control for measuring miR-29 mature transcripts. The horizontal line at 1 serves as the vehicle control. Brown bar, pri-miR-29a/b1 transcripts; blue bar, pri-miR-29b2/c transcripts; black bar, precursor transcripts; yellow bar, mature transcripts. Means ± standard errors are presented. The difference between the treatment and the control was analysed by unpaired two-tailed Student's t test. * $p<0.05$, ** $p < 0.01$, *** $p<0.001$, n=3.

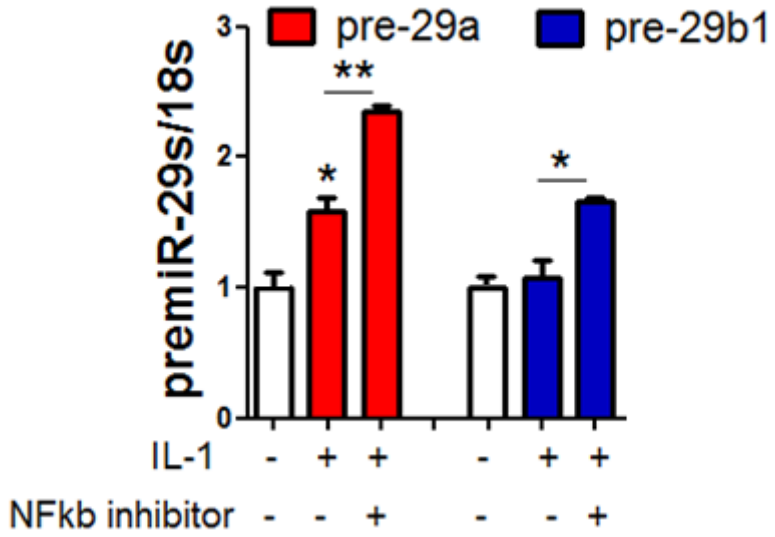

Figure 4.9 NFκB inhibition further increases the IL-1-induced expression of pre-miR-29a and pre-miR-29b1

SW1353 cells were plated in high glucose media with 10% (v/v) FCS in a 6 well-plate in monolayer and serum starved for 24 hours before treating with IL-1β (10ng/ml) in the presence or absence of NFκB inhibitor JSH-23 (10μM) for a further 8 hours. Cells were then harvested and the total RNA was isolated by Trizol. Relative expression of pre-miR-29a, -29b1 were measured by quantitative RT-PCR. 18S rRNA was the endogenous control. Red bar, pre-miR-29a; blue bar, pre-miR-29b1. Means ± standard errors are presented. The difference between the treatment and the control was analysed by unpaired two-tailed Student's t test * $p<0.05$, ** $p < 0.01$, *** $p<0.001$, n=6.

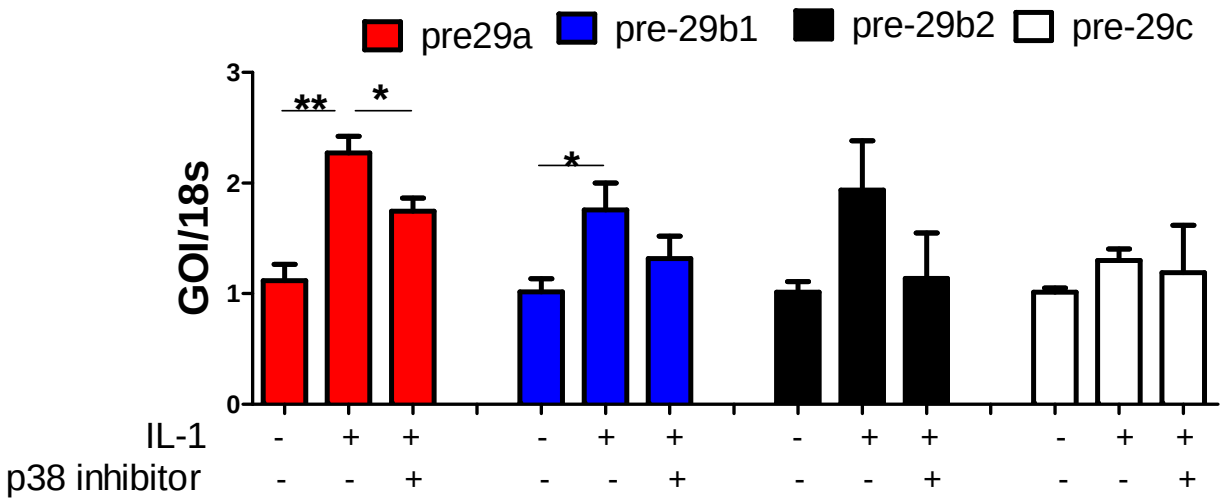

Figure 4.10 P38 inhibition suppresses the IL-1 induction of pre-miR-29s

SW1353 cells were plated in high glucose media with 10% (v/v) FCS in a 6 well-plate in monolayer and serum starved for 24 hours before treating with IL-1β (10ng/ml) in the presence or absence of p38 inhibitor SB203580 (10µM) for a further 8 hours. Cells were then harvested and the total RNA was isolated by Trizol. Relative expression of pre-miR-29a, -29b1, -29b2, -29c were measured by quantitative RT-PCR. 18S rRNA was the endogenous control. Red bar, pre-miR-29a; blue bar, pre-miR-29b1; black bar, pre-miR-29b2; white bar, pre-miR-29c. Means ± standard errors are presented. The difference between the treatment and the control was analysed by unpaired two-tailed Student's t test * $p<0.05$, ** $p < 0.01$, *** $p<0.001$, n=3.

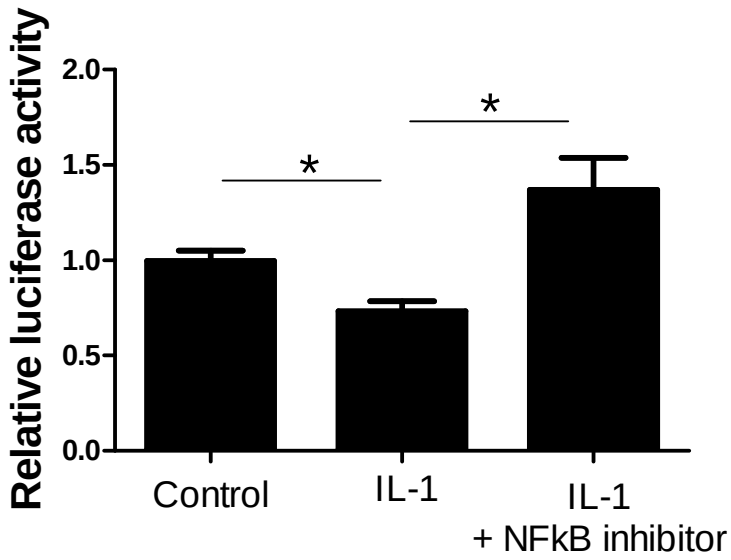

Figure 4.11: IL-1 suppresses the primary miR-29a/b1 promoter through NFκB

Pri-miR-29a/b1 promoter reporter (100ng) or pGL4 (control, 100ng) were transfected into SW1353 cells. After transfection, cells were serum starved for 24 hours, and followed by stimulating for another 6 hours with IL-1β (5ng/ml), IL-1β and NFκB inhibitor JSH-23 (10μM) or vehicle (0.5% (w/v) BSA) before measuring luciferase activity. Renilla was the endogenous control. Means ± standard errors are presented. The difference of luciferase activity was analysed by unpaired two-tailed Student's t test. * $p<0.05$, ** $p < 0.01$, *** $p<0.001$, n=6.

4.2.1. LPS suppressed the miR-29 family expression through NFκB signalling pathway

Toll-like receptors (TLRs) have important roles in activation of the innate and adaptive host defence against infections. TLR can bind to various damage-associated molecular patterns, which are endogenous danger signals or alarmins, leading to autoinflammatory conditions, and contributing to production of co-stimulatory signals necessary for adaptive immune reactions (Janeway *et al.* 2002). Lipopolysaccharide (endotoxin) (LPS) from bacteria is an example of a TLR-stimulating molecule. Chondrocytes are a potential source of several proinflammatory substances which may be TLR ligands: high-mobility group box 1, heat-shock proteins, and several components of the cartilage extracellular matrix (ECM) - e.g. low-molecular-weight hyaluronan, heparin sulphate, biglycan, and fibronectin fragments (Konttinen *et al.* 2012). From this point of view, OA could be considered as an autoinflammatory disease with the chondrocyte as its primary inflammatory cell (Konttinen et al. 2012). On this basis it was hypothesized that the activation of TLR-4, a receptor for LPS, may directly affect the biosynthetic activity of chondrocytes, including expression of the miR-29 family.

The level of miR-29 family expression was measured by qRT-PCR in HACs stimulated LPS (1µg/ml) in monolayer or micromass culture for a 24 hours or a 48 hour time course, respectively. Real-time PCR showed that the miR-29 family was significantly suppressed by LPS (Figure 4.12). Interesting, the levels of all processed miRNAs were strongly regulated by LPS in a time dependent manner: a significant decrease of the two miR-29 family clusters and their precursors were detected after 4 hours of treatment whilst decrease of the mature miRNAs was not detected until 24 hours. However, after 48 hours treating with LPS, all miR-29 family was tended to increase (Figure 4.12)

Again, the effect of LPS on the promoter of pri-miR-29a/b1 was also examined by luciferase assay. The pri-miR-29a/b1 promoter reporter was transfected into SW1353 cells for 24 hours before stimulation with LPS (1µg/ml) in the presence or absence of an NFκB inhibitor JSH-23 (10µM) for another 6 hours. Luciferase assay data showed that promoter activity of pri-miR-29a/b1 was significantly decreased by LPS and this effect was abolished with the NFκB inhibitor (Figure 4.13).

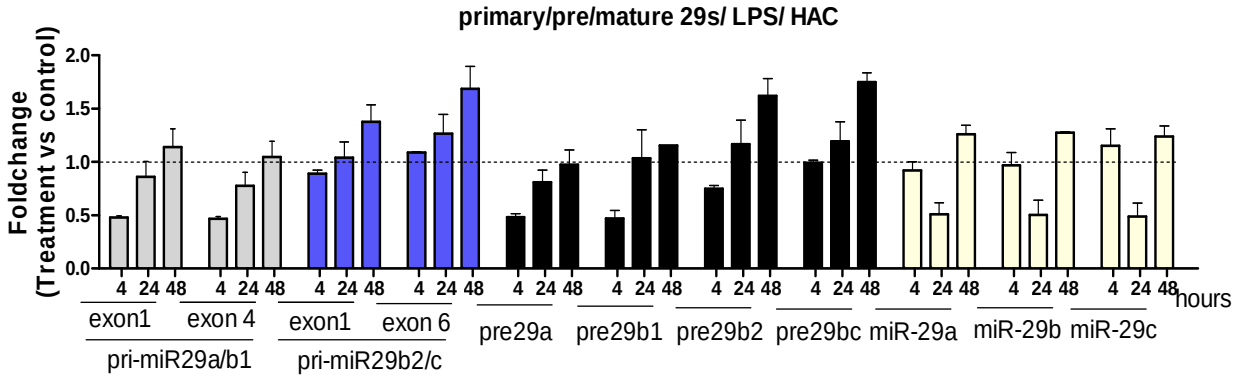

Figure 4.12: LPS suppresses expression of the miR-29 family

Human primary chondrocytes were cultured in high glucose media with 10% (v/v) FCS in monolayer. After 2 sequential passages, cells were put in micromass culture ($2.5x10^7$cells/ml) in high glucose media with 10% (v/v) FCS. After 24 hours in micromass, cells were stimulated for 4, 24, and 48 hours with LPS (1µg/ml) or vehicle (0.5% (w/v) BSA).
Relative expression of the primary miR-29a/b1, -29b2/c, precursor miR-29a, -29b1, -29b2, -29c, the mature miR-29a,- 29b, -29c was measured by quantitative RT-PCR. 18S rRNA was the endogenous control for measuring primary and precursor transcripts; U6 was the endogenous control for measuring miR-29 mature transcripts. The horizontal line at 1 serves as the vehicle control. Brown bar, pri-miR-29a/b1 transcripts; blue bar, pri-miR-29b2/c transcripts; black bar, pre-miR transcripts; yellow bar, mature miR transcripts. Means ± standard errors are presented. The difference between the treatment and the control was analysed by unpaired two-tailed Student's t test. * $p<0.05$, ** $p < 0.01$, *** $p<0.001$, n=3.

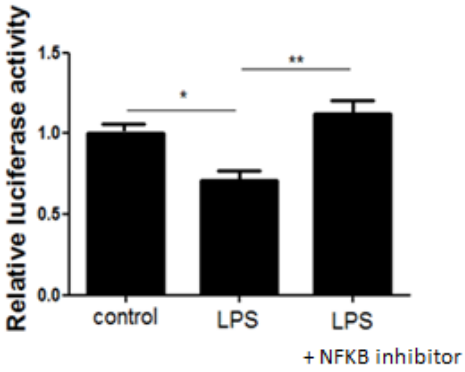

Figure 4.13: LPS suppresss the primary miR-29a/b1 promoter through NFκB

Pri-miR-29a/b1 promoter-reporter (100ng) or pGL4 (control, 100ng) was transfected into SW1353 cells. After transfection, cells were serum starved for 24 hours, followed by stimulatiion for another 6 hours with LPS (1µg/ml) in the absence or presence of an NFκB inhibitor JSH-23 (10µM) before measuring luciferase activity. Renilla was the endogenous control. Means ± standard errors are presented. The difference of luciferase activity was analysed by unpaired two-tailed Student's t test. * $p<0.05$, ** $p < 0.01$, *** $p<0.001$, n=6.

4.2.2. The microRNA-29 family targets Dicer giving a negative feedback loop for maturation of pre-miR-29

Previous data showed that expression of the miR-29 family was regulated by TGFβ, IL-1, LPS in which primary microRNA and precursor microRNA were modulated far ahead the mature microRNAs. In order to explain this, the 3'UTR regions of genes encoding for proteins involved in miRNA biogenesis were searched for putative binding site of the miR-29 family. Among these, of particular interest is the ribonuclease III enzyme Dicer, renowned for its central role in the biogenesis of microRNAs, converting the stem-loop pre-miRNA to mature miRNA (Bartel 2004). Bioinformatic analysis showed that there was a putative binding site of miR-29 in the *DICER* 3'UTR, suggesting the miR-29 family may regulate Dicer expression leading to the down-regulation of the Dicer level and as the consequence, the processing from precursors to mature miRNAs would potentially be slowed down. The 3'UTR region of *DICER* was therefore sub-cloned downstream of the firefly luciferase gene in the pmiR-GLO vector. The effect of the miR-29 family on the *DICER* 3'UTR was measured by luciferase assay after 24 hour co-transfection of the *DICER* 3'UTR- pmiR-GLO and the miR-29 family in SW1353 cells. Dual-luciferase reporter analysis showed the co-transfection of miR-29s significantly inhibited the wild type construct, whereas when the target site was mutated, the construct was not inhibited (Figure 4.14). This indicates that miR-29 may suppress expression of Dicer. The effect of the miR-29 family in *DICER* expression at transcriptional level was also investigated. Human primary chondrocyte was transfected with either miR-29b mimic (50nM) or non – targeting control (50nM). The transfected cells were then put in either monolayer or micromass culture for a further 48 hours. The expression of *DICER* was measured by qRT-PCR. Real-time qRT-PCR data showed that the expression of Dicer was not affected by miR-29s (data not shown), suggesting that the miR-29s does not control Dicer expression at mRNA level.

There is a growing body of work demonstrating that microRNAs can be processed independently of Dicer via Argonaute2 (Dueck *et al.* 2010). To evaluate whether or not miR-29s required Dicer to mature, the level of pre-miR-29s and mature miR-29s were measured in DLD, a Dicer-knockdown cell line. Data (Figure 4.15) showed that the levels of mature miR-29s were strongly reduced whilst the level of pre-miR-29s was not affected (Figure 4.15), demonstrating miR-29 processing is Dicer-dependent.

Taken together, these data show that the miR-29 family targets Dicer giving a negative feedback loop for its maturation.

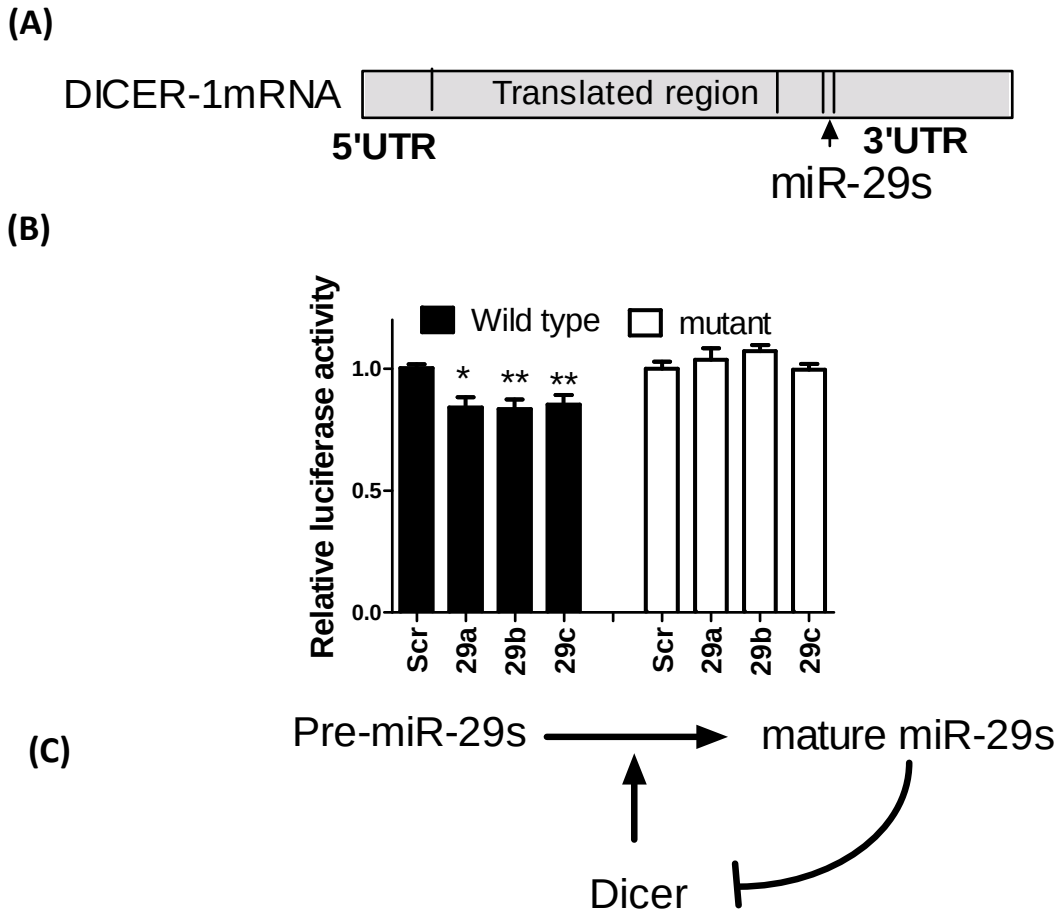

Figure 4.14: The miR-29 family targets Dicer

(A) Bioinformatic analysis reveals one binding site of the miR-29 family in the 3'UTR of Dicer. (B) miR-29 family targets Dicer: The Dicer 3'UTR containing the binding site of the miR-29 family (wild type) or a mutated, non-functional binding site for miR-29 family (mutant) were sub-cloned into the pmiR-GLO vector and were co-transfected with either miR-29a, -29b, -29c mimic (50nM) or non-targeting control (50nM) into SW1353 cells for 24 hours and luciferase activity was measured. Renilla was the endogenous control. (C) miR-29 targets Dicer giving a negative feedback loop for its maturation. Means ± standard errors are presented. The difference of luciferase activity was analysed by unpaired two-tailed Student's t test. * $p<0.05$, ** $p < 0.01$, *** $p<0.001$, n=6.

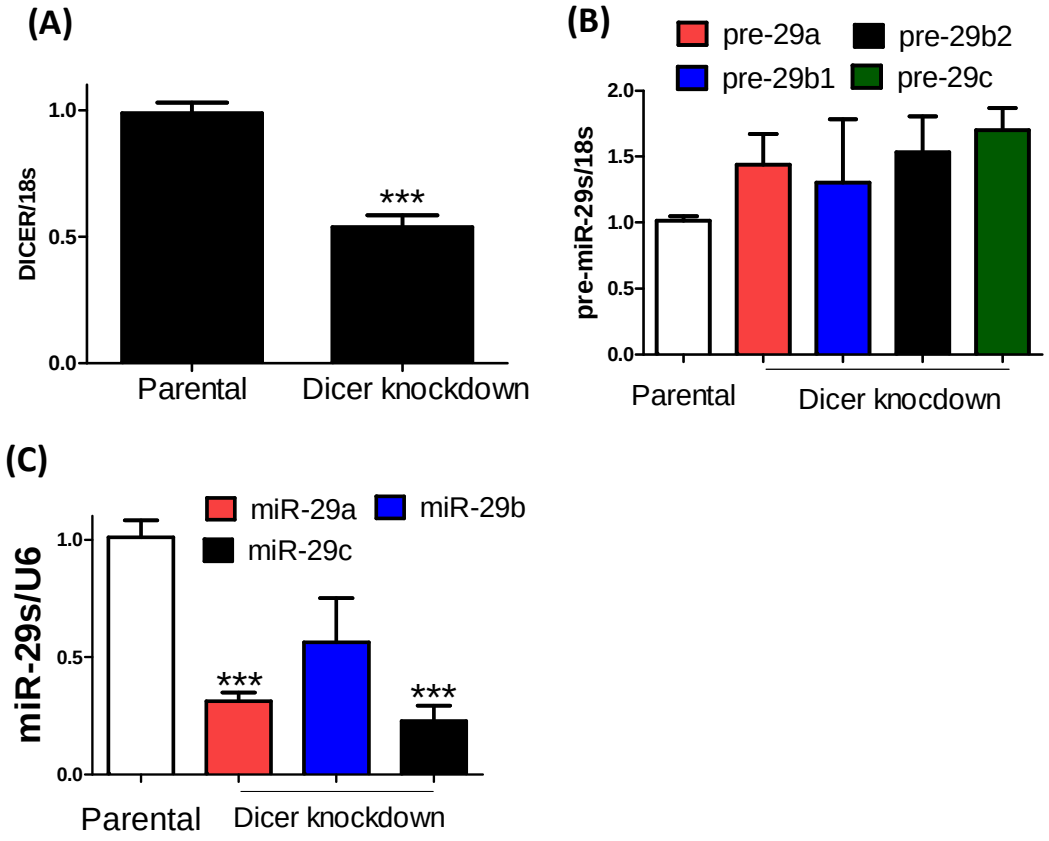

Figure 4.15: Dicer is required for the miR-29 family maturation

2

Level of Dicer, precursor and mature miR-29 were measured in DLD, Dicer knockdown cell line or parental control by quantitative RT-PCR. (A) Relative expression of Dicer; (B) Relative expression of precursor miR-29s (normalised to expression in parental control). 18S rRNA is endogenous control. Red, pre-29a; blue, pre-29b1; black, pre-29b2; green, pre-29c; white, levels of all precursors in control (set at 1); (C) Relative expression of mature miR-29 family (normalised to expression in parental control). U6 is endogenous control. Red, miR-29a; blue, miR-29b; black, miR-29c; white, levels of all mature miR-29 in control (set at 1). Means ± standard errors are presented. The difference of relative expression was analysed by unpaired two-tailed Student's t test. * $p<0.05$, ** $p < 0.01$, *** $p<0.001$, n=3.

4.3. Discussion

Since miRNAs have broad effects on cartilage homeostasis, and OA, it is particularly interesting to work out how miRNAs themselves are being regulated. Such data could provide crucial information for further understanding the mechanism underlying OA and for being able to manipulate these miRNAs in chondrocytes therapeutically. Generally, the expression of miRNAs can be regulated transcriptionally, epigenetically, or controlled by different stimuli e.g. cytokines and growth factors. In this study, just transcription factors, cytokines, and growth factors controlling the miR-29 family expression in chondrocytes were for the first time investigated. These studies were able to show that, in human chondrocytes, the master transcriptional regulator SOX9, TGFβ and LPS suppressed whilst IL-1 strongly induced the miRNA-29 family expression.

Several published data report the suppressive effect of SOX9 on the expression of individual members of the miR-29 family in other cellular contexts: in murine stem cells, overexpression of SOX9 or knockdown SOX9 in cell lines e.g. C3H10T1/2 or ATDC5 leads to suppression or induction of miR-29a and miR-29b expression (Yan et al. 2011), respectively; in human C-20/A4 chondrocytes, overexpression of SOX9 strongly down-regulated the level of miR-29a (Guerit et al. 2014). Herein, for the first time, suppressive effect of SOX9 on the expression of all members of the miR-29 family in primary human chondrocytes was shown. The effect was exerted, at least in part, through directly targeting the promoter of the miR-29a/b1 locus. In line with these data, Guerit et al (2014) reported that SOX9 can physically bind to at least 3 out of 4 putative binding sites within the proximal promoter of miR-29a/b1 cluster; also, another transcription factor YY1, was shown not to bind directly to the miR-29a/b1 promoter, but, physically interacted with SOX9 to suppress miR-29a/b1 expression (Guerit et al. 2014). The mechanism by which SOX9 negatively regulates the pri-miR-29b2/c cluster is still unknown. Several putative binding sites of SOX9 are found in the promoter of the pri-miR-29b2/c cluster, implicating a possible direct mechanism. However, this needs further investigation.

Alongside SOX9, other transcriptional regulatory mechanisms responsible for expression of the miR-29 family have also been reported: the pri-miR-29a/b1 locus was stimulated by the transcription factors CEBPA (Eyholzer et al, 2010), GATA3 (Chou et al. 2013), STAT1 (Schmitt et al, 2012) but suppressed by c-MYC (Mott et al. 2010, Parpart et al. 2014), NFκB

(Liu et al. 2010, Mott et al. 2010), Sp1(Liu et al. 2010, Amodio et al. 2012), HDAC1, HDAC3, and Gli (Mott et al. 2010); the pri-miR-29b2/c locus was inhibited by Smad3 (Qin et al. 2011), NFκB, YY1, Ezh2, H3K37, HDAC1 (Wang et al. 2008). Thus, it is likely that the transcriptional regulation of the miR-29a/b1 cluster is controlled by a combination of different transcription factors. Interestingly, in the chondrocyte context, miR-1247 together with miR-145 were reported to directly target and repress expression of SOX9 (Yang et al. 2011, Martinez-Sanchez and Murphy 2013), suggesting these miRNAs could contribute to the induction of the miR-29 family level in chondrocytes. Additionally, throughout the current project, the miR-29 family members exhibit different expression levels between the primary miR-29a/b1 and primary miR-29b2/c loci in different cellular contexts. This discrepancy could be explained in part by different transcription factor binding to each promoter.

Together with SOX9, TGFβ signalling was found to suppress the expression of all miR-29 family members in chondrocytes. Since TGFβ signalling induces SOX9 expression (Greco et al. 2011), the suppressive effect of TGFβ on the miR-29 family could be exerted through SOX9 and this TGFβ-SOX9 signalling could in part explain the down-regulation of the miR-29 family by TGFβ. The suppressive effect of TGFβ on the miR-29 family expression has also been observed in various cell types associated with fibrosis e.g. human aortic adventitial fibroblasts (Maegdefessel et al. 2012), renal fibrosis cells (Wang et al. 2012, Ramdas et al. 2013), murine hepatic stellate cells (Roderburg et al. 2011), rat hepatic stellate cells (Kwiecinski et al. 2011), human skin fibroblasts (Maurer et al. 2010), human tenon's fibroblast (Li et al. 2012), human lung fibroblast cell line (Cushing et al. 2011, Yang et al. 2013) in which either some members or the whole miR-29 family significantly decreased expression with TGFβ treatment. Apart from TGFβ-SOX9 signalling, the mechanism for the inhibition of TGFβ on the miR-29 family expression is currently unknown. There is some evidence that TGFβ inhibits miR-29 expression through SMAD3 signalling e.g. the inhibition effect of TGFβ on miR-29 expression was abolished when *Smad3* was knocked out in mouse embryonic fibroblast (Qin et al. 2011); SMAD3 could directly interact with at least two conserved SMAD3-binding sites in the promoter region of miR-29b2/c locus (Qin et al. 2011); activated TGFβ signalling induced SMAD3 translocate into nucleus and bind to miR-29b2/c promoter, resulting in the dissociation of MyoD and the stabilization of YY1 whose expression negatively regulated the miR-29b2/c expression through a conserved binding site

(Qin et al. 2011). However, this needs to be validated in chondrocytes. Besides the suppressive role, TGFβ also exerted an inductive effect on miR-29 expression at late time points. For instance, the primary miR-29b2/c locus was induced in human primary chondrocyte in micromass cultured with TGFβ1 for 48 hours (Figure 4.4b) though this increase did not reach significantly; the miR-29 family expression was increased at a late stage in the human chondrogenesis model with TGFβ3 as the major driver among others (Figure 3.12). That TGFβ induces miR-29 family expression suggests that there are may be several TGFβ-triggered signalling pathways, apart from TGFβ-SOX9, regulating the miRNA-29 expression. However, in this project, the molecular mechanisms by which TGFβ controls expression of the miR-29s are again not fully understood.

The TLR4 ligand, LPS, was found to repress the miR-29 family expression in chondrocytes. Importantly, this inhibition was facilitated by NFκB (p50/p65). Supporting the finding of this study, published data in cholangiocarcinoma cells and murine hepatic stellate cells also showed that LPS down-regulated expression of the miR-29 family (Mott et al. 2010, Roderburg et al. 2011) . Moreover, NFκB, activated by TLR ligands, was revealed to both directly or indirectly (cooperating with YY1) suppress the miR-29a/b1 or the miR-29b2/c locus, respectively (Wang et al. 2008, Mott et al. 2010). In contrast to LPS, it was surprising to find that IL-1β increased miR-29 expression and this stimulation was not NFκB but p38-dependent. However, the effect of inhibiting p38 signalling was only observed for miR-29a and miR-29b but not miR-29c, although all miR-29 family members were found strongly induced by IL-1β. Since IL-1β could activate the NFκB signalling pathway alongside p38 MAPK signalling (Aigner et al. 2006), the fact that an NFκB inhibitor further increased the IL-1 induction of the miR-29a/b1 locus implicates NFκB signalling in suppressing miR-29. It is likely that in human chondrocyte, for the period of time examined (48 hours), induction through 38 MAPK signalling was dominant over the NFκB, explaining why IL-1β induced (not suppressed) miR-29 expression. It therefore, made sense to expect a similar induction of the proximal promoter of miR-29a/b1 by IL-1β. However, a suppressive effect was observed. These data could be explained if the inductive p38-dependent transcription factors do not work through this 2kb proximal promoter of the miR-29a/b1, whilst several binding sites of NFκB in this promoter region are seen. This hypothesis needs experimental data to validate it. The mechanism responsible for the IL-1β induced miR-29b2/c cluster is still unclear and needed to be further explored. Notably, the IL-1β mRNA expression level was increased by

LPS/ TLR-4 and this is mediated by p38 MAP kinase in human chondrocytes (Bobacz *et al.* 2007). Therefore, that the miR-29 family expression was increased after 48 hours treatment with LPS could be explained in part by the accumulation of IL-1β which in turn up-regulated the miR-29 family expression.

This study also showed that the expression of all miR-29 members was not modulated by Wnt3a (β-catenin, canonical Wnt signalling), neither at the mRNA level by qRT-PCR or in the promoter assay. There are, several publications which have reported that either some members or the whole miR-29 family were Wnt3a-induced: In osteoblasts, Wnt3a positively modulates the expression of miR-29a and miR-29c though two T-cell factor/LEF-binding sites within the miR-29a/b1 promoter (Kapinas et al. 2009, Kapinas et al. 2010); in muscle progenitor cells (MPCs), Wnt3a treatment increased miR-29s expression in a time dependent manner (Hu et al. 2014); the promoter activities of both the miR-29a/b1 and miR-29b2/c cluster were strongly induced in MPCs where Wnt3a was overexpressed or added to media (Hu et al. 2014).Therefore, an interesting question that remains to be answered is why miR-29 expression is not modulated by Wnt3a in chondrocytes.

In contrast to the rapid change in expression of the pri-miR-29 or pre-miR-29 in response to stimuli, the modulation of the miR-29 family mature is quite slow. The posttranscriptional processing from the precursor to the mature form of the miR-29 family may be tightly controlled. Since the miR-29s has significant impact on a functional phenotype by regulating multiple genes that fall into the same or related pathways (which will be discussed more in Chapter 5), its expression must be regulated, potentially at more than one level. Interestingly, herein, Dicer was found to be the direct target of the miR29 family, suggesting a negative feedback loop for its maturation. In supporting this data, in T47D breast cancer cells, Dicer 1 was also reported as a miR-29a target (Cochrane *et al.* 2010). Apart from Dicer, other components of the microRNA precursor processing machinery e.g. Helicase, Exportin 4 and 5 are also predicted to be putative targets of the miR-29s as they have several binding sites in their 3'UTR regions (data not shown). Even though these have not been experimentally validated as the direct targets, this further supports the idea that miR-29 is involved in a negative feedback loop for its maturation.

In conclusion, the miR-29 family was found to be negatively regulated by the master regulator of chondrogensis SOX9, by TGFβ signalling and by LPS-NFκB signalling. It is

positively regulated by IL-1-p38 MAPK signalling. Interestingly, the canonical Wnt signalling pathway does not control expression of the miR-29 family. Furthermore, expression of the miR-29 family was tightly controlled at the level of posttranscriptional processing in which miR-29 directly targets Dicer, giving a negative feedback loop for its maturation.

CHAPTER 5
FUNCTIONS OF THE MICRORNA 29 FAMILY IN CHONDROCYTES

5.1 Introduction

The ability of a single miRNA to target multiple mRNAs especially those that function in the same intracellular pathways and/or diseases, adds an additional layer of regulation to gene expression. The aberrant expression of the miR-29 family has been found in multiple malignancies and fibroses, carcinogenesis. Also, an understanding of how miR-29 contributes to these processes has been revealed: miR-29 targets genes are involved in cellular proliferation, cell cycle, cell differentiation, and apoptosis at genetic and epigenetic levels. The following summarizes some functions of miR-29s in human disease.

In chondrogenesis or OA, around 30 miRNAs have been shown to have functions in cartilage homeostasis (Le et al, 2013), which is relatively small compared to the total number of miRNAs. Moreover, as mentioned in the previous chapter, for any potential miRNA therapeutic application, a combination of different miRNAs might be required for a complex disease like OA. Identifying novel miRNA targets and the cell signalling pathways and networks by which miRNAs exert their functions on disease phenotype are therefore, of particular importance both to have an insight into OA pathogenesis and also to ensure the specificity in any miRNA-based drug delivery method. Thus, this chapter places emphasis on identifying the function of the miR-29 family in chondrocytes including identifying the function of the miR-29 family in TGFβ/Smad, NFκB, and Wnt/β-catenin signalling pathways and novel targets of the miR-29s.

Aims:

- Investigate signalling pathways involved in chondrogenesis and osteoarthritis which are regulated by the miR-29 family
- Perform gain-and-loss of function of miR-29b experiments to identify potential targets of the miR-29 family
- Identify and validate novel direct targets of the miR-29 family

5.2 Results

5.2.1 The miR-29 family supress TGFβ/Smad signalling pathway

In articular cartilage, the canonical TGFβ/Smad signalling pathway has been shown to play a pivotal role in the maintenance of normal cartilage: it up-regulates the expression of several types of collagens and proteoglycan; and it down-regulates cartilage degrading enzymes. Importantly, disruption of the TGFβ pathway has been shown to lead to OA. Mice expressing a dominant negative TGFβRII exhibit articular cartilage degeneration similar to that observed in human OA with abnormal expression of type X collagen, an indicator of chondrocyte hypertrophy; mutant mice with targeted disruption of Smad3 (Smad3−/−) show a similar pathology in chondrocytes, including aberrant type X collagen expression in vivo; primary chondrocytes isolated from Smad3−/− mice demonstrate an accelerated differentiation process with up-regulated BMP signalling.

In Chapter 4, expression of the miR-29 family was found to be suppressed by TGFβ signalling. Here, I measure the impact of the miR-29 family on Smad signalling. The TGFβ/Smad signalling reporter (CAGA)12-luc (Figure 5.1a) containing 12 binding sites of the Smad2/3/4 (GAGAC) binding site upstream of the firefly luciferase-encoding gene was used. The principle of this experiment is based on the fact that: signals are transduced from TGFβ ligands to the Smad2/3/4 complex which subsequently regulates gene expression; the miR-29 family may change the expression or transcriptional activity of Smad2/3/4; thus altering luciferase levels. $(CAGA)_{12}$-luc (100ng) and Renilla (10ng) were co-transfected with either miR-29 mimic (50nM) or non-targeting control (50nM) into SW1353 cells for 24 hours and followed by serum starvation for another 24 hours. Cells were then treated with either TGFβ1 or TGFβ3 (4ng/ml) for another 6 hours before measuring the luciferase activity. Luciferase assay data (Figure 5.1b) showed that: stimulating cells with TGFβ1 strongly induced luciferase activity as compared with non-treatment control; pre-treatment with all members of the miR-29 family significantly decreased the luciferase activity at this 6 hour time point. A similar pattern was observed when treating cells with TGFβ3 (Appendix, Figure 7a). These data demonstrate that Smad signalling was successfully activated in SW1353 cells by TGFβ1or TGFβ3 and that the miR-29 family is a negative regulator of this signalling. As all miR-29 family members supressed the signalling, an experiment using only an inhibitor of miR-29b (50nM) was performed. Consistent with the mimic data above,

luciferase activity was significantly increased with the miR-29b inhibitor compared to control (Figure 5.1c and Appendix, Figure 7b).

The suppressive effect of the miR-29 family on the TGFβ signalling pathway was further confirmed by measuring the effect of the miR-29 family on a TGFβ responsive gene. ADAMTS4 was chosen since it is induced by TGFβ in chondrocytes, but was not a putative direct target of the miR-29 family. Human primary chondrocytes were transfected with miR-29 family mimics (50nM) in monolayer for 24 hours with 10% (v/v) FCS. The media was then replaced with media with 0.5% (v/v) FCS for another 24 hours before stimulating with TGFβ (4ng/ml) for a further 6 hours. The expression of ADAMTS4 was measured by qRT-PCR (Figure 5.2) showing that ADAMTS4 was strongly induced by TGFβ; the miR-29 mimics significantly decreased the expression of ADAMTS4 as compared with non-targeting control. These data again confirmed the suppressive effect of the miR-29 family on TGFβ signalling pathway.

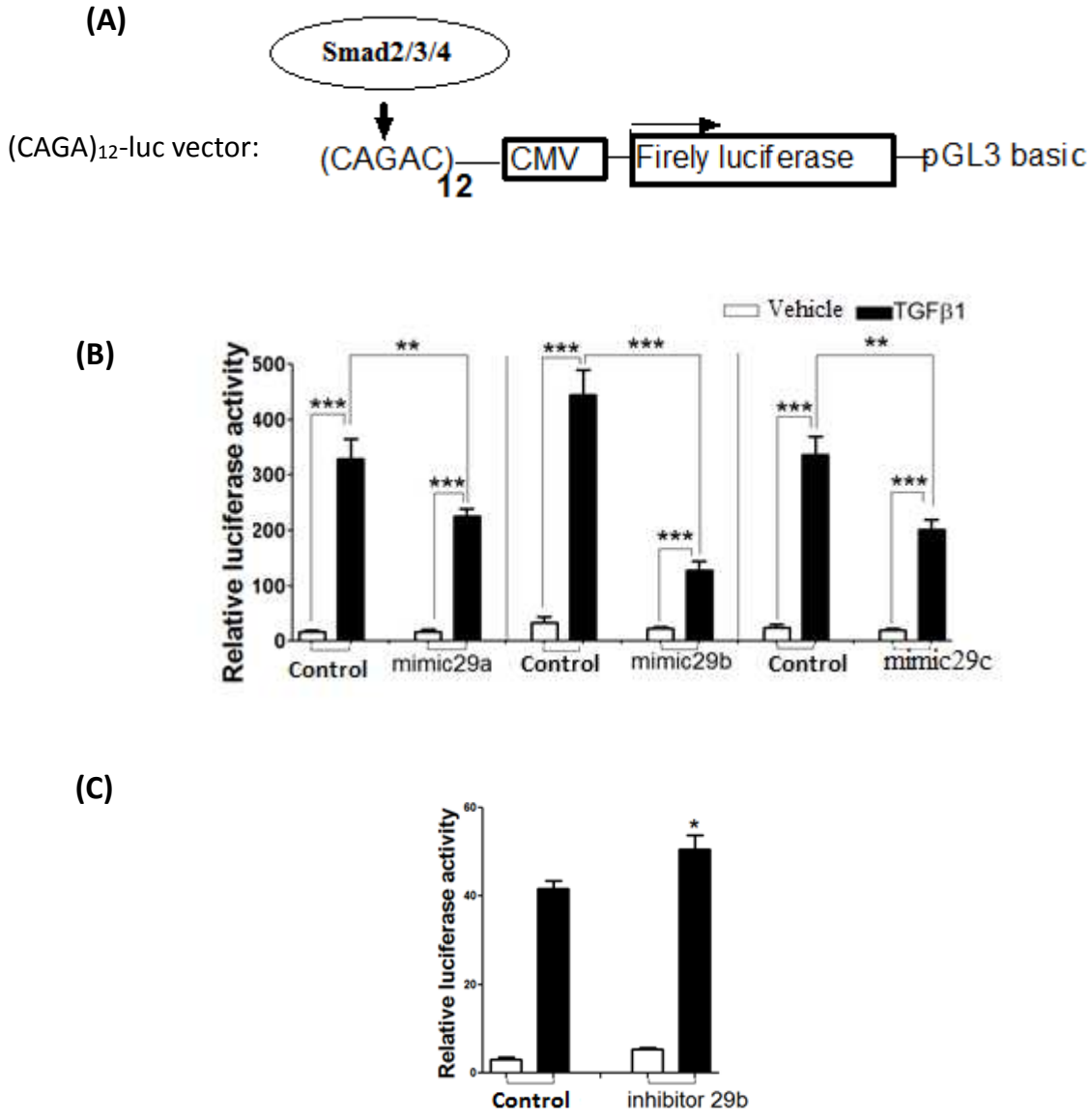

Figure 5.1 The miR-29 family suppress TGFβ signalling pathway

(A) The TGFβ signalling reporter ($CAGA_{12}$-luc) contains 12 binding sites of the Smad2/3/4 (GAGAC) binding consensus upstream of the firely luciferase-encoding gene in pGL3100ng $CAGA_{12}$-luc vector, and 10ng Renilla vector were co-transfected with either miR-29 family mimic (B) or miR-29b inhibitor (C) into SW1353 cells in monolayer. The non-targeting control (50nM) was also used as the negative control. 24 hours after transfection, cells were serum starved for another 24 hours, followed by treatment with TGFβ (4ng/ml) for another 6 hours before measuring luciferase activity. Renilla is the loading control for luciferase assay. Open bar: non – treatment control, close bar: TGFβ treatment. Means ± standard errors are presented, n=6. The difference of luciferase activity was analysed by Student's unpaired two-tailed t test. * $p<0.05$, ** $p < 0.01$, *** $p<0.001$

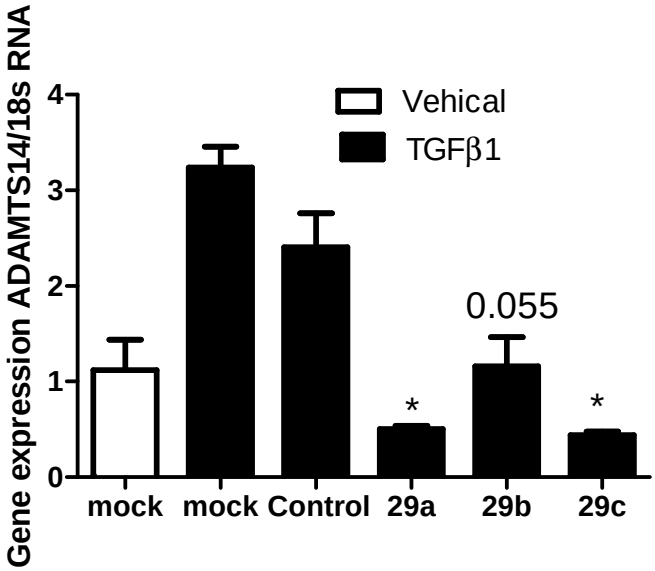

Figure 5.2 The miR-29 family suppresses the TGFβ induced gene ADAMTS4

Human primary chondrocytes were transfected with either miR-29 family mimics (50nM) or non – targeting control (50nM) for 24 hours. Cells were then changed into 0.5% (v/v) FCS for 24 hours and followed by stimulating with TGFβ1 (4ng/ml) for another 6 hours. Total RNA was isolated and the expression level of ADAMTS4 was measured by qRT-PCR. 18S rRNA was used as the endogenous control. Data were normalized to untreated, mock transfected cells. Open bar: non – treatment control, close bars: TGFβ treatment. Means ± standard errors are presented, n=3. The difference in expression level of ADAMTS was analysed by Student's unpaired two-tailed t test. * $p<0.05$, ** $p < 0.01$, *** $p<0.00$

5.2.2 The miR-29 family suppresses the NFκB signalling pathway

In Chapter 4, IL-1β was found to increase expression of the miR-29 family. It is, therefore, of importance to investigate how the miR-29 family regulates the signalling pathways triggered by IL-1β. There are at least three pathways triggered by IL-1β including NFκB, JNK, and p38 MAPK pathways. Nevertheless, in this project, just the interaction between the miR-29 family and NFκB signalling was investigated. The transcription factor NFκB is held in the cytoplasm in an inactive form associated with the inhibtory κB (IκB) protein. In response to IL-1β binding of the receptor, NFκB releases from IκB and the activated NFκB will then translocate to the nuclear, bind to DNA elements present in its target genes and facilitate their transcription.

Similar to the experiment for investigating the interacting between the miR-29 family and TGFβ signalling, the NFκB signalling reporter containing multiple binding sites for NFκB upstream of a luciferase-encoding gene was utilized (Figure 5.3a). The signal cascade from IL-1β will activate NFκB which consequently induces the transcription of the luciferase gene in the reporter and this may be modulated by the miR-29 family. The luciferase assay was set up similar to the experiment in 5.1.1 except the cells were treated with IL-1β (5ng/ml) instead of TGFβ1 (4ng/ml). Luciferase data (Figure 5.3b, c) showed that IL-1β strongly induced the luciferase activity of the κB reporter; all miR-29 family mimics significantly decreased activity (B) but the miR-29b inhibitor induced activity (C). These data show that NFκB signalling was successfully triggered in SW1353 cells by IL-1and that the miR-29 family is a negative regulator of the NFκB signalling pathway.

The suppressive effect of the miR-29 family on the NFκB signalling pathway was further confirmed by measuring the effect of the miR-29 family on an NFκB responsive gene. MMP3, which is induced expression by IL-1 and is not a putative direct target of the miR-29 family, was chosen. Again, the experiment was set up similar to the experiment in 5.1.1 except cells were stimulated with IL-1 (5ng/ml). The Taqman qRT-PCR (Figure 5.4) showed that MMP3 was strongly induced expression by IL-1β; the miR-29b and miR-29c mimics significantly decreased the expression of MMP3 as compared with non-targeting control, though the miR-29a mimic had no effect.

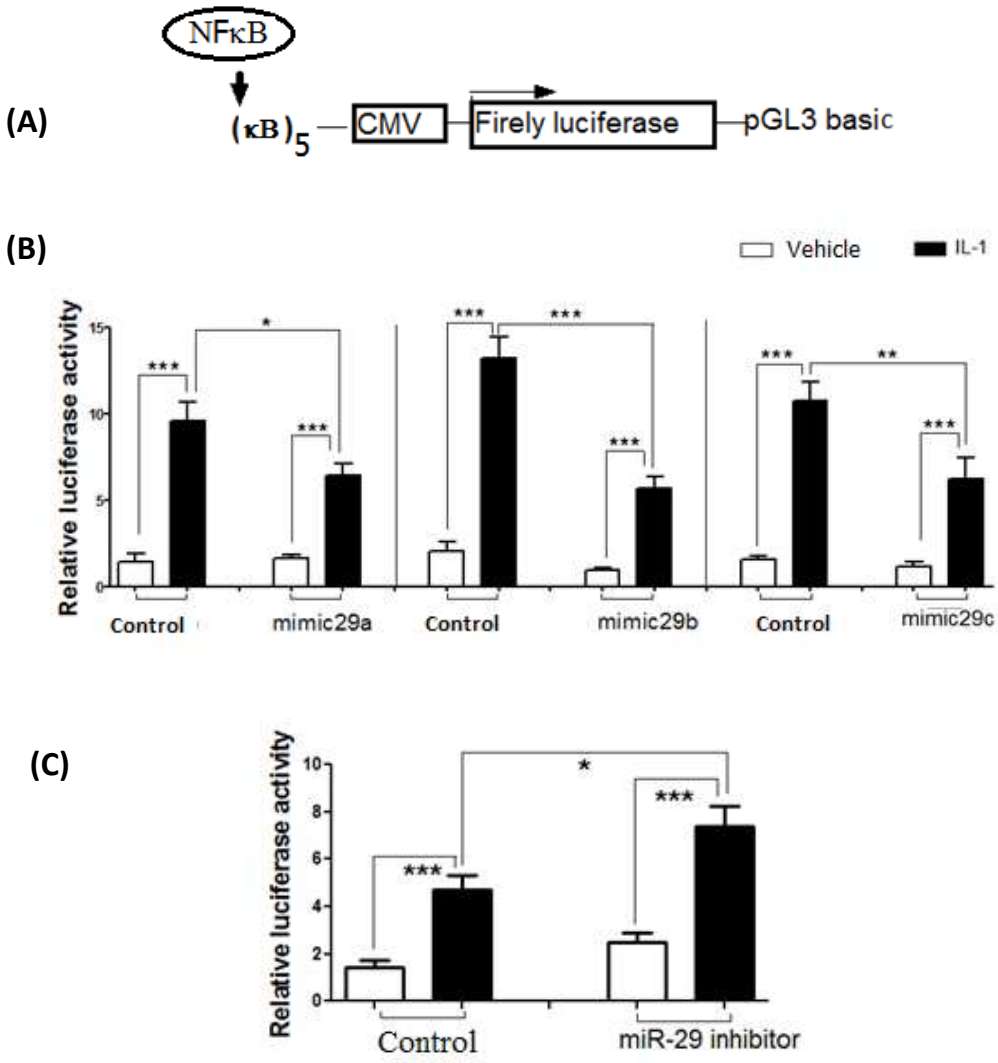

Figure 5.3 The miR-29 family suppresses NFκB signalling pathway

(A) The NFκB signalling reporter (κB vector) contains 5 binding sites of NFκB upstream of the firely luciferase-encoding gene in pGL3

100ng κB vector, and 10ng Renilla expression vector were co-transfected with either miR-29 family mimic (B) or miR-29b inhibitor (C) into SW1353 cells in monolayer. The non-targeting control (50nM) was also used as a negative control. 24 hours after transfection, cells were serum starved for further 24 hours, and followed by treating with IL-1 (5ng/ml) for another 6 hours before measuring luciferase activity. Renilla is the endogenous control for luciferase assay. Means ± standard errors are presented, n=6. The difference of luciferase activity was analysed by Student's unpaired two-tailed t test. * $p<0.05$, ** $p < 0.01$, *** $p<0.001$

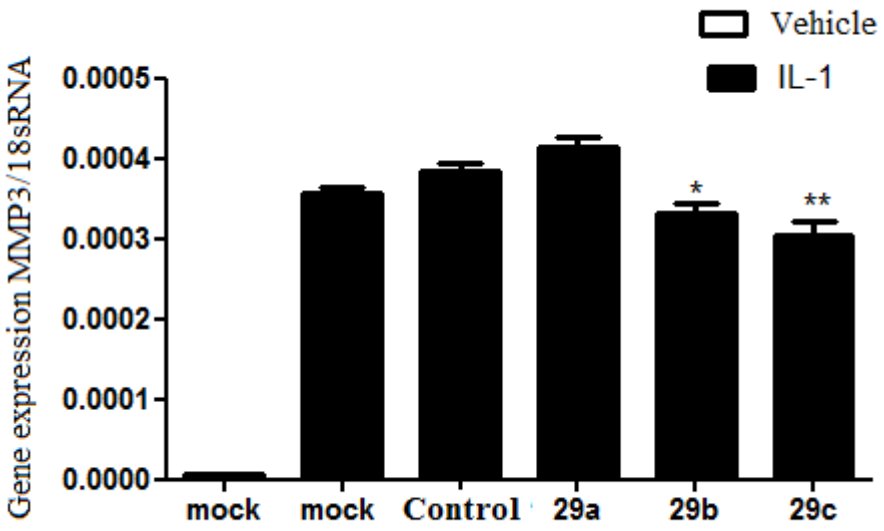

Figure 5.4 The miR-29 family suppresses expression of the IL-1-induced gene MMP3
Human primary chondrocytes were transfected with either miR-29 family mimic (50nM) or non – targeting control (50nM) for 24 hours. Cells were then changed into 0.5% (v/v) FCS for 24 hours, followed by stimulating with IL-1β (5ng/ml) for a further 6 hours. Total RNA was isolated and the expression of MMP3 was measured by qRT-PCR. 18S rRNA expression was used as the housekeeping gene. Open bar: non – treatment control, close bar: IL-1β treatment. Means ± standard errors are presented, n=3. The difference in expression level of IL-1β was analysed by unpaired two-tailed t test. * $p<0.05$, ** $p < 0.01$, *** $p<0.001$

5.2.3 The miR-29 family supresses the canonical Wnt signalling pathway

Even though expression of the miR-29 family is not regulated by Wnt3a in human chondrocyte, it is still of interest to investigate whether the WNT/β-catenin signalling is modulated by the miR-29 family because of the critical role of this signalling in OA development: balanced β-catenin levels are essential for maintaining homeostasis of articular cartilage and any factors impairing this balance could lead to pathological changes.

For investigating the interaction between the miR-29 family with the WNT/β-catenin signalling, the TOPFlash reporter (containing 7 binding sites of TCF/LEF driving the expression of the luciferase encoding gene) and FOPFlash reporter (control for TOPFlash where all the TCF/LEF binding sites are mutated) were used (Figure 5.5a). With the presence of e.g. Wnt3a, the signal transduced from the FZD receptor and LRP-5/6 co-receptor proteins will lead to the accumulation of β-catenin in the nucleus where it acts in concert with TCF/LEF transcription factors to generate a transcriptionally active complex inducing the expression of cognate genes and also therefore the TOPFlash reporter. Thus, any modulation of luciferase activity in the presence of the miR-29 family indicates that the miRNA family impacts on canonical signalling. Again the luciferase assay experiment was set up similarly to the assay in 5.1.1 but the TOPFlash (100ng) or FOPFlash (100ng) and Wnt3a (50ng/ml) were utilized. Luciferase assay data (Figure 5.5b, c) showed that Wnt3a strongly induced the luciferase activity from TOPFlash but not FOPFlash reporters; all members of the miR-29 family significantly decreased luciferase activity, whilst a miR-29b inhibitor increased the luciferase activity compared to control. These data show that the WNT/β-catenin pathway was induced in SW1353 cell with Wnt3a and that the miR-29 family is a negative regulator of this signalling.

The suppressive effect of the miR-29 family on the WNT/β-catenin signalling pathway was further confirmed by measuring the effect of the miR-29 family on the expression of *AXIN2*, a WNT/β-catenin responsive gene and not a putative direct target of the miR-29 family. The experiment was set up similarly to the experiment in 5.1.1 except cells were stimulated with Wnt3a (50ng/ml). The qRT-PCR data (Figure 5.6) showed that *AXIN2* expression was strongly induced by Wnt3a; the miR-29 family mimics significantly decreased the expression of *AXIN2* as compared with non-targeting control.

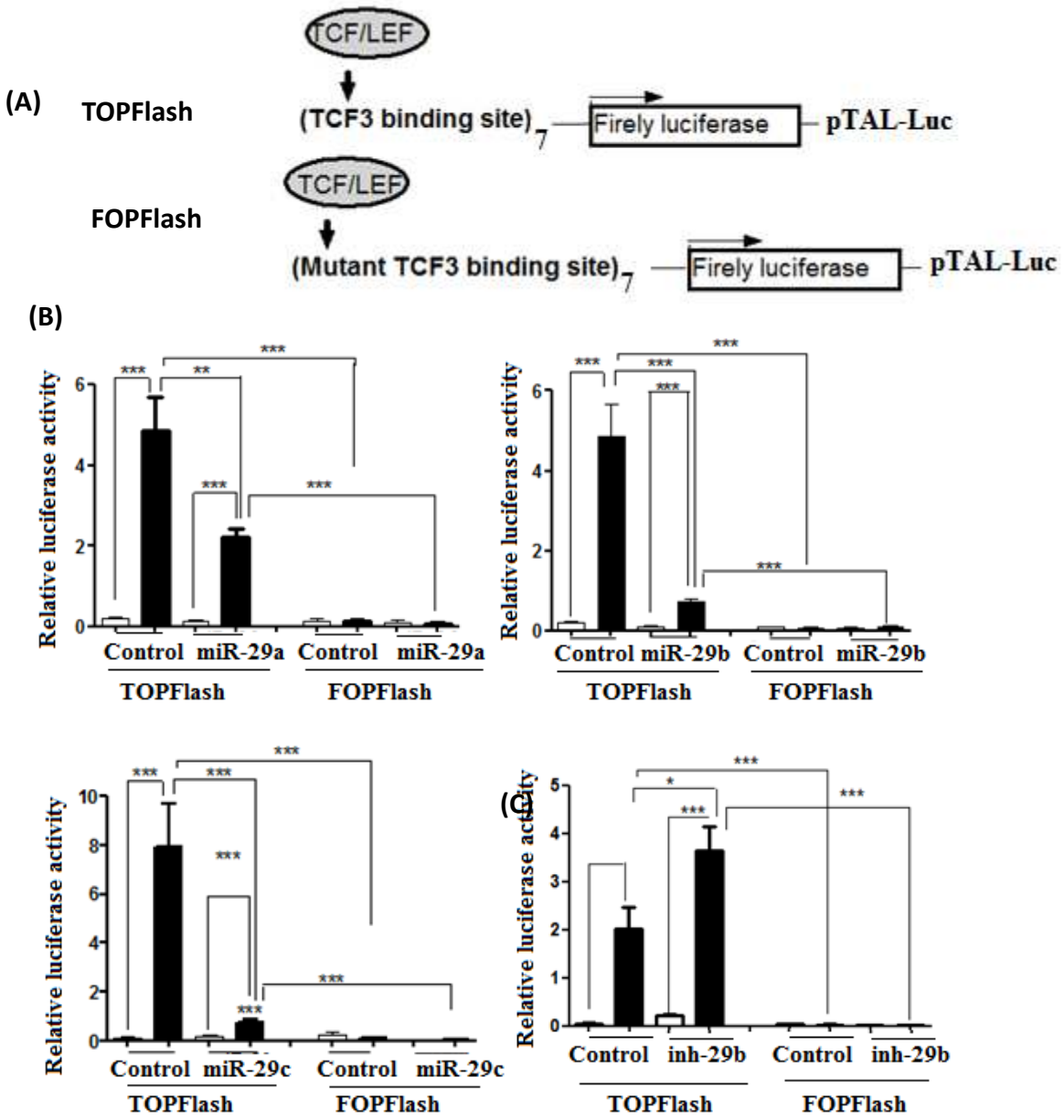

Figure 5.5 The miR-29 family suppresses the WNT/β-catenin signalling pathway

(A) The canonical WNT signalling reporter (TOPFlash vector) contains 7 binding sites of TCF/LEF upstream of the firely luciferase encoding gene in the pTAL-Luc vector. The FOPFlash vector is the control in which all binding sites of TCF/LEF are mutated.

100ng TOPFlash or FOPFlash vectors, and 10ng Renilla vector was co-transfected with either miR-29 family mimic (50nM) (B) or miR-29b inhibitor (50nM) (C) into SW1353 cells in monolayer. The non-targeting control (50nM) was also used as the control. 24 hours after transfection, cells were serum starved for another 24 hours, and followed by treatment with WNT3a (50ng/ml) for another 6 hours before measuring luciferase activity. Renilla is the endogenous control for luciferase assay. Means ± standard errors are presented, n=6. The difference of luciferase activity was analysed by Student's unpaired two-tailed t test. * $p<0.05$, ** $p < 0.01$, *** $p<0.001$

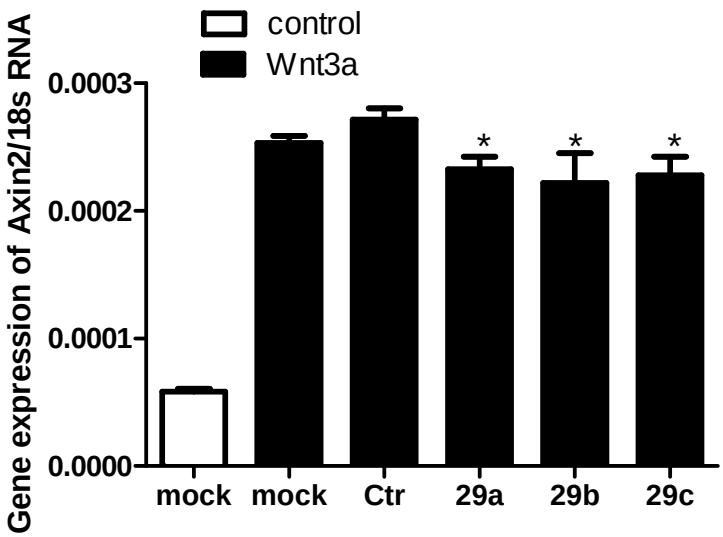

Figure 5.6 The miR-29 family suppresses expression of the WNT/β-catenin induced gene *AXIN2*

Human primary chondrocytes were transfected with either miR-29 family mimic (50nM) or non – targeting control (50nM) for 24 hours. Cells were then serum starved for 24 hours and followed by stimulating with Wnt3a (50ng/ml) for another 6 hours. The expression level of Axin2 was measured by qRT-PCR. 18S rRNA was used as the housekeeping gene. Open bar: non – treatment control, close bar: WNT3a treatment. Means ± standard errors are presented, n=3. The difference in expression level of *AXIN2* was analysed by unpaired two-tailed t test. * $p<0.05$, ** $p < 0.01$, *** $p<0.001$

5.2.4 Identification of miR-29 family targets

The miR-29 family was found to suppress the TGFβ/Smad, NFκB, and WNT/β-catenin signalling pathways. Nonetheless, it still remained unclear the direct mechanism by which the miR-29 family controlled these pathways. I therefore sought to identify novel targets of the miR-29 family to explain how the miR-29 family interacts with these pathways.

5.2.4.1 Gain- and loss- of function of miR-29b

For identifying new targets, a gain- and loss- of function experiment was performed. Since the miR-29 family shares the same seed binding site, it was deemed sufficient just to overexpress or silence miR-29b rather than all members of the family. Human primary chondrocytes were transiently transfected with miR-29b mimic or miR-29b inhibitor (50nM) and their non-targeting controls for 48 hours in triplicate and then total RNA was isolated. The transfection experiment was validated by measuring the miR-29b level by qRT-PCR. The data (data not shown) showed that the level of miR-29b strongly increased or decreased after transfection with either miR-29b mimic or inhibitor, respectively. These data suggest a good transfection efficiency into human chondrocytes. For performing a whole genome profile, an equal amount of total RNA from each sample in the triplicate was pooled together. These pooled samples were then subjected to whole genome array using Illumina human HT-12 V4.0 expression BeadChips to profile more than 47,000 human transcripts.

The global effect of the miR-29b mimic and inhibitor transfection on whole genome expression was first investigated by plotting the distribution of different expression values for all mRNAs in the miR-29b overexpression or knockdown experiments. Since the miRNA will exert its function by suppressing target gene expression, it was expected that the overexpression of miR-29b would significantly suppress target gene expression; conversely, a strong induction of target gene expression would be observed with the silencing of the miR-29b. Consistent with this hypothesis, data (Figure 5.7A) showed that in the miR-29b silencing experiment, the distribution of modulated genes was slightly skewed towards higher expression. Using an absolute 1.3 fold change (FC) as the cut off, there are 213 and 144 mRNA going up and down, respectively in this experiment (whilst just 9 and 10 mRNA going up and down respectively if the FC cut off was 1.5). Surprisingly, this pattern was also observed with the overexpression of the miR-29b (Figure 5.7B) with 703 and 518 mRNA

going up and down with 1.5 FC cut off, respectively. These data suggest that the miR-29b mimic has stronger effect than miR-29b inhibitor in chondrocytes and that the transfection with the miR-29b mimic strongly induced rather than supressed gene expression. Further analysis of the mRNAs strongly increased with miR-29b overexpression showed that the majority of these induced genes do not contain a binding site for the miR-29 family in their 3'UTR, suggesting that they are not direct targets of the miR-29 family. Indeed, a number of interferon responsive genes were strongly increased (Appendix, Table 7), suggesting a non-specific response to the synthetic oligonucleotide. This has been previously noted even for small RNAs (Karlsen et al. 2011). Interestingly, these genes were not modulated in the miR-29b silencing experiment, suggesting that a specific sequence in the miR-29b mimic is responsible.

The effect of the miR-29b mimic or inhibitor on whole genome expression was further analysed by examining the potential targets of the miR-29 family. The array data (Figure 5.8) revealed there were 12215 mRNAs in the intersection of the two experiments that increased in the miR-29b knockdown and decreased in miR-29b overexpression experiments. To further explore the effect of modulation of miR-29b on the transcriptome, the percentage of mRNAs containing seed sites (e.g. 6-mer, 7-mer, 8-mer) was calculated. It was a postulated that potential direct targets of miR-29s (those mRNA containing miR-29 seed sites) should be enriched in mRNA down-regulated by miR-29b and in mRNA up-regulated by miRNA-29b silencing. Particularly, this enrichment should be highest in genes that are decreased by miR-29b mimic and increased by miR-29b inhibitor. Data (Figure 5.8) showed that regardless of the length of the seed sequence, the percentage of mRNAs with seed sites is higher in the mRNAs which are decreased on overexpression or increased on silencing of miR-29b than in total mRNA. The percentage of mRNAs with seed sites is the highest in the intersection of the two experiments. These data confirm the hypothesis that taking the intersection containing mRNAs which decrease with the overexpression and increase with silencing of miR-29b is an effective way to filter the relevant miRNA targets.

Also, a subset of mRNA which was differentially expressed in the microarray analysis was selected for validating using RT-qPCR. Comparison of the expression levels between the microarray and RT-PCR results demonstrated a similar expression pattern between the two platforms (data not shown). These results confirmed the mRNA array data.

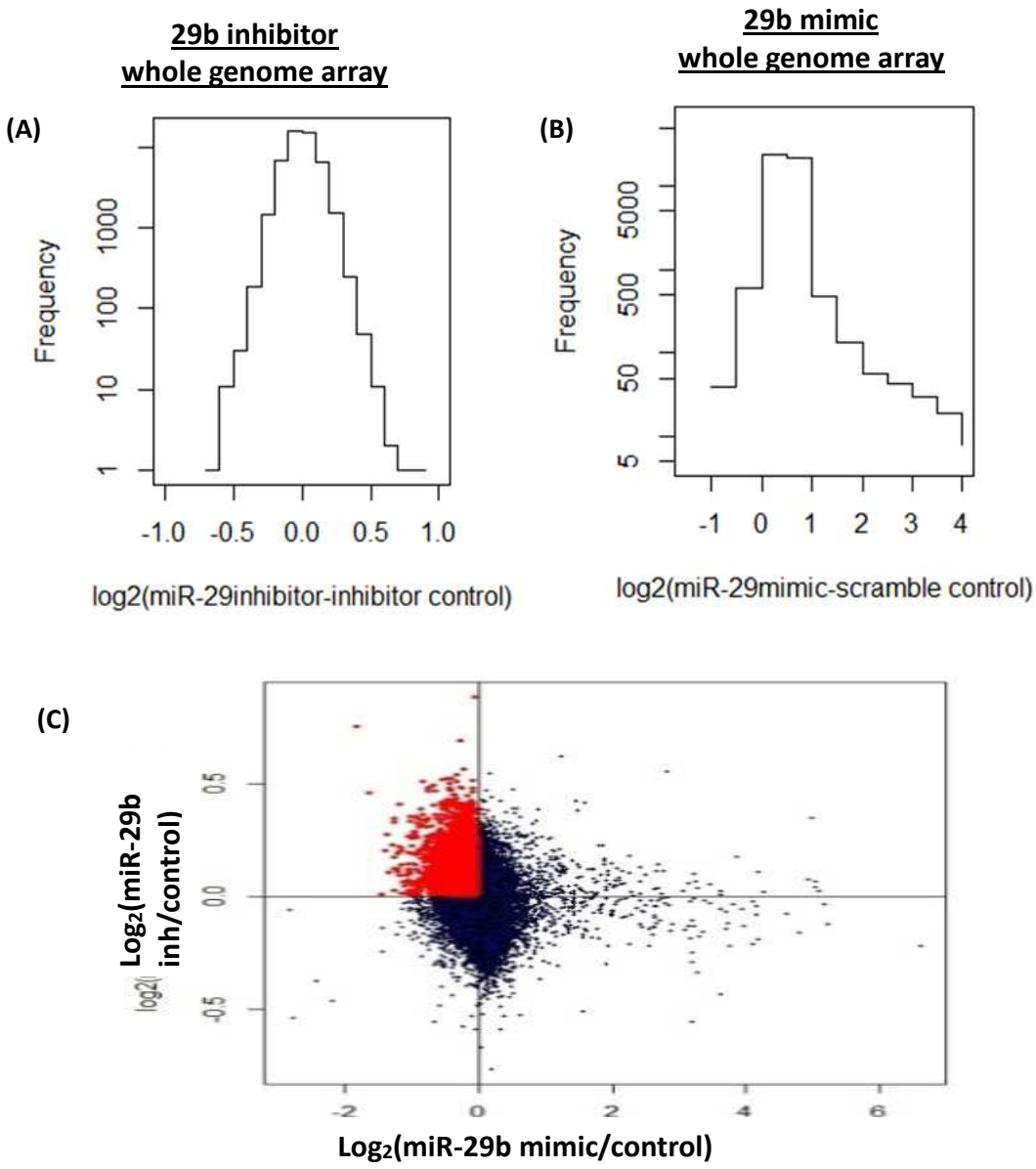

Figure 5.7 Gain- and loss- of function of miR-29b experiments

Human primary chondrocytes were cultured in high glucose media with 10% (v/v) FCS in monolayer until reaching 90% confluence. Cells were transfected with miR-29b mimic (50nM), miR-29b inhibitor (50nM), or non – targeting control (50nM) for 48 hours in triplicate. Cells were then harvested and total RNA was isolated from each sample. An equal amount of total RNA from each sample was pooled together. Pooled samples were subjected to whole genome array using Illumina humanHT-12 V4.0 expression BeadChip array. The Global effect of the miR-29b overexpression or silencing on whole genome expression was presented in (A) for the miR-29b silencing experiment and in (B) for the miR-29b overexpression experiment. Both datasets were plotted together on the same chart (C). The mRNAs which decreased in the miR-29 overexpression and increased in the miR-29b silencing experiment are highlighted in red.

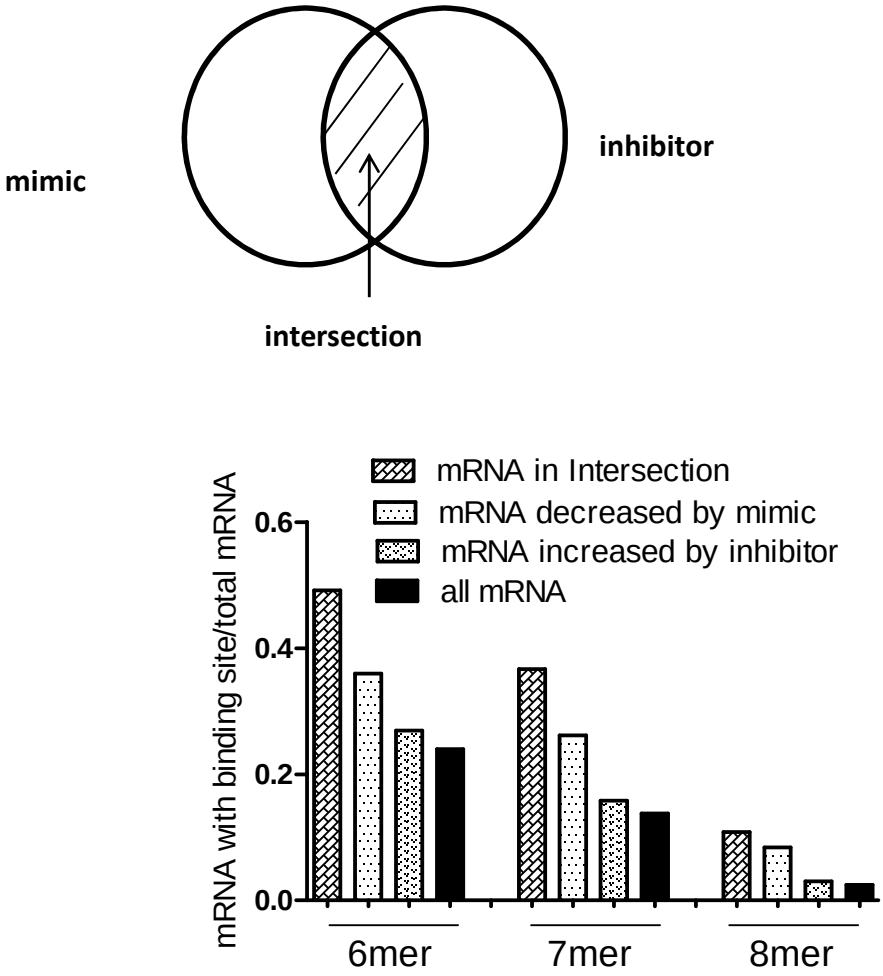

Figure 5.8: Enrichment of miR-29 putative direct targets in miR-29b gain – and loss – of function experiment.

From whole genome array data, the percentage of miR-29 putative direct targets was calculated for (i) mRNA decreased by the miR-29b mimic ; (ii) mRNA increased by the miR-29b inhibitor ; (iii) mRNA in the intersection of the two (decreased by miRN-29b mimic and increased by inhibitor) (iv) all the mRNAs detected from the whole genome array. The calculation was performed for the range of fold change (FC) and for each types of seed sequence e.g. 6-mer, 7-mer, 8-mer. The mRNA having more than one binding site for each type of seed sequence was always assigned as 1. When FC=k, the percentage of 6mer-seed-site targets increasing or decreasing expression was calculated: **6mer** = sum of mRNA having 6mer-seed site sequence in the 3'UTR with FC in the range of (k, FC max) if k >0, or (FC min, k) if k<0; **Total mRNA** = sum of mRNA with FC in the range of (k, FC max) if k>0, or (FC min, k) if k< 0; **mRNA with binding site/ total mRNA = 6mer/total mRNA.** The percentage of other seed site targets was calculated similarly. Here, calculation for the absolute FC 1.3 is presented.

5.2.4.2 Known targets of the miR-29 family

The miR-29 family has emerged as an important miRNA in a number of pathologic settings by regulating multiple genes that fall into the same or related pathways.

In the whole genome array of the overexpression and silencing of the miR-29b, a number of known direct targets of the miR-29 family were also identified in human chondrocytes (e.g. Table 5.1).

Gene	Binding sites				Fold change mimic (decrease)	Fold change inhibitor (increase)
	s6	s7m8	s7a1	s8		
COL1A1	**3**	**1**	**3**	**1**	**2.53**	**1.69**
COL1A2	**3**	**1**	**2**	**1**	**1.26**	**1.05**
COL2A1	**1**	**1**	**1**	**1**	**1.17**	**1.39**
COL3A1	**3**	**2**	**2**	**2**	**1.36**	**1.26**
COL4A1	**2**	**1**	**2**	**1**	**1.22**	**1.41**
COL5A1	**5**	**4**	**2**	**2**	**1.15**	**1.15**
COL5A2	**2**	**1**	**2**	**1**	**2.20**	**1.27**
COL6A1	**1**	**0**	**1**	**0**	**1.27**	**1.08**
COL6A2	**1**	**1**	**1**	**1**	**1.12**	**1.01**
COL6A3	**1**	**1**	**1**	**1**	**1.20**	**1.14**
COL8A1	**1**	**1**	**1**	**1**	**1.35**	**1.07**
COL11A1	**2**	**2**	**0**	**0**	**1.80**	**1.25**
COL15A1	**2**	**1**	**1**	**1**	**1.73**	**1.22**
COL16A1	**1**	**1**	**0**	**0**	**1.35**	**1.05**
COL20A1	**3**	**0**	**0**	**0**	**1.01**	**1.13**
ADAM19	**6**	**2**	**0**	**0**	**1.64**	**1.28**
CDK6	**3**	**2**	**1**	**0**	**1.61**	**1.07**

Table 5.1: Fold change expression of known targets of the miR-29 family in the miR-29b gain- and loss- of function experiment in human articular chondrocytes

5.2.4.3 Novel targets of the miR-29 family

5.2.4.3.1 The ADAMTS family

The miR-29 family is one example of the fact that a miRNA can regulate many functionally related genes. As shown above, a number of extracellular matrix-related genes were found to be direct targets of the miR-29 family. Since a miRNA can regulate the expression of several hundred genes, it was likely that the miR-29 family could directly target sets of novel genes within families. In chapter 4, TGFβ was found to suppress miR-29 family expression and the miR-29 family itself was also found to supress TGFβ signalling. These data suggest that the level of miR-29 and TGFβ-induced genes, may be inversely correlated and the miR-29 family might further inhibit the effect of TGFβ signalling on gene expression by exerting a second suppressive effect on the pathway through directly targeting inducible genes. This means that a number of TGFβ-inducible genes could potentially be direct targets of the miR-29 family. Herein, the ADAMTS family investigated as TGFβ inducible genes (except *ADAMTS 19*) (Figure 5.9) and genes which have roles in cartilage.

Human primary chondrocytes were stimulated with TGFβ1 for 24 hours in monolayer culture. The expression levels of members of the ADAMTS families were measured by qRT-PCR showing that *ADAMTS6*, *ADAMTS10*, *ADAMTS14* and *ADAMTS17* were significantly induced by TGFβ (Figure 5.9). Moreover, bioinformatic analysis found that there were a number of miR-29 binding sites in the 3'UTR regions of these ADAMTS genes (Table 5.2). Together with this, these TGFβ induced ADAMTS genes were predicted to be miR-29 potential direct targets by different bioinformatics algorithms e.g. Diana, Targetscan, Microcosm, miRDB, Picta (Table 5.2). Taken together, all of these data demonstrated that ADAMTS genes, including *ADAMTS6, ADAMTS10, ADAMTS14, ADAMTS17, ADAMTS19* are miR-29 potential direct targets.

In order to validate these ADAMTS genes as miR-29 direct targets, the expression levels of these genes were measured by qRT-PCR in human chondrocytes transfected with the miR-29b mimic for 48 hours. qRT-PCR (Figure 5.10) showed that the expression of these ADAMTS genes was significantly suppressed by overexpression of the miR-29b, again supporting that these genes are the miR-29 direct targets. To further validate these ADAMTS genes as miR-29 direct targets, the 3'UTR regions containing the miR-29 binding sties were

subcloned downstream of the luciferase encoding gene in pmiRGLO. These ADAMTS3'UTR-pmiRGLO reporter vectors (100ng) were co-transfected with the miR-29 family mimic (50nM) to DF1 cells. After 24 hours of transfection, the cells were harvested and luciferase assays were performed. Together with the ADAMTS 3'UTR-pmiRGLO reporter vectors, mutant vectors in which the miR-29 binding sites were mutated were constructed and tested. A 3'UTR was a direct target for the miR-29 family if the luciferase activity was suppressed with the overexpression of the miRNA in the wild-type construct and this effect was abolished when the miRNA binding sites were mutated. Luciferase assay data showed that *ADAMTS6* (Figure 5.14), *ADAMTS10* (Figure 5.15*), ADAMTS14* (Figure 5.11), *ADAMTS17* (Figure 5.12), *ADAMTS19* (Figure 5.13) were all direct targets of the miR-29 family.

Genes	8 -mer	7 -mer	6 -mer	Bioinformatic algorithm
ADAMTS6		2		Diana, Targetscan, Microcosm, miRDB,Picta
ADAMTS10		2		Diana, Microcosm, Picta
ADAMTS14		2	2	Diana, Picta
ADAMTS17		2	3	Targetscan, Microcosm, miRDB,Picta
ADAMTS19		2		Picta

Table 5.2: *ADAMTS6, ADAMTS10, ADAMTS14, ADAMTS17, ADAMTS19* are predicted to be miR-29 targets

A number of different binding sites for miR-29 were found in the 3'UTR regions of *ADAMTS6, ADAMTS10, ADAMTS14, ADAMTS17,* and *ADAMTS19*. These ADAMTSs were predicted to be miR-29 family targets by different bioinformatics algorithms.

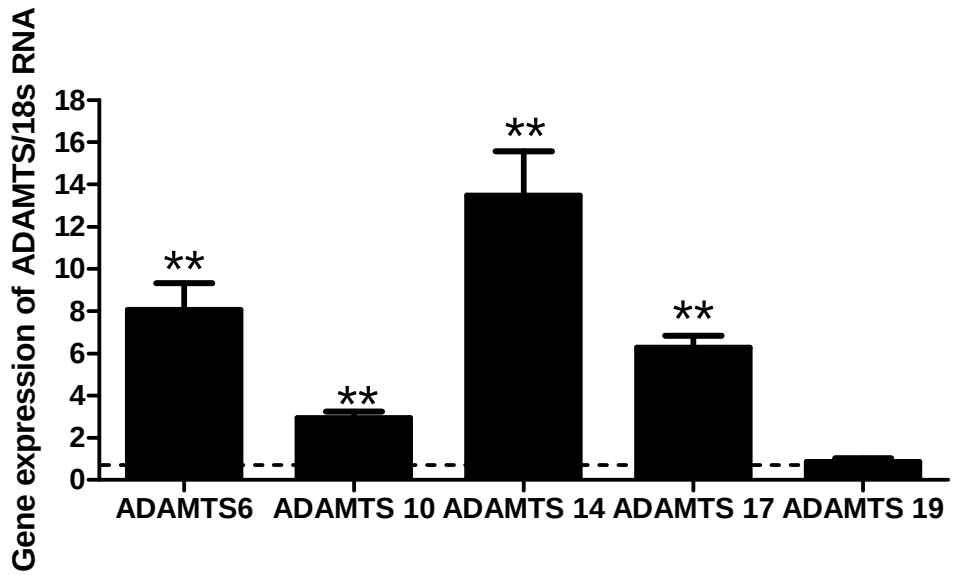

Figure 5.9 Members of ADAMTS family are TGFβ inducible genes

Human primary chondrocytes was cultured with 10% (v/v) FCS in monolayer until 90% confluence. Cells were switched to media with 0.5% (v/v) FCS for 24 hours before treating with TGFβ1 (4ng/ml) or vehicle (4mM HCl+0.5% (w/v) BSA) for another 24 hours. Cells were harvested and subjected to total RNA isolation. Relative expression of the ADAMTS genes was measured by quantitative RT-PCR. 18S rRNA was the housekeeping control. Relative expression value of each of the ADAMTSs in TGFβ stimulated cells was normalized to the vehicle control. The horizontal line at 1 serves as the vehicle control. Closed bar: TGFβ treatment, open bar: vehicle. Means ± standard errors are presented, n=3. The difference between the treatment and the control was analysed by Student's unpaired two-tailed t test. * $p<0.05$, ** $p < 0.01$, ***, $p<0.001$.

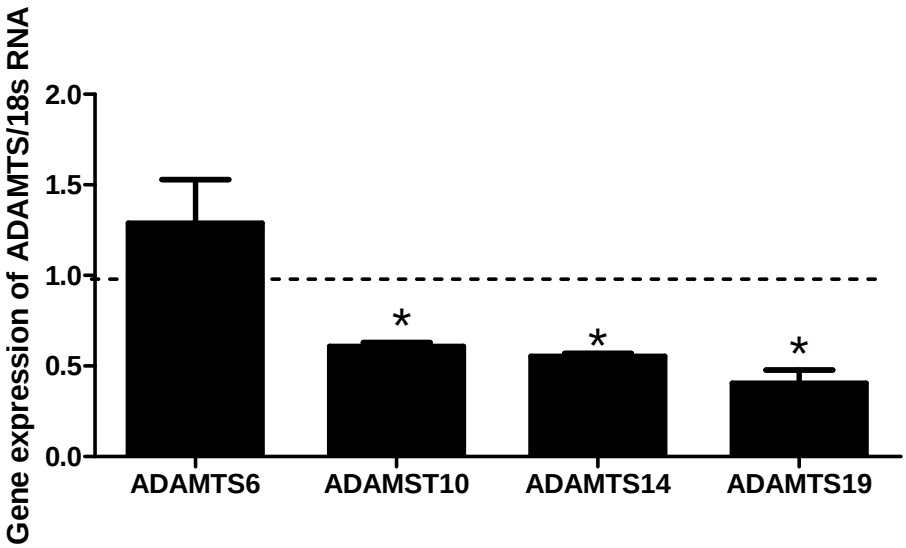

Figure 5.10 The expressions of members of the ADAMTS family were suppressed by miR-29b mimic

Human primary chondrocytes was cultured in media with 10% (v/v) FCS in monolayer until 90% confluence. Cells were then transfected with either miR-29b mimic (50nM) or non – targeting control (50nM) for 48 hours. Total RNA was isolated and the expression levels of the ADAMTS genes were measured by qRT-PCR. 18S rRNA was the housekeeping control. Relative expression value of each of the ADAMTS genes was normalized to non – targeting control. The horizontal line at 1 serves as the non-targeting control. Means ± standard errors are presented, n=3. The difference in expression between miR-29b overexpression and non – targeting control was analysed by Student's unpaired two-tailed t test. * $p<0.05$, ** $p < 0.01$, ***, $p<0.001$

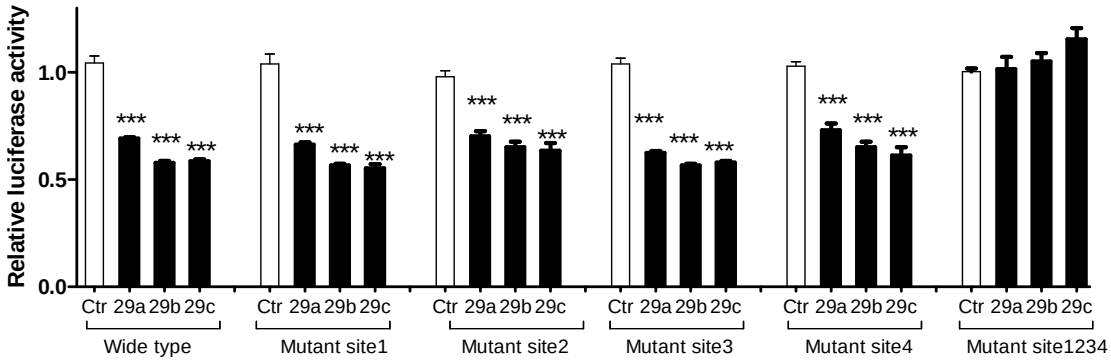

Figure 5.11: ADAMTS14 is a direct target of the miR-29 family

The ADAMTS14 3'UTR region containing 4 binding sites of the miR-29 family was subcloned downstream of the luciferase encoding gene in the pmiRGLO vector to create the ADAMTS14 3'UTR-pmiRGLO wide type (WT) vector. The mutant vectors were created from WT vector in which just single or quadruplicate binding sites of the miR-29 family were mutated. Either the WT or the mutants vectors (100ng) were co-transfected into chicken fibroblast DF1 cells with either miR-29b mimic (50nM) or non – targeting control (50nM). Luciferase assays were performed 24 hours after transfection. The relative luciferase value was normalised to the non-targetting control Open bar: non-targetting control, closed bar: miR-29 family mimic. Means ± standard errors are presented, n=6. The difference of luciferase activity was analysed by Student's unpaired two-tailed t test. * $p<0.05$, ** $p < 0.01$, *** $p<0.001$, Ctr, non-targetting control, 29a, 29b, 29c: miR-29a,-b,-c mimic.

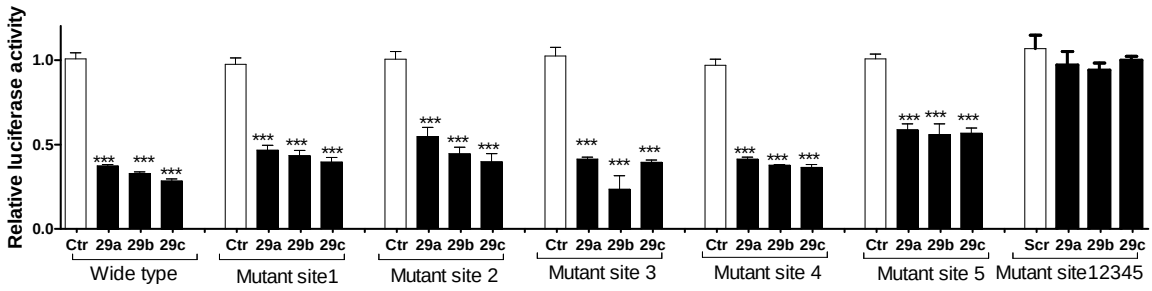

Figure 5.12: ADAMTS17 is a direct target of the miR-29 family

The ADAMTS17 3'UTR region containing 5 binding sites of the miR-29 family was subcloned downstream of the luciferase encoding gene in the pmiRGLO vector to create the ADAMTS17 3'UTR-pmiRGLO wide type (WT) vector. The mutant vectors were created from WT vector in which just single or quadruplicate binding sites of the miR-29 family were mutated. Either the WT or the mutants vectors (100ng) were co-transfected into chicken fibroblast DF1 cells with either miR-29b mimic (50nM) or non – targeting control (50nM). Luciferase assays were performed 24 hours after transfection. The relative luciferase value was normalised to the non-targetting control Open bar: non-targetting control, closed bar: miR-29 family mimic. Means ± standard errors are presented, n=6. The difference of luciferase activity was analysed by Student's unpaired two-tailed t test. * $p<0.05$, ** $p < 0.01$, *** $p<0.001$, Ctr, non-targetting control, 29a, 29b, 29c: miR-29a,-b,-c mimic.

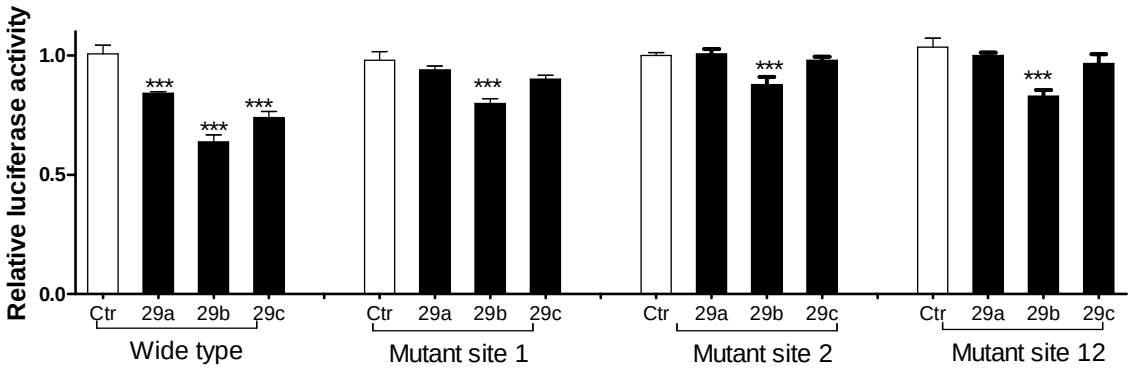

Figure 5.13: ADAMTS19 is a direct target of the miR-29 family

The ADAMTS19 3'UTR region containing 2 binding sites of the miR-29 family was subcloned downstream of the luciferase encoding gene in the pmiRGLO vector to create the ADAMTS19 3'UTR-pmiRGLO wide type (WT) vector. The mutant vectors were created from WT vector in which just single or duplicate binding sites of the miR-29 family were mutated. Either the WT or the mutants vectors (100ng) were co-transfected into chicken fibroblast DF1 cells with either miR-29b mimic (50nM) or non – targeting control (50nM). Luciferase assays were performed 24 hours after transfection. The relative luciferase value was normalised to the non-targetting control Open bar: non-targetting control, closed bar:

miR-29 family mimic. Means ± standard errors are presented, n=6. The difference of luciferase activity was analysed by Student's unpaired two-tailed t test. * $p<0.05$, ** $p < 0.01$, *** $p<0.001$, Ctr, non-targetting control, 29a, 29b, 29c: miR-29a,-b,-c mimic.

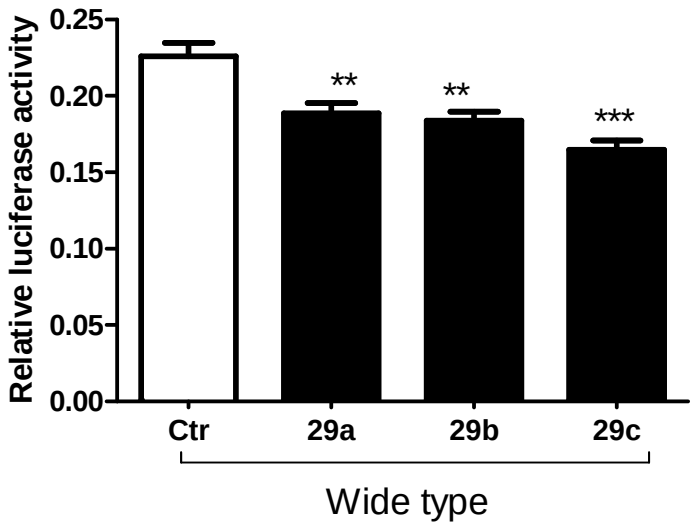

Figure 5.14: ADAMTS6 is a direct target of the miR-29 family

The ADAMTS6 3'UTR region containing 2 binding sites of the miR-29 family was subcloned downstream of the luciferase encoding gene in the pmiRGLO vector to create the ADAMTS6 3'UTR-pmiRGLO wide type (WT) vector. The WT vector (100ng) was co-transfected into chicken fibroblast DF1 cells with either miR-29b mimic (50nM) or non – targeting control (50nM). Luciferase assays were performed 24 hours after transfection. The relative luciferase value was normalised to the non-targeting control Open bar: non-targeting control, closed bar: miR-29 family mimic. Means ± standard errors are presented, n=6. The difference of luciferase activity was analysed by Student's unpaired two-tailed t test. * $p<0.05$, ** $p < 0.01$, *** $p<0.001$, Ctr, non-targeting control, 29a, 29b, 29c: miR-29a,-b,-c mimic.

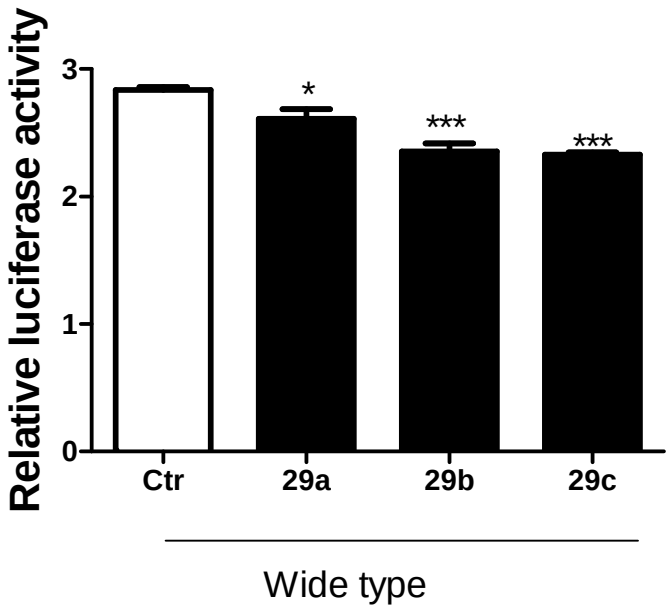

Figure 5.15: ADAMTS10 is a direct target of the miR-29 family
The ADAMTS10 3'UTR region containing 2 binding sites of the miR-29 family was subcloned downstream of the luciferase encoding gene in the pmiRGLO vector to create the ADAMTS10 3'UTR-pmiRGLO wide type (WT) vector. The WT vector (100ng) was co-transfected into chicken fibroblast DF1 cells with either miR-29b mimic (50nM) or non – targeting control (50nM). Luciferase assays were performed 24 hours after transfection. The relative luciferase value was normalised to the non-targeting control Open bar: non-targeting control, closed bar: miR-29 family mimic. Means ± standard errors are presented, n=6. The difference of luciferase activity was analysed by Student's unpaired two-tailed t test. * $p<0.05$, ** $p < 0.01$, *** $p<0.001$, Ctr, non-targeting control, 29a, 29b, 29c: miR-29a,-b,-c mimic.

5.2.4.3.2 WNT signalling pathway related genes

As shown previously, the miR-29 family was found to negatively regulate the TGFβ, NFκB, and WNT/β-catenin signalling pathways. The remaining question is how the miR-29 family supress these signalling pathways.

The whole genome array from the miR-29b gain – and loss – of function experiment found 12215 mRNAs that were the miR-29 putative targets. These consisted of 6925 mRNAs containing at least one 6-mer, 3400 mRNAs containing 7-mer, and 728 mRNAs containing 8-mer binding sites in their 3'UTR. Those mRNAs with miR-29 binding sites were considered as putative direct targets of the miR-29 family; the others without the miR-29 binding site were considered as indirect targets.

The miR-29 family suppression of TGFβ, NFκB, and WNT/β-catenin signalling pathways could be through a direct mechanism by targeting the mRNAs in the signalling cascade. In order to verify how miR-29 suppresses these signalling pathways, both putative miRNA-29 indirect and direct targets were analysed with DAVID functional analysis (web address) software to identify the most represented gene ontology (GO) categories. Analysing the miR-29 direct target sections found the enrichment for the Wnt signalling pathway together with MAPK kinase signalling pathway, apoptosis pathways, P53 signalling pathways. Since, NFκB and TGFβ pathways did not come up in this analysis, the miR-29 indirect targets were further analysed. However, neither NFκB nor TGFβ signalling pathways were enriched. In the scope of this project, the mechanisms by which the miR-29 suppressed these two signalling pathways remains unclear and need to be further explored.

All the miR-29 putative direct targets were selected regardless of the fold change cut off. In this manner, the Wnt signalling-related direct targets e.g. Dishevelled 3 (DVL3), casein kinase 2 alpha 2 polypeptide (CSNK2A2), GSK-3 binding protein frat2 (FRAT2), Frizzled family receptor 3 (FZD3), and Frizzled family receptor 5 (FZD5) were only modulated with a small fold change in the array (Fold change between 1 to 1.2). The expression of these mRNAs were measured by qRT-PCR, however in triplicate samples these data showed that the modulation of these genes under the control of the miR-29b did not reach statistical significance (Appendix, Figure 8).

Even though expression of these Wnt-related genes was not significantly modulated at the mRNA level, the genes were explored as miR-29 direct targets since miR-29 might exert its functions on these genes at the protein level. To verify these genes as the miR-29 direct targets, 3'UTR regions containing miR-29 binding sites of these genes were subcloned downstream of a luciferase encoding gene in the pmiRGLO vector. Constructs in which the miR-29 binding sites were mutated were also created. Either the 3'UTR-pmiRGLO vectors or the mutant 3'UTR-pmiRGLO vectors were co-transfected with the miR-29 family mimic (50nM) into DF1 cells for 24 hours. Then cells were harvested and the luciferase assays were performed. Luciferase assay data showed that FZD3 (Figure 5.19), FZD5 (Figure 5.18), FRAT2 (Figure 5.17), CK2A2 (Figure 5.16), DVL3 (Figure 5.15) were the direct targets of the miR-29 family since the luciferase activities were significantly decreased with the miR-29 family mimics and this effects were abolished when the miR-29 binding sites were mutated.

As mentioned above, qRT-PCR showed that the expression levels of these WNT signalling related genes were not significantly modulated with the miR-29b mimic at the mRNA level. However, the luciferase assay showed that miR-29 family could directly bind to the 3'UTR regions of these genes. It was postulated that the miR-29 family could directly target these genes at the protein level. Since all members of the miR-29 family directly targeted these genes, it was sufficient to check the effect of the miR-29b mimic on these genes at the protein level. In order to test this hypothesis, SW1353 cells were transfected with miR-29b mimic for 72 hours. Cells were then harvested and subjected to western blot. Time limitations meant that only expression levels of DVL3 were examined. Western blot data (Figure 5.15) showed that miR-29b supressed DVL3 expression level to 50% as compared to the non – targeting control, again confirming DVL3 is a direct target of miR-29 family.

Taken together, all of these data provide good evidence that the miR-29 family can inhibit the Wnt signalling, at least in part, via repression of these targets. Interestingly, DVL3, CSNK2A2 and FRAT2 were decreased in expression in hip OA cartilage compared to fracture controls, where the miR-29 family were increased in expression. Fzd3 expression however, was higher in expression in hip OA (Figure 5.20).

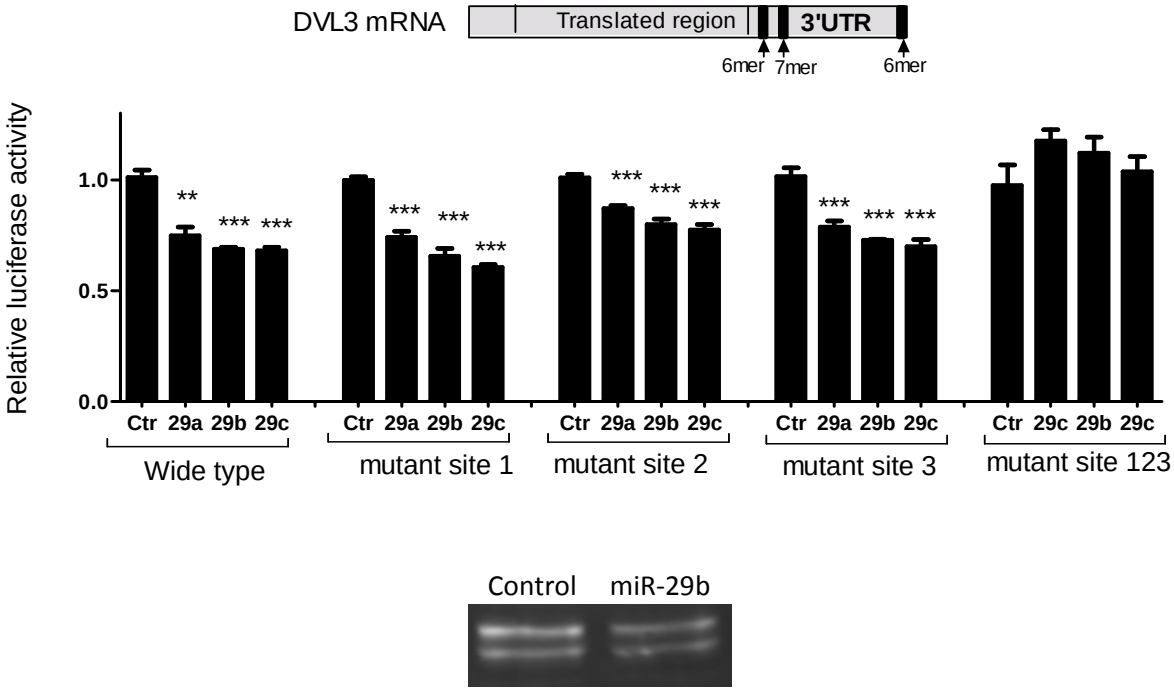

Figure 5.16: DVL3 is a direct target of the miR-29 family

(A) The DVL3 3'UTR region containing 3 binding sites of the miR-29 family was subcloned downstream of the luciferase encoding gene in the pmiRGLO vector to create the DVL3 3'UTR-pmiRGLO wide type (WT) vector. The mutant vectors were created from WT vector in which just single or triplicate binding sites of the miR-29 family were mutated. Either the WT or the mutants vectors (100ng) were co-transfected into chicken fibroblast DF1 cells with either miR-29b mimic (50nM) or non – targeting control (50nM). Luciferase assays were performed 24 hours after transfection. The relative luciferase value was normalised to the non-targetting control. Means ± standard errors are presented, n=6. The difference of luciferase activity was analysed by Student's unpaired two-tailed t test. * $p<0.05$, ** $p < 0.01$, *** $p<0.001$, Ctr, non-targetting control, 29a, 29b, 29c: miR-29a,-b,-c mimic.

(B) SW1353 was transfected with a miR-29b mimic (50nM) or non-targeting control (50nM) for 3 days. Protein was extracted and separated on 10 (w/v) SDS-PAGE, blotted onto PVDF and probed with an anti DVL3 antibody. The blot was stripped and re-probed with a GAPDH antibody to assess loading, n=2.

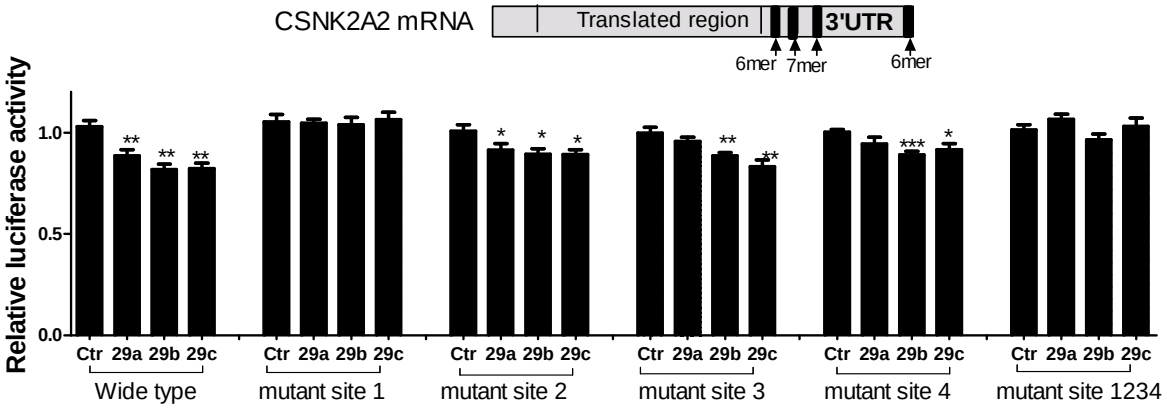

Figure 5.17: CK2A2 is a direct target of the miR-29 family

The CK2A2 3'UTR region containing 4 binding sites of the miR-29 family was subcloned downstream of the luciferase encoding gene in the pmiRGLO vector to create the CK2A2 3'UTR-pmiRGLO wide type (WT) vector. The mutant vectors were created from WT vector in which just single or quadruplicate binding sites of the miR-29 family were mutated. Either the WT or the mutants vectors (100ng) were co-transfected into chicken fibroblast DF1 cells with either miR-29b mimic (50nM) or non – targeting control (50nM). Luciferase assays were performed 24 hours after transfection. The relative luciferase value was normalised to the non-targeting control. Means ± standard errors are presented, n=6. The difference of luciferase activity was analysed by Student's unpaired two-tailed t test. * $p<0.05$, ** $p < 0.01$, *** $p<0.001$, Ctr, non-targeting control, 29a, 29b, 29c: miR-29a,-b,-c mimic.

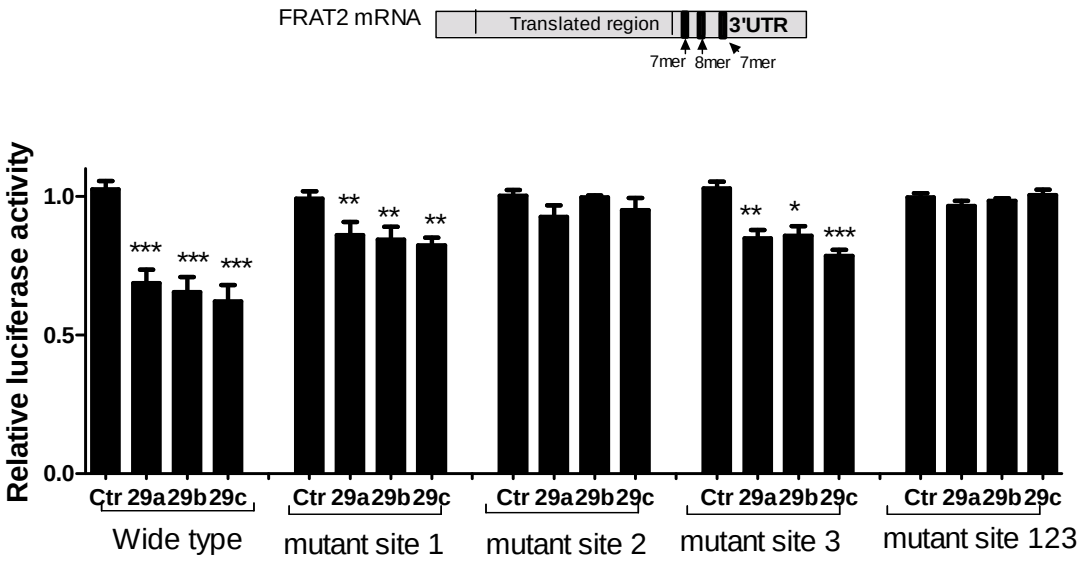

Figure 5.18: *FRAT2* is a direct target of the miR-29 family

The *FRAT2* 3'UTR region containing 4 binding sites of the miR-29 family was subcloned downstream of the luciferase encoding gene in the pmiRGLO vector to create the *FRAT2* 3'UTR-pmiRGLO wide type (WT) vector. The mutant vectors were created from WT vector in which just single or triplicate binding sites of the miR-29 family were mutated. Either the WT or the mutants vectors (100ng) were co-transfected into chicken fibroblast DF1 cells with either miR-29b mimic (50nM) or non – targeting control (50nM). Luciferase assays were performed 24 hours after transfection. The relative luciferase value was normalised to the non-targeting control. Means ± standard errors are presented, n=6. The difference of luciferase activity was analysed by Student's unpaired two-tailed t test. * $p<0.05$, ** $p < 0.01$, *** $p<0.001$, Ctr, non-targeting control, 29a, 29b, 29c: miR-29a,-b,-c mimic.

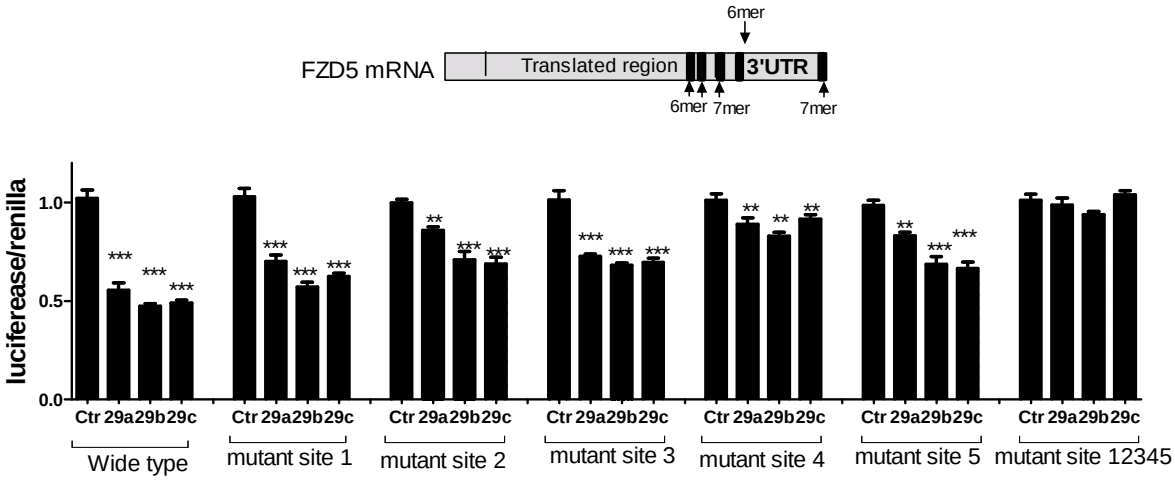

Figure 5.19: *FZD5* is a direct target of the miR-29 family

The *FZD5* 3'UTR region containing 5 binding sites of the miR-29 family was subcloned downstream of the luciferase encoding gene in the pmiRGLO vector to create the *FZD5* 3'UTR-pmiRGLO wide type (WT) vector. The mutant vectors were created from WT vector in which just single or quintuplicate binding sites of the miR-29 family were mutated. Either the WT or the mutants vectors (100ng) were co-transfected into chicken fibroblast DF1 cells with either miR-29b mimic (50nM) or non – targeting control (50nM). Luciferase assays were performed 24 hours after transfection. The relative luciferase value was normalised to the non-targeting control. Means ± standard errors are presented, n=6. The difference of luciferase activity was analysed by Student's unpaired two-tailed t test. * $p<0.05$, ** $p < 0.01$, *** $p<0.001$, Ctr, non-targeting control, 29a, 29b, 29c: miR-29a,-b,-c mimic.

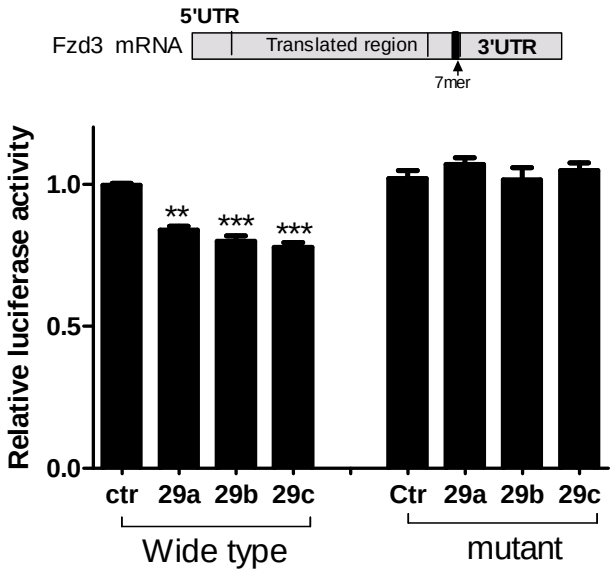

Figure 5.20: *FZD3* is a direct target of the miR-29 family

The *FZD3* 3'UTR region containing 1 binding sites of the miR-29 family was subcloned downstream of the luciferase encoding gene in the pmiRGLO vector to create the *FZD3* 3'UTR-pmiRGLO wide type (WT) vector. The mutant vectors were created from WT vector in which binding site of the miR-29 family were mutated. Either the WT or the mutants vectors (100ng) were co-transfected into chicken fibroblast DF1 cells with either miR-29b mimic (50nM) or non – targeting control (50nM). Luciferase assays were performed 24 hours after transfection. The relative luciferase value was normalised to the non-targeting control. Means ± standard errors are presented, n=6. The difference of luciferase activity was analysed by Student's unpaired two-tailed t test. * $p<0.05$, ** $p < 0.01$, *** $p<0.001$, Ctr, non-targeting control, 29a, 29b, 29c: miR-29a,-b,-c mimic.

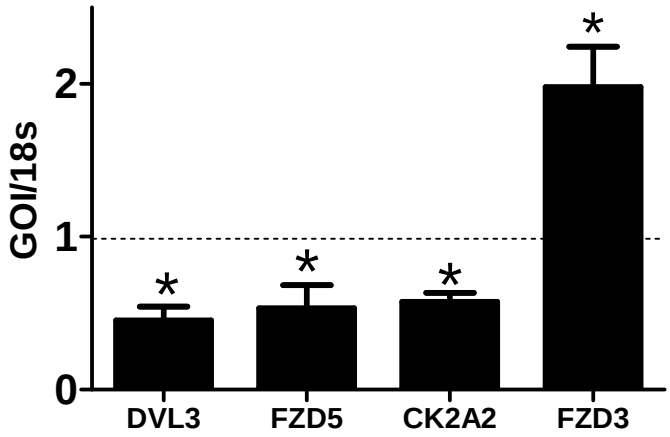

Figure 5.21: Expression of *FZD3, FZD5, DVL3,* and *CK2A2* in human cartilage

Total RNA was isolated from human hip articular cartilage of either end-stage OA patients or fracture controls and reverse transcribed to cDNA. Relative expressions of *FZD3, FZD5, DVL3,* and *CK2A2* were measured by real-time PCR where 18S rRNA was used as housekeeping control in hip osteoarthritis cartilage (HOA, n=8) and fracture to the neck of the femur (NOF, n=7). The horizontal line at 1 is the expression of these genes in NOF. Means ± standard errors are presented. Different in expression between HOA and control NOF was calculated by Student's unpaired two-tailed t test. * $p<0.05$, ** $p < 0.01$, *** $p<0.001$

5.3 Discussion

Previously, the miR-29 family has been shown to negatively interact with TGFβ signalling in several pathologic settings in which fibrosis development was the outcome of the disease such as liver, cardiac, renal fibrosis (van Rooij *et al.* 2008, Kwiecinski et al. 2011, Qin et al. 2011). In line with these studies, in the present study, the miR-29 family was also found to suppress the TGFβ signalling pathway in human chondrocytes. Noteworthy, miR-29 is one downstream mediator of TGFβ signalling in which the miRNA blocks the effect of the growth factor on gene expression. However, the direct mechanism by which miR-29 interferes with TGFβ signalling remains unclear in human chondrocytes. In fact, Smad3 was demonstrated to be a direct target of miR-29 in thyroid cells (Leone *et al.* 2012). In human chondrocytes, nevertheless, with transfection of miR-29 family mimics, the Smad3 mRNA level was not changed (data not shown); similarly, any decrease in luciferase activity when co-transfecting a Smad3-3'UTR reporter with miR-29 mimics was not statistically significant (data not shown), suggesting that Smad3 is not the target of miR-29 in the context of the chondrocyte. In addition, no obvious components of TGFβ signalling were regulated in the miR-29b gain- and loss-of function experiment with the whole genome array. This leads to the hypotheses that miR-29 may directly targets TGFβ signalling components at the protein level rather than mRNA level (similar to miR-140 (Pais et al. 2010)) or that the inhibition of miR-29 on TGFβ signalling is the consequence of the direct suppression of other factors inducing TGFβ signalling. To test this hypothesis, it may be best to perform miR-29b gain- and loss-of function experiment together with a proteomic assay. It may also be instructive to perform array experiments in the presence or absence of TGFβ itself

It has been shown that in the development and progression of OA, NFκB plays an active role e.g. mediating articular chondrocyte responses to proinflammatory cytokines (IL-1, TNF-α); inducing MMPs (e.g. MMP-1, MMP-3, MMP-13), cytokines (e,g, IL-6, IL-8) and chemokine expression (Marcu *et al.* 2010). Thus, NFκB is an attractive target for the treatment of OA. In this project, for the first time, NFκB signalling was confirmed as negatively regulated by the miR-29 family and miR-29 is also likely to serve as a downstream inhibitor of the signalling. Similar to TGFβ signalling, it is still not clear the direct mechanism by which miR-29 regulates NFκB signalling pathway. However, it suggests a potential therapeutic strategy for targeting NFκB signalling using miR-29. Further studies are needed to dissect the direct mechanism by which miR-29 interferes with NFκB signalling.

In this project, the miR-29 family was found to suppress the Wnt/β-catenin signalling pathway. In line with my data, the negative effect of the miR-29 on this signalling pathway is also reported. In human non-small-cell lung cancer cells, miR-29 directly targets DNMTs which in turn inhibited the methylation of Wnt inhibitory factor-1 (WIF-1) promoter; accordingly, miR-29 over-expression down-regulated β-catenin expression (Tan *et al.* 2013). In human colorectal cancer cells, miR-29b negatively regulated Wnt signalling and targeted B-cell CLL/lymphoma 9-like (BCL9L), thus decreasing its expression with a consequent decrease in nuclear translocation of β-catenin (Subramanian *et al.* 2014). In contrast to these studies, published data reports that the miR-29 family positively regulated canonical Wnt signalling by directly targeting its inhibitors in human embryonic kidney cells (Liu *et al.* 2011) and human fetal osteoblastic cells (Kapinas et al. 2010). This contradiction is not surprising as many miRNAs are known to act in a context-dependent manner depending on the relative availability of their targets in any cell type and this discordance could be a reflection of the differences in the miR-29 family regulatory networks in different cell lines.

Besides exerting function on several crucial signalling pathways implicated on chondrogenesis and OA, the crucial role of the miR-29 family was clearly shown through their target genes. In this project, miR-29b gain- and loss-of-function was applied to find miR-29 potential targets. Together with some novel and known targets which will be discussed later, the liposome – mediated transient transfection of the miR-29b-3p mimic surprisingly induced the expression of a number of immune genes which are not the miRNA targets. The Qiagen miR-29b-3p mimic used in the present study is double-stranded, 23 nucleotides in length with sequence identical to the sequence of the mature endogenous miRNA-29b-3p and does not contain any chemical modifications or overhangs, which makes it unlikely for any sequence difference between endogenous miRNA and Qiagen mimic to be responsible for the immune response. Moreover, the lack of immune response against the controls and the miR-29b inhibitor confirms that the immune response was specific and not due to a general response to small RNA. Indeed, it is likely that some specific GU- rich 4-mer sequences e.g. AUUU, UUGA, UGUU in the miR-29b-3p mature sequence (5'UAGCACCAUUUGAAAUCAGUGUU3') might be important for the immune gene up-regulation since these sequences have been shown to be potent immunostimulatory motifs mediated through TLR7 or TLR7/8 (Forsbach *et al.* 2008). Especially, it has been shown that the main effects induced upon activation of TLR7 in human immune cells are IFN- dependent

effects, proinflammatory cytokines and chemokines from cell expression only TLR7 or both TLR7 and 8 (Hertzog *et al.* 2003). Also, it is possible that this up-regulation of the immune genes could be attributed to the liposome alone besides the sequence of the synthetic miRNA since the levels of the immune genes were higher than the levels obtained for electroporation, and those observed in un-transfected controls (Karlsen *et al.* 2013). The explanation for this could be because liposomes fuse with the plasma membrane, which may trigger membrane – associated lipid receptors and/or distort the actin cytoskeleton which in turn up-regulates immune genes. However, it may depend on cellular context since electroporation could strongly trigger the increase of the immune genes in some cell types.

This study identifies FZD3, FZD5, FRAT2, CK2A2 and DVL3 as the critical targets of the miR-29 family in the Wnt signalling pathway. These genes have important roles in both canonical and/or non-canonical Wnt signalling pathways. **FZD3** and **FZD5** belong to the Frizzled proteins, which are the receptors for Wnt ligands. Wnt3a, Wnt5a, and Wnt2 can bind to FZD3 which in turn can activate both canonical and non-canonical WNT signalling pathways: Wnt3a activates the TOPFlash reporter in HEK293 cells overexpressing Wnt3a/FZD3/LRP6 (Lu *et al.* 2004) whist Wnt5a binding to FZD3 triggers downstream pathways independent of β-catenin (Hansen *et al.* 2009); Wnt2 can interact with FZD3 in human cumulus cells, but it is not known which downstream signalling pathways are activated after this binding interaction (Wang *et al.* 2009). **FZD5** functions as the receptor for Wnt5a, Wnt9b, and Wnt7a. Co-injection of hFZD5 and XWnt-5a induced the formation of dorsal axis duplication in *X. laevis* embryos; this axis duplication was suppressed after co-injection of RNA for human GSK-3β, suggesting the involvement β-catenin-dependent signalling in this receptor – ligand combination (He *et al.* 1997). Wnt9b was found in HEK293 cells as a binding partner for FZD5 to activate the TOPFlash reporter (Liu *et al.* 2008). Wnt7a was found to bind to FZD5 to activate the β-catenin signalling pathway and increase the proliferation of epithelial cells in the endometrium (Carmon *et al.* 2008). By targeting these two Frizzled proteins, miR-29 can interfere with Wnt signalling pathways. However, it will depend on the cellular context, whichWnt ligands are available to partner with, which will determine outcome. In line with these Frizzled proteins, another novel target of the miR-29 family, DVL3 (Disheveled 3), belonging to the Disheveled family including DVL1, 2 and 3, is a central component in mediating downstream events of both canonical and non-canonical Wnt signalling. Wnt ligands binding to Frizzled protein recruit Disheveled to the plasma membrane which leads to activation of downstream pathways. Disheveleds

includes DIX, PD2, and DEP domains: DIX and PDZ domains function together in canonical Wnt signalling to stabilize β-catenin; the DIX domain binds with Axin and results in inhibition of the β-catenin degradation complex in canonical Wnt signalling; PDZ and DEP domains cooperate in different subpathways of noncanonical Wnt signalling. Moreover, the other two targets FRAT2 and CSNK2A2 are potent activators of canonical Wnt signalling. **FRAT2** (Frequently rearranged in advanced T-cell lymphomas -2) belongs to the FRAT family including FRAT 1, 2, 3. By binding to GSK3, Frat prevents the phosphorylation and concomitant degradation of β – catenin (van Amerongen *et al.* 2005). **CSNK2A2** encodes for the subunit CK2α' of casein kinase 2 (CK2). CK2 has been shown to act as a positive modulator of WNT/β-catenin pathway, suppressing β-catenin degradation and β-catenin binding to APC (Price 2006). Several keys components of the WNT/β-catenin signalling are known substrates of CK2 in vitro including DVL (Willert *et al.* 1997), TEF/TCF (Homma *et al.* 2002, Miravet *et al.* 2002, Hammerlein *et al.* 2005), and β-catenin (Song *et al.* 2003). Taken together, it is likely that by directly targeting FZD3, FZD5, DVL3, FRAT2 and CSNK2A2, miR-29 could in part or in specific contexts, suppress the Wnt signalling pathway. Interestingly, in human cartilage, the expression levels of FZD5, CSNK2A2, and DLV3 were found to be down regulated in human OA, inversely correlating with the miR-29 expression level, suggesting a direct mechanism in which the suppression of these genes are controlled by miR-29 in human OA cartilage. However, FZD3 expression level was up-regulated in human OA cartilage which could be explained by the fact that there are many other factors which are involved in controlling gene expression together with miRNAs. Since the dys-regulation (either up-regulation or down-regulation) of the canonical Wnt signalling pathway can both lead to OA, there is a possible explanation for the disease development: the excessive amount of the miR-29 down-regulates the expression levels of a number of Wnt signalling related genes which consequently suppress the Wnt signalling pathway. Nevertheless, whether miR-29 targets all of these genes at the same time and the level at which the suppression of each gene contributing to the disease are still not explained in this project.

MicroRNA 29 has been suggested to serve as a master regulator in complex regulatory networks through fine-tuning a large set of functionally related genes, probably best illustrated by its extracellular matrix-related targets, whereby at least 16 ECM related genes are experimentally validated including collagen isoforms (van Rooij et al. 2008, Luna *et al.*

2009, Kwiecinski et al. 2011, Qin et al. 2011, Wang et al. 2012), laminin γ1 (Luna et al. 2009, Nishikawa *et al.* 2014), fibrillin 1, elastin (van Rooij et al. 2008), integrin β1 (Cushing et al. 2011). In line with these data, in this project, a number of ECM- related genes were highlighted as the direct targets of the miR-29 in human OA chondrocytes. However, there is not complete overlap since there are a number of genes that have been experimentally validated as direct targets of miR29 but not regulated when miR-29b was overexpressed or inhibited in human chondrocytes. For example, validated miR-29 direct target genes include DNMT3A, DNMT3B (Fabbri et al. 2007, Garzon *et al.* 2009, Amodio et al. 2012, Morita *et al.* 2013, Tan et al. 2013, Parpart et al. 2014), MMP2 (Liu et al. 2010, Steele et al. 2010, Fang *et al.* 2011), MMP9, ADAM12, ADAM19 (Luna et al. 2009, Ramdas et al. 2013), ADAMTS9 (Cushing et al. 2011). Nonetheless, in human chondrocyte, the expression levels of these genes were not modulated by the miR-29 family. The precise explanation for this difference is still not clear.

In this PhD thesis, members of ADAMTS family including *ADAMTS6, ADAMTS10 ADAMTS14, ADAMTS17, ADAMTS19* have been confirmed as novel direct targets of the miR-29 family. Interestingly, the miR-29 family is suppressed by TGFβ whist its direct targets, the ADAMTS family are strongly induced by TGFβ. However, except ADAMTS14 described as a procollagen N-propeptidase for pro-collagen type I, type II, and type III, the functions of ADAMTS 6, -17, and-19 remain unknown. Thus, further investigating the suppressive effect of miR-29 family on these ADAMTS becomes difficult both in vitro and in vivo. Moreover, ADAMTS14 and ADAMTS17 levels were reported to largely increase in hip OA cartilage and hip OA synovium, respectively (Davidson et al. 2006); the rs4747096 nsSNP in ADAMTS14 was over-represented in women requiring joint replacement because of knee OA and in patients with symptomatic hand OA (Rodriguez-Lopez *et al.* 2009, Poonpet *et al.* 2013), implicating the involvement of these ADAMTS on OA. The microRNA 29 family is, nevertheless, found to increase expression in hip OA cartilage in our sample set. Again, this could be explained in part by the fact that in cellular context, a miRNA is just one factor amongst others e.g. transcription, epigenetic silencing, differential biosynthesis, and extracellular stimuli controlling gene expression.

In summary, the miR-29 family was found to suppress the TGFβ/Smad3, NFκB, and Wnt/β-catenin signalling pathways. Gene expression profiles of gain- and-loss-of-function revealed the regulation of a large number of previously recognised extracellular matrix-associated

genes as well as an additional subset of protease and Wnt signalling pathway-related genes. Among these genes, the ADAMTS family e.g. *ADAMTS6, ADAMTS10, ADAMTS14, ADAMTS17, ADAMTS19,* and Wnt signalling related genes e.g. *FZD3, FZD5, DVL3, FRAT2, CK2A2* were validated as direct targets of the miR-29 family.

CHAPTER 6
GENERAL DISCUSSION

6.1 Summary

This project has identified the miR-29 family as important miRNAs involved in both cartilage homeostasis and OA (Chapter 3). In the murine DMM model of OA at 1, 3, and 7 days after surgery, miRNA profile data from total RNA isolated from the whole knee joints showed that miR-29b was significantly increased at day 1 and showed a trend to decrease at day 3 and 7 after surgery. Integrating analysis between the mRNA profiling and miRNA profiling data from the DMM model strongly highlighted the role of the miR-29 family since the expression of its putative targets inversely correlated with its expression across the time course. In human end-stage hip OA cartilage, the miR-29 family was increased compared with the facture to neck of femur controls. Furthermore, in a murine hip injury model, the expression of the miR-29 family was increased across a 48 hour time course. The miR-29 family was also found to be involved in chondrocyte phenotype since the expression of all members of the miR-29 family decreased across dedifferentiation of human chondrocytes. In chondrogenesis, the miR-29 family was found to significantly decrease at an early stage, suggesting a negative role in this phase of chondrogenesis in both human and murine models. The miR-29 family was also found to be expressed in murine limb development.

The factors controlling miR-29 family expression are another important finding of this project (Chapter 4). The master regulator of chondrogenesis SOX9 was found to negatively regulate miR-29 expression, at least in part through directly binding to the promoter region of miR-29a/b1. A number of growth factors and cytokines were identified which regulate expression of the miR-29 family in both human primary chondrocytes and SW1353 cell line: TGFβ supressed miR-29 family expression; IL-1 strongly increased the miRNA expression through the p38 MAPK signalling pathway; treatment with LPS for less than 24 hours decreased expression of miR-29 through NFκB signalling whilst treatment with LPS for longer times increased miR-29 expression. Interestingly, in response to cytokines and growth factors, the miR-29 primary and precursor transcripts were regulated ahead the mature transcripts. This was explained in part by the fact that several components taking part in the miRNA precursor processing were possibly the miR-29 targets. Among these, Dicer-1 was proven as a miR-29 direct target.

Crucially, the functions of the miR-29 family in chondrocyte were also revealed in which miR-29 served as the negative regulator of the TGFβ/SMAD, NFκB and WNT/β-catenin signalling pathways. A number of novel direct targets of the miR-29 family have been found e.g. the ADAMTS family (*ADAMTS6, -10, -14, -17, -19*) and components of the Wnt signalling pathway (*FZD3, -5, FRAT2, CK2A2, DVL3*) (Chapter 5).

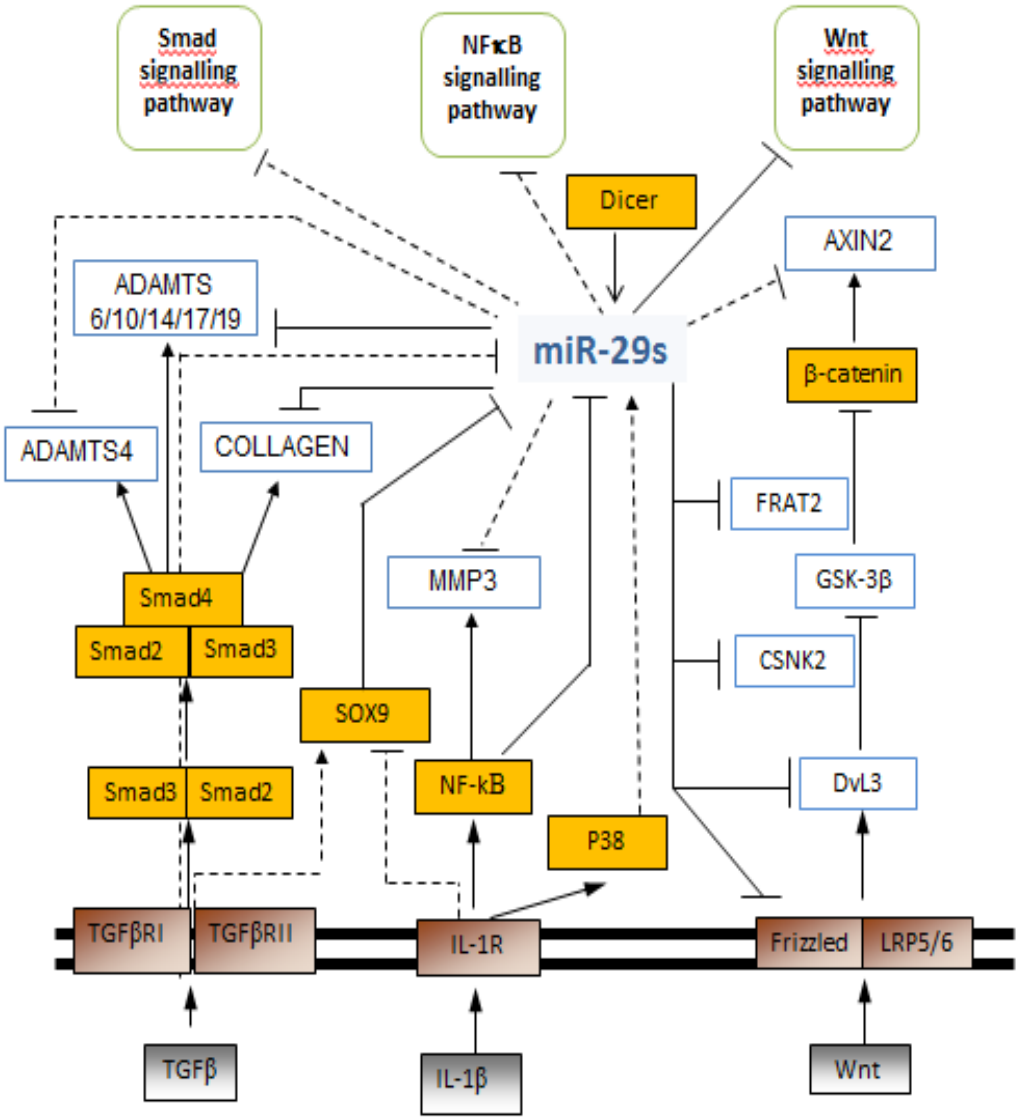

Figure 6.1. Summary of the role of the miR-29 family in chondrocytes

6.2 General discussion

6.2.1 Increased expression of the miR-29 family may contribute to the onset or progression of OA

The tight regulation of miRNA expression is crucial for cartilage homeostasis since the dysregulation of miRNAs may lead to OA. Especially, it has been shown that the aberrant expression of a single miRNA could have a profound effect on cartilage i.e. miR-140, with absence of miR-140 leading to premature OA (Miyaki et al. 2010). In the present study, all members of the miR-29 family have been implicated in cartilage homeostasis and OA. In both early and late stages of OA, an increase level of the miR-29 family was observed, suggesting that miR-29 may be involved in the onset of the disease. Moreover, in this study, the molecular mechanisms controlling this increased expression of miR-29 and the mechanisms by which increased miR-29 expression may lead to OA have been investigated: the miR-29 expression was up-regulated by IL-1, which is induced in both early and end stage OA, consequently suppressing both TGFβ and WNT/β-catenin signalling pathways. Since alteration of these two signalling pathways has been shown to be involved in OA development (Verrecchia et al. 2001, Verrecchia and Mauviel 2002, Zhu et al. 2008, Zhu et al. 2009), the increased expression level of the miR-29 family may contribute to this. In line with this, the miR-29 family was found to strongly suppress a number of ECM-related genes, especially collagens. Aggrecan was also found to be indirectly decreased by miR-29 (data not shown). However, more evidence is required to support this premise. If the increased expression level of miR-29 is a common observation in different OA models, this may also suggest that circulating miR-29 could be a biomarker for detecting early stage OA and also offers the possibility of using a miR-29 inhibitor as a novel treatment for OA. We are investigating the expression of the miR-29 family in the Str/ort model in collaboration with Dr Blandine Poulet (University College London, UK) and Professor Andy Pitsillides (Royal Veterinary College, London, UK).

The increased level of the miR-29 family may not be the only microRNA underlying the development of OA. In this project, miRNA profiling in the DMM model at 1, 3, and 7 days after surgery found a number of miRNAs modulated apart from miR-29s, suggesting these may also contribute to the pathogenesis of OA. Also, a number of miRNAs have been identified as differently expressed in human end stage OA cartilage as compared to the control counterparts. It is clear that in order to maintain cartilage homeostasis, miRNAs will interact with each other and mRNAs in a complex network that is tightly regulated. Thus, the up-regulation of miR-29 might be either the reason or the consequence of the deregulation of other networks of miRNAs. The question is how the other miRNAs interact with miR-29 and the effect of the increase expression of miR-29 on the miRNA/mRNA network in OA. This requires a computer modelling approach to resolve.

6.2.2 The signalling cascade IL-1/p38, IL-1/NFκB and the miR-29 family

Interestingly, in this study, it was found that whist IL-1 induced miR-29 expression through p38/MAPK, the NFκB pathway appears suppressive to miR-29 expression. In addition, the miRNA itself was found to suppress NFκB signalling. These data suggest that in response to the signalling cascade triggered by IL-1, the miR-29 expression level was induced through (i) induced expression of p38 MAPK and (ii) escape from the suppressive effect of NFκB through inhibiting the NFκB signalling pathway. However, the mechanism by which miR-29 suppressed NFκB signalling was not fully understood since the miR-29b gain- and loss- of function mRNA profiling experiment in human primary chondrocytes did not identify any potential targets related to the NFκB signalling pathway. It is a hypothesis that this suppressive effect could be an indirect effect or some potential targets could alter only at the protein level. Also, the direct mechanism through which p38 induced the miR-29 expression is not clear, even though in the promoter of miR-29a/b1 there are several binding sites for AP1 (data not shown). Interestingly, it is reported that p38 activation was found to induce NFκB activity in a dual way: by reducing IκB levels and by potentiating the translocation of p65/p50 (Baeza-Raja *et al.* 2004). Though evidence for this activation in human chondrocytes was not clear, the network controlling miR-29 expression in response to IL-1 becomes more complicated if this interaction is true in chondrocytes. Moreover, in this study, miR-29 was found to inhibit the pre-miRNA processing machinery to target Dicer and may also directly target other pre-miRNA processing genes, suggesting another regulatory layer for tightly

controlling the level of miR-29 in human chondrocytes. This could partly explain that the excessive amount of the miRNA in chondrocytes may lead to OA. Multiple regulatory layers are therefore needed for controlling miR-29 levels, clearly showed when the level of the primary miR-29 family was induced ahead of the level of mature miR-29 in chondrocytes stimulated with IL-1, TGFβ, and LPS. In the DMM model, miR-29 expression was induced 1 day after surgery together with the IL-1β expression level though this latter was not significant (data not shown), suggesting one possible explanation for the increase level of miR-29. However, it is unlikely that miR-29 was solely induced by IL-1 in the DMM model since the IL-1 level would have to be induced very early in order to then stimulate miR-29 expression. In line with this, mRNA profiling of DMM model 6 hours after surgery did not find a strongly induced expression of IL-1 (Burleigh et al. 2012). Similarly, in the murine hip injury model, the miR-29 expression level was also found to increase across the time course (reaching significance at 12 hours in culture). The precise mechanism for the increase expression of miR-29s in both DMM model and murine hip injury model are not clear and require further investigation.

6.2.3 The signalling cascade TGFβ/ Smad3 signalling pathway and the miR-29 family

In contrast with IL-1, TGFβ suppresses miR-29 expression. Since the miR-29 family directly targets a number of ECM-related genes, the suppressive effect TGFβ exerted on the miR-29 family is consistent with the well described protective effect of TGFβ in chondrocytes (Li et al. 2005). Interestingly, the miRNA itself gave a negative feedback loop on the TGFβ/Smad signalling pathway. This could be explained as an attempt to maintain miR-29 at homeostatic levels as TGFβ signalling becomes aberrant. This may also in part support the fact that an excessive amount of the miR-29 family could lead to OA: through suppressing Smad signalling and directly inhibiting responsive genes e.g. ECM related genes, the up-regulation of the miR-29s could strongly diminish the function of TGFβ in chondrocytes.

The precise mechanism by which TGFβ suppressed miR-29 expression and the mechanism by which miR-29 inhibited the TGFβ/Smad signalling were unclear. The miR-29b gain- and loss- of function mRNA profiling did not identify any TGFβ related potential targets, suggesting that this may also be at the protein level. Moreover, regarding the cellular context, when both IL-1 and TGFβ may be present, the cross talk between the two cytokines as well

as with other cytokines and growth factors in controlling the miR-29s expression levels are still unclear.

6.2.4 The canonical Wnt signalling and the miR-29 family

In this project, expression of the miR-29 family was not controlled by Wnt3a in chondrocytes. Since Wnt3a could trigger both canonical Wnt/β-catenin and CaMKII signalling pathways (Nalesso et al. 2011), it is likely that these two signalling pathways do not modulate the miR-29 levels in chondrocyte. However, expression ofmiR-29 was found to be induced by WNT3a in osteoblasts, suggesting a different mechanism controlling the miRNA-29 expression in the two cells types. The answer to this difference remains unknown and needs further investigation.

The canonical Wnt/β-catenin signalling pathway was inhibited by the miR-29 family in which some Wnt signalling related genes were validated as direct targets of the miRNA. Both over-activation and inhibition of Wnt signalling can lead to skeletal deformities and an early onset OA (Zhu et al. 2008, Zhu et al. 2009), illustrating that Wnt signalling needs to be tightly regulated in cartilage homeostasis. However, whether the decreasing of these direct targets is the mechanism for inhibition of the Wnt/β-catenin signalling pathway has not been confirmed in this study. This could be facilitated by utilizing siRNA to suppress the expression of each of these genes and measure this effect on the signalling though TOPFlash reporter.

6.2.5 Therapeautic applications for treating OA by targeting the miR-29 family

MicroRNAs have many advantages as a therapeutic modality. The mature miRNA sequences are short and often completely conserved across species. These characteristics make miRNAs relatively easy to target therapeutically and allow for using the same miRNA-modulating compound in preclinical efficacy and safety studies as well as in clinical trials. Moreover, miRNAs have typically many targets within cellular networks, which, in turn, enable modulation of entire pathways in a disease state via therapeutic targeting of disease – associated miRNAs.

The increase of the miR-29 family in OA potentially opens the door to develop a novel therapeutic strategy for OA. The therapeutic approach using **miRNA sponges** (transgenic

overexpression of RNA molecules harbouring complementary binding sites to a miRNA) or **miRNA-29 antagonists** to block the function of the endogenous miRNA-29s may have great promise as a novel treatment. The miRNA sponges have been proved to be successful in vivo whist the antagonists might have greater promise from a therapeutic perspective.

However, detailed examination of the miRNA therapy should be conducted before clinical use. Especially, the antagonists should have high binding affinity, and bio-stability. Indeed, this could be facilitated by chemically modifying them to increase the duplex melting temperature and improving nuclease resistance. Sugar modifications e.g. the 2'-O-methyl (2'-O-Me), 2'-O-Methoxyethyl (2'-MOE) 2'-fluoro and the bicyclic locked nucleic acid (LNA) modification are commonly used. Among these, the LNA exhibits the highest affinity toward complementary RNA with an increase in Tm of +2-8^{o}C per introduced LNA modification. In addition, by substituting the phosphodiester (PO) backbone linkages with phosphorothioate (PS) linkages in the antagonist oligonucleotides or by using peptide nucleic acid (PNA) or morpholino oligomers, respectively, their nuclease resistance properties might increase. Apart from nuclease resistance, PS backbone modifications also enhance binding to plasma proteins, leading to reduced clearance by glomerular filtration and urinary excretion. PNA oligomers are uncharged oligonucleotide analogues, in which the sugar-phosphate backbone has been replaced by a peptide-like backbone consisting of N-(2-aminoethyl)-glycine units. Polylysine-conjugated and nanoparticle-encapsulated PNA antimiRs have been shown to efficiently inhibit miRNA function in cultured cells and in mice (van Rooij *et al.* 2014). Morpholinos are uncharged and with slightly increased binding affinity to complementary miRNAs.

An effective way to deliver the miRNA-29 inhibitor to the arthritis joint to inhibit the endogenous miRNA-29 is needed. In particular, it is likely that the uptake of a synthetic antagonist into chondrocytes surrounded by the abundant matrix would be difficult in the treatment of damaged cartilage. The main challenge for development of miRNA - based therapeutics is efficient and safe delivery. Two strategies have been utilized to enhance in vivo delivery of antagonists: cholesterol conjugation and modification of the phosphate backbone with PS linkages. The 3' cholesterol conjugated, 2'-O-Me-modified antagonists have become a well-validated experimental tool for in vivo inhibition of miRNAs. PS backbone linkages can be employed to enhance the pharmacokinetic properties of antisense

oligonucleotides. The antagonist approach contains 2 PS modifications at the 5' end and 4 at the 3' end, which have been shown to be important for their in vivo activity, whereas complete replacement of the PO backbone by PS linkages decreased the antagonist efficiency. An increasing number of reports have described silencing of miRNA in vivo by unconjugated LNA-modified antagonists ranging from 8nt to 16nt in length as described in previous section. Administration of such antimiRs is either by intraperitoneal or subcutaneous injection resulted in antimiR uptake in the tissue of interest, which led to inhibition of miRNA function and derepression of direct target mRNAs. However, the mechanism of cellular uptake and distribution are still poorly understood. Directing uptake to cartilage is likely still to be difficult, and delivery by injection not pragmatic in OA.

6.3 Future direction

6.3.1 The modulation of the miR-29 family in OA

The miR-29 family was found to modulate expression in different animal models e.g. the DMM model, hip avulsion injury model, as well as human end stage OA cartilage. These data suggest that the increase in expression of the miR-29 family could be a common event in both early onset and end stage OA. However, care must be applied to conclude the up-regulation of miR-29s will lead to OA, with the expression level of miR-29s during OA progression remaining unclear. Thus, it is of importance to examine miR-29 expression in naturally occurring OA models too.

The miR-29 expression pattern increased in the hip avulsion injury across the time course in this study. Nonetheless, whether miR-29 potential targets were inversely correlated with the miR-29 expression level in this model has not been proven. Thus, we are performing mRNA profiling in the same samples in which the miR-29 expression was found to increase. This may also reveal additional mechanisms which lead to the increased expression of miR-29.

6.3.2 Biological functions of the miR-29 family in chondrocytes

The miR-29 family was found to suppress TGFβ/Smad, NFκB, and Wnt/β-catenin signalling pathways through using the reporters of these pathways together with measuring expression level of the responsive genes. However, whether interfering with the miR-29 effect on these signalling will lead to alter chondrocyte phenotype remains unclear. Overexpression and

knockdown of the miR-29 family in HACs in micromass culture in combination with measurement of chondrocyte markers e.g. *MMP13, COL2A1, SOX9, ADAMTS5* will help to address this.

From the miR-29b gain- and loss- of function mRNA data, apart from the Wnt signalling pathway, enrichment of some miR-29 potential targets which are related to MAPK signalling and apoptosis pathways was evident. Thus, validating these genes as the direct targets of the miR-29s is a priority in the future. It is now clear that miRNAs regulate gene expression at both mRNAs and protein levels. Also, the direct mechanisms the miR-29 supressing the two TGFβ and NFκB signalling pathways are unclear. Therefore, there is a need for proteomic analysis of the miR-29b gain- and loss- of function in HACs, likely in micromass culture. In addition, performing miR-29b gain – and loss - of function together with treatment with IL-1 and TGFβ could greatly help to find the mechanism miR-29 family interfering with NFκB and Smad signalling pathways. All of these experiments will give more information about biological functions of miR-29 in chondrocyte and the complex regulatory network the miR-29 is within.

A key step in understanding the biological functions of the miR-29 family in cartilage homeostasis and OA will be the development of multiple in vivo molecular tools to access gain – of – functions or loss – of – function in mouse models: A number of gain- of –function where the miR-29 family members are overexpressed through a transgenic model, such as the B cell – specific overexpression of the miR-29a/b1 cluster (Santanam et al. 2010), a viral transfection model such as the retroviral transfection of bone-marrow stem cells with miR-29a (Han *et al.* 2010) or systemic delivery of miR-29a have been reported (Wang *et al.* 2012). Also, loss-of-function models have been developed as a Cre-Lox-inducible knockout of the miR-29a/b-1 cluster or the expression of the miR-29 “sponge” sequence (either by transgene or lentivirus) (Ma et al. 2011). However, there is no information whether gain – and loss- of function of the miR-29s lead to OA in these models. Therefore, future studies in which these mice put on OA models e.g. DMM will provide more detail about the function of the miR-29 family.

6.3.3 The involvement of the miR-29 family expression in chick limb bud development and Zebrafish cartilage development.

The miR-29 family was suggested to be a negative regulator of early stage of chondrogenesis in both human and murine chondrogenesis models in this study. Nearly 16 collagen genes were validated as miR-29 direct targets in this study and others. Also, this miRNA was also expressed in murine limb development. It is likely that miR-29 would have a crucial role in cartilage and limb bud development and it is worthy of further investigation. This could be facilitated by again using the gain- and loss- of function of all members of the miR-29 family: a 500bp region around the mature sequence of the miR-29s or a sequence complementary to miR-29 can be subcloned and injected into the chicken limb. However, the involvement of the miR-29 family in chick limb development by in situ hybridization might be required to determine the stage in which miR-29 was expressed in the development process. In addition, ADAMTS14, a pro-collagen pro-peptidase, was validated as the miR-29 direct target. Overexpression or knockdown of the miR-29 family in chick limb could help to further investigate the functional outcome of the suppressive effect of the miR-29s on ADAMTS14 though the ADAMTS14 will need to be verified to be expressed in the chick limb first. This method could be useful for investigating the functional outcome of the interaction between miR-29 and other novel targets.

Interesting, the miR-29 family was found to be express in the cartilage of zebrafish (Wienholds et al. 2005). Thus, zebrafish might be a useful model for investigating the role of the miR-29s in cartilage development. Overexpression and knockdown of the miR-29 family could greatly help for answering this question.

6.3.4 The miR-29 family as the biomarker for OA

MicroRNAs exist in human body fluids such as plasma, urine, and saliva in a stable form which has the potential to be a novel diagnostic and prognostic biomarker. OA can be difficult to diagnose, but it is important to diagnose OA early and start treatment to prevent joint destruction in which the miR-29 based therapy could be an option. Indeed, there is growing evidence for future miRNA-based diagnostics: a number of miRNA in plasma were found at different levels between RA and OA patients. For examples, let-7e, miR-454, miR-886 were identified as differentially expressed circulating miRNAs in OA patients who underwent arthroplasty especially, let–7e emerged as potential predictor for severe knee or hip OA (Beyer et al. 2014). Since the miR-29 family was modulated at an early stage in DMM model, it could be a useful biomarker for OA in clinical use. Thus the expression level

of the miR-29 family in plasma should be determined to have an overview expression pattern of the miRNA.

REFERENCES

Abouheif, M., T. Nakasa, H. Shibuya, T. Niimoto, W. Kongcharoensombat and M. Ochi (2010). "Silencing microRNA-34a inhibits chondrocyte apoptosis in a rat osteoarthritis model in vitro." Rheumatology (Oxford, England) **49**(11): 2054-2060.

Abrahante, J., A. Daul, M. Li, M. Volk, J. Tennessen, E. Miller and A. Rougvie (2003). "The Caenorhabditis elegans hunchback-like Gene lin-57/hbl-1 Controls Developmental Time and Is Regulated by MicroRNAs." Developmental Cell **4**(5): 625-637.

Ahluwalia, J. K., S. Z. Khan, K. Soni, P. Rawat, A. Gupta, M. Hariharan, V. Scaria, M. Lalwani, B. Pillai, D. Mitra and S. K. Brahmachari (2008). "Human cellular microRNA hsa-miR-29a interferes with viral nef protein expression and HIV-1 replication." Retrovirology **5**: 117.

Aigner, T., W. Bertling, H. Stoss, G. Weseloh and K. von der Mark (1993). "Independent expression of fibril-forming collagens I, II, and III in chondrocytes of human osteoarthritic cartilage." J Clin Invest **91**(3): 829-837.

Aigner, T., A. Sachse, P. M. Gebhard and H. I. Roach (2006). "Osteoarthritis: pathobiology-targets and ways for therapeutic intervention." Adv Drug Deliv Rev **58**(2): 128-149.

Aigner, T., S. Soeder and J. Haag (2006). "IL-1beta and BMPs--interactive players of cartilage matrix degradation and regeneration." Eur Cell Mater **12**: 49-56; discussion 56.

Akhtar, N., Z. Rasheed, S. Ramamurthy, A. Anbazhagan, F. Voss and T. Haqqi (2010). "MicroRNA-27b regulates the expression of matrix metalloproteinase 13 in human osteoarthritis chondrocytes." Arthritis & Rheumatism **62**(5): 1361-1371.

(2010). "MicroRNA-27b regulates the expression of matrix metalloproteinase 13 in human osteoarthritis chondrocytes." Arthritis and rheumatism **62**(5): 1361-1371.

Akiyama, H., M. C. Chaboissier, J. F. Martin, A. Schedl and B. de Crombrugghe (2002). "The transcription factor Sox9 has essential roles in successive steps of the chondrocyte differentiation pathway and is required for expression of Sox5 and Sox6." Genes Dev **16**(21): 2813-2828.

Amarilio, R., S. V. Viukov, A. Sharir, I. Eshkar-Oren, R. S. Johnson and E. Zelzer (2007). "HIF1alpha regulation of Sox9 is necessary to maintain differentiation of hypoxic prechondrogenic cells during early skeletogenesis." Development **134**(21): 3917-3928.

Ambros, V. (2004). "The functions of animal microRNAs." Nature **431**(7006): 350-355.

Amodio, N., M. T. Di Martino, U. Foresta, E. Leone, M. Lionetti, M. Leotta, A. M. Gulla, M. R. Pitari, F. Conforti, M. Rossi, V. Agosti, M. Fulciniti, G. Misso, F. Morabito, M. Ferrarini, A. Neri, M. Caraglia, N. C. Munshi, K. C. Anderson, P. Tagliaferri and P. Tassone (2012). "miR-29b sensitizes multiple myeloma cells to bortezomib-induced apoptosis through the activation of a feedback loop with the transcription factor Sp1." Cell Death Dis **3**: e436.

Amodio, N., M. Leotta, D. Bellizzi, M. T. Di Martino, P. D'Aquila, M. Lionetti, F. Fabiani, E. Leone, A. M. Gulla, G. Passarino, M. Caraglia, M. Negrini, A. Neri, A. Giordano, P. Tagliaferri and P. Tassone (2012). "DNA-demethylating and anti-tumor activity of synthetic miR-29b mimics in multiple myeloma." Oncotarget **3**(10): 1246-1258.

Amos, N., S. Lauder, A. Evans, M. Feldmann and J. Bondeson (2006). "Adenoviral gene transfer into osteoarthritis synovial cells using the endogenous inhibitor IkappaBalpha reveals that most, but not all, inflammatory and destructive mediators are NFkappaB dependent." Rheumatology (Oxford) **45**(10): 1201-1209.

Arner, E. C. (2002). "Aggrecanase-mediated cartilage degradation." Curr Opin Pharmacol **2**(3): 322-329.

Arroyo, J., J. Chevillet, E. Kroh, I. Ruf, C. Pritchard, D. Gibson, P. Mitchell, C. Bennett, E. Pogosova-Agadjanyan, D. Stirewalt, J. Tait and M. Tewari (2011). "Argonaute2 complexes carry a

population of circulating microRNAs independent of vesicles in human plasma." Proceedings of the National Academy of Sciences **108**(12): 5003-5008.
Avasarala, S., M. Van Scoyk, J. Wang, M. Sechler, K. Vandervest, C. Brzezinski, C. Weekes, M. G. Edwards, J. Arcaroli, R. E. Davis, R. K. Bikkavilli and R. A. Winn (2013). "hsa-miR29b, a critical downstream target of non-canonical Wnt signaling, plays an anti-proliferative role in non-small cell lung cancer cells via targeting MDM2 expression." Biol Open **2**(7): 675-685.
Baeza-Raja, B. and P. Munoz-Canoves (2004). "p38 MAPK-induced nuclear factor-kappaB activity is required for skeletal muscle differentiation: role of interleukin-6." Mol Biol Cell **15**(4): 2013-2026.
Baker-Lepain, J. C., J. A. Lynch, N. Parimi, C. E. McCulloch, M. C. Nevitt, M. Corr and N. E. Lane (2012). "Variant alleles of the Wnt antagonist FRZB are determinants of hip shape and modify the relationship between hip shape and osteoarthritis." Arthritis Rheum **64**(5): 1457-1465.
Bartel, D. (2004). "MicroRNAs: genomics, biogenesis, mechanism, and function." Cell **116**(2): 281-297.
(2009). "MicroRNAs: target recognition and regulatory functions." Cell **136**(2): 215-233.
Benito, M. J., D. J. Veale, O. FitzGerald, W. B. van den Berg and B. Bresnihan (2005). "Synovial tissue inflammation in early and late osteoarthritis." Ann Rheum Dis **64**(9): 1263-1267.
Berezikov, E., W.-J. Chung, J. Willis, E. Cuppen and E. Lai (2007). "Mammalian mirtron genes." Mol Cell **28**(2): 328-336.
Beyer, C., A. Zampetaki, N. Y. Lin, A. Kleyer, C. Perricone, A. Iagnocco, A. Distler, S. R. Langley, K. Gelse, S. Sesselmann, R. Lorenzini, A. Niemeier, B. Swoboda, J. H. Distler, P. Santer, G. Egger, J. Willeit, M. Mayr, G. Schett and S. Kiechl (2014). "Signature of circulating microRNAs in osteoarthritis." Ann Rheum Dis.
Bi, W., J. M. Deng, Z. Zhang, R. R. Behringer and B. de Crombrugghe (1999). "Sox9 is required for cartilage formation." Nat Genet **22**(1): 85-89.
Billinghurst, R. C., L. Dahlberg, M. Ionescu, A. Reiner, R. Bourne, C. Rorabeck, P. Mitchell, J. Hambor, O. Diekmann, H. Tschesche, J. Chen, H. Van Wart and A. R. Poole (1997). "Enhanced cleavage of type II collagen by collagenases in osteoarthritic articular cartilage." J Clin Invest **99**(7): 1534-1545.
Blom, A. B., S. M. Brockbank, P. L. van Lent, H. M. van Beuningen, J. Geurts, N. Takahashi, P. M. van der Kraan, F. A. van de Loo, B. W. Schreurs, K. Clements, P. Newham and W. B. van den Berg (2009). "Involvement of the Wnt signaling pathway in experimental and human osteoarthritis: prominent role of Wnt-induced signaling protein 1." Arthritis Rheum **60**(2): 501-512.
Bobacz, K., I. G. Sunk, J. G. Hofstaetter, L. Amoyo, C. D. Toma, S. Akira, T. Weichhart, M. Saemann and J. S. Smolen (2007). "Toll-like receptors and chondrocytes: the lipopolysaccharide-induced decrease in cartilage matrix synthesis is dependent on the presence of toll-like receptor 4 and antagonized by bone morphogenetic protein 7." Arthritis Rheum **56**(6): 1880-1893.
Bohnsack, M., K. Czaplinski and D. Gorlich (2004). "Exportin 5 is a RanGTP-dependent dsRNA-binding protein that mediates nuclear export of pre-miRNAs." RNA (New York, N.Y.) **10**(2): 185-191.
Bondeson, J., A. B. Blom, S. Wainwright, C. Hughes, B. Caterson and W. B. van den Berg (2010). "The role of synovial macrophages and macrophage-produced mediators in driving inflammatory and destructive responses in osteoarthritis." Arthritis Rheum **62**(3): 647-657.
Bondeson, J., S. Lauder, S. Wainwright, N. Amos, A. Evans, C. Hughes, M. Feldmann and B. Caterson (2007). "Adenoviral gene transfer of the endogenous inhibitor IkappaBalpha into human osteoarthritis synovial fibroblasts demonstrates that several matrix metalloproteinases and aggrecanases are nuclear factor-kappaB-dependent." J Rheumatol **34**(3): 523-533.
Bossé, G. and M. Simard (2010). "A new twist in the microRNA pathway: Not Dicer but Argonaute is required for a microRNA production." Cell Res **20**(7): 735-737.

Brennecke, J., A. Stark, R. Russell and S. Cohen (2005). "Principles of MicroRNA–Target Recognition." PLoS Biol **3**(3): e85.

Brunner, A. M., C. M. Henn, E. I. Drewniak, A. Lesieur-Brooks, J. Machan, J. J. Crisco and M. G. Ehrlich (2012). "High dietary fat and the development of osteoarthritis in a rabbit model." Osteoarthritis Cartilage **20**(6): 584-592.

Buckwalter, J. A., H. J. Mankin and A. J. Grodzinsky (2005). "Articular cartilage and osteoarthritis." Instr Course Lect **54**: 465-480.

Burleigh, A., A. Chanalaris, M. Gardiner, C. Driscoll, O. Boruc, J. Saklatvala and T. Vincent (2012). "Joint immobilisation prevents murine osteoarthritis, and reveals the highly mechanosensitive nature of protease expression in vivo." Arthritis Rheum: n/a-n/a.

Burleigh, A., A. Chanalaris, M. D. Gardiner, C. Driscoll, O. Boruc, J. Saklatvala and T. L. Vincent (2012). "Joint immobilization prevents murine osteoarthritis and reveals the highly mechanosensitive nature of protease expression in vivo." Arthritis Rheum **64**(7): 2278-2288.

Burrage, P. S., K. S. Mix and C. E. Brinckerhoff (2006). "Matrix metalloproteinases: role in arthritis." Front Biosci **11**: 529-543.

Caetano-Lopes, J., H. Canhao and J. E. Fonseca (2007). "Osteoblasts and bone formation." Acta Reumatol Port **32**(2): 103-110.

Cai, J., G. Yin, B. Lin, X. Wang, X. Liu, X. Chen, D. Yan, G. Shan, J. Qu and S. Wu (2014). "Roles of NFkappaB-miR-29s-MMP-2 circuitry in experimental choroidal neovascularization." J Neuroinflammation **11**: 88.

Cai, X., C. Hagedorn and B. Cullen (2004). "Human microRNAs are processed from capped, polyadenylated transcripts that can also function as mRNAs." RNA (New York, N.Y.) **10**(12): 1957-1966.

Carmon, K. S. and D. S. Loose (2008). "Secreted frizzled-related protein 4 regulates two Wnt7a signaling pathways and inhibits proliferation in endometrial cancer cells." Mol Cancer Res **6**(6): 1017-1028.

Chalfie, M. (1981). "Mutations that lead to reiterations in the cell lineages of C. elegans." Cell **24**(1): 59-69.

Chang, T. C., D. Yu, Y. S. Lee, E. A. Wentzel, D. E. Arking, K. M. West, C. V. Dang, A. Thomas-Tikhonenko and J. T. Mendell (2008). "Widespread microRNA repression by Myc contributes to tumorigenesis." Nat Genet **40**(1): 43-50.

Chen, C., D. Ridzon, A. Broomer, Z. Zhou, D. Lee, J. Nguyen, M. Barbisin, N. Xu, V. Mahuvakar, M. Andersen, K. Lao, K. Livak and K. Guegler (2005). "Real-time quantification of microRNAs by stem–loop RT–PCR." Nucleic Acids Res **33**(20): e179-e179.

Chen, L. X., L. Lin, H. J. Wang, X. L. Wei, X. Fu, J. Y. Zhang and C. L. Yu (2008). "Suppression of early experimental osteoarthritis by in vivo delivery of the adenoviral vector-mediated NF-kappaBp65-specific siRNA." Osteoarthritis Cartilage **16**(2): 174-184.

Chen, X., Y. Ba, L. Ma, X. Cai, Y. Yin, K. Wang, J. Guo, Y. Zhang, J. Chen, X. Guo, Q. Li, X. Li, W. Wang, Y. Zhang, J. Wang, X. Jiang, Y. Xiang, C. Xu, P. Zheng, J. Zhang, R. Li, H. Zhang, X. Shang, T. Gong, G. Ning, J. Wang, K. Zen, J. Zhang and C.-Y. Zhang (2008). "Characterization of microRNAs in serum: a novel class of biomarkers for diagnosis of cancer and other diseases." Cell Res **18**(10): 997-1006.

Chendrimada, T., R. Gregory, E. Kumaraswamy, J. Norman, N. Cooch, K. Nishikura and R. Shiekhattar (2005). "TRBP recruits the Dicer complex to Ago2 for microRNA processing and gene silencing." Nature **436**(7051): 740-744.

Chong, K. W., A. Chanalaris, A. Burleigh, H. Jin, F. E. Watt, J. Saklatvala and T. L. Vincent (2013). "Fibroblast growth factor 2 drives changes in gene expression following injury to murine cartilage in vitro and in vivo." Arthritis Rheum **65**(9): 2346-2355.

Chou, J., J. H. Lin, A. Brenot, J. W. Kim, S. Provot and Z. Werb (2013). "GATA3 suppresses metastasis and modulates the tumour microenvironment by regulating microRNA-29b expression." Nat Cell Biol **15**(2): 201-213.

Clements, K. M., J. S. Price, M. G. Chambers, D. M. Visco, A. R. Poole and R. M. Mason (2003). "Gene deletion of either interleukin-1beta, interleukin-1beta-converting enzyme, inducible nitric oxide synthase, or stromelysin 1 accelerates the development of knee osteoarthritis in mice after surgical transection of the medial collateral ligament and partial medial meniscectomy." Arthritis Rheum **48**(12): 3452-3463.

Clevers, H. (2006). "Wnt/beta-catenin signaling in development and disease." Cell **127**(3): 469-480.

Cochrane, D. R., D. M. Cittelly, E. N. Howe, N. S. Spoelstra, E. L. McKinsey, K. LaPara, A. Elias, D. Yee and J. K. Richer (2010). "MicroRNAs link estrogen receptor alpha status and Dicer levels in breast cancer." Horm Cancer **1**(6): 306-319.

Colige, A., I. Vandenberghe, M. Thiry, C. A. Lambert, J. Van Beeumen, S. W. Li, D. J. Prockop, C. M. Lapiere and B. V. Nusgens (2002). "Cloning and characterization of ADAMTS-14, a novel ADAMTS displaying high homology with ADAMTS-2 and ADAMTS-3." J Biol Chem **277**(8): 5756-5766.

Cortez, M. A., M. S. Nicoloso, M. Shimizu, S. Rossi, G. Gopisetty, J. R. Molina, C. Carlotti, Jr., D. Tirapelli, L. Neder, M. S. Brassesco, C. A. Scrideli, L. G. Tone, M. M. Georgescu, W. Zhang, V. Puduvalli and G. A. Calin (2010). "miR-29b and miR-125a regulate podoplanin and suppress invasion in glioblastoma." Genes Chromosomes Cancer **49**(11): 981-990.

Cushing, L., P. P. Kuang, J. Qian, F. Shao, J. Wu, F. Little, V. J. Thannickal, W. V. Cardoso and J. Lu (2011). "miR-29 is a major regulator of genes associated with pulmonary fibrosis." Am J Respir Cell Mol Biol **45**(2): 287-294.

Davidson, R. K., J. G. Waters, L. Kevorkian, C. Darrah, A. Cooper, S. T. Donell and I. M. Clark (2006). "Expression profiling of metalloproteinases and their inhibitors in synovium and cartilage." Arthritis Res Ther **8**(4): R124.

DeLise, A. M., L. Fischer and R. S. Tuan (2000). "Cellular interactions and signaling in cartilage development." Osteoarthritis Cartilage **8**(5): 309-334.

Dell'accio, F., C. De Bari, N. M. Eltawil, P. Vanhummelen and C. Pitzalis (2008). "Identification of the molecular response of articular cartilage to injury, by microarray screening: Wnt-16 expression and signaling after injury and in osteoarthritis." Arthritis Rheum **58**(5): 1410-1421.

Diarra, D., M. Stolina, K. Polzer, J. Zwerina, M. S. Ominsky, D. Dwyer, A. Korb, J. Smolen, M. Hoffmann, C. Scheinecker, D. van der Heide, R. Landewe, D. Lacey, W. G. Richards and G. Schett (2007). "Dickkopf-1 is a master regulator of joint remodeling." Nat Med **13**(2): 156-163.

Dudek, K., J. Lafont, A. Martinez-Sanchez and C. Murphy (2010). "Type II collagen expression is regulated by tissue-specific miR-675 in human articular chondrocytes." The Journal of biological chemistry **285**(32): 24381-24387.

(2010). "Type II collagen expression is regulated by tissue-specific miR-675 in human articular chondrocytes." Journal of Biological Chemistry **285**(32): 24381-24387.

Dudhia, J. (2005). "Aggrecan, aging and assembly in articular cartilage." Cell Mol Life Sci **62**(19-20): 2241-2256.

Dueck, A. and G. Meister (2010). "MicroRNA processing without Dicer." Genome Biol **11**(6): 123.

Dunn, W., G. DuRaine and H. Reddi (2009). "Profiling microRNA expression in bovine articular cartilage and implications for mechanotransduction." Arthritis & Rheumatism **60**(8): 2333-2339.

(2009). "Profiling microRNA expression in bovine articular cartilage and implications for mechanotransduction." Arthritis and rheumatism **60**(8): 2333-2339.

Elmen, J., M. Lindow, S. Schutz, M. Lawrence, A. Petri, S. Obad, M. Lindholm, M. Hedtjarn, H. Hansen, U. Berger, S. Gullans, P. Kearney, P. Sarnow, E. Straarup and S. Kauppinen (2008). "LNA-mediated microRNA silencing in non-human primates." Nature **452**(7189): 896-899.

Esau, C., S. Davis, S. Murray, X. X. Yu, S. Pandey, M. Pear, L. Watts, S. Booten, M. Graham, R. McKay, A. Subramaniam, S. Propp, B. Lollo, S. Freier, F. Bennett, S. Bhanot and B. Monia (2006). "miR-122 regulation of lipid metabolism revealed by in vivo antisense targeting." Cell Metabolism **3**(2): 87-98.

Eyholzer, M., S. Schmid, L. Wilkens, B. U. Mueller and T. Pabst (2010). "The tumour-suppressive miR-29a/b1 cluster is regulated by CEBPA and blocked in human AML." Br J Cancer **103**(2): 275-284.

Fabbri, M., R. Garzon, A. Cimmino, Z. Liu, N. Zanesi, E. Callegari, S. Liu, H. Alder, S. Costinean, C. Fernandez-Cymering, S. Volinia, G. Guler, C. D. Morrison, K. K. Chan, G. Marcucci, G. A. Calin, K. Huebner and C. M. Croce (2007). "MicroRNA-29 family reverts aberrant methylation in lung cancer by targeting DNA methyltransferases 3A and 3B." Proc Natl Acad Sci U S A **104**(40): 15805-15810.

Fan, Z., S. Soder, S. Oehler, K. Fundel and T. Aigner (2007). "Activation of interleukin-1 signaling cascades in normal and osteoarthritic articular cartilage." Am J Pathol **171**(3): 938-946.

Fang, J. H., H. C. Zhou, C. Zeng, J. Yang, Y. Liu, X. Huang, J. P. Zhang, X. Y. Guan and S. M. Zhuang (2011). "MicroRNA-29b suppresses tumor angiogenesis, invasion, and metastasis by regulating matrix metalloproteinase 2 expression." Hepatology **54**(5): 1729-1740.

Fell, H. B. (1978). "Synoviocytes." J Clin Pathol Suppl (R Coll Pathol) **12**: 14-24.

Fenn, A. M., K. M. Smith, A. E. Lovett-Racke, M. Guerau-de-Arellano, C. C. Whitacre and J. P. Godbout (2013). "Increased micro-RNA 29b in the aged brain correlates with the reduction of insulin-like growth factor-1 and fractalkine ligand." Neurobiol Aging **34**(12): 2748-2758.

Fernandes, R. J., S. Hirohata, J. M. Engle, A. Colige, D. H. Cohn, D. R. Eyre and S. S. Apte (2001). "Procollagen II amino propeptide processing by ADAMTS-3. Insights on dermatosparaxis." J Biol Chem **276**(34): 31502-31509.

Ferracin, M., A. Veronese and M. Negrini (2010). "Micromarkers: miRNAs in cancer diagnosis and prognosis." Expert review of Molecular Diagnostics **10**(3): 297-308.

Forsbach, A., J. G. Nemorin, C. Montino, C. Muller, U. Samulowitz, A. P. Vicari, M. Jurk, G. K. Mutwiri, A. M. Krieg, G. B. Lipford and J. Vollmer (2008). "Identification of RNA sequence motifs stimulating sequence-specific TLR8-dependent immune responses." J Immunol **180**(6): 3729-3738.

Friedman, R., K. Farh, C. Burge and D. Bartel (2009). "Most mammalian mRNAs are conserved targets of microRNAs." Genome Res **19**(1): 92-105.

Frisbie, D. D., S. C. Ghivizzani, P. D. Robbins, C. H. Evans and C. W. McIlwraith (2002). "Treatment of experimental equine osteoarthritis by in vivo delivery of the equine interleukin-1 receptor antagonist gene." Gene Ther **9**(1): 12-20.

Garzon, R., C. E. Heaphy, V. Havelange, M. Fabbri, S. Volinia, T. Tsao, N. Zanesi, S. M. Kornblau, G. Marcucci, G. A. Calin, M. Andreeff and C. M. Croce (2009). "MicroRNA 29b functions in acute myeloid leukemia." Blood **114**(26): 5331-5341.

Gierman, L. M., F. van der Ham, A. Koudijs, P. Y. Wielinga, R. Kleemann, T. Kooistra, R. Stoop, M. Kloppenburg, G. J. van Osch, V. Stojanovic-Susulic, T. W. Huizinga and A. M. Zuurmond (2012). "Metabolic stress-induced inflammation plays a major role in the development of osteoarthritis in mice." Arthritis Rheum **64**(4): 1172-1181.

Gilad, S., E. Meiri, Y. Yogev, S. Benjamin, D. Lebanony, N. Yerushalmi, H. Benjamin, M. Kushnir, H. Cholakh, N. Melamed, Z. Bentwich, M. Hod, Y. Goren and A. Chajut (2008). "Serum MicroRNAs Are Promising Novel Biomarkers." PLoS One **3**(9): e3148.

Girkontaite, I., S. Frischholz, P. Lammi, K. Wagner, B. Swoboda, T. Aigner and K. Von der Mark (1996). "Immunolocalization of type X collagen in normal fetal and adult osteoarthritic cartilage with monoclonal antibodies." Matrix Biol **15**(4): 231-238.

Glasson, S. S., R. Askew, B. Sheppard, B. Carito, T. Blanchet, H. L. Ma, C. R. Flannery, D. Peluso, K. Kanki, Z. Yang, M. K. Majumdar and E. A. Morris (2005). "Deletion of active ADAMTS5 prevents cartilage degradation in a murine model of osteoarthritis." Nature **434**(7033): 644-648.

Goldring, M., K. Tsuchimochi and K. Ijiri (2006). "The control of chondrogenesis." J Cell Biochem **97**(1): 33-44.

Goldring, M. B. (2000). "Osteoarthritis and cartilage: the role of cytokines." Curr Rheumatol Rep **2**(6): 459-465.

(2012). "Chondrogenesis, chondrocyte differentiation, and articular cartilage metabolism in health and osteoarthritis." Ther Adv Musculoskelet Dis **4**(4): 269-285.

Goldring, M. B., J. Birkhead, L. J. Sandell, T. Kimura and S. M. Krane (1988). "Interleukin 1 suppresses expression of cartilage-specific types II and IX collagens and increases types I and III collagens in human chondrocytes." J Clin Invest **82**(6): 2026-2037.

Goldring, M. B. and S. R. Goldring (2007). "Osteoarthritis." J Cell Physiol **213**(3): 626-634.

Goldring, M. B., K. Tsuchimochi and K. Ijiri (2006). "The control of chondrogenesis." J Cell Biochem **97**(1): 33-44.

Goldring, S. R. and M. B. Goldring (2004). "The role of cytokines in cartilage matrix degeneration in osteoarthritis." Clin Orthop Relat Res(427 Suppl): S27-36.

Greco, K. V., A. J. Iqbal, L. Rattazzi, G. Nalesso, N. Moradi-Bidhendi, A. R. Moore, M. B. Goldring, F. Dell'Accio and M. Perretti (2011). "High density micromass cultures of a human chondrocyte cell line: a reliable assay system to reveal the modulatory functions of pharmacological agents." Biochem Pharmacol **82**(12): 1919-1929.

Griffin, T. M., J. L. Huebner, V. B. Kraus and F. Guilak (2009). "Extreme obesity due to impaired leptin signaling in mice does not cause knee osteoarthritis." Arthritis Rheum **60**(10): 2935-2944.

Grishok, A., A. E. Pasquinelli, D. Conte, N. Li, S. Parrish, I. Ha, D. L. Baillie, A. Fire, G. Ruvkun and C. C. Mello (2001). "Genes and mechanisms related to RNA interference regulate expression of the small temporal RNAs that control C. elegans developmental timing." Cell **106**(1): 23-34.

Grotle, M., K. B. Hagen, B. Natvig, F. A. Dahl and T. K. Kvien (2008). "Obesity and osteoarthritis in knee, hip and/or hand: an epidemiological study in the general population with 10 years follow-up." BMC Musculoskelet Disord **9**: 132.

Guan, Y.-J., X. Yang, L. Wei and Q. Chen (2011). "MiR-365: a mechanosensitive microRNA stimulates chondrocyte differentiation through targeting histone deacetylase 4." FASEB Journal **25**(12): 4457-4466.

Guerit, D., J. M. Brondello, P. Chuchana, D. Philipot, K. Toupet, C. Bony, C. Jorgensen and D. Noel (2014). "FoxO3a regulation by miRNA-29a controls chondrogenic differentiation of mesenchymal stem cells and cartilage formation." Stem Cells Dev.

Guilak, F., D. L. Butler and S. A. Goldstein (2001). "Functional tissue engineering: the role of biomechanics in articular cartilage repair." Clin Orthop Relat Res(391 Suppl).

Hammerlein, A., J. Weiske and O. Huber (2005). "A second protein kinase CK1-mediated step negatively regulates Wnt signalling by disrupting the lymphocyte enhancer factor-1/beta-catenin complex." Cell Mol Life Sci **62**(5): 606-618.

Hammond, S. M., E. Bernstein, D. Beach and G. J. Hannon (2000). "An RNA-directed nuclease mediates post-transcriptional gene silencing in Drosophila cells." Nature **404**(6775): 293-296.

Han, J., Y. Lee, K.-H. Yeom, Y.-K. Kim, H. Jin and N. Kim (2004). "The Drosha-DGCR8 complex in primary microRNA processing." Genes Dev **18**(24): 3016-3027.

Han, Y. C., C. Y. Park, G. Bhagat, J. Zhang, Y. Wang, J. B. Fan, M. Liu, Y. Zou, I. L. Weissman and H. Gu (2010). "microRNA-29a induces aberrant self-renewal capacity in hematopoietic progenitors, biased myeloid development, and acute myeloid leukemia." J Exp Med **207**(3): 475-489.

Hansen, C., J. Howlin, A. Tengholm, O. Dyachok, W. F. Vogel, A. C. Nairn, P. Greengard and T. Andersson (2009). "Wnt-5a-induced phosphorylation of DARPP-32 inhibits breast cancer cell migration in a CREB-dependent manner." J Biol Chem **284**(40): 27533-27543.

Harfe, B., M. McManus, J. Mansfield, E. Hornstein and C. Tabin (2005). "The RNaseIII enzyme Dicer is required for morphogenesis but not patterning of the vertebrate limb." Proc Natl Acad Sci U S A **102**(31): 10898-10903.

He, A., L. Zhu, N. Gupta, Y. Chang and F. Fang (2007). "Overexpression of micro ribonucleic acid 29, highly up-regulated in diabetic rats, leads to insulin resistance in 3T3-L1 adipocytes." Mol Endocrinol **21**(11): 2785-2794.

He, X., J. P. Saint-Jeannet, Y. Wang, J. Nathans, I. Dawid and H. Varmus (1997). "A member of the Frizzled protein family mediating axis induction by Wnt-5A." Science **275**(5306): 1652-1654.

Hebert, S. S., K. Horre, L. Nicolai, A. S. Papadopoulou, W. Mandemakers, A. N. Silahtaroglu, S. Kauppinen, A. Delacourte and B. De Strooper (2008). "Loss of microRNA cluster miR-29a/b-1 in sporadic Alzheimer's disease correlates with increased BACE1/beta-secretase expression." Proc Natl Acad Sci U S A **105**(17): 6415-6420.

Heimberg, A., L. Sempere, V. Moy, P. Donoghue and K. Peterson (2008). "MicroRNAs and the advent of vertebrate morphological complexity." Proceedings of the National Academy of Sciences **105**(8): 2946-2950.

Heinegard, D. and T. Saxne (2011). "The role of the cartilage matrix in osteoarthritis." Nat Rev Rheumatol **7**(1): 50-56.

Hertzog, P. J., L. A. O'Neill and J. A. Hamilton (2003). "The interferon in TLR signaling: more than just antiviral." Trends Immunol **24**(10): 534-539.

Homma, M. K., D. Li, E. G. Krebs, Y. Yuasa and Y. Homma (2002). "Association and regulation of casein kinase 2 activity by adenomatous polyposis coli protein." Proc Natl Acad Sci U S A **99**(9): 5959-5964.

Houard, X., M. B. Goldring and F. Berenbaum (2013). "Homeostatic mechanisms in articular cartilage and role of inflammation in osteoarthritis." Curr Rheumatol Rep **15**(11): 375.

Hu, Z., J. D. Klein, W. E. Mitch, L. Zhang, I. Martinez and X. H. Wang (2014). "MicroRNA-29 induces cellular senescence in aging muscle through multiple signaling pathways." AGING **6**(3): 15.

Hu, Z., J. D. Klein, W. E. Mitch, L. Zhang, I. Martinez and X. H. Wang (2014). "MicroRNA-29 induces cellular senescence in aging muscle through multiple signaling pathways." Aging (Albany NY) **6**(3): 160-175.

Hui, W., G. J. Litherland, M. S. Elias, G. I. Kitson, T. E. Cawston, A. D. Rowan and D. A. Young (2012). "Leptin produced by joint white adipose tissue induces cartilage degradation via upregulation and activation of matrix metalloproteinases." Ann Rheum Dis **71**(3): 455-462.

Hutvagner, G. (2005). "Small RNA asymmetry in RNAi: function in RISC assembly and gene regulation." FEBS Lett **579**(26): 5850-5857.

Hutvágner, G., J. McLachlan, A. Pasquinelli, É. Bálint, T. Tuschl and P. Zamore (2001). "A Cellular Function for the RNA-Interference Enzyme Dicer in the Maturation of the let-7 Small Temporal RNA." Science **293**(5531): 834-838.

Hutvagner, G. and M. Simard (2008). "Argonaute proteins: key players in RNA silencing." Nature Reviews. Molecular Cell Biology **9**(1): 22-32.

Iliopoulos, D., K. Malizos, P. Oikonomou and A. Tsezou (2008). "Integrative microRNA and proteomic approaches identify novel osteoarthritis genes and their collaborative metabolic and inflammatory networks." PLoS One **3**(11): e3740.

Inui, M., G. Martello and S. Piccolo (2010). "MicroRNA control of signal transduction." Nature Reviews. Molecular Cell Biology **11**(4): 252-263.

Janeway, C. A., Jr. and R. Medzhitov (2002). "Innate immune recognition." Annu Rev Immunol **20**: 197-216.

Jones, S. W., G. Watkins, N. Le Good, S. Roberts, C. L. Murphy, S. M. Brockbank, M. R. Needham, S. J. Read and P. Newham (2009). "The identification of differentially expressed microRNA in osteoarthritic tissue that modulate the production of TNF-alpha and MMP13." Osteoarthritis and Cartilage **17**(4): 464-472.

(2009). "The identification of differentially expressed microRNA in osteoarthritic tissue that modulate the production of TNF-alpha and MMP13." Osteoarthritis and cartilage / OARS, Osteoarthritis Research Society **17**(4): 464-472.

Kadler, K. E., D. F. Holmes, J. A. Trotter and J. A. Chapman (1996). "Collagen fibril formation." Biochem J **316 (Pt 1)**: 1-11.

Kapinas, K., C. Kessler and A. Delany (2009). "miR-29 suppression of osteonectin in osteoblasts: regulation during differentiation and by canonical Wnt signaling." J Cell Biochem **108**(1): 216-224.

Kapinas, K., C. Kessler, T. Ricks, G. Gronowicz and A. M. Delany (2010). "miR-29 modulates Wnt signaling in human osteoblasts through a positive feedback loop." J Biol Chem **285**(33): 25221-25231.

Karlsen, T., A. Shahdadfar and J. Brinchmann (2011). "Human primary articular chondrocytes, chondroblasts-like cells, and dedifferentiated chondrocytes: differences in gene, microRNA, and protein expression and phenotype." Tissue engineering. Part C, Methods **17**(2): 219-227.

Karlsen, T. A. and J. E. Brinchmann (2013). "Liposome delivery of microRNA-145 to mesenchymal stem cells leads to immunological off-target effects mediated by RIG-I." Mol Ther **21**(6): 1169-1181.

Karsdal, M. A., A. C. Bay-Jensen, R. J. Lories, S. Abramson, T. Spector, P. Pastoureau, C. Christiansen, M. Attur, K. Henriksen, S. R. Goldring and V. Kraus (2014). "The coupling of bone and cartilage turnover in osteoarthritis: opportunities for bone antiresorptives and anabolics as potential treatments?" Ann Rheum Dis **73**(2): 336-348.

Kawano, Y. and R. Kypta (2003). "Secreted antagonists of the Wnt signalling pathway." J Cell Sci **116**(Pt 13): 2627-2634.

Kent, O., R. Chivukula, M. Mullendore, E. Wentzel, G. Feldmann, K. Lee, S. Liu, S. Leach, A. Maitra and J. Mendell (2010). "Repression of the miR-143/145 cluster by oncogenic Ras initiates a tumor-promoting feed-forward pathway." Genes Dev **24**(24): 2754-2759.

Kerkhof, H. J., R. J. Lories, I. Meulenbelt, I. Jonsdottir, A. M. Valdes, P. Arp, T. Ingvarsson, M. Jhamai, H. Jonsson, L. Stolk, G. Thorleifsson, G. Zhai, F. Zhang, Y. Zhu, R. van der Breggen, A. Carr, M. Doherty, S. Doherty, D. T. Felson, A. Gonzalez, B. V. Halldorsson, D. J. Hart, V. B. Hauksson, A. Hofman, J. P. Ioannidis, M. Kloppenburg, N. E. Lane, J. Loughlin, F. P. Luyten, M. C. Nevitt, N. Parimi, H. A. Pols, F. Rivadeneira, E. P. Slagboom, U. Styrkarsdottir, A. Tsezou, T. van de Putte, J. Zmuda, T. D. Spector, K. Stefansson, A. G. Uitterlinden and J. B. van Meurs (2010). "A genome-wide association study identifies an osteoarthritis susceptibility locus on chromosome 7q22." Arthritis Rheum **62**(2): 499-510.

Ketting, R. F., S. E. Fischer, E. Bernstein, T. Sijen, G. J. Hannon and R. H. Plasterk (2001). "Dicer functions in RNA interference and in synthesis of small RNA involved in developmental timing in C. elegans." Genes Dev **15**(20): 2654-2659.

Khvorova, A., A. Reynolds and S. Jayasena (2003). "Functional siRNAs and miRNAs exhibit strand bias." Cell **115**(2): 209-216.

Kiani, C., L. Chen, Y. J. Wu, A. J. Yee and B. B. Yang (2002). "Structure and function of aggrecan." Cell Res **12**(1): 19-32.

Kim, D., J. Song and E.-J. Jin (2010). "MicroRNA-221 Regulates Chondrogenic Differentiation through Promoting Proteosomal Degradation of Slug by Targeting Mdm2." Journal of Biological Chemistry **285**(35): 26900-26907.
Kim, D., J. Song, S. Kim, C.-H. Chun and E.-J. Jin (2011). "MicroRNA-34a regulates migration of chondroblast and IL-1β-induced degeneration of chondrocytes by targeting EphA5." Biochem Biophys Res Commun **415**(4): 551-557.
Kim, D., J. Song, S. Kim, C.-H. Chun, J. Sonn and E.-J. Jin (2012). "MicroRNA-34a modulates cytoskeletal dynamics through regulating RhoA/Rac1 crosstalk in chondroblasts." The Journal of biological chemistry.
Kim, D., J. Song, S. Kim, S.-S. Kang and E.-J. Jin (2011). "MicroRNA-142-3p regulates TGF-β3-mediated region-dependent chondrogenesis by regulating ADAM9." Biochem Biophys Res Commun **414**(4): 653-659.
Kim, N. (2005). "MicroRNA biogenesis: coordinated cropping and dicing." Nature Reviews. Molecular Cell Biology **6**(5): 376-385.
Kim, N., J. Han and M. Siomi (2009). "Biogenesis of small RNAs in animals." Nature reviews. Molecular cell biology **10**(2): 126-139.
Kiriakidou, M., G. Tan, S. Lamprinaki, M. De Planell-Saguer, P. Nelson and Z. Mourelatos (2007). "An mRNA m7G cap binding-like motif within human Ago2 represses translation." Cell **129**(6): 1141-1151.
Knauper, V., C. Lopez-Otin, B. Smith, G. Knight and G. Murphy (1996). "Biochemical characterization of human collagenase-3." J Biol Chem **271**(3): 1544-1550.
Kobayashi, M., G. R. Squires, A. Mousa, M. Tanzer, D. J. Zukor, J. Antoniou, U. Feige and A. R. Poole (2005). "Role of interleukin-1 and tumor necrosis factor alpha in matrix degradation of human osteoarthritic cartilage." Arthritis Rheum **52**(1): 128-135.
Kobayashi, T., J. Lu, B. Cobb, S. Rodda, A. McMahon, E. Schipani, M. Merkenschlager and H. Kronenberg (2008). "Dicer-dependent pathways regulate chondrocyte proliferation and differentiation." Proc Natl Acad Sci U S A **105**(6): 1949-1954.
Kongcharoensombat, W., T. Nakasa, M. Ishikawa, A. Nakamae, M. Deie, N. Adachi, A. Mohamed and M. Ochi (2010). "The effect of microRNA-21 on proliferation and matrix synthesis of chondrocytes embedded in atelocollagen gel." Knee Surgery, Sports Traumatology, Arthroscopy **18**(12): 1679-1684.
Konttinen, Y. T., T. Sillat, G. Barreto, M. Ainola and D. C. Nordstrom (2012). "Osteoarthritis as an autoinflammatory disease caused by chondrocyte-mediated inflammatory responses." Arthritis Rheum **64**(3): 613-616.
Kosaka, N., H. Iguchi and T. Ochiya (2010). "Circulating microRNA in body fluid: a new potential biomarker for cancer diagnosis and prognosis." Cancer Sci **101**(10): 2087-2092.
Koshy, P. J., C. J. Lundy, A. D. Rowan, S. Porter, D. R. Edwards, A. Hogan, I. M. Clark and T. E. Cawston (2002). "The modulation of matrix metalloproteinase and ADAM gene expression in human chondrocytes by interleukin-1 and oncostatin M: a time-course study using real-time quantitative reverse transcription-polymerase chain reaction." Arthritis Rheum **46**(4): 961-967.
Kozomara, A. and S. Griffiths-Jones (2011). "miRBase: integrating microRNA annotation and deep-sequencing data." Nucleic Acids Research **39**(Database issue): D152-D157.
Kwiecinski, M., A. Noetel, N. Elfimova, J. Trebicka, S. Schievenbusch, I. Strack, L. Molnar, M. von Brandenstein, U. Tox, R. Nischt, O. Coutelle, H. P. Dienes and M. Odenthal (2011). "Hepatocyte growth factor (HGF) inhibits collagen I and IV synthesis in hepatic stellate cells by miRNA-29 induction." PLoS One **6**(9): e24568.
Lagos-Quintana, M., R. Rauhut, W. Lendeckel and T. Tuschl (2001). "Identification of novel genes coding for small expressed RNAs." Science (New York, N.Y.) **294**(5543): 853-858.

Lai, E. (2002). "Micro RNAs are complementary to 3' UTR sequence motifs that mediate negative post-transcriptional regulation." Nat Genet **30**(4): 363-364.
Lane, L. B., A. Villacin and P. G. Bullough (1977). "The vascularity and remodelling of subchondrial bone and calcified cartilage in adult human femoral and humeral heads. An age- and stress-related phenomenon." J Bone Joint Surg Br **59**(3): 272-278.
Lane, N. E., K. Lian, M. C. Nevitt, J. M. Zmuda, L. Lui, J. Li, J. Wang, M. Fontecha, N. Umblas, M. Rosenbach, P. de Leon and M. Corr (2006). "Frizzled-related protein variants are risk factors for hip osteoarthritis." Arthritis Rheum **54**(4): 1246-1254.
Lapiere, C. M., A. Lenaers and L. D. Kohn (1971). "Procollagen peptidase: an enzyme excising the coordination peptides of procollagen." Proc Natl Acad Sci U S A **68**(12): 3054-3058.
Lau, N. C., L. P. Lim, E. G. Weinstein and D. P. Bartel (2001). "An abundant class of tiny RNAs with probable regulatory roles in Caenorhabditis elegans." Science (New York, N.Y.) **294**(5543): 858-862.
Lau, P.-W. and I. MacRae (2009). "The molecular machines that mediate microRNA maturation." J Cell Mol Med **13**(1): 54-60.
Lawrie, C., S. Gal, H. Dunlop, B. Pushkaran, A. Liggins, K. Pulford, A. Banham, F. Pezzella, J. Boultwood, J. Wainscoat, C. Hatton and A. Harris (2008). "Detection of elevated levels of tumour-associated microRNAs in serum of patients with diffuse large B-cell lymphoma." Br J Haematol **141**(5): 672-675.
Le, L. T., T. E. Swingler and I. M. Clark (2013). "Review: the role of microRNAs in osteoarthritis and chondrogenesis." Arthritis Rheum **65**(8): 1963-1974.
Lee, D. A., G. Bentley and C. W. Archer (1993). "The control of cell division in articular chondrocytes." Osteoarthritis Cartilage **1**(2): 137-146.
Lee, I., S. Ajay, J. I. Yook, H. S. Kim, S. H. Hong, N. H. Kim, S. Dhanasekaran, A. Chinnaiyan and B. Athey (2009). "New class of microRNA targets containing simultaneous 5'-UTR and 3'-UTR interaction sites." Genome Res **19**(7): 1175-1183.
Lee, J. H., T. Ort, K. Ma, K. Picha, J. Carton, P. A. Marsters, L. S. Lohmander, F. Baribaud, X. Y. Song and S. Blake (2009). "Resistin is elevated following traumatic joint injury and causes matrix degradation and release of inflammatory cytokines from articular cartilage in vitro." Osteoarthritis Cartilage **17**(5): 613-620.
Lee, R. and V. Ambros (2001). "An Extensive Class of Small RNAs in Caenorhabditis elegans." Science **294**(5543): 862-864.
Lee, R. C., R. L. Feinbaum and V. Ambros (1993). "The C. elegans heterochronic gene lin-4 encodes small RNAs with antisense complementarity to lin-14." Cell **75**(5): 843-854.
Lee, Y., C. Ahn, J. Han, H. Choi, J. Kim, J. Yim, J. Lee, P. Provost, O. Radmark, S. Kim and N. Kim (2003). "The nuclear RNase III Drosha initiates microRNA processing." Nature **425**(6956): 415-419.
Lee, Y., K. Jeon, J.-T. Lee, S. Kim and N. Kim (2002). "MicroRNA maturation: stepwise processing and subcellular localization." The EMBO Journal **21**(17): 4663-4670.
Lee, Y., M. Kim, J. Han, K.-H. Yeom, S. Lee, S. Baek and N. Kim (2004). "MicroRNA genes are transcribed by RNA polymerase II." The EMBO Journal **23**(20): 4051-4060.
Lefebvre, V., W. Huang, V. R. Harley, P. N. Goodfellow and B. de Crombrugghe (1997). "SOX9 is a potent activator of the chondrocyte-specific enhancer of the pro alpha1(II) collagen gene." Mol Cell Biol **17**(4): 2336-2346.
Lefebvre, V., C. Peeters-Joris and G. Vaes (1990). "Modulation by interleukin 1 and tumor necrosis factor alpha of production of collagenase, tissue inhibitor of metalloproteinases and collagen types in differentiated and dedifferentiated articular chondrocytes." Biochim Biophys Acta **1052**(3): 366-378.

Leone, V., D. D'Angelo, P. Pallante, C. M. Croce and A. Fusco (2012). "Thyrotropin regulates thyroid cell proliferation by up-regulating miR-23b and miR-29b that target SMAD3." J Clin Endocrinol Metab **97**(9): 3292-3301.

Letamendia, A., E. Labbe and L. Attisano (2001). "Transcriptional regulation by Smads: crosstalk between the TGF-beta and Wnt pathways." J Bone Joint Surg Am **83-A Suppl 1**(Pt 1): S31-39.

Lewis, B., C. Burge and D. Bartel (2005). "Conserved Seed Pairing, Often Flanked by Adenosines, Indicates that Thousands of Human Genes are MicroRNA Targets." Cell **120**(1): 15-20.

Li, G., J. Yin, J. Gao, T. S. Cheng, N. J. Pavlos, C. Zhang and M. H. Zheng (2013). "Subchondral bone in osteoarthritis: insight into risk factors and microstructural changes." Arthritis Res Ther **15**(6): 223.

Li, H., H. Xie, W. Liu, R. Hu, B. Huang, Y.-F. Tan, K. Xu, Z.-F. Sheng, H.-D. Zhou, X.-P. Wu and X.-H. Luo (2009). "A novel microRNA targeting HDAC5 regulates osteoblast differentiation in mice and contributes to primary osteoporosis in humans." The Journal of clinical investigation **119**(12): 3666-3677.

Li, J., J. Huang, L. Dai, D. Yu, Q. Chen, X. Zhang and K. Dai (2012). "MiR-146a, an interleukin-1beta responsive microRNA, induces vascular endothelial growth factor and chondrocyte apoptosis by targeting Smad4." Arthritis Res Ther **14**(2): R75.

Li, N., J. Cui, X. Duan, H. Chen and F. Fan (2012). "Suppression of type I collagen expression by miR-29b via PI3K, Akt, and Sp1 pathway in human Tenon's fibroblasts." Invest Ophthalmol Vis Sci **53**(3): 1670-1678.

Li, T. F., R. J. O'Keefe and D. Chen (2005). "TGF-beta signaling in chondrocytes." Front Biosci **10**: 681-688.

Li, X., G. Gibson, J.-S. Kim, J. Kroin, S. Xu, A. van Wijnen and H.-J. Im (2011). "MicroRNA-146a is linked to pain-related pathophysiology of osteoarthritis." Gene **480**(1-2): 34-41.

Liang, Z.-J., H. Zhuang, G.-X. Wang, Z. Li, H.-T. Zhang, T.-Q. Yu and B.-D. Zhang (2012). "MiRNA-140 is a negative feedback regulator of MMP-13 in IL-1β-stimulated human articular chondrocyte C28/I2 cells." Inflammation Research **61**(5): 503-509.

(2012). "MiRNA-140 is a negative feedback regulator of MMP-13 in IL-1β-stimulated human articular chondrocyte C28/I2 cells." Inflammation research: 1-7.

Lim, L., N. Lau, P. Garrett-Engele, A. Grimson, J. Schelter, J. Castle, D. Bartel, P. Linsley and J. Johnson (2005). "Microarray analysis shows that some microRNAs downregulate large numbers of target mRNAs." Nature **433**(7027): 769-773.

Lin, E., L. Kong, X.-H. Bai, Y. Luan and C.-J. Liu (2009). "miR-199a, a bone morphogenic protein 2-responsive MicroRNA, regulates chondrogenesis via direct targeting to Smad1." The Journal of biological chemistry **284**(17): 11326-11335.

(2009). "miR-199a, a bone morphogenic protein 2-responsive MicroRNA, regulates chondrogenesis via direct targeting to Smad1." Journal of Biological Chemistry **284**(17): 11326-11335.

Lin, L., Q. Shen, C. Zhang, L. Chen and C. Yu (2011). "Assessment of the profiling microRNA expression of differentiated and dedifferentiated human adult articular chondrocytes." Journal of Orthopaedic Research **29**(10): 1578-1584.

Lin, S.-Y., S. Johnson, M. Abraham, M. Vella, A. Pasquinelli, C. Gamberi, E. Gottlieb and F. Slack (2003). "The C elegans hunchback homolog, hbl-1, controls temporal patterning and is a probable microRNA target." Developmental Cell **4**(5): 639-650.

Link, A., F. Balaguer, Y. Shen, T. Nagasaka, J. J. Lozano, R. Boland and A. Goel (2010). "Fecal MicroRNAs as novel biomarkers for colon cancer screening." Cancer Epidemiol Biomarkers Prev **19**(7): 1766-1774.

Liu, C., Y. Wang, P. M. Smallwood and J. Nathans (2008). "An essential role for Frizzled5 in neuronal survival in the parafascicular nucleus of the thalamus." J Neurosci **28**(22): 5641-5653.

Liu, S., L. C. Wu, J. Pang, R. Santhanam, S. Schwind, Y. Z. Wu, C. J. Hickey, J. Yu, H. Becker, K. Maharry, M. D. Radmacher, C. Li, S. P. Whitman, A. Mishra, N. Stauffer, A. M. Eiring, R. Briesewitz, R. A.

Baiocchi, K. K. Chan, P. Paschka, M. A. Caligiuri, J. C. Byrd, C. M. Croce, C. D. Bloomfield, D. Perrotti, R. Garzon and G. Marcucci (2010). "Sp1/NFkappaB/HDAC/miR-29b regulatory network in KIT-driven myeloid leukemia." Cancer Cell **17**(4): 333-347.

Liu, Y., T. Huang, X. Zhao and L. Cheng (2011). "MicroRNAs modulate the Wnt signaling pathway through targeting its inhibitors." Biochem Biophys Res Commun **408**(2): 259-264.

Lodewyckx, L., F. P. Luyten and R. J. Lories (2012). "Genetic deletion of low-density lipoprotein receptor-related protein 5 increases cartilage degradation in instability-induced osteoarthritis." Rheumatology (Oxford) **51**(11): 1973-1978.

Loeser, R., S. Goldring, C. Scanzello and M. Goldring (2012). "Osteoarthritis: A disease of the joint as an organ." Arthritis & Rheumatism: n/a-n/a.

Loeser, R. F., S. R. Goldring, C. R. Scanzello and M. B. Goldring (2012). "Osteoarthritis: a disease of the joint as an organ." Arthritis Rheum **64**(6): 1697-1707.

Long, J., Y. Wang, W. Wang, B. H. Chang and F. R. Danesh (2011). "MicroRNA-29c is a signature microRNA under high glucose conditions that targets Sprouty homolog 1, and its in vivo knockdown prevents progression of diabetic nephropathy." J Biol Chem **286**(13): 11837-11848.

Lories, R. J., J. Peeters, A. Bakker, P. Tylzanowski, I. Derese, J. Schrooten, J. T. Thomas and F. P. Luyten (2007). "Articular cartilage and biomechanical properties of the long bones in Frzb-knockout mice." Arthritis Rheum **56**(12): 4095-4103.

Loughlin, J., B. Dowling, K. Chapman, L. Marcelline, Z. Mustafa, L. Southam, A. Ferreira, C. Ciesielski, D. A. Carson and M. Corr (2004). "Functional variants within the secreted frizzled-related protein 3 gene are associated with hip osteoarthritis in females." Proc Natl Acad Sci U S A **101**(26): 9757-9762.

Lu, D., Y. Zhao, R. Tawatao, H. B. Cottam, M. Sen, L. M. Leoni, T. J. Kipps, M. Corr and D. A. Carson (2004). "Activation of the Wnt signaling pathway in chronic lymphocytic leukemia." Proc Natl Acad Sci U S A **101**(9): 3118-3123.

Luna, C., G. Li, J. Qiu, D. L. Epstein and P. Gonzalez (2009). "Role of miR-29b on the regulation of the extracellular matrix in human trabecular meshwork cells under chronic oxidative stress." Mol Vis **15**: 2488-2497.

Lund, E., S. Güttinger, A. Calado, J. Dahlberg and U. Kutay (2004). "Nuclear Export of MicroRNA Precursors." Science **303**(5654): 95-98.

Lytle, R., T. Yario and J. Steitz (2007). "Target mRNAs are repressed as efficiently by microRNA-binding sites in the 5′ UTR as in the 3′ UTR." Proceedings of the National Academy of Sciences **104**(23): 9667-9672.

Ma, F., S. Xu, X. Liu, Q. Zhang, X. Xu, M. Liu, M. Hua, N. Li, H. Yao and X. Cao (2011). "The microRNA miR-29 controls innate and adaptive immune responses to intracellular bacterial infection by targeting interferon-gamma." Nat Immunol **12**(9): 861-869.

Maegdefessel, L., J. Azuma, R. Toh, D. R. Merk, A. Deng, J. T. Chin, U. Raaz, A. M. Schoelmerich, A. Raiesdana, N. J. Leeper, M. V. McConnell, R. L. Dalman, J. M. Spin and P. S. Tsao (2012). "Inhibition of microRNA-29b reduces murine abdominal aortic aneurysm development." J Clin Invest **122**(2): 497-506.

Marcu, K. B., M. Otero, E. Olivotto, R. M. Borzi and M. B. Goldring (2010). "NF-kappaB signaling: multiple angles to target OA." Curr Drug Targets **11**(5): 599-613.

Martel-Pelletier, J., C. Boileau, J. P. Pelletier and P. J. Roughley (2008). "Cartilage in normal and osteoarthritis conditions." Best Pract Res Clin Rheumatol **22**(2): 351-384.

Martin, P. (1990). "Tissue patterning in the developing mouse limb." Int J Dev Biol **34**(3): 323-336.

Martinez-Sanchez, A., K. Dudek and C. Murphy (2012). "Regulation of human chondrocyte function through direct inhibition of cartilage master regulator SOX9 by microRNA-145 (miRNA-145)." Journal of Biological Chemistry **287**(2): 916-924.

(2012). "Regulation of human chondrocyte function through direct inhibition of cartilage master regulator SOX9 by microRNA-145 (miRNA-145)." The Journal of biological chemistry **287**(2): 916-924.
Martinez-Sanchez, A. and C. L. Murphy (2013). "miR-1247 functions by targeting cartilage transcription factor SOX9." J Biol Chem **288**(43): 30802-30814.
Martinez, J., A. Patkaniowska, H. Urlaub, R. Lührmann and T. Tuschl (2002). "Single-stranded antisense siRNAs guide target RNA cleavage in RNAi." Cell **110**(5): 563-574.
Matyas, J. R., L. J. Sandell and M. E. Adams (1997). "Gene expression of type II collagens in chondro-osteophytes in experimental osteoarthritis." Osteoarthritis Cartilage **5**(2): 99-105.
Maurer, B., J. Stanczyk, A. Jungel, A. Akhmetshina, M. Trenkmann, M. Brock, O. Kowal-Bielecka, R. E. Gay, B. A. Michel, J. H. Distler, S. Gay and O. Distler (2010). "MicroRNA-29, a key regulator of collagen expression in systemic sclerosis." Arthritis Rheum **62**(6): 1733-1743.
Meachim, G. and D. H. Collins (1962). "Cell counts of normal and osteoarthritic articular cartilage in relation to the uptake of sulphate (35SO4) in vitro." Ann Rheum Dis **21**: 45-50.
Messier, S. P., D. J. Gutekunst, C. Davis and P. DeVita (2005). "Weight loss reduces knee-joint loads in overweight and obese older adults with knee osteoarthritis." Arthritis Rheum **52**(7): 2026-2032.
Miravet, S., J. Piedra, F. Miro, E. Itarte, A. Garcia de Herreros and M. Dunach (2002). "The transcriptional factor Tcf-4 contains different binding sites for beta-catenin and plakoglobin." J Biol Chem **277**(3): 1884-1891.
Mitchell, P., R. Parkin, E. Kroh, B. Fritz, S. Wyman, E. Pogosova-Agadjanyan, A. Peterson, J. Noteboom, K. O'Briant, A. Allen, D. Lin, N. Urban, C. Drescher, B. Knudsen, D. Stirewalt, R. Gentleman, R. Vessella, P. Nelson, D. Martin and M. Tewari (2008). "Circulating microRNAs as stable blood-based markers for cancer detection." Proceedings of the National Academy of Sciences **105**(30): 10513-10518.
Miyaki, S., T. Nakasa, S. Otsuki, S. Grogan, R. Higashiyama, A. Inoue, Y. Kato, T. Sato, M. Lotz and H. Asahara (2009). "MicroRNA-140 is expressed in differentiated human articular chondrocytes and modulates interleukin-1 responses." Arthritis & Rheumatism **60**(9): 2723-2730.
(2009). "MicroRNA-140 is expressed in differentiated human articular chondrocytes and modulates interleukin-1 responses." Arthritis and rheumatism **60**(9): 2723-2730.
Miyaki, S., T. Nakasa, S. Otsuki, S. P. Grogan, R. Higashiyama, A. Inoue, Y. Kato, T. Sato, M. K. Lotz and H. Asahara (2009). "MicroRNA-140 is expressed in differentiated human articular chondrocytes and modulates interleukin-1 responses." Arthritis Rheum **60**(9): 2723-2730.
Miyaki, S., T. Sato, A. Inoue, S. Otsuki, Y. Ito, S. Yokoyama, Y. Kato, F. Takemoto, T. Nakasa, S. Yamashita, S. Takada, M. Lotz, H. Ueno-Kudo and H. Asahara (2010). "MicroRNA-140 plays dual roles in both cartilage development and homeostasis." Genes Dev **24**(11): 1173-1185.
Miyaki, S., T. Sato, A. Inoue, S. Otsuki, Y. Ito, S. Yokoyama, Y. Kato, F. Takemoto, T. Nakasa, S. Yamashita, S. Takada, M. K. Lotz, H. Ueno-Kudo and H. Asahara (2010). "MicroRNA-140 plays dual roles in both cartilage development and homeostasis." Genes Dev **24**(11): 1173-1185.
Miyazawa, K., M. Shinozaki, T. Hara, T. Furuya and K. Miyazono (2002). "Two major Smad pathways in TGF-beta superfamily signalling." Genes Cells **7**(12): 1191-1204.
Mooney, R. A., E. R. Sampson, J. Lerea, R. N. Rosier and M. J. Zuscik (2011). "High-fat diet accelerates progression of osteoarthritis after meniscal/ligamentous injury." Arthritis Res Ther **13**(6): R198.
Morita, S., T. Horii, M. Kimura, T. Ochiya, S. Tajima and I. Hatada (2013). "miR-29 represses the activities of DNA methyltransferases and DNA demethylases." Int J Mol Sci **14**(7): 14647-14658.
Mott, J. L., S. Kurita, S. C. Cazanave, S. F. Bronk, N. W. Werneburg and M. E. Fernandez-Zapico (2010). "Transcriptional suppression of mir-29b-1/mir-29a promoter by c-Myc, hedgehog, and NF-kappaB." J Cell Biochem **110**(5): 1155-1164.

Moulin, D., V. Salone, M. Koufany, T. Clement, P. Netter, I. Behm-Ansmant, B. Charpentier, C. Branlant and J.-Y. Jouzeau (2012). "miR-29b is overexpressed in osteoarthritic patients and targets type II collagen." Osteoarthritis and Cartilage **20**: S139 - S140.

Muniyappa, M. K., P. Dowling, M. Henry, P. Meleady, P. Doolan, P. Gammell, M. Clynes and N. Barron (2009). "MiRNA-29a regulates the expression of numerous proteins and reduces the invasiveness and proliferation of human carcinoma cell lines." Eur J Cancer **45**(17): 3104-3118.

Murata, K., H. Yoshitomi, S. Tanida, M. Ishikawa, K. Nishitani, H. Ito and T. Nakamura (2010). "Plasma and synovial fluid microRNAs as potential biomarkers of rheumatoid arthritis and osteoarthritis." Arthritis Res Ther **12**(3): R86.

Murata, K., H. Yoshitomi, S. Tanida, M. Ishikawa, K. Nishitani, H. Ito and T. Nakamura (2010). "Plasma and synovial fluid microRNAs as potential biomarkers of rheumatoid arthritis and osteoarthritis." Arthritis Res Ther **12**(3): R86.

Nah, S. S., I. Y. Choi, B. Yoo, Y. G. Kim, H. B. Moon and C. K. Lee (2007). "Advanced glycation end products increases matrix metalloproteinase-1, -3, and -13, and TNF-alpha in human osteoarthritic chondrocytes." FEBS Lett **581**(9): 1928-1932.

Nakamura, Y., X. He, H. Kato, S. Wakitani, T. Kobayashi, S. Watanabe, A. Iida, H. Tahara, M. L. Warman, R. Watanapokasin and J. H. Postlethwait (2012). "Sox9 is upstream of microRNA-140 in cartilage." Appl Biochem Biotechnol **166**(1): 64-71.

Nakamura, Y., J. Inloes, T. Katagiri and T. Kobayashi (2011). "Chondrocyte-specific microRNA-140 regulates endochondral bone development and targets Dnpep to modulate bone morphogenetic protein signaling." Mol Cell Biol **31**(14): 3019-3028.

Nakamura, Y., J. B. Inloes, T. Katagiri and T. Kobayashi (2011). "Chondrocyte-specific microRNA-140 regulates endochondral bone development and targets Dnpep to modulate bone morphogenetic protein signaling." Mol Cell Biol **31**(14): 3019-3028.

Nalesso, G., J. Sherwood, J. Bertrand, T. Pap, M. Ramachandran, C. De Bari, C. Pitzalis and F. Dell'accio (2011). "WNT-3A modulates articular chondrocyte phenotype by activating both canonical and noncanonical pathways." J Cell Biol **193**(3): 551-564.

Neu, C., A. Khalafi, K. Komvopoulos, T. Schmid and H. Reddi (2007). "Mechanotransduction of bovine articular cartilage superficial zone protein by transforming growth factor β signaling." Arthritis & Rheumatism **56**(11): 3706-3714.

Ng, L. J., S. Wheatley, G. E. Muscat, J. Conway-Campbell, J. Bowles, E. Wright, D. M. Bell, P. P. Tam, K. S. Cheah and P. Koopman (1997). "SOX9 binds DNA, activates transcription, and coexpresses with type II collagen during chondrogenesis in the mouse." Dev Biol **183**(1): 108-121.

Nicolas, F. E., H. Pais, F. Schwach, M. Lindow, S. Kauppinen, V. Moulton and T. Dalmay (2008). "Experimental identification of microRNA-140 targets by silencing and overexpressing miR-140." RNA (New York, N.Y.) **14**(12): 2513-2520.

Nishikawa, R., Y. Goto, S. Kojima, H. Enokida, T. Chiyomaru, T. Kinoshita, S. Sakamoto, M. Fuse, M. Nakagawa, Y. Naya, T. Ichikawa and N. Seki (2014). "Tumor-suppressive microRNA-29s inhibit cancer cell migration and invasion via targeting LAMC1 in prostate cancer." Int J Oncol **45**(1): 401-410.

Okamura, K., J. Hagen, H. Duan, D. Tyler and E. Lai (2007). "The mirtron pathway generates microRNA-class regulatory RNAs in Drosophila." Cell **130**(1): 89-100.

Okuhara, A., T. Nakasa, H. Shibuya, T. Niimoto, N. Adachi, M. Deie and M. Ochi (2011). "Changes in microRNA expression in peripheral mononuclear cells according to the progression of osteoarthritis." Modern rheumatology / the Japan Rheumatism Association: 1-12.

Pais, H., E. Francisco, S. Soond, T. Swingler, I. Clark, A. Chantry, V. Moulton and T. Dalmay (2010). "Analyzing mRNA expression identifies Smad3 as a microRNA-140 target regulated only at protein level." RNA **16**(3): 489-494.

Pais, H., F. E. Nicolas, S. M. Soond, T. E. Swingler, I. M. Clark, A. Chantry, V. Moulton and T. Dalmay (2010). "Analyzing mRNA expression identifies Smad3 as a microRNA-140 target regulated only at protein level." RNA **16**(3): 489-494.

Park, S. J., E. J. Cheon, M. H. Lee and H. A. Kim (2013). "MicroRNA-127-5p regulates matrix metalloproteinase 13 expression and interleukin-1beta-induced catabolic effects in human chondrocytes." Arthritis Rheum **65**(12): 3141-3152.

Parpart, S., S. Roessler, F. Dong, V. Rao, A. Takai, J. Ji, L. X. Qin, Q. H. Ye, H. L. Jia, Z. Y. Tang and X. W. Wang (2014). "Modulation of miR-29 expression by alpha-fetoprotein is linked to the hepatocellular carcinoma epigenome." Hepatology **60**(3): 872-883.

Pearle, A. D., C. R. Scanzello, S. George, L. A. Mandl, E. F. DiCarlo, M. Peterson, T. P. Sculco and M. K. Crow (2007). "Elevated high-sensitivity C-reactive protein levels are associated with local inflammatory findings in patients with osteoarthritis." Osteoarthritis Cartilage **15**(5): 516-523.

Pearle, A. D., R. F. Warren and S. A. Rodeo (2005). "Basic science of articular cartilage and osteoarthritis." Clin Sports Med **24**(1): 1-12.

Pelletier, J. P., J. P. Caron, C. Evans, P. D. Robbins, H. I. Georgescu, D. Jovanovic, J. C. Fernandes and J. Martel-Pelletier (1997). "In vivo suppression of early experimental osteoarthritis by interleukin-1 receptor antagonist using gene therapy." Arthritis Rheum **40**(6): 1012-1019.

Petersen, C., M.-E. Bordeleau, J. Pelletier and P. Sharp (2006). "Short RNAs repress translation after initiation in mammalian cells." Mol Cell **21**(4): 533-542.

Petrovich, O. n., S. L. llyich and M. S. Pavlovich (2014). "Connectic tissue: Histophysiology, Biochemistry, Molecular Biology ".

Pfander, D., T. Cramer, E. Schipani and R. S. Johnson (2003). "HIF-1alpha controls extracellular matrix synthesis by epiphyseal chondrocytes." J Cell Sci **116**(Pt 9): 1819-1826.

Poonpet, T., S. Honsawek, N. Tammachote, S. Kanitnate and R. Tammachote (2013). "ADAMTS14 gene polymorphism associated with knee osteoarthritis in Thai women." Genet Mol Res **12**(4): 5301-5309.

Presle, N., P. Pottie, H. Dumond, C. Guillaume, F. Lapicque, S. Pallu, D. Mainard, P. Netter and B. Terlain (2006). "Differential distribution of adipokines between serum and synovial fluid in patients with osteoarthritis. Contribution of joint tissues to their articular production." Osteoarthritis Cartilage **14**(7): 690-695.

Price, M. A. (2006). "CKI, there's more than one: casein kinase I family members in Wnt and Hedgehog signaling." Genes Dev **20**(4): 399-410.

Pujol, J.-P., C. Chadjichristos, F. Legendre, C. Bauge, G. Beauchef, R. Andriamanalijaona, P. Galera and K. Boumediene (2008). "Interleukin-1 and transforming growth factor-beta 1 as crucial factors in osteoarthritic cartilage metabolism." Connect Tissue Res **49**(3): 293-297.

Pullen, T. J., G. da Silva Xavier, G. Kelsey and G. A. Rutter (2011). "miR-29a and miR-29b contribute to pancreatic beta-cell-specific silencing of monocarboxylate transporter 1 (Mct1)." Mol Cell Biol **31**(15): 3182-3194.

Qin, W., A. C. Chung, X. R. Huang, X. M. Meng, D. S. Hui, C. M. Yu, J. J. Sung and H. Y. Lan (2011). "TGF-beta/Smad3 signaling promotes renal fibrosis by inhibiting miR-29." J Am Soc Nephrol **22**(8): 1462-1474.

Ramdas, V., M. McBride, L. Denby and A. H. Baker (2013). "Canonical transforming growth factor-beta signaling regulates disintegrin metalloprotease expression in experimental renal fibrosis via miR-29." Am J Pathol **183**(6): 1885-1896.

Reinhart, B. J., F. J. Slack, M. Basson, A. E. Pasquinelli, J. C. Bettinger, A. E. Rougvie, H. R. Horvitz and G. Ruvkun (2000). "The 21-nucleotide let-7 RNA regulates developmental timing in Caenorhabditis elegans." Nature **403**(6772): 901-906.

Riordan, E. A., C. Little and D. Hunter (2014). "Pathogenesis of post-traumatic OA with a view to intervention." Best Pract Res Clin Rheumatol **28**(1): 17-30.

Ro, S., C. Park, D. Young, K. Sanders and W. Yan (2007). "Tissue-dependent paired expression of miRNAs." Nucleic Acids Res **35**(17): 5944-5953.
Roderburg, C., G. W. Urban, K. Bettermann, M. Vucur, H. Zimmermann, S. Schmidt, J. Janssen, C. Koppe, P. Knolle, M. Castoldi, F. Tacke, C. Trautwein and T. Luedde (2011). "Micro-RNA profiling reveals a role for miR-29 in human and murine liver fibrosis." Hepatology **53**(1): 209-218.
Rodriguez-Lopez, J., M. Pombo-Suarez, J. Loughlin, A. Tsezou, F. J. Blanco, I. Meulenbelt, P. E. Slagboom, A. M. Valdes, T. D. Spector, J. J. Gomez-Reino and A. Gonzalez (2009). "Association of a nsSNP in ADAMTS14 to some osteoarthritis phenotypes." Osteoarthritis Cartilage **17**(3): 321-327.
Rodriguez, A., S. Griffiths-Jones, J. Ashurst and A. Bradley (2004). "Identification of mammalian microRNA host genes and transcription units." Genome Res **14**(10A): 1902-1910.
Roodman, G. D. (1999). "Cell biology of the osteoclast." Exp Hematol **27**(8): 1229-1241.
Rothwell, A. G. and G. Bentley (1973). "Chondrocyte multiplication in osteoarthritic articular cartilage." J Bone Joint Surg Br **55**(3): 588-594.
Ruby, G., C. Jan and D. Bartel (2007). "Intronic microRNA precursors that bypass Drosha processing." Nature **448**(7149): 83-86.
Sætrom, P., B. Heale, O. Snøve, L. Aagaard, J. Alluin and J. Rossi (2007). "Distance constraints between microRNA target sites dictate efficacy and cooperativity." Nucleic Acids Res **35**(7): 2333-2342.
Saini, H. K., S. Griffiths-Jones and A. J. Enright (2007). "Genomic analysis of human microRNA transcripts." Proc Natl Acad Sci U S A **104**(45): 17719-17724.
Sandell, L. J. and T. Aigner (2001). "Articular cartilage and changes in arthritis. An introduction: cell biology of osteoarthritis." Arthritis Res **3**(2): 107-113.
Sandell, L. J., N. Morris, J. R. Robbins and M. B. Goldring (1991). "Alternatively spliced type II procollagen mRNAs define distinct populations of cells during vertebral development: differential expression of the amino-propeptide." J Cell Biol **114**(6): 1307-1319.
Santanam, U., N. Zanesi, A. Efanov, S. Costinean, A. Palamarchuk, J. P. Hagan, S. Volinia, H. Alder, L. Rassenti, T. Kipps, C. M. Croce and Y. Pekarsky (2010). "Chronic lymphocytic leukemia modeled in mouse by targeted miR-29 expression." Proc Natl Acad Sci U S A **107**(27): 12210-12215.
Scanzello, C. R. and S. R. Goldring (2012). "The role of synovitis in osteoarthritis pathogenesis." Bone **51**(2): 249-257.
Schipani, E., H. E. Ryan, S. Didrickson, T. Kobayashi, M. Knight and R. S. Johnson (2001). "Hypoxia in cartilage: HIF-1alpha is essential for chondrocyte growth arrest and survival." Genes Dev **15**(21): 2865-2876.
Schmid, T. M. and T. F. Linsenmayer (1985). "Developmental acquisition of type X collagen in the embryonic chick tibiotarsus." Dev Biol **107**(2): 373-381.
Schmitt, M. J., C. Margue, I. Behrmann and S. Kreis (2013). "MiRNA-29: a microRNA family with tumor-suppressing and immune-modulating properties." Curr Mol Med **13**(4): 572-585.
Schwarz, D., G. Hutvágner, T. Du, Z. Xu, N. Aronin and P. Zamore (2003). "Asymmetry in the assembly of the RNAi enzyme complex." Cell **115**(2): 199-208.
Sengupta, S., J. A. den Boon, I. H. Chen, M. A. Newton, S. A. Stanhope, Y. J. Cheng, C. J. Chen, A. Hildesheim, B. Sugden and P. Ahlquist (2008). "MicroRNA 29c is down-regulated in nasopharyngeal carcinomas, up-regulating mRNAs encoding extracellular matrix proteins." Proc Natl Acad Sci U S A **105**(15): 5874-5878.
Serra, R., M. Johnson, E. H. Filvaroff, J. LaBorde, D. M. Sheehan, R. Derynck and H. L. Moses (1997). "Expression of a truncated, kinase-defective TGF-beta type II receptor in mouse skeletal

tissue promotes terminal chondrocyte differentiation and osteoarthritis." J Cell Biol **139**(2): 541-552.
Shioya, M., S. Obayashi, H. Tabunoki, K. Arima, Y. Saito, T. Ishida and J. Satoh (2010). "Aberrant microRNA expression in the brains of neurodegenerative diseases: miR-29a decreased in Alzheimer disease brains targets neurone navigator 3." Neuropathol Appl Neurobiol **36**(4): 320-330.
Sibley, C., Y. Seow, S. Saayman, K. Dijkstra, S. El Andaloussi, M. Weinberg and M. Wood (2012). "The biogenesis and characterization of mammalian microRNAs of mirtron origin." Nucleic Acids Res **40**(1): 438-448.
Silver, I. A. (1975). "Measurement of pH and ionic composition of pericellular sites." Philos Trans R Soc Lond B Biol Sci **271**(912): 261-272.
Smith, M. D., E. Barg, H. Weedon, V. Papengelis, T. Smeets, P. P. Tak, M. Kraan, M. Coleman and M. J. Ahern (2003). "Microarchitecture and protective mechanisms in synovial tissue from clinically and arthroscopically normal knee joints." Ann Rheum Dis **62**(4): 303-307.
Song, D. H., I. Dominguez, J. Mizuno, M. Kaut, S. C. Mohr and D. C. Seldin (2003). "CK2 phosphorylation of the armadillo repeat region of beta-catenin potentiates Wnt signaling." J Biol Chem **278**(26): 24018-24025.
Song, J., D. Kim and E.-J. Jin (2011). "MicroRNA-488 suppresses cell migration through modulation of the focal adhesion activity during chondrogenic differentiation of chick limb mesenchymal cells." Cell Biology International **35**(2): 179-185.
Song, R. H., M. D. Tortorella, A. M. Malfait, J. T. Alston, Z. Yang, E. C. Arner and D. W. Griggs (2007). "Aggrecan degradation in human articular cartilage explants is mediated by both ADAMTS-4 and ADAMTS-5." Arthritis Rheum **56**(2): 575-585.
Sorrentino, A., M. Ferracin, G. Castelli, M. Biffoni, G. Tomaselli, M. Baiocchi, A. Fatica, M. Negrini, C. Peschle and M. Valtieri (2008). "Isolation and characterization of CD146+ multipotent mesenchymal stromal cells." Exp Hematol **36**(8): 1035-1046.
Stanton, H., F. M. Rogerson, C. J. East, S. B. Golub, K. E. Lawlor, C. T. Meeker, C. B. Little, K. Last, P. J. Farmer, I. K. Campbell, A. M. Fourie and A. J. Fosang (2005). "ADAMTS5 is the major aggrecanase in mouse cartilage in vivo and in vitro." Nature **434**(7033): 648-652.
Steele, R., J. L. Mott and R. B. Ray (2010). "MBP-1 upregulates miR-29b that represses Mcl-1, collagens, and matrix-metalloproteinase-2 in prostate cancer cells." Genes Cancer **1**(4): 381-387.
Subramanian, M., S. R. Rao, P. Thacker, S. Chatterjee and D. Karunagaran (2014). "MiR-29b downregulates canonical Wnt signaling by suppressing coactivators of beta-catenin in human colorectal cancer cells." J Cell Biochem **115**(11): 1974-1984.
Sulzbacher, I. (2013). "Osteoarthritis: histology and pathogenesis." Wien Med Wochenschr **163**(9-10): 212-219.
Suomi, S., H. Taipaleenmäki, A. Seppänen, T. Ripatti, K. Väänänen, T. Hentunen, A.-M. Säämänen and T. Laitala-Leinonen (2008). "MicroRNAs regulate osteogenesis and chondrogenesis of mouse bone marrow stromal cells." Gene Regulation and Systems Biology **2**: 177-191.
Swingler, T., G. Wheeler, V. Carmont, H. Elliott, M. Barter, M. Abu-Elmagd, S. Donell, R. Boot-Handford, M. Hajihosseini, A. Münsterberg, T. Dalmay, D. Young and I. Clark (2011). "The expression and function of microRNAs in chondrogenesis and osteoarthritis." Arthritis & Rheumatism: n/a-n/a.
(2012). "The expression and function of microRNAs in chondrogenesis and osteoarthritis." Arthritis & Rheumatism **64**: 1909-1919.
Taganov, K., M. Boldin, K.-J. Chang and D. Baltimore (2006). "NF-kappaB-dependent induction of microRNA miR-146, an inhibitor targeted to signaling proteins of innate immune responses." Proc Natl Acad Sci U S A **103**(33): 12481-12486.

Tan, M., J. Wu and Y. Cai (2013). "Suppression of Wnt signaling by the miR-29 family is mediated by demethylation of WIF-1 in non-small-cell lung cancer." Biochem Biophys Res Commun **438**(4): 673-679.

Tardif, G., D. Hum, J.-P. Pelletier, N. Duval and J. Martel-Pelletier (2009). "Regulation of the IGFBP-5 and MMP-13 genes by the microRNAs miR-140 and miR-27a in human osteoarthritic chondrocytes." BMC Musculoskelet Disord **10**: 148.

Tetlow, L., D. Adlam and D. Woolley (2001). "Matrix metalloproteinase and proinflammatory cytokine production by chondrocytes of human osteoarthritic cartilage: Associations with degenerative changes." Arthritis & Rheumatism **44**(3): 585-594.

Tortorella, M. D., A. M. Malfait, C. Deccico and E. Arner (2001). "The role of ADAM-TS4 (aggrecanase-1) and ADAM-TS5 (aggrecanase-2) in a model of cartilage degradation." Osteoarthritis Cartilage **9**(6): 539-552.

Tuddenham, L., G. Wheeler, S. Ntounia-Fousara, J. Waters, M. Hajihosseini, I. Clark and T. Dalmay (2006). "The cartilage specific microRNA-140 targets histone deacetylase 4 in mouse cells." FEBS Lett **580**(17): 4214-4217.

Ugalde, A. P., A. J. Ramsay, J. de la Rosa, I. Varela, G. Marino, J. Cadinanos, J. Lu, J. M. Freije and C. Lopez-Otin (2011). "Aging and chronic DNA damage response activate a regulatory pathway involving miR-29 and p53." EMBO J **30**(11): 2219-2232.

Umlauf, D., S. Frank, T. Pap and J. Bertrand (2010). "Cartilage biology, pathology, and repair." Cellular and Molecular Life Sciences **67**(24): 4197-4211.

van Amerongen, R. and A. Berns (2005). "Re-evaluating the role of Frat in Wnt-signal transduction." Cell Cycle **4**(8): 1065-1072.

van Beuningen, H. M., H. L. Glansbeek, P. M. van der Kraan and W. B. van den Berg (1998). "Differential effects of local application of BMP-2 or TGF-beta 1 on both articular cartilage composition and osteophyte formation." Osteoarthritis Cartilage **6**(5): 306-317.

van der Kraan, P. M. and W. B. van den Berg (2007). "Osteophytes: relevance and biology." Osteoarthritis Cartilage **15**(3): 237-244.

van Rooij, E. and S. Kauppinen (2014). "Development of microRNA therapeutics is coming of age." EMBO Mol Med **6**(7): 851-864.

van Rooij, E., L. B. Sutherland, J. E. Thatcher, J. M. DiMaio, R. H. Naseem, W. S. Marshall, J. A. Hill and E. N. Olson (2008). "Dysregulation of microRNAs after myocardial infarction reveals a role of miR-29 in cardiac fibrosis." Proc Natl Acad Sci U S A **105**(35): 13027-13032.

Vasudevan, S. and J. Steitz (2007). "AU-rich-element-mediated upregulation of translation by FXR1 and Argonaute 2." Cell **128**(6): 1105-1118.

Vasudevan, S., Y. Tong and J. Steitz (2007). "Switching from repression to activation: microRNAs can up-regulate translation." Science (New York, N.Y.) **318**(5858): 1931-1934.

Ventura, A., A. Young, M. Winslow, L. Lintault, A. Meissner, S. Erkeland, J. Newman, R. Bronson, D. Crowley, J. Stone, R. Jaenisch, P. Sharp and T. Jacks (2008). "Targeted deletion reveals essential and overlapping functions of the miR-17 through 92 family of miRNA clusters." Cell **132**(5): 875-886.

Verrecchia, F., M. L. Chu and A. Mauviel (2001). "Identification of novel TGF-beta /Smad gene targets in dermal fibroblasts using a combined cDNA microarray/promoter transactivation approach." J Biol Chem **276**(20): 17058-17062.

Verrecchia, F. and A. Mauviel (2002). "Transforming growth factor-beta signaling through the Smad pathway: role in extracellular matrix gene expression and regulation." J Invest Dermatol **118**(2): 211-215.

Wang, B., R. Komers, R. Carew, C. E. Winbanks, B. Xu, M. Herman-Edelstein, P. Koh, M. Thomas, K. Jandeleit-Dahm, P. Gregorevic, M. E. Cooper and P. Kantharidis (2012). "Suppression of

microRNA-29 expression by TGF-beta1 promotes collagen expression and renal fibrosis." J Am Soc Nephrol **23**(2): 252-265.
Wang, F. S., P. C. Chuang, C. L. Lin, M. W. Chen, H. J. Ke, Y. H. Chang, Y. S. Chen, S. L. Wu and J. Y. Ko (2013). "MicroRNA-29a protects against glucocorticoid-induced bone loss and fragility in rats by orchestrating bone acquisition and resorption." Arthritis Rheum **65**(6): 1530-1540.
Wang, H., R. Garzon, H. Sun, K. J. Ladner, R. Singh, J. Dahlman, A. Cheng, B. M. Hall, S. J. Qualman, D. S. Chandler, C. M. Croce and D. C. Guttridge (2008). "NF-kappaB-YY1-miR-29 regulatory circuitry in skeletal myogenesis and rhabdomyosarcoma." Cancer Cell **14**(5): 369-381.
Wang, H. X., F. R. Tekpetey and G. M. Kidder (2009). "Identification of WNT/beta-CATENIN signaling pathway components in human cumulus cells." Mol Hum Reprod **15**(1): 11-17.
Wang, L., L. Zhou, P. Jiang, L. Lu, X. Chen, H. Lan, D. C. Guttridge, H. Sun and H. Wang (2012). "Loss of miR-29 in myoblasts contributes to dystrophic muscle pathogenesis." Mol Ther **20**(6): 1222-1233.
Wang, L. G. and J. Gu (2012). "Serum microRNA-29a is a promising novel marker for early detection of colorectal liver metastasis." Cancer Epidemiol **36**(1): e61-67.
Watanabe, T., T. Sato, T. Amano, Y. Kawamura, N. Kawamura, H. Kawaguchi, N. Yamashita, H. Kurihara and T. Nakaoka (2008). "Dnm3os, a non-coding RNA, is required for normal growth and skeletal development in mice." Dev Dyn **237**(12): 3738-3748.
Wei, W., H. B. He, W. Y. Zhang, H. X. Zhang, J. B. Bai, H. Z. Liu, J. H. Cao, K. C. Chang, X. Y. Li and S. H. Zhao (2013). "miR-29 targets Akt3 to reduce proliferation and facilitate differentiation of myoblasts in skeletal muscle development." Cell Death Dis **4**: e668.
Weng, L. H., C. J. Wang, J. Y. Ko, Y. C. Sun and F. S. Wang (2010). "Control of Dkk-1 ameliorates chondrocyte apoptosis, cartilage destruction, and subchondral bone deterioration in osteoarthritic knees." Arthritis Rheum **62**(5): 1393-1402.
Wermter, C., M. Howel, V. Hintze, B. Bombosch, K. Aufenvenne, I. Yiallouros and W. Stocker (2007). "The protease domain of procollagen C-proteinase (BMP1) lacks substrate selectivity, which is conferred by non-proteolytic domains." Biol Chem **388**(5): 513-521.
Westholm, J. and E. Lai (2011). "Mirtrons: microRNA biogenesis via splicing." Biochimie **93**(11): 1897-1904.
Wieland, H., M. Michaelis, B. Kirschbaum and K. Rudolphi (2005). "Osteoarthritis — an untreatable disease?" Nature Reviews Drug Discovery **4**(4): 331-344.
Wienholds, E., W. P. Kloosterman, E. Miska, E. Alvarez-Saavedra, E. Berezikov, E. de Bruijn, H. R. Horvitz, S. Kauppinen and R. H. Plasterk (2005). "MicroRNA expression in zebrafish embryonic development." Science **309**(5732): 310-311.
Wienholds, E., M. Koudijs, F. van Eeden, E. Cuppen and R. Plasterk (2003). "The microRNA-producing enzyme Dicer1 is essential for zebrafish development." Nat Genet **35**(3): 217-218.
Wightman, B., I. Ha and G. Ruvkun (1993). "Posttranscriptional regulation of the heterochronic gene lin-14 by lin-4 mediates temporal pattern formation in C. elegans." Cell **75**(5): 855-862.
Willert, K., M. Brink, A. Wodarz, H. Varmus and R. Nusse (1997). "Casein kinase 2 associates with and phosphorylates dishevelled." EMBO J **16**(11): 3089-3096.
Willert, K. and K. A. Jones (2006). "Wnt signaling: is the party in the nucleus?" Genes Dev **20**(11): 1394-1404.
Wittmann, J. and H.-M. Jäck (2010). "Serum microRNAs as powerful cancer biomarkers." Biochim Biophys Acta **1806**(2): 200-207.
Xiong, Y., J. H. Fang, J. P. Yun, J. Yang, Y. Zhang, W. H. Jia and S. M. Zhuang (2010). "Effects of microRNA-29 on apoptosis, tumorigenicity, and prognosis of hepatocellular carcinoma." Hepatology **51**(3): 836-845.
Xu, J., Y. Kang, W.-m. Liao and L. Yu (2012). "MiR-194 Regulates Chondrogenic Differentiation of Human Adipose-Derived Stem Cells by Targeting Sox5." PLoS One **7**(3): e31861.

Yamasaki, K., T. Nakasa, S. Miyaki, M. Ishikawa, M. Deie, N. Adachi, Y. Yasunaga, H. Asahara and M. Ochi (2009). "Expression of MicroRNA-146a in osteoarthritis cartilage." Arthritis and rheumatism **60**(4): 1035-1041.

Yamashita, S., S. Miyaki, Y. Kato, S. Yokoyama, T. Sato, F. Barrionuevo, H. Akiyama, G. Scherer, S. Takada and H. Asahara (2012). "L-Sox5 and Sox6 enhance chondrogenic miR-140 expression by strengthening dimeric Sox9 activity." Journal of Biological Chemistry.

Yan, C., Y. Wang, X.-Y. Shen, G. Yang, J. Jian, H.-S. Wang, G.-Q. Chen and Q. Wu (2011). "MicroRNA regulation associated chondrogenesis of mouse MSCs grown on polyhydroxyalkanoates." Biomaterials **32**(27): 6435-6444.

Yang, B., H. Guo, Y. Zhang, L. Chen, D. Ying and S. Dong (2011). "MicroRNA-145 Regulates Chondrogenic Differentiation of Mesenchymal Stem Cells by Targeting Sox9." PLoS One **6**(7): e21679.

Yang, B., H. Guo, Y. Zhang, S. Dong and D. Ying (2011). "The microRNA expression profiles of mouse mesenchymal stem cell during chondrogenic differentiation." BMB Reports **44**(1): 28-33.

Yang, J., S. Qin, C. Yi, G. Ma, H. Zhu, W. Zhou, Y. Xiong, X. Zhu, Y. Wang, L. He and X. Guo (2011). "MiR-140 is co-expressed with Wwp2-C transcript and activated by Sox9 to target Sp1 in maintaining the chondrocyte proliferation." FEBS Lett **585**(19): 2992-2997.

Yang, T., Y. Liang, Q. Lin, J. Liu, F. Luo, X. Li, H. Zhou, S. Zhuang and H. Zhang (2013). "miR-29 mediates TGFbeta1-induced extracellular matrix synthesis through activation of PI3K-AKT pathway in human lung fibroblasts." J Cell Biochem **114**(6): 1336-1342.

Yi, R., Y. Qin, I. Macara and B. Cullen (2003). "Exportin-5 mediates the nuclear export of pre-microRNAs and short hairpin RNAs." Genes Dev **17**(24): 3011-3016.

Zamli, Z. and M. Sharif (2011). "Chondrocyte apoptosis: a cause or consequence of osteoarthritis?" Int J Rheum Dis **14**(2): 159-166.

Zampetaki, A., S. Kiechl, I. Drozdov, P. Willeit, U. Mayr, M. Prokopi, A. Mayr, S. Weger, F. Oberhollenzer, E. Bonora, A. Shah, J. Willeit and M. Mayr (2010). "Plasma microRNA profiling reveals loss of endothelial miR-126 and other microRNAs in type 2 diabetes." Circ Res **107**(6): 810-817.

Zeng, Y. and B. Cullen (2004). "Structural requirements for pre-microRNA binding and nuclear export by Exportin 5." Nucleic Acids Res **32**(16): 4776-4785.

Zhang, Y. K., H. Wang, Y. Leng, Z. L. Li, Y. F. Yang, F. J. Xiao, Q. F. Li, X. Q. Chen and L. S. Wang (2011). "Overexpression of microRNA-29b induces apoptosis of multiple myeloma cells through down regulating Mcl-1." Biochem Biophys Res Commun **414**(1): 233-239.

Zhang, Z., J. Zou, G. K. Wang, J. T. Zhang, S. Huang, Y. W. Qin and Q. Jing (2011). "Uracils at nucleotide position 9-11 are required for the rapid turnover of miR-29 family." Nucleic Acids Res **39**(10): 4387-4395.

Zhao, Q., H. Eberspaecher, V. Lefebvre and B. De Crombrugghe (1997). "Parallel expression of Sox9 and Col2a1 in cells undergoing chondrogenesis." Dev Dyn **209**(4): 377-386.

Zhong, N., J. Sun, Z. Min, W. Zhao, R. Zhang, W. Wang, J. Tian, L. Tian, J. Ma, D. Li, Y. Han and S. Lu (2012). "MicroRNA-337 is associated with chondrogenesis through regulating TGFBR2 expression." Osteoarthritis and Cartilage.

Zhou, S., K. Eid and J. Glowacki (2004). "Cooperation between TGF-beta and Wnt pathways during chondrocyte and adipocyte differentiation of human marrow stromal cells." J Bone Miner Res **19**(3): 463-470.

Zhu, M., M. Chen, M. Zuscik, Q. Wu, Y. J. Wang, R. N. Rosier, R. J. O'Keefe and D. Chen (2008). "Inhibition of beta-catenin signaling in articular chondrocytes results in articular cartilage destruction." Arthritis Rheum **58**(7): 2053-2064.

Zhu, M., D. Tang, Q. Wu, S. Hao, M. Chen, C. Xie, R. N. Rosier, R. J. O'Keefe, M. Zuscik and D. Chen (2009). "Activation of beta-catenin signaling in articular chondrocytes leads to osteoarthritis-

like phenotype in adult beta-catenin conditional activation mice." J Bone Miner Res **24**(1): 12-21.

ENDICES

Genes	Accession number	Sequences (5'->3')
ADAMTS6	ENSG00000049192	Forward: ACGTGAGCTCTCTCATCGTCATGGTTCTGC Reverse: ACGTGAGCTCCAAGCAGGAGAATGAATGTAGG
ADAMTS14	ENSG00000138316	Forward: GAGCTCGCTGTGCCCTGCCATC GAGCTCGGGTCCAATGGCGATGTTA
ADAMTS17	ENSG00000140470	Forward: ACGTTCTAGAAACATGAGCGTGGACTTGG Reverse: ACGTTCTAGATGTAATGCAAGTTAACGAATGG
ADAMTS19	ENSG00000145808	Forward: ACGTGAGCTCAATCACAGCTCCAGGTAATC Reverse: ACGTGAGCTCCCAAGAGACATACTATCTTCCAAGG
FZD3	ENSG00000104290	Forward: ATGCGTCGACTATTAGATGCCCAGCCTTTCTC Reverse: ATGCGTCGACATGCCTACCAAGAGGATAACATTC
FZD5	ENSG00000163251	Forward: ATGCGTCGACGGCATCGGCTACAACCTGAC Reverse: ATGCGTCGACAGACCACACAGTTCAAAGA AACCTG
FRAT2	ENSG00000181274	Forward: ATGCGTCGACCAACAGCGTCCAGTTCCTAC Reverse: ATGCGTCGACGCCGTCAAGTTTCATACAGC
CK2A2	ENSG00000070770	Forward: ATGCGTCGACATGCAGGTACTAGAGTTGTGTGG Reverse: ATGCGTCGACAATAAGTTTGCTTGTTTCTGTGG
DVL3	ENSG00000161202	Forward: ATGCGTCGACGCTGCGTTCCTCTCTCCATC Reverse: ATGCGTCGACTACCATTTATTGAGCACCTACTCTACTG TG

Table 1: Primer sequences for PCR amplification 3'UTR region of potential targets of the miR-29 family. For subcloning purpose, restriction sites (bases underlined) were added to the 5'P of the primers. *Sac*I (GAGCTC), *Sal*I (GTCGAC), *Xba*I (TCTAGA).

Genes	Mutant	Primer sequence (5'->3')
ADAMTS6	Site 1	Forward: TATGTGATGCACTGACATGTAATTTAAGAAGCTTATGATGGAATCAAGTCAAACATGCTGTTTAACTGAAAG Reverse: CTTTCAGTTAAACAGCATGTTTGACTTGATTCCATCATAAGCTTCTTAAATTACATGTCAGTGCATCACATA
	Site 2	Forward: TATTTATTTCACCAGGGCACATTAAGCTTAAGTTAACTGTTCTTTGAAAAGGCGCAAGGGAATTCAGT Reverse: ACTGAATTCCCTTGCGCCTTTTCAAAGAACAGTTAACTTAAGCTTAATGTGCCCTGGTGAAATAAATA
ADAMTS10	Site 1	Forward: GGGGACACAGACCCGTTTGTAAGCTTACCCCTTGTCGATGGTGTGCG Reverse: CGCACACCATCGACAAGGGGTAAGCTTACAAACGGGTCTGTGTCCCC
	Site 2	Forward: GCTCGGTCCGGGCCAAGCTTATGACGATGAGAGATGCATTAATCGGTCC Reverse: GGACCGATTAATGCATCTCTCATCGTCATAAGCTTGGCCCGGACCGAGC
ADAMTS14	Site 1	Forward: GTTTGTCTTTGCTGGCCAGAAGAGTCGACTCATGGCCATACTCTGGCCTTG Reverse: CAAGGCCAGAGTATGGCCATGAGTCGACTCTTCTGGCCAGCAAAGAC
	Site 2	Forward: GGGTGCCAGCCCCTGGCCGTCGACTGGAGTGGGGAAGACAC Reverse: GTGTCTTCCCCACTCCAGTCGACGGCCAGGGGCTGGCACCC
	Site 3	Forward: CTAAACTCCTGCCAGGTGATAGAGAGCTCTCTCACTTCTTCCTTCCCCAAGGC

		Reverse: GCCTTGGGGAAGGAAGAAGTGAGAGAGCTCTCTATCACCTGGCAGGAGTTTAG
	Site 4	Forward: CTAAACTCCTGCCAGGTGATAGAGAGCTCTCTCACTTCTTCCTTCCCCAAGGC Reverse: GCCTTGGGGAAGGAAGAAGTGAGAGAGCTCTCTATCACCTGGCAGGAGTTTAG
ADAMTS17	Site 1	Forward: GCAATTACCGTTTCTTATGTCACAGTCGACTGAAGAGAGGCCCTTCTGTTTCCC Reverse: GGGAAACAGAAGGGCCTCTCTTCAGTCGACTGTGACATAAGAAACGGTAATTGC
	Site 2	Forward: CACCAACTTGGTGGGCATTTCATGTCGACTTATGTTCTAGGACTTTACCGTA Reverse: TACGGTAAAGTCCTAGAACATAAGTCGACATGAAATGCCCACCAAGTTGGTG
	Site 3	Forward: TAACAAAACAAAACACAGAAACACAGTCGACATAAATCAAGAAGCACAGGGAGATGATCCCATGG Reverse: CCATGGGATCATCTCCCTGTGCTTCTTGATTTATGTCGACTGTGTTTCTGTGTTTTGTTTTGTTA
	Site 4	Forward: GAAGTGTTGAGAAACTTCCGTGTCGACTCTGTGGAAAGAACCGAGGGT Reverse: ACCCTCGGTTCTTTCCACAGAGTCGACACGGAAGTTTCTCAACACTTC
	Site 5	Forward: CCAGAGTCTCACGACCCTACGGTCGCCTTTTTATTGGTGCAAAATTAAACC Reverse: GGTTTAATTTTGCACCAATAAAAAGGCGACCGTAGGGTCGTGAGACTCTGG
ADAMTS	Site 1	Forward: ATCAAATTAATTTATTTTTTTGCCTGCCAAACATCCAATGGTCGACTTGTTTTGGTTACACAAACATTTTGATTTATACTATATG

19		Reverse: CATATAGTATAAATCAAAATGTTTGTGTAACCAAAACAAGTCGACCATTGGATGTTTGGCAGGCAAAAAAATAAATTAATTTGAT
	Site 2	Forward: GTTGTTTGTTAGGGCTATCTCTAAGTCGACCCTCTCTCCCCACCAATAACATTGAATTATC Reverse: ATAATTCAATGTTATTGGTGGGGAGAGAGGGTCGACTTAGAGATAGCCCTAACAAACAACG
FZD3		Forward: GGATTTAGTCTAACTCACAGCTAAGGTAGAAAAGTACTCTGATGGCAAGAGAATGTCCAGACTAATATTTTC Reverse: GAAAATATTAGTCTGGACATTCTCTTGCCATCAGAGTACTTTTCTACCTTAGCTGTGAGTTAGACTAAATCC
FZD5	Site 1	Forward: CGGCGTCGCGGCCCAAGCTTGGGAGGCGGTCGCAG Reverse: CTGCGACCGCCTCCCAAGCTTGGGCCGCGACGCCG
	Site 2	Forward: GTGGACGTGGAGATGAAGCACAAGCTTGACCACAGGCCTATCCAGAAGG Reverse: CCTTCTGGATAGGCCTGTGGTCAAGCTTGTGCTTCATCTCCACGTCCAC
	Site 3	Forward: GCCCACCAGCAGGTAGAAGCTTAGCGGGCCCAGCACGAAGCC Reverse: GGCTTCGTGCTGGGCCCGCTAAGCTTCTACCTGCTGGTGGGC
	Site 4	Forward: CACATGAAGTACTTGAGCATGAAGCTTCAGTACTCGGGCTTGGCGCGCG Reverse: CGCGCGCCAAGCCCGAGTACTGAAGCTTCATGCTCAAGTACTTCATGTG
	Site 5	Forward: CGGGAGGGGGCAACAAGCTTATGAAGGTAAACGGAAGTGACCTTGGCA Reverse: TGCCAAGGTCACTTCCGTTTACCTTCATAAGCTTGTTGCCCCCTCCCG
FRAT2	Site 1	Forward: GCGTGGAGAAATGTATGCGCCAGAAGCTTTCCGTGGGGCATGAG

		AATTTCC Reverse: GGAAATTCTCATGCCCCACGGAAAGCTTCTGGCGCATACATTTCTCCACGC
	Site 2	Forward: CTTATTTTCTGGTGGAGGAGCTTAGTAAGTAAGCTTACAATTGCTGTGCAAAGAAATTCCAGAGG-3' Reverse: CCTCTGGAATTTCTTTGCACAGCAATTGTAAGCTTACTTACTAAGCTCCTCCACCAGAAAATAAG
	Site 3	Forward: GGGAGACTCCAAGCGGTGGTAAAAGCTTAACAGGGCTCTTCTTGGAGCAAG Reverse: CTTGCTCCAAGAAGAGCCCTGTTAAGCTTTTACCACCGCTTGGAGTCTCCC
CK2A2	Site 1	Forward: AGAGGAATATACAAGGGGCTTGGGGAAGAAAATAAGCTTCCCGGAGCAAGTGTTG Reverse: CAACACTTGCTCCGGGAAGCTTATTTTCTTCCCCAAGCCCCTTGTATATTCCTCT
	Site 2	Forward: TCTCCTCTAATCTATCAGTCTGAGAAGCTTTTCCTCTCTGCAAGGGAACACATTTGC Reverse: GCAAATGTGTTCCCTTGCAGAGAGGAAAAGCTTCTCAGACTGATAGATTAGAGGAGA
	Site 3	Forward: GCGCCTGACTCGAGAAGCTTACCTTTCAGTCCACTGGGACCAATCCA Reverse: TGGATTGGTCCCAGTGGACTGAAAGGTAAGCTTCTCGAGTCAGGCGC
	Site 4	Forward: CTGCTTCCATCCTTATCAACAGAAGCTTTGGGAGAACCTAAGTCATTTCCCTGAG Reverse: TCAGGGAAATGACTTAGGTTCTCCCAAAGCTTCTGTTGATAAGGATGGAAGCAG
DVL3	Site 1	Forward: GTGCGCTAACTGCTCGCAGAAGCTTGCGAGGGTGGGGTGCACC

		Reverse: GGTGCACCCCACCCTCGCAAGCTTCTGCGAGCAGTTAGCGCAC
	Site 2	Forward: CCCTTTTGTCTCTGGGACCAGACTTGTTAAGCTTACCCCTTACTCCCCTCTGC Reverse: GCAGAGGGGAGTAAGGGGTAAGCTTAACAAGTCTGGTCCCAGAGACAAAAGGG
	Site 3	Forward: GCACAGTGCCTGGCACACAGTAGAGTAAAGCTTCAATAAATGGTAGTCGACC Reverse: GGTCGACTACCATTTATTGAAGCTTTACTCTACTGTGTGCCAGGCACTGTGC
DICER		Forward: ACGTGAGCTCGTGTGCAGTAGTGCCAGTCC Reverse: ACGTGAGCTCTGCAATCACAGGAACACAGG

Table 2: Primers for mutating the binding sites of the miR-29 family

Genes	Accession number	Primer sequence (5'->3')	Probe
Arginase-1	ENSMUST00000020161	Forward: CCTGAAGGAACTGAAAGGAAAG Reverse: TTGGCAGATATGCAGGGAGT	2
IL-6	ENSMUST00000026845	Forward: TGATGGATGCTACCAAACTGG Reverse: TTCATGTACTCCAGGTAGCTATGG	6
SAA3	ENAMUST00000006956	Forward: GCTCGGGGGAACTATGATG Reverse: AACTTCTGAACAGCCTCTCTGG	26
Axin2		Forward: GCTGACGGATGATTCCATGT Reverse: ACTGCCCACACGATAAGGAG	56
SOX9	ENST00000245479	Forward: TACCCGCACTTGCACAAC Reverse: TCTCGCTCTCGTTCAGAAGTC	61
FZD3	NM_017412	Forward: ACAGCAAAGTGAGCAGCTACC Reverse: CTGTAACTGCAGGGCGTGTA	75
FZD5	NM_003468	Forward:ACCCCAGGGGAGAGAAACT Reverse: TGCAAATTGGGGGAAGTAAG	83
DVL3	NM_004423	Forward:CCCTGAGCACCATCACCT Reverse: GGATGGACAAGTGGAAGTCG	17
FRAT2		Forward: GTTCAAGGTCACGGTTTGCT Reverse: GAAAAGACTCCGGGGTGAGT	14
CK2A2	NM_001896	Forward: CCATGGAGCACCCATACTTC Reverse: CACAGCATTGTCTGCACAAG	68

Table 3: Primer sequence and the Universal Probe Library probe for gene of interest

Genes	Accession number	Primer sequence (5'-3')
ADAMTS4	MM_005099	Forward: CAAGGTCCCATGTGCAACGT Reverse: CATCTGCCACCACCAGTGTCT Probe: FAM-CCGAAGAGCCAAGCGCTTTGCTTC-TAMRA
ADAMTS6	NM_014273	Forward: GGCTGAATGACACATCCACTGTT Reverse: CAAACCGTTCAATGCTCACTGA Probe: FAM-AAGCGCTTCCGCCTCTGCAACC-TAMRA
ADAMTS10	NM_030957	Forward: AGAGAACGGTGTGGCTAACCA Reverse: TCTCTCGCGCTCACACATTC Probe: FAM-CAGTGCTCATCACACGCTATGACATCTGC-TAMRA
ADAMTS14	AF366351	Forward: CGCTGGATGGGACTGAGTGT Reverse: CGCGAACATGACCCAAACTT Probe: FAM-CCCGGCAAGTGGTGCTTCAAAGGT-TAMRA
ADAMTS17	NM_139057	Forward: GGTCTCAATTTGGCCTTTACCAT Reverse: GACCTGCCAGCGGCAAGAT Probe: FAM-CCACAACTTGGGCATGAACCACGA-TAMRA
ADAMTS19	AJ311904	Forward: GGTGTAAGGCTGGAGAATGTACCA Reverse: TGCGCTCTCGACTGCTGAT Probe: FAM-CCTCAGCACCTGAACATCTGGCCG-TAMRA
MMP3	NM002422	Forward: TTCCGCCTGTCTCAAGATGATAT Reverse: AAAGGACAAAGCAGGATCACAGTT Probe: FAM-TCAGTCCCTCTATGGACCTCCCCCTGAC-TAMRA

Table 4: Primer pairs and probe for gene of interest

Genes	Primer sequences (5'->3')
Pri-miR-29a/b1exon 1	Forward: TACTGAACTGTCACGGCAGA Reverse: TGTAGTTAGCGACCTCTGCT
Pri-miR-29a/b1Exon4	Forward: TTGCACCCTCACGACATGCT Reverse: TGACTCTCAGCAGGCCTCA
Pri-miR-29b2/c exon 1	Forward: ACTTCTTTAGGGGTGTGCGTA Reverse: ACCCATCTCCCTAGCATTCT
Pri-miR-29b2/c Exon6	Forward: TCAGACTTGCCACCTGGACT Reverse: AGTTGGCATGAGGCTTCGA
Pre-29a	Forward: CTGATTTCTTTTGGTGTTCAG Reverse: AACCGATTTCAGATGGTGC
Pre-29b1	Forward: CATATGGTGGTTTAGATTT Reverse: AACACTGATTTCAAATGGTG
Pre-29b2	Forward: GCTGGTTTCACATGGTGGC Reverse: AACACTGATTTCAAATGGTG
Pre-29c	Forward: CGATTTCTCCTGGTGTTCA Reverse: ACCGATTTCAAATGGTGC

Table 5: Primers for detecting the primary and the premature sequence of the miR-29 family

Names	24_DMM_R	24_DMM_L	log2 Fold change	Fold change
CYP2E1	9.0	10.2	-1.2	2.3
CES3	8.1	9.3	-1.2	2.3
TMEM45B	7.9	8.6	-0.8	1.7
CFD	12.9	13.6	-0.7	1.6
SCD1	10.1	10.7	-0.6	1.6
IGFBP6	8.9	9.6	-0.6	1.5
CHAD	12.4	13.0	-0.6	1.5
LOC100045005	9.6	10.2	-0.6	1.5
TENS1	8.5	9.1	-0.6	1.5
C130045I22RIK	8.2	8.8	-0.6	1.5
LOC667337	9.4	9.9	-0.6	1.5
CXCL1	9.1	7.3	1.9	3.6
CCL7	9.2	7.5	1.8	3.4
SAA3	8.9	7.3	1.6	3.1
TIMP1	12.0	10.5	1.5	2.9
SERPINA3N	11.2	9.7	1.5	2.8
GP38	10.8	9.4	1.4	2.6
MMP3	8.9	7.6	1.3	2.5
ARG1	8.0	7.1	0.8	1.8
CXCL14	9.4	8.8	0.7	1.6
MB	11.9	11.2	0.7	1.6
ANGPTL4	9.5	8.9	0.6	1.6
MT1	13.5	12.9	0.6	1.6
ANKRD23	9.5	8.9	0.6	1.5
MS4A6D	9.9	9.3	0.6	1.5
LOC386330	9.9	9.4	0.5	1.5
LOC270589	8.9	8.4	0.5	1.5
CCL9	11.2	10.6	0.5	1.5
CKM	12.3	11.8	0.5	1.5
LOC386144	9.6	9.1	0.5	1.4

Table 6: List genes changed expression at day 1 in DMM model

GENES	7_DMM_R	7_DMM_L	log2 Fold change	Fold change
MYL3	9.8	11.0	-1.2	2.3
ATP1A2	9.0	10.1	-1.2	2.3
NDRG2	10.0	11.2	-1.2	2.3
CKMT2	11.7	12.8	-1.2	2.2
ANKRD23	10.2	11.4	-1.2	2.2
2310003M01RIK	9.5	10.6	-1.1	2.2
ACTN2	11.1	12.2	-1.1	2.2
2310042D19RIK	9.2	10.3	-1.1	2.2
MYH2	11.0	12.1	-1.1	2.2
PFKM	11.5	12.6	-1.1	2.2
ABRA	8.6	9.7	-1.1	2.1
COX7A1	11.4	12.5	-1.1	2.1
ANKRD2	8.0	9.1	-1.1	2.1
COX8B	11.8	12.8	-1.1	2.1
MB	12.0	13.1	-1.1	2.1
ENO3	12.9	14.0	-1.1	2.1
DUSP26	8.1	9.2	-1.1	2.1
RTN2	10.0	11.1	-1.0	2.1
PKIA	10.4	11.5	-1.0	2.1
TCAP	12.5	13.6	-1.0	2.1
MYOZ1	10.4	11.5	-1.0	2.0
MYOM1	9.9	10.9	-1.0	2.0
ACTN3	11.3	12.3	-1.0	2.0
2310002L09RIK	8.6	9.6	-1.0	2.0
HRC	10.3	11.3	-1.0	2.0
MYOM2	9.1	10.1	-1.0	2.0
CKM	13.0	14.0	-1.0	2.0
CSRP3	8.5	9.5	-1.0	2.0
TMEM38A	9.3	10.3	-1.0	2.0
1110012N22RIK	9.2	10.2	-1.0	2.0
TPM2	11.3	12.3	-1.0	2.0
RYR1	10.1	11.1	-1.0	2.0
MLF1	9.5	10.5	-1.0	2.0
TTN	9.7	10.7	-1.0	2.0
TMOD4	10.7	11.7	-1.0	2.0
DYSFIP1	8.7	9.7	-1.0	2.0
NRAP	9.1	10.1	-1.0	2.0
CMYA5	10.8	11.8	-1.0	2.0
SMTNL2	8.5	9.5	-1.0	1.9
MYLK2	9.2	10.2	-1.0	1.9

MYL2	9.3	10.3	-0.9	1.9
LOC669660	8.6	9.6	-0.9	1.9
KBTBD10	9.8	10.7	-0.9	1.9
ASB2	10.6	11.5	-0.9	1.9
A530098C11RIK	8.7	9.6	-0.9	1.9
F730003H07RIK	9.3	10.3	-0.9	1.9
ZMYND17	8.5	9.4	-0.9	1.9
CPT1B	8.3	9.2	-0.9	1.9
2310079P10RIK	8.5	9.4	-0.9	1.9
EEF1A2	10.7	11.6	-0.9	1.9
YIPF7	8.5	9.4	-0.9	1.9
SCL0003151.1_1374	8.9	9.8	-0.9	1.9
INMT	7.6	8.5	-0.9	1.9
CES3	8.8	9.7	-0.9	1.9
PYGM	9.2	10.1	-0.9	1.8
MYBPC2	11.6	12.5	-0.9	1.8
8030451F13RIK	8.6	9.5	-0.9	1.8
FABP3	10.6	11.4	-0.9	1.8
NEURL	9.5	10.4	-0.9	1.8
PDLIM3	10.4	11.3	-0.9	1.8
SYPL2	9.6	10.5	-0.9	1.8
4833419K08RIK	9.0	9.9	-0.9	1.8
AMPD1	11.1	12.0	-0.8	1.8
CACNA1S	8.6	9.5	-0.8	1.8
SCL0002069.1_48	8.1	9.0	-0.8	1.8
C130073O12RIK	9.0	9.9	-0.8	1.8
GM1157	7.8	8.6	-0.8	1.8
MYH1	9.2	10.1	-0.8	1.8
SLC25A37	11.8	12.6	-0.8	1.8
LOC638935	8.1	9.0	-0.8	1.8
LOC386360	10.4	11.2	-0.8	1.8
BC030476	9.0	9.8	-0.8	1.8
MYH4	10.0	10.8	-0.8	1.7
SCL000959.1_2	13.3	14.1	-0.8	1.7
RPL3L	12.2	13.0	-0.8	1.7
COX6A2	12.7	13.5	-0.8	1.7
MTDNA_ND4L	8.7	9.5	-0.8	1.7
TNNT3	13.1	13.9	-0.8	1.7
AK1	9.8	10.6	-0.8	1.7
DES	11.1	11.9	-0.8	1.7
A2BP1	8.4	9.2	-0.8	1.7
KY	9.1	9.8	-0.8	1.7

UNC45B	8.4	9.2	-0.8	1.7
AI595366	8.7	9.4	-0.8	1.7
D830037I21RIK	7.3	8.1	-0.8	1.7
PGM2	12.0	12.8	-0.8	1.7
4933421G18RIK	9.7	10.4	-0.8	1.7
MYF6	8.3	9.0	-0.8	1.7
SCN4B	8.3	9.1	-0.8	1.7
ALPK3	8.5	9.3	-0.8	1.7
PGAM2	12.3	13.1	-0.8	1.7
ITGA2B	8.9	9.7	-0.8	1.7
CRYAB	9.8	10.6	-0.7	1.7
LOC386144	9.1	9.8	-0.7	1.7
LOC100047934	10.8	11.6	-0.7	1.7
SRL	9.3	10.0	-0.7	1.7
PHKG1	8.8	9.5	-0.7	1.7
ATP1B1	9.5	10.2	-0.7	1.7
HSPB7	8.2	8.9	-0.7	1.7
TNNC1	8.3	9.0	-0.7	1.6
CHCHD10	12.4	13.1	-0.7	1.6
GMPR	9.0	9.7	-0.7	1.6
S3-12	9.3	10.0	-0.7	1.6
9930004G02RIK	9.4	10.1	-0.7	1.6
TCEA3	10.3	11.0	-0.7	1.6
PPP1R3C	10.7	11.4	-0.7	1.6
TRIM54	9.0	9.7	-0.7	1.6
FBP2	8.3	9.0	-0.7	1.6
COQ10A	8.8	9.5	-0.7	1.6
TXLNB	7.8	8.5	-0.7	1.6
XIRP2	8.4	9.1	-0.7	1.6
FSD2	8.6	9.3	-0.7	1.6
PDE4DIP	9.9	10.6	-0.7	1.6
NDUFC1	10.9	11.6	-0.7	1.6
MSCP	11.9	12.6	-0.7	1.6
EG433229	9.2	9.9	-0.7	1.6
SMARCD3	8.2	8.9	-0.7	1.6
SCL0003073.1_164	8.2	8.8	-0.7	1.6
HHATL	8.6	9.3	-0.7	1.6
DNAJC7	8.9	9.6	-0.7	1.6
USP13	7.9	8.6	-0.7	1.6
ADSSL1	11.5	12.2	-0.7	1.6
ACADM	11.2	11.9	-0.7	1.6
MT-ATP6	11.3	12.0	-0.7	1.6
6430573H23RIK	8.2	8.9	-0.7	1.6
TUBA8	8.6	9.3	-0.7	1.6

DEDD2	9.8	10.4	-0.7	1.6
LOC100041835	12.3	12.9	-0.7	1.6
1300013J15RIK	7.9	8.6	-0.7	1.6
MACROD1	9.1	9.8	-0.7	1.6
ALDOA	13.2	13.9	-0.7	1.6
LOC667034	8.5	9.2	-0.7	1.6
MDH2	10.0	10.6	-0.7	1.6
PDK4	9.3	10.0	-0.7	1.6
ART5	7.7	8.4	-0.7	1.6
JSRP1	7.9	8.6	-0.7	1.6
PPM1L	8.4	9.0	-0.7	1.6
MFN2	10.1	10.8	-0.7	1.6
RILPL1	8.8	9.4	-0.6	1.6
EHBP1L1	8.8	9.4	-0.6	1.6
NDUFA5	10.3	10.9	-0.6	1.6
MTDNA_ND2	11.5	12.2	-0.6	1.6
MTDNA_ND5	11.5	12.2	-0.6	1.6
TRIM72	9.7	10.4	-0.6	1.6
B930008G03RIK	10.0	10.7	-0.6	1.6
2310040G24RIK	7.9	8.5	-0.6	1.6
ALAD	12.0	12.7	-0.6	1.6
SGCA	8.4	9.0	-0.6	1.5
LOC385959	8.3	8.9	-0.6	1.5
LOC547380	8.3	8.9	-0.6	1.5
NDUFS7	11.8	12.4	-0.6	1.5
1300017J02RIK	8.9	9.5	-0.6	1.5
LOC381792	7.7	8.3	-0.6	1.5
FLNC	8.5	9.1	-0.6	1.5
DHRS7C	8.1	8.7	-0.6	1.5
ART1	8.0	8.6	-0.6	1.5
EG245190	8.8	9.5	-0.6	1.5
A530020A01RIK	7.9	8.5	-0.6	1.5
PRKAA2	7.8	8.4	-0.6	1.5
VLDLR	8.7	9.3	-0.6	1.5
1110002E22RIK	8.1	8.7	-0.6	1.5
NDUFB9	7.8	8.4	-0.6	1.5
MYO18B	8.1	8.7	-0.6	1.5
ITGB1BP3	8.3	8.9	-0.6	1.5
PHLDA3	9.4	10.0	-0.6	1.5
GPT2	8.5	9.1	-0.6	1.5
LOC386256	7.9	8.5	-0.6	1.5
TSC22D3	9.4	10.0	-0.6	1.5
NDUFA4	12.4	13.0	-0.6	1.5

4CYTL1	9.4	10.0	-0.6	1.5
PTP4A3	9.0	9.6	-0.6	1.5
FBXO32	7.9	8.5	-0.6	1.5
CNKSR1	7.7	8.3	-0.6	1.5
ZXDA	9.0	9.6	-0.6	1.5
LOC100044934	8.4	9.0	-0.6	1.5
KBTBD5	7.8	8.4	-0.6	1.5
SRR	11.0	11.6	-0.6	1.5
CACNG1	8.1	8.7	-0.6	1.5
SCL0002124.1_39	7.7	8.3	-0.6	1.5
DEB1	11.0	11.6	-0.6	1.5
LMOD3	7.9	8.5	-0.6	1.5
9830134C10RIK	8.2	8.8	-0.6	1.5
TYKI	9.3	9.9	-0.6	1.5
UFSP1	8.6	9.2	-0.6	1.5
SMPX	7.7	8.2	-0.6	1.5
LOC100047214	9.1	9.7	-0.6	1.5
VGLL2	7.6	8.2	-0.6	1.5
CAR3	10.3	10.9	-0.6	1.5
SLC25A12	9.1	9.7	-0.6	1.5
EG622339	13.4	14.0	-0.6	1.5
CIB2	9.4	9.9	-0.6	1.5
A630006E02RIK	9.5	10.1	-0.6	1.5
UGP2	9.4	10.0	-0.6	1.5
4933428A15RIK	8.6	9.2	-0.6	1.5
CHKA	9.4	10.0	-0.6	1.5
SNTA1	8.5	9.0	-0.6	1.5
SLC6A9	9.3	9.9	-0.6	1.5
2410076I21RIK	8.4	8.9	-0.6	1.5
TPI1	12.1	12.6	-0.6	1.5
SMTNL1	7.9	8.4	-0.6	1.5
TMOD1	8.7	9.3	-0.6	1.5
TSPAN8	8.5	9.1	-0.6	1.5
MTDNA_COXII	12.8	13.4	-0.6	1.5
NDUFS2	8.7	9.3	-0.6	1.5
SLC2A4	8.1	8.7	-0.6	1.5
MYOT	7.8	8.4	-0.6	1.5
A230005G17RIK	8.3	8.9	-0.6	1.5
TNNT1	8.9	9.4	-0.6	1.5
FHL1	11.6	12.1	-0.6	1.5
SPNB1	9.5	10.0	-0.6	1.5
5830496L11RIK	9.1	9.6	-0.6	1.5
ENSMUSG00000054212	9.5	10.1	-0.6	1.5

5430434G16RIK	8.9	9.4	-0.6	1.5
IDH3A	8.9	9.4	-0.6	1.5
SLC38A5	11.1	11.7	-0.6	1.5
LDB3	8.1	8.6	-0.6	1.5
E430039I23RIK	11.1	11.6	-0.6	1.5
KEL	10.5	11.0	-0.6	1.5
2310039E09RIK	8.2	8.7	-0.6	1.5
D530007E13RIK	8.9	9.4	-0.6	1.5
1110018J23RIK	7.9	8.5	-0.6	1.5
TMEM45B	8.2	8.7	-0.6	1.5
BC022224	10.2	10.7	-0.6	1.5
RBM38	9.9	10.5	-0.6	1.5
2810484G07RIK	10.9	11.5	-0.5	1.5
ACO2	10.8	11.4	-0.5	1.5
1700021F05RIK	10.3	10.8	-0.5	1.5
VEGFB	9.8	10.4	-0.5	1.5
STXBP3	8.2	8.7	-0.5	1.5
AGL	9.3	9.8	-0.5	1.5
TAL1	9.3	9.8	-0.5	1.5
MYOZ2	7.7	8.2	-0.5	1.5
NCTC1	7.8	8.3	-0.5	1.5
ABCA7	9.4	10.0	-0.5	1.5
SAR1B	10.3	10.9	-0.5	1.5
3632431M01RIK	8.6	9.1	-0.5	1.5
FCHO1	10.0	10.5	-0.5	1.5
P2RY1	8.8	9.3	-0.5	1.5
B230387C07RIK	9.1	9.7	-0.5	1.5
TRIM63	7.5	8.0	-0.5	1.5
1810020D17RIK	9.5	10.0	-0.5	1.4
FYCO1	8.1	8.6	-0.5	1.4
RABGEF1	10.3	10.8	-0.5	1.4
ITGB1BP2	8.2	8.8	-0.5	1.4
IFT140	9.1	9.6	-0.5	1.4
SAMD11	8.2	8.7	-0.5	1.4
ABCB10	8.2	8.8	-0.5	1.4
LOC100046690	9.0	9.5	-0.5	1.4
PFN2	8.9	9.5	-0.5	1.4
C1QTNF3	11.0	7.5	3.5	11.3
LRRC15	10.6	8.4	2.2	4.7
ANGPTL1	9.7	7.6	2.1	4.4
MFAP5	10.2	8.1	2.1	4.4
THBS2	11.8	9.7	2.1	4.3
FSTL1	11.1	9.0	2.0	4.1

COL6A2	10.4	8.4	2.0	4.1
MMP2	13.7	11.7	2.0	3.9
COL6A1	12.4	10.4	2.0	3.9
CAPN6	9.7	7.7	2.0	3.9
COL3A1	9.8	7.9	1.9	3.8
MMP3	9.3	7.4	1.9	3.8
TIMP1	11.8	9.9	1.9	3.8
COL5A1	12.6	10.7	1.9	3.7
CTHRC1	9.5	7.6	1.9	3.7
AEBP1	10.9	9.1	1.9	3.6
COL18A1	9.8	8.0	1.8	3.5
DKK3	10.2	8.5	1.7	3.4
COL14A1	9.3	7.6	1.7	3.3
E430002G05RIK	9.9	8.1	1.7	3.3
PCOLCE	10.9	9.2	1.7	3.3
LUM	12.2	10.5	1.7	3.3
DPT	10.3	8.6	1.7	3.2
MMP14	11.9	10.2	1.7	3.2
GP38	11.0	9.3	1.7	3.2
FCRLS	9.9	8.2	1.6	3.1
MFAP4	9.2	7.6	1.6	3.1
CSRP2	11.0	9.4	1.6	3.1
LOX	11.4	9.8	1.6	3.1
SPON2	11.2	9.6	1.6	3.0
ITM2A	9.8	8.2	1.6	3.0
LY6A	12.8	11.3	1.6	3.0
DDAH1	9.3	7.7	1.6	3.0
MUP2	9.7	8.2	1.6	3.0
GPNMB	9.5	8.0	1.6	3.0
CD248	9.9	8.3	1.5	2.9
ANTXR1	9.9	8.3	1.5	2.9
6330406I15RIK	9.7	8.1	1.5	2.9
LOXL1	10.8	9.2	1.5	2.9
MUP1	9.2	7.7	1.5	2.9
NBL1	10.3	8.8	1.5	2.9
MFAP2	9.2	7.7	1.5	2.8
CCL21A	10.6	9.1	1.5	2.8
FN1	10.4	8.9	1.5	2.8
MEST	8.8	7.3	1.5	2.8
MRGPRF	9.5	8.0	1.5	2.8
CCL21C	10.0	8.5	1.5	2.8
SAA3	8.7	7.2	1.5	2.8
LOC100048554	9.2	7.7	1.5	2.8
THY1	10.0	8.5	1.5	2.7

HTRA1	10.5	9.1	1.5	2.7
OSR2	9.3	7.8	1.5	2.7
LOC100041504	9.9	8.4	1.4	2.7
GPX7	9.8	8.4	1.4	2.7
KDELR3	10.4	8.9	1.4	2.7
H19	11.4	10.0	1.4	2.7
PDLIM4	10.3	8.9	1.4	2.6
C1QTNF2	9.3	7.9	1.4	2.6
COL6A3	11.3	9.9	1.4	2.6
FBLN2	9.4	8.0	1.4	2.6
MXRA8	10.5	9.1	1.4	2.6
SCL0001849.1_2273	9.0	7.6	1.4	2.6
VKORC1	11.1	9.7	1.3	2.5
PPIC	12.3	11.0	1.3	2.5
ITGBL1	9.6	8.3	1.3	2.5
EMP1	12.7	11.4	1.3	2.5
KNSL5	11.8	10.5	1.3	2.5
SERPINH1	12.8	11.5	1.3	2.5
2310016C16RIK	10.3	9.0	1.3	2.5
WISP2	10.4	9.1	1.3	2.5
MAGED1	11.6	10.3	1.3	2.5
COL16A1	11.6	10.3	1.3	2.5
LEPREL2	9.2	7.9	1.3	2.4
GPX8	10.7	9.4	1.3	2.4
BGN	14.3	13.0	1.3	2.4
SRPX2	10.2	8.9	1.3	2.4
ITGA11	9.9	8.6	1.3	2.4
CCDC80	11.0	9.7	1.3	2.4
CLEC11A	10.4	9.2	1.3	2.4
SMOC1	9.7	8.5	1.2	2.4
OGN	10.3	9.0	1.2	2.4
CRTAP	10.1	8.9	1.2	2.4
VIM	11.1	9.8	1.2	2.3
COL4A2	11.3	10.0	1.2	2.3
FKBP11	10.0	8.7	1.2	2.3
CD276	9.3	8.1	1.2	2.3
PRKCDBP	10.1	8.9	1.2	2.3
CCL7	8.4	7.2	1.2	2.3
NFATC4	9.4	8.1	1.2	2.3
ECM1	10.8	9.6	1.2	2.3
COL15A1	9.4	8.2	1.2	2.3
2610027C15RIK	10.0	8.8	1.2	2.3

PRELP	13.1	11.9	1.2	2.3
TIMP2	12.6	11.4	1.2	2.3
GRB10	9.4	8.2	1.2	2.3
FBN1	9.6	8.4	1.2	2.3
COPZ2	10.0	8.8	1.2	2.3
SCARF2	12.0	10.8	1.2	2.3
ENPP1	9.6	8.4	1.2	2.3
COL4A1	11.7	10.5	1.2	2.3
IGF1	9.6	8.4	1.2	2.2
SULF2	9.2	8.0	1.2	2.2
SERPINA3N	10.2	9.0	1.2	2.2
FKBP9	11.1	9.9	1.2	2.2
RNASE4	9.8	8.6	1.2	2.2
COMP	12.8	11.6	1.2	2.2
MS4A6D	9.8	8.6	1.2	2.2
CPXM1	9.3	8.2	1.1	2.2
DAB2	9.7	8.5	1.1	2.2
EFEMP2	10.0	8.9	1.1	2.2
LOC100047053	8.4	7.3	1.1	2.2
COL8A1	9.5	8.4	1.1	2.2
SERPING1	11.9	10.7	1.1	2.2
ANGPTL4	10.2	9.1	1.1	2.2
THBS3	8.7	7.6	1.1	2.1
HSPG2	10.5	9.4	1.1	2.1
PTN	8.9	7.8	1.1	2.1
GM22	9.3	8.2	1.1	2.1
NNMT	9.6	8.6	1.1	2.1
LGMN	10.9	9.8	1.1	2.1
4930533K18RIK	9.8	8.7	1.1	2.1
VASN	10.9	9.8	1.1	2.1
ELN	8.5	7.5	1.1	2.1
FMOD	10.2	9.1	1.1	2.1
LOC100046883	10.8	9.8	1.1	2.1
CLEC4N	8.6	7.6	1.1	2.1
NDN	10.0	8.9	1.1	2.1
ACAN	9.7	8.6	1.1	2.1
OLFML1	8.8	7.8	1.1	2.1
C1QTNF1	8.7	7.6	1.1	2.1
SOCS3	9.3	8.3	1.0	2.1
1500015O10RIK	11.9	10.8	1.0	2.0
FKBP10	9.7	8.7	1.0	2.0
TREM2	9.4	8.4	1.0	2.0
MGP	13.5	12.5	1.0	2.0
COL10A1	10.7	9.6	1.0	2.0

ADAMTS12	8.7	7.7	1.0	2.0
CRLF1	8.5	7.5	1.0	2.0
HTRA3	9.6	8.6	1.0	2.0
P4HA2	9.0	8.0	1.0	2.0
FSCN1	9.0	8.1	1.0	2.0
NUPR1	12.0	11.0	1.0	2.0
SCARA3	11.9	10.9	1.0	2.0
SYNPO	10.1	9.1	1.0	2.0
NID2	8.8	7.8	1.0	2.0
TSPAN6	8.9	7.9	1.0	2.0
LGALS1	12.5	11.5	1.0	2.0
IGFBP7	10.5	9.5	1.0	2.0
TMEM119	9.7	8.7	1.0	2.0
COL2A1	13.6	12.6	1.0	2.0
MS4A7	8.8	7.8	1.0	2.0
ANXA5	12.4	11.4	1.0	2.0
RAMP2	10.0	9.1	1.0	2.0
MMP23	9.5	8.5	1.0	1.9
SLC1A4	8.5	7.6	1.0	1.9
LOC100047856	9.1	8.2	1.0	1.9
AHNAK2	9.1	8.2	1.0	1.9
CDKN1C	11.0	10.0	1.0	1.9
APOE	11.0	10.0	1.0	1.9
SPARC	13.1	12.1	1.0	1.9
BC020108	8.5	7.5	0.9	1.9
C1QB	11.5	10.5	0.9	1.9
FNDC3B	10.2	9.3	0.9	1.9
IGSF10	8.8	7.9	0.9	1.9
COL12A1	9.1	8.2	0.9	1.9
9030024J15RIK	9.7	8.7	0.9	1.9
1110036O03RIK	8.9	8.0	0.9	1.9
LRIG3	9.4	8.5	0.9	1.9
FAM129B	10.2	9.3	0.9	1.9
EDNRA	9.5	8.5	0.9	1.9
IL33	8.3	7.4	0.9	1.9
IGFBP6	10.0	9.0	0.9	1.9
LGALS3BP	10.8	9.9	0.9	1.9
OLFML3	11.5	10.6	0.9	1.9
COL1A2	11.1	10.2	0.9	1.9
GPR176	8.4	7.5	0.9	1.9
CERCAM	9.9	9.0	0.9	1.9
CNRIP1	9.7	8.8	0.9	1.9
GALNTL1	8.5	7.7	0.9	1.9

KERA	8.2	7.3	0.9	1.9
PRG4	12.7	11.8	0.9	1.9
IGKV3-2_X16954_IG_KAPPA_VARIABLE_3-2_18	9.0	8.1	0.9	1.9
LOC676136	9.5	8.6	0.9	1.9
ABI3BP	8.6	7.7	0.9	1.9
PKD2	8.9	8.0	0.9	1.8
COL1A1	13.2	12.3	0.9	1.8
SCX	8.6	7.7	0.9	1.8
IGF2	10.3	9.4	0.9	1.8
SFRP1	8.3	7.4	0.9	1.8
KCTD17	9.1	8.2	0.9	1.8
IGFBP4	12.0	11.2	0.9	1.8
MFGE8	12.3	11.5	0.9	1.8
EFS	9.2	8.4	0.9	1.8
BC064033	8.4	7.6	0.9	1.8
LOC243431	9.8	9.0	0.9	1.8
MAGED2	11.1	10.2	0.9	1.8
DPYSL3	9.3	8.4	0.9	1.8
ANPEP	8.4	7.6	0.9	1.8
A430110N23RIK	8.2	7.4	0.9	1.8
CXCL1	8.1	7.2	0.8	1.8
LTBP3	9.0	8.2	0.8	1.8
LRRC17	8.3	7.4	0.8	1.8
LOC100047583	9.3	8.5	0.8	1.8
UTS2R	8.3	7.4	0.8	1.8
TNN	8.3	7.5	0.8	1.8
CALU	10.0	9.2	0.8	1.8
BMP1	9.9	9.1	0.8	1.8
SCARA5	9.7	8.9	0.8	1.8
TXNDC5	10.7	9.9	0.8	1.8
SDC2	10.4	9.6	0.8	1.8
IFITM2	12.1	11.3	0.8	1.8
PRDX4	11.0	10.1	0.8	1.8
DLK1	8.2	7.3	0.8	1.8
0610007N19RIK	9.4	8.6	0.8	1.8
TPST1	9.9	9.0	0.8	1.8
NT5DC2	9.1	8.3	0.8	1.8
SULF1	8.9	8.1	0.8	1.8
HTRA4	9.0	8.2	0.8	1.8
AKR1B8	8.3	7.4	0.8	1.8
SRPX	8.8	8.0	0.8	1.8

MARCKS	11.2	10.4	0.8	1.8
PARVA	9.6	8.8	0.8	1.7
TGFB3	8.8	8.0	0.8	1.7
LOC232060	8.7	7.9	0.8	1.7
WISP1	9.5	8.7	0.8	1.7
LXN	10.0	9.2	0.8	1.7
D14ERTD449E	9.2	8.5	0.8	1.7
MDK	8.6	7.8	0.8	1.7
TGFBI	11.3	10.5	0.8	1.7
SH3PXD2B	9.4	8.6	0.8	1.7
EMP2	9.0	8.2	0.8	1.7
IGHG	9.7	9.0	0.8	1.7
RIN2	9.1	8.3	0.8	1.7
1700023M03RIK	9.9	9.2	0.8	1.7
WBP5	10.9	10.1	0.8	1.7
CD68	10.3	9.5	0.8	1.7
1200009O22RIK	8.6	7.8	0.8	1.7
IL1RL1	8.1	7.3	0.8	1.7
ADAMTS2	11.0	10.2	0.8	1.7
A730054J21RIK	8.3	7.5	0.8	1.7
4732462B05RIK	10.0	9.3	0.8	1.7
LBP	9.9	9.1	0.8	1.7
IL13RA1	8.7	7.9	0.8	1.7
FER1L3	8.4	7.6	0.8	1.7
C4A	10.0	9.2	0.8	1.7
SOX9	9.8	9.0	0.8	1.7
1810055G02RIK	10.2	9.4	0.8	1.7
PANX3	10.7	10.0	0.8	1.7
FKBP14	8.5	7.7	0.8	1.7
SERPINF1	12.8	12.1	0.8	1.7
TUBB6	9.9	9.2	0.8	1.7
C1QC	10.8	10.0	0.8	1.7
OLFML2B	11.5	10.7	0.8	1.7
TCEAL8	9.9	9.2	0.8	1.7
PDGFRA	9.4	8.6	0.8	1.7
NOX4	8.3	7.5	0.8	1.7
SFRP2	8.1	7.3	0.7	1.7
6720469N11RIK	10.1	9.3	0.7	1.7
LOC380799	8.7	8.0	0.7	1.7
CSTB	12.6	11.8	0.7	1.7
CYB561	8.7	8.0	0.7	1.7
LHFPL2	9.7	9.0	0.7	1.7
LOC98434	10.3	9.5	0.7	1.7

CD14	8.5	7.7	0.7	1.7
PMP22	9.4	8.7	0.7	1.7
RBP1	8.6	7.8	0.7	1.7
2310008M10RIK	11.4	10.6	0.7	1.7
MT1	13.4	12.7	0.7	1.7
EXT1	9.9	9.2	0.7	1.7
LIMA1	9.0	8.3	0.7	1.7
MATN4	8.3	7.5	0.7	1.7
EDG5	9.3	8.6	0.7	1.7
SPSB1	8.7	8.0	0.7	1.7
ARMCX2	9.4	8.7	0.7	1.7
SVEP1	8.3	7.6	0.7	1.7
HMGN3	10.5	9.8	0.7	1.6
GPR23	8.7	8.0	0.7	1.6
FOLR2	8.6	7.8	0.7	1.6
UBE2E2	9.3	8.6	0.7	1.6
RHOJ	9.4	8.7	0.7	1.6
PROS1	9.9	9.2	0.7	1.6
STAB1	9.6	8.9	0.7	1.6
LOC637227	9.6	8.8	0.7	1.6
MYADM	10.8	10.1	0.7	1.6
ANXA8	8.4	7.7	0.7	1.6
PLOD1	8.3	7.6	0.7	1.6
MEOX2	8.9	8.2	0.7	1.6
LOC381629	10.7	10.0	0.7	1.6
LOC384413	9.4	8.7	0.7	1.6
TAX1BP3	10.5	9.8	0.7	1.6
6330404C01RIK	9.3	8.6	0.7	1.6
FRMD6	9.8	9.1	0.7	1.6
COL9A2	10.6	9.9	0.7	1.6
NT5E	9.0	8.3	0.7	1.6
MYO1E	9.0	8.3	0.7	1.6
LMAN1	9.5	8.8	0.7	1.6
GRN	12.1	11.4	0.7	1.6
LOC669053	9.3	8.6	0.7	1.6
CUL7	9.5	8.8	0.7	1.6
P4HB	13.1	12.4	0.7	1.6
TWSG1	10.1	9.4	0.7	1.6
D4BWG0951E	8.3	7.7	0.7	1.6
BICC1	9.6	8.9	0.7	1.6
WTIP	9.3	8.6	0.7	1.6
IL11RA1	11.3	10.7	0.7	1.6
LOC636944	9.9	9.3	0.7	1.6
PLVAP	10.2	9.5	0.7	1.6

EGFR	8.5	7.8	0.7	1.6
RFTN2	8.6	8.0	0.7	1.6
TMED3	9.9	9.2	0.7	1.6
TUBB2B	8.7	8.1	0.7	1.6
C130021I20	7.9	7.3	0.7	1.6
CXCL16	8.2	7.5	0.7	1.6
CDON	8.2	7.6	0.7	1.6
SDC3	11.1	10.5	0.7	1.6
5430435G22RIK	8.4	7.8	0.7	1.6
ADRA2A	8.6	7.9	0.7	1.6
C1QA	9.3	8.7	0.7	1.6
PRRC1	9.8	9.2	0.7	1.6
TPBG	8.3	7.7	0.6	1.6
BOK	8.5	7.8	0.6	1.6
NID1	8.8	8.1	0.6	1.6
FXYD6	11.3	10.7	0.6	1.6
TGFBR2	9.8	9.2	0.6	1.6
LAMC1	9.2	8.5	0.6	1.6
ZFP521	8.4	7.7	0.6	1.6
GPR125	9.4	8.8	0.6	1.6
COL5A2	8.0	7.4	0.6	1.6
PAPSS2	9.2	8.6	0.6	1.6
BDH2	9.5	8.9	0.6	1.6
MIA1	10.1	9.4	0.6	1.6
SOCS2	9.9	9.2	0.6	1.6
GLT8D1	9.4	8.8	0.6	1.6
PLOD2	8.5	7.9	0.6	1.6
FSTL	8.0	7.4	0.6	1.6
IGFBP3	8.1	7.5	0.6	1.5
2410146L05RIK	8.0	7.3	0.6	1.5
GSTM2	10.2	9.5	0.6	1.5
ISLR	8.0	7.4	0.6	1.5
PPIB	11.3	10.7	0.6	1.5
PDGFRB	8.6	7.9	0.6	1.5
DLG5	9.5	8.9	0.6	1.5
CAV1	10.4	9.8	0.6	1.5
CCL4	8.2	7.6	0.6	1.5
TMEM176B	10.1	9.4	0.6	1.5
RAB34	8.4	7.7	0.6	1.5
CDKN1A	8.7	8.1	0.6	1.5
CYB5R3	9.6	9.0	0.6	1.5
SEPN1	10.2	9.6	0.6	1.5
LOC630253	8.2	7.6	0.6	1.5

PRRX2	8.1	7.5	0.6	1.5
RHOC	8.4	7.8	0.6	1.5
PRSS35	8.8	8.2	0.6	1.5
GPRC5B	8.4	7.8	0.6	1.5
PDIA5	8.1	7.5	0.6	1.5
PMEPA1	8.2	7.6	0.6	1.5
ADAMTS4	7.9	7.3	0.6	1.5
RRBP1	9.3	8.7	0.6	1.5
FAM171B	8.4	7.8	0.6	1.5
SERTAD4	8.1	7.5	0.6	1.5
CRABP2	7.8	7.2	0.6	1.5
5430433G21RIK	9.4	8.9	0.6	1.5
RAB11FIP5	9.3	8.7	0.6	1.5
4933421H10RIK	8.7	8.1	0.6	1.5
DCN	12.3	11.7	0.6	1.5
2610009E16RIK	9.1	8.5	0.6	1.5
3110079O15RIK	12.8	12.2	0.6	1.5
VAT1	9.6	9.1	0.6	1.5
COL8A2	8.2	7.6	0.6	1.5
LOC100047162	9.9	9.4	0.6	1.5
HOXC6	9.1	8.5	0.6	1.5
ZFYVE21	10.3	9.7	0.6	1.5
BGLAP-RS1	13.8	13.2	0.6	1.5
9430028L06RIK	7.9	7.3	0.6	1.5
ACTA2	10.3	9.7	0.6	1.5
GLT25D1	10.7	10.1	0.6	1.5
RCN3	8.3	7.7	0.6	1.5
CLEC3B	8.2	7.6	0.6	1.5
GMDS	8.8	8.2	0.6	1.5
BMPER	8.3	7.7	0.6	1.5
2300002D11RIK	8.0	7.4	0.6	1.5
PLAT	8.0	7.4	0.6	1.5
TWIST1	8.4	7.8	0.6	1.5
6230400G14RIK	8.8	8.2	0.6	1.5
PLOD3	10.2	9.7	0.6	1.5
CAPG	10.0	9.5	0.6	1.5
LOC626583	8.1	7.5	0.6	1.5
ALG14	8.9	8.4	0.6	1.5
MMP12	7.8	7.2	0.6	1.5
TNXB	8.5	7.9	0.6	1.5
TUBA1A	9.4	8.9	0.6	1.5
CD81	12.8	12.2	0.6	1.5
TMEM86A	9.9	9.4	0.6	1.5
C1QTNF5	7.9	7.3	0.6	1.5

ERGIC1	9.4	8.8	0.6	1.5
5031439A09RIK	8.9	8.4	0.6	1.5
S100A10	9.2	8.6	0.6	1.5
CBR2	9.1	8.6	0.6	1.5
FBLN7	7.8	7.3	0.6	1.5
B9D1	8.3	7.7	0.6	1.5
ALG5	9.6	9.1	0.6	1.5
RRAS	9.9	9.3	0.6	1.5
CHMP4B	10.4	9.8	0.6	1.5
GNS	10.9	10.4	0.6	1.5
H47	10.8	10.3	0.6	1.5
IFITM5	9.2	8.7	0.6	1.5
WWTR1	8.8	8.2	0.5	1.5
CRIP2	11.0	10.4	0.5	1.5
ANXA2	13.6	13.1	0.5	1.5
A730017D01RIK	8.5	7.9	0.5	1.5
PRRX1	8.1	7.6	0.5	1.5
COL22A1	10.4	9.9	0.5	1.5
MANBAL	10.3	9.8	0.5	1.5
POFUT2	8.1	7.6	0.5	1.5
APLNR	8.3	7.7	0.5	1.5
FBLIM1	8.7	8.2	0.5	1.5
LMNA	10.4	9.9	0.5	1.5
PLCD1	8.7	8.1	0.5	1.5
RHBDF1	9.9	9.4	0.5	1.5
LOC100039175	8.8	8.2	0.5	1.5
EBPL	8.8	8.3	0.5	1.5
KDELR2	8.5	8.0	0.5	1.5
FAH	8.9	8.3	0.5	1.5
PDIA3	11.7	11.1	0.5	1.5
PLA1A	8.1	7.6	0.5	1.5
GAS6	11.3	10.8	0.5	1.5
BC065085	8.3	7.8	0.5	1.5
D10ERTD610E	8.6	8.1	0.5	1.4
IFIT3	8.5	8.0	0.5	1.4
PDGFRL	7.9	7.4	0.5	1.4
3632451O06RIK	8.0	7.5	0.5	1.4
TPM4	11.3	10.8	0.5	1.4
PLP2	10.0	9.5	0.5	1.4
C4B	8.7	8.1	0.5	1.4

Table 7: Genes changed expression in DMM model at day 7

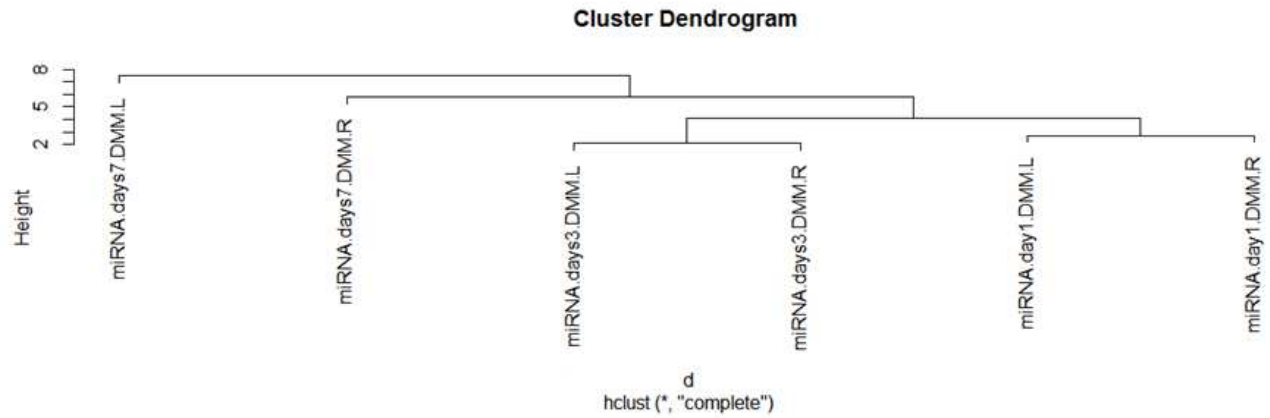

Figure 1: Hierarchical cluster analysis for DMM models at 1, 3, and 7 days after surgery

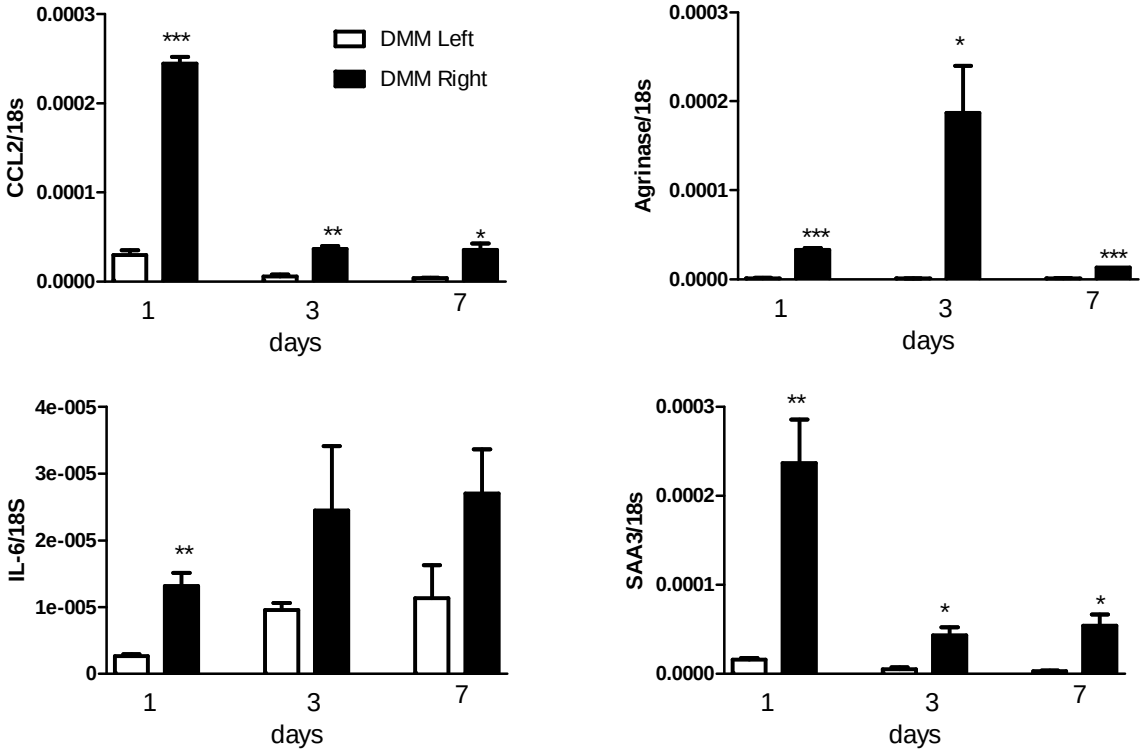

Figure 2: CCL2, Agrinase, IL-6 and SAA-3 were significantly induced expression in DMM model at 1, 3, and 7 days after surgery

Total RNA was reversed transcribed to cDNA and gene expression was measured by real-time qRT-PCR in individual samples of DMM left knee (un-operated, open bar), and DMM right knee (DMM, close bar). 18S was used as endogenous control. The data show mean +/- SEM, n=3. The expression of genes of interest between each group was analysed by unpaired two-tailed t test * $p<0.05$, ** $p < 0.01$, *** $p<0.001$.

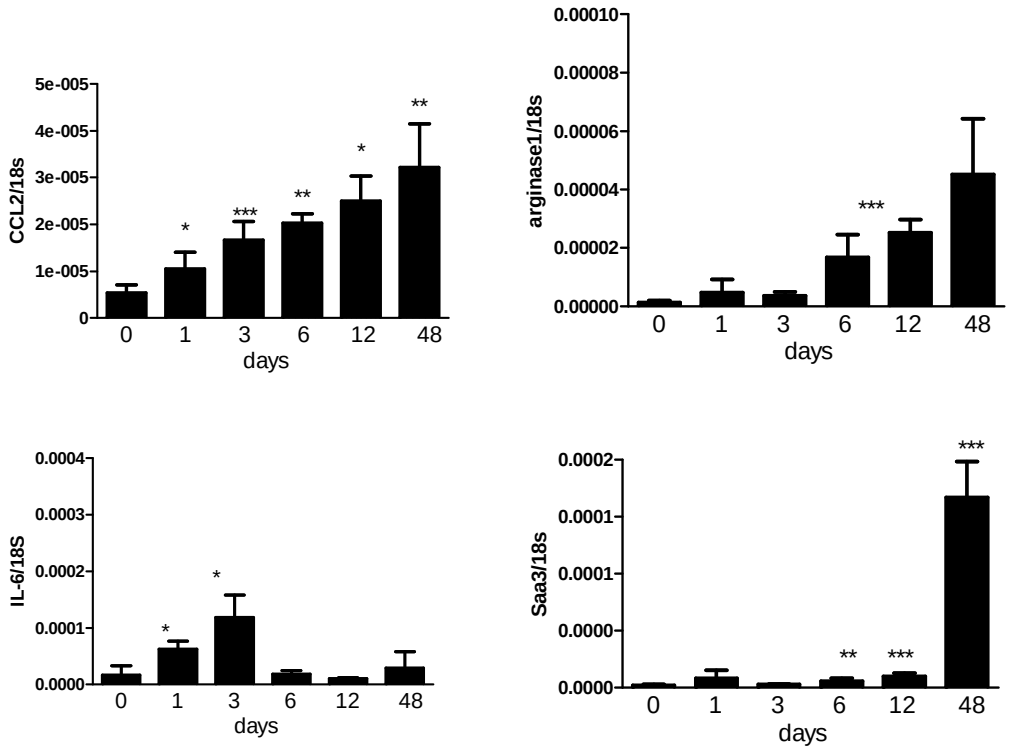

Figure 3: Gene expression in hip avulsion injury model

The femoral caps of C57Bl/6 mice aged 4 weeks were avulsed and put in culture. At each of 3, 6, 12, 48 hour time points, the femoral caps were harvested. Total RNA was isolated using Trizol and reverse transcribed to cDNA. Gene expression was measured by real-time qRT-PCR where 18S was used as an endogenous control. Assays were repeated 3 times. At least triplicate samples were measured at each time. Means ± standard errors are presented. Difference in expression between each time point against control (t=0) was calculated by unpaired two-tailed t test. * $p<0.05$, ** $p < 0.01$, *** $p<0.001$.

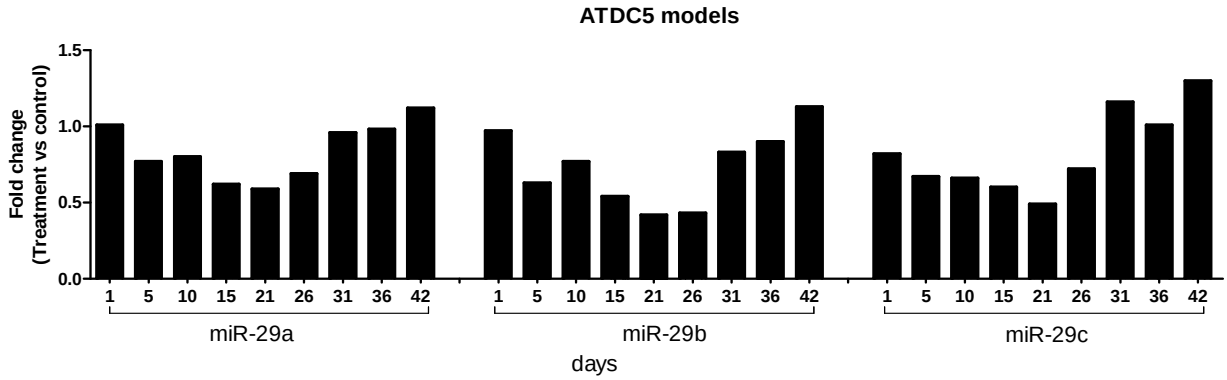

Figure 4: The expression of the miR-29 family in ATDC5 model

The embryonic carcinoma cell line ATDC5 was stimulated to from chondrocytes using insulin for 42 days. Total RNA was isolated, reverse transcribed to cDNA and used for miRNA microarray.

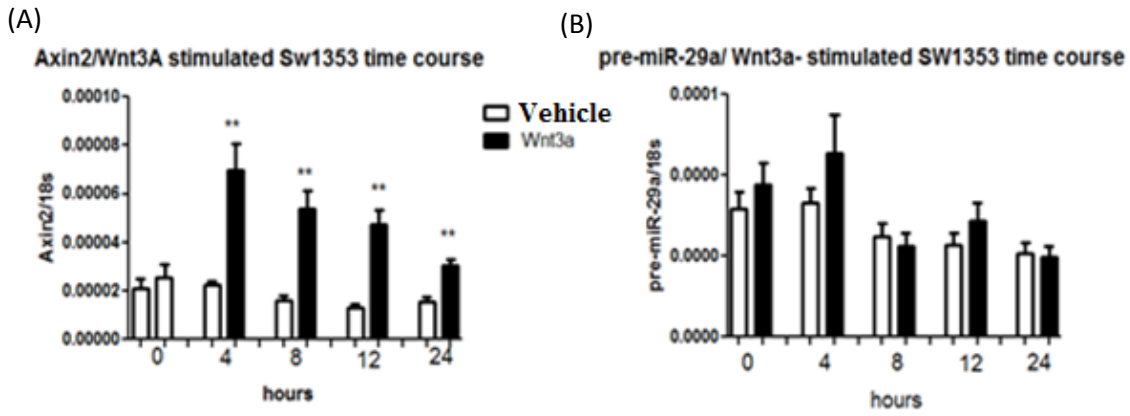

Figure 5: Expression of the miR-29 family was not controlled by Wnt3a

SW1353 cells were cultured in high glucose media with 10% (v/v) FCS in monolayer until 90% confluence. Cells were serum starved for 24 hours before treating with Wnt3a or vehicle (0.5% (w/v) BSA) across 24 hour course.

Relative expression of the precursor miR-29a and axin2 was measured by quantitative RT-PCR. 18S rRNA was the endogenous control for measuring the precursor transcripts. Open bar, control; close bar, WNT3a. (A) Expression level of axin2. (B) Expression level of precursor miR-29a. Means ± standard errors are presented. The difference between the treatment and the control was analysed by unpaired two-tailed t test. * $p<0.05$, ** $p < 0.01$, *** $p<0.001$, n=3.

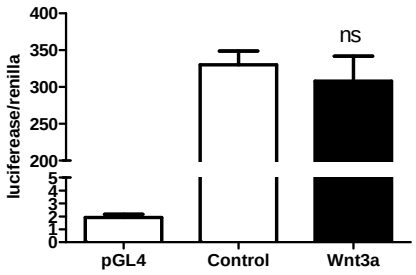

Figure 6: Wnt3a does not control the expression from the primary miR-29a/b1 promoter

The pri-miR-29a/b1 promoter-reporter (100ng) or the empty vector pGL4 (control, 100ng) were transfected into SW1353 cells. After transfection, cells were serum starved for 24 hours, followed by stimulating for another 6 hours with WNT3a (100ng/ml), or vehicle (0.5% BSA) before measuring luciferase activity. Renilla was use as endogenous control. Open bar: vehicle, black bar: Wnt3a. Means ± standard errors are presented, n=3. The difference of luciferase activity was analysed by unpaired two-tailed Student's t test. * $p<0.05$, ** $p < 0.01$, *** $p<0.00$.

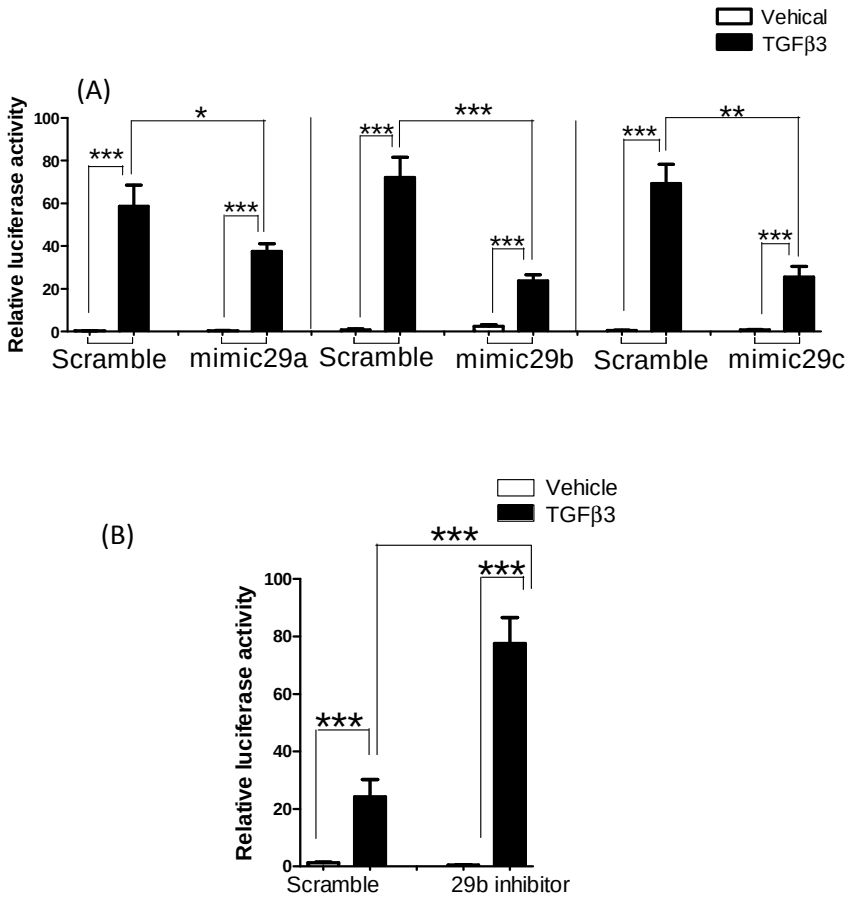

Figure 7 The miR-29 family suppress TGFβ signalling pathway

(A) The TGFβ signalling reporter ($CAGA_{12}$-luc) contains 12 binding sites of the Smad2/3/4 (GAGAC) binding consensus upstream of the firely luciferase-encoding gene in pGL3100ng $CAGA_{12}$-luc vector, and 10ng Renilla vector were co-transfected with either miR-29 family mimic (B) or miR-29b inhibitor (C) into SW1353 cells in monolayer. The non-targeting control (50nM) was also used as the negative control. 24 hours after transfection, cells were serum starved for another 24 hours, followed by treatment with TGFβ3 (4ng/ml) for another 6 hours before measuring luciferase activity. Renilla is the loading control for luciferase assay. Open bar: non – treatment control, close bar: TGFβ3 treatment. Means ± standard errors are presented, n=6. The difference of luciferase activity was analysed by Student's unpaired two-tailed t test. * $p<0.05$, ** $p < 0.01$, *** $p<0.001$

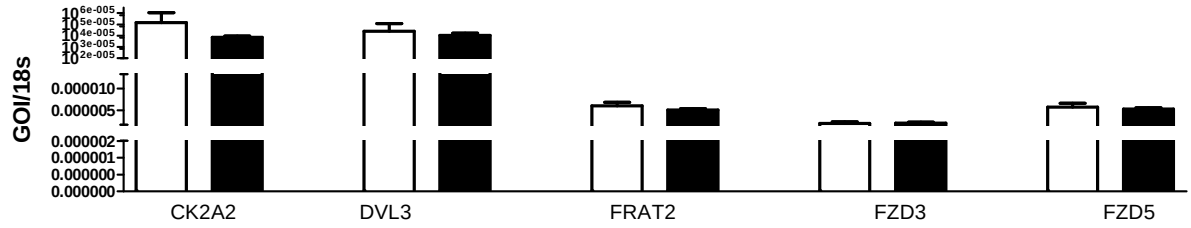

Figure 8 The miR-29 family does not target some of its putative targets at mRNA level Human primary chondrocytes was cultured in media with 10% (v/v) FCS in monolayer until 90% confluence. Cells were then transfected with either miR-29b mimic (50nM) or non – targeting control (50nM) for 48 hours. Total RNA was isolated and the expression levels of GOI were measured by qRT-PCR. 18S rRNA was the housekeeping control. Relative expression value of each of these genes was normalized to non – targeting control. Means ± standard errors are presented, n=3. The difference in expression between miR-29b overexpression and non – targeting control was analysed by Student's unpaired two-tailed t test. * $p<0.05$, ** $p < 0.01$, ***, $p<0.001$